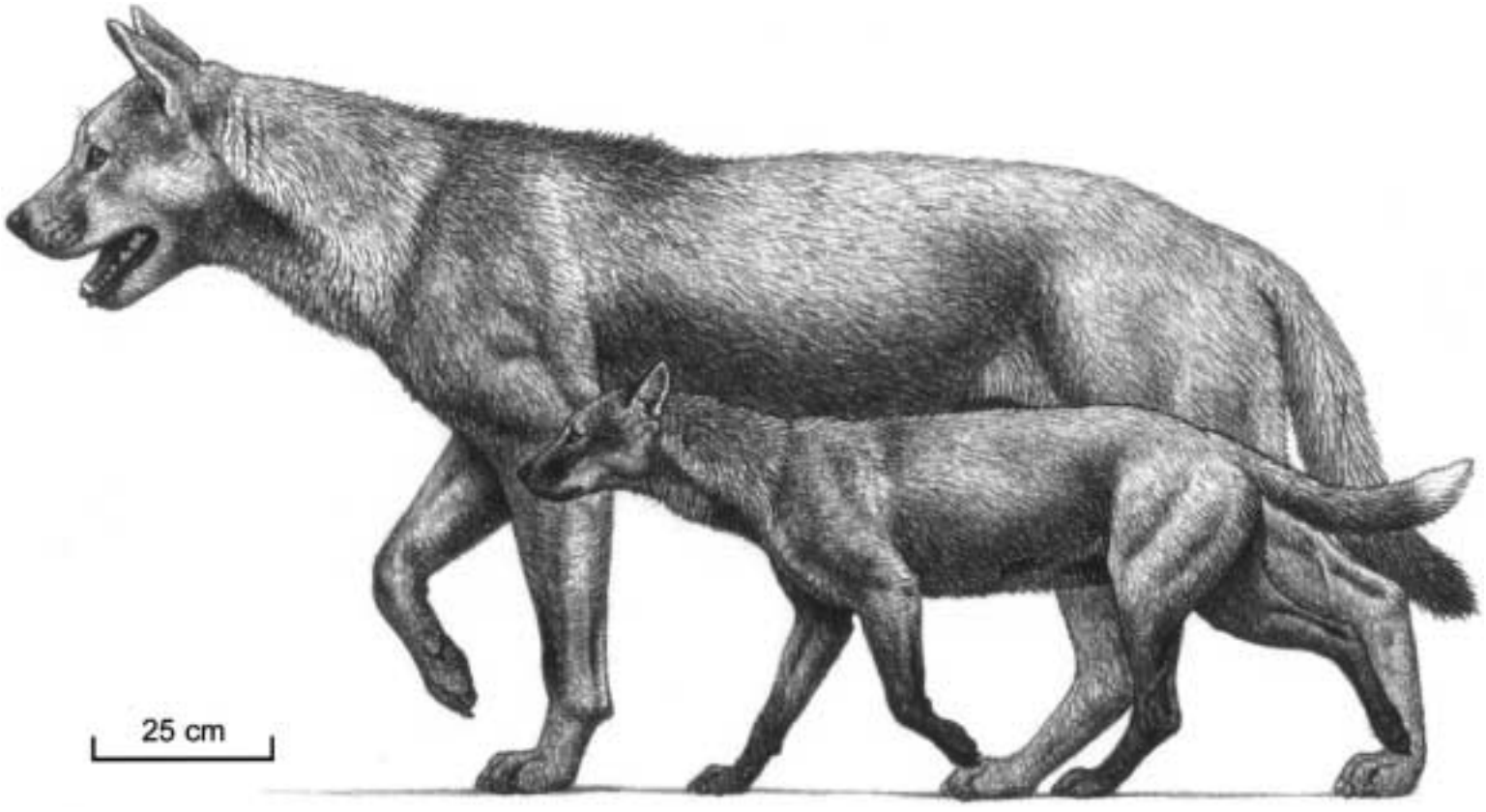

Reconstruction of *Epicyon saevus* (small individual, based on AMNH 8305) and *Epicyon haydeni* (large individual, composite figure, based on specimens from Jack Swayze Quarry). These two species co-occur extensively during the late Clarendonian and early Hemphillian of western North America. Illustration by Mauricio Antón.

CONTENTS

FIGURES

TABLES

ABSTRACT

The subfamily Borophaginae (Canidae, Carnivora, Mammalia) was erected by G. G. Simpson in 1945 to include seven genera of large, bone-crushing ''dogs'' in the late Tertiary of the northern continents. As a monophyletic group of canids, the Borophaginae is now known to be much more diverse than was originally envisioned but is confined within the middle to late Tertiary of North America. Fossil records of the borophagines are well represented and members of this prolific clade are often the most common predators in the late Tertiary deposits.

Largely due to the Childs Frick Collection at the American Museum of Natural History, borophagines are represented by some of the best materials among fossil carnivorans in anatomical representation, sample size, and stratigraphic density. As a result of this explosive growth of new information, borophagine systematics is now in need of a complete rethinking at a level that could not have been attempted by previous studies.

A detailed study of borophagine phylogenetic systematics is presented here, publishing for the first time the entire Frick Collection. A total of 66 species of borophagines, including 18 new species, ranging from Orellan through Blancan ages, are presently recognized. A phylogenetic analysis of these species is performed using cladistic methods, with Hesperocyoninae, an archaic group of canids, as an outgroup. At its base, the Borophaginae has a sister relationship with the subfamily Caninae, which includes all living canids and their most recent fossil relatives. The Borophaginae–Caninae clade is in turn derived from the subfamily Hesperocyoninae.

Apart from some transitional forms, most of the Borophaginae can be organized in four major clades (all erected as new tribes or subtribes): Phlaocyonini, Cynarctina, Aelurodontina, and Borophagina. The Borophaginae begins with a group of small fox-sized genera, such as *Archaeocyon*, *Oxetocyon*, *Otarocyon*, and *Rhizocyon*, in the Orellan through early Arikareean. Relationships among these genera are difficult to resolve due to their primitiveness. Slightly more derived, but still near the base of the Borophaginae, is the Phlaocyonini, a hypocarnivorous clade of the Arikareean and Hemingfordian that includes *Cynarctoides* and *Phlaocyon*. These two genera represent divergent approaches toward hypocarnivory. Species of *Cynarctoides* trend toward selenodonty and remain small in size, whereas species of *Phlaocyon* specialize toward bunodont dentitions but of increasing size, with an unusual trend toward hypercarnivory by two terminal species in the clade.

Four transitional taxa (species of *Cormocyon* and *Desmocyon*) occupy intermediate positions between the Phlaocyonini and Cynarctina, and represent a gradual size increase toward medium-size individuals. The subtribe Cynarctina, the second hypocarnivorous clade, includes *Paracynarctus* and *Cynarctus* in the Hemingfordian through Clarendonian, and represents a larger size group than the Phlaocyonini, although there is a tendency toward size reduction among advanced species of *Cynarctus*. The cynarctines feature the most bunodont dentition known among canids.

The next series of transitional taxa (*Metatomarctus*, *Euoplocyon*, *Psalidocyon*, *Microtomarctus*, *Protomarctus*, and *Tephrocyon*) are of medium size and occupy a pectinated sequence that contains a rather diverse set of dental morphology. These include the most hypercarnivorous borophagine *Euoplocyon*, the peculiarly trenchant *Psalidocyon*, and the dwarf lineage *Microtomarctus*. The next clade, Aelurodontina, is the first major hypercarnivorous group and is represented by *Tomarctus* and *Aelurodon* in the Barstovian and Clarendonian. The aelurodontines evolve around a more consistent theme of increasingly more hypercarnivorous dentitions with strong premolars, forming a rather linear series from *Tomarctus* to various species of *Aelurodon*.

The terminal clade Borophagina, sister to the Aelurodontina, begins with the mostly mesocarnivorous *Paratomarctus* and *Carpocyon* in the late Barstovian through late Hemphillian. The terminal species of *Carpocyon*, *C. limosus*, shows some hypocarnivorous adaptations. *Protepicyon* in the Barstovian initiates the hypercarnivorous trend in the terminal clade. *Epicyon*, the largest known canid, is the dominant predator in the Clarendonian and Hemphillian. Finally, an enlarged concept of *Borophagus* consists of a series of pectinated species terminated by *B. diversidens* in the late Blancan. *Epicyon* and *Borophagus* are the most highly evolved in their capacity to crush bones.

Phylogenetic reconstruction was greatly aided by the high quality of fossil records and the large number of transitional forms. The latter ensures a morphological continuity that facilitates the identification of homoplasies that otherwise could easily be mistaken as synapomorphies. Confidence in the phylogeny is further enhanced by a high congruence between the cladistic rank and the stratigraphic sequence. The temporal and morphological continuity in many borophagine lineages also permits further postulation about their evolutionary processes, such as cladogenetic and anagenetic events.

Our considerably enlarged concept of the Borophaginae indicates a much broader trophic diversity than has previously been envisioned. In addition to the commonly recognized hyenalike forms, members of the Borophaginae acquired a wider spectrum of morphologies that surpassed either the hesperocyonine or canine canids. The Borophaginae played broad ecological roles that are performed by at least three living carnivoran families, Canidae, Hyaenidae, and Procyonidae.

INTRODUCTION

Members of the subfamily Borophaginae, an archaic group in the dog family Canidae, are common carnivorans in North America from the middle Oligocene through the Pliocene. Together with the extinct bear dogs (Amphicyonidae) and occasional immigrant bears and cats from the Eurasia, borophagines were the dominant predators during much of this time. These ''hyenoid dogs'' are most commonly known for their specialized predatory features, such as robust, bone-cracking dentitions and jaws that parallel those of some Old World hyenas. On the other hand, certain omnivorous borophagines are noted for their specializations toward bunodont dentitions, which led them to be regarded as possible precursors to the raccoon family Procyonidae. Between these extreme forms of trophic adaptations is a wide spectrum of cranial and dental patterns that seems to fill every conceivable intermediate morphology, a striking demonstration of morphological flexibility unequaled by modern families of Carnivora.

Despite the diverse ecological roles of the borophagines and the presence of abundant fossil remains, no detailed phylogenetic study has been attempted since G. G. Simpson first erected the subfamily in 1945 (see History of Study below). This is especially notable in light of the fact that fossil borophagines are often the most common carnivorans in many Neogene deposits of North America. Nonetheless, carnivorans, being on top of the food chain, represent a small portion of the biomass and their fossil remains are relatively scarce.

It is therefore fortunate that Tertiary carnivorans attracted the keen interest of the late Dr. Childs Frick, who, with his personal fortune, launched a massive collection program unequaled in the history of vertebrate paleontology. With the help of a dedicated staff, the Frick Laboratory brought together a magnificent collection of Tertiary mammals, known as the Frick Collection (Galusha, 1975a). The impact of the Frick Collection can be felt in the vastly increased quality, quantity, and stratigraphic density of fossil records of many taxa. Significantly, the increased density permits the recognition of numerous intermediate taxa, which fill gaps in the previously known morphology and geological range, and represents a quantum leap in our ability to reconstruct their phylogeny.

In collaboration with his long-time assistant Beryl E. Taylor, Childs Frick intended to publish a comprehensive account of late Cenozoic carnivorans of North America, an ambitious project that remained incomplete at the time of his death in 1965. Since then, the Frick Collection at the American Museum of Natural History became available to the general scientific public. In the 1970s, two of the present authors, B. E. Taylor and R. H. Tedford, began a reanalysis of the systematics and phylogeny of two subfamilies of fossil canids, the Borophaginae and Caninae, under the then new cladistic paradigm. Under this new partnership, every taxon was examined anew and hypodigms were reassembled, and a preliminary phylogenetic analysis was produced without the benefit of computer programs. By the time of Taylor's retirement in 1980, the borophagine manuscript consisted of diagnoses and hypodigms of most taxa, measurements of approximately 80% of the specimens, and 89 plates of illustrations. In 1995, a renewed effort on the borophagine phylogeny became possible with the support from the National Science Foundation to Wang and Tedford. As Wang joined this latest collaboration, all specimens in the Taylor and Tedford manuscript were critically reexamined once again and additional material from more recent collections in several institutions was added to the hy-

podigm. Although the resulting phylogeny is in many ways consistent with the main framework of the Taylor and Tedford manuscript, significant differences exist in the number of taxa recognized, contents of hypodigms, and positions of some clades. In addition, descriptive sections for all taxa have been added. In the final stage of collaboration, the two senior authors did not attempt to persuade Taylor to share the views expressed in the present form, which differs substantially from his previous manuscript, and therefore they must bear responsibility for all of the errors in this monograph.

As the final product of a long search for a historical explanation of a complex group of carnivorans, this monograph represents the fruit of labors of three generations. The evolution of the ideas in each generation broadly reflects its own times in phylogenetic methodology and in the state of knowledge of particular taxa. The task of assembling all relevant information, morphologic and stratigraphic, on thousands of specimens proved to be daunting even with the energetic pursuit of the three generations. Although every effort was made to examine all relevant materials, we undoubtedly have missed some and probably misidentified others. While there surely are alternative hypotheses that we did not fully explore, especially in ways of constructing species, we are confident of the essential validity and internal consistency of our phylogeny given the current state of knowledge.

INSTITUTIONAL ABBREVIATIONS

ACM	Amherst College Museum (Pratt Museum), Amherst
AMNH	Department of Vertebrate Paleontology, American Museum of Natural History, New York
ANSP	Academy of Natural Science of Philadelphia, Philadelphia
BF	Private collection of Barbara Fite, Lutz, Florida
CMNH	Carnegie Museum of Natural History, Pittsburgh
DMNH	Denver Museum of Natural History, Denver
F:AM	Frick Collection, Department of Vertebrate Paleontology, American Museum of Natural History, New York
FMNH	Field Museum of Natural History, Chicago
HAFO	Hagerman Fossil Beds National Monument, Hagerman
IGM	Instituto de Geologia Museo, Universidad Nacional Autonoma de Mexico, Mexico D.F.
IMNH	Idaho Museum of Natural History, Pocatello
JODA	John Day Fossil Beds National Monument, John Day
KUVP	Division of Vertebrate Paleontology, Museum of Natural History, University of Kansas, Lawrence
LACM	Natural History Museum of Los Angeles County, Los Angeles
LACM-CIT	California Institute of Technology, now in the collection of the LACM
MCZ	Museum of Comparative Zoology, Harvard University, Cambridge
MSU	Midwestern State University, Wichita Falls
NMC	National Museum of Canada, Ottawa
OMNH	Oklahoma Museum of Natural History, Norman (= OMP or OUSM, Stoval Museum of Science and History, University of Oklahoma)
PPHM	Panhandle-Plains Historical Museum, Canyon
SDSM	Museum of Geology, South Dakota School of Mines and Technology, Rapid City
TMM	Texas Memorial Museum, University of Texas, Austin
TMM-BEG	University of Texas Bureau of Economic Geology, now in the collection of the TMM
TMM-TAMU	Texas A&M University, now in the collection of the TMM
TRO	Timberlane Research Organization, Florida
UA	University of Arizona, Tucson
UCMP	Museum of Paleontology, University of California at Berkeley
UCM	University of Colorado Museum, Boulder
UCR	University of California at Riverside
UF	University of Florida, Gainesville
UF V-	Formerly Florida Geological Survey, Tallahassee, now part of the University of Florida collection
UM	University of Michigan, Ann Arbor
UMMP	University of Montana Museum of Paleontology, Missoula

UNM	University of New Mexico, Albuquerque
UNSM	Nebraska State Museum, University of Nebraska, Lincoln
UO	University of Oregon Condon Museum of Geology, Eugene
USGS D	United States Geological Survey, Denver register
USGS M	United States Geological Survey, Menlo Park register
USNM	United States National Museum of Natural History, Smithsonian Institution, Washington, D.C.
UW	University of Wyoming, Laramie
UWBM	University of Washington Burke Museum, Seattle
WTSU	West Texas A&M University, formerly WTM, West Texas State University Museum, Canyon
YPM	Yale Peabody Museum of Natural History, Yale University, New Haven
YPM-PU	Princeton University Natural History Museum, now in the collection of the YPM

ACKNOWLEDGMENTS

It is obvious that the most critical asset in a project such as this is the presence of the magnificent fossil carnivoran collections at the American Museum of Natural History. Our foremost gratitude thus goes to Dr. Childs Frick, whose lifelong passion for fossil carnivorans helped produce the legendary Frick Collection. Borophagines were part of a larger plan by Frick to revise the entire North American Carnivora, an ambitious project that was never published. While we are the direct beneficiaries of his collection, the ideas in this volume are solely our own.

It is equally apparent that the Frick Collection would not be possible without the dedicated staff of the Frick Laboratory. The professionalism exhibited by these people in their exhaustive sampling and field documentation greatly enriches our knowledge of these canids. Among the most exceptional are Morris S. Skinner and Ted Galusha, assisted by Marie Skinner and Marian Galusha, whose collections and stratigraphic studies laid down the foundation of faunal successions.

We are deeply indebted to Raymond J. Gooris, who accomplished the monumental task of illustrating nearly all of the specimens and who painstakingly compiled much of the bibliography (except as noted otherwise, all specimen illustrations are drawn by Gooris). Sincere thanks are also due to the Frick Laboratory registrar George Krochak, to preparators Otto Simonis and Ernest Heying, and more recently to Edward Pederson for their skillful preparations of important specimens and casts of materials from many other institutions, to Alejandra Lora for her patience in typing the initial draft of this manuscript, to Lorrain Meeker for her excellent photographic plates used in this paper, and to Robert L. Evander for database input and cross-checking. We also thank Henry Galiano, Barbara Fite, and Jim Ranson for donations or loans of their private casts and specimens.

For their permission to study the collections in their care and their assistance in arranging loans and casts (and their patience with overdue loans) and in supplying locality data or measurements, we express our gratitude to the following individuals: Lawrence G. Barnes, Samuel A. McLeod, and David P. Whistler, Natural History Museum of Los Angeles County; Phil Bjork and James E. Martin, South Dakota School of Mines and Technology; C. S. Churcher, University of Toronto; Richard Cifelli, University of Oklahoma; Margery Coombs, University of Massachusetts; Walter W. Dalquest, Midwestern University; Mary R. Dawson, Carnegie Museum of Natural History; Robert J. Emry, United States National Museum of Natural History; John Flynn, William Turnbull, and William Simpson, Field Museum of Natural History; Lawrence J. Flynn and Charles R. Schaff, Harvard University; C. David Frailey, Johnson County Community College; Theodore J. Fremd, John Day Fossil Beds National Monument; Frederic G. Hayes, Marc S. Frank, Bruce J. MacFadden, and S. David Webb, University of Florida; Robert M. Hunt, Jr., Michael R. Voorhies, Richard G. Corner, and Bruce E. Bailey, University of Nebraska; John H. Hutchison and Pat Holroyd, University of California at Berkeley; Everett H. Lindsay, University of Arizona; Spencer G. Lucas, New Mexico Museum of Natural History and Science; Larry D. Martin and Desui Miao, University of Kansas; H. Gregory McDonald, Hager-

man Fossil Beds National Monument; Guy G. Musser, Department of Mammalogy, American Museum of Natural History; William N. Orr, University of Oregon; John M. Rensberger, University of Washington; Mary Ann Turner and John Ostrom, Yale University; and John A. Wilson and Ernest L. Lundelius, Jr., University of Texas at Austin.

We owe a deep debt of gratitude to our reviewers, Jon A. Baskin and Annalisa Berta, for their kindness to take up such a daunting task with good humor. We also greatly appreciate the moral support and encouragement by Berta during her tenure as program director of the NSF. We are especially grateful to Jon Baskin for sharing his insights on the evolution of *Aelurodon* and *Epicyon* and for his sensible comments that greatly improved the substance and presentation of this paper.

Finally, we gratefully acknowledge financial supports from the National Science Foundation (DEB-9420004, to Wang and Tedford; DEB-9707555, to Tedford and Wang), and a Frick Postdoctoral Fellowship to Wang. Additional financial assistance was provided by the Frick Endowment Fund.

HISTORY OF STUDY

In 1858, Joseph Leidy described two partial lower jaws and an isolated upper fourth premolar (carnassial) collected from deposits exposed along the Niobrara River in north-central Nebraska by F. V. Hayden, pioneer geological explorer of the west. Leidy named two genera based on this material, *Aelurodon* and *Epicyon*, thus beginning a series of discoveries of the ''hyenoid dogs'' in the Tertiary of North America. In the ensuing decades

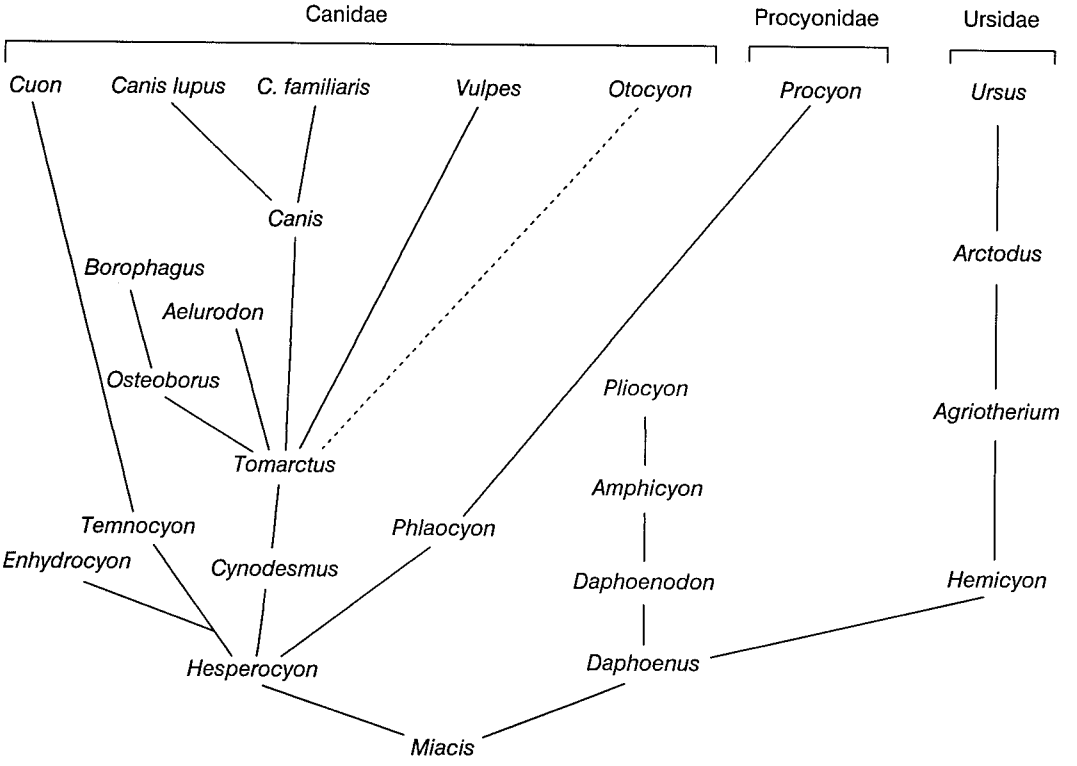

Fig. 1. Phylogeny of Canidae, Procyonidae, and Ursidae by W. D. Matthew, redrawn from Matthew (1930). Some taxa are substituted with current usages (e.g., *Tomarctus* for *Tephrocyon*, *Borophagus* for *Hyaenognathus*).

TABLE 1

Previous Classifications (or Phylogenies Modified into Classifications) of Borophagine Canids

1. Cope (1883: 247)
- Family Canidae
  - Basal lineage
    - *Megalotis* (= *Otocyon*)
    - *Amphicyon*
    - *Galecynus* (= *Cormocyon* sensu Cope)
  - *Galecynus–Hyaenocyon* lineage
    - *Temnocyon* (including *Mesocyon*)
    - *Enhydrocyon*
    - *Hyaenocyon* (= *Enhydrocyon*)
  - *Galecynus–Aelurodon* lineage
    - *Canis*
    - *Aelurodon*
    - *Oligobunis* and others

2. Scott (1895: 75)
- Cynoids
  - *Miacis–Cynodictis* lineage
    - *Cynodictis* (= *Hesperocyon*)
  - *Miacis–Canids* lineage
    - *Daphoenus*
    - *Temnocyon*
    - *Cynodesmus*
    - *Aelurodon*
    - *Canis*

3. Wortman and Matthew (1899: 139, taken from phylogeny)
- Family Canidae
  - *Uintacyon–Cuon* lineage
    - *Daphoenus*
    - *Enhydrocyon*
    - *Hyaenocyon*
    - *Temnocyon*
    - *Cuon*
  - *Procynodictis–Canis* lineage
    - *Cynodictis* (= *Hesperocyon*) *lippincottianus*
    - *Cynodesmus*
    - *Hypotemnodon* = *Mesocyon*
    - *Canis*
  - *Vulpavus–Nothocyon* lineage
    - *Cynodictis* (= *Hesperocyon*) *gregarius*
    - *Nothocyon* (= *Cormocyon*)

4. Matthew (1930: 132, taken from phylogeny in fig. 1, canid part only)
- Family Canidae
  - *Miacis–Cuon* lineage (trenchant talonid)
    - *Temnocyon*
    - *Enhydrocyon*
    - *Cuon*
  - *Miacis–Canis* lineage (basined talonid)
    - *Cynodictis*
    - *Cynodesmus* (= *Tomarctus thomsoni*)
    - *Tephrocyon* (= *Tomarctus*)
    - *Vulpes*
    - *Canis*
    - *Aelurodon*
    - *Osteoborus*
    - *Borophagus*

5. Loomis (1936: 50, taken from phylogeny in fig. 6)
- Canids with trenchant talonid
  - *Daphoenus–Amphicyon* group (amphicyonids)
  - *Temnocyon* group
    - *Temnocyon*
    - *Cuon*
    - *Icticyon* (= *Speothos*)
    - *Lycaon*
  - *Mesocyon* group
    - *Mesocyon*
  - *Enhydrocyon* group
    - *Brachyrhynchocyon*
    - *Enhydrocyon*
- Canids with basined talonid
  - *Nothocyon* group
    - *Cynodictis* (= *Hesperocyon*)
    - *Nothocyon* (= *Cormocyon*)
    - *Cynodesmus* (sensu stricto for *Tomarctus thomsoni*)
    - *Tomarctus*
    - *Canis*
  - *Tephrocyon* group
    - *Tephrocyon*
  - *Aelurodon* group
    - *Aelurodon*
    - *Borophagus*
    - *Hyaenognathus*
    - *Pliocyon*
  - *Allocyon* group (ursids)
    - *Allocyon*
    - *Hemicyon*

6. VanderHoof and Gregory (1940: 144)
- Hyaenoid dogs
  - *Cynodesmus*
  - *Tomarctus* (including *Tephrocyon*)
  - *Aelurodon*
  - *Osteoborus*
  - *Borophagus* (including *Hyaenognathus* and *Porthocyon*)

7. Simpson (1945: 108–111, in part)
- Superfamily Canoidea
  - Family Canidae
    - Subfamily Caninae
      - *Cynodictis*
      - *Pseudocynodictis* (= *Hesperocyon*)
      - *Nothocyon* (= *Cormocyon*)
      - *Cynodesmus*
      - *Mesocyon*
      - *Tomarctus*
      - *Leptocyon*
    - Subfamily Simocyoninae
      - *Brachyrhynchocyon*
      - *Enhydrocyon*
      - *Philotrox*
      - *Euoplocyon*

TABLE 1—*(Continued)*

Subfamily Borophaginae
Aelurodon
Borocyon (= *Daphoenodon*)
Borophagus
Gobicyon
Hadrocyon
Osteoborus
Pliocyon
Pliogulo

8. Macdonald (1963: 201, taken from phylogeny in fig. 23)
Trenchant talonid group
Hesperocyon
Mesocyon
Enhydrocyon
Sunkahetanka
Basined talonid group
Nothocyon
Cynodesmus
Neocynodesmus
Tomarctus
Other Borophaginae unspecified

9. Tedford (1978)
Family Canidae
Subfamily Hesperocyoninae
Hesperocyon
Mesocyon
Enhydrocyon
Subfamily Borophaginae
Nothocyon (= *Cormocyon*)
Tomarctus
Cynarctus
Prohyaena (= *Aelurodon*)
Aelurodon (= *Epicyon*)
Osteoborus
Borophagus
Subfamily Caninae
Leptocyon
Vulpes
Nyctereutes
Canis
Lycaon

10. Munthe (1989: fig. 1)
Subfamily Borophaginae
Tomarctus sensu lato
Euoplocyon
Cynarctus
Carpocyon
Aelurodon
Strobodon
Epicyon
Osteoborus
Borophagus

11. McKenna and Bell (1997: 244–245)
Infraorder Cynoidea
Family Canidae
Subfamily Borophaginae
Oxetocyon
Cormocyon
Euoplocyon
Phlaocyon
Tomarctus
Aletocyon
Bassarriscops
Cynarctoides
Strobodon
Aelurodon
Carpocyon
Epicyon
Cynarctus
Osteoborus
Borophagus

around the turn of the twentieth century, generic names such as *Tomarctus* (Cope, 1873), *Tephrocyon* (Merriam, 1906), and *Borophagus* (Cope, 1892) became well established in the literature. Taxonomic studies during this early period were mainly revisions of individual genera, e.g., *Tomarctus* (including *Tephrocyon*) by Matthew (1924), *Borophagus* (including *Hyaenognathus*) by Matthew and Stirton (1930), *Osteoborus* by Stirton and VanderHoof (1933), and *Aelurodon* by VanderHoof and Gregory (1940). Although these forms were frequently compared with one another or linked together in phylogenies (Matthew, 1924, 1930; VanderHoof and Gregory, 1940; McGrew, 1935; fig. 1), there was no explicit proposal to include them in a higher taxon, other than with informal references such as ''hyenoid dogs.''

In his influential classification of mammals, Simpson (1945: 111) listed seven extinct genera under a newly erected subfamily Borophaginae: *Borocyon*, *Aelurodon*, *Gobicyon*, *Pliocyon*, *Osteoborus*, *Pliogulo*, and *Borophagus*, with an additional genus, *Hadrocyon*, as Borophaginae incertae sedis. Simpson (1945: 224) informally defined his new subfamily as including ''large, later Tertiary canids with heavy jaws, rather distantly convergent toward the hyenas and so sometimes called 'hyenoid dogs.' '' Although Simpson considered that borophagines might be polyphyletic ''in detailed origin,'' citing the study by VanderHoof and Gregory (1940) as evidence, he nonetheless concluded that the included genera ''must have had a common origin very little, if at all, before the rise of the morphological family'' (Simpson, 1945: 224).

Of his original list of seven genera, four are now commonly regarded to be amphicyonids: *Borocyon*, *Gobicyon*, *Hadrocyon*, and *Pliocyon*. The remaining three genera, *Aelurodon*, *Osteoborus*, and *Borophagus* (including *Pliogulo*), were generally considered a natural group, in so far as higher level relationships of Canidae are concerned. More recent taxonomic studies of borophagines were mostly limited to these few highly hypercarnivorous forms plus a few mesocarnivorous forms such as *Tomarctus* (Williams, 1967; Dalquest, 1968; Webb, 1969b; Richey, 1979). A summary of previous classifications is presented in table 1.

Earlier studies of canid phylogeny generally follow a theme of bipartite division based on talonid structure of the lower carnassial, i.e., those with a basined, bicuspid talonid vs. those with a trenchant, unicuspid talonid, as championed by Matthew (1924, 1930) and followed until rather recently (e.g., Macdonald, 1963). A strict adherence to this dichotomy had led Matthew (1924, 1930) to divide the entire Canidae (plus some noncanids) into these two main categories, and to envision a highly heterogeneous group with trenchant talonids that includes such distantly related taxa as *Temnocyon* (an Arikareean amphicyonid), *Enhydrocyon* (an Arikareean hesperocyonine), and *Cuon* (Asiatic dhole, a living canine).

The concept of the Borophaginae was generally confined to a few highly specialized, bone-eating, hyenoid dogs until a brief review by Tedford (1978), who proposed a phylogenetic framework of selected genera of fossil and living canids. Two of his critical points are relevant in the present project. First, a tripartite division of the Canidae was proposed, which included the existing subfamilies Borophaginae and Caninae, and a new, more primitive, subfamily Hesperocyoninae. Such a division of canids has since been more or less adopted by contemporary vertebrate systematists (Berta, 1988; Martin, 1989; Munthe, 1989, 1998; Wang, 1990, 1994; Van Valkenburgh, 1991). The central concept of this phylogeny envisions three successive, partially overlapping radiations of canids replacing each other during the Tertiary (fig. 2). The earliest radiation is represented by the hesperocyonines, which first appeared in the late Eocene (Duchesnean, about 40 Ma) of North America, flourished during the Arikareean–Hemingfordian, and became extinct in the early Barstovian (Wang, 1994). During the Orellan, two lineages arose from *Hesperocyon*. One is represented by small fox-sized, *Cormocyon*-like animals that eventually gave rise to the borophagines. The other lineage is represented by *Leptocyon*, which became the precursor of the canines (including all living canids). The borophagines diversified before the canines, attained their maximal species richness during the Clarendonian, and became extinct by the start of the Pleistocene. The canines, on the other hand, maintained an inconspicuous presence during much of this time and did not achieve their present diversity until they had successfully dispersed into the Old World and South America in the Plio-Pleistocene.

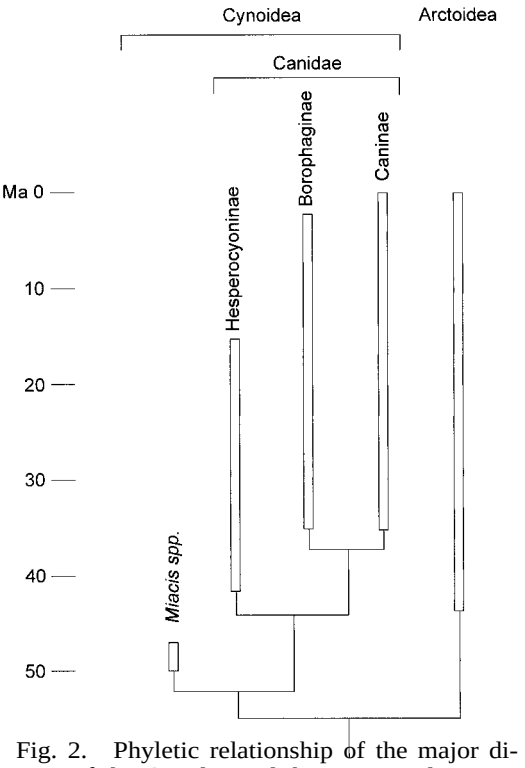

Fig. 2. Phyletic relationship of the major divisions of the Canidae and their temporal ranges. Relationships with other Caniformia are as developed in Wang and Tedford (1994: fig. 9).

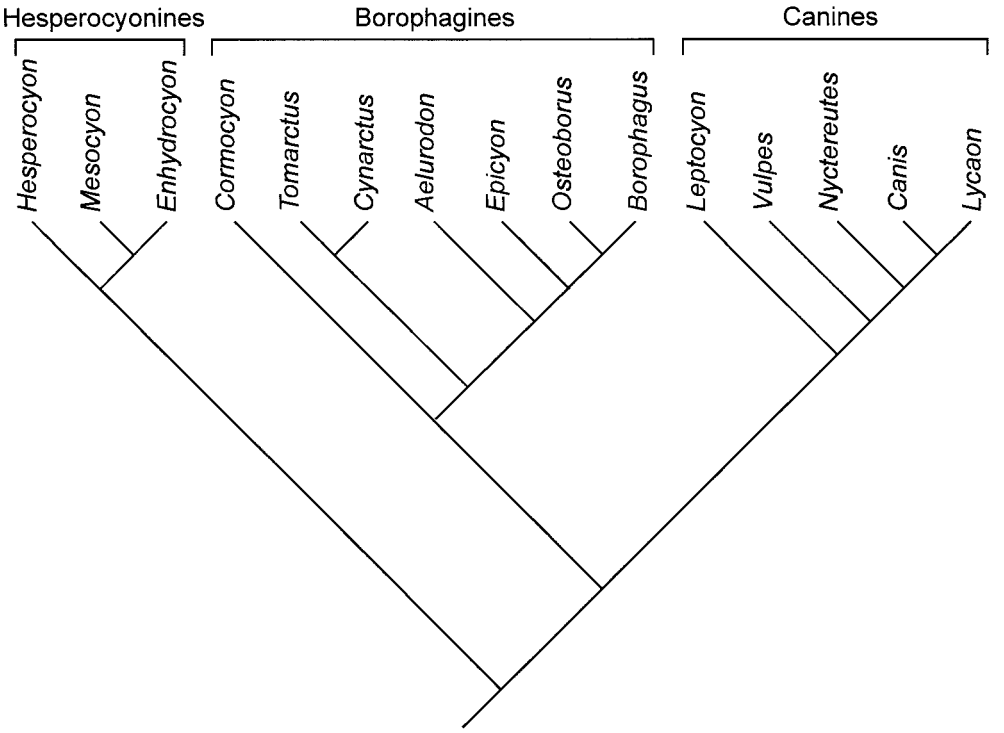

Fig. 3. Phylogeny of Canidae proposed by R. H. Tedford (redrawn from Tedford, 1978). Some taxa are substituted with current usages (e.g., *Cormocyon* for *Nothocyon*, *Aelurodon* for *Prohyaena*, *Epicyon* for *Aelurodon*).

Second, Tedford (1978: fig. 3) broadened the original concept of the Borophaginae (Simpson, 1945) to include such stem taxa as *Cormocyon* (formerly *Nothocyon*, see Wang and Tedford, 1992) and *Tomarctus* (formerly including *Cynodesmus*), as well as hypocarnivorous taxa such as *Phlaocyon* and *Cynarctus*. The small, generalized borophagines *Tomarctus* and *Cormocyon* had previously been regarded as directly ancestral to both the living canines as well as the derived borophagines (Matthew, 1924, 1930). The hypocarnivorous *Phlaocyon* and *Cynarctus*, on the other hand, were formerly thought to be related to the procyonids (the raccoon family), again on the basis of dental similarities only (Wortman and Matthew, 1899; Matthew, 1930; McGrew, 1937, 1941; Simpson, 1945), but were later conclusively demonstrated to be canids by Hough (1948) and Dahr (1949). A recent update by McKenna and Bell (1997: 244) on the Simpson's 1945 classification of Borophaginae has significantly expanded the original list of genera and is largely consistent with that proposed in this paper.

Munthe (1979, 1989) studied the functional morphology of borophagine postcranial skeletons. Her systematic framework is broadly consistent with that presented here, although her selected taxa are limited to a few forms that have adequate postcranial materials (see table 1). Munthe found a diverse array of postcranial adaptations among borophagines, in contrast to the stereotypical view that these hyenoid dogs were noncursorial, bone-crushing scavengers. Besides the obvious reason of better or more complete postcranial materials available, this is partly due to her modern view of borophagine systematics (see also Munthe, 1998), i.e., some of the included meso- and hypocarnivorous taxa were simply not considered borophagines in the past. The spectrum of cursorial capabilities and trophic adaptations is surely further enlarged in light of a much larger

content of the Borophaginae identified in this study (Munthe began her analysis with ''*Tomarctus*'' *thomsoni* as the most primitive borophagine and did not attempt to study such basal forms as *Archaeocyon*, *Cormocyon*, *Phlaocyon*, *Cynarctoides*, etc.).

MATERIALS AND METHODS

SCOPE

Because their specimens are usually the most common carnivorans in the middle to late Tertiary of North America, borophagines are present in nearly every institution housing a collection of Tertiary mammals. Although a completely exhaustive study is not practical, every effort was made to ensure a comprehensive review of all significant collections and all published materials, through loans, casts, or personal visits by at least one of us. Despite the fact that material comes from nearly 40 present or former institutions (see list under Institutional Abbreviations), the Frick Collection at the American Museum of Natural History comprises the largest single collection of borophagines and constitutes our primary database.

SPECIES DETERMINATION

Morphological criteria are the only available means for discrimination of fossil species. Most species can be distinguished by a combination of qualitative and quantitative characters and morphometrics. Discontinuity in the morphospace is still a convenient criterion in species discrimination, whose usefulness has been demonstrated in recent studies of living sympatric canids (Dayan et al., 1989, 1992). In these studies, the lower carnassial length of coexisting species of desert canids in the Middle East was found to differ by approximately 18%, which was postulated to reflect character displacement in niche partitioning. Such a living analog can be usefully applied in fossil canids (e.g., Wang, 1994).

Studies of morphological variation in living canids also offer quantitative guides for the present study (e.g., Lawrence and Bossert, 1967, 1975; Kolenosky and Standfield, 1975; Clutton-Brock et al., 1976; Nowak, 1979). Species delineations, however, are rarely completely precise when variations through geologic range and among different geographic regions are intermingled in large samples. Quantitative variations typically include one or more components, such as ontogenetic, sexual, geographic, and geologic variation. The latter often entails a moderate amount of size increase over the life-span of a species. Our evaluations of morphological variation in borophagines indicate that coefficients of variance in lower carnassial lengths generally fall within a range of 4 to 7, comparable to those in the hesperocyonines and living canids. Larger values would thus signal the possibility of a mixed sample, although allowance is sometimes made for cases in widespread taxa with long durations that have undergone noticeable size change. Furthermore, divisions of chronospecies along an anagenetic lineage (morphological change without cladogenetic event) contain a certain degree of arbitrariness when the fossil record is more or less continuous. Geological hiatuses sometimes serve as convenient breaks but may later be shown to be artifacts of poor records when transitional samples are obtained.

Except in rare cases when fossil material can be positively sexed through association of a baculum (e.g., some skeletons of *Desmocyon thomsoni* and *Carpocyon compressus*), sexual identity in most instances can only be inferred from a few dental and osteological features, most of which are quite subtle and thus do not offer unambiguous identification. Sexual dimorphism of canids is relatively subtle and appears strongly constrained by the phylogeny, in contrast to the markedly more dimorphic arctoids (Gittleman and Van Valkenburgh, 1997). Dimorphisms in cranial and dental measurements of living canids range from 3 to 6% in *Vulpes* (Churcher, 1960; Gingerich and Winkler, 1979; Dayan et al., 1989, 1992; Gittleman and Van Valkenburgh, 1997; personal obs.), 3 to 8% in *Canis* (Jolicoeur, 1975; Gittleman and Van Valkenburgh, 1997), and nearly 0% in *Urocyon* (Gittleman and Van Valken-

burgh, 1997; personal obs.); such differences are often well within the adult size variation of the population as a whole. Qualitatively, males of living canids tend to have slightly stronger canines, broader and deeper muzzles, more robust jaws, stronger postorbital processes and sagittal crest, and possibly broadly concave caudal edge of pubis (Munthe, 1989; Gittleman and Van Valkenburgh, 1997; personal obs.). Such morphological tendencies are useful as a general guide for allowance of intraspecific variation.

TAXONOMIC NOMENCLATURE

Ideally, higher level nomenclatures (genus and above) should be consistent with phylogenetic relationships. Traditional usage of some generic names, e.g., *Tomarctus* and *Cormocyon* (formerly *Nothocyon*), often reflects an evolutionary grade rather than strict genealogical relationships. For the most part, we use generic names for monophyletic clades only, although it is not practical to completely eliminate paraphyletic taxa. In fact, some species, as defined in this study, represent segments of a single lineage, and as such, recognition of more than one species along a continuous spectrum of morphological change is necessarily arbitrary and paraphyletic. Thus we do not designate a genus for every pectinated species unless it represents a distinct lineage (usually supported by autapomorphies) from adjacent species.

Above the generic level, we use the ranks of tribe or subtribe for several well-defined clades (e.g., Phlaocyonini, Cynarctina, Aelurodontina, and Borophagina) that represent specializations toward hypo- or hypercarnivory. These names are also convenient for discussions about relationships or functional morphology. However, we do not attempt to assign every taxon to a tribe or subtribe, leaving segments of pectinated clades without a higher level designation, except that they are within the subfamily Borophaginae.

Throughout the text we frequently use the conventional terms ''primitive'' or ''derived'' to describe certain taxa. These terms are convenient in discussions about relationships between phylogenetic positions and morphological features. It should be obvious that the relative primitiveness or derivedness of a taxon is defined within the context of our phylogeny.

FORMAT

Owing to the large number of species and specimens involved in this study, as well as our emphasis on phylogenetic relationships, we adopt an abbreviated format for economical presentation of morphological information. Instead of the traditional bone-by-bone and tooth-by-tooth descriptions, we figure all historically important specimens (types) as well as anatomically well-preserved ones. In most instances, we illustrate multiple specimens for each species so that they complement each other in anatomical details and permit a sense of variations. The illustrations are done in a consistent manner to enable the reader to make certain morphological comparisons directly. The subtler proportional differences are more easily demonstrated in the log-ratio diagrams (sensu Simpson, 1941) that we compile for all species described in this paper. These proportional relationships can also be examined in tables of cranial and dental measurements presented in appendices II and III. In the tables for dental measurements, we list measurements for the holotype as well as all primary statistics to show quantitative variations. In the tables for cranial measurements, on the other hand, we present the original data, since measurable skulls are far more rare than are dental specimens. Together, the illustrations, ratio diagrams, and tables of measurements comprise the primary database for morphological information on all taxa. To supplement this system, we sometimes make brief comparisons among related species on relevant features that are not easily gathered from the above sources, or we note qualitative variations in a section labeled ''Description and Comparison'' under each species. Finally, a ''Discussion'' section is used to briefly comment on the phylogenetic implications and/or other important information about the taxon. Likewise, historical developments of each taxon are not presented in great detail. Instead, we strive to provide a comprehensive synonym list for past references of all taxa whenever an author's concept of the taxon is unambiguous (i.e., not just taxonomic lists). Readers

can thus look for such information from the synonym lists. We hope that this system is a viable alternative to detailed verbal descriptions and that it forms an adequate basis from which the reader can verify the data matrix in the phylogenetic analysis.

We attempt to make the diagnoses close reflections of our phylogenetic framework. However, the purpose of our diagnoses is to contrast and delineate closely related taxa and is not meant to be a mirror image of the characters mapped on the phylogenetic tree. Thus, while we point out the polarities of the diagnostic features whenever possible, these features tend to be more descriptive than are the characters coded in the matrix or mapped on the phylogenetic tree, and a character complex, sometimes coded as one character, may be split into several diagnostic features. In addition, the diagnosis is more directed toward contrasts of anatomies from actual materials rather than the assumed character transformations for missing data as demanded by the phylogenetic algorithm.

CHRONOLOGICAL FRAMEWORK

The time scale used in this work to calibrate the geologic ranges of borophagine (fig. 141) is derived from data in Tedford et al. (1987) as modified by new knowledge of the position of epoch boundaries and the placement of the boundaries of the North American Land Mammal ages (NALMa).

A significant reinterpretation of the position of the Eocene–Oligocene boundary places it now at about 34 Ma at the Chadronian–Orellan NALMa boundary (Prothero and Swisher, 1992). The revision of the geomagnetic polarity timescale (Cande and Kent, 1995) yields an Oligocene–Miocene boundary at 24 Ma (rounded from 23.8 Ma), a Miocene–Pliocene boundary of 5 Ma (rounded from 5.4 Ma), and a Pliocene–Pleistocene boundary of 1.8 Ma.

Continuing calibration of the NALMa using newly gathered correlations with the geomagnetic polarity timescale of Cande and Kent (1992, 1995) now allows placement of the Chadronian–Orellan boundary (Prothero and Swisher, 1992) nearly identical to the Eocene–Oligocene boundary at 34 Ma, the Orellan–Whitneyan boundary (Prothero and Swisher, 1992, Tedford et al., 1996) at 32 Ma (rounded from 32.2 Ma), the Whitneyan–Arikareean boundary (Tedford et al., 1996) at 30 Ma (30.1 Ma), the Arikareean–Hemingfordian boundary (MacFadden and Hunt, in press) at 19 Ma, the Hemingfordian–Barstovian boundary at 16 Ma (15.9 Ma), the Barstovian–Clarendonian boundary (data discussed in Whistler and Burbank, 1992) about 12 Ma, the Clarendonian–Hemphillian boundary (see Whistler and Burbank, 1992) about 9 Ma, the Hemphillian–Blancan boundary (Repenning, 1987) at 5 Ma (approximately at the top of the Therra subchron within the Gilbert chron), and the Blancan–Irvingtonian boundary (Repenning, 1987) at 2 Ma (base of the Olduvai subchron, 1.95 Ma, within the Matuyama chron).

Subdivision of the NALMa follows the definition and characterization proposed by Tedford et al. (1987). Although the content of these subdivisions remains valid, calibration of their boundaries needs revision following reassessment of the ages of the NALMa boundaries. Work on the Whitneyan–Arikareean transition (Tedford et al., 1996) provided an approximate data on the faunal turnover marking the beginning of the medial Arikareean at 28 Ma. A 4-m.y.-long episode follows that lacks biochronologic typification but ends approximately at the beginning of the Miocene (late Arikareean) at 24 Ma. The Hemingfordian is divided into two parts. The first by immigration events and the second by the explosive cladogenesis of equine horses at approximately 17.5 Ma. Likewise, the Barstovian is divided into two parts with the rise of the medial Miocene Great Plains chronofauna at about 14.8 Ma. The Clarendonian is divided at about 10 Ma by the immigration of shovel-tusk mastodonts. A two-fold division of the Hemphillian recognizes the increase in immigrants during the later part of the age beginning around 7 Ma. We have chosen to divide the Blancan at approximately 4 Ma at the boundary between Blancan II and III of Repenning (1987), placed in the late Gilbert above the Cochiti subchron recording the first appearance of muskrats in mid-latitude North America.

The geochrons of the taxa shown in the phylogenetic chart (fig. 141) were established using the above criteria and other spe-

cific chronological data related to their occurrence (stratigraphic association with radioisotopically dated rocks or relevant magnetostratigraphy). In some cases the precise position in time of the site or fauna containing borophagines is established by biological correlation with other sites with better chronological data. In cases where the taxon is a member of a fauna characteristic of a whole stratigraphic unit, the chronological limit of that unit is used as the temporal span of the taxon. These conventions will lead to some over-estimation of the geologic ranges for some taxa, which should be born in mind when assessing the average species longevity for the borophagines.

DEFINITIONS

Unless otherwise stated, anatomical terminology, particularly the soft anatomy, follows that of Evans and Christensen (1979). The notation for dental formula is as follows: I1 I2 I3 C1 P1 P2 P3 P4 M1 M2 for upper teeth and i1 i2 i3 c1 p1 p2 p3 p4 m1 m2 m3 for lower teeth. Dental nomenclature follows Van Valen (1966). Frequently used terms are defined in figure 4. Most of these represent conventional usage that needs no further explanation. We use the term hypocone in the upper molars, whether it is a discrete, conate cusp arising from the lingual cingulum as in certain hypocarnivorous lineages, or is simply an enlargement of the internal (lingual) cingulum as is the primitive condition for all canids. Such usage is different from that in the hesperocyonine volume (Wang, 1994), in which the term internal cingulum is used to indicate its homology with the structure in the miacoid carnivorans.

The terms hyper- and hypocarnivory, convenient concepts for describing dental adaptation in carnivorans, were proposed by Crusafont-Pairó and Truyols-Santonja (1956) on the basis of two angles on the upper and lower carnassial teeth. Our own use of these terms, however, is somewhat broader in meaning, not limited to the tooth angles of their original definition, and refers to the dental tendencies that emphasize shearing vs. grinding functions. By hypercarnivory we mean any dental tendency toward increased efficiency in shearing, which in canids commonly involves elongated shearing blade of carnassial teeth, reduction or loss of m1 metaconid, shortened and simplified m1 talonid, reduction of M2 and m2–m3. In contrast, hypocarnivorous tendencies include shortening of shearing blade, as well as enlargement and increasing complexity of grinding part of the dentition (m1 talonid and m2–m3). We also employ the coordinate term mesocarnivory to indicate a dentition lacking these specializations. Mesocarnivorous canids approach the primitive condition in dental structure.

SYSTEMATIC PALEONTOLOGY

CLASS MAMMALIA LINNAEUS, 1785
ORDER CARNIVORA BOWDICH, 1821
SUBORDER CANIFORMIA KRETZOI, 1943
INFRAORDER CYNOIDEA FLOWER, 1869
FAMILY CANIDAE FISCHER DE WALDHEIM, 1817

INCLUDED SUBFAMILIES: Hesperocyoninae Martin, 1989; Borophaginae Simpson, 1945; and Caninae Fischer de Waldheim, 1817.

DIAGNOSIS: The following synapomorphies uniting the canid clade are present in *Prohesperocyon* and *Hesperocyon*, the most basal members of the Canidae, although some of the characters are further modified in later and more derived taxa: presence of a low septum derived from the entotympanic bordering the suture of the ectotympanic with the caudal entotympanic; presence of a small and shallow suprameatal fossa; presence of an inflated entotympanic bulla; medial expansion of the petrosal in full contact with the basioccipital and basisphenoid; ossification of the tegmen tympani; extrabullar position of the internal carotid artery and loss of the stapedial artery; presence of posterior accessory cusps on the upper and lower third premolars; reduction of the M1 parastyle; and loss of the M3.

DISCUSSION: Phylogenetic analyses of basal cynoids and their higher taxonomic grouping follow recent studies by us (Wang, 1994; Wang and Tedford, 1994, 1996). Thus defined, our concept of the Canidae, especially

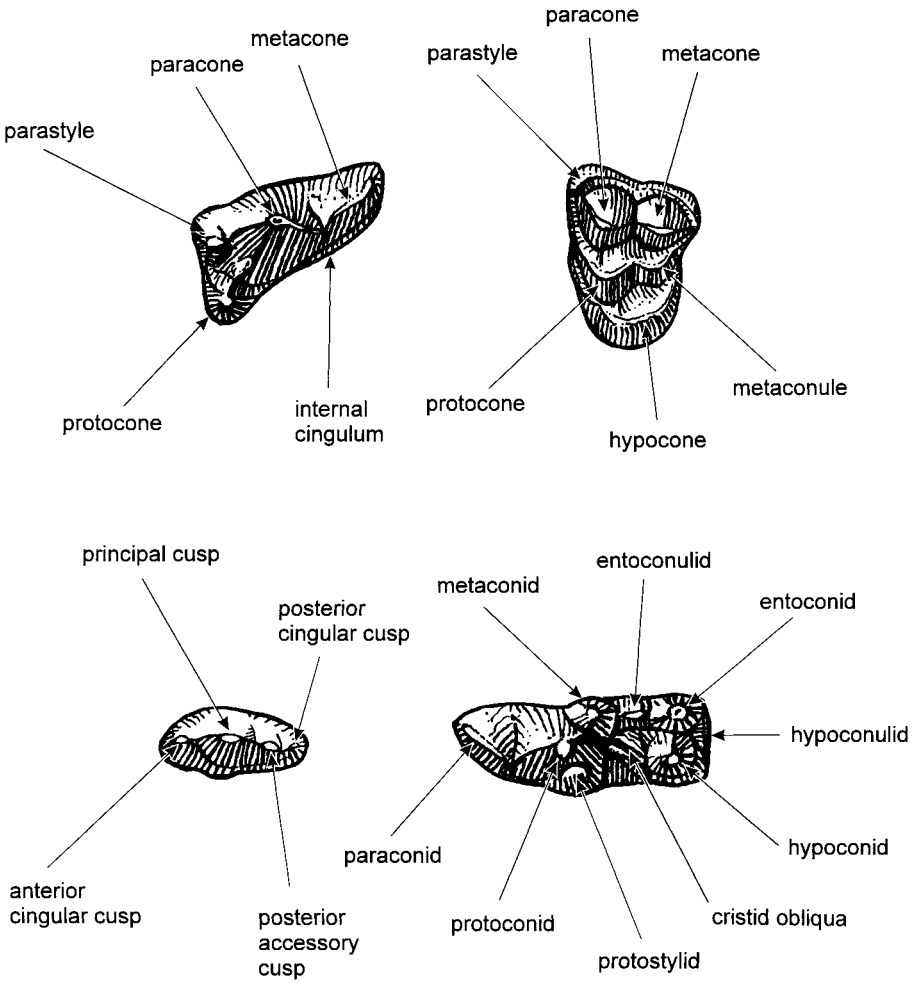

Fig. 4. Dental terminology for P4–M1 (upper part) and p4–m1 (lower part) in the present study.

as concerned with the extinct taxa, differs markedly from traditional treatments such as in Matthew (1924, 1930), Simpson (1945), and Piveteau (1961). Much of the difference can be attributed to a recent renewal of interest in the basicranial characters as a useful tool to unravel the fundamental relationships of caniform carnivores (see references cited in Wang and Tedford, 1994). The above canid basicranial characters remain quite stable throughout the history of Canidae, with the exception of a highly modified middle ear in *Otarocyon*, a new genus described below. We exclude amphicyonids from the Canidae because of their arctoid basicranium (Hough, 1948; Ginsburg, 1966; Hunt, 1977).

At the subfamily level, we follow a tripartite division of the Canidae proposed by one of us (Tedford, 1978) and substantiated later (Wang and Tedford, 1996). Such a scheme has gained some recent acceptance (e.g., Martin, 1989), and forms the basic framework of canid phylogeny in this study. According to this phylogenetic framework, all living canids and closely related fossil taxa (such as *Leptocyon* Matthew, 1918 and *Eucyon* Tedford and Qiu, 1996) belong to the Subfamily Caninae, whose living members were recently analyzed by Tedford et al. (1995) and whose fossil members are being monographed by Tedford, Taylor, and Wang (MS). Among early diverging lineages, a

North American radiation of early canids from late Eocene to middle Miocene comprises the Subfamily Hesperocyoninae, which was extensively treated by Wang (1994). Standing between the above two subfamilies (both in terms of phylogeny and in ecological replacement) is the Borophaginae, the subject of this study. See further comments about the interrelationship of the three subfamilies of the Canidae in the Discussion section under the subfamily Borophaginae.

SUBFAMILY BOROPHAGINAE SIMPSON, 1945

INCLUDED GENERA: *Archaeocyon*, new genus; *Oxetocyon* Green, 1954; *Otarocyon*, new genus; *Rhizocyon*, new genus; *Cynarctoides* McGrew, 1938a; *Phlaocyon* Matthew, 1899; *Cormocyon* Wang and Tedford, 1992; *Desmocyon*, new genus; *Paracynarctus*, new genus; *Cynarctus* Matthew, 1902; *Metatomarctus*, new genus; *Euoplocyon* Matthew, 1924; *Psalidocyon*, new genus; *Microtomarctus*, new genus; *Protomarctus*, new genus; *Tephrocyon* Merriam, 1906; *Tomarctus* Cope, 1873; *Aelurodon* Leidy, 1858; *Paratomarctus*, new genus; *Carpocyon* Webb, 1969b; *Protepicyon*, new genus; *Epicyon* Leidy, 1858; and *Borophagus* Cope, 1892.

DISTRIBUTION: Orellan through Blancan of North America and Hemphillian of Central America.

DIAGNOSIS: Borophagines and canines are distinguished from the hesperocyonines in further reduction of M1 parastyle, anteriorly extended lingual cingulum of M1, basined talonid of the m1, and tall m2 metaconid relative to protoconid. Compared to the canines, borophagines lack certain synapomorphies possessed by that subfamily: slender, elongated mandible, narrow and long premolars separated by diastemata, reduced or absent posterior accessory cusps on premolars, reduced P4 protocone, elongated trigonid of m1, and elongated m2, although most of these characters have been independently acquired by some derived borophagines. Except for the basal species, many borophagines progressively acquired additional synapomorphies that readily distinguish them from both hesperocyonine and canine canids: upper incisors with lateral cusps, more robust premolars with strong accessory cusps, presence of a distinct parastyle on P4, quadrate M1 with enlarged metaconule, and strong posterior process of the premaxillary that eventually meets the frontal.

DISCUSSION: Although we exclude *Borocyon*, *Gobicyon*, and *Pliocyon* from Simpson's Borophaginae, we substantially expand his concept to include a much larger array of taxa. With the possible exception (see Phylogeny section) of the three most basal genera (*Archaeocyon*, *Oxetocyon*, and *Otarocyon*) our cladistic analysis suggests it is a monophyletic clade and a sister group of the Subfamily Caninae.

The tendency toward a basined, bicuspid talonid on the m1 appears to be a key innovation that initiates the borophagine and canine clades. The elevation of the entoconid (from a primitively low ridge in *Hesperocyon*) to a cusp that, together with the hypoconid, encloses the talonid basin is the first step toward an increased grinding function for the dentition. The basined talonid may have been the most critical structure that enabled the early borophagines to avoid competition with the medium- to large-size hesperocyonines that dominate the hypercarnivorous niches—they were able to explore hypocarnivorous niches almost immediately after they diverged from *Hesperocyon*. Such a dental morphology forms the basis of repeated evolution of hypocarnivorous dentitions not only in borophagines (such as *Cynarctoides*, *Phlaocyon*, *Cynarctus*, and *Carpocyon*), but also in certain living canines (such as *Urocyon* and *Nyctereutes*). The basined, bicuspid talonid is thus a key innovation similar to the development of hypocones in the upper dentitions of many orders of eutherian mammals (Hunter and Jernvall, 1995). On the other hand, this basic talonid structure in the borophagines is noticeably modified toward more trenchant talonids in certain highly advanced taxa, such as *Euoplocyon*, *Aelurodon*, and *Borophagus*. These exceptions are clearly phylogenetic reversals as a result of the repeated evolution of hypercarnivorous tendencies.

Archaeocyon, new genus

TYPE SPECIES: *Pseudocynodictis pavidus* Stock, 1933.

ETYMOLOGY: Greek: *archaeo,* beginning; *cyon,* dog.

INCLUDED SPECIES: *A. pavidus* (Stock, 1933); *A. leptodus* (Schlaikjer, 1935); and *A. falkenbachi,* new species.

DISTRIBUTION: Whitneyan of Nebraska, South Dakota, and Wyoming; late Whitney or early Arikareean of California; early Arikareean of Nebraska, Wyoming, Montana, South Dakota, North Dakota, and Oregon; and medial Arikareean of Wyoming.

DIAGNOSIS: As a basal taxon in the Caninae–Borophaginae clade, *Archaeocyon* possesses all the synapomorphies that unite these two subfamilies and differentiate them from the hesperocyonines: M1 parastyle weak, M1 lingual cingulum anteriorly extended to surround protocone, basined talonid of m1, and m2 metaconid slightly higher than protoconid. In contrast to the Caninae clade (*Leptocyon* through living canids), *Archaeocyon* lacks derived characters for that clade: a slender horizontal ramus, narrow and elongated premolars that are set apart by diastemata, premolar posterior accessory cusps reduced or absent, reduced P4 protocone, more open trigonid of m1, and elongated m2. *Archaeocyon* remains primitive relative to most borophagines (*Rhizocyon* and higher sister taxa) in its unenlarged auditory bulla, posteriorly oriented paroccipital process that does not articulate with the bulla (except in some of the latest individuals of *A. pavidus*), posteriorly restricted M1 hypocone, and M2 lingual cingulum not connected to metaconule.

DISCUSSION: Phylogenetically, *Archaeocyon* is similar to *Hesperocyon* in its basal position to more than one clade. *Hesperocyon* is a paraphyletic genus that includes species which gave rise to the common ancestor of the Caninae–Borophaginae clade as well as to members of the Hesperocyoninae (Wang, 1994). Likewise, *Archaeocyon* is basal to both the Borophaginae and Caninae. Lacking a derived character of its own, *Archaeocyon* is a paraphyletic genus that does not exhibit a clear morphological tendency toward either the Caninae or Borophaginae. Considering that the dental morphology of basal borophagines tends to be more conservative (i.e., more similar to *Hesperocyon*) than their counterparts in the canines (*Leptocyon*), we place *Archaeocyon* in the Borophaginae along with *Oxetocyon* and *Otarocyon,* which occupy a similarly ambiguous position in the cladogram. The earliest occurrence of *Leptocyon* is in the Orellan (Wang and Tedford, 1996); records of *Archaeocyon* postdate the Orellan. It is thus unlikely that *Archaeocyon* had given rise to the Caninae. Instead, the genus is morphologically and stratigraphically in the right position to be the most basal member of the Borophaginae.

Of the few derived dental characters of *Archaeocyon* (more basined talonid, expanded lingual cingulum on M1, etc.), all are pointed toward an initial tendency of hypocarnivory relative to the condition in *Hesperocyon*. Such a tendency enabled the early borophagines to exploit hypocarnivorous niches bypassed by the far more hypercarnivorous hesperocyonines.

Lacking any clearly defined morphological trends, the species of *Archaeocyon* do not easily lend themselves to cladistic analysis. This kind of difficulty is not uncommon in small, basal caniforms that are conservative in just about every aspect of their morphology and show little inclination toward hyper- or hypocarnivory (see Phylogeny section for further discussion).

Archaeocyon pavidus (Stock, 1933)

Figures 5, 6

Pseudocynodictis (?) *pavidus* Stock, 1933: 31, pl. 1, figs. 1–5.

''*Hesperocyon*'' *pavidus* (Stock): Wang, 1994: 34 (in part), fig. 11A–C.

Cormocyon pavidus (Stock): Wang and Tedford, 1996: 446 (in part), fig. 7.

HOLOTYPE: LACM-CIT 466, crushed anterior half of skull and mandible with left P2–M1, right P3–M2, left and right p2–m2, and alveoli for p1 and m3 (Wang, 1994: fig. 11A, B), Kew Quarry Local Fauna (LACM-CIT loc. 126), Las Posas Hills, Sespe Formation (late Whitneyan or early Arikareean), Ventura County, California.

REFERRED SPECIMENS: From type locality: LACM 1338, partial ramus with p4–m1; and LACM 5276, partial ramus with p3–m1.

Whitneyan of northwestern Nebraska: F: AM 50338, partial left maxillary with I1–I3,

P2–M2, and associated partial mandible with left and right c1–m3, 1 mi northeast of Crow Butte, Dawes County, 30 ft above a gray, ashy layer in Whitney Member of Brule Formation; F:AM 63970 (Wang and Tedford, 1996: fig. 7), crushed skull with I3–P1, P2 broken–P4, M1–M2 both broken, both partial rami with c1–m3 (p1 alveolus) (figs. 5A–E, 6), articulated partial skeleton including atlas and incomplete vertebral column, humerus, radius, ulna, and distal end of femur through metatarsals I–V, east side of Roundhouse Rock, 5 mi southwest of Bridgeport, Morrill County, 20 ft below contact of the Whitney and Horn members of the Brule Formation; F:AM 63976, right ramus fragment with m2–m3, Plunkett-Parson Locality, 8 mi north of Harrison, Sioux County, below lower Whitney ash in a paleo-valley fill that cuts through the Orellan clays; F:AM 63990, partial left ramus with p4 broken–m2 and m3 alveolus, northeast of Crow Butte, 30 ft above green layer, Dawes County; UNSM 26142 (AMNH cast 96708), partial right ramus with p3 broken–m3, White River Group, probably Whitney Member of Brule Formation, Scotts Bluff County.

Whitneyan of southwestern South Dakota: F:AM 50342, fragment of left ramus with m1–m2, 6 mi southeast of Oelrichs, Fall River County, 20 ft above first gray nodule zone in Poleslide Member of Brule Formation; F:AM 63360, right ramus fragment with m1, 0.25 mi west of Cedar Pass, Jackson County, in basal Poleslide Member, Brule Formation; and LACM 9602 (AMNH cast 129651), right ramal fragment with m1–m2, LACM loc. 1973, Godsell Ranch.

Southeast corner of Sheep Mountain, uppermost part of Poleslide Member, Brule Formation, 3 ft below base of Rockyford Ash (late Whitneyan), Shannon County, South Dakota: F:AM 63220, partial crushed skull with C1–M2 (M1 broken) and both partial rami with p1–m2 and m3 alveolus.

Southeast corner of Sheep Mountain in lower part of Sharps Formation (early Arikareean), Shannon County, South Dakota: F:AM 63221, articulated partial skull and mandible with worn C1–M2, mandible with c1 (broken)–m3, articulated partial scapula through partial ulna, partial femur, and limb fragments, 15 ft above base of Rockyford Ash; and F:AM 63222, skull with I2 (broken)–M2 (fig. 5F–I), left ramus with c1–m3 (fig. 5J, K), humerus, distal end femur, partial scapula, and articulated cervical vertebrae, 18 ft above the base of the Rockyford Ash.

Picture Gorge 30, Blue Basin level 1, UCMP loc. V4849-1, Turtle Cove Member, John Day Formation, Oregon: UCMP 76652, maxillary and mandible fragments with left C1, P1–P2 alveoli, P3–M2, right P3–M2, left m1, and right p2–m2.

DISTRIBUTION: Whitneyan of Nebraska and South Dakota, early Arikareean of South Dakota and Oregon, and late Whitneyan or early Arikareean of California.

EMENDED DIAGNOSIS: *Archaeocyon pavidus* lacks derived borophagine characters other than those uniting the Borophaginae and Caninae clades. Being possibly the most primitive member of the genus, *A. pavidus* possesses all the synapomorphies of *Archaeocyon* as contrasted to the primitive conditions in the hesperocyonines: reduced M1 parastyle, anteriorly extended lingual cingulum on M1, incipient development of basined talonid on m1, and tall m2 metaconid. *A. pavidus* has an autapomorphy that distinguishes it from other species of the genus: presence of a lateral groove on the lower canine. Additionally, it is distinguished from *A. leptodus* in its smaller size and shorter m1, and from *A. falkenbachi* in its unshortened rostrum. *A. pavidus* differs from *Rhizocyon oregonensis* in having a smaller size, narrower upper molars, and M2 lingual cingulum not connected to metaconule.

DESCRIPTION AND COMPARISON: A detailed description of dental morphology of this species can be found in Wang (1994: fig. 11A, B). A significant addition of new material to the present study is four complete or partial skulls and skeletons from the latest Whitneyan to earliest Arikareean of Nebraska and South Dakota (figs. 5, 6). As expected from its phylogenetic position, *Archaeocyon pavidus* differs little from a small *Hesperocyon*. It retains an uninflated auditory bulla, a small suprameatal fossa, a posteriorly oriented paroccipital process, and relatively small braincase, all of which are primitive characters present in basal canids such as *Prohesperocyon* and *Hesperocyon*. A slightly enlarged bulla and ventrally oriented paroccipital pro-

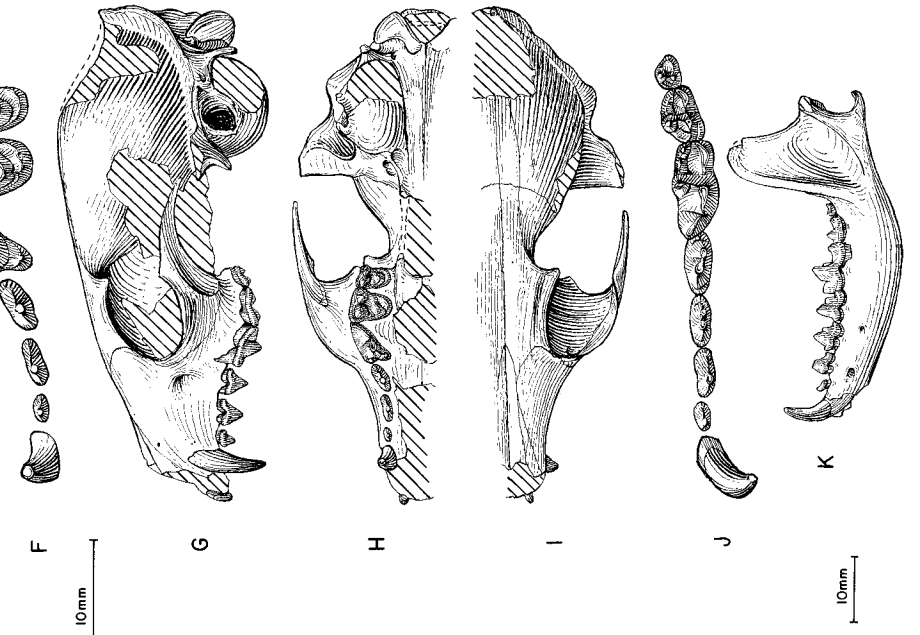

Fig. 5. *Archaeocyon pavidus*. **A**, Upper teeth, **B**, lateral and **C**, ventral views of skull, **D**, lower teeth, and **E**, ramus of F:AM 63970 (I1, P1, lingual parts of M1–M2, c1, and paroccipital process reversed from right side), east side of Roundhouse Rock, Whitney Member, Brule Formation (Whitneyan), Morrill County, Nebraska. **F**, Upper teeth, **G**, lateral, **H**, ventral, and **I**, dorsal views of skull, **J**, lower teeth, and **K**, ramus of F: AM 63222, Sheep Mountain, lower part of Sharps Formation (early Arikareean), Shannon County, South Dakota. The longer (upper) scale is for A, D, F, and J, and the shorter (lower) scale is for the rest.

Fig. 6. Partial articulated skeleton of *Archaeocyon pavidus*, F:AM 63970 (skull reversed from that of the left side), east side of Roundhouse Rock, Whitney Member, Brule Formation (Whitneyan), Morrill County, Nebraska. Photograph by Lorraine Meeker.

cess in individuals from the latest Whitneyan through earliest Arikareean of South Dakota indicate their slightly more derived morphology relative to individuals of older geologic age. The paroccipital process in the South Dakota specimens, although fully bent toward the ventral side, is still only partially fused with the bulla, i.e., there is a free tip at the distal end (fig. 5G).

Archaeocyon pavidus is smaller than *Hesperocyon gregarius*. Additionally, it has acquired some subtle dental features that signal its advance toward the Caninae–Borophaginae clade. *A. pavidus* is less hypercarnivorous than *Hesperocyon*, as is reflected in its slight increase in grinding dentition such as broadening of the M1 by reduction of the parastyle and anterior expansion of the lingual cingulum to surround the protocone, lowering of the m1 trigonid, lowering of the hypoconid and elevation of the entoconid on m1 to form a more basined talonid, and elevation of metaconid on m2 so that it is higher than the protoconid. Many of above features are in an initial stage of development and subject to variation that may be reminiscent of conditions in *Hesperocyon*. For example, although the M1 of F:AM 50338 has a reduced parastyle, it still has the lingual cingulum restricted to the posterolingual corner.

The postcranial skeleton of *Archaeocyon pavidus* is also much like that of *Hesperocyon*. The humerus is somewhat bowed and has an entepicondylar foramen. The olecranon of ulna lacks a prominent medial process. The digits are closely appressed for both metacarpals and metatarsals. Such a limb structure suggests an initial adaptation toward a scansorial life that probably has not quite achieved the full digitigrade posture (Wang, 1993).

DISCUSSION: Aside from the few subtle dental features that ally it with the borophagine–canine clade, *Archaeocyon pavidus* is rather *Hesperocyon*-like in size and proportions. *A. pavidus* was recognized by Wang (1994) as possibly a very primitive borophagine, but was tentatively referred to ''*Hesperocyon*'' to indicate its primitive sim-

ilarity to *H. gregarius*. Wang and Tedford (1996) adopted the interim name *Cormocyon pavidus* to express its basal borophagine position. In both papers, a small sample of fragmentary jaws from the Cedar Creek Member (Orellan) of White River Formation of Colorado in the KUVP collection [referred to as ''*Pseudocynodictis* sp. (small form)'' by Galbreath, 1953: 76] was included in the hypodigm of *C. pavidus*. Our present analysis of this sample, however, indicates that Wang's earlier reference, mainly based on size considerations, lacks the morphological basis established in this study. Most importantly, the talonid structure of the Colorado sample is basically that of a *Hesperocyon*. Such morphology is inconsistent with our phylogenetic hypothesis of early borophagines, which predicts that if a sister relationship between the Borophaginae and Caninae is correct, the basined talonid should have evolved during Orellan, since it occurs in the earliest *Leptocyon*. The small form in the Orellan of Colorado may represent a distinct species of *Hesperocyon* after all, although the fragmentary materials are not suitable for establishment of a new species.

Presence of *Archaeocyon pavidus* in the John Day Formation of Oregon is suggested by one individual, UCMP 76652, from the basal part of the Turtle Cove Member. Other than its slightly larger size, UCMP 76652 compares well with its counterparts in the Great Plains.

Archaeocyon leptodus (Schlaikjer, 1935)

Figures 7–11

Nothocyon leptodus Schlaikjer, 1935: 131, fig. 6.
Hesperocyon leptodus (Schlaikjer): Macdonald, 1963: 203; 1970: 54.
Nothocyon geismarianus (Cope, 1877): Macdonald, 1970: 55 (in part).

HOLOTYPE: MCZ 2878 (AMNH cast 129680), left partial ramus with c1–p2 alveoli, p3 root, p4–m2, and m3 root (fig. 9A, B). Schlaikjer (1935: 131) reported that the type was from ''Lower Harrison Formation, approximately 15 ft above the Brule-lower Harrison contact,'' 4.5 mi southeast of Fort Laramie, Goshen County, Wyoming. As pointed out by McKenna (1966: 6), these ''Lower Harrison'' sediments of Schlaikjer belong to the lower Arikaree Group of other authors (early Arikareean).

REFERRED SPECIMENS: Schomp Ranch, north of Mitchell, lower ash of the Whitney Member of the Brule Formation (Whitneyan), Sioux County, Nebraska: F:AM 63971, crushed partial skull with I3–M2 (P1 alveolus) (fig. 7A–D), mandible with i1–i3 alveoli and p1–m3 (fig. 7E, F), articulated partial skeleton including most of the vertebral column, partial scapula through manus with most of phalanges, partial femur, partial tibia and fibula, and pes with most of the phalanges.

Whitney Member of Brule Formation (Whitneyan), Morrill County, Nebraska: UNSM 25699, right partial ramus with p3 alveolus–m1, UNSM loc. Mo-107 or Mo-108.

Horn Member of the Brule Formation (early Arikareean), Morrill County, Nebraska: Redington Gap area (UNSM loc. Mo-108): F:AM 99287, left ramus with i1–p3 alveoli, p4–m2, and m3 alveolus, 92 ft above the base of upper Whitney ash and 5 ft below the contact with the Gering Formation; UNSM 4486, left ramus with incisor and c1 alveoli, p1–m1, and m2 broken (fig. 7K, L), 13 ft above the base of the Horn Member; UNSM 4487, right partial maxillary with P4–M1 and M2 alveolus, west of Reddington Gap, from 30 to 40 ft above the base of the Horn Member; UNSM 25126, right partial ramus with c1–p1 alveoli, p2–p3 broken, p4, m1 broken, m2, and m3 alveolus, north of Reddington Gap, from 30 to 40 ft above the base of the Horn Member; UNSM 25398, left ramus with i3, c1–p1 alveoli, p2–m1, and m2 root, 1.25 mi west of Reddington Gap, 50 ft above base of the Horn Member; and UNSM 25399 (AMNH cast 96705), skull with I1–I2, I3 alveolus, and C1–M2 (fig. 7G–J), 100 yd west of road, from 10 ft above base of the Horn Member. One mi east of Birdcage Gap (UNSM loc. Mo-105): UNSM 25707, skull with I1–M2 and mandible with i2 broken–m3. Round House Rock (UNSM loc. Mo-104): FMNH P14797, skull with I1 alveolus–M2 and both rami with i1 broken–m3 (fig. 8C–G); and UNSM 25394, right partial ramus with m1–m2 and m3 alveolus, astragalus, and fragments, 15 ft above marl,

upper part of the Horn Member; and UNSM 25709, palate with C1–M2 (M1 broken).

Horn Member of Brule Formation (early Arikareean), Banner County, Nebraska: Three mi northeast of Wrights Gap: UNSM 26097, anterior part of skull I1–I2, I3 alveolus, C1, and P1 alveolus–M2 (fig. 8A, B). North side of point between Shobar and Logan Canyons: UNSM 25708, partial skull with I1–C1 and P1 alveolus–M2, right and left rami with i2–c1 and p1 alveolus–m3, distal end of humerus, and partial radius and ulna. Bayard Quarry (UNSM loc. Bn-102): UNSM 25710, right partial ramus with p3–p4 alveoli, m1 broken, and m2–m3 alveoli.

Three Tubs locality, north side of 66 Mountain, Whitney Member, Brule Formation (Whitneyan), Goshen County, Wyoming: F:AM 50298, articulated skull with I3–M2 and mandible with c1–m3 and articulated partial skeleton with cervical vertebrae, partial scapula, both humeri, and incomplete radii and ulnae, from 10 ft above the lower ash in the middle Whitney; F:AM 50299, right incomplete side of skull with C1–M2 (P1 alveolus) articulated with right ramus with i3–m3 and distal ends of both tibiae, distal fibula, and both articulated incomplete pes, 3 ft above the base of the lower ash in the middle Whitney; and F:AM 50300, right incomplete side of skull with I3–C1 alveoli, P1, P2 broken, and P4–M1, and right partial ramus with p1–m3 (m1 and m2 broken), 8 ft above the base of the lower ash in the middle Whitney.

Wounded Knee Area, middle and upper parts of the Sharps Formation (early Arikareean), Shannon County, South Dakota: LACM 5900, left partial ramus with p3 broken–m2, LACM loc. 1829; LACM 9200, right partial ramus with p2, alveolus p3–p4, and m1 broken–m2, LACM loc. 1861; LACM 9283 (AMNH cast 129647), right partial ramus with p2 alveolus–m1, LACM loc. 1966; LACM 9297, left partial ramus with p4 (broken)–m1, LACM loc. 1980; LACM 9360, left maxillary fragment with P3–M1, LACM loc. 1819; LACM 9371 (AMNH cast 129650), left maxillary fragment with P4–M1, LACM loc. 1955; LACM 9389, right ramal fragment with m1 and m2 alveolus, LACM loc. 1982; LACM 9408, left ramal fragment with m1, LACM loc. 1959; LACM 9426, right ramal fragment with m1 and m2 broken alveolus, LACM loc. 1984; LACM 9446, right partial ramus with p4 broken–m2 (m3 alveolus), LACM loc. 1959; LACM 9518, right partial ramus with p2–m3, LACM loc. 1984; LACM 21661, right partial ramus with m1–m2, LACM loc. 1959; LACM 28982, left partial ramus with m1–m2 and m3 alveolus, LACM loc. 1956; SDSM 53323, crushed fragment of skull with P1–P3 alveoli and P4, SDSM loc. V5353; SDSM 53331, left maxillary fragment with M1, SDSM loc. V541; SDSM 54261, left ramal fragment with p4 (root)–m1, SDSM loc. V5357; SDSM 54272, left partial ramus with p3–p4 alveoli and m1–m2, SDSM loc. V5361; SDSM 54280, right partial ramus with p2 (alveolus) and p3–m2 (p4 broken), SDSM loc. V5359; SDSM 54292, skull with C1 alveolus, P1–P2 roots, and P3–M2, SDSM loc. V541; SDSM 54338, skull with I1 and I3, C1 alveolus, and P1–M2, SDSM loc. V541; SDSM 55101, right partial ramus with p2 (alveolus) p3, p4 root, and m1–m2, SDSM loc. V5351; and SDSM 56110, partial ramus with m1–m2 (both broken) and m3 alveolus, SDSM loc. V541.

East side of Cedar Pass, clay lens in capping channel, base of upper part of the Sharps Formation (early Arikareean), Jackson County, South Dakota: F:AM 49447, skull with I1–P3 alveoli and roots, P4–M1, and M2 alveolus (fig. 9J, K).

White Butte (Chalky Buttes), lower Arikaree Group (early Arikareean), Slope County, North Dakota: AMNH 8084, right partial ramus with p4–m1.

Little Muddy Creek, lower Arikaree Group (early Arikareean), Niobrara County, Wyoming: F:AM 49028, left partial ramus with m1 broken–m2 and m3 alveolus; F:AM 49044, partial skull with C1–P1 and M2 broken, both partial jaws with p2, p3–m1 (all broken or alveoli), and m2; F:AM 49045, skull with I1–M2 and both rami with c1–m3 (fig. 9C–H); F:AM 49047, right partial maxillary with P4–M2; F:AM 49048, left partial ramus with p1 alveolus and p2–m2 all broken; F:AM 49049, right partial ramus with m1–m2 and m3 root; F:AM 49051, left partial ramus with c1 broken, p1–p3 alveoli, p4–m1, and m2 root; F:AM 49052, left par-

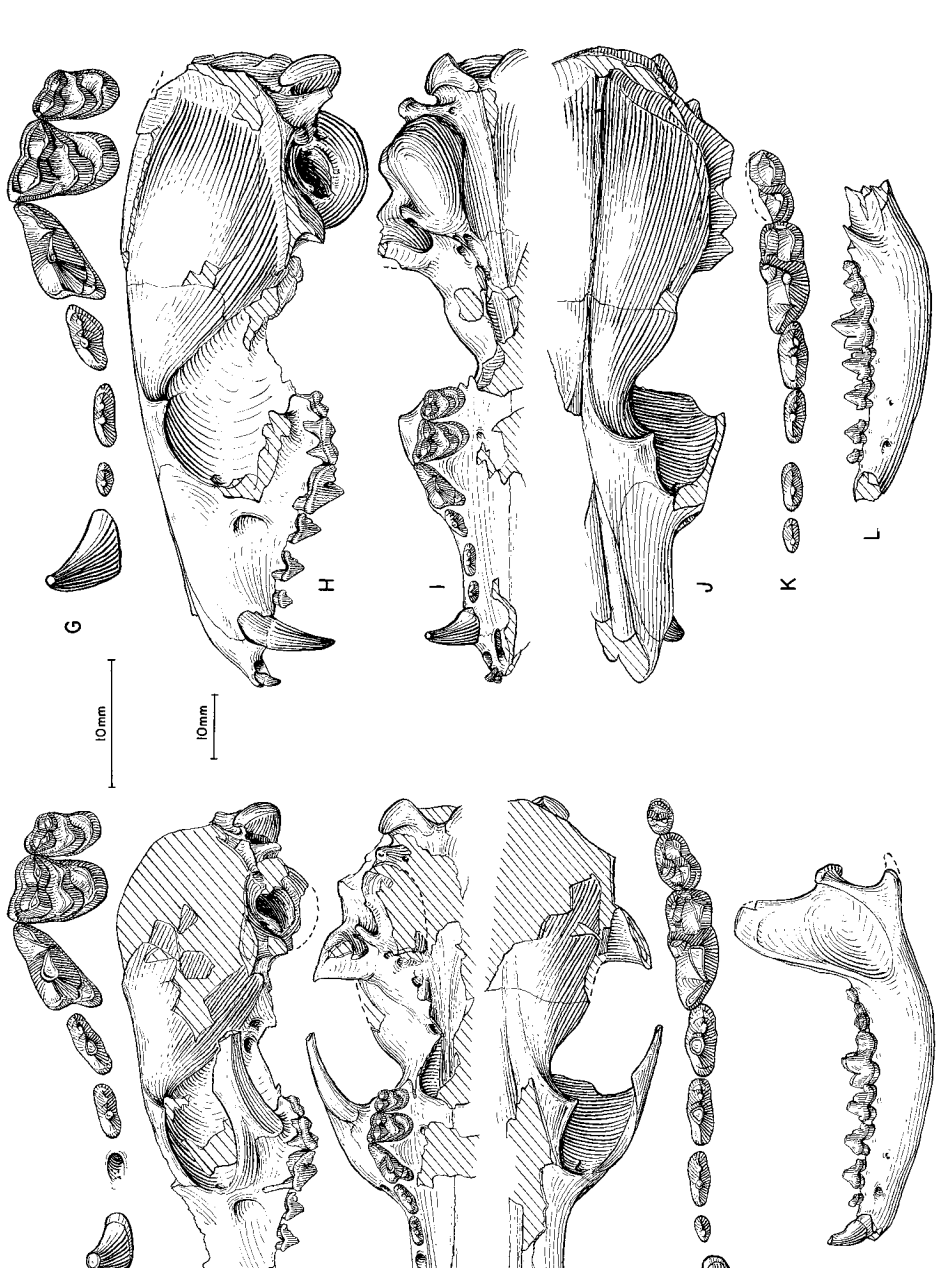

Fig. 7. *Archaeocyon leptodus*. **A**, Upper teeth, **B**, lateral, **C**, ventral, and **D**, dorsal views of skull, **E**, lower teeth, and **F**, ramus, F:AM 63971, Schomp Ranch, Whitney Member, Brule Formation (Whitneyan), Sioux County, Nebraska. **G**, Upper teeth, **H**, lateral, **I**, ventral, and **J**, dorsal views of skull (auditory bulla reversed from right side), UNSM 25399, Redington Gap, Horn Member, Brule Formation (early Arikareean), Morrill County, Nebraska. **K**, Lower teeth and **L**, ramus, UNSM 4486, Redington Gap, Horn Member of Brule Formation (early Arikareean), Morrill County, Nebraska. The longer (upper) scale is for A, E, G, and L, and the shorter (lower) scale is for the rest.

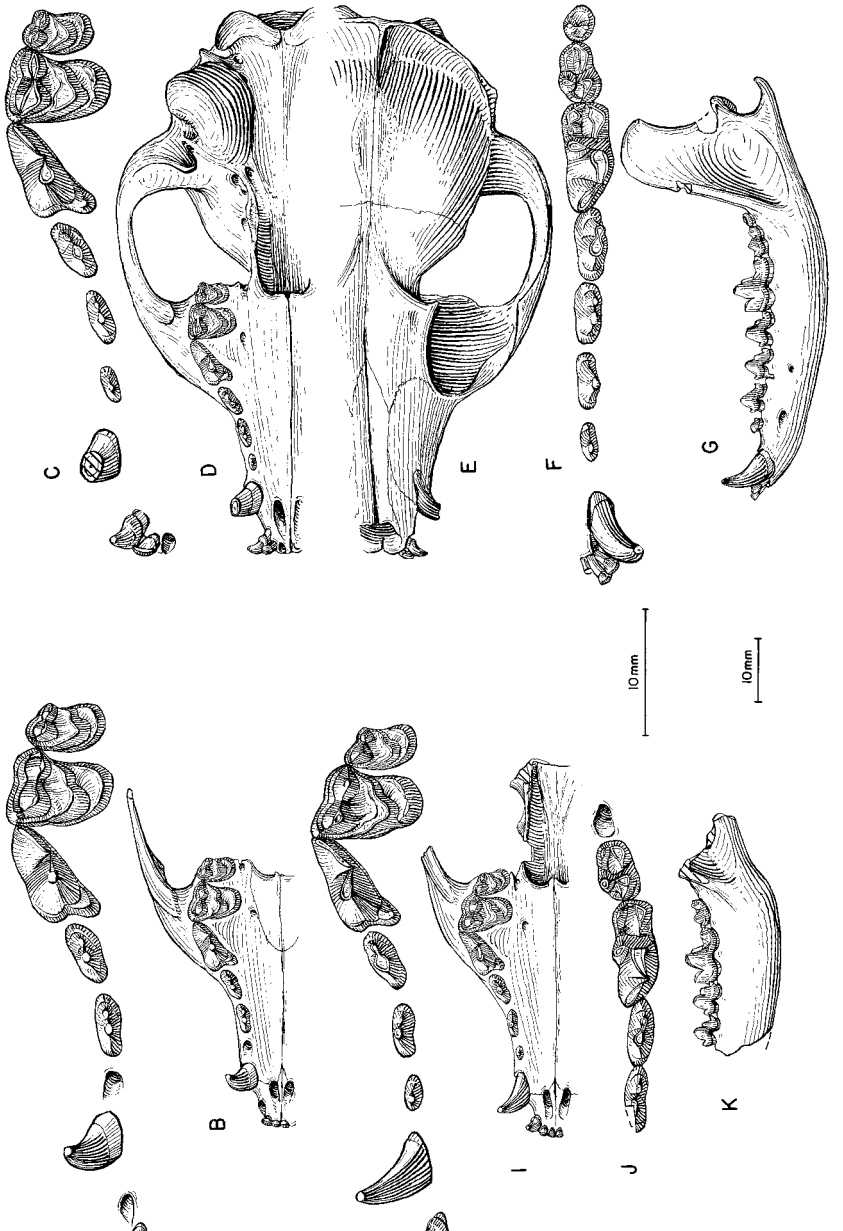

Fig. 8. *Archaeocyon leptodus*. **A**, Upper teeth and **B**, palate (P3 reversed from right side), UNSM 26097, 3 mi northeast of Wrights Gap, Horn Member, Brule Formation (early Arikareean), Banner County, Nebraska. **C**, Upper teeth, **D**, ventral, and **E**, dorsal views of skull, **F**, lower teeth (c1 reversed from right side), and **G**, ramus (reversed from right side), FMNH P14797, Round House Rock, Horn Member, Brule Formation (early Arikareean), Morrill County, Nebraska. **H**, Upper teeth, **I**, palate, **J**, lower teeth, and **K**, ramus (reversed from right side), F:AM 50221, south side of Bear Mountain, lower Arikaree Group (early Arikareean), Goshen County, Wyoming. The longer (upper) scale is for A, C, F, H, and J, and the shorter (lower) scale is for the rest.

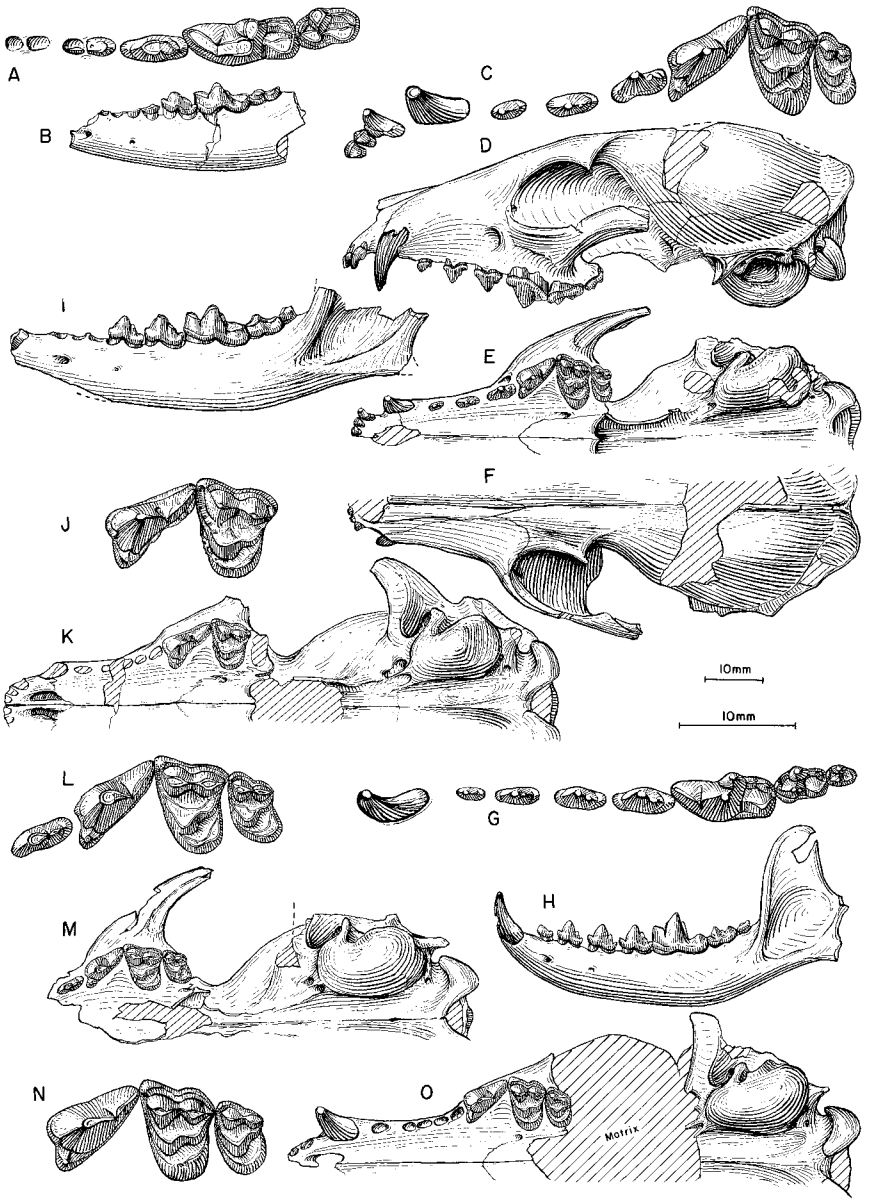

Fig. 9. *Archaeocyon leptodus*. **A**, Lower teeth and **B**, ramus, MCZ 2878, holotype, lower Arikaree Group (early Arikareean), Goshen County, Wyoming. **C**, Upper teeth, **D**, lateral, **E**, ventral, and **F**, dorsal views of skull, **G**, lower teeth, and **H**, ramus (all reversed from right side), F:AM 49045, Little Muddy Creek, lower Arikaree Group (early Arikareean), Niobrara County, Wyoming. **I**, Ramus, F:AM 49052, Little Muddy Creek. **J**, P4–M1, and **K**, ventral view of skull, F:AM 49447, east side of Cedar Pass, Sharps Formation (early Arikareean), Jackson County, South Dakota. **L**, Upper teeth and **M**, ventral view of skull (reversed from right side), F:AM 49032, Muddy Creek, lower Arikaree Group (medial Arikareean), Niobrara County, Wyoming. **N**, Upper teeth and **O**, ventral view of skull (reversed from right side), F:AM 49033, Muddy Creek. The longer (lower) scale is for A, C, G, J, L, and N, and the shorter (upper) scale is for the rest.

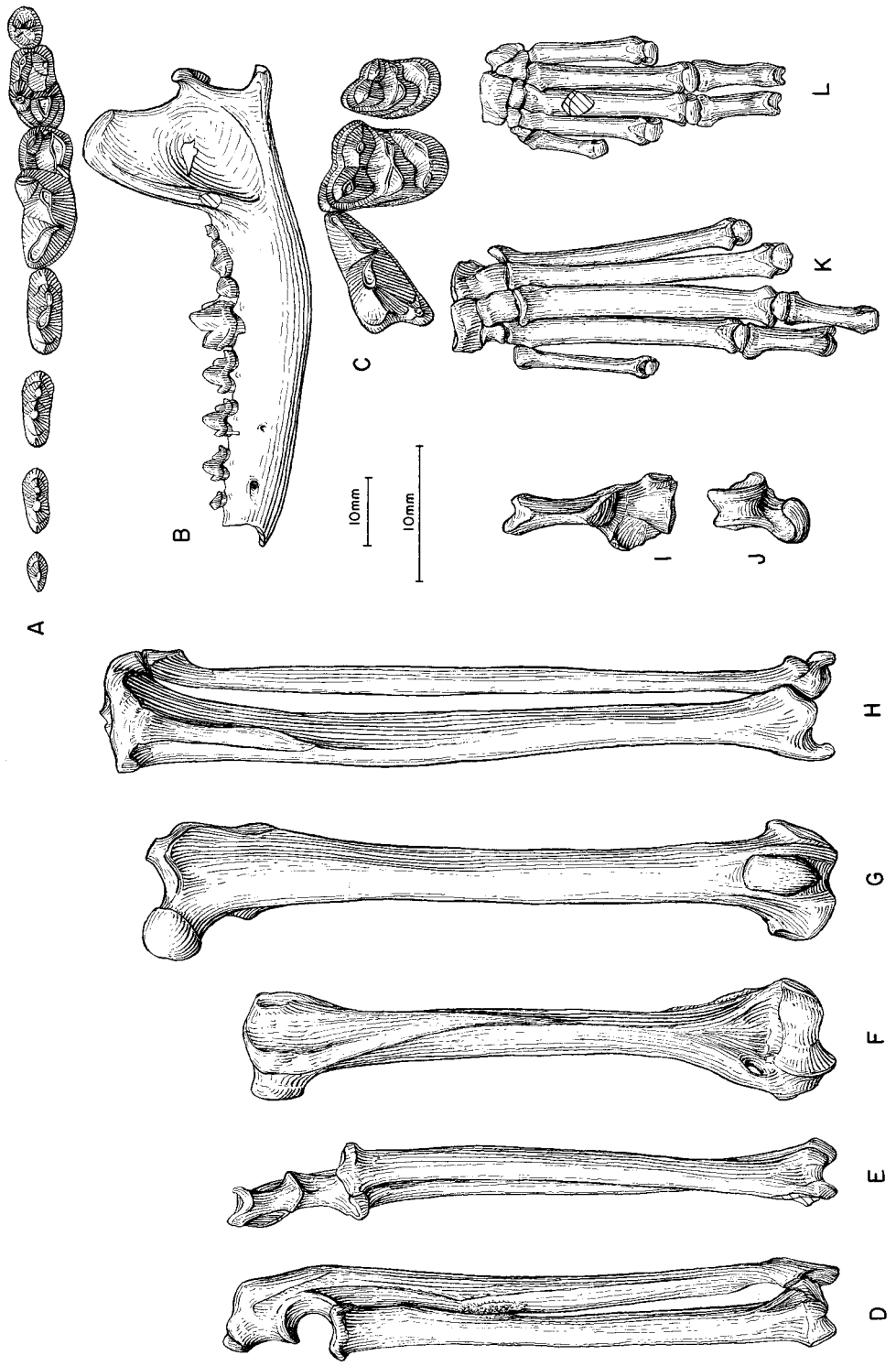

Fig. 10. *Archaeocyon leptodus*. **A**, Lower teeth, **B**, ramus, **C**, upper teeth, **D**, lateral and **E**, anterior views of radius and ulna, **F**, humerus, **G**, femur, **H**, tibia and fibula, **I**, calcaneum, **J**, astragalus, **K** partial foot, and **L**, partial hand, F:AM 49060, Muddy Creek, lower Arikaree Group (medial Arikareean), Niobrara County, Wyoming (I–L reversed from right side). The longer (lower) scale is for A and C, and the shorter (upper) scale is for the rest.

Fig. 11. Partial articulated skeleton of *Archaeocyon leptodus*, F:AM 49060, Muddy Creek, lower Arikaree Group (medial Arikareean), Niobrara County, Wyoming. Photograph by Lorrain Meeker.

tial ramus with c1 broken, p1–p2 alveoli, and p3–m3 (fig. 9I); and F:AM 49053, left partial ramus with p3–m1 all broken and m2.

Willow Creek, lower Arikaree Group (early Arikareean), Niobrara County, Wyoming: F:AM 49076, right ramal fragment with p4 broken–m1.

Muddy Creek Area, lower Arikaree Group (medial Arikareean), Niobrara and Platte counties, Wyoming: F:AM 49021, left partial ramus with p3–p4 and m1–m2 both broken; F:AM 49026, right maxillary fragment with M1–M2 and right ramal fragment with m2; F:AM 49030, partial skull with P2 broken–M2, right and left partial rami with p3–m3, both humeri, radius, partial ulna, and carpals with the proximal ends of metacarpals II–IV; F:AM 49031, incomplete edentulous skull, humerus, tibia, and calcaneum; F:AM 49032, partial skull with right P3–M2 (fig. 9L, M); F:AM 49033, partial skull with I2–I3 alveoli, C1, P1–P3 alveoli, and P4–M2 (fig. 9N, O); F:AM 49035, right partial ramus with p1–p4 alveoli and roots and m1–m2; F:AM 49036, left partial maxillary with P4 broken–M2, left partial ramus with p2 alveolus–m3, right ramal fragments, detached broken bullae, and fragments; F:AM 49037, left partial ramus with p1–p3 alveoli and p4 broken–m2; F:AM 49038, right partial maxillary with P3–M2; F:AM 49039, right partial maxillary with P4–M2 (M1 broken); F:AM 49040, left partial ramus with c1–p1 broken and p2–m1; F:AM 49040A, left partial maxillary with P3 broken–M2; F:AM 49050, right and left partial rami with p4 broken–m3; F:AM 49060, partial skull with P3 broken–M2 (fig. 10C), partial mandible with c1 broken–m3 (fig. 10A, B), and partial postcranial skeleton (fig. 11) including articulated vertebrae, scapula, humerus (fig. 10F), radius and ulna (fig. 10D, E), nearly complete manus including metacarpals I–V and two first phalanges (fig. 10L), pelvis, femora (fig. 10G), tibiae and fibulae (fig. 10H), calcaneum (fig. 10I), astragalus (fig. 10J), tarsals, and metatarsals I–V and two first phalanges (fig. 10K); F:AM 50224, right partial ramus with c1 broken

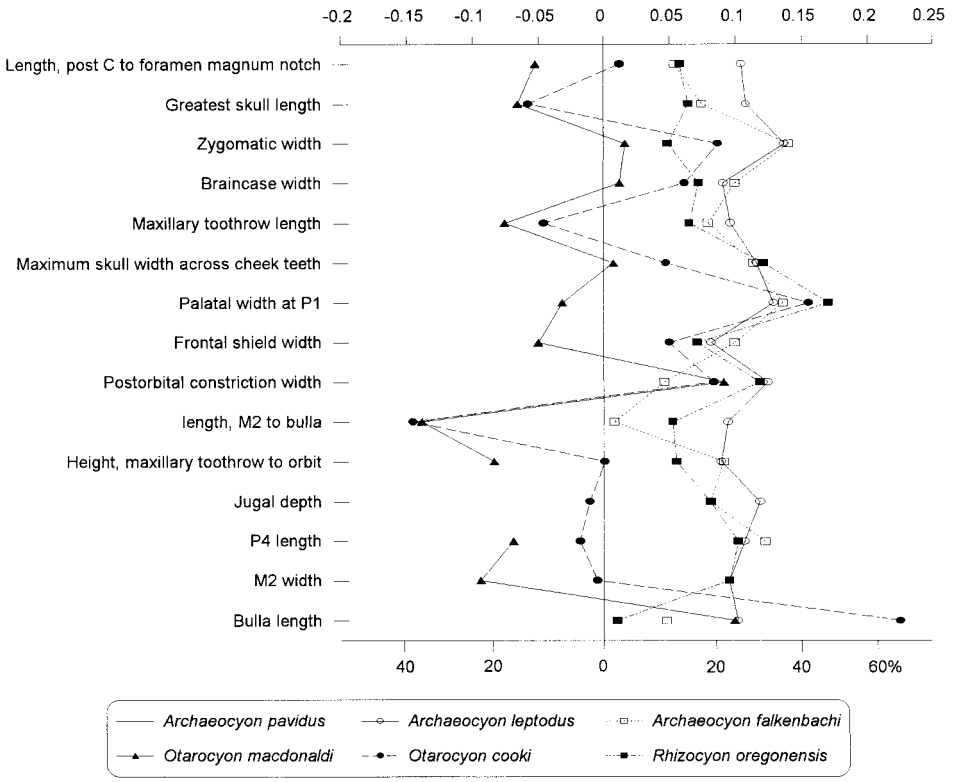

Fig. 12. Log-ratio diagram for cranial measurements of *Archaeocyon*, *Otarocyon*, and *Rhizocyon* using *A. pavidus* as a standard for comparison (straight line at zero). See text for explanations and appendix II for measurements and their definitions.

and p1 alveolus–m2; and F:AM 50226, right partial ramus with m1 broken.

South side of Bear Mountain, lower Arikaree Group (early Arikareean), Goshen County, Wyoming: F:AM 50221, anterior half of skull with I1–M2 and right partial ramus with p3–m2 and m3 alveolus (fig. 8H–K).

Horse Creek area, lower Arikaree Group (early Arikareean), Goshen County, Wyoming: F:AM 49069, right and left partial rami with p2–m2; F:AM 49072, left partial ramus with p2 alveolus, p3–m1 all broken, m2, and m3 alveolus; F:AM 50222, left partial ramus with i1–c1 broken, p1 alveolus, p2 broken–p4, and m1 broken–m2; and F:AM 99286, partial palate with P3 broken–M2 and associated partial cranium.

Canyon Ferry Area, Toston Formation (early Arikareean), Lewis and Clark County, Montana: USNM 19097, right partial ramus with i1–p2 alveoli, p2–m1 all broken, m2, and m3 alveolus; and USNM 20144, right partial ramus with p1 alveolus–m2.

DISTRIBUTION: Whitneyan of Nebraska and Wyoming; early Arikareean of Nebraska, Wyoming, Montana, South Dakota, and North Dakota; and medial Arikareean of Wyoming.

EMENDED DIAGNOSIS: *Archaeocyon leptodus* differs from *A. pavidus* in its larger size and elongated lower first molar with an open trigonid. The rostrum in *A. leptodus* is not shortened, as contrasted with that of *A. falkenbachi*. *A. leptodus* is distinct from the phlaocyonine clade by its possession of the following primitive characters: posteriorly oriented paroccipital process that is not fused with the bulla, weak metaconule of M1, lack of a connection between metaconule and lingual cingulum of M2, and lack of a protostylid on m1.

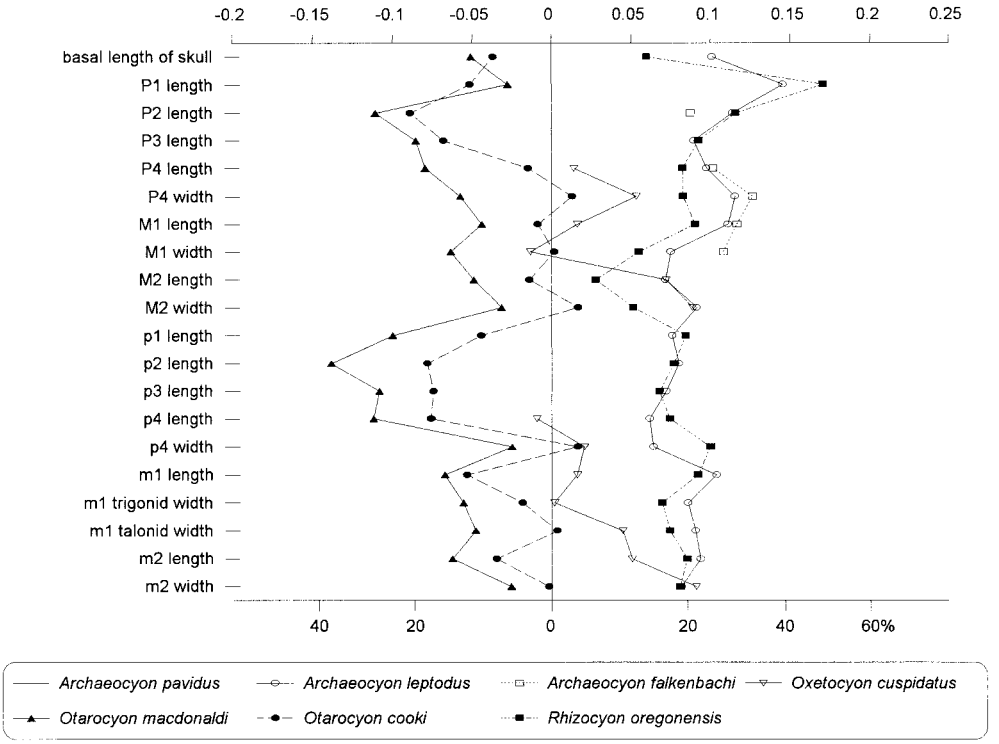

Fig. 13. Log-ratio diagram for dental measurements of *Archaeocyon*, *Oxetocyon*, *Otarocyon*, and *Rhizocyon* using *A. pavidus* as a standard for comparison (straight line at zero). See text for explanations and appendix III for summary statistics of measurements and their definitions.

DESCRIPTION AND COMPARISON: The present reference of a large number of specimens from the Whitneyan and early Arikareean of the northern Great Plains transforms *Archaeocyon leptodus* from that of an obscure species to one that has the best representation among early borophagines both in terms of its anatomy and in the continuity of its fossil record. Nearly complete skulls demonstrate the generalized morphology of this basal borophagine. The skull is primitive in its unshortened snout, a single temporal crest, a wide masseteric scar on the jugal, and lack of fusion between the paroccipital process and the auditory bulla. In overall cranial proportions, *A. leptodus* is very similar to *Rhizocyon* and *Cormocyon* (fig. 12). The UNSM sample from the Horn Member of Brule Formation tends to have a more ventrally oriented paroccipital process, whereas individuals from the Muddy Creek locality of the lower Arikaree Group have a less ventrally oriented process (two specimens, F:AM 49032 and 49060, still have fully posteriorly directed process). Even in individuals that have a mainly ventrally oriented paroccipital process, however, the base of the process is mostly free of contact with the posterior aspect of the bulla. There is a slight tendency in *A. leptodus* to enlarge its bulla relative to the primitive condition in *A. pavidus*.

Teeth of *Archaeocyon leptodus* are overall 24% larger than those of *A. pavidus*, 21% larger than those of *Rhizocyon oregonensis*, and 24% smaller than those of *Cormocyon copei* (average percentage of all measurements). Besides its intermediate size, *A. leptodus* is also intermediate in its possession of an open trigonid on m1 as opposed to the more closed trigonid in *A. pavidus* and *R. oregonensis*, but it lacks a distinct metaconule on M1 and a connection between the metaconule and lingual cingulum of M2 seen in *Cormocyon*.

The most prominent feature on the holotype of *A. leptodus* is its elongated, open tri-

gonid of m1. Its paraconid is more longitudinally oriented in contrast to the primitively more oblique orientation in other *Archaeocyon*. Related to this long trigonid, the p4 also becomes slender. In this latter feature, the holotype is the most extreme among referred specimens (see discussion below). Within the hypodigm, there is a gradual lengthening of the trigonid through time. Our sample from the Whitney and Horn Members of the Brule Formation shows little change in this feature, whereas those from the lower Arikaree Group of Wyoming tend to have a more open trigonid.

DISCUSSION: We recognize *Archaeocyon leptodus* from the Whitneyan through medial Arikareean of the northern Great Plains as distinct from *Rhizocyon oregonensis* of similar age from the John Day Basin. Earlier (from Whitney and Horn Members of Brule Formation) individuals of *A. leptodus* are not easily distinguished in the dentitions, both in quantitative and qualitative traits, from individuals of *R. oregonensis*. The main distinction between these lies in a few subtle characters in *A. leptodus*: more posteriorly oriented paroccipital process, slightly larger bulla, M1 hypocone more posteriorly positioned, M2 lacking a connection between metaconule and internal cingulum, and a more elongated m1. We thus recognize two similar, but morphologically distinguishable, species on either side of the continental divide, similar in this regard to the *Cormocyon copei* and *C. haydeni* species pair.

The elongated trigonid and slender premolars, especially prominent in the holotype of *Archaeocyon leptodus*, are more typically seen in the canine clade, as in the contemporaneous *Leptocyon*. However, the ramus of *A. leptodus* is relatively robust and its premolars are not widely spaced, unlike those in *Leptocyon*, which has a much more gracile horizontal ramus and long diastemata between premolars. Elsewhere, we (Wang and Tedford, 1996) have identified a *Leptocyon* specimen from the Orella Member of the Brule Formation as the earliest record of the subfamily Caninae. This fragmentary lower jaw, UNSM 25354, has the simplified premolars typical of *Leptocyon* but still has a relatively unelongated m1. If our recognition of this Orellan specimen as the most primitive Caninae is correct, the elongation of the m1 must have happened after the simplification of the premolars. This would imply that the elongation of the m1 in *A. leptodus*, which lacks simplified premolars, was probably independently acquired, as it surely had happened at least once in *Cormocyon haydeni* and in more derived borophagines (see further discussion under Phylogenetic Analysis).

Archaeocyon falkenbachi, new species

Figure 14

HOLOTYPE: F:AM 49029, partial skull with C1–P1 alveoli and P2–M1 (P3 alveolus) (fig. 14) from the Muddy Creek Area, 1.5 mi west of bridge, 65 ft below the white layer, lower Arikaree Group (medial Arikareean), Niobrara County, Wyoming.

ETYMOLOGY: Named for the late Charles H. Falkenbach, who led the Frick Laboratory parties collecting extensively in Wyoming.

REFERRED SPECIMEN: Holotype only.

DISTRIBUTION: Medial Arikareean of Wyoming.

DIAGNOSIS: *Archaeocyon falkenbachi* differs from all other species of *Archaeocyon* in its inflated, more bulbous bulla with little anterolateral compression that characterize other species; short temporal fossa; wide zygoma; closely spaced premolars; reduced P2 posterior accessory cusp; and M1 very wide for its length.

DESCRIPTION AND COMPARISON: The single skull of the holotype constitutes the only specimen of this rare species. The shortening of its skull affects several proportional relationships of its cranium. Compared to most species of *Archaeocyon*, *Rhizocyon*, and *Cormocyon*, it has a shortened temporal fossa and a broadened zygomatic arch (fig. 12). The paroccipital process is posteriorly oriented in contrast to the ventrally oriented processes in *Cormocyon*. The bulla is shorter and less anteriorly narrowed than in *A. leptodus*. The opening for the external auditory meatus is more rounded, due to the development of a short meatal tube, than in most individuals of *A. leptodus*. Other than these differences, *A. falkenbachi* is very close to the general stage of evolution of *A. leptodus*.

Dental morphology of *Archaeocyon fal-*

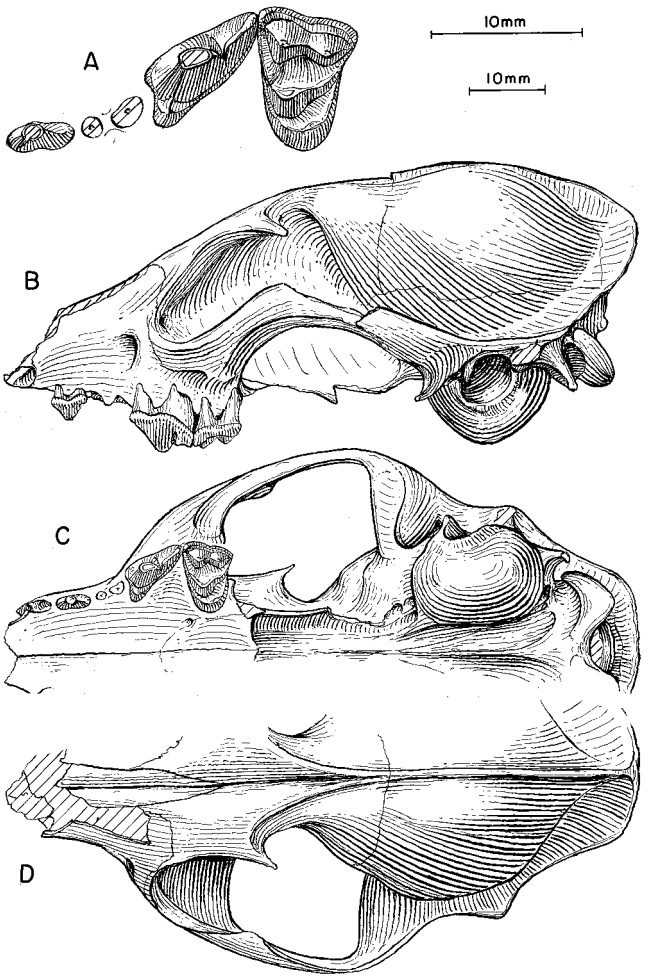

Fig. 14. *Archaeocyon falkenbachi*. **A**, upper teeth, **B**, Lateral, **C**, ventral and **D**, dorsal views of skull, and F:AM 49029, holotype, Muddy Creek, lower Arikaree Group (medial Arikareean), Niobrara County, Wyoming. The longer (upper) scale is for A, and the shorter (lower) scale is for the rest.

kenbachi is also very close to that of *A. leptodus*. The only differences between the two species are a simplified P2 (lacking a posterior accessory cusp) and a mediolaterally wider M1 in *A. falkenbachi*.

DISCUSSION: Slight wear on the tips of the upper molars and the presence of a low but distinct sagittal crest indicate that F:AM 49029 is an adult. It is unlikely that its unique cranial proportions cited above (features related to brachycephally) are due to young age. *Archaeocyon falkenbachi* thus represents a lineage divergent from *A. leptodus*, which does not appear to lead to other lineages.

Oxetocyon Green, 1954

TYPE SPECIES: *Oxetocyon cuspidatus* Green, 1954.

INCLUDED SPECIES: Type species only.

DISTRIBUTION: Whitneyan of South Dakota and Nebraska, and early Arikareean of Nebraska.

EMENDED DIAGNOSIS: In contrast to *Archaeocyon*, *Oxetocyon* shares with *Otarocyon* such derived characters as taller P4 parastyle, conate talonid cusps on m1, m1 entoconid separated from the metaconid by a notch, and m2 metaconid larger than protoconid. In addition, *Oxetocyon* has several au-

tapomorphies related to its unusual mode of hypocarnivory: enlarged and quadrate upper molars, strong anterolingual cingulum on M1, distinct cleft on the lingual cingulum that isolates the large conate hypocone on the M1, and a distinct metaconule on M1. *Oxetocyon* is primitive relative to *Rhizocyon* and more derived borophagines in its lack of a connection between metaconule and posterior lingual cingulum on M2, and absence of a protostylid on m1.

Oxetocyon cuspidatus Green, 1954

Figure 15

Oxetocyon cuspidatus Green, 1954: 218, fig. 1. Galbreath, 1956: 375. Tanner, 1973: 66, fig. 1. Wang and Tedford, 1996: 446, fig. 8. Munthe, 1998: 134.

HOLOTYPE: SDSM 2980 (AMNH cast 80132), left maxillary fragment with M1 and broken alveoli of P4 and M2 (fig. 15A), from 7 mi east of Rockyford, Protoceras Channels, Poleslide Member of Brule Formation (Whitneyan), Shannon County, South Dakota.

REFERRED SPECIMENS: Whitney Member of Brule Formation (Whitneyan), Morrill and Sioux counties, Nebraska: UNSM 2665, partial skull with C1 broken alveolus, P1–P3 alveoli, and P4–M2 (Tanner, 1973: fig. 1A–C; fig. 15F–H) from UNSM loc. Mo-104, base of Roundhouse Rock, 8.5 ft below the base of the Upper Ash; UNSM 25081, left ramal fragment with p3–m1 all broken, UNSM loc. Sx-28; UNSM 25381, left maxillary fragment with P3 alveolus–M2 (fig. 15B, C) and fragment of dorsal roof cranium, UNSM loc. Mo-0, 7 mi southeast of Broadwater, 10 ft above railroad grade; and UNSM 25698 (AMNH cast 96707), right partial ramus with p3 alveolus–m3 (fig. 15D, E), UNSM loc. Mo-107 or Mo-108.

Gering Formation (early Arikareean), Morrill County, Nebraska: UNSM 11695 (AMNH cast 104655), right partial ramus with p4–m1 and alveoli of c1–p3.

DISTRIBUTION: Whitneyan of South Dakota and Nebraska, and early Arikareean of Nebraska.

EMENDED DIAGNOSIS: As for monotypic genus.

DESCRIPTION AND COMPARISON: Although Tanner's (1973) referred partial skull (UNSM 2665) substantially increased knowledge of *Oxetocyon cuspidatus*, which was established on a single M1, much remains to be learned about this rare species. Tanner's description of UNSM 2665 is still the main source of information on the cranial morphology of *Oxetocyon*. To this we can only add a fragment of skull roof associated with upper teeth (UNSM 25381), which only preserves the posterior segment of the sagittal crest (single crested) and partial nuchal crest. UNSM 25381 (fig. 15B, C) is a somewhat larger individual with primitive dental features compared to the holotype and UNSM 2665: it has a smaller protocone of P4, a less pronounced notch on the labial cingulum of M1, a less deep cleft anterior to the hypocone on the lingual cingulum of M1 and absence of such a cleft on M2, lack of a discrete hypocone on M1, metaconule less enlarged on M1–M2, and overall less transverse division of the M1. While certainly introducing additional dental variations, our inclusion of UNSM 25381 helps to bridge the large morphological gap between the holotype of *O. cuspidatus* and other basal borophagines such as *Archaeocyon*.

The present referral of two ramal fragments is largely based on their conate cusps of the lower molars and on the generally good occlusion between the upper and lower teeth. The rounded shape of the cusps of m1 talonid and m2 are in sharp contrast to the crestlike cusps of the contemporaneous *Hesperocyon* and to a lesser extent those of *Otarocyon*, but is consistent with the cusp shape of the upper teeth of *O. cuspidatus*. Furthermore, the high m2 entoconid occludes well with the basin between the enlarged lingual cingulum and protocone of the M2. Besides these salient features, the referred lower jaws and teeth are quite similar to those of *Archaeocyon* species.

Our reference of these jaws to *O. cuspidatus* has some interesting phylogenetic implications. While the upper teeth of *Oxetocyon* bear certain similarities to those of *Cynarctoides* and *Phlaocyon*, such as the quadrate appearance of M1 and the presence of a M1 hypocone (however, *Cynarctoides* and *Phlaocyon* do not have the transverse cleavage across the M1 so characteristic of *Oxetocyon*), the referred lower teeth lack the cor-

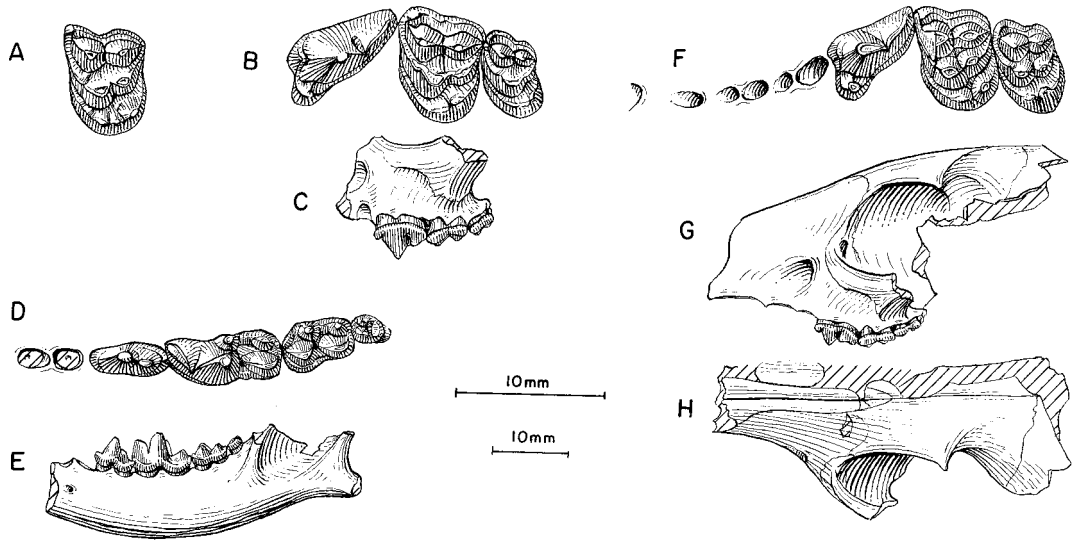

Fig. 15. *Oxetocyon cuspidatus*. **A**, M1, SDSM 2980, holotype, 7 mi east of Rockyford, Poleslide Member of Brule Formation (Whitneyan), Shannon County, South Dakota. **B**, Upper teeth and **C**, lateral view of maxillary, UNSM 25381, 7 mi southeast of Broadwater, Whitney Member, Brule Formation (Whitneyan), Morrill County, Nebraska. **D**, Lower teeth and **E**, ramus (reversed from right side), UNSM 25698, Whitney Member, Brule Formation (Whitneyan), Morrill County, Nebraska. **F**, Upper teeth, and **G**, lateral and **H**, dorsal views of partial skull, UNSM 2665, Roundhouse Rock, Whitney Member, Brule Formation (Whitneyan), Sioux County, Nebraska. The longer (upper) scale is for A, B, D, and F, and the shorter (lower) scale is for the rest.

responding specializations of the Phlaocyonini, such as the presence of a protostylid on m1–m2. *Oxetocyon* thus possesses a mixture of features that suggests an evolutionary pathway independent from the phlaocyonine clade.

DISCUSSION: *Oxetocyon* represents one of the first of many trends toward hypocarnivory within the subfamily Borophaginae. During the Whitneyan, it is also the most hypocarnivorous canid, with its own peculiar way of enlarging and squaring up the upper molars and dividing them into roughly symmetrical parts along a transverse cleavage in the middle of the crown. The absence of a connection between the metacone and lingual cingulum on M2 and the lack of a protostylid on m1 indicate only a basal relationship with regard to the phlaocyonine clade, despite the common possession of a similarly developed hypocone on M1.

Oxetocyon and *Otarocyon* share a few derived features, such as conate cusps on lower molars, lingually opened talonid basin on m1, and high m2 metaconid. Although our cladistic analysis indicates a sister relationship of the two genera because of these characters, it is conceivable that the hypocarnivorous characters may have been independently acquired since the dissimilarity between the upper molars of these genera is so great. Such speculation may be confirmed with knowledge of the basicranium of *Oxetocyon*. Meanwhile, we maintain two distinct genera in the recognition that they represent two distinct clades, even though they may be sister taxa.

Otarocyon, new genus

TYPE SPECIES: *Cynodesmus cooki* Macdonald, 1963.

ETYMOLOGY: Greek: *otaros*, large eared; *cyon*, dog.

INCLUDED SPECIES: *Otarocyon macdonaldi*, new species; and *Otarocyon cooki* (Macdonald, 1963).

DISTRIBUTION: Orellan of South Dakota and Montana, early Arikareean of South Da-

kota, and early to medial Arikareean of Wyoming.

DIAGNOSIS: Species of the highly derived *Otarocyon* are united by many synapomorphies: hypertrophied auditory bulla, anteroposteriorly flattened paroccipital process that is ventrally oriented, large suprameatal fossa, shortened rostrum, broadened braincase, short temporal fossa, paired temporal crests, single-cusped, short, and tall crowned premolars, enlarged P4 protocone, elevated lingual cingulum of M1, conical entoconid of m1 separated anteriorly from metaconid by a deep notch (lingually opened talonid basin), m2 metaconid much larger and higher than protoconid. *Otarocyon* is primitive compared to *Rhizocyon* and more derived borophagines in its transversely elongated upper molars and lack of a connecting ridge between the lingual cingulum and metaconule of M2.

DISCUSSION: The abrupt appearance of the morphologically highly derived *Otarocyon* in the Orellan without any apparent predecessor presents a problem for phylogenetic interpretation. Although *Otarocyon* shares with *Archaeocyon* derived characters of the canine–borophagine clade (reduced M1 parastyle, anteriorly extended M1 lingual cingulum, more basined talonid of m1, and high m2 entoconid), the ways that these morphologies are achieved, however, seem to suggest independent development of these characters. For example, the highly conate m1 entoconid is interrupted anteriorly by a deep notch separating the entoconid from the metaconid, and is in sharp contrast to a ridgelike entoconid, which reaches anteriorly to the base of the metaconid and fully encloses a talonid basin in all primitive hesperocyonines, canines, and borophagines. This peculiarity of the bicuspid talonid is not seen elsewhere in the borophagines. In absence of more transitional forms, however, we must assume for the purpose of parsimony that these derived characters in *Otarocyon* are synapomorphies shared with other borophagines, rather than being homoplasies.

For all its unique morphology, *Otarocyon* has a living canine analog, fennec fox (*Vulpes* (*Fennecus*) *zerda*), from desert regions of northern Africa and the Arabian Peninsula. In addition to being among the smallest foxes, the fennecs share with *Otarocyon* a striking list of derived similarities: expanded braincase, short nasal process of frontal, parasagittal temporal crests, enlarged bulla and narrowed interbullar space, loss of low septum inside bulla, paroccipital process fully cupping bulla, simplified premolars, and enlarged m2 metaconid. The list is long enough to raise the intriguing possibility of the origin of ancestral fennecs from *Otarocyon*. The implicit long hiatus in the fossil record (approximately 25 m.y.) notwithstanding, such a proposition, however, would have to overcome a longer list of derived characters in fennecs that indicates their position within the Vulpini (Tedford et al., 1995: characters 4–18), although some of these characters are not unique to vulpines or cannot be observed in available materials of *Otarocyon*. For example, *Otarocyon* does not possess such canine characters as slender horizontal ramus, narrow premolars, elongated P4 and m1, m2 anterolabial cingulum, or loss of entepicondylar foramen of humerus. Furthermore, fennecs differs from *Otarocyon* in additional details that require explanation if they are postulated as sister-groups: presence of a frontal depression (seen in most vulpines), lack of a suprameatal fossa, presence of a short bony external auditory meatus, and an extension of the ectotympanic ring to form the dorsal passage of auditory meatus. It is therefore more parsimonious to view the similarities between *V. zerda* and *Otarocyon* as independently derived. Such conclusion is also consistent with studies of chromosomes, allozymes, and mitochondrial DNA of living canids (Wayne et al., 1987a, 1987b; Wayne and O'Brien, 1987; Wayne et al., MS), which place the fennec within the clade of living foxes but not in a more basal position as would be predicted by an *Otarocyon–Fennecus* sister relationship.

This remarkable convergence in two subfamilies of Canidae provides a valuable living analog (*Vulpes zerda*) of a fossil group (*Otarocyon*) for inference of its soft anatomy and ecology. For example, we can reasonably infer that *Otarocyon* must have had a very large external ear, as have the fennecs, and that the auditory apparatus was sensitive to low-frequency hearing (Lay, 1972; Webster and Webster, 1980). The implication that *Otarocyon* may have lived in an open envi-

ronment, as do the living fennecs, is inherently less testable with the fossil alone, but no less interesting. The peculiar middle ear morphology in *Otarocyon* was already present in Orellan (in *O. macdonaldi*) and seems to indicate at least patchy presence of open environments at the time, as also concluded by Retallack (1983) in a study of soils of Orellan age in South Dakota.

Otarocyon macdonaldi, new species

Figure 16G–L

HOLOTYPE: AMNH 38986, skull with I1–M2 (C1 broken) and mandible with i1–m3 (fig. 16G–L) from Scenic Member of Brule Formation (Orellan), south of White River, near Scenic, Pennington County, South Dakota.

ETYMOLOGY: Named for J. Reid Macdonald for his singular contributions to the Cenozoic paleontology and stratigraphy of South Dakota.

REFERRED SPECIMEN: Cooper Gulch Locality No. 1, Toston Formation (?Orellan), Lewis and Clark County, Montana: UMMP 7933 (AMNH cast 127173), partial rostrum with left P4–M2 and right P2–M2, UMMP loc. MV8303.

DISTRIBUTION: Orellan of South Dakota and Montana.

DIAGNOSIS: *O. macdonaldi* is easily distinguishable from *Archaeocyon* and other primitive borophagines by several derived characters shared with *O. cooki*: brachycephalic skull, shortened nasal process of frontal, laterally expanded braincase, paired temporal crests, enlarged auditory bulla, large suprameatal fossa, flattened paroccipital process hugging the bulla, short, simple, and high-crowned premolars, enlarged P4 protocone, high M1–M2 lingual cingulum, short trigonid, high hypoconid and entoconid, lingually opened talonid basin on m1, and high metaconids of m1–m2. *O. macdonaldi* is more primitive than *O. cooki* in its lesser development of some of the above characters: smaller size; longer and narrower muzzle; P1–P3 and p1–p3 anteroposteriorly longer with crown height lower relative to length; P4 protocone smaller; braincase less expanded relative to length of skull; parasagittal crests weaker and more widely separated; m1 with trigonid more elongate and shear less oblique, metaconid smaller and lower crowned, and entoconid less conical and lower crowned.

DESCRIPTION AND COMPARISON: As in *Otarocyon cooki*, *O. macdonaldi* is easily distinguished from the far more conservative *Archaeocyon* in the numerous synapomorphies shared between *O. cooki* and *O. macdonaldi* (see Diagnosis above). Distinctions between *O. cooki* and *O. macdonaldi*, however, are far more subtle. Besides its slightly smaller size (3% in basal length of skull, but 9% in average dental measurements; see appendices II, III), *O. macdonaldi* is mainly distinct from *O. cooki* in its slightly lesser degree of development of the advanced features: skull less brachycephalic, parasagittal crests less prominent, braincase less expanded, m1 trigonid less shortened, and lower molar cusps lower. Similarly, the teeth of *O. macdonaldi* are little different from those of *O. cooki* other than their smaller size.

The single referred specimen from Montana (UMMP 7933) displays certain subtle variations that are not present in the holotype: a weak lingual cingulum on P2, presence of an additional (third) root on the P3 and a distinct lingual cingulum supported by this extra root, presence of a narrow labial cingulum on the P4, better developed P4 parastyle, and better developed M1 metaconule.

DISCUSSION: In a thesis on the evolution of mammalian molars, Patterson (1956: 48) used AMNH 38986 to illustrate the field concept of dental development and its interactions with phylogenetic constraints (he did not give a formal taxonomic identification of this specimen and merely called it ''an undescribed Oligocene dog''). To him, the increased size and height of P4 protocone and M1–M2 hypocones (lingual cingula) and similar enlargements of m1 entoconid and m1–m2 metaconids are all related to a genetic process of increasing size of the lingual portions of the cheekteeth. It is relevant to note that Patterson's observation is even better illustrated in UMMP 7933, in which the lingual cingula of the entire upper toothrow, including that of the P2–P3, are well-developed.

Despite its much earlier appearance in the Orellan and being separated from its early

Arikareean sister-species *Otarocyon cooki* by at least 2 m.y., *O. macdonaldi* basically possesses all the morphological specializations present in *O. cooki*, although usually to a slightly lesser degree. In other words, once the major adaptive features were acquired, the *Otarocyon* lineage remained essentially unchanged except for slight size increase and slightly greater emphasis on the various features (e.g., greater expansion of braincase, stronger temporal crests, shorter premolars and m1 trigonid). These minor adjustments probably reflect an anagenetic series stretching from the Orellan to the early Arikareean.

Otarocyon cooki (Macdonald, 1963)
Figures 16A–F, 17, 18

Cynodesmus cooki Macdonald, 1963: 210, figs. 26, 27. 1970: 58.

HOLOTYPE: SDSM 54308, right partial ramus with p4–m2 (fig. 17A, B), from the Wounded Knee area, SDSM loc. V5359, upper part of the Sharps Formation (early Arikareean), Shannon County, South Dakota (Macdonald, 1963).

REFERRED SPECIMENS: From the type area: LACM 13975, right partial ramus with m1 broken, m2, and m3 alveolus, LACM loc. 1955; SDSM 55132, right partial ramus with p4 broken–m3, SDSM loc. V5410, upper part of the Sharps Formation (early Arikareean).

Little Muddy Creek, lower Arikaree Group (early Arikareean), Niobrara County, Wyoming: F:AM 49041, right partial ramus with c1 (broken), p1–p3 alveoli, and p4–m3; F:AM 49042, partial skull with I2–M2, right and left partial rami with i3–m3 (fig. 17H–J), articulated right humerus and radius and ulna (fig. 17K–M), left humerus and incomplete radius and ulna and first phalanx; F:AM 49043, posterior part of skull, left ramus with c1 (broken) and p1–m3 (fig. 17C–G), and distal part of tibia; F:AM 49046, left partial maxillary with P3 (broken)–M2; and F:AM 49055, right partial ramus with p3–m2 (m1 broken) and m3 (alveolus).

Muddy Creek, lower Arikaree Group (medial Arikareean), Niobrara County, Wyoming: F:AM 49020, skull with I1 (alveolus) and I2–M2, mandible with i2–m3 (fig. 16A–F), articulated left distal partial humerus, and broken radius and ulna; F:AM 49022, left partial maxillary with P4–M2; F:AM 49023, partial skull with P1–P3 alveoli and P4 (broken)–M2; F:AM 49024, left partial ramus with p1–p2 (both broken) and p3–m1; F:AM 49025, right partial ramus with c1–m3; F:AM 49027, fragmentary skull with P4–M2, right partial ramus with c1–p1 both broken, p2–m2, and m3 alveolus, and postcranial fragments including articulated tarsals and metatarsals I–V, from 25 ft above the ''Gering–Monroe Creek'' contact; and F:AM 49034, left partial maxillary with P4–M1, from 25 ft below white layer.

North of Jeriah, lower Arikaree Group (?medial Arikareean), Niobrara County, Wyoming: F:AM 49071, right partial ramus with p3 (broken alveolus), p4 (broken), m1–m2, and m3 alveolus.

DISTRIBUTION: Early Arikareean of South Dakota, and early to medial Arikareean of Wyoming.

EMENDED DIAGNOSIS: As the terminal species in the *Otarocyon* clade, *O. cooki* has, relative to *O. macdonaldi*, more brachycephalic skull, more expanded braincase, and more prominent temporal crests.

DESCRIPTION AND COMPARISON: The present reference of more complete material than was available in the topotype series (Macdonald, 1963) reveals a remarkable animal with highly derived cranial morphology mixed with a relatively primitive, unspecialized dentition. This extraordinary combination of cranial and dental structures is unique in many ways and requires a more detailed description.

The brachycephally of *Otarocyon cooki* affects the skull shape in several ways. Besides having a relatively short and broad rostrum, the braincase is also considerably expanded laterally (fig. 12). The nasal process of the frontal between the maxillary and nasal is also shortened. The parallel temporal crests are strong.

The most prominent feature of the basicranium of *Otarocyon cooki* is its hypertrophied auditory bulla (fig. 16, 17). The external dimensions of the bulla far exceed in relative size of skull those of most carnivorans. The bulla is nearly twice as large as that of a similar-size *Hesperocyon* in linear dimensions and thus must be approximately eight

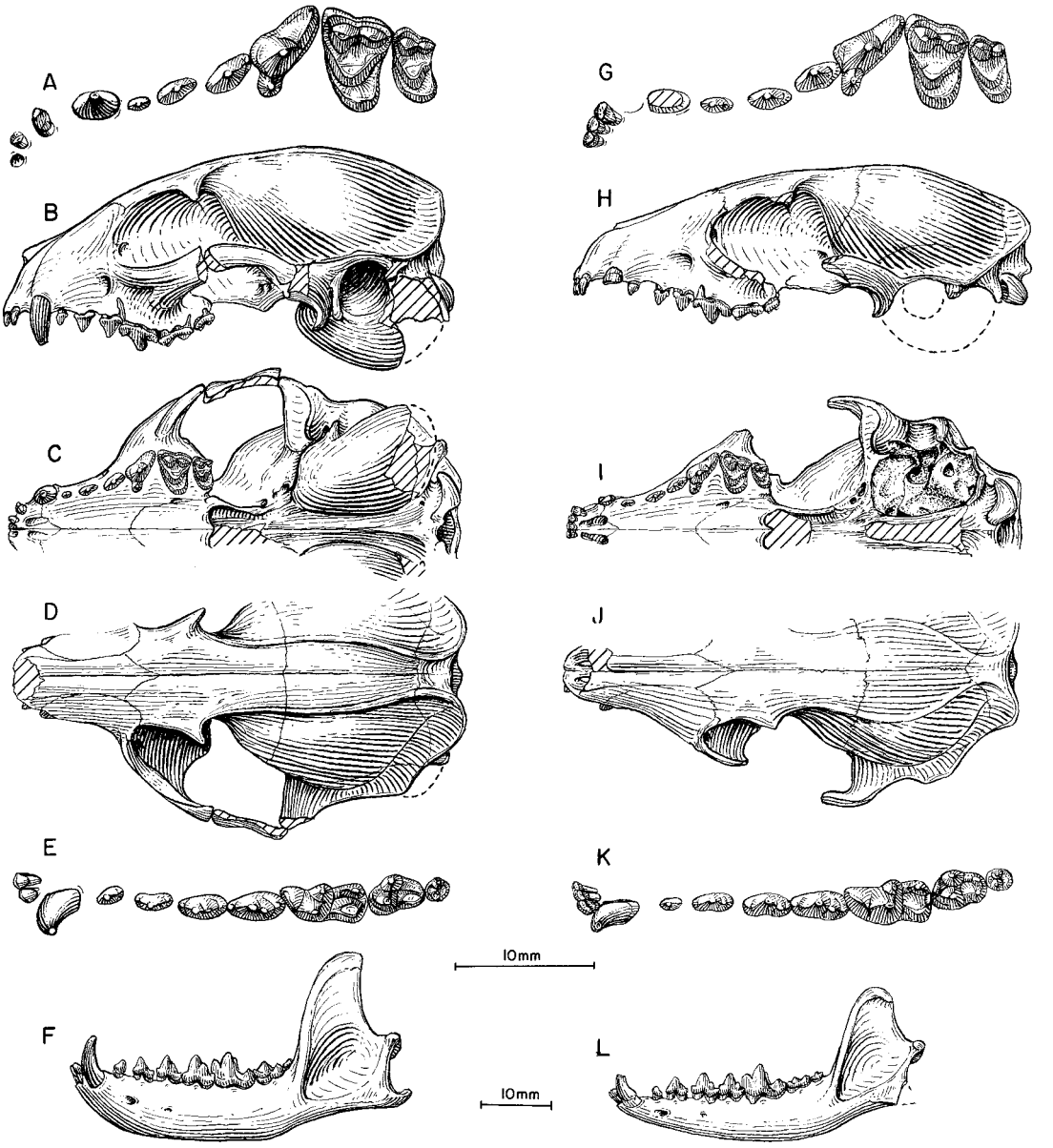

Fig. 16. **A**, Upper teeth, **B**, lateral, **C**, ventral and **D**, dorsal views of skull, **E**, lower teeth, and **F**, ramus, *Otarocyon cooki*, F:AM 49020 (P1, paroccipital process, p2, and p3 reversed from right side), Muddy Creek, lower Arikaree Group (medial Arikareean), Niobrara County, Wyoming. **G**, Upper teeth, **H**, lateral, **I**, ventral, and **J**, dorsal views of skull, **K**, lower teeth, and **L**, ramus, *Otarocyon macdonaldi*, AMNH 38986, holotype, south of White River near Scenic, Scenic Member, Brule Formation (Orellan), Pennington County, South Dakota. The longer (upper) scale is for A, E, G, and K, and the shorter (lower) scale is for the rest.

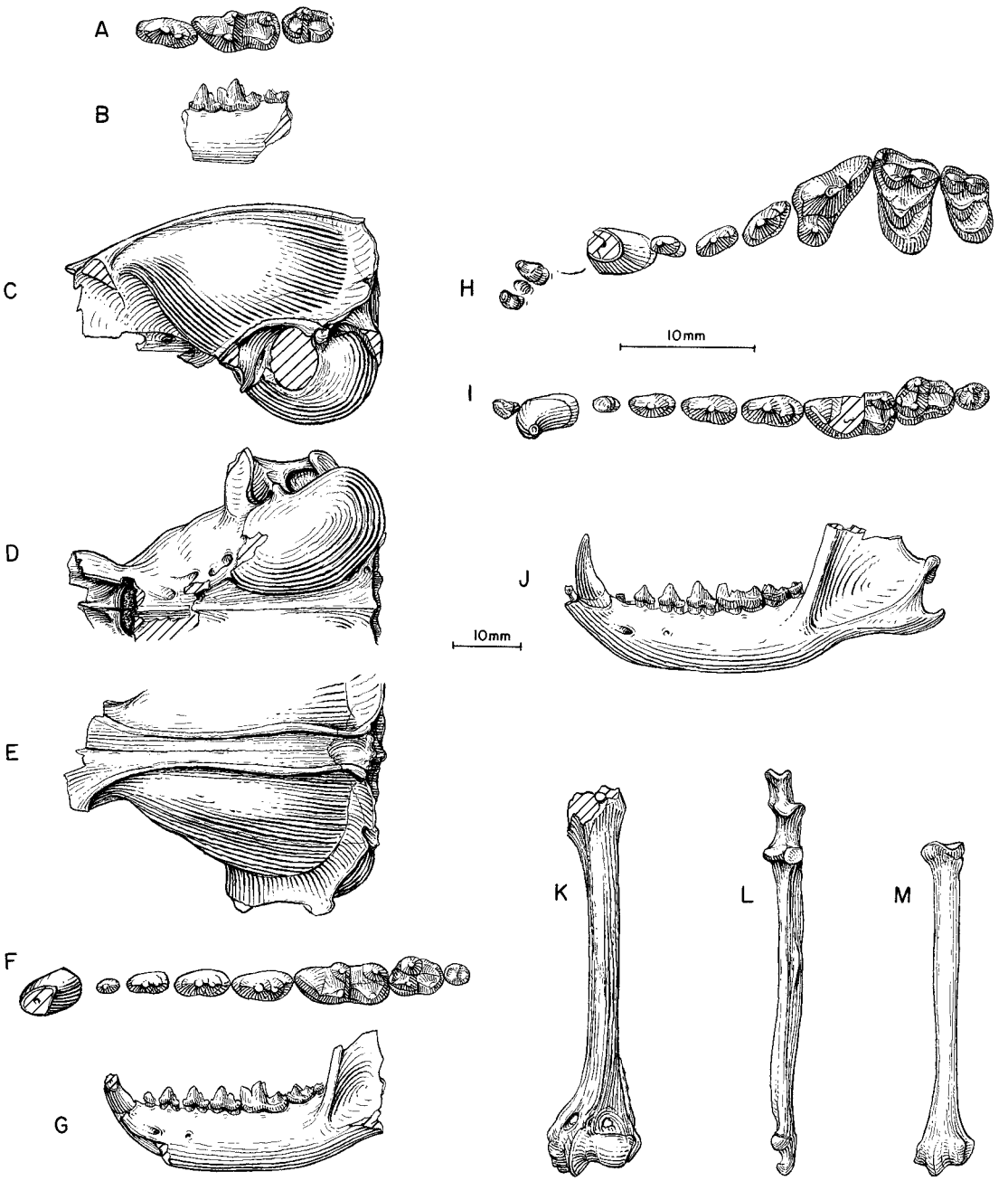

Fig. 17. *Otarocyon cooki*. **A**, Lower teeth and **B**, ramus (reversed from right side), SDSM 54308, holotype, Wounded Knee area, Sharps Formation (early Arikareean), Shannon County, South Dakota. **C**, Lateral, **D**, ventral, and **E**, dorsal views of partial skull (bulla from right side), **F**, lower teeth, and **G**, ramus, F:AM 49043, Little Muddy Creek, lower Arikaree Group (early Arikareean), Niobrara County, Wyoming. **H**, Upper teeth, **I**, lower teeth, **J**, ramus, **K**, humerus, **L**, ulna, and **M**, radius, F:AM 49042 (I1, I3, P4–M2, and all limb bones reversed from right side), Little Muddy Creek. The longer (upper) scale is for A, F, H, and I, and the shorter (lower) scale is for the rest.

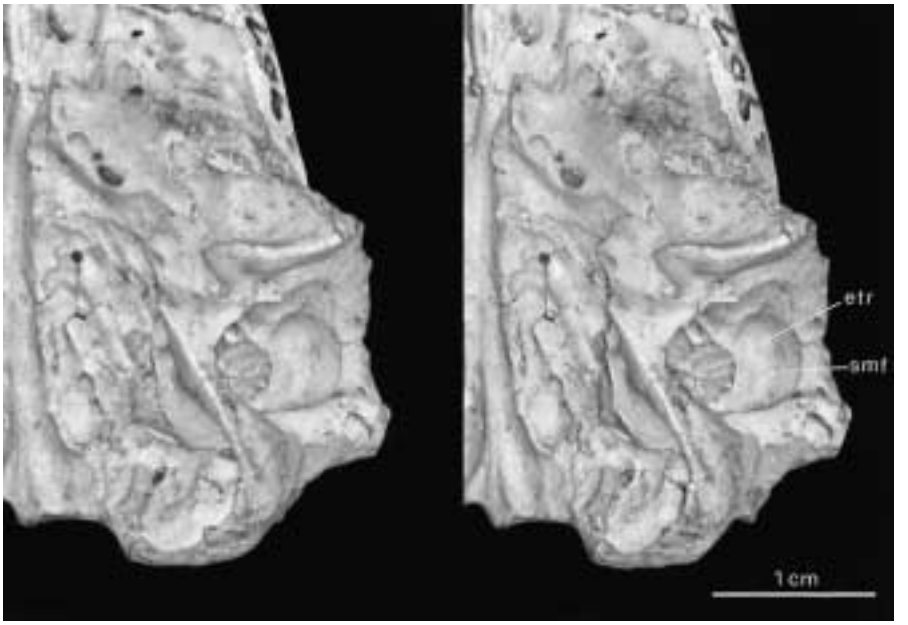

Fig. 18. Stereophotograph of basicranial region of *Otarocyon cooki*, F:AM 49043, Little Muddy Creek, lower Arikaree Group (early Arikareean), Niobrara County, Wyoming. Abbreviations: etr, epitympanic recess; smf, suprameatal fossa. Photograph by Lorrain Meeker.

times larger in volume. Exact proportions of the bullar components are difficult to ascertain due to fusion of the sutures, but expansion of the caudal entotympanic is presumably the primary cause of the bullar inflation, since this has been the case in living canids that expand their bullae (Hunt, 1974). There is no indication on the internal bullar surface of a low septum, a unique structure present in nearly all canids (Wang and Tedford, 1994). This absence of the septum is presumably a result of the extreme inflation of the thin-walled bulla, as also occurs in the living fennecs. The space between the two bullae is narrowed to about half the distance were the bullae not inflated. The opening of the external auditory meatus is also considerably enlarged. The paroccipital process is ventrally oriented, completely hugs the bulla, and has no free tip.

Another outstanding feature in the middle ear region of *O. cooki* is a large, deep, rounded suprameatal fossa (fig. 18), a condition thought to be diagnostic of the procyonids (Riggs, 1942, 1945; Segall, 1943; Hough, 1944, 1948). Although Schmidt-Kittler (1981) and Wolsan (1993) demonstrated a more extensive presence and varying patterns of the suprameatal fossa in many lineages of musteloids, such a structure had not been reported in a canid except for a rudimentary stage of development in *Hesperocyon* (Wang and Tedford, 1994), which serves well as a morphological precursor for the structural elaboration in *Otarocyon*. The fossa in *Otarocyon* is dorsally excavated into the squamosal shelf of the external auditory meatus and is expanded posteriorly into the mastoid process, a condition found in the procyonids but not the mustelids (see Schmidt-Kittler, 1981 and Wolsan, 1993). Yet little else in the basicranium of *Otarocyon*, besides the suprameatal fossa, suggests any arctoid characters. The mastoid process, although excavated by the suprameatal fossa, is not enlarged, as is the case in many arctoids. There is an alisphenoid canal, which is lost in living procyonids and mustelids. *Otarocyon* thus becomes one more example of independent acquisition of a hypertrophied suprameatal fossa, and is the only canid known to have elaborated this structure to such an extent.

Dental morphology of *Otarocyon cooki*,

on the other hand, is for the most part that of a basal canid with certain autapomorphies. Associated with the brachycephalic skull, the cheekteeth also become shortened, resulting in short, simple, high-crowned premolars (fig. 13; appendix III). The trigonid of m1 is also shortened and the shearing blade is rather obliquely oriented. The cusps of the lower molars also become high-crowned, including metaconids of m1–m2, hypoconid and entoconid of m1, and entoconid of m2. In particular, a deep notch between the high entoconid and metaconid of m1 is a peculiar feature not seen in other borophagines.

DISCUSSION: *Otarocyon cooki* has remained in obscurity since its first description from the Wounded Knee area of South Dakota (Macdonald, 1963), partly because of the fragmentary topotype material. Although generally primitive, the lower teeth of the topotype material offer sufficiently diagnostic characters that our reference of more complete skulls and mandibles to this rare species is secure and reveals a surprising combination of cranial and dental characteristics.

In addition to the incomplete nature of the holotype, Macdonald's (1963) reference of this species to *Cynodesmus* further compounds the problem of its relationship among canids. Since its initial establishment by Scott (1893), the genus *Cynodesmus* (type species *C. thooides*) has gradually included more borophagine species, particularly because of the early reference of *Desmocyon thomsoni* (see further comments under this taxon) to this genus. Macdonald's alliance of *cooki* with *Cynodesmus* further stretched the concept of this genus. *Cynodesmus* is now restricted to two species within the Hesperocyoninae (Wang, 1994) and has a very distant relationship to any borophagine.

Rhizocyon, new genus

TYPE SPECIES: *Cynodictis* (?) *oregonensis* Merriam, 1906.

ETYMOLOGY: Greek: *rhiza*, root; *cyon*, dog.

INCLUDED SPECIES: Type species only.

DISTRIBUTION: Early Arikareean of Oregon.

DIAGNOSIS: *Rhizocyon* is derived relative to *Archaeocyon*, *Oxetocyon*, and *Otarocyon* in having a wider frontal shield, more quadrate upper molars with anteriorly expanded lingual cingulum, and a connection between the lingual cingulum and metaconule on M2. It differs from members of the Phlaocyonini in its unenlarged bulla, posteriorly directed paroccipital process, small metaconule on M1, and lack of protostylids on lower molars. In contrast to *Cormocyon* and more derived borophagines, *Rhizocyon* lacks an elongated m1 trigonid.

Rhizocyon oregonensis (Merriam, 1906)

Figure 19

Canis gregarius Cope, 1879a: 58.
Canis lippincottianus Cope, 1879a: 58.
Galecynus gregarius (Cope): Cope, 1883: 241 (in part); 1884: 916 (in part), pl. 68, figs. 5–8.
Galecynus lippincottianus (Cope): Cope, 1884: 920 (AMNH 6883 only).
Cynodictis gregarius (Cope): Wortman and Matthew, 1899: 130.
Cynodictis (?) *oregonensis* Merriam, 1906: 4, 5, 11, pl. 2, fig. 4. Merriam and Sinclair, 1907: 184. Thorpe, 1922a: 162–164.
Cynodictis oregonensis (Merriam): Matthew, 1909: 106.
Nothocyon oregonensis (Merriam): Hall and Martin, 1930: 283.
Nothocyon lemur (Cope, 1879b): Macdonald, 1970: 56–57 (in part).
Cormocyon oregonensis (Merriam): Fremd and Wang, 1995: 75.

LECTOTYPE: AMNH 6879, skull with I1–I2 both broken, I3–M2, and left ramus with c1 broken–m3 (Cope, 1884: 917, pl. LXVIII, figs. 5–8; fig. 19), John Day Basin, John Day Formation, ?early Arikareean of Oregon.

Merriam (1906) did not designate a holotype in his original description of *Cynodictis*(?) *oregonensis*, although he did indicate that UCMP 316, a partial left ramus with i3–c1 and p2–m2 (Merriam, 1906: pl. 2, fig. 4), was the ''most important'' among a series of jaw fragments in the UCMP collection. Museum labels associated with UCMP 316 have labeled it the holotype, even though no subsequent publication has selected it as such. Unfortunately, some of the most diagnostic elements of UCMP 316 have been lost. The entire p3, part of the principal cusp of p4, the entire m1, and partial m2 (originally incomplete) are missing from UCMP 316, and the published line drawing of a lateral view

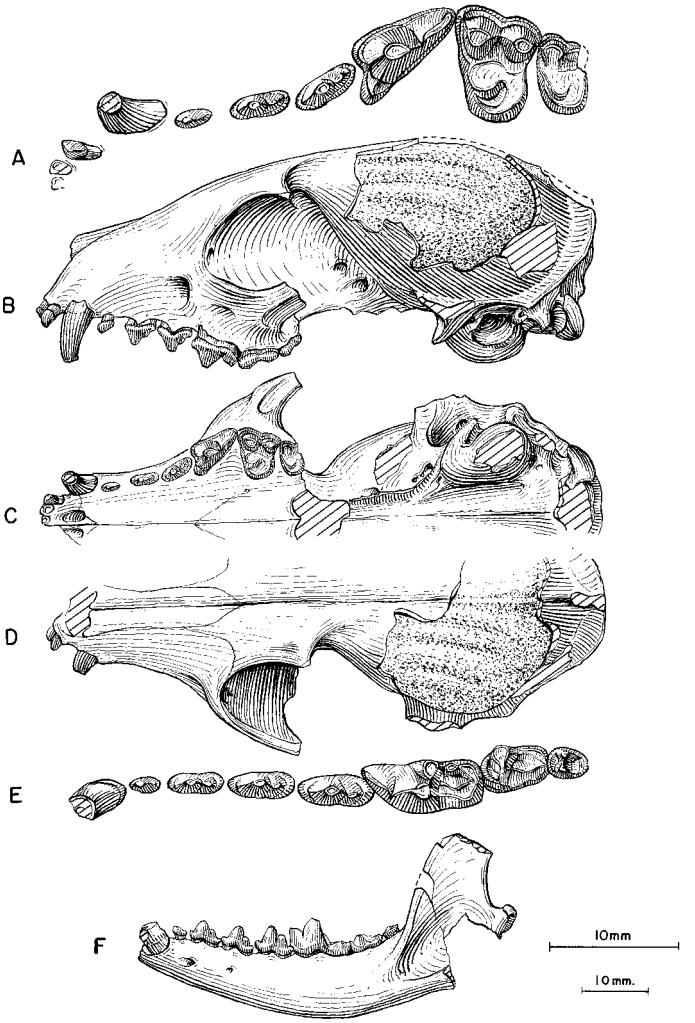

Fig. 19. *Rhizocyon oregonensis*. **A**, Upper teeth (P4–M2 reversed from right side), **B**, lateral, **C**, ventral, and **D**, dorsal views of skull, **E**, lower teeth, and **F**, ramus, AMNH 6879, lectotype, John Day Basin, John Day Formation (?early Arikareean), Oregon. The longer (upper) scale is for A and E, and the shorter (lower) scale is for the rest.

is the only information available on these structures. The remaining i3–c1, p2, and p4 are difficult to distinguish from similar-size John Day canids (e.g., *Phlaocyon latidens*). We choose AMNH 6879 as a lectotype, not only because of its far more complete and superior preservation, but also because the original diagnosis (Merriam, 1906: 11, fn. 3) included skull characteristics that could only have been observed on AMNH 6879, which thus must be part of the original syntype series.

REFERRED SPECIMENS: From Turtle Cove Member of John Day Formation (early Arikareean), Wheeler and Grant counties, Oregon (biostratigraphic positions of some JODA specimens in the Turtle Cove Member are placed within a letter system by Fremd et al., 1994 and Fremd and Wang, 1995): AMNH 6881, fragmentary palate with P3 broken, P3–M2, and right and left partial rami with p4–m3, from Camp Creek; AMNH 6883, right ramus fragment with worn m1–m2; AMNH 6914a, right ramus

fragment with p3–p4; JODA 398, left ramus fragment with p3–p4; JODA 688 (AMNH cast 129655), left maxillary fragment with M1–M2; JODA 735, left ramus fragment with m2; JODA 791 (AMNH cast 129654), right m1, Bed E; JODA 1624, right ramus fragment with p4–m2, Bed K; JODA 1639, left ramus fragment with p4–m2, Bed F; JODA 1654, rostral part of skull with nearly complete dentitions, Bed J; JODA 1847, right m1, Bed E; JODA 3041, right ramus fragment with m1–m2, Bed E2; JODA 3433, skull and mandible fragments with right P3–M1 and left p4–m1, Bed E; JODA TF10922, left ramus fragment with m1, Bed C; UCMP 316, partial left ramus with i3–c1 and p2–m2 (Merriam, 1906: pl. 2, fig. 4), from UCMP loc. 818, Blue Basin, Turtle Cove Member; UCMP 365, right ramus fragment with m1 and erupting p4 (Merriam, 1906: pl. 2, fig. 5); UCMP 79365, rostral part of skull with left and right P2–M2, UCMP loc. V-6322, Haystack 8-63, level 2; and YPM 12760, right ramus with p2–p3 and m1–m2 from Turtle Cove.

DISTRIBUTION: Early Arikareean of Oregon. Recent JODA collections suggest that *Rhizocyon oregonensis* is mostly restricted to the lower part (Beds B–J of Fremd and Wang, 1995) of the Turtle Cove Member in the John Day Formation, and this is in essential agreement with Merriam and Sinclair (1907: 188), who listed it as from the ''Middle John Day.''

EMENDED DIAGNOSIS: Same as for monotypic genus.

DESCRIPTION AND COMPARISON: *Rhizocyon oregonensis* is 22% larger (average of all dental measurements, appendix III) and has a slightly more robust construction (fig. 12) than *Archaeocyon pavidus*. In addition, the anterior expansion of the braincase yields a wider postorbital constriction. Proportionally, *R. oregonensis* is most notable for having both a broad rostrum and short bulla as compared to other basal borophagines (palate width at P1 and bulla length in fig. 12). The basicranium is primitive in its small bulla with a V-shape notch on the auditory meatus, as well as posteriorly oriented paroccipital process lacking contact with the posterior part of the bulla. Breakage of the entotympanic bulla reveals a partial entotympanic septum at the ento- and ectotympanic suture.

The m1 entoconid is crestlike, and about the same height as the hypoconid. Metaconid of the m2 is higher than the protoconid. Although of larger size, the proportions of the teeth are similar to those in *A. pavidus*, with the exception of a longer P1 and slightly shorter M2 (fig. 13). The m1 trigonid in *Rhizocyon* is not as longitudinally oriented (i.e., more opened) as in *A. leptodus* or *Cormocyon* and more derived forms.

DISCUSSION: Earlier references of this Oregon species either directly to *Hesperocyon gregarius* (Cope, 1879a, 1883, 1884) or as a distinct species of *Hesperocyon* (*Cynodictis*) (Merriam, 1906; Matthew, 1909; Thorpe, 1922a) reinforced the idea of a relationship of *oregonensis* to the small canids in the White River, as was also suspected of *Archaeocyon pavidus*. Our cladistic analysis, however, suggests that *Rhizocyon* represents a basal borophagine with some of the initial synapomorphies of the borophagine clade.

Phlaocyonini, new tribe

Type Genus: *Phlaocyon* Matthew, 1899.

INCLUDED GENERA: *Cynarctoides* McGrew, 1938a; and *Phlaocyon* Matthew, 1899.

DISTRIBUTION: Early Arikareean through early Barstovian of North America.

DIAGNOSIS: Derived characters that distinguish early Phlaocyonini from *Archaeocyon* and *Rhizocyon* include a large M1 metaconule and presence of a protostylid on m1. Phlaocyonines differ from *Cormocyon* in possessing a primitively short, closed m1 trigonid.

Cynarctoides McGrew, 1938

TYPE SPECIES: *Cynarctus acridens* Barbour and Cook, 1914.

INCLUDED SPECIES: *C. lemur* (Cope, 1879b); *C. roii* (Macdonald, 1963); *C. harlowi* (Loomis, 1932); *C. luskensis*, new species; *C. gawnae*, new species; *C. acridens* (Barbour and Cook, 1914); and *C. emryi*, new species.

DISTRIBUTION: ?Whitneyan of South Dakota; early Arikareean of Oregon, Nebraska, and South Dakota; medial or late Arikareean of South Dakota and Florida; late Arikareean

of Colorado, Nebraska, Wyoming, and New Mexico; early Hemingfordian of Nebraska, Idaho, Texas, and New Mexico; late Hemingfordian of Nebraska, Wyoming, and New Mexico; and early Barstovian of Nebraska, New Mexico, and California.

EMENDED DIAGNOSIS: Shared derived characters that distinguish all species of *Cynarctoides* include parasagittal crests and slender, shallow horizontal ramus. Advanced species of *Cynarctoides* (*C. luskensis* and more derived forms) further developed narrow rostrum, long jaws, narrow and long premolars, conical and high-crowned cusps in the lower molars, laterally shifted p4 accessory cusp, long M2 and m2, progressive larger hypocones in upper molars, higher metaconids in lower molars, and larger protostylids in lower molars, although the slender jaws and premolars are later reversed in *C. emryi*.

DISCUSSION: The type species *Cynarctoides acridens* was originally recognized as a species of *Cynarctus* (Barbour and Cook, 1914; Matthew, 1932; McGrew, 1937), mostly because of the fragmentary nature of the holotype (a ramal fragment with a single m1). The discovery of the upper teeth allowed direct comparisons of the relevant taxa and led to the establishment of the genus *Cynarctoides* by McGrew (1938a). However, McGrew regarded *Cynarctoides* as a primitive procyonid, as he did all other hypocarnivorous borophagines then known (e.g., *Phlaocyon* and *Cynarctus*). With only dental materials available to her, Hough (1948) challenged this arrangement and considered *Cynarctoides* a canid, a view that won firm support from Galbreath (1956) in his analysis of a basicranial fragment of *C. acridens* from Colorado. Past discussions about *Cynarctoides* systematics, however, were mostly based on a few specimens reported in the literature, and large morphological gaps left room for speculation.

Such a deficiency in the fossil record is partially bridged in this study—large numbers of specimens including skulls are now available from a wide range of geographic and geologic distributions. Additionally, three new species are described below, which, together with *C. acridens*, represent a nearly continuous series of intermediate stages of development toward a peculiar form of hypocarnivory quite different from that of both *Phlaocyon* and *Cynarctus*. For example, the upper carnassial (P4) of *Cynarctoides* remains largely primitive without a hypocone and has never gone beyond the addition of a slightly widened lingual cingulum. Its M1–M2, however, usually have a discrete hypocone (except the basal species of *C. lemur* through *C. luskensis*), which is often surrounded lingually by a narrow cingulum, a peculiarity not seen in *Phlaocyon* and *Cynarctus*. The tendency to develop distinct crests (e.g., crista obliqua) in the lower molars is another reason for its unique appearance. Together, these features help to define a unique clade of borophagines and increase our confidence about the appearance of independently acquired hypocarnivorous characters, such as the presence of a discrete hypocone on M1–M2.

Cynarctoides lemur (Cope, 1879b)

Figure 20D–P

Canis lemur Cope, 1879b: 371.

Galecynus lemur (Cope): Cope, 1881b: 181; 1883: 241, fig. 7; 1884: 915, 931, pl. 70, figs. 6–8.

Cynodictis lemur (Cope): Scott, 1898: 400.

Nothocyon lemur (Cope): Wortman and Matthew, 1899: 127, 130. Matthew, 1899: 62; 1932: 3. Merriam, 1906: 13, pl. 2. Peterson, 1907: 53. Thorpe, 1922a: 165 (in part). Hall and Martin, 1930: 283. Hough, 1948: 100. Macdonald, 1963: 209; 1970: 56 (in part). Munthe, 1998: 138.

Cynodictis (?) *oregonensis* Merriam, 1906: 12, fig. 5 (in part).

Bassariscops willistoni (Peterson, 1924): Peterson, 1928: 97, fig. 7 (CMNH 11334 only).

Bassariscops achoros Frailey, 1979 (in part): 134, figs. 3B, 4C.

''Cormocyon'' lemur (Cope): Fremd and Wang, 1995: 74.

HOLOTYPE: AMNH 6888, skull with I1–C1 alveoli and P1–M2 (P2 alveolus) (fig. 20D–F) from the John Day Basin, John Day Formation (early Arikareean), Wheeler or Grant counties, Oregon.

REFERRED SPECIMENS: From the type area (biostratigraphic positions of some JODA specimens in the Turtle Cove Member are placed within a letter system by Fremd and Wang, 1995): AMNH 6889, partial skull with P2–P3 alveoli and P4–M2 (fig. 20G–I);

AMNH 6890, fragmentary skull with P4 alveolus and M1 broken–M2; AMNH 6891, anterior part of skull with I3–P2 alveoli, P3–P4, and M1–M2 both broken; AMNH 6892, left partial ramus with p2–p3 alveoli and p4–m2 (fig. 20J, K), Camp Creek; AMNH 6893, right partial ramus with p4 broken, m1, and m2 alveolus; AMNH 6895, right ramal fragment with m2 broken; AMNH 6898, left isolated p4 and jaw fragment with m1; AMNH 6900, right ramal fragment with m1 broken–m2; AMNH 6914b, left ramal fragment with m2 and m3 alveolus; KUVP 600, partial skull with C1–M2 (Hall and Martin, 1930: figs. 1–3) and right ramus with p3–m2, from ''Haystack Valley, below Turtle Cove''; JODA 355, edentulous right ramus fragment, unit E1; JODA 690, right P4; JODA 731, left M1; JODA 790, right ramus fragment with broken p4–m1, unit E1; JODA 825, rostral part of skull with left P3–M2 and right P4–M1, unit E2; JODA 1243, left ramus fragment with m1, unit E1; JODA 1352, partial skull, unit E2; JODA 1373, right ramus fragment with m1, unit E1; JODA 1390, right P4, unit E2; JODA 1401, left maxillary fragment with M1, unit C; JODA 1918, left M1, unit E1; JODA 2769, right ramus fragment with p3–p4, unit D; JODA 2856, left M1, unit C; JODA 2859, right P4, unit C; JODA 2918, right M1, unit E1; JODA 2971, right maxillary fragment with M1–M2, unit E2; JODA 2977, broken right P4, unit E2; JODA 2990, right ramus fragment with m1, unit E2; JODA 3049, p3, unit E3; JODA 3051 (AMNH cast 129656), rostral part of skull with left P4–M2 and right P4–M1, unit E1; JODA 3090, left ramus fragment with m1, unit E2; JODA 3380, left m1, unit D; JODA 3394, left ramus fragment with m1, unit E; JODA 3442, broken left M1; JODA TF8923, right M1; JODA TF3924PC, left ramus with p3–m1, unit E3; UCMP 352, left partial maxillary with P3 broken–M1 and M2 alveolus, Black Rock 3, loc. 839; UCMP 1104, left partial maxillary with P4–M2, Rudio Creek 1, UCMP loc. 869; UCMP 10208, partial skull with C1–M1 all broken, Logan Butte 1, UCMP loc. 898 (Merriam, 1906: pl. 2, fig. 2); UCMP 75217, left ramal fragment with m1, South Canyon Level 4, UCMP loc. V6600; uncataloged YPM specimen, field number 493, left partial maxillary with C1–P3 alveoli, P4–M1, and M2 broken; uncataloged YPM specimen, field number 785, left ramal fragment with m1 broken–m2; uncataloged YPM specimen, field number 903, left maxillary fragment with M1–M2 (fig. 20L) and left ramal fragment with m1; uncataloged YPM specimen, field number 940, Box 11-118, right isolated M1 and right ramal fragment with m1 broken–m2, from Turtle Cove.

Cedar Pass, ?Poleslide Member of Brule Formation (?Whitneyan), South Dakota: UCMP loc. V7228: UCMP 4130, anterior part of skull with C1–M2 (P1 alveolus) and partial mandible with c1 broken–m3 (p2 and m2 all broken).

Sharps Formation (early Arikareean), Shannon County, South Dakota: F:AM 50356, left partial maxillary with P3–M2, lower part of Sharps Formation, 12 ft above the Rockyford Ash; LACM 9368, right partial maxillary with P4 broken–M1, LACM loc. 1955; SDSM 54307, right partial ramus with p4–m2 (fig. 20M, N), SDSM loc. V5359, south side of Sharps Cutoff road, upper part of Sharps Formation; and SDSM 55134, left ramal fragment with m1, SDSM loc. V5410, Godsell Ranch channel, base of upper part of Sharps Formation.

Browns Park Formation (?early Arikareean), Moffat County, Colorado: CMNH 11334 (AMNH cast 89666) (fig. 20O, P), left partial ramus with c1 and m1–m2, and alveoli of p1–p4 and m3, 1.5 mi southwest of Sunbeam (referred to *Bassariscops willistoni* Peterson, 1928: 96, fig. 7; this specimen is presumably lower in stratigraphic level than the better dated faunas found by Honey and Izett, 1988).

Buda Local Fauna (medial Arikareean), Alachua County, Florida: UF 171368, right p4; UF 16969, left M1; UF 160799, left ramal fragment with talonid of m1, m2, and m3 alveolus; UF 18403 (AMNH cast 105034; Frailey, 1979: figs. 3B, 4C), left maxillary fragment with M1–M2; UF 160796, right P4; and UF 160797, left P4.

DISTRIBUTION: ?Whitneyan of South Dakota, early Arikareean of Oregon and South Dakota, ?early Arikareean of Colorado, and medial Arikareean of Florida.

EMENDED DIAGNOSIS: In contrast to *Rhizocyon*, *Archaeocyon*, and other basal boro-

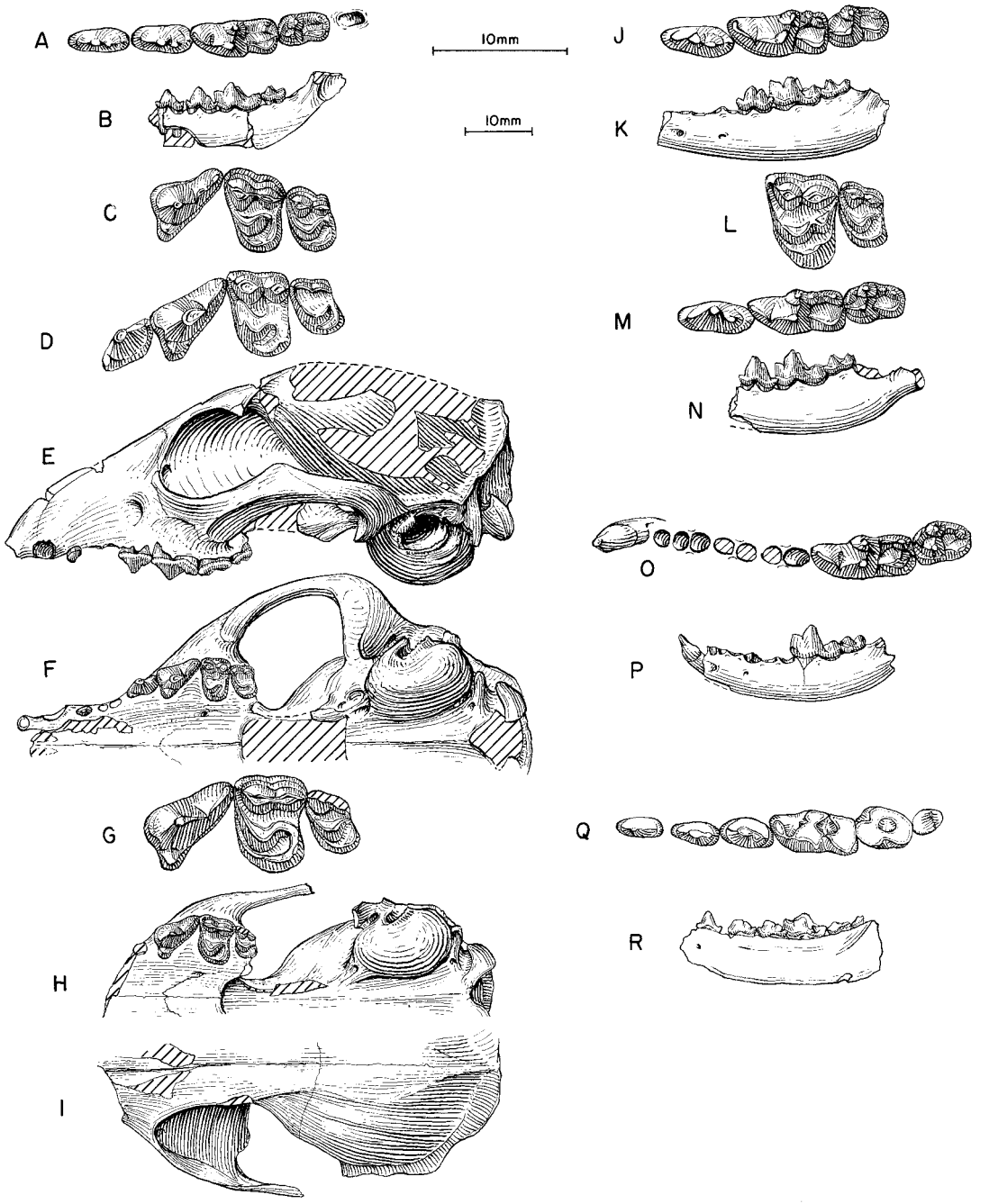

Fig. 20. **A**, Lower teeth and **B**, ramus (reversed from right side), *Cynarctoides roii*, SDSM 53321, holotype, Wounded Knee, Sharps Formation (early Arikareean), Shannon County, South Dakota. **C**, Upper teeth, *C. roii*, SDSM 54132, Wounded Knee, Sharps Formation. **D**, Upper teeth, and **E**, lateral and **F**, ventral views of skull, *C. lemur*, AMNH 6888, holotype, John Day Basin, John Day Formation (early Arikareean), Wheeler or Grant counties, Oregon. **G**, Upper teeth, and **H**, ventral and **I**, dorsal views of skull, *C. lemur*, AMNH 6889, John Day Formation. **J**, Lower teeth and **K**, ramus, *C. lemur*, AMNH 6892, Camp Creek, John Day Formation. **L**, M1–M2, *C. lemur*, YPM 903, John Day Formation.

phagines, derived characters of *Cynarctoides lemur* shared with other species of *Cynarctoides* and the *Phlaocyon* clades include a large M1 metaconule and the presence of a protostylid on m1–m2. *C. lemur* shows the initial tendency of the genus: slender ramus and separate temporal crests. *C. lemur* primitively lacks derived characters in more advanced species of the *Cynarctoides* clade: elongate premolars, conical talonid cusps of m1, and a protostylid on m2. It also primitively lacks other features that are synapomorphies of *Phlaocyon*: short and robust premolars, shortened P4 with enlarged lingual shelf, quadrate M1–M2, and wide m1 talonid.

DESCRIPTION AND COMPARISON: Descriptions of the general cranial and dental morphologies of *Cynarctoides lemur* have been available for some time (Cope, 1884; Merriam, 1906; Hall and Martin, 1930; Hough, 1948). In skull length, *C. lemur* is slightly larger than *Archaeocyon*. The most conspicuous feature often noted about *C. lemur* is its enlarged bulla, which is larger than that in *A. pavidus* and *Rhizocyon oregonensis*. Other relevant features in the present phylogenetic analysis are concerned with two subtle dental characters: (1) a more distinct metaconule on M1 begins to take shape in most specimens of *C. lemur*, and (2) a protostylid begins to appear on the m1 of *C. lemur*. The latter is a derived feature that signals the initiation of a hypocarnivorous clade, which quickly diverged into *Cynarctoides* and *Phlaocyon*. The skull roof of *C. lemur* has paired temporal crests instead of a single sagittal crest in the primitive condition. The double temporal crests do not seem to be related to ontogenetic age, as is common in small carnivorans, because individuals with modest (AMNH 6889) and advanced (AMNH 6888 and 6891) wear on the permanent molars all exhibit this trait.

DISCUSSION: A protostylid on the m1 has been traditionally used to differentiate *Cynarctoides lemur* (considered absent) from the contemporaneous *Phlaocyon latidens* (e.g., Cope, 1884; Merriam, 1906; Macdonald, 1963). Both species have been closely linked in almost all past discussions. Our observations suggest that the protostylid is variably present in both species, although those in *P. latidens* tend to be better developed than in *C. lemur*. The protostylid therefore is a synapomorphy of a clade that includes *Cynarctoides* and *Phlaocyon*, and this cusp is further elaborated in the species of *Cynarctoides*.

Matthew (1932: 3) was the first to speculate that the origin of *Cynarctoides acridens* may be found in the John Day ''*Nothocyon*'' *lemur* or ''*Nothocyon*'' (= *Phlaocyon*) *latidens* (however, he did not think his new species, *Cynarctus mustelinus* [presently synonymized under *C. acridens*], was in the same group). In fact, he went so far as to suggest that the holotype of *C. acridens* be placed in the same genus (*Nothocyon*) as the two John Day species. Matthew's suggestion is generally confirmed by our phylogenetic conclusions.

Collections made by JODA field teams in recent years restrict the stratigraphic distribution of *Cynarctoides lemur* to a narrow range within the Turtle Cove Member of the John Day Formation, as opposed to the more vague ''John Day Basin'' frequently used in the literature. The species is found in units A–F below the Picture Gorge Ignimbrite (Fremd and Wang, 1995), now estimated to be around 28.7 Ma (Woodburne and Swisher, 1995). Such a restricted range is consistent with the occurrence of representatives of this taxon in the Great Plains (Sharps Formation, South Dakota).

Fragmentary materials (including specimens referred to *Phlaocyon achoros*) from

---

←

M, Lower teeth and **N**, ramus (reversed from right side), *C. lemur*, SDSM 54307, Sharps Cutoff road, Wounded Knee, Sharps Formation. **O**, Lower teeth and **P**, ramus, *C. lemur*, CMNH 11334, Browns Park Formation (?early Arikareean), Moffat County, Colorado. **Q**, Lower teeth and **R**, ramus, *C. harlowi*, ACM 31-34, holotype, 3 mi southeast of Van Tassel, Upper Harrison beds, Niobrara County, Wyoming. The longer (upper) scale is for A, C, D, G, J, L, M, O, and Q, and the shorter (lower) scale is for the rest.

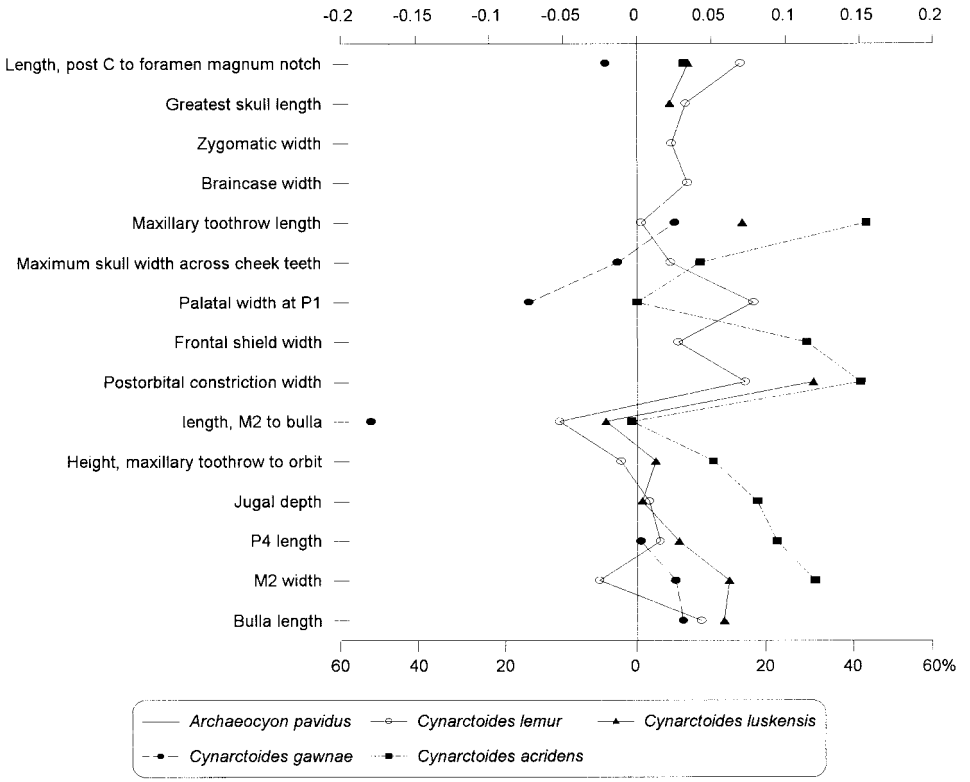

Fig. 21. Log-ratio diagram for cranial measurements of four species of *Cynarctoides* using *A. pavidus* as a standard for comparison (straight line at zero). See text for explanations and appendix II for measurements and their definitions.

the Buda Local Fauna, Florida, are provisionally referred to this species. It is of interest to note that JODA 3051, referred here to *Cynarctoides lemur*, exhibits certain initial features toward the development of *Phlaocyon achoros*, which is known only in the Buda Local Fauna (see discussion under that species).

Cynarctoides roii (Macdonald, 1963)

Figure 20A–C, O, P

?*Phlaocyon* Peterson, 1924: 303, fig. 2.
Nothocyon roii Macdonald, 1963: 206, figs. 24, 25. 1970: 54.

HOLOTYPE: SDSM 53321 (AMNH cast 129863), right partial ramus with p3–m2 and m3 alveolus (fig. 20A, B) from the Wounded Knee Area, SDSM loc. V5354, from near the top of the Sharps Formation (early Arikareean), Shannon County, South Dakota.

REFERRED SPECIMENS: From the Wounded Knee Area, upper part of the Sharps Formation (early Arikareean), Shannon County, South Dakota: LACM 9196 (AMNH cast 129646), right partial ramus with p2–m1 (p4 broken), LACM loc. 1959; LACM 9284, right ramal fragment with m1 broken, LACM loc. 1966; LACM 9462, left detached m1, LACM loc. 1982; LACM 9507, left partial ramus with m1–m2 and m3 alveolus, LACM loc. 1984; SDSM 5581, right partial ramus with p4–m1, SDSM loc. V5350; SDSM 5583, right partial ramus with c1–p2 alveoli and p3–p4, SDSM loc. V5341; SDSM 53322, left partial ramus with p4 broken–m2 and m3 alveolus, SDSM loc. V5358; SDSM 54132, fragmentary skull with P4–M2 (Macdonald, 1963: fig. 25; fig. 20C), SDSM loc. V5354; SDSM 54252, left partial ramus with P4–M1, SDSM loc. V5354; SDSM 54273, left ramal fragment with m1, SDSM loc. V5360; UCMP 114775, left ramus fragment

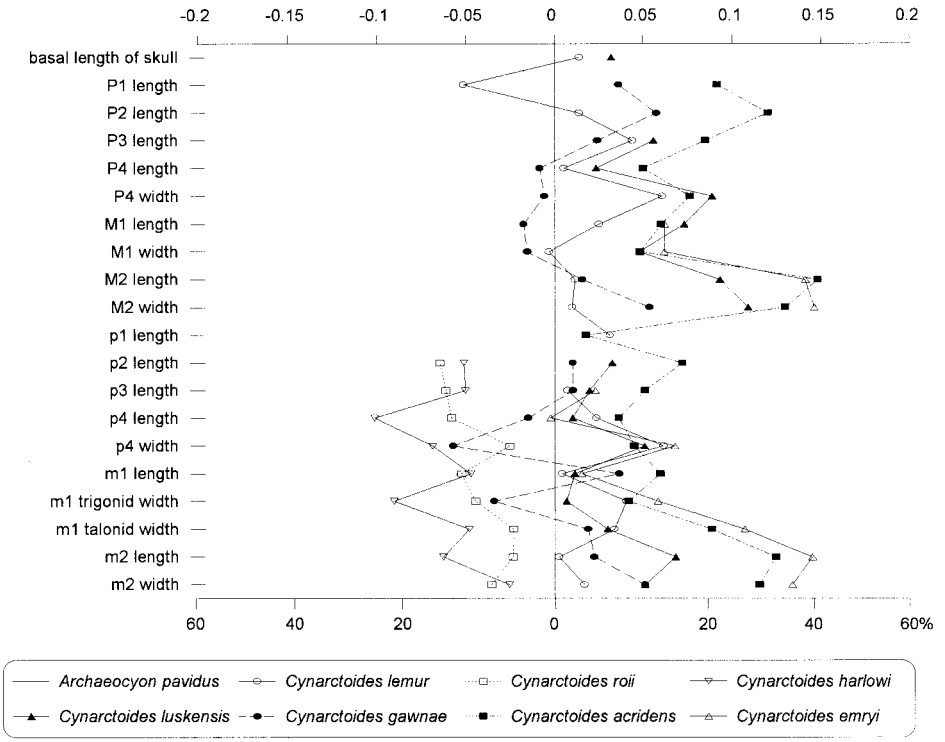

Fig. 22. Log-ratio diagram for dental measurements of seven species of *Cynarctoides* using *A. pavidus* as a standard for comparison (straight line at zero). See text for explanations and appendix III for summary statistics of measurements and their definitions.

with m1–m2, UCMP loc. V76043, Wolff Camp 2; and UCMP 121784, partial left ramus with p3 broken–m2 and m3 alveolus, UCMP loc. V75201 (= SDSM V5354).

One mi east of Nebraska/Wyoming line, Horse Creek Basin, lower Arikaree Group (early Arikareean), Banner County, Nebraska: F:AM 49070, left partial ramus with p3–m2, from 20 ft above White Layer.

DISTRIBUTION: Early Arikareean of South Dakota and Nebraska.

EMENDED DIAGNOSIS: *C. roii* differs from *C. lemur* in its smaller size, entoconid of m1 less prominent, protostylid on m2, and protoconid and metaconid of m2 close together. Compared to *C. harlowi*, *C. roii* is slightly larger and has longer premolars.

DESCRIPTION AND COMPARISON: *C. roii* is still poorly known and little can be added to the topotype series from the Wounded Knee Area, other than a questionable reference of a ramus from the early Arikareean of Nebraska and possibly one from younger rocks of the Browns Park Formation of Colorado. Macdonald's (1963) characterization of this species is thus still essentially valid, although his phylogenetic framework is quite different from ours. In general, *C. roii* is so primitive in its overall morphology that few characters can be identified to distinguish it from other basal borophagines.

In light of our phylogeny, *C. roii* is close to the base of the *Cynarctoides* clade. The only features that suggest it to be on this side of the clade (as opposed to the *Phlaocyon* side) are its slender ramus and development of a labial cingulum (precursor of a protostylid) lateral to the m2 protoconid. However, *C. roii* still lacks a protostylid on the m1, a character present in all other more derived phlaocyonines.

DISCUSSION: Much remains to be learned about this rare and tiny borophagine. Its small size and generally primitive morphol-

ogy call for comparisons with *C. lemur* and *C. harlowi*. Although the poorly preserved specimens of *C. roii* and *C. harlowi* do not lend themselves to a rigorous phylogenetic analysis, we may speculate that these two species, possibly including *C. lemur*, form a small clade of their own, within which continued size reduction seems to be the main trend.

Cynarctoides harlowi (Loomis, 1932)

Figure 20Q, R

Pachycynodon harlowi Loomis, 1932: 326, fig. 9.

HOLOTYPE: ACM 31-34 (AMNH cast 48830), right partial ramus with p2–m3 and alveoli of c1–p1 (fig. 20Q, R), from 3 mi southeast of Van Tassel, in the ''Upper Harrison'' beds (late Arikareean), Niobrara County, Wyoming.

DISTRIBUTION: Late Arikareean of Wyoming.

REFERRED SPECIMEN: Holotype only.

EMENDED DIAGNOSIS: *Cynarctoides harlowi* differs from *C. roii* in its smaller size and shorter premolars.

DESCRIPTION AND COMPARISON: The holotype of *C. harlowi* is still the only specimen known in the late Arikareean of Wyoming. It is the smallest borophagine and closest in size and morphology to *C. roii*. In fact, in all its dental measurements it is either near or slightly outside the lower end of corresponding measurements in *C. roii*. The only observable difference between these two species is shorter p2–p4 in *C. harlowi* (fig. 22).

DISCUSSION: The advanced stage of wear, especially on molars, and poor state of preservation of the holotype of *C. harlowi* make the determination of its taxonomic status difficult. Although ACM 31-34 matches reasonably well with some specimens of *C. roii*, its much younger age (late Arikareean) and proportional differences of the lower teeth suggest a distinct species. Macdonald (1963: 208) compared *C. harlowi* with *C. roii*, and commented that ''*Nothocyon roii* is ideally an ancestor to *N. harlowi*, as there is very little modification of the lower molars during the intervening time, and the major difference is the reduction of the premolars in the younger species [*N. harlowi*].'' In any case, wear on ACM 31-34 is so severe that to use it as the holotype of a species is dubious at best. Until more and better-preserved materials are found, the status of *C. harlowi* cannot be clarified beyond the present recognition that it probably represents a small borophagine.

Cynarctoides luskensis, new species

Figure 23N–T

HOLOTYPE: F:AM 49005, partial skull with C1–P2 alveoli, P3–M2, and partial mandible with c1, p1–p3 alveoli, and p4–m3 (fig. 23N–R) from 18 mi southeast of Lusk, Upper Harrison Beds (late Arikareean), Goshen County, Wyoming.

ETYMOLOGY: In reference to the locality of the holotype near the town of Lusk in Goshen County, southeastern Wyoming.

REFERRED SPECIMENS: Upper Harrison Beds (late Arikareean), Wyoming: F:AM 49003, right partial ramus with p2–m2 and m3 alveolus (fig. 23S, T), 7 mi southeast of Chugwater, Platte County; and F:AM 50225, right partial maxillary with P3–M2, from Jay Em area, high brown sand, Goshen County.

DISTRIBUTION: Late Arikareean of Wyoming.

DIAGNOSIS: In contrast to *Cynarctoides lemur* and *C. roii*, *C. luskensis* has derived characters shared with all other more advanced species of *Cynarctoides*: long, slender horizontal ramus, P3 and p3 posterior cusplet weak or absent, long and narrow premolars, m1 talonid cusps high-crowned and conical, m1 entoconid exceeding height of the hypoconid, and presence of a protostylid on m2. *C. luskensis* lacks derived characters found in *C. gawnae* and more derived species: fully encircled ectotympanic ring forming the roof of the external auditory meatus, cleft on M1–M2 lingual cingulum and large conical hypocone, M2 paraconule, and strong m2 protostylid.

DESCRIPTION AND COMPARISON: The skull of the holotype, although laterally compressed, is the best preserved among all species of *Cynarctoides*. In contrast to other hypocarnivorous borophagines (such as *Otarocyon* and derived species of *Phlaocyon*, and, to a lesser extent, *Rhizocyon*), the rostrum of *Cynarctoides* is slightly elongated as first shown in *C. luskensis*. The temporal

crests, trailing behind the small postorbital processes, are poorly defined, although the crests seem to be separate, as is consistent with the similar pattern in taxa more primitive (*C. lemur*) and more derived (*C. gawnae* and *C. acridens*). The bulla is moderately inflated, although its form is modified due to the mediolateral compression. The mastoid process is not enlarged and there is no suprameatal fossa. The ectotympanic does not extend dorsally to form a full ring. The paroccipital process is ventrally oriented and fully fused with the bulla, a derived state shared with *C. lemur* and the rest of the *Cynarctoides–Phlaocyon* clade. The masseteric scar (for origination of the superficial masseter muscle) on the anterior part of the jugal is wide, occupying approximately two-fifth of the total depth of the zygomatic arch. Beginning in *C. luskensis*, the mandible of *Cynarctoides* species becomes very slender (shallow) and long, to accommodate the elongated premolars. On the holotype, the anterior crest of the ascending ramus extends ventrally and anteriorly to form an elongated ridge below the lower molars (fig. 23R).

Dental morphology of *Cynarctoides luskensis* possesses an interesting mixture of primitive and derived characteristics. Besides the slender premolars, the upper teeth remain primitive and are close to the overall shape of those in *C. lemur*. The lingual cingulum in M1–M2 lacks a deep cleft that creates a conical hypocone in later species of *Cynarctoides* (beginning in *C. gawnae*), although the posterior end of the cingulum is slightly swollen (on the holotype, the left M1 has a vague indication of a cleft, whereas that on the right side is less conspicuous). The M2 metaconule is fully connected to the end of the lingual cingulum. The lower molars, on the other hand, are more derived, resembling advanced species of *Cynarctoides*. The m1 protostylid is still weakly developed. The m2 begins to develop a protostylid as well. Cusps on the m2 and on the talonid of m1 show signs of becoming conical and higher crowned, instead of the crestlike and low crowned as in *C. lemur* and basal *Phlaocyon* species (*P. minor* and *P. latidens*).

DISCUSSION: Presently identified as a transitional species of *Cynarctoides*, *C. luskensis* provides a crucial phylogenetic link between the advanced species of *Cynarctoides* and the primitive *C. lemur*. Its slender ramus and premolars and its pattern of lower molars are unmistakably those of *Cynarctoides*, whereas its upper molars are little more advanced than those in *C. lemur*. An elevated entoconid on the lower molars thus precedes the emergence of an isolated hypocone on the upper molars, as is a general rule in other hypocarnivorous borophagines. The more cuspidate cheekteeth seem to indicate an emphasis toward puncturing, instead of shearing or grinding, reflecting an increasingly insectivorous diet.

Cynarctoides gawnae, new species

Figure 23G–I

Cynarctoides, new species B Gawne, 1975: 2.

HOLOTYPE: F:AM 49249, partial skull with C1 alveolus–M2 and both partial rami with c1 broken and p1 alveolus–m3 (fig. 23G–I) from Jeep Quarry, upper part of Chamisa Mesa Member of the Zia Formation (early Hemingfordian), Arroyo Pueblo drainage, Sandoval County, New Mexico.

ETYMOLOGY: In honor of Dr. C. E. Gawne for her earlier recognition of this species in her dissertation on the Zia Sand faunas.

REFERRED SPECIMENS: Jeep Quarry and Jeep Quarry horizon, upper part of the Chamisa Mesa Member of the Zia Formation (early Hemingfordian), Arroyo Pueblo drainage, Sandoval County, New Mexico: F:AM 49233, left ramus fragment with c1–p1, left detached m1, and p2–m3 alveoli; F:AM 62775, right edentulous ramus fragment with p1–p4 alveoli.

Jemez Creek drainage, southwest corner of *Blickomylus* Hill, local green zone near base of hill, near middle of Chamisa Mesa Member, Zia Formation (early Hemingfordian), Arroyo Pueblo drainage, Sandoval County, New Mexico: F:AM 49213, left partial ramus with c1 broken, p1 alveolus, p2–p3 both broken, and p4–m2.

DISTRIBUTION: Early Hemingfordian of New Mexico.

DIAGNOSIS: Relative to the more primitive *Cynarctoides luskensis*, *C. gawnae* has acquired a fully encircled ectotympanic ring, a discrete hypocone on M1–M2, and an enlarged protostylid of m2. It is, on the

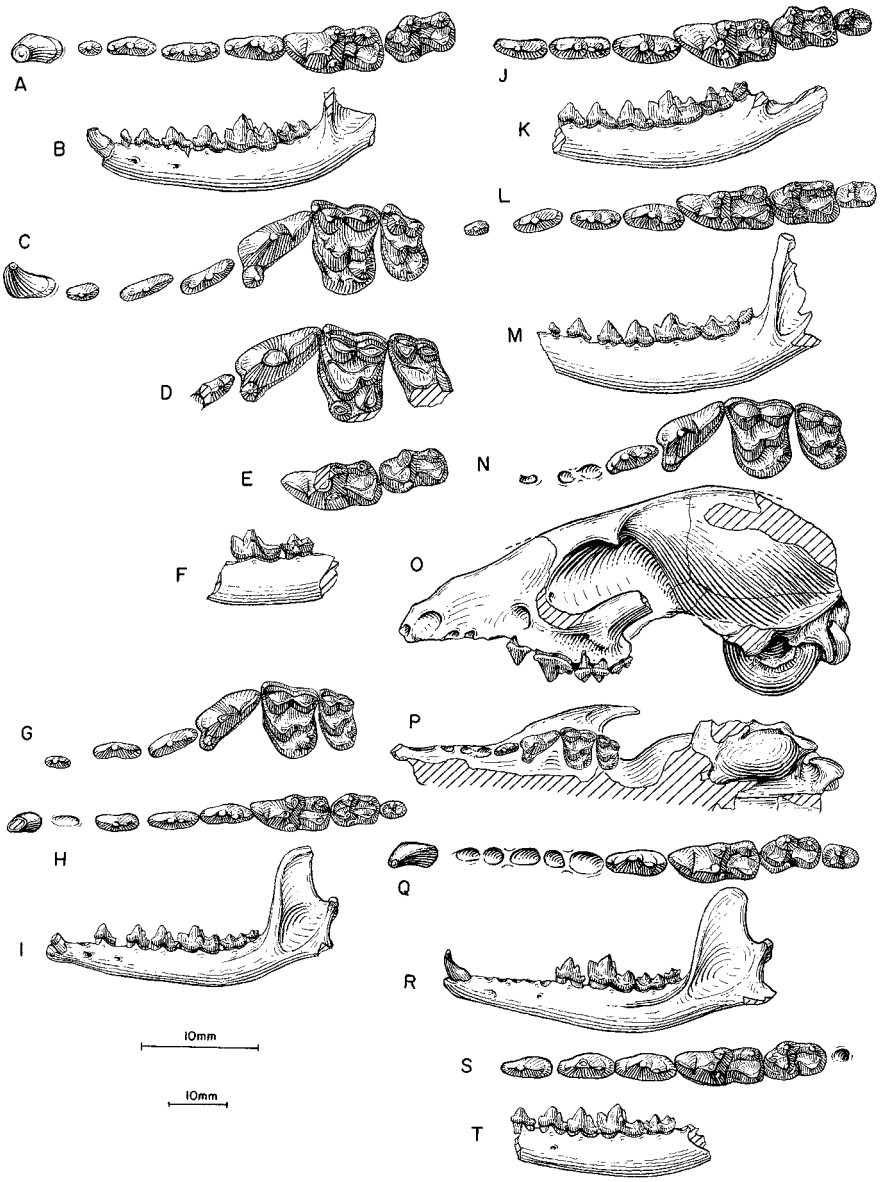

Fig. 23. **A**, Lower teeth, **B**, ramus, and **C**, upper teeth, *Cynarctoides acridens*, F:AM 63140, *Cynarctoides* Quarry, Chamisa Mesa Member, Zia Formation (early Hemingfordian), Sandoval County, New Mexico. **D**, Upper teeth, *C. acridens*, F:AM 49109, Ginn Quarry, temporally equivalent to Sheep Creek Formation (late Hemingfordian), Dawes County, Nebraska. **E**, Lower teeth and **F**, ramus (reversed from right side), *C. acridens*, AMNH 20502 (holotype of *C. mustelinus*), Stonehouse Draw, Sheep Creek Formation (late Hemingfordian), Sioux County, Nebraska. **G**, Upper teeth, **H**, lower teeth, and **I**, ramus (P1 and p2 reversed from right side), *C. gawnae*, F:AM 49249, holotype, Jeep Quarry, Chamisa Mesa Member, Zia Formation. **J**, Lower teeth and **K**, ramus (reversed from right side), *C. acridens*, F:AM 49112, Long Quarry, Sheep Creek Formation. **L**, Lower teeth and **M**, ramus (reversed from right side), *C. acridens*, F:AM 49126, Boulder Quarry, Olcott Formation (early Barstovian), Sioux County, Nebraska. **N**, Upper teeth (P3 reversed from right side), **O**, lateral and **P**, ventral views of skull, **Q**, lower teeth, and **R**, ramus, *C. luskensis*, F:AM 49005, holotype, 18 mi southeast of Lusk, Upper Harrison beds (late Arikareean), Goshen County, Wyoming. **S**, Lower teeth and **T**, ramus (reversed from right side), *C. luskensis*, F:AM 49003, 7 mi southeast of Chugwater, Upper Harrison beds (late Arikareean), Platte County, Wyoming. The longer (upper) scale is for A, C–E, G, H, J, L, N, Q, and S, and the shorter (lower) scale is for the rest.

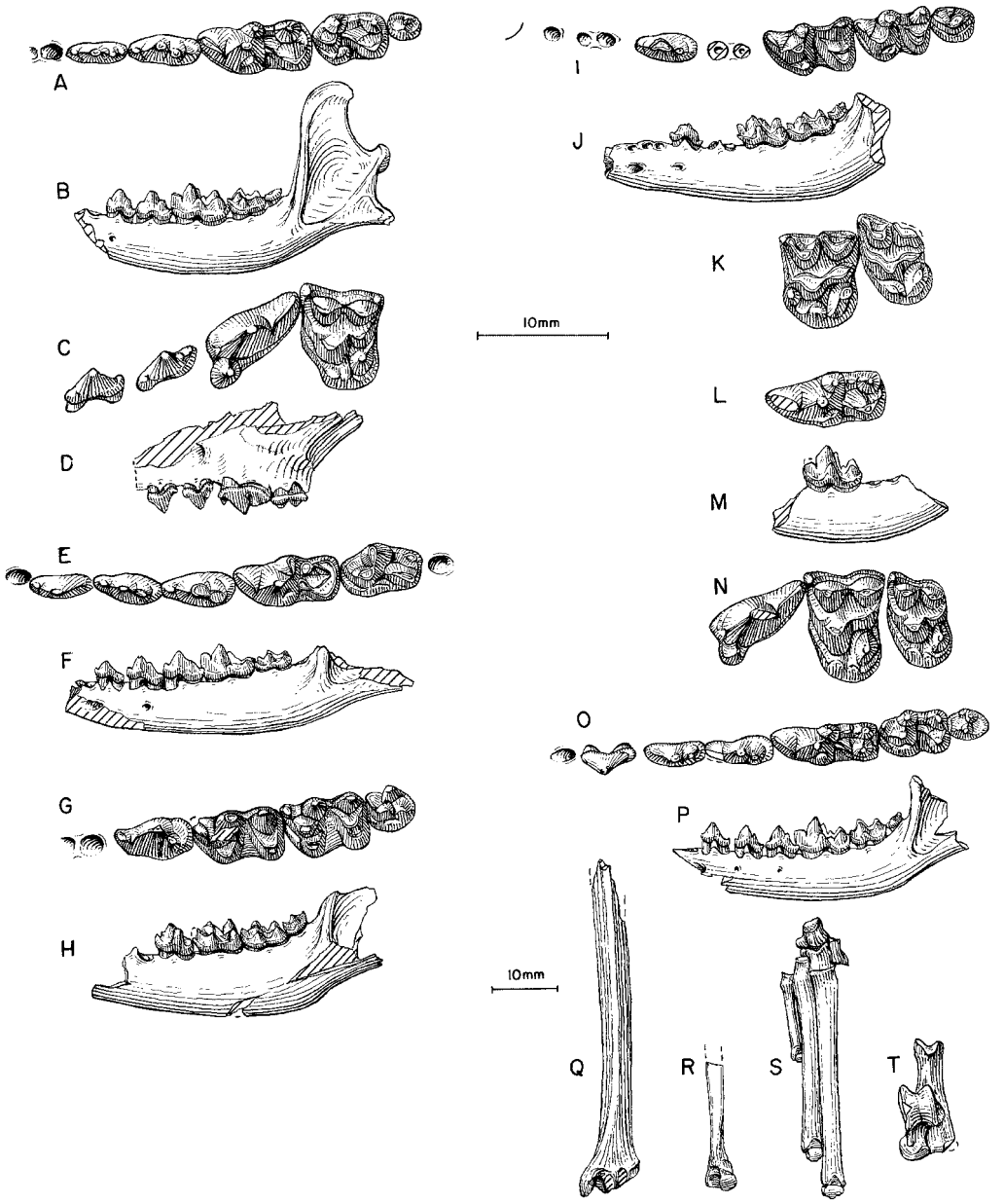

Fig. 24. **A**, Lower teeth and **B**, ramus (reversed from right side), *Cynarctoides acridens*, FMNH UC1547, east of Agate, Upper Harrison beds (late Arikareean), Sioux County, Nebraska. **C**, Upper teeth and **D**, lateral view of maxillary, *C. acridens*, FMNH UC1564, Agate area, Upper Harrison beds (late Arikareean), Sioux County, Nebraska. **E**, Lower teeth and **F**, ramus (reversed from right side), *C. acridens*, F:AM 49001, 18 mi southeast of Lusk, Upper Harrison beds (late Arikareean), Goshen County, Wyoming. **G**, Lower teeth and **H**, ramus (reversed from right side), *C. emryi*, UNSM 25455, holotype, Hemingford Quarry, Runningwater Formation (early Hemingfordian), Box Butte County, Nebraska. **I**, Lower teeth and **J**, ramus (reversed from right side), *C. emryi*, UNSM 25456, Hemingford Quarry. **K**, M1–M2, *C. emryi*, UNSM 25615, Hemingford Quarry. **L**, Crown view of m1, and **M**, ramus, *C. acridens*, AMNH 82558 (HC 144), holotype, 4 mi northeast of Agate, Upper Harrison beds (late Arikareean), Sioux County, Nebraska. **N**, Upper teeth, **O**, lower teeth, **P**, ramus, **Q**, distal tibia, **R**, distal fibula, **S**, partial foot, and **T**, astragalus-calcaneum, *C. acridens*, F:AM 99360, Runningwater Formation (early Hemingfordian), Dawes County, Nebraska. The longer (upper) scale is for A, C, E, G, I, K, L, N, and O, and the shorter (lower) scale is for the rest.

other hand, primitive relative to *C. acridens* in that its M1 hypocone is not surrounded by a narrow lingual cingulum, and in that it has a less complex and smaller M2 without a distinct paraconule and an m1 without a metastylid and with a weaker protostylid.

DESCRIPTION AND COMPARISON: The holotype skull was severely flattened dorsoventrally, obscuring much of the original proportions. The dorsal skull roof, however, is relatively intact and reveals a smooth temporal area with separate (although rather weak) temporal crests as in *C. acridens* and *C. luskensis*. Both bullae are crushed but seem to show no enlargement over that seen in *C. luskensis*. As in *C. acridens*, the ectotympanic forms a fully closed ectotympanic ring (dorsal extension to the roof of the external auditory meatus) as opposed to the open, half ring in the primitive condition. In cranial proportion, *C. gawnae* is notable for its long and slender rostrum (length P1–M2 vs. palate width at P1 in fig. 21), characteristic of most advanced species of *Cynarctoides*.

The upper and lower teeth and the mandible are well preserved and clearly show intermediate characters between *C. luskensis* and *C. acridens*. Slight deepening of a transverse cleft on the lingual cingulum of M1 coupled with the rising of the posterior end of the cingulum creates a prominent hypocone, an advancement over that in *C. luskensis*. However, the hypocone still shows no sign of encirclement by a narrow cingulum on the lingual side, a derived condition that begins in *C. acridens*. The hypocone development on the M2 is also intermediate between *C. luskensis* (crestlike) and *C. acridens* (conate). The m1 protostylid remains small and fully attached to the protocone base. The m2 protostylid, on the other hand, is enlarged (in occlusal view) relative to that in *C. luskensis*. As in *C. luskensis*, the crista obliqua on m1 is still more or less sagittally oriented, instead of a more oblique orientation as in *C. acridens* and *C. emryi*.

DISCUSSION: In her unpublished dissertation on the geology and paleontology of the Zia Sand, Gawne (1973) described a new species of *Cynarctoides*, which was later referred to as ''*Cynarctoides*, new species B'' (Gawne, 1975), but never formally published. The content of her new species is the same as this study, and we take this opportunity to formally describe it.

Cynarctoides gawnae is an example of a transitional form that bridges the gap between *C. acridens*, which has many of the advanced characteristics of the genus, and *C. luskensis*, which has few. This combination of transitional features allows a sense of the actual steps shown by species of *Cynarctoides* in acquiring their peculiar morphology. The fact that the earliest records of *C. acridens* are from the late Arikareean of New Mexico and Nebraska suggests that *C. gawnae* must have had an equally long history, going back into the Arikareean (see further comments under *C. acridens*).

Cynarctoides acridens (Barbour and Cook, 1914)

Figures 23A–F, J–M, 24A–F, L–T

Cynarctus acridens Barbour and Cook, 1914: 226, pl. 1, figs. c, d. McGrew, 1937: 444, fig. 1.
Nothocyon annectens Peterson, 1907: Thorpe, 1922b: 429 (in part).
Cynarctus mustelinus Matthew, 1932: 2, figs. 2, 3.
''*Cynarctus*'' *acridens* (Barbour and Cook): Matthew, 1932: 3.
Cynarctoides acridens (Barbour and Cook): McGrew, 1938a: 324, fig. 87 (in part). Galbreath, 1956: 373, fig. 1. Munthe, 1988: 98, figs. 23, 24; 1998: 134.
Cynarctoides mustelinus (Matthew): Galbreath, 1956: 373. Munthe, 1998: 134.
Nothocyon near *latidens* (Cope, 1881b): Macdonald, 1963: 209; 1970: 56.
Nothocyon aff. *minor* (Matthew, 1907): Gawne, 1975: 2.
Cynarctoides, new species A: Gawne, 1975: 2.
Cynarctoides cf. *C. acridens* (Barbour and Cook): Galusha, 1975b: 57.

HOLOTYPE: AMNH 82558 (HC 144), right partial ramus with m1 and m2 alveolus from 4 mi northeast of Agate, Upper Harrison Beds of Peterson (1907) (late Arikareean), Sioux County, Nebraska (fig. 24L, M).

REFERRED SPECIMENS: East of Porcupine Creek, lower part of Rosebud Formation (equivalent to Monroe Creek Formation or Harrison Formation of Macdonald, 1963:

157) (medial or late Arikareean), AMNH locality ''Rosebud'' 32, Shannon County, South Dakota: AMNH 12873, right ramal fragment with m1 (referred to *Nothocyon* near *latidens* by Macdonald, 1963: 209).

First hill south of *Syndyoceras* Hill, 0.5 mi west of Agate, Harrison Formation (late Arikareean), Sioux County, Nebraska: AMNH 81035 (HC 488), right ramus fragment with p4–m1.

Agate area, Upper Harrison beds (late Arikareean), Sioux County, Nebraska: F:AM 50229, partial left and right rami with c1–m3 (m1s broken), limb bone fragments, 9 mi southwest of Harrison, in high brown sand; F:AM 107600, isolated left M1; FMNH UC1547 (AMNH cast 88393), right ramus with p1–p2 alveoli and p3–m3, from east of Agate (fig. 24A, B); FMNH UC1564 (AMNH cast 88392), left maxillary and skull fragment with C1–P1 alveoli broken and P2–M1 (fig. 24C, D); and FMNH P26201, right partial ramus with p2–m3.

Eighteen mi southeast of Lusk, Upper Harrison beds (late Arikareean), Goshen County, Wyoming: F:AM 49001, right partial ramus with c1–p1 alveoli, p2–m2, and m3 alveolus (fig. 24E, F); and F:AM 49002, right isolated m1 from below high brown sand.

Runningwater Formation (early Hemingfordian), Box Butte County, Nebraska: F:AM 99364, right partial ramus with m2 and alveoli of c1–m1 and m3, Dry Creek, Prospect B; UNSM 25417, partial left ramus with c1, p2, p3–m2, and alveoli of p1, p3, and m3, UNSM loc. Bx-7; UNSM 25424, right partial ramus with p2–m2 and alveoli of c1–p1 and m3, UNSM loc. Bx-7; UNSM 25462, left partial ramus with c1–p3 alveoli and p4–m2, UNSM loc. Bx-22, 12 mi west and 4 mi north of Hemingford; UNSM 25463, left M1, Marsland Quarry, UNSM loc. Bx-22; UNSM 25464, right ramus fragment with m1–m2 and alveolus of m3, Marsland Quarry, UNSM loc. Bx-22; UNSM 25612, left partial ramus with c1–p3 alveoli and p4–m2, Hemingford area, UNSM loc. Bx-0; UNSM 25666, right ramus with c1–p1 alveoli, p2–m2, and m3 alveolus, Hemingford Quarry 7B, UNSM loc. Bx-7B; UNSM 25723, right partial ramus with p2–p3 and p4–m2 all broken, Hemingford Quarry 7B, UNSM loc. Bx-7B; UNSM 25724, right partial ramus with m1–m2, and m3 alveolus, Hemingford Quarry 12B, UNSM loc. Bx-71; UNSM 25766, left M1, UNSM loc. Bx-7; UW 4141, left isolated broken M1, UW loc. V-34001, Marsland Quarry; UW 4142, left isolated m1, UW loc. V-34001, Marsland Quarry; UW 4143, left isolated broken m1, UW loc. V-34001, Marsland Quarry; and UW 4144, right ramus fragment with broken p4–m1, UW loc. V-34001, Marsland Quarry.

Runningwater Formation (early Hemingfordian), Cherry County, Nebraska: F:AM 49178, left partial ramus with p4–m2 and m3 alveolus, Antelope Creek; F:AM 107608, isolated left m1 (broken); YPM 12781, right partial ramus with p4 broken–m2 and m3 alveolus (referred to *Nothocyon annectens* by Thorpe [1922b: 429]), Antelope Creek.

Runningwater Formation (early Hemingfordian), Dawes County, Nebraska: AMNH 85956 (HC 1325), right ramus fragment with p4, Havorka Quarry; F:AM 25331, left ramus fragment with m1–m2 and alveolus of m3, from Belmont area; F:AM 25428, skull and ramus fragments with left P4–M1, right M1–M2, left p2–m1, and right p1–m3, Elder Ranch; F:AM 25429, partial right ramus with p2–p3, p4 broken, and m1–m2 broken, Marshall Ranch; F:AM 49098, left partial ramus with p3–m1, Woods Canyon Quarry; F:AM 49107, left partial ramus with p3–m1 and alveoli of p1–p2 and m2; F:AM 49108, left partial ramus with c1–m2 (broken); F:AM 49121, right partial ramus with p2, p4–m1, and alveoli of p1, p2, and m2–m3, Dunlap Camel Quarry; F:AM 49122, right ramus fragment with p4–m1, Dunlap Camel Quarry; F:AM 49123, left ramus fragment with m1 and alveolus of m2, ''B'' Quarry; F:AM 99360, skull fragments, isolated left and right P4–M2, right and left rami with p1 alveolus–m3, distal tibia and fibula, calcaneum, astragalus, tarsals, and metatarsals I, II, and III (fig. 24N–T); F:AM 99361, right partial ramus with p3–m1 and m2 broken, Pebble Creek; F:AM 99363, left ramus fragment with m2–m3, Woods Canyon; F:AM 99365, left partial ramus with p1–p2 both broken and p3–m3, Cottonwood Creek Quarry; F:AM 99366, right partial ramus with p1–p3 all broken, p4–m1, and m2 broken, Cottonwood Creek Quarry; F:AM 99367, right par-

tial ramus with m1 broken, Cottonwood Creek Quarry; F:AM 99368, isolated left m1, Cottonwood Creek Quarry; F:AM 99369, left ramus fragment with p4 root–m1, Cottonwood Creek Quarry; and F:AM 99371, left partial ramus with p3 alveolus–m2 and m3 alveolus, Cottonwood Creek Quarry.

Runningwater Formation (early Hemingfordian), Bridgeport Quarry (UNSM loc. Mo-115), Morrill County, Nebraska: UNSM 25434, right ramal fragment with m1 broken–m2 and m3 alveolus; UNSM 25435, left ramal fragment with p4–m1; UNSM 25437, right M1; UNSM 25444, left dp4; UNSM 25446, left M1; UNSM 25450, left M1; and UNSM 25460, right ramal fragment with m1–m3.

Schoolhouse Prospect No. 2, Box Butte Formation (late Hemingfordian), Dawes County, Nebraska: F:AM 99372, right partial ramus with p4–m3.

Dry Creek, Prospect A, Red Valley Member, Box Butte Formation (late Hemingfordian), Box Butte County, Nebraska: F:AM 95277, left partial ramus with p4 broken, m1, and m2 broken.

Ginn Quarry, in rocks temporally equivalent to the Sheep Creek Formation (late Hemingfordian), Dawes County, Nebraska: F:AM 49109, left partial maxillary with P3 broken–M1 and M2 broken (fig. 23D).

Split Rock Formation (late Hemingfordian), Granite Mountain, Fremont County, Wyoming (as listed in Munthe, 1988: 99): CMNH 14710, M2 fragment from UCMP V69190; CMNH 14371, M1 fragment from UCMP loc. 69190; CMNH 14172, c1 from UCMP loc. V69190; CMNH 14713, m1 from UCMP loc. V69190; CMNH 15844, mandible fragment with p3, broken p2, and root of p1, from UCMP loc. V69190–69192; CMNH 15845, M1 fragment from UCMP loc. V69190–69192; CMNH 15846, m1 from UCMP loc. V69190–69192; KUVP 20350, m2 fragment from UCMP loc. V69190–69192; KUVP 20358, m1 fragment, from UCMP loc. V69190–69192; MCZ 7317, maxillary fragment with P3–M2 and isolated P4, from UCMP loc. V69191; UCMP 21589, m2 from UCMP loc. V69191; UCMP 30084, m3 from UCMP loc. V77145; UCMP 121919, P4 fragment from UCMP loc. V69190; UCMP 121920, mandible fragment with m1 from UCMP loc. V69190; UCMP 121921, m1 from UCMP loc. V69191; and UWBM 62576, left ramus with p3-m2.

Martin Canyon Local Fauna (early Hemingfordian), Logan County, Colorado: KUVP 9970, partial left and right basicranium, left maxillary with P3–M1 and M2 alveolus, left ramus fragment with m1–m2 and m3 alveolus, and right ramus fragment with m2–m3 (Galbreath, 1956: fig. 1).

Lemhi Valley, 40 mi south of Salmon, in talus about 15 ft below white zone, Geertson Formation (early Hemingfordian), Lemhi County, Idaho: F:AM 63270B, right ramal fragment with broken m1 and isolated M2.

Hidalgo Bluff, Oakville Formation (early Hemingfordian), Washington County, Texas: TMM-BEG 40067-180 (AMNH cast 99659), left isolated M1.

Sheep Creek Formation (late Hemingfordian), Sioux County, Nebraska: AMNH 20502, right partial ramus with m1–m2 (fig. 23E, F), holotype of *Cynarctus mustelinus* Matthew (1932: 2), Stonehouse Draw; AMNH 20503, right partial ramus with p2 alveolus, p3–p4, m1 alveolus, and m2–m3, paratype of *Cynarctus mustelinus* Matthew (1932: 2), Stonehouse Draw; AMNH 22399, right ramus with c1–p2 alveoli and p3–m3, Ashbrook Pasture near Sinclair Draw; AMNH 22399A, right partial edentulous ramus, Ashbrook Pasture near Sinclair Draw; AMNH 96677, partial left ramus with p4 and m1–m3 alveoli, Agate area; F:AM 49110, left partial ramus with c1–p1 alveoli and p2–m2 (m1 broken), Greenside Quarry; F:AM 49111, right partial ramus with p2–p3, p4 broken, and m1–m3 alveolus, Thomson Quarry; F:AM 49112, right partial ramus with p2–m3, Long Quarry (fig. 23J, K); and F:AM 49114, right partial ramus with p1 alveolus–m1 (p2, p4, and m2 all broken), Ravine Quarry.

Olcott Formation (early Barstovian), Sioux County, Nebraska: F:AM 49105, left ramus with i1–i3 broken alveoli and c1 broken–m3, *Synthetoceras* Quarry; F:AM 49126, right ramus with c1 alveolus–m3, Boulder Quarry (fig. 23L, M); F:AM 49127, left partial ramus with p1 alveolus–m2, Humbug Quarry; F:AM 49128, left ramus with c1–m3, Humbug Quarry; F:AM 49129,

left partial ramus with c1, p1–p4 alveoli, broken m1, m2, and m3 alveolus, Humbug Quarry; F:AM 49130, right ramus fragment with p1 alveolus, p2, and p3 alveolus–p4, Humbug Quarry; F:AM 49131, left partial ramus with m1–m2 and m3 alveolus, Humbug Quarry; F:AM 49136, right and left partial rami with c1–m1 and m2 broken, floor of Mill Quarry; F:AM 49137, left partial ramus with unerupted p2–p4, m1–m2 alveolus, and m3 unerupted, floor of Mill Quarry; F:AM 49138, right partial ramus with p4–m2 and m3 alveolus, Mill Quarry; and F:AM 49139, left ramus fragment p4 and m1 broken, Mill Quarry.

Observation Quarry, Sand Canyon Formation (early Barstovian), Dawes County, Nebraska: F:AM 25383, left isolated M1; F:AM 25384, left isolated M1; and F:AM 49120, right maxillary fragment with P4 broken.

Standing Rock Quarry, lower part of the Piedra Parada Member of the Zia Formation (late Arikareean), Sandoval County, New Mexico: F:AM 49203, crushed skull with I1–I3 all broken, C1, P1 alveolus–M2, and mandible with i3, c1 broken, and p1–m3 (p2 broken).

Blick Quarry, near the middle of the Chamisa Mesa Member of the Zia Formation (early Hemingfordian), Arroyo Pueblo drainage, Sandoval County, New Mexico: F:AM 49200, left ramus fragment with broken m1; F:AM 49202, left and right partial rami with i3 broken–m3 (p4–m1 both broken); F:AM 49211, left P4; F:AM 49212, partial mandible with c1–m3; F:AM 49234, left ramus fragment with m1 and isolated right m1; F:AM 49235, partial mandible with c1–m3, southwest corner of hill containing Blick Quarry, low; F:AM 49236, left partial ramus with c1–p1 alveoli and p2–m1 (p3 and m1 broken); F:AM 49237, right partial ramus with i1–c1 and p1 broken–m1 (p3 and m1 broken); F:AM 49242, left partial ramus with p3 root–m3; and F:AM 50161, right ramus fragment with m2 broken.

Cynarctoides Quarry, near the middle of the Chamisa Mesa Member of the Zia Formation and the same level as Blick Quarry (early Hemingfordian), Arroyo Pueblo drainage, Sandoval County, New Mexico: F:AM 49204, right and left ramus fragment with p2 and m2–m3 both broken; F:AM 49238, right and left partial rami with c1 broken–m2; F:AM 50160, left partial ramus with p4–m2 all broken; F:AM 63140, anterior part of skull with I1–I3 alveoli and C1–M2 and both partial rami with c1–m2 and m3 alveolus (fig. 23A–C); F:AM 63141, right partial ramus with p4–m1 both broken and m2; F:AM 63142, right and left partial maxillae with P4–M2; F:AM 63143, right isolated M1; F:AM 63150, anterior fragment of skull with I1–P1 alveoli and P2–M2; F:AM 63151, right partial ramus with c1–m2 (m1–m2 both broken) and m2 alveolus; F:AM 63152, right partial ramus with c1 broken, p1 alveolus, and p2–m3 (p4–m1 both broken); F:AM 63153A, two ramus fragment with p1–p3, p4, and m1 broken; F:AM 63153B, ramus fragment with broken c1 and broken base of teeth; and F:AM 63153C, ramus fragment and detached teeth including c1, p3, and broken p4.

South of Santa Cruz River, 50 ft below the Nambe White Ash Stratum, Nambe Member, Tesuque Formation (late Hemingfordian), Santa Fe County, New Mexico: F:AM 63144, right and left partial rami with c1 broken, p1–p3 alveoli, p4 broken, m1, and m2 broken.

Tesuque Grant, Skull Ridge Member of Tesuque Formation (early Barstovian), Santa Fe County, New Mexico: F:AM 49201, left ramal fragment with m1 broken and alveoli of m2–m3; and F:AM 63138, right partial ramus with c1 root, p1–p2 alveoli, p3 broken–m2, and m3 broken alveolus.

Barstow Formation (early Barstovian), San Bernardino County, California: F:AM 27497, left maxillary fragment with P4–M1, Yermo Quarry, 5 mi east of Yermo; and F:AM 27539, left partial maxillary with P4–M2, Sandstone Quarry, ''Second Division.''

DISTRIBUTION: Medial or late Arikareean of South Dakota; late Arikareean of Nebraska, Wyoming, and New Mexico; early Hemingfordian of Nebraska, Colorado, Idaho, Texas, and New Mexico; late Hemingfordian of Nebraska, Wyoming, and New Mexico; and early Barstovian of Nebraska, New Mexico, and California.

EMENDED DIAGNOSIS: Besides the larger size, derived characters that distinguish *Cynarctoides acridens* from *C. gawnae* are M1

hypocone surrounded by a narrow cingulum, M2 larger and more complex with a larger paraconule, broader p4, a metastylid on m1, and a stronger protostylid on m1. This species, however, lacks the extreme specializations in *C. emryi* such as the stylar cusps on the labial border of M1; M2 and m2 nearly equal in size to M1 and m1; robust p4 with laterally shifted posterior accessory cusp; selenodont-like lower molars with lingually directed crista obliqua; and talonid cusps nearly equal in height to those of the trigonids.

DESCRIPTION AND COMPARISON: Despite the large number of referred specimens listed above, the overall skull morphology of this species remains poorly known. Besides the basicranial fragments described by Galbreath (1956), a dorsoventrally flattened skull from the Zia Formation in New Mexico (F:AM 49203) supplies additional cranial morphology. As demonstrated by Galbreath (1956), the middle ear region of *C. acridens* is essentially that of a primitive canid. It has a moderately inflated bulla and a ventrally directed paroccipital process that is fully fused with the bulla. The ectotympanic extends dorsally to form a full tympanic ring. The mastoid process is not enlarged and there is no suprameatal fossa. The skull roof has paired temporal crests except for a small segment near the nuchal crest. The masseteric scar on the zygomatic arch is wide, making up two-fifth of its depth.

With the large sample of lower jaws available, a better appreciation of variation is possible. Although most of the horizontal rami remain slender (a derived character acquired since *C. luskensis*), some individuals of *C. acridens* show a stronger ramus, such as developed in *C. emryi*. These individuals also tend to broaden their p4 slightly, but not quite to the degree of robustness of the p4 in *C. emryi*.

The dentition of *Cynarctoides acridens* is highly derived. The M1 hypocone not only becomes higher but also is surrounded lingually by a narrow cingulum. The anterior end of the lingual cingulum is also enlarged, but not quite to the stage of an isolated cusp as in *C. emryi*. The m1 protostylid is enlarged at the expense of the protoconid. The protostylid is a distinct cusp fully detached from the base of the protoconid, in contrast to being more closely appressed to the protoconid in *C. gawnae* and *C. luskensis*. A small metastylid is present on m1–m2 for the first time, and tends to be better developed in specimens from New Mexico than in those from the Great Plains. Cusps on m2 are higher-crowned and more conical than in *C. luskensis* and *C. gawnae*.

DISCUSSION: Despite the nearly identical size and shape of the holotypes of *Cynarctoides acridens* and *C. mustelinus*, Matthew (1932: 3) considered his *Cynarctus mustelinus* to differ generically from the former, which he thought to be nearer to ''*Nothocyon*'' *lemur* from John Day. Galbreath (1956) and Munthe (1988), on the other hand, failed to see any distinction even at the species level. As pointed out by Munthe (1988: 103), Matthew apparently allowed stratigraphic relationships to be a major factor in his taxonomic determination. At the time, *C. acridens* was known only from the Upper Harrison beds, whereas Matthew's two specimens of *C. mustelinus* (AMNH 20502 and 20503) were from the Sheep Creek Formation. In light of the present records, it is clear that *C. acridens* had a nearly continuous range from the medial Arikareean through early Barstovian of the Great Plains and the southwestern United States. Furthermore, despite the multiple species of *Cynarctoides* newly described here, *C. acridens* remains the most persistent among all species of the genus both in terms of geologic range and geographic distribution. In fact, *C. acridens* coexisted with all advanced species of *Cynarctoides* (*C. luskensis* and above) in one area or at one time, and it was always more abundant and outlasted all other species when they did co-occur (fig. 141). It thus seems no coincidence that *C. acridens* was the first to be discovered and that it remained the only valid species recognized of the genus until this study.

Cynarctoides emryi, new species

Figure 24G–K

Cynarctoides acridens (Barbour and Cook, 1914): McGrew, 1938a: 328, fig. 88 (in part).

HOLOTYPE: UNSM 25455 (F:AM cast 96711), right partial ramus with p3 broken alveolus–m3 (m1 broken) (fig. 24G, H), from

Hemingford Quarry 7B (UNSM loc. Bx-7B), Runningwater Formation (early Hemingfordian), Box Butte County, Nebraska.

ETYMOLOGY: Named for Dr. Robert J. Emry of the National Museum of Natural History, the Smithsonian Institution, in recognition of his important fieldwork in Nebraska.

REFERRED SPECIMENS: From the type locality, Hemingford Quarry 7B (UNSM loc. Bx-7B), Runningwater Formation (early Hemingfordian), Box Butte County, Nebraska: UNSM 25456, right partial ramus with c1 broken, p1–p2 alveoli, p3, and p4 root–m3 (fig. 24I, J); UNSM 25615 (F:AM cast 96710), left partial maxillary with M1–M2 (fig. 24K); and UNSM 25722, right partial ramus with c1–m1 all broken.

Woods Canyon, Runningwater Formation (early Hemingfordian), Dawes County, Nebraska: F:AM 25432, right partial ramus with c1 broken, p1 alveolus, p2 broken–m1, and m2 alveolus; and F:AM 49106, right and left partial rami with p2–m1.

Stamen Ranch, Runningwater Formation (early Hemingfordian), Sioux County, Nebraska: F:AM 99362, right partial ramus with p4–m3.

Upper Harrison Beds (late Arikareean), Sioux County, Nebraska: FMNH P25548, right maxillary fragment with P4 alveolus and M1–M2 (McGrew, 1938a: fig. 88), from near Agate.

DISTRIBUTION: Late Arikareean to early Hemingfordian of Nebraska.

DIAGNOSIS: Derived characters that distinguish this species from *Cynarctoides acridens* and other more primitive species of the genus are: M1 with anterolabial stylar cusps and M2 with minute anterolabial stylar cusp; lack of connecting crest between paracone and metacone of M1–M2 (i.e., complete transverse division by a valley); p4 posterior accessory cusp laterally displaced; selenodont m1–m2; m1 trigonid shorter, protostylid larger relative to protoconid, entoconid extremely tall, much taller than hypoconid and about equal to height of metaconid; further enlargement of m2 to almost the same size as m1; m2 protostylid larger and entoconid extremely tall, much taller than hypoconid and approximating height of metaconid; and m3 large with strong labial cingulum and protostylid.

DESCRIPTION AND COMPARISON: Teeth of *Cynarctoides emryi* reveal an animal with highly unique dental morphology. In almost every aspect of the dentition, *C. emryi* shows the extreme modifications of the *Cynarctoides* clade. The most obvious is the development of the almost selenodont-like upper and lower molars. Other species of *Cynarctoides* have upper molars whose cusps remained conical. In *C. emryi*, however, the paracone and metacone have developed an anterior and a posterior crista extending labially to form stylar cusps. The lingual cingulum in front of the hypocone has further differentiated into two additional cusps, one immediately lingual to the protocone (this cusp was probably independently acquired in certain population of *C. acridens*, e.g., F:AM 49109, fig. 23D) and one slightly more anterior and labial. Such enlargements of the cingular cusps contributed to the reduction of the protocone.

The M2 and m2 in *C. emryi* are almost identical in size and morphology to the M1 and m1 (fig. 24G, I, K), an obvious trend toward increasing the grinding surfaces that began in *C. acridens*. The m1–m2 also become relatively short and broad, and their talonid cusps have nearly the same height as the trigonid cusps. In correlation with the further enlarged protostylids in the m1–m2, the posterior accessory cusp of the p4 is also enlarged and laterally shifted to resemble a protostylid of the lower molars.

DISCUSSION: *Cynarctoides emryi* from the late Arikareean and early Hemingfordian of Nebraska coexists with *C. acridens*. It is interesting to note, however, that the more primitive *C. acridens* outlasted *C. emryi* and survived well into the early Barstovian. The former also had a much wider distribution (New Mexico and California, in addition to the states in the northern Great Plains).

As the phylogenetically terminal member of the *Cynarctoides* clade, *C. emryi* is the most hypocarnivorous of all species. In fact, the dental morphology of this small carnivoran has in many ways gone beyond the normal repertoire of a hypocarnivorous carnivoran and shows adaptations to insectivory or herbivory in its rather selenodont lower mo-

lars. Such a specialization is extremely rare among carnivorans, and is known only in lophocyonine viverrids in the Miocene of Europe (Fejfar and Schmidt-Kittler, 1984, 1987; Koufos et al., 1994).

Phlaocyon Matthew, 1899

Bassariscops Peterson, 1924.
Aletocyon Romer and Sutton, 1927.

TYPE SPECIES: *Phlaocyon leucosteus* Matthew, 1899.

INCLUDED SPECIES: *P. minor* (Matthew, 1907); *P. latidens* (Cope, 1881b); *P. annectens* (Peterson, 1907); *P. achoros* (Frailey, 1979); *P. multicuspus* (Romer and Sutton, 1927); *P. marslandensis* McGrew, 1941; *P. leucosteus* Matthew, 1899; *P. yatkolai*, new species; and *P. mariae*, new species.

DISTRIBUTION: Early Arikareean of Oregon and Wyoming; medial Arikareean of South Dakota and Florida; late Arikareean of South Dakota, Nebraska, Wyoming, Colorado, Florida and Texas; early Hemingfordian of Nebraska and Colorado; and late Hemingfordian of Nebraska.

EMENDED DIAGNOSIS: Synapomorphies that unite *Phlaocyon* are robust premolars, widened P4, quadrate (elongated) upper molars relative to P4, and wide m1 talonid. In cranial proportions, all *Phlaocyon* tend to have a deep jugal, a wide rostrum, and a wide zygomatic arch.

DISCUSSION: Because *Phlaocyon* and *Procyon* share convergent adaptations toward hypocarnivorous dentitions, earlier discussions on the phylogenetic relationships of *Phlaocyon* (mainly *P. leucosteus*) are mostly in the context of the evolution of procyonids. *Phlaocyon* was considered an intermediate form between the living raccoon (*Procyon*) and primitive canids (Wortman and Matthew, 1899; McGrew, 1938a, 1939, 1941). In her landmark study of the basicrania of fossil North American carnivorans, Hough (1948) first demonstrated the essentially canid middle ear region in *P. leucosteus*, a conclusion independently reached by Dahr (1949). Consistent with this conclusion, our present reference to *Phlaocyon* of several species, previously regarded as unrelated, fills much of the large gap between *P. leucosteus* and more primitive borophagines (such as *Archaeocyon*). Our descriptions of three new species below further demonstrate a hypocarnivorous clade that is considerably more diverse than previously thought, and our cladistic concept of *Phlaocyon* encompasses a morphological spectrum far beyond the traditional boundary of the genus (e.g., Peterson, 1928; Stevens, 1977: 34–35).

Phlaocyon minor (Matthew, 1907)
Figures 25, 26H–N

Cynodesmus minor Matthew, 1907: 189. Macdonald, 1963: 212.
Tephrocyon sp. Wood and Wood, 1937: 139, fig. 1 (13).
Tomarctus minor White, 1941b: 95.
Nothocyon minor Cook and Macdonald, 1962: 561. Macdonald, 1970: 57.

HOLOTYPE: AMNH 12877, right partial maxillary with P4–M2, left partial ramus with c1–p1 alveoli, p2–m1 (fig. 25C–F), and limb fragments, from 4 m. E. of Porcupine P.O. . . . E. of Porc[upine] Cr'k . . . upper Rosebud, AMNH ''Rosebud'' 22, Rosebud Formation (late Arikareean), Shannon County, South Dakota (Macdonald, 1963: 156).

REFERRED SPECIMENS: From the Wounded Knee-Rosebud fauna (late Arikareean), Shannon County, South Dakota: AMNH 12878, left partial ramus with p3 alveolus and p4–m3, from AMNH ''Rosebud'' 5, east of Porcupine Butte, upper Rosebud beds (''Rosebud Formation'' of Macdonald [1963: 154]); and AMNH 13800, right and left rami with i1–m3, 2 mi west of American Horse Creek, Upper Rosebud Beds.

Little Muddy Creek, lower Arikaree Group (early Arikareean), Niobrara County, Wyoming: F:AM 49054 (fig. 25A, B), left partial ramus with p3 broken–m1 and m2 broken.

Turtle Butte Formation (medial Arikareean), Tripp County, South Dakota: SDSM 8540 (AMNH cast 98586), left partial ramus with p4–m2 and alveoli of p3 and m3.

Syndyoceras Hill, 0.5 mi west of Agate, Harrison Formation (late Arikareean), Sioux County, Nebraska: AMNH 81033 (HC 489), left ramus fragment with c1 broken–p1, p2–p4 alveoli, and m1 from first hill south in *Syndyoceras* layer.

Upper Harrison beds (late Arikareean),

south of Lusk, Wyoming: F:AM 27578, right and left partial rami with p1 alveolus–m2, Sand Gulch, Goshen County; F:AM 49073, right partial ramus with c1 broken, p1–p2 alveoli, and p4–m1, Royal Valley, Niobrara County; F:AM 49081, left partial ramus with p4 broken–m2 and m3 alveolus (fig. 25G, H), Silver Springs, Niobrara County; and F:AM 50223, right partial ramus with p3–m2, Jay Em Section, high, Goshen County.

Upper Harrison beds (late Arikareean), Van Tassel area, Niobrara County, Wyoming: F:AM 49004, skull with I3–M2 (P3 broken, fig. 26H–K), partial mandible with c1 broken–m3 (fig. 26L, M) and left humerus (fig. 26N) articulated with proximal end of ulna and radius, right distal end humerus, isolated vertebrae, and limb fragments, 1.5 mi southwest of Van Tassel, low.

Upper Harrison beds (late Arikareean), Guernsey area, Platte County, Wyoming: F:AM 50218, skull fragment with P4–M2 and partial mandible with c1–m3 (fig. 25I–K) from 3 mi southeast of Guernsey, 7 ft below the green-white layer.

Cedar Run Local Fauna, Cedar Creek, Oakville Formation (late Arikareean), Washington County, Texas: AMNH 30087, isolated right broken M1 (Wood and Wood, 1937: fig. 1 [13]).

DISTRIBUTION: Early Arikareean of Wyoming; medial to late Arikareean of South Dakota; late Arikareean of Nebraska, Wyoming, and Texas.

EMENDED DIAGNOSIS: As the most basal species of *Phlaocyon*, *P. minor* possesses all the synapomorphies (mostly in their initial stage of development) of the genus that can be used to distinguish it from primitive borophagines such as *Archaeocyon*, *Rhizocyon*, and *Cynarctoides*: robust and shortened premolars, quadrate M1, and widened m1 talonid. Additionally, *P. minor* has two autapomorphies, double temporal crests, and an elongated m2 relative to that of m1. On the other hand, *P. minor* lacks derived features in *P. latidens* and more derived species: widened P4 with a distinct lingual cingulum or hypocone, a cleft on lingual cingulum of M1 isolating the hypocone, and more distinct protostylid on m1.

DESCRIPTION AND COMPARISON: The present reference of F:AM 49004, a nearly complete skull and mandible, furnishes morphologies previously unknown in *P. minor*. Although imperfectly preserved, especially in its fragmentary teeth, F:AM 49004 shows a cranium very close to that of *P. latidens*. The most prominent feature of the skull is the inflated braincase (braincase width in fig. 27). Such an expansion of the braincase seems to cause the temporal crests (very weak) to remain separate anterior to the inion. Other cranial proportions that suggest membership in the *Phlaocyon* clade include a deep jugal, a broad palate, and a wide zygomatic arch (see fig. 27). The temporal fossa is short (length M2 to bulla in fig. 27), which appears to be a feature in F:AM 49004 alone among *Phlaocyon* species. The paroccipital process is rodlike, ventrally oriented, and has almost no free tip (i.e., it is completely fused with the bulla). The mastoid process is not inflated. Both bullae are crushed inward, creating an appearance of much smaller bullae than is indicated by the position of their attachment to the surrounding bones. The anterior zygomatic arch still has a rather wide masseteric scar.

At the base of the *Phlaocyon* clade, *P. minor* shares only the initial development of the diagnostic features of the genus, and some of these dental characters are also variable. For example, the robustness of premolars, the widening of m1 talonid, and the enlarged m2 are only variably present in the known sample of *P. minor*. In contrast to the usually well-developed protostylids on m1 of *P. latidens*, this cusp occurs in *P. minor* only rarely (4 of 13 individuals) and is usually poorly developed or shows a rudimentary impression only when present. Such a stage of development of the protostylid is here postulated to be equivalent to that in *Cynarctoides lemur* (see further discussion under that species), although a larger sample is certainly desirable to improve statistical inference.

DISCUSSION: Cook and Macdonald (1962) commented on the close resemblance of *P. minor* to *P. latidens*, and this was their reason for including *minor* in *Nothocyon*. An editorial error in Macdonald (1963) left *minor* in *Cynodesmus*, but this was later corrected (Macdonald, 1970). White (1941b) noted the confusion about *Cynodesmus* created by Matthew's (1907) reference of *C. mi-*

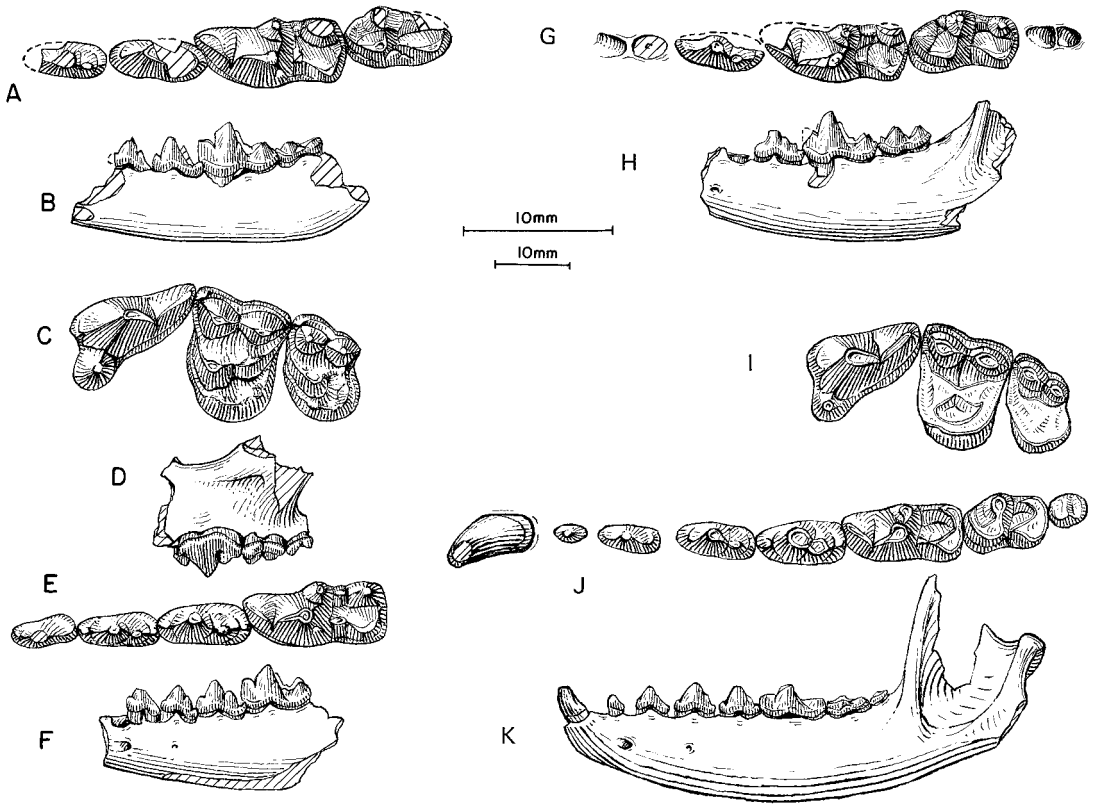

Fig. 25. *Phlaocyon minor*. **A**, Lower teeth and **B**, ramus, F:AM 49054, Little Muddy Creek, lower Arikaree Group (early Arikareean), Niobrara County, Wyoming. **C**, Upper teeth, **D**, lateral view of maxillary (reversed from right side), **E**, lower teeth, and **F**, ramus, AMNH 12877, holotype, Rosebud Formation (late Arikareean), Shannon County, South Dakota. **G**, Lower teeth and **H**, ramus, F:AM 49081, Upper Harrison beds (late Arikareean), Silver Springs, Niobrara County, Wyoming. **I**, Upper teeth, **J**, lower teeth, and **K**, ramus (M1–M2 and p1 reversed from right side), F:AM 50218, Upper Harrison beds (late Arikareean), Guernsey area, Platte County, Wyoming. The longer (upper) scale is for A, C, E, G, I, and J, and the shorter (lower) scale is for the rest.

nor and *C. thomsoni* to this genus. However, White's paper was overlooked by most subsequent authors, and the confusion continued until quite recently. *Cynodesmus* is now recognized as belonging to the Hesperocyoninae (Wang, 1994: 61–62).

Phlaocyon latidens (Cope, 1881b)

Figure 26A–G

Galecynus latidens Cope, 1881b: 181. Cope, 1884: 915, pl. 70, figs. 4, 5.
Cynodictis latidens (Cope): Scott, 1898: 400.
Nothocyon latidens (Cope): Matthew, 1899: 62; 1932: 3. Wortman and Matthew, 1899: 127–130. Merriam, 1906: 15, pl. 2, figs. 6, 7. Peterson, 1907: 53. Thorpe, 1922a: 164. Hall and Martin, 1930: 283. Munthe, 1998: 138.
''*Cormocyon*'' *latidens* (Cope): Fremd and Wang, 1995: 74.

HOLOTYPE: AMNH 6896, crushed partial skull with P3 alveolus, P4–M2, and left ramus with p1–p2 alveoli, p3–m2, and m3 alveolus (fig. 26A–E) from the John Day Basin, John Day Formation (?early Arikareean), Grant or Wheeler counties, Oregon.

REFERRED SPECIMENS: John Day Formation (early Arikareean), Grant or Wheeler counties, Oregon (biostratigraphic positions of some JODA specimens in the Turtle Cove Member are placed within a letter system by

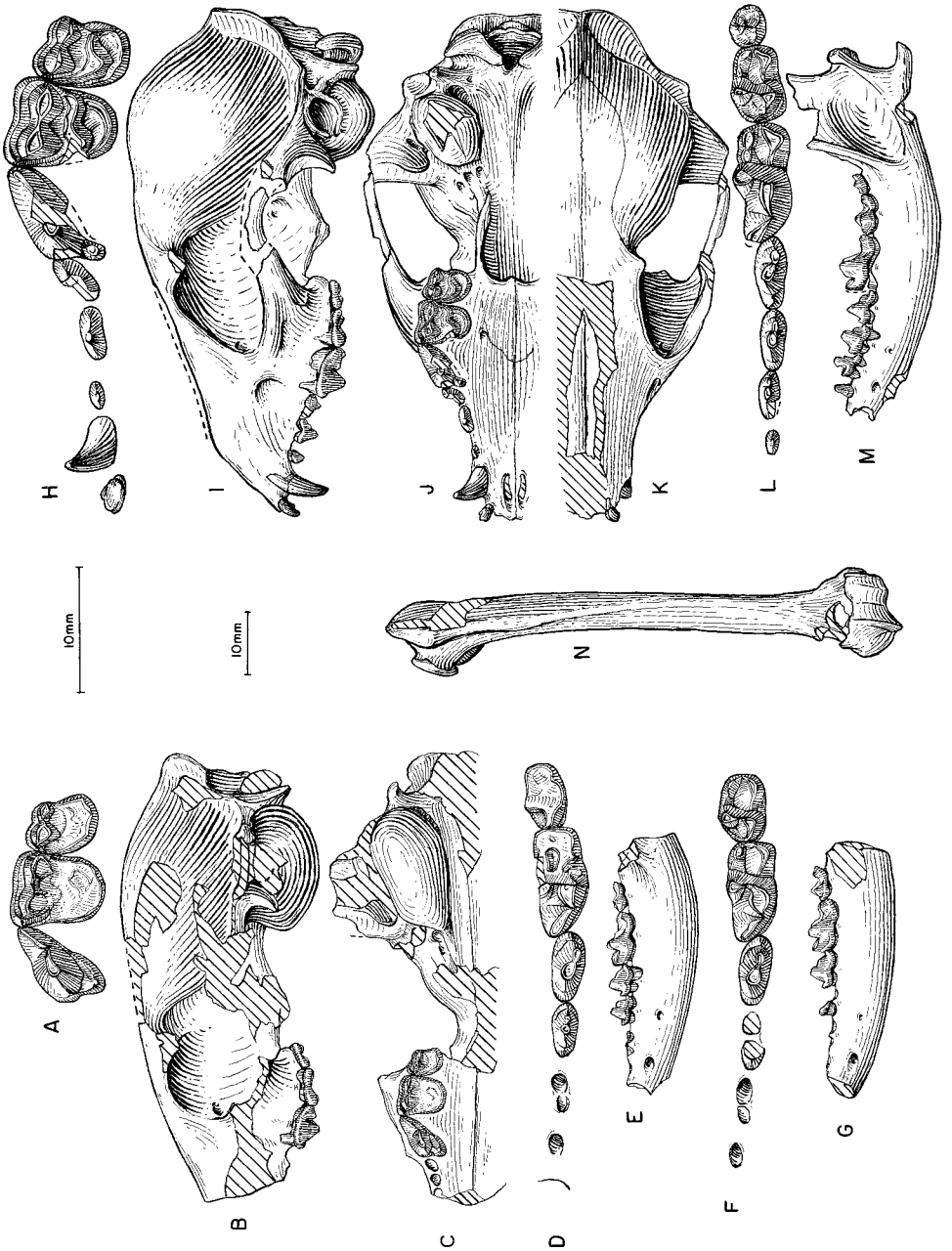

Fig. 26. **A**, Upper teeth, **B**, lateral view and **C**, ventral view of skull, **D**, lower teeth, **E**, ramus, *Phlaocyon latidens*, AMNH 6896, holotype, John Day Basin, John Day Formation (?early Arikareean), Oregon. **F**, Lower teeth and **G**, ramus (reversed from right side), *P. latidens*, AMNH 6897, John Day Basin. **H**, Upper teeth, **I**, lateral, **J**, ventral, and **K**, dorsal views of skull, **L**, lower teeth, **M**, ramus, and **N**, humerus, *Phlaocyon minor*, F:AM 49004 (zygomatic arch, P1, P2, P4, M1, and entire lower jaw reversed from right side), Upper Harrison beds (late Arikareean), Van Tassel area, Niobrara County, Wyoming. The longer (upper) scale is for A, D, F, H, and L, and the shorter (lower) scale is for the rest.

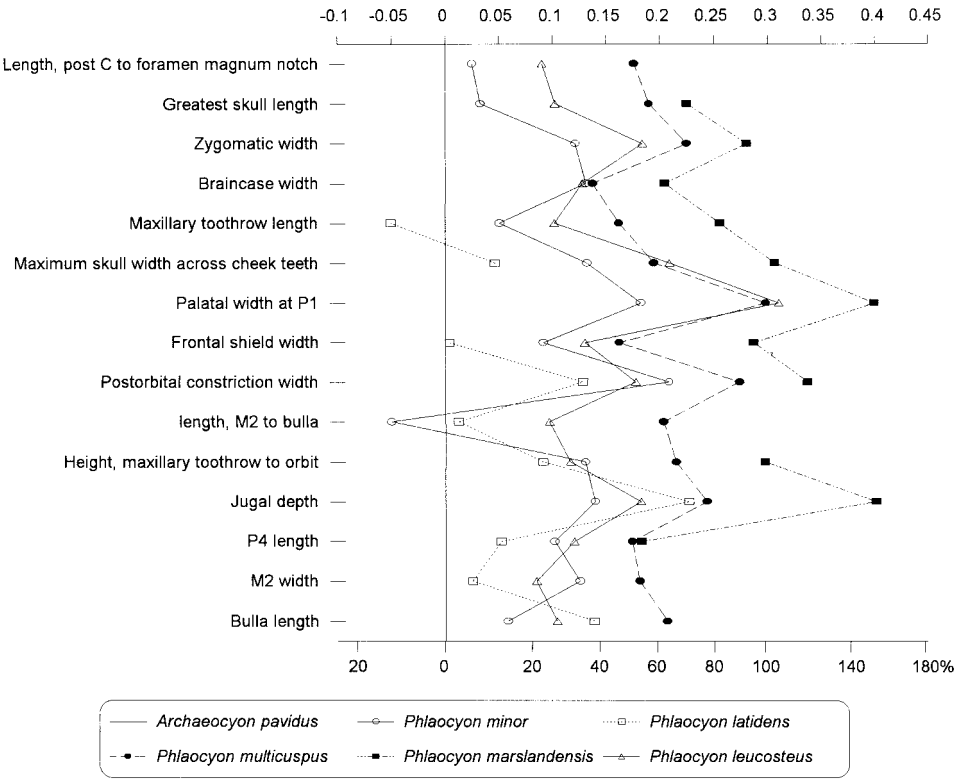

Fig. 27. Log-ratio diagram for cranial measurements of five species of *Phlaocyon* using *Archaeocyon pavidus* as a standard for comparison (straight line at zero). See text for explanations and appendix II for measurements and their definitions.

Fremd and Wang, 1995): AMNH 6836B, left ramus fragment with m1; AMNH 6897, right partial ramus with c1–p2 alveoli and p3 broken–m2 (fig. 26F, G); AMNH 6907, left ramus fragment with p4–m1; JODA 351, skull and mandible fragments with left C1, P3–M2, left c1–p1, and right c1 and p2–p4, unit F; JODA 363, right ramus fragment with p4–m1, unit E; JODA 711, right maxillary fragment with M1–M2; JODA 1251, broken left M1, unit E3; JODA 2753, left P4–M2, right p3–p4, unit E2; JODA 2809, left ramus fragment with m1–m2; JODA 2975 (AMNH cast 129657), right maxillary fragment with P4–M1, unit E2; JODA 3266, left ramus fragment with m1, unit E1; JODA 3384, left ramus fragment with p4–m2, unit E; JODA 3522, left M1, unit E1; JODA TF10921, right P4, unit A; JODA TF4924, right ramus fragment with m1, unit B; JODA TF4931, left ramus fragment with m1, unit D; UCMP 4094, right ramal fragment with p4–m1, UCMP loc. V76102; UCMP 760, right maxillary with P4–M2, and left and right rami with p1–m3 (p4 missing), UCMP loc. V76102; UCMP 10256, partial left ramus with p4–m1, Logan Butte loc. 898, Crook County; UCMP 76296, left ramus fragment with m1–m2, V-4849, Sheep Rock loc. 2; YPM 12699, skull fragment with P3 root and P4–M2; YPM 12794, right and left partial rami with p2, p3 broken–m1, and m2 alveolus; YPM 12795, right partial ramus with p4–m2; and YPM 12797, left ramal fragment with p4–m1.

DISTRIBUTION: Early Arikareean of Oregon.

EMENDED DIAGNOSIS: *P. latidens* possesses derived features distinct from *P. minor*: presence of a transverse cleft on the M1 lingual cingulum to delineate a conate hypocone, strong postprotoconal P4 lingual shelf, and more consistent presence of protostylid on

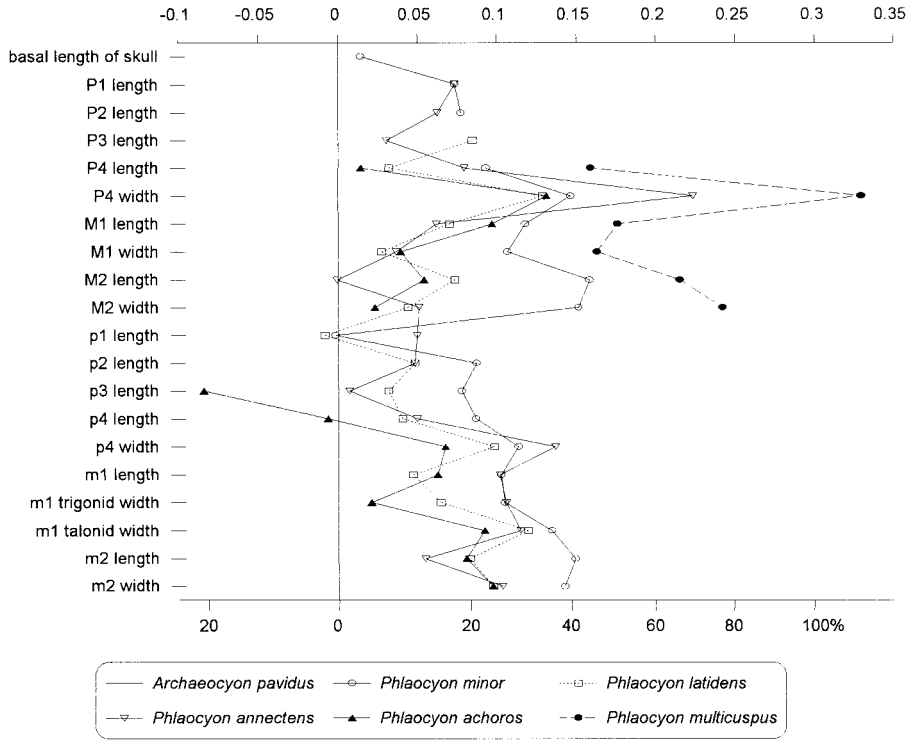

Fig. 28. Log-ratio diagram for dental measurements of five species of primitive *Phlaocyon* using *Archaeocyon pavidus* as a standard for comparison (straight line at zero). See text for explanations and appendix III for summary statistics of measurements and their definitions.

m1. Two autapomorphic characters that further distinguish *P. latidens* from *P. minor* and advanced *Phlaocyon* are an inflated tympanic bulla with a weak external auditory meatus lip and an enlarged m2. On the other hand, *P. latidens* still has a longer snout (as inferred from associated ramus), well-developed premolar cusplets, and crestlike talonid cusps on m1, in contrast to the shortened snout, simplified premolars, and conical talonid cusps in *P. annectens* and more derived species of *Phlaocyon*.

DESCRIPTION AND COMPARISON: The crushed holotype skull is still the main source of information about the cranial morphology of this species. Besides an enlarged bulla, ventrally oriented paroccipital process, and single temporal crest, little else can be learned about the general cranial morphology of AMNH 6896 because of the crushing and loss of the snout.

Dentally, *P. latidens* shows several derived characters of the *Phlaocyon* clade, although most of them are still somewhat weak at this stage of development. The lingual cingulum of P4 is in an early stage of widening, especially toward the anterior end, in most specimens. The outlines of the upper molars are rather quadrate. There is a transverse cleft on the lingual cingulum of most of the M1s that helps to define an isolated hypocone, a feature not present in *P. minor*. The lower premolars show tendencies toward the robustness typical of the *Phlaocyon* clade, but still retain small cusplets on p2–p3. The frequency of occurrence of a protostylid on m1 (10 of 12 individuals; from AMNH, UCMP, and YPM collections only) is higher than in *P. minor* (4 of 13), and this cusp is also more distinct in *P. latidens*. Similar to *P. minor*, *P. latidens* also has an elongated m2, a shared derived feature not seen in other species of *Phlaocyon*.

DISCUSSION: For more than a century after their initial description by Cope (1879b, 1881b), *Cynarctoides lemur* and *Phlaocyon*

latidens have been considered as a pair of closely related species (mostly under the genus *Nothocyon*), co-occurring in the Turtle Cove Member of the John Day Formation. Indeed, their similar sizes and numerous shared primitive characters make differentiation of fragmentary dental materials difficult. In light of the phylogeny presented here, we recognize a number of derived features in *latidens* that individually may seem homoplastic or too weakly developed, but collectively point rather strongly to membership within the *Phlaocyon* clade.

Phlaocyon annectens (Peterson, 1907)

Figure 29

Nothocyon (*Galecynus*) *annectens* Peterson, 1907: 53, figs. 14, 15. Cook, 1909: 268.
Phlaocyon willistoni Peterson, 1924: 300, fig. 1. Untermann and Untermann, 1954: 186.
Bassariscops willistoni (Peterson): Peterson, 1928: 96, fig. 6 (in part). Frailey, 1979: 134. Munthe, 1998: 134.
Nothocyon annectens (Peterson): Hough, 1948: 106. Galbreath, 1956: 375.
?*Nothocyon* cf. *N. lemur* (Cope, 1879b): Stevens et al., 1969: 21, fig. 7A–C.
?*Nothocyon* cf. *N. annectens* (Peterson): Stevens, 1977: 30, fig. 9.
‘‘*Nothocyon*’’ *annectens* (Peterson): Munthe, 1998: 134.

HOLOTYPE: CMNH 1602 (AMNH cast 89668), left and right partial maxillae with I1 broken–M2 and right and left partial rami with c1 broken–m3 (fig. 29F–I) from Carnegie Quarry 3, southeast of Carnegie Hill, Upper Harrison beds (late Arikareean), Sioux County, Nebraska.

REFERRED SPECIMENS: Upper Harrison beds (late Arikareean), Sioux County, Nebraska: AMNH 81030, left partial ramus with m1, 2 mi north of Agate Spring Quarry; and F:AM 49006, palate with I1–M1 and M2 broken and partial mandible with c1 and p1 alveolus–m3 (fig. 29C–E), 3 mi east and 2 mi south of Van Tassel.

Browns Park Formation (?medial or late Arikareean; exact stratigraphic position in relation to the better dated local faunas in Honey and Izett, 1988 is not clear), 1.5 mi southwest of Sunbeam, Moffat County, Colorado: CMNH 11332 (AMNH cast 89665) (holotype of *Phlaocyon willistoni* Peterson, 1924: fig. 1), partial palate with I2–C1 broken, P1 root, P2 broken alveolus, and P3–M2 (M1 broken) (fig. 29A, B); and CMNH 11333 (AMNH cast 89667), right partial ramus with c1–m2 (all teeth broken or represented by alveoli).

Castolon Local Fauna, lower part of Delaho Formation (late Arikareean), Big Bend National Park, Brewster County, Texas: TMM 40635-66, right ramal fragment with p3 and m1 (Stevens et al., 1969: fig. 7A–C); TMM 40693-23, ramal fragment with m1; TMM 40849-10, right and left partial maxillary with P3–M2 (Stevens, 1977: fig. 9); TMM 40879-2, ramal fragment with m1; and TMM 40918-35, ramal fragment with alveoli for premolars.

DISTRIBUTION: Late Arikareean of Nebraska and Texas, and medial or late Arikareean of Colorado.

EMENDED DIAGNOSIS: *Phlaocyon annectens* is derived with respect to *P. latidens* and *P. minor* in its short snout; simplified, robust premolars; shorter P4 with enlarged protocone and an incipient hypocone or wide lingual shelf; and more conical talonid cusps of m1. *P. annectens* is primitive relative to more derived species of *Phlaocyon* in its unenlarged I3, incipient hypocone on P4, smaller P4 protocone, lack of a fully isolated hypocone on M1 lingual cingulum, lack of a cristid connection between entoconid and hypoconid of m1, and extremely weak protostylids on m1–m2.

DESCRIPTION AND COMPARISON: Beginning in *P. annectens*, the accessory and cingular cusplets on the premolars are reduced or lost in front or behind the main cusp, except on the p4; the P4 protocone is slightly enlarged; the P4 lingual cingulum is more widened or even begins to form a small hypocone as seen in CMNH 11332 (holotype of *Phlaocyon willistoni*); and the entoconid and hypoconid of m1 become more conical in contrast to the more crestlike cusps in *P. latidens* and *P. minor*. Other than the above derived characters, *P. annectens* remains primitive in all other aspects.

DISCUSSION: The overall size and shape of the holotype of *P. willistoni* is quite close to specimens of *P. annectens* from Nebraska. The Browns Park specimen, however, has a slightly more derived P4 with a larger,

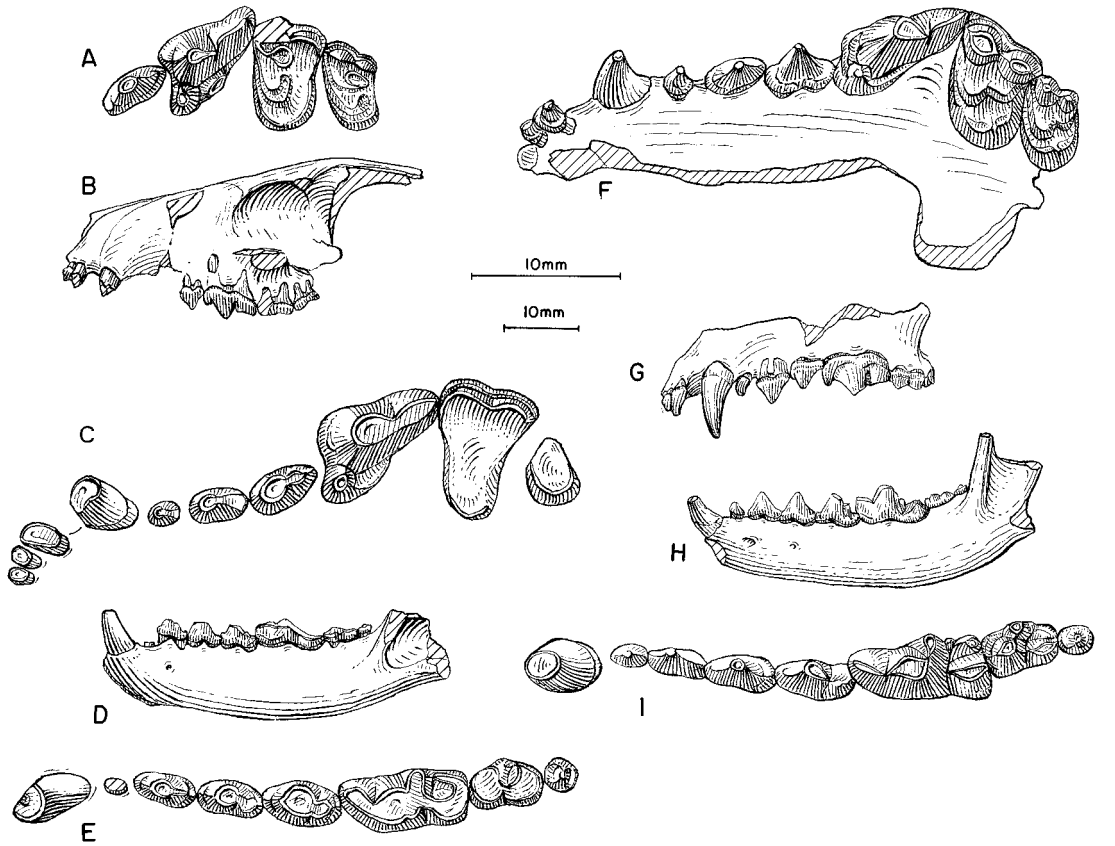

Fig. 29. *Phlaocyon annectens*. **A**, Upper teeth and **B**, lateral view of partial skull (reversed from right side), CMNH 11332 (holotype of *Phlaocyon willistoni*), Browns Park Formation (?medial or late Arikareean), 1.5 mi southwest of Sunbeam, Moffat County, Colorado. **C**, Upper teeth, **D**, ramus, and **E**, lower teeth, F:AM 49006, Upper Harrison beds (late Arikareean), 3 mi east and 2 mi south of Van Tassel, Sioux County, Nebraska. **F**, Upper teeth and **G**, lateral view of maxillary, **H**, ramus, and **I**, lower teeth, *P. annectens*, CMNH 1602, holotype, Carnegie Quarry 3, southeast of Carnegie Hill, Upper Harrison beds (late Arikareean), Sioux County, Nebraska. The longer (upper) scale is for A, C, E, F, and I, and the shorter (lower) scale is for the rest.

more distinct protocone, and a small hypocone. These features are within a normal range of species variation and represent intermediate stages in a trend toward more advanced taxa (e.g., *P. leucosteus* and *P. marslandensis*).

We follow Peterson (1924) in referring a second specimen from Brown's Park (CMNH 11333, an essentially edentulous ramus with a partial p3) to *Phlaocyon willistoni* (= *P. annectens*), based mainly on its size and robustness of the p3. If such a reference is correct, CMNH 11333 indicates a very shallow ramus in the type series. A third, smaller specimen, CMNH 11334 (a partial ramus with m1–m2), was also described by Peterson, who acknowledged that it ''undoubtedly represents an additional species'' and called it ''?*Phlaocyon*'' (Peterson, 1924: 302–303, fig. 2). However, he was subsequently convinced that CMNH 11334 should belong to *P. willistoni* after all (Peterson, 1928: 98). We share with Peterson's earlier hesitation and place CMNH 11334 in *Cynarctoides roii* because of its primitive lower molar morphology that shows none of the signs of robustness characteristic of *Phlaocyon*.

The present reference of the materials from Castolon Local Fauna, Texas, is based

on the figures and descriptions by Stevens et al. (1969) and Stevens (1977). Although we follow Stevens (1977) in tentatively placing the Texas specimens in *P. annectens*, we note here that the Texas materials suggest a taxon of somewhat smaller size. For example, the lower carnassial in TMM 40635-66 is 8.2 mm long (Stevens et al., 1969: 21) as opposed to 9.7 mm for the holotype of *P. annectens*. That Stevens and her colleagues earlier (Stevens et al., 1969) equated the Castolon specimens with ''*Nothocyon*'' *lemur* is further evidence of the size problem. However, qualitatively, the Texas specimens have a widened P4 lingual cingulum and simplified premolars, derived characters that suggest the stage of development in *P. annectens*.

Phlaocyon achoros (Frailey, 1979)

Figure 30A–F

Bassariscops achoros Frailey, 1979 (in part): 134, figs. 3A, C–E, 4A, B, D. Munthe, 1998: 134.
Cynarctoides sp. Frailey, 1979: 140, fig. 5A.

HOLOTYPE: UF 18389 (AMNH cast 105035), left P4 (fig. 30A), Buda Local Fauna (medial Arikareean), Alachua County, Florida (Frailey, 1979: figs. 3A, 4A, B).

REFERRED SPECIMENS: From type locality: UF 171365, left p4 (fig. 30D); UF 171366, left p4 (Frailey, 1979: fig. 3C); UF 171367, right p3; UF 16963, right M2 (fig. 30C); UF 171361, right M2; UF 171362, right M2; UF 16964, right m2; UF 16989 (AMNH cast 105036), isolated left m1 (Frailey, 1979: fig. 3D); UF 16991, right ramus with p2–m1 alveoli, m2 (fig. 30F), and m3 alveolus (Frailey, 1979: figs. 3E, 4D); UF 18390, talonid of left m1; UF 18415 (AMNH cast 105033), left isolated m1 (fig. 30E) (referred to *Cynarctoides* sp. by Frailey, 1979: fig. 5A); UF 18501, right maxillary fragment with M1 (fig. 30B); and UF 22778, right P4.

DISTRIBUTION: Medial Arikareean of Florida.

EMENDED DIAGNOSIS: *P. achoros* is more derived than *P. annectens* in its enlarged P4 protocone and initial development of a small hypocone on P4. *P. achoros* shares with its sister-species *P. multicuspus* several derived features: a distinct cingulum-like parastyle on P4, a well-developed paraconule and metaconule on M1–M2, and a metaconule split into two cusps. Besides its much smaller size, *P. achoros* is distinguishable from *P. multicuspus* in its lack of a conical hypocone on M2.

DESCRIPTION AND COMPARISON: Although individual teeth in Frailey's (1979: fig. 3) composite figure are within the approximate size ranges of each other, we identify two taxa in his hypodigm of *Bassariscops achoros*. One is represented by teeth with consistent hypocarnivorous features, such as extra cusps on upper molars, which we associate with the holotype. The other has more mesocarnivorous dentition, which we refer to *Cynarctoides lemur*. Under this new association, we redescribe *P. achoros* below.

In dental proportions, *P. achoros* is not much different from *P. annectens* (fig. 28). As noted by Frailey (1979), the P4 in the holotype of *P. achoros* is quite similar to that in *P. willistoni* (here synonymized with *P. annectens*). *P. achoros*, however, has a more elevated parastyle, which is even more developed in *P. multicuspus*. The M1–M2 are the most distinct with their cuspidate crown patterns. The paraconule is enlarged to form a distinct cusp. The metaconule is also enlarged and split into two smaller cusps. The P4–M2 thus assembled (fig. 30A–C) are far more consistent with the morphological pattern in *P. multicuspus*. The only major dental difference between *P. achoros* and *P. multicuspus* is the former's lack of a distinct hypocone on M2.

Allocation of the lower teeth is more difficult, partly due to the lack of comparable materials in *P. multicuspus* (known from a single skull). The lower premolars are referred to *P. achoros* with more confidence because of the ready differentiation of two morphotypes. Those referred to *P. achoros* have typically advanced *Phlaocyon* features of shorter, broader, and higher-crowned main cusps and more reduced posterior accessory cusps (fig. 30D), as contrasted to those referred to *Cynarctoides lemur*. Reference of the lower molars, however, is less certain. We chose UF 18415 and UF 16991 as representatives of the m1 and m2, respectively. Their enlarged talonids relative to trigonids and well-developed talonid cusps (especially en-

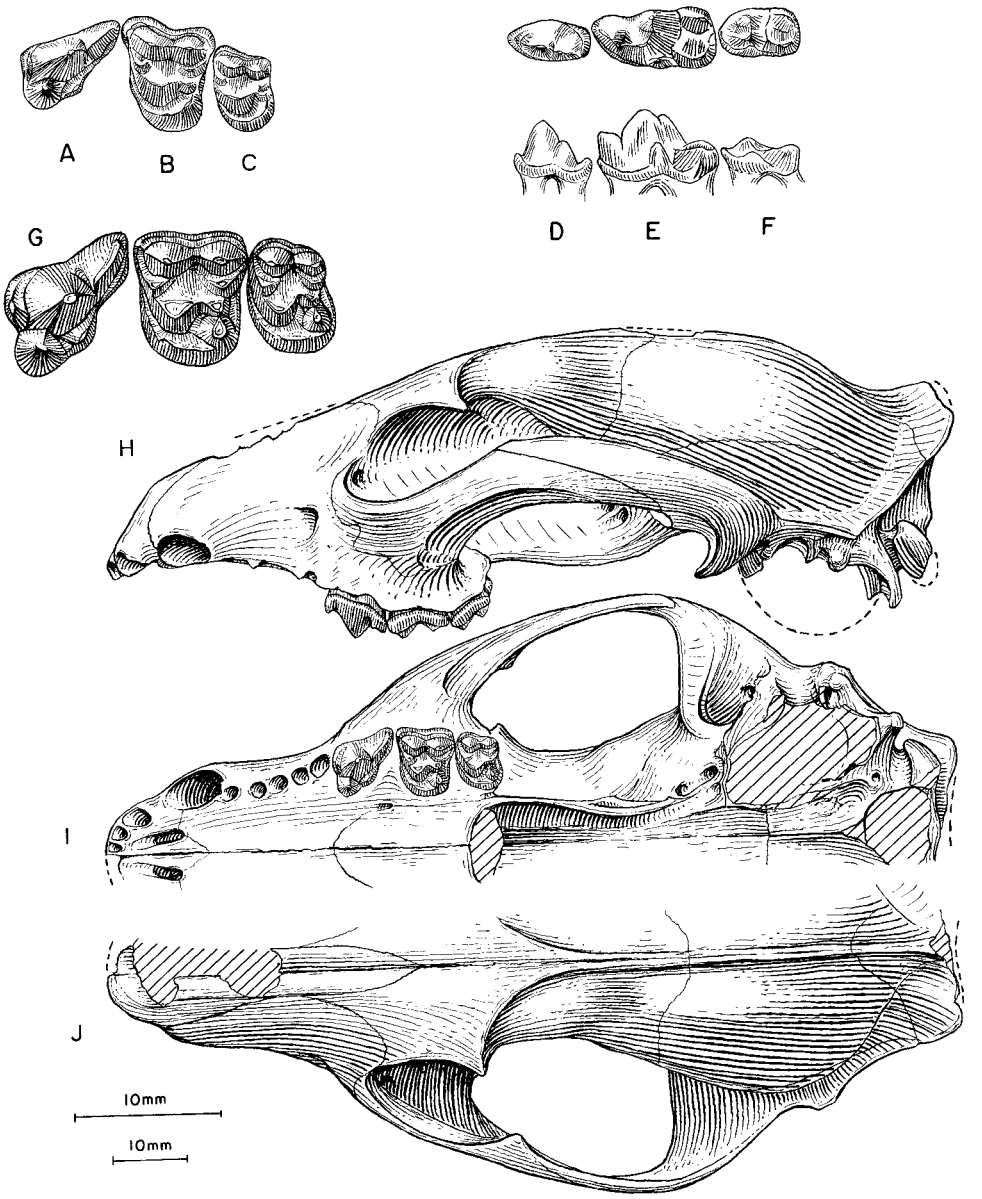

Fig. 30. **A–F**, *Phlaocyon achoros*, composite illustration of upper and lower teeth; **A**, P4, UF 18389, holotype; **B**, M1, UF 18501; **C**, M2, UF 16963; **D**, p4, UF 171365; **E**, m1, UF 18415; and **F**, m2, UF 16991 (M1, M2, and m2 reversed from right side), Buda Local Fauna (late Arikareean), Alachua County, Florida. **G**, Upper teeth, and **H**, lateral, **I**, ventral and **J**, dorsal views of skull, *Phlaocyon multicuspus*, FMNH UC1482, holotype, 3 mi southeast of Rawhide Buttes, ?Upper Harrison beds (late Arikareean), Goshen County, Wyoming. The longer (upper) scale is for A–G, and the shorter (lower) scale is for the rest. Illustrations for *P. achoros* by X. Wang.

toconid) and protostylids are commonly found in advanced *Phlaocyon*.

DISCUSSION: Reanalysis of the Buda materials, some of which were not included in Frailey's (1979) original descriptions, reveals at least three taxa among the small canids: *Cynarctoides lemur, Phlaocyon achoros*, and *Cormocyon* cf. *C. copei* (represented by a single M2). If our new hypodigm of *P. achoros* is correctly assembled, it becomes rather apparent that this Florida species, although still poorly known, is closely related to another rare taxon, *Aletocyon multicuspus* Romer and Sutton, 1927.

Small borophagines from the Buda Local Fauna seem to rather closely resemble those from the John Day Formation of Oregon, although it should be cautioned that the references to *Cynarctoides* and *Cormocyon* are based on very incomplete materials. This connection to the northwest is further suggested by a specimen from the Turtle Cove Member of John Day Formation, JODA 3051, a left maxillary fragment with P4–M2 (presently referred to *Cynarctoides lemur*). Incipient developments of features on JODA 3051 seem to suggest possible relationship to *P. achoros*: a raised P4 parastyle and incipient development of an extra cusp between metaconule and metacone on M1. While it may be tempting to trace the origin of the *achoros–multicuspus* clade to Oregon, we treat this specimen as a variation of *C. lemur* until additional material becomes available.

Phlaocyon multicuspus (Romer and Sutton, 1927)

Figure 30G–J

Aletocyon multicuspus Romer and Sutton, 1927: 460, figs. 1, 2. McGrew, 1938a: 331, fig. 91; 1941: 33. Hough, 1948: 104, fig. 11.

Aletocyon multicuspidens (Romer and Sutton): Dahr, 1949: 2.

Aletocyon multicuspis (Romer and Sutton): Munthe, 1998: 134.

HOLOTYPE: FMNH UC1482 (AMNH cast 108069), partial skull with incisor alveoli, C1, P1–P3 alveoli, and P4–M2 (fig. 30G–J) from 3 mi southeast of Rawhide Buttes, ''Lower Harrison,'' but more likely Upper Harrison beds (late Arikareean), Goshen County, Wyoming.

DISTRIBUTION: Late Arikareean of Wyoming.

EMENDED DIAGNOSIS: In addition to its much larger size, derived characters that distinguish *Phlaocyon multicuspus* from *P. annectens* and more primitive species include a further enlarged protocone and hypocone of P4. *P. multicuspus* shares with its sister-species *P. achoros* several derived characters: presence of a parastyle on P4, a paraconule on M1, a more distinct M1 metaconule, and a extra cusp between the metaconule and metacone of M1. *P. multicuspus* is unique among all species of *Phlaocyon* in its longer skull (a reversal) and a conate hypocone on M2. In addition, *P. multicuspus* lacks derived characters that are present in *P. leucosteus* and *P. marslandensis*: narrowed masseteric scar and enlarged I3. On the other hand, *P. multicuspus* is easily distinguished from *P. yatkolai* and *P. mariae* in its much smaller size and less massive premolars.

DESCRIPTION AND COMPARISON: *Phlaocyon multicuspus* is unique within the *Phlaocyon* clade in its mixture of a primitive-looking skull and a highly derived dentition. The proportional relationships of the skull of *P. multicuspus* are quite *Phlaocyon*-like, with a deep zygomatic arch of jugal, broad anterior palate, and narrow braincase (fig. 27). The posterior premaxillary process is widely separated from the frontal, as opposed to the near meeting of these two bones in *P. leucosteus*. Other primitive features include a wide masseteric scar on the lateral face of the zygomatic arch and a rodlike paroccipital process, in contrast to a much narrowed and ventrally facing masseteric scar and a platelike paroccipital process in *P. leucosteus*. Also notable is a slightly domed forehead in *P. multicuspus*, indicating a small frontal sinus beneath the frontal bone.

Dental morphology of *P. multicuspus*, on the other hand, is very hypocarnivorous. In some ways, its teeth are the most advanced among species of the genus. This is mostly related to the cuspidate nature of its cheekteeth. There are extra cusps that are not normally seen in other species of *Phlaocyon*: a small, but distinct parastyle on P4, a paraconule on M1–M2, a more distinct metaconule on M1–M2, an additional cusp between metaconule and metacone of M1–M2, and a

conical hypocone on M2. These derived features are also shared by *P. achoros*, indicating a sister-group relationship. Additionally, the M2 in *P. multicuspus* is enlarged to nearly the same size as the M1, in contrast to smaller M2s in other species of *Phlaocyon*.

DISCUSSION: McGrew (1941: 35) noted that ''The similarity in general skull structure and basic tooth pattern between *Phlaocyon* and *Aletocyon* leaves no doubt that the two are closely related,'' a conclusion also reached by Dahr (1949). Nonetheless, McGrew agreed with Romer and Sutton (1927) that *Aletocyon* should be a distinct genus from *Phlaocyon*, apparently based on the perceived morphological distances. Although we do not recognize such distances as a criterion for taxonomy, the genus *Aletocyon* could be used to represent a small clade of its own consisting of *achoros* and *multicuspus*. Such a practice, however, would require the creation of additional generic names for pectinated species near the base of *Phlaocyon*, an option we chose not to use.

Phlaocyon marslandensis McGrew, 1941

Figure 31C–I

Phlaocyon marslandensis McGrew, 1941: 33, figs. 12, 13. Dahr, 1949: 4. Frailey, 1978: 9.

HOLOTYPE: FMNH P26314 (AMNH cast 95585), left partial maxillary and premaxillary with I3–C1, P1–P3 alveoli, and P4–M1 (fig. 31G–I) from near Dunlap, Runningwater Formation (''Upper Marsland beds'' of McGrew, 1941) (early Hemingfordian), Dawes County, Nebraska.

REFERRED SPECIMENS: Runningwater Formation (early Hemingfordian), Box Butte County, Nebraska: F:AM 99370 (fig. 31C–F), right fragment of skull with P1–M2, right partial ramus with i1 broken–m3 (p1 alveolus), right distal part of humerus, first phalanx, and fragments, below Dry Creek Prospect B; UNSM 25607, right partial maxillary with P4–M1, UNSM loc. Bx-7; UNSM 25641, right ramus with c1 broken, p1 alveolus, p2, p3–m1 alveoli, m2, and m3 alveolus, UNSM loc. Bx-27; UNSM 25659, left partial maxillary with P4–M1, M2 alveolus, UNSM loc. Bx-28; UNSM 26153 (AMNH cast 95577), partial palate with I1–I3 alveoli, C1, P1 alveolus, P2–M1, and M2 alveolus, UNSM loc. Bx-7.

Runningwater Formation (early Hemingfordian), Sheridan County, Nebraska: Clinton Highway Locality, UNSM loc. Sh-101B: UNSM 5010-70, left ramus with c1 broken, p1–p2 alveoli, and p3–m3.

DISTRIBUTION: Early Hemingfordian of Nebraska.

EMENDED DIAGNOSIS: *Phlaocyon marslandensis* shares several derived characters with its sister-species *P. leucosteus* but differs from *P. multicuspus*, *P. annectens*, and more primitive species of the genus in having a relatively shorter rostrum such that the premolars are imbricated, a large I3, a lateral groove on the lower canine, tall crowned premolars, narrow and mostly ventrally oriented masseteric scar on the jugal, a cristid between the entoconid and hypoconid of m1, and a protostylid on m2. The premolar characteristics and the m2 protostylid can also be used to distinguish *P. marslandensis* from the *yatkolai–mariae* group. In addition to its larger size, *P. marslandensis* is distinguished from its sister-species *P. leucosteus* in its larger P4 protocone and less prominent protostylids on m1–m2.

DESCRIPTION AND COMPARISON: The partial skull of UNSM 26153 has much of the skull roof preserved, supplying cranial morphologies unknown in the holotype. In general, it has a heavier construction with deeper jugal, broader palate, broader snout, and stronger sagittal crest than that in *P. leucosteus* (fig. 27). The posterior premaxillary process does not meet the frontal. There is a modest inflation of the frontal area, indicating the presence of a frontal sinus beneath the frontal bone. The masseteric scar on the zygomatic arch is less than one-fourth of the total depth, being much more reduced than in *P. multicuspus*. Although the I3s in UNSM 26153 are missing, their alveoli clearly suggest an enlarged incisor. In F:AM 99370, a distal part of a humerus shows the presence of a small entepicondylar foramen.

DISCUSSION: McGrew (1941) suggested a close relationship between *Phlaocyon leucosteus* and his newly erected *P. marslandensis*, a conclusion consistent with the present phylogeny, even though characters in support of his conclusion (lack of a P4 par-

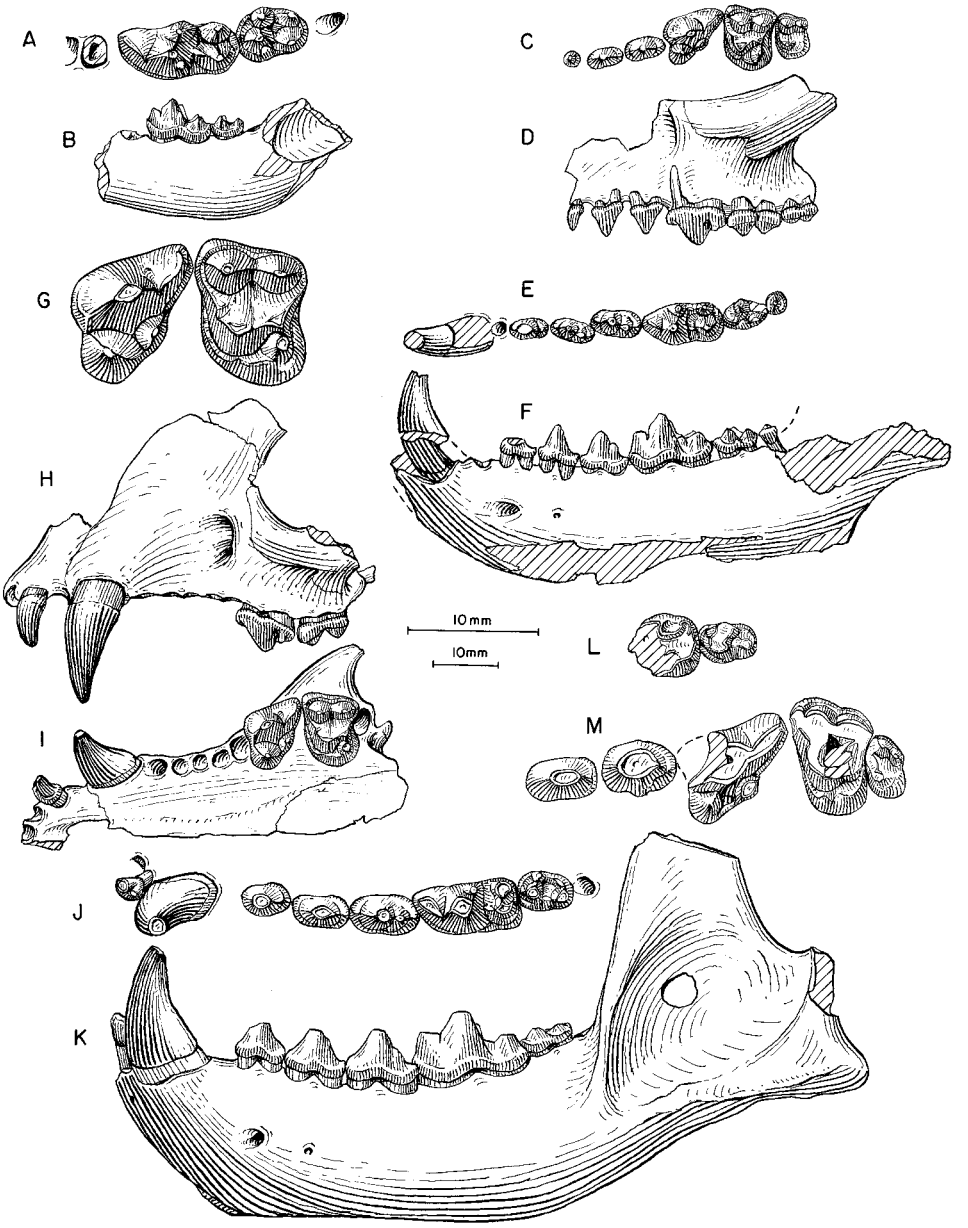

Fig. 31. **A**, Lower teeth and **B**, ramus (reversed from right side), *Phlaocyon leucosteus*, YPM 12801 (holotype of *Nothocyon latidens multicuspis*). **C**, Upper teeth, **D**, lateral view of maxillary, **E**, lower teeth, and **F**, ramus (all reversed from right side), *P. marslandensis*, F:AM 93370, Runningwater Formation (early Hemingfordian), Box Butte County, Nebraska. **G**, P4–M1, and **H**, lateral and **I**, ventral views of partial skull, *P. marslandensis*, FMNH P26314, holotype, from Dunlap, Runningwater Formation (early Hemingfordian), Dawes County, Nebraska. **J**, Lower teeth and **K**, ramus (reversed from right side), *P. yatkolai*, UNSM 62546, holotype, Runningwater Quarry, Runningwater Formation (early Hemingfordian), Box Butte County, Nebraska. **L**, Lower teeth and **M**, upper teeth, *P. mariae*, F:AM 25466, holotype, *Aletomeryx* Quarry, Runningwater Formation (early Hemingfordian), Cherry County, Nebraska. The longer (upper) scale is for A and G, and the shorter (lower) scale is for the rest.

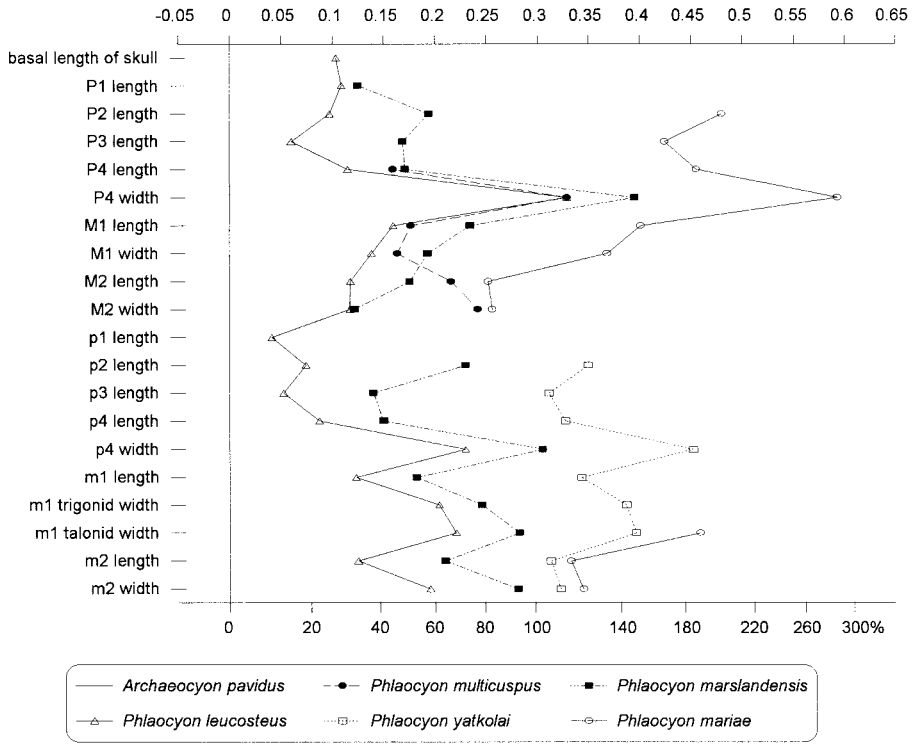

Fig. 32. Log-ratio diagram for dental measurements of five species of advanced *Phlaocyon* using *A. pavidus* as a standard for comparison (straight line at zero for y-axis). See text for explanations and appendix III for summary statistics of measurements and their definitions.

astyle and reduced anterolingual cingulum) turn out to be primitive in our analysis (see Phylogenetic Analysis below). McGrew further speculated that *P. marslandensis* was directly descendant from *P. leucosteus* partly because of a perceived age difference between the two species. Such a relationship, however, is presently contradicted by autapomorphies in *P. leucosteus*; that is, broadened p4 and better developed m2 protostylid.

Phlaocyon leucosteus Matthew, 1899

Figures 31A, B, 33–35

Phlaocyon leucosteus Matthew, 1899: 54. Wortman and Matthew, 1899: 131, pl. 6, fig. 10. McGrew, 1938a: 331; 1941: 33. Hough, 1948: 97. Dahr, 1949: 1. Frailey, 1978: 9. Munthe, 1998: 135.

Nothocyon latidens multicuspis Thorpe, 1922b: 430, fig. 3.

Phlaocyon sp.: Frailey, 1978: 8.

HOLOTYPE: AMNH 8768, skull with I1–M2, mandible with i1–m3, and partial skeleton including scapula, right humerus, both radii, left ulna, right partial ulna, both front feet including carpals, metacarpals I–V and phalanges, both femora, both tibiae, both fibula, both rear feet including tarsals, metatarsals I–V with some phalanges, vertebrae, ribs, etc. (figs. 33, 35) from Martin Canyon, head of Dorby Creek, Martin Canyon beds (sensu Matthew, 1901; late Arikareean), Logan County, Colorado. Found with five partial skeletons of *Merycochoerus proprius magnus* thought to be part of ''White River formation'' and disconformably overlain by the Pawnee Creek beds of the Loup Fork Formation (Matthew, 1901: 401).

REFERRED SPECIMENS: South side of Dry Creek, Upper Harrison beds (late Arikareean), Box Butte County, Nebraska: F:AM 99349, anterior part of skull with C1–P3 alveoli and P4–M2.

Runningwater Formation (early Heming-

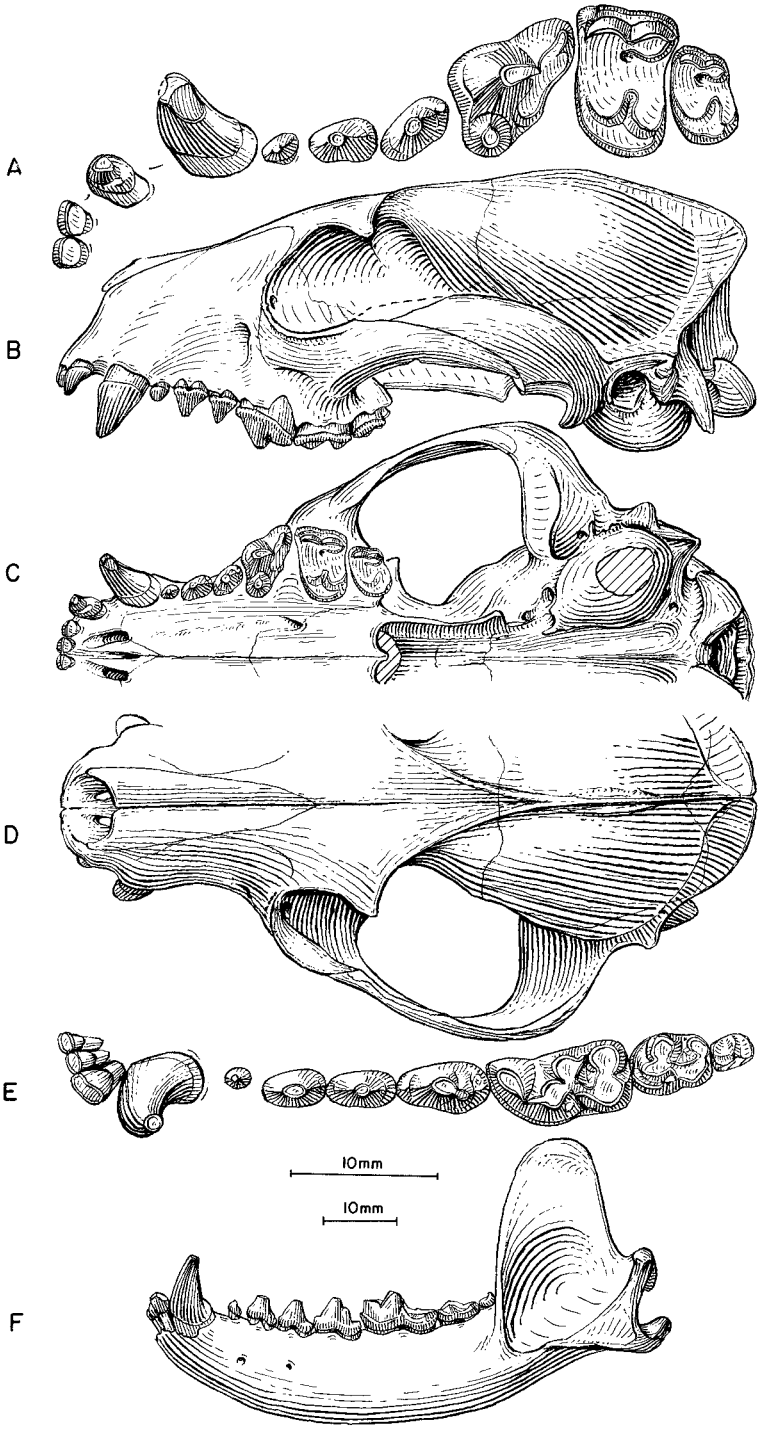

Fig. 33. *Phlaocyon leucosteus*. **A**, Upper teeth (C1 reversed from right side), **B**, lateral, **C**, ventral and **D**, dorsal views of skull, **E**, lower teeth, and **F**, ramus, AMNH 8768, holotype, Martin Canyon beds (early Hemingfordian), Logan County, Colorado. The longer (upper) scale is for A and E, and the shorter (lower) scale is for the rest.

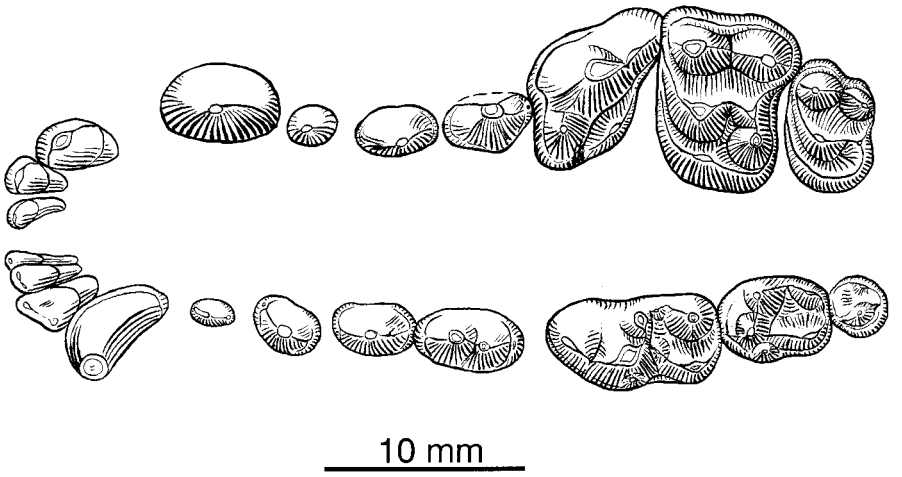

Fig. 34. *Phlaocyon leucosteus*, UNSM 26524, Runningwater Formation (early Hemingfordian), Cherry County, Nebraska. Illustration by X. Wang.

fordian), Cherry and Dawes counties, Nebraska: Antelope Creek: YPM 12801 (AMNH cast 88395), right partial ramus with p4 alveolus–m2 and m3 alveolus (fig. 31A, B) (holotype of *Nothocyon latidens multicuspis* Thorpe, 1922b. *Aletomeryx* Quarry: F:AM 49184, left ramus with i1–i3 alveoli, c1 broken, p1 alveolus, p2 broken–m1, and m2–m3 alveoli. Cottonwood Creek: F:AM 54467, right partial ramus with p4–m1 and m2 alveolus. Cottonwood Creek Quarry: F:AM 99348, right maxillary with P1–M2. UNSM loc. Cr-128: UNSM 26524, crushed skull with I1–M2, left and right rami with i1–m3 (fig. 34), five cervicals, partial left humerus, and other skeletal fragments.

Sand Canyon Region, Runningwater Formation (early Hemingfordian), Dawes County, Nebraska: F:AM 49118, right partial maxillary with P4–M1.

Sand Canyon Quarry, Red Valley Member, Box Butte Formation (late Hemingfordian), Dawes County, Nebraska: F:AM 99347, left ramus with c1–m1 alveoli, m2, and m3 alveolus (possibly reworked from the Runningwater Formation).

SB-1A Local Fauna (?late Arikareean), 1 mi north of Live Oak, Suwannee County, Florida: TRO 392, isolated right P4 (*Phlaocyon* sp. in Frailey, 1978: 8–9, fig. 2A, B).

DISTRIBUTION: Late Arikareean of Nebraska, ?late Arikareean of Florida, early Hemingfordian of Colorado and Nebraska, and late Hemingfordian of Nebraska.

EMENDED DIAGNOSIS: Like its sister-species *Phlaocyon marslandensis*, *P. leucosteus* is derived with respect to *P. multicuspus* and other more primitive species of *Phlaocyon* in a relatively shorter rostrum with imbricated premolars, narrow masseteric scar, a large I3, a lateral groove on c1, tall premolars, and a cristid between entoconid and hypoconid of m1. Some of these characters can also be used to distinguish it from the *yatkolai–mariae* species group: relatively large I3, a lateral groove on c1, narrowed masseteric scar on the zygomatic arch, tall crowned premolars that are imbricated, and presence of a protostylid on m2. Within the *leucosteus–marslandensis* species group, *P. leucosteus* is distinguishable from *P. marslandensis* in its smaller size and slightly better developed m2 protostylid.

DESCRIPTION AND COMPARISON: After nearly 100 years since its initial description, the remarkable holotype of *Phlaocyon leucosteus* is still the best preserved and most complete specimen of all known species of the genus, and is also the only specimen of this species from the type locality. However, the holotype suffers from heavy wear on its teeth, obscuring much of the crown pattern on the molars. We are thus fortunate to have available a nearly complete skull and man-

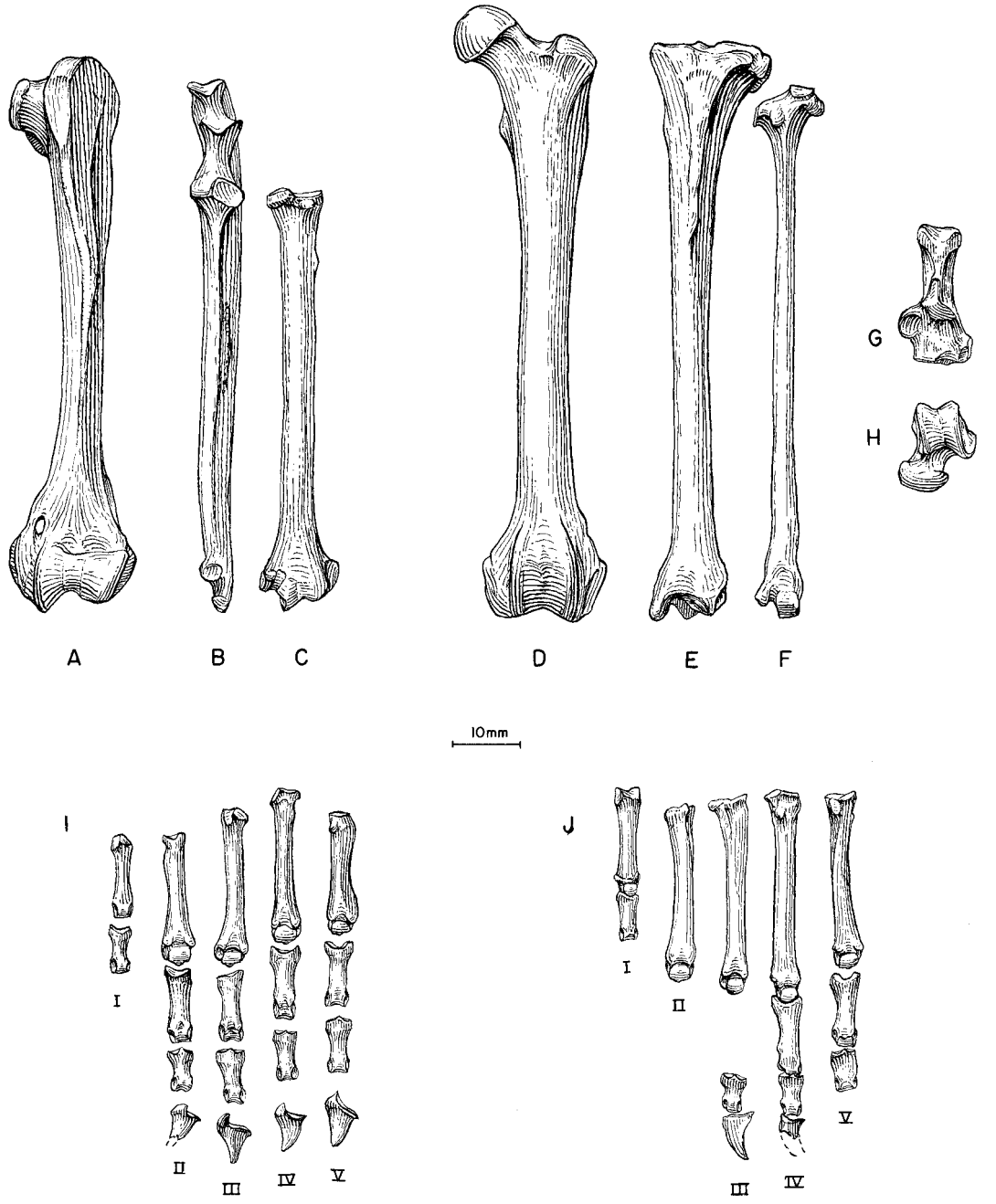

Fig. 35. *Phlaocyon leucosteus*. **A**, Humerus (reversed from right side), **B**, ulna (reversed from right side), **C**, radius, **D**, femur, **E**, tibia, **F**, fibula, **G**, calcaneum, **H**, astragalus, **I**, hand, and **J**, foot, AMNH 8768, holotype, Martin Canyon beds (early Hemingfordian), Logan County, Colorado.

dible of a younger individual from Nebraska with little wear on the teeth (UNSM 26524). With this additional specimen, plus other fragmentary materials, *P. leucosteus* is unquestionably the best known species of *Phlaocyon*.

Cranial morphologies peculiar to *P. leucosteus* (as compared to closely related species such as *P. multicuspus* and *P. marslandensis*) include a strong posterior process of premaxillary that nearly touches the frontal, large postorbital process of frontal, a laterally expanded paroccipital process to form a flat plate around the bulla, and slightly inflated mastoid process. Many of these features are probably related to the brachycephalic development of the skull. On the younger individual (UNSM 26524), however, these features are either less well-developed (premaxillary process and postorbital process) or not preserved (paroccipital process and mastoid process). Another cranial feature of *P. leucosteus* indicating its advanced status (shared with *P. marslandensis*) is a narrowed masseteric scar on the anterior portion of the zygomatic arch.

The angular process of the mandible is highly variable through age. Thus, the young individual (USNM 26524) has a slender process similar to the condition of most primitive borophagines, whereas that in the much older AMNH 8768 consists of an extremely broadened internal ridge forming a large fossa on its dorsal face for the insertion of the medial pterygoid muscle. This latter condition is also in sharp contrast to that of another old individual, F:AM 49184, which has a posteriorly elongated angular process instead of the broadened one in AMNH 8768. In absence of other related cranial or dental differences, such differences in angular process construction are here regarded as variations within the species.

Dentally, *P. leucosteus* has the most hypocarnivorous teeth in the *Phlaocyon* clade. *P. leucosteus* shares with *P. marslandensis* such derived features as an enlarged I3, c1 with a lateral groove, high-crowned premolars, and a protostylid on m2. In contrast to *P. marslandensis*, the hypocone on M1 of *P. leucosteus* is partially connected to the metaconule but is more isolated from the lingual cingulum, due to a distinct cleft on the cingulum. There is, however, no conate hypocone on the M2. A well-developed protostylid is present in m1–m2.

In *P. leucosteus*, the maximum length of the tibia is shorter than that of the femur. This shortened distal segment of the hindlimb is a derived condition relative to that in *Hesperocyon*, *Cormocyon copei*, *Archaeocyon leptodus*, and others. However, we do not know when this happened within the Phlaocyonini clade because of our lack of knowledge of the postcrania of other intermediate species.

DISCUSSION: See discussion under the genus *Phlaocyon* for a brief summary of past controversies on this species and the historical role it played in the debate of the origin of procyonids.

Frailey (1978: 9) commented that a single P4 from the SB-1A Fauna in Florida ''could be within the limits of variation for *P. leucosteus*,'' but refrained from referring the specimen as such because of its somewhat smaller size. In view of the present expanded hypodigm of *P. leucosteus* from the Hemingfordian of western Nebraska, the Florida specimen does fall within its size range and thus is tentatively referred to this species.

Phlaocyon yatkolai, new species

Figure 31J, K

HOLOTYPE: UNSM 62546, right ramus with i1–i2 alveoli, i3–c1, p2–m2, and m3 alveolus (fig. 31J, K) from Runningwater Quarry (UNSM loc. Bx-58), 19 mi east of Agate, base of the Runningwater Formation (early Hemingfordian), Box Butte County, Nebraska.

ETYMOLOGY: Named in honor of the late Daniel Yatkola who collected the type and made a landmark study of the stratigraphy of this area.

DISTRIBUTION: Early Hemingfordian of Nebraska.

DIAGNOSIS: In addition to its larger size, derived characters of this new species relative to the *leucosteus–marslandensis* species pair and other species of *Phlaocyon* are loss of p1, massive premolars, compression of m1 entoconid and hypoconid, and reduction of m1 metaconid. An unreduced m2 (relative to m1), presence of an m3, and lower and less

erect ascending ramus in *P. yatkolai* are the only observable differences (all primitive for *P. yatkolai*) between it and *P. mariae*.

DESCRIPTION AND COMPARISON: Lack of upper teeth in *Phlaocyon yatkolai* severely limits the scope of comparison. Membership of *yatkolai* within the *Phlaocyon* clade is indicated by only two observable characters: simplified and robust premolars and cristid connections between the entoconid and hypoconid of m1. The massiveness of its premolars seems not merely a proportional enlargement relative to its size, and, as shown in fig. 32, the premolars are larger relative to m1. *P. yatkolai* is also distinct from all other species of *Phlaocyon* in its reduced m1 metaconid and loss of p1, features commonly associated with hypercarnivory. The entoconid and hypoconid of m1 are closely compressed together instead of being separated by a deep valley as in all other species of *Phlaocyon*.

DISCUSSION: Despite the lack of comparable parts between the holotypes of *P. yatkolai* and *P. mariae* (mostly upper teeth), the basis of a sister relationship for these two species, as proposed in our phylogeny, is not limited to their massive premolars, which is the only codable character shown in the phylogeny, but also includes their common tendency toward hypercarnivorous dentition. Each, however, expresses this tendency by different parts (upper or lower) of the teeth that do not lend themselves to direct comparison. Our phylogeny predicts more dental synapomorphies when the question marks in the data matrix (table 2) left by the missing teeth are filled. Of the few common teeth that can be compared, those in *P. yatkolai* are more primitive, as indicated by its unreduced m2 and presence of m3.

Phlaocyon mariae, new species

Figure 31L, M

HOLOTYPE: F:AM 25466, upper and lower worn teeth and skull fragments including C1 broken, maxillary fragment with P2 broken–P3, detached broken P4s, maxillary fragment with M1 broken–M2, and left ramus fragment with m1 broken–m2 (fig. 31L, M) from *Aletomeryx* Quarry, near mouth of Antelope Creek, Runningwater Formation (early Hemingfordian), Cherry County, Nebraska.

ETYMOLOGY: Named in honor of S. Marie Skinner in recognition of her long career in assembling and documenting the collections from Nebraska.

DISTRIBUTION: Early Hemingfordian of Nebraska.

DIAGNOSIS: *Phlaocyon mariae* is the most apomorphic taxon with highly derived characters not seen in any other species of *Phlaocyon*: large size, high and erect ascending ramus, P4 elongate relative to length of molars with protocone relatively small, P4 hypocone larger than protocone, M1 transversely elongated, M1 parastyle enlarged, M1 hypocone reduced, M2 and m2 reduced relative to M1 and m1, and loss of m3. In addition, *P. mariae* shares with *P. yatkolai* the development of massive premolars.

DESCRIPTION AND COMPARISON: Besides being the largest *Phlaocyon* species, *P. mariae* is rather unusual in its curious mixture of hypo- and hypercarnivorous characters. On the one hand, it retains several hypocarnivorous characters acquired in more primitive species of *Phlaocyon* such as robust premolars and a P4 hypocone. On the other hand, it has a somewhat hypercarnivorous M1. Thus, the outline of the M1 is more transversely elongated than is usually the case in all species of *Phlaocyon* owing to an enlargement of its parastyle, a narrowing of the angle between labial and anterior borders of M1, and a shortening of its lingual cingulum, which nearly lost its anterior segment. Also, the conical hypocone on M1, a constant in all *Phlaocyon* except in *P. minor*, is almost lost—only a minor swelling is left on the lingual cingulum. Correlated with this hypercarnivorous trend is the reduction of the posterior molars: the upper and lower second molars are extremely small, compared to the larger M2s and m2s in most *Phlaocyon*, and the m3 is lost. In contrast to its anteroposteriorly shortened molars, the P4 is relatively elongated (fig. 32), and its protocone is reduced.

DISCUSSION: Breakage, wear, and poor preservation on the type and only specimen of this species hinder more complete assessment of its phylogenetic relationships. However, it is clear that this is an unusual taxon with a mixture of features as described above. The presence of hypercarnivorous

characters within a predominantly hypocarnivorous clade is puzzling and raises questions about its phylogenetic position. However, based on the limited codable characters, our cladistic analysis consistently places *P. mariae* in the terminal part of the *Phlaocyon* clade, and singles out the presence of massive premolars (more so than the already robust premolars in most *Phlaocyon*) as a derived feature to support a *P. yatkolai–P. mariae* sister relationship.

If our phylogeny is correct, *P. mariae* provides an example of a hypocarnivorous clade evolving to large body size and then reversing toward a more hypercarnivorous diet. *P. mariae* and *P. yatkolai* appear to be the first and earliest borophagine to attempt hypercarnivory.

Borophagini, new tribe

TYPE GENUS: *Borophagus* Cope, 1892.

INCLUDED GENERA: *Cormocyon* Wang and Tedford, 1992; *Desmocyon*, new genus; *Paracynarctus*, new genus; *Cynarctus* Matthew, 1902; *Metatomarctus*, new genus; *Euoplocyon* Matthew, 1924; *Psalidocyon*, new genus; *Microtomarctus*, new genus; *Protomarctus*, new genus; *Tephrocyon* Merriam, 1906; *Tomarctus* Cope, 1873; *Aelurodon* Leidy, 1858; *Paratomarctus*, new genus; *Carpocyon* Webb, 1969b; *Protepicyon*, new genus; *Epicyon* Leidy, 1858; and *Borophagus* Cope, 1892.

DISTRIBUTION: Arikareean through Blancan of North America.

DIAGNOSIS: In contrast to Phlaocyonini and other basal Borophaginae, Borophagini has a derived character of an elongated m1 trigonid. Most members of Borophagini also acquired synapomorphies, such as premaxillary contact with frontal, lack of laterally flared orbital rim of zygomatic arch, elaborate lateral accessory cusps on I3, and a cristid between the hypoconid and entoconid of m1.

DISCUSSION: Members of this clade embody the traditional sense of the subfamily Borophaginae. In contrast to its sister-clade Phlaocyonini, which primarily exploits the hypocarnivorous niches, the Borophagini clade is consisted of mostly meso- to hypercarnivorous taxa that often became progressively larger and terminated in durophagous taxa.

Cormocyon Wang and Tedford, 1992

TYPE SPECIES: *Cormocyon copei* Wang and Tedford, 1992.

INCLUDED SPECIES: *Cormocyon haydeni*, new species; and *Cormocyon copei* Wang and Tedford, 1992.

DISTRIBUTION: Early Arikareean of Oregon, early to late Arikareean of South Dakota, medial to late Arikareean of Wyoming, late Arikareean of Florida, and ?late Arikareean of Colorado.

EMENDED DIAGNOSIS: The paraphyletic *Cormocyon* differs from *Archaeocyon* and *Rhizocyon* in its derived characters, such as ventrally directed paroccipital process, enlarged M1 metaconule, and elongated m1 trigonid. Compared to the phlaocyonines, *Cormocyon* lacks the following hypocarnivorous characters of that clade: m1 protostylid and slender horizontal ramus for *Cynarctoides*, and shortened premolars, short upper carnassial, and widened m1 talonid for *Phlaocyon*. Primitive characters that distinguish *Cormocyon* from *Desmocyon* and more derived taxa are absence of a frontal sinus, lack of an encircling ectotympanic for the auditory meatus, and crestlike talonid cusps on m1.

DISCUSSION: In a short paper, Wang and Tedford (1992) attempted to clarify the concept of *Nothocyon*, which has become a taxonomic wastebasket for many small fossil canids ever since Matthew (1899) informally erected the genus [type species *N. geismarianus* (Cope, 1881b) by subsequent designation]. Much of the past confusion surrounding *Nothocyon* stems from the poorly preserved genoholotype (AMNH 6884, a single m1). A much better preserved specimen (AMNH 6885) was later referred to *geismarianus* by Cope (1883, 1884). Through the reference of YPM 12733 to *N. geismarianus*, we demonstrated that these two AMNH specimens represented quite different caniforms. *N. geismarianus* is a highly derived subparictine ursoid (Baskin and Tedford, 1996), whereas *Cormocyon copei* is a borophagine canid based on AMNH 6885. Wang and Tedford (1992), however, did not attempt to define the precise content of *Cormocyon*, pending results of this study, and it has served in similarly vague capacity as had *Nothocyon* (Wang, 1994; Wang and Tedford,

1996) as a basal borophagine. In the present study, *Cormocyon* is a paraphyletic genus at the base of the tribe Borophagini.

Cormocyon haydeni, new species

Figures 36–38

Nothocyon geismarianus (Cope, 1878): Macdonald, 1963: 209.

HOLOTYPE: F:AM 49448, skull with I1–M2 (fig. 36A–D), both rami with I1–I2 alveoli and i3–m3 (fig. 36E, F), right humerus (fig. 37C) and partial left humerus, radius and ulna (fig. 37A, B), articulated lumbar, sacrum and pelvis, both femora (fig. 37E), left tibia (fig. 37G) and right partial tibia with articulated distal remnant of fibula and astragalus, left astragalus (fig. 37F), left partial pes including tarsals, metatarsals I–IV, and 4 first, 3 second, and 1 third phalanges (fig. 37D), Eagle Nest Butte, 260 ft above the base of the exposed section in rocks equivalent to the Harrison Formation (late Arikareean), Washabaugh County, South Dakota.

ETYMOLOGY: Named for Ferdinand Vanderveer Hayden, pioneer geologist of the Great Plains.

REFERRED SPECIMENS: Wounded Knee area, upper part of Sharps Formation (early Arikareean), 8 mi south of Porcupine, Shannon County, South Dakota: F:AM 49436, left maxillary with P3–M2.

Wounded Knee area, lower part of Rosebud Formation equivalent to the Monroe Creek Formation by Macdonald (1963) (medial Arikareean), Shannon County, South Dakota: AMNH 12872, right ramus with c1, p1–p2 alveoli, and p3–m2 (referred to *Nothocyon geismarianus* by Macdonald, 1963: 209), Porcupine Creek, ''Rosebud 8'' of Macdonald (1963: 154).

West of Spanish Diggings, upper part of the lower Arikaree Group (medial Arikareean), Niobrara County, Wyoming: F:AM 50228, left partial ramus with m1 broken–m2, and m3 alveolus.

Northwest and northeast of Lusk, in rocks referred to the Harrison Formation (late Arikareean), Niobrara County, Wyoming: F:AM 27575, left ramal fragment with m1–m2, north of Keeline; F:AM 49058 (in AMNH permanent exhibition), skull with I1–I3 alveoli and C1–M2 (fig. 38A–C) and right and left partial rami with isolated c1, p1 alveolus–m2, and m3 alveolus (fig. 38D, E), north of Keeline; F:AM 49064, partial skull with I1–M2 (P1 root) (fig. 38F) and partial mandible with i3–m3 (c1 broken) (fig. 38G, H), from North Ridge; F:AM 54138, right partial ramus with p1–p3 alveolus, p4 broken–m1, and m2 alveolus, north of Keeline; and F:AM 105247, partial mandible with c1 broken–p2 and p3–p4 both broken. Ellicott Ranch, Steer Pasture: KUVP 32380, nearly complete skull with I1–P3 all broken and P4–M2.

DISTRIBUTION: Early to late Arikareean of South Dakota, and medial to late Arikareean of Wyoming.

DIAGNOSIS: *Cormocyon haydeni* is distinguished from the Phlaocyonini and more basal Borophaginae in its possession of an elongated m1. In contrast to *C. copei* and more derived forms, on the other hand, *C. haydeni* has a primitively flared dorsal rim of the anterior zygomatic arch. *C. haydeni* also has a relatively short temporal fossa as compared to *C. copei*.

DESCRIPTION AND COMPARISON: *Cormocyon haydeni* is larger than *Archaeocyon leptodus* and *A. falkenbachi*. Other than this size difference, the cranial proportions of *C. haydeni* are very similar to those of *A. leptodus*. *C. haydeni* has a slightly downturned paroccipital process that does not yet fully fuse with the bulla. The bulla is less anteriorly expanded as in *A. leptodus*. The M1–M2 are more quadrate in outline with a more symmetrical distribution of the internal cingulum.

Compared to the John Day *Cormocyon copei*, *C. haydeni* is smaller and has a relatively short temporal fossa. A direct measurement of the length of this fossa is the distance between the posterior margin of the M2 and the glenoid fossa (length of M2 to bulla in fig. 39). In this measurement, individuals of *C. copei* are consistent in having longer temporal fossae than in *C. haydeni*. As shown in the ratio diagram (fig. 40), dental measurements of *C. haydeni* are nearly indistinguishable from those of *C. copei*, except for somewhat smaller size of the lower cheekteeth of the former.

DISCUSSION: *Cormocyon haydeni* seems to be the most basal species of the Boro-

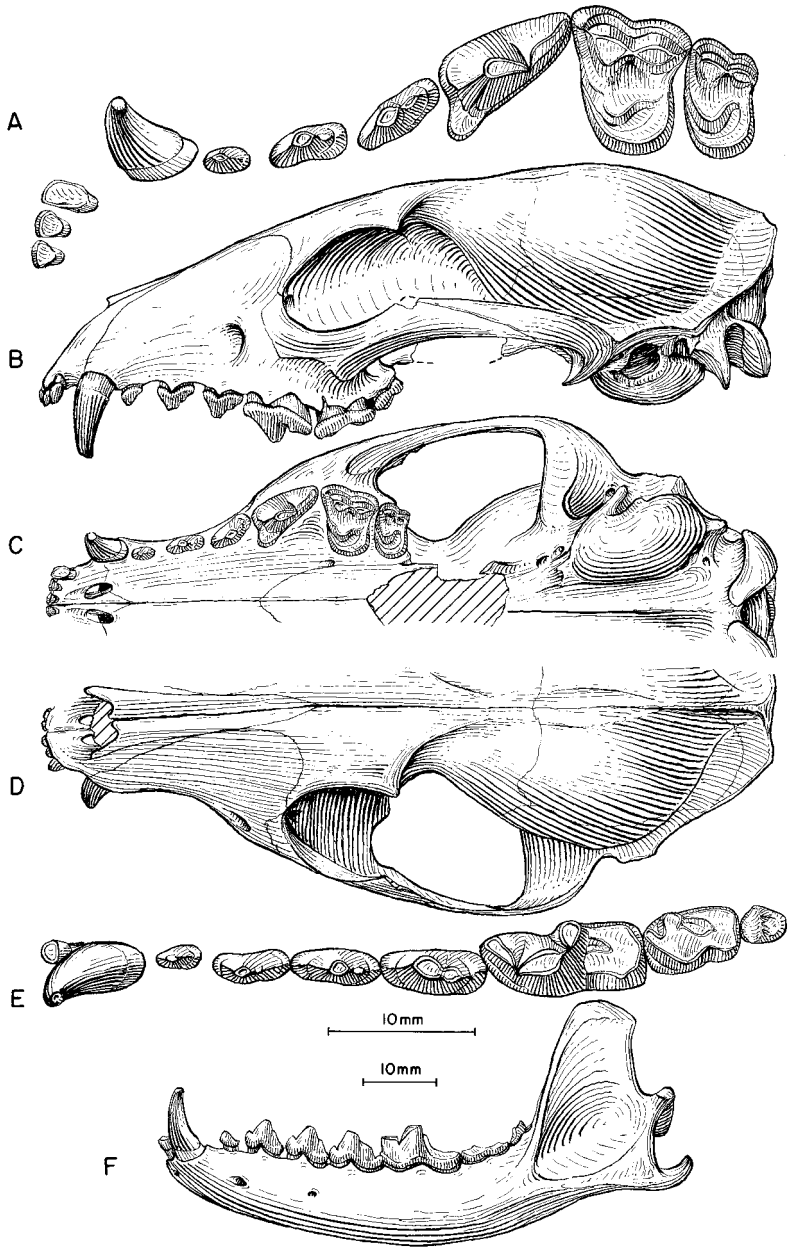

Fig. 36. *Cormocyon haydeni*. **A**, Upper teeth (M1–M2 reversed from right side), **B**, lateral, **C**, ventral, and **D**, dorsal views of skull, **E**, lower teeth, and **F**, ramus (reversed from right side), F:AM 49448, holotype, Eagle Nest Butte, in rocks equivalent to Harrison Formation (late Arikareean), Washabaugh County, South Dakota. The longer (upper) scale is for A and E, and the shorter (lower) scale is for the rest.

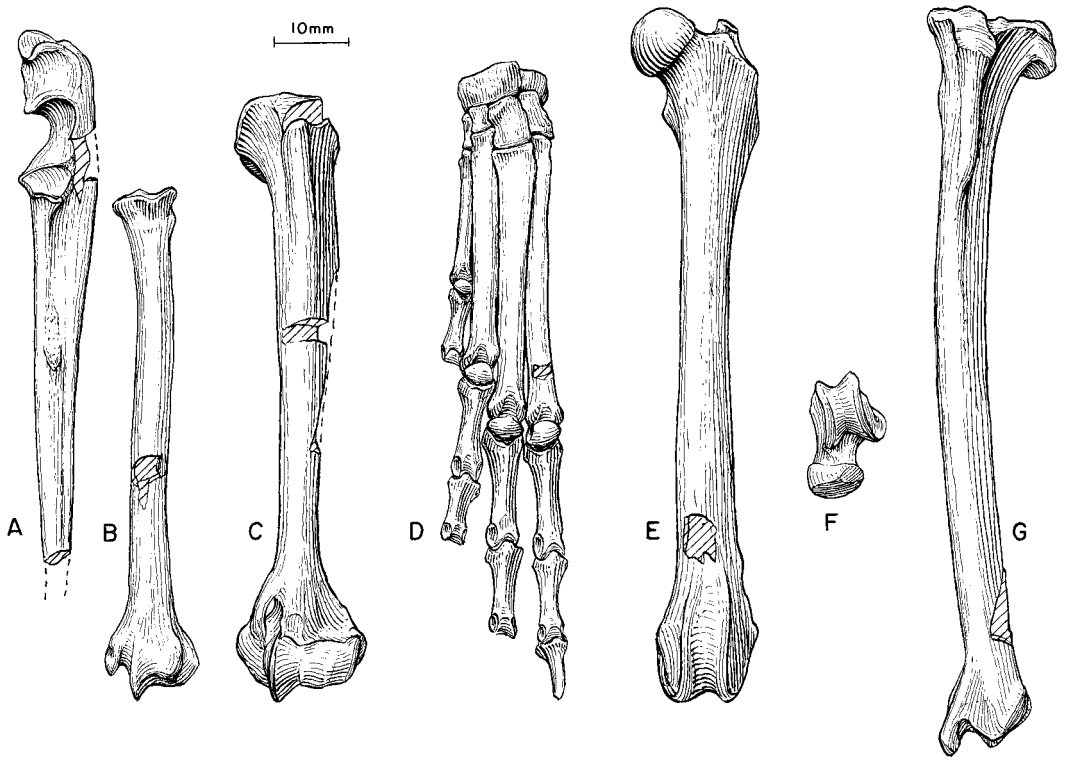

Fig. 37. *Cormocyon haydeni*. **A**, Partial ulna, **B**, radius, **C**, humerus (reversed from right side), **D**, partial foot, **E**, femur (reversed from right side), **F**, astragalus, and **G**, tibia, F:AM 49448, holotype, Eagle Nest Butte, in rocks equivalent to Harrison Formation (late Arikareean), Washabaugh County, South Dakota.

phagini clade that gave rise to most of the borophagines. This lineage of small, fox-like canids remains conservative throughout the Arikareean. Slight increase in size, downturned paroccipital process, and more cuspidate molars are a few characters that mark the difference of *C. haydeni* from such basal borophagines as *Archaeocyon* and *Rhizocyon*.

Reference of materials from the lower Rosebud Formation of South Dakota (AMNH 12872 and F:AM 49436) to *Cormocyon haydeni* is problematic. If correct, the early Arikareean occurrence of this species may be contemporaneous with the earliest occurrence of *C. copei*, as is predicted in our phylogeny. These two Rosebud specimens, however, have some peculiarities of their own (e.g., elongated carnassials) and may prove to be a different taxon given additional materials.

Cormocyon copei Wang and Tedford, 1992

Figure 41

Galecynus geismarianus Cope, 1881b: 180 (in part); 1883: 240, figs. 5, 6 (in part); 1884: 915, 920.

Cynodictis geismarianus (Cope): Cope, 1889: 233, fig. 59 (in part).

Nothocyon (*Galecynus*) *geismarianus* (Cope): Matthew, 1899: 62 (faunal list).

Nothocyon geismarianus (Cope): Wortman and Matthew, 1899: 125 (in part). Matthew, 1909: 106 (faunal list). Thorpe, 1922a: 164. Hough, 1948: 100.

Cormocyon copei Wang and Tedford, 1992: 225. Fremd and Wang, 1995: 76. Munthe, 1998: 135.

Leptocyon mollis (Merriam, 1906): Fremd and Wang, 1995: 76 (in part).

HOLOTYPE: AMNH 6885, complete skull with I1–M2, mandible with i2–m3 (fig. 41), and articulated partial lumbar and sacral vertebrae and partial pelvis, from the John Day

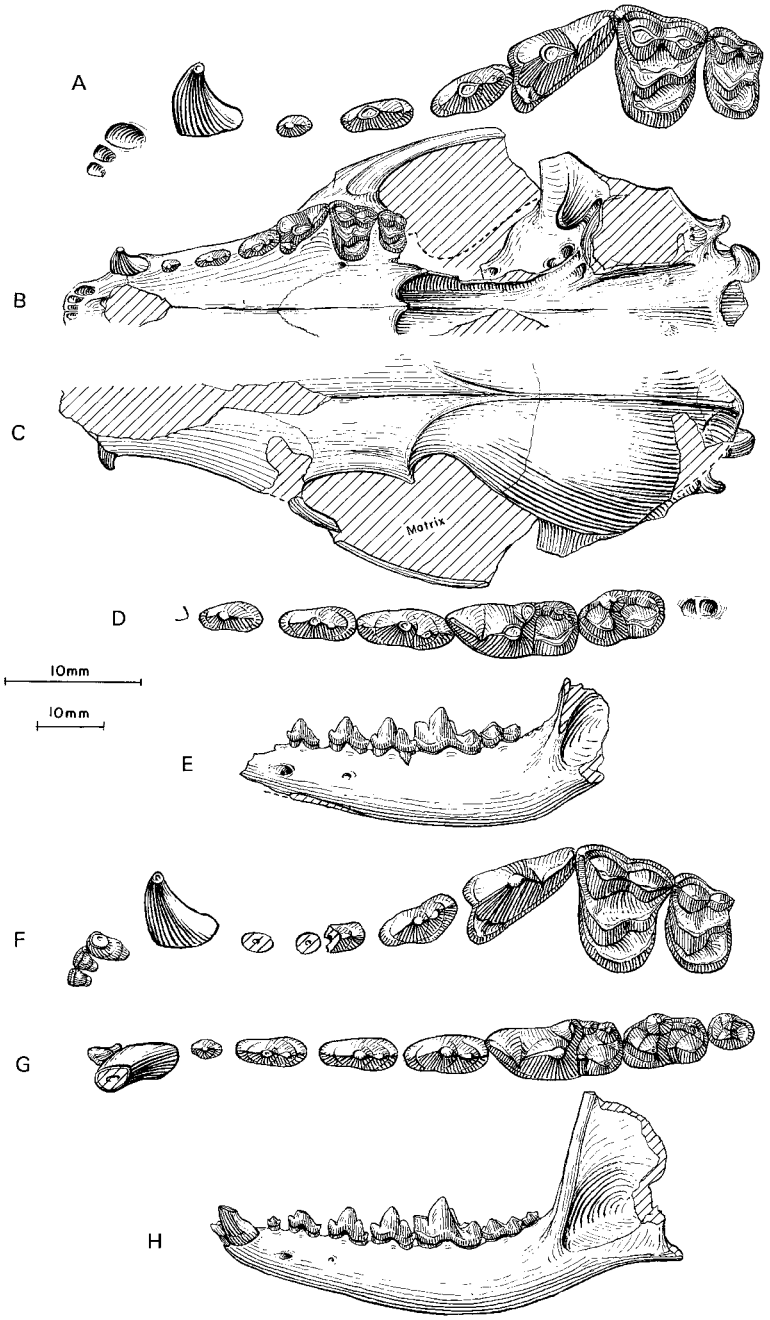

Fig. 38. *Cormocyon haydeni*. **A**, Upper teeth, **B**, ventral and **C**, dorsal views of skull, **D**, lower teeth, and **E**, ramus, F:AM 49058, north of Keeline, in rocks referred to Harrison Formation (late Arikareean), Niobrara County, Wyoming. **F**, Upper teeth, **G**, lower teeth, and **H**, ramus, F:AM 49064, North Ridge, in rocks referred to Harrison Formation. The longer (upper) scale is for A, D, F, and G, and the shorter (lower) scale is for the rest.

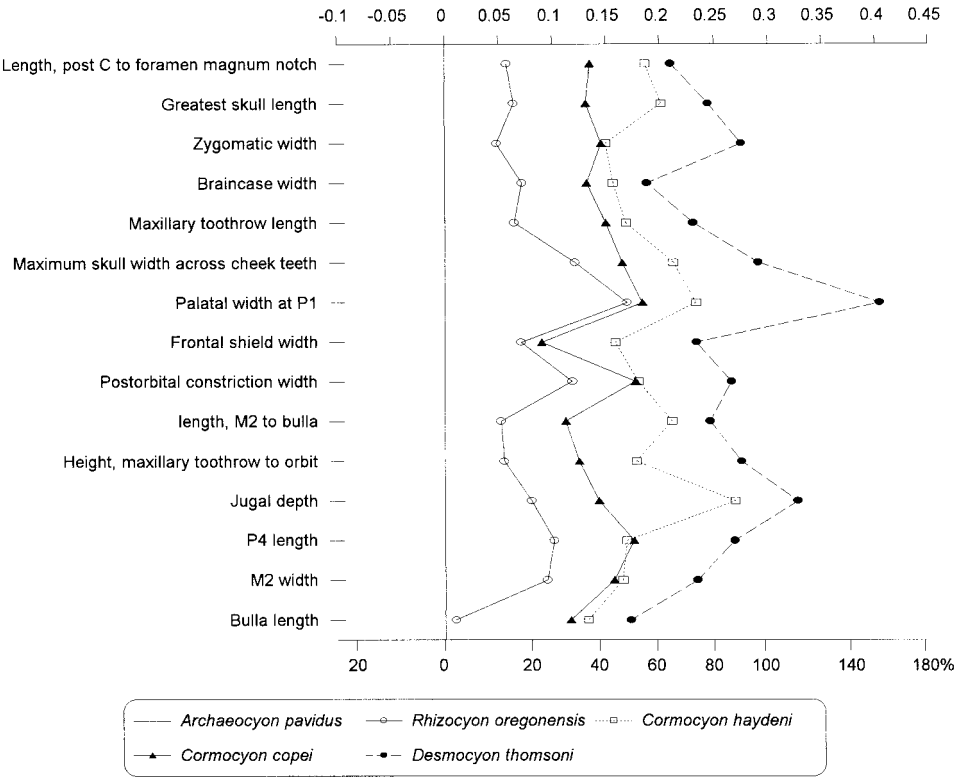

Fig. 39. Log-ratio diagram for cranial measurements of *Rhizocyon*, *Cormocyon*, and *Desmocyon* using *A. pavidus* as a standard for comparison (straight line at zero for y-axis). See text for explanations and appendix II for measurements and their definitions.

Basin, John Day Formation (?early Arikareean), Wheeler or Grant counties, Oregon.

REFERRED SPECIMENS: From the locality of the type (biostratigraphic positions of some JODA specimens in the Turtle Cove Member are placed within a letter system by Fremd et al., 1994): AMNH 6886, greater part of an articulated postcranial skeleton, including incomplete vertebral column, partial scapula, humerus, radius, ulna, metacarpals I, II, IV, and V, three first phalanges, partial pelvis, femur, and tibia (Cope, 1884: pl. LXXa, figs. 10–12); AMNH 6887, partial skull with P3–M2 all represented by roots; AMNH 6947, posterior half of skull; AMNH 6947A, rostral part of skull with alveoli for C1–P4; JODA 771, left ramal fragment with m1 and m2 alveolus; JODA 924, left P4, unit H; JODA 1630, right maxillary fragment with P4–M2, unit I; JODA 1750 (AMNH cast 129652), right partial ramus with p1–m1 and broken c1 and m2, unit F; JODA 1755, left ramus with c1–m2, unit J; JODA 1809, right maxillary fragment with P4–M1, unit G; JODA 3004, left m2, unit K; UCMP 76608, right and left partial rami with p1 root–m3, Picture Gorge Locality 7, Zone 3, UCMP loc. V6681; UCMP 76748, partial skull with P2 broken–M2, right and left rami with c1 broken, p1–p2 alveoli, p3–m2, and m3 alveolus, and fragments of vertebrae, UCMP loc. V6505, Haystack loc. no.7; UCMP 76931, fragmentary palate with P3–M2 and both partial rami with c1–m2 (p2 broken), Picture Gorge loc. 22, UCMP loc. V66116; UCMP 77161, partial skull with P1 alveolus–M2, and right and left partial rami with p3–m3 (m1 broken), right and left distal part of humeri, and left distal part tibia, from UCMP loc. V6322, Haystack loc. no.8, level 2; UCMP 112181, rostral part of skull with C1 alveolus–M2, and right and left partial rami

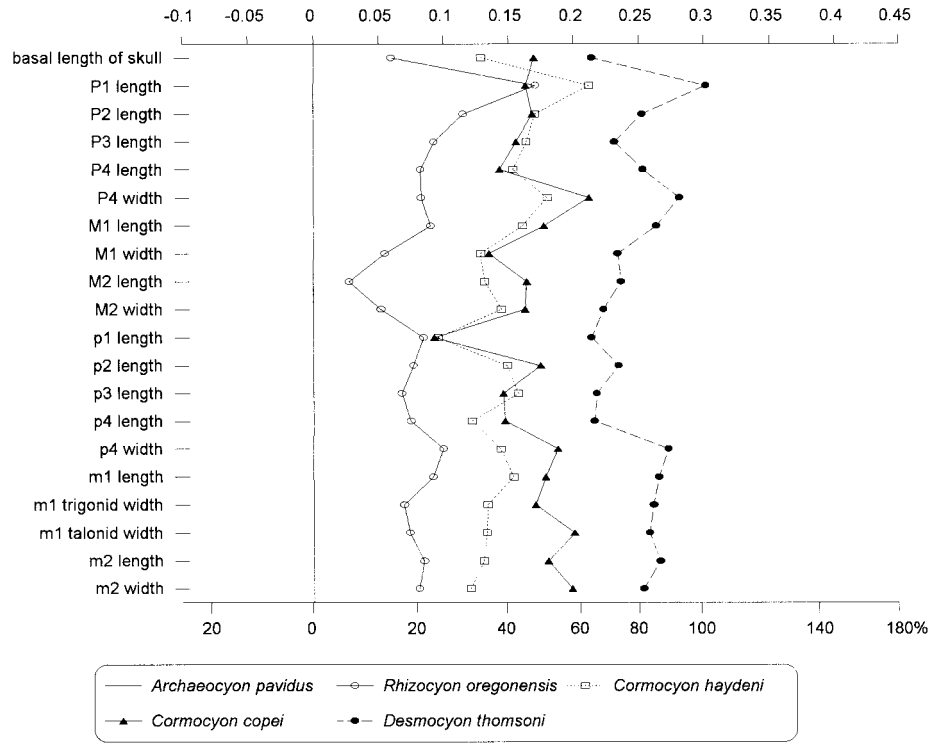

Fig. 40. Log-ratio diagram for dental measurements of *Rhizocyon*, *Cormocyon*, and *Desmocyon* using *A. pavidus* as a standard for comparison (straight line at zero for y-axis). See text for explanations and appendix III for summary statistics of measurements and their definitions.

with c1–m2, from UCMP loc. V6691, Haystack loc. no.12; YPM 12679, partial skull with C1 alveolus, P1–P4 roots, and M1–M2, Haystack Valley area; YPM 12679-1, anterior part of skull with I1–P1 alveoli, and P2–M2; and YPM 12700, skull fragment with P4–M2 and articulated right partial ramus with c1–p2 all alveoli, p3 (from left side), p4–m1, and m2–m3 alveoli, Camp Watson.

Buda Local Fauna (medial Arikareean), Alachua County, Florida: UF 16963c, left M2.

Troublesome Formation (?late Arikareean), Grand County, Colorado: UCMP 26770 (AMNH cast 129864), right maxillary fragment with P3–M2, Granby Locality, UCMP loc. 77027; UCMP 47873 (AMNH cast 129865), left partial ramus with p2 alveolus and p3–m1, Substation Locality, UCMP loc. 82045.

DISTRIBUTION: Early Arikareean of Oregon, medial Arikareean of Florida, and ?late Arikareean of Colorado.

EMENDED DIAGNOSIS: A synapomorphy that distinguishes *Cormocyon copei* and later borophagines from *C. haydeni* and more basal taxa is the lack of a laterally flared orbital rim of the zygomatic arch. Additionally, *C. copei* has a long temporal fossa, an autapomorphy that distinguishes it from *C. haydeni*.

DESCRIPTION AND COMPARISON: The holotype of *Cormocyon copei* is probably a female, judging from its small size and relatively gracile canines. It has the shortest P4 among all referred specimens (appendix III), and its P4 protocone is also very small. These proportional differences may reflect sexual dimorphism, but rigorous statistical testing is not possible with the small sample size.

Besides its larger size, *Cormocyon copei* is advanced over *C. haydeni* in its loss of a lateral flare on the orbital rim of the zygomatic arch and its deeper jugal contribution to the zygomatic arch (jugal depth in fig. 39). In some individuals (e.g., AMNH 6885 and

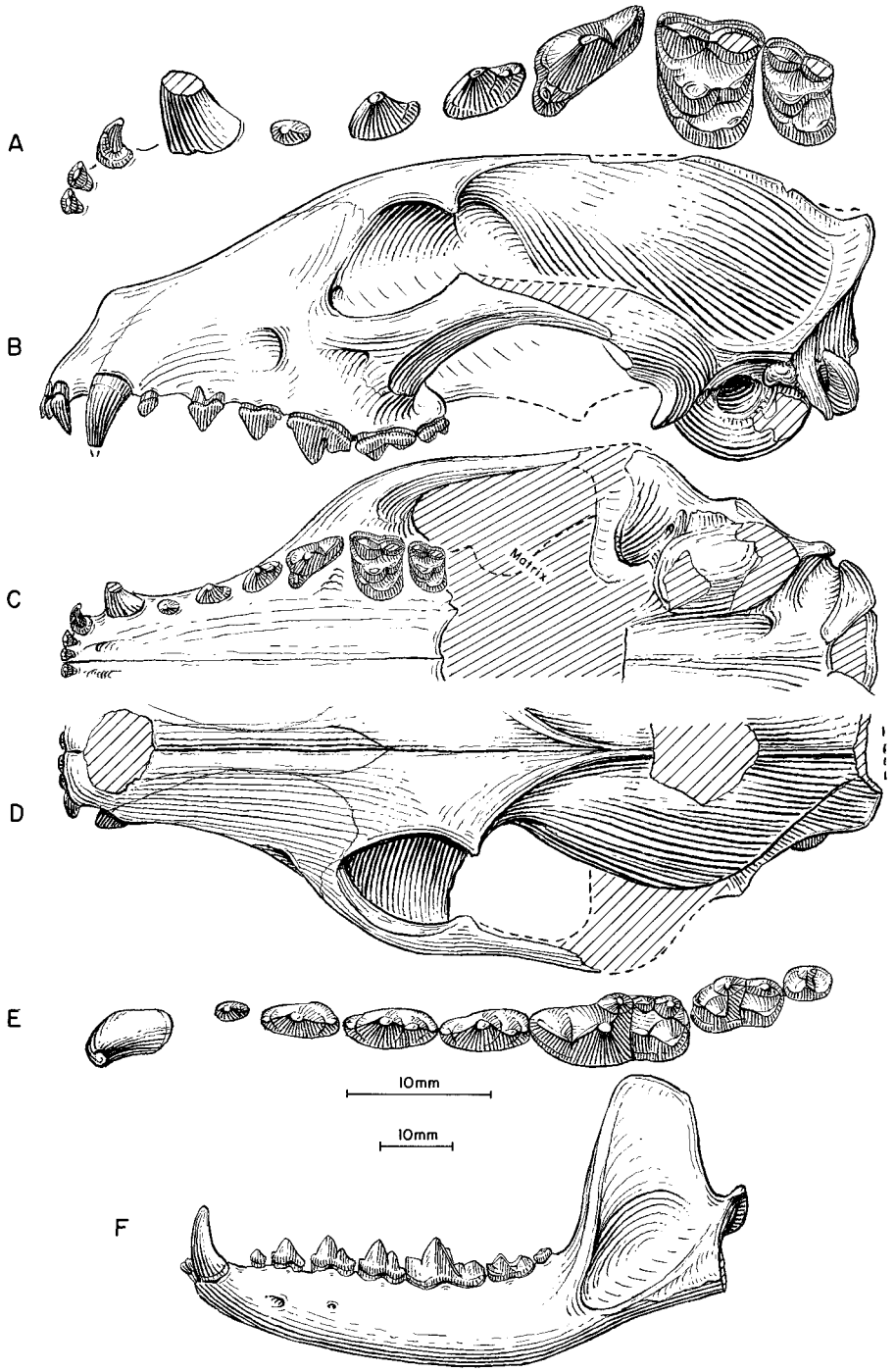

Fig. 41. *Cormocyon copei*. **A**, Upper teeth, **B**, lateral, **C**, ventral, and **D**, dorsal views of skull, **E**, lower teeth, and **F**, ramus, AMNH 6885, holotype, John Day Basin, John Day Formation (?early Arikareean), Oregon. The longer (upper) scale is for A and E, and the shorter (lower) scale is for the rest.

UCMP 77161) the anterior section of the jugal has a rounded dorsal border (rather than a flat and tilted surface in primitive forms), a character that is fully fixed in *Desmocyon thomsoni*. Additional John Day specimens referred to this species allow a better appreciation of variation and show incipient development of characters present in more derived taxa. Some individuals (AMNH 6885 and YPM 12700) display a gently domed forehead that suggests initial development of a frontal sinus shown in *D. thomsoni*. Although most individuals show a distinct metaconule on M1–M2, the lower molar talonids of some individuals still retain rather crestlike cusps. The holotype has the most conate talonid cusps.

Another consistent character that permitted us to distinguish the John Day *Cormocyon copei* from the Great Plains species *C. haydeni* is an elongated temporal fossa (length M2 to bulla in fig. 39). This long fossa and its associated long (anteroposteriorly) ascending ramus of the mandible is even more pronounced among the referred specimens (e.g., UCMP 76748 and 77161, YPM 12679). On the other hand, these referred specimens tend to have more primitive dental morphology in their crestlike talonid cusps of m1, in contrast to the conate cusps in the holotype.

DISCUSSION: Our present concept of *Cormocyon copei* is primarily based on specimens from the John Day Basin but includes some questionably referred specimens from Florida and Colorado. Two specimens from the Troublesome Formation of north-central Colorado are here referred to *C. copei* because of their size and dental morphology. The maxillary fragment (UCMP 26770) is undoubtedly a primitive borophagine with *copei*-like characteristics such as shortened P4, distinct metaconules of M1–M2, and a connection between the M2 metaconule and its lingual cingulum. The ramus fragment (UCMP 47873), however, has an m1 with a rather trenchant talonid that is quite hesperocyonine-like. Another peculiarity of the Colorado specimens is an elevated lingual cingulum on M2 and a transverse cleft on M1 that is similar to the initial development of a conate hypocone in *Phlaocyon*. On the other hand, its P4 completely lacks a hypocone or a widened lingual cingulum that is characteristic of *Phlaocyon*. The above combination of peculiarities may suggest a distinct species for the Colorado materials, or even two species. We refrain from erecting a new taxon for lack of better materials and of larger series for evaluation of variation. As presently referred, the Colorado materials indicate the presence of a *C. copei*-like form outside the John Day Basin, but still to the west of the continental divide. A single M2 from the Buda Local Fauna of Florida is tentatively referred to *Cormocyon*.

Cormocyon copei is very close, in stage of evolution, to *C. haydeni* from the northern Great Plains. The *copei–haydeni* pair appears to mark an instance of sister-species on either side of the continental divide. As part of a nearly linear series of borophagines from *Cormocyon* to *Tomarctus*, this species pair occupies the starting point of a long evolutionary trend toward medium- to large-size predators. The possession of a derived condition on the zygomatic arch shows *C. copei* to be slightly more advanced than *C. haydeni*.

Desmocyon, new genus

TYPE SPECIES: *Cynodesmus thomsoni* Matthew, 1907.

ETYMOLOGY: Greek: *desmo*, bond, suggesting relationship; *cyon*, dog, an anagram of the genus *Cynodesmus*, to which the type species was originally referred.

INCLUDED SPECIES: *Desmocyon thomsoni* (Matthew, 1907), and *Desmocyon matthewi*, new species.

DISTRIBUTION: Late Arikareean of South Dakota, Wyoming, Nebraska, and Oregon; early Hemingfordian of Nebraska, New Mexico, and Florida.

DIAGNOSIS: Derived characters distinguishing *Desmocyon* and more derived taxa from *Cormocyon* are broad rostrum and palate, frontal sinus present but not penetrating postorbital process, encircling ectotympanic forming an external auditory meatus ring, and deep zygoma. Compared to the Cynarctina, *Desmocyon* lacks the hypocarnivorous characters of that clade: a prominent subangular lobe, high mandibular condyle, short P4, m1 protostylid, wide m1 talonid, and

large m2. *Desmocyon* is primitive relative to *Metatomarctus* in that the I3 is not enlarged and lacks a well-developed lateral cusplet, and the P4 has only a weak anterior crest on the paracone.

Desmocyon thomsoni (Matthew, 1907)

Figures 42–44, 46E, F

Cynodesmus thomsoni Matthew, 1907: 186, figs. 4, 5; 1909: 112. Peterson, 1910: 267, fig. 62. Cook, 1912: 42. Hough, 1948: 103.
Nothocyon sp. Cook, 1909: 266; 1912: 42.
Tomarctus thomsoni (Matthew): White, 1941b: 95. Cook and Macdonald, 1962: 562. Macdonald, 1963: 209; 1970: 57.
Nothocyon regulus Cook and Macdonald, 1962: 560, fig. 1.
Tomarctus thompsoni [sic] (Matthew): Munthe, 1989: 13; 1998: 135.

HOLOTYPE: AMNH 12874, skull with I1–M2 (fig. 42A–C), mandible with i1–m3 (fig. 42D, E) and associated skeletal fragments including partial tibia, partial radius and ulna, carpals and incomplete metacarpals II–V, and phalanges. Matthew reported that the type was from the Upper Rosebud beds. Macdonald (1963: 209) listed the type locality as AMNH ''Rosebud 24'' and located the type locality by quoting from the 1906 field notes as ''8 m. E. of Porcupine P.O. . . . N. of Porc[upine] Cr'k . . . upper Rosebud'' (Macdonald, 1963: 156). He concluded that ''Rosebud 24'' is ''probably Rosebud Formation'' in the sense used by him (1963, 1970), late Arikareean.

REFERRED SPECIMENS: Wounded Knee area, Rosebud Formation (late Arikareean), Shannon County, South Dakota: AMNH 12874A, left ramal fragment with m1 broken; AMNH ''Rosebud 17''; AMNH 12885, partial palate with C1, P1 alveolus, P2–P3, and P4–M1 broken, and left ramal fragment with m1; SDSM 5584 right isolated P4 from SDSM V5341; and SDSM 5585, right partial ramus with p3 alveolus and p4–m1 from SDSM V554.

Syndyoceras Hill, 0.5 mi west of Agate, Harrison Formation (late Arikareean), Sioux County, Nebraska: AMNH 81008 (HC 115, holotype of *Nothocyon regulus* Cook and Macdonald, 1962), right partial ramus with p4 alveolus, m1, and m2 alveolus.

Lusk area, Upper Harrison beds (late Arikareean), Niobrara County, Wyoming: AMNH 13763, partial skull with P2–M2 and right and left partial rami with c1 broken–m3, 9 mi south of Lusk; F:AM 27566, right ramal fragment with m1 broken and m2; F:AM 27566A, partial right ramus with m1 broken and m2–m3 alveoli, north of Lusk; F:AM 49078, left ramal fragment with m2, Royal Valley; F:AM 49085, right partial ramus with p4 root–m1 broken, Royal Valley; F:AM 50207, partial mandible with c1, p1 alveolus, p2 broken–m2, and m3 alveolus, Royal Valley in white line; F:AM 50209, anterior part of skull with I3, C1 alveolus, and P1–M2 (P4 broken) and right ramus with c1 broken, p1–p3 alveoli, p4–m2, and m3 alveolus, Royal Valley; F:AM 50210, articulated fragment of skull with C1 and P4–M2 and partial mandible with c1, p2–p4 all broken, and m1–m2, Silver Springs; F:AM 50211, left ramus with c1, p1 alveolus, and p2 broken–m2, Freeman Ranch, south of Lusk; F:AM 50212, right partial ramus with c1 root and p1 broken–m1, Royal Valley; and F:AM 50213, fragmentary skull, right partial ramus with p3–m1, fragmentary limbs including an incomplete articulated pes with tarsals and proximal part of metatarsals II–IV, detached partial metatarsal V and isolated phalanges, and partial baculum, Silver Springs area.

Lusk area, Upper Harrison beds (late Arikareean), Goshen County, Wyoming: F:AM 27551, partial skull with C1–M2 and partial mandible with c1–m2 and m3 root, 16–20 mi southeast of Lusk; F:AM 27552, partial skull with P3–M2 (all broken) and articulated partial right ramus with m1 broken–m2; F:AM 27553, right partial ramus with c1 and p1 alveolus–m1, 18 mi southeast of Lusk; F:AM 27564, anterior part of skull with I1–I2 alveoli and I3–M1, 2 mi west of Jay-Em; F:AM 27569, anterior part of skull with I1–M1 and M2 broken, partial mandible with i1–m3, right partial humerus, right partial radius, right ulna, right incomplete manus with metacarpals II–V and phalanges, left metacarpal I, right femur, right tibia, partial pelvis, and vertebrae, 21 mi southeast of Lusk; F:AM 27570, left partial maxillary with C1–P2, isolated M1, both partial rami with c1 broken–p3 and m1–m2, 12–15 mi southeast of Lusk; F:AM 27571, partial skull with I3–

C1, P1–P2 roots, and P3–M2, 16–20 mi southeast of Lusk; F:AM 27572, partial palate with P2 root–M2 and both partial rami with p2–m2 and m3 alveolus, 12–15 mi southeast of Lusk; F:AM 27574, left ramal fragment with p4–m1 (broken), North Ridge on Highway 85; F:AM 49018; skull fragment, left metacarpals I, II, and V, incomplete left metacarpal III, left metatarsals III, IV, and V, and left calcaneum, 25 mi southeast of Lusk; F:AM 49065, left premaxillary-maxillary fragment with I3–C1 and partial maxillary with P3–M1, M2 broken, right and left partial rami with p2–m1 all broken and m2–m3, atlas, axis, distal fragment of humerus, proximal part of radius and ulna, articulated calcaneum and astragalus, and articulated tarsals and metatarsals II–IV, Jay-Em, high in section; F:AM 49066, right partial ramus with p2–m2, 20 mi southeast of Lusk, high Middle Brown Sand; F:AM 49067, partial skull with I1–M2, mandible with i1–m3, and associated limbs including partial humerus, radius, ulna, articulated manus with carpals, metacarpals I–V, some phalanges, partial femora, tibia, astragalus, and calcaneum, 18 southeast of Lusk, high in section; F:AM 49068, left partial maxillary with P4–M1 and M2 alveolus, right and left partial rami with c1 and p2–m1, partial radius and ulna, carpals, metacarpals III, IV, and V, calcaneum, astragalus, tarsals, incomplete metatarsals III, IV, and V, and vertebrae, Sand Gulch, high in section; F:AM 49082, right partial maxillary with P4–M2 (M1 broken) and right partial ramus with p2–p3 alveoli and m1–m3, 25 mi southeast of Lusk; F:AM 49083, right partial ramus with m1, 18 mi southeast of Lusk, middle brown sand; F:AM 49084, right partial ramus with p4 root and m1–m2, Jay-Em; F:AM 49087, left isolated p4, m1, and right m2, 18 mi southeast of Lusk; F:AM 49089, partial skull with C1 broken–M2 and partial mandible with c1–p1 both broken and p2–m3, 16 mi southeast of Lusk, high brown sand; F:AM 49090, left partial ramus with c1–p2 roots, p3, and p4–m1 both broken, 16 mi southeast of Lusk, middle brown sand; F:AM 49091, right ramus with p3 alveolus and p4–m2, 18 mi southeast of Lusk, high brown sand; F:AM 49092, left partial maxillary with P1, P2–P3 alveoli, P4, M1 broken, and M2 alveolus, Jay-Em, high brown sand; F:AM 49094, partial skull with I3 broken, and C1–M2 (P1 alveolus) and left ramus with i1, i2–p2 alveoli, p3 broken, p4 alveolus–m2, and m3 alveolus, Jay-Em, high in section; F:AM 49095, partial left ramus with i2–m2 and m3 alveolus, 18 mi southeast of Lusk, high in section; F:AM 49097, skull with I1, I2 alveolus, I3–M2 (P1 alveolus), left ramus with c1–m3 (p4 alveolus), left humerus, right partial humerus, both radii and ulnae, carpals articulated with metacarpals II and III, detached metacarpal V, phalanges, both femora, right tibia, calcaneum, astragalus, tarsals articulated with proximal ends of metatarsals III–V, and partial baculum, Jay-Em, high in section; F:AM 50205, partial palate with P3–M2, 16 mi southeast of Lusk; F:AM 50206, partial right ramus with i2–m1 (all broken) and m2–m3, Sand Gulch, south end; F:AM 50208, right partial ramus with p2–p4 all broken, m1–m2, and m3 alveolus, 16 mi southeast of Lusk, light sand, west end; F:AM 54118, right partial ramus with c1, p1–p3 alveoli, p4, m1 broken, and m2 alveolus, Jay-Em, below white layer; and F:AM 105250, left partial ramus with c1, p1–p4 alveoli, m1, and m2–m3 alveoli, roadcut about 1 mi southeast of Podelack Ranch headquarters.

Spoon Buttes area, Upper Harrison beds (late Arikareean), Goshen County, Wyoming: F:AM 49086, right ramal fragment with m1, Spoon Buttes; and F:AM 54142, right and left partial maxillae with I1–M1, southwest of Spoon Buttes.

Lusk area, 18 Miles District, 18 mi southeast of Lusk, high brown sand, Upper Harrison beds (late Arikareean), Goshen County, Wyoming (The following four skulls and jaws, F:AM 49096A–D, were found associated with the limb elements in one field block. No direct association between limb elements and skulls was apparent; however, those limb elements marked F:AM 49096-1 [smaller] and F:AM 49096-2 [larger] are tentatively considered as representing two or more individuals. Additional limb elements are placed in F:AM 49096 that may represent one or more individuals.): F:AM 49096A, skull with I1–M2 and mandible i1–m3; F:AM 49096B, skull with I1–M2 (fig. 43A, B) and mandible i1–m3 (fig. 43C, D); F:AM

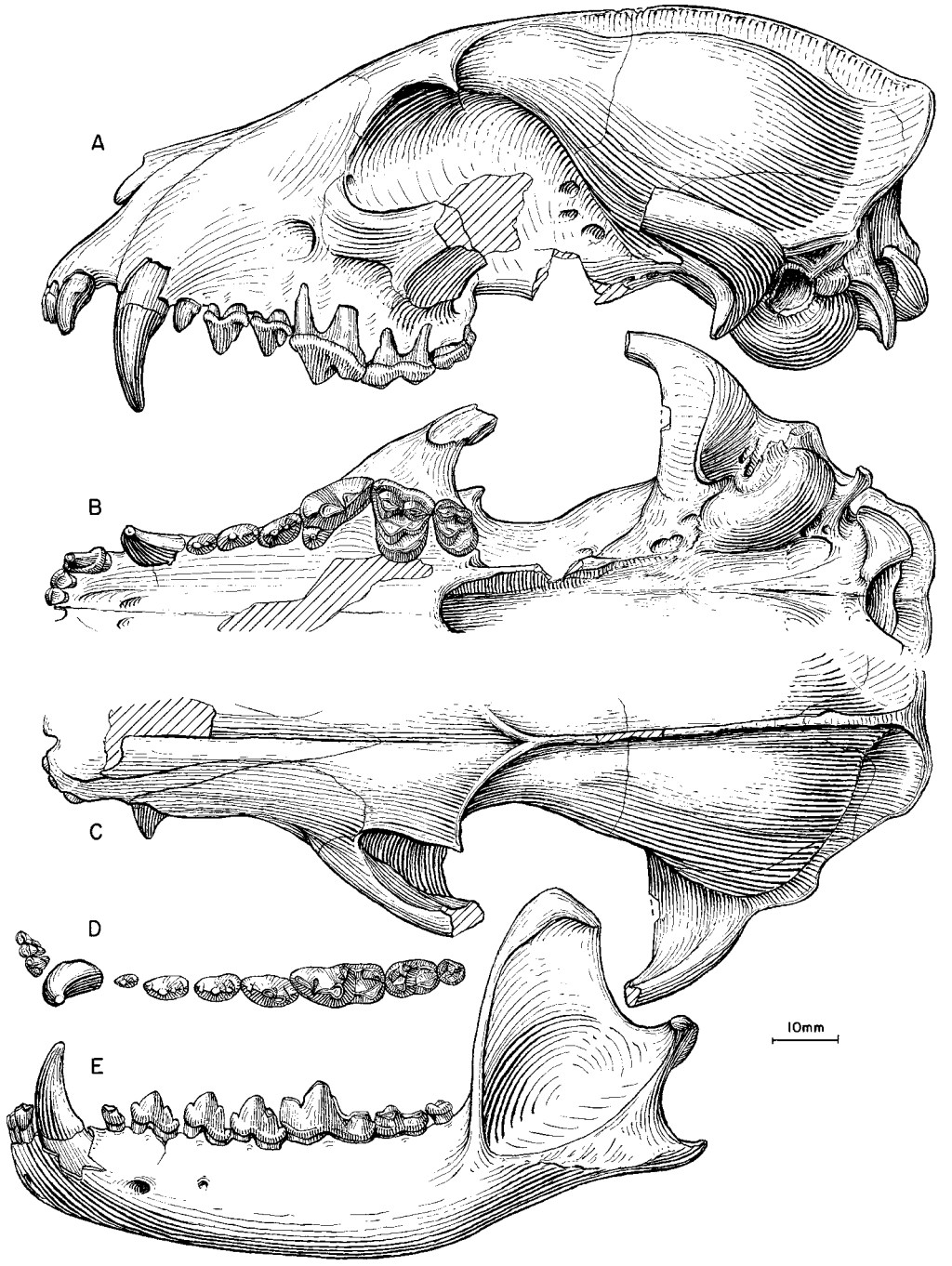

Fig. 42. *Desmocyon thomsoni*. **A**, Lateral, **B**, ventral, and **C**, dorsal views of skull (I1–I2 reversed from right side), **D**, lower teeth, and **E**, ramus (angular process reversed from right side), AMNH 12874, holotype, 8 mi east of Porcupine, Rosebud Formation (late Arikareean), Shannon County, South Dakota.

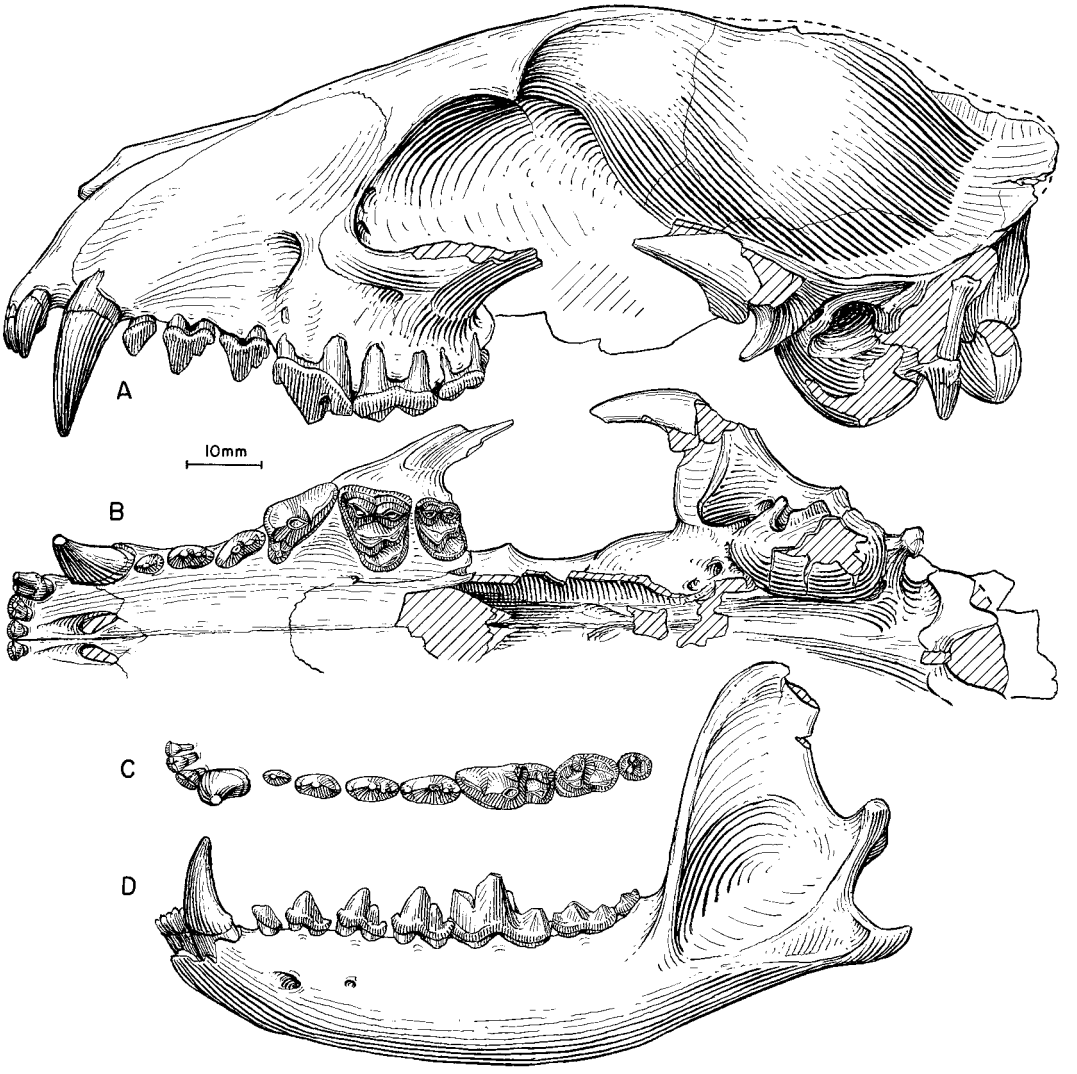

Fig. 43. *Desmocyon thomsoni*. **A**, Lateral and **B**, ventral views of skull (C1 reversed from the right side), **C**, lower teeth, and **D**, ramus (c1 and i1–i2 reversed from the right side), F:AM 49096B, 18 Miles District, Upper Harrison beds (late Arikareean), Goshen County, Wyoming.

49096C, skull with I1–M2 and mandible with i1–m3; F:AM 49096D, anterior half of skull with I1–M2 and partial mandible with i1–m3; F:AM 49096-1, right and left humeri, right partial radius, and two left femora; F:AM 49096-2, right and left humeri (fig. 44A) (?two individuals), left radius and ulna (fig. 44B, C), right femur (fig. 44D), right and left tibia both with fibula (fig. 44E, F); and F:AM 49096, following limbs associated with the above and may represent either the same or other individuals included right proximal part of radius and ulna, left incomplete ulna, two right partial femora, right proximal part of tibia, right and left partial articulated pes with tarsals and metatarsals I–V (fig. 44G), and right partial articulated pes with calcaneum, astragalus, incomplete metatarsals III and IV, and complete metatarsal V.

Wheatland area, Upper Harrison beds (late Arikareean), Platte County, Wyoming: F:AM 27565, left partial ramus with p4–m3; F:AM

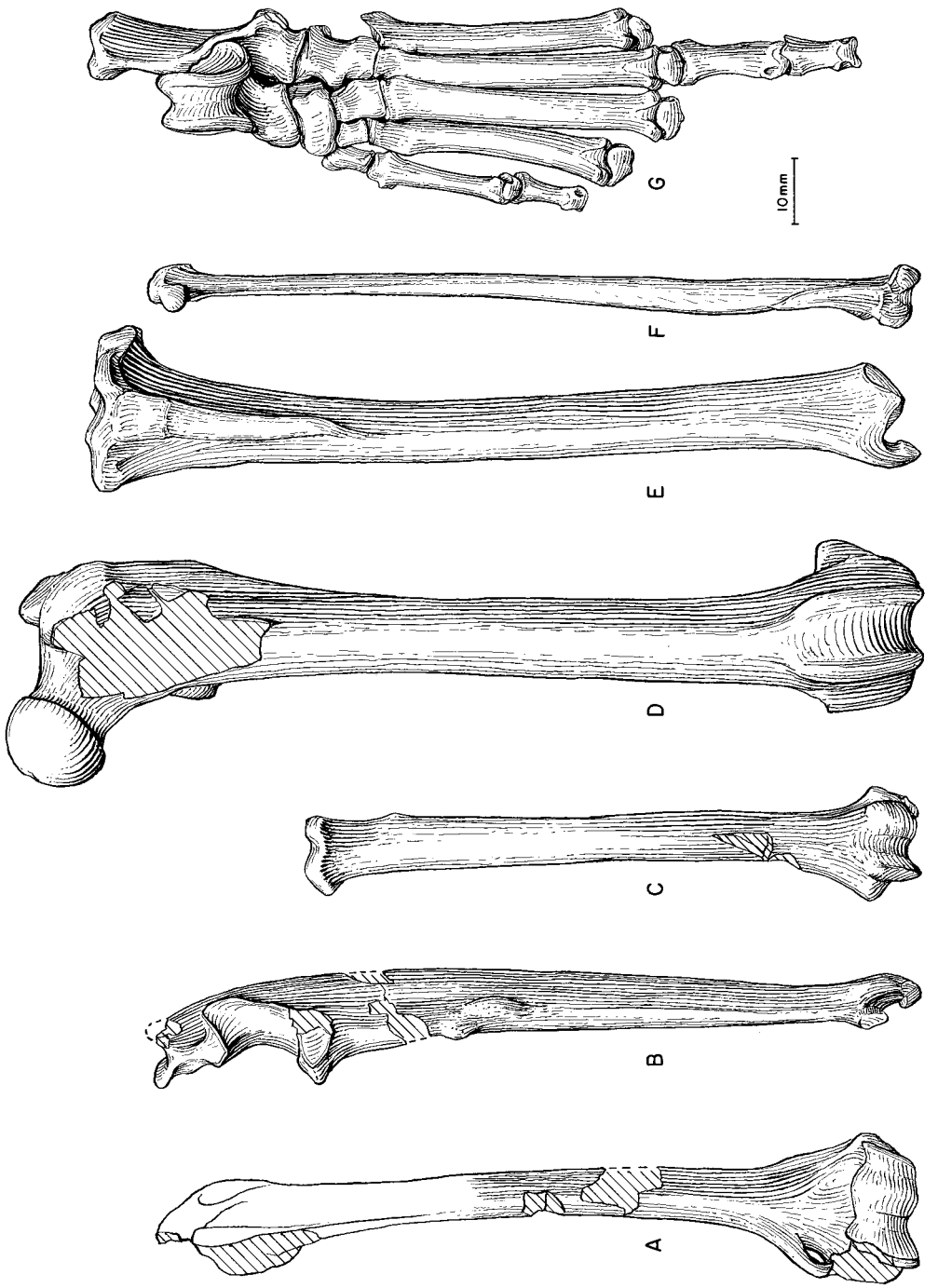

Fig. 44. *Desmocyon thomsoni*. **A**, Humerus, **B**, ulna, **C**, radius, **D**, femur (reversed from right side), **E**, tibia, **F**, fibula, and **G**, tarsi, metatarsi, and partial phalanges, F:AM 49096(2), 18 Miles District, Upper Harrison beds (late Arikareean), Goshen County, Wyoming.

49017 (referred to *Tomarctus thomsoni* by Munthe, 1989: 13), associated postcranial skeleton with partial axis, pelvis fragment, left humerus, right partial radius and ulna, right partial manus with carpals and metacarpals II, III, and IV, left femur, left tibia and fibula, left articulated pes with calcaneum, astragalus, tarsals, metatarsal I, incomplete metatarsals II, III, IV, and V, Uva Breaks, 10 ft above white layer; and F:AM 54119, partial skull with I1–I3 alveoli, C1–P4, partial mandible with c1 broken, p1–m2, and m3 alveolus and associated limb including distal end of both humeri, right and left radii, left ulna and right partial ulna, right metacarpal I, partial metacarpal III, left metacarpal IV and right partial metacarpal IV, left metacarpal V, and left calcaneum, Uva Breaks.

Guernsey area, Upper Harrison beds (late Arikareean), Platte County, Wyoming: F:AM 49088, posterior part of skull, both partial rami with p4–m3, axis, atlas, cervicals, and vertebrae, 6 mi west of Guernsey, high brown sand; and F:AM 49093, right and left rami with i1–m3, 2 mi southwest of Guernsey, 20 ft above white layer.

Upper Harrison beds (late Arikareean), Sioux County, Nebraska: AMNH 81026 (HC 485), right partial ramus with i1–i3 alveoli, c1–p1 broken, p2–m2, and m3 alveolus; AMNH 81027 (HC 240), left partial ramus with p3 root, p4–m1, and m2–m3 alveoli, 3 mi northeast of Agate, 15 ft above the contact with the lower Harrison; F:AM 49182, left partial ramus with p4–m1 both broken, m2, and m3 alveolus, 5–7 mi northeast of Agate, low in section; F:AM 49183, left ramus with i1–p3 alveoli, p4–m1, and m2–m3 alveoli, Morava Ranch; F:AM 49189, left ramal fragments with c1–p3 all broken and p4 broken–m2, south of Harrison, high brown sand; F:AM 49190, left maxillary with C1–M1, south of Harrison, high in section; F:AM 105251, left partial ramus with p2 alveolus, p3–m2, and m3 alveolus, northeast of Agate, surface below grayish low channel; KUVP 27672, partial skull and mandible with complete upper and lower teeth, partial postcranial skeleton with atlas, axis, two lumbars, distal left humerus, proximal left ulna, left radius, left and right femora, left and right tibiae, partial left foot with calcaneum, tarsals, metatarsals II–IV, and phalanges, from locality KU-NE-028, Dout Ranch, Sitting Hen and vicinity; and KUVP 27673, partial skull and mandible with most upper and lower teeth except for P1 and p1, and postcranial skeleton with partial atlas, axis, one cervical, three thoracics, four lumbars, left and right humeri, left and right ulna and radius, partial right manus with metacarpals II–V, and one medial phalanx, Dout Ranch.

Upper Harrison beds (late Arikareean), Cherry County, Nebraska: UNSM 26550, complete skull and mandible with entire upper and lower dentition and partial articulated skeleton, UNSM loc. Cr-127; UNSM 26664, complete skull with left and right I1–M2, partial left ramus with p4–m1, m2 broken, m3 alveolus, partial vertebral column with one cervical, one thoracic, five lumbars, sacrum, pelvis, partial right scapula, left radius, nearly complete left and right hindlimbs with femora, tibiae, fibulae, tarsals and metatarsals, and phalanges; and UNSM 6865-86, skull fragments with I3–M2 and left and right rami with i1–m3.

John Day Formation (?late Arikareean), Oregon: AMNH 7238, isolated right M1–M2 (No stratigraphic information is available on this specimen, which was collected by E. D. Cope parties. Based on the known range of this species, AMNH 7238 is probably from the Haystack Valley Member of the John Day Formation, i.e., late Arikareean).

Lower part of Runningwater Formation (early Hemingfordian), Dawes County, Nebraska: F:AM 49180, left partial ramus with p2–m3 (p4–m1 broken), 1.25 mi northwest of Marsland; F:AM 49188, left partial ramus with m1–m2, Cross Cut Prospect, Sand Canyon System; F:AM 54496, right partial ramus with p4–m1 and m2 broken, Hay Springs Creek; and F:AM 105096, right isolated P2 and two maxillary fragments with P3–P4, M1, and M2 alveolus, Hay Springs Creek.

Lower part of Runningwater Formation (early Hemingfordian), Box Butte County, Nebraska: F:AM 62890, partial skull with I1–I3 alveoli, C1–M2 (p1 alveolus) (fig. 46E, F), East Channel Prospect, type section of Runningwater Formation; and F:AM 99693, left partial ramus with p4 alveolus–m2 and m3 alveolus, Runningwater Quarry.

Lower part of Runningwater Formation (early Hemingfordian), Morrill County, Nebraska: Bridgeport Quarry 1 (UNSM loc. Mo-113): UNSM 25711, right ramal fragment with m1–m2; UNSM 25792, left partial maxillary, with P3 alveolus–M1; UNSM 25797 (F:AM cast 97147), left partial maxillary with P3–M1 and M2 alveolus; UNSM 25798, right partial maxillary with M1–M2; and UNSM 25799, left ramal fragment with m1–m2 and m3 alveolus.

Spiers Quarry, ?Runningwater Formation (early Hemingfordian), Dawes County, Nebraska: F:AM 49191, left partial ramus with m1 broken and m2–m3.

Jeep Quarry, Arroyo Pueblo drainage, upper part of Chamisa Mesa Member, Zia Formation (early Hemingfordian), Sandoval County, New Mexico: F:AM 50138, right ramal fragment with p4–m1; and F:AM 62775A, right edentulous ramus fragment with p1–m2 alveoli.

DISTRIBUTION: Late Arikareean of South Dakota, Wyoming, Nebraska, and Oregon; early Hemingfordian of Nebraska and New Mexico.

EMENDED DIAGNOSIS: Characters of *Desmocyon thomsoni* that are primitive with respect to *D. matthewi* are small frontal sinus that does not penetrate the postorbital process, frontal shield narrow relative to width of braincase, postorbital width of frontals narrow, and m1 talonid without transverse crest between entoconid and hypoconid and hypoconulid shelf absent.

DESCRIPTION AND COMPARISON: Besides its larger size, *Desmocyon thomsoni* has several cranial features that set itself apart from *Cormocyon* and more basal taxa. In cranial proportions, *D. thomsoni* has a relatively broader muzzle and wide palate, a deeper jugal contribution to the zygomatic arch, and a smaller bulla (fig. 39). An inflated frontal sinus first appears in *D. thomsoni*, as reflected by a slightly domed forehead and verified by dissected individuals (F:AM 49067, 49094, 49096A, 49097). In all of these individuals and others whose postorbital processes are broken, the sinus does not invade the postorbital process and generally ends before the postorbital constriction, rather than expanding behind the constriction. Also first appearing in *D. thomsoni* is a complete ectotympanic ring, which bridges the top of external auditory meatus. Thus, the roof of the meatus is now formed by the dorsal extension of the ectotympanic instead of the squamosal. Fusion between the ectotympanic and squamosal sometimes obscure this relationship; however, a bony thickening in this part of the meatus is always visible in such cases to indicate the encircling ectotympanic.

On the other hand, isolated individuals of *Desmocyon thomsoni* begin to display the initial development of certain derived features seen in *D. matthewi*. For example, two specimens (the holotype and F:AM 49067) show an expanded posterior process of the premaxillary whose tip touches the nasal process of the frontal, a derived character fully established in *D. matthewi*. While such cases of advanced features suggest what is to come in phylogeny, they are judged to be interspecific variation since most specimens still show the primitive state.

The presence of *Desmocyon thomsoni* in the Runningwater Formation of Nebraska is established by excellent materials (under study by Bruce Bailey), which have none of the derived characters for *D. matthewi*. Such a recognition of *D. thomsoni* in the Runningwater Formation creates a problem of identification of more fragmentary materials. The nearly identical size of *D. thomsoni* and *D. matthewi* makes the differentiation difficult. We are forced to use more subtle dental criteria for species recognition, such as a slightly better developed anterior ridge of the paracone on P4 tending toward a parastyle and the presence of a transverse crest between the hypoconid and entoconid of m1, as indicative of *D. matthewi*. Stratigraphically, *D. thomsoni* generally occurs in the lower part of the Runningwater Formation whereas *D. matthewi* is mostly found in the upper part.

A much larger series of specimens is now referable to *Desmocyon thomsoni* than was available when the taxon was first described, mostly due to the contributions from the Frick Collection. Particularly noteworthy is the presence of a group of four individuals (F:AM 49096A–D) in a single block of matrix from southeast of Lusk, Wyoming, that affords a rare instance of observing individuals from a real population. All four individuals are adults with differing degree of wear

on their teeth. Although dental dimensions of the four individuals are very close, there are significant size differences in their limbs (we cannot, however, associate the skulls with particular sets of postcranial skeleton).

Two specimens, F:AM 49097 and 50213, can be positively sexed due to associations of a baculum. Two other individuals, UNSM 26550 and 26664 (under study by Bruce Bailey), lack a baculum, and they are here regarded as females. Our inference that the UNSM specimens truly lack a baculum is based on their excellent preservation. The postcranial skeleton in UNSM 26664 includes well-preserved, completely undistorted lumbar vertebrae and an intact sacrum-pelvis, in addition to articulated hindlimbs on both sides—the posterior half of the skeleton surrounding the baculum region is completely preserved. Both male individuals display markedly stronger canines, more robust lower jaws, and slightly broader (transversely) cheekteeth than do those of the female. Based on such criteria, we may infer the sex of other referred specimens.

DISCUSSION: Initial reference of *thomsoni* to *Cynodesmus* by Matthew (1907), along with ''*C.*'' *minor*, significantly expanded the concept of *Cynodesmus* and was followed by a series of other species later referred to this genus by other authors (e.g., Simpson, 1932; Macdonald, 1963). Such an expanded concept of *Cynodesmus* became an important feature of a phylogeny of canids proposed by Matthew (1924, 1930), in which *Cynodesmus* serves as a key link between *Hesperocyon* and *Tomarctus*, the latter being in turn postulated to be ancestral to almost all living canids. As a well-known taxon at the time, ''*Cynodesmus*'' *thomsoni* played an important role in past studies on canid phylogeny. Our own analysis suggests that *thomsoni* has no relevance in the initiation of the living canine clade, but is related to a long series of borophagines.

Certain individuals of *Desmocyon thomsoni* from the Upper Harrison beds of Nebraska (e.g., UNSM 26550 and 26664) are noticeably smaller than those from equivalent beds in Wyoming. Individuals from the late Arikareean of Wyoming can be up to 15% larger in total skull length than found in the Nebraska samples, and samples from the Runningwater Formation tend to retain the small size. Such a size difference is generally beyond the sexual dimorphism encountered in living canids. Lacking any morphological characters to separate these samples, however, we must consider the possibility of size reduction within the species. It seems possible that the co-occurrence of *D. thomsoni* with the larger *Metatomarctus canavus* (and sometimes with *Paracynarctus kelloggi*) in some quarries in the Runningwater Formation may have caused size reduction in *D. thomsoni*.

Desmocyon matthewi, new species

Figures 45, 46A–D

HOLOTYPE: F:AM 49177, articulated skull and mandible with all teeth represented (fig. 45), postcranial elements including the first four cervical vertebrae, partial humerus, partial radius and ulna, partial pelvis, and partial femur from Marshall Ranch, Cottonwood Creek, upper part of the Runningwater Formation (early Hemingfordian), Dawes County, Nebraska.

ETYMOLOGY: Named in honor of William Diller Matthew for his pioneering studies on canid phylogeny and his fundamental contributions to paleomammalogy.

REFERRED SPECIMENS: Upper part of the Runningwater Formation (early Hemingfordian), Dawes County, Nebraska: F:AM 49176, left maxillary fragment with isolated C1, P3 broken, isolated P4 broken, right and left partial rami with c1, p1–p2 alveoli, p3–m3 (m2 broken), partial humerus, radius (fig. 46A), partial ulna (fig. 46B), metacarpal I and partial metacarpal III, metatarsal II and incomplete metatarsals I and III, vertebrae, and phalanges, Elder Ranch, Cottonwood Creek; F:AM 49194, right ramus with c1–m2 and m3 alveolus, ''B'' Quarry; F:AM 61300, partial skull with I2–M2, ''B'' Quarry; F:AM 61301, left partial maxillary with P3–M1, D. C. Quarry; F:AM 104693, left partial ramus with p1–p3 alveoli, m1 broken–m2 and m3 alveolus, Cottonwood Creek Quarry; F:AM 104695, left partial ramus with p1 alveolus, p2–p3 broken, p4–m2, and m3 alveolus, Cottonwood Creek Quarry; F:AM 104699, right maxillary fragment with C1–P1 alveoli and P2–P3, ''B'' Quarry; F:

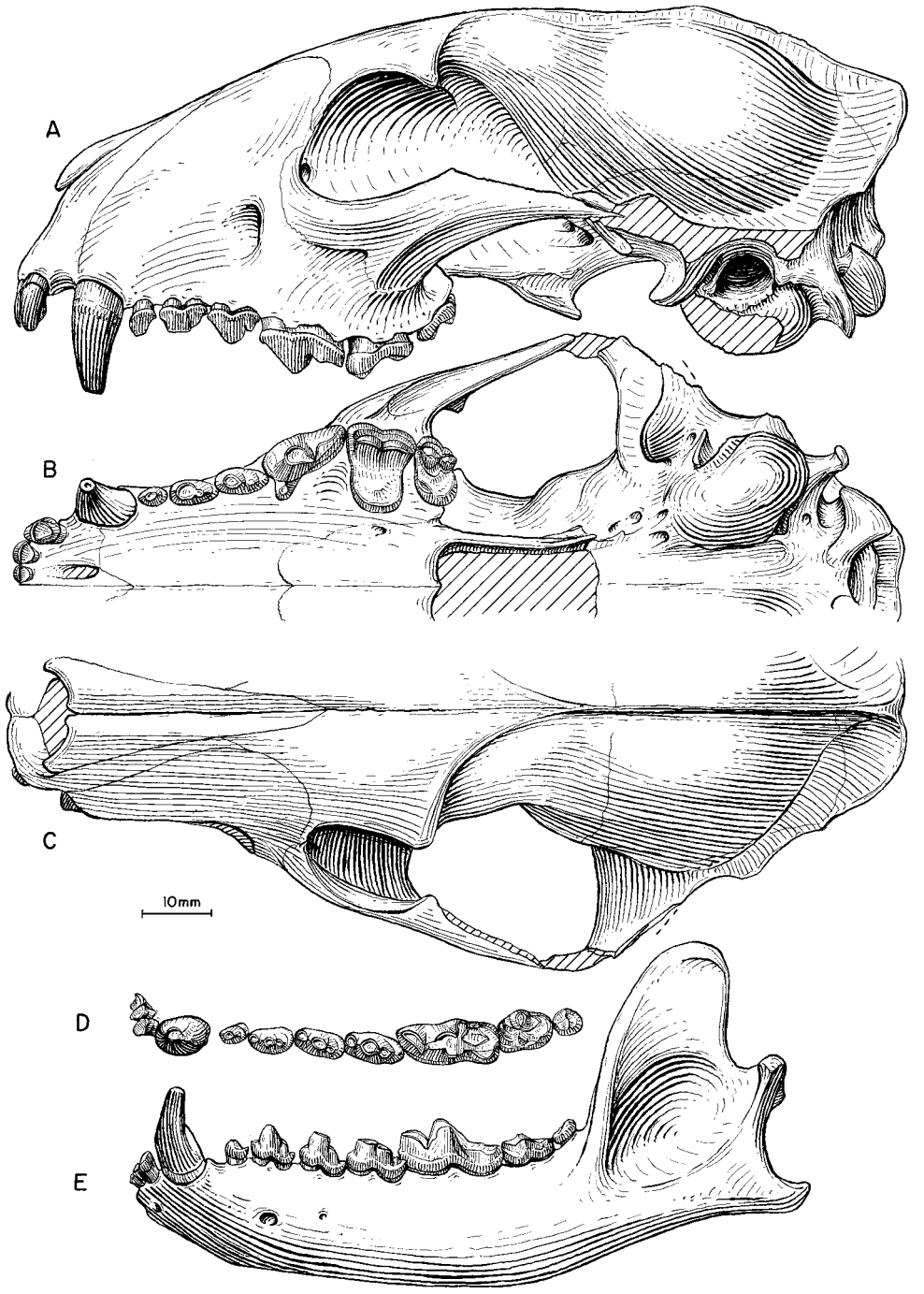

Fig. 45. *Desmocyon matthewi*. **A**, Lateral, **B**, ventral, and **C**, dorsal views of skull, **D**, lower teeth, and **E**, ramus, F:AM 49177, holotype, Marshall Ranch, Runningwater Formation (early Hemingfordian), Dawes County, Nebraska.

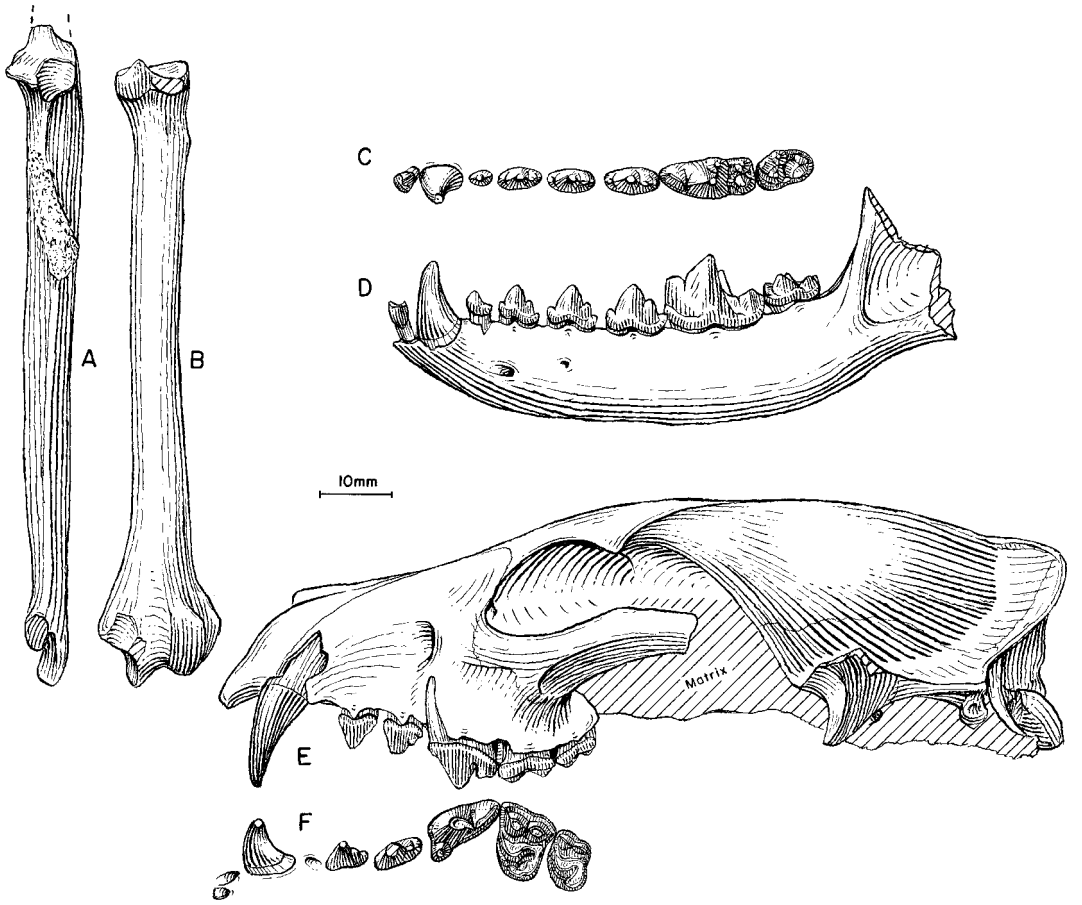

Fig. 46. **A**, Partial ulna and **B**, radius, *Desmocyon matthewi*, F:AM 49176, Elder Ranch, Runningwater Formation (early Hemingfordian), Dawes County, Nebraska. **C**, Lower teeth and **D**, ramus, *D. matthewi*, F:AM 49181, 4 ft above *Aletomeryx* Quarry, Runningwater Formation (early Hemingfordian), Cherry County, Nebraska. **E**, Lateral view of skull and **F**, upper teeth (M2 reversed from right side), *D. thomsoni*, F:AM 62890, East Channel Prospect, Runningwater Formation (early Hemingfordian), Box Butte County, Nebraska.

AM 104701, right ramal fragment with m1 broken, m2, and m3 alveolus, northwest of Marsland; F:AM 105335, left partial maxillary with P4–M1, Cottonwood Creek Quarry; and F:AM 105336, right ramus fragment with m1, Cottonwood Creek Quarry.

Upper part of the Runningwater Formation (early Hemingfordian), Cherry County, Nebraska: F:AM 25439, left partial ramus with i1–i3 alveoli and c1 broken–m2 (m1 broken and m3 alveolus), above *Aletomeryx* Quarry; F:AM 25467, right isolated M1, *Aletomeryx* Quarry, Antelope Creek; F:AM 49181, right and left rami with i3–m2 and m3 alveolus (fig. 46C, D), 4 ft above *Aletomeryx* Quarry; F:AM 49185, left maxillary fragment with M1, right ramal fragment with m1–m2 and left isolated m2, upper *Aletomeryx* zone, 18 mi east of *Aletomeryx* Quarry; and F:AM 61299, right partial ramus with p1–p3 alveoli, p4–m1 both broken, m2, and m3 alveolus, 10 ft above *Aletomeryx* Quarry zone.

Upper part of Runningwater Formation (early Hemingfordian), Box Butte County, Nebraska: UNSM 25627 (F:AM cast 97146), right partial ramus with p4–m2 and m3 alveolus, Hemingford Quarry (UNSM loc. Bx-7).

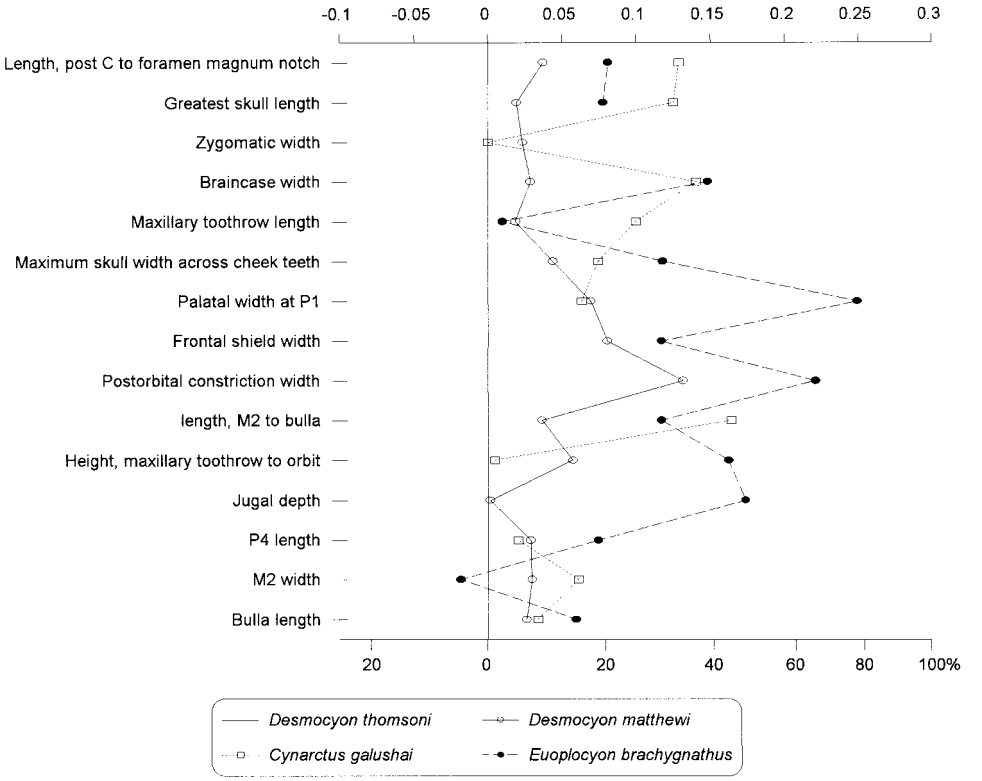

Fig. 47. Log-ratio diagram for cranial measurements of *Desmocyon*, *Cynarctus*, and *Euoplocyon* using *Desmocyon thomsoni* as a standard for comparison (straight line at zero). See text for explanations and appendix II for measurements and their definitions.

Runningwater Formation (early Hemingfordian), 2 mi west of Pole Creek, Cherry County, Nebraska: F:AM 61312, right ramus with c1 and p1 alveolus–m3; and F:AM 62880, isolated left m1.

Miller Locality (early Hemingfordian), Suwannee River, Dixie? County, Florida: KUVP 11453, right ramus with p1–p3 alveoli, p4–m1, and m2–m3 alveoli; KUVP 114454, right ramus with p2, p4, and alveoli of the rest of teeth; KUVP 114455, right ramus with p4–m1 and alveoli of the rest of cheekteeth; KUVP 114456, left ramal fragment with m1–m2; KUVP 114458, left ramus with c1–p2 alveoli and p3–m1; KUVP 114462, right ramal fragment with p1–p3 alveoli and p4; KUVP 114466, right ramus with p4–m1 and alveoli of the rest cheekteeth; KUVP 114467, left ramal fragment with c1–p3 alveoli and p4–m1 broken; KUVP 114472, left ramus with m1–m2, and p4 and m3 alveoli; and KUVP 116621 (cast), left ramus with c1–p2 alveoli, p3–m2, and m3 alveolus.

DISTRIBUTION: Early Hemingfordian of Nebraska and Florida.

DIAGNOSIS: Synapomorphic features that distinguish *Desmocyon matthewi* and higher taxa from *D. thomsoni* are posterior process of premaxillary meeting nasal process of frontal; frontal sinus enlarged, penetrating postorbital process and extending posteriorly to near frontal-parietal suture; frontal shield wide relative to width of braincase; postorbital width of frontals greater; and m1 talonid usually with transverse cristid between entoconid and hypoconid.

DESCRIPTION AND COMPARISON: Although the tips of the premaxillary and frontal may begin to touch each other in some individuals of *Desmocyon thomsoni* and also in *Phlaocyon leucosteus* (probably due to its brachy-

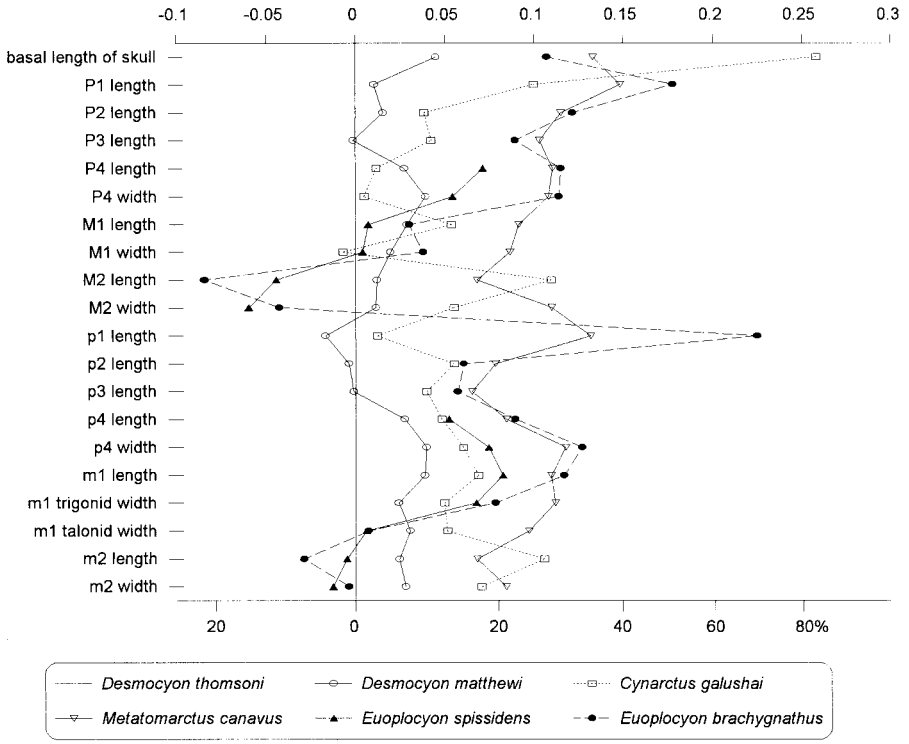

Fig. 48. Log-ratio diagram for dental measurements of *Desmocyon*, *Cynarctus*, *Metatomarctus*, and *Euoplocyon* using *Desmocyon thomsoni* as a standard for comparison (straight line at zero). See text for explanations and appendix III for summary statistics of measurements and their definitions.

cephalic skull), the contact of these two bones are firmly established only in *D. matthewi* and higher taxa—the transverse width of this zone of contact is 2 mm or more. The more extensive frontal sinus in *D. matthewi* can be inferred from its broader and more domed frontal shield in the holotype and can be observed in a dissected specimen, F:AM 61300. The sinus in the latter can be seen to invade the postorbital process extending back toward the frontal-parietal suture. Quantitatively, this sinus expansion is readily demonstrated in the ratio diagram of cranial measurements, which shows a conspicuously broadened postorbital constriction (fig. 47).

Dentally, *Desmocyon matthewi* is little different from *D. thomsoni* both in size and proportions (fig. 48), and as discussed under *D. thomsoni*, differentiation of fragmentary materials between *D. thomsoni* and *D. matthewi* is sometimes difficult. The only derived feature in *D. matthewi* is the usual possession of a transverse crest between the hypoconid and entoconid in m1. Presence of this transverse crest delineates a small basin on the posterior end of the talonid—a hypoconulid shelf. Heavy wear on some specimens referred to *D. matthewi*, however, prevents direct observation of this feature.

The small sample, mostly fragmentary lower jaws, from the Miller Local Fauna of Florida is closely comparable with those from Nebraska. Nearly all (5 of 6 individuals) have acquired the transverse crest between the hypoconid and entoconid on m1s, a character of the species. The only noticeable variation is in the slightly longer m2s in the Florida sample.

DISCUSSION: Specimens of *Desmocyon matthewi* are rather rare and are confined to a few quarries in the upper part of the Runningwater Formation of Nebraska and the correlative Miller Local Fauna of Florida. This phylogenetically transitional species quickly gave rise to the more derived Cynarctina and *Metatomarctus*. Both *Metato-*

marctus and early members of the Cynarctina co-occur with *Desmocyon matthewi* in the early Hemingfordian of Nebraska.

SUBTRIBE CYNARCTINA MCGREW, 1937, new rank

TYPE GENUS: *Cynarctus* Matthew, 1902.

INCLUDED GENERA: *Paracynarctus*, new genus; and *Cynarctus* Matthew, 1902.

DISTRIBUTION: Early Hemingfordian through early Clarendonian of North America.

EMENDED DIAGNOSIS: The Cynarctina shares with *Metatomarctus* a single derived character of a lateral accessory cusp on the I3 that distinguishes it from the more primitive *Desmocyon*. The cynarctine clade is distinguished from *Metatomarctus* and *Euoplocyon* in its hypocarnivorous characteristics: a small subangular lobe on mandible, high mandibular condyle, short P4 relative to upper molars, enlarged M2, m1 protostylid, elongated m2 with strong anterolabial cingulum, and m3 elongate with basined trigonid. In addition, the Cynarctina primitively lacks a distinct parastyle crest on the P4, as is present in *Metatomarctus* and more derived taxa.

Paracynarctus, new genus

TYPE SPECIES: *Paracynarctus sinclairi*, new species.

ETYMOLOGY: Greek: *para*, near; *Cynarctus*, indicating relationship to the genus *Cynarctus*.

INCLUDED SPECIES: *Paracynarctus kelloggi* (Merriam, 1911) and *Paracynarctus sinclairi*, new species.

DISTRIBUTION: Early Hemingfordian of Nebraska and Delaware; medial to late Hemingfordian of New Mexico; late Hemingfordian of Wyoming and Nevada; late Hemingfordian or early Barstovian of Colorado; Hemingfordian of California; early Barstovian of Nebraska, Nevada, California, and New Mexico; and late Barstovian of Nevada.

DIAGNOSIS: In addition to the derived characters shared by *Paracynarctus* and *Cynarctus* (see diagnosis of subtribe Cynarctina), three derived characters are possessed by all species of *Paracynarctus*: diastemata between premolars, P4 with strong lingual cingulum or hypocone, and cleft on lingual cingulum of M1 and M2 separating near cusplike development of anterolingual cingulum from hypocone. In addition, most *Paracynarctus* lacks a transverse cristid on m1 talonid (a reversal). *Paracynarctus* is distinguishable from *Cynarctus* in its lack of synapomorphies of the latter clade: narrowed auditory opening, recurved c1, and elongated M1.

DISCUSSION: The presence of a small hypocone on the P4 and quadrate upper molars in *Paracynarctus* (especially in *P. sinclairi*), in contrast to the lack of these features in *Cynarctus*, suggests that *Paracynarctus* arrived at a moderate level of hypocarnivory in a way that differs from *Cynarctus*. Furthermore, *Paracynarctus* entirely lacks the numerous synapomorphies in the *Cynarctus* clade that are related to further reduction of premolars, enlargement of complex lower molars, narrowed auditory meatus, and other features. Despite such divergent approaches to hypocarnivory, there are several shared derived characters between *Paracynarctus* and *Cynarctus* that suggest a sister relationship (diagnosis of Cynarctina).

Paracynarctus kelloggi (Merriam, 1911)

Figures 49, 50, 51A–H

Tephrocyon kelloggi Merriam, 1911 (in part): 235, pl. 32, figs. 1, 2, 6, and 7; 1913: 367, fig. 9a, b. Green, 1948: 81.

Tephrocyon near *kelloggi* (Merriam): Merriam, 1911: 237, fig. 7; 1913: 368, fig. 13; 1916: 174, fig. 2a, b.

Tomarctus kelloggi (Merriam): Bode, 1935: 87. Munthe, 1988: 91, figs. 21, 22 (in part).

Cynodesmus kelloggi (Merriam): Stirton, 1939a: 628–629. Downs, 1956: 236.

Cynodesmus casei Wilson, 1939: 315, figs. 1, 2.

Tomarctus casei (Wilson): White, 1941b: 95.

Tomarctus ? *kelloggi* (Merriam): Henshaw, 1942: 108, figs. 1, 1a, 2, 2a. Munthe, 1998: 135.

Tomarctus cf. *T. thomsoni* (Matthew, 1907): Emry and Eshelman, 1998: 160, fig. 2M, L.

HOLOTYPE: UCMP 11562 (AMNH cast 27873), right and left partial rami with c1 broken–m2 (p3–p4 broken and m3 alveolus) (fig. 49G, H), from UCMP loc. 1065, Virgin Valley, Virgin Valley Formation (early Barstovian), Humboldt County, Nevada.

REFERRED SPECIMENS: From the type area, Virgin Valley, Virgin Valley Formation (early Barstovian), Humbolt County, Nevada: UCMP 11474 (Merriam, 1911: fig. 6), right

ramus with c1–m1 all broken and m2, UCMP loc. 1065; and UCMP 15546 (IT 114), right maxillary fragment with P4–M1.

From Split Rock Formation (late Hemingfordian), Fremont County, Wyoming (listed by Munthe, 1988, in part): ACM 11391 (AMNH cast 89734) (Munthe, 1988: figs. 21, 22), partial skull with P4–M2 (fig. 49A, B), basicranium, occiput, right and left rami with c1–m3 (fig. 49C, D), scapholunar, trapezium, trapezoid and metacarpal I, from UCMP loc. V69191, 15 ft above *Brachycrus* Quarry of Falkenbach (1936–1938); CMNH 14708, m3, from UCMP loc. V69190; KUVP 20356, m2, from V69190–69192; MCZ 7321, P4, and two p4s, from V69190–V69192; UCMP 121912 and F:AM 95409 (one individual), P4 fragment, lingual halves of both M1s, both M2s, c1, both p2s, p4, fragments of both m1s, and m2 from UCMP loc. V77149; UCMP 121913, ramal fragment with m1–m2, from V77149; UCMP 121914, ramal fragment with m1, from V77149; UCMP 121915, ramal fragment with p1–p2 from V69190; UCMP 121916 and 121917, M2s, from V69192; UCMP 121918, p4, from V69192; and KUVP 20355, M1, from V69190-69192.

Upper part of the Runningwater Formation (early Hemingfordian), Dawes County, Nebraska: F:AM 99351, left partial ramus with p2–p3, p4 alveolus, and m1 broken, Warren Barnum Ranch.

Canyada Pilares, northern Ceja del Rio Puerco area, local green zone, in Canyada Pilares Member, Zia Formation (early Hemingfordian), New Mexico: F:AM 27352, left premaxillary-maxillary with I1–I2, I3 broken, and C1–M2 (fig. 49E, F).

Pollack Farm Site (Delaware Geological Survey locality Id11-a), lower shell bed of Cheswold sands, lower Calvert Formation (late early Hemingfordian), near Cheswold, Delaware: USNM 475812, isolated right P4 (referred to *Tomarctus* cf. *T. thomsoni* by Emry and Eshelman, 1998: fig. 2M, L).

Kiva Quarry near the divide between Canyada de Zia and Canyada Piedra Parada, Zia Formation (late Hemingfordian), Jemez Creek Area, Sandoval County, New Mexico: F:AM 50142, left ramus with i1–i3 broken and c1–m3 (p1 broken); and F:AM 50144, right ramus with c1–m3 (fig. 49I, J).

Massacre Lake Local Fauna (late Hemingfordian), Washoe County, Nevada: UCMP loc. V6161: UCMP 75844, left maxillary with P1–P3 alveoli and P4–M1. Big Basin: USGS M1094, left maxillary fragment with M1–M2.

White Operation Wash, ''Double Purple'' layer of the Nambe Member, Tesuque Formation (late Hemingfordian), Santa Fe County, New Mexico: F:AM 50140, right partial ramus with p4 broken, m1, m2 alveolus, and m3 unerupted.

Spruce Gulch, 5 mi south of State Bridge, in a volcanic tuff in North Park Formation, late Hemingfordian or early Barstovian (presence of *Brachycrus* and *Mylagaulus* in this locality [Robinson, 1968] suggests a late Hemingfordian or early Barstovian age instead of the late Arikareean estimated by Wilson, 1939), Eagle County, Colorado: UM 18955 (holotype of *Cynodesmus casei* Wilson, 1939), premaxillary-maxillary with C1–P1 broken and P2–M2.

Santa Fe Area, Skull Ridge Member and correlatives, Tesuque Formation (early Barstovian), Santa Fe County, New Mexico: F:AM 27394, right partial ramus with c1–p3 alveoli, p4–m1, and m2 broken; F:AM 27396, anterior part of skull with I1–C1 all broken, P1–P3, and P4–M2 all broken, 3 mi from Cuyamunque; F:AM 27399, left partial ramus with c1 and p2–m2, Tesuque; F:AM 27487, palate with I1–C1 all broken and P1–M2, and mandible with i1–i3 all broken and c1–m3, west of Tesuque (fig. 51A–D); F:AM 27488, left partial ramus with p2–p3 alveoli, p4, and m1 broken–m2, Cuyamunque; F:AM 50135, right premaxillary-maxillary with I2–P4 broken and M1–M2, lower part of light band, east of Tesuque Fault; F:AM 50136, right partial ramus with p4 root and m1–m3 all broken, west of Tesuque, Tesuque Boundary wash, light band east of Tesuque Fault; F:AM 50137, anterior part of skull with I1–M1 and M2 broken (fig. 51E, F), 1 mi east of Cuyamunque; F:AM 50187, right partial ramus with c1 alveolus and p1–m3 all broken, partial left ulna, Tesuque; and F:AM 105097, right partial ramus with p3–m2 (broken) and alveoli of i1–p2, 5 ft below Ash A in block no. 3 south of Arroyo Seco, Skull Ridge.

Phillips Ranch, UCMP loc. 2577, Bopesta

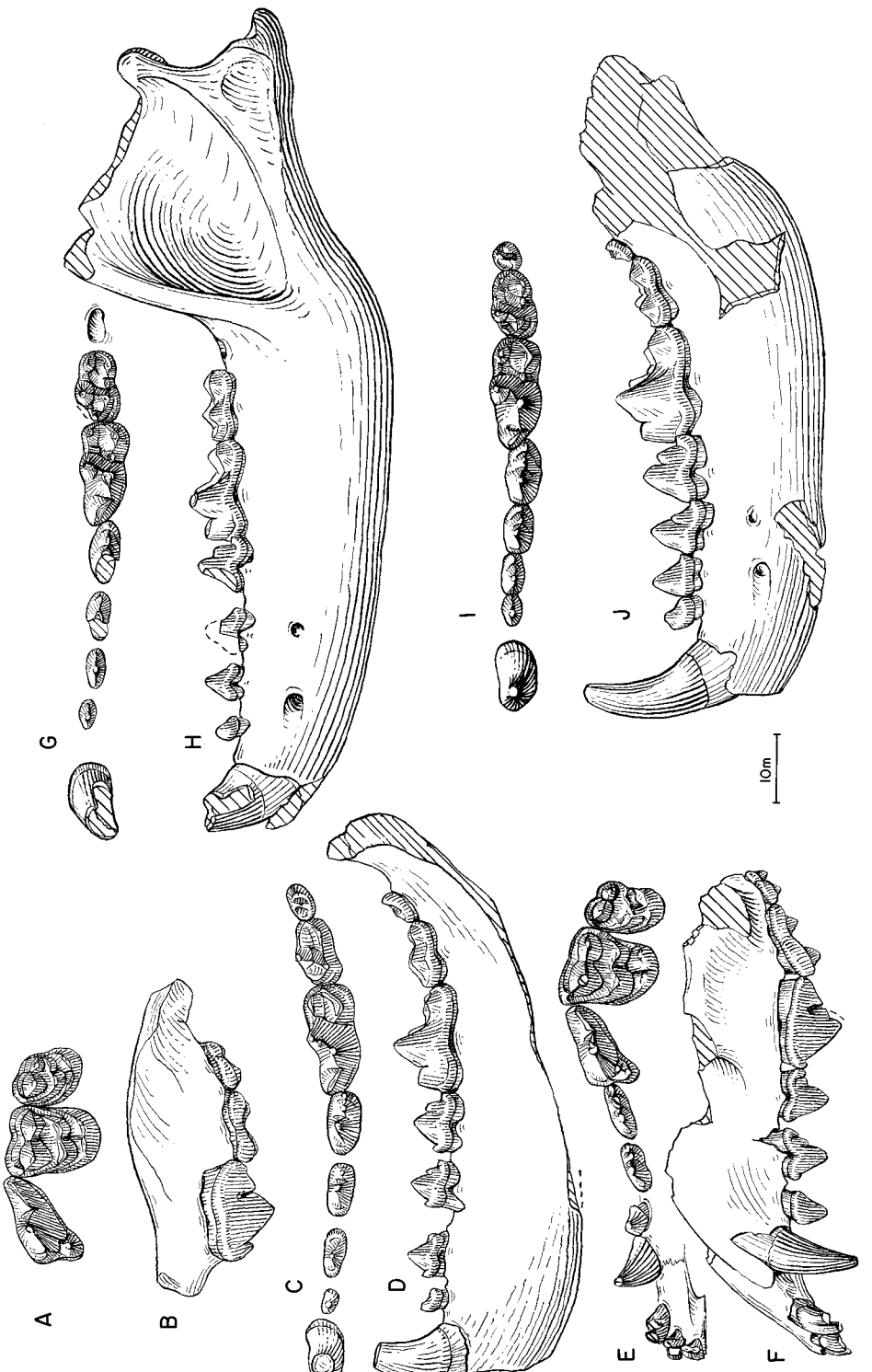

Fig. 49. *Paracynarctus kelloggi*. **A**, Upper teeth, **B**, lateral view of maxillary, **C**, lower teeth, and **D**, ramus, ACM 11391 (all reversed from right side), 15 ft above *Brachycrus* Quarry, Split Rock Formation (late Hemingfordian), Fremont County, Wyoming. **E**, Upper teeth and **F**, lateral view of partial skull, F:AM 27352, Canyada Pilares, Canyada Pilares Member, Zia Formation (medial Hemingfordian), New Mexico. **G**, Lower teeth and **H**, ramus, UCMP 11562, holotype, Virgin Valley, Virgin Valley Formation (early Barstovian), Humboldt County, Nevada. **I**, Lower teeth and **J**, ramus, F:AM 50144 (all reversed from right side), Kiva Quarry, Zia Formation (late Hemingfordian), Sandoval County, New Mexico.

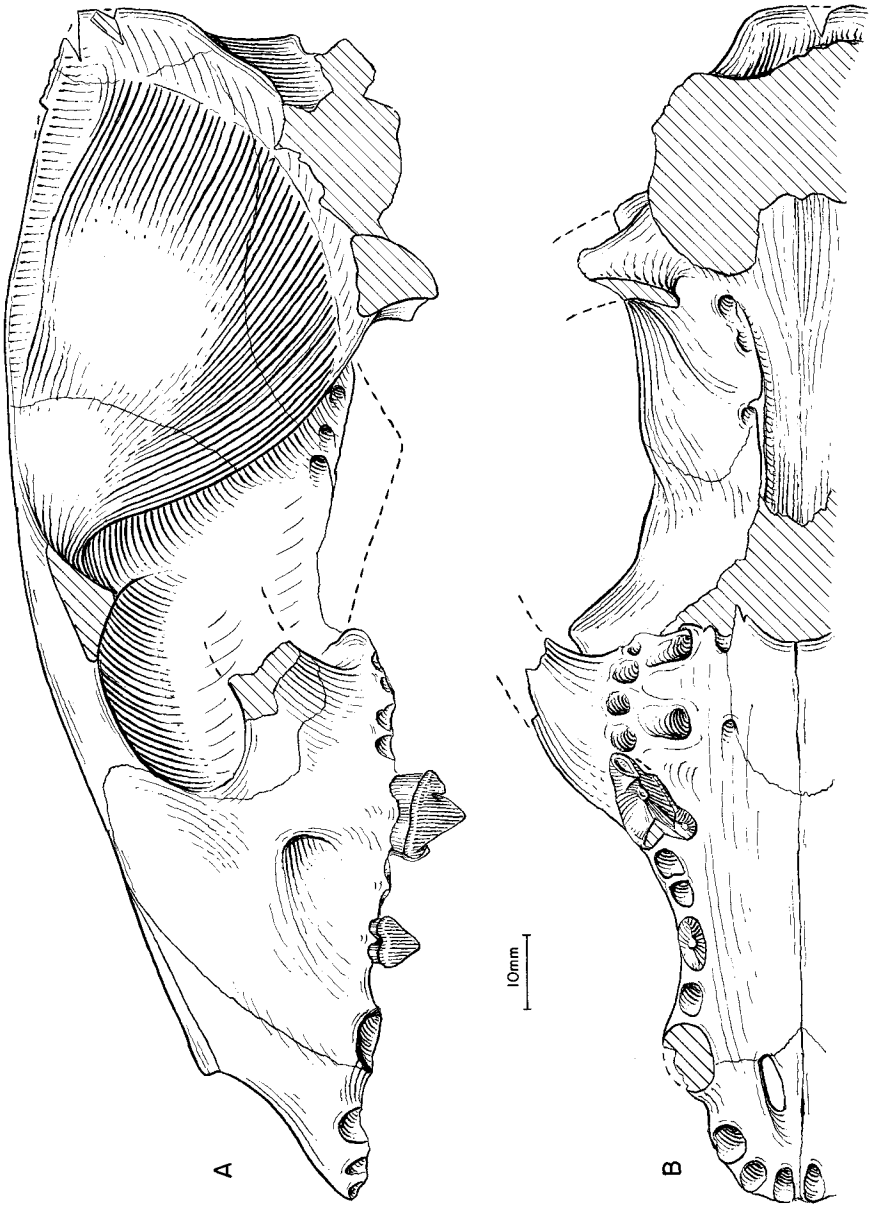

Fig. 50. *Paracynarctus kelloggi*. **A**, Lateral and **B**, ventral views of skull (crushing of skull partially restored), F:AM 61001, Steepside Quarry, Barstow Formation (early Barstovian), San Bernardino County, California.

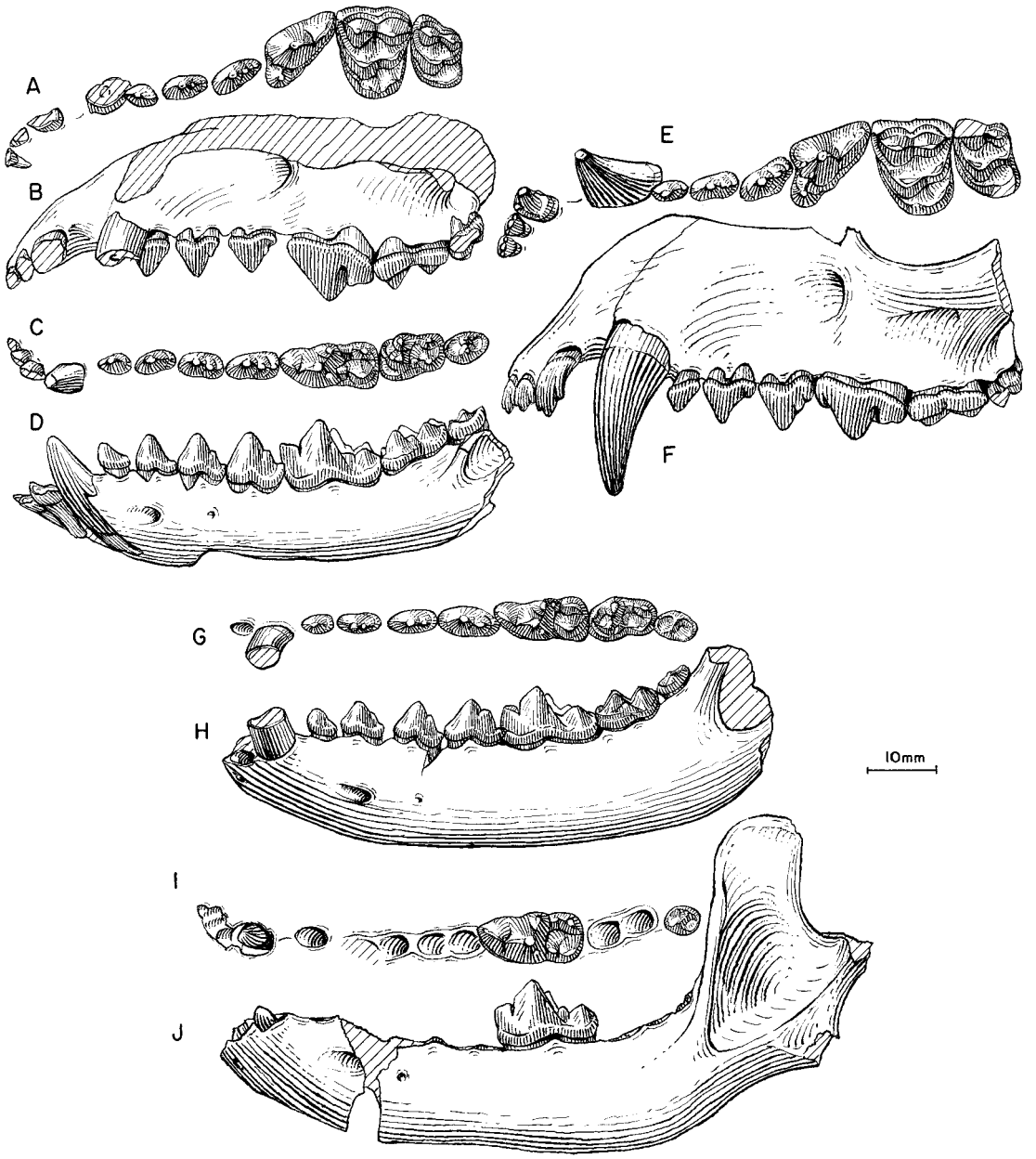

Fig. 51. **A**, Upper teeth (M2 reversed from right side), **B**, lateral view of partial skull, **C**, lower teeth, and **D**, ramus (reversed from right side), *Paracynarctus kelloggi*, F:AM 27487, Santa Fe area, Skull Ridge Member, Tesuque Formation (early Barstovian), Santa Fe County, New Mexico. **E**, Upper teeth (reversed from right side) and **F**, lateral view of partial skull, *P. kelloggi*, F:AM 50137, 1 mi east of Cuyamunque, Skull Ridge Member, Tesuque Formation. **G**, Lower teeth and **H**, ramus, *P. kelloggi*, F:AM 61000 (all reversed from right side), Steepside Quarry, Barstow Formation (early Barstovian), San Bernardino County, California. **I**, Lower teeth and **J**, ramus, *Paracynarctus sinclairi*, F:AM 61007, Humbug Quarry, Olcott Formation (early Barstovian), Dawes County, Nebraska.

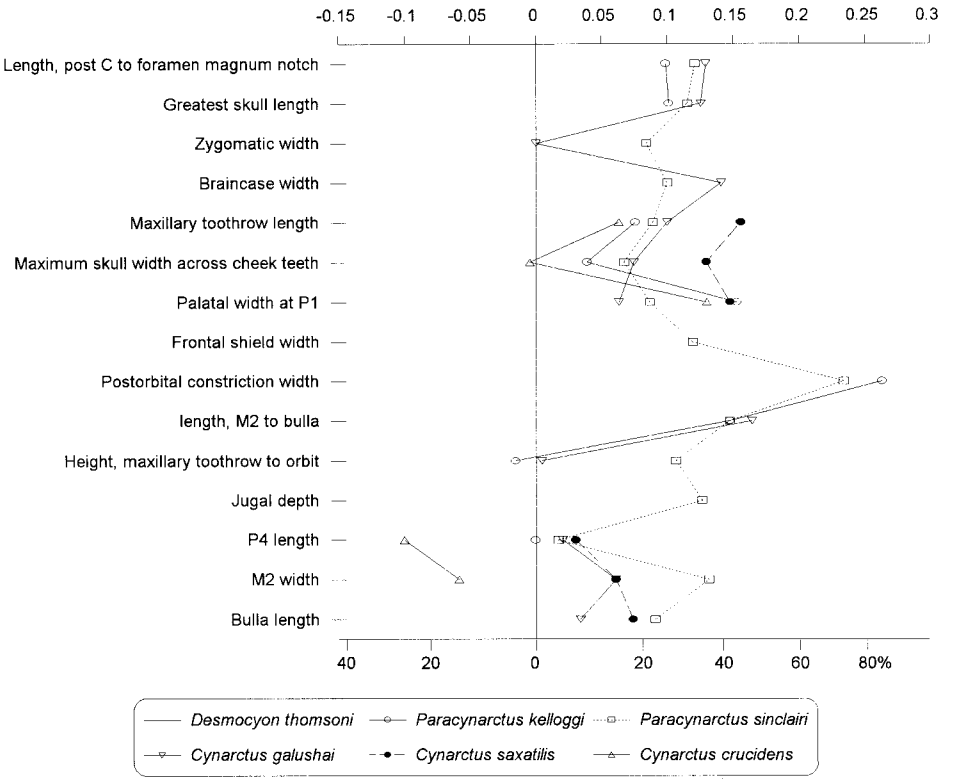

Fig. 52. Log-ratio diagram for cranial measurements of *Paracynarctus* and *Cynarctus* using *Desmocyon thomsoni* as a standard for comparison (straight line at zero). See text for explanations and appendix II for measurements and their definitions.

Formation (late Hemingfordian), Kern County, California: UCMP 45119, left ramal fragment with p4–m1.

Steepside Quarry, Barstow area, Barstow Formation (early Barstovian), San Bernardino County, California: F:AM 61000, left and right partial rami with i3–m3 (fig. 51G, H); F:AM 61001, crushed skull with P2, P4, and alveoli of the rest of teeth (fig. 50); F:AM 61002, right partial ramus with c1, p2–p3 broken, p4–m2, and m3 alveolus; F:AM 61003, left partial ramus with c1–p1 alveoli and p2–m3 (m1–m2 broken); F:AM 61004, right partial ramus with i2 root–c1, p1–p4 broken, m1, and m2 broken; and F:AM 61005, left partial ramus with c1 and p1 root–m3 (m1 broken).

Siebert Formation, Tonopah Local Fauna (LACM loc. 172) (late early Barstovian), San Antonio Mountains, near Tonopah, Nye County, Nevada: LACM-CIT 789 (Henshaw, 1942: pl. 3, figs. 2, 2a), left ramal fragment with m1–m2; LACM-CIT 1235 (Henshaw, 1942: pl. 3, figs. 1, 1a), left partial ramus with p1–m1 and m2 alveolus; UCMP 15972, right and left ramal fragments with m1 and m2; and UCMP 15975, left maxillary fragment with P4–M1 and M2 broken and an isolated M1.

Home Station Pass, unnamed formation (late Barstovian), Pershing County, Nevada: F:AM 49299, right isolated M2; and F:AM 49299A, left isolated M2.

DISTRIBUTION: Early Hemingfordian of Nebraska and Delaware; early to late Hemingfordian of New Mexico; late Hemingfordian of Wyoming, Nevada, and California; late Hemingfordian or early Barstovian of Colorado; early Barstovian of Nevada, California, and New Mexico; and late Barstovian of Nevada.

EMENDED DIAGNOSIS: Synapomorphies

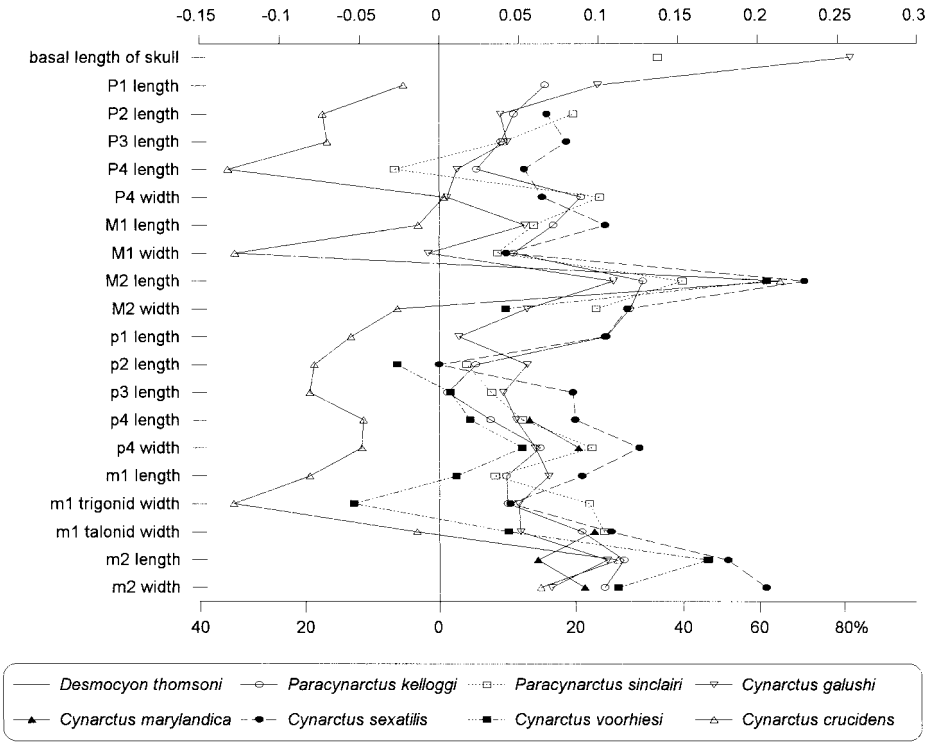

Fig. 53. Log-ratio diagram for dental measurements of *Paracynarctus* and *Cynarctus* using *Desmocyon thomsoni* as a standard for comparison (straight line at zero). See text for explanations and appendix III for summary statistics of measurements and their definitions.

uniting *P. kelloggi* and *P. sinclairi* are a small diastemata between premolars, P4 with strong lingual cingulum or hypocone, and enlarged M1 lingual cingulum which has a transverse cleft. Characters of *P. kelloggi* that are primitive with respect to *P. sinclairi* are horizontal ramus not narrowed, P4 lacking a conical hypocone, and smaller and less quadrate M1 and M2.

DESCRIPTION AND COMPARISON: Despite the numerous referred specimens above, our knowledge of the cranial morphology of this species is still incomplete. The best cranial material available is a crushed skull from the Barstow Formation of California (F:AM 61001). Supplemented by other cranial fragments (e.g., F:AM 50137 and descriptions of ACM 11391 in Munthe, 1988), we may observe the following cranial and dental features. The premaxillary is in full contact with the nasal process of frontal. The frontal sinus reaches the frontal-parietal suture. The nuchal crest is broadly fan-shaped in posterior view, and the lambdoidal crest above the mastoid area is not reduced as in *Microtomarctus* and *Tomarctus*. The opening for the external auditory meatus is large, in contrast to markedly reduced opening in *Cynarctus*.

Upper incisors of *P. kelloggi* are complex. The I3 has small lateral and lingual accessory cusps in addition to the two cusps on the tip. In some individuals, the P1–P3 are slightly reduced in size and are simple in morphology as compared to those in *Desmocyon matthewi* and *Metatomarctus*. The P4 is short and wide (except F:AM 27352), and has a strong lingual cingulum. Such cingulum is particularly well-developed in all Barstovian specimens. All M1s consistently have an elongated lingual cingulum, which is divided by a transverse cleft to delineate a conical hypocone (at this stage, it is still a slight enlargement on the posterolingual corner of the cingulum). The M2 is slightly enlarged relative to the M1 (fig. 53).

The lower canine lacks the sharply re-

curved condition in *Cynarctus*. Lower premolars are small, and some are separated by short diastemata, although individuals from California and New Mexico tend to have more closely spaced premolars, as seen in *Desmocyon matthewi* and more basal taxa. The talonid of m1 is relatively wide. A transverse crest between the entoconid and hypoconid is either lacking or only vaguely developed, and as a result, the talonid basin is wider and deeper than those in *Cynarctus*. The m2 is markedly elongated, often with a well-developed anterolabial cingulum. The m3 is also long.

DISCUSSION: Previous studies of *Paracynarctus kelloggi* placed it in *Tomarctus*, *Tephrocyon*, or *Cynodesmus* (see synonym list above). As summarized by Munthe (1988: 96–98), the low-crowned premolars in *P. kelloggi* seemed at odds with other species of *Tomarctus* in the traditional sense (*Desmocyon* through *Tomarctus* in this study), which tend to have strong, high-crowned, multicuspid premolars. In the broader view afforded by this study, *P. kelloggi* has a combination of meso- and hypocarnivorous characters (including the low-crowned premolars) to be a cynarctine, and, more specifically, its development of a strong P4 lingual cingulum and a cleft on the M1 lingual cingulum further ally itself to *P. sinclairi*.

The early Hemingfordian presence of *P. kelloggi* is indicated by a jaw fragment from the upper part of the Runningwater Formation of Nebraska (F:AM 99351). This individual agrees in some aspects of the dental morphology of *P. kelloggi* (reduction of premolars, widening of the m1 talonid, presence of a protostylid on m1, and a deep talonid basin). Pending additional materials from this locality, it may be viewed as an early representative of this species.

Wilson's (1939) *Cynodesmus casei* from Spruce Gulch, Colorado, is here synonymized with *Cynarctus galushai*. Based on his descriptions and illustrations (Wilson, 1939: 315–317, figs. 1, 2), the holotype of *casei* possesses all the diagnostic characters of *Paracynarctus kelloggi*, although it is slightly smaller in dental dimensions.

Emry and Eshelman (1998: 160, fig. 2M, L) recently referred a single P4 from the Pollack Farm Site, Delaware, to *Tomarctus* cf. *T. thomsoni*. Their published figure shows that this upper carnassial has a strong cingulum on both anterior and lingual sides, and a narrower cingulum on the labial side. Furthermore, the P4 has a large protocone and a small parastyle. All of these features suggest a cynarctine affinity, although the limited material available prevents from a secure identification. If our reference of the Delaware specimen to *Paracynarctus kelloggi* is correct, it is only the second record of cynarctine in the east coast of United States (the other is *Cynarctus marylandica*; see below).

Paracynarctus sinclairi, new species

Figures 51I, J, 54

HOLOTYPE: F:AM 61009, skull with I1–I3 alveoli and C1–M2 (P1 alveolus) (fig. 54), from Quarry 2, Olcott Formation (early Barstovian), Sioux County, Nebraska.

ETYMOLOGY: Named for the eminent vertebrate paleontologist W. J. Sinclair of Princeton University who directed collecting in the Sioux County area early in the twentieth century.

REFERRED SPECIMENS: Olcott Formation (early Barstovian), Dawes County, Nebraska: F:AM 49135, right partial maxillary with P4–M2, New Surface Quarry; F:AM 61007, left partial ramus with c1 erupting, m1, m3 unerupted, and alveoli of i1–i3, p1–p4, and m2 (fig. 51I, J), Humbug Quarry; F:AM 61008, left partial ramus with p2 and p4 and alveoli for p1, p3, and m1–m3, Quarry 2; F:AM 61008A, left ramus with i1–p1 alveoli, p2, p3–p4 alveoli, m1 broken, and m2–m3 alveoli, Boulder Quarry; and F:AM 61040, partial right ramus with c1–p1 alveoli and p2–m3 (m2 broken), West Sinclair Draw.

Observation Quarry, Sand Canyon Formation (early Barstovian), Dawes County, Nebraska: F:AM 54480, right isolated M2; F:AM 61006, right isolated P4; and F:AM 105095, left broken isolated M1.

DISTRIBUTION: Early Barstovian of Nebraska.

DIAGNOSIS: Derived characters that distinguish *P. sinclairi* from *P. kelloggi* are the presence of a P4 hypocone and larger and subquadrate M1–M2.

DESCRIPTION AND COMPARISON: The excel-

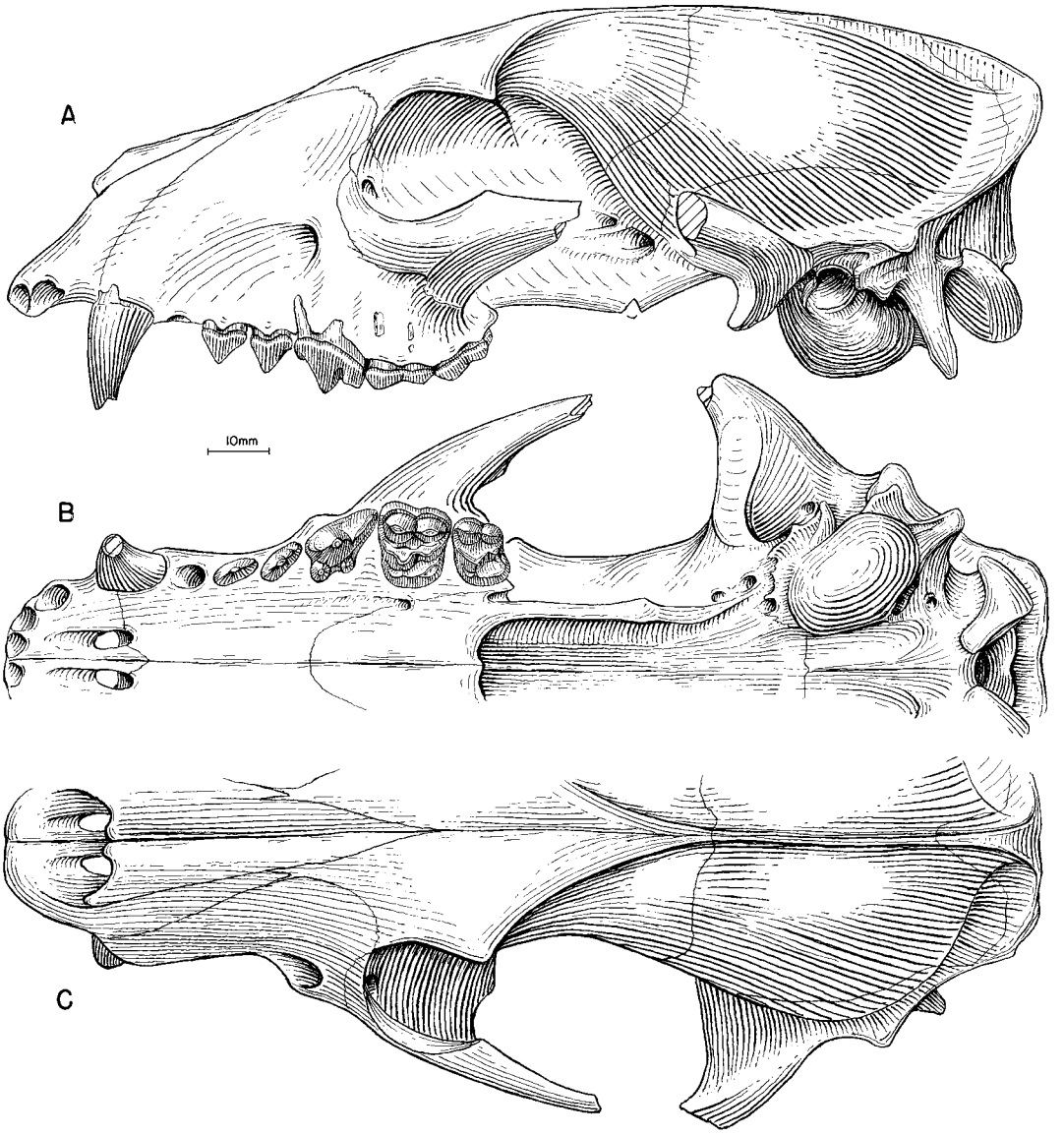

Fig. 54. *Paracynarctus sinclairi*. **A**, Lateral, **B**, ventral, and **C**, dorsal views of skull, F:AM 61009, holotype, Quarry 2, Olcott Formation (early Barstovian), Sioux County, Nebraska.

lently preserved skull of the holotype affords a suitable basis of comparison of the cranial morphology of this species. The premaxillary process is in full contact with the nasal process of the frontal, and the contact region is 2.5 mm in the narrowest section. The frontal sinus is well developed and extends to the frontal-parietal suture. The nuchal crest is not expanded posteriorly as it is in *Microtomarctus* and *Tomarctus*, and its outline forms a broad fan as in *Cynarctus*, *Psalidocyon*, and more primitive forms. The bulla is moderately inflated but not as bulbous as in *Cynarctus*. The opening for the external auditory meatus is relatively large and still has a V-shape notch toward the postglenoid process, in contrast to narrowed, rounded external openings in *Cynarctus*.

The upper premolars are slightly reduced, both in size and accessory cusplets, relative to those in *Metatomarctus*. The P4 is short relative to the M1, and has a distinct hypocone (F:AM 61009) or a prominent enlargement of the anterior segment of the lingual cingulum just behind the protocone (F:AM 49135, 61006). The M1 in the holotype is nearly quadrate because of the widening of the lingual cingulum, especially toward the anterolingual corner. This expansion of the lingual border, however, is not as prominent in F:AM 49135 and 105095. F:AM 49135 and 61006 are also significantly smaller in size than the holotype (averaging 21% smaller in all dental measurements), and may represent a distinct species when more complete materials are known. The M2 is large, as in *P. kelloggi*.

No associated lower jaw exists for *P. sinclairi*, and the present reference to this species of four partial rami is necessarily provisional. A weak subangular lobe is present in F:AM 61008A but is less developed in F:AM 61007 because of the younger age of the latter. The m1 in F:AM 61007 is somewhat peculiar in its prominent development of a conical cristid obliqua anterior to the hypoconid behind the protoconid. This cusp is not present in F:AM 61008A or is weakly developed in most other Cynarctina. There is a protostylid in F:AM 61007, but it is so weak that no more than a slight impression is visible. The m1 in F:AM 61007 is also highly crenulated. As in *P. kelloggi*, the m2 is enlarged.

DISCUSSION: The moderately hypocarnivorous dentition in *P. sinclairi* has a distinctly different configuration from those of *Cynarctus*. In *P. sinclairi* the form of the P4 hypocone and the quadrate M1 with its strong lingual cingulum, but not a distinct, conical hypocone, is opposite to the case in *Cynarctus*. Both forms of hypocarnivory in *Paracynarctus* and *Cynarctus* are evidently derived features with respect to primitive conditions in *Metatomarctus* and *Desmocyon matthewi*, and that in *P. kelloggi* and *P. sinclairi* thus helps to define a clade distinct from *Cynarctus*.

Cynarctus Matthew, 1902

TYPE SPECIES: *Cynarctus saxatilis* Matthew, 1902.

INCLUDED SPECIES: *Cynarctus galushai*, new species; ?*Cynarctus marylandica* (Berry, 1938); *Cynarctus saxatilis* Matthew, 1902; *Cynarctus voorhiesi*, new species; and *Cynarctus crucidens* Barbour and Cook, 1914.

DISTRIBUTION: Early Barstovian of Maryland and California; late Barstovian of Nebraska, Colorado, and California; early Clarendonian of Nebraska, South Dakota, and Texas; late Clarendonian of Nebraska; and Clarendonian of Texas.

EMENDED DIAGNOSIS: Derived characters that distinguish *Cynarctus* from *Paracynarctus* are an auditory meatus of small diameter with a small lip, M1 transversely narrow and subquadrate, c1 strongly recurved, and p4 posterolingual shelf with weak ''metastylid'' sometimes present. In addition, *Cynarctus* and *Paracynarctus* share several derived dental features distinguishable from those of *Metatomarctus* and more primitive taxa: a weak subangular lobe, a high mandibular condyle, short P4 relative to M1, enlarged M2, presence of a m1 protostylid, widened m1 talonid, and elongated m2 and m3.

DISCUSSION: Of the several independent attempts by the borophagines to develop hypocarnivorous dentitions, *Cynarctus* has gone the farthest. As the name implies, *Cynarctus* is rather ursidlike in many features, such as in the reduction of its premolars, posterior expansion of M2, shortening of m1 trigonid, and enlargement of the m1 talonid. Matthew (1902) initially thought *Cynarctus* was an amphicyonid, and did not mention this genus in his subsequent treatment of the canid phylogeny (Matthew, 1924, 1930). McGrew (1937, 1938a), on the other hand, was impressed by its hypocarnivorous dentition and placed *Cynarctus*, along with *Cynarctoides* and *Phlaocyon*, in the Procyonidae.

Basicranial morphology of *Cynarctus*, available for *C. galushai* and *C. crucidens* from the F:AM collection, shows a typical canid middle ear (i.e., inflated entotympanic bulla, presence of an alisphenoid canal, absence of a deep suprameatal fossa). Coupled with typical borophagine cranial and dental features, more clearly seen in *C. galushai*, these morphologies firmly place *Cynarctus* within the borophagine clade.

Cynarctus galushai, new species

Figure 55

HOLOTYPE: F:AM 27543, crushed skull with I1–I3 alveoli, C1, and P1 alveolus–M2 and right and left partial rami with i1–m2 (fig. 55A, B), Valley View Quarry, ''Second Division,'' Barstow Formation (late early Barstovian), San Bernardino County, California.

ETYMOLOGY: Named in honor of Ted Galusha, Frick Curator Emeritus, American Museum of Natural History, who collected many of the specimens cited in this paper.

REFERRED SPECIMENS: ''Second Division,'' Barstow Formation (late early Barstovian), San Bernardino County, California: F:AM 27542, left ramus with i3 root–m3 (p1 alveolus and p3 broken) (fig. 55E, F), Valley View Quarry.

''First Division,'' Barstow Formation (early late Barstovian), San Bernardino County, California: F:AM 27268, right and left partial rami with i1–p1 alveoli, p2–m2, and m3 alveolus, no data but preservation suggests *Hemicyon* Quarry; F:AM 27283, left partial maxillary with P4 broken–M1 and M2 alveolus, no locality data; F:AM 27312, right partial ramus with p4–m2 and alveolus of p3; F:AM 27545, left partial ramus with c1, p1 and p3 alveoli, p2 broken, and p4–m2, Skyline Quarry; F:AM 27546, left partial ramus with p2–p4, m1 broken, m2 root, and m3 alveolus, Skyline Quarry; F:AM 27547A, right partial ramus with c1 broken, p2, m1, and alveoli of p1, p3, p4, and m2, Skyline Quarry; F:AM 27547B, right partial ramus with p4–m1 and roots of p1–p3 and m2, Skyline Quarry; F:AM 27550, palate with I1–C1 alveoli, P1–M2, and isolated left I3 (fig. 55C, D), Skyline Quarry; F:AM 61011, left partial ramus with c1–p2 alveoli, p3–m1 broken, and m2, Skyline Quarry; F:AM 61015, partial mandible with c1 and p1 alveolus–m3 (p3 broken), Skyline Quarry; F:AM 67130, left ramal fragment with p4–m1, Skyline Quarry; and F:AM 67367, left partial ramus with c1 broken, p3–m1, associated isolated m2 (p2, m2, and m3 alveoli), Sunnyside Quarry.

DISTRIBUTION: Early to late Barstovian of California.

DIAGNOSIS: *Cynarctus galushai*, the basalmost species of the genus, shares with *C. saxatilis* through *C. crucidens* derived characters for the genus: small external auditory meatus, M1 transversely narrow, recurved c1, and presence of a weak cusp on p4 posterolingual shelf. *C. galushai* can be further distinguished from *Paracynarctus* in its primitive state of the following characters: absence of a widened P4 lingual cingulum and lack of anteriorly expanded M1 lingual cingulum. No autapomorphic characters are recognized for *C. galushai*. Characters of *C. galushai* that are primitive with respect to *C. saxatilis* through *C. crucidens* are premolars more closely spaced; P4 protocone of moderate size and lingual cingulum weak; M1 and M2 labial cingulum strong; m1 protostylid and metastylid weak, metaconid of moderate size and low relative to height of protoconid; and m2 metaconid moderately high, anterolabial cingulum weak, protostylid weak, and metastylid weak or absent.

DESCRIPTION AND COMPARISON: The holotype, although severely crushed dorsoventrally, represents the best cranial material available. Much of the skull roof is collapsed onto the basicranium. Despite this damage, the frontal sinus can still be seen to extend to the frontal-parietal suture. The nuchal crest is fan-shaped in outline, as is in *Psalidocyon*, and the lambdoidal crest is complete. The bullae are not crushed (better preserved on the left side) and show a narrow opening for the external auditory meatus, as is characteristic of *Cynarctus*. The mandible in the holotype is less distorted than is the cranium. It has a rather elevated ventral border of the masseteric fossa (nearly to the level of the upper border of the horizontal ramus). However, some referred specimens of this species (e.g., F:AM 27542, 27546, 61015) have lower masseteric fossae. There is a weak subangular lobe.

Dental morphology of *C. galushai* is only slightly modified toward the hypocarnivorous dentition that characterizes the advanced species from *C. saxatilis* and above. Premolars are generally short and lower crowned, although not as markedly so as in more derived species such as *C. voorhiesi* and *C. crucidens*. The M1 begins to show a slightly transversely narrowed appearance, but this proportional trait is still subtle at this stage

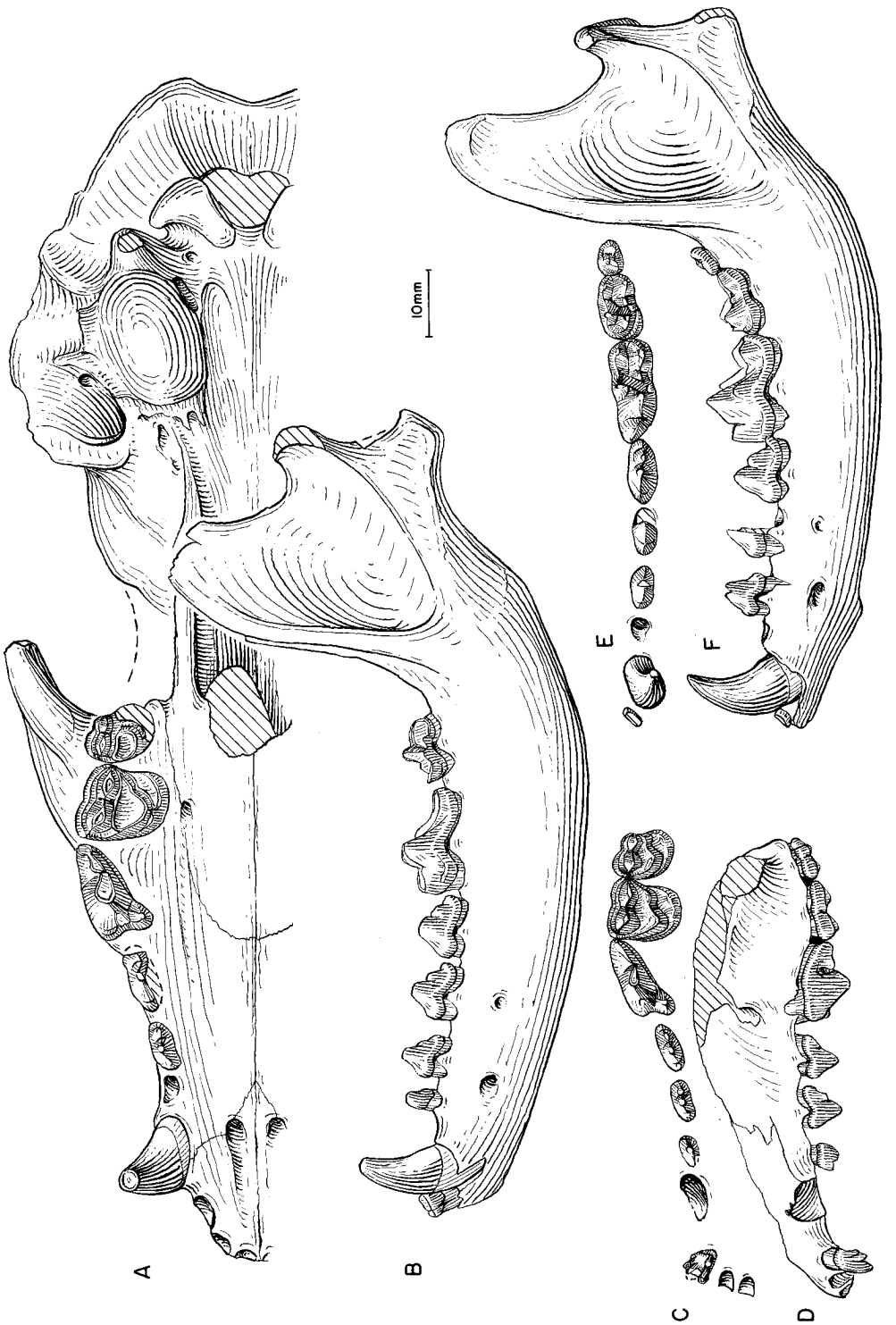

Fig. 55. *Cynarctus galushai*. **A**, Ventral view of skull and **B**, ramus, F:AM 27543, holotype, ''Second Division,'' Barstow Formation (late early Barstovian), San Bernardino County, California. **C**, Upper teeth and **D**, lateral view of partial skull, F:AM 27550, Skyline Quarry, ''First Division,'' Barstow Formation (early late Barstovian), San Bernardino County, California. **E**, Lower teeth and **F**, ramus, F:AM 27542, Valley View Quarry, ''Second Division,'' Barstow Formation (late early Barstovian), San Bernardino County, California.

(see fig. 53). Similarly, the enlargement of the M2 is only in the beginning stage, which is more readily observable in the ratio diagram (fig. 53). The metaconule of M1–M2 is slightly enlarged relative to those in *Desmocyon matthewi*, and the lingual cingulum of M1–M2 is thickened to suggest an initiation of a conate hypocone.

Besides the slight decrease in size, the lower premolars remain largely unmodified from those in *Desmocyon matthewi*. In some individuals there is a tiny cusp on the lingual base of the principal cusp of the p4. The lower molars begin to show the proportions of the genus, but only in the most rudimentary way: slight widening of m1 talonid and elongation of m2–m3. An additional hypocarnivorous character is a small protostylid present on the m1s of all individuals.

DISCUSSION: *C. galushai* represents an early stage of hypocarnivorous specializations in the *Cynarctus* clade. Characters indicative of membership in this clade include the presence of a narrow external meatus, a transversely narrowed M1, a recurved c1, as well as less well-defined features such as the occasional occurrence of a small cusp on the posteromedial side of the p4 main cusp. While these characters in *C. galushai* permit recognition of a cladogenetic event branching off a mesocarnivorous lineage close to *Metatomarctus*, there remains a rather large morphological gap between *C. galushai* and the extremely derived morphology in *C. saxatilis* through *C. crucidens* (see further discussion under *C. saxatilis*).

?*Cynarctus marylandica* (Berry, 1938)

Figure 56A, B

Tomarctus marylandica Berry, 1938: 159, fig. 68a–d. Downs, 1956: 236. Munthe, 1998: 135.
Cynarctus marylandica (Berry): Tedford and Hunter, 1984: 137.
Tomarctus kelloggi (Merriam, 1911): Munthe, 1988: 97.

HOLOTYPE: USNM 15561 (AMNH cast 48836), left m2 and m1 lacking paraconid (fig. 56A, B) from 1.25 mi south of Plum Point Wharf, Calvert Formation (early Barstovian), Calvert County, Maryland.

REFERRED SPECIMEN: 1.5–2 mi north of Parker Creek, Calvert Formation (early Barstovian), Calvert County, Maryland: USNM 299471 (AMNH cast 127312), left ramal fragment with p4 and alveoli of p3 and m1.

DISTRIBUTION: Early Barstovian of Maryland.

EMENDED DIAGNOSIS: Two autapomorphic features that separate this species from other *Cynarctus* are a strong crest on the posterior face of protoconid on m1 and a strong transverse crest between the entoconid and hypoconid of m2. Primitive characters in common with *C. galushai* are unreduced p4, m1 protostylid very weak and metastylid lacking, and m2 metaconid not enlarged and approximating protoconid in size, with anterolabial cingulum weak, protostylid weak, and metastylid absent.

DESCRIPTION AND COMPARISON: The only feature of this species that is indicative of *Cynarctus* is a protostylid on the m1. However, this protostylid is less developed than those in *C. galushai*, and at such initial stage of development it can be found in isolated individuals of other medium-size, mesocarnivorous borophagines such as *Metatomarctus canavus* (e.g., F:AM 49197, 99358, 99359).

DISCUSSION: Tedford and Hunter (1984: 137) suggested that the Maryland materials may be a primitive member of *Cynarctus*, comparable with early Barstovian species elsewhere. The meager materials available shroud the true identity of this taxon, which is one of only three known borophagine dogs from the Miocene of the northeast coast (the other two are *Paracynarctus kelloggi* and *Metatomarctus canavus*). The available materials do not even permit confident assignment of its generic position, although its placement within the medium-size Borophaginae seems likely. The distinct crest on the posterior face of the m1 trigonid, however, is not seen in other borophagines. Such peculiarity suggests the distinctness of this species, which may prove different in other aspects as well when more is known about it.

Cynarctus saxatilis Matthew, 1902

Figures 56G, H, 57A–D

Cynarctus saxatilis Matthew, 1902: 281, fig. 1; 1932: 2. Barbour and Cook, 1914: 225. Evan-

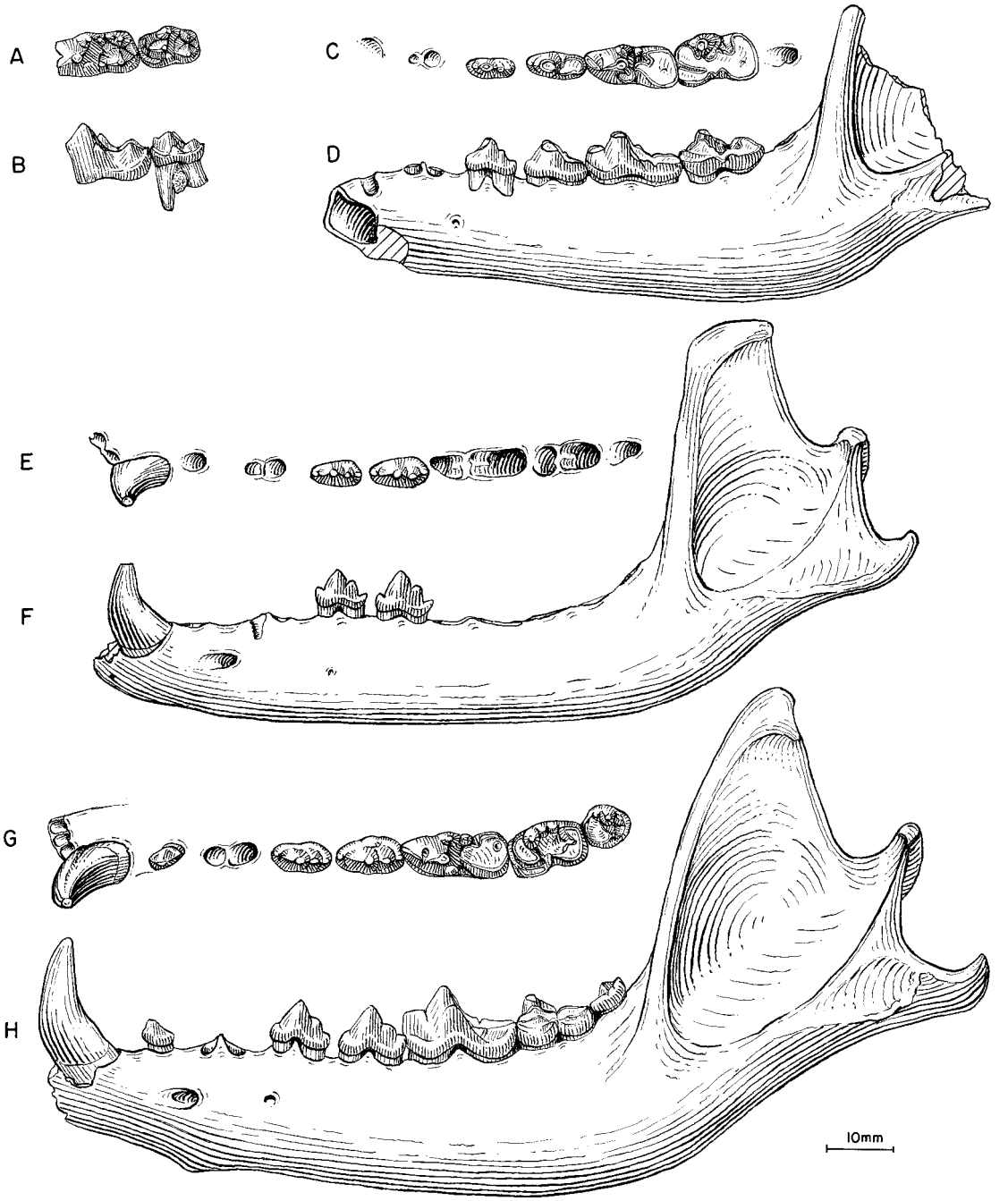

Fig. 56. **A**, Occlusal and **B**, buccal views of m1–m2, ?*Cynarctus marylandica*, USNM 15561, holotype, 1.25 mi south of Plum Point Wharf, Calvert Formation (early Barstovian), Calvert County, Maryland. **C**, Lower teeth and **D**, ramus (reversed from right side), *Cynarctus voorhiesi*, F:AM 105094, holotype, Lucht Quarry, Burge Member, Valentine Formation (late Barstovian), Brown County, Nebraska. **E**, Lower teeth and **F**, ramus (reversed from right side), *C. voorhiesi*, F:AM 49144, Lucht Quarry. **G**, Lower teeth and **H**, ramus, *C. saxatilis*, AMNH 9453 (part of the ascending ramus and p1 reversed from right side), holotype, Cedar Creek, Ogallala Group (late Barstovian), Logan County, Colorado.

der, 1986: 28, fig. 4. Voorhies, 1990a: A134; 1990b: 122. Munthe, 1998: 135.
Cynarctus crucidens Barbour and Cook, 1914: McGrew, 1938a: 329.
Carpocyon cuspidatus (Thorpe, 1922b): Evander, 1986: 27, fig. 8C (in part).

HOLOTYPE: AMNH 9453, right and left rami with i1–i3 alveoli and c1–m3 (p2 alveolus) (fig. 56G, H), Cedar Creek, 40 mi north of Sterling, Ogallala Group (late Barstovian), Logan County, Colorado.

REFERRED SPECIMENS: Pawnee Creek area, Ogallala Group (late Barstovian), Weld or Logan County, Colorado: AMNH 6836, left isolated m1.

Norden Bridge Quarry, Niobrara River, Cornell Dam Member, Valentine Formation (early late Barstovian), Brown County, Nebraska (listed by Voorhies, 1990a: A134): USNM 352392, right ramus with p4–m1 and partial m2 alveolus.

Crookston Bridge Member, Valentine Formation (early late Barstovian), Cherry and Knox counties, Nebraska: Railway Quarry A (UNSM loc. Cr-12): UCMP 29891 (Evander, 1986: fig. 4), left ramus with i1–i3 alveoli, and c1–m3 (fig. 57A, B); and UNSM 25834, right partial maxillary with P3–M2 (referred to *Carpocyon cuspidatus* by Evander, 1986: fig. 8C). Stewart Quarry (UNSM loc. Cr-150): UNSM 1061-96, left maxillary fragment with M1–M2. Sand Lizard Quarry (UNSM loc. Kx-120): left ramus with p2–m2 and m3 alveolus. West Valentine Quarry (UNSM loc. Cr-114): UNSM 2685-87, right maxillary with P3 broken–M2.

Devil's Gulch, upper part of Devil's Gulch Member, 10 ft below the Burge Member, Valentine Formation (late Barstovian), Brown County, Nebraska: FMNH P25537 (AMNH cast 97782), rostral part of skull with I1 alveolus–M2 (fig. 57C, D) (referred to *Cynarctus crucidens* by McGrew, 1938a: 329, fig. 89) and crushed posterior half of skull. (The latter is an uncataloged F:AM specimen with field data of ''Box 152, Elliot Quarry, Neb. 1935.'' According to the recollection of M. F. Skinner [personal commun.], a complete skull was discovered by the F:AM field party in the Devil's Gulch and left uncollected for some time. The Field Museum field party later collected the front half, i.e., FMNH P25537, and the F:AM crews got what remained of the skull. The morphology, bone preservation and breakage, and enclosing rock matrix are generally consistent with the assumption that the two halves belong to a single individual, although the field label, ''Elliot Quarry,'' is not [the possibility of mislabeling is likely]. The F:AM half skull is now deposited in the FMNH.)

Valentine Formation (late Barstovian), Webster County, Nebraska: Myers Farm (UNSM loc. Wt-15A): UNSM 21669, right m2.

DISTRIBUTION: Late Barstovian of Colorado and Nebraska.

EMENDED DIAGNOSIS: Characters of *C. saxatilis* shared with *C. voorhiesi* and *C. crucidens* that are derived with respect to *C. galushai* are premolars anteroposteriorly short and more widely spaced, with p2 isolated by diastemata; P4 protocone strong; M1 and M2 labial cingulum weak to absent lateral to metacone; M1 hypocone large and well delineated; M2 large with length approximating that of M1; m1 with distinct protostylid and strong metastylid; m2 protoconid small, extremely strong metaconid, strong metastylid, extremely large anterolabial cingulum, and strong protostylid; and m3 with well-developed metaconid. Primitive characters of *C. saxatilis* relative to those in *C. voorhiesi* and *C. crucidens* are premolars large and transversely wide; P4 lacking parastyle and lingual cingulum weak; M1 metastyle weak with a cingulum surrounding protocone; M2 not exceeding M1 in length, metacone relatively small and not expanded posteriorly; p4 posterior cusplet moderate in size; m1 trigonid moderately long relative to length of talonid; m2 relatively short; and coronoid process of mandible tall and depth of mandible below masseteric line shallow.

DESCRIPTION AND COMPARISON: Nearly a century after its first description, specimens of *C. saxatilis* remain rare in museum collections. The holotype is still the best mandible available, and the present reference of FMNH P25537 to this species permits observation of the skull and upper teeth. Consistent with cranial characteristics of other species of *Cynarctus* (e.g., *galushai* and *crucidens*), the skull of *C. saxatilis* has a well-developed frontal sinus extending to the frontal-parietal suture and invading the post-

orbital processes. The bulla is bulbous and has a narrow opening of the external auditory meatus. The palate is not narrowed, and the infraorbital foramen is not compressed into a vertical slit as is in *C. crucidens*.

Dentally, *C. saxatilis* has begun to acquire the highly hypocarnivorous characters typical of later species of the genus. The following features first appear in the upper cheekteeth of this species: enlargement of P4 protocone, a distinct hypocone on M1–M2, elongation of M2, and reduction of labial cingulum of M1–M2. Modifications in the lower molars are even more dramatic, leading to an increased grinding area. A distinct anterolabial cingulum is formed on the m1, and this cingulum similarly becomes a broad shelf on the m2 that displaces the trigonid far to the lingual side. The trigonid of m1 is low and short in contrast to a much enlarged talonid. Accessory cusps, such as the protostylid and metastylid, are well developed on both m1 and m2. The m2 has a high, lingually positioned metaconid that dominates the trigonid, and its protoconid and paraconid form a low ridge curving anteriorly around the metaconid. The m3 has a broad, semicircular basin in front of a transverse ridge formed by the protoconid and metaconid.

On the other hand, the dental morphology of *C. saxatilis* still shows a certain primitiveness relative to *C. voorhiesi* and *C. crucidens*. The premolars are not as extremely reduced as in the latter two species. The M1–M2 still have a lingual and labial cingulum. The M2 hypocone is not posteriorly expanded, and thus the length of the M2 does not exceed that of the M1. The m1 trigonid is not as greatly reduced as in the more advanced species, and the m1 protostylid is not detached from the protocone to form a discrete cusp.

DISCUSSION: In his study of FMNH P25537, McGrew (1938a: 323) stated that the agreement in size and proportion between his Field Museum specimen and the holotype of *C. crucidens* is so close that the assignment of this specimen to *C. crucidens* is ''practically certain.'' Our own observations, however, suggest that FMNH P25537 is significantly larger than all other specimens assigned to *C. crucidens*, and its dentition occludes more precisely with the holotype of *C. saxatilis*, which although mentioned by McGrew (1938a), was not critically compared. The generally more primitive dental morphology of FMNH P25537 lends further support to its reference to *C. saxatilis*.

Such reference, however, is not without problems. Besides the larger size and stronger premolars, the lower molar morphology of the holotype of *C. saxatilis* is very close to that of *C. crucidens*. This is, however, in contrast to the more primitive upper molars in FMNH P25537, which lacks the extreme hypocarnivorous features shown in *C. crucidens*, such as reduction of upper molar cingulum, elongation of M2, and posterior expansion of M2 hypocone. Therefore, the possibility exists that FMNH P25537 may represent yet another species more primitive than *C. saxatilis*. Until associated upper and lower jaws become available, FMNH P25537 is best referred to *C. saxatilis*.

In *C. saxatilis*, most of the dental characteristics of advanced species of *Cynarctus* are established. Toward the more primitive side of the *Cynarctus* clade, however, there exists a large morphological gap between *saxatilis* and *galushai*, as reflected by the numerous apomorphic characters separating the two species (fig. 140).

Cynarctus voorhiesi, new species

Figure 56C–F

HOLOTYPE: F:AM 105094, right partial ramus with c1–p2 alveoli, p3–m2, and m3 alveolus (fig. 56C, D), Lucht Quarry, Burge Member, Valentine Formation (late late Barstovian), Brown County, Nebraska.

ETYMOLOGY: Named for Michael R. Voorhies in recognition of his studies of late Cenozoic faunas and stratigraphy of Nebraska.

REFERRED SPECIMENS: Burge Member, Valentine Formation (late late Barstovian), Brown and Cherry counties, Nebraska: F:AM 49143, left isolated M2, Lucht Quarry, Brown County; F:AM 49144, right ramus with i1–i3 alveoli, c1, p1–p2 alveoli, p3–p4, and m1–m3 all alveoli (fig. 56E, F), Lucht Quarry, Brown County; F:AM 49151, right partial ramus with i1–i3 alveoli, c1 broken, p1 root–m1, and m2–m3 alveoli, June Quarry, Brown County; F:AM 49152, left partial

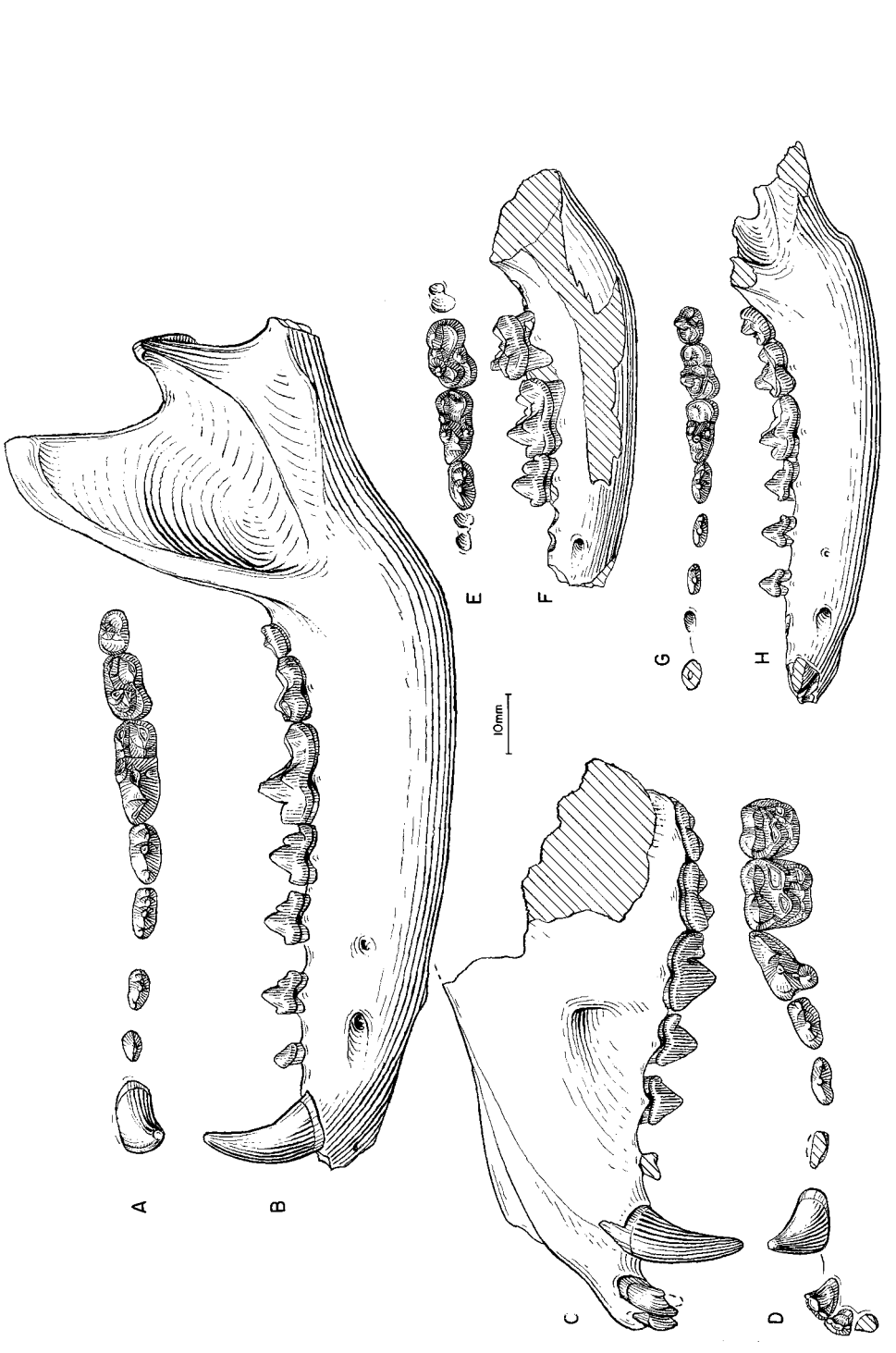

Fig. 57. **A**, Lower teeth and **B**, ramus, *Cynarctus saxatilis*, UCMP 29891, Railway Quarry A, Crookston Bridge Member, Valentine Formation (early late Barstovian), Cherry County, Nebraska. **C**, Lateral view of partial skull and **D**, upper teeth, *C. saxatilis*, FMNH P25537, Devil's Gulch, Devil's Gulch Member, Valentine Formation (late Barstovian), Brown County, Nebraska. **E**, Lower teeth and **F**, ramus (reversed from right side), *C. crucidens*, F:AM 49307, MacAdams Quarry, Clarendon Beds (early Clarendonian), Donley County, Texas. **G**, Lower teeth and **H**, ramus (reversed from right side), *C. crucidens*, UNSM 25465, holotype, Williams Canyon, Cap Rock Member, Ash Hollow Formation (early Clarendonian), Brown County, Nebraska.

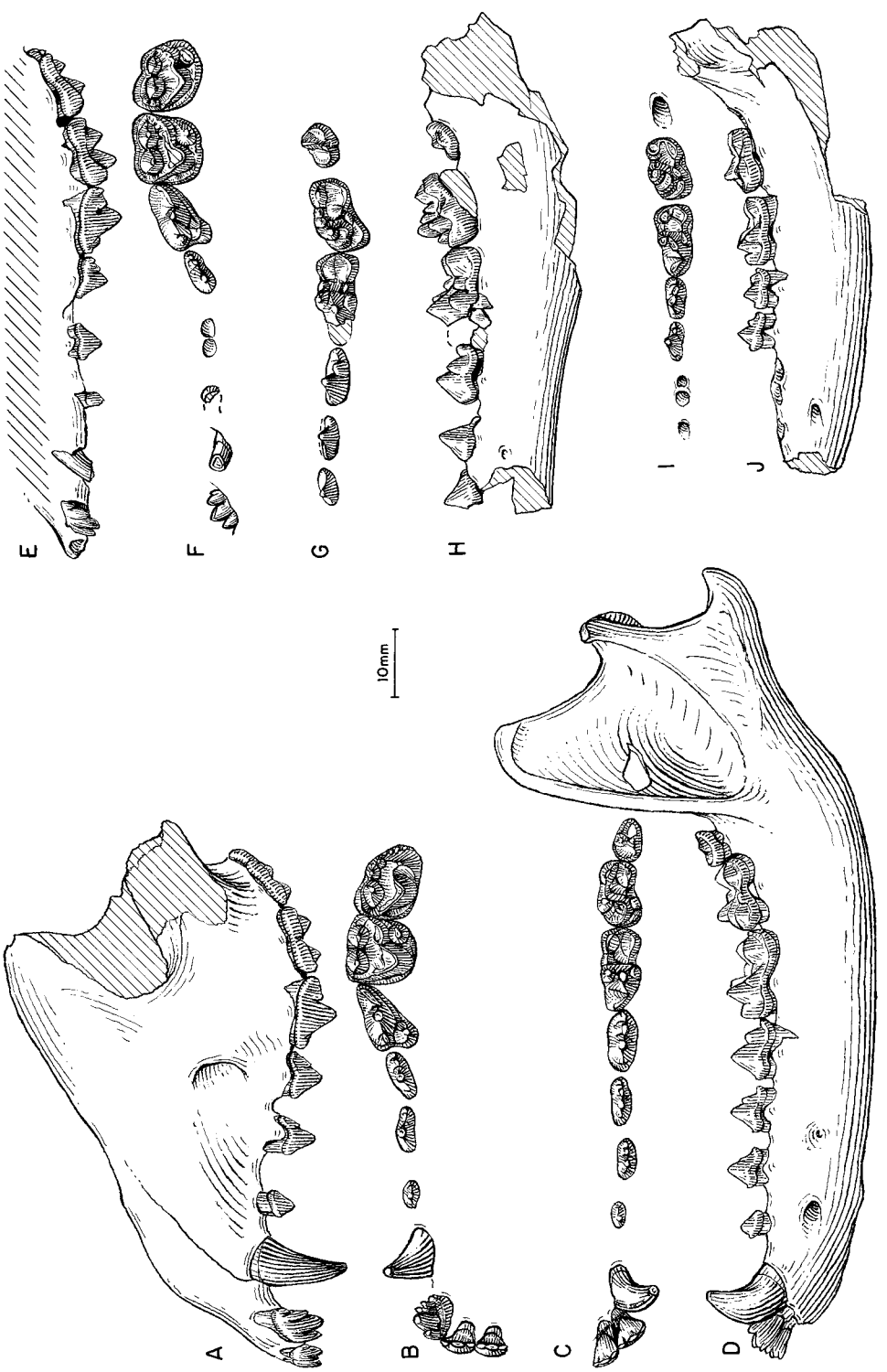

Fig. 58. *Cynarctus crucidens*. **A**, Lateral view of partial skull, **B**, upper teeth, **C**, lower teeth, and **D**, ramus, F:AM 49172 (C and D reversed from right side), Medicine Creek, Cap Rock Member, Ash Hollow Formation (early Clarendonian), Cherry County, Nebraska. **E**, Lateral and **F**, occlusal views of upper teeth, **G**, lower teeth, and **H**, ramus, F:AM 49312, Quarry 6, Clarendon Beds (early Clarendonian), Donley County, Texas. **I**, Lower teeth and **J**, ramus, F:AM 49146, Bear Creek Quarry, Merritt Dam Member, Ash Hollow Formation (late Clarendonian), Cherry County, Nebraska.

ramus with p1 alveolus, p2 broken–m2, and m3 alveolus, June Quarry, Brown County; F:AM 49153, right partial ramus with i1–p2 alveoli and p3–m2 all broken, 300 yd south of Lucht Quarry; and F:AM 105093, right ramal fragment with c1–p2 alveoli, p3–p4, and m1 alveolus, Midway Quarry, Cherry County.

DISTRIBUTION: Late late Barstovian of Nebraska.

DIAGNOSIS: *C. voorhiesi* is derived with respect to *C. saxatilis* in having a smaller size; premolars more widely spaced, smaller, and transversely narrower; p3–p4 posterior accessory cusplets weaker; m1 trigonid, especially the paraconid, shorter relative to length of talonid; and m2 more elongate relative to m1. The above derived characters of *C. voorhiesi* are shared with *C. crucidens*. Primitive characters in contrast to *C. crucidens* are coronoid process tall, more robust horizontal ramus, less posteriorly expanded M2 hypocone, and broader and larger premolars.

DESCRIPTION AND COMPARISON: Specimens of *C. voorhiesi* are limited to a few ramal fragments and an isolated M2. This new species from the latest Barstovian is transitional between the late Barstovian *C. saxatilis* and Clarendonian *C. crucidens* in its intermediate status in size, reductions of premolars, and enlargement of molars. Thus, *C. voorhiesi* still has a rather robust horizontal ramus instead of the slender ramus in *C. crucidens*. On average, dental measurements are 13% larger than those of *C. crucidens* but 13% smaller than those of *C. saxatilis* (appendix III). The premolars are more reduced and narrower than in *C. saxatilis* but are still larger than in *C. crucidens*. The M2 is close to the stage of evolution in *C. crucidens* except for the slightly less posteriorly expanded hypocone. Lower molars of all specimens are heavily worn. The proportions of different parts, however, are still readily observable. Most m1s are larger than those of *C. crucidens* and have relatively longer trigonids.

DISCUSSION: Although poorly represented by fragmentary materials, *C. voorhiesi* fills a morphological gap between *C. saxatilis* and *C. crucidens*. It is almost exactly intermediate, both in size and shape, between the latter two species. Stratigraphically, *C. voorhiesi* (Burge Member of Valentine Formation) is also intermediate between the occurrences of *C. saxatilis* (Devil's Gulch and Crookston Bridge members of Valentine Formation) and *C. crucidens* (mostly Ash Hollow Formation or equivalent strata), and there is no known overlap in their occurrences in Nebraska (fossil records in other states are too poor to see any pattern). These morphological and stratigraphic intermediacies, coupled with the lack of any apparent autapomorphies in *C. voorhiesi*, suggest an anagenetic lineage in the advanced *Cynarctus*.

Cynarctus crucidens
Barbour and Cook, 1914

Figures 57E–H, 58

Cynarctus crucidens Barbour and Cook, 1914: 225, pl. 1, figs. a, b. Matthew, 1932: 2. Munthe, 1998: 135.

Cynarctus fortidens Hall and Dalquest, 1962: 137, figs. 1, 2. Munthe, 1998: 135.

HOLOTYPE: UNSM 25465 (AMNH cast 14307), right partial ramus with i1–i3 alveoli, c1 broken, and p1 alveolus–m3 (fig. 57G, H) from Williams Canyon (or Quinn Canyon), tributary of Plum Creek, level equivalent to Clayton Quarry, Cap Rock Member, Ash Hollow Formation (early Clarendonian), Brown County, Nebraska (M. F. Skinner, personal commun.).

REFERRED SPECIMENS: Cap Rock Member, Ash Hollow Formation (early Clarendonian), Antelope, Cherry, and Brown counties, Nebraska: Clayton Quarry: F:AM 49148, right isolated m1. East Clayton Quarry: F:AM 49150, right and left m1s; F:AM 49170, right ramal fragment with i1–i3 alveoli, c1 root, and p1–p4 all alveoli; and F:AM 49174, right isolated M2. Medicine Creek, south side of Niobrara River: F:AM 49172, anterior part of skull with I1–M2 (fig. 58A–D), basicranium with bulla, right ramus with i2–m3, first five cervical vertebrae, both partial scapulae, right partial humerus, both radii and ulnae with distal epiphyses missing, and both partial tibiae. Poison Ivy Quarry (UNSM loc. Ap-116): UNSM 2000-78, anterior partial skull with I1–M2; and UNSM PI1597, left ramal fragment with i1–p3.

Merritt Dam Member, Ash Hollow Formation (late Clarendonian), Cherry County, Nebraska: F:AM 25142, right partial ramus

with m1 and alveoli for p3–p4 and m2–m3, Kat Quarry; F:AM 49145, left premaxillary maxillary with I1–I3 alveoli, C1, and P1 alveolus–M2, Bear Creek Quarry; F:AM 49146, left partial ramus with p1–p2 alveoli, p3–m2, and m3 alveolus (fig. 58I, J), Bear Creek Quarry; F:AM 49147, right partial ramus with c1, p1–p2 alveoli, p3–m1, and m2–m3 alveoli, Bear Creek Quarry; and F:AM 105092, left isolated m1, Gallup Gulch Quarry.

Hollow Horn Bear Quarry, undifferentiated beds of the Ogallala Group, temporally equivalent to the Cap Rock Member of the Ash Hollow Formation (early Clarendonian), Todd County, South Dakota: F:AM 49401, right partial maxillary with M1–M2; F:AM 49402, right partial maxillary with P4–M1 alveoli and M2; F:AM 49403A, left isolated M1; F:AM 49403B, left isolated M1; F:AM 49403C, left isolated M1; F:AM 49403D, left isolated M1; F:AM 49403E, left isolated M1; F:AM 49404, right ramus with i1–i3 alveoli and c1–m3; F:AM 49405, left ramus with i1–i3 alveoli and c1–m3; F:AM 49406, left partial ramus with i1–i3 alveoli, c1 broken, p1 alveolus, p2–p3, p4 alveolus, m1–m2, and alveolus of m3; F:AM 49407, left isolated M2; F:AM 49408, right isolated M1; F:AM 49409, left isolated m1; F:AM 49419, left isolated m1; F:AM 49419A, left isolated M2; F:AM 49419B, left isolated P4; F:AM 49420, right broken isolated m1; F:AM 105091, left isolated m1; and F:AM 105091A, right isolated m1.

Kilpatrick Quarry (= Quarry 7), Laucomer Member, Snake Creek Formation (early Clarendonian), Sioux County, Nebraska: AMNH 22405, left isolated m1.

Clarendon Beds (early Clarendonian), Donley County, Texas: F:AM 49302, left immature maxillary fragment with dP3 broken–dP4, MacAdams Quarry; F:AM 49303, left premaxillary fragment with I1 alveolus–I3, detached teeth including canines and right M1–M2, Quarry 2, Lewis Place, Spade Flats; F:AM 49304, right isolated M1, MacAdams Quarry; F:AM 49305, right maxillary fragment with M1–M2, MacAdams Quarry; F:AM 49306, right and left rami with i1 alveolus–m2 and m3 alveolus, MacAdams Quarry; F:AM 49307, right partial ramus with p3 alveolus–m2 and m3 alveolus (fig. 57E, F), MacAdams Quarry; F:AM 49308, left partial ramus with i1–p3 alveoli, p4–m2, and m3 alveolus, MacAdams Quarry; F:AM 49309, left partial ramus with p2–p4 alveoli, m1 broken–m2, and m3 alveolus, MacAdams Quarry; F:AM 49310, left partial ramus with p1–p3 all broken, p4–m2 (m1 broken), MacAdams Quarry; F:AM 49311, right isolated M1, Quarry 1 of Gidley; F:AM 49312, articulated crushed partial skull with I3 erupting, C1–P1 both broken, P3–M2, lower jaws with c1 broken–m3 (fig. 58E–H), partial left and right humeri articulated with incomplete radius and ulna, and partial pelvis articulated with femur and partial tibia, White Fish Creek, Quarry 6; F:AM 49313, left ramal fragment with c1, p1–p3 alveoli, p4, and m1 alveolus–m2, MacAdams Quarry; F:AM 70768, crushed immature skull with dC1, P1 alveolus, and dP2–dP4, MacAdams Quarry; F:AM 105089, right ramal fragments with p3 broken–p4 and detached broken m1 and m2, MacAdams Quarry, 10 mi north of Clarendon; F:AM 105090, left partial ramus with c1 broken and p1 alveolus–m3 (p4 broken), MacAdams Quarry; KUVP 11353 (holotype, *Cynarctus fortidens* Hall and Dalquest, 1962: fig. 1), right maxillary fragment with P3–M1, in ''bluff on west side of Turkey Creek, approximately 75 ft above stream, Raymond Farr Ranch'' (Hall and Dalquest, 1962: 137); and KUVP 11354 (Hall and Dalquest, 1962: fig. 2), right ramal fragment with m2, same locality as above.

Highway Pit, 0.75 mi north of Lipscomb, Ogallala Group (Clarendonian), Lipscomb County, Texas: F:AM 105088, left ramal fragment with m2.

DISTRIBUTION: Early Clarendonian of Nebraska, South Dakota, and Texas; late Clarendonian of Nebraska; and Clarendonian of Texas.

EMENDED DIAGNOSIS: Unique or further development of derived characters that distinguish *Cynarctus crucidens* from all other species are P1–P2 and p1–p2 small and narrow and isolated by longer diastemata; P4 parastyle; M1 strong metastyle, labial cingulum at metacone lacking; M2 anteroposteriorly elongate and exceeding M1 length, hypocone large and posteriorly situated, metastyle well developed, and strong posterior cingulum; p4 with large, low posterior ac-

cessory cusplet; m1 trigonid extremely short and narrow relative to length and width of talonid; m2 entoconid and hypoconid strong, conical cusps; coronoid process of mandible low; and horizontal ramus slender and depth of mandible below masseteric line deep (elevated lower border of the masseteric fossa).

DESCRIPTION AND COMPARISON: The cranial morphology of *C. crucidens* is still incompletely known. Skull fragments of F:AM 49172 show that the maxillary region of the palate is narrowed compared to *C. saxatilis*, whereas the anterior tip of the palate is not. This narrowing of the cheek region also causes a compression of the infraorbital canal, which becomes slitlike in cross-section rather than more open as in *C. saxatilis* and more primitive taxa. The basicranial fragment in F:AM 49172 has a well-preserved bulla, which is very bulbous and has a very narrow opening for the external auditory meatus. In the mandible the lower border of masseteric fossa is elevated to the level of the base of lower molars, and the coronoid crest is relatively low.

As the terminal species of the *Cynarctus* clade, *C. crucidens* possesses the most hypocarnivorous dental features of all species. The upper and lower incisors are highly cuspidate, together forming a comblike structure. In addition to more prominent developments of individual cusps, the I3 has added another small accessory cusp on the lateral ridge, totaling two lateral accessory cusps instead of one, as in *C. saxatilis*. Correspondingly, the i3 has an additional cusplet between the lateral and central cusps. These multicuspid incisors form a longer transverse blade and together they occupy a broader anterior tip of the snout. The upper and lower premolars (except P4) are widely spaced from each other and are considerably reduced compared to those of *C. saxatilis*, *C. voorhiesi*, and other cynarctines. Advanced features of the P4 include a distinct parastyle and a wider lingual cingulum (especially prominent in F:AM 49145). Advancement of the M1, relative to that in *C. saxatilis*, is mainly in the reduction of the cingula: both the lingual cingulum surrounding the protocone and the labial cingulum are lost or extremely reduced. The M2 is greatly expanded posteriorly due to enlargement of the hypocone, slightly more so than in *C. voorhiesi*, such that its outline is anteroposteriorly elongated, compared to the more or less quadrate M2 in *C. saxatilis*. Besides the much smaller size and more reduced premolars, the lower cheekteeth of *C. crucidens* are quite similar to those of *C. saxatilis* and *C. voorhiesi* in both proportions and cusp morphologies.

DISCUSSION: Hall and Dalquest's (1962) contrast of their *C. fortidens* with *C. crucidens* was apparently based on FMNH P25537 (a partial skull), which was referred to *C. crucidens* by McGrew (1938a: 330) but is presently assigned to *C. saxatilis* (see further comments under that species). Therefore, the few diagnostic characters cited by Hall and Dalquest are differences between their *C. fortidens* and *C. saxatilis* (contrary to Hall and Dalquest [1962: 138], however, the holotype of *C. fortidens* is smaller, not larger, than FMNH P25537). A larger sample of the Clarendon materials is now available in the Frick Collection, and they show unambiguously the characteristics of *C. crucidens*, which has seniority over *C. fortidens*.

There is a tendency toward decreasing size from earlier species of *Cynarctus* (such as *saxatilis* and *galushai*) to the terminal species *crucidens*. Superposed on this overall size reduction is the reduction of the premolars, which may help explain the rather large coefficients of variance in most measurements of the premolars in *C. crucidens* (appendix III), especially for the upper premolars.

Metatomarctus, new genus

TYPE SPECIES: *Cynodesmus canavus* Simpson, 1932.

ETYMOLOGY: Greek: *meta*, between; in allusion to the intermediate position of this genus between *Tomarctus* and the more primitive borophagines.

INCLUDED SPECIES: *Metatomarctus canavus* (Simpson, 1932), *Metatomarctus* sp. A, and *Metatomarctus* sp. B.

DISTRIBUTION: Early Hemingfordian of Nebraska, New Mexico, Florida, and Delaware; late Hemingfordian of Wyoming and California; and early Barstovian of Nevada.

DIAGNOSIS: Derived characters that distinguish *Metatomarctus* and higher taxa from

Desmocyon matthewi are I3 with one lateral accessory cusplet (shared with the Cynarctina) and initial development of an anterior crest on the P4. *Metatomarctus* is primitive with respect to *Euoplocyon*, *Psalidocyon*, and higher taxa in its less elaborate I3 with a single accessory cusp. In contrast to the Cynarctina clade, *Metatomarctus* lacks such derived characters as subangular lobe of the mandible, high mandibular condyle, reduced premolars, shortened P4, small protostylid of m1, wide m1 talonid, and elongated m2.

Metatomarctus canavus (Simpson, 1932)

Figure 59

Cynodesmus canavus Simpson, 1932: 19, fig. 4. White, 1941b: 91.
Tomarctus thomasi White, 1941b: 94, pl. 14, fig. 3; 1942: 8, pl. 7, fig. 1. Downs, 1956: 236.
Tomarctus canavus (Simpson): White, 1942: 8, pl. 2, fig. 2, pl. 6, figs. 1–3; 1947: 502. Olsen, 1956a: 2, figs. 1, 4. Downs, 1956: 236. Wang, 1994: 125. Munthe, 1998: 135.
Nothocyon insularis White, 1942: 7, pl. 1, fig. 3; 1947: 502, fig. 2.
Tomarctus kelloggi (Merriam, 1911): Munthe, 1988: 91 (in part).
Tomarctus sp. Reynolds et al., 1995: 108.
Tomarctus cf. *T. canavus* (Simpson): Emry and Eshelman, 1998: 160, fig. 2N–P.

HOLOTYPE: UF V-5260, right partial ramus with p2, p3 alveolus, p4–m2, m3 alveolus (fig. 59A, B), from Thomas Farm Local Fauna, Hawthorn Formation (late early Hemingfordian), Gilchrist County, Florida.

REFERRED SPECIMENS: Thomas Farm Local Fauna, Hawthorn Formation (late early Hemingfordian), Gilchrist County, Florida: AMNH 27674, partial left ramus with p2–p3 alveoli, p4–m1, and m2 alveolus; AMNH 27674A, isolated right m1; MCZ 3628 (AMNH cast 129643), partial skull with P4–M1, partial right ramus with c1–p1 alveoli, p2 broken, p3–m2, and m3 alveolus (White, 1942: pl. 6; Olsen, 1956a: fig. 1); MCZ 3641, M1; MCZ 3673, maxillary with P4–M1; MCZ 3674, maxillary with P4–M1; MCZ 3682 (AMNH cast 129681) (holotype of *Tomarctus thomasi* White, 1941b), partial left maxillary with P4–M2; MCZ 3712 (White, 1942: pl. 7), partial right ramus with c1–p1 alveoli, p2–m2, and m3 alveolus; MCZ 3713, ramus with p2 and p4–m2; MCZ 3728, maxillary with P2–M2; MCZ 3812 (AMNH cast 129682) (holotype of *Nothocyon insularis* White, 1942), partial right maxillary with P4 broken–M2; MCZ 3813 (White, 1942: pl. 2, fig. 2), left maxillary with P2, P3 alveolus, P4–M1, and M2 alveolus; MCZ 3924, ramus with p4–m1; MCZ 4242 (White, 1947: fig. 2D, E), partial right ramus with c1–p1 alveoli, p2–m1, and m2–m3 alveoli; MCZ 4334, ramus with p2–m2; MCZ 4507, ramus with m1; MCZ 5814, ramus with m1; MCZ 7146, maxillary with P4–M1; MCZ 7147, ramus with p4–m1; MCZ 7148, ramus with m1–m2; MCZ 7307, ramus with p2–m1; MCZ 7308, ramus with p4–m2; SDSM 525 (formerly MCZ 3967), right partial ramus with p2, p3 alveolus, and p4–m2; UF 926, right M1; UF 927, left broken M1; UF 3532, right ramus with c1–m2 alveoli; UF 17652, left M1; UF 17654, left m1; UF 17655, left P4; UF 19781, right ramus with c1–m3 alveoli; UF 19788, right immature ramus with c1 erupting, dp4 broken, and m1–m2 erupting; UF 19795, right ramus with p2–p4 alveoli, m1–m2, and m3 alveolus; UF 19952, right ramus with p2–p3 alveoli, p4–m1, and m2 alveolus; UF 58957, left maxillary fragment with P4–M2; UF 59089, left and right maxillary fragments with P4 broken–M2; UF 60527, left ramus fragment with p2–p4 (p3 broken); UF 66925, right ramal fragment with p1–p3 alveoli and p4; UF 94786, right m1; UF 94854, right ramal fragment with m2; UF 94855, left maxillary with P1–P3 alveoli and P4–M2; UF 94856, right m1; UF 94857, left ramus with c1–p3 alveoli, p4, m1 alveolus, m2, and m3 alveolus; UF 94858, left M1; UF 94859, left P2; UF 94860, left M2; UF 94861, right P3; UF 94862, talonid of right m1; UF 94866, right ramus with p3 alveolus, and p4–m2; UF 94868, right ramus with c1–p3 alveoli, p4–m2, and m3 alveolus; UF 94869, left immature ramus with c1 and p2–p4 erupting and dp3; UF 94870, left M2; UF 94873, left m2; UF 94875, right ramal fragment with p4; UF 94886, left P4; UF 94887, left broken M1; UF 94888, right M1; UF 94889, right p4; UF 94891, right ramal fragment with p2, p3 alveolus, and p4 broken; UF 94899, left M1; UF 95001, broken left m1; UF 95002, talonid of left m1; UF 95003, talonid of left m1; UF 154100, right ramus with c1–p1 al-

veoli, p2, p3 alveolus, and p4–m1; UF 165879, left ramus with p1–p2, p3 alveolus, p4–m1, and m2–m3 alveoli; UF V-5653, left and right maxillae with P1 alveolus, P2, P3 alveolus, and P4–M2; UF V-5658 (AMNH cast 48841), isolated right m1; UF V-5668, right M1; UF V-5669, right M2; UF V-5670, right P4; UF V-5707, partial crushed skull with C1–P3 alveoli and P4–M2; UF V-5766 (AMNH cast 48837), partial right maxillary with P4–M2; UF V-5767 (AMNH cast 48832), partial right ramus with p1–m2 and m3 alveolus; UF V-6266, partial right ramus with p1–p2 alveoli and p3 broken–p4; UF V-6267, right ramal fragment with i1–p3 alveoli and p4; UF V-6282, partial right ramus with p4–m1 all broken and m2 alveolus; UF V-6283, right ramal fragment with m2; UF V-6284, left ramal fragment with p1–p2 alveoli and p3; UF V-6288, left ramal fragment with m2 and m3 alveolus; UF V-6331, right ramus with p1–m1 alveoli, m2, and m3 alveolus; UF V-8946, right M1; UF V-9162, left ramal fragment with p4; UF V-9173, broken left M1; UF V-9174, left M1.

Pollack Farm Site (Delaware Geological Survey locality Id11-a), lower shell bed of Cheswold sands, lower Calvert Formation (late early Hemingfordian), near Cheswold, Delaware: USNM 475817, isolated right m1 (referred to *Tomarctus* cf. *T. canavus* by Emry and Eshelman, 1998: fig. 2O, P); and USNM 475930, isolated left m2 (referred to *Tomarctus* cf. *T. canavus* by Emry and Eshelman, 1998: fig. 2N).

Jeep Quarry or Jeep Quarry horizon, Arroyo Pueblo drainage, upper part of Chamisa Mesa Member, Zia Formation (early Hemingfordian), Sandoval County, New Mexico: F:AM 50139A, left ramal fragment with broken c1, p1 alveolus, and broken p2; and F:AM 50141, right ramal fragment with c1–m1 all broken, and isolated m3.

Hemingford Area, upper part of the Runningwater Formation (late early Hemingfordian), Box Butte, Cherry, and Dawes counties, Nebraska: UNSM 25597, left partial ramus with p1–p2 alveoli and p3–m1, UNSM loc. Bx-7; UNSM 25600, partial right ramus with p1 alveolus–m2 and m3 alveolus, UNSM loc. Bx-7B; UNSM 25601, right ramus with c1, p1–p3 alveoli, p4–m1, and m1–m2 alveoli, UNSM loc. Bx-7; UNSM 25602, right ramus with c1 alveolus–m2 and m3 alveolus, UNSM loc. Bx-7B; UNSM 25605, right partial maxillary with P4–M1 and M2 alveolus, UNSM loc. Bx-9; UNSM 25609, left partial ramus with p1 alveolus–m1 and m2–m3 alveoli (fig. 59S, T), UNSM loc. Bx-7; UNSM 25613, right partial ramus with p3 alveolus, p4–m1 both broken, and m2, UNSM loc. Bx-7; UNSM 25614, left partial ramus with m1, Bx-12; UNSM 25616 (F:AM cast 97102), right partial ramus with p1 alveolus–m2, UNSM loc. Bx-7; UNSM 25620, right partial maxillary with P4 broken–M2, UNSM loc. Bx-7; UNSM 25621, partial left ramus with c1 broken–m2 and m3 alveolus, UNSM loc. Bx-7B; UNSM 25623, right ramal fragment with m1 broken and m2–m3, Hemingford Quarry 11A (UNSM loc. Bx-11); UNSM 25626, partial right ramus with p1 alveolus–m2, UNSM loc. Bx-22; UNSM 25635, left ramus with i1–i3 alveoli, c1, p1 alveolus, p2–p4, and m1–m3 alveoli, UNSM loc. Bx-7; UNSM 25640, partial left maxillary with P3 alveolus–M2, UNSM loc. Bx-12; UNSM 25653, right maxillary with P2 broken–M2, UNSM loc. Bx-7; UNSM 25654, right partial ramus with p4–m1 and m2 root, UNSM loc. Bx-7; UNSM 25655, right and left partial maxillary with P1 alveolus–M2, UNSM loc. Bx-12; UNSM 25658 (AMNH cast 107922), left ramus with c1–p1 alveoli, p2–m1, and m2 broken–m3 alveolus (fig. 59Q, R), UNSM loc. Bx-7; UNSM 25660, partial ramus with p1–m3 alveolus, UNSM loc. Bx-7; UNSM 25662 (AMNH cast 107923), partial skull with C1 root–M2 (P1 alveolus) (fig. 59P), UNSM loc. Bx-51; UNSM 25669, left partial ramus with p3–m1, UNSM loc. Bx-27; UNSM 25813, left partial maxillary with P3 broken–M2 and left partial ramus with p2–m3 (p4 broken), near Nonpareil Sand Pit; UNSM 25814, right partial ramus with p3–m2, UNSM loc. Bx-7B; UNSM 25815, left partial ramus with c1–p1 broken, p2–p4, and m1 broken, UNSM loc. Bx-7B; UNSM 25816, partial right ramus with i1 alveolus–m1, UNSM loc. Bx-7B; UNSM 25817, right partial ramus with p4–m2, UNSM loc. Bx-12D; UNSM 25818, left partial ramus with c1, p1 alveolus–m1 broken, and m2 alveolus, no locality data; UNSM 25827 (AMNH cast 124024), right partial ramus with p4 root–m2 and m3

alveolus, UNSM loc. Cr-101; and UNSM 26159, right partial ramus with c1, p1–p3 alveoli, p4, m1–m2 both broken, and m3 alveolus, no data, Dawes County.

Clinton Highway Locality (UNSM loc. Sh-101B), Runningwater Formation (early Hemingfordian), Sheridan County, Nebraska: UNSM 5008-70, partial left and right maxillary with I2–M2.

Dry Creek Prospect B, Runningwater Formation (early Hemingfordian), Box Butte County, Nebraska: F:AM 99353, left isolated m2; F:AM 99354, right isolated p4; F:AM 99355, left isolated p4; F:AM 99356, right ramal fragment with p4; F:AM 99357, left partial ramus with p1 alveolus–p4 and m1 broken; F:AM 99358, left ramus with i1–i3 alveoli, c1, p1 alveolus–m2, and m3 alveolus; and F:AM 99359, left ramus with i1–i3 alveoli, c1, p1 alveolus–m2, and m3 alveolus.

Other localities in the Runningwater Formation (early Hemingfordian), Dawes County, Nebraska: F:AM 25419, right partial ramus with p2 alveolus, p3–p2, and m3 alveolus, Ahren Prospect, Cottonwood Creek; F:AM 49197, partial adolescent skull with I2–P3 all erupting, dP4, P4 erupting, both partial rami with p3–p4 erupting, m1–m2, and m3 erupting (fig. 59C–F) and postcranial fragments, Elder Ranch, Cottonwood Creek; F:AM 49198, premaxillary and partial maxillary with I1 alveolus, I2–P1, p2 alveolus, and P4–M2, Pepper Creek; F:AM 49199, left ramus with c1–m3 (fig. 59G, H), both partial humeri (fig. 59K), right radius (fig. 59J), both ulnae (fig. 59I), metacarpal III (fig. 59M), partial pelvis, partial right femur, distal ends of both tibiae (fig. 59N, O), calcaneum (fig. 59L), broken astragalus, and vertebrae, Pebble Creek; F:AM 104694, right partial ramus with c1 broken, p1 alveolus, p2–p3, m1, and m2–m3 alveoli, NW¼, sect. 36, T30N, R49W; and F:AM 104700, right and left partial rami with c1 broken, p1 alveolus, and p2–p4, Sand Canyon Region.

Two mi west of Pole Creek, Runningwater Formation (early Hemingfordian), Cherry County, Nebraska: F:AM 61313, right partial ramus with i1–p1 alveoli, p2–m2 (m1 broken), and m3 alveolus; and F:AM 61314, right partial ramus with p4–m1.

Bridgeport Quarries, Runningwater Formation (early Hemingfordian), Morrill County, Nebraska: UNSM loc. Mo-113: UNSM 25713, left ramal fragment with m1–m2 and m3 alveolus; UNSM 25800, right maxillary with P3 alveolus–M1 and M2 alveolus; UNSM 25802, left maxillary with C1–P3 alveoli and P4 broken–M2; UNSM 25803, right maxillary with P4–M1; UNSM 25804, left ramus with c1, p1 alveolus, p2–m1 all broken, and m2–m3 alveoli; UNSM 25805, right ramus with p2–m2 and m3 alveolus; UNSM 25835, right ramal fragment with m1 broken and m2–m3 alveoli; UNSM 25-6-7-34-SP, right maxillary with P3 broken–M2; UNSM 37-6-7-34-SP, right M1; and UNSM 24-6-7-34-SP, left maxillary fragment with M1–M2. UNSM loc. Mo-114: UNSM 25735, left ramus with p1–m1 all broken and m2. UNSM loc. Mo-116: UNSM 25734, right ramus with c1–p3 alveoli, p4–m1 broken, and m2 alveolus.

Split Rock Formation (late Hemingfordian), Fremont County, Wyoming: UW 926, partial skull and mandible with complete dentition (referred to *Tomarctus kelloggi* by Munthe, 1988), Rattlesnake Hills, UW loc. 50001.

Hackberry Local Fauna (late Hemingfordian), Lanfair Valley, eastern Mohave, California: AMNH 129879 (cast of San Bernardino County Museum collection), left ramus with i2–c1 and p2–m2 (referred to *Tomarctus* sp. by Reynolds et al., 1995).

DISTRIBUTION: Early Hemingfordian of Nebraska, New Mexico, Florida, and Delaware; and late Hemingfordian of Wyoming and California.

EMENDED DIAGNOSIS: Only known species and its characters are those listed for the genus.

DESCRIPTION AND COMPARISON: Despite the large number of referred specimens, our knowledge of *Metatomarctus canavus* is still mostly limited to teeth and jaws. *M. canavus* is significantly larger than the contemporaneous *Desmocyon matthewi*, with dental measurements on average 23% larger. In *M. canavus*, a lateral cusplet is present on the I3. Another derived character first appearing in *M. canavus* is a more distinct anterior crest on the paracone on P4 than those seen in most *D. matthewi*, initiating a trend toward a distinct parastyle in later taxa. This initial

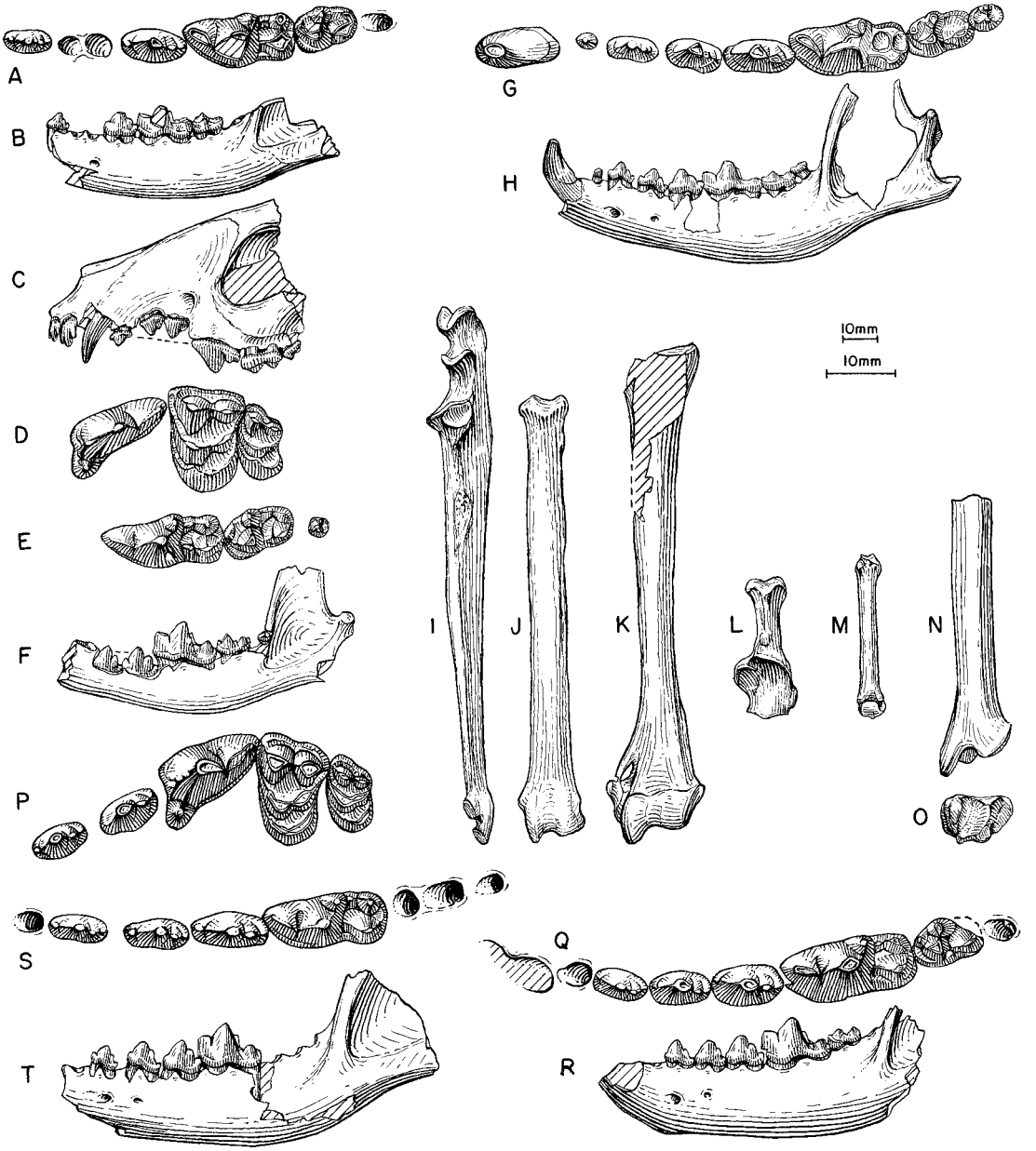

Fig. 59. *Metatomarctus canavus*. **A**, Lower teeth and **B**, ramus (reversed from right side), UF V-5260, holotype, Thomas Farm Local Fauna, Hawthorn Formation (early Hemingfordian), Gilchrist County, Florida. **C**, Lateral view of partial skull, **D**, upper teeth, **E**, lower teeth, and **F**, ramus, F:AM 49197, Elder Ranch, Runningwater Formation (early Hemingfordian), Dawes County, Nebraska. **G**, Lower teeth, **H**, ramus, **I**, ulna, **J**, radius, **K**, partial humerus, **L**, calcaneum, **M**, metacarpal III, and **N**, anterior and **O**, distal views of distal tibia, F:AM 49199 (J, K, L, N and O reversed from right side), Pebble Creek, Runningwater Formation. **P**, Upper teeth, UNSM 25662, Hemingford Area, Runningwater Formation. **Q**, Lower teeth and **R**, ramus, UNSM 25658, Hemingford Quarry, Runningwater Formation. **S**, Lower teeth and **T**, ramus, UNSM 25609, Hemingford Quarry, Runningwater Formation. The longer (lower) scale is for A, D, E, G, P, Q, and S, and the shorter (upper) scale is for the rest.

development of a parastyle varies from a rather distinct parastyle in UNSM 25662 (fig. 59P) to a weak anterior crest in F:AM 49198. The crest leading to the protocone and lingual to the anterior crest is also distinct.

Compared to *Euoplocyon* and later taxa, *Metatomarctus canavus* is primitive in its less elaborate I3 lateral accessory cusplet (i.e., one cusplet vs. two or more in *Euoplocyon* and others). Compared to the cynarctine clade, on the other hand, *M. canavus* has a primitively undeveloped subangular lobe, low mandibular condyle, unshortened P4, no protostylid on m1, and a normally proportioned m2 that is not elongated.

Specimens from the early Hemingfordian of New Mexico are too poorly preserved to be certain about their identity. The size and morphology of F:AM 50141 is in general agreement with the type series from Florida.

DISCUSSION: Six nominal species had been proposed for the median-size canids from the Thomas Farm local fauna, not counting other carnivorans such as amphicyonids. The last synthesis of Thomas Farm canids was by Olsen (1956a), who recognized only two species: ''*Cynodesmus*'' *iamonensis* Sellards (see Wang, 1994: 120) and ''*Tomarctus*'' *canavus*. We agree with Olsen's assessment, and the contrasting characters listed by him underline some of the fundamental differences between hesperocyonine and borophagine canids, such as the presence in *M. canavus* of a distinct metaconule and a broader lingual cingulum on M1, as well as a transverse crest between the hypoconid and entoconid of m1. Furthermore, the premolars of *M. canavus* have more distinct anterior accessory cusplets. These characters are lacking in all hesperocyonines, including ''*Cynodesmus*'' *iamonensis*, which was referred to the genus *Osbornodon* by Wang (1994). *Osbornodon iamonensis* is known to occur both in the Thomas Farm Local Fauna and in the Runningwater Formation of Nebraska (Wang, 1994). It is thus of interest that *Metatomarctus canavus* is also recognizable in both locations. The coexistence of both species in the early Hemingfordian of Florida and Nebraska is further evidence of the broad zoogeographic distribution of these medium-size canids.

Metatomarctus sp. A

Tomarctus cf. *T. optatus* (Matthew, 1924): Stirton, 1939a: 633.

REFERRED SPECIMENS: High Rock Canyon 2 (UCMP loc. 1107) (early Barstovian), Humboldt County, Nevada: UCMP 38290, left ramal fragment with crushed m1–m2; and UCMP 38301, right ramal fragment with m1 and broken m2.

DISTRIBUTION: Early Barstovian of Nevada.

DESCRIPTION AND COMPARISON: The most conspicuous features of this species and *Metatomarctus* sp. B are their slender cheekteeth with narrow premolars and nearly longitudinally oriented shearing blade of m1. The two species are probably closely related and form a small clade of their own. Their relationships to other borophagines, however, are difficult to determine, owing to the paucity of materials. Although the longitudinally oriented shearing blades resemble those of *Psalidocyon*, we chose to view this as a parallel development because of other morphological differences. For example, this species pair lacks the anteriorly canted p3 main cusp (seen only in *Metatomarctus* sp. B) and m1 paraconid, features that are unique to *Psalidocyon*. Besides the extremely trenchant m1 trigonids, these two species seem to fall within the stage of evolution of *Metatomarctus*. It is likely that they form a small clade derivable from the base of *Metatomarctus*, and when more is known about their morphology, they may deserve a generic status of their own.

Only the m1–m2 are available from the two referred specimens of *Metatomarctus* sp. A. Although mediolateral compression of UCMP 38290 has certainly contributed to its slender appearance, the m1 on UCMP 38301 is essentially not deformed. The shearing blade (trigonid) on both specimens is even more longitudinally oriented than in *Psalidocyon*. Our scant knowledge of this form makes it inappropriate to erect a new species.

Metatomarctus sp. B

Tephrocyon? compare *rurestris* (Condon, 1896): Merriam, 1911: 239, fig. 8a, b; 1913: 370, fig. 15a, b.

Tephrocyon? sp: Merriam, 1911: 241, fig. 9a, b; 1913: 370, fig. 16a, b.

Tomarctus large species: Downs, 1956: 236.

REFERRED SPECIMENS: High Rock Canyon 2 (UCMP loc. 1107) (early Barstovian), Humboldt County, Nevada: UCMP 12503, left ramal fragment with p4–m1 (Merriam, 1911: fig. 8; 1913: fig. 15a, b); and UCMP 12504, left ramal fragment with p4–m1 (Merriam, 1911: fig. 9; 1913: fig. 16a, b).

DISTRIBUTION: Early Barstovian of Nevada.

DESCRIPTION AND COMPARISON: Preservation of the above referred specimens is slightly better than for *Metatomarctus* sp. A. With the presence of the p3, the trenchant morphology of the lower cheekteeth is even more evident than in *Metatomarctus* sp. A. The sharp-edged p3 and m1 trigonid once again remind one of the conditions in *Psalidocyon*, but other details are inconsistent with the latter genus. As noted for *Metatomarctus* sp. A above, we consider the trenchant cheekteeth in this species an independent character from *Psalidocyon*, an assertion to be verified by future discoveries.

As noted by Stirton (1939a: 633), there is a large size difference among the High Rock Canyon dogs. There are clearly two size groups (e.g., m1 length of UCMP 38290 is 19.3 mm as compared to 24.5 mm in UCMP 10254), indicating the coexistence of two sister-species of this peculiar clade. Close examination also reveals that there may be more than one taxon among the large-size group (*Metatomarctus* sp. B). UCMP 10253 has a relatively wider m1 talonid than in UCMP 10254, a feature seen in hypocarnivorous clades such as *Cynarctus*. As is the case in *Metatomarctus* sp. A, we refrain from formally erecting a new species for *Metatomarctus* sp. B because of insufficient materials.

Euoplocyon Matthew, 1924

TYPE SPECIES: *Aelurocyon*? *brachygnathus* Douglass, 1903.

INCLUDED SPECIES: *Euoplocyon spissidens* (White, 1947) and *Euoplocyon brachygnathus* (Douglass, 1903).

DISTRIBUTION: Early Hemingfordian of Florida; and early Barstovian of Montana, Nebraska, California, and Oregon.

EMENDED DIAGNOSIS: A single derived character that distinguishes *Euoplocyon* from *Metatomarctus* and more primitive taxa is the presence of two lateral cusplets on I3. *Euoplocyon* lacks the enlarged parastyle on P4 that is present in *Psalidocyon* and others. It does not have a posteriorly extended nuchal crest, as found in *Microtomarctus* and later clades. On the other hand, it has a primitively large opening for the external auditory meatus, in contrast to the narrow openings in *Cynarctus* and *Metatomarctus* and more derived taxa. Autapomorphies of *Euoplocyon* include an elongated paroccipital process with a long free tip (seen only in *E. brachygnathus*) and a hypercarnivorous dentition with reduced M1 metaconule, m1 protoconid tall and trenchant, m1 metaconid usually absent but occasionally present as a weak crest (but never a distinct cusp), m1 talonid trenchant with a dominant and centrally located hypoconid, m1 entoconid reduced to a weak cingulum, and m2 metaconid reduced or absent.

DISCUSSION: Among medium-size borophagines, *Euoplocyon* is the most hypercarnivorous in terms of its trenchant lower carnassial. The development of a trenchant talonid of carnassial in *Euoplocyon* and other extinct and living taxa such as *Enhydrocyon*, *Cuon*, *Speothos*, and one species of *Aelurodon* (e.g., *A. taxoides magnus* Thorpe, synonymized with *A. ferox* in this study) inspired Matthew (1924, 1930) to place them all in a group to be distinct from the ''typical'' canids with basined talonids. Recent studies by us on the extinct hesperocyonines (Wang, 1994) and living canines (Tedford et al., 1995) demonstrate that hypercarnivorous dentitions, as in hypocarnivorous and mesocarnivorous ones, are equally subject to parallelisms. A completely trenchant talonid developed at least five times in the two other major clades of canids: three times among the living canines (in *Speothos*, the *Cuon–Lycaon* clade, and the extinct South American *Protocyon* [Berta, 1988]), and twice among the hesperocyonines (in *Enhydrocyon* and *Ectopocynus*), although the hesperocyonines initially had a rather trenchant talonid. The borophagines independently developed trenchant heels at least twice: in *Euoplocyon* and in advanced *Aelurodon*.

Tedford and Frailey (1976) first pointed out a possible relationship of *Euoplocyon*

with advanced borophagines such as *Tomarctus* and *Aelurodon*, based mostly on dental similarities. We now have cranial materials that show a generalized skull without the advanced cranial features in advanced borophagines such as *Aelurodon*. Such cranial structures suggest a relatively basal position in the phylogeny, near *Psalidocyon* and *Microtomarctus*.

Dentally, the hypercarnivorous morphology in *Euoplocyon* appears rather suddenly without intermediate forms, given the phylogenetic position postulated in this study. When the relatively more primitive *E. spissidens* first appears in the late early Hemingfordian Thomas Farm Local Fauna, its lower carnassial is already that of a highly advanced form. None of the other Hemingfordian or earlier borophagines display any tendency toward a trenchant talonid on m1 (most are in the opposite direction toward a more basined talonid). This may suggest that *Euoplocyon* originated in the southern part of North America, where vertebrate fossils earlier than the Thomas Farm Local Fauna are poorly represented. The fact that similar-size canids, such as *Osbornodon iamonensis* and *Metatomarctus canavus*, occur in both the Hawthorn Formation in Florida and the Runningwater Formation in Nebraska, whereas *E. spissidens* is restricted to Florida, further suggests that *E. spissidens* could have dispersed to the northern Great Plains but did not.

Euoplocyon spissidens (White, 1947)

Figure 60N–Q

Aelurocyon spissidens White, 1947: 497, fig. 1A, B.
Parictis bathygenus White, 1947 (in part): 500, fig. 2A.
Enhydrocyon spissidens (White): Olsen, 1958: 597, fig. 3A–C.
Euoplocyon spissidens (White): Tedford and Frailey, 1976: 5, fig. 2C, D. Munthe, 1998: 136.
Osbornodon iamonensis (Sellards, 1916): Wang, 1994 (in part): 120 (MCZ 3930 only).

HOLOTYPE: MCZ 4246, (AMNH cast 56015), left partial ramus with p2–p3 alveoli, p4–m1, and m2 alveolus (fig. 60N, O) from the Thomas Farm Local Fauna, Hawthorn Formation (late early Hemingfordian), Gilchrist County, Florida.

REFERRED SPECIMENS: From the type locality: MCZ 3930 (AMNH cast 129639), left partial maxillary with P4–M2 (referred to *Parictis bathygenus* White, 1947: fig. 2A); and MCZ 7310 (AMNH cast 56017) (Tedford and Frailey, 1976: fig. 2C, D), left partial ramus with p4–m2 (fig. 60P, Q).

DISTRIBUTION: Late early Hemingfordian of Florida.

EMENDED DIAGNOSIS: Primitive characters that distinguish *E. spissidens* from *E. brachygnathus* are p4 less robust, m1 and m2 talonids longer and wider, m2 metaconid distinct but smaller than protoconid, and lower toothrow and anterodorsal part of horizontal ramus less deflected laterally.

DESCRIPTION AND COMPARISON: Almost no additional material is available except the present reference of a maxillary fragment (MCZ 3930) previously referred to *Parictis bathygenus* by White (1947: 500) and to *Osbornodon iamonensis* by Wang (1994: 120). This maxillary has canidlike upper molars and cannot belong to the same species represented by the holotype lower jaw of the ursoid *Parictis* (?*Cynelos*) *bathygenus*. The size of the upper carnassial is significantly smaller than the type of *O. iamonensis*, and its relatively small M2 is in sharp contrast to the enlarged M2 in *O. iamonensis*. The upper teeth of MCZ 3930 compare favorably, both in size and shape, to those of *E. brachygnathus*. The only subtle difference is a more posteriorly positioned P4 protocone than is the case in *E. brachygnathus*. If the present reference is correct, reduction of the metaconule of M1 in *E. spissidens* is already as advanced as that in *E. brachygnathus*, as would be expected for the highly trenchant m1 of *E. spissidens*.

The anterior horizontal ramus of *Euoplocyon spissidens* is not laterally deflected as in *E. brachygnathus*. Of the few known lower teeth, *E. spissidens* is little different from *E. brachygnathus* in dental dimensions (appendix III)—the two species are almost indistinguishable on the ratio diagram (fig. 48). Qualitatively, however, the early Hemingfordian *E. spissidens* possesses a few primitive features relative to the early Barstovian *E. brachygnathus*: the m1 entoconid shelf, although considerably reduced, is slightly wider than in *E. brachygnathus*; and the m2 metaconid is not yet completely lost.

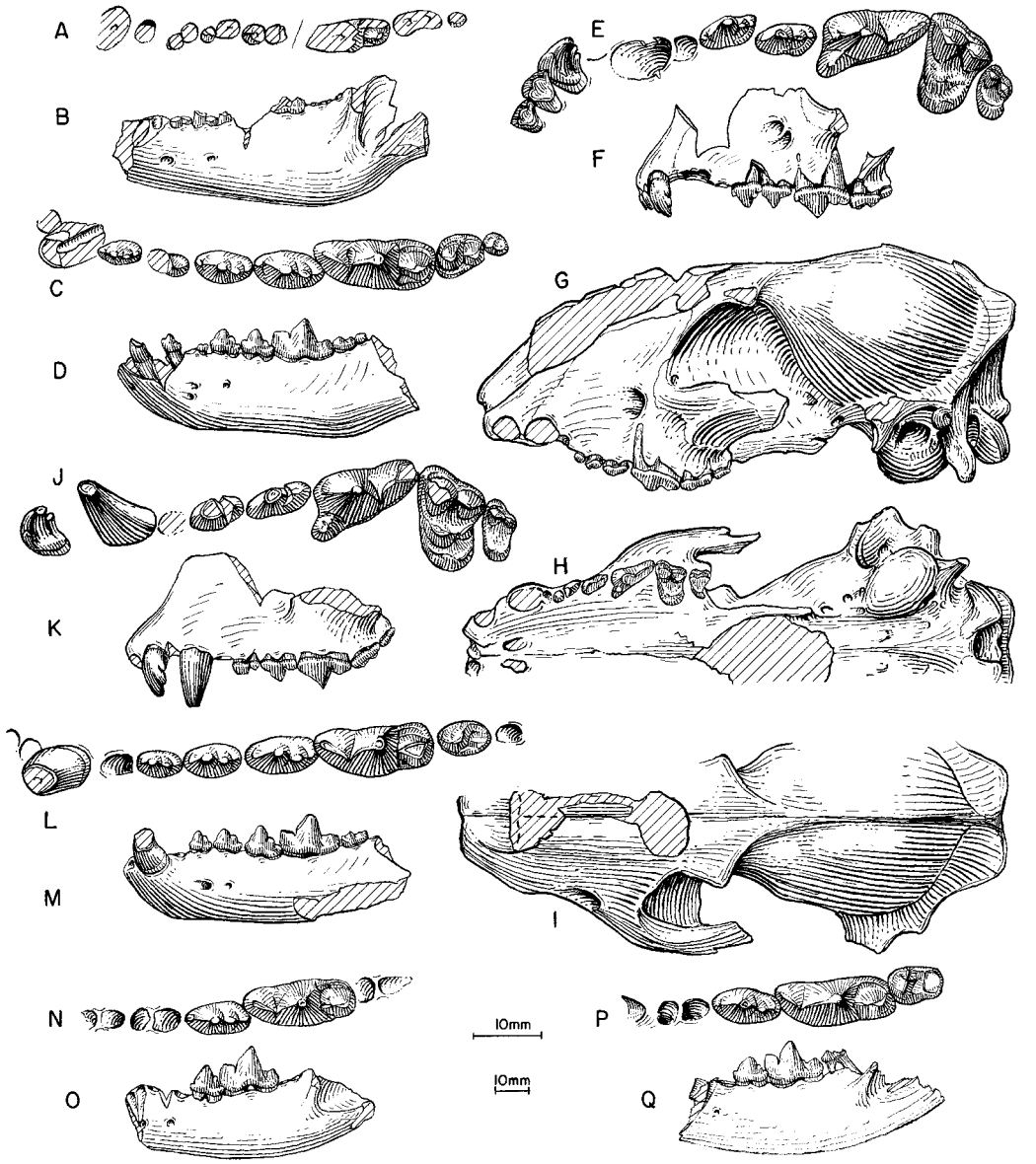

Fig. 60. **A**, Occlusal and **B**, lateral views of ramus, *Euoplocyon brachygnathus*, CMNH 752, holotype, near New Chicago, Flint Creek beds (early Barstovian), Granite County, Montana. **C**, Lower teeth and **D**, ramus, *E. brachygnathus*, AMNH 18261 (holotype of *E. praedator*), Sheep Creek Quarry, Olcott Formation (early Barstovian), Sioux County, Nebraska. **E**, Upper teeth and **F**, lateral view of maxillary, *E. brachygnathus*, F:AM 25489, Trojan Quarry, Olcott Formation, Sioux County, Nebraska. **G**, Lateral, **H**, ventral, and **I**, dorsal views of skull (reversed from right side), *E. brachygnathus*, F:AM 50120, Steep Side Quarry, Green Hills Fauna, Barstow Formation (early Barstovian), San Bernardino County, California. **J**, Upper teeth and **K**, lateral view of maxillary, *E. brachygnathus*, F:AM 50123, Steep Side Quarry. **L**, Lower teeth and **M**, ramus (m2 reversed from right side), *E. brachygnathus*, F: AM 27314, Barstow Formation. **N**, Lower teeth and **O**, ramus, *E. spissidens*, MCZ 4246, holotype, Thomas Farm Local Fauna, Hawthorn Formation (early Hemingfordian), Gilchrist County, Florida. **P**, Lower teeth and **Q**, ramus, *E. spissidens*, MCZ 7310, Thomas Farm Local Fauna. The longer (upper) scale is for A, C, E, J, L, N, and P, and the shorter (lower) scale is for the rest.

DISCUSSION: With the fragmentary materials available, we have little more information than when this species was last examined by Tedford and Frailey (1976). Consequently, the various arguments proposed in that paper for assignment of this Thomas Farm species to *Euoplocyon* are still valid, and little can be added except the larger phylogenetic perspective afforded in this study.

If *spissidens* is correctly referred to *Euoplocyon* as a primitive species of that genus, it follows that the broadened palate and the associated lateral deflection on the lower jaw of *E. brachygnathus* must have been derived within the *Euoplocyon* clade, independent from those in advanced borophagines such as *Aelurodon* and *Epicyon*. As commented under the genus *Euoplocyon*, these features, as commonly associated with hypercarnivorous dentitions, have been developed several times during the history of the Canidae.

Euoplocyon brachygnathus (Douglass, 1903)

Figure 60A–M

Aelurocyon? *brachygnathus* Douglass, 1903: 173, fig. 16.

Euoplocyon praedator Matthew, 1924: 103. Tedford and Frailey, 1976: 6, fig. 2A, B. Munthe, 1998: 136.

Euoplocyon? sp. Gazin, 1932: 50, fig. 3.

?*Aelurodon brachygnathus* (Douglass): VanderHoof and Gregory, 1940: 152.

Aelurodon brachygnathus (Douglass): McGrew, 1944b: 79.

HOLOTYPE: CMNH 752 (AMNH cast 101208), left partial ramus with i1–i3 broken alveoli and c1–m3 all represented by roots or broken teeth (fig. 60A, B), near New Chicago, Flint Creek beds (early Barstovian), Granite County, Montana.

REFERRED SPECIMENS: From the Olcott Formation (early Barstovian), Sioux County, Nebraska: AMNH 18261, left ramus with i1–i3 alveoli, c1 broken, and p1–m3 (p2 broken) (fig. 60C, D), Sheep Creek Quarry (holotype of *Euoplocyon praedator* Matthew, 1924); F:AM 25488, left partial ramus with i1–p1 alveoli and p2–m1 (p4 alveolus), Humbug Quarry; F:AM 25489, left premaxillary and maxillary with I1–M2 (C1–P1 alveoli) (fig. 60E, F), Trojan Quarry (Sinclair Quarry No. 4, horizon A); F:AM 25442, left ramus with i1–i3 alveoli, c1–m2, and m3 alveolus, Echo Quarry; F:AM 25443, left ramus with i1–m3 (p1 and p3 alveoli), Echo Quarry; F:AM 105333, left partial ramus with i1–p1 alveoli, p2, and p3–m1 all broken, Echo Quarry; and F:AM 129867, left ramus with i1–i3 alveoli, broken c1, p1 alveolus, and broken p2–m3, Quarry 2.

Green Hills Fauna, Barstow Formation (early Barstovian), San Bernardino County, California: F:AM 27225, left ramus with c1 broken–m2 and m3 alveolus, Green Hills; F:AM 27314, partial mandible with c1–m2 (p1 and m3 alveoli) (fig. 60L, M), ?Second Division; F:AM 27315, right and left partial rami with unerupted p4–m3, Green Hills; F:AM 27315A, left immature partial ramus with c1 erupting, unerupted p3 and p4, and m2–m3; F:AM 27315B, right and left rami with i3–m1 and m2–m3 alveoli, Green Hills; F:AM 27532, left premaxillary and left and right partial maxillae with I1–I2 roots and I3–M2, Green Hills; F:AM 50120, crushed skull with I3–P1 alveoli and P2 broken–M2 (fig. 60G–I), Steep Side Quarry; F:AM 50122, left partial maxillary with I3 broken–P3 and P4 broken, Steep Side Quarry; F:AM 50123, left premaxillary-maxillary with I1–I2 alveoli and I3–M2 (P1 alveolus and P2 broken) (fig. 60J, K), Steep Side Quarry; F:AM 67325, right partial ramus with p2–p3 alveoli and p4 broken–m1, Steep Side Quarry, upper level; and F:AM 67326, left partial ramus with p1 alveolus, p2–p3 both broken, p4–m1, and m2 alveolus (F:AM 67325 and 67326 being possibly one individual), Steep Side Quarry; and F:AM 67327, right partial premaxillary-maxillary with I1–P2, Steep Side Quarry.

Skull Spring Local Fauna (LACM-CIT loc. 57), Butte Creek Formation (early Barstovian), Malheur County, Oregon: LACM-CIT 392, left isolated m1 (Gazin, 1932: fig. 3).

DISTRIBUTION: Early Barstovian of Montana, Nebraska, California, and Oregon.

EMENDED DIAGNOSIS: Derived characters that separate *Euoplocyon brachygnathus* from *E. spissidens* are p4 more robust; m1–m2 talonids shorter and narrower, metaconid absent; and lower toothrow and anterodorsal part of the horizontal ramus strongly deflected laterally. Autapomorphies for *E. brach-*

ygnathus (although their status in *E. spissidens* is unknown) include mastoid large and knoblike, long free tip of paroccipital process, and partitioned infraorbital canal.

DESCRIPTION AND COMPARISON: Cranial morphology of this species is known only from a crushed skull from the Barstow Formation (F:AM 50120). Reference of this skull is based on its short snout and broad palate, which correspond to similarly shortened mandible and lateral deflected lower premolars, and secondarily on the entirely shearing mode of wear on its premolars, as would be expected for a highly hypercarnivorous lower dentition. Furthermore, its narrowed heel of M1 that lacks a metaconule is what would be expected for a trenchant talonid of m1. F:AM 50120 suffers from heavy crushing on top of the skull. This distortion and the advanced age of this individual (as indicated by heavy wear) make many bony sutures difficult to recognize. Thus, it is not clear whether the premaxillary is in contact with the frontal, although this is likely because of well-developed lateral cusplets on I3, which seem related to a stronger, more securely anchored premaxillary process. A moderate frontal sinus is probably present on F:AM 50120, judging from the slightly enlarged supraorbital region. However, the sinus does not seem to extend behind the postorbital constriction because of a lack of inflation in this area typically associated with a large sinus. The nuchal crest is low and lacks the posterior extension seen in *Microtomarctus* and more advanced taxa. The most unambiguous hypercarnivorous feature of the skull is its broadened palate and shortened rostrum (palate width at P1 and length of P1–M2 in fig. 47), apparently in parallel with similar features in *Aelurodon* and the *Epicyon–Borophagus* clade. The opening for the external auditory meatus is large with a V-shape notch on the anterior edge of the opening, and lacks a bony lip for the meatus. The mastoid process of *E. brachygnathus* is inflated, as in *Enhydrocyon*, but in contrast to the latter, the paroccipital process is prominently elongated so that it has a free tip 9 mm long. These peculiarities in the mastoid and paroccipital processes are apparently autapomorphies, since taxa above and below *Euoplocyon* lack these features. Another autapomorphous feature is a tendency for the infraorbital canal to be partitioned into two foramina by a septum—a complete septum is present in F:AM 25489, and a partial septum is seen on the right side of F:AM 50120 (the left canal is undivided).

Except for the highly hypercarnivorous lower carnassial, teeth of *Euoplocyon brachygnathus* exhibit typical medium-size borophagine characteristics, with well-developed cusplets on incisors and premolars. Two distinct lateral cusplets are present on I3 (seen on F:AM 25489, 50123, and 67327), and the premolars are similarly cuspidate with distinct cingular and accessory cusplets, even on P1 and p1, features that are not seen in *Enhydrocyon*. A parastyle on P4 is almost entirely lacking in the Barstow sample, and it is weakly developed in only one individual (F:AM 25489) from the Snake Creek sample. The wear on the upper premolars in F:AM 50120 (fig. 60H) represents mostly a shearing mode (a longitudinal, nearly vertical facet on the lingual face of all premolars that are self-sharpening), in contrast to a predominantly crushing mode of wear in most mesocarnivorous borophagines (flattening of the principal cusps of the premolars). The M1 is slender and its metaconule is conspicuously absent among closely related borophagines that always have a distinct metaconule. Reduction of the metaconule is consistently correlated with a trenchant m1 talonid, as seen in hypercarnivorous canines (e.g., *Speothos*) and hesperocyonines (e.g., *Enhydrocyon*). The M2 is reduced relative to the M1.

Evidence for hypercarnivory is more clearly seen on the lower teeth, especially the m1. As in *Euoplocyon spissidens*, the metaconid is lost in all individuals. In general, the talonid of m1 is more reduced (narrowed) than in *E. spissidens*. The entoconid either is completely lacking or is represented by a narrow and low cingulum on the lingual edge of the talonid. In all individuals, the metaconid on m2 is lost except for a transverse crest leading down the apex of the protoconid, in contrast to the small metaconid in *E. spissidens*.

DISCUSSION: No additional material of *Euoplocyon brachygnathus* is known from the type locality. Although the only tooth fragment remaining on the holotype is a partial

talonid of m1, as well as the roots of the cheekteeth, the horizontal ramus (fig. 60A, B) displays the characteristic shape of this species, which is much better represented in material from the Olcott Formation of Nebraska and the Barstow Formation of California. The combination of a short and deep horizontal ramus with a laterally deflected anterodorsal region is not seen in other contemporaneous canids. Its narrow and trenchant m1 talonid and its close spacing of the cheekteeth provide additional evidence that *E. brachygnathus* is conspecific with *E. praedator* from the Lower Snake Creek Fauna. As such, *E. brachygnathus*, a fitting name but based on a poorly preserved holotype, has priority over Matthew's *E. praedator*.

As the terminal member of a small, precociously hypercarnivorous clade, *Euoplocyon brachygnathus* displays several traits convergent with those in the *Aelurodon* clade. For example, a broadened palate and the associated lateral eversion of the anterior mandible are typical features of the latter clade. Dentally, *E. brachygnathus* also shares with the *Aelurodon* clade a reduced M2 and m2, as well as a general trend of a reduced M1 metaconule and narrowed m1 talonid. However, the generally primitive cranial configuration of *E. brachygnathus* (e.g., relatively small frontal sinus, nuchal crest not expanded, and large opening for auditory meatus) indicates a phylogenetic position close to *Metatomarctus*, not to *Aelurodon*.

Psalidocyon, new genus

TYPE SPECIES: *Psalidocyon marianae*, new species.

ETYMOLOGY: Greek: *psalido*, scissors; *cyon*, dog.

INCLUDED SPECIES: Type species only.

DISTRIBUTION: Early Barstovian of New Mexico and Nebraska.

DIAGNOSIS: A synapomorphic feature shared with *Microtomarctus* and higher taxa is a pronounced P4 parastyle, which is absent in *Euoplocyon* and more primitive taxa. Derived characters unique to this genus are incisors tall-crowned and complex; canine large with lingual surface compressed and concave, anterolingual crest and posterolingual crest present; P1–P3 and p1–p4 tall-crowned and complex with sharp anterior and posterior blades; m1 trigonid very open with sectorial paraconid-protoconid blade and metaconid very large; m2 metaconid large, much taller than protoconid; and deep horizontal ramus. Characters of *Psalidocyon* that are primitive relative to *Microtomarctus* are nuchal crest not posteriorly expanded and lambdoidal crests unreduced.

Psalidocyon marianae, new species

Figure 61

HOLOTYPE: F:AM 27397, skull with I1–M2, mandible with i1–m3 (fig. 61A–F) and associated limbs, including partial scapula, humerus, femur, tibia, and questionably associated partial manus and nearly complete pes, from southeast of White Operation, Skull Ridge Member, Tesuque Formation (early Barstovian), Santa Fe County, New Mexico.

ETYMOLOGY: Named in honor of Marian Galusha for her contributions in the field and office during and following the work of the Frick Laboratory in the southwestern United States.

REFERRED SPECIMENS: From Olcott Formation (early Barstovian), Sioux County, Nebraska: F:AM 25490, right partial ramus with c1–p4 and m1 broken, Trojan Quarry (= Quarry 4 of Horizon A); F:AM 61295, left partial ramus with i1–p1 alveoli and p2–m1, Humbug Quarry; F:AM 61296, right partial ramus m1–m2 and m3 alveolus (fig. 61G, H), Echo Quarry; F:AM 61297, left partial ramus i2–m1 (p1–p2 broken), Echo Quarry; and F:AM 61298, right partial ramus with m1–m2 and m3 alveolus, Quarry 2.

DISTRIBUTION: Early Barstovian of New Mexico and Nebraska.

EMENDED DIAGNOSIS: As for genus.

DESCRIPTION AND COMPARISON: The holotype skull and mandible are only slightly crushed laterally. In overall cranial proportions, *Psalidocyon* closely resembles *Desmocyon matthewi* (fig. 62). The premaxillary process appears to be in contact with the nasal process of the frontal, although breakage in this area makes the observation less certain. The dorsal profile of the skull indicates a well-developed frontal sinus extending posteriorly to the frontal-parietal suture. The nu-

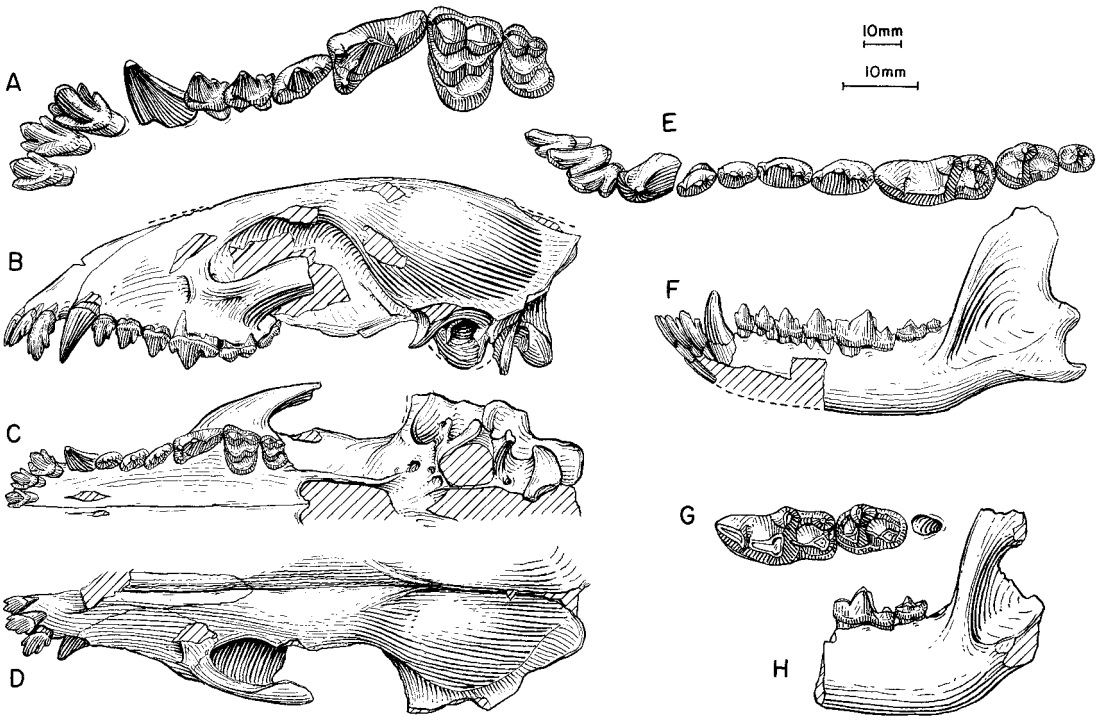

Fig. 61. *Psalidocyon marianae*. **A**, Upper teeth (I1–I2 reversed from right side), **B**, lateral, **C**, ventral, and **D**, dorsal views of skull, **E**, lower teeth, and **F**, ramus (p2, m2, and ascending ramus reversed from right side), F:AM 27397, holotype, southeast of White Operation, Skull Ridge Member, Tesuque Formation (early Barstovian), Santa Fe County, New Mexico. **G**, Lower teeth and **H**, ramus (reversed from right side), F:AM 61296, Echo Quarry, Olcott Formation (early Barstovian), Sioux County, Nebraska. The shorter (upper) scale is for B, C, D, F, and H, and the longer (lower) scale is for the rest.

chal crest is fan-shaped in the posterior view. The lambdoidal crest is sharp and unreduced. Both bullae are broken, especially the caudal entotympanic part. The opening for the external auditory meatus is large and lacks an external lip. The paroccipital process is laterally expanded and forms a deep pocket between it and the bulla. The mastoid process is small and recedes beneath a prominent horizontal shelf. The horizontal ramus has a weak subangular lobe.

The entire dentition of the holotype is nearly perfectly preserved. Although all permanent teeth are fully erupted, there is little trace of wear on any tooth. Dental morphology of this species is quite unusual in its development of sharp blades along the entire dental battery from incisors through premolars. These sharp blades are formed on the lateral edges of the incisors and on the anterior and posterior edges of the main cusps of canines and premolars. The cutting edges are further enhanced by the high crowns of these teeth. Despite the sharp blades on the premolars, the tips of these teeth usually indicate apical rather than shearing wear, as is common in most borophagines of similar size. The upper incisors are procumbent and have a prominent main cusp with one or two accessory cusps on either side. The C1 is short and straight with a strong anterolingual ridge that bends lingually to form a lingual groove on the canine. The large upper and lower premolars are imbricated within the jaws in young individuals. Premolar accessory and cingular cusps are distinct, and the right P2 in the holotype even has two posterior accessory cusplets that create a serrated posterior cutting edge. The premolars also have a narrow lingual cingula. The P4 has a

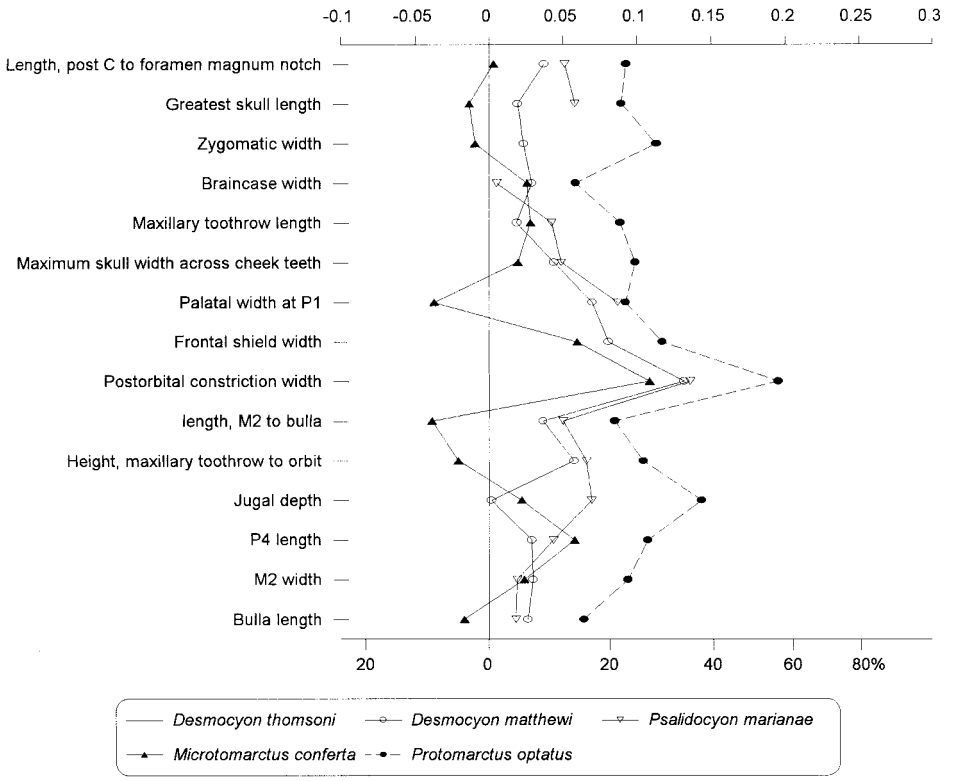

Fig. 62. Log-ratio diagram for cranial measurements of *Desmocyon*, *Psalidocyon*, *Microtomarctus*, and *Protomarctus* using *Desmocyon thomsoni* as a standard for comparison (straight line at zero). See text for explanations and appendix II for measurements and their definitions.

distinct parastyle, and its protocone is reduced. Like other premolars, the anterior and posterior blades of the P4 paracone are sharp-edged. The upper molars remain primitive and are indistinguishable from those of *Metatomarctus*.

The lower incisors have a large medial cusp and smaller, but distinct lateral cusps. Like the upper canines, the anterolingual ridge of the lower canine bends lingually to form a prominent groove. The outline of the m1 is more slender than for taxa of similar size. The cutting blade on m1 is more longitudinally oriented than in *Metatomarctus*, and the talonid cusps are more cuspidate with a strong transverse crest. The m2 has a dominant metaconid, exceeded only by advanced species of *Cynarctus*.

DISCUSSION: Although represented by a few ramal fragments only, *Psalidocyon marianae* is positively identified in the Olcott Formation of Nebraska because of the highly characteristic dental morphology. Besides the autapomorphies mostly related to the bladelike incisors and premolars, the skull and upper molars of *Psalidocyon* are rather typical of medium-size, mesocarnivorous borophagines, not unlike those of *Desmocyon matthewi* and *Metatomarctus*. This combination of primitive and derived characters best places it above *Metatomarctus* and below *Microtomarctus*.

Rudimentary development of the bladelike premolars and canines can be found in a partial mandible (F:AM 49181; fig. 46C, D) from the early Hemingfordian of Nebraska, presently referred to *Desmocyon matthewi*. This individual shows sharp anterior crests on the premolars, a distinct anterolingual crest on the c1, and a thin-bladed lower carnassial. In the absence of upper dentitions, which are critical in evaluating relationships

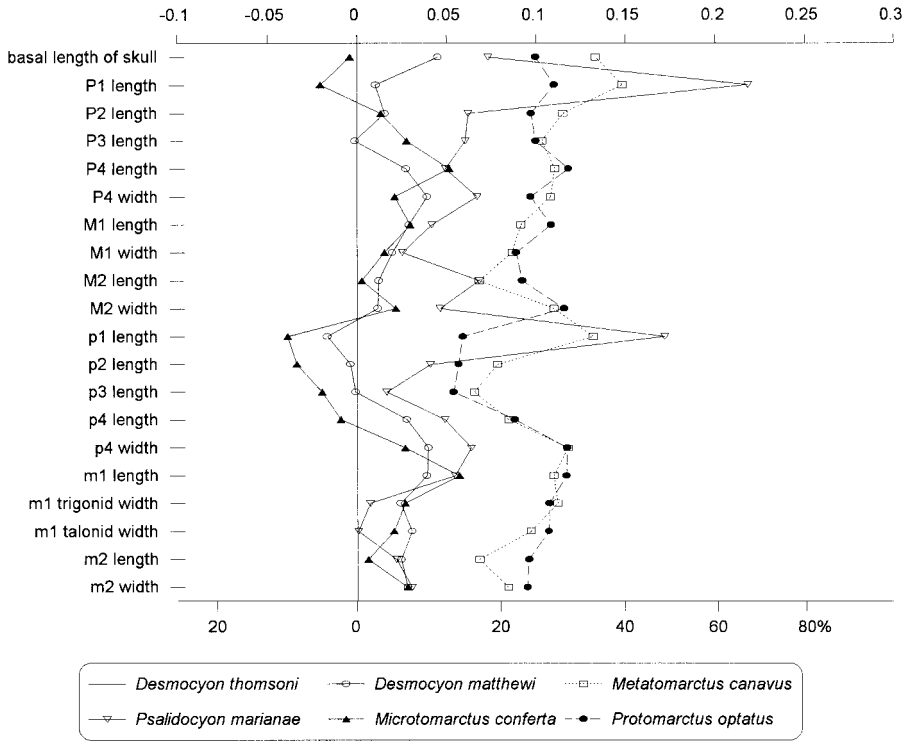

Fig. 63. Log-ratio diagram for dental measurements of *Desmocyon*, *Metatomarctus*, *Psalidocyon*, *Microtomarctus*, and *Protomarctus* using *Desmocyon thomsoni* as a standard for comparison (straight line at zero). See text for explanations and appendix III for summary statistics of measurements and their definitions.

of closely related species, we chose to explain these features on F:AM 49181 as an individual variation of *D. matthewi*, rather than as an early occurrence or a primitive species of *Psalidocyon*. Such an earlier appearance of *Psalidocyon*-like features in a more primitive taxon of *D. matthewi* is roughly consistent with our phylogenetic conclusions, which place these two genera not far apart.

Microtomarctus, new genus

TYPE SPECIES: *Tephrocyon conferta* Matthew, 1918.

ETYMOLOGY: Greek: *micro*, small, plus *tomarctus*.

INCLUDED SPECIES: Type species only.

DISTRIBUTION: Late Hemingfordian of New Mexico; early Barstovian of Nevada, California, New Mexico, Nebraska, and Colorado; late Barstovian of Texas, California, Colorado, and New Mexico.

DIAGNOSIS: Synapomorphic features shared with *Metatomarctus* and higher taxa are posterior expansion of the nuchal crest that overhangs the occipital condyle, and lambdoidal crests suppressed. Characters unique to this genus are small size, brachycephalic skull, and small, short canines. Characters of *Microtomarctus* that are primitive relative to *Protomarctus* are frontal sinus relatively smaller and less complex, auditory meatus of large diameter with V-shaped opening, and a single lateral accessory cusplet on I3 (here interpreted as a reversal).

Microtomarctus conferta (Matthew, 1918)

Figures 64–66

?*Tephrocyon* cf. *temerarius* (Leidy, 1858): Matthew and Cook, 1909: 376 (AMNH 13859).

Tephrocyon confertus Matthew, 1918: 189, fig. 1.
Nothocyon vulpinus coloradoensis Thorpe, 1922b: 430, fig. 2.
Tomarctus confertus (Matthew): Matthew, 1924: 96, fig. 17. Hough, 1948: 107. Downs, 1956: 237.
Tomarctus paulus Henshaw, 1942: 105, pl. 2, figs. 3, 4a. Downs, 1956: 237. Munthe, 1998: 135.
Nothocyon vulpinus (Matthew, 1907): Galbreath, 1953: 100.
Tomarctus cf. *T. paula* (Henshaw): Honey and Izett, 1988: 20, fig. 8.
Tomarctus? *confertus* (Matthew): Munthe, 1998: 135.

HOLOTYPE: AMNH 17203, right ramus with i1–i3 alveoli, c1–m2 (p1 and p3 alveoli) (fig. 64A, B), 23 mi south of Agate, Lower Snake Creek Fauna, Olcott Formation (early Barstovian), Sioux County, Nebraska.

REFERRED SPECIMENS: Lower Snake Creek Fauna, Olcott Formation (early Barstovian), Sioux County, Nebraska: AMNH 13859, left ramal fragment with c1–p4 alveoli, m1 broken, and m2–m3, 23 mi south of Agate (referred to ?*Tephrocyon* cf. *temerarius* by Matthew and Cook, 1909: 376); AMNH 17204, left partial ramus with p3–m2, 23 mi south of Agate; AMNH 17205, left ramus with c1 and p1 alveolus–m2, 23 mi south of Agate; AMNH 17206, left partial ramus with m1–m2 and m3 alveolus, 23 mi south of Agate; AMNH 18253, partial skull, premaxillary missing, C1–P2 alveoli, and P3–M2, Quarry B, figured by Matthew (1924, fig. 17); AMNH 18254, left partial ramus with p3–p4 and all alveoli, Quarry A; AMNH 20056, 3 isolated teeth of two or more individuals, right M1 and two right m1s, 23 mi south of Agate; AMNH 20064, right ramal fragment with p4–m1, West Sinclair Draw; F:AM 61024, left partial ramus with c1, p1–p2 alveoli, p3–m1, and m2–m3 alveoli, Version Quarry; F:AM 61025, right partial ramus with i1–i3 alveoli, c1, p1 alveolus, p2–m2, and m3 alveolus, Humbug Quarry; F:AM 61026, right partial ramus with c1–p4, m1 broken–m2, and m3 alveolus, Echo Quarry; F:AM 61027, left partial ramus with c1 and p1 alveolus–m1, Quarry 2; F:AM 61028, right partial ramus with m1–m2 and m3 alveolus, New Surface Quarry; F:AM 61029, left partial ramus with c1–p3 alveoli, p4–m2, and m3 alveolus, Echo Quarry; F:AM 61030, right ramal fragment with c1 alveolus and p2–p3, New Surface Quarry; F:AM 61031, partial skull with C1–P3 alveoli, P4, and M1–M2 alveoli, Echo Quarry; F:AM 61032, left partial maxillary with P2–P4, Echo Quarry; F:AM 61033, right ramus with i1–p1 all alveoli, p2–m2, and m3 alveolus, Echo Quarry; F:AM 61034, left partial ramus with p1–p2 alveoli, p3 broken–m2, and m3 alveolus, Quarry 2; F:AM 61035, left partial ramus with p2–p3 alveoli, p4–m1, and m2–m3 alveoli, Echo Quarry; F:AM 61036, right partial ramus with i3–c1 broken, p1 alveolus–m2 (p2 broken), Echo Quarry; F:AM 61037, left ramus with i1–i3 alveoli, c1, p1 alveolus–m2, and m3 alveolus, Echo Quarry; F:AM 61038, partial skull with P2–M2, Echo Quarry; F:AM 61039, partial skull with P2–M2 (fig. 64C–E), Echo Quarry; F:AM 67776, partial humerus, Echo Quarry; F:AM 67776B, partial humerus, Quarry 2; F:AM 67777A, partial radius, West Sand Quarry; F:AM 67778 and 67778A, partial ulna; F:AM 67787, femur, Echo Quarry; F:AM 67787A, partial femur, Echo Quarry; F:AM 67788, tibia, Echo Quarry; F:AM 67789, partial femur, New Surface Quarry; and AMNH 97232, detached teeth including P4, M2, and m1, Quarry A.

Green Hills Fauna, Barstow Formation (early Barstovian), San Bernardino County, California: F:AM 27272A, left and right maxillary fragments with P4–M2, second layer above Rak Division; F:AM 27284, right broken isolated P4, ?Second Division lower layer; F:AM 27297, left partial ramus with i3 broken–c1, p1 alveolus–m1, and m2 broken–m3 alveolus; F:AM 27297A, right and left rami with c1–m2, lower Green Hills Quarry; F:AM 27299, crushed skull with I1 broken–M2 and mandible with i1–m2, Deep Quarry; F:AM 27299A, crushed anterior part of skull with I3–P3 alveoli, P4–M1, and M2 alveolus, second layer above Third Division; F:AM 27299B, mandible with i1–m2 and m3 alveolus, Deep Quarry; F:AM 27299C, right crushed partial ramus with c1 broken, p2–p4, and m1–m2 broth broken, Deep Quarry; F:AM 27530, crushed anterior part of skull with C1–P2 alveoli and P3–M2, lower Green Hills Quarry; F:AM 50121, fragmentary skull with P4 broken–M2, upper level of Steepside Quarry; F:AM 61019, right ramal

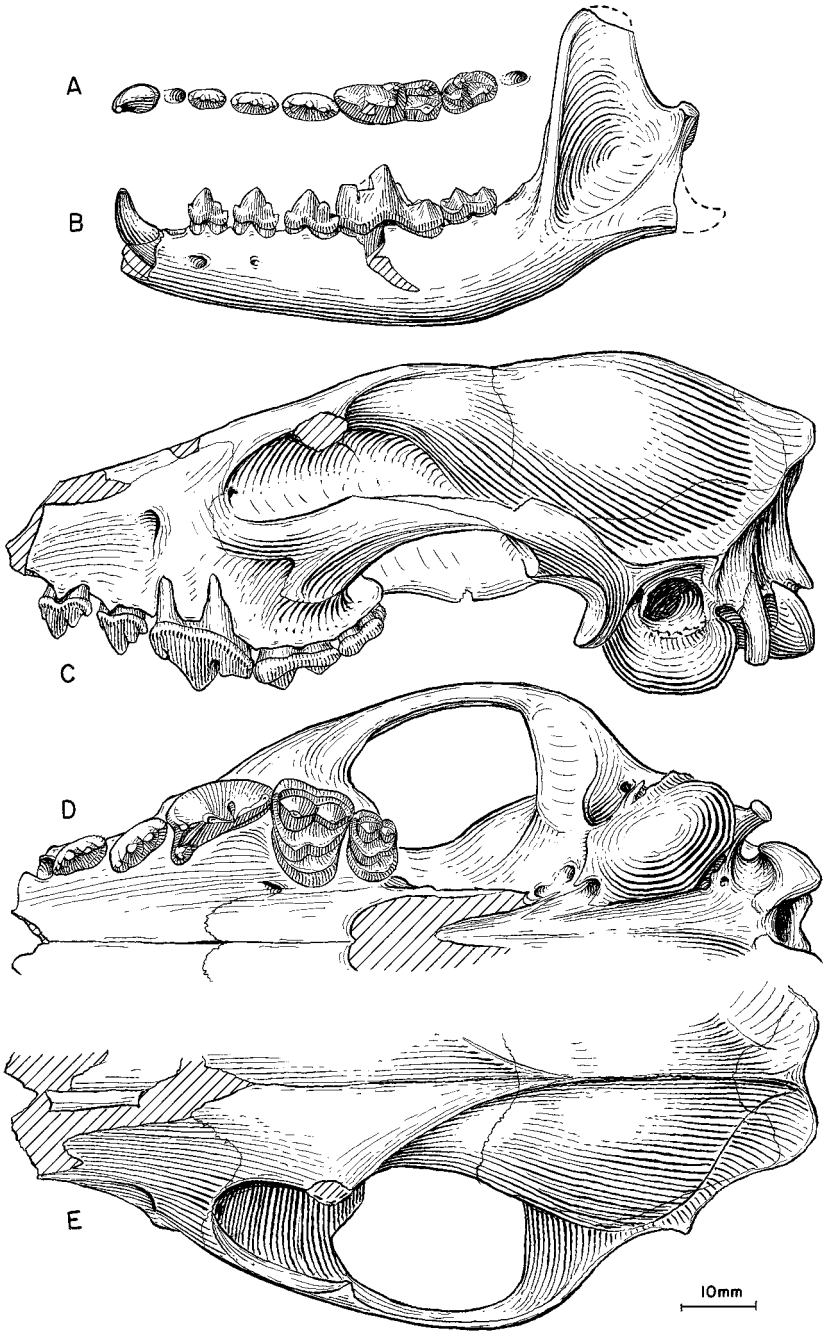

Fig. 64. *Microtomarctus conferta*. **A**, Lower teeth and **B**, ramus (reversed from right side), AMNH 17203, holotype, 23 mi south of Agate, Olcott Formation (early Barstovian), Sioux County, Nebraska. **C**, Lateral, **D**, ventral, and **E**, dorsal views of skull (bulla and P2 reversed from right side), F:AM 61039, Echo Quarry, Olcott Formation.

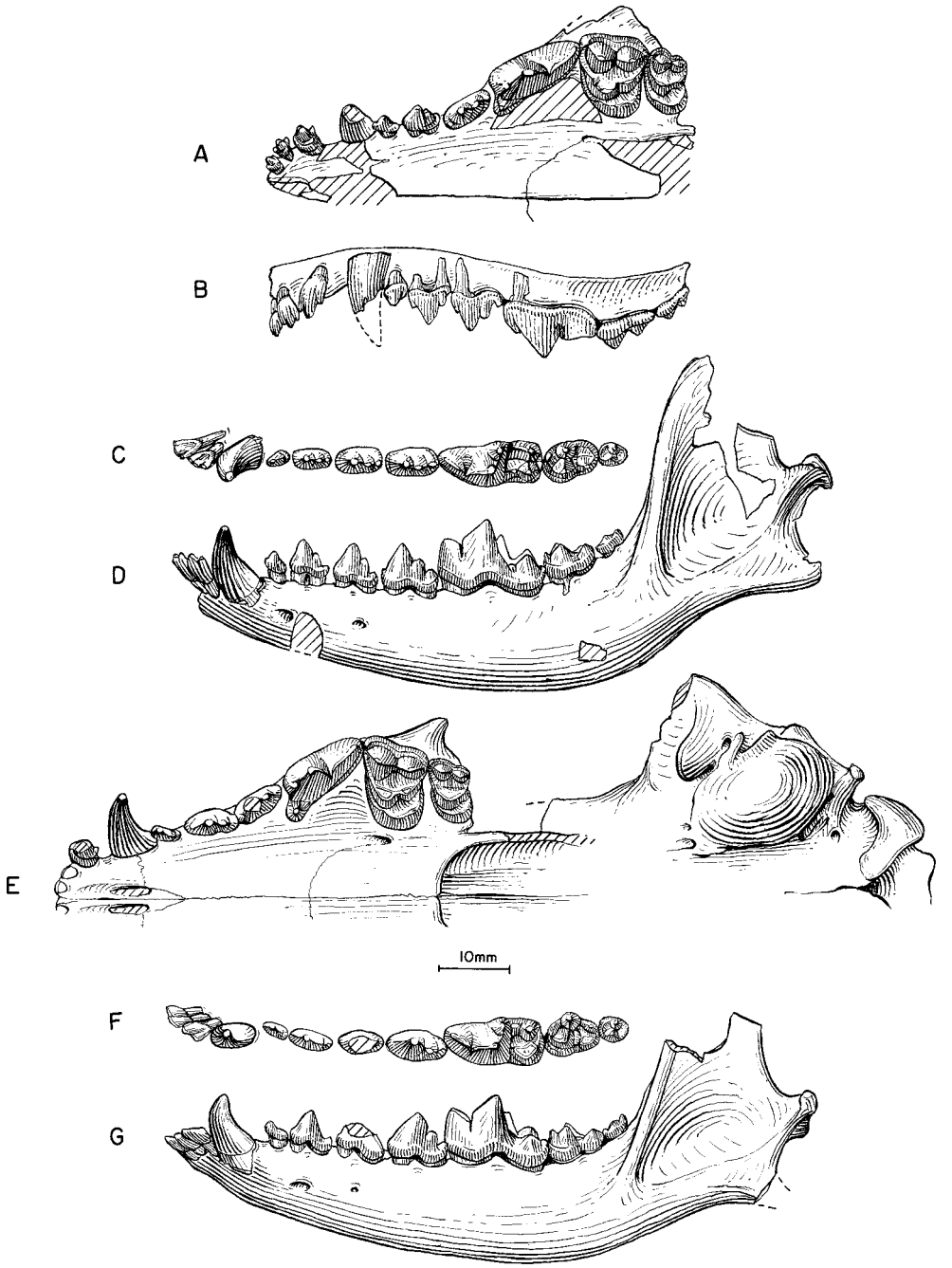

Fig. 65. *Microtomarctus conferta*. **A**, Ventral and **B**, lateral views of maxillary and upper teeth, **C**, lower teeth, and **D**, ramus, LACM-CIT 1229 (holotype of *Tomarctus paulus*), Siebert Formation, Tonopah Local Fauna (late early Barstovian), San Antonio Mountains, Nye County, Nevada. **E**, Ventral view of skull, **F**, lower teeth, and **G**, ramus, F:AM 27548, Skyline Quarry, ''First Division,'' Barstow Formation (early late Barstovian), San Bernardino County, California.

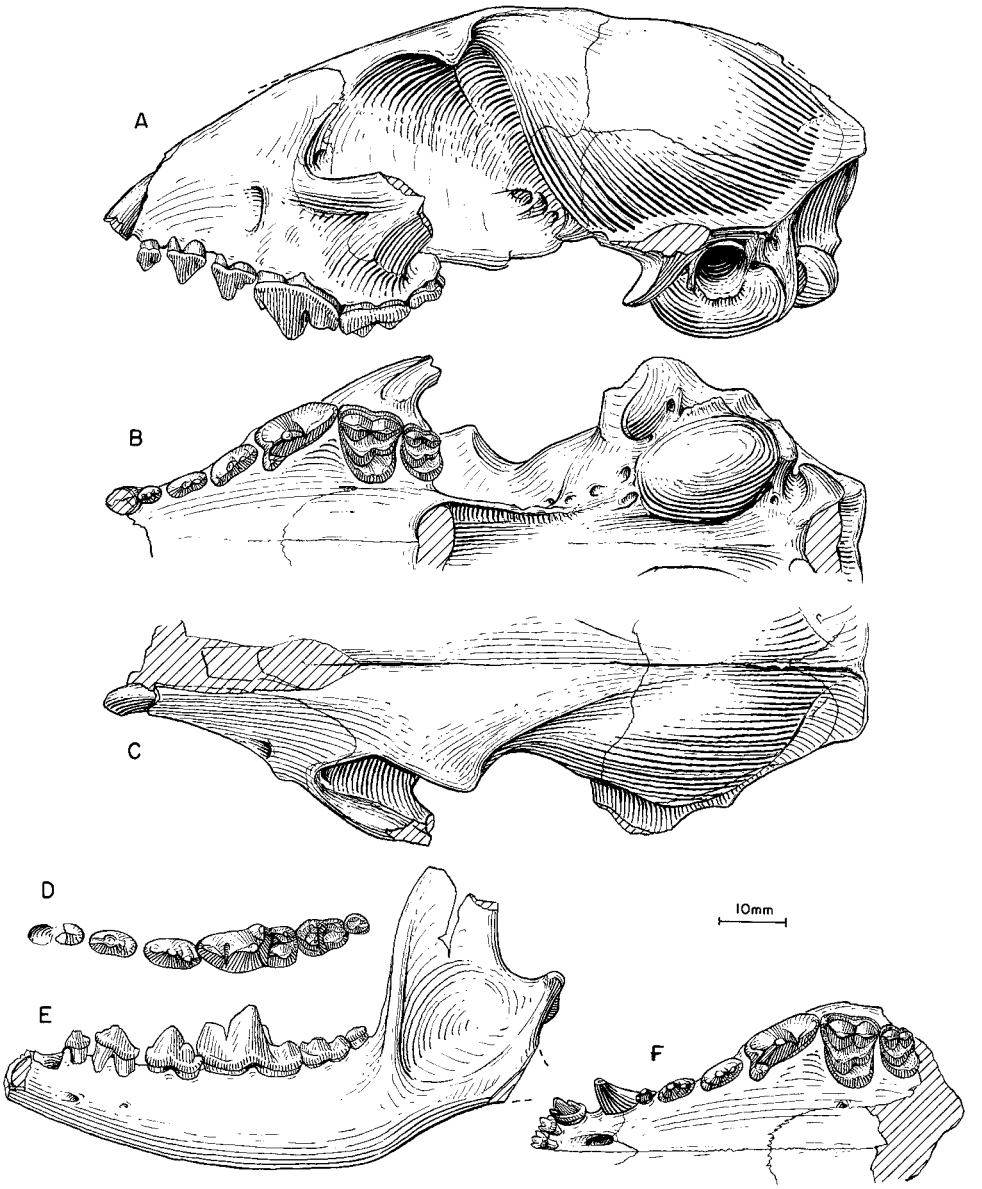

Fig. 66. *Microtomarctus conferta*. **A**, Lateral, **B**, ventral, and **C**, dorsal views of skull, **D**, lower teeth, and **E**, ramus (anterior part of ramus and p2–p3 reversed from right side), F:AM 27398X, Pojoaque Bluffs, Pojoaque Member, Tesuque Formation (early late Barstovian), Santa Fe County, New Mexico. **F**, Ventral view of partial skull (reversed from right side), F:AM 27398, Santa Cruz, Pojoaque Member, Tesuque Formation.

fragments with c1, p1 alveolus, p2, broken p3, and m1–m2, upper level of Steepside Quarry; F:AM 61019A, left ramal fragment with c1–m1 broken, upper level of Steepside Quarry; F:AM 61020, anterior half of skull with I1–P1 alveoli, P2, and P3 alveolus–M2 (M1–M2 broken), Steepside Quarry upper level; F:AM 61021, right partial maxillary with P4 broken–M2, Steepside Quarry upper level; F:AM 61022, left partial maxillary with P3–M2, Steepside Quarry upper level; and F:AM 61023, right partial ramus with c1

broken, p1 alveolus–m2, and m3 alveolus, Steepside Quarry upper level.

Yermo Local Fauna, 5 mi east of Yermo, Barstow Formation (early Barstovian), San Bernardino County, California: F:AM 27522, crushed anterior part skull with I1–P3 alveoli and P4–M2; F:AM 27527, right partial ramus with p3 broken–m3; F:AM 27527A, left partial ramus with c1, and p1 alveolus–m1; F:AM 27527B, left partial ramus with p2, p4 broken, and m1; F:AM 27527C, right partial ramus with c1–p1 alveoli, p2–m1 (p4 broken), and m2–m3 alveoli; 27527D, left partial ramus with p3 broken–m2 and m3 alveolus; F:AM 61063, right partial ramus with p2–p3 alveoli, p4–m1 both broken, and m2–m3 alveoli; F:AM 61063A, right partial ramus with m1 broken–m2 and m3 alveolus; F:AM 61063B, right partial maxillary with P4–M2; and F:AM 61063C, left partial maxillary with P4 broken–M2.

Kiva Quarry, 2 mi southwest of Zia Pueblo, Jemez Creek area, Zia Formation (late Hemingfordian), Sandoval County, New Mexico: F:AM 50143, right and left partial rami with c1–m2 and m3 alveolus.

Nambe Member, Tesuque Formation (late Hemingfordian), Santa Fe County, New Mexico: F:AM 67373, right partial ramus with i1–p2 all broken, p3, p4–m1 both broken, and m2–m3, north side of fault block south of Santa Cruz River drainage, 35 ft below No. 1 White Ash; and F:AM 105257, right partial ramus with m1–m2 both broken, East Cuyamunque, Nambe Pueblo Grant.

Skull Ridge area, Skull Ridge Member, Tesuque Formation (early Barstovian), Santa Fe County, New Mexico: F:AM 27383B, right partial ramus with p1–p2 alveoli, p3, p4 broken, and m1–m3 alveoli, Santa Cruz; F:AM 27391, right partial ramus with c1–m2 all broken; 27391A, left partial ramus with c1–p1 alveoli, and p2–m2 all broken; F:AM 27396A, left partial ramus with p3 broken–m3 (m1 broken); F:AM 27396B, right partial ramus with c1–p1 alveoli, and p2–m2 all broken, South Skull Ridge; F:AM 27396C, left partial ramus with p4–m2, 3 mi from Cuyamunque, left side of road; F:AM 27396D, anterior part of skull with I1–P3 alveoli and P4–M2 all broken; F:AM 27398Z, right partial maxillary with P4–M2 and right partial ramus with c1 broken–m3, south Skull Ridge; F:AM 27473, skull with C1, P1–P3 alveoli, and P4–M2; F:AM 27478, right and left partial rami with p2 root and p3–m3, Upper Skull Ridge; F:AM 50164, anterior part of mandible with i1–c1 all broken, p1–p4, and m1 broken, west Cuyamunque, Tesuque Pueblo just south of north boundary; F:AM 50165, associated partial rami with p4–m3, Cuyamunque; F:AM 50166, right partial ramus with c1–p1 alveoli, p2, p3 alveolus, p4–m1 both broken, and m2 alveolus, base of channel above Ash ''F''; F:AM 50167, partial mandible with i1–c1 all broken, p1 alveolus–p4, and m1–m2 both broken, Joe Rack Wash; F:AM 50168, left partial ramus with c1 broken, p1–p2 alveoli, and p3–m2 all broken, Skull Ridge, Nambe Creek side of Divide, 12 ft above Ash ''B''; F:AM 50169, left partial ramus with p1–p2 alveoli, p3–m2, and m3 alveolus, 8 ft below Ash ''B''; F:AM 50170, partial mandible with c1–m3 alveoli; F:AM 50171, left partial ramus with i3–c1 both broken, p1–p2 alveoli, p3 broken, P4, and m1 broken; F:AM 50172, partial skull with I3–M2, White Operation District above white layer; F:AM 50173, right partial ramus with c1–p3 all broken, p4, and m1–m3 all broken; F:AM 50174, right partial ramus with p4 broken–m2 and m3 alveolus; F:AM 50175, right partial ramus with c1–m2 all broken or roots, Skull Ridge area; F:AM 50176, right partial ramus with p4 and m1 broken; F:AM 50177Y, right m1, White Operation District; F:AM 50178, partial palate with left and right P4 broken and M1–M2, west Cuyamunque, white ash east of central fault; F:AM 50179, anterior part of skull with P3 broken–M2, North Skull Ridge, 40 ft above white layer; F:AM 50180, right and left partial maxillary with C1 and P2–M2, no locality data; F:AM 50182, left ramus with i1–m3, below white layer; F:AM 50188, crushed anterior part of skull with I1–M2 and both partial rami with c1 broken–m3 (m1 broken), Tesuque Grant between Arroyo Ancho and Rio Tesuque; F:AM 67336, left partial ramus with i1–p3 alveoli and p4–m3 all broken, north of Tesuque Grant, north boundary Tesuque East, Cuyamunque; F:AM 67337, right partial ramus with p4–m1 roots and m2 broken–m3, Joe Rack Wash, channel above

Ash ''F''; and F:AM 67338, left ramus fragment with p4–m1 all broken.

Cold Spring Fauna, Fleming Formation (early late Barstovian), 8 mi south of Livingston, Polk County, Texas: F:AM 63292, right and left partial rami with p1, p2–p3 both broken, p4, m1 broken, m2, and m3 alveolus.

UCMP loc. V5433, Raine Ranch Formation (late early Barstovian), 3.5 mi south of Carlin, Elko County, Nevada: UCMP uncataloged (AMNH cast 80131), right ramus with c1–m2 and m3 alveolus.

Siebert Formation, LACM-CIT loc. 172, Tonopah Local Fauna (late early Barstovian), San Antonio Mountains, near Tonopah, Nye County, Nevada: LACM-CIT 1229 (AMNH cast 116109) (holotype of *Tomarctus paulus* Henshaw, 1942), anterior part of skull with I1–M2 with fragments and mandible with i2–m3 (fig. 65A–D); LACM-CIT 1232, right and left rami with c1, p1 alveolus, and p2–m3; LACM 15973, right ramus with c1–p4 alveoli and m1 broken; LACM 15975, left maxillary fragment with P4–M2 broken; and LACM 15976, left partial ramus with p3 broken–m1 and m2 root.

Valley View Quarry, ''Second Division,'' Barstow Formation (late early Barstovian), San Bernardino County, California: F:AM 27533, skull with I1–C1 alveoli and P1–M2 and partial mandible with i2–c1 broken and p1–m3 (p3–m1 all broken); F:AM 27549, left ramus with c1 broken, p1 alveolus–m1, and m2 broken–m3 alveolus; F:AM 61042, crushed anterior part of skull with I3–P3 alveoli and P4–M2; F:AM 61043, left premaxillary-maxillary and right partial maxillary with I1–M2 (P1 alveolus); and F:AM 61056, left partial ramus with p1–p4 alveoli, m1 broken, and m2–m3 alveoli.

''First Division,'' Barstow Formation (early late Barstovian), San Bernardino County, California: F:AM 18012, right and left partial rami with c1 broken–p3 and p4 broken–m2, Mayday Quarry; F:AM 27253A, left ramus with i1–i3 alveoli, c1 broken, p1 alveolus–m2, and m3 alveolus, North End lower layer; F:AM 27270, right partial ramus with c1–p3 roots, p4, and m1 broken–m2 alveolus, Barstow area; F:AM 27291, right partial ramus with i3–c1 alveoli, p1, p2 alveolus–m1, and m2 alveolus, North End lower layer; F:AM 27294, crushed partial skull with P1 alveolus–M2 (P2 broken), North End; F:AM 27296, left partial ramus with p2–m1, *Hemicyon* Stratum; F:AM 27298, right partial ramus with i1–p1 alveoli, p2–m2, and m3 alveolus, North End lower layer; F:AM 27298A, right partial ramus with i1–i3 alveoli and c1–m1 (p1 alveolus and p2 broken), *Hemicyon* Stratum; F:AM 27298B, left ramus fragment with p4–m1, *Hemicyon* Stratum; F:AM 27524, right maxillary fragment with P3 broken, P4–M2, North End; F:AM 27525, right ramus fragment with i1–i3 roots, c1 root, p1–p3, p4–m1 roots, and m2–m3, North End; F:AM 27526, right maxillary fragment with P4–M2 (M1 broken); F:AM 27528, right and left partial rami c1, p2–m2, and m3 alveolus; F:AM 27534, partial skull with I1–I3, C1 broken, and P1–M2, Mayday Quarry; F:AM 27541, right partial ramus with i1–p1 alveoli, p2–m2, and m3 alveolus, Skyline Quarry; F:AM 27547, left partial ramus with p1 alveolus, p2–m1, and m2–m3 alveoli, Skyline Quarry; F:AM 27548, crushed skull with I1–I2 alveoli and I3–M2 and mandible with i1–m3 (fig. 65E–G), Skyline Quarry; F:AM 61010, right partial maxillary P4–M1 all broken, New Year Quarry; F:AM 61044, left partial ramus with c1, p1–p2 alveoli, p3 broken–m1, and m2 broken, North End; F:AM 61045, right partial ramus with c1 and p1 alveolus–m1, Skyline Quarry; F:AM 61046, right partial maxillary with P4–M2, Hidden Hollow Quarry; F:AM 61047, left partial maxillary with P4–M2 (M1 alveolus), Leader Quarry; F:AM 61048, left partial maxillary with P4 broken–M2, Mayday Quarry; F:AM 61049, right and left rami with i2–i3 alveoli and c1–m3 (p1 alveolus), Skyline Quarry; F:AM 61050, left partial ramus with p3 alveolus, p4 broken–m2, and m3 alveolus, Skyline Quarry; F:AM 61051, right partial ramus c1–p4 alveoli, m1 broken, and m2–m3 alveoli, North End; F:AM 61052, left partial ramus c1 broken, p1–p2 alveoli, p3–m1, and m2–m3 alveoli, Skyline Quarry; F:AM 61053, right partial ramus with p2–m1 all broken, and m2 alveolus, Yule Tide Quarry; F:AM 61054, right partial ramus c1 broken–p1 alveolus and p2–m2, New Hope Quarry; F:AM 61055, left partial ramus with p3–m2 all erupting, Leader Quarry; F:AM 61057, crushed skull with I1–P3 alveoli and P4 broken–M2, Hidden Hollow

Quarry; F:AM 61058, crushed partial skull with P3–M2 all broken, Skyline Quarry; F:AM 61058A, crushed partial skull with C1–P1 alveolus and P2–M2, Skyline Quarry; F:AM 61058B, left partial ramus with c1–p3 alveoli, p4–m2, and m3 alveolus, Skyline Quarry; F:AM 61058C, right partial ramus with p4 broken–m1, Skyline Quarry; F:AM 61059, anterior part of skull with I1–I2, I3–C1 both broken, and P1–M2 and both partial rami with c1 broken–m3, Leader Quarry; F:AM 61060, left partial maxillary P3–M2, Leader Quarry; F:AM 61061, left partial maxillary with P3 alveolus–M2, Leader Quarry; F:AM 61062, right partial ramus with i3–p4 and m1 broken, Leader Quarry; F:AM 67129, right partial ramus c1 broken–m2 (p3, p4, and m1 all broken), 2 ft above Skyline Quarry; F:AM 67131, right ramus fragment with p2–p3 alveoli and p4–m1 both broken, Skyline Quarry; and F:AM 67146, left partial ramus with p1–p3 alveoli and p4–m1, Leader Quarry.

Pawnee Creek Formation (late early Barstovian), near Grover, Weld County, Colorado: F:AM 28322, left isolated M1, Pawnee Creek area; F:AM 28346, left partial maxillary with P4 broken–M2, north of 3 Points Pit and 40 ft above East and West Pits; F:AM 67877, distal part humerus, Pawnee Quarry; F:AM 67878, left radius, Pawnee Quarry; and F:AM 105258, left partial ramus with c1 alveolus, p2–p4 all broken, m1–m2, and m3 alveolus, R. Day Ranch, 3 Points, west side.

''Gerrys Ranch'' (see Galbreath, 1953: 100), Ogallala Group (?early Barstovian), Weld County, Colorado: YPM 12812, left ramal fragment with p3–m1 (holotype of *Nothocyon vulpinus coloradoensis* Thorpe, 1922b: 430, fig. 2).

Horse Quarry, Pawnee Creek Formation (early late Barstovian), near Grover, Weld County, Colorado: F:AM 28320A, left partial ramus with p1–p2 alveoli, p3 broken–p4, and m1 broken; F:AM 28321, right and left edentulous rami with p2–m3 alveoli; F:AM 28353, left ramus with c1, p1–p2 alveoli, p3–m2, and m3 alveolus; and F:AM 61041, right partial ramus with p3 broken, p4, m1 broken, and m2 alveolus.

Martin Canyon, Ogallala Group (early late Barstovian), Cedar Creek, horizon E, Weld County, Colorado: AMNH 9041, right partial ramus with p2–m1 (p3 broken) and m2 alveolus.

Pojoaque Member of the Tesuque Formation (early late Barstovian), Santa Fe and Rio Arriba counties, New Mexico: F:AM 27376, right partial ramus with c1 root and p1–m1 all broken; F:AM 27377, right partial ramus with c1 broken, and p2–m1 all broken, Camel Area; F:AM 27378, right and left partial rami with c1 and p2–m3, Third Division; F:AM 27392, right partial ramus with m2–m3, lower Pojoaque Bluffs; F:AM 27393, right partial ramus with p2–m2 all broken and m3, Santa Fe general area; F:AM 27398, palate with I1–M2 (fig. 66F), Santa Cruz; F:AM 27398X, partial skull with C1 broken–M2 and both rami with c1–p1 alveoli and p2 broken–m3 (fig. 66A–E), Pojoaque Bluffs; F:AM 27398Y, partial skull with I3 alveolus, C1 broken, P1–P2 alveoli, and P3 broken–M2, Pojoaque; F:AM 50184, partial mandible with i1–p2 roots and p2–m3 all broken, Santa Cruz, east of Tesuque fault, top of light band; F:AM 50185, partial left ramus with c1 broken, p1–p2 alveoli, and p3–m1, Tesuque area; F:AM 50186, right partial ramus with p3 alveolus, p4–m1 both broken, and m2–m3 alveoli, Tesuque area; F:AM 50203, anterior part of skull with I1–M2 all broken and eroded and associated (but possibly not from the same individual) right and left partial rami with c1 broken–m3 (m2 broken), south Santa Cruz; F:AM 62770, partial skull with I1–I3 alveoli, C1 broken, P1–P3 alveoli, and P4–M2, West Cuyamunque; F:AM 62772, right ramal fragment with p4 alveolus–m1 and m2 root, West Cuyamunque; and F:AM 67339, right and left partial rami with i1–m2 all broken, seventh wash, Santa Cruz area.

South fork of Three Sands Hills Wash, Rio del Oso–Abiquiu locality, Chama El Rito Member, Tesuque Formation (late Barstovian), Rio Arriba County, New Mexico: F:AM 50181, left partial maxillary with P1–P4 alveoli and M1 broken–M2.

Jemez Creek Area, tributary of Canyada De Zia, Zia Formation (unnamed beds above the Zia Sand of Galusha, 1966) (late early Barstovian), Sandoval County, New Mexico: F:AM 50191, crushed partial skull with P2–M2, greenish sand; and F:AM 50193, right

partial ramus with i1–p4 and m1–m3 alveoli, greenish sand.

Jemez Creek Area, tributary of Canyada De Zia, Zia Formation (unnamed beds above the Zia Sand of Galusha, 1966) (early late Barstovian), Sandoval County, New Mexico: F:AM 50190, skull fragment, incomplete atlas and axis, left maxillary fragment with P4–M2 and right isolated P4–M1, and right and left partial rami with p2 alveolus–m2 (m1 broken) and m3 alveolus, channel above the cliff-forming sands.

Cedar Springs Draw Local Fauna (early late Barstovian), Browns Park Formation, Moffat County, Colorado (list following Honey and Izett, 1988: 20): USGS D856-1, anterior part of skull with M1 broken and M2, right ramus with c1–p2 alveoli, and p3 broken–m3; and USGS D856-2, right premaxillary and maxillary with I3–P1.

DISTRIBUTION: Late Hemingfordian of New Mexico; early Barstovian of Nevada, California, New Mexico, Nebraska, and Colorado; late Barstovian of Texas, California, Colorado, and New Mexico.

EMENDED DIAGNOSIS: As for genus.

DESCRIPTION AND COMPARISON: Although earlier descriptions of this species by Matthew (1918, 1924) were based on fairly complete skull and lower jaws, a much larger sample of *Microtomarctus conferta* is now available that covers a much larger geographic region than was originally known. The most conspicuous feature about *M. conferta* is its small size as compared to most other *Tomarctus*-like taxa, both more primitive and derived than *M. conferta*. This reduction in size is also accompanied by a slightly brachycephalic skull with a short temporal fossa (length of M2 to bulla in fig. 62). Thus, the rostrum is relatively short and the premolars tend to imbricate slightly. Besides this small size, the only other derived cranial character of *M. conferta* that distinguishes it from the more primitive *Psalidocyon*, cynarctines, and *Metatomarctus* is a posteriorly expanded nuchal crest, which overhangs the occipital condyle. In posterior view, the nuchal crest is more quadrate instead of the fan-shape crest in *Psalidocyon*, *Paracynarctus*, *Cynarctus*, and other genera. Accompanying this expansion of the nuchal crest is a reduction of the lambdoidal crest above the mastoid process. The lambdoidal crest becomes indistinct and does not project to form a thin crest as in more primitive taxa. A dissected frontal area (F:AM 61038) shows that the frontal sinus lacks an elaborate system of septa first seen in *Protomarctus*, but is relatively more expanded in the postorbital constriction than in *Psalidocyon* and more primitive taxa (fig. 62). Also primitive is a relatively large opening of external auditory meatus in *M. conferta*, in contrast to the reduced openings in *Protomarctus*.

Dentally, *Microtomarctus conferta* shares with *Psalidocyon* a distinct P4 parastyle that is formed from the raised anterior cingulum. This parastyle is sharp-edged and distinctly triangular in anterior view. The I3 has a small lateral cusplet only, in contrast to the larger and more numerous cusplets in *Tomarctus*. Corresponding to the smaller body size, the sizes of the teeth are more or less proportionally reduced as compared with those of *Metatomarctus*.

DISCUSSION: Henshaw (1942: 105) contrasted his *Tomarctus paula* (emended by Honey and Izett, 1988: 23; see also etymology under *T. brevirostris*) from *conferta* in the following manner: ''P4 elongate with protocone set very far forward. Upper molars very wide transversely. Lower dentition differs from *T. conferta* type in narrower premolars with only moderately high cusps. m1 short, not compressed. m2 moderately long and narrow.'' Such differences are quite subtle between the Lower Snake Creek and Tonopah samples, and are readily subsumed within the normal range of variation of a species given the large sample from the wide geologic and geographic distribution determined in this study. Therefore, on morphological ground, *T. paulus* is considered synonymous with *Microtomarctus conferta*.

A few individuals presently referred to *Protomarctus optatus* from the Sheep Creek Formation (e.g., AMNH 20498, F:AM 61281) have nearly identical dental dimensions as some of the large individuals of *Microtomarctus conferta*. These individuals, however, have a narrowed external auditory meatus, and thus belong to *P. optatus* rather than *M. conferta*.

The small size of *Microtomarctus conferta* is here interpreted to be a result of size re-

duction, as is implied in our phylogeny. The successively more primitive outgroups (*Psalidocyon*, primitive species of cynarctines, and *Metatomarctus*) are all larger than *Microtomarctus*, as are *Protomarctus* and more derived taxa. Size reduction is rare in canids, and occurs only within *Cynarctus* (see further discussion under *C. crucidens*) up to this point of phylogeny of the borophagines (later, *Aelurodon stirtoni* and *Borophagus orc* also underwent size reduction). The presence of large samples of *M. conferta* suggests the prevalence of a species in the early Barstovian that successfully occupied a mesocarnivorous niche previously held by mostly hesperocyonine canids and amphicyonids.

This size reduction is especially pronounced in the New Mexico sample. Thus, the late Hemingfordian individuals (e.g., F:AM 50143, 67373) are among the largest *Microtomarctus conferta* (m1 length of 17 mm), whereas a few individuals from the late Barstovian of Santa Cruz area (F:AM 50203, 62770, 62772, 67339) are among the smallest (m1 length of 13.0–14.5 mm). These individuals are, on average, 12% smaller than the rest of specimens referred to *M. conferta*. Although such size difference may be more than that between some closely related species recognized in this study, we failed to find any other morphological features to indicate divergence within *conferta*. We thus regard the small size of these individuals as intraspecific variation, or due to anagenetic processes near the end of the *M. conferta* lineage.

Protomarctus, new genus

TYPE SPECIES: *Tomarctus optatus* Matthew, 1924.

ETYMOLOGY: Greek: *pro*, before; in allusion to its ancestral status to *Tomarctus*.

INCLUDED SPECIES: Type species only.

DISTRIBUTION: Early Hemingfordian of Colorado and New Mexico; and late Hemingfordian of Nebraska, Wyoming, and California.

DIAGNOSIS: *Protomarctus* is derived with respect to *Microtomarctus* and more primitive taxa in its multichambered frontal sinus that reaches to, or slightly passes, the frontal-parietal suture and its narrowed opening for external auditory meatus. On the other hand, *Protomarctus* is primitive with respect to *Tephrocyon*, Aelurodontina, and Borophagina in its less enlarged postorbital process of frontal. *Protomarctus* can be further distinguished from Aelurodontina in its primitive features such as less broadened forehead, palate not widened, nuchal crest not laterally compressed, premolars not enlarged, M1 paracone not high-crowned and with a distinct metaconule, m1 metaconid and entoconid unreduced, and m2 metaconid unreduced. *Protomarctus* is distinct from primitive members of Borophagina, such as *Paratomarctus* and *Carpocyon*, in its absence of the following derived characters: prominently domed forehead, a short tube for auditory meatus, reduced premolars with weakened cusplets, p4 enlarged relative to p2–p3, and reduced P4 protocone.

Protomarctus optatus (Matthew, 1924)

Figure 67

Tomarctus optatus Matthew, 1924: 98, figs. 18, 19. Skinner et al., 1977: 342. Munthe, 1988: 87; 1998: 135.

Tephrocyon (*Canis*) *temerarius* (Leidy, 1858): Peterson, 1910: 268, fig. 63 (CMNH 2404).

Tephrocyon temerarius (Leidy): Merriam, 1913: 366, fig. 7 (CMNH 2404).

Tomarctus brevirostris (Cope, 1873): Downs, 1956: 233.

Tomarctus cf. *T. optatus* (Matthew): Galusha, 1975b: 56.

HOLOTYPE: AMNH 18916, mandible with i1–c1, p1 alveolus, and p2–m3 (fig. 67A, B) from Thomson Quarry (Skinner et al., 1977: 342), east side of Stonehouse Draw, Sheep Creek Formation (late Hemingfordian), Sioux County, Nebraska.

REFERRED SPECIMENS: Martin Canyon Quarry A (KUVP loc. CO-48), Martin Canyon beds (early Hemingfordian), Logan County, Colorado: KUVP 45128, left maxillary with P4–M2.

Sheep Creek Formation (late Hemingfordian), Sioux County, Nebraska: Stonehouse Draw: AMNH 14175, right partial ramus with p4–m1 and p3 and m2 alveoli; AMNH 14176, right partial maxillary with P4–M1 and M2 alveolus (Matthew, 1924: fig. 19); AMNH 18236, right immature partial ramus with c1 erupting, dp3 broken–dp4, and m1

unerupted, Ashbrook Pasture, Sinclair Draw; AMNH 18669, right partial maxillary with P4–M2 and left partial maxillary with P4 root and M1–M2 (another individual), Ashbrook Pasture; AMNH 18915, right ramus with c1–m3; AMNH 18917, right partial ramus with m1–m2 and m3 alveolus; AMNH 18918, right partial ramus with p4–m2 (m1 broken) and m3 alveolus; AMNH 20494, left partial maxillary with M1–M2; AMNH 20498, partial skull with I1–P1 alveoli, P2, P3 alveolus, and P4–M1; AMNH 20499, right maxillary with P4–M2; AMNH 20500, right partial ramus with p3 alveolus–m2; AMNH 21445, right partial ramus with c1, p1–p2 alveoli, p3–m2, and m3 alveolus; AMNH 26904, left partial ramus with m1 (c1–p4 and m2 all alveoli); AMNH 26905, left partial ramus with c1–p2 alveoli and m1. Thomson Quarry: F:AM 61244, left partial ramus with p2–p4 alveoli and m1–m3; F:AM 61245, right partial ramus with p1–p3 alveoli, p4–m2, and m3 alveolus; F:AM 61246, left partial ramus with c1, p1 alveolus–m1 (p4 broken), and m2 alveolus; F:AM 61247, right partial ramus with i1–p3 alveoli, p4–m1, and m2 broken–m3 alveolus; F:AM 61254, right partial ramus with i1–p1 alveoli, p2–m2, and m3 alveolus; F:AM 61255, right partial ramus with i1 alveolus–m2 (p3 broken) and m3 alveolus; F:AM 61257, left partial ramus with c1–p2, p3 alveolus–m2, and m3 alveolus; F:AM 61266, right partial ramus with i1–p1 alveoli, p2 broken–m2, and m3 alveolus; F:AM 61271, left partial ramus with c1 broken, p2, p3–m2, p1, and p3 and m3 alveoli; F:AM 61272, right ramus with c1–p1 alveoli, p2–m2, and m3 alveolus (fig. 67C, D); F:AM 61273H, left partial ramus with m1–m2; F:AM 61273I, right partial ramus with p2–m1 all broken, m2, and m3 alveolus; F:AM 61279, posterior part of skull, premaxillary-maxillary fragment with I1 alveolus, I2–I3, and broken C1 alveolus, right and left detached maxillary fragments with P3 broken–M1 and associated limbs (61279A–D) of two or more individuals including F:AM 61279A, humerus and partial femur; F:AM 61279B, immature right partial femur; F:AM 61279C, immature left tibia; F:AM 61279D, left tibia and right partial tibia, patella, left calcaneum and astragalus, tarsals, metatarsal I, right and left metatarsals IV (two individuals), and two first phalanges; F:AM 61281, partial skull with I1–I3 alveoli, C1–P4 (P1 alveolus), and M1–M2 alveoli; F:AM 61287, right partial maxillary with P3 broken–M2; F:AM 61291, left partial maxillary with P4–M1; and F:AM 61294, right partial maxillary with P2–P4. Greenside Quarry: F:AM 61249, left ramus with c1–m2 (p1 and m3 alveoli); F:AM 61250, right partial ramus with i1–p1 alveoli, p2, p3 alveolus, p4–m1, and m2–m3 alveoli; F:AM 61251, left ramus with c1–m3 (p1 alveolus); F:AM 61252, left partial ramus with i3–p1 alveoli, p2–m2, and m3 alveolus; F:AM 61253, left partial ramus with i1–p2 alveoli, p3, p4 alveolus, m1, and m2–m3 alveoli; F:AM 61260, left partial ramus with c1–m1 (p1 alveolus); F:AM 61262, right ramus with i1–i3 alveoli, c1–m2, and m3 alveolus; F:AM 61267, left ramus with i1–i3 alveoli, c1–p2 broken, and p3–m3; F:AM 61269, left ramus with c1–p1 alveoli, p2–m2, and m3 alveolus; F:AM 61273G, left partial ramus with p4–m2 and m3 unerupted; F:AM 61273J, right ramal fragments with c1–m1 broken (p1 alveolus), and m2 broken–m3; F:AM 61273K, right partial ramus with m2 and m3 alveolus; F:AM 61273L, left ramal fragment with p3–p4 and m1–m3 alveoli; F:AM 61273N, left ramal fragment with m2–m3; F:AM 61274, skull with I1 alveolus–M2; F:AM 61275, right partial maxillary with C1–P1 alveoli and P2–M2; F:AM 61277, right partial maxillary with C1–P3 alveoli, P4–M1, and M2 alveolus; F:AM 61278, skull with I1–I2 alveoli and I3–M2 (P1 alveolus) (fig. 67E–G); F:AM 61280, partial skull with I1–I3 alveoli and C1–M2 (P3 alveolus); F:AM 61285, right partial maxillary with P4–M2; and F:AM 61289, right partial maxillary with P4–M2. Long Quarry: F:AM 25288, left partial ramus with c1 and p1 alveolus–m1; F:AM 61018, left partial ramus with p1 alveolus–m2 (p3 root and m1 broken); F:AM 61258, left partial ramus with c1 broken, p1 alveolus–m1, and m2 broken–m3 alveolus; F:AM 61261, right partial ramus with c1 broken–p1 alveolus and p2–m1; F:AM 61263, left ramus with c1–p2 alveoli, p3–m2, and m3 alveolus; F:AM 61264, right ramus with c1, p1–p3 alveoli, p4–m2, and m3 alveolus; F:AM 61268, right partial ramus with c1–m3 (p1 alveolus); F:AM 61273B, left partial ra-

mus with p1–p3 alveoli and p4–m1; F:AM 61273D, right partial ramus with m1; F:AM 61282, left maxillary with C1–P1 alveoli, P2 broken–M1, and M2 broken; F:AM 61284, left premaxillarymaxillary with I1–I2 alveoli, I3 broken–C1, P1 alveolus–P3, and P4 broken; F:AM 61288, skull fragments and left partial maxillary with P4–M2; and F:AM 61293, left partial maxillary with P4 broken–M2. Hilltop Quarry: F:AM 61248, right ramus with i1–i3 alveoli, c1, p1–p2 alveoli, and p3–m3; F:AM 61256, right partial ramus with c1, p1–p2 alveoli, and p3–m2; F:AM 61265, right ramus with i3–c1 all broken, p1–m2, and m3 alveolus; F:AM 61273, left partial ramus with p3–m1, and m2 alveolus; F:AM 61273E, right partial ramus with p3–p4 alveoli, m1–m2, and m3 alveolus; F:AM 61273F, right partial ramus with m1 and m2–m3 alveoli; F:AM 61286, left isolated P4; and F:AM 61290, left partial maxillary with P4–M1. Ashbrook Quarry: F:AM 61270, right ramus with c1–m2 and m3 alveolus; F:AM 61273C, right ramal fragment with detached p4 and m1–m2; F:AM 61273M, left partial ramus with c1–p3 all broken or alveoli and p4; and F:AM 61276, left maxillary with C1–P3 alveoli, P4–M1 both broken, and M2. Watson Ranch: F:AM 61292, right partial maxillary with P4–M2. Thistle Quarry: F:AM 61273A, right ramal fragment with m1 and m2 alveolus; and F:AM 61283, left maxillary with C1–M2 (P1–P2 alveoli). Vista Quarry: F:AM 61259, right ramus with c1–m1 (p1 alveolus) and m2–m3 alveoli. Ravine Quarry: F:AM 61135, left partial ramus with i3–p1 alveoli, p2, p3 alveolus–m1, m2 broken, and m3 alveolus. Conference Quarry: F:AM 105255, right partial ramus with p4–m1 both broken, m2, and m3 alveolus. Northwest of Snake Den Hill, 55 ft above base of Sheep Creek Formation: F:AM 105256, right ramal fragment with p4 broken and m1–m2.

Whistle Creek, Runningwater or Sheep Creek Formation (Hemingfordian), Sioux County, Nebraska: CMNH 2404, left partial ramus with p4–m2 and m3 alveolus (referred to *Tephrocyon* (*Canis*) *temerarius* by Peterson, 1910: 268, fig. 63 and Merriam, 1913: 366, fig. 7).

Rocks temporally equivalent to the Sheep Creek Formation (late Hemingfordian), Dawes County, Nebraska: Ginn Quarry: F:AM 54493, right maxillary with C1–M2 (P1 alveolus); F:AM 54494, right partial maxillary with P4–M1 and M2 alveolus; F:AM 54495, left ramus with c1 broken, p1–p3 alveoli, p4–m2, and m3 alveolus; F:AM 61183, anterior part of skull with I1–P1 alveoli, P2, and P3 alveolus–M2; and F:AM 61184, left partial maxillary with M1–M2. ''G'' Quarry: F:AM 49195, right ramus with c1–p4, m1 alveolus, m2, and m3 alveolus.

Sand Canyon Region, Red Valley Member, Box Butte Formation (late Hemingfordian), Box Butte County, Nebraska: F:AM 95279, crushed palate with I1–M2 and mandible with i1–m1, and m2 broken (referred to *Tomarctus* cf. *T. optatus* by Galusha, 1975b: 56).

Box Butte Formation (late Hemingfordian), Box Butte County, Nebraska: UNSM 25652 (AMNH cast 97101), left partial maxillary with P4–M1 and M2 alveolus, UNSM loc. Bx-0.

Split Rock Formation (late Hemingfordian), Granite Mountain, Fremont County, Wyoming (as listed in Munthe, 1988: 87): CMNH 14709, M2, from UCMP loc. V69192; UCMP 121910, partial skull with I3–M2 (P1 alveolus), UCMP loc. V77155; and UCMP 121911, M1, from UCMP loc. V69190.

Arroyo Pueblo drainage, near middle of Chamisa Mesa Member, Zia Formation (early Hemingfordian), Sandoval County, New Mexico: Blick Quarry: F:AM 50198, immature partial skull with dC1, P1, dP2–dP4, P2–P3 unerupted, and P4–M2 erupting, and mandible with di1–di2, i3 broken, dc1, p1, dp2 broken–dp4, p2–p4 unerupted, and m1–m2 erupting. *Cynarctoides* Prospect: F:AM 62777, palate with C1–P2 alveoli, and P3 broken–M2.

Barstow area, Barstow Formation (late late Hemingfordian), San Bernardino County, California: Rak Division: F:AM 27149, crushed skull with I3 alveolus–C1 broken, P1–P3 broken, and P4–M2. Third Division: F:AM 27288, right and left partial rami with c1, p1–p2 alveoli, and p3–m2.

DISTRIBUTION: Early Hemingfordian of Colorado and New Mexico; and late Hemingfordian of Nebraska, Wyoming, and California.

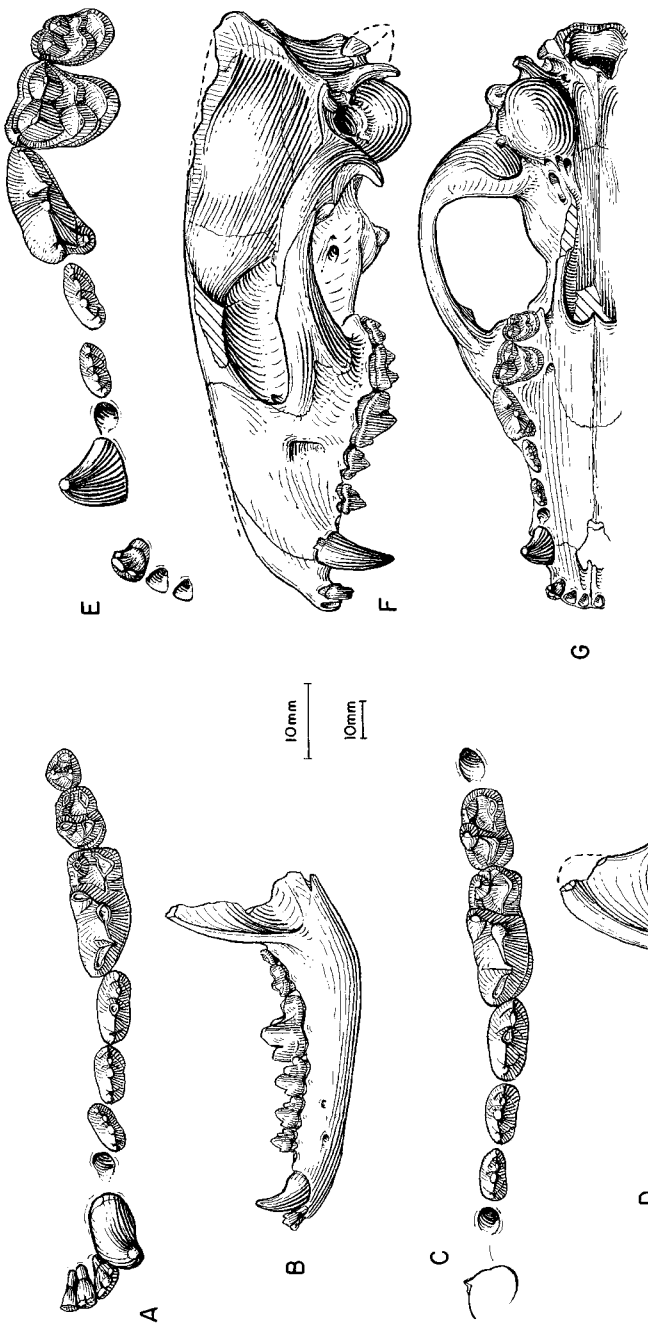

Fig. 67. *Protomarctus optatus*. **A**, Lower teeth and **B**, ramus (i3 reversed from right side), AMNH 18916, holotype, Thomson Quarry, Sheep Creek Formation (late Hemingfordian), Sioux County, Nebraska. **C**, Lower teeth and **D**, ramus (reversed from right side), F:AM 61272, Thomson Quarry. **E**, Upper teeth and **F**, lateral and **G**, ventral views of skull, F:AM 61278, Greenside Quarry, Sheep Creek Formation (late Hemingfordian), Sioux County, Nebraska. The longer (upper) scale is for A, C, and E, and the shorter (lower) scale is for the rest.

EMENDED DIAGNOSIS: As for genus.

DESCRIPTION AND COMPARISON: Numerous upper and lower jaws as well as several skulls permit good knowledge of the cranial and dental morphology of *Protomarctus optatus* and its variation. Most of the specimens are represented by materials from the Sheep Creek Formation or equivalent strata in the northern Great Plains. Specimens from the various quarries in the Sheep Creek Formation constitute a fairly uniform sample, except for a few individuals (e.g., AMNH 20498, F:AM 54493, 61184, 61281) that approach the upper range of *Microtomarctus conferta*.

Protomarctus optatus is on average 27% (basal length of skull) larger than *Microtomarctus conferta* and is approximately the same size as *Desmocyon*, whereas it is about 12% (basal length of skull; 11% for m1 length) smaller than *Tomarctus hippophaga*. The frontal sinus is noticeably more inflated than in *Desmocyon* and *Microtomarctus*. Externally, the forehead is more domed than the latter genera, and this inflation can be seen to pass behind the frontal-parietal suture. A dissected specimen of *P. optatus* (F:AM 61278) reveals that the sinus extends beyond the frontal-parietal suture by more than 5 mm. The frontal bone in this skull also bears partial septa (at least two) that partition the sinus into chambers. The diagonally oriented septa form either a vertical partitioning of the sinus or they bend horizontally to enclose a partial chamber. Skulls from Thomson Quarry (F:AM 61279 and 61281) generally show less inflation than those from Greenside Quarry (F:AM 61274, 61278, 61280), despite the higher stratigraphic position of the former.

The premaxillary process is in full contact with the nasal process of the frontal. As in *Microtomarctus conferta*, the nuchal crest of *Protomarctus optatus* is posteriorly expanded to overhang the occipital condyle. The bulla is inflated ventrally and in the posterolateral corner in front of the paroccipital process. The external auditory meatus has a smaller opening than in *M. conferta*, and the ectotympanic forms a short lip surrounding the meatus.

Dentally, *Protomarctus optatus* is little more derived than *Desmocyon matthewi* and *Microtomarctus* except for its two additional lateral cusplets on I3. On the other hand, premolars of *P. optatus* are primitive with respect to both Aelurodontina and Borophagina clades: they are not as uniformly enlarged as in the Aelurodontina (first developed in *Tomarctus hippophaga*), nor as uniformly reduced as in *Paratomarctus* in the Borophagina clade.

Two specimens from the early Hemingfordian Chamisa Mesa Member of the Zia Formation, New Mexico, are referred to this species (Munthe [1988: 89] listed ''Zia Sand'' under the geographic distribution of *Tomarctus optatus*, probably based on the same F:AM specimens, but did not elaborate). The New Mexico individuals are slightly larger than those from the northern Great Plains, but their P4 parastyles are less distinctly formed. Other than these variations, the New Mexico specimens are a close match with the topotype series from Nebraska.

DISCUSSION: Matthew (1924) compared his newly erected *Tomarctus optatus* with ''*T. brevirostris*'' (now *T. hippophaga*) and *T. temerarius* (*Paratomarctus*) and found it to be somewhat intermediate in size and morphology. He (1924: 100) noted that the ''smaller size and somewhat more slender proportions'' were the only distinctions of *T. optatus* when compared to *T. hippophaga*. In fact, he suggested that *T. optatus* may be a ''primitive mutant'' of *T. hippophaga*, but preferred to hold the names distinct pending further evidence. Even with the complete cranial materials available to this study, Matthew's observation is essentially correct; that is, differences between these two species are small (as also are between *Protomarctus optatus* and *Paratomarctus temerarius*). Besides the small size and slender teeth noted by Matthew, the only cranial features we can add are the primitively narrow frontal shield and the less enlarged postorbital process of the frontal in *optatus*. As indicated by the primitive states of these features in *optatus*, we recognize it as a critically positioned taxon on the verge of giving rise to two great Borophagini clades: Aelurodontina and Borophagina. *Protomarctus optatus* possesses the right combination of morphology and is in the right stratigraphic level to be ancestral to both clades.

Galusha (1975b: 56) noted the transitional nature of an anterior skull fragment and its associated mandible (F:AM 95279) from the Red Valley Member of Box Butte Formation. Its dental morphology is intermediate between that of *Desmocyon matthewi* of the Runningwater Formation and that of *Protomarctus optatus* from the Sheep Creek Formation. The teeth of F:AM 95279 are very close to the average dental dimensions of both *Metatomarctus canavus* and *P. optatus*. Its I3 has two lateral accessory cusplets, in contrast to one cusplet in *Protomarctus* and *Microtomarctus*, and its P4 bears a distinct parastyle, although the latter still does not assume the prominence shown by most individuals of *P. optatus* from the Sheep Creek Formation. We agree with Galusha (1975b) that despite its intermediate morphology and stratigraphic relationship, F:AM 95279 has essentially reached the general stage of development of *P. optatus*.

Tephrocyon Merriam, 1906

TYPE SPECIES: *Canis rurestris* Condon, 1896.

INCLUDED SPECIES: Type species only.

DISTRIBUTION: Early Barstovian of Oregon and Texas.

EMENDED DIAGNOSIS: *Tephrocyon* is derived with respect to *Protomarctus* and more primitive taxa in its larger size, more pronounced postorbital process of frontal (a character also shared with Aelurodontina and Borophagina), slightly more broadened palate, and an elongated m2 (an autapomorphy). *Tephrocyon* is distinguishable from Aelurodontina in its primitive characters such as nuchal crest not laterally compressed, premolars not enlarged, M1 paracone not high-crowned and with a distinct metaconule, m1 metaconid and entoconid unreduced, and m2 metaconid unreduced. On the other hand, *Tephrocyon* differs from members of Borophagina in its lack of the following derived characters: domed forehead, short tube for auditory meatus, small premolars with reduced cusplets, p4 enlarged relative to p2–p3, and reduced P4 protocone.

DISCUSSION: Shortly after Merriam's (1906) establishment of *Tephrocyon*, a number of medium-size taxa were referred to it by him (Merriam, 1913) and *Tephrocyon* quickly became a taxonomic wastebasket for many *Canis*-like taxa. The popularity of the genus, however, was diminished soon after Matthew's (1924, 1930) influential studies of canid evolution. Matthew's resurrection of Cope's (1873) *Tomarctus*, which has priority over *Tephrocyon*, proved to be more enduring. *Tephrocyon* had since been rarely mentioned in the literature, except in connection with its type species *T. rurestris*.

Tephrocyon rurestris (Condon, 1896)

Figure 68

Canis rurestris Condon, 1896: 11, pl. 1.

Tephrocyon rurestris (Condon): Merriam, 1906: 6, pl. 1, figs. 1–3; 1913: 362, figs. 1–5. Thorpe, 1922a: 175. Matthew, 1924: 89.

Tomarctus rurestris (Condon): Downs, 1956: 231, figs. 10, 11. Munthe, 1998: 135.

Tomarctus cf. *rurestris* (Condon): Shotwell, 1968: 37, fig. 14A.

Tomarctus cf. *T. kelloggi* (Merriam): Shotwell, 1968: 37, fig. 17E, F.

HOLOTYPE: UO 23077 (AMNH cast 97225), skull with C1 broken, P1 alveolus–M2 (P3 broken), and mandible with c1–p1 alveoli and p2–m3 (fig. 68) from near Cottonwood Creek, Mascall Formation (early Barstovian), Grant County, Oregon.

REFERRED SPECIMENS: From the Mascall type area, Oregon (referred by Downs, 1956; Shotwell, 1968): UCMP 39297, partial left m1 (Downs, 1956: fig. 12c), UCMP loc. V4834; UO 24191, partial ramus with p4–m1; UO 24192, maxillary fragment with P4; YPM 12713, left P4, M1–M2, right P4, and left m2 and m3 (Downs, 1956: fig. 12a), Cottonwood Creek; YPM 12720, right m1 (Downs, 1956: fig. 12b), Crooked Creek; and YPM 14312, left M1 (Downs, 1956: fig. 12d).

Red Basin Local Fauna, Butte Creek Volcanic Sandstone (early Barstovian), Malheur County, Oregon: UO 20552, left ramal fragment with m1 and m2–m3 alveoli; UO 21499, isolated left m2; UO 21559 (Shotwell, 1968: fig. 17E, F), right ramal fragment with m1–m2; UO 22837, crushed right maxillary fragment with P4–M1; UO 23132, isolated right M1; UO 23386, isolated right P3; UO 23496, isolated left m1; and UO 23497, isolated left m2.

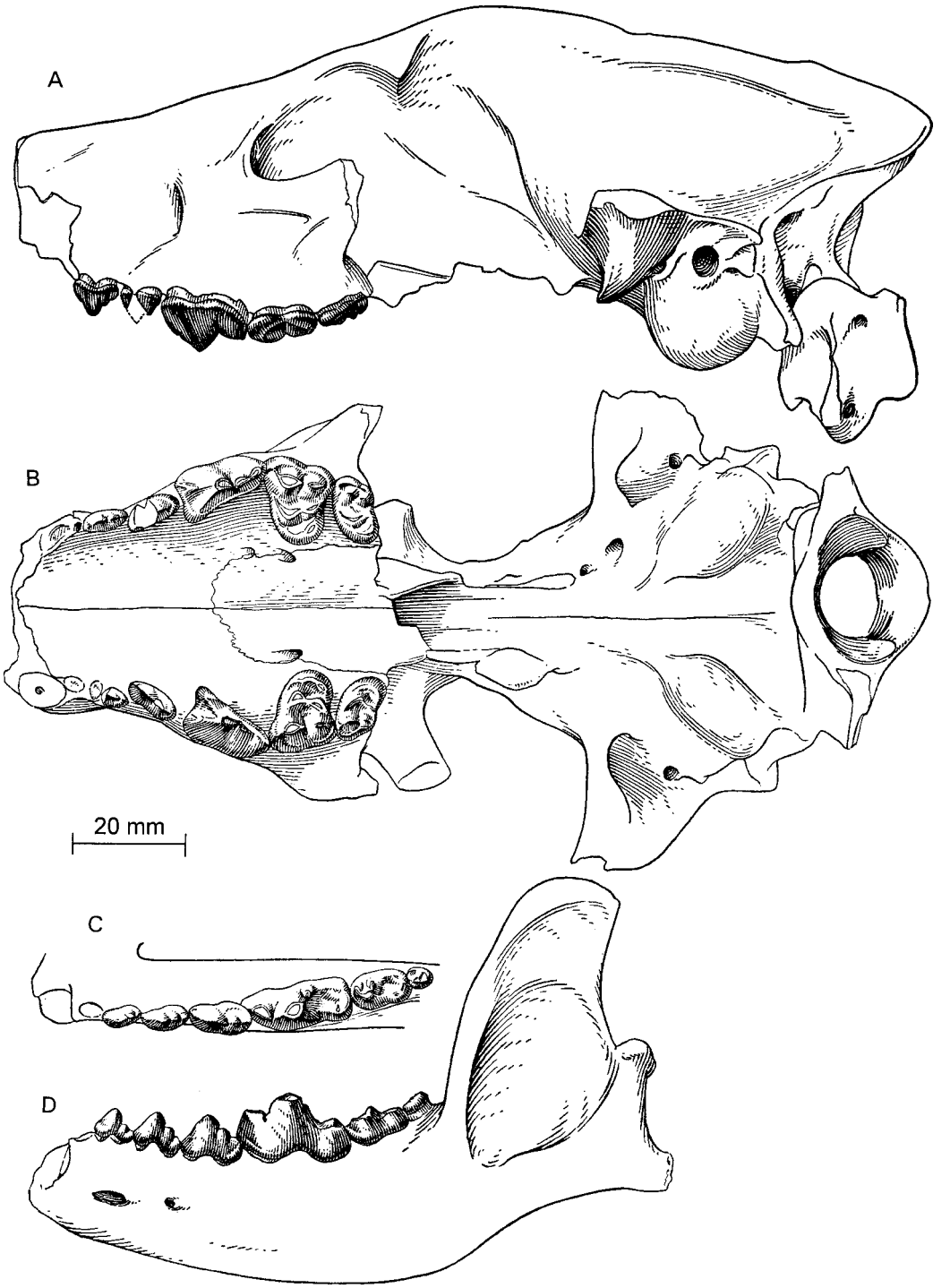

Fig. 68. *Tephrocyon rurestris*. **A**, Lateral and **B**, ventral views of skull, **C**, lower teeth, and **D**, ramus, UO 23077, holotype, near Cottonwood Creek, Mascall Formation (early Barstovian), Grant County, Oregon. Modified from Downs (1956: fig. 10).

DISTRIBUTION: Early Barstovian of Oregon.

EMENDED DIAGNOSIS: As for genus.

DESCRIPTION AND COMPARISON: The well-preserved holotype, UO 23077, is still the best material for this species. The geologically younger *Tephrocyon rurestris* (early Barstovian) is larger than the older (Hemingfordian) *Protomarctus optatus* (14% larger in m1 length, but a much smaller percentage in premolar length). The skull seems slightly more derived toward the Aelurodontina clade. There is a moderate frontal sinus, probably reaching to the frontal-parietal suture as suggested by its external profile. The forehead is quite flat, as is commonly the case in Aelurodontina but is in contrast to the domed profile in the Borophagina clade. The postorbital process of frontal is laterally expanded in contrast to a narrowed postorbital constriction, also a common occurrence of the aelurodontine clade (fig. 71). The sagittal crest is higher than in *P. optatus* and slightly overhangs the occipital condyle. The opening for the external auditory meatus is narrow. The palate shows an initial stage in the broadening seen in the aelurodontine clade.

Dentally, *Tephrocyon rurestris* and *Protomarctus optatus* are quite similar. Cheek-teeth for *T. rurestris* are proportionally slender (see fig. 72). The m1–m2 are also more elongated than in *P. optatus*. The premolars of *T. rurestris* are neither enlarged, as in the aelurodontines, nor reduced, as in *Paratomarctus*.

DISCUSSION: As the genoholotype of *Tephrocyon* (Merriam, 1906), *T. rurestris* played an important role in shaping the early concept of a centrally positioned genus in the canid phylogeny, mostly because Merriam (1913) referred a number of mesocarnivorous taxa to it. Matthew's (1924, 1930) authoritative study on canid phylogeny, however, resurrected Cope's earlier (1873) genus *Tomarctus* as having priority. The Mascall *T. rurestris* has since been mostly regarded as just another species of *Tomarctus* (Downs, 1956; Shotwell, 1968). Although our present phylogeny places *T. rurestris* in a trichotomy with the Aelurodontina and Borophagina clades, subtle features, such as flat forehead, broadened palate, and heightened sagittal crest, indicate that *T. rurestris* may be closer to the Aelurodontina side. However, *T. rurestris* does not have the widened premolars that are a derived character for the aelurodontine clade. Lacking better samples of *T. rurestris*, it is not clear if the above-cited aelurodontine features are independent developments or simply individual variation. In any case, the presence of an autapomorphy (i.e., an elongated m2) in *T. rurestris* and its entirely Columbia Plateau distribution suggest that it was not an anagenetic lineage leading directly to *Tomarctus*.

Fragmentary specimens from the Red Basin Local Fauna (Shotwell, 1968) are slightly smaller than the holotype of *Tephrocyon rurestris*, but are otherwise consistent with most aspects of dental morphology of *T. rurestris*, especially the slender, elongated m2. On the other hand, two rami from Trail Creek Quarry, Wyoming, referred to *Tomarctus rurestris* by Voorhies (1965), are presently placed in *Paratomarctus temerarius*.

Aelurodontina, new subtribe

TYPE GENUS: *Aelurodon* Leidy, 1858.

INCLUDED GENERA: *Tomarctus* Cope, 1873 and *Aelurodon* Leidy, 1858.

DISTRIBUTION: Early Barstovian through late Clarendonian of North America.

DIAGNOSIS: A single synapomorphy unites all members of Aelurodontina: uniformly robust lower premolars with distinct accessory cusplets. Advanced members of this clade further acquire derived characters, such as broadened palate, paroccipital process elongated with long free tip, anteromedial part of ramus strongly deflected laterally, high sagittal crest, nuchal crest laterally compressed and overhanging occipital condyle, I3 with three lateral accessory cusplets, M1 paracone high crowned, M1 metaconule small to absent, m1 metaconid reduced to absent, m1 talonid short and narrow, m1 entoconid small to absent, and m2 metaconid small to absent. Members of Aelurodontina generally lack the derived characters for the Borophagina clade: prominently domed forehead, shortened rostrum, reduced I3 lateral cusplets, reduced anterior premolars, reduced premolar cusplets, p4 enlarged relative to p2–p3, and reduced P4 protocone.

Tomarctus Cope, 1873

TYPE SPECIES: *Tomarctus brevirostris* Cope, 1873.

INCLUDED SPECIES: *Tomarctus hippophaga* (Matthew and Cook, 1909) and *Tomarctus brevirostris* Cope, 1873.

ETYMOLOGY: Simpson (in Honey and Izett, 1988) has pointed out that *Tomarctus* is feminine in gender and the International Commission on Zoological Nomenclature (1985: article 31) states that adjectival species names must conform in gender with that of their genus. Although *Tomarctus* was assembled by Cope from Greek roots, he placed the Latin neuter *brevirostris* as its adjective. In this work we have tried to abide by ICZN article 31 and its directive article 34 to provide justified emendation of species names associated with *Tomarctus* or its derivatives.

DISTRIBUTION: Early Barstovian of Colorado, Nebraska, New Mexico, and California; and late Barstovian of Colorado and Texas.

EMENDED DIAGNOSIS: The single derived character that unites *Tomarctus* and the *Aelurodon* clade is the enlarged premolars. *Tomarctus* is also distinguishable from *Protomarctus* by its larger size, wider forehead, and more complex septa within the frontal sinus. Primitive characters that distinguish *Tomarctus* from *Aelurodon* are sagittal crest lower, bulla not hypertrophied, mastoid process small, P4 protocone less reduced, P4 parastyle smaller, upper molars not reduced relative to P4, M1 lingual cingulum not restricted to the posterolingual border, m1 talonid not narrowed, m2 less reduced, and m2 metaconid approximately equal to protoconid in height.

DISCUSSION: *Tomarctus* is one of the most confused taxa in the studies of Tertiary canids, both because of the many species that had been erected under this genus and because of its purported central position in the line of descent to the living wolves (*Canis*) and foxes (*Vulpes*). This confusion originated from Matthew's (1924, 1930) early syntheses of the phylogeny of the Canidae, which followed a scheme that recognized two dichotomous lines of canids, i.e., taxa with basined vs. trenchant m1 talonids—a structure highly homoplastic throughout the history of canid evolution. *Tomarctus*, with a fully basined talonid, was thus postulated to be ancestral to not only all large borophagines, but also to all living canids with a basined talonid. Matthew's scheme proved to be profoundly influential, and *Tomarctus* played an important role in nearly all past interpretations of the geological history of dogs. It is clear from our phylogenetic analysis that, even allowing a horizontal (or gradational) classification, the various species referred to *Tomarctus* (sensu lato) occupy primitive positions in various clades of advanced borophagines and are far removed from any living canid. Cladistically, *Tomarctus* is still a paraphyletic genus in the present classification and pertains to the Aelurodontina clade only.

Tomarctus hippophaga (Matthew and Cook, 1909)

Figures 69, 70

Tephrocyon hippophagus Matthew and Cook, 1909: 373, fig. 4. Cook, 1912: 44. Merriam, 1913: 364, fig. 6. Sinclair, 1915: 76. Matthew, 1918: 185. Munthe, 1998: 135.

Tomarctus brevirostris (Cope, 1873): Matthew, 1924: 91, figs. 11–16 (in part). Colbert, 1939: 65. Hough, 1948: 107 (AMNH 18243, mislabeled by Hough as AMNH 18234).

Tomarctus hippophagus (Matthew and Cook): VanderHoof, 1931: 19.

HOLOTYPE: AMNH 13836, right ramus with i2–i3 alveoli and c1–m2 (p1 and m3 alveoli) (fig. 69G, H), Quarry 2, East Sinclair Draw, Lower Snake Creek Fauna, Olcott Formation (early Barstovian), Sioux County, Nebraska.

REFERRED SPECIMENS: Lower Snake Creek Fauna, Olcott Formation (early Barstovian), Sioux County, Nebraska: Quarry A: AMNH 18249, partial left ramus with c1–p1 alveoli, p2–m2, and m3 alveolus; AMNH 18250, left partial maxillary with P4–M1; and AMNH 18251A, right ramus fragment with m1. Quarry B: AMNH 18242, skull with I1–P1 alveoli and P2–M2 (Matthew, 1924: figs. 12, 13); AMNH 18247, right partial maxillary with P4 broken–M2; and AMNH 18248, left partial ramus with c1, p1–p3 alveoli, p4–m2, and m3 alveolus. Sheep Creek Quarry: AMNH 18243, skull with C1–M2 (P1 alveolus) (Matthew, 1924: figs. 14, 15); and

AMNH 18244, skull with I1, I2–P1 alveoli, and P2–M2, and right partial ramus with c1–p1 alveoli, p2–m2, and m3 alveolus (Matthew, 1924: figs. 11, 16; fig. 70E–J). Echo Quarry: F:AM 61114, right partial ramus with i1–p4 alveoli, m1–m2, and m3 alveolus; F:AM 61116, left partial ramus with c1–p4 alveoli, m1, and m2–m3 alveoli; F:AM 61131, left partial ramus with i1–i3 alveoli, c1, p1–p3 alveoli, p4, m1 broken, and m2–m3 alveoli; F:AM 61132, left ramus with i1–p4 alveoli, m1, and m2 broken–m3 alveolus; F:AM 61133, right partial ramus with p4–m2 and m3 alveolus; F:AM 61134, left partial ramus with i3–p4, m1–m2 roots, and m3 alveolus; F:AM 61137, right ramus with c1–p3 alveoli, p4–m1, and m2–m3 alveoli; F:AM 61138, left partial ramus with i3–p3 alveoli, p4–m1, and m2–m3 alveoli; F:AM 61149, right partial ramus with c1–m1; F:AM 61154, left ramus with i1–p1 alveoli, and p2–m1 (p3 alveolus, p4 broken, and m2–m3 alveoli); F:AM 61155, left ramus with c1–m1 and m2–m3 alveoli; F:AM 61156, skull with I1 alveolus, I2, I3 alveolus, C1 root, P1 alveolus, and P2–M2 (fig. 70A–D); F:AM 61174, left ramus with c1, p1 alveolus, p2–m2, and m3 alveolus (fig. 69C, D); F:AM 61174A, partial right premaxillary-maxillary with I3–P1 alveoli and P2–M2 (fig. 69E, F); F:AM 61176, right partial ramus with i1–i3 alveoli and c1 broken–m1 (p1 alveolus and p2 broken); F:AM 61177B, right ramal fragment with m1 and m2 alveolus; F:AM 61177H, left partial ramus with p3 broken–m2; F:AM 61177K, left partial ramus with m1–m2; and F:AM 61181, posterior part of skull. Mill Quarry: F:AM 61145, right partial ramus with i2 alveolus, i3–m1, and m2–m3 alveoli; F:AM 61152, right ramus with c1–m2 (p1 and p3 alveoli, m1 broken, and m3 alveolus); F:AM 61177D, left partial ramus with m1–m2 and m3 alveolus; and F:AM 61180, posterior part of skull. Sinclair Draw: F:AM 61177G, left ramal fragment with m1 and m2–m3 alveoli. East Sinclair Draw: AMNH 81526 (HC 1168), left isolated m1; AMNH 83440 (HC 616), right partial ramus with c1–p1 alveoli and p2–m2; F:AM 25486, right ramus with i1–i3 alveoli, c1 broken, p1 alveolus–m1, and m2–m3 alveoli; F:AM 61173, right partial maxillary with P4–M1; and F:AM 61177E, right partial ramus with m1 and m2 alveolus. Quarry 2, East Sinclair Draw: AMNH 13837, right partial ramus with c1–p1 alveoli, p2, p3 alveolus–m1, and m2–m3 alveoli; AMNH 13838, right partial ramus with m1–m2 and m3 alveolus; AMNH 13839, right partial ramus with c1–p2 alveoli, p3–p4, and m1–m3 alveoli; AMNH 13840, right partial ramus with c1–p4 alveoli, m1, and m2–m3 alveoli; AMNH 83420 (HC 336), right ramal fragment with c1–m1 (all broken); F:AM 25495, left partial ramus with p2 broken–m3; F:AM 25497, right partial ramus with i1–i3 alveoli, c1, p2–m1, and m2 broken; F:AM 61115, right partial ramus with i1–i3 alveoli, c1, p1–p3 alveoli, p4–m1, and m2–m3 alveoli; F:AM 61118, left partial ramus with i1–c1 alveoli, p2–m1, and m2–m3 alveoli; F:AM 61119, left partial ramus with c1–m1 (p1 and m2–m3 alveoli); F:AM 61120, right partial ramus with c1–m2 (p1 and m3 alveoli); F:AM 61144, right ramus with i1–p1 alveoli and p2–m3 (m1 broken); F:AM 61150, right partial ramus with c1 alveolus–m1 and m2–m3 alveoli; F:AM 61161, right partial maxillary with P1 alveolus–P4 and M1 alveolus; F:AM 61164, right partial maxillary with P4–M1 and M2 alveolus; F:AM 61170, right maxillary fragment with P3–P4 both broken; F:AM 61177, left partial ramus with p4 broken–m2 and m3 alveolus; F:AM 61177M, left partial ramus with m1 and m2–m3 alveoli; F:AM 61177O, right partial ramus with p1–p3 alveoli, p4 broken–m1, and m2 broken; F:AM 61178A, right partial ramus with i1–i3 alveoli and c1 broken–p4; and F:AM 61179H, posterior cranial fragment. West Sinclair Draw: F:AM 25496, right ramus fragment with m1. Humbug Quarry: F:AM 61136, right partial ramus with c1–p1 alveoli and p2 broken–m1; F:AM 61139, right ramus with c1–m2 (p1 and m3 alveoli); F:AM 61140, left partial ramus with c1 alveolus and p2–m1 (p3 alveolus); F:AM 61141, right ramus with c1 broken–m2 (p1 and m3 alveoli); F:AM 61142, right ramus with i1–p1 alveoli, and p2–m2 (m1 broken and m3 alveolus); F:AM 61143, left partial ramus with i2–p1 alveoli and p2–m2 (m1 broken); F:AM 61146, right ramus with i1–i3 alveoli, c1, p1 alveolus, and p2–m3 (fig. 69A, B); F:AM 61147, right partial ramus with p1 alveolus–m1 (p3 alveolus); F:AM

61148, left partial ramus with i3–c1 alveoli, p3 broken–m2, and m3 alveolus; F:AM 61160, posterior part of skull and separate premaxillary-maxillary with I1–P1 alveoli and P2–M2; F:AM 61162, right maxillary fragment with P3–P4; F:AM 61165, left partial maxillary with P4–M2; F:AM 61166, left partial maxillary with P3–M1 (both P4 and M1 broken); F:AM 61177A, left partial ramus with p2 broken–m2 (p4 broken and m3 alveolus); F:AM 61177F, right partial ramus with m1–m3; F:AM 61177I, right partial ramus with p2 broken–m1; F:AM 61177J, right partial ramus with p3–m1; F:AM 61177U, left partial ramus with i1–p1 alveoli, p2–p4, m1 alveolus, m2 broken, and m3 alveolus; F:AM 61177W, right partial ramus with p1 alveolus, p2–p3 both broken, p4, m1 alveolus, m2, and m3 alveolus; F:AM 61177X, left partial ramus with p1 alveolus, p2 broken–p4, and m1 alveolus; F:AM 61178D, left immature partial ramus with c1–p1 alveoli, dp2–dp4, and m1 unerupted; F:AM 61179, posterior part of skull; F:AM 61179A, posterior part of skull; F:AM 61179B, posterior part of skull; F:AM 61179E, cranial fragment; F:AM 61179D, posterior part of skull; and F:AM 61179I, cranial fragment. Quarry 3: F:AM 61153, left partial ramus with p2–m2 and m3 alveolus. Quarry 6: AMNH 22370, right partial ramus with c1–p3 alveoli, p4, and m1–m3 alveoli. Quarry 7, Kilpatrick Pasture: AMNH 21477A, isolated left M1, left M2, and m2. Grass Root Quarry: F:AM 21448C, left and right maxillary fragments with P2–P3, P4 root, and M1–M2. Jenkins Quarry: F:AM 61157, right and left partial maxillary with C1–P1 alveoli, P2 broken–M2, and skull fragments. Boulder Quarry: F:AM 61113, left partial ramus with i1 alveolus, and c1 broken–m2 (p3, p4, and m3 alveoli); F:AM 61163, right partial maxillary with P3–M1; F:AM 61167, left partial maxillary with P4–M2; F:AM 61177Y, right partial ramus with c1–p4 alveoli, m1 broken, and m2–m3 alveoli; and F:AM 61177Z, left partial ramus with c1–p4 (p1 alveolus). Surface Quarry: F:AM 61177C, right ramus fragment with m1–m2. East Sand Quarry: F:AM 61168, right partial maxillary with P4–M1; F:AM 61177L, right partial ramus m1–m2 and m3 alveolus; F:AM 61179J, posterior part of skull; and F:AM 104806, right ramal fragment with p4–m1 alveoli and m2–m3, below East Sand Quarry. West Sand Quarry: F:AM 61117, right ramus with c1 broken–m2 (p1 and m3 alveoli).

Lower Snake Creek Fauna, Olcott Formation (early Barstovian), unallocated, Sioux County, Nebraska: AMNH 13841, right partial ramus with p1 alveolus, p2–p3, and roots of p4–m1; AMNH 13850, right isolated upper M1, left isolated lower m1, two left ramal fragments with p2–p4; AMNH 20058, three isolated lower m1s; AMNH 20059, left and right ramal fragments with m1–m2; AMNH 20069, left isolated P4; AMNH 22377, left partial maxillary with P3–M1, ''Ashbrook Pasture, Olcott Hill'' (although label as from the Upper Snake Creek, this specimen was probably mislabeled); AMNH 83417, isolated left P4, left p3, and left m2; AMNH 83434, right partial ramus with p2 alveolus–m2 and m3 alveolus; AMNH 96682A, left ramal fragment with m1–m2; AMNH 96682B, right ramal fragment with m1–m2 and m3 alveolus; and AMNH 96682C, left isolated lower m1.

Observation Quarry, Sand Canyon Formation (early Barstovian), Dawes County, Nebraska: F:AM 54485, left isolated P4; F:AM 61187, right maxillary fragment with P3 alveolus–P4; F:AM 61188, right partial ramus with c1 broken, p2–p4, m1–m2 both broken, and m3 alveolus; F:AM 61189, left partial ramus with c1, p1–p3 alveoli, p4–m2, and m3 alveolus; F:AM 67987, left incomplete humerus; F:AM 67988, metacarpal I; F:AM 67988A, metacarpal II; F:AM 67988B, incomplete metacarpal III; F:AM 67988D, metacarpal V; F:AM 67988E, metacarpal V; F:AM 67988G, calcaneum; F:AM 67988H, broken astragalus; and F:AM 104805, right partial ramus with c1 broken, p1 alveolus–p4, and m1–m2 both broken.

Sand Canyon Formation (early Barstovian), Dawes County, Nebraska: Expectation Prospect: F:AM 61185, right premaxillary-maxillary with I1–I3 alveoli, and C1–M2 (P1 alveolus, P2 and P4 broth broken). Survey Quarry: F:AM 61186, right isolated M1; F:AM 67988C, partial metacarpal II; and F:AM 67988I, first phalanx. School House Prospect, Pepper Creek: F:AM 61315, right ramus with c1–m2 and m3 alveolus; F:AM

61316, left ramus with i1–c1 all broken and p1–m3; F:AM 61317, left partial maxillary with P4–M2; F:AM 61318, left maxillary fragment with P4–M1 alveoli and M2; and F:AM 67990, incomplete radius.

Mud Hills Area, Green Hills and Second Division faunas, Barstow Formation (early Barstovian), San Bernardino County, California: Steepside Quarry: F:AM 61190, left ramus with c1 broken–m2 (m1 broken); F:AM 61191, right partial ramus with c1 broken, p1–p2 alveoli, p3 broken–m2, and m3 alveolus; F:AM 61192, right and left partial rami with i3–m3 (p1 alveolus); F:AM 61193, left partial maxillary with P4–M2 (M1 broken), left ramus with c1–m2 (p1 and p3 alveoli and p4–m1 both broken), m3 alveolus, and associated cervical vertebrae (F:AM 61193A); F:AM 61194, right partial ramus with c1–m1; F:AM 61195, right partial ramus with c1–p3 alveoli, p4 broken–m1, and m2–m3 both broken; F:AM 61196, crushed mandible with i2–m3 (i2–c1 and m1–m2 all broken); F:AM 61197, left ramus with c1–m3; F:AM 61198, right partial ramus with p2 alveolus–m2 (p3 and m1 broken); F:AM 61199, left partial ramus with i3–p3 roots and p4 broken–m1; F:AM 61200, left ramus with c1 broken–m2 (m1–m2 both broken) and m3 alveolus; F:AM 61201, right ramus fragment with m1 broken and m2–m3; F:AM 61201A, left ramal fragments with c1–m2 all broken; F:AM 61202, right ramus with c1–p1 alveoli, p2–m2 (m1 broken), and m3 alveolus; F:AM 61203, right and left partial rami with c1–m2 (p3–m1 all broken); F:AM 61204, right ramus with premolar alveoli and m1–m2 both broken; F:AM 61205, left partial ramus with i2–m2 (p1 alveolus and m1–m2 broken); F:AM 61206, right and left partial rami with c1 broken–m3 (p1 broken); F:AM 61207, maxillary fragment with C1 and both rami with i3–c1 broken and p1 alveolus–m2; F:AM 61208, left partial ramus with p1–p3 alveoli, p4–m2, and m3 alveolus; F:AM 61209, right partial ramus with c1–p3 alveoli, p4–m1, and m2 alveolus; F:AM 61210, right partial ramus with p2 broken–m1; F:AM 61211, right partial ramus with p4 broken–m2; F:AM 61212, right partial ramus with i3–p4 and m1 broken; F:AM 61215, skull with I1–P1 alveoli, P2–P4 all broken, M1, and M2 broken; F:AM 61216, partial skull with P3 broken–M2; F:AM 61217, crushed partial skull with P2–M2; F:AM 61218, crushed partial skull with P4–M1 both broken and M2; F:AM 61219, anterior part of skull with I1–P1 alveoli and P2 broken–M2; F:AM 61220, crushed skull with I1–P3 alveoli and P4–M2; F:AM 61221, left partial maxillary with P4–M2 (M1 broken); F:AM 61222, right partial maxillary with P3 alveolus–M2; F:AM 61223, right partial maxillary with P4, M1 broken, and M2 root; F:AM 61225, left partial maxillary with P3 broken–M2 (M1 broken); F:AM 61226, right and left partial maxillae with P3 broken–M2 and detached C1; F:AM 61227, right partial maxillary with P3 broken–M2; F:AM 61228, left partial maxillary with P4 broken–M2; F:AM 61229, right and left broken and incomplete maxillae and left partial premaxillary-maxillary with I1–I2 roots, and C1–M2; F:AM 61230, left partial maxillary with I1–P1 alveoli, P2 broken–P3, and a separate maxillary fragment with P4–M1; F:AM 61231, two associated left maxillary fragments with C1–P2 and M1–M2 and teeth fragments; F:AM 61231A, left premaxillary fragment with C1; F:AM 61232, right partial maxillary with P4 broken–M2; F:AM 61233, crushed fragment of skull with P2–P3 alveoli and P4–M2 all broken; F:AM 61234, crushed partial skull with C1–P3 alveoli and P4–M2 all broken; F:AM 61235, skull fragment with C1 broken, P1 and P3 alveoli, and P4–M2 all broken; F:AM 61236, posterior part of skull; and F:AM 105302, posterior part of skull. Green Hills: F:AM 27150, palate with P2 broken–M2 and mandible with i3–m3; F:AM 27505, left partial ramus with c1 broken–m2 (p1 and p2 broken); F:AM 27510, crushed partial skull with P3–M2 and both rami with c1 broken–m3 (p1 alveolus and m1 broken); F:AM 27512, left partial maxillary with P4–M2; F:AM 27513, left maxillary fragment with P3–P4; F:AM 27514, right ramus with i3 alveolus–m1 and m2 root; F:AM 27515, right partial ramus with p1 alveolus–m2 (m1 broken); F:AM 27516, left partial ramus with p1–p3 alveoli, p4–m2, and m3 alveolus; F:AM 27517, left partial ramus with c1–p4 and m1 broken; F:AM 27518, right partial ramus with i3 broken–m2 (p1 alveolus and p2 broken); F:AM 27519, right and left rami with c1–m2 and m3 alveolus; F:AM 27520, left

partial ramus with c1–p2 alveoli, p3–m2, and m3 alveolus; F:AM 27521, right partial ramus with p4–m3; F:AM 27531, right and left partial maxillae with P4 broken–M2; and F:AM 67335, left partial ramus with c1–p4 alveoli and m1–m2. First layer above Third Division: F:AM 27272, partial palate with P3 broken–M2; and F:AM 27285, immature left and right partial rami with dp2 broken, dp3, and m1 unerupted. Second layer above Third Division: F:AM 27263, right and left partial rami with i2–m3 (c1 broken). Lower Second Division: F:AM 27511, crushed partial palate with P2–M2 (P3 broken). Sunder Ridge Quarry: F:AM 61213, right and left partial rami with c1–m2 (p1 broken). Turbin Quarry: F:AM 61214, right ramal fragment with m1 broken–m2. No locality data: F:AM 27262, right partial ramus with p3–m2; F:AM 27262A, right partial ramus with c1–p4 and m1–m2 both broken; F:AM 27264, right partial ramus with P4–M2; F:AM 27265, right maxillary fragment with M1; F:AM 27271, left ramus with i1–c1 broken, p1 broken, p2–m1 all broken, and m2; and F:AM 27271A, isolated left m1.

Yermo Quarry, Barstow Formation (early Barstovian), San Bernardino County, California: F:AM 27507, right partial maxillary with P4–M2; F:AM 27509, right partial ramus with p4 root–m2; F:AM 27529, right and left partial rami with c1–m3 (p1 and p4 alveoli); F:AM 61237, anterior part of skull with I1–M2; F:AM 61238, partial skull with P1–P3 alveoli and P4–M2 all broken; F:AM 61239, left partial maxillary with P4–M1 and M2 broken; F:AM 61240, right and left partial maxillae with P4–M2; F:AM 61242, left partial ramus with p2–m2 all broken; and F:AM 61243, left isolated m1.

Skull Ridge Member, Tesuque Formation (early Barstovian), Santa Fe County, New Mexico: Southeast of White Operation Wash: F:AM 27379, partial skull with P1–P3 alveoli, P4 broken, and M1–M2; F:AM 27381, right partial ramus with p3–m2 (p4 broken) and m3 alveolus; F:AM 27382, left and right ramal fragments with broken p2–m3 (p2–m2 all broken); F:AM 27383, right partial ramus with p4–m1 both broken, m2, and m3 unerupted; and F:AM 27384, edentulous left partial ramus with c1–m3 alveoli. Skull Ridge: F:AM 27383A, right partial maxillary with P4–M2. Cuyamunque: F:AM 27470, skull with I1–M2 (most teeth broken or heavily worn). One mi north of White Operation: F:AM 50154, left and right partial rami with c1 broken–m2 (p1–p2 and m3 alveoli).

Kent Quarry (UCMP loc. V5666), Dry Canyon West Side 2, Cuyama Valley, Caliente Formation (early Barstovian), Ventura County, California: UCMP 50670, partial anterior skull with I1–M2 (I3 broken) and mandible with i3–m2 and m3 alveolus; and UCMP 51104, skull fragments with P3–M1 and partial left and right bullae.

DISTRIBUTION: Early Barstovian of Nebraska, New Mexico, and California.

EMENDED DIAGNOSIS: Compared to *Tomarctus brevirostris*, *T. hippophaga* is primitive in having palate not widened, nuchal crest not laterally narrowed, and M1 paracone less high-crowned.

DESCRIPTION AND COMPARISON: The numerous previously undescribed materials from the Olcott Formation represent a marked improvement in quantity and quality of specimens over that available to Matthew (1924, his *Tomarctus brevirostris*). This is especially true for the exquisitely preserved materials from the Echo Quarry. In addition, large samples from the lower part of the Barstow Formation are referred to this species for the first time. These and a small sample from the Tesuque Formation, New Mexico, suggest that *Tomarctus hippophaga* was widespread in the early Barstovian.

A nearly perfect skull (F:AM 61156; fig. 70A–D) from the Echo Quarry permits an undistorted view of this species, as opposed to the crushed skulls from other quarries described by Matthew (1924). With the increased fidelity of cranial structures, it is possible to ascertain that *Tomarctus hippophaga* has a relatively narrower palate than does *T. brevirostris* (as exemplified by a similarly undistorted skull, F:AM 61158) (see Description and Comparison under *T. brevirostris*). Apparently a young adult, because of the lack of wear on teeth, F:AM 61156 has relatively narrow forehead (distance between the supraorbital rim) in contrast to older individuals (AMNH 18242–44) that have broader foreheads (fig. 70E–H). On a dissected partial skull (F:AM 61181), the large

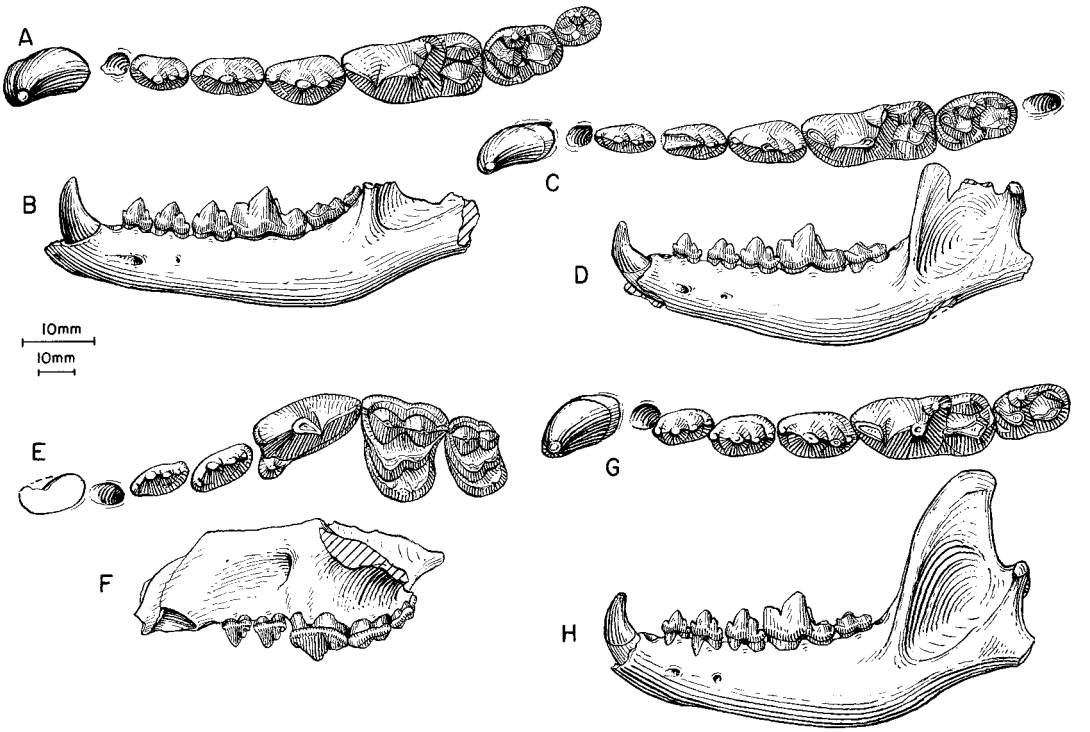

Fig. 69. *Tomarctus hippophaga*. **A**, Lower teeth and **B**, ramus (reversed from right side), F:AM 61146, Humbug Quarry, Olcott Formation (early Barstovian), Sioux County, Nebraska. **C**, Lower teeth and **D**, ramus, F:AM 61174, Echo Quarry, Olcott Formation (early Barstovian), Sioux County, Nebraska. **E**, Upper teeth and **F**, lateral view of maxillary (reversed from right side), F:AM 61174A, Echo Quarry. **G**, Lower teeth and **H**, ramus (reversed from right side), AMNH 13836, holotype, Quarry 2, East Sinclair Draw, Olcott Formation (early Barstovian), Sioux County, Nebraska. The longer (upper) scale is for A, C, E, and G, and the shorter (lower) scale is for the rest.

frontal sinus can be seen to be partitioned by a horizontal septum into anterodorsal and posteroventral chambers including a sinus in the postorbital process that communicates through a restricted passage with the posteroventral chamber. Other than the above-noted features, *T. hippophaga* is quite similar in cranial proportions to *Protomarctus optatus* and *Tomarctus brevirostris* (fig. 71).

Tomarctus hippophaga is larger than *Protomarctus optatus* (13% in basal skull length and 11% in m1 length, all pooled averages). Signaling its affinity with the Aelurodontina, *T. hippophaga* has enlarged lower premolars and this enlargement is rather uniform on all premolars instead of differential enlargement of p4 over p2–p3 as in the Borophagina. The massiveness of the premolars is mainly reflected in the width of the tooth and is in clear contrast to the immediate primitive state in *P. optatus*. Other than the robust premolars, teeth of *T. hippophaga* are little different from those of *P. optatus*.

Specimens from the Barstow Formation are on the whole 5% (pooled average of all dental measurements) smaller than their counterparts in the Lower Snake Creek Fauna in Nebraska. The California individuals also tend to be more primitive in their narrower foreheads and less massive premolars. Such minor differences aside, the California sample is closest, both in size and overall morphology, to the topotypical materials of *Tomarctus hippophaga* in Nebraska. We interpret these variations from the California sample as representing a primitive population of the lineage.

Referred individuals from the Tesuque

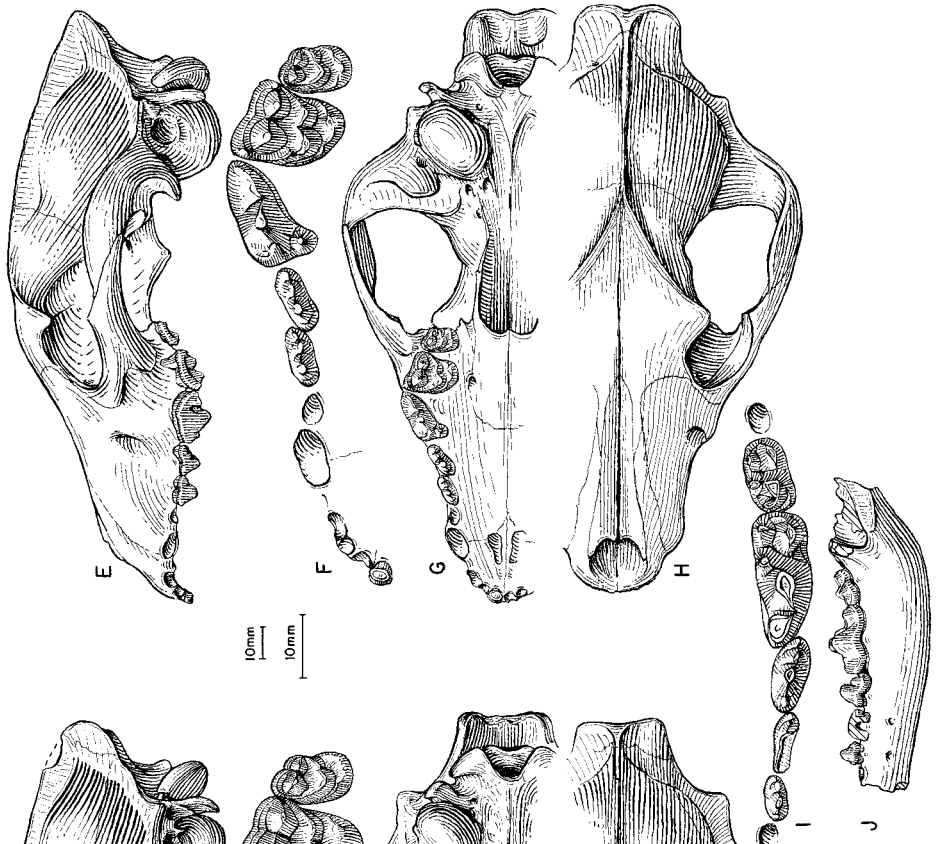

Fig. 70. *Tomarctus hippophaga*. **A**, Lateral, **B**, enlarged occlusal, **C**, ventral and **D**, dorsal views of skull and upper teeth, F:AM 61156, Echo Quarry, Olcott Formation (early Barstovian), Sioux County, Nebraska. **E**, Lateral, **F**, enlarged occlusal, **G**, ventral, and **H**, dorsal views of skull and upper teeth (I1 and P2–P3 reversed from right side), **I**, lower teeth, and **J**, ramus (reversed from right side), AMNH 18244, Sheep Creek Quarry, Olcott Formation (early Barstovian), Sioux County, Nebraska. The shorter (upper) scale is for A, C, D, E, G, H, and J, and the longer (lower) scale is for the rest.

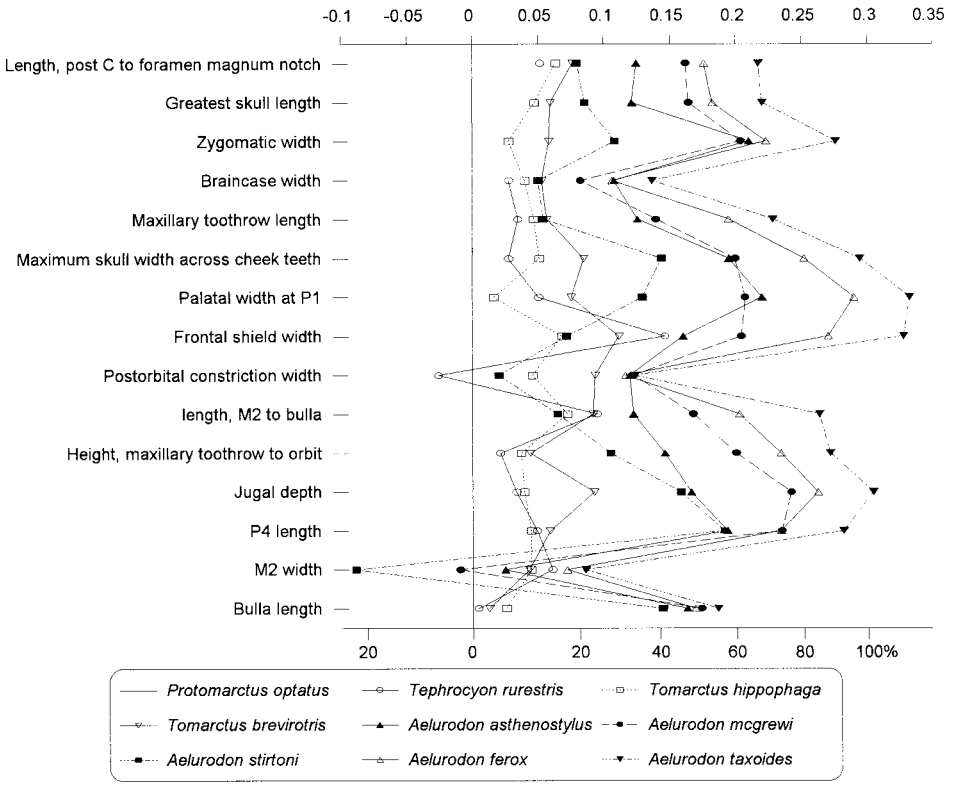

Fig. 71. Log-ratio diagram for cranial measurements of *Tephrocyon*, *Tomarctus* and *Aelurodon* using *Protomarctus optatus* as a standard for comparison (straight line at zero). See text for explanations and appendix II for measurements and their definitions.

Formation are less well represented both in quantity and quality of materials. Most of the specimens match very well, in size and shape, with the topotype series from Nebraska. One skull (F:AM 27470), however, is substantially larger and is in the same size category as *Tomarctus brevirostris*. Teeth of F:AM 27470 are severely worn and badly broken. This large individual has an unbroadened palate and its nuchal crest is not narrowed laterally, features that suggest its assignment to *T. hippophaga*.

DISCUSSION: *Tomarctus hippophaga* was initially compared with *Tephrocyon rurestris* from the Mascall Formation of Oregon by Matthew and Cook (1909), who made no reference to *Tomarctus brevirostris*. Shortly afterward, Matthew began to suspect that *brevirostris* from the Pawnee Creek area of Colorado might be conspecific with *hippophaga*. However, he did not act on this suspicion until the publication of his influential treatise on the Snake Creek faunas, when he was finally convinced that the faunas from the Pawnee Creek and Snake Creek were very close in age, and *T. hippophaga* was thus synonymized under *T. brevirostris* (Matthew, 1924). Matthew's authoritative treatment on the relationships of canids in the 1924 volume proved to be very influential, and except for one brief mention of *Tomarctus hippophaga* by VanderHoof (1931: 19), his taxonomic decision was followed by all subsequent students. Thus, *T. hippophaga* has all but disappeared from the literature.

Matthew himself, however, still harbored some lingering doubts about this decision. Indeed, there is a substantial size difference between the holotypes of *Tomarctus brevirostris* and *T. hippophaga*—the lower carnassial of the former is 16% longer than that of the latter. Furthermore, there are individ-

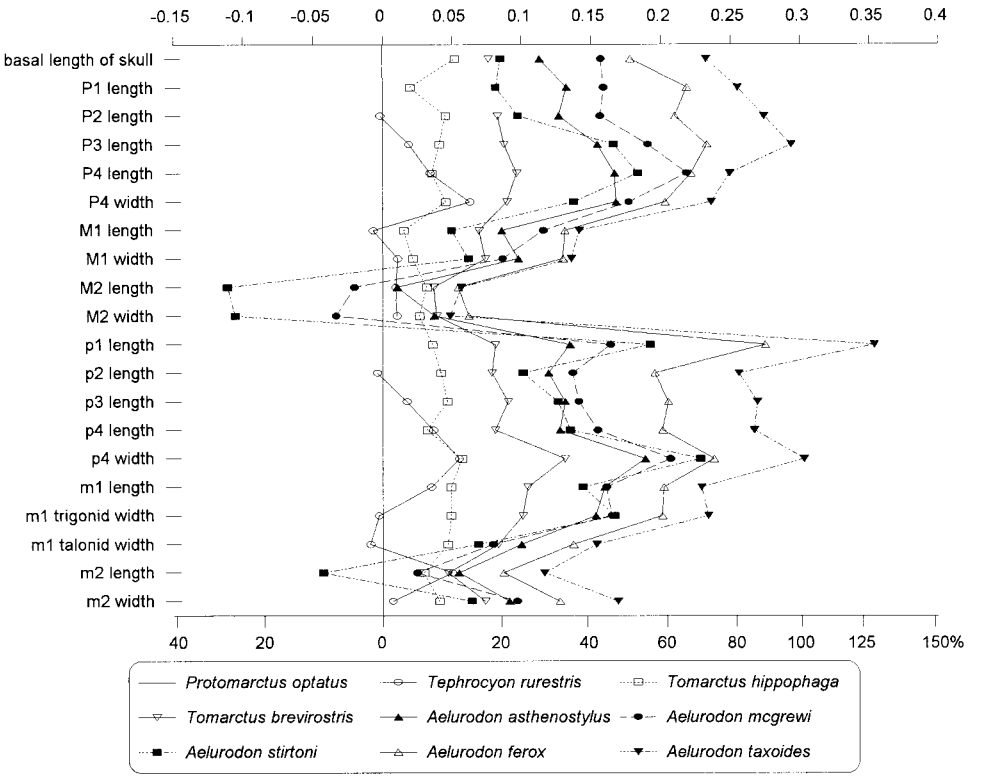

Fig. 72. Log-ratio diagram for dental measurements of *Tephrocyon*, *Tomarctus*, and *Aelurodon* using *Protomarctus optatus* as a standard for comparison (straight line at zero). See text for explanations and appendix III for summary statistics of measurements and their definitions.

uals in the Lower Snake Creek Fauna that possess even smaller carnassials than that of the holotype of *T. hippophaga*, making the variation in size even greater. Associated with the size differences are some cranial characters in certain large individuals from the Olcott Formation that suggest more than one species is present in the Snake Creek Fauna. Our resurrection of *T. hippophaga* is thus an attempt to account for these quantitative and qualitative differences (see further discussion under *Tomarctus brevirostris*).

Without explicit reference to specimens, Barbour and Cook (1917: 180) listed *Tephrocyon* cf. *hippophaga* to occur in the Valentine beds in Nebraska. We could find no such occurrence in these younger strata.

Tomarctus brevirostris Cope, 1873

Figure 73

Tomarctus brevirostris Cope, 1873: 2. Matthew, 1899: 68; 1901: 359; 1924: 91 (in part). Hay, 1902: 775. Cope and Matthew, 1915: pl. CXIXc, fig. 4. Munthe, 1998: 135.

Aelurodon francisi Hay, 1924: 2, pl. 3, figs. 1, 2. Wilson, 1960: 991 (in part). Munthe, 1998: 136.

Aelurodon simulans Hay, 1924: 2, fig. on p. 3.

?*Aelurodon francisi* (Hay): Vanderhoof and Gregory, 1940: 153.

Tomarctus sp.: Repenning and Vedder, 1961: table 235.1.

HOLOTYPE: AMNH 8302, right ramal fragment with p4 alveolus–m1 (fig. 73O, P) from Court House Butte, Pawnee Creek Formation (probably early Barstovian), Weld County, Colorado.

REFERRED SPECIMENS: Pawnee Creek Formation (late early Barstovian), Weld County, Colorado: Middle Horizon near Hereford: F:AM 28302, left partial ramus with p4–m1 (fig. 73M, N). Question Mark Pit, southwest side: F:AM 67319, right ramus with c1–m3 (fig. 73E, F); F:AM 67320, right partial ramus with i1–i3 alveoli, c1 broken, p1–p3 al-

veoli, p4 broken–m1, and m2–m3 alveoli; and F:AM 67322, left partial ramus with c1 broken, m1 broken, and alveoli of the remaining teeth. Three Point, East Side Pit: F:AM 67321, left partial ramus with c1–p1 alveoli, and p2 broken–m2 (p3 alveolus, p4–m1 broken, and m3 alveolus). Pawnee Quarry: F:AM 105304, left partial maxillary with P4–M2 all broken. Big Spring Quarry: F:AM 105305, right isolated M1. No locality data: F:AM 28314, left and right partial maxillary with C1–M2 (molars extremely worn); and F:AM 28319, immature right ramal fragment with dp4 and m1.

Pawnee Creek Formation (early late Barstovian), Logan and Weld counties, Colorado: Cedar Creek: AMNH 9455, immature left ramus with di1, dc1, dp2, dp4, and m1 unerupted. Horse Quarry: F:AM 28315, right partial maxillary with P4 and M1–M2 alveoli; and F:AM 28317, left partial ramus with i1–p2 alveoli, p3–m1, and m2 alveolus.

Olcott Formation (early Barstovian), Sioux County, Nebraska: Humbug Quarry: F:AM 61158, partial skull with C1, P4–M2, and alveoli of all other teeth (fig. 73A–D); F:AM 61169, left partial maxillary with P2–P4 (P3 alveolus and M1 broken); F:AM 61177Q, left partial ramus with p2–p3 alveoli, p4–m1, and m2 alveolus; F:AM 61177V, right partial ramus with i1–p1 alveoli and p2–p4. Boulder Quarry: F:AM 61123, left ramus with i1–i3 alveoli, c1, p1 alveolus–m1, and m2 alveolus. Echo Quarry: F:AM 61121, left ramus with i1–i3 alveoli, and c1–m1 (p1 alveolus and m2–m3 alveoli); F:AM 61122, right ramus with i1–i3 alveoli, and c1–m2 (p1 and m3 alveoli). Ashbrook Pasture: AMNH 13834, left partial maxillary with M1–M2; AMNH 20057, right isolated M1; AMNH 22400, left maxillary with P4 broken–M2, right ramus with i1–p1 alveoli, p2–m2, and m3 alveolus; and AMNH 81031 (HC 273), right partial maxillary with C1–P1 alveoli and P2–P4. East Sinclair Draw: F:AM 25487, partial left ramus with p2–p3 alveoli, p4–m1, and m2 alveolus, Horizon C. East Sand Quarry: F:AM 61151, right ramus with i3–p1 alveoli, p2, p3 alveolus–m1, and m2–m3 alveoli. Jenkins Quarry: F:AM 61177R, left isolated m1. West Sand Quarry: F:AM 61129, right ramus with i2–m2 (p1 and m3 alveoli). Quarry A: AMNH 18251, left partial ramus with p3–m2 and right partial ramus with m1 and m2–m3 alveoli. Quarry B: AMNH 18246, left partial maxillary with P1–P3 alveoli and P4–M2 (fig. 73G, H). Quarry 2: F:AM 61125, left ramus with i1–p1 alveoli, and p2–m2 (m1 broken and m3 alveolus); F:AM 61130, left ramus with c1–p1 alveoli, p2–m2, and m3 alveolus (fig. 73I, J); F:AM 61171, right maxillary fragment with M1 broken–M2; F:AM 61177P, left partial ramus with m1–m2; F:AM 61178, left partial ramus with i1–i3 alveoli, c1, and p1 alveolus–p4; and F:AM 61179C, posterior part of skull. Quarry 8: F:AM 61127, right partial ramus with i1–i3 alveoli, c1, p1–p2 alveoli, and p3–m2. New Surface Quarry: F:AM 61124, right partial ramus with c1–p3 alveoli, p4–m1, and m2 roots; F:AM 61126, left partial ramus with c1–p1 alveoli, p2–m2, and m3 alveolus; F:AM 61128, left partial ramus with c1–p1 alveoli, p2–m1, and m2–m3 alveoli; F:AM 61175, partial left maxillary with P2 alveolus and P3 broken–M2; F:AM 61177N, left ramal fragment with m1; F:AM 61177S, left ramal fragment with m1–m2 and m3 alveolus; F:AM 61178B, right ramal fragment with p2 alveolus–p4; F:AM 61179F, skull fragments, posterior part; and F:AM 61179G, posterior part of skull. Version Quarry: F:AM 61159, right maxillary with P1 alveolus–M2; and F:AM 61177T, right partial ramus with p4 broken–m2 and m3 alveolus, ?Version Quarry or Pocket 34. Seventeen mi south of Agate (from Upper Snake Creek beds, but probably reworked): AMNH 81096 (HC 515), isolated right m1.

Second Division Fauna, Barstow Formation (late early Barstovian), San Bernardino County, California: Valley View Quarry: F:AM 27502, right ramus with c1–m2 (p1 alveolus) and m3 alveolus; F:AM 27538, right and left rami with i1–c1 all broken and p1–m3; F:AM 27544, right partial ramus with i1–p1 roots and p2–m2 (p3 and m3 alveoli); F:AM 27544A, left partial ramus with p4 broken–m3; and F:AM 31100, right ramus with i2–i3 roots and c1–m2. No locality data: F:AM 27260, left maxillary with P4–M2; and F:AM 27261, right partial ramus with p2–p4 all broken and m1–m3.

East Caliente Range, Caliente Formation (early Barstovian), San Luis Obispo County,

California: USGS M1005, isolated P4 and M1 (referred to *Tomarctus* sp. by Repenning and Vedder, 1961: table 235.1), 4 ft below middle Triple Basalt.

Skull Ridge Member, Tesuque Formation (early Barstovian), Santa Fe County, New Mexico: Skull Ridge: F:AM 61182, crushed anterior part skull with I3–M2, partial left and right rami with p3–m2, and limb fragments including metapodial fragments and 9 phalanges. Third District: F:AM 27368, left maxillary fragment with P3–M1.

J. Niscavit Farm, from a well at a depth of 22 ft, Grimes Prairie, 12 mi east of Navasota and 3 mi north of Stoneham, possibly equivalent to the Cold Spring fauna (Wilson, 1960: 991) of Fleming Formation (late Barstovian), Grimes County, Texas: TMM-TAMU 2379 (AMNH cast 97240) (holotype of *Aelurodon francisi* Hay, 1924), left partial ramus with p3–m3 (fig. 73K, L).

Noble Farm fauna (late Barstovian) (stratigraphically equivalent to Grimes Prairie, the type locality of *A. francisi*, according to VanderHoof and Gregory, 1940: 153), Moore County, Texas: TMM-TAMU 2186 (AMNH cast 97772) (holotype of *Aelurodon simulans* Hay, 1924), right partial ramus with p3–m2 (m1 broken) and m3 alveolus.

DISTRIBUTION: Early Barstovian of Colorado, Nebraska, New Mexico, and California; and early late Barstovian of Colorado; late Barstovian of Texas.

EMENDED DIAGNOSIS: Synapomorphies shared by *Tomarctus brevirostris* and *Aelurodon* but distinguishing it from *T. hippophaga* are broadened palate, posterodorsally produced nuchal crest that is laterally compressed, reduction of lambdoidal crest, and high-crowned M1 paracone relative to metacone. Primitive characters that distinguish *T. brevirostris* from *Aelurodon* are sagittal crest lower, bulla not hypertrophied, mastoid process small, P4 protocone less reduced, P4 parastyle smaller, upper molars not reduced relative to P4, M1 lingual cingulum not restricted to the posterolingual border, m1 talonid not narrowed, m2 less reduced, and m2 metaconid approximately equal to protoconid in height.

DESCRIPTION AND COMPARISON: Our reshuffling of the hypodigm of *Tomarctus* admits, in addition to the topotype materials from Colorado, only a small portion of the total Lower Snake Creek samples and excludes all of the specimens described by Matthew (1924, see Discussion below). The newly referred skull from Humbug Quarry (F:AM 61158, fig. 73A–D) is entirely undistorted, unlike the crushed skulls figured in Matthew (1924), and affords secure knowledge about its cranial morphology. In overall cranial proportions, *T. brevirostris* is slightly more advanced than *T. hippophaga* toward the *Aelurodon* clade. In the ratio diagram figure 71, the pattern for *T. brevirostris* begins to assume the shape for various species of *Aelurodon*, although still in its initial stage. The most obvious difference is a broader palate. This broadening of the palate is not merely due to its overall larger size; there is a 17% increase in palate breadth across widest points of cheekteeth (P4–M1 juncture) vs. a 7% increase in basal length of skulls (only the undistorted skulls are measured: F:AM 61158 for *T. brevirostris* and F:AM 61156 for *T. hippophaga*). The broadened palate is also indicated by the laterally deflected horizontal rami of the lower jaws. The frontal sinus has about the same degree of inflation as in *T. hippophaga*, and the postorbital process is similarly well developed. The nuchal crest is slightly more produced posteriorly and narrower laterally than that in *T. hippophaga*. The external auditory meatus has a slightly longer lip, and the paroccipital process is more posteriorly expanded, increasing the area of the lateral scar.

Dental differences between *Tomarctus brevirostris* and *T. hippophaga* are subtle and often involve proportional relationships. *T. brevirostris* is on average 10% larger (pooled average of all dental measurements) than *T. hippophaga*. Signaling the further advancement toward the *Aelurodon* clade, the premolars of *T. brevirostris* are stronger than those of *T. hippophaga*; its M2 and m2 are slightly reduced relative to M1 and m1, and the M1 shows an appreciable crown height difference between paracone (higher) and metacone. Other than these subtle proportional differences, the cusp morphology of upper and lower molars is quite similar to those of *T. hippophaga*.

Compared with *Aelurodon*, on the other hand, *T. brevirostris* is more easily distin-

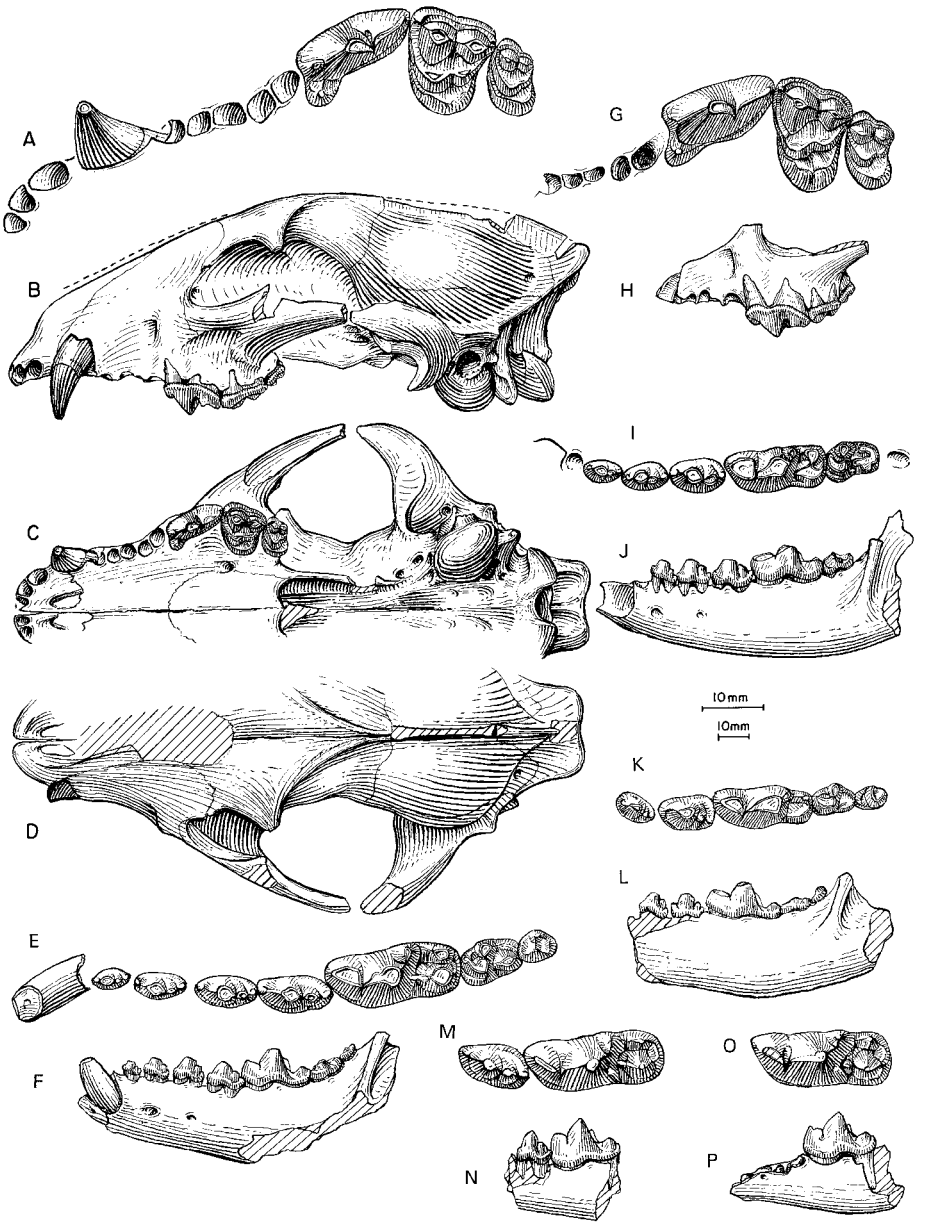

Fig. 73. *Tomarctus brevirostris*. **A**, Upper teeth and **B**, lateral, **C**, ventral, and **D**, dorsal views of skull, F:AM 61158, Humbug Quarry, Olcott Formation (early Barstovian), Sioux County, Nebraska. **E**, Lower teeth and **F**, ramus (reversed from right side), F:AM 67319, Question Mark Pit, Pawnee Creek Formation (late early Barstovian), Weld County, Colorado. **G**, Upper teeth and **H**, lateral view of maxillary, AMNH 18246, Quarry B, Olcott Formation. **I**, Lower teeth and **J**, ramus, F:AM 61130, Quarry 2, Olcott Formation. **K**, Lower teeth and **L**, ramus, TMM 2379 (holotype of *Aelurodon francisi*), J. Niscavit Farm, beds possibly equivalent to the Cold Spring Fauna of Fleming Formation (late Barstovian), Grimes County, Texas. **M**, Lower teeth and **N**, ramus, F:AM 28302, middle Horizon near Hereford, Pawnee Creek Formation (late early Barstovian), Weld County, Colorado. **O**, Occlusal and **P**, lateral views of ramus and m1 (reversed from right side), AMNH 8302, holotype, Court House Butte, Pawnee Creek Formation (probably early Barstovian), Weld County, Colorado. The longer (upper) scale is for A, E, G, I, K, M, and O, and the shorter (lower) scale is for the rest.

guished by its primitive cranial and dental morphology. The sagittal crest in *T. brevirostris* is still low, the bulla is not prominently inflated, and the paroccipital process is not quite as elongated as in *Aelurodon*. The P4 parastyle is not strong. The m1 talonid remains broad, and the m2 metaconid is still large.

DISCUSSION: Established on a ramal fragment with a single m1 from the Pawnee Creek Formation in Colorado, *Tomarctus brevirostris* was largely ignored by subsequent students until Matthew's (1924) reference of complete cranial and dental materials from the Lower Snake Creek Fauna of Nebraska. These referred materials played an important role in establishing *T. brevirostris* as a primitive ancestor to nearly all later canids (see further discussion under the genus).

After many years of hesitation following the establishment of *Tephrocyon hippophaga* (Matthew and Cook, 1909), Matthew (1924) finally concluded that *Tomarctus brevirostris* and *T. hippophaga* were probably conspecific, mainly because of his increasing confidence that the Pawnee Creek beds (now Formation), where the type of *T. brevirostris* was recovered, and the Lower Snake Creek beds (now Olcott Formation) were roughly coeval. However, he did have some lingering doubts about this conclusion: ''it is quite probable that the species [*T. brevirostris* and *T. hippophaga*] are identical, but adequate proof of this is lacking, and they may yet prove to be distinct'' (Matthew, 1924: 89). Although Matthew's observation was based on quite good materials (three lightly crushed skulls) from the Lower Snake Creek Fauna, considerably more materials from both the Olcott Formation and the Pawnee Creek Formation have been accumulated since his last review. With the additional materials, we now recognize the validity of both *T. brevirostris* and *T. hippophaga* and the presence of both within the Lower Snake Creek Fauna.

Our reestablishment of these two species comes from two lines of evidence. First, there is a wide range of variation in size among the Lower Snake Creek samples, and it exceeds the normal variation of a species, even if one takes into account the temporal dimension of the fauna (see appendices II and III). Second, a well-preserved skull from the Humbug Quarry (F:AM 61185) demonstrates that *Tomarctus brevirostris* possesses the initial development of several derived characters normally found only in *Aelurodon*, such as broadened palate, narrowed nuchal crest, and elongated paroccipital process, that contrast with the absence of these features in other skulls from the Lower Snake Creek quarries (including those described by Matthew, 1924). This advanced-looking skull is near the higher end of the size range among the Lower Snake Creek materials and is about the same size as the topotype series from Colorado. We thus hypothesize that among the Lower Snake Creek samples there is a small proportion of large-size individuals referable to *T. brevirostris* that are distinct from most individuals typified by the holotype of *T. hippophaga*. Such a hypothesis engenders a problem in the allocation of hypodigms—fragmentary specimens of intermediate size are difficult to allocate to one species or another—but is preferable to the alternative that does not discriminate the morphological differences within the samples, i.e., lumping everything into a single species, as proposed by Matthew (1924).

At a size almost identical to that of *Tomarctus brevirostris*, *Aelurodon francisi* (Hay, 1924) is almost indistinguishable from the former except in a few subtle features: a reduced metaconid, a slightly narrowed talonid, and a relatively reduced lingual side of the talonid that restricts the entoconid to a more anterior position. Although these features may suggest a taxon in the initial stage of development toward the *Aelurodon* clade, we tentatively place the Texas material in *Tomarctus* because of its lack of robust premolars so typical of *Aelurodon*.

Hay (1924: 2) also proposed *Aelurodon simulans* as a species distinct from *A. francisi*, even though he admitted that ''at first this specimen [holotype of *A. simulans*] was taken to belong to *Ae. francisi*.'' Subsequent authors (VanderHoof and Gregory, 1940; Wilson, 1960) had all failed to see any distinction between the two species, a conclusion with which we agree. The only observable difference between the poorly preserved holotypes of these two Texas species is a rela-

tively more slender p3–p4 in *A. simulans*, a distinction easily encompassed by variation within species of similar size.

The referred specimens of *A. francisi* (Wilson, 1960) from the Cold Spring Fauna, however, clearly represent a large, more derived form (see *A. ferox*). The Cold Spring specimens agree well in size with *A. ferox*, and their advanced dental features, such as three lateral accessory cusplets on I3 (Wilson, 1960: fig. 4h), high-crowned M1 paracone, and prominent P4 parastyle, indicate the presence of this widespread species of *Aelurodon* in the late Barstovian of Texas.

Henshaw (1942) referred one upper canine and one m1 (LACM-CIT 774) to *Tomarctus brevirostris* from late early Barstovian sites near Tonopah in the San Antonio Mountains, Nevada. According to his figure (Henshaw, 1942: fig. 3), the upper canine is too long to be a canid. The m1, on the other hand, is too worn to be sure of its identity, and its size and proportions are slightly smaller than *T. brevirostris* as defined in this study (its size is closer to *Tomarctus hippophaga*). Its occurrence in the early Barstovian of Nevada is thus questionable.

Aelurodon Leidy, 1858

Prohyaena Schlosser, 1890: 25.
Strobodon Webb, 1969a: 43.

TYPE SPECIES: *Aelurodon ferox* Leidy, 1858.

INCLUDED SPECIES: *A. asthenostylus* (Henshaw, 1942); *A. mcgrewi*, new species; *A. stirtoni* (Webb, 1969a); *A. ferox* Leidy, 1858; and *A. taxoides* Hatcher, 1893.

DISTRIBUTION: Early Barstovian of Nebraska, Colorado, Nevada, and California; late Barstovian of Colorado, Nebraska, South Dakota, New Mexico, Texas, and California; early Clarendonian of South Dakota, Nebraska, New Mexico, Oklahoma, Texas, Florida, and Nevada; late Clarendonian of Nebraska, New Mexico, and California; and Clarendonian of Kansas.

EMENDED DIAGNOSIS: Species of *Aelurodon* share many derived features that differ from *Tomarctus*: high sagittal crest, enlarged bulla, enlarged mastoid process, P4 parastyle strong, P4 protocone reduced, reduced M1–M2 and m2, M1 lingual cingulum reduced anteriorly, m1 talonid narrowed, shortened m2, and m2 metaconid reduced. Besides the *A. mcgrewi–stirtoni* clade, advanced species of *Aelurodon* acquire further derived characters, such as extremely broadened palate, transversely straight upper incisor row, massive premolars with very strong cusplets, extremely high sagittal crest, and more posterodorsally produced nuchal crest.

DISCUSSION: The strikingly robust skull and teeth of *Aelurodon*, mirroring in many ways the cranial and dental construction of bone-crushing hyaenids, attracted the attention of early vertebrate paleontologists (see Baskin, 1980, for a recent summary). Such attention quickly resulted in a proliferation of names during the pioneering era of North American vertebrate paleontology. In the first comprehensive review, VanderHoof and Gregory (1940) listed more than a dozen nominal species of ''*Aelurodon*'' (including *Epicyon*) but went little beyond reiteration of many of the previous ''species,'' essentially following the phylogenetic scheme advanced by Matthew (1924, 1930). Shortly afterward, McGrew (1944b) offered the insight that the multiple species of *Aelurodon* may be divided into two groups—the *A. taxoides* species group and the ''*A.*'' *saevus* species group—an idea further elaborated by Mawby (1964, 1965). In attempting to determine to which of these two groups the type species *A. ferox* belongs, Richey (1979: 108) took note of a crest between the P4 protocone and paracone in the *taxoides* group and concluded that the holotype of *A. ferox*, lacking this crest, probably belonged to the *saevus* group. Baskin (1980), however, investigated the P4 morphology in greater depth and determined that the genus *Aelurodon* should be restricted to the *A. taxoides* group, and *Epicyon* should be resurrected for the ''*A.*'' *saevus* group. Baskin's phylogenetic outline is basically consistent with our own analysis, although his P4 protocone synapomorphy is not completely unique within *Epicyon* and is also shared by *Borophagus*.

Aelurodon asthenostylus (Henshaw, 1942), new rank

Figures 74–76

Aelurodon wheelerianus asthenostylus Henshaw, 1942: 111, pl. 4, figs. 1, 2.

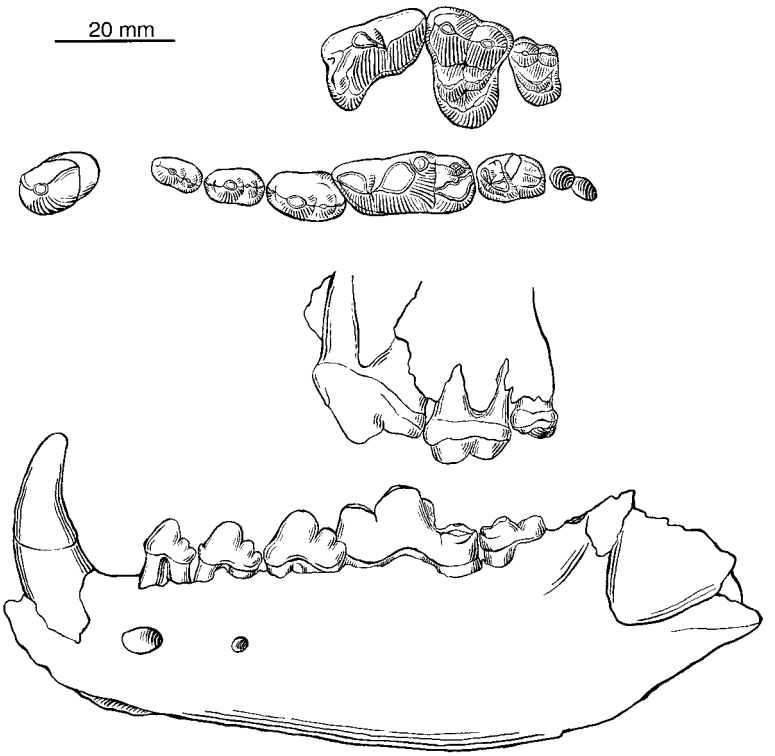

Fig. 74. *Aelurodon asthenostylus*. LACM-CIT 781, holotype, Siebert Formation (late early Barstovian), San Antonio Mountains, near Tonopah, Nye County, Nevada. Ramus and lower teeth reversed from right side. Illustration by X. Wang.

HOLOTYPE: LACM-CIT 781 (formerly LACM-CIT 2816), partial palate with left and right P4–M2 and partial mandible with left and right c1–m2 (fig. 74), from Tonopah Local Fauna, LACM-CIT loc. 172-C, Siebert Formation (late early Barstovian), San Antonio Mountains, near Tonopah, Nye County, Nevada.

REFERRED SPECIMENS: From the type locality: LACM-CIT 775, left maxillary with P4 broken–M1; and LACM-CIT 776, partial mandible with p3–m2.

Second Division Fauna, Mud Hills, Barstow Formation (late early Barstovian), San Bernardino County, California: F:AM 27161, partial skull with C1–P1 alveoli, P2–M2, and partial mandible with c1–p1 alveoli and p2–m3 (fig. 75A–F); F:AM 27221, left maxillary with I1 broken–M2 (P1–P2 broken); F:AM 27223, left partial ramus with i2–p1 all broken and p2–m2 (p3, m1, and m2 all broken); and F:AM 27162 and 27162A, fragmentary posterior partial skull with P4 broken–M2, mandible with i2–c1 all broken, p1–m2, and m3 alveolus, radius, partial ulna, metacarpals III, IV, and V, calcaneum, astragalus, and proximal part of metatarsals IV and V.

Barstow Fauna, Barstow Formation (early late Barstovian), San Bernardino County, California: North End: F:AM 27154, palate with I1–I2 alveoli, I3–M2, and mandible with i2–m3; F:AM 27158, left partial maxillary with P4–M2 and right partial ramus with p1 alveolus–m2 (p4 alveolus) (upper and lower jaws probably do not belong to the same individual); F:AM 27174, left ramus with c1 broken and p2 broken–m3; F:AM 67070, right partial ramus with p3–m2 all broken. Skyline Quarry: F:AM 31106, left partial ramus with c1–m2. Four ft below New Year Quarry: F:AM 61709, right and left maxillary with I1 alveolus, I2, I3–P2 alveoli, P3 broken–M2, and both rami with c1–m2 (p1 alveolus, m1–m2 both broken).

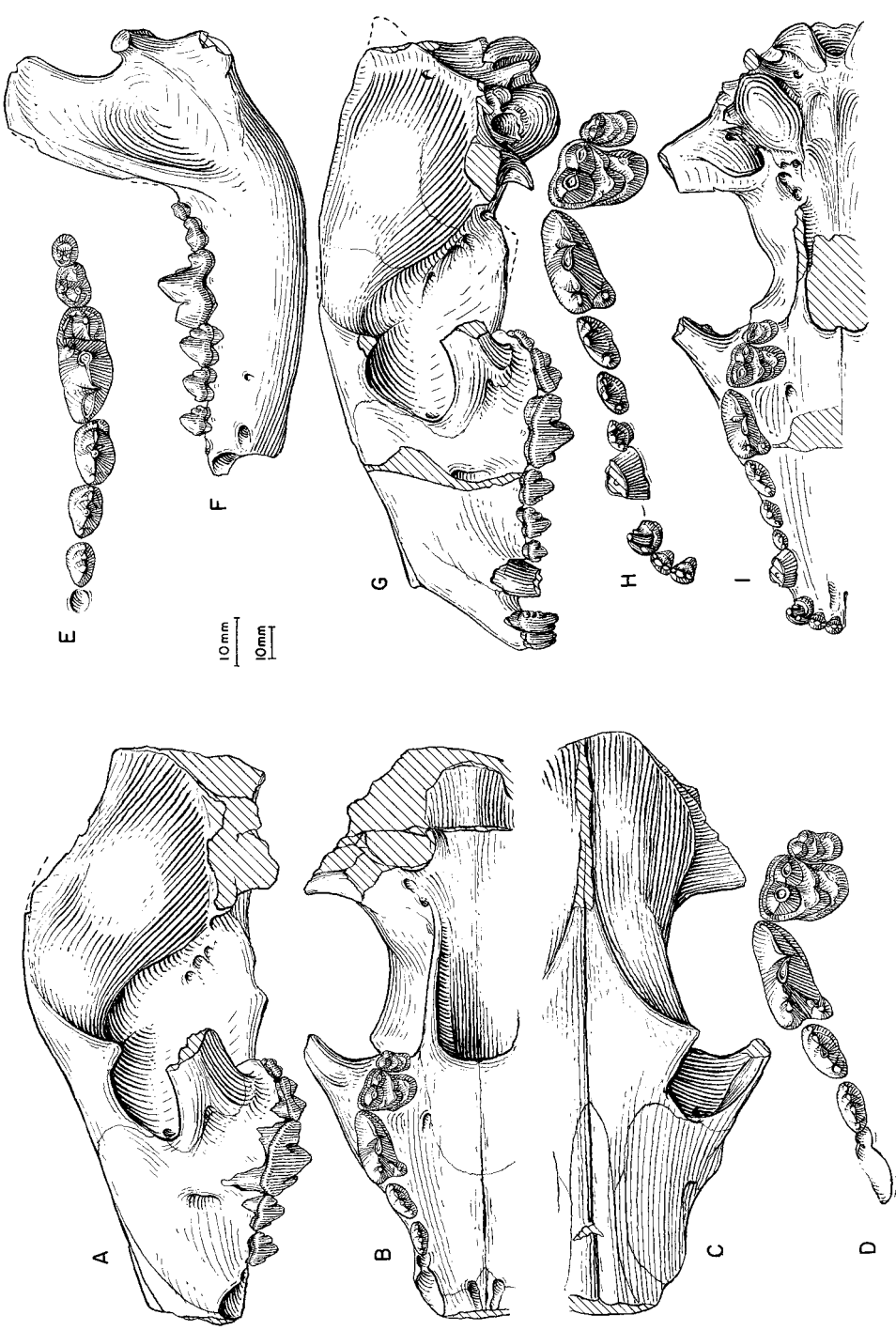

Fig. 75. *Aelurodon asthenostylus*. **A**, Lateral, **B**, ventral, and **C**, dorsal views of skull, **D**, upper teeth, **E**, lower teeth, and **F**, ramus, F:AM 27161, Second Division Barstow Bluffs, Barstow Formation (late early Barstovian), San Bernardino County, California. **G**, Lateral view of skull, **H**, upper teeth, and **I**, ventral view of skull, F:AM 27159, *Hemicyon* Stratum, Barstow Formation (early late Barstovian), San Bernardino County, California. The longer (upper) scale is for D, E, and H, and the shorter (lower) scale is for the rest.

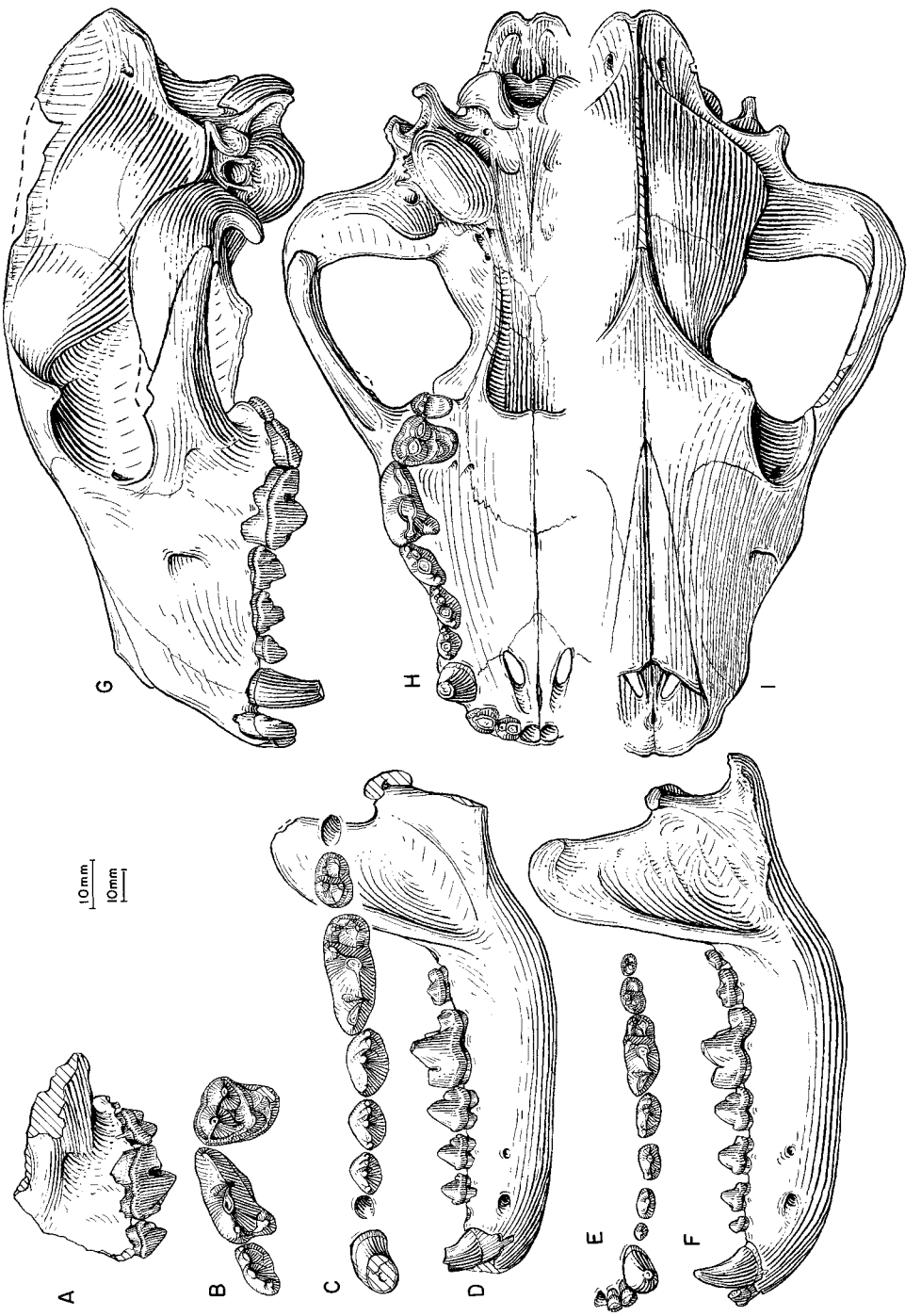

Fig. 76. *Aelurodon asthenostylus*. **A**, Lateral and **B**, enlarged occlusal views of maxillary and upper teeth, **C**, lower teeth, and **D**, ramus, F: AM 27170A, *Hemicyon* Stratum, Barstow Formation (early late Barstovian), San Bernardino County, California. **E**, Lower teeth and **F**, ramus, F:AM 28356, Horse Quarry, Pawnee Creek Formation (early late Barstovian), Weld County, Colorado. **G**, Lateral, **H**, ventral, and **I**, dorsal views of skull (crushed frontal area restored), F:AM 28351, Pawnee Buttes, Pawnee Creek Formation (late early Barstovian), Weld County, Colorado. The longer (upper) scale is for B and C, and the shorter (lower) scale is for the rest.

New Year Quarry: F:AM 67072, right partial ramus with c1–m2 (p1 alveolus). Prospect near Chert Ridge: F:AM 67063, left partial maxillary with P4–M2; F:AM 67065, right partial ramus with i1–p1 roots and p2–m2 (m2 broken and m3 alveolus). New Hope Quarry: F:AM 67068, left partial ramus with c1 broken and p2–m2; F:AM 67077, left partial ramus with i3–c1 both broken and p1 alveolus–m2 (p2, p4, and m1 all broken). Hidden Hollow Quarry: F:AM 67062, partial skull with C1–M2 (P1 and P4 both broken); F:AM 67071, right and left rami with i1–c1 (i3 broken), p1 alveolus, and p2–m3; F:AM 67074, right and left rami with c1–m3; F:AM 67075, right ramus with c1 and p4–m3; F:AM 67079, left partial ramus with i1–m1 (p1 alveolus); and F:AM 67080, palate with I2–I3, C1–P2 alveoli, and P3–M2. Leader Quarry: F:AM 67064, right and left partial maxillae with C1–M2 (P1 alveoli) and skull fragments; and F:AM 67076, right ramus with i1–i3 alveoli, c1 broken, p1 alveolus, p2 broken–m2, and m3 alveolus. First Division: F:AM 67067, right maxillary fragment with P4–M1 both broken, detached broken premolars and incisors, and left partial ramus with p3 broken–m3 (m1 broken). *Hemicyon* Stratum (some specimens are questionably referred to this quarry): F:AM 27155, anterior part of skull with I1–P1 alveoli and P2–M2; F:AM 27155A, left partial maxillary with P3–M2; F:AM 27157, anterior part of skull with I1–P1 alveoli and P2–M2; F:AM 27157A, right partial maxillary with P4–M2 (M1 broken); F:AM 27158A, left partial maxillary with P4–M1; F:AM 27159, skull with I1–M2 (fig. 75G–I); F:AM 27160, crushed partial skull with I1–P2 alveoli and P3–M2; F:AM 27163, anterior part of skull with I2 broken–M2; F:AM 27164, partial skull with C1–P2 alveoli, P3–M1 both broken, and M2 alveolus; F:AM 27165, partial skull with P1–P3 alveoli and P4–M2 (M1 broken); F:AM 27166, anterior part of skull with C1–P1 alveoli and P2 broken–M2; F:AM 27166A, crushed partial skull with P4 broken–M2; F:AM 27168, left partial maxillary with P2 broken–M2; F:AM 27169, right partial maxillary with P3–M2; F:AM 27170, left maxillary fragment with P3–M1; F:AM 27170A, left partial maxillary with P3–M1, right and left rami with c1–m2 (p1 and m3 alveoli) (fig. 76A–D); F:AM 27171, crushed partial skull with P3 alveolus and P4 broken–M2; F:AM 27172, partial skull with P2 broken, P3 alveolus, and P4–M2; F:AM 27173, right and left partial rami with c1 broken–m3; F:AM 27178, left partial ramus with m1–m3; F:AM 27181, right partial ramus with c1 broken–m2 (p2 broken) and m3 alveolus; F:AM 27182, right ramus with c1–p3, p4–m2 all broken, and m3; F:AM 27186, left partial ramus with m1–m3; F:AM 27187, left partial ramus with m1 broken–m3; F:AM 27188, left ramus with c1–m3 (p1 alveolus); F:AM 27190, right partial ramus with p1 alveolus–m3; F:AM 27191, right partial ramus with c1 broken–p1 alveolus, p2–m2, and m3 alveolus; F:AM 27192, left partial ramus with c1–m2 (p1 and m3 alveoli); F:AM 27193, left partial ramus with p1 alveolus–m2; F:AM 27194, left partial ramus with p4–m3; F:AM 27195, left partial ramus with c1–m1 (p2 alveolus); F:AM 27196, left partial maxillary with P4–M2; F:AM 27198, right partial ramus with c1 broken–m2 (p1 alveolus and p2–p3 both broken); F:AM 27199, left partial ramus with c1–m2 (p1 alveolus and p4 broken); F:AM 27200, left partial ramus with p3–m2 (m1 broken) and m3 alveolus; F:AM 27201, left partial ramus with c1–m2 (p1 and m3 alveoli); F:AM 27203, left partial ramus with c1 broken–m2 (p1 alveolus and p4–m1 both broken); F:AM 27204, right partial ramus with p2–p3 and p4–m1 both broken; F:AM 27206, left partial ramus with p3–m2; F:AM 27207, right ramal fragment with m1–m2 both erupting; F:AM 27208, left ramal fragment with p3–m2 (p4–m1 both broken); F:AM 27209, right partial ramus with c1 broken–m3 (p1 and p3 alveoli and p2 broken); F:AM 27215, left partial immature ramus with dp4 broken and c1–m1 all unerupted; F:AM 31101, partial mandible with i1–m2 (p1 alveolus) and m3 alveolus; F:AM 67069, left partial ramus with c1 alveolus and p2 broken–m3; and F:AM 67084, posterior part of skull. Horizon below Split Ridge: F:AM 67073, right and left rami with c1–m3 (p3 and p4 both broken).

Pawnee Creek Formation (late early Barstovian), Weld County, Colorado: Pawnee Buttes: AMNH 9359, immature anterior part of skull with dI3, dC1, dP3–dP4, erupting

I1–I2, P1, and erupting P4. Two mi west of Quarry: F:AM 28351, skull with I1 alveolus–M2 (fig. 76G–I). Davis Ranch, first canyon east of the Kiota Road: F:AM 67323, right partial ramus with c1, p1–p3 alveoli, p4–m2 and m3 alveolus. Hereford, middle horizon: F:AM 28301, right and left rami with c1 broken, p1, p2 broken, p4–m2, and m3 alveolus. No locality data: F:AM 28310, right partial maxillary with P3 broken–M2; F:AM 28312, left maxillary fragment with broken M1; F:AM 28312A, right partial maxillary with P4–M2; and F:AM 70800, right isolated M1.

Pawnee Creek Formation (early late Barstovian), Weld County, Colorado: Horse Quarry: F:AM 28309, left maxillary with I1–I2 alveoli, I3 broken, and C1 alveolus–M1 (P2–P3 broken and M2 alveolus); F:AM 28311, right ramus with i1–i3 alveoli, c1, p2–m1, and m2–m3 alveoli; F:AM 28313 and 28313A, left partial maxillary with P2–P3 alveoli, P4, and M1–M2 both broken, and right metacarpal II; F:AM 28329, right broken m1; F:AM 28354, left partial ramus with c1 and p2–m1; F:AM 28355, right isolated M2, mandible with i1–m2 and m3 alveolus, both femora, left tibia and fibula, both calcanea and astragali, left metatarsals II, IV, and V, and right metatarsals III and IV, vertebrae, and ribs; F:AM 28356, mandible with i1 alveolus–m3 (fig. 76E, F) and associated limb elements of more than one individual including, left humerus, two left radii, left ulna with distal end missing, and left metacarpals III, IV, and V; F:AM 28357, left partial maxillary with M1–M2; and F:AM 107720, posterior part of skull.

Surprise Quarry, Hay Springs Creek Drainage, Sand Canyon Formation (early Barstovian), Dawes County, Nebraska: F:AM 25417, left partial maxillary with P4–M2.

Driftwood Creek, Ogallala Group (early late Barstovian), Hitchcock County, Nebraska: AMNH 96687, left partial ramus with i2–p1 alveoli, p3–p4 both broken, m1 alveolus, m2, and m3 alveolus.

DISTRIBUTION: Early Barstovian of Nebraska, Colorado, Nevada, and California; and early late Barstovian of Nebraska, Colorado, and California.

EMENDED DIAGNOSIS: As distinguished from *Tomarctus*, derived characters of *Aelurodon asthenostylus* that are shared with advanced species of *Aelurodon* include sagittal crest high, bulla enlarged, mastoid process enlarged, P4 protocone reduced, P4 parastyle strong, M1 and M2 smaller relative to carnassial, M1 lingual cingulum reduced anteriorly, m1 talonid narrowed, m2 reduced, and m2 metaconid low relative to protoconid. *A. asthenostylus*, on the other hand, is primitive relative to the derived species of *Aelurodon* in its smaller size (except *A. stirtoni*), paroccipital process less elongated, I3 less enlarged, premolars less massive and lacking distinct anterior cingular cusps, and M1 with large metaconule. In addition, *A. asthenostylus* lacks the synapomorphy for the *A. mcgrewi–stirtoni* clade, that is, extremely reduced M2 and m2. Compared to the *A. ferox–taxoides* clade, *A. asthenostylus* is primitive in its less broadened contact of premaxillary and frontal, lower sagittal crest, nuchal crest less posterodorsally produced, and I3 with two lateral accessory cusplets only. An autapomorphy for *A. asthenostylus* is its prominently broadened palate.

DESCRIPTION AND COMPARISON: Large samples of skulls and jaws from the Barstovian of California and Colorado greatly increase our knowledge of this species, originally named from Tonopah, Nevada. Unlike *Tomarctus*, which shows only the initial developments of aelurodontine cranial proportions, the skull of *Aelurodon asthenostylus* displays many derived characteristics of the clade. The pattern of cranial proportions of *A. asthenostylus* in the ratio diagram (fig. 71) is consistent with other species of *Aelurodon*, with a relatively deep and wide zygomatic arch, broad rostrum, and reduced M2. The palate is noticeably broadened relative to that in *Tomarctus* and the *A. mcgrewi–stirtoni* clade. Contact between the premaxillary and frontal is strong, but less than that in the *A. ferox–taxoides* clade. The frontal sinus is at a stage of development similar to *Tomarctus*, in which the sinus is extended posteriorly slightly beyond the frontal-parietal suture. The sagittal crest can be as low as in *Tomarctus*, but some individuals (F:AM 67062, F:AM 28351, and probably F:AM 27161) have acquired a crest as high as those in *A.*

mcgrewi. The nuchal crest is narrow in posterior view, but not as posteriorly expanded as in the *A. ferox–taxoides* clade. The mastoid process is enlarged. The paroccipital process is strongly built, sometimes with a long free tip.

Aelurodon asthenostylus has the dental proportions of later aelurodontines with its strong premolars, large P4 parastyle, high-crowned M1 paracone, reduced M1 metaconule, and reduced size of M1–M2 and m2, characters that readily distinguish themselves from those in *Tomarctus*. The premolars, however, generally lack the strong development of accessory cusps, especially the anterior cusplets, that are better developed in more derived species of *Aelurodon*. The P4 has a more reduced protocone than in *Tomarctus*. Other tendencies toward hypercarnivory include long shearing blades for upper and lower carnassials, reduced m1 metaconid, reduced m1 entoconid relatively to the hypoconid, reduced m1 talonid, reduced m2 metaconid, and smaller m2–m3—all evolved to enhance the shearing part of dentition at the expense of the grinding part.

DISCUSSION: Most of the derived features possessed by *Aelurodon asthenostylus* are those of the traditional concept of *Aelurodon*. It appears to have gradually evolved to *A. ferox* and, if so, our division of these two forms is more out of convenience of reflecting an anagenetic rather than a cladogenetic event. On the other hand, there is a larger morphological gap between *Tomarctus brevirostris* and *A. asthenostylus*. This gap is of interest since we can observe a rapid replacement of *Tomarctus* by *Aelurodon* with a brief coexistence of these two in the Barstow and Pawnee Creek formations. Although still poorly known, several partial lower jaws from the Valley View Quarry of the Second Division Fauna are tentatively identified as *Tomarctus brevirostris* (see referred specimens under the species). Most specimens of *A. asthenostylus*, on the other hand, are from the Barstow Fauna, suggesting a replacement of *Tomarctus* by *A. asthenostylus* in the late early Barstovian of southern California. In the Pawnee Creek Formation of Colorado, however, these two taxa apparently coexisted (at least found together in Horse and Mastodon quarries, see also Discussion under *Protepicyon raki* for its distinctions from *A. asthenostylus*).

Individuals from the Pawnee Creek Formation in Colorado are in general slightly larger and more derived than those from the Barstow Formation, and they bridge the gap between the typical members of *A. asthenostylus* and *A. ferox*. The link provided by the Colorado form suggests a rather continuous transformation from *A. asthenostylus* to *A. ferox*, with the implication that the division between these taxa is somewhat arbitrary.

Aelurodon mcgrewi, new species

Figure 77C–G

Aelurodon wheelerianus (Cope, 1877): Cope, 1881a: 388 (in part); 1883: 245, fig. 11a, b (in part). Matthew and Gidley, 1904: 250, fig. 3 (in part). Cope and Matthew, 1915: pl. CXIXa, figs. 1–3 (in part). Barbour and Cook, 1917: 179, fig. 6 (in part). Colbert, 1939: 65 (in part).

Prohyaena wheelerianus (Cope): Schlosser, 1890: 25 (in part).

Strobodon stirtoni (Webb, 1969a): Evander, 1986: 28, figs. 5, 7E, 8E (in part).

Aelurodon cf. *A. wheelerianus* (Cope): Voorhies, 1990a: A118 (in part).

HOLOTYPE: AMNH 22410, partial skull with I1–I2 alveoli and I3–M2, right ramus and left partial ramus with i1–i2 alveoli and i3–m3 (p1 broken) (fig. 77E–G), complete cervical vertebrae, partial right scapula, left humerus, and postcranial fragments, south of Norden, Devil's Gulch Member, Valentine Formation (late Barstovian), Brown County, Nebraska.

ETYMOLOGY: Named for Paul O. McGrew in recognition of his many contributions to knowledge of the Neogene rocks and faunas of the Great Plains and for his study, with R. A. Stirton, of the Borophaginae.

REFERRED SPECIMENS: Crookston Bridge Member, Valentine Formation (late Barstovian), Cherry and Keyapaha counties, Nebraska (following list by Evander, 1986): Railway Quarry A (UNSM loc. Cr-12): UNSM 76620, right immature ramus with c1 erupting, p1–p4 alveoli, m1 broken, m2 alveolus, and m3 erupting (Evander, 1986: figs. 5, 7E). Railway Quarry B (UNSM loc. Cr-13): UCMP 63657, right partial maxillary with P2–M2 (Evander, 1986: fig. 8E) (fig.

77C, D). Stewart Quarry (UNSM loc. Cr-150): UNSM 1481-95: right ramus with i1–m2 (p1 alveolus) and m3 alveolus. Devil's Jump Off: F:AM 25174, left partial ramus with i3–p2 alveoli, p3–m1, m2 broken, and m3 alveolus. Ripple Quarry: F:AM 70600, left partial ramus with c1–p1 alveoli, p2–p4 all broken, and m1–m2. Schoettger Quarry: F:AM 61744, left partial ramus with p3 alveolus, and p4–m2.

Devil's Gulch Member, Valentine Formation (late Barstovian), Brown and Cherry counties, Nebraska: Three mi above the Garner Bridge on the north side of the Niobrara River: F:AM 61778, skull with I1–M2 and associated right incomplete m1 and left humerus. Fairfield Creek, North Fork: F:AM 35131, left partial ramus with p1–m1, m2 root, and m3 alveolus.

Republican River beds (late Barstovian), Ogallala Group, Red Willow County, Nebraska: AMNH 8307 (referred to *Aelurodon wheelerianus* by Cope, 1883: fig. 11a, b), anterior part of skull with I3 broken–M2, mandible with i1–m3, skull fragments, partial radius and ulnae, carpus, and cervical vertebrae.

DISTRIBUTION: Late Barstovian of Nebraska.

DIAGNOSIS: *Aelurodon mcgrewi* shares with most species of *Aelurodon* derived features that are distinct from the more primitive *A. asthenostylus*: long free tip on the paroccipital process, enlarged I3, P1–P3 and p1–p4 massive and with more distinct anterior cingular cusplets, and M1 metaconule reduced or absent. In addition, *A. mcgrewi* shares a derived character with *A. stirtoni* that is distinct from the *A. ferox–taxoides* clade: M2 metacone reduced or absent. *A. mcgrewi* is distinguishable from *A. stirtoni* in its primitive status of the following characters: larger size, higher sagittal crest, nuchal crest more posteriorly expanded, posterior border of M1 not prominently recurved, m2 not extremely shortened, and m2 metaconid present. In contrast to the *A. ferox–taxoides* clade, *A. mcgrewi* lacks derived characters of that clade: broad contact between premaxillary and frontal, extremely high sagittal crest, extremely broad palate, transversely straight upper incisor row, and I3 with three lateral accessory cusplets.

DESCRIPTION AND COMPARISON: *Aelurodon mcgrewi* is overall quite similar to *A. ferox*, especially to its earlier representatives. *A. mcgrewi* is close to *A. ferox* not only in size, but in cranial proportions, as shown in the ratio diagrams (fig. 71). However, derived features such as a reduced M2 and m2 and a broadened p4 show *A. mcgrewi* to be a member a small clade with *A. stirtoni*. The increasingly stronger premolars at the expense of the grinding part the dentition (M1–M2 and m1 talonid–m3) is a general trend within the aelurodontine clade, but in *A. mcgrewi* this is manifested in a slightly different way. Thus, its p4 is relatively more broadened (fig. 72) and its M2 has a more reduced metacone. *A. mcgrewi* has only a moderately broadened palate, a primitive character relative to *A. asthenostylus*, suggesting that the narrower palate in *A. stirtoni* may have been a character reversal.

DISCUSSION: Cope (1881a, 1883) referred a partial rostrum and mandible, AMNH 8307, from the Republican River of Nebraska to his earlier erected species *Canis wheelerianus* Cope, 1877, and changed the generic assignment of this species to *Aelurodon*. *A. wheelerianus* was based on a partial ramus lacking all the teeth from Santa Fe, New Mexico, and the poor status of preservation of the holotype became the source of considerable uncertainty surrounding its identity (see also discussion under *A. ferox*). Cope's referred specimen from Nebraska has since been illustrated repeatedly (Cope, 1883: fig. 11a, b; Matthew and Gidley, 1904: fig. 3; Cope and Matthew, 1915: pl. CXIXa, figs. 1–3; Barbour and Cook, 1917: fig. 6), and with its well-preserved teeth became the focus of attention of this species instead of its poorly preserved holotype. In this sense *A. wheelerianus* thus symbolized a small-size *Aelurodon*, in contrast to the larger *A. taxoides*, and even became the basis of a new genus *Prohyaena* proposed by Schlosser (1890: 25). Although lacking much of the posterior and dorsal parts of the skull, AMNH 8307 preserves such derived dental features as reduced M2 with a vestigial metacone, relatively widened p4, and shortened m2. These subtle features signal its position in *A. mcgrewi*, despite its general similarity to *A.*

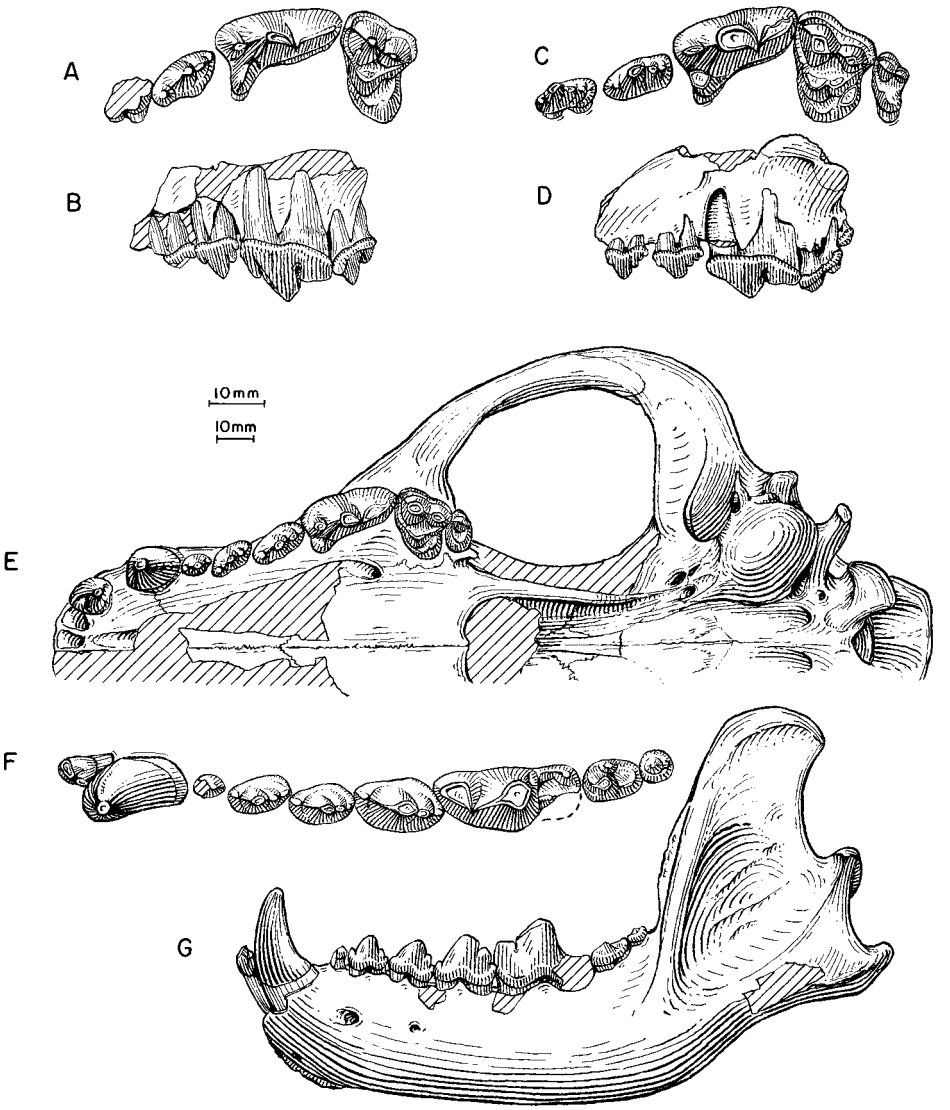

Fig. 77. **A**, Enlarged occlusal and **B**, lateral views of maxillary and upper teeth, *Aelurodon stirtoni*, UCMP 33473, holotype, Fence Line Locality, Burge Member, Valentine Formation (late late Barstovian), Cherry County, Nebraska. **C**, Enlarged occlusal and **D**, lateral views of maxillary and upper teeth, *A. mcgrewi*, UCMP 63657, Railway Quarry B, Crookston Bridge Member, Valentine Formation (late Barstovian), Cherry County, Nebraska. **E**, Ventral view of skull, **F**, lower teeth, and **G**, ramus (reversed from right side), *A. mcgrewi*, F:AM 22410, holotype, south of Norden, Devil's Gulch Member, Valentine Formation (late Barstovian), Brown County, Nebraska. The longer (upper) scale is for A, C, and F, and the shorter (lower) scale is for the rest.

ferox (*A. wheelerianus* of most past references).

Evander (1986: 28, figs. 5, 7E, 8E) referred two specimens from the Railway quarries, Crookston Bridge Member of Valentine Formation, to *Strobodon stirtoni*. His reference was mainly based on UCMP 63657, a maxillary fragment with P2–M2 (another figured specimen is UNSM 76220, a partial ramus with a broken m1). Evander's figure of this specimen (fig. 8E), however, shows a M1 with a rather unreduced metaconule and un-

shortened internal cingulum. The only dental features that suggest *A. stirtoni* appear to be its overall small size (compared to *A. ferox* from the same Railway quarries; see Evander, 1986: table 2) and its relatively small M2, which still has a distinct metacone in contrast to the loss of this cusp in *A. stirtoni*. It seems possible that the two specimens from the Railway quarries represent a primitive form of *A. mcgrewi*.

Our identification of *Aelurodon mcgrewi*, from the Devil's Gulch Member of the Valentine Formation, that gave rise to *A. stirtoni*, from the Burge Member of the Valentine Formation, helps to bridge the morphological gap between *A. stirtoni* and other species of *Aelurodon*. It also provides evidence for character reversals, such as smaller size, lower sagittal crest, and narrow palate, in *A. stirtoni*.

Aelurodon stirtoni (Webb, 1969)

Figures 77A, B, 78, 79

Strobodon stirtoni Webb, 1969a: 43, fig. 8a, b. Voorhies, 1990a: 40. Munthe, 1998: 136.

HOLOTYPE: UCMP 33473, left partial maxillary with P2 broken–M1 and M2 alveolus (fig. 77A, B) from Fence Line Locality (UCMP loc. V3331), Burge Member, Valentine Formation (late late Barstovian), Cherry County, Nebraska.

REFERRED SPECIMENS: Burge Member, Valentine Formation (late late Barstovian), Cherry County, Nebraska: Swallow Quarry (UNSM loc. Cr-16): UNSM 25789 (AMNH cast 97286), skull with I1–M2 (P1 alveolus) and left and right rami with c1–m3 (p1 alveolus) (fig. 78); F:AM 25171, right ramus with i3 alveolus–m2 (p1 alveolus) and m3 alveolus; and F:AM 25175, skull with I2 broken–M2 (P1 alveolus and P2–P3 both broken), and left ramus with c1 broken–m2 (p1–p3 alveoli and p4–m1 both broken). Burge Quarry: F:AM 25177, right partial ramus with c1, p1–p2 alveoli, p3–m2 (m1 broken), and m3 alveolus; F:AM 25178, right ramus with i1–i3 alveoli, c1, p1 alveolus–m2, and m3 alveolus (fig. 79A, B); F:AM 25179, left ramus with i1–i3 alveoli, c1 broken–p1 alveolus, p2–m2, and m3 alveolus; and F:AM 25181, partial left ramus with c1 broken, p1 alveolus, and p2–m1. Gordon Creek: F:AM 25182, left ramus with i1–i3 alveoli, c1, p1 alveolus–m1, and m2–m3 alveoli. Deep Creek: F:AM 25110, left ramus with i1 alveolus–c1, p1–p2 alveoli, p3–m2, and m3 alveolus. June Quarry: USNM 215320 (AMNH cast 129868), partial skull with I1–M2 and mandible with i1–m3, and incomplete skeleton with baculum (Munthe, 1989: figs. 5D, 6C, 7C, 9C, 11D, 12D–F, 13, 14B, 15C, 17D, 18A). Spring Canyon, 1 mi from mouth of Snake River: UNSM 25694, anterior half skull with I2–I3, C1–P1 alveoli, and P2–M2.

Pojoaque and Chama El Rito members of Tesuque Formation (late Barstovian), Santa Fe and Rio Arriba counties, New Mexico: West Santa Cruz: F:AM 27492, partial skull with I1–I2 alveoli and I3–M2 (P1 alveolus and P3 broken) and both rami with i3–c1 both broken, and p1 alveolus–m3 (m1 broken) (fig. 79C–G). Santa Cruz, Second Wash: F:AM 27367, left maxillary fragment with erupting P4; and F:AM 27474, immature palate with dC1, dP3–dP4 both broken, I2 erupting, C1 erupting, and P2–M1 all erupting. Santa Clara: F:AM 27481, crushed articulated fragments of skull with I1 root–M2 (I3, C1, and P2–M2 all broken). *Aelurodon* Wash, Rio del Oso, Abiquiu: F:AM 70501, left partial ramus with p1 (detached), p2–m2, and premaxillary fragment with C1.

DISTRIBUTION: Late late Barstovian of Nebraska and late Barstovian of New Mexico.

EMENDED DIAGNOSIS: *Aelurodon stirtoni* is distinguished from the more primitive *A. mcgrewi* in its autapomorphous features: smaller size, sagittal crest low (a reversal), nuchal crest not posteriorly expanded (reversal), extremely recurved posterior border of M1, further shortened m2, and m2 metaconid absent.

DESCRIPTION AND COMPARISON: Through collections at the AMNH, UNSM, and USNM, *Aelurodon stirtoni* is now much better known than when it was first described more than 25 years ago. Three nearly complete skulls and several well-preserved rami are available. All northern Great Plains specimens are from the Burge Member of the Valentine Formation and, consistent with this short interval, the sample is rather uniform in size and morphology.

The overall size of *Aelurodon stirtoni* is

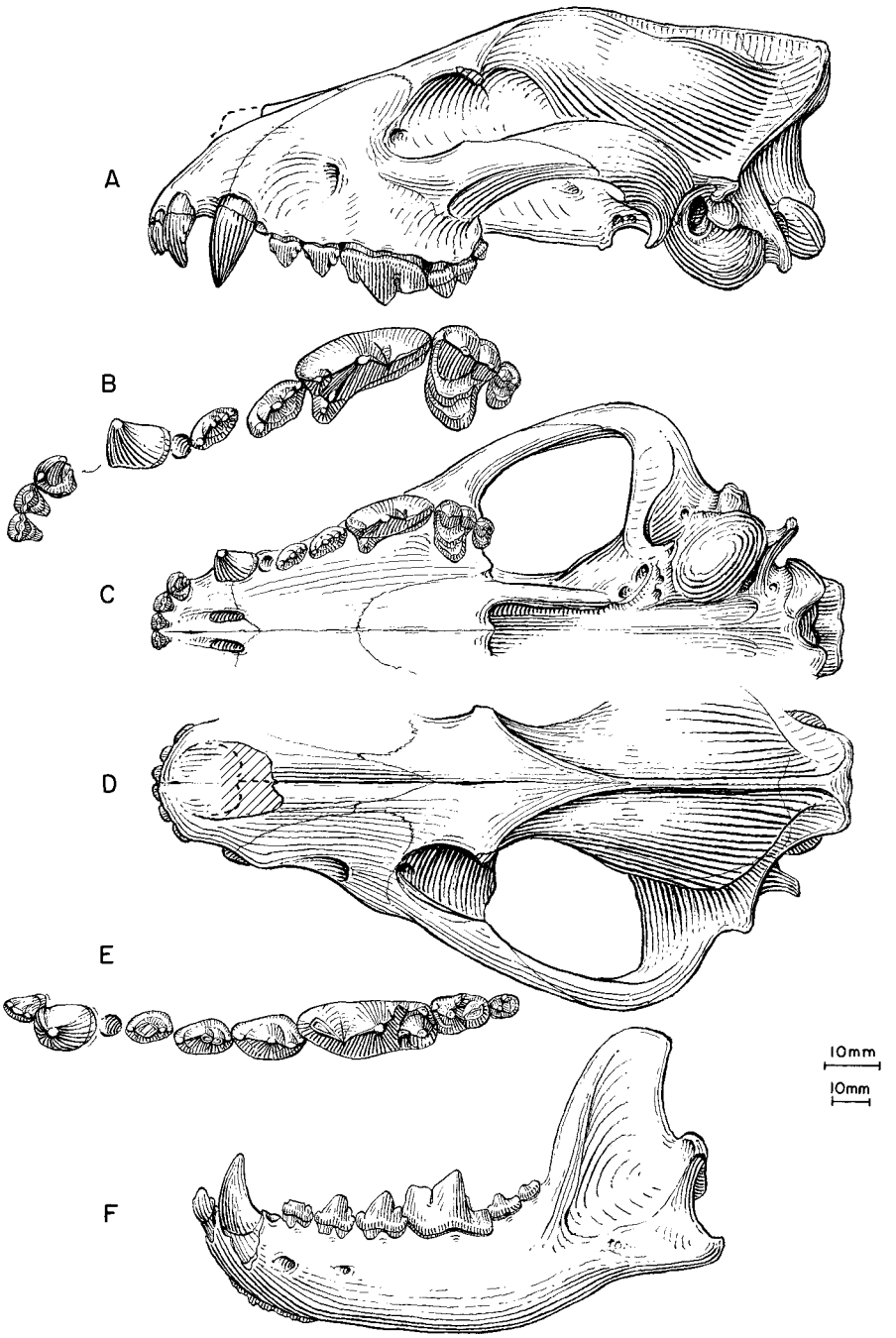

Fig. 78. *Aelurodon stirtoni*. **A**, Lateral, **B**, enlarged occlusal, **C**, ventral, and **D**, dorsal views of skull (zygomatic arch reversed from right side) and upper teeth (M2 reversed from right side), **E**, lower teeth and **F**, ramus (m3 reversed from right side), UNSM 25789, Swallow Quarry, Burge Member, Valentine Formation (late late Barstovian), Cherry County, Nebraska. The longer (upper) scale is for B and E, and the shorter (lower) scale is for the rest.

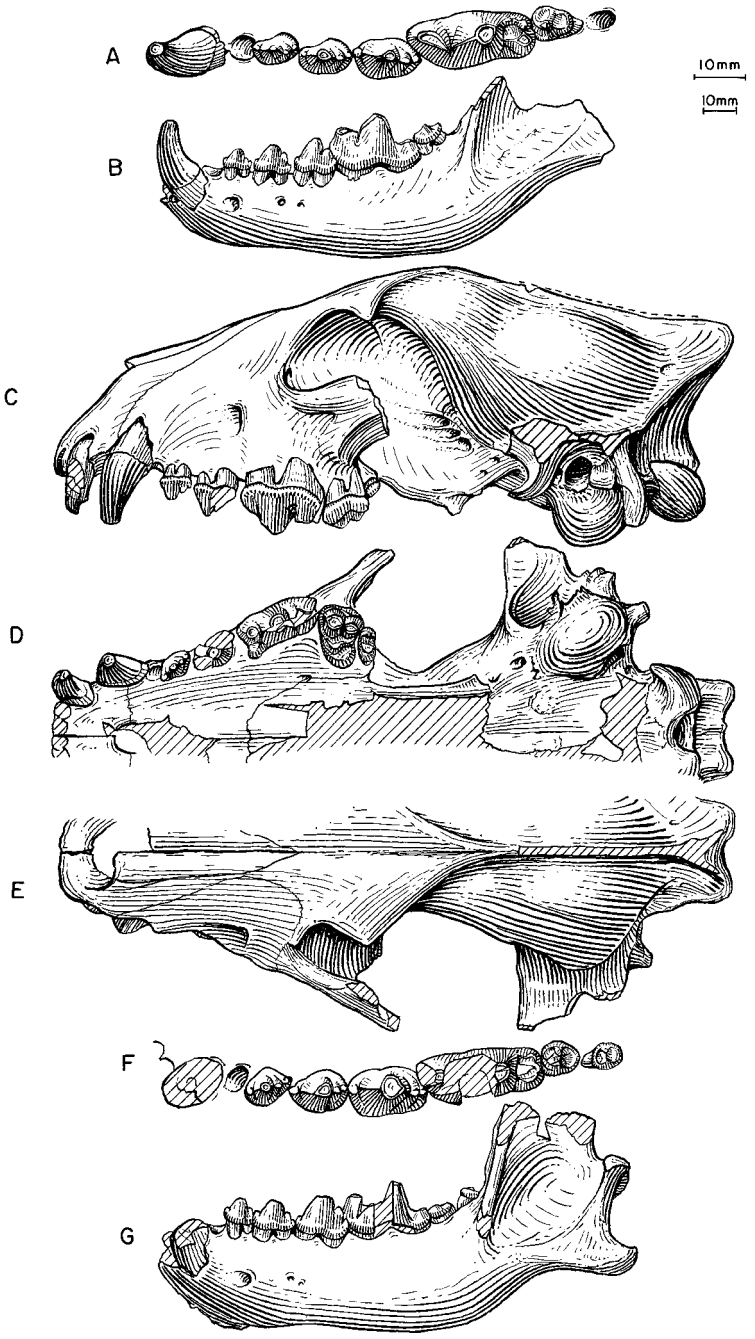

Fig. 79. *Aelurodon stirtoni*. **A**, Lower teeth and **B**, ramus (reversed from right side), F:AM 25178, Burge Quarry, Burge Member, Valentine Formation (late late Barstovian), Cherry County, Nebraska. **C**, Lateral, **D**, ventral, and **E**, dorsal views of skull (reversed from right side), **F**, lower teeth, and **G**, ramus (reversed from right side), F:AM 27492, West Santa Cruz, Pojoaque Member, Tesuque Formation (late Barstovian), Santa Fe County, New Mexico. The longer (upper) scale is for A and F, and the shorter (lower) scale is for the rest.

significantly smaller than that of *A. mcgrewi* (which is 18% larger than the former in average basal length of skull, although dental dimensions average only 9% larger). The general skull proportions of *A. stirtoni* are not very different from *Tomarctus*: the palate is only slightly broadened, the sagittal crest is low (probably a reversal), and the nuchal crest only slightly overhangs the occipital condyle. On the other hand, the proportional patterns of the ratio diagram of the skull of *A. stirtoni* (fig. 71) are unmistakably *Aelurodon*-like, with a broad muzzle, wide and deep zygomatic arch, narrow postorbital constriction, narrow braincase, enlarged bulla, and large mastoid process.

Dentally, this species is not difficult to recognize because of the distinctive shape of M1 and very reduced M2 and m2. The P4 is relatively longer than either of the more anterior premolars (P1–P3) or the molars, as compared to those in *Aelurodon asthenostylus* and more derived *A. ferox–taxoides* clade (fig. 72). The P4 parastyle has a distinct lateral ridge from its apex leading up to the crown base in contrast to the lack of such a ridge in the latter clade. The uniquely ''twisted'' appearance of M1, i.e., a sharp curve on the posterior border, is largely due to the combination of a shortened talon, a reduced metaconule (practically lost), and a more posterolingually restricted lingual cingulum (hypocone). The M2 is extremely reduced (but still double-rooted) and simple in cusp morphology. It is dominated by a paracone, and the metacone is absent. As in *A. mcgrewi*, the p4 is broadened, mostly due to a small lingual ''lip'' at the posterolingual corner of the tooth. Hypercarnivorous tendencies on the m1 are mainly manifested in the reduced talonid relative to a long shearing blade of the trigonid. In all except two individuals (F:AM 25182 and UNSM 25789), the m1 metaconid is reduced to a mere vertical ridge, and, correspondingly, the m2 metaconid is lost except in F:AM 25179. In most individuals, the m1 entoconid is reduced to a low longitudinal ridge to allow more space for a prominent hypoconid.

Specimens from the Pojoaque Member of the Tesuque Formation, New Mexico, are almost identical to the Burge sample both in size and dental morphology. F:AM 27474 and 27481 have the characteristically twisted M1s (as for their northern Plains counterparts), whereas F:AM 27492 has a slightly more primitive looking M1 (less sharply recurved posterior border), as in *A. mcgrewi*. The latter has otherwise the typical cranial and dental morphology of the species.

DISCUSSION: The distinctly ''twisted'' M1 of a maxillary fragment from the Burge Member of the Valentine Formation led Webb (1969a) to erect a new genus *Strobodon*. The M1 is so uniquely shaped among Borophagini that, even with the fragmentary holotype, a new genus seemed warranted. We now recognize an *A. mcgrewi–stirtoni* clade that is linked to the *A. ferox–taxoides* clade. Among the limited sample of the *Aelurodon mcgrewi–stirtoni* clade, we can observe a rather distinct morphological transformation from *A. mcgrewi* in the Devil's Gulch Member to *A. stirtoni* in the Burge Member of the Valentine Formation. The geologically older *A. mcgrewi* is closer in morphology to *A. asthenostylus* and the presumed primitive ancestor of *A. ferox*. *A. mcgrewi* seems to have the right combination of primitive and derived morphology and to be the right geological age to be an ancestor of *A. stirtoni*. If this scenario is correct, we are also witnessing a size reduction in *A. stirtoni*, probably in response to the dominant, large-size *A. ferox–taxoides* clade.

The relatively brief span represented by the Devil's Gulch and Burge members implies that morphological transformation from *Aelurodon mcgrewi* to *A. stirtoni* must have happened quickly, in less than 500,000 m.y. Such a high rate of evolution is in contrast to that in the much longer lasting species pair *A. ferox* and *A. taxoides* for more than 5 million years from the early late Barstovian through the Clarendonian. Such a rapid emergence of *A. stirtoni*, in the face of what must have been formidable competition from *A. ferox*, is achieved by size reduction and exploiting more hypercarnivorous niches.

Aelurodon ferox Leidy, 1858

Figures 80, 81, 82D, E

Aelurodon ferox Leidy, 1858: 22; 1869: 68, pl. 1, figs. 13, 14. VanderHoof and Gregory, 1940: 148, fig. 4a–c. McGrew, 1944b: 79. Baskin,

1980: 1349, fig. 1A. Evander, 1986: 29, figs. 6, 7F, 8F. Munthe, 1998: 136.
Canis wheelerianus Cope, 1877: 302, pl. 69, figs. 2, 2b.
Aelurodon wheelerianus (Cope): Cope, 1881a: 388. Scott, 1890: 67. VanderHoof and Gregory, 1940: 148. Gregory, 1942: 347. McGrew, 1944b: 79. Voorhies, 1990a: A118, figs. A25–A30 (in part).
Prohyaena wheelerianus (Cope): Schlosser, 1890: 25 (in part).
Aelurodon platyrhinus Barbour and Cook, 1917: 173, figs. 1–4.
Aelurodon near *wheelerianus* (Cope): Thorpe, 1922b: 439.
Aelurodon taxoides magnus Thorpe, 1922b: 440, figs. 9–11.
Tephrocyon marshi Thorpe, 1922b: 436, fig. 6.
Euoplocyon taxoides magnus (Thorpe): Matthew, 1924: 104.
Aelurodon marshi (Thorpe): VanderHoof and Gregory, 1940: 153. Evander, 1986: 30. Munthe, 1998: 136.
Aelurodon taxoides (Hatcher, 1893): VanderHoof and Gregory, 1940: 149 (in part). Webb, 1969a: 41 (in part). Baskin, 1980: 1349 (in part).
Aelurodon francisi (Hay, 1924): Wilson, 1960: 991, fig. 4b–k (in part).
Aelurodon haydeni (Leidy, 1858): Messenger and Messenger, 1977: 98, fig. 1g–i.
Aelurodon cf. *A. ferox* (Leidy): Voorhies et al., 1987: 62.

HOLOTYPE: USNM 523 (AMNH cast 9960), right isolated P4 (fig. 80F, G), ''in the valley of the Niobrara River'' (Leidy, 1858: 22), Nebraska. VanderHoof and Gregory (1940: 143) suggested that the type locality ''is probably the exposure about 1 mi east of Fort Niobrara, near Valentine, Nebraska.'' Skinner and Johnson (1984: 244), however, found no evidence that the Hayden Expedition had collected in the vicinity of Fort Niobrara, which was not founded until April of 1880.

REFERRED SPECIMENS: Hottell Ranch Quarry (UNSM loc. Bn-10), undifferentiated bed in Ogallala Group temporally equivalent to the Cornell Dam Member of the Valentine Formation (early late Barstovian), Banner County, Nebraska: UNSM 3029-47, left ramus with i2–c1, p1 alveolus, p2–m2, and m3 alveolus.

Cornell Dam Member, Valentine Formation (early late Barstovian), Brown County, Nebraska: Norden Bridge Quarry (UNSM loc. Bw-106): F:AM 107754, left isolated incomplete m1; F:AM 107755, left maxillary fragment with C1–P1 alveoli and P2–P3; UNSM 2091-77, right maxillary with P4–M2; UNSM 2519-76, left maxillary fragment with M1–M2; UNSM 83891, partial skull with I1–M2 (Voorhies, 1990a: fig. A29); UNSM 83892, right maxillary with P4–M2; UNSM 83898, right ramus with c1–m3; UNSM 83899, right ramus with p3–m2 and m3 alveolus; UNSM 83900, right ramus with i1–i3 alveoli, c1, p1 alveolus, p2–m2, and m3 alveolus; UNSM 83901, right ramus with c1, p1 root, p2–m2; UNSM 83902, right ramus with i2–c1, p1–p2 alveoli, and p3–m1; UNSM 83903, left ramus with i1–i3 alveoli, c1, p1 alveolus, p2–m2, and m3 alveolus; UNSM 83904, right ramal fragment with m1–m2; UNSM 83905, left ramal fragment with c1–p2, p3 alveolus, and p4–m1 broken; UNSM 83906 immature left ramus with erupting c1 and p2–m2 (Voorhies, 1990a: fig. A31C, D); USNM 352360, skull with I1–M2 (Voorhies, 1990a: figs. A25–27); USNM 352361, partial left rostrum with I1–M2 (P1 alveolus) (Voorhies, 1990a: fig. A28); and USNM 352364, right ramus with i2, i3 alveolus, c1, p1 alveolus–m2, and m3 alveolus (Voorhies, 1990a: fig. A30).

Crookston Bridge Member, Valentine Formation (late Barstovian), Boyd, Cherry, and Knox counties, Nebraska: Railway Quarry A (UNSM loc. Cr-12; list following Evander, 1986): F:AM 61742, left ramus with i1–i3 alveoli, c1, p1 alveolus, p2–m2, and m3 alveolus (fig. 80D, E); F:AM 61743, left partial ramus with c1–p3 alveoli, p4–m2, and m3 alveolus; F:AM 61745, left partial maxillary with P3–M2; F:AM 67476, right metacarpal IV; UCMP 33188, left maxillary fragment with P3 and P4 broken; UNSM 1093, skull with complete dentition (holotype of *A. platyrhinus* Barbour and Cook, 1917) (fig. 80A–C); UNSM 25931, right premaxillary fragment with I3 and right isolated M1; UNSM 26020, right ramus with c1, p1 alveolus–m1, and m2–m3 alveoli (Evander, 1986: figs. 6, 7F); UNSM 76621, anterior part of skull with I1–I2 alveoli and I3–M2 (P1 and P3 alveoli) (Evander, 1986: fig. 8F); UNSM 76622, left partial ramus with c1 broken–p3; UNSM 76623, right P4 broken; UNSM 76624, left humerus; UNSM 76625,

left ulna; UNSM 76626, right ulna, distal end missing; UNSM 76627, left distal part of humerus; UNSM 76628, left proximal end of femur; UNSM 76629, left distal part of tibia; UNSM 76630, right calcaneum; UNSM 76631, right calcaneum; UNSM 76632, right metatarsal III; UNSM 76633, left metacarpal III; UNSM 76634, left metacarpal IV; UNSM 76635, right metacarpal III; and UNSM 76636, left metatarsal II. Crookston Bridge Quarry (UNSM loc. Cr-15): F:AM 107719, left isolated m2. Jamber Quarry (UNSM loc. Bd-6): UNSM 9401, left ramus with c1–m2 and m3 alveolus (referred to *Aelurodon haydeni* by Messenger and Messenger, 1977: fig. 1g–i). Four Gate Quarry (UNSM loc. Kx-148): UNSM 2126-90, nearly complete skull with I1–I2, I3–P1 alveoli, and P2–M2. Sand Lizard Quarry (UNSM loc. Kx-120): UNSM 2137-75, left ramus with i1–i3 alveoli and c1–m3 (p1 alveolus); and UNSM 2155-95, right ramus with p3–m1 and m2 alveolus. West Valentine Quarry (UNSM loc. Cr-114): UNSM 2330-87, nearly complete skull with entire upper dentition; UNSM 2556-87, left ramus with p4–m1, m2 alveolus, and erupting m3; UNSM 2569-87, left ramus with p2–m2; and UNSM 3700-86, right ramal fragment with i1–p1 alveoli and p2–p4.

Devil's Gulch Member, Valentine Formation (late Barstovian), Brown, Cherry, and Keyapaha counties, Nebraska: Devil's Gulch below Horse Quarry: F:AM 25230, skull with I1–M2 and mandible with i1–m3, partial axis, and atlas. Devil's Gulch upper zone: F:AM 25127, left partial ramus with i2–c1 broken, p1–p4, and m1–m2 both broken. Devil's Gulch Horse Quarry: F:AM 25226, partial skull with I3–P1 alveoli and P2–M1; F:AM 25227, left partial ramus with p2–m2; F:AM 25228, left ramus with i3 broken–m3; F:AM 25229, left partial ramus with c1 and p1 alveolus–m2; F:AM 61747, left partial ramus with p2 alveolus, p3–m2, and m3 alveolus; F:AM 61748, left ramal fragment with m1 erupting and detached p4 unerupted; F:AM 67002, posterior part of skull; F:AM 67003, posterior part of skull; F:AM 67343, right maxillary fragment with P4; and F:AM 107718, right detached P4. West fork of Deep Creek: F:AM 61746, skull with I1 alveolus–M2, left ramus with c1 broken, p2 broken–m2, and m3 alveolus, and partial skeleton including the entire cervical vertebrae, five broken thoracics, most lumbars, partial left and right scapulae, left humerus, left radius, left ulna, right pelvis, metacarpal III, both metacarpals V, carpals, tarsals, calcaneum, metatarsals II, IV, and V, and phalanges, 25 ft below the Burge Member; and F:AM 70624, anterior part of skull with I1–I2, I3–C1 alveoli, and P1–M2, left ramus with i2–m2 and m3 alveolus, axis, third–fourth cervicals, broken thoracics and lumbars, left humerus, right radius, partial left radius, partial right ulna, metacarpals II and V, metatarsals III and incomplete IV, scapholunar, and two proximal phalanges, 20 ft below the Burge Member. Ten ft below the Burge Member, first canyon of Snake River: F:AM 67346, immature partial skeleton including skull with dI2, dC1, dP2–dP4, and P4–M1 unerupted, left and right rami with di2–c1, dp2–dp4, and m1 unerupted, atlas through fifth cervical vertebrae, partial manus, partial tibia, and partial pes. Steer Creek: F:AM 67344, posterior part of skull, 40 ft below Burge Member. White Cliffs on Plum Creek: F:AM 70610, left partial ramus with p3–m2. Nenzel Quarry: F:AM 70609, right partial ramus with m1–m2 and m3 alveolus. Sawyer Quarry: F:AM 54203, right ramus with c1–p1 alveoli, p2–m2 (p4 broken), and m3 alveolus; and F:AM 54204, right partial ramus with p3–m2. Meisner Quarry: F:AM 25247, crushed skull with I1–I2 alveoli and I3–M2 (P4 broken) and left ramus with c1–p3 alveoli, p4–m1, m2 broken, and m3 alveolus. First canyon west of Bailing Springs, south side of Niobrara River, South of Cody: F:AM 61749, right partial ramus with c1–p2 alveoli, p3–m2, and m3 broken. Southeast of Springview in Keyapaha County: UNSM 1222-91, left ramus with c1–p4 all broken and m1–m2.

Burge Member, Valentine Formation (late late Barstovian), Cherry and Knox counties, Nebraska: Burge Quarry: F:AM 61753, skull with I2–M2 (fig. 81); F:AM 61754, partial skull with I1–M2; F:AM 61755, partial skull with I1–I2 alveoli, I3, C1–P1 alveoli, and P2–M2; F:AM 61756, right maxillary with P1–M2; F:AM 61757, skull with I1–M2 (P1 root); F:AM 61759, left isolated M1; F:AM 61762, left ramus with c1 broken, p1 alveo-

lus–m2 (p3 broken and m3 alveolus); F:AM 61763, right ramus with i2 broken, i3–p1 alveoli, p2–m2, and m3 alveolus; F:AM 61766, left ramus with m1 and alveoli of all other teeth; F:AM 61767, left ramus with c1 broken, p1 alveolus–m2, and m3 alveolus; F:AM 61770, right ramus with i1–p1 alveoli, p2–m1, and m2–m3 alveoli; F:AM 61771, left ramus with i1–i3 alveoli and c1–m3 alveolus (fig. 82D, E); F:AM 67004, immature right maxillary fragment with P1 alveolus, dP2–dP4, and P4–M1 unerupted; F:AM 67005, immature right maxillary fragment with dP3–dP4, and M1 unerupted (this may be the same individual as F:AM 67004); UCMP 32241 (referred to *Aelurodon taxoides* by Webb, 1969a: 41), nearly complete right ramus with i1–i3 alveoli, c1–m2, and m3 alveolus; and UCMP 32558, left ramus with c1 alveolus, p2–m1 all broken, and m2–m3 alveoli. June Quarry: F:AM 61758, right partial maxillary with P2–M2; F:AM 61775, right isolated m1; and F:AM 107717, right partial ramus with i1–i3 alveoli, c1 broken, p1 alveolus–p4, and m1 broken. East fork of Deep Creek: F:AM 61772, left ramus with i2–m1, m2 broken, and m3 alveolus. White Point Quarry: F:AM 61776, left partial ramus with i1–i3 alveoli, c1, and p1 alveolus–p4. Lucht Quarry: F:AM 61774, left partial ramus with m1 broken–m2 and m3 alveolus. Midway Quarry: F:AM 61768, right partial ramus with c1–p1 alveolus, p2–m2, and m3 alveolus; F:AM 61765, right and left rami with i1–i3 alveoli and c1–m3 alveolus; and F:AM 61773, left ramus with c1–p1 alveoli, p2–m1, m2 broken, and m3 alveolus. East fork of Fairfield Creek: F:AM 61761, right and left rami with i1–m2 and m3 alveolus, broken atlas, partial fibula, and phalanges; and F:AM 107716, right ramal fragment with m2 and m3 alveolus. Gordon Creek Quarry (UNSM loc. Cr-14): F:AM 61764, right partial ramus with i1 and p2 unerupted, dp3–dp4 both broken, and m1–m2 both erupting; and UNSM 25932, left ramus with c1, p1–p2 alveoli, p3 broken–m1, and m2–m3 alveoli. Meisner Slide: F:AM 61777, left partial ramus with i1–i3 alveoli, c1 broken, p1 alveolus–p4, and m1 broken. Talus in connection with Moore Creek Quarry No. 1: F:AM 25128, right partial ramus with m1 broken–m2. Bug Prospect (UNSM loc. Kx-119): UNSM 46815, partial skull and complete mandible with I1–M2 and i1–m2.

Valentine Formation, Nebraska: Tihen Locality (UCMP loc. 6259), Keyapaha County: UCMP 64726, isolated right P1–M2 (P4 broken), left and right rami with c1, p1 alveolus–m2, and m3 alveolus. A few mi east of mouth of Antelope Creek, Cherry County: YPM 10057 (holotype for *Aelurodon taxoides magnus* Thorpe, 1922b: 440, figs. 9–11), partial right maxillary-premaxillary with I1–C1 alveoli and P1 broken–M1, both rami with c1–m3. West of mouth of Minnechaduza Creek, Cherry County: YPM 12787 (holotype of *Tephrocyon marshi* Thorpe, 1922b: 436, fig. 6), left ramus with p2–p3, p4 alveolus, and m1–m2. ''Niobrara River'': YPM 10060 (referred to *Aelurodon* near *wheelerianus* by Thorpe, 1922b: 439), partial maxillary with P4–M1, left ramus with c1, p1 alveolus, p2–p3, and part of m1–m2.

Hardin Bridge, Niobrara River, Ogallala Group, temporally equivalent to the Burge Member of the Valentine Formation (late Barstovian), Sheridan County, Nebraska: F:AM 70604, right ramus with i3 alveolus, c1, p1 alveolus–m2, and m3 alveolus.

From 2.9 mi east of White Clay, along the Nebraska–South Dakota state line, Ogallala Group, temporally equivalent to the upper part of the Valentine Formation (late Barstovian), Nebraska and South Dakota: F:AM 61750, crushed fragmentary skull with both partial maxillae with P4–M2 and broken detached teeth, and both rami with c1 broken–m3 (p1–p3 broken), 14 mi north of Nebraska–South Dakota state line; F:AM 61751, right and left partial rami with c1–m3 (p1 alveolus), south side of the Nebraska–South Dakota state line; and F:AM 61752, left partial maxillary with P4–M2.

Hazard Homestead Locality (UNSM Hk-104), Driftwood Creek, Republic River, Ogallala Formation (late Barstovian, temporally equivalent to Crookston Bridge Member of Valentine Formation), Hitchcock County, Nebraska: UNSM 8539, right maxillary fragment with P3–p4 broken; UNSM 91072, left premaxillary-maxillary with I1–P1 alveoli, P2, P3 alveolus, and P4–M2; UNSM 91073, fragmentary skull with P3–M2; UNSM 91074, right maxillary with P3–M2 (P3–M1 all broken); UNSM 91076, par-

tial anterior skull with I1–P1 alveoli and P3–M2; UNSM 91077, left ramus with i1–i3 alveoli, c1, p1 alveolus, and p2–m2 broken; UNSM 2015-90, left m1; UNSM 1000-89, right ramus with p2–m1; and UNSM 1255-91, partial mandible with i2, c1–m1, and m2–m3 alveoli.

Ogallala Group (late Barstovian), Knox County, Nebraska: Spatz Quarry (UNSM Kx-103): UNSM 26126, partial left and right rami with p2–m2. 1.1 mi west of Miller Creek on Devil's Nest Road (UNSM loc. Kx-116): UNSM 8538, left ramus with c1–m2 and m3 alveolus.

Niobrara River, NE¼ of SE of sect. 20, T29N, R45W, ?Valentine Formation (?late Barstovian), Sheridan County, Nebraska: F:AM 61779, isolated right I2, broken right P4, and isolated left p4–m2.

Cold Spring Fauna, Fleming Formation (early late Barstovian), San Jacinto and Polk counties, Texas (referred to *Aelurodon francisi* by Wilson, 1960: 991): TMM-BEG 31191-9 (AMNH cast 89630), left ramal fragment with c1–p1 broken and p2–p3 (Wilson, 1960: fig. 4b, c); TMM-TAMU 2634B (AMNH cast 89630), partial left ramus with p4–m2 (m1 broken); TMM-BEG 31191-23 (AMNH cast 89624), right partial maxillary with P4–M1 (Wilson, 1960: fig. 4d, e), Site 2; TMM-BEG 31191-30 (AMNH cast 89617), left isolated P4 (Wilson, 1960: fig. 4f, g) and left isolated P3, Site 2; and TMM-BEG 31183-72 (AMNH cast 89620), isolated I1, I2, and I3 (Wilson, 1960: fig. 4h–k), and right maxillary fragment with P4 alveolus and M1, Site 2.

Santa Cruz area, Pojoaque Member of Tesuque Formation (late Barstovian), Rio Arriba and Santa Fe counties, New Mexico: F:AM 27340A, right and left rami with i3–m3, partial right scapula, both humeri (crushed), partial left and right ulnae, both radii, partial left hand with carpals, metacarpals I, IV, and V, proximal through distal phalanges, partial left and right femuri, partial left and right tibia, partial left and right feet with calcaneum, astragalus, tarsals, metatarsals I–V, and proximal through distal phalanges, between Second and Third washes; F:AM 27341, fragmentary skull with I1–P3 alveoli and P4–M2 all broken, Red Sand; F:AM 27343, left ramus with i1–p1 alveoli and roots, p2–m1 all broken, and m2–m3, Second District; F:AM 27345, partial crushed skull with C1 broken–M2 (P1 alveolus and P3 broken); F:AM 27346, skull with I1–I3 alveoli and C1–M2 (P3 and M2 broken), and mandible with c1–m3 (p1 alveolus), Red Sand; F:AM 27347, crushed posterior part of skull with M1–M2 and detached maxillary fragments with C1 alveolus and P1 broken–P4, Red Layer, ?Second Wash; F:AM 27349, right and left rami with i1–i2 alveoli, i3–m2, and m3 alveolus, Third Wash; F:AM 27350, immature right and left maxillary fragments with dP4 and P3–M1 unerupted, both rami with di3, dp3–dp4, p1, and unerupted p4–m2; F:AM 27351A, edentulous left ramus with all alveoli; F:AM 27351B, left partial ramus with p3–m1 all broken; F:AM 27356, immature skull with dI2 broken–dP4 and unerupted P4–M1, and mandible with di3–dp4 and unerupted p4–m1; F:AM 27357, crushed partial skull with I1–P1 alveoli, P2, and P4 broken–M2, and left partial ramus with i1–p1 alveoli, p2–p4, and m1–m3 alveoli, Rio Grande Slope; F:AM 27358, partial mandible with c1–m2 and m3 unerupted, between First and Second washes; F:AM 27360, partial palate with I1–M1 (M2 broken); F:AM 27479, mandible with i1–m2 and m3 alveolus, isolated upper canine, atlas, caudal vertebrae, both scapulae, left and partial right humeri, both ulnae, both radii, carpals, metacarpals I–V, pelvis, both femora, both tibiae, both calcaneum, astragalus, tarsals, metatarsals I, incomplete II, III–V, phalanges, and fragments, Rio Grande Slope; F:AM 27491, broken maxillary fragments and teeth including I3–C1 and P2–M2 all broken, ''green,'' east of Red Layer; F:AM 61722, left partial maxillary with P4–M1 both broken and M2, Second Wash; F:AM 61723, right ramus with i1 alveolus–m2 (p2–p4 broken) and m3 alveolus, two partial thoracics, two lumbars, seven caudals, partial left and right scapulae, left and partial right humeri, pelvis, partial baculum, right femur, patella, right tibia, nearly complete right foot with calcaneum, astragalus, tarsals, metatarsals I–V, and proximal, middle, and distal phalanges, Santa Cruz Grant, 100 yd west of survey stake; F:AM 61733, left partial ramus with p2 broken–m2 and m3 alveolus, First Wash; F:AM 61734, left ramal fragment with p4 broken–

m1, head of First Wash; and F:AM 107708, left partial maxillary with P4 broken–M2, Third Wash.

Pojoaque Bluffs area, Pojoaque Member of Tesuque Formation (late Barstovian), Rio Arriba and Santa Fe counties, New Mexico: AMNH 8309, left partial maxillary with P2 alveolus and P3–M2 all broken; F:AM 27351, right partial ramus with m1–m2 both broken, Pojoaque, right side of Santa Fe Road, 2 mi from Tesuque; F:AM 27351C, right and left partial rami with c1 broken and p3–m2 all broken, lower Pojoaque Bluffs; F:AM 27490, skull with I1–I3 alveoli and C1–M2 (P4 broken), south Pojoaque Bluffs; F:AM 61721, right and left partial maxillae with P3–M2 and detached broken C1, southwest Pojoaque Bluffs; F:AM 61724, right ramus with i2–m3 (m1 broken), southwest Pojoaque Bluffs; F:AM 61725, left partial ramus with p2–m2 all broken, central Pojoaque Bluffs; F:AM 61729, left ramus with all teeth represented by alveoli or broken, south Pojoaque Bluffs; F:AM 61730, partial skull with I1–P1 alveoli and P2–M2, West Pojoaque; F:AM 61736, fragmentary skull with I1–I2, I3 alveolus, and C1–M1 (P1 alveolus), southeast of Pojoaque Bluffs; F:AM 107705, right partial ramus with c1–p4 and m1 alveolus, head of the tributary of first large wash; F:AM 107706, left ramus with c1 broken, p1 alveolus, p2–m2 (p3 and m1 broken), and m3 alveolus, south Pojoaque Bluffs; and F:AM 107707, crushed partial skull with C1 and P2–M1, both partial rami with c1 and p2–m2, partial humerus, incomplete right radius and ulna, right calcaneum, metacarpals II, III, and IV, and phalanges, middle of Jacona Grant, west of Jacona Fault.

Rio del Oso–Abiquiu area, Chama el Rito Member of Tesuque Formation (late Barstovian), Rio Arriba County, New Mexico: F:AM 61719, crushed skull with I3–M2 and both rami with c1 broken–m3 (p1 alveolus), near the head of Three Sands Hills Wash; F:AM 61720, anterior part of skull with I1 alveolus, I2–C1 all broken, P1 alveolus–M1, and M2 alveolus, south fork of Three Sands Hills Wash; F:AM 61731, right immature ramal fragment with c1 and p2–p4 unerupted and m1 broken, South Ojo Caliente; F:AM 61732, right maxillary fragment with M1 broken, mandible with i1–m3, both partial humeri, left radius, and right partial femur, Chama el Rito area; F:AM 61735, left ramal fragment with m1 broken, middle Ojo Caliente; F:AM 61737, two left maxillary fragments with left P4 and M1–M2, Ojo Caliente; F:AM 67362, left immature partial ramus with dc1 broken, dp2–dp4 all broken, and p4–m1 unerupted, Ojo Caliente; and F:AM 107736, left partial ramus with m1 broken and m2–m3, Chama el Rito area.

Lower part of the Ojo Caliente Member, Tesuque Formation (late Barstovian), Rio Arriba County, New Mexico: Conical Hill Quarry: F:AM 67370, crushed partial skull with I1 alveolus, I2 broken–C1, P1 alveolus–P4, and M1–M2 both broken; F:AM 67371, right ramus with c1 broken, p1 alveolus, p2–p3 both broken, p4–m2, and m3 alveolus; and F:AM 67372, left ramus with i1–i3 alveoli, c1, p1 alveolus–m1, m2 broken, and m3 alveolus.

Jemez Creek area, undifferentiated beds in the Zia Formation (late Barstovian), Sandoval County, New Mexico: Rincon Quarry: F:AM 61726, immature skull with C1 and P2–P3 all erupting, dP4, P4 unerupted, and M1; F:AM 61727, right partial maxillary with P4 alveolus and M1–M2; and F:AM 61728, right and left rami with c1–p1 alveoli and p2–m3 (p3 broken). East fork of the Canyada de las Milpas: F:AM 107704, right ramal fragment with p2–m2 (p3 broken) and partial left ulna.

Upper part of the Pojoaque Member of the Tesuque Formation and possibly Chamita Formation (Clarendonian), Rio Arriba and Santa Fe counties, New Mexico: F:AM 27340, crushed skull with I2–I3 alveoli and C1–M2 (P1 and P3 alveoli), no locality data; F:AM 27344, right ramus with c1 broken, p1–p2 alveoli, p3 broken–m2 (m1 broken), and m3 alveolus, 1 mi upriver from San Juan Bridge; F:AM 27348, partial skull with I1–M2 and mandible with i1–m3, Chimayo; F:AM 27351D, left ramal fragment with m1–m2 both broken, Battleship Mountain; F:AM 50159, right premaxillary fragment with I1–I2 alveoli and I3, and right maxillary fragment with P4–M1 both broken, Battleship Mountain District; F:AM 67057, left ramus with c1–m3 all broken or alveoli, red layer, north Santa Clara River; and F:AM 67059,

right and left partial maxillae with P2–M2, near springs, west of San Ildefonso.

DISTRIBUTION: Late Barstovian of Nebraska, South Dakota, Texas, and New Mexico; and Clarendonian of New Mexico.

EMENDED DIAGNOSIS: *Aelurodon ferox* shares with *A. taxoides* derived characters that distinguish it from other species of *Aelurodon*: larger size; broad contact of premaxillary and frontal; strong, laterally expanded postorbital process of frontal; extremely high and thin-bladed sagittal crest and more posterodorsally produced nuchal crest; more broadened palate; incisive battery aligned in straight transverse line; I3 larger with three lateral accessory cusplets; and premolars larger and more massive. *A. ferox* lacks the following advanced features that are present in *A. taxoides*: a weak symphyseal flange on the horizontal ramus, a more reduced P4 protocone, and an m2 metaconid extremely reduced or absent.

DESCRIPTION AND COMPARISON: Abundant materials from the Frick Collection, together with those in the UNSM and USNM collections, constitute an adequate sample for evaluation of the temporal and spatial variations of this species. Except for its smaller size, the proportional patterns of the cranium of *A. ferox* are almost identical to those of *A. taxoides* (fig. 71). Particularly noteworthy in the ratio diagram are the high contrasts between a wide frontal shield and a narrow postorbital constriction and between a wide zygomatic arch and a narrow braincase. As in *A. asthenostylus*, the skull takes a front-heavy appearance with a very broad palate, robust rostrum, and wide open external and internal nares, in contrast to the relatively slender construction of its posterior half of the skull. The forehead in *A. ferox* is also broadened, partly due to the laterally expanded postorbital process of frontal. Specimens with dissected frontals (F:AM 25230 and 61746) reveal essentially the same degree of complexity in frontal sinus as those in *Tomarctus brevirostris*. The multichambered sinus extends into the postorbital process but does not expand much beyond the frontal-parietal suture posteriorly, in contrast to the more elaborate sinus in the *Epicyon–Borophagus* clade. This enlargement of the supraorbital area, coupled with a deep zygomatic arch, results in a relatively small orbit. Beginning in *A. ferox*, the sagittal crest is extremely high and forms a thin blade with a relatively straight dorsal edge. The posterior expansion of the nuchal crest overhangs the occipital condyle by more than 20 mm. Basicranially, *A. ferox* has an enlarged mastoid process and an elongated paroccipital process with a long free tip, characteristic of the aelurodontine clade.

Dentally, *A. ferox* continues the tendency toward a larger and more complex I3—three lateral accessory cusps are common in this species, in contrast to two or fewer in more primitive taxa. The premolars are strong relative to the molars, a tendency that began in *A. asthenostylus*, and there is a slight tendency for the anterior premolars to become disproportionately larger than in *A. asthenostylus* (fig. 72). These robust premolars also have more distinct accessory and cingular cusplets. More noticeable is the addition of a small anterior cingular cusp in all premolars, which is shared by the *A. mcgrewi–stirtoni* clade but is generally absent in *A. asthenostylus*. As in the more primitive species of *Aelurodon*, the P4 protocone is rather reduced. However, most individuals still retain a small cuspidate protocone rather than the almost complete absence of a protocone as in *A. taxoides*. The M1 continues the trend toward increased crown height of the paracone relative to the talon, as well as a reduced metaconule and internal cingulum. The M2 is small, as in *A. asthenostylus*, but not as strongly reduced as in *A. stirtoni*.

Although still retaining the fundamentally bicuspid talonid, the lower carnassial is increasingly hypercarnivorous in its long trigonid blade vs. reduced metaconid, short and narrowed talonid, and lower, anteriorly restricted entoconid (as contrasted to a higher and larger hypoconid). All these features vary to a greater or lesser extent within the presently defined hypodigm, which encompasses a span of approximately 3 m.y. in the late Barstovian. However, the apparent general tendency is that geologically younger individuals have a greater degree of development of these features. The m2 still has a distinct metaconid, in contrast to its near loss in *A. taxoides*.

DISCUSSION: The single isolated P4 of USNM 523, the genoholotype of *Aelurodon*

ferox, has been the source of frustration for generations of paleontologists, with the question of the identity of *Aelurodon* being generally at issue (see Baskin, 1980, for a recent review). Such uncertainty about the holotype may have been responsible for the general reluctance of most authors to refer additional materials to this species (except Evander, 1986). On the other hand, the status of Cope's (1877) *Aelurodon wheelerianus* is equally uncertain. The holotype from the ''Santa Fe marls'' is a partial ramus with all cheekteeth broken near the base and may properly belong to the category of nomen vanum (sensu Chorn and Whetstone, 1978; Mones, 1989). However, the subsequent reference (Cope, 1883: 245, fig. 11a, b) to *A. wheelerianus* of a partial palate and nearly complete mandible (AMNH 8307, presently referred to *A. mcgrewi*; see further discussion under this species) from Red Willow County, Nebraska, helped to perpetuate the application of this name for the small-size *Aelurodon* in the Valentine Formation (e.g., Voorhies, 1990a, 1990b).

Despite the lack of a clear concept of the type species, the name *Aelurodon* has been in such wide usage that even authors who regarded the genoholotype as specifically indeterminate (VanderHoof and Gregory, 1940; McGrew, 1944b) were unwilling to discard *A. ferox*, just to be able to continue the use of the generic name. Recently, Baskin (1980) demonstrated that even the meager USNM 523 preserves the highly diagnostic feature in which the P4 protocone lacks a connection to the parastyle, and is thus distinct from *Epicyon* (McGrew's ''*A.*'' *saevus* species group), contrary to Richey's (1979) interpretation of USNM 523. In light of our phylogenetic framework, Baskin's diagnosis remains a valid characterization of these large hyenalike borophagines. Thus, even though the lack of a protocone to parastyle connection on P4 is a primitive condition in *Aelurodon*, this feature, coupled with its large size and the bulbous shape of the parastyle (in contrast to the often triangular parastyle in *Epicyon*), is sufficient to permit a reasonable conclusion that the genoholotype is very close to, if not synonymous with, *A. platyrhinus* (Evander, 1986) or *A. taxoides* (Voorhies, 1990a).

Questions still remain, however, with regard to its specific identity. Within the present hypodigm, based on large series of well-preserved materials, the size of USNM 523 falls within the two most derived species of *Aelurodon*: ''*platyrhinus*'' and *taxoides*. The size of P4 in both of these species overlap extensively, and USNM 523 falls in the middle of the range of overlap (fig. 83). Our specific assignments of individual specimens are largely based on stratigraphic relationships (see below). Therefore, our decision to retain *A. ferox* as distinct from *A. taxoides* continues to be somewhat arbitrary, and is motivated by the desire to maintain generic stability. In this, we are in partial agreement with VanderHoof and Gregory (1940), who voiced the suspicion that *A. ferox*, *A. platyrhinus*, and *A. taxoides* are synonymous, but they nevertheless decided to retain *A. ferox* as a distinct species.

As we cannot recognize any autapomorphic features for *A. ferox*, and we can observe that larger size and other derived features for *A. taxoides* are acquired through geologically successively younger individuals in the northern Great Plains, it seems possible that the latter gradually evolved from *A. ferox* anagenetically. Such a succession can also be observed in parallel in other parts of North America. In fact, there seems to be no natural break in the morphology to mark the boundary of the *ferox–taxoides* species pair (fig. 84), and fragmentary specimens were assigned to one species or another based mainly on the association of fauna (i.e., Mammal Age) rather than morphology. As such, our presentation of the hypodigm assumes a sense of chronospecies for these two taxa. If this was indeed the case, our division of these two species, mostly along the Barstovian–Clarendonian boundary (sensu Tedford et al., 1987), would be somewhat arbitrary and affected by the controversy of the placement of the boundary in Nebraska (see Voorhies, 1990a, 1990b). An exception to this theme involves a few specimens from Battleship Mountain and San Ildefonso sites (Clarendonian) of New Mexico. These specimens come from high in the Pojoaque Member of the Tesuque Formation or possibly from the Chamita Formation. These localities and levels produce taxa of Clarendonian age,

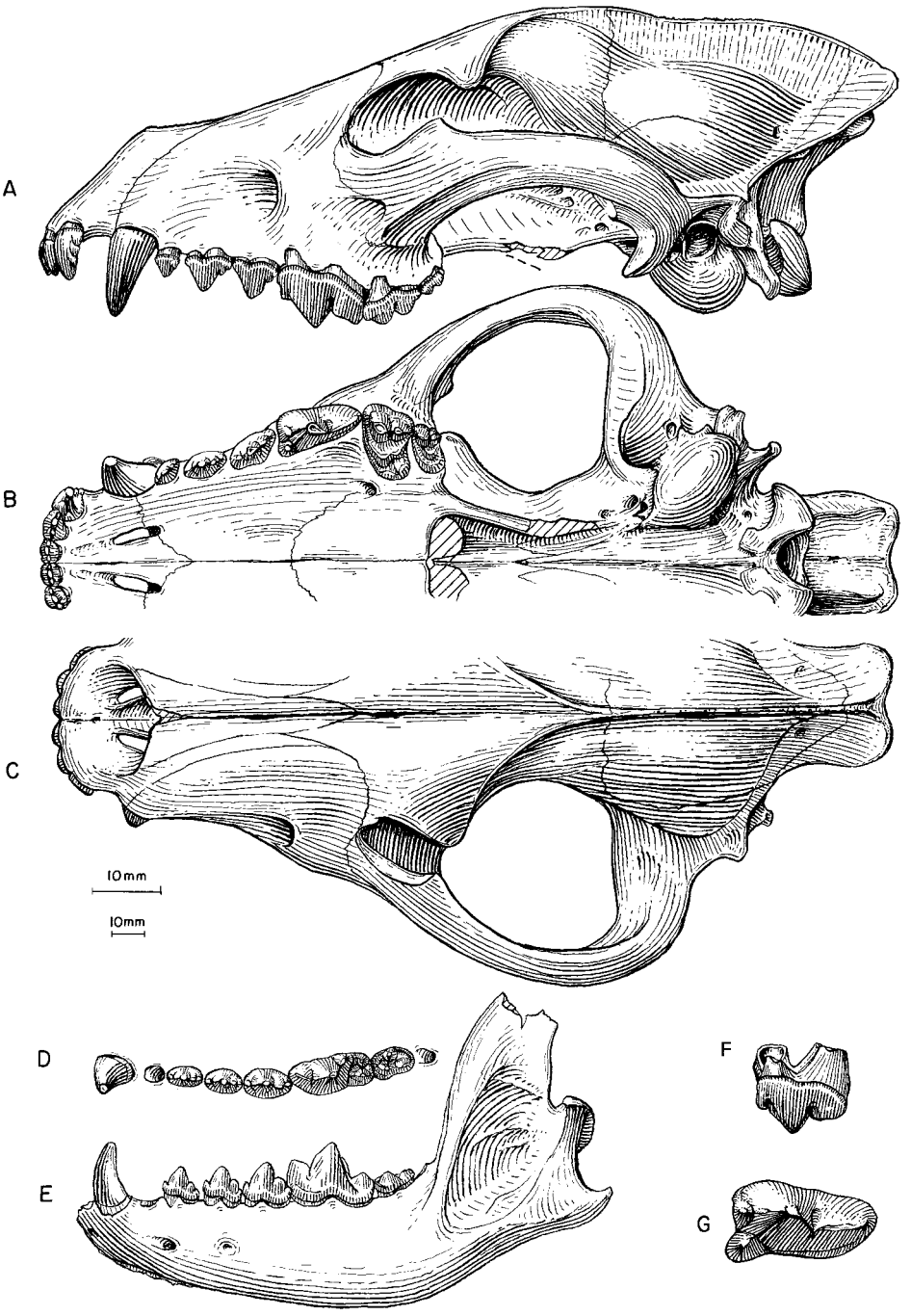

Fig. 80. *Aelurodon ferox*. **A**, Lateral, **B**, ventral, and **C**, dorsal views of skull, UNSM 1093 (holotype of *A. platyrhinus*), Railway Quarry A, Crookston Bridge Member, Valentine Formation (late Barstovian), Cherry County, Nebraska. **D**, Lower teeth and **E**, ramus, F:AM 61742, Railway Quarry A. **F**, Lateral and **G**, enlarged occlusal views of P4 (reversed from right side), USNM 523, holotype, ''valley of the Niobrara River,'' Nebraska. The longer (upper) scale is for G, and the shorter (lower) scale is for the rest.

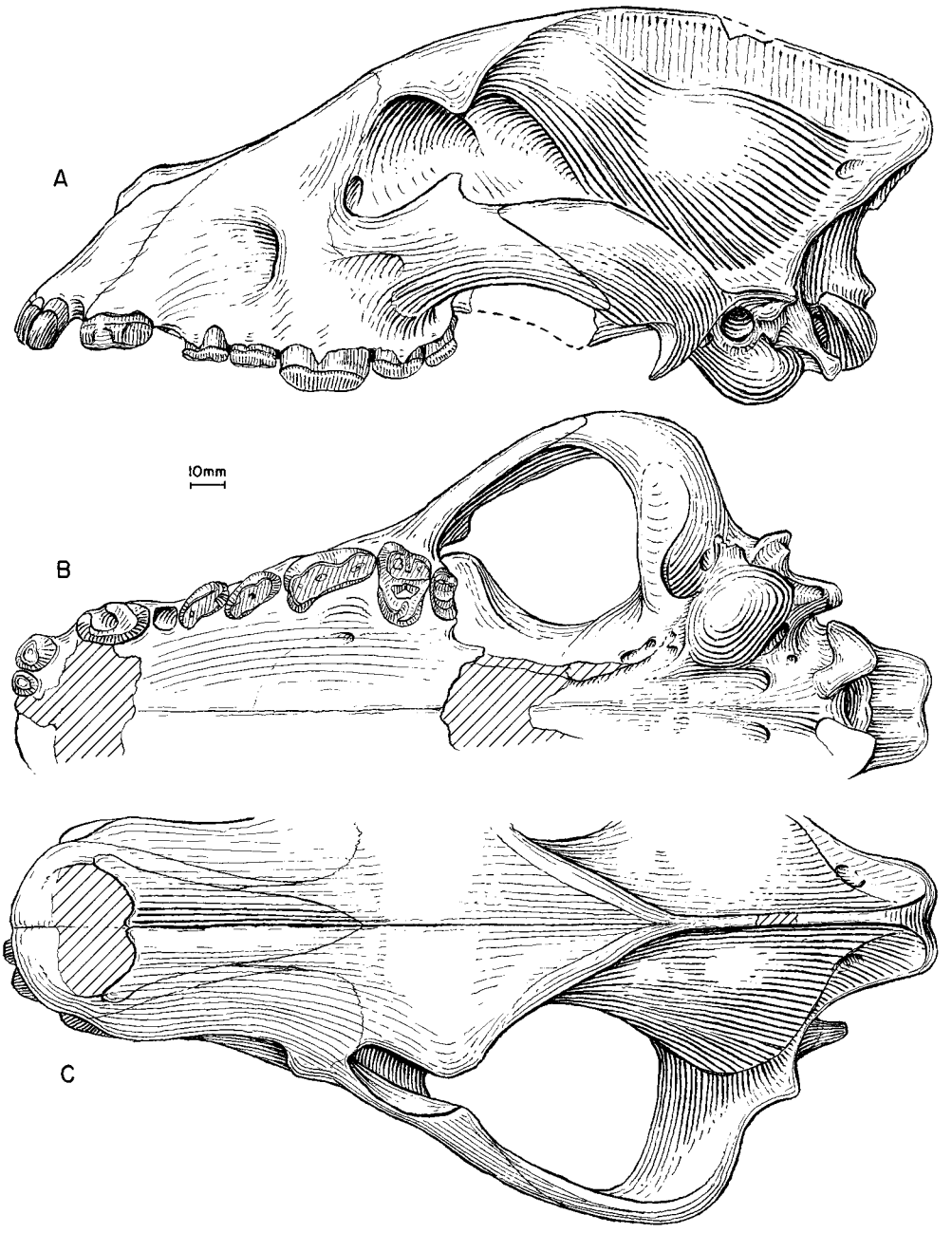

Fig. 81. *Aelurodon ferox*. **A**, Lateral, **B**, ventral, and **C**, dorsal views of skull, F:AM 61753, Burge Quarry, Burge Member, Valentine Formation (late late Barstovian), Cherry County, Nebraska.

but lack of precise biostratigraphy lends some uncertainty to the age of individual specimens. Individuals from these localities are comparable in size to *A. ferox* and are markedly smaller than *A. taxoides* from other Clarendonian localities.

The resulting division of the two morphospecies represents approximately the

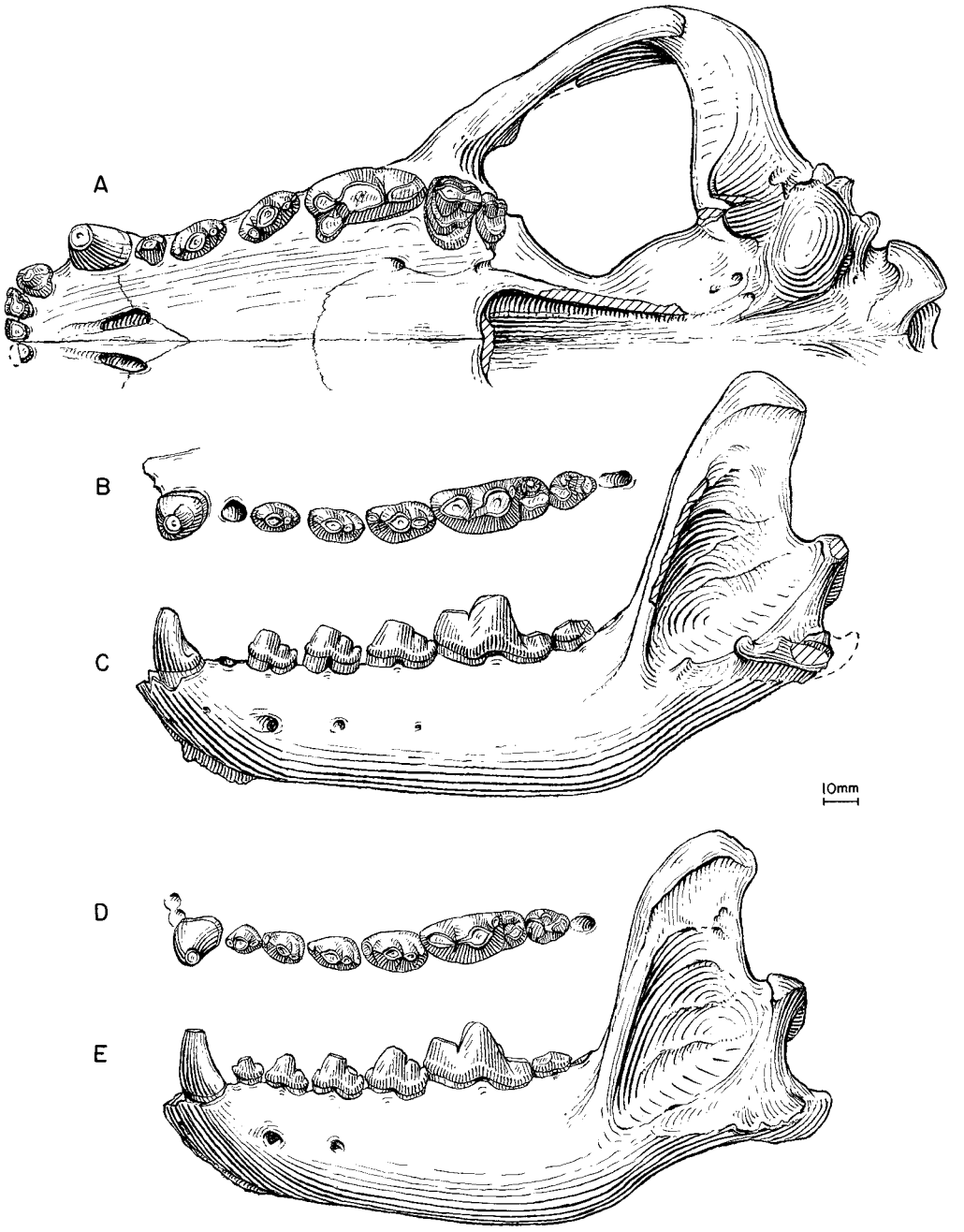

Fig. 82. **A**, Ventral view of skull, *Aelurodon taxoides*, F:AM 67047, 1 mi west of Dixon, Dixon Member, Tesuque Formation (late Barstovian–Clarendonian), Rio Arriba County, New Mexico. **B**, Lower teeth and **C**, ramus, *A. taxoides*, YPM-PU 10635, holotype, ''Loup Fork,'' Ash Hollow Formation (Clarendonian), Sheridan County, Nebraska. **D**, Lower teeth and **E**, ramus, *A. ferox*, F:AM 61771, Burge Quarry, Burge Member, Valentine Formation (late late Barstovian), Cherry County, Nebraska.

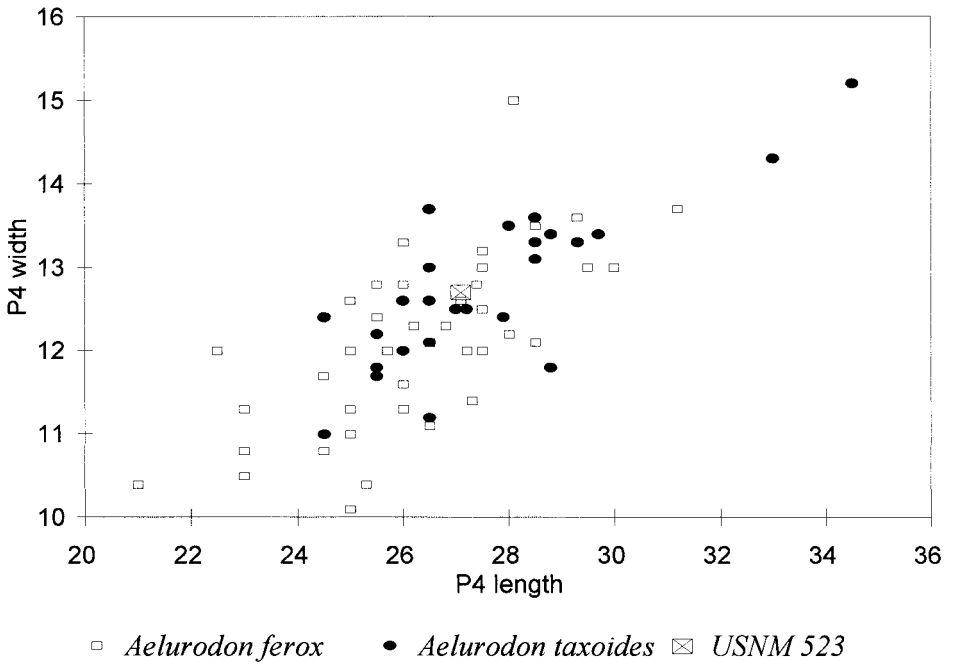

Fig. 83. Scatter diagram of P4 length vs. P4 width for *Aelurodon ferox* and *A. taxoides* showing the position of the holotype of *A. ferox* (USNM 523).

same amount of variation in size (e.g., coefficient of variation for m1 length is 5.5 in *ferox* and 6.9 in *taxoides*; see other CVs in appendix III) shown by most other borophagines in this study. In the present hypodigm, there is a significant size difference from the oldest individuals in the Cornell Dam Member of the Valentine Formation to the youngest individuals in the Burge Member of the Valentine Formation. At the extreme ends, the size difference can be as large as 23% (in basal lengths of skull, see appendix II), an amount of variation we attribute to the approximately 3 m.y. span of steady evolution of this species in the late Barstovian (fig. 84).

Similarly, at the lower end of the stratigraphic range of *A. ferox*, individuals from the Cornell Dam and Crookston Bridge members of the Valentine Formation are transitional between *A. asthenostylus* (especially the Pawnee Creek sample in Colorado) and individuals from the upper part of the Valentine Formation. Besides a slightly larger size, the specimens from the lower members of the Valentine Formation are only slightly more advanced toward hypercarnivory than is *A. asthenostylus*, and distinctions between *A. asthenostylus* and the more ''typical'' members of *A. ferox* in the upper Valentine Formation are blurred by these intermediate forms.

Aelurodon taxoides Hatcher, 1893

Figures 82A–C, 85, 86

Aelurodon taxoides Hatcher, 1893: 236, pl. 1, figs. 2, 2a. Matthew and Gidley, 1904: 250. VanderHoof and Gregory, 1940: 149 (in part). Gregory, 1942: 345, figs. 8, 9. McGrew, 1944b: 79. Macdonald, 1960: 967, fig. 4. Wilson, 1960: 993, fig. 5c, d. Webb, 1969a: 41. Baskin, 1980: 1349 (in part). Munthe, 1998: 136.

?*Tephrocyon* sp. Matthew and Cook, 1909: 376, fig. 5.

?*Cuon* sp. Matthew and Cook, 1909: 376.

Aelurodon cf. *A. aphobus* (Merriam): Macdonald, 1948: 57, figs. 3, 4.

Tomarctus propter Cook and Macdonald, 1962: 562, fig. 2. Skinner et al., 1977: 356.

Aelurodon cf. *taxoides* (Hatcher): Dalquest and Hughes, 1966: 80, fig. 2. Dalquest et al., 1996: 131.

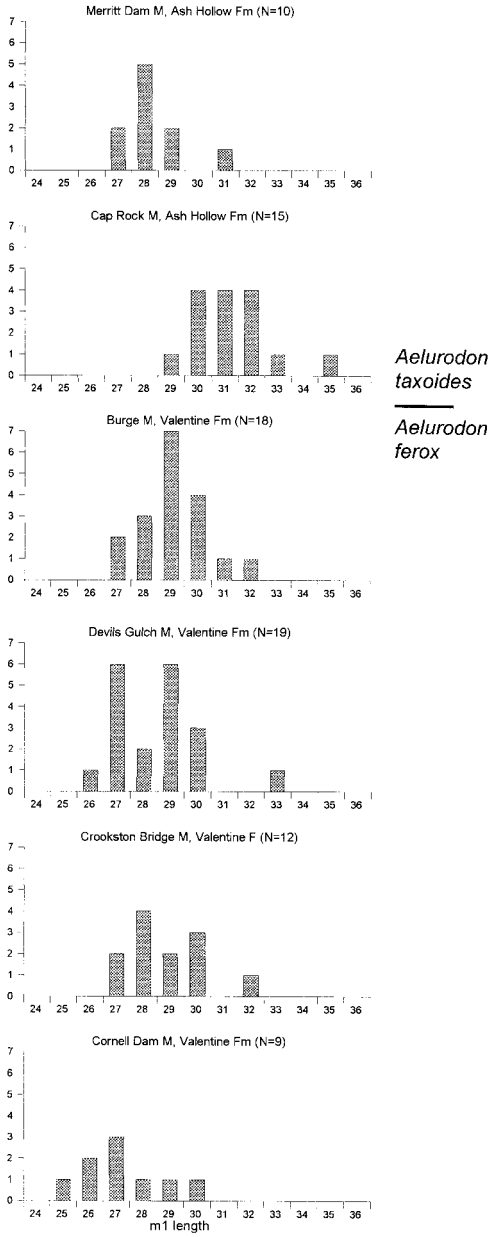

Fig. 84. Histograms of the length of m1 in *Aelurodon ferox* and *A. taxoides* in different stratigraphic positions (members of the Valentine and Ash Hollow formations) in the late Barstovian through Clarendonian of Nebraska. Note the general increase in size through time except in the end member (Merritt Dam Member), where this tendency is reversed.

Aelurodon cf. *A. taxoides* Hatcher, 1893: Skinner and Johnson, 1984: 299.

HOLOTYPE: YPM-PU 10635 (AMNH cast 97777), left ramus with i1–i3 alveoli, c1, p1 alveolus–m2, and m3 alveolus (fig. 82B, C), and atlas from the ''Loup Fork'' (Ash Hollow Formation, Clarendonian), south side of the Niobrara River, midway between the mouths of Pine and Box Butte creeks, Sheridan County, Nebraska.

REFERRED SPECIMENS: Undifferentiated beds of the Ogallala Group temporarily equivalent to the Ash Hollow Formation (early Clarendonian), Thomas Fox Ranch, Mission Local Fauna, Mellette County, South Dakota (list follows Macdonald, 1960): SDSM 553, left ramus with i1–i3 alveoli, c1–m2, and m3 alveolus (Macdonald, 1960: fig. 4); SDSM 572, left ramal fragment with m2–m3; SDSM 573, left ramal fragment with c1 and p4; SDSM 5652, partial skull with P3–M2; SDSM 53277, right ramus with c1, roots of p1–p4, and m1; SDSM 53278, right ramal fragment with p1 alveolus and p2–p3; SDSM 53279, right ramal fragment with p1 alveolus, p2, p3 alveolus, and p4; and SDSM 55185, isolated left P4. George Thin Elk Gravel Pits (same locality as above): F:AM 67328, crushed partial skull with I1–P2 alveoli and P3–M2; and F:AM 107715, right partial maxillary with P4–M2 all broken.

Undifferentiated beds of the Ogallala Group temporally equivalent to Ash Hollow Formation (early Clarendonian), South Dakota: AMNH 10813, left maxillary fragment with P1 and P2 broken. Canyon of the Little White River: AMNH 97737, left isolated P4. Spring Creek: F:AM 67029, skull fragments with I1–P1 alveoli, P2 broken, and P3 alveolus, talus of slide on Little White River; F:AM 67439, left distal tibia; and F:AM 67440, left metacarpal II. Rosebud Agency Quarry: F:AM 67483, right femur.

Undifferentiated beds of the Ogallala Group temporally equivalent to Ash Hollow Formation (early Clarendonian), Big Springs Canyon, Bennett County, South Dakota: AMNH 10891A, partial tibia; F:AM 67481, left humerus; F:AM 67482, right tibia; and UCMP 32588, complete mandible with left and right i1–i3 alveoli, c1–m2, and m3 al-

veolus (referred to *Aelurodon taxoides* by Gregory, 1942: figs. 8, 9), UCMP loc. V3322.

Undifferentiated beds (early Clarendonian) of the Ogallala Group, temporally equivalent to the Cap Rock Member of the Ash Hollow Formation, Hollow Horn Bear Quarry, Todd County, South Dakota: F:AM 67006, right and left maxillae with I1–I3 alveoli and C1–M2 (P1 alveolus) (fig. 85A, B); F:AM 67007, left maxillary fragment with P4; F:AM 67008, right and left rami with i2–m3 (fig. 85C, D); F:AM 67009, left partial ramus with c1, p1 alveolus, p2–p4, m1 alveolus, m2, and m3 alveolus; F:AM 67010, right maxillary fragment with P3; F:AM 67010A–C, detached right P1, detached right P3, and detached left p4; F:AM 67427, left partial humerus; F:AM 67427A, left partial humerus; F:AM 67428, left radius; F:AM 67429 and 67429A, B, three partial ulnae; F:AM 67430, right partial femur; F:AM 67484, right tibia; F:AM 67431, proximal part of metatarsal V; and 67431A, left calcaneum.

Undifferentiated beds (early Clarendonian) of the Ogallala Group, temporally equivalent to the Cap Rock Member of the Ash Hollow Formation, 0.25 mi west of Wounded Knee Creek, 0.5 mi south of South Dakota state line, Cherry County, Nebraska: UNSM 50792, left maxillary with P4–M1 and mandible with i3–m3 (p1 alveolus).

Cap Rock Member, Ash Hollow Formation (early Clarendonian), Brown County, Nebraska: Clayton Quarry: F:AM 67012, right partial maxillary with P3–M1; F:AM 67019, right ramal fragment with m2 and m3 alveolus; F:AM 67434, right radius; and F:AM 107714, left isolated p4. East Clayton Quarry: F:AM 67011, left partial maxillary with P3–P4 both broken and M1–M2; and F:AM 67018, right ramus with c1 broken, p1 alveolus–m2, and m3 alveolus. Fairfield Creek No. 3: F:AM 25100, left ramus with i2 and c1–m3, both radii, partial right ulna, partial metacarpals II and V, partial left tibia, partial pes with metatarsal II and incomplete III and IV, tarsals, and phalanges (referred to *Aelurodon* cf. *A. taxoides* by Skinner and Johnson, 1984: 299).

Cap Rock Member, Ash Hollow Formation (early Clarendonian), Cherry, Keyapaha, and Knox counties, Nebraska: West fork of Deep Creek: F:AM 67042, right partial ramus with i1–p1 alveoli, p2–p3, p4–m1 both broken, and m2–m3 alveoli; and F:AM 67455H, left calcaneum. Between Garner and Crane bridges: F:AM 67028, right partial ramus with p3–m1 (p4 broken) and m2–m3 alveoli. Spring Canyon: F:AM 67026, left partial ramus with p2–m1; and F:AM 67027, left ramal fragment with p3 broken–p4. Mensinger Quarry: F:AM 70615, left detached M1; and F:AM 107713, left ramal fragment with m1 broken–m2. Garner Quarry: F:AM 67330, right partial ramus with c1, p1 alveolus, p2–m1 (p3 alveolus), and m2–m3 alveoli; and F:AM 107712, right isolated m2. Northeast of Springview: F:AM 67030, left partial maxillary with P4 broken–M2, and isolated left P1. West of Boiling Spring flat: F:AM 67345, right and left partial rami with i2, i1 and i3 alveoli, c1–m2 (p1–p2 alveoli), and m3 alveolus, canyon on south side of Niobrara River about due west of Boiling Spring flat. Jonas Wilson Ranch: F:AM 107711, right partial ramus with m1 broken–m2 and m3 alveolus, talus near June Quarry, base of Cap Rock. Above Bug Prospect (UNSM loc. Kx-119B): UNSM 2061-84, right ramus with i1, c1 broken, p1 alveolus, and p2–m2. No locality data: F:AM 25101, left partial ramus with p4–m1; and F:AM 25129, right partial ramus with p4–m2.

Merritt Dam Member, Ash Hollow Formation (late Clarendonian), Sheridan, Brown, Cherry, and Hitchcock counties, Nebraska: Rhino Horizon No. 3 Quarry: F:AM 25111, right ramus with i2–p1 alveoli, p2–m2, and m3 alveolus (fig. 85E, F); F:AM 67022, right partial ramus with i2–p2 alveoli, p3–m1, and m2 alveolus; F:AM 67023, right broken m1; F:AM 67522, left partial humerus; and F:AM 67523, right partial ulna. Bear Creek Quarry: F:AM 67013, crushed skull with I1–M2; F:AM 67014, right and left partial maxillae with P3–M1; F:AM 67015, partial posterior skull; F:AM 67016, right ramus with i1–i3 alveoli and c1–m2 (p1–p2 broken and m3 alveolus); F:AM 67017, right and left rami with c1–m2 (p1 alveolus) and m3 alveolus; F:AM 67020, left ramus with c1–m2 and m3 alveolus; F:AM 67021, right and left rami with c1–m1 (p1 alveolus) and m2–m3 alveoli; F:AM 67024, right isolated P3; F:AM 67432, left humerus; F:AM 67432A,

right partial humerus; F:AM 67432B, left partial humerus; F:AM 67433, right proximal part of radius; F:AM 67433A–C, three proximal parts of ulnae; F:AM 67435, left metacarpal III; F:AM 67436, left metatarsal IV; and F:AM 67455C, left astragalus. Volcanic Ash Pit, north side of Bear Creek: F:AM 67329, right premaxillary-maxillary with I1 root–M2 (P2 broken). *Leptarctus* Quarry: F:AM 67031, fragmentary skull with I1–P1 alveoli, P2–M1, and M2 alveolus; F:AM 67032, left partial maxillary with P2 broken–P4 (P3 alveolus) and M1–M2 both broken; F:AM 67033, partial skull with I1–M2 (p1 alveolus); F:AM 67034, left P4; F:AM 67036, crushed skull with I1–M2; F:AM 67040, right ramus with i1–i3 alveolus, c1–m2 (p1 alveolus), and m3 alveolus; and F:AM 67446, left femur. Kat Quarry: F:AM 25153, right partial ramus with c1–p2 alveoli and p3–m3; and F:AM 25203, right maxillary fragment with P3–M2 alveoli. Kat Quarry Channel: F:AM 67038, right ramus with i1–i3 alveoli, c1–m1, and m2–m3 alveoli; and F:AM 67039, right ramus with i1–p1 alveoli and p2–m3 (fig. 85G, H); F:AM 67443, right radius; F:AM 67444, left radius; F:AM 67445D, right distal end of radius; F:AM 67448A, right partial femur; F:AM 67449, right tibia; F:AM 67450A, left tibia; and F:AM 67452A, left metacarpal III. West line Kat Quarry: F:AM 67043, right ramal fragment with p4; F:AM 67445A, right radius with distal end missing; and F:AM 67455E, proximal phalanx. Quarter Kat Quarry Channel: F:AM 67043A, right isolated p4; F:AM 67447, left femur; and F:AM 67448, left femur. Xmas Quarry: F:AM 25155, left immature ramus with dp2–dp4 and p4–m2 unerupted; F:AM 67445, left radius; F:AM 67445B, right proximal part of radius; F:AM 67445E, right partial ulna; F:AM 67451, left metacarpal II; F:AM 67455A, left calcaneum; and F:AM 67455D, proximal phalanx. Hans Johnson Place: F:AM 67035, right partial maxillary with P3–M2 and skull fragments; F:AM 67450, right tibia; F:AM 67452, left metacarpal IV; F:AM 67453, left metacarpal V; F:AM 67454, right metatarsal IV; F:AM 67455, right calcaneum; and F:AM 67455F, proximal phalanx. J. Wilson Ranch, 4 mi north of Johnstown: F:AM 67037, posterior part of skull. *Machairodus* Quarry: F:AM 67041, left partial ramus with p2, m1, and all alveoli; and F:AM 67442, right humerus. Gallup Gulch Quarry: F:AM 107710, left isolated M1. *Platybelodon* Slide: F:AM 67445C, left proximal end of radius. West fork of Indian Creek: AMNH 98216, left I3 and medial phalanx. Driftwood Creek: AMNH 96678, left ramal fragment with i1–i3 alveoli, c1 broken, and p1 alveolus–p2. Snake River, 5 mi below mouth of Clifford Creek: F:AM 67455B, right calcaneum. Mastodon Prospect: F:AM 61780, right maxillary fragment with P3.

Lower part of Ash Hollow Formation (Clarendonian), Banner County, Nebraska: Harrisburg Locality A1 (UNSM loc. Bn-104): UNSM 25933, complete skull with I1–P2 alveoli, P3–M1, and M2 alveolus. Near Harrisburg (UNSM loc. Bn-103): UNSM 25726, left ramal fragment with p2–p4.

South side of Niobrara River, northeast of River View School, 1 mi east of Peters Farm, 60 ft above ash bed, Ash Hollow Formation (Clarendonian), Sheridan County, Nebraska: UNSM 1486, nearly complete skull with I3–M2 (P1 alveolus).

Snake Creek area, Laucomer Member, Snake Creek Formation (late Clarendonian), Sioux County, Nebraska: Olcott Quarry: F:AM 61398, right isolated broken m1; and F:AM 67044, left ramus with i1, c1–m2, and m3 alveolus. ?Olcott Hill: AMNH 13857, right isolated m1 (referred to ?*Cuon* sp. by Matthew and Cook, 1909: 376). Ashbrook Pasture: F:AM 67995, right femur, *Hipparion* Affine Channel. East fork of *Phiohippus* Draw: F:AM 107709, right ramal fragment with p1–p3 alveoli and p4, middle *Hipparion* Affine Channel. Quarry 7, Kilpatrick Pasture: AMNH 108532, isolated left M1, and isolated right m1. No locality data: AMNH 13843, left ramal fragment with p4–m1 (referred to ?*Tephrocyon* sp. by Matthew and Cook, 1909: 376, fig. 5; Merriam, 1913: 369, fig. 14).

Dixon Member, Tesuque Formation (late Barstovian), Rio Arriba County, New Mexico: F:AM 67047, crushed skull with I1–M2 (fig. 82A), 1 mi west of Dixon, 200 ft below Ojo Caliente Sandstone.

Round Mountain Quarry, Chamita Formation (early Clarendonian), Rio Arriba County, New Mexico: F:AM 67048, left ra-

mus with i1–m3 (i2 alveolus, c1, p3, and m1 all broken); F:AM 67049, right and left rami with c1, p3–m1, and m2 alveolus; F:AM 67052, left partial ramus with c1–p2 alveoli, p3, p4–m2 all broken, and m3 alveolus; F:AM 107703, right maxillary fragment with P4 alveolus, M1 root, and M2, 50 ft below Round Mountain Quarry.

MacAdams Quarry (Location 17, Quarry 1), 10 mi north of Clarendon, Clarendon beds (early Clarendonian), Donley County, Texas: F:AM 61781, skull with I1–I2 alveoli and I3–M2 (C1 root and P1 alveolus) and mandible with i1–i3 alveoli, c1, p1 alveolus–m2, and m3 alveolus (fig. 86A–E); F:AM 61782, skull with I1–I2 alveoli, I3–C1, P1 alveolus–P4, and M1 broken–M2 alveolus; F:AM 61783, right partial maxillary with P2–M2; F:AM 61784, right partial maxillary with P1–P2 alveoli and P3–P4 and right partial ramus with c1–m1 (p1 alveolus); F:AM 61785, left partial maxillary with P2–M2; F:AM 61786, left partial maxillary with C1, P3–M2, detached I3, and skull fragments; F:AM 61787, right partial maxillary with P2, P3 alveolus, and P4–M1; F:AM 61788, left partial maxillary with P4–M2; F:AM 61790, left partial maxillary with P2–P3 and P4–M1 both broken; F:AM 61791, left partial maxillary with C1–P2 (P1 alveolus); F:AM 61793, left ramus with i1–i3 alveoli and c1–m3 (p1 alveolus); F:AM 61794, right ramus with i1–i3 alveoli, c1, p1 alveolus, p2–m1, and m2–m3 alveoli; F:AM 61795, left partial ramus with i1–m1 (p1 alveolus); F:AM 61796, right ramus with c1, p1 alveolus–m1, and m2–m3 alveoli, and atlas; F:AM 61797, right partial ramus with i1–p1 alveoli and p2–m1 (p3–m1 all broken); F:AM 61798, left partial ramus with p4–m1; F:AM 61799, left partial ramus with c1–m1 (p2–m1 all broken); F:AM 67001, left partial ramus with p2–m2 all broken; F:AM 67001A, left partial ramus with c1–p4 (p1 alveolus); F:AM 67001B, right partial ramus with c1–p3 roots and p4–m1 both broken; F:AM 67001C, left partial ramus with i2–p1 roots, p2–m1 broken, and m2–m3 roots; F:AM 67395, anterior part of skull with I1 alveolus–M2 (fig. 86F, G); F:AM 67943, right ulna; F:AM 67943A, left partial ulna; F:AM 67943B, right metacarpal III; F:AM 67943C, right metacarpal IV; F:AM 67943D, left calcaneum; F:AM 67943E, right astragalus; and F:AM 70775, partial skull with I1 alveolus–M2.

White Fish Creek, Clarendon beds (early Clarendonian), Donley County, Texas: Quarry 7: F:AM 70755, skull with I1–M2 (C1 broken and P1 alveolus); F:AM 70756, right ramus with i1–i3 alveoli, c1–m1 (p1 alveolus), m2 broken, and m3 alveolus; F:AM 70757, left ramus with i1 alveolus–m3 (c1 broken); F:AM 70776, right ramus with i1–i3 alveoli, c1, p1 alveolus–m1, and m2–m3 alveoli; F:AM 107702, left ramus with i1–i3 alveoli, and c1–m2 (p4–m2 all broken). Quarry 4: F:AM 61792, right isolated M1. Hill top west of California Quarry: F:AM 61792A, left isolated I3.

Mill Iron Ranch, Turkey Creek (early Clarendonian), Hall County, Texas: F:AM 70754, left partial ramus with p1 alveolus–m1 and m2–m3 alveoli.

Amarillo area, Ogallala Group (early Clarendonian), Texas: Bivins Ranch: F:AM 67045, left ramus with c1 broken, p1 alveolus–m2 (m1 broken), and m3 alveolus, north end about 100 ft below the Cap; and F:AM 67948, postcranial elements including incomplete vertebral column, pelvis, incomplete femur, right tibia and left partial tibia, calcaneum, astragalus, both crushed pes including metatarsals II–V, and one proximal, middle, and distal phalanges. No locality data (private donation by Floyd V. Studer): F:AM 67046, isolated left m1 and m2.

Channing area, Ogallala Group (Clarendonian), Texas: F:AM 67324, left ramus with c1 root–m3, approximately 6 mi southeast of Four Way locality.

Goliad Formation, near Normanna, Lapara Creek Fauna (early Clarendonian), Bee County, Texas: TMM-BEG 31132-458, left ramus with i1–i3 alveoli, c1, p1 alveolus, p2–m2, and m3 alveolus (Wilson, 1960: 993, fig. 5c, d).

Sanford Pit (Clarendonian), 12 mi southwest of Borger, Carson County, Texas: F:AM 107701, left maxillary fragment with C1–P1 alveoli and P2, and isolated left C1.

Exell Local Fauna, Ogallala Group (Clarendonian), 30 mi north of Amarillo, north of Canadian River, Moore County, Texas: PPHM P174-18 (Dalquest and Hughes,

1966: fig. 2), right ramus with c1, p1 alveolus, and p2–m2.

Noble Ranch, UCMP loc. V69145, Ogallala Group (Clarendonian), Moore County, Texas: WTSU 1099 (UCMP cast 85341), left maxillary with C1, P1 alveolus, and P2–M1.

Beaver Local Fauna (early Clarendonian), Whisenhunt Quarry, Laverne Formation, Beaver County, Oklahoma (list following Dalquest et al., 1996): WTSU-V-7036, 2 right premolars.

Republican River beds, Ogallala Group (Clarendonian), Bow Creek, 12.5 mi southeast of Logan, Rooks County, Kansas: F:AM 30902, skull with I1–M2 and mandible with i1–m3, partial skeleton with axis, atlas, 4 cervicals, 10 thoracics, 5 lumbars, right humerus (Munthe, 1989: figs. 6B, 7B), partial pelvis, left calcaneum, and right metacarpals III–V (skull and mandible in permanent exhibition).

Agricola Road Locality, Agricola Fauna (early Clarendonian), Bone Valley Formation, Polk County, Florida: UF 98354, left ramal fragment with p3–m1; UF 98355, left ramal fragment with m2–m3; UF 98356, partial right m1; UF 98357, right maxillary fragment with M1–M2; and UF 102644, left m1 talonid.

Johnson Member, Snake Creek Formation (late Clarendonian? *Aelurodon* specimens from these localities have the appearance of reworked materials—they are more likely to be originally from the underlying Laucomer Member), Sioux County, Nebraska: *Pliohippus* Draw, Snake Creek Quarry: AMNH 20487, left partial ramus with c1–p3 broken. ?*Aphelops* Quarry 1: AMNH 20061, right isolated p4 and right ramal fragment with p2–p3. ''Western fossiliferous exposures, 17 mi south and 1.5 mi east of Agate'': AMNH 81007 (HC 658), right isolated m1 (holotype of *Tomarctus propter* Cook and Macdonald, 1962: 562, fig. 2).

Snowball Valley North, UCMP loc. V6019, Cedar Mountain, Esmeralda Formation (early Clarendonian), Mineral County, Nevada: UCMP 59272, complete skull with I1–M2, left and right partial rami with p2–m3, partial vertebral column, partial right forelimb, and partial left and right hindlimbs (referred to *Aelurodon taxoides* by Mawby, 1965).

South side of Mount Diablo, Green Valley Formation (late Clarendonian), Contra Costa County, California: Black Hawk Ranch Quarry (UCMP loc. V3310): UCMP 33475, left ramus with c1 and p1 alveolus–m2 (Macdonald, 1948: fig. 3); UCMP 33478, left ramus with p3 broken–m2 (Macdonald, 1948: fig. 4); UCMP 34689a, isolated right M1; UCMP 34689b, left maxillary fragment with M1; UCMP 34693, isolated M1; UCMP 34694, right maxillary with P4–M1; UCMP 39498, broken left m1; UCMP 44963, broken left m1; UCMP 47256, left ramus with p4–m2; and UCMP 58678, left ramal fragments with p3–m2. Kendall-Mallory Locality (UCMP loc. V6107): UCMP 58222, right ramus with p4–m2.

DISTRIBUTION: Late Barstovian of New Mexico; early Clarendonian of South Dakota, Nebraska, New Mexico, Oklahoma, Texas, Florida, and Nevada; late Clarendonian of Nebraska, New Mexico, and California; and Clarendonian of Kansas.

EMENDED DIAGNOSIS: *A. taxoides* is derived with respect to its ancestral species *A. ferox* in its larger size, mandible with a weak anteroventral flange at the symphysis, P4 protocone reduced to a mere basal swelling, and m2 metaconid small to near absent and talonid short.

DESCRIPTION AND COMPARISON: Besides a few maxillary fragments previously described (e.g., Macdonald, 1960), much of the cranial morphology of *A. taxoides* has not been described. We are now in possession of several partial skulls to fill this void.

As the most derived species in the aelurodontine clade, *A. taxoides* is the largest in the lineage, reaching the size of a tiger, although later individuals in Nebraska may show a size reduction (fig. 84). The overall cranial proportions are similar to those of *A. ferox* (fig. 71), most noticeably with a broad rostrum and forehead, resulting in a front-heavy skull construction relative to the posterior half. Such broadening of the rostrum also results in widened external and internal nares. The frontal is not prominently domed as is in the *Epicyon–Borophagus* clade. The postorbital process of the frontal is strong and laterally expanded such that the orbit becomes relatively small. Both the external appearance of the forehead and a dissected

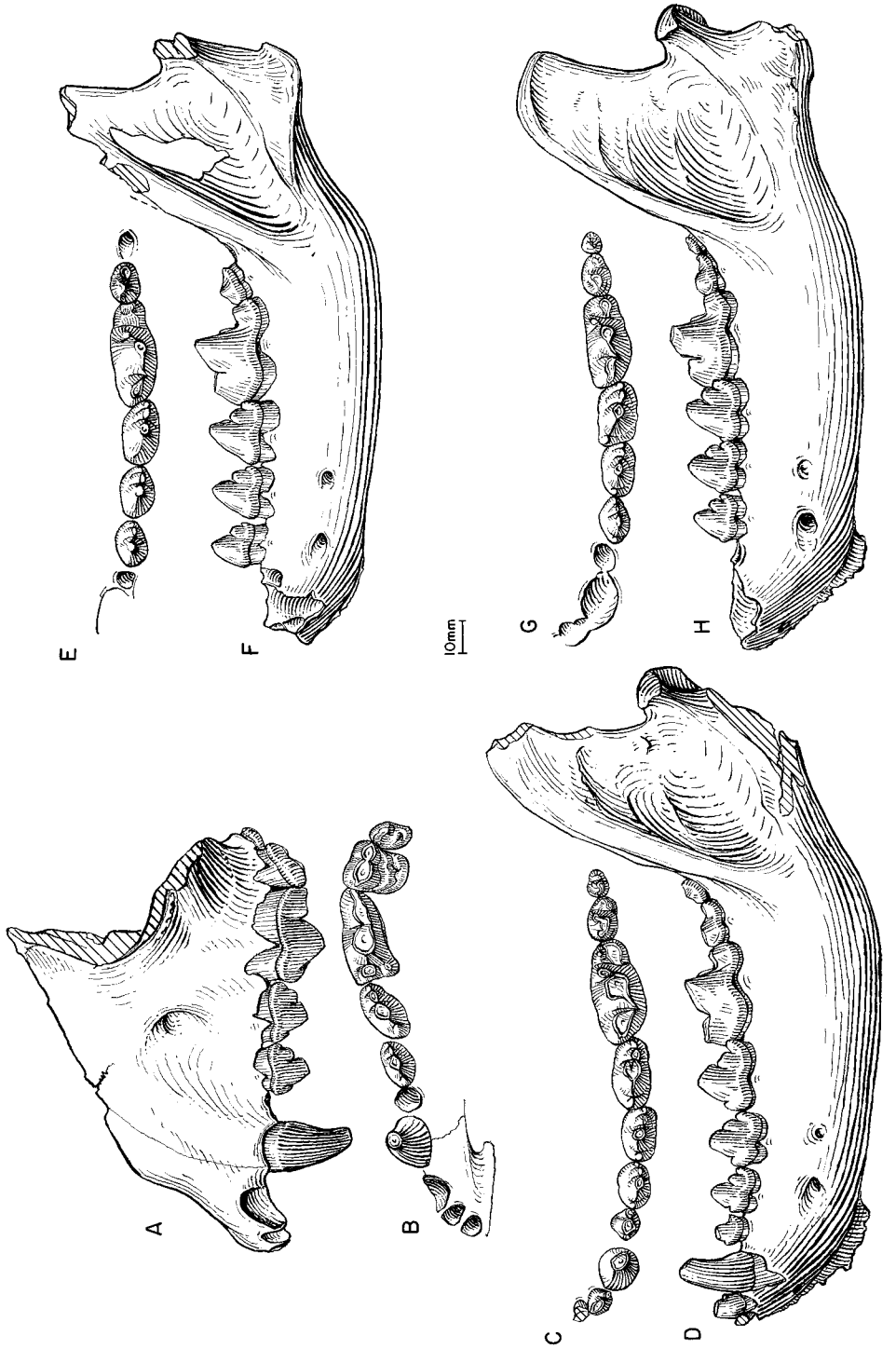

Fig. 85. *Aelurodon taxoides*. **A**, Lateral view of partial skull and **B**, upper teeth, F:AM 67006, Hollow Horn Bear Quarry, Ogallala Group (early Clarendonian), Todd County, South Dakota. **C**, Lower teeth and **D**, ramus, F:AM 67008, Hollow Horn Bear Quarry. **E**, Lower teeth and **F**, ramus, F:AM 25111, Rhino Horizon no. 3 Quarry, Merritt Dam Member, Ash Hollow Formation (late Clarendonian), Brown County, Nebraska. **G**, Lower teeth and **H**, ramus, F:AM 67039, Kat Quarry Channel, Merritt Dam Member, Ash Hollow Formation (late Clarendonian), Brown County, Nebraska.

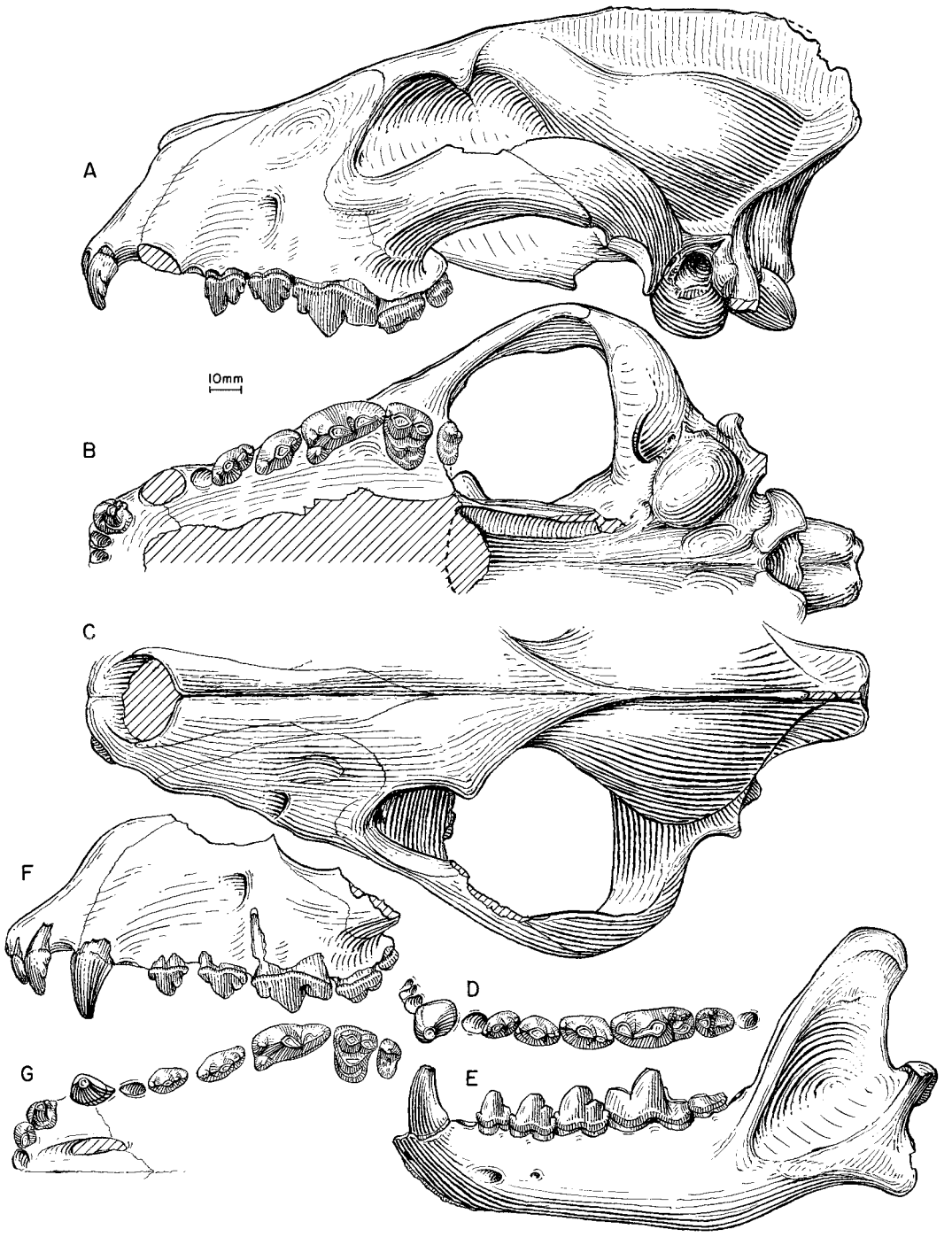

Fig. 86. *Aelurodon taxoides*. **A**, Lateral, **B**, ventral and **C**, dorsal views of skull, **D**, lower teeth, and **E**, ramus, F:AM 61781, MacAdams Quarry, Clarendon beds (early Clarendonian), Donley County, Texas. **F**, Lateral and **G**, occlusal views of partial skull and upper teeth, F:AM 67395, MacAdams Quarry.

specimen (F:AM 67015) indicate a frontal sinus no more elaborate than that in *A. ferox* (i.e., multichambered sinus that expands slightly beyond the frontal-parietal suture). Mandibles of *A. taxoides* differ from those of *A. ferox* in the development of a weak boss on the anteroventral border at the symphysis. Predictably, such a growth is more prominent in older individuals.

As the result of the trend toward enlargement of the pre-carnassial premolars and reduction of the post-carnassial molars, *A. taxoides* is characterized by massive premolars and relatively small molars (except m1). Thus, *A. taxoides* has the largest P1–P3 and p1–p4 in the aelurodontine clade, both relative to the length of carnassials and in absolute terms (fig. 72). These massive premolars have distinct accessory and cingular cusplets both anterior and posterior to the principal cusp. On the whole, the P4 protocone is extremely reduced, often to no more than a mere protuberance at the anterolingual base of the tooth. The parastyle is prominent, as in most other species of the *Aelurodon* clade. The M1 has a similarly high-crowned paracone and reduced internal cingulum as in *A. ferox*. Its metaconule is also very weak, mostly reduced to no more than a narrow postprotocrista without a distinct cusp. Individuals from the Clarendon beds of Texas have the most reduced m1s, possibly as a reflection of a geographic variation. In most specimens, the m1s still have a small metaconid and entoconid, a status not much different from *A. ferox*. The talonid, however, is noticeably reduced, especially in the lingual side where the entoconid is often restricted to an anterior location in contrast to the unshortened hypoconid, i.e., the posterolingual corner of the talonid is reduced (fig. 85). Nearly all m2s in *A. taxoides* have extremely reduced metaconids or have lost them altogether, in contrast to their more distinct presence in *A. ferox*. The talonid of m2 is also conspicuously reduced, being both shortened and narrowed.

Fragmentary materials from early Clarendonian of Florida (Agricola Fauna) have a dental morphology of advanced *Aelurodon*, but lie in the lower end of the size spectrum of *A. taxoides*. Although it is tempting to regard these as a population of small individuals in the south, lack of sufficient specimens (only three specimens are measurable) prevents a statistical evaluation.

Individuals from the Green Valley Formation of California exhibit, for the most part, the typical morphology of this species from the Great Plains. There are, however, tendencies for the California individuals to have a higher crowned and more posteriorly sloped p4 principal cusp with less distinct anterior cingular cusplet and occasionally a long m2 (e.g., UCMP 33478 and 58222), features more often encountered in *Epicyon* and *Borophagus*. The late Clarendonian California sample is still limited to mostly fragmentary jaws and teeth, and these distinct morphologies are here treated as regional variations of *Aelurodon taxoides* until demonstrated otherwise by more complete materials.

DISCUSSION: As the end member of a long line toward hyenalike dental adaptations, *A. taxoides* has highly distinct cranial and dental morphologies. Its giant size and massive premolars permit easy recognition of this species. Thus, except for occasional junior synonyms proposed earlier in the century, more recent authors generally have no difficulty in recognizing this species (e.g., Macdonald, 1960; Wilson, 1960; Webb, 1969a). The relatively well-preserved holotype of *A. taxoides* avoids taxonomic controversies experienced with other species of *Aelurodon*.

The distinct morphology of *A. taxoides* (together with *A. ferox*) helped to polarize the divergent morphologies between the so-called *A. taxoides* species group and the ''*A.*'' *saevus* species group, an idea initially outlined by McGrew (1944b) and more firmly established by Baskin (1980). As its front-heavy cranial proportions, the teeth of *A. taxoides* are also front-heavy with massive premolars at the expense of reduced molars (except m1 trigonid). The opposite is generally true for the *Epicyon–Borophagus* clade, whose anterior premolars are greatly reduced but whose molars remain unreduced until very late in the phylogeny.

Cook and Macdonald (1962: 562, fig. 2) described a single m1 (AMNH 81007 = HC 658) from the Upper Snake Creek beds and named it *Tomarctus propter*. Skinner et al. (1977: 356) listed it as from the Johnson

Member of the Snake Creek Formation. Largely indeterminable based on the holotype alone, it nonetheless has the hypercarnivorous morphology of an *Aelurodon*. Presence of an *A. taxoides*-like form in the Johnson Member is further indicated by two more specimens (AMNH 20061 and 20487), both of which are represented by lower premolars and a canine only. Of the three specimens, however, two (AMNH 20061 and 81007) have the clear indications of water-worn polish, common in the Upper Snake Creek materials, and are likely to be reworked from the underlying Laucomer Member (late Clarendonian). Such an interpretation and the lack of Hemphillian occurrence of *Aelurodon* elsewhere in North America led us to conclude that *Aelurodon* was extinct at the end of Clarendonian.

Borophagina, new subtribe

TYPE GENUS: *Borophagus* Cope, 1892.

INCLUDED GENERA: *Paratomarctus*, new genus; *Carpocyon* Webb, 1969b; *Protepicyon*, new genus; *Epicyon* Leidy, 1858; and *Borophagus* Cope, 1892.

DISTRIBUTION: Late Hemingfordian through late Blancan of North America.

DIAGNOSIS: Derived characters uniting the Borophagina as a monophyletic group include dorsally enlarged frontal sinus producing a domed forehead, premolar cingular cusplets reduced or absent, and P4 protocone reduced or absent. Advanced Borophagina are further derived in such morphological trends as reduction of I3 lateral cusplets, P4 parastyle connected to protocone by a ridge, and progressively lower crowned P2–P3 and p2–p3 relative to higher crowned and larger p4. Borophagina generally lack the derived characters of the Aelurodontina in its high sagittal crest, posteriorly extended and laterally narrowed nuchal crest, elaborate lateral cusplets on I3, uniformly enlarged premolars, reduced m1 entoconid and m2 metaconid, and reduced M2 and m2.

Paratomarctus, new genus

TYPE SPECIES: *Cynodesmus euthos* McGrew, 1935.

ETYMOLOGY: Greek: *para*, near, plus *tomarctus*.

INCLUDED SPECIES: *Paratomarctus temerarius* (Leidy, 1858) and *Paratomarctus euthos* (McGrew, 1935).

DISTRIBUTION: Late Hemingfordian of Nebraska; early Barstovian of California, Nevada, Oregon, and Montana; late Barstovian of Nebraska, Wyoming, Nevada, California, and New Mexico; early Clarendonian of Nebraska, South Dakota, and Texas; and late Clarendonian of Nebraska.

DIAGNOSIS: As the stem taxon of the Borophagina, *Paratomarctus* differs from the Aelurodontina in the following derived characters: dorsally enlarged frontal sinus producing a domed forehead, premolar cingular cusplets reduced or absent, and P4 protocone reduced or absent. It can be distinguished from the *Carpocyon–Borophagus* clade in the following primitive features: bulla not greatly enlarged, external auditory meatus lacking a short tube, I3 lateral cusplets unreduced, and P4 parastyle not enlarged. *Paratomarctus* is further distinguished from *Carpocyon* in its lack of autapomorphies of the latter clade: enlarged upper molars relative to P4, anteriorly extended M1 lingual cingulum, and enlarged m2. *Paratomarctus* has one autapomorphy: premolars uniformly reduced.

Paratomarctus temerarius (Leidy, 1858)

Figures 87, 88C–J

Canis temerarius Leidy, 1858: 21; 1869: 29, pl. 1, fig. 12; 1871: 341. Hayden, 1858: 158. Cope, 1883: 242.

?*Canis anceps* Scott, 1893: 660; 1895: 75. Matthew, 1899: 67. Hay, 1902: 775.

?*Canis temerarius* (Leidy): Matthew, 1899: 67.

‘‘*Canis*’’ *anceps* (Scott): Matthew, 1901: 374.

‘‘*Canis*’’ *temerarius* (Leidy): Matthew, 1909: 115.

?*Tephrocyon* cf. *temerarius* (Leidy): Matthew and Cook, 1909: 376.

Tephrocyon temerarius (Leidy): Merriam, 1913: 365, figs. 7, 8a, b. Matthew, 1918: 188; 1924: 98.

Tephrocyon near *kelloggi* (Merriam, 1911): Merriam, 1913: 368, fig. 10; 1916: 173, fig. 2a, b.

Tomarctus cf. *T. brevirostris* (Cope, 1873): Gazin, 1932: 48, fig. 2 (LACM-CIT 379).

Cynodesmus cf. *C. kelloggi* (Merriam): Stirton, 1939a: 632.

Tomarctus cf. *T. rurestris* (Condon, 1896): Downs, 1956: 235 (LACM-CIT 379).

Tomarctus temerarius (Leidy): Downs, 1956: 236. Voorhies, 1990a: A128. Munthe, 1998: 135.
Tomarctus canavus (Simpson, 1932): Wilson, 1960: 986, fig. 2a–c (TMM 31190-67).
Tomarctus rurestris (Condon, 1896): Voorhies, 1965: 21, pls. 1, 2 (in part). Forsten, 1970: 42 (in part).
Tomarctus near *T. euthos* (McGrew, 1935): Evander, 1986: 26, fig. 2.

LECTOTYPE: USNM 768, right ramal fragment with m1 (fig. 87A, C) from the ''sands of the Niobrara River, Loup Fork'' (?late Barstovian), Nebraska.

REFERRED SPECIMENS: Cornell Dam Member, Valentine Formation (early late Barstovian), Brown County, Nebraska: Norden Bridge Quarry (UNSM loc. Bw-106; list of USNM specimens follows Voorhies, 1990a: A128): UNSM 83931, right ramus with c1, p1 alveolus, p2, p3 broken, and p4–m3; UNSM 83932, right ramus with p2–p4, m1 broken–m2, and m3 alveolus; UNSM 83933, left immature ramus with unerupted m1–m2; UNSM 83934, left immature ramus with unerupted c1, p2, and m1–m2; UNSM 83936, right broken m1; UNSM 83937, left I3; UNSM 83945, left ramal fragment with broken m2; UNSM 83946, left p4; UNSM 83951, left M1; USNM 352353, left m1; USNM 352390, skull with I1–M2; USNM 352394, right ramus with p4–m2; USNM 352395, left ramus with c1 and p2–p4; and USNM 352397, left ramus with c1, p2–p3, and p4 broken.

Crookston Bridge Member, Valentine Formation (late Barstovian), Cherry and Brown counties, Nebraska: Mouth of Snake River: F:AM 61070, skull with I1–M2 (fig. 87D–G) (in permanent exhibition). Crookston Bridge Quarry (UNSM loc. Cr-15): UNSM 25720 (AMNH cast 97142), right partial ramus with c1, p1–p4 alveoli, m1–m2, and m3 unerupted; and UNSM 25880 (AMNH cast 97249), left partial maxillary with P3 alveolus and P4 broken–M1. Dutch Creek, 8 mi north of Long Pine: F:AM 25123, left partial maxillary with P3 alveolus–M2 (P4 and M1 broken) and right partial ramus with i3–p1 alveoli and p2–m3; F:AM 25124, left partial ramus with c1 broken–m2 (p1 and p3 alveoli); F:AM 61064, posterior part of skull, right premaxillary-maxillary and left partial maxillary with I1 alveolus–M2 (M1 missing), skull fragment, and right partial ramus with c1–p1 alveoli and p2 broken–m3 (p4 broken); F:AM 67351, left partial maxillary with P4–M2, detached C1, P2, and P3, partial radius and ulna, both partial tibia, and foot bone fragments; and UNSM 25887 (AMNH cast 97144), left partial ramus with m1 broken–m2 (p4 and m3 alveoli). Miesner Slide: F:AM 61071, crushed skull with I1–M2, mandible with i1 alveolus–m3, atlas, axis, one cervical and one dorsal vertebrae, right ulna, and right femur. Railway Quarry A (UNSM loc. Cr-12; list following Evander, 1986: 26): F:AM 61066, right ramus with c1–m2 (p1 and p3 alveoli) (in permanent exhibition); USNM 25881 (AMNH cast 97250), right partial maxillary with P4–M1; UNSM 25882 (AMNH cast 97251), right partial maxillary with P3–M2 (referred to *Tomarctus* near *T. euthos* by Evander, 1986: fig. 8B); UNSM 25884 (AMNH cast 97143), right partial ramus with p1–p3 alveoli, p4–m2, and m3 alveolus (referred to *Tomarctus* near *T. euthos* by Evander, 1986: figs. 2, 7B); UNSM 25885, left ramus with p2 broken–m2; UNSM 25886, left ramus with p3–p4 and m1–m3 alveoli; UNSM 76615, posterior part of skull; and UNSM 76616, left humerus. Railway Quarry B (UNSM loc. Cr-13): UCMP 124377 (UCMP 29926 in Evander, 1986), left ramal fragment with m1 and m2–m3 alveoli; and UNSM 76614, left partial maxillary with P4 broken–M2. Garner Bridge, Niobrara River: F:AM 70616, left partial ramus with m1–m3; and F:AM 70617, right isolated m1. Nenzel Quarry: F:AM 61067, right partial ramus with m1–m2 and m3 alveolus. West Valentine Quarry (UNSM loc. Cr-114): UNSM 2383-87, right ramus with p4 broken–m1 and m2–m3 alveoli; UNSM 2611-87, left ramus with p1–p3 alveoli, p4–m1, and m2–m3 alveoli; UNSM 3502-86, right ramus with c1–m1 (p1 alveolus and m1 broken); and UNSM 3840-86, left maxillary with P4–M2.

Devil's Gulch Member, Valentine Formation (late Barstovian), Brown and Cherry counties, Nebraska: Fairfield Falls Quarry: F:AM 61065, left partial ramus with i3–p1 alveoli, p2–m1, and m2–m3 alveolus; F:AM 61068, left ramus with c1 broken, p1 alveolus, p2–m2, and m3 alveolus; and F:AM 61069, partial skull with I1–M2. Devil's

Gulch Horse Quarry: F:AM 25221, right ramus with c1–m2 (p1, p3, and m3 alveoli). Devil's Gulch: F:AM 25132, left partial ramus with c1–p3 alveoli, p4 broken–m1, and m2–m3 alveoli.

Valentine Formation (late Barstovian), Brown County, Nebraska: Elliot Place, 4 mi north of Long Pine: F:AM 25222, left ramus with c1–m2 (p1 and m3 alveoli).

Valentine Formation (late Barstovian), Webster County, Nebraska: Myers Farm (UNSM loc. Wt-15A) (referred to *Tomarctus* cf. *T. optatus* by Corner, 1976): UNSM 20844, right ramus with p1 alveolus–m2 and m3 alveolus; UNSM 20845, right ramal fragment with p1–p2 alveoli and p3–m1; UNSM 20846, right maxillary with P3 alveolus–M2; UNSM 20983, left ramus with p1 alveolus–m2; UNSM 21664, left ramus with c1–m2 (p1 alveolus); UNSM 21665, right ramal fragment with p1–p2 alveoli and p3–p4; UNSM 21666, right ramal fragment with m2 and m3 alveolus; and UNSM 45158, right ramal fragment with p4–m1.

Trail Creek Fauna, Ogallala Group (late Barstovian), Laramie County, Wyoming: UW 834, left ramus with c1 broken, p4–m2, and alveoli of p1–p3 and m3 (referred to *Tomarctus rurestris* by Voorhies, 1965: pl. 2); and UW 849, left ramus with c1 broken, p2–m2, and alveoli of p1 and m3 (referred to *Tomarctus rurestris* by Voorhies, 1965: pl. 1).

Smith River Valley, ''Upper beds'' or ''*Cyclopidius* beds,'' in Deep River beds (?early Barstovian), Meagher County, Montana: YPM-PU 10453 (AMNH cast 97241) (holotype of *Canis anceps* Scott, 1893), left partial ramus with p4 broken–m2 and m3 alveolus (fig. 88I, J).

East of New Chicago, in north draw, Flint Creek Fauna (early Barstovian), Granite County, Montana: F:AM 67359, right ramal fragment with p3–m1; and F:AM 67359a, left ramal fragment with m1 broken–m2 and m3 alveolus.

Barstow area, Barstow Formation (early late Barstovian), San Bernardino County, California: Skyline Quarry: F:AM 67121, crushed skull with I1–M2 and mandible with i3–m3 (fig. 87H–K); F:AM 67122, crushed partial skull with P2–M1 all broken and M2; F:AM 67125, posterior part of skull and right partial maxillary with P4–M2; F:AM 67140, right partial ramus with c1–p1 alveoli, and p2 broken–m2 (p3, p4, and m2 all broken); and F:AM 67141, right partial ramus with c1–p2 alveoli and p4 broken–m2. North End: F:AM 27289, partial skull with P1–P2 alveoli and P3 broken–M2; F:AM 27290, partial skull with P2 alveolus–M2; F:AM 27292, right partial ramus with c1 and p3–m1; and F:AM 27295, right partial maxillary with P4–M2. New Hope Quarry: F:AM 67120, skull with I1–P1 alveoli and P2–M2; F:AM 67126, right partial maxillary with C1–P1 alveoli and P2 broken–M2 (P3 alveolus and P4 broken); and F:AM 67127, both partial maxillae with P1 alveolus, P2–P3 both broken, P4–M2, and both rami with c1 broken–m2 (p1 alveolus). Hidden Hollow Quarry: F:AM 61012, both premaxillae-maxillae with I1–M2; F:AM 61013, left partial maxillary with P2 broken–M2; F:AM 61014, right partial maxillary with P4–M1; F:AM 67124, both partial maxillae with P4–M2, both partial rami with p3–m2, and associated detached canines, incisors, and premolars; F:AM 67128, left partial ramus with c1–p1 alveoli and p2–m1; F:AM 67132, both rami with c1–m2 (p1–p2 and m3 alveoli); F:AM 67133, left partial ramus with p4–m1 and m2–m3 alveoli; F:AM 67136, right partial ramus with c1–p1 alveoli and p2–m3; F:AM 67137, left partial ramus with c1–p1 alveoli and p2–m2 (p3 and m3 alveoli); F:AM 67138, left partial ramus with p2–p3 both broken, p4, and m1 broken; F:AM 67139, left partial ramus with c1–m1 (p1–p2 alveoli and m2 broken); and F:AM 67149, right partial ramus with p3–m1. Leader Quarry: F:AM 67123, anterior part of skull with I1–P1 alveoli and P2–M2; F:AM 67134, left partial ramus with i1–c1, p1 alveolus–m1 (p3 alveolus), and m2 broken; F:AM 67143, right partial maxillary with P4–M2; F:AM 67144, left partial ramus with m1–m2 both broken; F:AM 67145, right partial ramus with p4–m2 (m1 broken) and m3 alveolus; F:AM 67147, partial left ramus with c1–m3 all broken or alveoli; F:AM 67150, right partial ramus with c1, p1–p4 alveoli or broken, and m1–m2; F:AM 67151, left ramus with c1 broken–m3; and F:AM 67152, left and right rami with p2–m1. Sunnyside Quarry: F:AM 67142, skull with I1–M2 (fig. 87L–N) and

cervical vertebrae; and F:AM 67368, immature left and right ramal fragments with p3–p4 unerupted and m1. Mayday Quarry: F:AM 67148, right and left partial rami with c1 broken–m2 (p1 alveolus). First Division, localities unspecified: F:AM 27226, anterior part of skull with I3–M2 (P3–P4 broken); F:AM 27228, right ramus with i1–i3 roots, c1–m2, and m3 alveolus; F:AM 27229, left partial ramus with c1 broken–m2 (p1–p2 alveoli); F:AM 27233A, right ramus fragment with m1–m2; F:AM 27235, right partial ramus with c1 broken–m2 (p1 alveolus); F:AM 27237, skull with C1–M2; F:AM 27238, crushed skull with I2–M2; F:AM 27239, crushed partial skull with I3–P3 all broken, P4–M1, and M2 broken; F:AM 27240, crushed partial skull with I1–P3 alveoli and P4 broken–M2; F:AM 27241, posterior part of skull with P3–M2 (P4 broken) and both partial rami with c1 broken–m1 (p1–p2 alveoli) and m2–m3 both broken; F:AM 27242, partial cranium and associated teeth including M1–M2; F:AM 27245, partial skull with I1–I2 alveoli, I3–M2 (p1 alveolus and both C1 and M2 broken); F:AM 27246, left partial maxillary with P3–M2; F:AM 27247, left partial maxillary with P3–M2; F:AM 27248, anterior part of skull with C1–P1 alveoli and P2–M2; F:AM 27248A, left partial maxillary with P3–M2; F:AM 27250, left partial maxillary with P3 broken and P4 alveolus–M2; F:AM 27254, right partial ramus with c1–m3 (p1 alveolus and p3 broken); and F:AM 27269, left partial ramus with p4 broken–m2 and m3 root. *Hemicyon* Quarry and *Hemicyon* Stratum: F:AM 27233, left partial ramus with m1 broken–m2; F:AM 27234, left ramal fragment with m1 unerupted; F:AM 27244, skull with I1 alveolus–M2 (I3 broken and C1 alveolus); F:AM 27249, partial skull with C1 broken, and P3 alveolus–M2 (M1 broken); F:AM 27251, left ramus with c1 broken–m2 (p1 alveolus); F:AM 27251A, right partial ramus with c1–p3 alveoli, p4–m2, and m3 alveolus; F:AM 27252, right partial ramus with c1–p1 alveoli, p2–m2, and m3 alveolus; F:AM 27253, left partial ramus with c1, p1–p2 alveoli, p3–m2, and m3 alveolus; F:AM 27255, skull with I1 broken–M2 (P1 alveolus) and mandible with i1–m3 (fig. 88C–H); F:AM 27293, left partial ramus with c1, p1 alveolus–p4, m1 broken, and m2 detached; F:AM 27501, skull with C1–M2 (P1 alveolus); F:AM 27506, right partial ramus with c1, p3, m1, and alveoli for p1–p2 and p4; F:AM 27508, left ramus with c1 broken–m2; and F:AM 27523, partial palate with P2–M2. Starlight Quarry: F:AM 67366, left partial ramus with p2–p3 alveoli and p4–m2. No locality data: F:AM 27227, left ramus with p2–m2 (p4 broken); F:AM 27230, right ramus with p1–m1 and m2 broken; F:AM 27231, right partial ramus with p3–m2; F:AM 27236, left partial ramus with p4–m3; F:AM 27243, anterior part of skull with P4–M2 all broken; F:AM 27246A, right maxillary with P4–M2; F:AM 27253B, right partial ramus with p2–p3 alveoli, p4–m1, and m2 alveolus; F:AM 27256, left and right ramal fragments with m1–m3; F:AM 27256A, four ramal fragments with m1; F:AM 27259, right partial ramus with p4–m1 and m2–m3 alveoli; and F:AM 67135, left partial premaxillary-maxillary with I1 broken–C1 and P4–M2. UCMP loc. 1307 (Barstow area): UCMP 19402, right ramus with p3–m2 (Merriam, 1913: fig. 8a, b). UCMP loc. 2301 (Barstow area): UCMP 32824, partial left and right rami with c1–p1 alveoli, p2–m2, and m3 alveolus. Hell Gate Basin No. 4 (UCMP loc. V66160): UCMP 79198, left and right maxillary fragments with P4–M2, left and right rami with i1–p1 alveoli, p2–m3, atlas, axis, and one cervical.

Pojoaque Member of the Tesuque Formation (late Barstovian), Santa Fe or Rio Arriba counties, New Mexico: Santa Cruz, First Wash: F:AM 27386, right partial ramus with m1 and m2 alveolus; and F:AM 50150, anterior part of skull with I1–I2 alveoli and I3–M2. Santa Cruz: F:AM 27390, partial palate with C1 broken and P1 alveolus–M2 (P2–P3 broken). Red layer, Santa Cruz, Second Wash: F:AM 27472, left ramus with c1 broken–m2 (p1 alveolus and p3 broken). Half mi west of Santa Cruz Dam, red layer: F:AM 50151, left partial ramus with m1–m2. Pojoaque Bluffs: F:AM 27389, right partial ramus with i1–p1 alveoli, p2–m2 all broken, and m3 alveolus; F:AM 50149, left partial ramus with p2–p4, m1 broken, and m2–m3 alveoli; F:AM 50155, left partial ramus with c1 alveolus, p1–m1 all broken, m2, and m3 alveolus; F:AM 27480, both partial pes in-

cluding calcaneum, metatarsal I, incomplete metatarsals II and III, metatarsals IV and V, and two first phalanges; F:AM 67895, calcaneum; F:AM 67901 and 67901A, two calcanea. North Pojoaque Bluffs: F:AM 50147, left partial ramus with c1–p2 broken, p3, p4–m1 both broken, and m2; and F:AM 50158, right partial maxillary with P4 broken and M1–M2 alveoli. South Pojoaque Bluffs: F:AM 50148, left ramus with i1–c1 broken and p1–m3. West Pojoaque Bluffs: F:AM 67894, left partial manus including metacarpals I, III, and V, incomplete metacarpals II and IV, three first phalanges, and one second phalanx. San Ildefonso: F:AM 27471, anterior part of skull with I1–M2. Santa Fe area: F:AM 27380, right immature partial ramus with c1 and p3–p4 all erupted, dp4, and m1–m2; F:AM 27387, left ramal fragment with p4 root–m1; and F:AM 50152, left ramal fragment with m1 unerupted.

Chama El Rito Member, Tesuque Formation (late Barstovian), Rio Arriba County, New Mexico: *Aelurodon* Wash, Rio del Oso–Abiquiu: F:AM 67374, right and left partial maxillae with P1 alveolus–M2; F:AM 67375, isolated I3 right and left partial maxillae with P2–M2; F:AM 67376, left partial maxillary with C1 broken–P3 and P4 broken; F:AM 67377, right partial maxillary with P4 broken–M2; F:AM 67378, right isolated upper P4 and right maxillary fragment with M1–M2 alveolus; F:AM 67379, left isolated M1; F:AM 67380, right ramus with c1 broken, p1–p4 alveoli, m1–m2, and m3 alveolus; F:AM 67381, left partial ramus with c1–m2 (p1 alveolus); F:AM 67382, right ramus with c1–m2 and m3 alveolus; F:AM 67383, left partial ramus with p2–m2 and m3 alveolus; F:AM 67384, right ramal fragment with m1 and associated detached m2; and F:AM 70500, premaxillary with I1 broken–I3, maxillary fragment, and detached teeth including C1–M1 and M2 broken and left partial ramus with p2 broken–p4 and m1 broken. Three-Sand Hills Wash, Rio del Oso locality, Green Sand Stratum: F:AM 50153, left ramus with i1–m2 (p1 broken and m3 alveolus).

Ojo Caliente Member, Tesuque Formation (late Barstovian), Rio Arriba County, New Mexico: Conical Hill Quarry, 15 mi northwest of Espanola: F:AM 67369, left partial ramus with c1–m1 all broken and m2. Middle of Ojo Caliente locality: F:AM 104813, right isolated m1.

Jemez Creek area, unnamed member of Zia Formation (late Barstovian), Sandoval County, New Mexico: Rincon Quarry: F:AM 50195, right and left partial maxillae with P2 and P4 both broken, M1, and M2 alveolus; F:AM 50196, right partial maxillary with M1 broken–M2; F:AM 50197, right partial ramus with p2 alveolus, p3 broken–m2, and m3 alveolus; F:AM 104812, left isolated broken M1; and F:AM 67897, left incomplete humerus. West tributary of Canyada de Zia: F:AM 50192, right and left partial rami with p1–p3 all broken, p4, and m1–m3 all broken; and F:AM 50194, partial skull with C1–M1 all broken and M2. Red Cliff Prospect in main fork, Canyada Piedra Parada: F:AM 50146, right and left partial rami with c1–m2 (p1 and m3 alveoli).

Cedar Mountain, UCMP loc. 2027, Stewart Spring Fauna (late Barstovian), Esmeralda Formation, Mineral County, Nevada: UCMP 19767, partial left m1 (referred to *Tephrocyon* near *kelloggi* by Merriam, 1913: fig. 10; 1916: fig. 2a, b).

Fleming Formation (early Barstovian), Trinity River Local Fauna, San Jacinto County, Texas: Kelly Farm: F:AM 63291, left maxillary fragment with P4–M2. Trinity River Pit 1, upper part of the Fleming Formation: F:AM 67392, right partial ramus with p2 alveolus–m1 and m2 root; F:AM 67393, right isolated broken M1; F:AM 67394, partial skull with C1–P3 alveoli and P4–M2 (M1 broken); F:AM 70700, right partial ramus with p2–p4 alveoli and m1–m2 both broken; F:AM 70705, left partial ramus with c1, p1 alveolus–m1, and m2–m3 alveoli; F:AM 104809, left partial ramus with i1–i3 alveoli, c1, p1 alveolus, p2, p3 alveolus, p4–m1 both broken, and m2 root; F:AM 104810, right partial ramus with i1–p3 alveoli, p4–m2, and m3 root; F:AM 104811, left ramal fragment with m2 broken; F:AM 104819, right partial ramus with c1, and p1 alveolus–m1 (p4 broken and m2–m3 alveoli); and F:AM 105358, posterior part of skull fragment. Near Pointblank, Pointblank Local Fauna: TMM-BEG 31190-67 (AMNH cast 89629), right partial ramus with p1 alveolus, p2, and p3 alveolus–m1 (referred to *Tomarctus canavus* by Wilson, 1960: fig. 2a–c).

Skull Spring Local Fauna (LACM-CIT loc. 57), Butte Creek Formation (early Barstovian), Malheur County, Oregon: LACM-CIT 379, right maxillary fragment with M1–M2 (referred to *Tomarctus brevirostris* by Gazin, 1932: fig. 2).

DISTRIBUTION: Early Barstovian of California, Oregon, Nevada, Texas, and Montana; and late Barstovian of Nebraska, Wyoming, New Mexico, Nevada, and California.

EMENDED DIAGNOSIS: Besides its smaller size, *Paratomarctus temerarius* is primitive with respect to *P. euthos* in its less enlarged postorbital process of frontal, narrow frontal shield, narrower palate, short tubular auditory meatus, and lack of a symphyseal boss on the inferior ramus.

DESCRIPTION AND COMPARISON: *Paratomarctus temerarius* is now a much better known species, with the present reference of nearly complete cranial materials from a large series of specimens from Nebraska, New Mexico, and the Barstow Formation of California. These more complete materials demonstrate that this species shows the initial development of the dorsal inflation of the frontal sinus characteristic of the prominently domed forehead of the Borophagina clade. Besides their similar size, the cranial proportions of *P. temerarius* are also close to those of *Protomarctus optatus* (fig. 89). Noticeable differences in cranial measurements include a slightly narrower zygomatic arch and narrower palate at the P1 in the former. Dentally, *P. temerarius* has the distinctly reduced premolars characteristic of the genus. The pre-carnassial premolars are uniformly small with a backward hook of their main cusp, instead of the much larger p4 vs. p2–p3 in *Epicyon* and derived species of *Carpocyon*, and have reduced (or absent) anterior and posterior stylar cusplets on p2–p3. Other than the domed forehead and reduced premolars, *P. temerarius* is quite similar to *P. optatus*.

Individuals from the Barstow Formation tend to have a less inflated frontal sinus, but have a well-developed P4 parastyle with distinct lateral ridges converging toward the apex. The parastyle appears to be an independent development from that in *Carpocyon* and more derived taxa, because individuals in the lower stratigraphic level (Second Division Fauna) have both distinct and indistinct parastyles, whereas individuals from higher levels (e.g., *Hemicyon* Stratum) tend to have a uniformly distinct parastyle. On the other hand, parastyles from individuals in the Valentine Formation, including those from the Devil's Gulch Member, are indistinct. We thus interpret a distinct parastyle on P4 of *Paratomarctus temerarius* as an aspect of intraspecific variation.

In the F:AM collection, there is a modest sample of cranial and postcranial materials referable to *Paratomarctus temerarius* from the early Barstovian Fleming Formation, Texas. A well-preserved skull (F:AM 67394) clearly indicates the presence of a prominently domed forehead typical of the species, although this doming is slightly exaggerated by the lateral crushing suffered by this specimen. The sagittal crest is slightly concave in lateral profile, reminiscent of the condition in *Epicyon*. The bulla is greatly inflated with a modest development of a tubular external auditory meatus. The teeth of the Texas specimens, however, are generally more primitive with unreduced premolars, in contrast to those from the Valentine Formation of Nebraska, and are more comparable to those of *Protomarctus optatus*. One individual, F:AM 67392, has a larger p4 and smaller p3, a character for *Carpocyon* and more derived taxa, but most other individuals (F:AM 70705, 104810, 104819) do not have much size differentiation among the premolars. Similarly, the P4 (in F:AM 63291, 67394) still shows the primitively small parastyle as in *Protomarctus optatus*. Overall, the Texas individuals seem to have the cranial morphology of *Paratomarctus temerarius* but with a dentition more like *Protomarctus optatus*. If our present systematic assignment is correct, the Texas materials reveal the primitive morphology of this species and represent the earliest record of this lineage in the early Barstovian.

DISCUSSION: Leidy's (1858) type series of *Canis temerarius* consisted of two poorly preserved specimens (both cataloged as USNM 768). One is a ramal fragment with an m1 (fig. 87A, C) and the other a maxillary fragment with broken P4 and M1 (fig. 87B). The lower jaw was subsequently figured by Leidy (1869: pl. 1, fig. 12) but the maxillary was described first by Leidy (1858) and thus

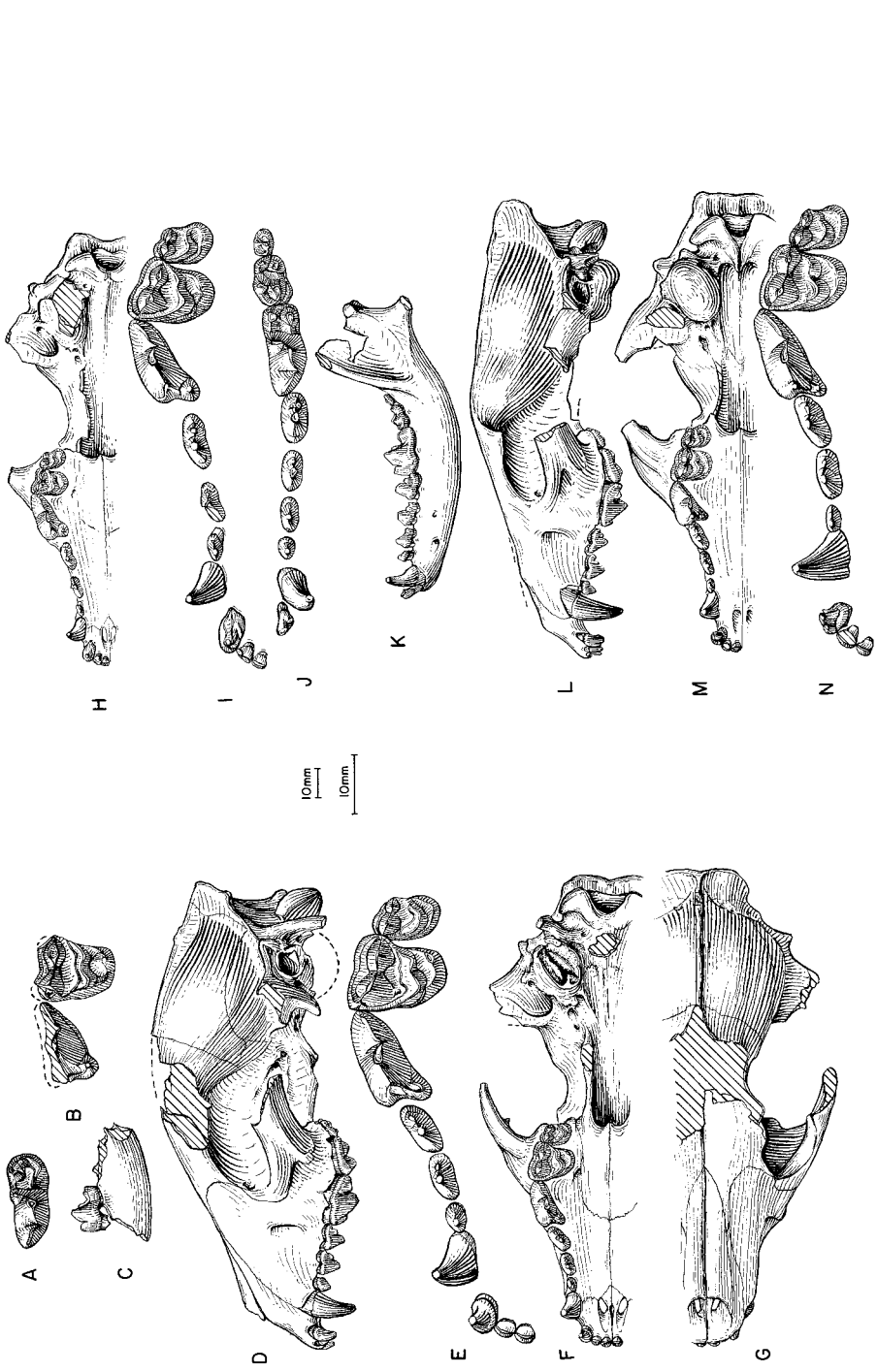

Fig. 87. *Paratomarctus temerarius*. **A**, Enlarged occlusal and **C**, lateral views of ramus and lower teeth, USNM 768, holotype, ''sands of the Niobrara River, Loup Fork'' (?late Barstovian), Nebraska. **B**, Occlusal view of upper teeth, USNM 768 (presumably a different individual from the ramus with the same number). **D**, Lateral, **E**, enlarged occlusal, **F**, ventral, and **G**, dorsal views of skull and upper teeth, F:AM 61070, mouth of Snake River, Crookston Bridge Member, Valentine Formation (late Barstovian), Cherry County, Nebraska. **H**, Ventral view of skull, **I**, upper teeth (P3 reversed from right side), **J**, lower teeth, and **K**, ramus (i3 reversed from right side), F:AM 67121, Skyline Quarry, Barstow Formation (late early Barstovian), San Bernardino County, California. **L**, Lateral, **M**, ventral, and **N**, enlarged occlusal views of skull and upper teeth, F: AM 67142, Sunnyside Quarry, Barstow Formation (early late Barstovian), San Bernardino County, California. The shorter (upper) scale is for C, D, F, G, H, K, L, and M, and the longer (lower) scale is for the rest.

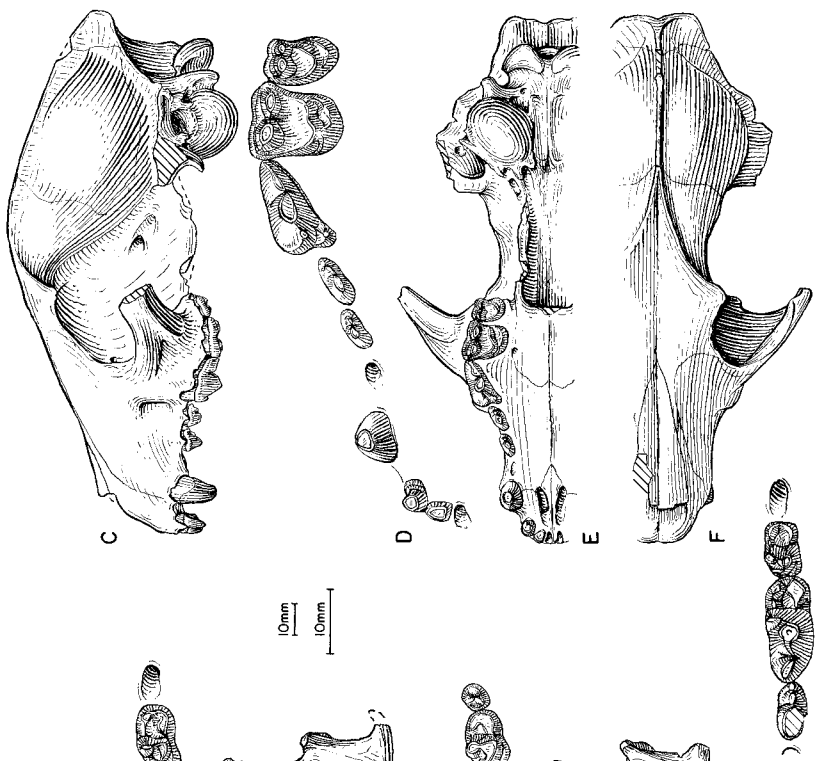

Fig. 88. **A**, Lower teeth and **B**, ramus (reversed from right side), *Paratomarctus euthos*, F:AM 61075, June Quarry, Burge Member, Valentine Formation (late Barstovian), Brown County, Nebraska. **C**, Lateral, **D**, enlarged occlusal, **E**, ventral, and **F**, dorsal views of skull and upper teeth, **G**, lower teeth, and **H**, ramus (angular process reversed from right side), *P. temerarius*, F:AM 27255, *Hemicyon* Stratum, Barstow Formation (early late Barstovian), San Bernardino County, California. **I**, Lower teeth and **J**, ramus, *P. temerarius*, YPM-PU 10453 (holotype of *Canis anceps*), Smith River Valley, "Upper beds," Deep River beds (?early Barstovian), Meagher County, Montana. The shorter (upper) scale is for B, C, E, F, H, and J, and the longer (lower) scale is for the rest.

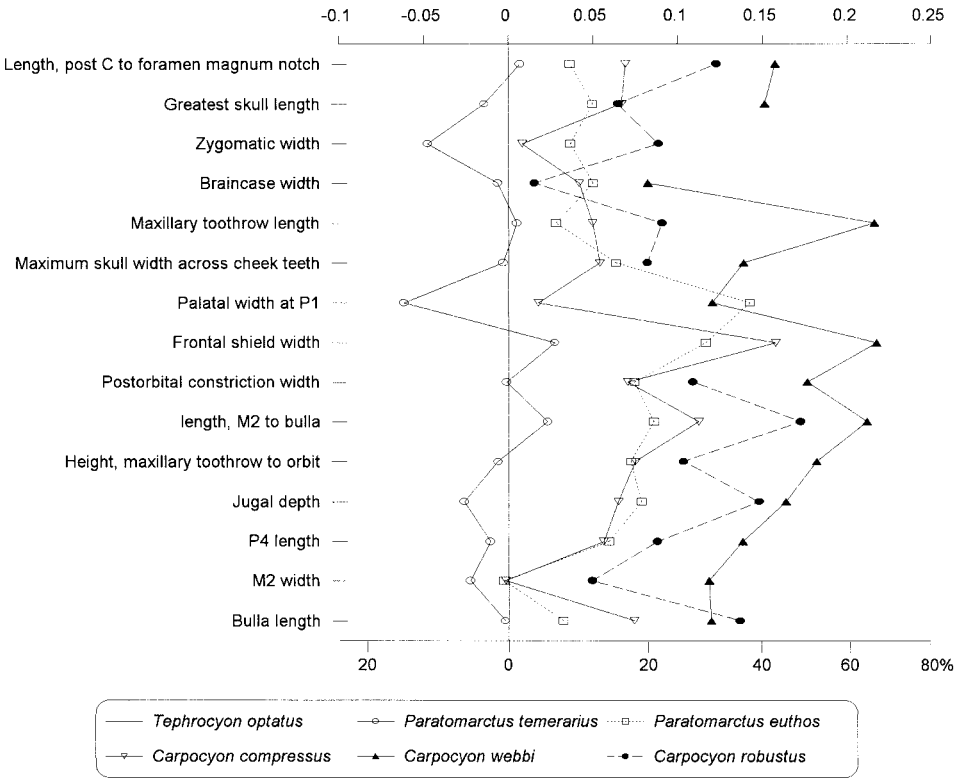

Fig. 89. Log-ratio diagram for cranial measurements of *Paratomarctus* and *Carpocyon* using *Protomarctus optatus* as a standard for comparison (straight line at zero). See text for explanations and appendix II for measurements and their definitions.

has ''page priority.'' Matthew (1924: 98) attempted to clarify this ambiguity, stating that ''many authors would consider that the figuring of the lower jaw fragment by Leidy [1869] and its implicit selection as type by Matthew, Peterson and Merriam constitute a selection of type which must stand, in accordance with the rules.'' However, Voorhies (1990a: A130) most recently still considered the maxillary as the holotype, citing the same Matthew (1924) paper but arguing for page priority. The International Code of Zoological Nomenclature (International Commission on Zoological Nomenclature, 1985: art. 24) does not recognize page priority, and Matthew (1924) is here regarded as the first reviser, that is, the lower jaw was explicitly selected as the lectotype.

Fixing the lower jaw as the lectotype still leaves the question of its identity unanswered (the upper teeth that share the same number as the lectotype have a more hypocarnivorous appearance, with a short and wide P4 and a distinct hypocone on M1, and may not belong to the same species; see fig. 87B). Assuming that the lectotype was from the Valentine Formation of Nebraska, its lower carnassial is difficult to distinguish from the contemporaneous and morphologically similar *Carpocyon compressus*. Size is the only criterion that helps to place USNM 768 in our hypodigm of *Paratomarctus temerarius*. Although there is a significant overlap of the ranges of these two species (m1 length is 15.5–21 mm for *P. temerarius* and 19.5–22.5 mm for *C. compressus*), USNM 768 (m1 length of 16.0 mm) happens to be close to the lower limit of *P. temerarius* and falls outside the overlapping part of the ranges of these two species.

Peterson (1910: fig. 63) was the first to refer a partial ramus (CMNH 2404) from

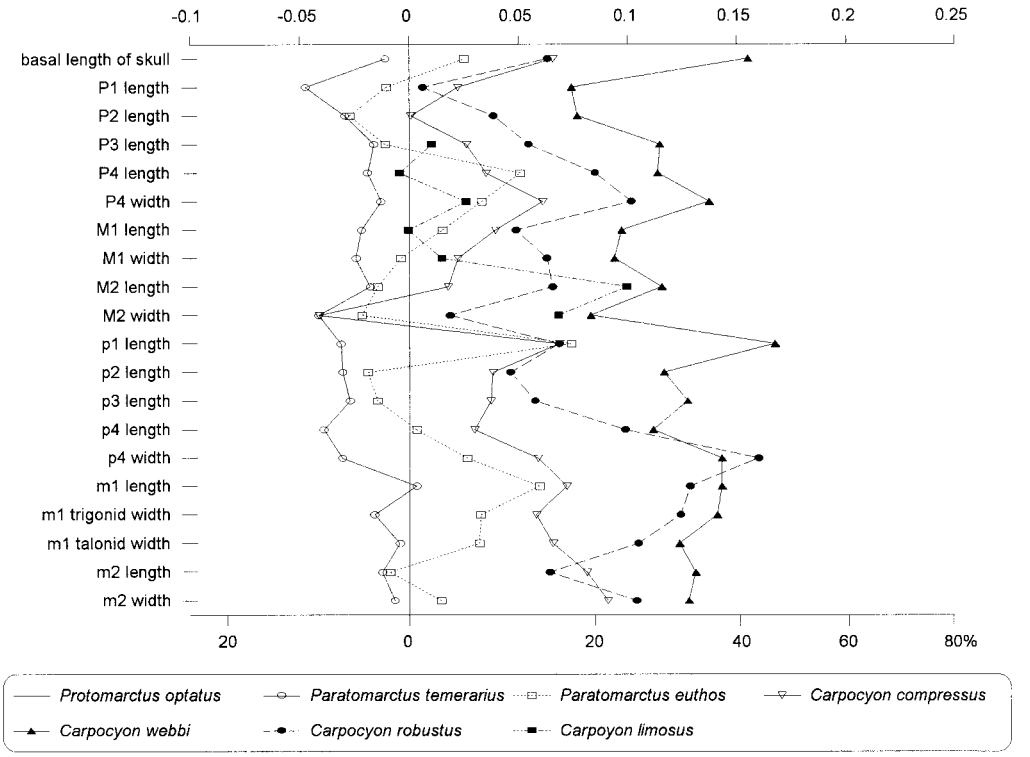

Fig. 90. Log-ratio diagram for dental measurements of *Paratomarctus* and *Carpocyon* using *Protomarctus optatus* as a standard for comparison (straight line at zero). See text for explanations and appendix III for summary statistics of measurements and their definitions.

Whistle Creek, Sioux County, Nebraska, to *Paratomarctus temerarius*. Judging from his published figure, however, CMNH 2404 has an unreduced p4 and probably belongs to *Protomarctus optatus*. Shortly afterward, Merriam (1913: fig. 8) referred a second ramus (UCMP 19402) with shortened premolars from the ''Mohave Beds'' (now Barstow Formation) of California to ''*Tephrocyon temerarius*.'' Voorhies (1965; and also Forsten, 1970) referred two rami from the Trail Creek Quarry, Wyoming, to *Tomarctus rurestris*. The Wyoming specimens appear to compare well, both in size and shape, with *Paratomarctus temerarius*. Additional materials (upper and lower jaws) from the Railway Quarries near Valentine, Nebraska, were recently described by Evander (1986: figs. 7B, 8B), who assigned them to *Tomarctus* near *T. euthos*. We now consider these lower Valentine materials to belong to *P. temerarius*. Most recently, Voorhies (1990a: A128) referred a large sample of specimens from the Norden Bridge Quarry, extending the known range of this species in the Great Plains to the base of the Valentine Formation.

Scott (1893) described ?*Canis anceps* from the ''*Cyclopidius* beds'' (?early Barstovian) of Montana as a new form. The holotype, YPM-PU 10453, is still the only specimen known from this locality, and its poor preservation permits no knowledge beyond the three lower teeth (fig. 88I, J). The main distinction of *C. anceps* is its peculiar m2, which features a small trigonid due to the very anteriorly located protoconid and metaconid, as well as a widened talonid with a large basin surrounded by a distinct entoconid on the lingual border. Other than these peculiarities, its dental proportions match well with those of *Paratomarctus temerarius*.

In the late Hemingfordian Sheep Creek Formation of Nebraska, a partial ramus

(AMNH 18915, presently referred to *Protomarctus optatus*) shows the distinctly reduced premolars with a backward hook of their main cusps in *Paratomarctus temerarius*. In fact, this individual, in which the entire lower cheekteeth series is preserved, is so similar to the topotype series of *P. temerarius*, both in size and shape, that were it found in the Valentine Formation there would be no doubt about its taxonomic assignment to *P. temerarius*. We chose to view AMNH 18915 as an individual variation of *Protomarctus* from an otherwise uniform sample from the Sheep Creek, rather than treating it as an early occurrence of *P. temerarius*. Such an occurrence of a *temerarius*-like individual within the population of *Protomarctus* in the Sheep Creek Formation is not surprising given our postulated phylogeny, which shows that *Protomarctus* may have given rise to *P. temerarius*.

Paratomarctus euthos (McGrew, 1935)

Figures 88A, B, 91–93

Cynodesmus euthos McGrew, 1935: 305, figs. 1–3; 1938b: 311.

Tomarctus euthos (McGrew): VanderHoof and Gregory, 1940: 159, figs. 7d, 8d. White, 1941b: 95. Downs, 1956: 235. Macdonald, 1960: 965, fig. 3. Webb, 1969a: 37, fig. 6. Munthe, 1998: 135.

Tomarctus sp.: Munthe, 1989: 42, figs. 11A, 17A (F:AM 61088).

HOLOTYPE: UCMP 29282, skull with I1–I2 alveoli and I3–M2 (fig. 91) from Gordon Creek Quarry, UCMP loc. V3313, Burge Member of the Valentine Formation (late Barstovian), Cherry County, Nebraska.

REFERRED SPECIMENS: Burge Member of the Valentine Formation (late Barstovian), Cherry and Brown counties, Nebraska: Burge Quarry: F:AM 61072, left ramus with c1–p2 alveoli, p3–m2, and m3 alveolus; F:AM 61074, right partial ramus with m1–m2 and m3 alveolus; F:AM 61078, left ramus with i2–m3; F:AM 61079, right ramus with c1 broken–m1 and m2–m3 alveoli; F:AM 61080, right partial ramus with p1–p2 alveoli, p3–m1, and m2–m3 alveoli; F:AM 61082, right partial ramus with p2–p3 alveoli, p4 broken–m1, and m2 broken; F:AM 61084, right partial ramus with p2–p3 roots and p4–m1; F:AM 61086, immature skull with I3, C1 erupting, and P4–M2; F:AM 67340, left isolated m1; F:AM 67350, partial skull with I3–P2 alveoli, P3–P4, and M1 alveolus; F:AM 67352, posterior part of skull; and UCMP 32242, right ramus with c1, p1 alveolus, p2–m1, and m2–m3 alveoli (VanderHoof and Gregory, 1940: figs. 7d, 8d; Webb, 1969a: fig. 6). Gordon Creek Quarry: F:AM 67353, right immature partial ramus with dp4 broken and m1–m2 unerupted. South side of Niobrara River: F:AM 61087, left partial maxillary with P3–P4. June Quarry: F:AM 61073, right partial ramus with p3–m2 and m3 alveolus; F:AM 61075, right ramus with c1, p1–p2 alveoli, p3–m2, and m3 alveolus (fig. 88A, B); F:AM 61076, right ramus with c1 erupting, p1–p2 alveoli, p3–m2, and m3 alveolus; F:AM 61077, right partial ramus with c1–m2 (p1, p3, and m3 alveoli); F:AM 61081, left ramus with c1–p1 alveoli and p2–m2 (m1 broken and m3 alveolus); F:AM 61083, left partial ramus with c1–p3 alveoli, p4–m2, and m3 alveolus; F:AM 61085, posterior part of skull with P4–M2; and F:AM 70618, right partial ramus with p3–m1. Lucht Quarry: F:AM 70602, right partial ramus with p1–p3 alveoli and p4–m1; F:AM 70603, left partial ramus with p4–m2 and m3 unerupted; F:AM 70605, posterior part of skull; and F:AM 105308, right ramus with i1–i3 alveoli, c1 broken, p1–p3 alveoli, p4–m2, and m3 alveolus. Talus on south side of the Niobrara River above Garner Bridge: F:AM 61352, right partial maxillary with P4–M1 both broken.

Equivalent to the Burge Member of the Valentine Formation (late Barstovian), Sheridan County, Nebraska: Extension Quarry: F:AM 67355, posterior part of skull and fragments including left partial maxillary with P4–M1 both broken and M2. Paleo Channel Quarry: F:AM 67357, right immature ramus with c1 erupting, p1 alveolus, p2 erupting, dp3–dp4, m1–m2 alveoli, and m3 unerupted.

Clayton or East Clayton quarries, Cap Rock Member, Ash Hollow Formation (early Clarendonian), Brown County, Nebraska: F:AM 61095, anterior part of skull with I1–P1 alveoli and P2–M2; F:AM 61096, left ramus with c1 broken, p1 alveolus–m1, and m2–m3 alveoli; F:AM 61097, left partial ramus with c1–p1 alveoli and p2 broken–m1 (p4 bro-

ken); F:AM 61098, left isolated m1; F:AM 61099, left partial ramus with p4–m2 (m1 broken and m3 alveolus); F:AM 61099A, right partial ramus with p1–p2 alveoli, p3 broken–p4, and m1 broken; and F:AM 61099B, right partial maxillary with P4–M1.

Undifferentiated beds of Ogallala Group, equivalent to the Cap Rock Member (early Clarendonian) of Ash Hollow Formation, Todd County, South Dakota: Hollow Horn Bear Quarry: F:AM 61089, partial skull with P1 alveolus–M2 and mandible with i1 alveolus–m2 (p1 and m3 alveoli) (fig. 92); F:AM 61092, right partial ramus with c1–p2 alveoli, p3–m1, and m2–m3 alveoli; F:AM 61093, left partial ramus with i1–i3 alveoli and c1–m1 (p1 and p3 alveoli); F:AM 61094, right partial ramus with c1 broken–p1, p2 alveolus–p4, m1 broken, and m2–m3 alveoli; F:AM 61100, right partial maxillary with P4–M1; F:AM 67536, right humerus; F:AM 67536A, left distal part of humerus; F:AM 67536B, partial right humerus; F:AM 67537, partial radius; F:AM 67538, left proximal part of femur; F:AM 67539, left tibia; F:AM 67539A, left distal part of tibia; F:AM 67539B, distal end of fibula; F:AM 67540, right metacarpal II; F:AM 67540A, left proximal part metacarpal IV; F:AM 67540B, left broken metacarpal V; F:AM 67540C, left metacarpal II; F:AM 67541, right metatarsal I; F:AM 67542, right metatarsal II; F:AM 67542A, left proximal part of metatarsal II; F:AM 67543, right metatarsal V; F:AM 67543A, right broken metatarsal V; F:AM 67544, 67544A, and 67544B, three calcanea; F:AM 67544C, D, two astragali; and F:AM 67544E–G, three first phalanges. Canyon of Little White River: AMNH 10808, right partial ramus with p4–m2 (all broken) and m3 alveolus; and AMNH 10809, left partial ramus with p4–m2 (all broken) and m3 alveolus.

Driftwood Creek, 16 mi southeast of Trenton, south side of Republic River, temporally equivalent to the Cap Rock Member, Ash Hollow Formation (early Clarendonian), Hitchcock County, Nebraska: F:AM 30905, left ramal fragment with p1 alveolus–p4 and m1 broken.

Thomas Fox Ranch, Mission Fauna, Ogallala Group undivided (early Clarendonian), Mellette County, South Dakota: SDSM 53250 (referred to *Tomarctus euthos* by Macdonald, 1960: fig. 3), left ramus with p1 alveolus, p2–m2, and m3 alveolus.

Clarendon Beds (early Clarendonian), Donley County, Texas: White Fish Creek, Quarry 6: F:AM 70750, articulated skull and mandible with I1–M2 and i1–m3, and articulated partial skeleton including partial vertebrae, ribs, broken scapula through nearly complete manus, and partial pelvis through pes; F:AM 70751, immature articulated skull and mandible with broken deciduous C1 and premolars, and P4–M2 unerupted, and broken deciduous c1–premolar and p4–m3 unerupted, and articulated partial skeleton with crushed front and hindlimbs; F:AM 70752, crushed articulated skull and partial mandible with I1–M2 and i1–m3 (some teeth broken); and F:AM 70753, articulated skull and mandible with I1–M2 and i1–m3, and nearly complete articulated skeleton. Quarry 7, Ro Ranch: F:AM 61090, right partial ramus with m1–m3. Location 5, Quarry 3: F:AM 61108, left partial ramus with i2 broken, c1, p1 alveolus–m1, and m2–m3 alveoli. Quarry 1: F:AM 61107, left ramus (with healed wound) with i1–c1, p1–p3 alveoli, m1–m2, and m3 alveolus. MacAdams Quarry (Location 17, Quarry 1), 10 mi north of Clarendon: F:AM 61109, left partial ramus with p2–p4, m1–m2 both broken, and m3 alveolus; and F:AM 61110, right immature partial maxillary with dP4 broken.

Merritt Dam Member, Ash Hollow Formation (late Clarendonian), Brown and Cherry counties, Nebraska: North of Crane Bridge, Niobrara River: F:AM 61088, skull fragments, right premaxillary-maxillary with I3–P4 (P1 alveolus and M1 broken), mandible with i3–m2 (c1 broken and m3 alveolus), fragmentary scapula, both ulnae (Munthe, 1989: fig. 11A), distal end of right radius, fragment of pelvis, baculum, distal end of femur, right tibia (Munthe, 1989: fig. 17A) and partial left tibia, both calcanea, incomplete metacarpal III, metacarpals IV and V, metatarsals II, III, IV, and incomplete V, carpals, tarsals, vertebrae, and incomplete ribs. Bear Creek Quarry: F:AM 61111, left ramus and right partial ramus with i3–m2 and m3 alveolus; and F:AM 61112, right partial ramus with c1–m1 (p1 alveolus and m1 broken). Talus slope near Old Wilson Quarry: F:AM 105307, left isolated P4. *Leptarctus*

Quarry: F:AM 61102, partial crushed skull with I1–I3 alveoli, C1–P1 broken, P2–P4, and M1–M2 alveoli; and F:AM 61103, left ramus with i1–i3 alveoli and c1–m3. *Machairodus* Quarry: F:AM 61101, skull with I1–I3 alveoli and C1–M2 (P1 and P3 alveoli) and left ramus with i1–i3 alveoli, c1, p2–m2, and m3 alveolus (fig. 93). Trailside Kat Quarry: F:AM 61106, right partial maxillary with P2–P3 and P4 broken. East Kat Quarry: F:AM 61105, left partial ramus with m1 and m2–m3 alveoli; and F:AM 67354, left maxillary fragment with P4. Quarter Kat Quarry Channel: F:AM 67354A, right isolated P4. West Line Kat Quarry Channel: F:AM 61104, left partial ramus with p3 broken–m1 and m2–m3 alveoli. Xmas Quarry Zone: F: AM 25146, left partial ramus with c1–p1 alveoli and p2–m3 (p3–p4 broken).

DISTRIBUTION: Late late Barstovian of Nebraska; early Clarendonian of Nebraska, South Dakota, and Texas; and late Clarendonian of Nebraska.

EMENDED DIAGNOSIS: *Paratomarctus euthos* can be distinguished from *P. temerarius* by larger size, enlarged postorbital process of frontal, wide frontal shield, broadened palate and laterally flared dorsal border of ramus, more elongated external auditory meatus, and weak symphyseal boss on anteroventral border of ramus.

DESCRIPTION AND COMPARISON: Unlike the poorly founded *Paratomarctus temerarius*, *P. euthos* was established on a well-preserved skull. Associated skulls and lower jaws in the present study, however, permit a more complete knowledge of the entire cranial and dental morphology. In addition, through reference of a much larger sample in the hypodigm, we are in a better position to evaluate its variation.

Paratomarctus euthos is 8% (average of all dental measurements) larger than *Paratomarctus temerarius*. The most noticeable difference between *P. temerarius* and *P. euthos* is the broader palate and forehead of the latter (palate width at P1 and frontal shield width in fig. 89), especially shown by individuals in the Ash Hollow Formation. Associated with the broad palate is a widened anterior part of the skull relative to the posterior part, as well as a laterally flared anterior ramus. These features parallel similar developments in *Euoplocyon* and *Aelurodon*. Furthermore, *P. euthos* has a weak boss at the ventral border of the mandibular symphysis, as also occurs in *A. taxoides*. However, in contrast to *Euoplocyon*, and to a lesser degree to *Aelurodon*, *P. euthos* still possesses a fully bicuspid talonid on the m1, and its reduced premolars are characteristic of the Borophagina clade.

Individuals in the Burge Member of the Valentine Formation are transitional between *P. temerarius* and the Clarendonian individuals of *P. euthos*. The Burge individuals tend to have a more gracile appearance with narrower palates and less flared lower jaws than the more robust skulls and broader palates in individuals from the Ash Hollow Formation. The Clarendonian individuals also display initial tendencies toward hypercarnivory in their reduction of the m1 entoconid and m2 metaconid and smaller M2 and m2.

One individual from the *Machairodus* Quarry, F:AM 61101 (fig. 93), has a rather flat forehead and reduced m2 metaconid, features commonly seen in *Aelurodon*. Furthermore, its P4 parastyle is poorly developed and its p1 is absent. F:AM 61101 has otherwise typical *P. euthos* features (e.g., small premolars, a boss on the ramus), and its peculiarities are here considered as variations within the species.

A ramal fragment with p2–p4 (F:AM 30905) from Driftwood Creek, Nebraska, is also questionably referred to this species. Its large size is not seen in more typical individuals from the early Clarendonian of Nebraska.

DISCUSSION: *Cynodesmus euthos* was initially conceived to be in a direct line of descent to modern *Canis* (McGrew, 1935: fig. 4), in contrast to the then popular view that the latter was derived from *Tomarctus*, which was in turn derived from *Cynodesmus* (Matthew, 1924, 1930). McGrew (1935) cited an indistinct P4 parastyle on the holotype of *euthos* (a primitive character in our analysis) as his main evidence of a direct relationship with *Canis*, as opposed to better developments of the parastyle in *Tomarctus*. VanderHoof and Gregory (1940: 160), however, suggested that size of the P4 parastyle tends to be variable and that *Tomarctus* (sensu lato) is the proper generic name for *eu-*

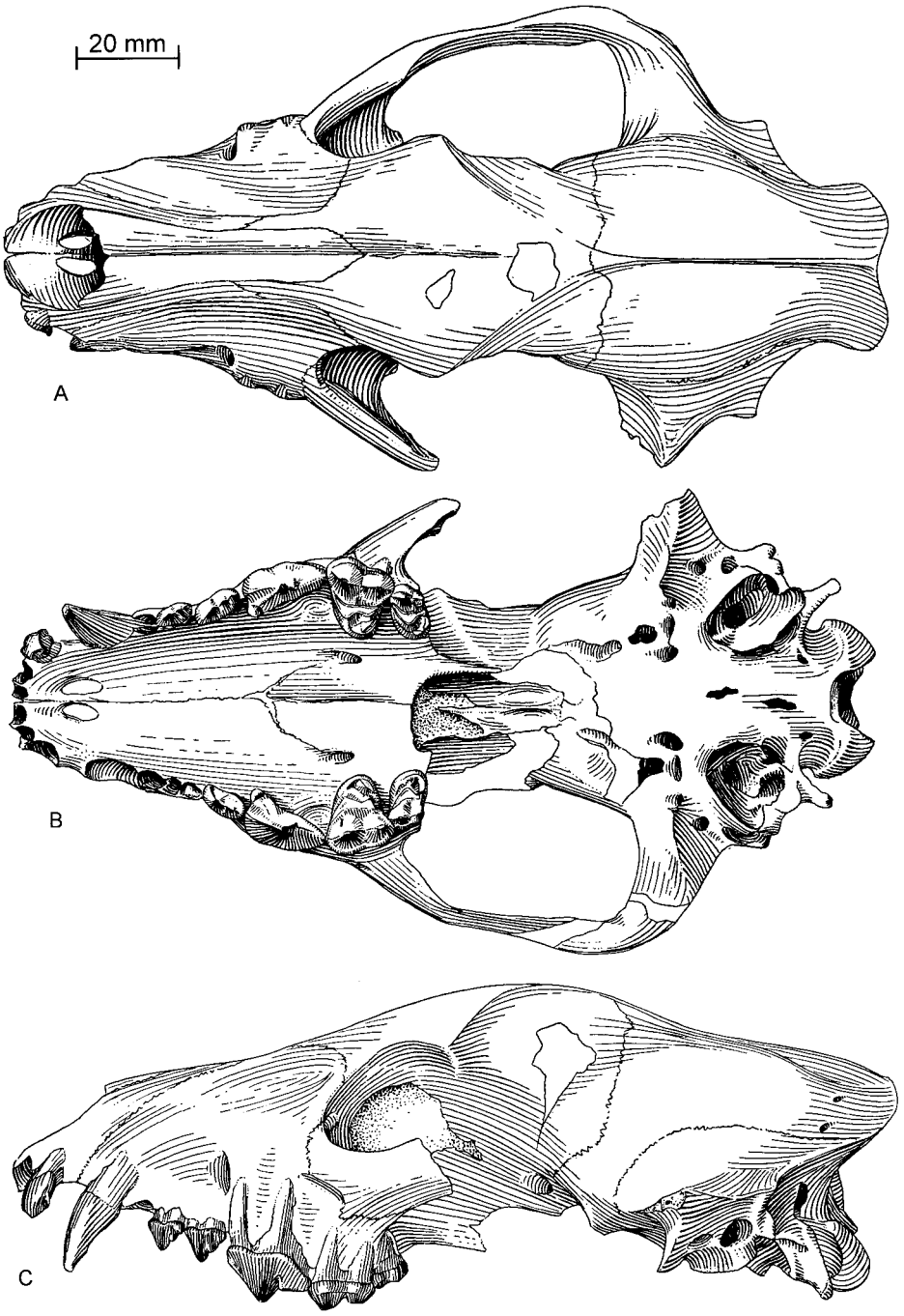

Fig. 91. *Paratomarctus euthos*. **A**, Dorsal, **B**, ventral, and **C**, lateral views of skull, UCMP 29282, holotype, Gordon Creek Quarry, Burge Member, Valentine Formation (late late Barstovian), Cherry County, Nebraska. Adopted from McGrew (1935: figs. 1–3).

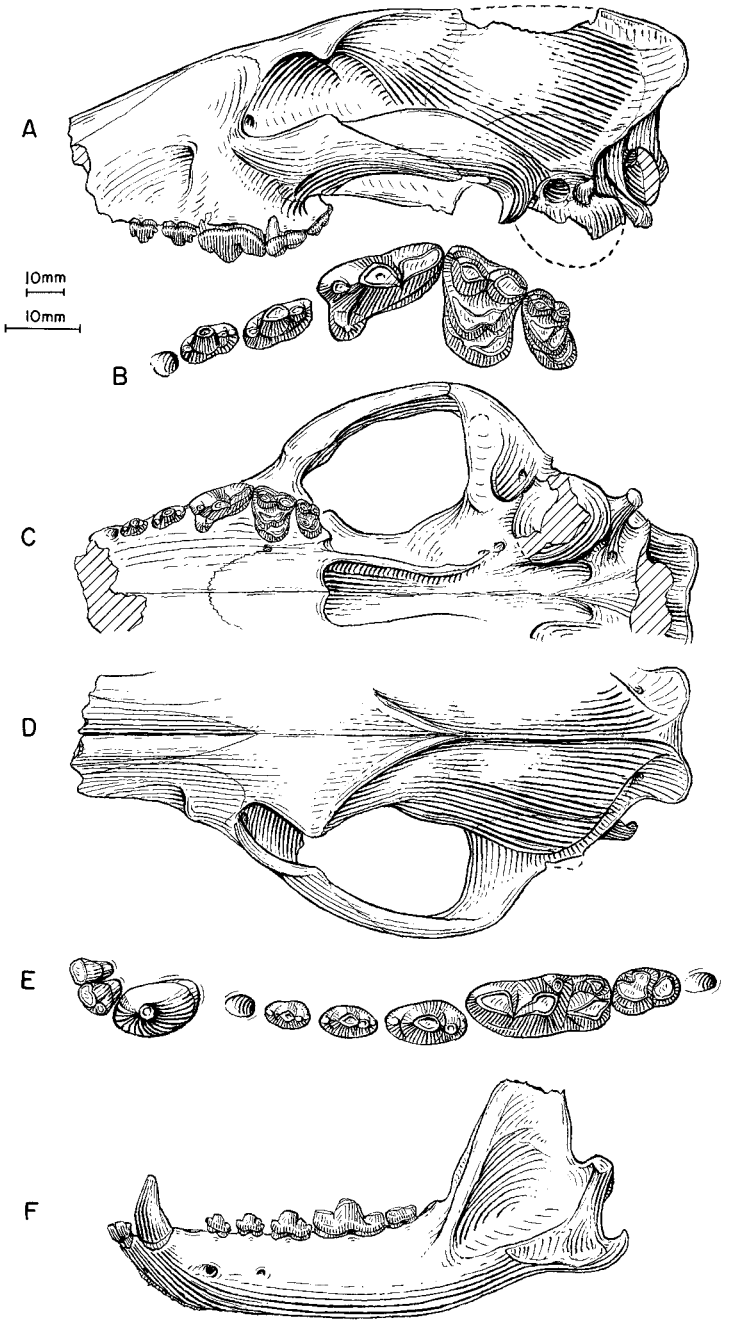

Fig. 92. *Paratomarctus euthos*. **A**, Lateral, **B**, enlarged occlusal, **C**, ventral, and **D**, dorsal views of skull and upper teeth, **E**, lower teeth, and **F**, ramus, F:AM 61089, Hollow Horn Bear Quarry, Ogallala Group (early Clarendonian), Todd County, South Dakota. The shorter (upper) scale is for A, C, D, and F, and the longer (lower) scale is for the rest.

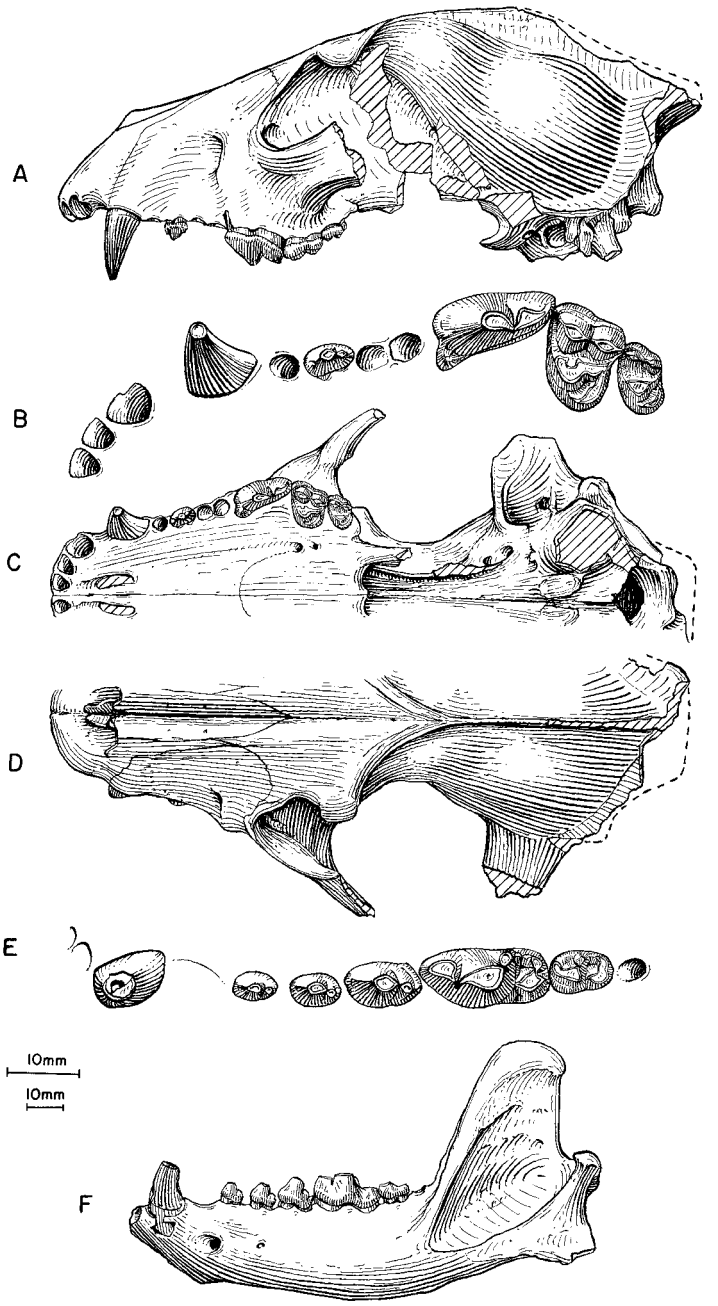

Fig. 93. *Paratomarctus euthos*. **A**, Lateral, **B**, enlarged occlusal, **C**, ventral and **D**, dorsal views of skull and upper teeth, **E**, lower teeth, and **F**, ramus, F:AM 61101, *Machairodus* Quarry, Merritt Dam Member, Ash Hollow Formation (late Clarendonian), Cherry County, Nebraska. The longer (upper) scale is for B and E, and the shorter (lower) scale is for the rest.

thos. Although we recognize no close relationship among *Cynodesmus*, *Tomarctus* and *Canis* (each belongs to separate subfamilies of canids), the controversy over the parastyle is relevant in a different context. As in *Paratomarctus temerarius*, development of P4 parastyle in *P. euthos* is somewhat variable before it becomes more stabilized in the next step of the phylogeny (*Carpocyon*). The indistinct parastyle in the holotype of *P. euthos* seems to be a rare exception (one only other occurrence of this feature is found in F:AM 61101 as mentioned above), and most individuals possess a small but distinct parastyle.

Despite the lack of association of skulls and jaws, VanderHoof and Gregory (1940: figs. 7d, 8d) correctly referred a lower jaw (UCMP 32242, also figured in Webb, 1969a: fig. 6) to *P. euthos*. This ramus became the critical link in later reference of additional materials from the Mission Fauna, South Dakota (Macdonald, 1960) and from the Burge Member of the Valentine Formation, Nebraska (Webb, 1969a). These new materials, plus the more extensive hypodigm available to the present study, indicate that the species was confined to the latest Barstovian through Clarendonian of the Great Plains.

Lack of autapomorphies for *P. temerarius* and stratigraphic continuity between *P. temerarius* and *P. euthos* indicate a linear ancestral-descendent relationship of these two taxa (i.e., they form a chronospecies). Our division between these two species along the boundary of Devil's Gulch/Burge members of the Valentine Formation is thus motivated by the available name for *euthos* in the Burge Member. Trends along this anagenetic series include a slight increase in size, more robust skull and jaws (particularly its anterior portion), and incipient tendency toward hypercarnivorous dentitions (reduced m1 entoconid and m2 metaconid, and smaller M2 and m2).

Carpocyon Webb, 1969

TYPE SPECIES: *Carpocyon limosus* Webb, 1969b.

INCLUDED SPECIES: *Carpocyon compressus* (Cope, 1890); *Carpocyon webbi*, new species; *Carpocyon robustus* (Green, 1948); and *Carpocyon limosus* Webb, 1969b.

DISTRIBUTION: Early Barstovian of New Mexico, Nevada and Texas; late Barstovian of Nebraska, Kansas, Colorado, and New Mexico; early Clarendonian of Nebraska, South Dakota, and Texas; late Clarendonian of Nebraska and Colorado; early Hemphillian of Oklahoma; and late Hemphillian of Florida.

EMENDED DIAGNOSIS: Four synapomorphies unite *Carpocyon* with the *Epicyon–Borophagus* clade and distinguish it from *Paratomarctus* and more primitive taxa: greatly inflated bulla, short tube for external auditory meatus, I3 lateral accessory cusplets reduced to one, and enlarged parastyle on P4. Characters of *Carpocyon* that are primitive with respect to *Protepicyon* and higher taxa are palate narrow, masseteric fossa without anterior excavation (except in *C. robustus*), M1 paracone low-crowned, and p4 less enlarged relative to p2–p3 (except *C. robustus*). Autapomorphic characters of *Carpocyon* further distinguishing it from *Paratomarctus* and the *Protepicyon–Borophagus* clade include P4 paracone-metacone shearing blade short relative to width of tooth, M1–M2 large relative to P4, M1 quadrate with anteriorly thickened lingual cingulum, and m2 enlarged.

DISCUSSION: The present recognition of three more species (besides the type species *Carpocyon limosus*) provides a rather continuous, although still somewhat sketchy, record for this lineage of medium-size Borophagina. Webb's (1969b) inclusion of *Cynodesmus cuspidatus* Thorpe (here included in *Carpocyon compressus*) as a species of *Carpocyon* is confirmed by our phylogenetic analysis. However, too little is known about the type species *C. limosus* to permit a firm connection between it and the more primitive species referred here. Dental morphology and stratigraphic position of *C. limosus* seem to suggest that it has a Clarendonian predecessor such as *C. robustus*.

As discussed by Webb (1969b), *Carpocyon* has certain superficial similarities to some species of *Cynarctus*, owing to their convergent adaptations toward hypocarnivory. Webb went to some length to contrast the differences between these genera (and also *Alopecocyon*, which is probably a simocyonine procyonid [Beaumont, 1964]). Many of

the dental features listed by Webb, such as elongation of M1–M2 and loss of labial cingulum in *Cynarctus*, are apparently differences between advanced species of *Cynarctus* (e.g., *C. saxatillis* through *C. crucidens*) and *Carpocyon*, and these differences tend to diminish when compared with primitive species of *Cynarctus*. In our analysis, *Carpocyon* differs from *Cynarctus* in the presence of a prominently domed forehead, a distinct P4 parastyle, and a more robust p4, characters that indicate a relationship with the *Protepicyon–Borophagus* clade.

As in the *Cynarctus* clade, size reduction also occurred in *Carpocyon*, mainly in the youngest species, *Carpocyon robustus* and *Carpocyon limosus*. From *C. compressus* to *C. webbi*, there is a size increase in early *Carpocyon* that parallels similar size increases in *Aelurodon* during the late Barstovian. Beyond *C. webbi*, however, the *Carpocyon* lineage began to decrease in size (*C. robustus* and *C. limosus*) despite the continued enlargement in the *Aelurodon ferox–taxoides* lineage. In the case of *C. robustus*, the interaction with *Epicyon saevus* in the Clarendonian may have driven *C. robustus* to a smaller size to avoid competitive interaction. In the case of *C. limosus*, the reason may lie more in its further advancement in hypocarnivory, a tendency also seen in the *Cynarctus* clade.

Carpocyon compressus (Cope, 1890)

Figures 94, 95

Aelurodon compressus Cope, 1890: 1067.
?*Aelurodon compressus* (Cope): Matthew, 1909: 115.
Cynodesmus cuspidatus Thorpe, 1922b: 433, figs. 4, 5. Webb, 1969a: 35.
?*Cynodesmus* or ?*Tomarctus compressus* (Cope): VanderHoof and Gregory, 1940: 158.
Tomarctus cuspidatus (Thorpe): White, 1941b: 95.
Carpocyon cuspidatus (Thorpe): Webb, 1969b: 275. Evander, 1986: 27, figs. 3, 7C (in part). Voorhies, 1990a: A130, fig. A-31A, B. Munthe, 1998: 136.
Tomarctus cf. *brevirostris* (Cope): Messenger and Messenger, 1977: 95, fig. 1a–f.

HOLOTYPE: AMNH 8543, left partial ramus with i3 alveolus, c1 broken, p1–p3 alveoli, p4, m1 broken, and m2–m3 alveoli (fig. 94A, B) from ''Loup Fork,'' presumably Valentine Formation (late Barstovian), Cherry County, Nebraska.

REFERRED SPECIMENS: Norden Bridge Quarry (UNSM loc. Bw-106), Cornell Dam Member, Valentine Formation (early late Barstovian), Brown County, Nebraska: UNSM 83949, left ramus with p4–m1 and alveoli of the rest teeth; UNSM 83956, right M1–M2; and UNSM 83957, right M2.

Crookston Bridge Member, Valentine Formation (late Barstovian), Boyd and Cherry counties, Nebraska: Railway Quarry A (UNSM loc. Cr-12): UNSM 25883 (AMNH cast 97252), left partial skull with P4–M2 (fig. 94E, F); UNSM 76613, left ramus with c1–p3 alveoli, p4 broken–m2, and m3 alveolus (referred to *Carpocyon cuspidatus* by Evander, 1986: figs. 3, 7C); and UNSM 76619, right distal part humerus. Railway Quarry B (UNSM loc. Cr-13): UNSM 3074-86, left ramus with p2–p3 alveoli, p4–m2, and m3 alveolus; and UNSM 3196-86, left ramus with c1 broken–m3 (p1 and p3 alveoli and m1 broken). Jamber Quarry (UNSM loc. Bd-6): UNSM 9403 (including UNSM 9404), right ramus with c1–m2 and m3 alveolus (referred to *Tomarctus* cf. *brevirostris* by Messenger and Messenger, 1977: 95, fig. 1a–f). Garner Bridge South (UNSM loc. Cr-123): UNSM 1213-89, left ramal fragment with p1 alveolus and p2–p4. Northeast of Garner Bridge (UNSM loc. Cr-139): UNSM 1231-89: right maxillary with P4–M2. West Valentine Quarry (UNSM loc. Cr-114): UNSM 2520-87, left maxillary with M1–M2; and UNSM 2750-87, left m1.

Bone Creek, 7 mi north and 5 mi east of Ainsworth, undifferentiated beds of the Valentine Formation temporally equivalent to the Crookston Bridge Member (M. R. Voorhies, personal commun. 1997) (late Barstovian), Brown County, Nebraska: UNSM 2556-90, complete skull and mandible with complete upper and lower dentition (fig. 95), partial skeleton with nearly complete vertebrate column, partial left and right scapulae, left forelimb, partial pelvis, baculum, and both hindlimbs.

Niobrara River, presumably from Crookston Bridge Member (M. F. Skinner, personal commun.), Valentine Formation (late Barsto-

vian), Cherry County, Nebraska: YPM 12788, right and left partial maxillary with P2 broken–M2 (holotype of *Cynodesmus cuspidatus* Thorpe, 1922b: figs. 4, 5) (fig. 94C, D).

Hazard Homestead Locality (UNSM Hk-104), Driftwood Creek, Republic River, Ogallala Formation (late Barstovian, temporally equivalent to Crookston Bridge Member of Valentine Formation), Hitchcock County, Nebraska: UNSM 91102, left ramus with i1–p3 alveoli, p4–m1, and m2–m3 alveoli; and UNSM 1112-92, right ramus with p2 broken–m1 and m2 alveolus.

Devil's Gulch Member, Valentine Formation (late Barstovian), Brown and Keyapaha counties, Nebraska: Devil's Gulch Horse Quarry: F:AM 25220, left partial ramus with p2–p3 alveoli, p4–m1, and m2–m3 alveoli; F:AM 61351, left isolated M1; and F:AM 67356, right isolated unerupted M1. Moore Creek: F:AM 25120, right maxillary fragment with P3 broken–P4 and isolated M2, and right and left rami with i1–m2 (p1 alveolus) and m3 alveolus (fig. 94G–I). No locality data: F:AM 25121, two parts of left ramus with c1 broken–p4 (p1 alveolus and p3 broken) and m1–m2 (m3 broken), axis, and right tibia. Horsethief Canyon No. 2: F:AM 25122, right partial ramus with m2 and m3 alveolus, and left distal part of humerus. Talus of Devil's Gulch: F:AM 61327, right ramal fragment with m1–m2 both broken and m3 alveolus. Half mi west and 40 ft above the Devil's Gulch Horse Quarry: F:AM 61319, left partial ramus with c1 broken, p1–p2 alveoli, p3–m1 all broken, m2, and m3 alveolus. Two and one-half mi northeast of Burton, 30 ft below Burge Channel: F:AM 61320, left partial ramus with p3–m2 (m1 broken).

H. A. Davis Ranch, east side of Snake River, 150 ft below top of Cap Rock, Valentine Formation (late Barstovian), Cherry County, Nebraska: UNSM 25888 (AMNH cast 97152), left ramus with c1 broken, p1–p3 alveoli, p4 broken–m1, and m2 broken.

Horse Quarry, Pawnee Creek Formation (late Barstovian), Weld County, Colorado: F:AM 28320, left ramal fragment with m1 broken–m3.

Silica Mine, Ogallala Group (?late Barstovian), Calvert, Kansas: F:AM 30903, left isolated m1, left calcaneum, and two metapodials.

Stewart Spring Fauna (late early Barstovian), UCMP loc. V5570, Esmeralda Formation, Mineral County, Nevada: UCMP 45236, left ramus with p1–p3 alveoli, p4–m2, and m3 alveolus.

DISTRIBUTION: Late Barstovian of Nebraska, Colorado, and Kansas.

EMENDED DIAGNOSIS: *Carpocyon compressus* possesses derived characters for the genus: inflated bulla, short tube for auditory meatus, P4 wide relative to length, large P4 parastyle, large upper molars relative to P4, anteriorly extended lingual cingulum of M1 giving the tooth a more quadrate outline, and large m2. *C. compressus* is generally smaller and more primitive in all known characters with respect to other species of *Carpocyon*, such as less prominent subangular lobe of mandible and less expanded posterior cingulum of M2.

DESCRIPTION AND COMPARISON: Until quite recently, knowledge of this species from the topotype area was mostly derived from fragmentary jaws. It is thus fortunate that a complete skull and skeleton from Bone Creek (USNM 2556-90; fig. 95) preserves nearly every part of its skeletal morphology. Furthermore, the presence of a baculum in this specimen permits positive identification of it as a male. Two bite marks on top of its head, one at the frontal–nasal juncture, and another (larger, deeper, and penetrating into the olfactory lobe of the brain cavity) behind the postorbital process of frontal seem to be the cause of its death (no sign of healing), and judging from the distance between the bite marks were from an animal of much larger size.

Except for its tendency toward a hypocarnivorous dentition, the skull of *Carpocyon compressus* is that of a generalized, medium-size Borophagina. The postorbital process of the frontal is well developed. It has a rather domed forehead, but not as prominently domed as in *C. webbi*. The frontal sinus extends slightly behind the frontal–parietal suture. The bulla is well inflated compared to those in *Paratomarctus*, but is not as hyperinflated as in *C. webbi*. There is a short external auditory meatus. The mastoid process

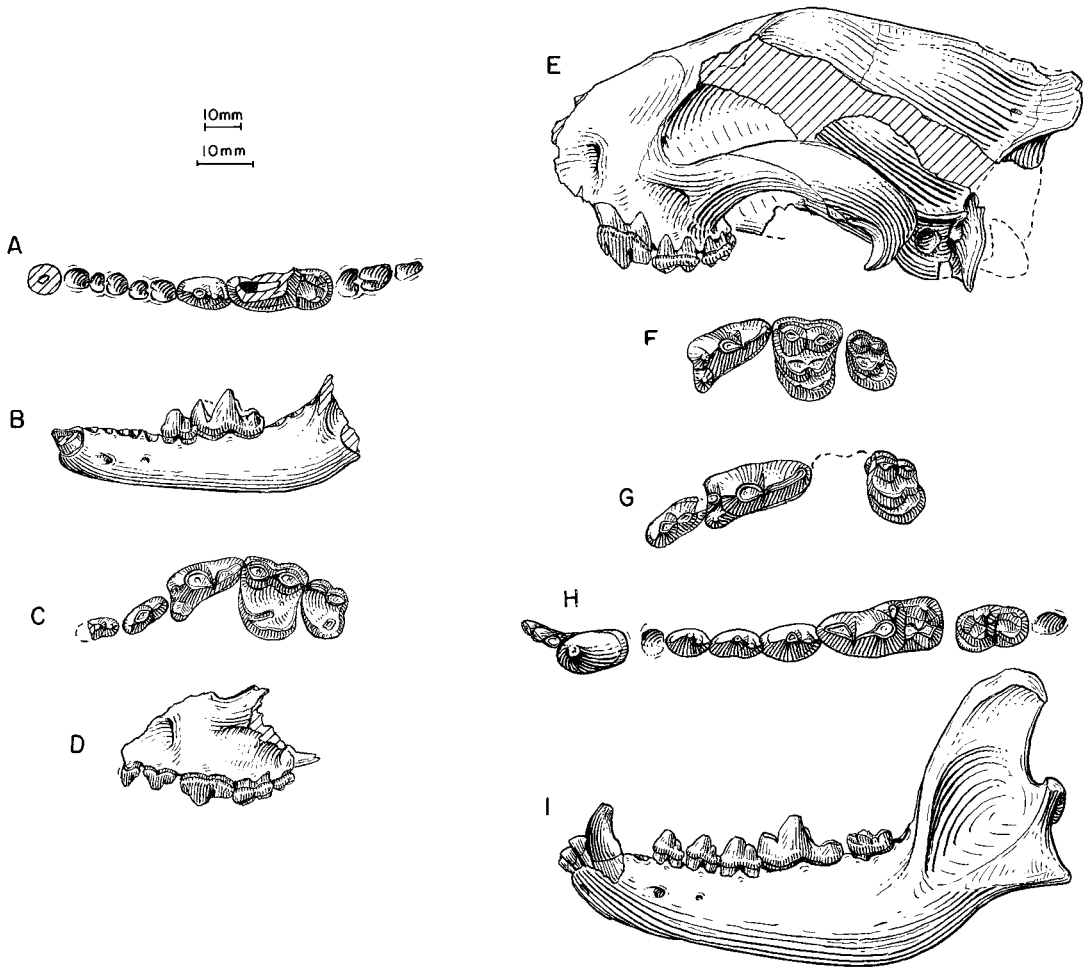

Fig. 94. *Carpocyon compressus*. **A**, Lower teeth and **B**, ramus, AMNH 8543, holotype, ''Loup Fork,'' ?Valentine Formation (late Barstovian), Nebraska. **C**, Upper teeth and **D**, lateral view of maxillary, YPM 12788 (holotype of *Cynodesmus cuspidatus*), Niobrara River, ?Crookston Bridge Member, Valentine Formation (late Barstovian), Cherry County, Nebraska. **E**, Lateral view of skull and **F**, upper teeth, UNSM 25883, Railway Quarry A, Crookston Bridge Member, Valentine Formation (late Barstovian), Cherry County, Nebraska. **G**, Upper teeth, **H**, lower teeth, and **I**, ramus, F:AM 25120, Moore Creek, Devil's Gulch Member, Valentine Formation (late Barstovian), Brown County, Nebraska. The shorter (upper) scale is for B, D, E, and I, and the longer (lower) scale is for the rest.

is not enlarged. The palate remains narrow as compared to those in *Epicyon* and *Borophagus*.

As the earliest member of *Carpocyon*, *C. compressus* has the basic dental configuration of the genus: distinct P4 parastyle, P4 protocone without a ridge connecting it with the parastyle, upper molars enlarged with a quadrate outline, M1 paracone and metacone low-crowned and subequal, and m2 large. *C. compressus* also lacks the more distinct subangular lobe and has an m1 paraconid more anteriorly oriented, features that first appear in *C. webbi*.

Among the Nebraska samples, individuals of *Carpocyon compressus* from the Crookston Bridge Member are the smallest, followed by individuals of larger size in the Devil's Gulch Member. This size increase is continued by *C. webbi* in the Burge Member,

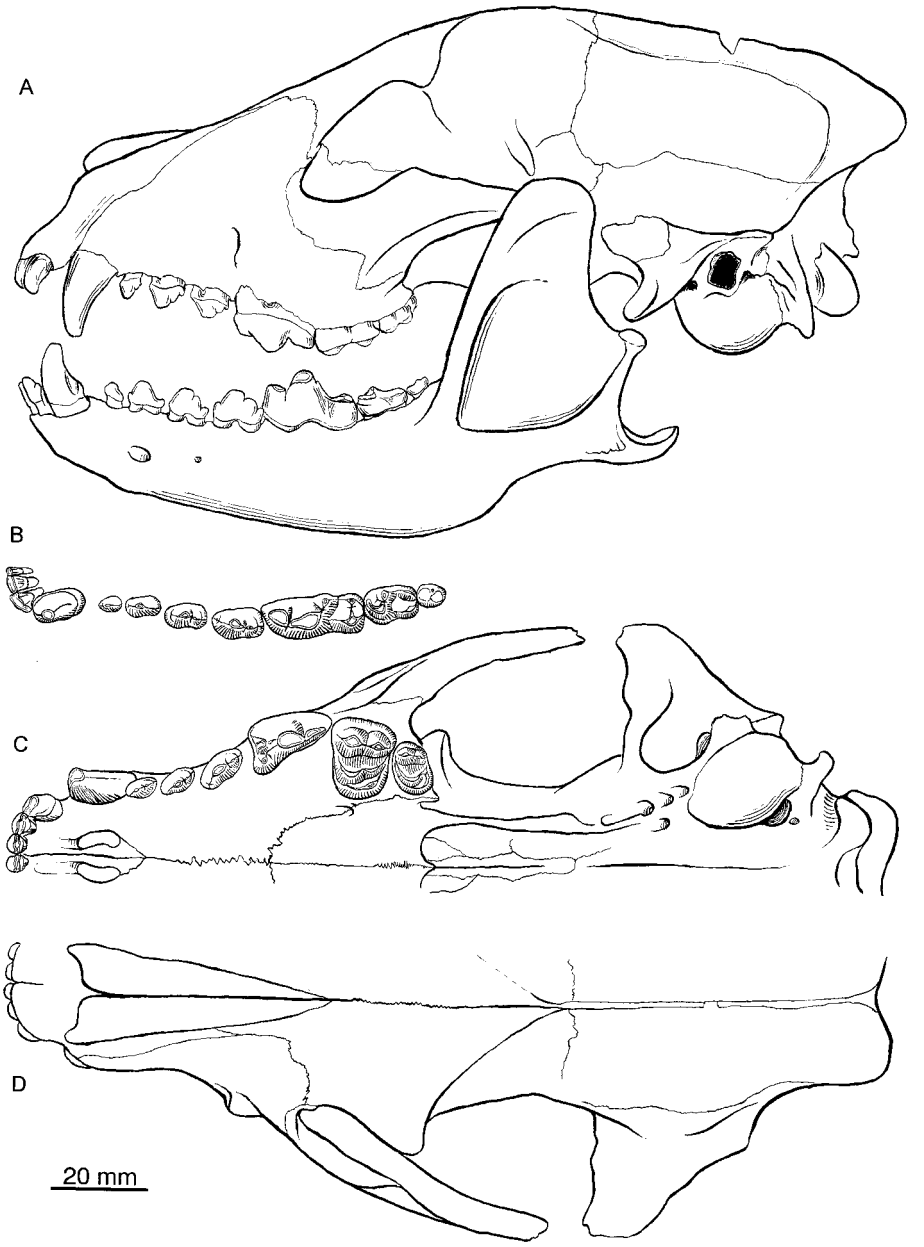

Fig. 95. *Carpocyon compressus*. **A**, Lateral, **B**, occlusal, **C**, ventral, and **D**, dorsal views of skull and mandible, UNSM 2256-90, Bone Creek, undifferentiated beds of Valentine Formation temporally equivalent to Crookston Bridge Member (late Barstovian), Brown County, Nebraska. Illustration by X. Wang.

which is otherwise quite similar to *C. compressus*.

DISCUSSION: Cope (1890) initially compared *compressus* with *Aelurodon* (mainly *A. saevus*, which is presently referred to *Epicyon saevus*), a proposition questioned by Matthew (1909: 115) and rejected by VanderHoof and Gregory (1940). The one

and a half cheekteeth (plus root of c1) in Cope's holotype of *Aelurodon compressus* are inadequate for a positive identification beyond the recognition that this specimen belongs to a young adult (absence of heavy wear) of a medium-size borophagine. The partial ramus in the holotype occludes well with a cranial fragment (UNSM 25883) from the Crookston Bridge Member of the Valentine Formation, which is nearly identical in dental proportions to Thorpes' holotype of *Cynodesmus cuspidatus* (probably also from the Crookston Bridge Member; M. F. Skinner, personal commun.). Although there is always a slight chance that these specimens represent more than one species, we consider them conspecific for lack of other borophagines within this size range and morphology (the contemporaneous *Paratomarctus temerarius* is closest in size range but has much more reduced p4s than shown on the alveoli of the holotype of *C. compressus*).

Webb (1969b: 281) included *Cynodesmus cuspidatus* in his newly established *Carpocyon*, having regarded *cuspidatus* as the ''first clear-cut embodiment'' of a postulated lineage from *Paratomarctus temerarius* to *Carpocyon limosus*. Webb's basic phylogenetic framework is substantiated by our own analysis, which provides two transitional taxa, *C. webbi* and *C. robustus*, linking the beginning and end members of the genus.

Carpocyon webbi, new species
Figures 96, 97A–E

HOLOTYPE: F:AM 61328, skull with I1–C1 alveoli and P1–M2 (fig. 96) from Midway Quarry, Burge Member, Valentine Formation (late late Barstovian), Cherry County, Nebraska.

ETYMOLOGY: Named for S. David Webb in recognition of his research on canids from Nebraska and Florida.

REFERRED SPECIMENS: Burge Member, Valentine Formation (late late Barstovian), Brown and Cherry counties, Nebraska: June Quarry: F:AM 61322, left ramus with c1–p3 alveoli, p4–m2, and m3 alveolus (fig. 97A, B); F:AM 61323, right partial ramus with p1–p2 alveoli, p3–m2 (p4–m1 both broken), and m3 alveolus; F:AM 61324, right partial ramus with p4 broken–m2 and m3 alveolus; F:AM 61326, left partial ramus with c1, p1–m1, and m3 alveoli; F:AM 61329, partial skull with C1–P1 alveoli and P2–M2; F:AM 61330, right partial maxillary with P4–M2; F:AM 61333, left partial ramus with p2, p4, and p1 and p3 alveoli; F:AM 70601, right partial ramus with m1–m2 and m3 alveolus. Lucht Quarry: F:AM 61325, left partial ramus with c1–p3 alveoli, p4–m2 all broken, and m3 alveolus; F:AM 67342, right partial ramus with i3–p1 alveoli, p2–m1 all broken, and m2 alveolus; F:AM 70606, left partial maxillary with P3–M2 (M1 alveolus); and F:AM 105334, left ramus with i1 alveolus and i2–m2 (p1, p3, and m3 alveoli). Burge Quarry: F:AM 61321, left partial ramus with m1–m2; F:AM 61331, left isolated M1; F:AM 61332, left ramal fragment with i1–p1 and p3 alveoli, p2, and p4; and UNSM 8535, left and right partial rami with p1–m2. Ewert Quarry: F:AM 61334, right ramal fragment with m2. Burge Talus, 1.5 mi below Steer Creek: F:AM 67341, left partial ramus with c1 broken–m2 (p1 alveolus). White Point Quarry, on the south fork of Deep Creek: F:AM 70623, right partial maxillary with P1 alveolus–M2 (P4 broken).

Thayer Ranch, 2 mi below Lion Bridge on Niobrara River, ?Cap Rock Member, Ash Hollow Formation (Clarendonian), Cherry County, Nebraska: F:AM 107753, left partial ramus with i1–p1 alveoli and p2–p4.

Pojoaque Member, Tesuque Formation (late Barstovian), Santa Fe County, New Mexico: Santa Cruz: F:AM 27371 and 27372, right and left maxillae with I1–I3 roots and C1–M2, and left partial ramus with p4–m3 of a single individual. Santa Cruz, Rio Grande Slope: F:AM 27366B, right ramus with c1 broken–m2 (p1, p4, and m3 alveoli) (fig. 97C, D). Santa Cruz Red Layer: F:AM 27366, right partial ramus with i1–p4 alveoli and roots, m1 broken–m2, and m3 alveolus. Santa Cruz First Wash: F:AM 61335, incomplete anterior part of skull with I1–I3 alveoli, C1 broken, P1–P3 alveoli, and P4 broken–M2, and posterior part of skull (fig. 97E); F:AM 61380, left partial ramus with i3–p3 alveoli, p4–m1 broken, and m2–m3 alveoli. South Pojoaque Bluffs: F:AM 50157, left partial maxillary with P1–P3 al-

veoli and P4 broken–M2, and right and left partial rami with p1 root–m2. Lower Pojoaque Bluffs, west of Huerfano Fault, San Ildefonso Grant: F:AM 61336, right partial ramus with c1 broken, p1 alveolus, p2–p4, m1 broken–m2, and m3 alveolus. ?Santa Cruz: F:AM 27369, left ramal fragment with p4–m1 both broken and m2–m3 alveoli; and F:AM 27370, left partial maxillary with P4–M1 both broken and M2 alveolus. No locality data: F:AM 27364, partial mandible with i1–m2 (c1 broken and m3 alveolus); and F:AM 61337, left partial ramus with c1–m2 (p1, p3, and m3 alveoli).

Conical Hill Quarry, base of Ojo Caliente Member, Tesuque Formation (late Barstovian), 15 mi northwest of Espanola, Rio Arriba County, New Mexico: F:AM 70502, left partial maxillary with C1–P2 alveoli, P3, and P4–M2 all broken.

Black Mesa, San Ildefonso, rocks referred to the Chamita Formation (Clarendonian), Rio Arriba County, New Mexico: F:AM 27365, left ramal fragment with m1 broken–m2 and m3 alveolus.

DISTRIBUTION: Late Barstovian of Nebraska and New Mexico, and Clarendonian of Nebraska and New Mexico.

DIAGNOSIS: Aside from its larger size and relatively and actually longer m1 as compared to other species, *C. webbi* is derived with respect to *C. compressus* in that the m1 paraconid is broad with the labial side at an oblique angle (nearly 45) to the protoconid, and the mandibular ramus has a more prominent subangular process. Compared to *C. robustus*, *C. webbi* is larger in size and lacks a deeply excavated masseteric fossa on the anterior rim, an expanded M2 posterior cingulum, and an enlarged p4.

DESCRIPTION AND COMPARISON: The beautifully preserved skull of the holotype unequivocally shows a highly domed and wide forehead in *Carpocyon*. The top of this prominent dome is almost 30 mm above the tip of the inion, in contrast to a much lower forehead in *C. compressus*. Beneath this domed forehead is a greatly expanded frontal sinus, which pushes slightly beyond the frontal–parietal suture but does not penetrate to the posterior part of the braincase, as it does in *Borophagus*. The skull in *C. webbi* is more domed than in some early individuals of *Epicyon saevus*, and represents an independent development within the *Carpocyon* lineage. Besides the vaulted forehead, the skull of *C. webbi* has the general construction of primitive Borophagina: palate narrow; nuchal crest slightly overhanging occipital condyle, but not laterally restricted as in *Aelurodon*; very inflated bulla; short free tip of the paroccipital process; mastoid process not inflated; and a moderate development of an auditory meatus tube. In general, the cranial proportions of *C. webbi* are most notable for an elongated skull with a long rostrum and long temporal fossa (length of P1–M2 and length of M2 to bulla in fig. 89) and a narrow braincase.

Dentally, the premolars are slightly reduced and not crowded. The P4 has a distinct parastyle and a reduced protocone. The ridge leading from the protocone points toward the apex of the paracone, not the parastyle, except in one individual, F:AM 70606, whose protocone ridge is directed laterally toward the parastyle but does not fully connect with the parastyle. The upper molars are quadrate in outline and enlarged relative to the P4. The p1–p3 are not as sharply reduced relative to the p4 as in *Carpocyon robustus*. The m1 paraconid tends to have a rather transversely oriented lateral border, in contrast to the more anteriorly oriented paraconid (in dorsal view) in *C. compressus*. The m2 is large.

The relatively large sample from the Pojoaque Member of the Tesuque Formation is similar in cranial and dental morphology to the Burge sample. Materials from the Conical Hill Quarry (F:AM 70502, a partial left maxillary with P3–M2), however, suffer from considerable postmortem deformation such that its premolars become extremely slender while its M1–M2 remain normally proportioned.

DISCUSSION: *Carpocyon webbi* attains the largest size in the genus—*Carpocyon* species both earlier and later than *C. webbi* are smaller in size. Individuals from the Pojoaque Member of the Tesuque Formation are more consistently of large-size. On average, the dental measurements of *C. webbi* are 16% larger than those of *C. compressus* and 10% larger than those of *C. robustus*.

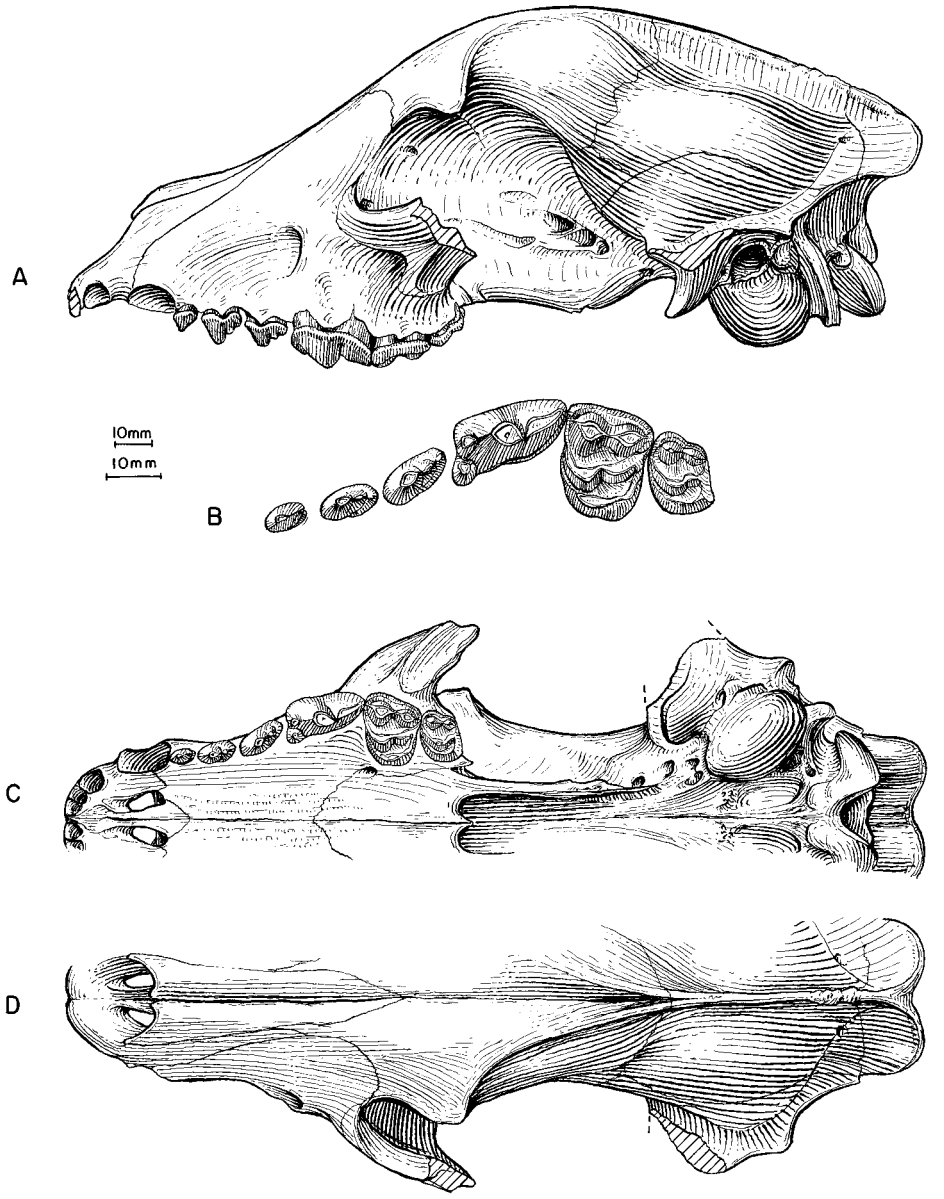

Fig. 96. *Carpocyon webbi*. **A**, Lateral, **B**, enlarged occlusal, **C**, ventral, and **D**, dorsal views of skull and upper teeth, F:AM 61328, holotype, Midway Quarry, Burge Member, Valentine Formation (late late Barstovian), Cherry County, Nebraska. The shorter (upper) scale is for A, C, and D, and the longer (lower) scale is for B.

The size increase culminated at *C. webbi*, and decreasing size and greater hypocarnivory seem to be the trend in *C. robustus* and *C. limosus*.

Samples from New Mexico are in general very close to those from Nebraska both in size and morphology. However, the New Mexico individuals tend to have more primitive proportions of the premolars, i.e., the p2–p3 is less reduced relative to p4. The relationship between the New Mexico and Nebraska samples remains poorly understood.

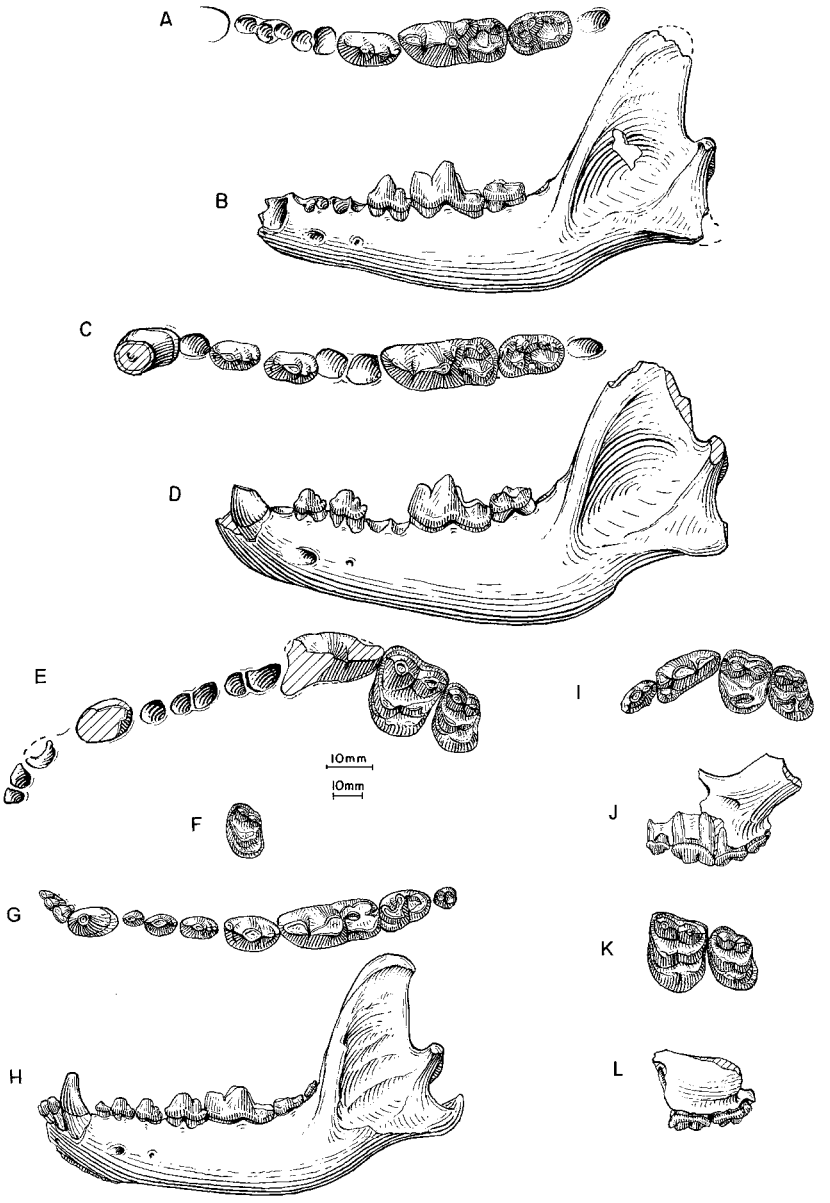

Fig. 97. **A**, Lower teeth and **B**, ramus, *Carpocyon webbi*, F:AM 61322, June Quarry, Burge Member, Valentine Formation (late late Barstovian), Brown County, Nebraska. **C**, Lower teeth and **D**, ramus (reversed from right side), *C. webbi*, F:AM 27366B, Santa Cruz, Pojoaque Member, Tesuque Formation (late Barstovian), Santa Fe County, New Mexico. **E**, Upper teeth, *C. webbi*, F:AM 61335, Santa Cruz First Wash, Pojoaque Member, Tesuque Formation (late Barstovian), Santa Fe County, New Mexico. **F**, Occlusal view of M2, **G**, lower teeth, and **H**, ramus, *C. robustus*, UCMP 33569, holotype, Red Rock Canyon, Dove Spring Formation (Clarendonian), Kern County, California. **I**, Upper teeth (M2 reversed from right side) and **J**, lateral view of maxillary, *C. limosus*, UF 12069, holotype, *Hexameryx* Locality, Bone Valley Formation (late Hemphillian), Polk County, Florida. **K**, Enlarged occlusal and **L**, lateral views of maxillary and upper teeth, *C. limosus*, F:AM 61017, Port of Entry Pit, Ogallala Group (early Hemphillian), Ellis County, Oklahoma. The longer (upper) scale is for A, C, E, F, G, I, and K, and the shorter (lower) scale is for the rest.

Carpocyon robustus (Green, 1948)
Figure 97F–H

Tomarctus robustus Green, 1948: 82, figs. 1, 3. Downs, 1956: 235. Munthe, 1989: 13, figs. 5A, 8K, 10A, 10M, 16I.
Aelurodon saevus (Leidy, 1869): Green, 1971: 489 (SDSM 6853).
Tomarctus? *robustus* (Green): Munthe, 1998: 135.

HOLOTYPE: UCMP 33569 (AMNH cast 80158), partial skeleton including left mandible with i1–m2 and m3 alveolus, right mandible with alveoli for incisors and canine, p1–m3 in place, an isolated left P2 and left M2 (fig. 97F–H), and an isolated I3, all cervical, thoracic, lumbar, and a few sacral vertebrae, pelvis, both scapulae, ribs, manubrium, sternebrae, left humerus, right radius and ulna, right and left scapholunar, magnum, unciform, cuneiform, pisiform, right trapezoid, metacarpals, left tibia, right calcaneum and cuboid, left navicular, right entocuneiform and ectocuneiform, metatarsals, phalanges, and sesamoids, from Red Rock Canyon, approximately 1 mi north of the Ricardo Post Office, UCMP loc. V3732, Dove Spring Formation (Clarendonian), Kern County, California.

REFERRED SPECIMENS: Gallup Gulch, 35 ft above spring level, massive sand, Ash Hollow Formation (early Clarendonian), Cherry County, Nebraska: F:AM 107858, right partial ramus with c1–m1.

First canyon above the Boiling Springs Bridge, south side of Niobrara River, marly zone, base of Ash Hollow Formation (early Clarendonian), Cherry County, Nebraska: F:AM 61350, partial skull with I3–P3 (all broken and P1 alveolus), P4–M2, and right partial ramus with m1 broken–m3.

Mission Local Fauna, George Thin Elk Gravel Pit, Thin Elk Gravels (early Clarendonian), northwest of Mission, Mellette County, South Dakota: F:AM 70622, left partial maxillary with P1–P3 alveoli, P4, and M1 broken alveolus; and SDSM 6853 (AMNH cast 93462), left ramus with c1, p3 alveolus, p4–m1, and m2 alveolus (referred to *Aelurodon saevus* by Green, 1971: 489).

Hollow Horn Bear Quarry, undifferentiated beds of Ogallala Group, temporally equivalent to the Cap Rock Member of the Ash Hollow Formation (early Clarendonian), Todd County, South Dakota: F:AM 61349, left partial ramus with p4 broken–m1 and m2–m3 alveoli.

Clarendon beds, Quarry 1, Spade Flats, Ogallala Group (early Clarendonian), Donley County, Texas: F:AM 70758, crushed partial skull with C1 alveolus–M2, and both rami with i1–i3 all broken and c1–m2 (p1 and m3 alveoli).

Merritt Dam Member, Ash Hollow Formation (late Clarendonian), Brown and Cherry counties, Nebraska: Platybelodon Quarry (UNSM loc. Cr-22): UNSM 25889, left ramal fragment with p1 alveolus and p2–p4. West Line Kat Quarry Channel: F:AM 61342, left ramus with c1–p1 alveoli and p2–m3; and F:AM 61348, left partial maxillary with P4–M2. *Leptarctus* Quarry: F:AM 61343, right ramus with c1, p1–p2 alveoli, p3–p4 both broken, m1, and m2–m3 alveoli. Wade Quarry: F:AM 61345, right partial ramus with p4–m2. Below Bear Creek: F:AM 61346, left partial ramus with p1 root, p2–m1 (m1 broken), and m2–m3 alveoli. No locality data: F:AM 25148, left ramus with c1–m2 (p1 and m3 alveolus).

Near Craig, 75 ft below the Weller Cap, upper end of Swelter Draw, Browns Park Formation (late Clarendonian), Moffat County, Colorado: F:AM 61338, crushed right and left rami with i1–m3; F:AM 61339, crushed mandible with i1–m3; F:AM 61340, crushed fragmentary skull with C1–P3 all broken and P4–M2 (M1 broken); F:AM 61341, crushed fragmentary skull with badly broken teeth; and F:AM 107857, broken tibia.

Milk Creek Formation, Milk Creek Quarry (Clarendonian), Yavapai County, Arizona: F:AM 129869, right ramal fragment with m1–m3 and isolated p4.

DISTRIBUTION: Early Clarendonian of Nebraska, South Dakota, and Texas; late Clarendonian of Nebraska and Colorado; and Clarendonian of California and Arizona.

EMENDED DIAGNOSIS: Besides its smaller size, *Carpocyon robustus* shares with *C. limosus* an expanded posterior cingulum of M2, in contrast to the more primitive *C. webbi* and *C. compressus*. In addition, *C. robustus* acquired autapomorphies of a strong pocket on the anterior rim of masseteric fossa and an enlarged p4 relative to p2–p3. Primitive characters that distinguish *C. robustus* from

C. limosus are less enlarged molars relative to P4, higher crowned M1 paracone and metacone, and weak development of a M2 hypocone.

DESCRIPTION AND COMPARISON: Although most newly referred materials are also lower jaws, a specimen from the Clarendon Beds of Texas, F:AM 70758, preserves much of the cranium with associated mandible. The mediolateral crushing on this skull is severe, but did not obscure several important features: a prominently domed forehead, an inflated bulla, well-developed tube for the auditory meatus, small mastoid process, and short tip of the paroccipital process. Except for a relatively narrow M2 and a short distance between orbit and M1, the overall pattern of cranial proportions is similar to those of *Carpocyon webbi* as exemplified in the ratio diagram of figure 89. In *C. robustus*, there is a deep, elongated pocket behind the anterior rim of the masseteric fossa. In the holotype, the degree of reduction in p1–p3 relative to the p4 is quite pronounced, more so than in *Protepicyon raki*. In another individual, F:AM 70758, the lower premolar reduction is nearly as pronounced as in the holotype. Furthermore, the basal cingulum of P3 in F:AM 70758 is markedly offset from that of the P4 in lateral view, such that the two teeth are no longer in the same horizontal plane. This latter feature is typically seen in the *Epicyon–Borophagus* clade. Through the more transitional forms from the early Clarendonian of Nebraska, the premolar reduction in the holotype seems to represent a temporal variation within the species. If the fragmentary materials from the Ash Hollow Formation are correctly referred, they are likely to represent the primitive condition of this character in *C. robustus*—the degree of premolar reduction in the Nebraska sample is comparable to that in *C. webbi*.

DISCUSSION: While *C. robustus* is still inadequately sampled, present reference of fragmentary materials from the Great Plains not only indicates a far more widely distributed species than its originally known occurrence in southern California, but also extends its temporal range to the late Clarendonian, to overlap with the early members of *Carpocyon limosus*.

Green (1948) recognized the incipient reduction of p1–p3 in the holotype of *Tomarctus robustus* as indicating a relationship to *Osteoborus*, but chose a horizontal classification to include *robustus* in *Tomarctus*, as was the common practice of the day. Furthermore, presence of an excavated anterior rim of masseteric fossa in the holotype seems also to suggest affinity to the *Protepicyon–Borophagus* clade. While our phylogenetic analysis suggests that these characters in *Carpocyon robustus* may have independently evolved within *Carpocyon*, the possibility that they are synapomorphies for a sister relationship between *robustus* and the *Protepicyon–Borophagus* clade should not be lightly dismissed, i.e., characters shared between *robustus* and other species of *Carpocyon* may be homoplastic. This latter alternative may be further entertained when more is known about its hypothesized sister-species *C. limosus*.

Faced with the competition of large and more numerous predators such as *Epicyon* and *Aelurodon*, *C. robustus* reduced its size from its larger predecessor *C. webbi*, and probably subsisted on smaller vertebrates such as lagomorphs and rodents. Near the rib basket of the holotype a ''mass of mangled small bones and teeth with some recognizable fragments includes I1–I2, an upper molar, and a left p3 of *Hypolagus* cf. *vetus* (Kellogg), plus some unidentifiable rodent material'' (Green, 1948: 86). Green identified these as ''stomach bolus or fossil fecal material,'' which is one of only two instances where direct dietary evidence for a borophagine are found (the other is found associated with a skeleton of *Aelurodon stirtoni*; see Munthe, 1989: 96).

Carpocyon limosus Webb, 1969

Figure 97I–L

Carpocyon limosus Webb, 1969b: 276, fig. 1. Munthe, 1998: 136.

HOLOTYPE: UF 12069 (AMNH cast 97775), two maxillary fragments with P3–M2 (fig. 97I, J) from Palmetto mine, *Hexameryx* Locality, 7 mi southeast of Brewster, Palmetto Fauna (''Upper Bone Valley Fauna'' of Tedford et al., 1987), Bone Valley Formation (late Hemphillian), Polk County, Florida.

REFERRED SPECIMEN: Port of Entry Pit (Arnett Locality), Ogallala Group (early Hemphillian), 5 mi east of Higgins, Texas, in Ellis County, Oklahoma: F:AM 61017, left maxillary fragment with M1–M2 (fig. 97K, L).

DISTRIBUTION: Early Hemphillian of Oklahoma, and late Hemphillian of Florida.

EMENDED DIAGNOSIS: Unique derived characters that distinguish *C. limosus* from all other species of *Carpocyon* are molars large and more quadrate with M1 length-to-width ratio ranging between 80 and 85%; M1 paracone and metacone low crowned, subequal, and conical; M2 hypocone distinct and separate from lingual cingulum; and M2 posterolingual cingulum strong.

DESCRIPTION AND COMPARISON: Webb's (1969b) original descriptions and illustrations of the holotype contain all details about the dental morphology of *C. limosus*. To the holotype, we can add only one maxillary fragment (F:AM 61017) from Oklahoma. In addition to indicating presence of *C. limosus* in the early Hemphillian of Oklahoma, the new material provides a measure of variation in its slightly larger size and a better developed posterior cingulum on M2. This referred specimen also furnishes a temporal link between the last occurrence of *C. robustus* in the late Clarendonian and the late Hemphillian holotype of *C. limosus*. Continued size reduction seems to be the trend from *C. webbi* to *C. limosus*, as also seen in another hypocarnivorous lineage, *Cynarctus*.

DISCUSSION: Besides the limited sense of temporal and geographic variation due to the presence of one referred specimen, knowledge of this rare species is still very incomplete. These meager records suggest a relic form of *Carpocyon* surviving in the Hemphillian of the southern United States, as the last hypocarnivorous member of the Borophaginae.

Webb (1969b: 278) correctly recognized a close relationship between his *Carpocyon limosus* and Thorpe's (1922b) *Cynodesmus cuspidatus* (presently *Carpocyon compressus*). Our present recognition of intermediate species, *C. webbi* and *C. robustus*, in the late Barstovian through Clarendonian further fills a long gap in the fossil record between *C. compressus* and *C. limosus*.

Protepicyon, new genus

TYPE SPECIES: *Protepicyon raki*, new genus and species.

ETYMOLOGY: Greek: *protos*, before; plus *Epicyon*.

INCLUDED SPECIES: Type species only.

DISTRIBUTION: Late early to late Barstovian of California and New Mexico.

DIAGNOSIS: In contrast to *Carpocyon* and *Paratomarctus*, derived characters that *Protepicyon* shares with the *Epicyon–Borophagus* clade include masseteric fossa deep and excavated into anterior rim, high-crowned M1 paracone, and widened p4 relative to p2–p3. Primitive characters that distinguish *Protepicyon* from *Epicyon* are palate narrow; auditory meatus less tubular and less laterally extended; P2–P3 and p2–p3 less reduced, with higher crowned main cusps; P4 protocone and parastyle mostly separate but maybe weakly connected; M1 labial cingulum at paracone unreduced; and p4 less enlarged relative to p2–p3. *Protepicyon* has a unique feature of its own—I3 with two distinct lateral cusplets, as compared to more reduced cusplets in taxa both more primitive and derived.

Protepicyon raki, new species

Figure 98

HOLOTYPE: F:AM 61705, crushed partial skull with I1–P1 alveoli, P2–M2, and right partial ramus (fig. 98F–I) with c1–m1 from Mayday Quarry, Barstow Formation (early late Barstovian), San Bernardino County, California.

ETYMOLOGY: Named in honor of Joseph Rak who made significant collections in the Barstow, California area for the Frick Laboratory.

REFERRED SPECIMENS: Barstow Formation (early late Barstovian), San Bernardino County, California: Mayday Quarry: F:AM 31102, right and left partial maxillae with detached P4 and M1–M2; F:AM 31107, left partial ramus with p1–m2 and m3 alveolus; F:AM 31108, left ramus with c1–m2 and m3 alveolus; F:AM 31109, right partial ramus with i2–c1, p1 alveolus, p2 broken–m1, and m2 broken; F:AM 61706, crushed partial skull with I1–M2 and both partial rami with c1 root, p1 alveolus, and p2–m3; F:AM

61707, crushed skull with I1–I2 alveoli, I3–C1 both broken, and P2–M2; F:AM 61710, right partial maxillary with P4–M2; F:AM 61711, right and left partial maxillae with P3 broken–M2; F:AM 61713, right partial ramus with c1 alveolus, p1–p2 both broken, and p3–m2; F:AM 61714, left partial ramus with c1, p1 alveolus, p2–m2, and m3 alveolus; F:AM 61715, right partial ramus with p2–m2; F:AM 61717, left ramus with c1 broken–m1, m2 broken, and m3 alveolus; F:AM 61718, left partial ramus with p1–m2 (p2 and m1 broken, m3 alveolus); F:AM 67060, left partial maxillary with P4 and M1 broken; F:AM 67061, premaxillary-maxillary fragment with I1–I3 alveoli and C1; F:AM 67082, right partial maxillary with P4–M2; and F:AM 67083, right partial ramus with m1–m3. Skyline Quarry: F:AM 31103, right and left partial maxillary with P4–M2. Four ft above New Year Quarry: F:AM 61708, crushed partial skull with P2–P3, P4–M1 both broken, and M2, and right partial ramus with c1, p1–p2 alveoli, and p3–m2 all broken. New Year Quarry: F:AM 61712, right ramus with c1 broken–m3 (p4 broken). New Hope Quarry: F:AM 61716, left ramus with c1 broken, p1 alveolus–m2; and F:AM Bx 319-1661, partial femori and partial tibiae of two or more individuals. North End: F:AM 27175, partial palate with I1–I3, C1–P1 alveoli, and P2–M2 (fig. 98A, B), and both rami with c1 erupting and p1–m2 (p2 broken and m3 erupting); and F:AM 27175A, right ramus with i3–p1 alveoli, p2–m2, and m3 alveolus. No locality data: F:AM 27156, crushed palate with P1 broken–M2; F:AM 27180, right partial ramus with c1–m1 (m2 broken); and F:AM 27189, right ramus with c1–m2 (p1 alveolus) and m3 alveolus.

Jemez Creek area, unnamed beds in upper part of the Zia Formation (late early Barstovian), Sandoval County, New Mexico: F:AM 61738, skull with I1 alveolus–M2 (I3 broken and P1 alveolus), and right and left rami with i2–m2 and m3 alveolus (fig. 98C–E, J); F:AM 61739, partial skull with I1 broken–M2; and F:AM 61740, right ramal fragment with p4–m3 all broken.

North Rio Puerco, unnamed beds upper part of the Zia Formation (late early Barstovian), Sandoval County, New Mexico: Pilares Quarry: F:AM 61741 and 61741A, right and left partial rami with p1–m2 all broken.

DISTRIBUTION: Late early Barstovian of New Mexico and early late Barstovian of California.

DIAGNOSIS: As for genus.

DESCRIPTION AND COMPARISON: Although represented by specimens suffering from various degrees of crushing, the topotypical materials of *Protepicyon raki* in the Barstow Formation consist of enough partial crania and jaws to permit a good sense of its overall morphology and variation. Referred materials from New Mexico, although rare, are better preserved.

The general cranial construction of *Protepicyon raki* begins to take the shape of primitive *Epicyon* in its domed forehead above the orbit, long rostrum, narrow palate (relative to *Aelurodon*), and enlarged bulla. In relative cranial and dental proportions, *P. raki* also approaches *Epicyon*: narrow braincase, long P4, and short M2 (figs. 99, 100). Except in young individuals, the mandible generally develops a deep pocket behind the anterior rim of the masseteric fossa. Teeth of *P. raki* begin to take the robust proportions of larger Borophagina. The I3 has two distinct lateral cusplets. The upper and lower first through third premolars are still quite strong and not as reduced as in *Epicyon*. The P4 is long compared to M1 and M2, and has a reduced protocone. Most individuals have P4 protocones that are not connected to the parastyle by a ridge. At least one individual (e.g., F:AM 27175), however, has a protocone with a lateral ridge directed toward the parastyle. The M1 paracone is higher crowned both absolutely and relatively than the metacone. All M2s in the Barstow Formation are enlarged due to transverse elongation. The p4 is broad, as is typical for *Epicyon*. The entoconid and hypoconid of m1 are about equal in height, as are the protoconid and metaconid of m2.

An undistorted skull (lacking dorsal part) plus mandible (F:AM 61738, fig. 98C–E, J), as well as a partial skull and ramus, from the Jemez Creek area, New Mexico, allows a sense of variation outside the Barstow area. The most noticeable difference of the New Mexico specimen is their smaller, less

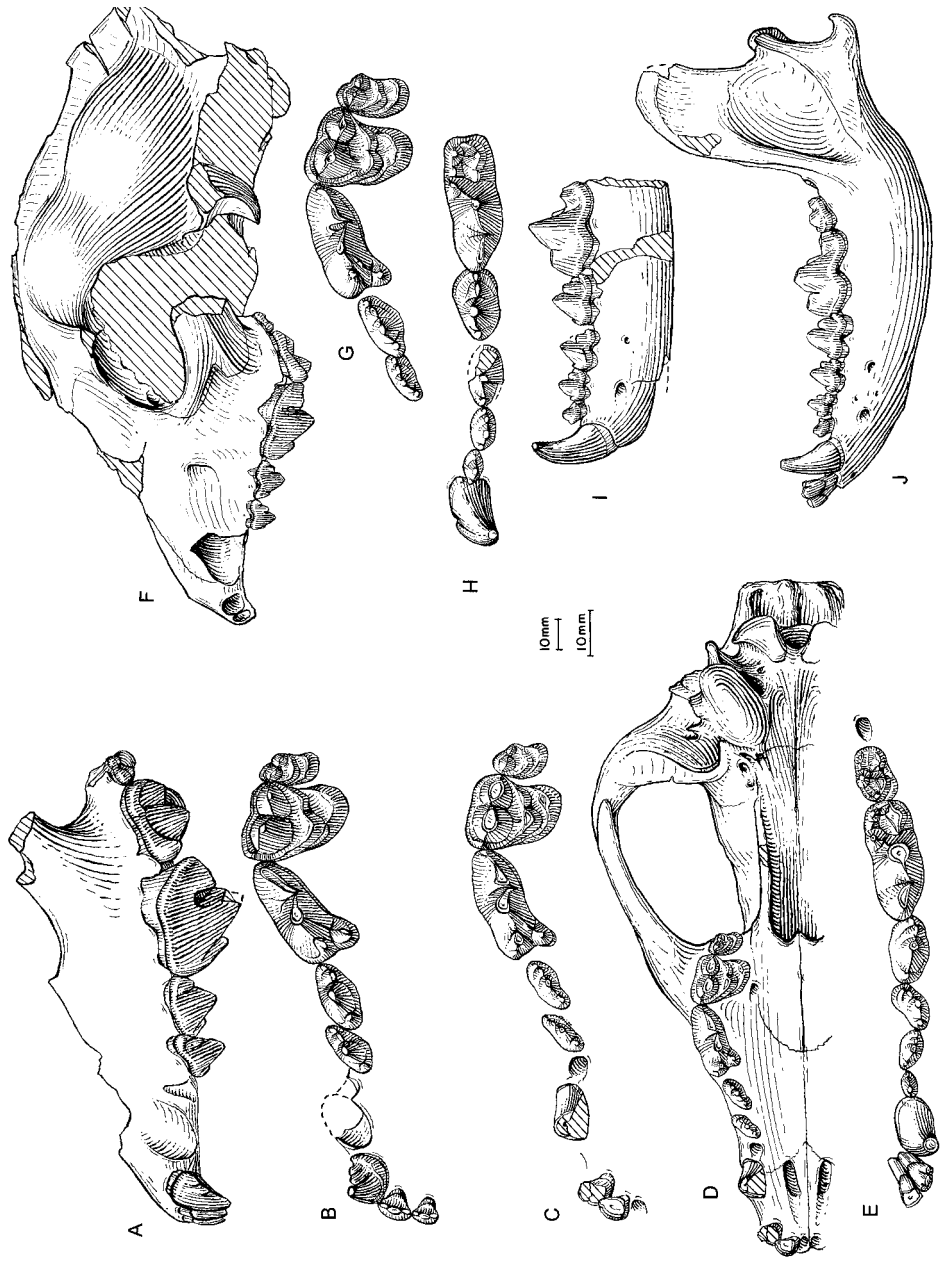

Fig. 98. *Protepicyon raki*. **A**, Lateral view of partial skull and **B**, upper teeth, F:AM 27175, North End, Barstow Formation (late early Barstovian), San Bernardino County, California. **C**, Upper teeth, and **D**, ventral view of skull, **E**, lower teeth, and **J**, ramus, F:AM 61738, Jemez Creek area, unnamed beds in upper part of Zia Formation (late early Barstovian), Sandoval County, New Mexico. **F**, Lateral view of skull, **G**, upper teeth (reversed from right side), **H**, lower teeth and **I**, ramus (reversed from right side), F:AM 61705, holotype, Mayday Quarry, Barstow Formation (early late Barstovian), San Bernardino County, California. The shorter (upper) scale is for D, F, I, and J, and the longer (lower) scale is for the rest.

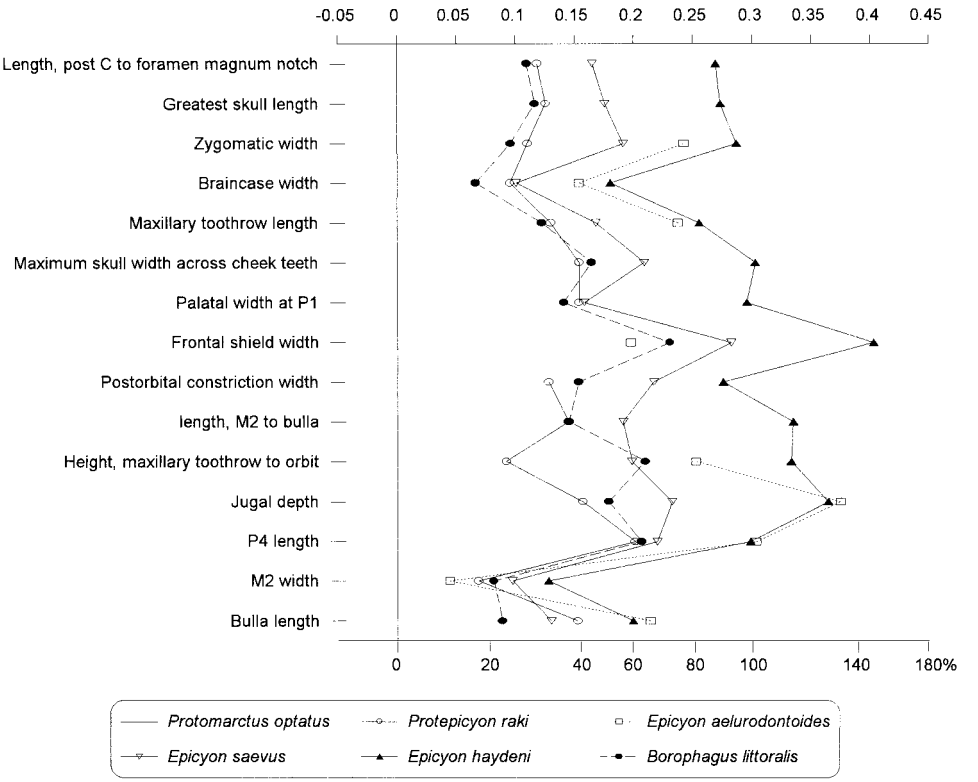

Fig. 99. Log-ratio diagram for cranial measurements of *Protepicyon* and *Epicyon* using *Protomarctus optatus* as a standard for comparison (straight line at zero for y-axis). See text for explanations and appendix II for measurements and their definitions.

transversely elongated M2s. Other than this difference, the New Mexico materials are morphologically close to those from California.

DISCUSSION: *Protepicyon raki* has a short range in the early part of the Barstow Fauna in the Barstow Formation. This coincides with the lower part of the range of *Aelurodon asthenostylus*, which extends to the *Hemicyon* Stratum as its highest occurrence. During this co-occurrence, both species are of approximately the same size and are not always easy to distinguish when specimens are fragmentary. In general, *P. raki* has a more domed forehead, narrower palate, less well-developed I3 accessory cusplets, less well-developed P1–P3 and p1–p4 cusplets, more transversely elongated M2, less reduced entoconid of m1, less reduced metaconid of m2, and more elongated m2. Such differences generally correspond to the morphological patterns of the *Epicyon* clade. We also note that certain individuals of *A. asthenostylus* from the *Hemicyon* Stratum or equivalent level (F:AM 27160, 27161, 27166, 27172) tend to have a P4 protocone that is connected to the parastyle, a derived character for *Epicyon* (Baskin, 1980). These individuals otherwise have typical *Aelurodon*-like cranial and dental features. The balance of the morphological evidence seems to indicate independent acquisition of the P4 protocone connection in certain populations of the *A. asthenostylus* lineage.

As a transitional species, *Protepicyon* has a brief occurrence in the late early Barstovian of New Mexico through early late Barstovian of California. It gave rise to *Epicyon*, which becomes more widely distributed in the Clar-

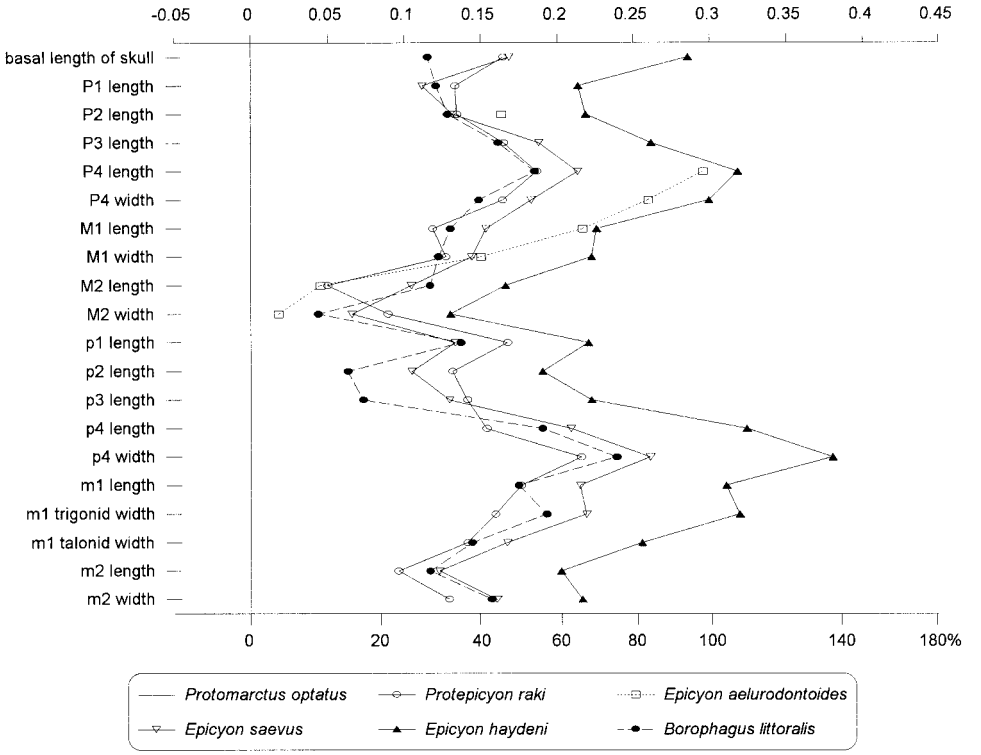

Fig. 100. Log-ratio diagram for dental measurements of *Protepicyon* and *Epicyon* using *Protomarctus optatus* as a standard for comparison (straight line at zero for y-axis). See text for explanations and appendix III for summary statistics of measurements and their definitions.

endonian through early Hemphillian of North America.

Epicyon Leidy, 1858

TYPE SPECIES: *Epicyon haydeni* Leidy, 1858.

INCLUDED SPECIES: *E. aelurodontoides*, new species; *E. saevus* (Leidy, 1858); and *E. haydeni* Leidy, 1858.

DISTRIBUTION: Late Barstovian or early Clarendonian of New Mexico; early Clarendonian of Nebraska, South Dakota, New Mexico, Nevada, and Texas; late Clarendonian of Nebraska, Montana, Oklahoma, New Mexico, Nevada, California, and Florida; Clarendonian of Arizona; early Hemphillian of Nebraska, Colorado, Kansas, Oklahoma, Texas, Idaho, Oregon, and Florida; late Hemphillian of Florida; and ?Hemphillian of Montana.

EMENDED DIAGNOSIS: Synapomorphies that unite *Epicyon* with the *Borophagus* clade are wider palate, I3 lateral cusplets weak or absent, P1–P3 and p1–p3 small and low-crowned, P4 protocone and parastyle connected by a ridge, absence of M1 labial cingulum at paracone, and p4 further enlarged relative to anterior premolars. Autapomorphies for *Epicyon* are a long free tip of the paroccipital process and elongated limbs. *Epicyon* is distinguished from *Borophagus* by the following primitive features: longer face; less dorsally expanded frontal sinus; lack of a boss below mandibular symphysis; narrow angular process; P1–P3 and p1–p3 more widely spaced, and relatively smaller P4 and p4; posterior cusplets on P2–P3 and p2–p3 not reduced; less reduced P4 protocone; p4 narrower relative to other premolars and carnassial, less tilted posteriorly, stronger posterior cusplet, and transverse diameter less than that of trigonid of m1; m2 paraconid usually larger and more distinct; and tibia more slender and elongate with the radius-

to-tibia ratio of 90% (vs. 100% in *Borophagus*).

DISCUSSION: *Epicyon* was originally named by Leidy (1858) as a subgenus of *Canis*, but was soon abandoned by the same author (Leidy, 1869). The type species was placed in *Aelurodon* by Scott (1890) and remained assigned to that genus for most of its history. *Epicyon* was resurrected and elevated to generic status by Baskin (1980) for the ''*Aelurodon*'' *saevus* species group, as a result of his analysis of the upper carnassials, following an earlier suggestion by McGrew (1944b) and Mawby (1964, 1965). Baskin's conclusion is confirmed by our phylogenetic analysis, which is based on a larger series of characters and taxa. In addition to the P4 protocone structures noted by Baskin, we can identify many cranial and dental features of *Epicyon* that distinguish it from *Aelurodon*: narrower palate, narrower external and internal nares, more prominently domed forehead, lower sagittal crest, less posteriorly extended nuchal crest, nuchal crest not laterally compressed, lack of accessory cusps on I3, reduction of P1–P3 and p1–p3, enlarged p4, and less reduced M2 and m2.

Dentitions of both *Aelurodon* and *Epicyon* appear to have been quite capable of crushing bones. However, there is a considerable difference between these genera in the construction of their dentitions. The focus of bone crushing in *Epicyon* is at the P4/p4 pair (as is also in *Borophagus*), whereas in *Aelurodon* there seems to be a wider range of focus among the anterior pairs of premolars (such as P3/p3 and P2/p2; see Werdelin [1989] for a further analysis of function).

Epicyon aelurodontoides, new species

Figure 101

HOLOTYPE: F:AM 67025 (fig. 101), partial skull with C1, P1 alveolus, P2, P3 alveolus, P4–M2, and detached premaxillary-maxillary with I1–I3 alveoli, 2 mi south of Young Brothers Ranch, vicinity of Ashland, Ogallala Group (early Hemphillian), Clark County, Kansas.

REFERRED SPECIMEN: Holotype only.

ETYMOLOGY: In allusion to its similarities to *Aelurodon*.

DISTRIBUTION: From type locality only.

DIAGNOSIS: Unique characters of *Epicyon aelurodontoides* that distinguish it from *E. saevus* and *E. haydeni* include reduced postorbital process of frontal, high sagittal crest, laterally compressed lambdoidal crest, an enlarged fossa at entrance of hypoglossal canal, large ventral facet on mastoid process, greatly enlarged I3, narrowed talon of M1, and reduced M2. *E. aelurodontoides* is further distinguishable from the *E. saevus–haydeni* clade in its lack of a synapomorphy of the latter: a concave dorsal edge of sagittal crest.

DESCRIPTION AND COMPARISON: F:AM 67025 consists of a partial posterior cranium, frontal shield, premaxillary, and maxillary fragments. The frontal is moderately domed, in both lateral and anterior views, but not very broadened, as it is in *Aelurodon* or advanced species of *Epicyon*. The postorbital process of frontal is very small, solid on the left side, and is penetrated by the frontal sinus on the right. The multichambered frontal sinus reaches backward to more than 10 mm behind the frontal–parietal suture. The sagittal crest is more than 20 mm high and has a straight dorsal edge. The laterally constricted nuchal crest is narrow and projects backward to slightly overhang the occipital condyle. In dorsal view, the zygomatic arch lacks a sharp angle in the posterior segment, as occurs in *Aelurodon*.

Although fragmentary, the left premaxillary and maxillary of F:AM 67025 form an essentially continuous dental battery. The alveoli of the incisors suggest a greatly enlarged I3 and an arched external profile, in contrast to the transversely straight incisor row in *Aelurodon*. Also indicative of its difference from *Aelurodon* is a relatively narrow palate at the anterior premolars (the width across the P1s is approximately 36 mm). On the other hand, the palate at P4 is not abruptly widened relative to that at P1–P3, as it is in *Borophagus*. In the ratio diagram (fig. 99), the few cranial measurements available for *E. aelurodontoides* are consistent with the general pattern of *Epicyon* except for a narrow frontal shield.

The basicranial region is most notable for an unusually enlarged hypoglossal canal. The canal (also called condyloid foramen), which holds the vertebral vein, is expanded to form a rounded bony fossa with a maximum di-

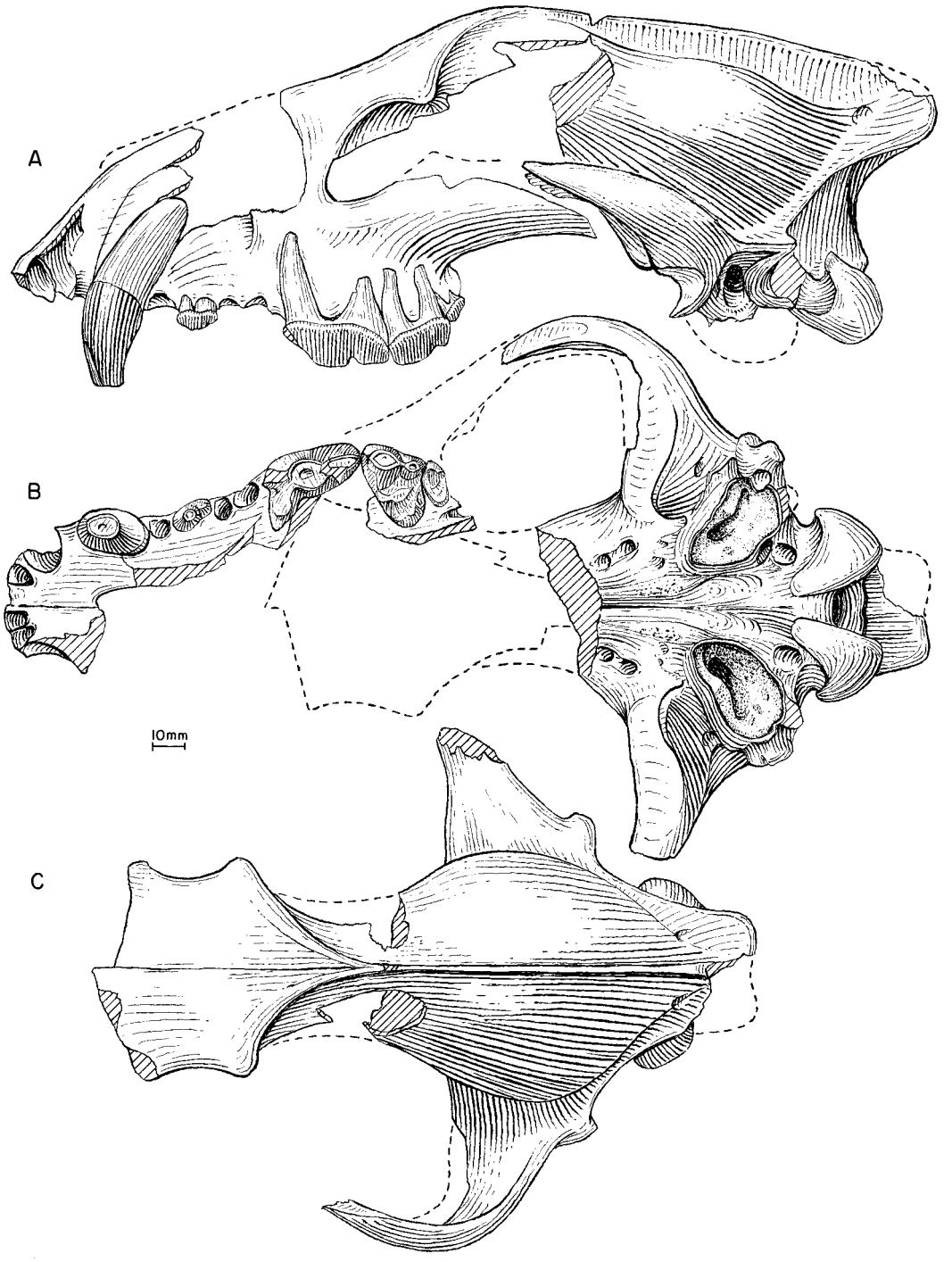

Fig. 101. *Epicyon aelurodontoides*. **A**, Lateral, **B**, ventral, and **C**, dorsal views of skull, F:AM 67025, holotype, 2 mi south of Young Brothers Ranch, Ogallala Group (early Hemphillian), Clark County, Kansas.

ameter of 10 mm at its ventral entrance. Toward the posterodorsal aspect of this fossa is the condyloid foramen, 4 mm in diameter, opening into the foramen magnum. Presumably, the vertebral vein forms a large, rounded sinus within this fossa immediately outside the condyloid foramen. Such an enlarged sinus for the vertebral vein at the hypoglossal canal is not known in other canids. The mastoid process has a thin lateral crest and an expanded ventral facet that protrudes posteriorly.

The dental morphology of this species is equally paradoxical. On the one hand, F:AM 67025 has *Aelurodon*-like upper molars with reduced internal cingulum on M1 and a very small M2. On the other hand, it has *Epicyon*-like reduced premolars that lie dorsal to the base of the P4. Heavy wear on the P4 does not permit determination of a possible connection between protocone and parastyle, a derived character for *Epicyon*.

DISCUSSION: This species possesses a curious mixture of cranial and dental features of *Aelurodon* and *Epicyon*. It has *Aelurodon*-like characters such as a high sagittal crest with a horizontal dorsal edge, a posteriorly projecting nuchal crest that overhangs the occipital condyle, a reduced lingual cingulum on M1, and a very reduced M2. On the other hand, F:AM 67025 seems to show affinities to the *Epicyon–Borophagus* clade because of its derived characters such as slightly domed forehead, reduced labial cingulum on M1, and small, low-crowned premolars. In particular, the premolar reduction is a unique character not seen in the *Aelurodon* clade, which features the opposite trend toward premolar enlargement. Other features that tip the balance toward an *Epicyon–Borophagus* affinity include upper incisor row arched, anterior muzzle narrow, and zygomatic arch not sharply angled near the posterior end (in dorsal view). These characters are primitive conditions relative to *Aelurodon* that generally do not characterize that genus. Although both of the P4s are present, heavy wear on these teeth does not permit clear observation of the protocone in relation to the parastyle. Lack of a ridge leading toward the protocone on the remaining enamel of the right P4, however, may suggest the *Epicyon* condition.

If the above analysis is correct, *E. aelurodontoides* may be placed within *Epicyon* because of its reduced anterior premolars and reduced M2, although the latter character is also independently developed in *Aelurodon*. On the other hand, F:AM 67025 lacks derived characters of the *Borophagus* clade, such as a shortened rostrum and elaborate frontal sinus. Within the *Epicyon* clade, *E. aelurodontoides* seems to be in a basal position because of its lack of a concave dorsal edge of the sagittal crest, a character shared by *E. saevus* and *E. haydeni*.

Epicyon saevus (Leidy, 1858)

Figures 102–107, 108A–F

Canis saevus Leidy, 1858: 21; 1869: 28, pl. 1, fig. 9.

Aelurodon saevus (Leidy): Cope, 1881a: 387; 1883: 243, fig. 9; 1890: 1067, pl. 32. Scott, 1890: 66, fig. 1. Matthew, 1899: 67. Cope and Matthew, 1915: pls. 68, 69. VanderHoof and Gregory, 1940: 145, fig. 2. McGrew, 1944b: 79 (in part). Mawby, 1964: 43.

Aelurodon haydeni (Leidy, 1858): Matthew and Gidley, 1904: 250, figs. 2, 5 (in part). Stirton, 1932: 61 (in part).

Aelurodon inflatus VanderHoof and Gregory, 1940: 154, figs. 7c, 8c. Gregory, 1942: 344, fig. 7. McGrew, 1944b: 79. Webb, 1969a: 41.

Osteoborus diabloensis Richey, 1938: Macdonald, 1956: 192, fig. 6.

Aelurodon n. sp.? Webb, 1969a: 41.

Aelurodon cf. *A. haydeni* (Leidy): Webb, 1969a: 42 (in part).

Aelurodon validus (Matthew and Cook, 1909): Skinner et al., 1977: 356 (in part).

Aelurodon mortifer (Cook, 1914): Skinner et al., 1977: 352 (in part).

Epicyon saevus (Leidy): Baskin, 1980: 1350. Munthe, 1989: 13, figs. 5B, 9A, 11B, 14A, 15B, 17B. Voorhies, 1990a: A127. Munthe, 1998: 136.

Epicyon cf. *E. saevus* (Leidy): Baskin, 1980: 1350, fig. 1B.

Aelurodon cf. *A. saevus* (Leidy): Webb et al., 1981: 523.

Epicyon haydeni (Leidy): Munthe, 1989: 14, figs. 6A, 7A (in part).

HOLOTYPE: USNM 126 (AMNH cast 97243), left partial ramus with p2–p3 roots, p4 broken, and m1–m2 (fig. 102E, F) from ''the sands of the Niobrara River'' (Leidy, 1869: 28), ?Cap Rock Member, Ash Hollow Formation (early Clarendonian), north central Nebraska.

REFERRED SPECIMENS: Cap Rock Member, Ash Hollow Formation (early Clarendonian), Brown and Cherry counties, Nebraska: Quinn Ranch Quarry: F:AM 25102, left ramus with c1 broken, p1 alveolus–m2, and m3 alveolus (fig. 102A, B); F:AM 25103, right partial ramus with i1–p2 alveoli, p2–m2, and m3 alveolus; F:AM 25104, right partial ramus with c1–p3 alveoli, p4–m1, and m2 alveolus; F:AM 25105, left ramus with c1, p2–p3, p4 alveolus–m2, and m3 alveolus; F:AM 25106, left partial ramus with c1–p1 alveoli, p2–m2, and m3 alveolus; F:AM 25107, left partial ramus with p2–p3 alveoli, p4–m2, and m3 alveolus; F:AM 25108, right partial ramus with c1–p1 alveoli, p2 root–m2 (p4 broken), and m3 alveolus; and F:AM 25140, left anterior part of skull with I1–M2 (fig. 105F, G). Deep Creek: F:AM 25108A, right ramus with c1–p1 alveoli, p3, p4 broken–m1, and m2–m3 alveoli. Head of Pole Creek: F:AM 61389, right partial ramus with i1–i3 alveoli, c1, p1–p4 alveoli, m1, and m2–m3 alveoli. Base of Cap Rock Member above Burge Quarry: F:AM 107869, left ramal fragment with c1–p1 alveoli and p2–p3. McConnel Place: F:AM 25099, immature skull with I1–I2, I3 erupting, dC1, P1, dP2–dP3, P3 unerupted, and P4–M2 all erupting, and mandible with i1–i3, dc1, c1 unerupted, p1, dp2–dp4, p2–p4 unerupted, m1–m2 erupting, and m3 unerupted. Little Beaver B Quarry: UCMP 63878 (referred to *Aelurodon* cf. *haydeni* by Webb, 1969a: 42), left ramal fragment with p4 and m2.

Driftwood Creek, Republican River beds, temporally equivalent to the Cap Rock Member, Ash Hollow Formation (early Clarendonian), Hitchcock County, Nebraska: AMNH 8305 (Cope, 1883: fig. 9; Cope and Matthew, 1915: pls., 68, 69; Munthe, 1989: figs. 5B, 9A, 11B, 14A, 15B, 17B, and reconstruction in front page), skull with I1–M2 (fig. 102G–I), mandible with i1–m2 and m3 alveolus (fig. 103A, B), postcranial elements including axis, posterior cervicals, thoracics, lumbars, sacrum, caudals, scapulae, right radius (fig. 103D) and ulna (fig. 103C), left incomplete ulna (another individual), metacarpals II and V (fig. 103J, K), pelvis, left femur (fig. 103F) and right partial femur, left tibia and partial fibula (fig. 103E), two left metatarsals IV (fig. 103I; larger one probably represents another individual), right metatarsal V, right calcaneum (fig. 103G) and astragalus (fig. 103H), right and left astragali (larger probably represents another individual), 5 phalanges, and rib fragments; AMNH 8311, posterior part of skull; AMNH 8312 (Cope and Matthew, 1915: pl. 69, fig. 9), left partial ramus with p4 broken–m2 and m3 alveolus.

Patton Ranch (UNSM loc. Bn-105), Ogallala Group, probably equivalent to lower part of Ash Hollow Formation (Clarendonian), Banner County, Nebraska: UNSM 26096, left ramus with i2–c1 broken, p1–m2 (p3 and m2 broken), and m3 alveolus.

Big Spring Canyon, UCMP loc. V-3322, Ogallala Group (early Clarendonian), Bennett County, South Dakota: AMNH 10805 (referred to *Aelurodon haydeni* by Matthew and Gidley, 1904: 250, fig. 5), right partial ramus with c1–p1 alveoli, p2 broken–m1, and m2–m3 alveoli; AMNH 10807, posterior part cranium; UCMP 32328 (fig. 104A, B), left ramus with i1–i2 alveoli, i3–m2, and m3 alveolus (holotype of *Aelurodon inflatus* Vanderhoof and Gregory, 1940: figs. 7c, 8c); and UCMP 33328, partial ramus with p1–m2.

Canyon of Little White River (early Clarendonian), Ogallala Group, South Dakota: AMNH 10804, left partial maxillary with C1–P1 alveoli and P2–M2 (Matthew and Gidley, 1904: fig. 3); AMNH 10806, right ramus with p1 alveolus, p2–m2 (p4–m1 broken), and m3 alveolus; and AMNH 10812, left ramal fragment with c1 alveolus and detached broken c1, p1 alveolus, and p2–p4 all broken.

Rosebud Agency Quarry (early Clarendonian), Ogallala Group, South Dakota: F:AM 61377, left partial ramus with c1–p2 alveoli and p3–m2; and F:AM 61378, left partial ramus with p2–p4 and m1 broken.

Hollow Horn Bear Quarry, undifferentiated beds (early Clarendonian) in Ogallala Group, temporally equivalent to Cap Rock Member of the Ash Hollow Formation, Todd County, South Dakota: F:AM 49439, right maxillary fragment with P4; F:AM 61369 and 61370 (one individual), right and left maxillae with C1, P1–P2 alveoli, and P3–M2; F:AM 61371, right isolated M1; F:AM 61371A, left isolated M1; F:AM 61371B,

left isolated M1; F:AM 61372, right ramus with i1 alveolus, i2, i3 alveolus, c1 broken, p1–p2 alveoli, p3–m1, m2 broken, and m3 alveolus; F:AM 61373, right ramus with i1–i3 alveoli, and c1–m3 (p1 and p3 alveoli); F:AM 61374, left ramus with c1–p3 alveoli, p4 broken–m2, and m3 alveolus; F:AM 61375, right partial ramus with c1–p2 alveoli, p3–m1, and m2–m3 alveoli; F:AM 61376, left isolated m2; F:AM 61376A, left isolated m2; F:AM 67489, right humerus; F:AM 67489A, right distal part humerus; F:AM 67489B, left distal part humerus; F:AM 67490, left radius; F:AM 67491, left radius; F:AM 67491B, proximal part radius; F:AM 67491C, left distal part radius; F:AM 67492, right ulna; F:AM 67492A–E, five partial ulnae; F:AM 67494, right distal part tibia; F:AM 67495 and 67495A, B, right and left partial right metacarpal II; F:AM 67496 and 67496A, B, two left and one right incomplete metacarpal III; F:AM 67497, left metacarpal IV; F:AM 67498, left metacarpal V; F:AM 67500, right metatarsal III; F:AM 67501, left incomplete metatarsal IV; F:AM 67501A, right metatarsal I; F:AM 67502, right metatarsal V; F:AM 67503 and 67503A, B, three isolated calcanea; and F:AM 67503C–F, four proximal phalanges.

Pojoaque Member, Tesuque Formation (late Barstovian or early Clarendonian), Santa Fe County, New Mexico: San Ildefonso: F:AM 61417, crushed anterior part of skull with I1–M2 (I2 and P1 alveoli), both rami with c1–m3 (p1 alveolus), and left partial radius and ulna; and F:AM 98629, right partial ramus with i1–p1 alveoli, p2–p3, p4 broken, and m1–m3 alveoli. Santa Cruz Red Layer: F:AM 27362, right ramal fragment with p2 broken–p4.

Santa Ana Wash, Jemez Creek area, unnamed beds of Zia Formation (late Barstovian or early Clarendonian), Sandoval County, New Mexico: F:AM 67363, right ramus with i2–m2 (m1 broken) and m3 alveolus.

Round Mountain Quarry, Chamita Formation (early Clarendonian), Rio Arriba County, New Mexico: F:AM 61418, left ramus with i3, c1 broken–m2; F:AM 61638, left partial ramus with i1–i3 alveoli, c1 root, p4–m1 broken base, and m2–m3 alveoli; F:AM 67050, left crushed partial ramus with c1 broken–p1 alveolus and p2–m2 (m1 broken); F:AM 67051, left partial ramus with c1–p4 all broken, m1–m2, and m3 alveolus; F:AM 67053, right partial ramus with p4–m1 both broken and m2–m3; F:AM 67053A, right partial ramus with c1–m2 all broken; F:AM 67054, left partial maxillary with I3 alveolus, C1 broken, P1 alveolus, and P2–M2 all broken; F:AM 67055, left partial maxillary with P3–M1 and M2 broken; and F:AM 67056, left partial maxillary with I2–I3 alveoli and C1–P4 all broken.

Clarendon beds (early Clarendonian), Donley County, Texas: MacAdams Quarry (= Location 17, Quarry 1), 10 mi north of Clarendon: F:AM 55416, left ramal fragment with c1 and p2 erupting; F:AM 61402, skull with I1–M2 (P1 alveolus); F:AM 61403, partial skull with I1–C1, P1 alveolus, P2, and P3 alveolus–M2; F:AM 61404, partial skull with I1–C1 all broken, P1 alveolus, P2, P3 alveolus, and P4–M2; F:AM 61405, right premaxillary and maxillary with I1 alveolus–M2 (P2 broken); F:AM 61406, right partial ramus with c1–p4 and m1 broken; F:AM 61407, right ramus with c1, p1–p2 alveoli, and p3–m2; F:AM 61408, left ramus with i3 broken, c1, and p2–m3 (p3 broken); F:AM 61409, right ramus with c1–m2 and m3 alveolus; F:AM 61410, left ramus with p2–m2 and m3 alveolus; F:AM 61411, right ramus with i3–m2 (p1 broken); F:AM 61412, left partial ramus with c1 alveolus and p1–m2 (m1 broken); F:AM 61413, left partial ramus with p2–m1; F:AM 61414, right partial ramus with c1–p2 all roots, p4, and m1–m2 both broken; F:AM 61415, left ramus with c1 broken, p1 alveolus, and p2–m1; F:AM 61789, right isolated P4; F:AM 61789A, right isolated P4; F:AM 67396, partial skull with I1–I3 alveoli, C1, P1–P3 alveoli, and P4–M2; F:AM 67397, partial skull with I1–I3 broken, C1, P1 alveolus, and P2–M2; F:AM 67941, left femur; F:AM 67941A, right partial femur; F:AM 67941B, left tibia; and F:AM 70765, right ramus with c1–m2 and m3 alveolus. Whitefish Creek, Quarry 7: F:AM 70767, skull with I1 root–M2 (P1 alveolus) (fig. 104C–F). Whitefish Creek, Quarry 1: F:AM 67385, right ramus with i2 alveolus–c1, p2–m2, and m3 alveolus; F:AM 67940, right proximal part radius; F:AM 67942A, left metatarsal III; and F:AM 70701, left ramus with i1–i2, i3 alveolus, c1

broken–p4, and m1–m2 both broken, fragments of axis. Lewis Place, Location 5, Quarry 2: F:AM 67939, right radius, partial ulna, metacarpal I, incomplete metacarpal II, scapho-lunar, and phalanges.

Sanford Pit, 12 mi southwest of Borger, Channing area, Ogallala Group (?early Hemphillian), Carson County, Texas: F:AM 97705, left ramal fragment with p1 alveolus, p2 broken–p4, and m1 alveolus.

Merritt Dam Member, Ash Hollow Formation (late Clarendonian), Brown and Cherry counties, Nebraska: Clayton Quarry: F:AM 61353, right partial maxillary with P4–M2; F:AM 61355, cranial fragment with detached P3–M2; F:AM 61361, right partial ramus with c1–p1 alveoli, p2–m1 (p4 root), and m2–m3 alveoli; F:AM 61362, left partial ramus with p2 broken–m1; F:AM 61365, left ramal fragment with m2 and m3 alveolus; F:AM 61366, right isolated m1; F:AM 67514, left distal humerus; F:AM 67514A, left distal humerus; F:AM 67514B, left distal humerus; F:AM 67515, left radius; F:AM 67515A, proximal part radius; F:AM 67515B, proximal part radius; and F:AM 67517, right distal part tibia. East Clayton Quarry: F:AM 61354, left partial maxillary with P4–M2; F:AM 61356, right isolated P4; F:AM 61357, right maxillary fragment with P1–P3; F:AM 61358, right isolated M1; F:AM 61358A, right isolated M1; F:AM 61358B, left isolated M1; F:AM 61358C, isolated right c1; F:AM 61359, right ramal fragment with m1; F:AM 61360, left ramus with i1–i3 alveoli, c1, p1 alveolus–m1, and m2–m3 alveoli; F:AM 61363, left immature partial ramus with dp4, c1 and p2–p4 all unerupted, and m1–m2 erupting; F:AM 61364, right partial ramus with p2–m2 all erupting; F:AM 61368, left isolated m2; F:AM 67515C, proximal part radius; F:AM 67516, left ulna; F:AM 67518, right immature metatarsal IV with distal end missing; F:AM 67520A, calcaneum; and F:AM 67520B, proximal phalanx. Mensinger Quarry: F:AM 67331, partial skull with I1–P1 alveoli and P2–M2 (fig. 105A–D); and F:AM 70612, left ramal fragment with p2–p4. Rhino Horizon No. 3 Quarry: F:AM 25109, right partial ramus with c1, p1–p4 alveoli, m1–m2, and m3 alveolus. Bear Creek Quarry: F:AM 61379, left ramus with i1–i3 alveoli, c1 broken, p1–p2 alveoli, p3–m2, and m3 alveolus; and F:AM 97703, right and left maxillary fragments with P4–M1 both broken and M2. Bear Creek Quarry slide: F:AM 61385, skull fragments and right and left partial rami with c1 alveolus, p1 root, p2–p4, m1–m2 broken, and m3 alveolus. Volcanic Ash pit on Bear Creek: F:AM 70614, right isolated m1. Pratt Quarry: F:AM 67506, distal left tibia; and F:AM 107870, right maxillary fragment with P4 and M1 alveolus. Pratt Slide, Plum Creek: F:AM 67507, left humerus (Munthe, 1989: fig. 8D); F:AM 67508, left radius; F:AM 67510, right incomplete ulna; and F:AM 97704, left maxillary fragment with P4–M1 and M2 alveolus. Morton Ranch, channel above Cap Rock: F:AM 70613, right immature partial maxillary with dP3–dP4 broken and M1 erupting. Bolling Quarry: F:AM 25217, left partial ramus with p1–p3 all broken and p4–m2; and F:AM 61367, right partial ramus with p2–p3 alveoli, p4–m1, and m2–m3 alveoli. West Line Kat Quarry Channel: F:AM 61381, skull with I1–P1 alveoli and P2–M2 (fig. 106C–F). East Kat Quarry Channel: F:AM 61386, right partial ramus with p2–m1 and m2 alveolus; F:AM 61387, left ramus with i2–m2 (p1 broken) and m3 alveolus (fig. 108A, B); and F:AM 67508B, left proximal end radius. Horn Quarry: F:AM 70621, right ramus with i1–m3 (fig. 102C, D). Wade Quarry: F:AM 61382, left ramus with c1–m2 and m3 alveolus (fig. 106A, B). Jonas Wilson Quarry: F:AM 61347, left ramal fragment with m1–m2 and m3 alveolus. *Leptarctus* Quarry: F:AM 61384, right ramus with i2–i3, c1 broken, p2–m2, and m3 alveolus. Gallup Gulch Quarry: F:AM 25218, right partial maxillary with P4–M1 and partial medial phalanx; F:AM 62893, right ramus with c1 alveolus, p1–m1, and m2–m3 alveoli; F:AM 62894, left partial ramus with c1 broken, p1–p3 alveoli, p4–m1, and m2 alveolus; F:AM 107871, right maxillary fragment with P1 alveolus and P2–P3; and F:AM 107872, right isolated m1. Five mi below mouth of Clifford Creek: F:AM 61383, right ramus with c1–m2 and m3 alveolus. First canyon, south side Niobrara River, below Crane Bridge: F:AM 97735, left ramal fragment with p2–p4. Madison Bridge on Niobrara River: F:AM 97736, right partial ramus with p3–p4 and m1–m2 alveoli. Jonas Wilson Place: F:AM

67508A, right partial radius, distal end missing; F:AM 67510A, left proximal part ulna; F:AM 67505, left femur; and F:AM 67506A, right distal part tibia. Hans Johnson Quarry: F:AM 67508C, left distal part radius; F:AM 67511, right metacarpal II; F:AM 67513, right calcaneum. *Machairodus* Quarry: F:AM 67508D, left distal end radius. Xmas Quarry: F:AM 67510B, left proximal part ulna.

Ash Hollow Formation (late Clarendonian), Antelope and Keith counties, Nebraska: Blue Jay Quarry (UNSM loc. Ap-112): UNSM 9503-79, left ramus with p1–p4 alveoli, m1, and m2 alveolus. North Shore Locality (UNSM loc. Kh-106), north shore of Lake McConaughy (Leite, 1990: 7): UNSM 2011-91, right ramal fragment with p1–p3; UNSM 2032-91, right p4; UNSM 8107-92, right ramus with c1–m1; UNSM 8137-90, left ramal fragment with c1, p2, and p4; UNSM 9033-88, left m1; and UNSM 9034-88, left m1.

Laucomer Member, Snake Creek Formation (late Clarendonian), Sioux County, Nebraska: Six mi southeast of Olcott Hill, *Hipparion* Affine Channel: F:AM 61391, right ramus with i1–i3 alveoli, c1 broken, p1 alveolus–m2 (p4–m1 broken), and m3 alveolus; and F:AM 61395, right ramal fragment with c1–p4 all broken. Sinclair Draw (same level as holotype of *Aelurodon mortifer* Cook): AMNH 81028 (HC 269), left ramal fragment with m1–m2 and m3 alveolus. Olcott Hill (UNSM loc. Sx-71): UNSM 25594, left m1. Top of Olcott Hill: AMNH 83432, right isolated P4. Quarry C, Olcott Hill: AMNH 18262 (referred to *Aelurodon mortifer* by Skinner et al., 1977: 353), left ramus with c1–p1 alveolus and p2–m3; AMNH 18262A, left isolated m1; AMNH 108509, right isolated M1; and AMNH 108510, right isolated p4. Olcott Hill, Ashbrook Pasture: AMNH 21438, left isolated m2; AMNH 81024 (HC 375), right partial maxillary with P4–M1; AMNH 81037 (HC 374), left partial maxillary with P4–M1; AMNH 81515, left ramal fragment with p3 alveolus and p4–m1; AMNH 22363, left ramal fragment with m1 and other isolated teeth, and postcranial elements; and AMNH 108514, right isolated m1. Olcott Quarry: F:AM 61393, right ramal fragment with m1–m2. Near west boundary fence between Kilpatrick and Ashbrook ranches: AMNH 81501 (HC 661), left isolated p4. ''23 mi south of Agate'': AMNH 13842, right isolated p4 and m1; AMNH 13844, right ramal fragment with m1–m2 both broken; AMNH 82409, right ramal fragment with c1–p1 both broken and p2–p3; and AMNH 83499, right partial ramus with c1 alveolus, p1–m1 all broken, and m2–m3 alveoli. Quarry 7, Kilpatrick Pasture: AMNH 21448, right partial ramus with c1 broken, p1 alveolus, p2, p3–m1 all broken, m2, and other ramal and teeth fragments; AMNH 22032, left partial ramus with i3–c1 both broken, p1–p4, and m1 broken; AMNH 22032A, right partial maxillary with P4 broken, M1, and M2 broken; AMNH 22397, right isolated P4; AMNH 22402, left ramus with c1–p2 alveoli, p3–m2, and m3 alveolus; AMNH 22402A (referred to *Aelurodon mortifer* by Skinner et al., 1977: 353), left partial ramus with m1 and m2–m3 alveoli; AMNH 22402B, left ramal fragment with p4 alveolus and m1; AMNH 108515, left ramal fragment with m1–m2 and m3 alveolus; AMNH 108516A–C, 4 right isolated m1s; AMNH 108517A, B, right and left P4s (two individuals) and left M1; AMNH 108518, right isolated m1; and AMNH 108520, right partial ramus with p4–m1. No locality data: UNSM 8544, right ramal fragment with p4–m1.

Truckee Formation (late Clarendonian), Churchill County, Nevada: Nightingale Road Locality: F:AM 63210, left ramus with c1–m2 all broken; and F:AM 63211, right and left rami with c1–m3, skull fragments and broken teeth, right and left incomplete radii and ulnae, fragmentary humerus, metacarpals II, III, and incomplete IV, distal end of fibula, calcaneum, broken astragalus, patella, and phalanges. Brady Pocket, UCMP loc. V4845: UCMP 38666, right maxillary with P2 alveolus–M1 and M2 alveolus (referred to *Osteoborus diabloensis* by Macdonald, 1956: fig. 6).

Fish Lake Valley, Esmeralda Formation (early Clarendonian), Esmeralda County, Nevada: UCMP 29683, nearly complete skull with I3–M2, and partial left ramus with m1–m2 and m3 alveolus, and incomplete skeleton, UCMP loc. V2804; and UCR 13336 (AMNH cast 92536) (listed as *Aelurodon haydeni* by Stirton, 1932: 61), left ramus

with c1–p1 alveoli, p2–m2 (p2–p4 all broken), and m3 alveolus, UCR loc. RV6304.

The Dalles Basin, The Dalles Formation (Clarendonian), Wasco County, Oregon: UO 21353, nearly complete left ramus with i1–i3 alveoli, c1 root, p1 alveolus, p2 broken–m2, and m3 alveolus.

Ricardo Fauna, Dove Spring Formation (early and ?late Clarendonian), Mohave Desert, Kern County, California: Red Rock Canyon (LACM loc. 1414): LACM 127794, right ramal fragment with m1. Red Rock Canyon (LACM loc. 1553): immature left and right rami with dp3–dp4 and erupting m1. Red Rock Canyon (LACM loc. 3458): LACM 4266, right ramal fragment with m1–m2. Red Rock Canyon (LACM loc. 4790): LACM 143521, right ramus with roots i1–i3, c1, p1–p3 roots, p4, and m1–m3 roots. Red Rock Canyon (LACM loc. 4696): LACM 143522, edentulous right ramal fragment. Ricardo Amphitheater (LACM loc. 5713): LACM 59813, partial skull with I1–P2, P3 alveolus, and P4 broken–M2.

Love Bone Bed (late Clarendonian), Alachua Formation, Alachua County, Florida: UF 24483, left ramus with c1, p1 alveolus, p2–m1, and m2–m3 alveoli; UF 24484, left ramal fragment with p4–m1 and m2 alveolus; UF 24485, left ramal fragment with m1–m2; UF 24486, left ramal fragment with p3–p4; UF 24487, left ramus with p4–m1; UF 24489, left ramus with p2–m1; UF 24496, right ramus with p1 alveolus, p2–m2, and m3 alveolus; UF 24497, right ramus with p1 alveolus, p2–m1, and m2–m3 alveolus; UF 24498, right ramus with m1–m2 (both broken) and m3 alveolus; UF 24499, right ramus with i1–p1 alveoli and p2–m1 (p4 broken); UF 24500, right ramus with m1 and m2 alveolus; UF 24501, right ramus with c1–p2 alveoli and p3–m1; UF 24502, right ramus with p2–m1; UF 24503, right ramus with m1–m2; UF 24507, right ramus with p4–m1 (both broken); UF 24524, right P4 (Baskin, 1980: fig. 1B); UF 24525, right P4; UF 24526, left P4; UF 24527, right P4; UF 24528, right P4; UF 24529, partial left P4; UF 24530, partial right P4; UF 24531, left P4; UF 24532, partial left P4; UF 24533, partial right P4; UF 24534, partial right P4; UF 24535, partial right P4; UF 24536, partial left P4; UF 24537, right maxillary fragment with P4 and M1 alveolus; UF 24538, left maxillary with P4 and M1–M2 alveoli; UF 24539, right maxillary with P4 and M1 alveolus; UF 24541, right M1; UF 24543, left M1; UF 24544, left M1; UF 24546, left M1; UF 24547, partial left M1; UF 24549, partial left M1; UF 24550, partial left M1; UF 24551, left m1; UF 24552, partial left M1; UF 24553, left maxillary fragment with M1 broken; UF 24554, right maxillary fragment with M1, and P4 and M2 alveoli; UF 24555, left maxillary with M1 and M2 alveolus; UF 24556, left maxillary with P4 alveolus and M1; UF 24558, right ramal fragment with m1; UF 24560, right m1; UF 24561, right m1; UF 24562, left m1; UF 24563, left m1; UF 24564, right m1; UF 24565, right m1; UF 24566, rostrum with I1–I2 alveoli, I3–C1, P1–P3 alveoli, and P4–M2; UF 24567, skull fragments with P2–P3 alveoli, P4–M1, and M2 alveolus; UF 24568 and 24569, right maxillary fragment with P4–M1; UF 24571, left ramus with p1 alveolus and p2–m2; UF 24572, right ramus with p1–p4 alveoli, m1, and m2–m3 alveoli; UF 24573, left ramus with p4 alveolus, m1, and m2 alveolus; UF 24578, left maxillary with P4 alveolus and M1 broken; UF 24580, skull fragments with P2–M2; UF 25826, left ramus with c1–p3 alveoli and p4–m1; UF 25827, right ramus with p2–p3 alveoli, p4–m2, and m3 alveolus; UF 25828, right ramus with p2–p3 alveoli, p4–m1, and m2–m3 alveoli; UF 25829, right ramus with c1–p2 alveoli and p3–m1; UF 25830, left ramus with c1–p1 alveoli, p2, p3 alveolus, p4–m1, and m2 alveolus; UF 25832, left m1; UF 25912, right p4; UF 25914, left p4; UF 25915, left p4; UF 25918, right p4; UF 25919, right p4; UF 25920, right p4; UF 33301, right half skull with I1–I3 alveoli, C1, P1 alveolus, and P2–M1; UF 37160, left P4; UF 37161, right P4; UF 37162, right P4; UF 37165, right M1; UF 37167, left M1; UF 37168, right M1; UF 37169, partial left P4; UF 37170, trigonid of right m1; UF 37172, right p4; UF 37173, trigonid of left m1; UF 37174, left p4; UF 37177, partial left P4; UF 37178, right m1; UF 37179, right m1; UF 37182, right p3; UF 37185, right M1; UF 37186, right M1; UF 37187, left M2; UF 37188, right M2; UF 37189, right M2; UF 37190, left M1; UF 37191, partial left M1; UF 37192, left p4;

UF 37193, right m2; UF 37194, right M2; UF 37195, left m2; UF 37198, left M2; UF 37199, left P3; UF 37200, left p2; UF 37201, left m2; UF 37203, left m2; UF 37204, left m2; UF 37206, left P2; UF 37208, left m2; UF 37209, left m2; UF 37210, left M2; UF 37211, right p3; UF 37213, left P3; UF 37214, right M1; UF 37216, partial right m1; UF 37218, left M2; UF 37221, left p4; UF 37222, right m2; UF 37225, right p3; UF 37226, left m2; UF 37227, partial right P4; UF 37228, left M2; UF 37229, left M2; UF 37230, left m2; UF 37231, right m2; UF 37232, left p3; UF 37233, left m3; UF 37235, left p2; UF 37236, left m3; UF 37238, right m3; UF 37239, right p4; UF 37240, right m3; UF 37241, trigonid of right m1; UF 37242, partial left m1; UF 37243, right P4; UF 37244, right ramal fragment with p4; UF 37245, trigonid of left m1; UF 37247, partial right m1; UF 37248, left P3; UF 37249, left ramus with m1–m2 and m3 alveolus; UF 37250, left ramus with c1–p1 alveoli, p2–m1, and m2–m3 alveoli; UF 37253, right ramus with p2–p3 (both broken) and p4–m1; UF 37254, right ramus with c1–p1 alveoli, p2–p4, and m1 alveolus; UF 37255, left ramus with p4–m2; UF 37256, immature right ramal fragment with c1 and p3 erupting; UF 37257, right ramus with p2–p3 alveoli, p4, and m1 alveolus; UF 37259, left ramus with c1–p3 alveoli, p4, and m1–m2 alveoli; UF 37262, right ramus with p3–m1; UF 37263, right ramus with p2–p4; UF 37264, left ramal fragment with m1 broken and m2–m3 alveoli; UF 37265, right ramus with c1, p1 alveolus, p2–m2, and m3 alveolus; UF 37266, right ramus with c1, p1 alveolus, p2–m2, and m3 alveolus; UF 37267, left ramal fragment with c1–p2 alveoli and p3–p4; UF 37269, left ramus with p4–m2 and m3 alveolus; UF 37271, left ramus with c1–p3 alveoli, p4–m1, and m2–m3 alveoli; UF 37272, right ramus with c1–p1 alveoli, p2–m2 (m1 broken), and m3 alveolus; UF 37273, left ramus with c1–p1 alveoli, p2, p3 alveolus, p4–m1, and m2 alveolus; UF 37274, right ramus with c1–p1 alveoli, p2–p4, and m1 alveolus; UF 37276, left maxillary fragment with P4, and M1–M2 alveoli; UF 37277, left maxillary with P4–M1 and M2 alveolus; UF 37280, left maxillary fragment with M1–M2; UF 37281, right maxillary with P1–P4 alveoli and M1; UF 37282, right ramus with p3–m2 and m3 alveolus; UF 37283, rostrum with I1–I3 alveoli, C1, P1 alveolus, P2, P3 alveolus, and P4–M2; UF 37285, trigonid of left m1; UF 37286, left m1; UF 37288, right m1; UF 37289, trigonid of left m1; UF 37290, trigonid of left m1; UF 37291, trigonid of right m1; UF 37292, trigonid of left m1; UF 41990, left p4; UF 41991, left p4; UF 41992, left m2; UF 41993, right M2; UF 41994, right m2; UF 41995, left m2; UF 41996, right ramal fragment with m2 and m3 alveolus; UF 41997, trigonid of right m1; UF 41998, trigonid of right m1; UF 41999, trigonid of right m1; UF 43076, partial left m1; UF 43077, trigonid of right m1; UF 43078, trigonid of right m1; UF 43079, trigonid of left m1; UF 43080, trigonid of right m1; UF 43081, partial left m1; UF 43082, talonid of left m1; UF 43083, trigonid of left m1; UF 124501, right M1; UF 124502, left m1; and UF 124503, right ramus with m1 broken and m2–m3 alveoli.

Aphelops Draw Fauna, Johnson Member, Snake Creek Formation (early Hemphillian), Sioux County, Nebraska: *Aphelops* Quarry (Quarry 1): AMNH 17581, right partial maxillary with P4 and M1 broken (referred to *Aelurodon validus* by Skinner et al., 1977: 356); AMNH 20061A, left ramal fragment with p2–p3, and other teeth fragments; and AMNH 108511, right isolated broken P4. *Merychippus* Draw, *Hipparion* Affine Channel: F:AM 61392, right partial ramus with m1–m2 and m3 alveolus; and F:AM 61394, right ramal fragment with m1 and m2 broken. *Aphelops* Draw, *Hipparion* Affine Channel: F:AM 61396, right ramal fragment with c1–p2 alveoli and p3; F:AM 61399, left isolated p4; F:AM 108507, right ramal fragment with p4–m1 both broken; and F:AM 108508, left ramal fragment with m1. *Aphelops* Draw, upper sand channel: F:AM 61397, right isolated m1; and F:AM 61401, left isolated P4. ''The Pits'' south of *Pliohippus* Draw: AMNH 20483, right ramus fragment with p4 and m1–m2 alveoli; AMNH 21140A, right ramal fragment with m1; AMNH 108512, left isolated P4; and AMNH 108513, left isolated M1. ''Western fossiliferous exposures, 17 mi south and 1.5 mi east of Agate'': AMNH 81519 (HC 659), broken

left m1. Sand channel, West Draw: F:AM 61639, left partial maxillary with P3–M2 (M1 broken);

Turtle-Carnivore Quarry (UNSM loc. Ft-48), Ogallala Group (late early Hemphillian), Frontier County, Nebraska: UNSM 2688, left ramus with c1–m3 (m2 alveolus).

Port of Entry Pit (Arnett Locality), Ogallala Group (early Hemphillian), Ellis County, Oklahoma: F:AM 61420, partial skull with I1–C1 alveoli and P1–M2 (fig. 107); F:AM 61421, partial skull with I1 alveolus–M2 (all badly worn); F:AM 61422, right and left partial maxillae with I3–M1 (P1 and M2 alveoli); F:AM 61423, left isolated P4; F:AM 61424, left maxillary with I1–I2 alveoli and I3–M2; F:AM 61425, right partial maxillary with P4–M1 and M2 broken; F:AM 61426, right partial maxillary with P2 alveolus–P4 and M1 alveolus; F:AM 61427, left partial maxillary with P4–M2; F:AM 61428, right maxillary with I1–I2 alveoli and I3–M2 (P1 alveolus and P2–P3 both broken); F:AM 61429, left partial maxillary with P2–M1 (P3 alveolus); F:AM 61430, left maxillary fragment with P1 alveolus–P3; F:AM 61431, right and left immature maxillae with dP3–dP4 and C1, P3, P4, and M1 unerupted; F:AM 61432, right, and left rami with i1–i3 alveoli, and c1–m2 (p1 and m3 alveoli) (fig. 108C, D); F:AM 61433, right ramus with c1 alveolus–p4 (p1 broken), m1 broken, and m2–m3 alveoli; F:AM 61434, right ramus with i2–m2 (p3–p4 broken) and m3 alveolus; F:AM 61435, left ramus with i3 root, c1–m1 (p1 and p4 broken), and m2–m3 alveoli; F:AM 61436, right ramus with p1 broken–m2 and m3 alveolus; F:AM 61438, right partial ramus with m1 and m2–m3 alveoli; F:AM 61439, right ramus with c1–p2 alveoli, p3–m2, and m3 alveolus; F:AM 61440, left partial ramus with p1 root and p2 broken–m1; F:AM 61441, left partial ramus with p1–p4 and m1–m3 alveoli; and F:AM 61515, right partial maxillary with P3–M2.

Bridge Creek, Box T Ranch, north of Higgins, Hemphill Beds, Ogallala Group (early Hemphillian), Lipscomb County, Texas: F:AM 61566, left ramus with c1 and p1 alveolus–m3; F:AM 61567 and 61568 (one individual), right and left rami with i1–c1, p1 alveolus, p2–m2, and m3 alveolus; F:AM 61569, left ramus with i1–i3, c1 broken, p1 alveolus–m2 (m1 broken), and m3 alveolus; F:AM 61570, left ramus with c1 broken–p3, p4–m1 both broken, and m2–m3 alveoli; F:AM 61571, right ramus with i1–i3 alveoli, c1, p1 alveolus–m2, and m3 alveolus; F:AM 61573, right ramus with c1 broken–m1 and m2–m3 alveoli; F:AM 61574, right ramus with c1–p1 alveoli, p2–m2, and m3 alveolus (fig. 108E, F); F:AM 61575, right partial ramus with c1–p3, p4 root, and m1–m3 alveoli; F:AM 61578, right maxillary fragment with M1–M2; F:AM 67707, left distal end humerus; F:AM 67709A right radius and right proximal end of radius; F:AM 67709B, left proximal part of ulna; F:AM 67710, left femur; F:AM 67710A, right proximal part femur; and F:AM 67711A, right and left tibiae.

V. V. Parker Place, Pit 1, 10 mi northeast of Higgins, Ogallala Group (early Hemphillian), Lipscomb County, Texas: F:AM 61576, left partial ramus with p2–p3 alveoli, p4–m1, and m2 alveolus; and F:AM 61577, left partial ramus with p4 and m1 broken.

North Pit, Ogallala Group (early hemphillian), Ellis County, Oklahoma: F:AM 61572, right ramus with c1–m1 (p2 alveolus) and m2–m3 alveoli.

McGehee Farm Locality (early Hemphillian), 5 mi north of Newberry, Alachua County, Florida: UF 12304, right ramus with p2–p3 alveoli, and p4–m2 (p4–m1 all broken); UF 12305, broken right P4; UF 12306, broken left M1; UF 12312, right m1; UF 16163, broken left P3; UF 57530, left ramal fragment with m2 and m3 alveolus; and UF 57531, broken right M1.

Thousand Creek Fauna, Thousand Creek Formation (early Hemphillian), Humboldt County, Nevada: F:AM 61636, right ramal fragment with p2–m2 all broken and m3; and F:AM 67360, left ramal fragment with p4 broken and m1 alveolus, and detached teeth including c1, m1 broken, and m2–m3.

South of the Coso Mountains, LACM-CIT loc. 4102 (Clarendonian or Hemphillian; no detailed locality information available; this specimen is unlikely to be from the Blancan Coso Formation), Inyo County, California: LACM-CIT 5128, right ramal fragment with p3–p4.

DISTRIBUTION: Late Barstovian or early Clarendonian of New Mexico; early Claren-

donian of Nebraska, South Dakota, New Mexico, Nevada, and Texas; late Clarendonian of Nebraska, Nevada, California, and Florida; Clarendonian of Oregon; early Hemphillian of Nebraska, Oklahoma, Texas, Nevada, and Florida; early and ?late Clarendonian and Clarendonian or Hemphillian of California.

EMENDED DIAGNOSIS: *Epicyon saevus* shares with *E. haydeni* a concave dorsal edge of sagittal crest not present in *E. aelurodontoides*. Furthermore, it lacks the autapomorphies of *E. aelurodontoides*: enlarged fossa at entrance of hypoglossal canal, enlarge ventral facet of mastoid process, narrowed talon of M1, and reduced M2. Primitive characters that distinguish *E. saevus* from *E. haydeni* are smaller size; shorter auditory meatus; mandibular ramus less robust with horizontal ramus narrower anteriorly; less reduced P4 protocone; M2 metacone larger; more distinct anterior accessory cusp on p4; m1 with metaconid larger, trigonid shorter, and talonid longer; and m2 metaconid usually larger relative to protoconid.

DESCRIPTION AND COMPARISON: The large series of specimens of *Epicyon saevus* from many late Tertiary localities permits a far better appreciation of its temporal and geographic variation than had been possible in previous studies. Its long geological range and increasing size through time is the cause of large variation among dental measurements (appendix III), as is also the case for *E. haydeni* (see further discussion under *E. haydeni* about the *E. saevus–haydeni* species pair).

Cranially, *Epicyon saevus* is in the initial stage (as compared to *Borophagus*) of development of a vaulted forehead through dorsal inflation of the frontal sinus, although later individuals (e.g., F:AM 61420 from the Port of Entry Pit, fig. 107) can have a significantly more domed forehead than individuals from the Ash Hollow Formation and equivalent beds. Associated with the domed forehead is an enlarged postorbital process of the frontal. Other than the inflated frontal sinus, the skull proportions remain rather primitive, especially for the Clarendonian individuals. Individuals of this age tend to have narrower palates and rather pointed premaxillary tips, in contrast to the heavily built rostrum in *Aelurodon* and *Borophagus*. Those from early Hemphillian strata (e.g., F:AM 61420), however, have independently broadened the palate, as have many individuals of *E. haydeni*. As in *Aelurodon*, the paroccipital process is elongated and has a long free tip extending beyond the bulla. In relative cranial proportions, *E. saevus* closely follows the pattern of *E. haydeni* with the exception of a relatively less elongated temporal fossa and a shallower zygomatic process of the jugal (fig. 99).

Dentally, *Epicyon saevus* shows reduction and eventual loss of the lateral accessory cusplets on I3, a trend opposite in direction from *Aelurodon*, which tends to further strengthen these cusplets. *E. saevus* also shows the initial stages of premolar reduction—not only does it have smaller P1–P3 and p1–p3 relative to P4 and p4, but these teeth are low-crowned and there is a vertical offset between the basal cingula of P3 and P4 in lateral view, in which the tip of P3 lies dorsal to that of P4, leaving a gap between the upper and lower anterior premolars when the mouth is closed (e.g., fig. 107, F:AM 61420). There is much variation in premolar reduction, especially noticeable among individuals from the Box T Ranch of Texas (fig. 108E, F). Certain of these specimens (e.g., F:AM 61571, 61574) have premolars that are almost in the stage of reduction as in *Borophagus*. These premolar reductions are clearly independent from those in the *Borophagus* clade, as the Box T individuals have otherwise typical *Epicyon* dental morphology and unshortened lower jaws.

As noted by Baskin (1980), a ridge from the protocone of P4 is directed labially toward the parastyle instead of toward the tip of the paracone, as is primitively the case in *Aelurodon*. Although we note some variation of this feature (see also discussion under *Aelurodon asthenostylus*), Baskin's characterization of the differences between *Aelurodon* and *Epicyon* is still valid. This derived condition is fully established in *E. saevus*.

DISCUSSION: The dental morphology of the holotype of *Epicyon saevus* is limited to two worn teeth in the ramus and broken roots and alveoli of the rest (fig. 102E, F). This deficiency in knowledge was remedied, soon after Leidy's initial announcement of this spe-

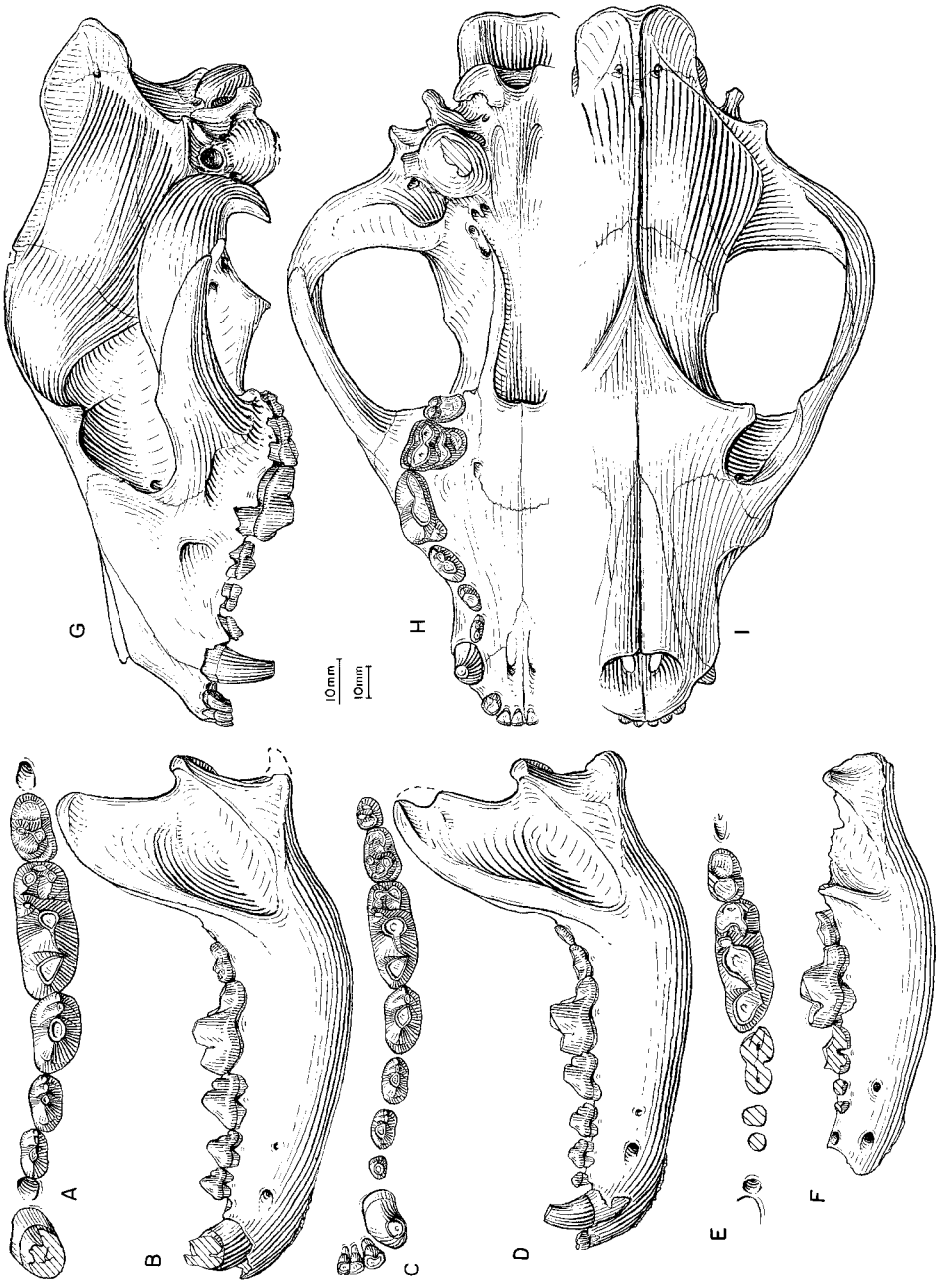

Fig. 102. *Epicyon saevus*. **A**, Lower teeth and **B**, ramus, F:AM 25102, Quinn Ranch Quarry, Cap Rock Member, Ash Hollow Formation (early Clarendonian), Cherry County, Nebraska. **C**, Lower teeth and **D**, ramus, F:AM 70621, Horn Quarry, Merritt Dam Member, Ash Hollow Formation (late Clarendonian), Cherry County, Nebraska. **E**, Lower teeth and **F**, ramus, USNM 126, holotype, "sands of the Niobrara River," ?Cap Rock Member, Ash Hollow Formation (early Clarendonian), north-central Nebraska. **G**, Lateral, **H**, ventral, and **I**, dorsal views of skull, AMNH 8305, Driftwood Creek, Republican River beds (early Clarendonian), Hitchcock County, Nebraska. The longer (upper) scale is for A, C, and E, and the shorter (lower) scale is for the rest.

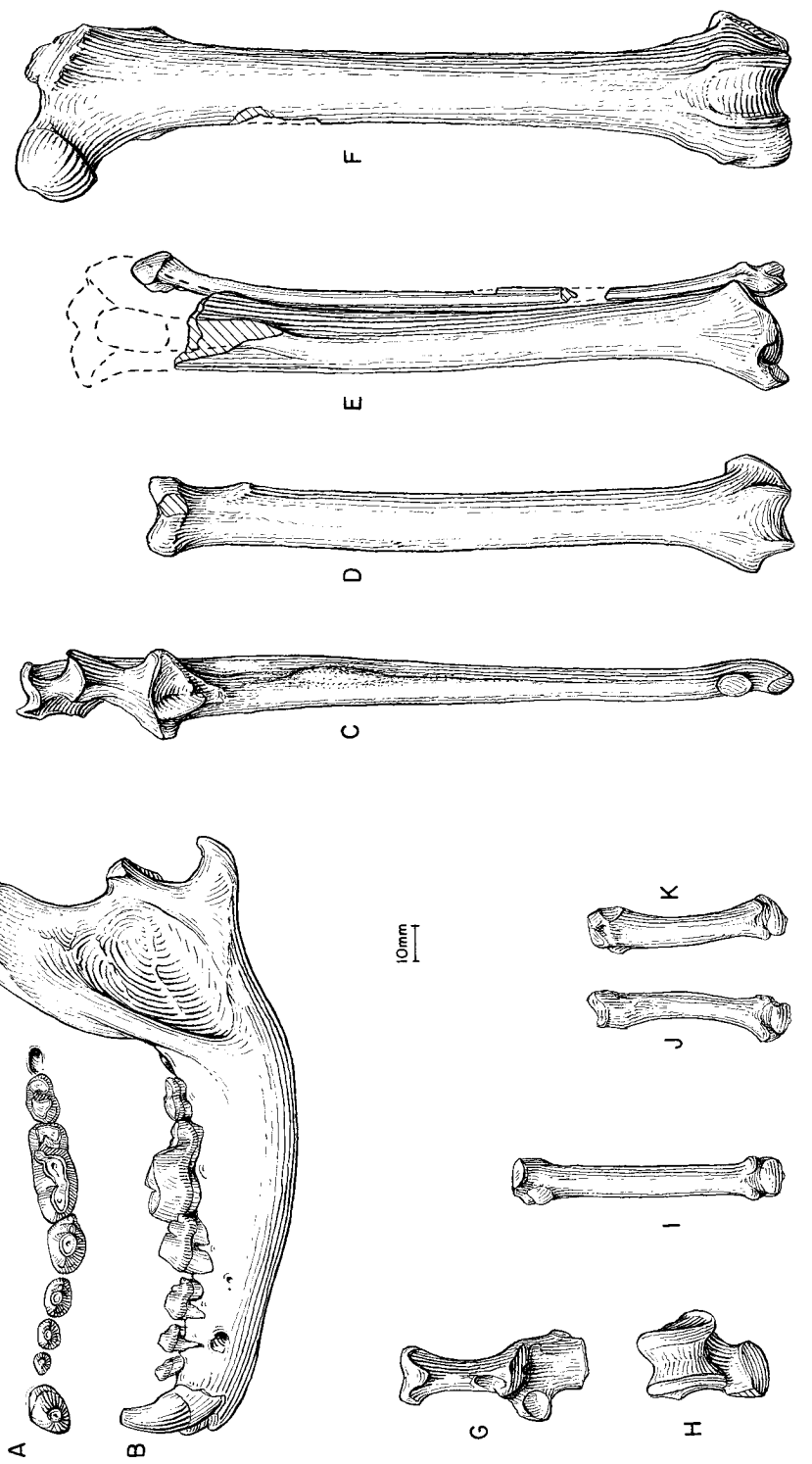

Fig. 103. *Epicyon saevus*. **A**, Lower teeth, **B**, ramus, **C**, ulna, **D**, radius, **E**, partial tibia and fibula, **F**, femur, **G**, calcaneum, **H**, astragalus, **I**, metatarsal IV, **J**, metacarpal II, and **K**, metacarpal V, AMNH 8305 (C, D, G, H, J, and K reversed from right side), Driftwood Creek, Republican River beds (early Clarendonian), Hitchcock County, Nebraska.

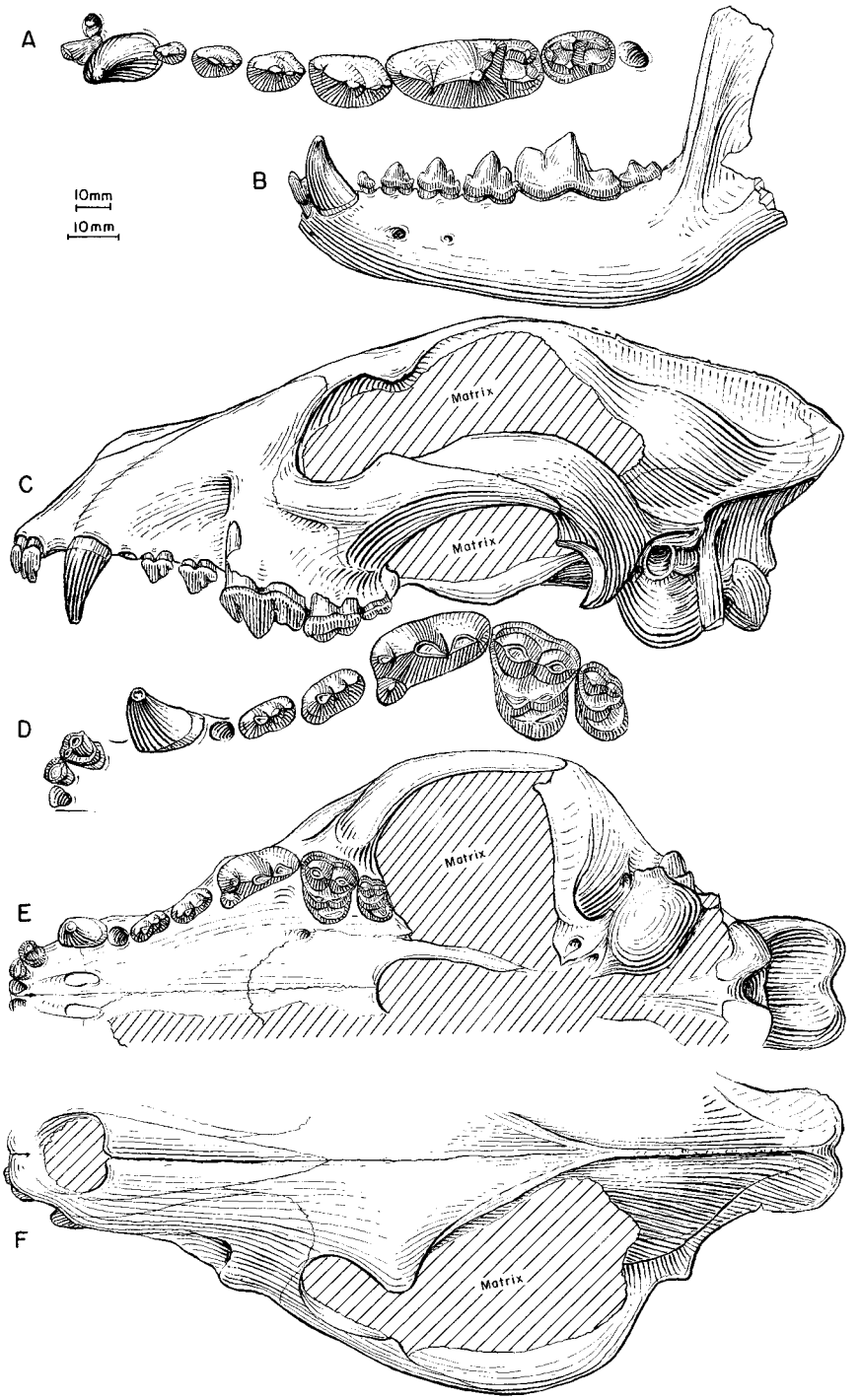

Fig. 104. *Epicyon saevus*. **A**, Lower teeth and **B**, ramus, UCMP 32328 (holotype of *Aelurodon inflatus*), Big Spring Canyon, Ogallala Group (early Clarendonian), Bennett County, South Dakota. **C**, Lateral, **D**, enlarged occlusal, **E**, ventral, and **F**, dorsal views of skull and upper teeth (I2–I3 and C1 reversed from right side), F:AM 70767, Whitefish Creek, Quarry 7, Clarendon beds (early Clarendonian), Donley County, Texas. The shorter (upper) scale is for B, C, E, and F, and the longer (lower) scale is for the rest.

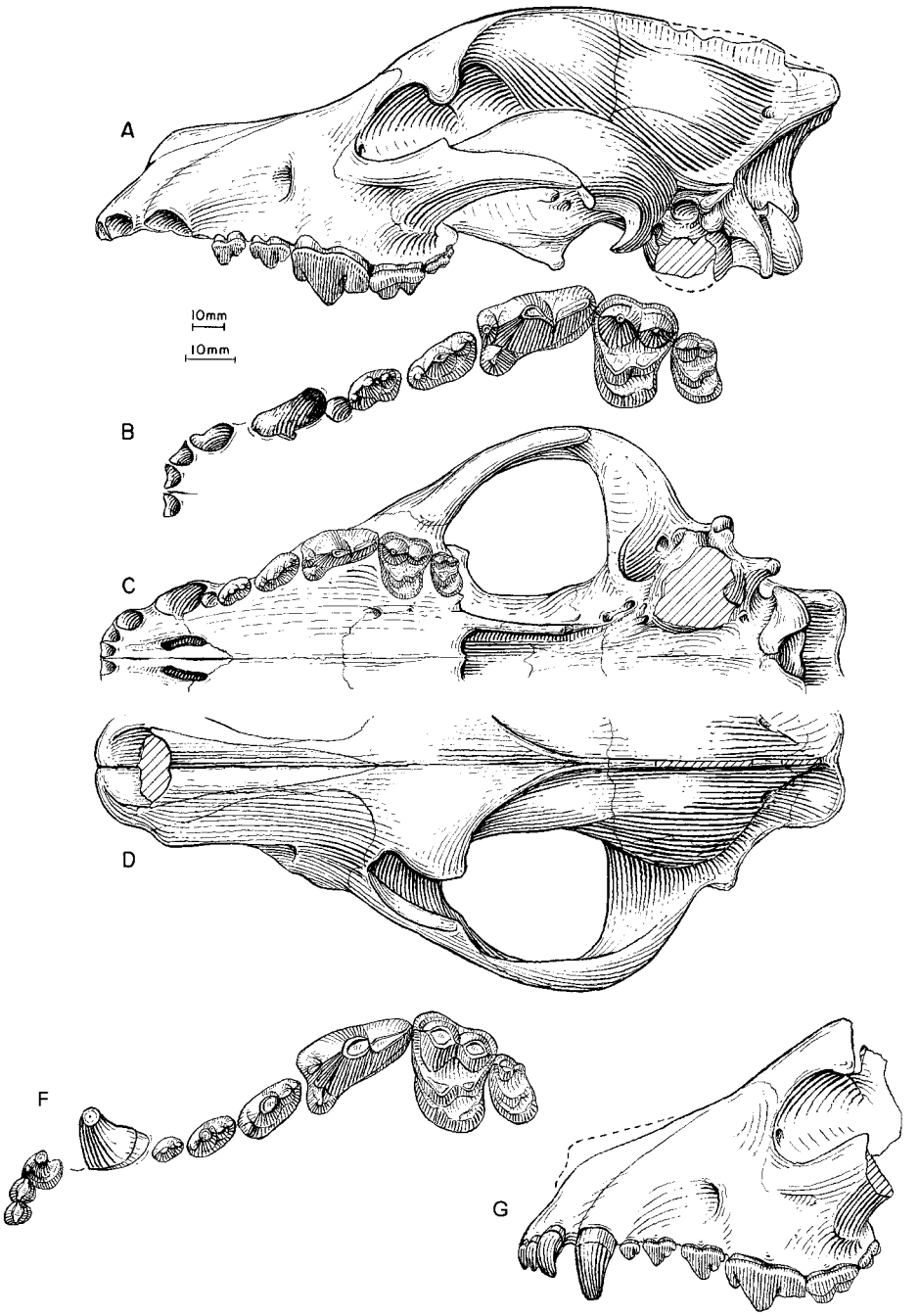

Fig. 105. *Epicyon saevus*. **A**, Lateral, **B**, enlarged occlusal, **C**, ventral, and **D**, dorsal views of skull and upper teeth, F:AM 67331, Mensinger Quarry, Merritt Dam Member, Ash Hollow Formation (late Clarendonian), Cherry County, Nebraska. **F**, Upper teeth and **G**, lateral view of partial skull, F:AM 25140, Quinn Ranch Quarry, Cap Rock Member, Ash Hollow Formation (early Clarendonian), Cherry County, Nebraska. The shorter (upper) scale is for A, C, D, and G, and the longer (lower) scale is for B and F.

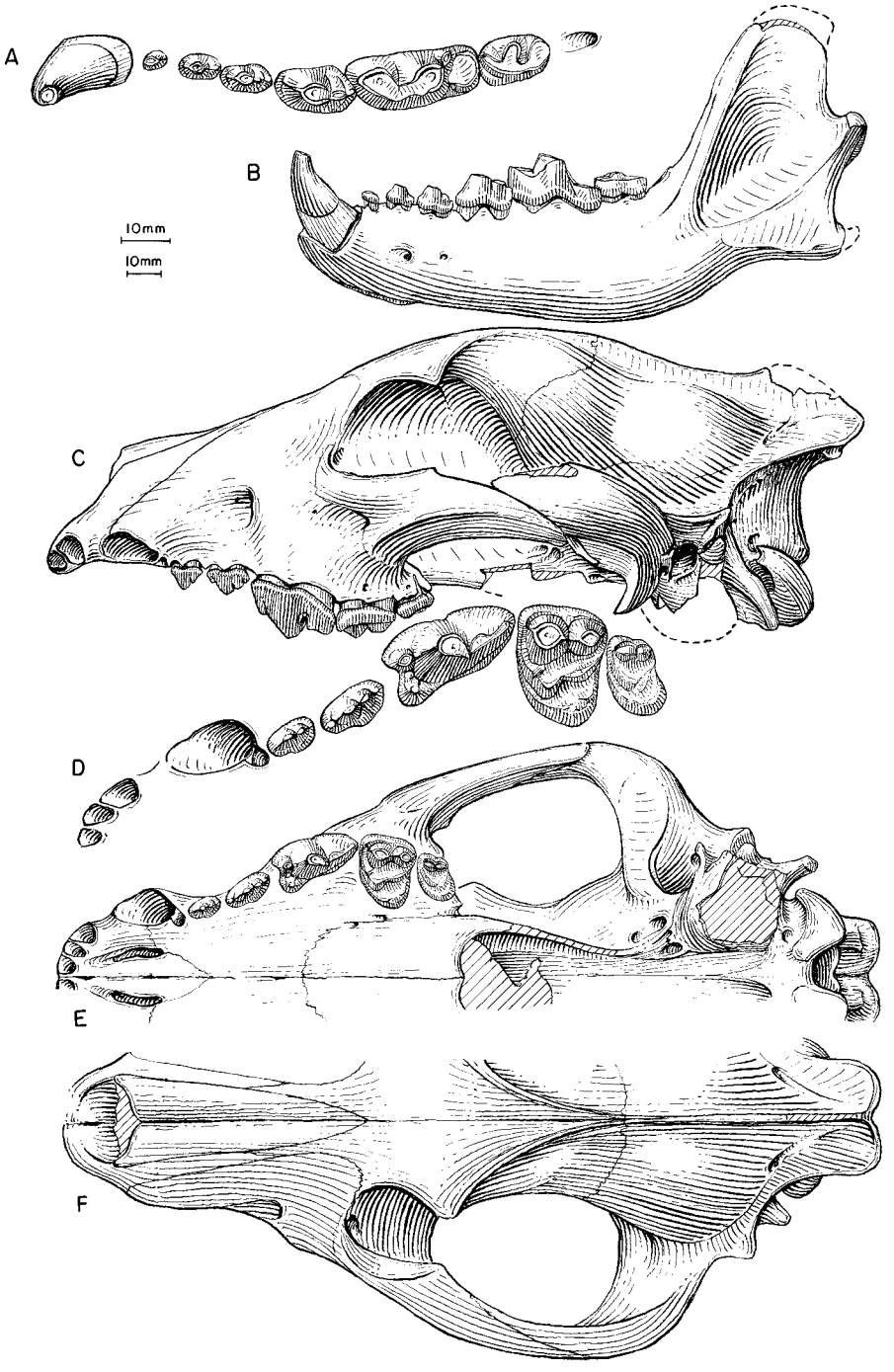

Fig. 106. *Epicyon saevus*. **A**, Lower teeth and **B**, ramus, F:AM 61382, Wade Quarry, Merritt Dam Member, Ash Hollow Formation (late Clarendonian), Cherry County, Nebraska. **C**, Lateral, **D**, enlarged occlusal, **E**, ventral, and **F**, dorsal views of skull and upper teeth, F:AM 61381, West Line Kat Quarry Channel, Merritt Dam Member, Ash Hollow Formation (late Clarendonian), Cherry County, Nebraska. The longer (upper) scale is for A and D, and the shorter (lower) scale is for the rest.

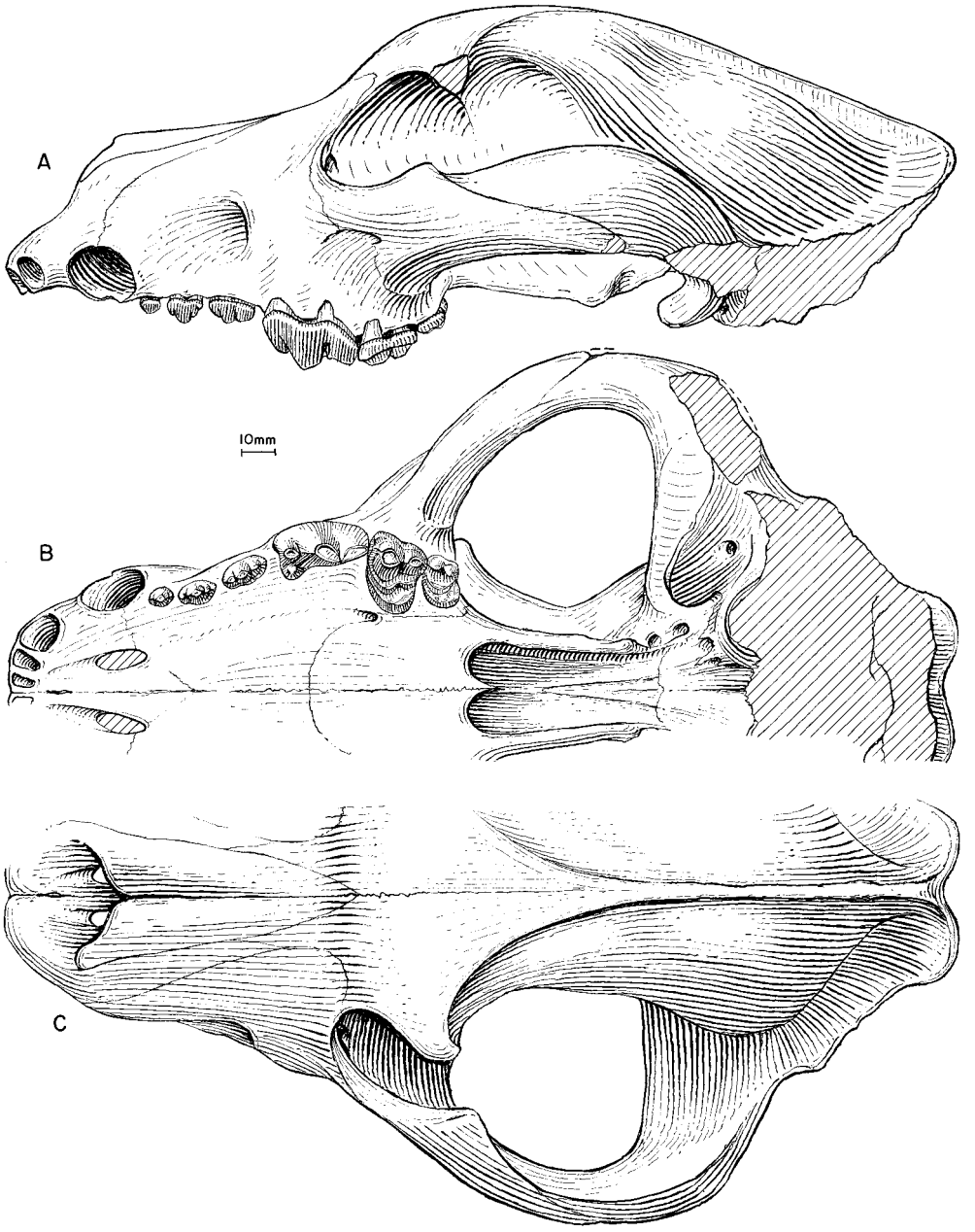

Fig. 107. *Epicyon saevus*. **A**, Lateral, **B**, ventral and **C**, dorsal views of skull (zygomatic arch and glenoid fossa reversed from right side), F:AM 61420, Port of Entry Pit, Ogallala Group (early Hemphillian), Ellis County, Oklahoma.

cies, by a complete skull and mandible with substantial part of associated skeleton (AMNH 8305) from the Republican River (Cope, 1883, 1890; Cope and Matthew, 1915). This latter specimen is still the most complete individual of the species, and it became the main material basis for the so-called *saevus* species group of McGrew (1944b) that was later referred to *Epicyon* (Baskin, 1980; Munthe, 1989). Recently,

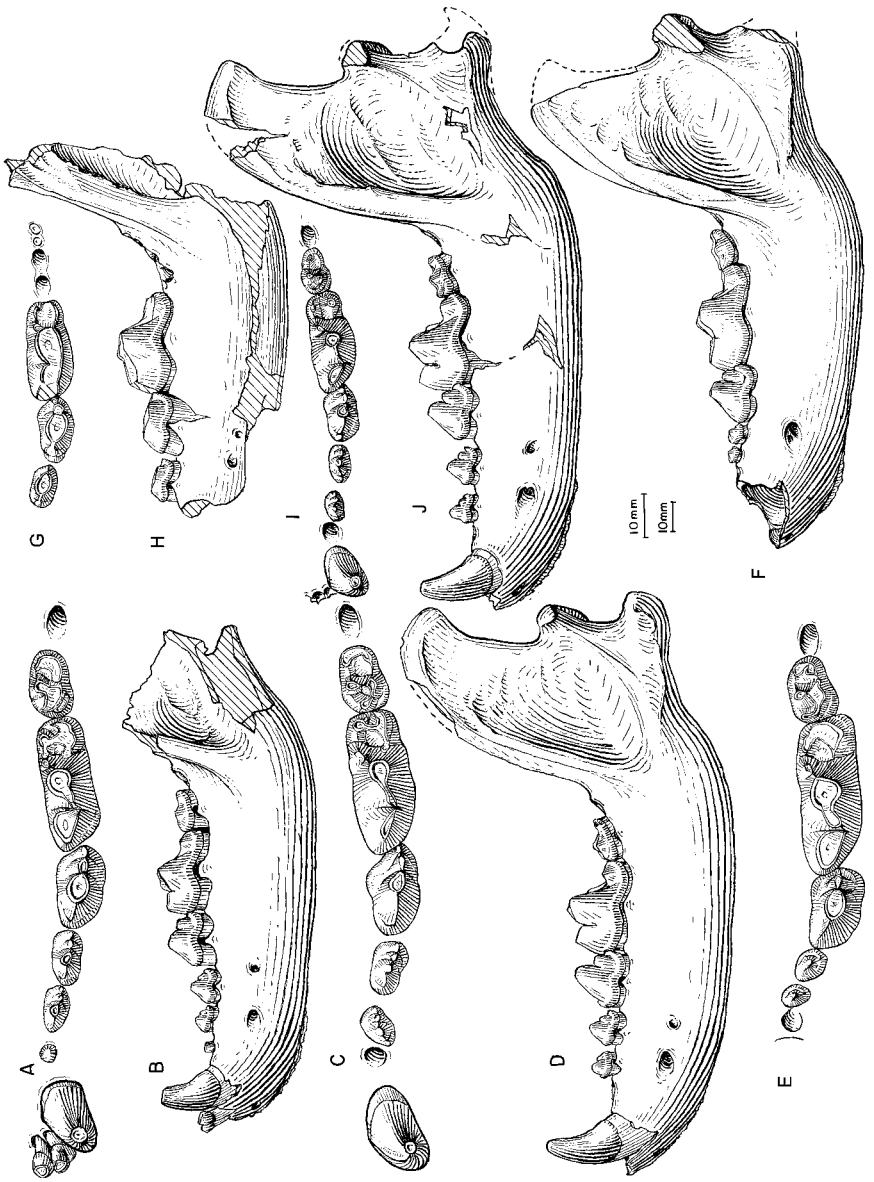

Fig. 108. **A**, Lower teeth and **B**, ramus, *Epicyon saevus*, F:AM 61387, East Kat Quarry Channel, Merritt Dam Member, Ash Hollow Formation (late Clarendonian), Cherry County, Nebraska. **C**, Lower teeth (c1 reversed from right side) and **D**, ramus, *E. saevus*, F:AM 61432, Port of Entry Pit, Ogallala Group (early Hemphillian), Ellis County, Oklahoma. **E**, Lower teeth and **F**, ramus, *E. saevus*, F:AM 61574, Box T Ranch, Ogallala Group (early Hemphillian), Lipscomb County, Texas. **G**, Lower teeth and **H**, ramus (reversed from right side), *E. haydeni*, USNM 127, holotype, ''Valley of the Niobrara River,'' possibly Merritt Dam Member, Ash Hollow Formation (late Clarendonian), Nebraska. **I**, Lower teeth and **J**, ramus, *E. haydeni*, F:AM 61453, Kat Quarry Channels, Merritt Dam Member, Ash Hollow Formation (late Clarendonian), Cherry County, Nebraska. The longer (upper) scale is for A, C, and E, and the shorter (lower) scale is for the rest.

Voorhies (1990a: A128) commented that AMNH 8305 is closely comparable to *Aelurodon wheelerianus* (*A. ferox* of this study) from the Norden Bridge Quarry. Voorhies' suggestion, however, appears to be based mainly on Cope and Matthew's (1915) figures, whereas our examination of AMNH 8305 clearly shows that it is an *Epicyon* (see Baskin [1980] for a recent summary of the complex history of this group).

When it first appears in the Clarendonian of the Great Plains, *Epicyon saevus* does not have an immediate predecessor there. Instead, its predecessor, *Protepicyon raki*, is from the late Barstovian of California and New Mexico. This is similar to the case of *Aelurodon*, whose oldest species is the early Barstovian *A. asthenostylus* of the Barstow Formation and Tonopah Local Fauna of Nevada. Such a western origin of large, hyena-like forms is also repeated in the *Borophagus* lineage, whose first member is *Borophagus littoralis* from coastal California.

Munthe's (1989) recent study of skeletal materials of *Epicyon saevus* suggests that it (and also her *E. haydeni*, which is in the same size range as the present *saevus* and is markedly smaller than individuals she referred to *E. validus*, here referred to *E. haydeni*) has relatively slender limbs and probably was cursorially adapted, preferring more open habitat (see also fig. 144). The robust dental construction of *E. saevus* was suitable for powerful bone crushing, indicating a lifestyle of active predation and scavenging.

Epicyon haydeni Leidy, 1858

Figures 108G–J, 109–113

Canis (*Epicyon*) *haydeni* Leidy, 1858: 21.
Canis haydeni Leidy, 1869: 30, pl. 1, fig. 10.
Aelurodon haydeni (Leidy): Scott, 1890: 66, fig. 2B. Matthew, 1899: 67. Matthew and Gidley, 1904: 250 (in part). VanderHoof and Gregory, 1940: 146, figs. 3, 5c, 6c. McGrew, 1944b: 82. Becker, 1980: 34.
Aelurodon haydeni validus Matthew and Cook, 1909: 371, fig. 2.
Tephrocyon mortifer Cook, 1914: 49, pls. 1–3.
Aelurodon? *aphobus* Merriam, 1919: 535, fig. 144a, b.
Aelurodon? possibly *aphobus* Merriam, 1919: 537, fig. 145.
Tomarctus mortifer (Cook): Matthew, 1924: 65. Cook, 1930: 50.
Aelurodon haydenianus validus (Matthew and Cook): Matthew, 1924: 100.
Aelurodon aphobus (Merriam): Stock, 1928: 41, pl. 1, fig. A. VanderHoof and Gregory, 1940: 152.
?*Osteoborus validus* (Matthew and Cook): Stirton and VanderHoof, 1933: 179.
Osteoborus validus (Matthew and Cook): Johnston, 1939b: 526, figs. 1–7. Hesse, 1940: 675, fig. 105. VanderHoof and Gregory, 1940: 158. Kitts, 1957: 7. Webb, 1969b: 302, fig. 7A–D.
Osteoborus ricardoensis Stirton and VanderHoof, 1933: 178.
Aelurodon mortifer (Cook): McGrew, 1944b: 79. Skinner et. al., 1977: 352.
Aelurodon cf. *A. mortifer* (Cook): Kitts, 1957: 10, pl. 1, figs. 1, 2, 5, 6. Kitts, 1964: 76, fig. 1.
Aelurodon validus (Matthew and Cook): Skinner et al., 1977: 356 (in part).
Epicyon haydeni (Leidy): Baskin, 1980: 1350. Leite, 1990: 7. Munthe, 1998: 136.
Aelurodon cf. *A. haydeni* (Leidy): Webb et al., 1981: 524.
Epicyon validus (Matthew and Cook): Munthe, 1989: 14, figs. 5C, 6F, 7F, 9F, 11G, 15F, 17G. Munthe, 1998: 137.
Epicyon cf. *E. validus* (Matthew and Cook): Leite, 1990: 15, fig, 9C, D.

HOLOTYPE: USNM 127 (AMNH cast 97244), right partial ramus with p3–p4, m1 broken, and m2–m3 alveoli (fig. 109G, H) from the ''Valley of the Niobrara River'' (Leidy, 1858: 21), possibly Merritt Dam Member, Ash Hollow Formation (late Clarendonian), Nebraska.

REFERRED SPECIMENS: White Fish Creek, Clarendon beds (early Clarendonian), Donley County, Texas: F:AM 61558, articulated crushed skull with I3–M2 and mandible with i3–m3, Quarry 1.

Merritt Dam Member, Ash Hollow Formation (late Clarendonian), Brown and Cherry counties, Nebraska: Xmas Quarry: F:AM 25149, immature maxillary fragment with dP3, detached premolar and incisor unerupted, and left ramus with c1 and p4–m2 all erupting; F:AM 25150, right ramus with c1 broken–m3 (p1 alveolus); F:AM 25151, right ramus with c1–p2 roots, p3, p4–m2 all broken, and m3 alveolus; F:AM 25152, left immature ramus with dp3–dp4, c1–p1 erupting, p4 unerupted, and m1–m2 erupting; F:AM 25223, right ramus with i2–m1 (p1 and p3 broken); F:AM 25224, left maxillary fragment with M1–M2; F:AM 25225, left isolat-

ed M1; F:AM 61451, posterior part of skull; F:AM 61458, left ramus with p2–m1 and m2–m3 alveoli; F:AM 67403, right humerus; F:AM 67403E, right distal part humerus; F:AM 67407A, right proximal part radius; F:AM 67407B, right proximal part radius; F:AM 67413A, right partial femur; F:AM 67420A, left metacarpal III; F:AM 67421, left metacarpal V; and F:AM 97734, left partial ramus with c1–p3 alveoli, p4, and m1 broken. Kat Quarry Channels: F:AM 61444, right maxillary with C1–P1 alveoli and P2–M2; F:AM 61446, right maxillary with P1 alveolus–P4, M1 broken, and M2 alveolus; F:AM 61447, left partial maxillary with P2, P3–P4 both broken, and M1; F:AM 61448, left maxillary fragment with P4; F:AM 61453, left ramus with i1–i3 alveoli and c1–m2 (p1 and p3 alveoli) (fig. 108I, J); F:AM 61461, right and left rami with i1–m2 and m3 alveolus (fig. 109A, B); F:AM 61462, right ramus with i1–i3 alveoli, c1–m1 (p2 alveolus), and m2 broken; F:AM 61463, right partial ramus with p2 alveolus, p3 broken–m2, and m3 alveolus; F:AM 61464, left partial ramus with c1–p1 alveoli, p2 broken–m1, and m2–m3 alveoli; F:AM 61465, right isolated m1; F:AM 61466, right partial ramus with p2–p3 alveoli, p4–m1, and m2–m3 alveoli; F:AM 61468, left ramus with i1–i3 alveoli, c1 broken, p1 alveolus–m1 (p1 alveolus), and m2–m3 alveoli; F:AM 61473, left ramus with c1–p1 alveoli, p2–m2, and m3 alveolus; F:AM 25138, right humerus; F:AM 67403D, left distal part of humerus; F:AM 67403F, left distal part of humerus; F:AM 67404, left radius; F:AM 67405, right radius; F:AM 67407D, right proximal end of radius; F:AM 67408, right ulna; F:AM 67413, left femur; F:AM 67417, right tibia, proximal end broken; F:AM 67418A, left distal part of tibia; F:AM 67422A, B, two right metatarsals II; F:AM 67423B, left metatarsal III; F:AM 67424, right metatarsal IV; F:AM 67425, right metatarsal V; and F:AM 67426A, left calcaneum. *Leptarctus* Quarry: F:AM 61388, right partial ramus with i1–i3 alveoli, c1 broken–p4 (p1 alveolus), m1 broken, and m2–m3 alveolus; F:AM 61443, partial skull with I1 alveolus, I2, I3 alveolus, and C1–M2 (P1 alveolus and P3 broken) (fig. 109C, D); F:AM 61454, right partial ramus with p1–m1 and m2 alveolus; F:AM 61455, right ramus with i3 alveolus–m2 (p1 alveolus); F:AM 61456, right partial ramus with c1 and p2 alveoli, p3–m2, and m3 alveolus; F:AM 61457, left partial ramus with p2–p3 alveoli, p4–m2, and m3 alveolus; F:AM 61459, left partial ramus with p4–m1 and m2–m3 alveoli; F:AM 61460, left partial ramus with i1–i3 alveoli, c1 broken–m1, and m2–m3 alveoli; F:AM 61467, right partial ramus with i1–i2 both broken, i3 alveolus, c1 broken, and p1–m3 (p2–m1 all broken); F:AM 61469, left partial ramus with c1–m2 (p1, p3, and m3 alveoli); F:AM 61470, right partial ramus with m1–m2; F:AM 61471, left partial ramus with p4–m1; F:AM 61472, left partial ramus with c1 broken–p4 (p3 alveolus) and m1 broken; F:AM 67347, right immature partial ramus with dp3–dp4, c1, and p2–p3 unerupted; F:AM 67349, right immature partial ramus with dp4; F:AM 67403A, left distal part of humerus; F:AM 67403G, right distal part of humerus; F:AM 67406, left radius; F:AM 67407, left radius; F:AM 67407C, left proximal radius; F:AM 67407F, left distal radius; F:AM 67409, left ulna; F:AM 67410, left ulna; F:AM 67411, left incomplete ulna; F:AM 67411A, left partial ulna; F:AM 67411B, right partial ulna; F:AM 67412, right femur; F:AM 67416, left tibia; F:AM 67421A, metacarpal V; F:AM 67423A, metatarsal III; and F:AM 67426C, proximal phalanx. Hans Johnson Quarry: F:AM 25141, partial skull with I1–I2 alveoli, I3–P3 all broken, and P4–M2; F:AM 67348, left immature ramus with dp4, c1, p2–p4 and m3 all erupting, and m1–m2 alveoli; F:AM 67441, associated skeletal elements of two front limbs, including both distal parts of humeri, both radii and ulnae, scapho-lunar, unciform, left metacarpal I, both metacarpals II–IV, right metacarpal V, and phalanges, including all phalanges for right manus except those for metacarpal I; F:AM 67401, left humerus, radius, and ulna; F:AM 67403C, right partial humerus; F:AM 67411C, left partial ulna; F:AM 67418, right tibia; F:AM 67419, left metacarpal II; F:AM 67420, left metacarpal III; F:AM 67421B, left metacarpal V; F:AM 67422, left metatarsal II; F:AM 67423, left metatarsal III; F:AM 67426, left calcaneum; and F:AM 67426B, medial phalanx. East Kat Creek Quarry: F:AM 61390, right isolated m2. Eggers Quarry: F:AM

70607, right partial ramus with c1–p3 alveoli, p4, m1 broken, and m2–m3 alveoli; and F:AM 70608, right ramus with c1, p2–m1, and m2–m3 alveoli. High channel at narrows of Snake River: F:AM 61449, both partial maxillae with I3–P1 alveoli, P2, P3 broken, left ramal fragment with c1–p1 alveoli, p2, and p3 broken, skull fragments, and broken teeth. Pratt Slide Quarry: F:AM 61452, right partial ramus with c1 broken, p1 alveolus, p2–p4 all broken, m1, and m2 alveolus. Pratt Quarry: F:AM 67414, left tibia. Pratt Place: F:AM 67403B, right distal end humerus. Wade Quarry: F:AM 61445, left maxillary fragment with P4 and M1 alveolus; and F: AM 61450, right broken P4. Jonas Wilson Quarry: F:AM 67415, left tibia.

Ash Hollow Formation (late Clarendonian), Keith County, Nebraska: Lonergan Creek (UNSM loc. Kh-107) and North Shore (UNSM loc. Kh-106) localities, north shore of Lake McConaughy (Leite, 1990: 7): UNSM 50826, left m1; UNSM 94203, maxillary with P4–M2; UNSM 96239, right ramus with p3–m2; UNSM 96268, right m1; UNSM 1125-90, left maxillary fragment with P3–P4 all broken; UNSM 8084-90, left p4; UNSM 8093-90, right ramal fragment with p1–p2 alveoli, p3, and p4 roots; UNSM 8126-92, right ramus with m1–m2; UNSM 8127-92, right ramal fragment with i3–c1, p1 alveolus, and p2; UNSM 8135-92, right p4; UNSM 9499-89, complete skull with I3–M2 (P1 and P3 broken); UNSM 9516-89, right broken m1; and UNSM 9500-89, right ramus with c1–m2 all broken.

Turtle Canyon, upper sandstone layer, Ash Hollow Formation (late Clarendonian), Sheridan County, Nebraska: F:AM 67402, right humerus.

Driftwood Creek (Clarendonian), Hitchcock County, Nebraska: AMNH 8313, left ramal fragment with m1–m3 alveoli; AMNH 8320, two right proximal part ulnae; and AMNH 8468a, right distal part radius.

Madison River, ''Loup Fork'' (late Clarendonian), Montana: AMNH 9744, left partial ramus with p1–p4 and m1 broken–m2.

Ricardo Fauna, Dove Spring Formation (late Clarendonian), Mohave Desert, Kern County, California: Opal Canyon (LACM loc. 5537): LACM 127790 (AMNH cast 117196), anterior partial skull with I1–M1 (P1 alveolus) and M2 alveolus. One-fourth mi south of North Last Chance Canyon (LACM-CIT loc. 1003): LACM-CIT 6 (AMNH cast 132801) (referred to *Aelurodon aphobus* by Stock, 1928: 41, pl. 1, fig. A; holotype of *Osteoborus ricardoensis* Stirton and VanderHoof, 1933: 178), right partial ramus with c1–m2 (p1 alveolus). Red Rock Canyon (LACM loc. 1553): LACM 143519, left and right maxillae with P4–M2. Red Rock Canyon (LACM loc. 6041): LACM 131855 (AMNH cast 129873), complete skull with entire dentition. Red Rock Canyon (LACM loc. 5428): LACM 138256, left ramus with c1–m2 all broken. Western El Paso Range: UCMP 21507, left partial maxillary with P3–P4 both broken and M1–M2 (holotype of *Aelurodon*? *aphobus* Merriam, 1919: 535, fig. 144). Power Line Ranch 3 (UCMP loc. V2769): UCMP 22470, left partial ramus with p4–m2 (referred to ''*Aelurodon*?, possibly *aphobus*'' by Merriam, 1919: 537, fig. 145); and UCMP 22471, left ramal fragment with m2 broken. Dove Spring: F:AM 18100, left ramal fragment with c1–p1 alveoli and p2–p4 (p2 and p4 broken).

Durham Local Fauna, Ogallala Group (?late Clarendonian or early Hemphillian), Roger Mills County, Oklahoma: OUSM 40-4-S50, right ramus with c1 broken, p1–p2 alveoli, and p3–m2 all broken (referred to *Aelurodon* cf. *A. mortifer* by Kitts, 1964: 76, fig. 1).

Pojoaque Member, Tesuque or Chamita formations (Clarendonian), Santa Fe County, New Mexico: Spring west of San Ildefonso: F:AM 27489, left maxillary with C1 broken and P1 alveolus–M2 (P4–M1 broken). San Ildefonso area: F:AM 67058, posterior part of skull and left partial ramus with p2–m2 all broken. Half mi south of Battleship Mountain: F:AM 61419, immature partial skull with dP3–dP4 and P3–M2 erupting, left and right partial rami with dp4 broken and p3–m2 erupting, incomplete vertebral column, humerus articulated with proximal ends of radius and ulna, and fragments. Santa Fe area: F:AM 27359A, right partial ramus with p4–m2 all broken and m3 alveolus. Ojo Caliente, under lava mesa: F:AM 21110, right ramal fragment with c1 broken, p1 alveolus, p2–p3, and p4 broken. No locality data: F:

AM 61555, right ramal fragment with c1 and p2–p3 all broken.

Milk Creek area, Milk Creek Formation (Clarendonian), Yavapai County, Arizona: Shields Ranch Quarry: F:AM 97151A, left partial ramus with c1 broken, p1 alveolus–p3, and p4 broken; and F:AM 97151B, left radius. Milk Creek Quarry: F:AM 97148, left ramus with i2–i3, c1 broken–p3, p4–m1 both broken, and m2–m3 alveoli. Deep Springs Quarry: F:AM 97150, left isolated M1. Manzanita Quarry: F:AM 97149, left immature partial ramus with broken deciduous incisors, dc1, dp2 broken–dp4, c1 unerupted, and m1 erupting.

President Wilson Springs, Jeddito Valley, Bidahochi Formation (Clarendonian), Navajo County, Arizona: F:AM 61559, right ramus with i1–i3 alveoli, c1 broken, p1 alveolus, p2, p3–p4 alveoli, m1 broken, and m2–m3 alveoli; and F:AM 61560, left posterior part of ramus with m2–m3 alveoli.

Love Bone Bed (late Clarendonian), Alachua Formation, Alachua County, Florida: UF 24542, left M1; UF 24545, partial right M1; UF 24548, right M1; UF 24574, left ramal fragment with m1; UF 24575, right ramal fragment with p4–m1 (both broken); UF 24570, left ramus with c1–p3 alveoli and p4 broken–m1; UF 24577, right maxillary with P4–M1 alveoli; UF 25921, right ramal fragment with p4; UF 25922, right p4; UF 37163, left P4; UF 37164, right P4; UF 37166, partial left m1; UF 37171, partial right m1; UF 37175, partial left m1; UF 37181, left p3; UF 37183, left m2; UF 37184, left p2; UF 37196, right M2; UF 37197, left P3; UF 37205, left P3; UF 37212, right p2; UF 37215, right P3; UF 37217, left P3; UF 37219, left P3; UF 37220, left p2; UF 37223, right P3; UF 37224, right M2; UF 37234, right P3; UF 37237, right P3; UF 37268, left ramus with c1, p1–p2 alveoli, p3–m2, and m3 alveolus; UF 37270, right ramus with p3–m3; UF 37284, left m1; UF 37287, left m1; UF 37293, left P4; and UF 43084, partial right P4.

Laucomer Member, Snake Creek Formation (late Clarendonian), Sioux County, Nebraska: Olcott Hill (see Skinner et. al., 1977: 352): AMNH 81004 (HC 270) (holotype of *Tephrocyon mortifer* Cook, 1914: 49, pls. 1–3), left ramus with c1–m2 and m3 alveolus (fig. 110A, B); and AMNH 81099 (HC 452), right isolated m1; Quarry 7, Kilpatrick Pasture: AMNH 21443, left partial ramus with i1–i3 alveoli, c1 broken, p1–p3 alveoli, and p4–m1 both broken; and AMNH 22378, right partial ramus with c1–p4 all broken. Surface of West Jenkins Quarry: F:AM 61562, right ramal fragment with m1–m2 and m3 alveolus (referred to *Aelurodon mortifer* by Skinner et al. [1977: 353], who considered the specimen ''likely reworked from deposits of a Snake Creek channel on the southwest side of Olcott Hill'').

North Tejon Hills, Chanac Formation, Kern County (late Clarendonian), California: LACM 16581, nuchal fragment of skull.

Aphelops Draw Fauna, Johnson Member, Snake Creek Formation (early Hemphillian), Sioux County, Nebraska: Twenty-three mi south of Agate: AMNH 14147 (holotype of *Aelurodon haydeni validus* Matthew and Cook, 1909: 371, fig. 2), left partial ramus with p3 root, p4–m2 (m1 broken), and m3 alveolus (fig. 110C, D). South of *Pliohippus* Draw: AMNH 20484, right ramal fragment with m1 and m2 alveolus; and AMNH 20484A, right isolated m1. ''The Pits,'' south of *Pliohippus* Draw: AMNH 21440, right ramal fragment with m1–m2 both broken. *Pliohippus* Draw, Snake Creek Quarry: AMNH 20485, right partial maxillary with I2–I3 alveoli, C1 broken, and P1–P3; AMNH 20486, left ramal fragment with m1 broken; AMNH 20486A, left ramal fragment with m1; and AMNH 20486B, left ramal fragment with m1. Snake Creek Quarry: AMNH 20068, right ramal fragment with c1–p1 alveoli and p2–m1 all broken, and other isolated canines and premolars; AMNH 20068A, left ramal fragment with p1 alveolus and p2–m1 (p3–m1 all broken); AMNH 20482, left partial maxillary with P3–M1 and M2 alveolus; AMNH 20482A, right partial maxillary with P4–M1 and M2 broken; and AMNH 21523, two right maxillary fragments with broken P4s and M1 alveolus. *Aphelops* Quarry No. 1.: AMNH 17580, left partial maxillary with P4–M1 (referred to *Aelurodon haydenianus validus* by Matthew, 1924: 100).

Lemoyne Quarry (UNSM loc. Kh-101), Ash Hollow Formation (early Hemphillian),

Keith County, Nebraska: UNSM 62880, isolated right P4 (Leite, 1990: fig. 9C, D).

Wray area, Ogallala Group (late early Hemphillian), Yuma County, Colorado: Locality B-1, Beecher Island: F:AM 61501, skull with I1 alveolus–M2 (fig. 110E, F); F:AM 61501A, right ramus with c1 broken–m2 (m1 broken and m3 alveolus) (fig. 111A, B); F:AM 61501B, right distal end of humerus; and F:AM 61502, basicranial area and right and left maxillae with I3 alveolus–M1. Locality C: F:AM 61503, skull with I1–M2 represented by broken teeth or alveoli; F:AM 61504, right ramus with c1 broken–m2 (p1 alveolus) and m3 alveolus; F:AM 61505, partial mandible with c1–m2 (p4 broken and m3 alveolus); F:AM 61506, left partial ramus with p4–m2; F:AM 61507, right ramal fragment with p3–m1; F:AM 61508, one canine; F:AM 61509, one canine; and F:AM 61510, one canine. Localities B and C: F:AM 67825, left humerus; F:AM 67826, left humerus; F:AM 67826A, left distal end of humerus; F:AM 67827, partial left radius; F:AM 67827A, left distal end of radius; F:AM 67828, left crushed femur; F:AM 67829, right tibia; F:AM 67829A, right tibia; F:AM 67829B, left tibia; F:AM 67830, right metacarpal III; DMNH 194 (F:AM cast 67830A), left metacarpal III; F:AM 67830B, right metacarpal III; F:AM 67831, right metacarpal IV; F:AM 67831A, left metacarpal IV; F:AM 67832, right metatarsal II; F:AM 67832A, right metatarsal II; DMNH A104 (F:AM cast 67833), right metatarsal III; F:AM 67833A, left metatarsal III; F:AM 67834A, right metatarsal IV; F:AM 67834B, left metatarsal IV and incomplete metatarsal V; F:AM 67835, right calcaneum; F:AM 67835A, left calcaneum; F:AM 67835B, right calcaneum; F:AM 67835C, left calcaneum; F:AM 67835D, left calcaneum; DMNH 713 (F:AM cast 67835E), right calcaneum; DMNH 713 (F:AM cast 67835G), left calcaneum; F:AM 67835H, right astragalus; F:AM 67835I, left astragalus; F:AM 67835J, right astragalus; and F:AM 67836A–N, proximal, medial, and distal phalanges.

Jack Swayze Quarry, Ogallala Group (early Hemphillian), Clark County, Kansas: F:AM 61475, left premaxillary-maxillary with I1 alveolus–M2 (C1 and P3 alveoli) and both rami with i1–i3 alveoli, c1–m1, and m2–m3 alveoli; F:AM 61476, left premaxillary-maxillary with I1–M2 (P2 alveolus and M1 broken); F:AM 61476A, two posterior parts of skulls; F:AM 61477, right and left partial maxillae with C1 alveolus, P1–M1 (P3 alveolus), and skull fragments; F:AM 61478, right partial maxillary with P4–M1 alveolus; F:AM 61479, left premaxillary-maxillary fragment with I1–I2 alveoli, I3–C1 both broken, P1 alveolus, and P2 broken; F:AM 61480, right maxillary fragment with M1–M2; F:AM 61481, left partial maxillary with P3 alveolus, P4–M1 both broken, and M2 alveolus; F:AM 61482, left partial maxillary with P1 alveolus, P2 broken, and P3 alveolus–M2; F:AM 61483, left partial maxillary with C1–P3 (P1 alveolus) and P4 broken; F:AM 61484, left maxillary fragment with P2–P3; F:AM 61485, right maxillary fragment with M2; F:AM 61486, broken occiput and basicranial region; F:AM 61487, right premaxillary-maxillary fragment with I1 alveolus–I3 and C1 alveolus; F:AM 61488, left premaxillary with I1 alveolus–I3; F:AM 61489 and 61489A, B, three detached canines; F:AM 61490, left partial maxillary with P4–M2; F:AM 61493, right ramus with c1–p1 alveoli, p2–p4, m1 broken, and m2 alveolus; F:AM 61494, right ramus with c1–m1 and m2 alveolus; F:AM 61494A, left ramus with i1–i3 alveoli, c1–m1 (p1 alveolus), and m2–m3 alveoli; F:AM 61495, mandible with i1–m2 and m3 alveolus; F:AM 61496, left ramus with c1–m1 and m2–m3 alveoli; F:AM 61498, left ramus with c1 alveolus–m1 and m2–m3 alveoli; F:AM 61499, right partial ramus with p3 alveolus, p4–m1, m2 alveolus, and m3 erupting; F:AM 61500, right and left rami with i1 alveolus, i2 broken–m2, and m3 alveolus; F:AM 67601, left humerus; F:AM 67602, left humerus; F:AM 67603, right humerus (Munthe, 1989: figs. 6F, 7F); F:AM 67604, left humerus; F:AM 67605, right humerus with proximal end broken; F:AM 67605A–C, three left distal part humeri; F:AM 67605D, left proximal end humerus; F:AM 67606, right radius; F:AM 67607, right radius (Munthe, 1989: fig. 9F); F:AM 67608 and 67608A, B, one right and two left proximal ends of radii; F:AM 67608C–G, one right and four left distal part radii; F:AM 67609, left ulna; F:AM 67610, left ulna; F:AM 67611 right ulna (Munthe,

1989: fig. 11G); F:AM 67612A–E, three right and three left proximal part ulnae; F:AM 67613, right femur (Munthe, 1989: fig. 15F); F:AM 67613A, B, two distal part tibiae; F:AM 67614, right tibia; F:AM 67615, right tibia; F:AM 67616, right and left tibiae (Munthe, 1989: fig. 17G); F:AM 67616A–C, right proximal end and one right and two left distal ends tibiae; F:AM 67617, left metacarpal I (fig. 111E); 67618D, two right four right and one incomplete metacarpals II (fig. 111F); F:AM 67619B, right partial metacarpal II; F:AM 67619A, one right and one left metacarpals III (fig. 111G); F:AM 67620B, one complete and two proximal part metacarpals IV (fig. 111H); F:AM 67621A, two left metacarpals V (fig. 111I); F:AM 67622A, one right and two left metatarsals I (fig. 112D); F:AM 67623A–C, two left and one left incomplete metatarsals II (fig. 112E); F:AM 67624A–C, one left and three right metatarsals III (fig. 112F); F:AM 67625, left metatarsal IV; F:AM 67625A, B, one right and one left metatarsal IV with distal end broken (fig. 112G); F:AM 67626, right metatarsal V (fig. 112H); F:AM 67626A, right metatarsal V (pathological); F:AM 67627, left calcaneum (fig. 112B); F:AM 67627A–C, two complete and one broken calcanea; F:AM 67628D, five astragali (fig. 112A); F:AM 67628E–G, cuboid (fig. 112C), scapholunar and unciform (fig. 111C, D); uncataloged skeleton fragments, carpals, tarsals, and phalanges (fig. 111J–O, 112I–N); and F:AM 100083, left partial scapula (Munthe, 1989: fig. 5C).

Vicinity of Ashland, Ogallala Group (early Hemphillian), Clark County, Kansas: Rhino Quarry, Young Brothers Ranch: F:AM 61491, left partial maxillary with P4 broken–M2; F:AM 61497, left ramus with p2 alveolus–m1 and m2–m3 alveoli; F:AM 67630, metacarpal IV; F:AM 67630A, metacarpal IV with proximal end broken; F:AM 67631, left metatarsal V. John Dakin Quarry: F:AM 61492, right and left rami with i1–i3 alveoli, c1–m2 (p1 alveolus), and m3 alveolus.

F. Sebastian Place, 1 mi southwest of Oberlin, Ogallala Group (early Hemphillian), Decatur County, Kansas: F:AM 61474, anterior half of skull with I1–I2, I3 broken–M1 (P1 alveolus), and M2 alveolus, and right metacarpal II (fig. 113A–C).

Vicinity of Hall Cope's Ranch, 6 mi southwest of Norton, Ogallala Group (early Hemphillian), Norton County, Kansas: F:AM 30901, partial anterior half skull with I3–M2; F:AM 30901A, right ramal fragment with p3 broken–m1 and m2–m3 both broken; and F:AM 30901B, partial atlas, left tibia, partial right hand, partial left calcaneum, and other fragments.

Port of Entry Pit (Arnett Locality), Ogallala Group (early Hemphillian), Ellis County, Oklahoma: F:AM 61442, left ramal fragment with c1 broken, p1 alveolus, and p2–p3; F:AM 61511, right ramus with i1–i3 alveoli and c1–m2 (p1 and m3 alveoli); F:AM 61512, left partial maxillary with P2–P3 alveoli and P4–M2; F:AM 61513, left premaxillary-maxillary with I1–I2 broken, I3, C1 broken–P3 (P1 alveolus), and P4–M2 alveoli; F:AM 61516, left partial maxillary with P4–M2 (M1 broken); F:AM 61518, left isolated P4; F:AM 61519, right partial maxillary with P4, M1 broken, and M2 alveolus; F:AM 61520, right partial maxillary with P3 alveolus–M1; F:AM 61521, right partial maxillary with P4–M1 both broken and M2; F:AM 61523, right maxillary fragment with P4–M1; F:AM 61523B, left partial maxillary with M1–M2; F:AM 61523C, right isolated M1; F:AM 61524, right ramus with c1 broken, p1–m2, and m3 alveolus; F:AM 61525, right ramus with c1, p2–p3 roots, and p4–m1; F:AM 61526, right ramus with c1–m2 (p1–p2 and m3 alveoli); F:AM 61527, left partial ramus with p3 alveolus, p4–m2 (m1 broken), and m3 alveolus; F:AM 61528, left ramus with p2 alveolus, p3–m2, and m3 alveolus; F:AM 61529, right ramal fragment with m1 and m2–m3 alveoli; F:AM 61530, left partial ramus with c1–p1 alveolus, p2–p4, m1 broken, and m2–m3 alveoli; F:AM 61531, right partial ramus with p3–m2 and m3 alveolus; F:AM 61532, right partial ramus with p4–m1 and m2–m3 alveoli; F:AM 61533, right ramus with i2 alveolus–m2 (p1 alveolus) and m3 alveolus; F:AM 61534, left ramus with c1–m2 (p1 alveolus) and m3 alveolus; F:AM 61535, left partial ramus with p4–m2 and m3 alveolus (fig. 113D, E); F:AM 61538, left ramus with i1 alveolus–m2 (p1 alveolus, p2 broken, and p4 root) and m3 alveolus; F:AM 61540, right ramus with c1, p2–m2, and m3 alveolus; F:AM 61541, right

ramus with i1–i2 alveoli, i3–m2 (c1 broken, p1 alveolus, and p3–p4 broken), and m3 alveolus; F:AM 61542, left ramus with c1–p2 alveoli, p3, p4–m1 both broken, and m2–m3 alveoli; F:AM 61543, left partial ramus with c1–p3 alveoli and p4–m1 broken; F:AM 61544, left partial ramus with p1 alveolus–m1 (p4 broken); F:AM 61547, left partial ramus with p1 alveolus–m1 and m2–m3 alveoli; F:AM 61551, right partial ramus with i1–p1 alveoli, p2 root–p3, and p4–m1 both broken; F:AM 61552, left partial ramus with i3, c1 broken, p1 alveolus, p2 broken–p4, and m1 broken; F:AM 61553 and 61554 (?one individual), right and left rami with c1 broken, p1–p4, m1 alveolus, m2 broken, and m3 alveolus; F:AM 67391, anterior parts of palate with I2–P3 and crushed posterior part of skull; OMNH 15174 (OUSM 40-1-S40), right maxillary with P3–M2 (referred to *Aelurodon* cf. *A. mortifer* by Kitts, 1957: 10, figs. 1, 2); OUSM 40-4-S26, left ramus with c1–m1 (referred to *Aelurodon* cf. *A. mortifer* by Kitts, 1957: figs. 5, 6); and OUSM 40-4-S52, partial ramus with i1–p1 alveoli and p2–m1 (referred to *Osteoborus validus* by Kitts, 1957: 7).

Ogallala Group (early Hemphillian), Ellis County, Oklahoma: Schwab Place, 0.5 mi north of highway, state line, east of Higgins: F:AM 61522, left partial maxillary with P4–M2. Fritzler Place, southwest of Giger Pit: F:AM 61537, left partial ramus with i3–c1 both broken and p1 alveolus–m1 (p4–m1 both broken). Five mi east of Higgins: F:AM 61545, left partial ramus with p3–m1 broken.

Ogallala Group (early Hemphillian), Lipscomb County, Texas: V. V. Parker Place, Pit 1, 10 mi northeast of Higgins: F:AM 61517, left isolated P4; F:AM 61536, left ramus with p1 alveolus–m1 and m2–m3 alveoli; F:AM 61539, right partial ramus with c1–m1 (p1 alveolus and m1 broken) and m2 alveolus; and F:AM 61549, left ramal fragment with p3 alveolus and p4. Parker Pit 2: F:AM 61523A, left maxillary fragment with P4 broken. V. V. Parker, Pit 4: F:AM 61514, left premaxillary-maxillary with I1–I2 alveoli, I3–C1, P1 root, P2, P3 alveolus, and P4–M1. Martin Sebit Ranch, 2 mi south of Higgins: F:AM 61523D, right premaxillary-maxillary with I1–I3 alveoli, C1, and P1–P3 alveoli; F:AM 61550, right partial ramus with c1–m1 (p4–m1 both broken); and WTSU 1100, skull with I3, P1–P2, and P4, and partial left and right rami with p1–m1 (referred to *Osteoborus validus* by Johnston, 1939b: 526, figs. 1–7). Bridge Creek, Box T Ranch, north of Higgins: F:AM 61546, right ramal fragment with m1 broken and m2 alveolus; and F:AM 61548, left ramal fragment with c1, p2 broken, and p3–p4. Higgins Loc. B (UCMP loc. V2825?): UCMP 30177, left ramal fragment with broken m1 and m2–m3 alveoli; and UCMP 30178, partial left m1.

Star Valley Quarry (early Hemphillian), unnamed beds in Banbury Basalt, Little Owyhee River, Owyhee County, Idaho (referred to *Aelurodon haydeni* by Becker, 1980: 34): IMNH 24542 (AMNH cast 108172), left ramus with i1–i3 alveoli, c1 broken, p1–p4 broken, and m1–m2 alveoli; and IMNH 24632 (AMNH cast 108172), broken left m1, questionably associated with IMNH 24542.

Prison Farm Gravel Pit, UMMP loc. 7403 (?Hemphillian), Powell County, Montana: MPUM 5085 (UCMP cast 113724), left ramus with c1 broken–m3 (p1 alveolus).

Rome Fauna, Rome beds (early Hemphillian), Dry Creek (LACM-CIT loc. 62), Malheur County, Oregon: LACM 6565, left maxillary with C1–P3.

Haile 19A Locality, Alachua Formation (early Hemphillian), Alachua County, Florida: UF 24201, anterior rostrum with I1–P1 alveoli and P2; UF 47312, right C1; UF 47351, right maxillary fragment with P4–M1 and M2 alveolus; UF 92000, partial skull with I1–I2 alveoli, I3, C1–P1 alveoli, and P2–M2; UF 114675, left C1; and UF 117700, right ramal fragment with m1 and m2–m3 alveoli.

McGehee Farm Locality (early Hemphillian), 5 mi north of Newberry, Alachua County, Florida (list following Webb, 1969b: fig. 7A, D; all were referred to *Osteoborus validus*): UF 12307, right c1; and UF 12308, partial right ramus with c1–m1 alveoli.

Mixson's Bone Bed, Williston, Alachua Formation (early Hemphillian), Levy County, Florida: F:AM 61556, right isolated p4 (referred to *Osteoborus validus* by Webb, 1969b: 302, fig. 7B, C); F:AM 61557, right premaxillary fragment with i1–c1 alveoli; and F:AM 67952, right metacarpal III.

Palmetto Fauna (''Upper Bone Valley Fauna'' of Tedford et al., 1987), Bone Valley Formation (late Hemphillian), Hardee and Polk counties, Florida: CF Industries Mine: UF 130117, right M1. District Grade Mine: UF 57301, left M1. Fort Green Mine: UF 60821, partial left m1; and UF 68040, partial right p4. Nichols Mine: UF 24009, left p4; and UF 24595, right p4. Phosphoria Mine: UF 40088, left c1. Silver City Mine: UF 53826, left ramal fragment with p4–m1 alveoli.

DISTRIBUTION: Early Clarendonian of Texas; late Clarendonian of Nebraska, Montana, New Mexico, Oklahoma, California, and Florida; Clarendonian of New Mexico and Arizona; early Hemphillian of Nebraska, Kansas, Colorado, Oklahoma, Texas, Idaho, Oregon, and Florida; late Hemphillian of Florida; and ?Hemphillian of Montana.

EMENDED DIAGNOSIS: Derived features distinguishing *Epicyon haydeni* from *E. aelurodontoides* and *E. saevus* are larger size; longer tube for external auditory meatus; mandibular ramus more robust, with horizontal ramus deeper anteriorly; P4 protocone more reduced; M2 metacone reduced; p4 wider and its anterior accessory cusp more reduced or lost; m1 metaconid smaller, trigonid more elongate, and talonid narrower and shorter relative to length of trigonid; and m2 metaconid usually smaller relative to protoconid. *E. haydeni* can be further distinguished from *E. aelurodontoides* by the lack of a large fossa in hypoglossal canal, a generally unenlarged mastoid process, and dorsal edge of the sagittal crest concave.

DESCRIPTION AND COMPARISON: Large samples of referred specimens available for this study permit rather complete knowledge about *Epicyon haydeni* both in dental and skeletal morphology and in temporal and geographic variation. As the largest canid ever evolved, *E. haydeni* reached the size of a grizzly bear. The large size and bone-crushing dental morphology make this species easy to recognize. For the most part, *E. haydeni* is an enlarged version of *E. saevus*, and differences reflected in their ratio diagrams indicate the relatively more elongated temporal fossa and deepened jugal in *E. haydeni* (fig. 99). Coevolution of the *saevus–haydeni* species pair during the early Clarendonian through early Hemphillian (see Discussion below) toward an ever larger size, however, presents some problems in identification. Some late Clarendonian individuals of *E. haydeni* are nearly the same size as those of the early Hemphillian *E. saevus*, but individuals of these two species from the same quarry or stratigraphic interval commonly do not overlap in size (fig. 114). In addition to this size difference, *E. haydeni* is more derived than *E. saevus* in several dental proportions (fig. 100), with its relatively smaller P1–P3 and p1–p3, larger and broader P4 and p4, and smaller M2 and m2. Qualitatively, *E. haydeni* tends to have a more reduced anterior cingular cusp on p4 and slightly more hypercarnivorous m1–m2 with more reduced metaconids.

DISCUSSION: Abundant fossils, large size variations, widespread geographic distribution, and long geological history combine to provide a fertile ground for taxonomic controversies regarding *Epicyon haydeni* (see synonym list). Thus, *Tephrocyon mortifer* Cook, 1914 was named from the Snake Creek Fauna (Laucomer Member of Snake Creek Formation), *Aelurodon haydeni validus* Matthew and Cook, 1909 from the *Aphelops* Draw Fauna (Johnson Member of Snake Creek Formation), and *Aelurodon aphobus* Merriam, 1919 and *Osteoborus ricardoensis* Stirton and VanderHoof, 1933 from the Dove Spring Formation (formerly Ricardo Formation), as well as various combinations of these names. VanderHoof and Gregory's (1940) attempt to clarify this nomenclatural proliferation resulted in only one synonym for *E. haydeni* (*T. mortifer*). Our own analysis suggests that all of above taxa fall within the species lineage of *E. haydeni*, which increased its size throughout its existence and was widespread over much of the North American continent.

Baskin (1998) demonstrated a co-occurrence of the *Epicyon saevus–haydeni* species pair in the late Clarendonian to early Hemphillian and the parallel increase of body size throughout their coexistence, a conclusion in essential agreement with our own analysis (fig. 114). Besides the larger sample available to us, our results differ from Baskin's only in minor details. For example, AMNH 81004 (holotype of *E. mortifer*) was ques-

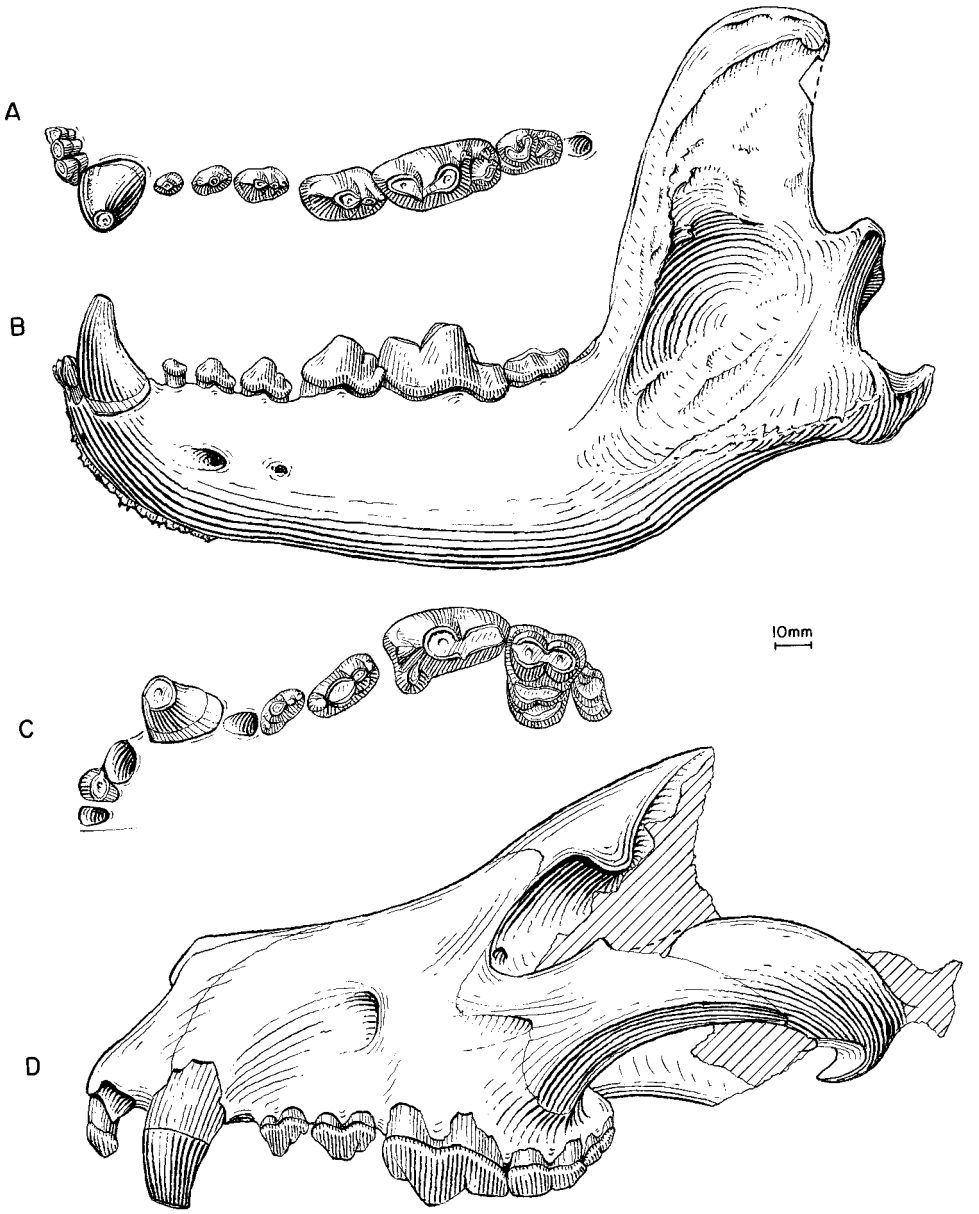

Fig. 109. *Epicyon haydeni*. **A**, Lower teeth and **B**, ramus, F:AM 61461, Kat Quarry Channels, Merritt Dam Member, Ash Hollow Formation (late Clarendonian), Cherry County, Nebraska. **C**, Upper teeth and **D**, lateral view of partial skull (nasal and frontal crushing restored), F:AM 61443, *Leptarctus* Quarry, Merritt Dam Member, Ash Hollow Formation (late Clarendonian), Cherry County, Nebraska.

tionably placed in *E. saevus* by Baskin, whereas we place it under *E. haydeni* mainly based on Skinner et al.'s (1977: 352) stratigraphic determination that it was probably collected from the Laucomer Member of the Snake Creek Formation. Given such stratigraphic context, AMNH 81004 is significantly larger than most of the referred specimens of *E. saevus* from the same strata, and as suggested by VanderHoof and Gregory (1940), we synonymized *E. mortifer* under *E. haydeni*.

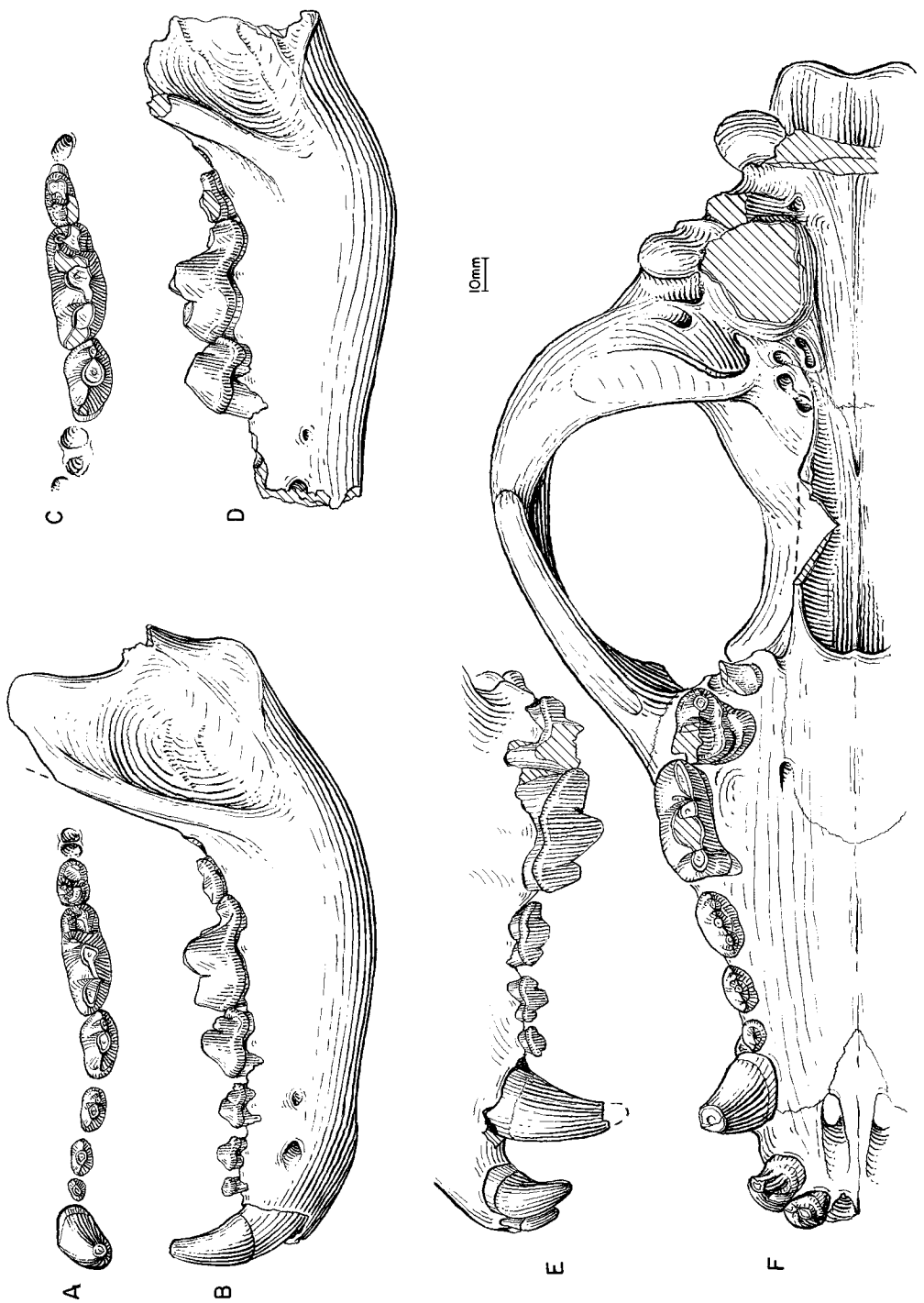

Fig. 110. *Epicyon haydeni*. **A**, Lower teeth and **B**, ramus, AMNH 81004 (holotype of *Tephrocyon mortifer*), Olcott Hill, Laucomer Member, Snake Creek Formation (late Clarendonian), Sioux County, Nebraska. **C**, Lower teeth and **D**, ramus, AMNH 14147 (holotype of *Aelurodon haydeni validus*), 23 mi south of Agate, Johnson Member, Snake Creek Formation (early Hemphillian), Sioux County, Nebraska. **E**, Lateral and **F**, ventral views of skull (combined from both sides), F:AM 61501, Beecher Island, Wray area, Ogallala Group (early Hemphillian), Yuma County, Colorado.

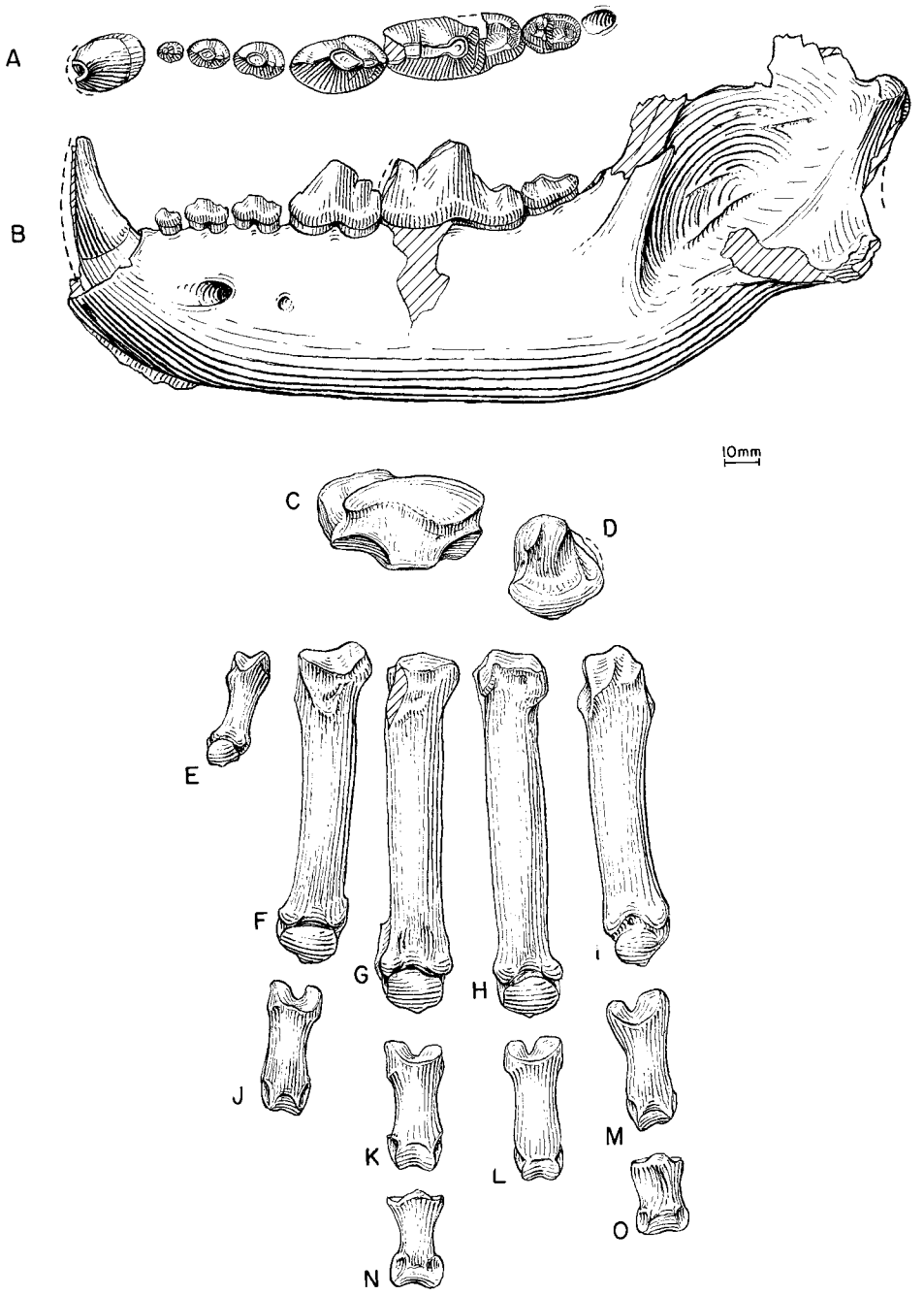

Fig. 111. *Epicyon haydeni*. **A**, Lower teeth and **B**, ramus, F:AM 61501A, Beecher Island, Wray area, Ogallala Group (late early Hemphillian), Yuma County, Colorado. **C**, Scapho-lunar, F:AM 67628F. **D**, Unciform, F:AM 67628G. **E**, Metacarpal I (reversed from right side), F:AM 67617. **F**, Metacarpal II, F:AM 67618D. **G**, Metacarpal III, F:AM 67619A. **H**, Metacarpal IV, F:AM 67620B. **I**, Metacarpal V, F:AM 67621A. **J**–**O**, Proximal and medial phalanges, uncataloged; C–O from Jack Swayze Quarry, Ogallala Group (early Hemphillian), Clark County, Kansas.

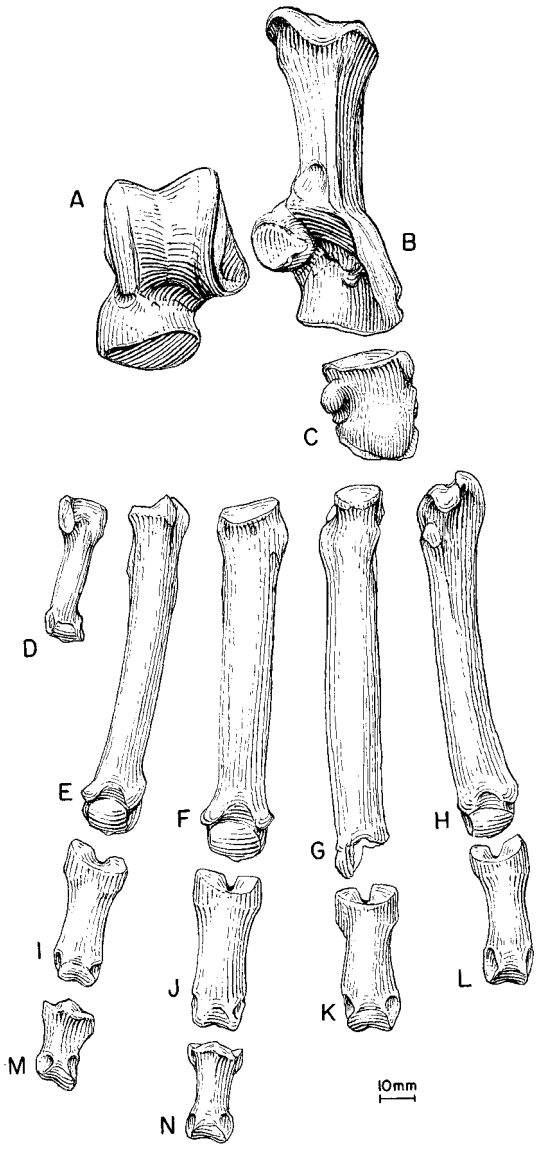

Fig. 112. *Epicyon haydeni*. **A**, Astragalus, F:AM 67628D. **B**, Calcaneum, F:AM 67627. **C**, Cuboid, F:AM 67628E. **D**, Metatarsal I, F:AM 67622A. **E**, Metatarsal II, F:AM 67623A. **F**, Metatarsal III, F:AM 67624. **G**, Metatarsal IV, F:AM 67625A. **H**, Metatarsal V, F:AM 67626 (reversed from right side). **I–N**, Proximal and medial phalanges, uncataloged. All from Jack Swayze Quarry, Ogallala Group (early Hemphillian), Clark County, Kansas.

Beginning in the late Clarendonian, *E. saevus* is accompanied by a larger *E. haydeni* in many localities. We thus recognize two distinct size groups that were maintained throughout the late Clarendonian and early Hemphillian despite the continued size increase by both groups. Known localities that have co-occurrence of the two morphs include Merritt Dam Member (late Clarendonian) of Ash Hollow Formation in north-central Nebraska, Pojoaque Member (Clarendonian) of Tesuque Formation in the Española Basin of New Mexico, Dove Spring Formation (late Clarendonian) in the western Mojave Desert of California, Love Bone Bed (late Clarendonian) of Alachua Formation in Florida, Johnson and Laucomer members (late Clarendonian through early Hemphillian) of Snake Creek Formation in western Nebraska, Port of Entry Quarry (early Hemphillian) in Oklahoma, and McGehee Farm (early Hemphillian) in Florida. Many other localities (see referred specimens listed under both species), mostly with small samples, contain only one morph. A notable exception to this *Epicyon* species pair is in the Black Hawk Ranch (late Clarendonian) of coastal California, where a different pair of Borophagini coexist: a large *Aelurodon taxoides* and a small *Borophagus littoralis*. The size ranges of the latter two species are nearly the same as the *saevus–haydeni* pair, and presumably they occupied similar ecological niches as their counterparts in the continental interior.

Although the size differences between *Epicyon saevus* and *E. haydeni* may possibly be explained as sexual dimorphisms of a single species (in which case the dimorphism must have started from a nondimorphic *E. saevus* in the early Clarendonian), we chose to view them as distinct species for three reasons. First, no living canids have exhibited such great size differences between opposite sexes, nor have we been compelled to consider this for other borophagines. Linear dimensions of common dental measurements are normally within 5% of each other among living canid species (e.g., Gingerich and Winkler , 1979; and personal obs.), whereas they are 16–23% in most quarry samples where the two species coexist. For example, *haydeni* is 22% larger, in m1 length, than *saevus*

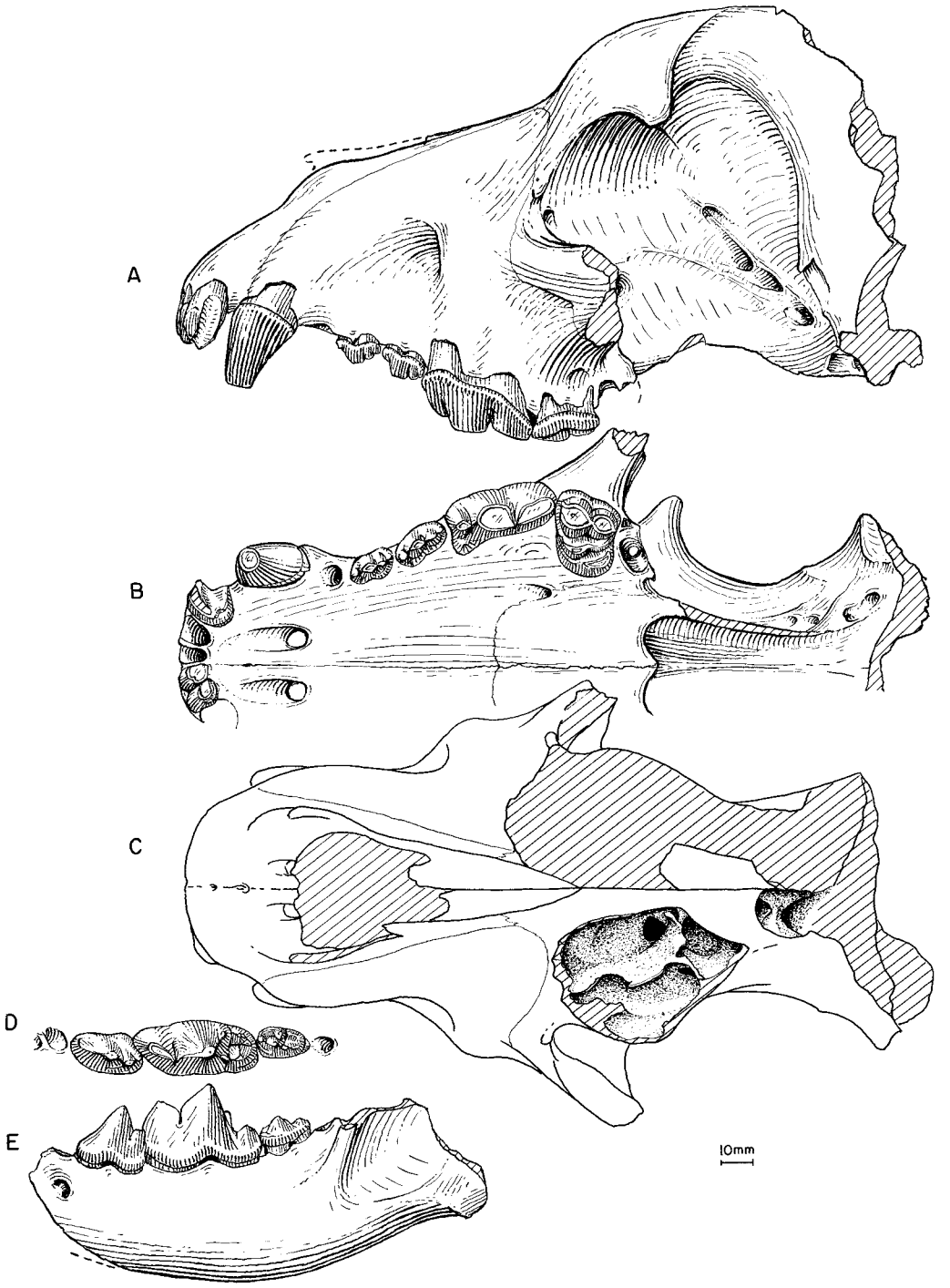

Fig. 113. *Epicyon haydeni*. **A**, Lateral, **B**, ventral, and **C**, dorsal views of partial skull, F:AM 61474, F. Sebastian Place, Ogallala Group (early Hemphillian), Decatur County, Kansas. **D**, Lower teeth and **E**, ramus, F:AM 61535, Port of Entry Pit, Ogallala Group (early Hemphillian), Ellis County, Oklahoma.

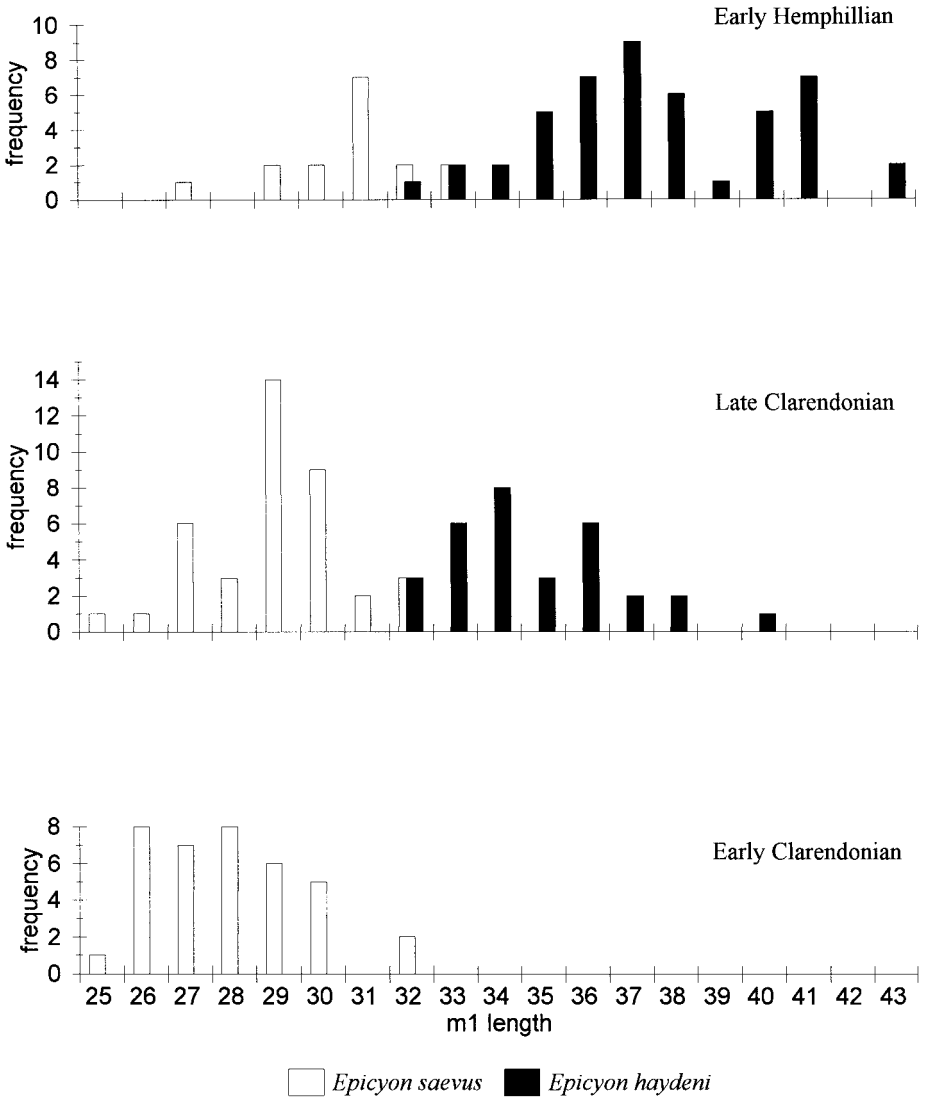

Fig. 114. Histogram of the length of m1 for *Epicyon saevus* and *E. haydeni*. Both species increase in size through time but maintain a distance among themselves. The apparent bimodal distribution within the early Hemphillian *E. haydeni* is mainly caused by the very large individuals from the latest early Hemphillian in the Wray area of Colorado and the Jack Swayze Quarry of Kansas. The Early Clarendonian (lower) part is pooled from samples in various quarries in the Cap Rock Member of the Ash Hollow Formation in Nebraska and equivalent horizon in South Dakota, and in the MacAdams Quarry in Texas. The Late Clarendonian (middle) part is combined from the Laucomer Member of the Snake Creek Formation and Merritt Dam Member of the Ash Hollow Formation in Nebraska. The Early Hemphillian (upper) part is combined from the Johnson Member of the Snake Creek Formation in Nebraska and various quarries in the Ogallala Group in Colorado, Kansas, Oklahoma, and Texas (see Referred Specimens under both species).

in the Johnson Member of the Snake Creek Formation, 20% in the Laucomer Member of Snake Creek Formation, 23% in the Merritt Dam Member of Ash Hollow Formation, and 16% in the Port of Entry Quarry (all ratios are based on pooled averages). The magnitudes of these differences are similar to those among living sympatric canids (Dayan et al., 1989, 1992). Second, qualitative dental features can be found that are present in one size group but not in the other. Therefore, the larger *haydeni* is more likely to exhibit the more derived features listed in the diagnosis, although enough variation is present within the two species to prevent confident assignments based on isolated specimens. Finally, despite the continued increase in size by both species, the two forms seem to maintain a rather constant size difference, and overlaps are rare (fig. 114). Such a constant size difference without overlap is best explained as morphological displacement by sympatrically distributed species. This view is also in basic agreement with a recent study by Baskin (1998), whose morphometric analysis further substantiates our conclusion.

Apart from some regional variation, the morphological integrity of this species pair seems maintained throughout their coexistence. Parallel trends within the two species, in addition to their increase in size, include progressive doming of the forehead, dorsal inflation of frontal sinus and postorbital process of the frontal, enlargement of p4s relative to anterior premolars, and elongation of the external auditory meatus. Our interpretation of these two species coevolving together toward larger size for more than 6 m.y. seems also consistent with the cursorial nature of this lineage (Munthe, 1989).

In most of western North America, *Epicyon haydeni* is last seen in the early Hemphillian deposits, and its general absence in the late Hemphillian has been used to characterize a faunal turnover, between the early and late Hemphillian, that eliminated many elements of the Clarendonian chronofauna (Tedford et al., 1987: 190). One exception to this generality is the occurrence of *E. haydeni* in the Upper Bone Valley Fauna of Florida. This late Hemphillian occurrence may be the last relic of this great lineage surviving in the Gulf Coast. Importantly, specimens from the Upper Bone Valley Fauna often lack stratigraphic control because of the commercial mining operations in various phosphate pits, and the possibility of faunal mixing needs to be kept in mind.

Borophagus Cope, 1892

Hyaenognathus Merriam, 1903: 278.
Porthocyon Merriam, 1903: 283.
Osteoborus Stirton and VanderHoof, 1933: 177.
Pliogulo White, 1941a: 67.
Cynogulo Kretzoi, 1968: 164 (replacement for *Pliogulo* White, 1941).

TYPE SPECIES: *Borophagus diversidens* Cope, 1892.

INCLUDED SPECIES: *Borophagus littoralis* VanderHoof, 1931; *B. pugnator* (Cook, 1922); *B. orc* (Webb, 1969b); *B. parvus*, new species; *B. secundus* (Matthew and Cook, 1909); *B. hilli* (Johnston, 1939a); *B. dudleyi* (White, 1941a); and *B. diversidens* Cope, 1892.

DISTRIBUTION: Early Clarendonian of California; late Clarendonian of California; early Hemphillian of Colorado, Nebraska, Kansas, Florida, Idaho, Oregon, Nevada, Honduras, and El Salvador; late Hemphillian of Kansas, Nebraska, New Mexico, Oklahoma, Texas, Arizona, California, Florida, Mexico; early Blancan of Washington, Idaho, Kansas, Nebraska, New Mexico, and Mexico; late Blancan of Washington, Idaho, California, Arizona, Nevada, Texas, Nebraska, and Florida; and ?late Blancan of Florida and Mexico.

EMENDED DIAGNOSIS: Synapomorphies that unite species of *Borophagus* are highly domed forehead; short muzzle with crowded premolars; p4 large relative to premolars and carnassial with transverse diameter nearly equal to or exceeding that of the m1 trigonid, tall-crowned, and posteriorly sloped; mandibular ramus short and robust with large masseteric fossa and weak symphyseal boss; and radius and tibia short and robust, with tibia especially short relative to length of femur. In cranial proportions, the braincase in *Borophagus* is not as narrowed relative to the length of skull, as it is in *Epicyon* and *Aelurodon*.

DISCUSSION: For many years after Cope's (1892, 1893) initial description of *Borophagus diversidens* from the Blanco beds, Texas,

the genoholotype was thought to have been lost until its discovery and redescription by VanderHoof in 1936. In the meantime, Merriam (1903) proposed two generic names of his own, *Hyaenognathus* and *Porthocyon*, despite his recognition that dentitions of the newly named genera bore a ''striking resemblance'' (p. 280) to Cope's *Borophagus*. Merriam's *Hyaenognathus*, based on far better materials from California, was more widely used in the next 30 years until VanderHoof (1936) demonstrated that *Hyaenognathus* is congeneric with *Borophagus*. At about the same time, Stirton and VanderHoof (1933) erected a new genus, *Osteoborus*, mainly to group the somewhat more primitive bone-crushing species in the Hemphillian, in contrast to the more advanced species of *Borophagus* in the Blancan. Since then, nearly every new record or new species from the Hemphillian has been referred to *Osteoborus*, whereas *Borophagus* was used as the last taxon of this lineage. Authors generally agree that *Borophagus* represents a terminal lineage derived from *Osteoborus*, a conclusion readily born out by our phylogenetic analysis. The usage of *Osteoborus* was thus meant to be gradational. For example, Johnston (1939a) and Hibbard (1944) both recognized that their newly erected species *O. hilli* and *O. progressus* (= *hilli*) probably gave rise to *B. diversidens*, but both still chose a horizontal classification and placed them in *Osteoborus*. Our nomenclatural decision to enlarge the scope of *Borophagus* and to abandon *Osteoborus* strives to maintain generic monophyly.

Borophagus gained the symbolic status as the nominal genus of a new subfamily, Borophaginae, in Simpson's (1945) influential classification of mammals. The highly mixed nature of the taxa grouped into the Borophaginae notwithstanding, Simpson's selection of *Borophagus* as the type genus is appropriate, as it represents the culmination of a long line of canid evolution whose range of morphological adaptations is unsurpassed by other groups of canids.

Recently, Richey (1979) attempted to quantitatively define the various species of *Osteoborus* and *Borophagus* based on the relative width of p4 but concluded that the exercise ''has proved vain'' (p. 121). While there obviously exists a morphocline toward increasing robustness of the p4 through time, extensive overlaps of the p4 width limit its usefulness as a single reliable criterion for species discrimination. Combinations of characters, both cranial and dental, are still necessary for a more accurate assessment of phylogenetic position.

Munthe's (1979) functional study indicates that *Borophagus* (her *Osteoborus* and *Borophagus*) has the shortest limbs among Borophagini. Her conclusion, however, was based on two species of the genus, *B. secundus* and *B. diversidens*, both of which are highly advanced forms within the *Borophagus* clade. Munthe's generalizations can now be extended to the more primitive forms, *B. pugnator* and *B. parvus*. There appears to be some proportional differences in the limbs between *Epicyon* and *Borophagus* (fig. 144). Whether such a divergence of locomotor adaptations reflects a preference to open habits by *Epicyon* vs. wooded habitat by *Borophagus* as suggested by Munthe (1979: 96) needs closer examination of individual localities in light of the more extensive distribution for both taxa in the present study.

Borophagus littoralis VanderHoof, 1931

Figures 115–117

Borophagus littoralis VanderHoof, 1931: 16, pls. 1–3. Barbat and Weymouth, 1931: 32.
Osteoborus littoralis (VanderHoof): Stirton and VanderHoof, 1933: 177. Macdonald, 1948: 65. Richey, 1979: 107.
Osteoborus diabloensis Richey, 1938: 304, fig. 1; 1979: 107. Macdonald, 1948: 61, figs. 5–9.
Epicyon diabloensis (Richey): Munthe, 1998: 136.
Epicyon littoralis (VanderHoof): Munthe, 1998: 136.

HOLOTYPE: UCMP 31503 (AMNH cast 30073), nearly complete skull with I1–P1 alveoli and P2–M2 (fig. 115) from UCMP loc. V3101, on Crocker Springs Creek, northeast side of Temblor Range, near Crocker Springs, 13 mi northwest of Taft, Kern County, California; in rocks referred to the Monterey Formation, mollusks associated with the holotype are typical of those restricted to the Santa Margarita Formation (''Faunizone D'' of Adegoke, 1969; ''Margaritan Stage'' of Addicott, 1972) elsewhere in the southern

San Joaquin Basin, California, early late Miocene (early Clarendonian).

REFERRED SPECIMENS: South Tejon Hills Local Fauna (LACM-CIT loc. 303), Santa Margarita Formation (early Clarendonian), Kern County, California: LACM-CIT 16734, partial palate with P2–M2 (P4 broken).

Black Hawk Ranch Quarry, UCMP loc. V3310, south side of Mount Diablo, Green Valley Formation (late? Clarendonian), Contra Costa County, California: UCMP 33476 (holotype of *Osteoborus diabloensis* Richey, 1938: fig. 1a, b), right ramus with c1–p1 alveoli, p2–m1, and m2–m3 alveoli (fig. 115C, D); UCMP 33477 (paratype of *Osteoborus diabloensis* Richey, 1938: fig. 1c, d; Macdonald, 1948: fig. 7a), right maxillary with P2–M1 (fig. 117A, B); UCMP 33484, left ramus with c1, p2, and p4–m2; UCMP 33492, right maxillary with C1, P2–P3 alveoli, and M1–M2 (Macdonald, 1948: fig. 7c); UCMP 33493, left maxillary with P2–M2 (Macdonald, 1948: fig. 7b); UCMP 33494, right immature partial ramus with dp2, dp4, and p3–p4 unerupted (Macdonald, 1948: fig. 8b); UCMP 33711, right immature ramus with dp3–dp4, c1, and p2–p4 all erupting (Macdonald, 1948: fig. 8a); UCMP 34515, skull with I3, C1 alveolus, and P1–M2 (Macdonald, 1948: fig. 5; fig. 116); UCMP 34623, right immature partial ramus with dp4 and p4–m1 unerupted (Macdonald, 1948: fig. 8c); UCMP 34640, right ramus with p3–m2; UCMP 34695, right isolated m1 (Macdonald, 1948: fig. 9); UCMP 34716, left ramus with m1; UCMP 38169, ramus with c1–m2; UCMP 39404, left maxillary with P4–M2; UCMP 39491, right maxillary with P3–M2; UCMP 39493, right maxillary with C1 erupting and P4–M1; UCMP 58085, right maxillary with P4–M1; UCMP 64414, left ramus with p4–m1; UCMP 78399, left ramus with m1–m2; and UCMP 131615, fragmentary skull with P4–M2.

Red Rock Canyon (LACM loc. 4771), Dove Springs Formation (late Clarendonian), Kern County, California: LACM 143520, left maxillary with C1, P1–P3, P4 broken, and M1–M2 broken.

Ingram Creek 8, UCMP loc. V3952, San Pablo Group (late? Clarendonian), Stanislaus County, California: UCMP 36011, left maxillary with P4–M2 broken.

North Tejon Hills (LACM CIT loc. 104), Chanac Formation (late Clarendonian), Kern County, California: LACM 16585, left M2.

Red Rock Canyon (LACM loc. 3620), rocks correlated with the Bedrock Springs Formation (early Hemphillian), southwest of the mouth of Red Rock Canyon, Kern County, California: LACM 61116, crushed anterior partial skull with I1–M1, partial cervical vertebrae, and fragmentary mandible.

DISTRIBUTION: Early and late Clarendonian or possibly early Hemphillian of California.

EMENDED DIAGNOSIS: As the most basal species of the *Borophagus* clade, *B. littoralis* has all of the derived characters for the genus. These can be used to distinguish it from *Epicyon* and all other more primitive Borophagina (see Diagnosis for *Borophagus*). *B. littoralis* differs from *B. pugnator* and more derived species in its primitively unreduced P1–P3 and p1–p3 with more distinct accessory and cingular cusplets.

DESCRIPTION AND COMPARISON: The present reference of *Borophagus diabloensis* from the Black Hawk Ranch Quarry to *B. littoralis* adds to the hypodigm a complete skull and many lower jaws. Possession of several *Borophagus* characters by this species suggests its derived status relative to *Epicyon*. The frontal is highly domed, more so than most *Epicyon* except highly advanced and geologically late individuals. The frontal sinus extends beyond the frontal-parietal suture. The rostrum is slightly shortened relative to skull length (length P1–M2 in fig. 118), as is also indicated by slightly imbricated upper premolars. The palate is beginning to be widened, although recognizable only in the ratio diagram (fig. 118). The mandible has a weak symphyseal boss, another character of *Borophagus*.

The P2–P3 and p2–p3 begin to have the extremely low-crowned appearance of the genus. In this regard, the Black Hawk Ranch individuals are more primitive than the holotype from Crocker Springs in their higher crowned principal cusps on premolars. To further separate the upper premolars from the lower ones, the P2–P3 are set above the base of the P4 such that they are in a different horizontal plane from that of the P4. The P4 protocone is reduced to a faint ridge. The protocone is slightly better developed in the

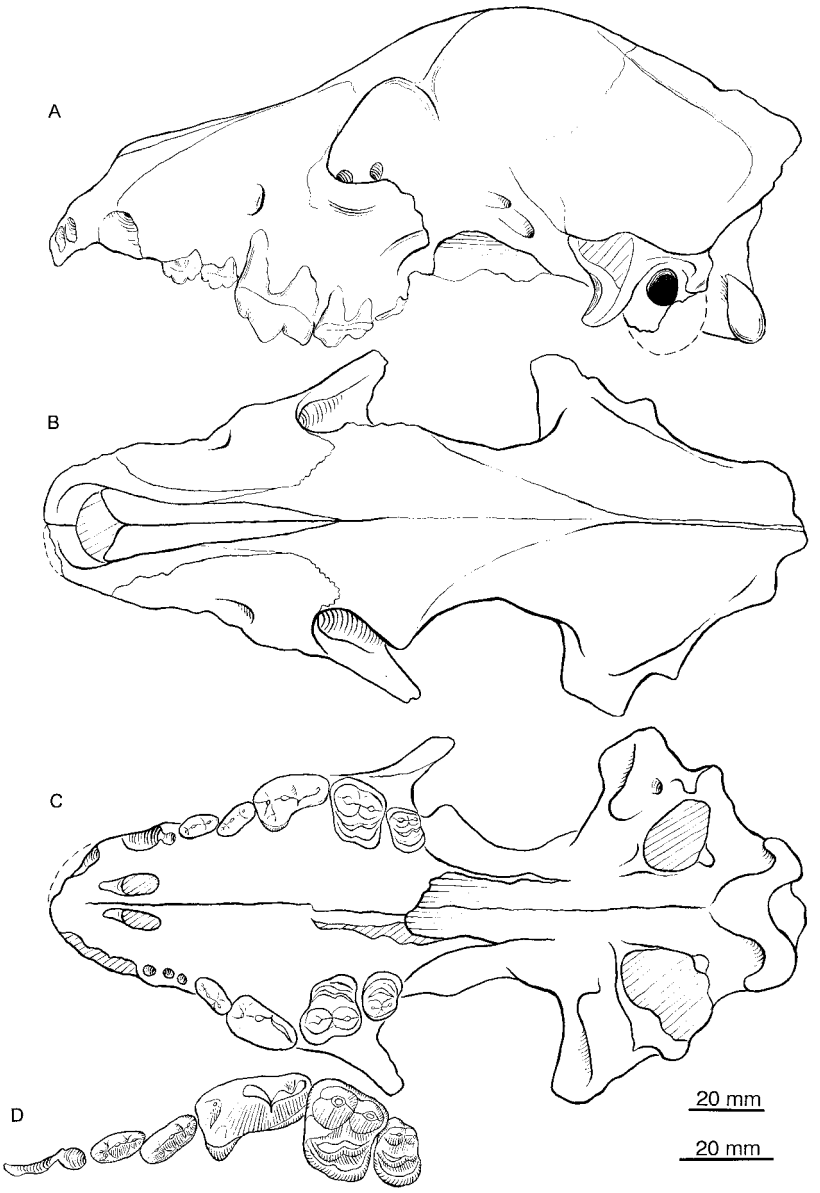

Fig. 115. *Borophagus littoralis*. **A**, Lateral, **B**, dorsal, and **C**, ventral views of skull, and **D**, occlusal view of upper teeth, UCMP 31503, holotype, near Crocker Springs, rocks referred to Santa Margarita Formation (Clarendonian), Kern County, California. The shorter (upper) scale is for A, B, and C, and the longer (lower) scale is for D. Illustration by X. Wang.

Black Hawk Ranch individuals. The M1 assumes a rather quadrate appearance mainly due to an anterior extension of the lingual cingulum, especially prominent in the holotype, a derived character also found in *Carpocyon*.

Lower teeth are known from the Black Hawk Ranch materials only. Little can be added to Macdonald's (1948) detailed descriptions of their morphology and variation. In general, the Black Hawk Ranch materials show primitive morphology for *Borophagus*:

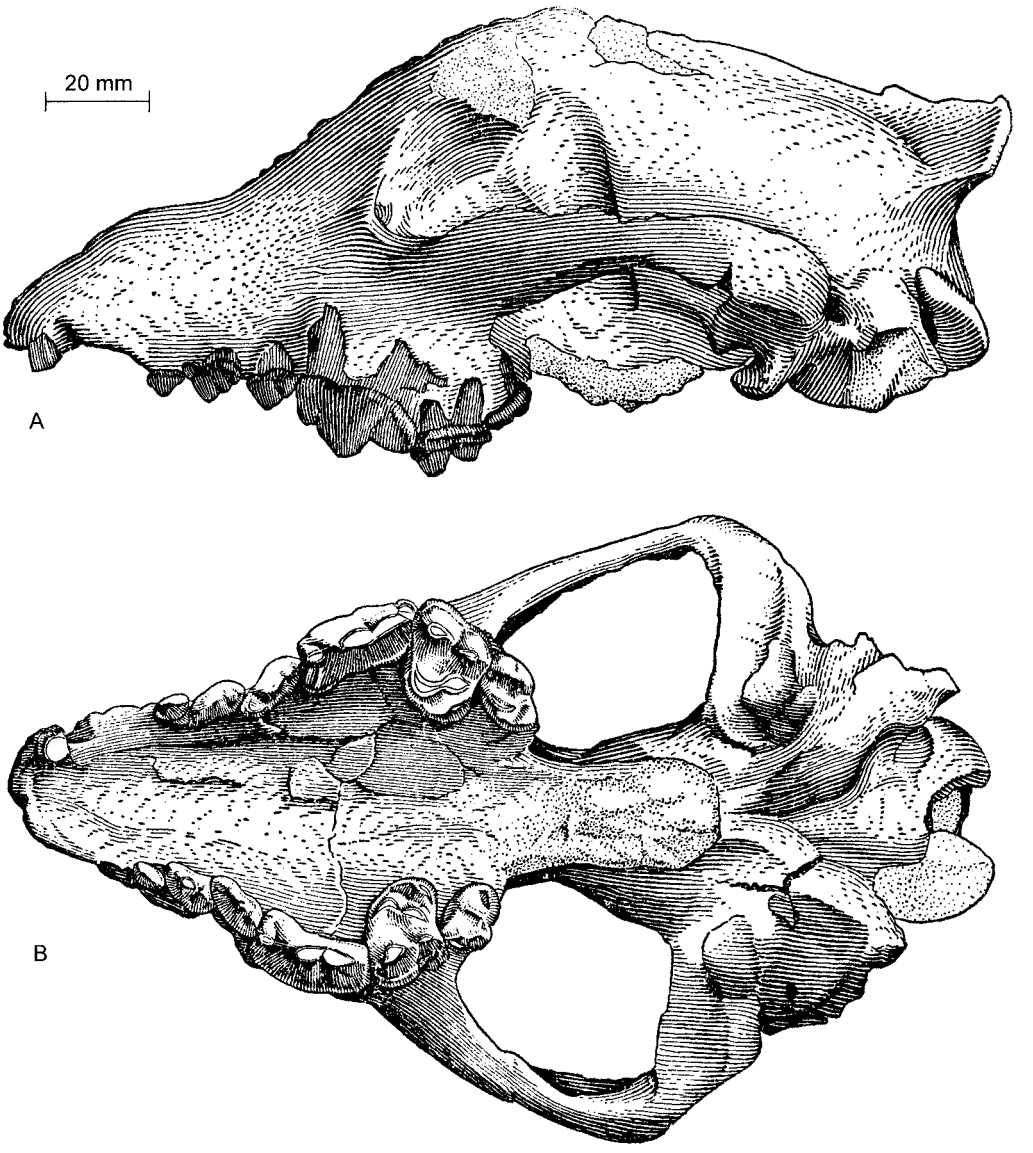

Fig. 116. *Borophagus littoralis*. **A**, Lateral and **B**, ventral views of skull, UCMP 34515, Black Hawk Ranch Quarry, Green Valley Formation (late Clarendonian), Contra Costa County, California. Modified from Macdonald (1948: fig. 5), both reversed from the original figures.

relatively unshortened p2–p3 with higher crowned main cusps and distinct posterior accessory cusps, and p4 not greatly enlarged and its main cusp not reclined.

DISCUSSION: As long maintained by their original authors, *Borophagus littoralis* and *B. diabloensis* from the Clarendonian of California represent the most primitive form in the *Borophagus* clade (VanderHoof, 1931; Richey, 1938), a conclusion consistent with our own analysis. This suggests that the origin of the terminal clade of the bone-crushing dog began in the late medial Miocene of the West Coast.

A partial palate (LACM-CIT 16734) from South Tejon Hills is provisionally referred to *Borophagus littoralis*. The limited material shows the derived conditions for *B. littoralis*:

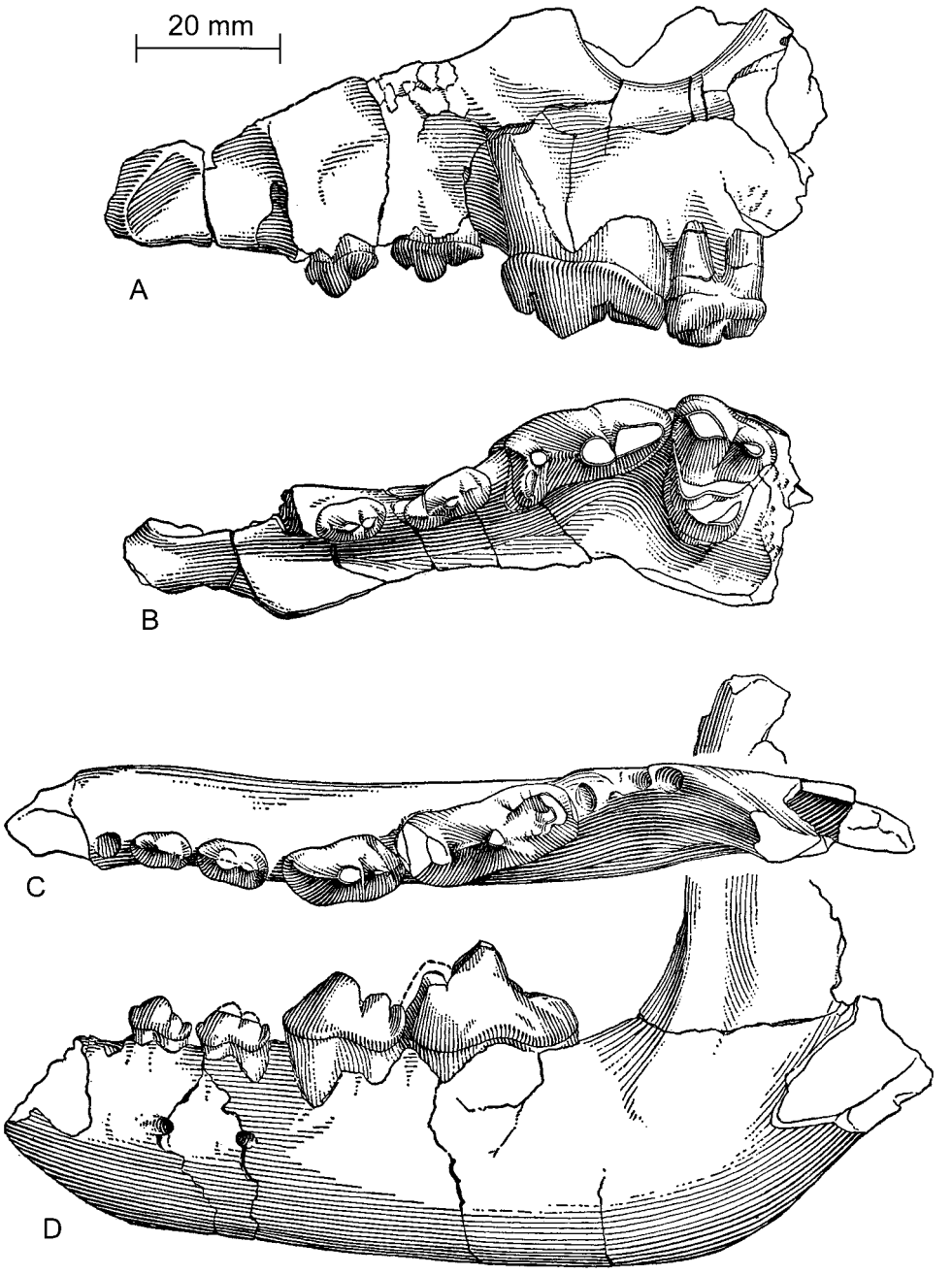

Fig. 117. *Borophagus littoralis*. **A**, Lateral and **B**, occlusal views of maxillary, UCMP 33477, Black Hawk Ranch Quarry, Green Valley Formation (late Clarendonian), Contra Costa County, California. **C**, Occlusal and **D**, lateral views of ramus, UCMP 33476 (holotype of *Osteoborus diabloensis*), Black Hawk Ranch Quarry. Modified from Richey (1938: fig. 1), all reversed from the original figures.

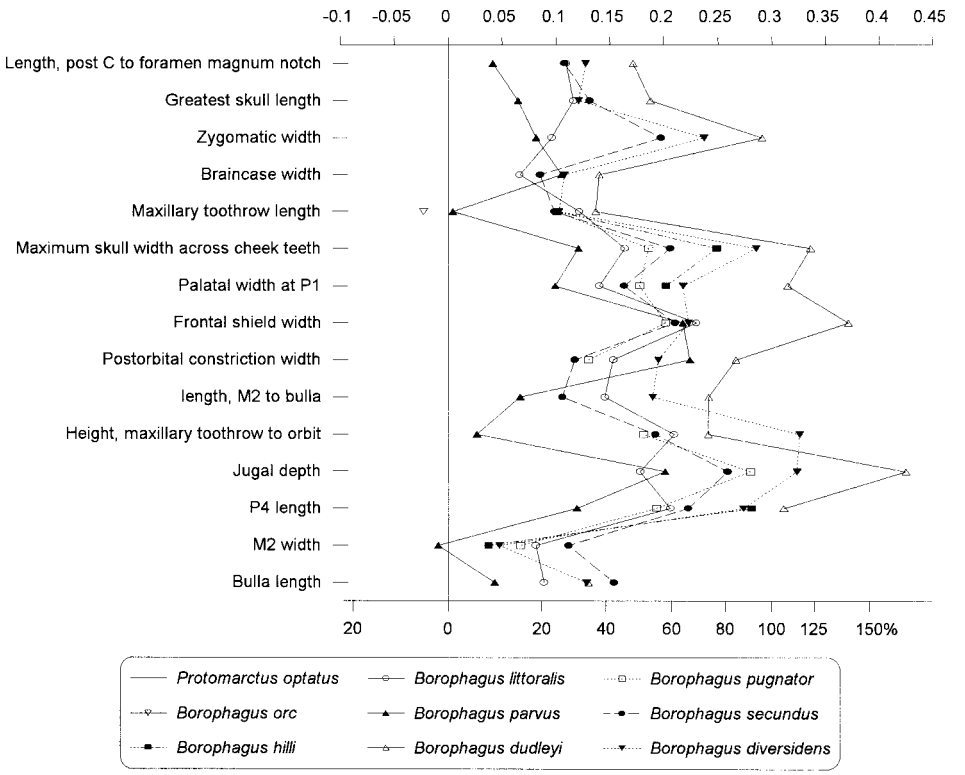

Fig. 118. Log-ratio diagram for cranial measurements of eight species of *Borophagus* using *Protomarctus optatus* as a standard for comparison (straight line at zero). See text for explanations and appendix II for measurements and their definitions.

shortened rostrum (as indicated by its imbricate P2–P3) and reduced P4 protocone.

Borophagus pugnator (Cook, 1922)

Figures 120, 121

Porthocyon pugnator Cook, 1922: 4, 3 figs.
Aelurodon (''*Porthocyon*'') *pugnator* (Cook): Matthew, 1924: 103.
Borophagus pugnator (Cook): VanderHoof, 1931: 17.
Osteoborus pugnator (Cook): Stirton and VanderHoof, 1933: 178. Richey, 1979: 107. Munthe, 1998: 137.
Osteoborus dudleyi (White): Webb, 1969b: 281 (in part).
Osteoborus galushai Webb, 1969b: 296, fig. 5. Richey, 1979: 107.
?*Osteoborus* cf. *O. galushai* (Webb): Webb, 1969b: 299, fig. 6.

HOLOTYPE: DMNH 184 (no. 3) (AMNH cast 113864), anterior part of skull with I1–I2 alveoli, I3–M2 (C1 alveolus), and incomplete basicranial region (fig. 120A–C) from Beecher Island Fauna, near Wray, Ogallala Group (late early Hemphillian), Yuma County, Colorado.

REFERRED SPECIMENS: From the vicinity of Wray, Ogallala Group (late early Hemphillian), Yuma County, Colorado: DMNH (2) 182, palate with I1–C1 alveoli and P1–M2 (AMNH cast 113863); DMNH 184 (no. 3) (AMNH cast 113864B), right ramus with c1, p1–p2 alveoli, p3–m1, and m2–m3 alveoli (same number as the holotype, but different individual; fig. 120D, F); F:AM 61613, left partial ramus with c1–m1 (p1 alveolus); F:AM 61614, right ramus with c1–p1 alveoli, p2–m1, and m2–m3 alveoli; F:AM 61615, left ramus with c1–p2 alveoli, p3–m2, and m3 alveolus; F:AM 61616, right partial ramus with p1–p3 alveoli, p4–m1 both broken, and m2–m3 alveoli; F:AM 61617, right partial ramus with p2–p3 alveoli, p4–m1, and

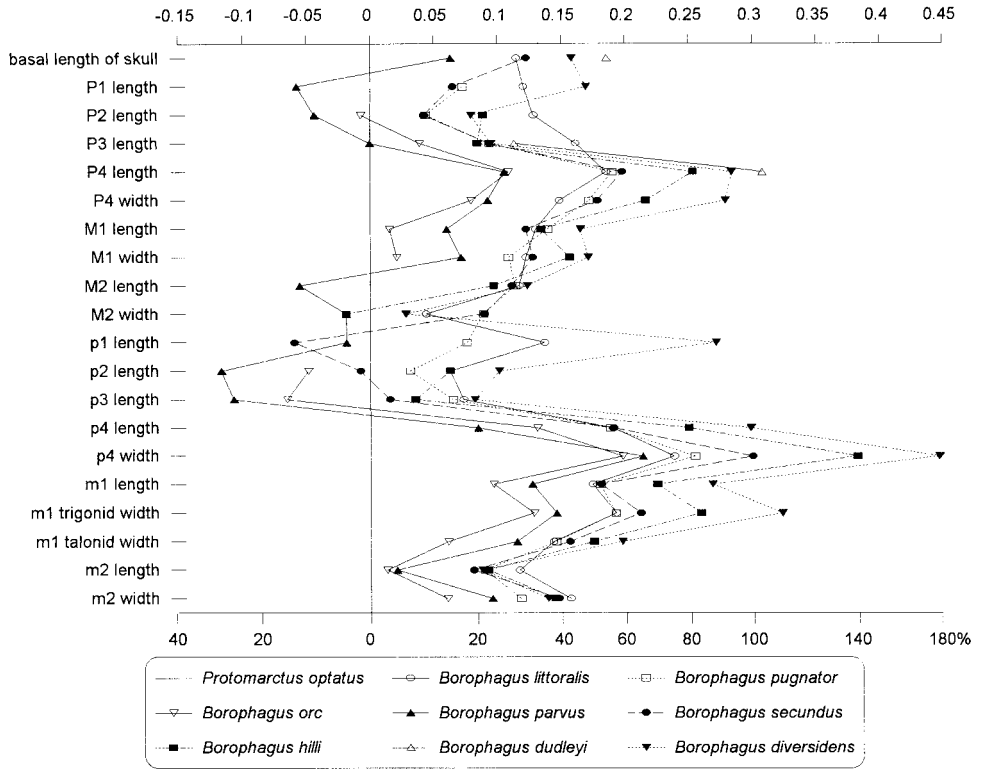

Fig. 119. Log-ratio diagram for dental measurements of eight species of *Borophagus* using *Protomarctus optatus* as a standard for comparison (straight line at zero). See text for explanations and appendix III for summary statistics of measurements and their definitions.

m2–m3 alveoli; F:AM 61618, left partial ramus with p4–m1 both broken; F:AM 61619, right ramus with c1 broken, p1–p4 alveoli, m1, and m2 alveolus; F:AM 61620, left partial ramus with p4–m1; F:AM 61621, left ramus with c1 broken, p2 root–m2 (p3–p4 broken), and m3 alveolus; F:AM 61622, left partial ramus with m1; F:AM 61623, left partial ramus with c1 alveolus–p3 and p4 broken; F:AM 61624, left partial ramus with p2 alveolus–m1 and m2 alveolus; F:AM 61625, right partial ramus with p1 alveolus–p4 and m1 alveolus; F:AM 61626, right partial ramus with c1–m3 all represented by alveoli or broken teeth; F:AM 61627, left partial maxillary with P4–M1 and M2 alveolus; F:AM 61628, right partial maxillary with P4 alveolus and M1 broken–M2; F:AM 61629, right partial maxillary with M1–M2; F:AM 61630, left partial maxillary with M1–M2; F:AM 61631, right isolated broken M1; F:AM 61632, left maxillary fragment with M1 broken and M2 alveolus; F:AM 61633, left premaxillary-maxillary fragments with I3–P2 and M1 broken; F:AM 61634, right premaxillary-maxillary fragment with I1–I3 alveoli, C1, and P1–P2 alveoli; F:AM 61635, right isolated M2; F:AM 67837, right humerus; F:AM 67838, left humerus; F:AM 67838A–D, three left and one right distal part humeri; DMNH 215 (AMNH cast 67839), left radius; F:AM 67840, right radius; F:AM 67841, right radius; F:AM 67842, left radius; F:AM 67843, right radius; F:AM 67843A–F, four proximal and two distal part radii; F:AM 67844, right partial ulna; F:AM 67844A, right proximal part ulna; DMNH 713T (AMNH cast 67844B), left proximal part ulna; F:AM 67845, right femur; F:AM 67846, left tibia; F:AM 67847, left tibia; F:AM 67848 and 67848A, B, two right and one left metacarpals I; F:AM 67849, left metacarpal II; F:AM 67850, left metacarpal III; F:AM 67850A, left proximal part metacarpal

III; F:AM 67851, left metacarpal IV; F:AM 67852, left metacarpal V; F:AM 67853, left metatarsal II; F:AM 67854 and 67854A, B, two right and one left metatarsals III; F:AM 67855, right metatarsal IV; F:AM 67856 and 67856A–E, two left and four right calcanea; F:AM 67856F, G, right and left astragali; and F:AM 67856H–K, three first and one second phalanges.

Reynolds Creek, Poison Creek Formation (?early Hemphillian), Owyhee County, Idaho: HAFO 2701 (AMNH cast 129876), partial right ramus with p2 alveolus, p3 broken, p4, and m1–m2 both broken (referred to *Osteoborus pugnator* by McDonald, ms).

Rome Fauna, Rome beds (early Hemphillian), Dry Creek (LACM-CIT loc. 62), Malheur County, Oregon: LACM 6564, left partial ramus with p3–m3 alveolus (p4–m2 all broken).

Head of Blue Creek, Ogallala Group (late early Hemphillian), Garden County, Nebraska: UNSM 25890, right ramus with c1–p2 alveoli and p3–m1.

Medicine Creek (UNSM loc. Ft-104), Ogallala Group (late early Hemphillian), Frontier County, Nebraska: UNSM 1094, left ramus with i1–m3.

Jack Swayze Quarry, Ogallala Group (early Hemphillian), Clark County, Kansas: F:AM 61662, anterior half skull with complete dentition and associated left and right rami with i1–i3 alveoli, c1–m2, and m3 alveolus (fig. 121A–F), two partial thoracic, six lumbars, sacrum, pelvis, right ulna, left distal radius, right humerus, and rib fragments; F:AM 61663, right partial ramus with p1–m2 and m3 alveolus; F:AM 61664, left ramus with p1 alveolus, p2 broken–m1, and m2–m3 alveoli and associated right distal part humerus (61664B) and right radius (61664A); F:AM 61665, right partial ramus with p4–m1; F:AM 61666, left partial ramus with c1, p1–p3 alveoli, and p4; F:AM 61667, left ramal fragment with m1; F:AM 61668, left partial maxillary with P4–M1; F:AM 61669, left ramus with c1–p1 alveoli, p2, and p3–m3 alveoli; F:AM 61669A, right partial ramus with p1–p3 alveoli, p4–m1 both broken, and m2 alveolus; F:AM 61669B, left partial ramus with p4 broken and m1–m3 alveoli; F:AM 67632 and 67632A, left humerus and radius; F:AM 67633, right humerus; F:AM 67633A–D, four left distal part humeri; F:AM 67633E, right proximal part humerus; F:AM 67634 and 67634A–E, two left proximal part radii, and two left and two right distal part radii; F:AM 67635 and 67635A–E, two left and four right proximal part ulnae; F:AM 67636 and 67636A, B, three distal part femori; F:AM 67637, left tibia; F:AM 67637A, B, two left distal part tibiae; F:AM 67638, left metacarpal II; F:AM 67639 and 67639A–D, one incomplete and five complete metacarpals V; F:AM 67640, right metacarpal V; F:AM 67641, left metatarsal I; F:AM 67642, right metatarsal II; F:AM 67643 and 67643A, right and left metatarsals III; F:AM 67644, left metatarsal IV; F:AM 67644A, left incomplete metatarsal V; F:AM 67645 and 67645A, B, three calcanea; 67645C, astragalus; F:AM 67645D–H, two tarsals and three first phalanges.

Rhino Hill Quarry (KUVP loc. Wal-004), Ogallala Group (early Hemphillian), Wallace County, Kansas: KUVP 3472, nearly complete mandible with left and right c1–m2 (p1–p2 alveoli) and m3 alveoli.

Vicinity of John Dakin Quarry, Ogallala Group (early Hemphillian), Clark County, Kansas: F:AM 61659, right isolated P4; F:AM 61660, left isolated m1; and F:AM 61661, left isolated m1.

Bridge Creek, Box T Ranch, north of Higgins, Hemphill Beds, Ogallala Group (early Hemphillian), Lipscomb County, Texas: F:AM 61565, right ramus with c1 alveolus–m1 and m2–m3 alveoli.

Mixson's Bone Bed, Alachua Formation (early Hemphillian), northeast of Williston, Levy County, Florida: F:AM 61671 and 61672 (one individual, holotype of *Osteoborus galushai* Webb, 1969b: fig. 5), right and left rami with i1–c1 broken alveoli, p1 alveolus–p4, m1–m2 both broken, and m3 alveolus (fig. 121G, H); F:AM 61673, right partial ramus with p4 alveolus, m1, and m2–m3 alveoli; F:AM 61674, right ramal fragment with m1 broken–m2; F:AM 61675, right partial maxillary with P1 alveolus, P2, and P3 alveolus–P4; F:AM 61676, left partial maxillary and detached teeth including P3, P4–M1 both broken, and right detached M2; F:AM 61677, right partial maxillary with M1–M2; F:AM 61678, left c1; F:AM 67949, left proximal and distal ends of hu-

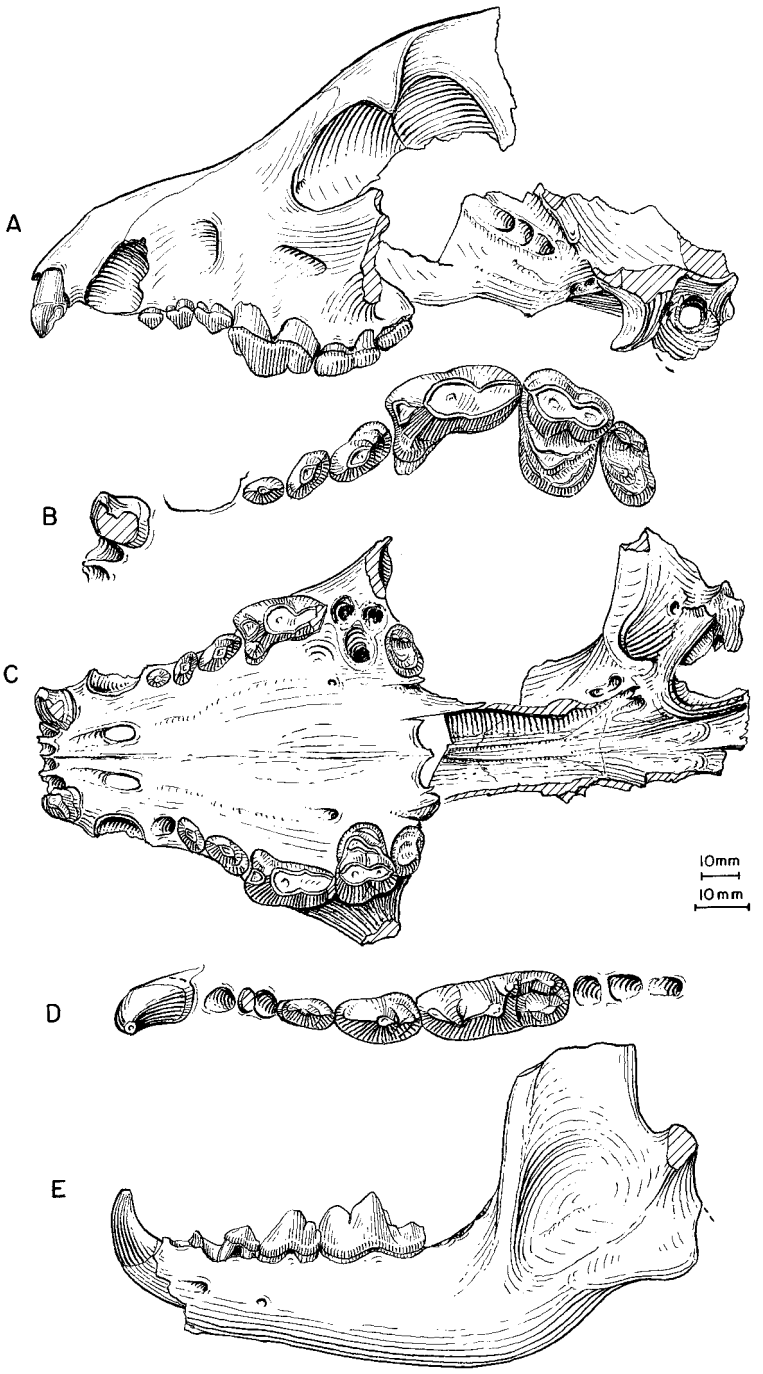

Fig. 120. *Borophagus pugnator*. **A**, Lateral, **B**, enlarged occlusal, and **C**, ventral views of skull and upper teeth, **D**, lower teeth, and **E**, ramus, DMNH 184(3), holotype, near Wray, Ogallala Group (late early Hemphillian), Yuma County, Colorado. The shorter (upper) scale is for A, C, and E, and the longer (lower) scale is for the rest.

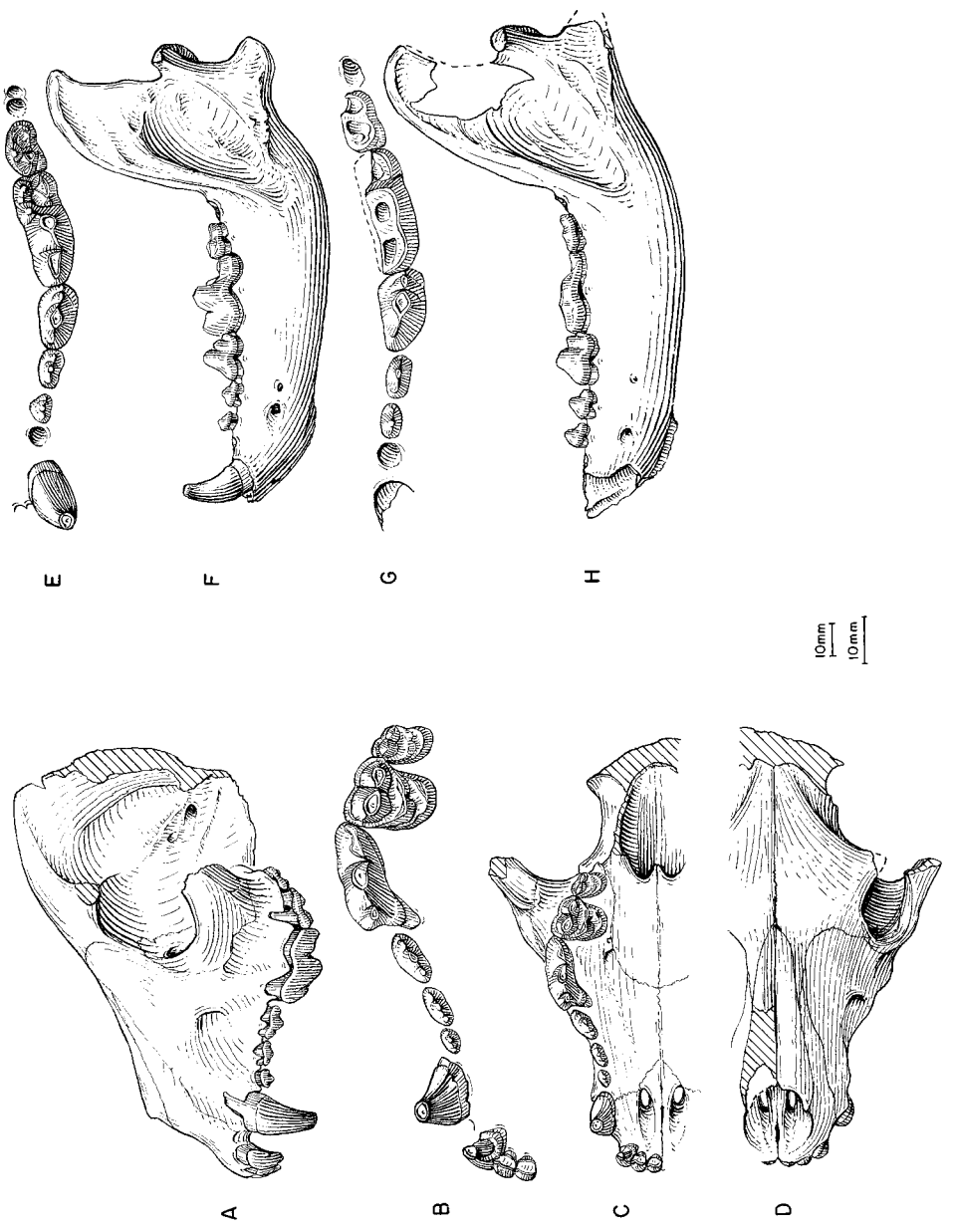

Fig. 121. *Borophagus pugnator*. **A**, Lateral, **B**, enlarged occlusal, **C**, ventral and **D**, dorsal views of partial skull (zygomatic arch reversed from right side) and upper teeth, **E**, lower teeth, and **F**, ramus, F:AM 61662, Jack Swayze Quarry, Ogallala Group (early Hemphillian), Clark County, Kansas. **G**, Lower teeth and **H**, ramus, F:AM 61671 (holotype of *Osteoborus galushai*), Mixson's Bone Bed, Alachua Formation (early Hemphillian), Levy County, Florida. The shorter (upper) scale is for A, C, D, F, and H, and the longer (lower) scale is for the rest.

merus; F:AM 67949A–C, one proximal and two distal ends humeri; F:AM 67949D, E, two distal ends femori; F:AM 67950 and 67950A, right and left tibiae; F:AM 67951, left metacarpal II; F:AM 67951A, left metacarpal V; F:AM 67951B, left metatarsal III with fused distal part of metatarsal II (pathological); F:AM 67951C, left metatarsal IV; F:AM 67951F, first phalanx; and F:AM 67951G, second and third phalanges.

Withlacoochee River 4A and 4X, Alachua Formation (late early Hemphillian), Citrus County, Florida: UF 14783, right ramal fragment with m1 broken–m2; and UF 20047 (AMNH cast 103344), complete mandible with c1, p2–m2, and m3 alveolus.

Palmetto Fauna (''Upper Bone Valley Fauna'' of Tedford et al., 1987), Bone Valley Formation (late Hemphillian), Hardee and Polk counties, Florida: Cargill (formerly Gardner) Phosphate Mine, Bird Clog Site, near Fort Meade: BF OB-10, right ramal fragment with m1. AMAX Phosphate Mine: UF 116070, left M1. Palmetto Mine: UF 124521, left ramus with p1–p2 alveoli and p3–m1. Fort Green Mine: UF 60823, partial right M1; UF 102047, partial left P4; UF 117435, left maxillary with P1–M2 alveoli; UF 124505, left ramal fragment with m1; UF 124506, right c1; and UF 124520, partial left m1. Palmetto Washer: UF 12401, right M1. Mulberry Phosphate Mines: UF 10335 (AMNH cast 98082), right maxillary fragment with P4–M2 (referred to *Osteoborus dudleyi* by Webb, 1969b: 283). Phosphoria Mine: UF 102084, partial right P4. No locality data: UF 49041 (cast of private collection of H. W. Smith), left ramus with c1, p1–p2 alveoli, and p3–m1; UF 50757 (cast of private collection of G. Heslep), left ramal fragment with m1; and USNM 184101 (AMNH cast 129872), left ramus with c1 and p2–p3 alveoli, and p4–m2.

DISTRIBUTION: Early Hemphillian of Colorado, Idaho, Oregon, Nebraska, Kansas, Texas, and Florida; and late Hemphillian of Florida.

EMENDED DIAGNOSIS: *Borophagus pugnator* is slightly more derived relative to *B. littoralis* in its more reduced anterior premolars with lower crowns on the main cusps and more reduced accessory and cingular cusps. *B. pugnator* is distinguishable from most other species of *Borophagus* in several primitive characteristics: frontals less abruptly elevated; muzzle more elongate; p1 usually present; p4 less robust, lower crowned, more upright, with stronger posterior accessory cusplet that is less compressed against posterior cingulum, and transverse diameter usually less than that of m1 trigonid; mandibular ramus more elongate and less massive, with less lateral deflection of the horizontal ramus and toothrow; and ascending ramus more erect.

DESCRIPTION AND COMPARISON: Significant additional materials from the Wray area are available in the Frick Collection to augment the holotype. The anterior partial skull of the holotype, however, is still the best specimen from the topotype area. Additional materials from Jack Swayze Quarry of Kansas and Mixson's Bone Bed of Florida (as the synonym *Osteoborus galushai*) further demonstrate the widespread distribution of this species.

Even with the addition of F:AM 61662, our knowledge of this species is still limited to the anterior half of the skull. The overall cranial construction of *Borophagus pugnator* is little different from that of *B. littoralis*. The forehead is in the same degree of frontal inflation as in *B. littoralis*, and the multichambered frontal sinus invades into the postorbital process of the frontal.

The overall dental proportions in *Borophagus pugnator* are also very similar to those of *B. littoralis*, except for its more reduced premolars (fig. 119). The lateral ridge on I3 (seen in F:AM 61662) is only weakly serrated approximately two-thirds from the base, and thus has practically lost all accessory cusplets. In lateral view, the P2–P3 are markedly elevated with respect to the base of the P4. Besides their smaller size, the premolars of *B. pugnator* have weaker accessory and cingular cusps than those of *B. littoralis*. The P4 protocone is extremely reduced (in the holotype) or lost (e.g., F:AM 61662, UCMP 31503). There is still a small p1 present in materials from Colorado and Kansas, whereas some individuals (USNM 184101 and UF 20047) from Florida have lost it.

DISCUSSION: Cook's *Borophagus pugnator* was either ignored or received only cursory

mention in subsequent studies of the *Osteoborus–Borophagus* lineage. Thus, new species, such as *B. galushai*, were erected mainly by demonstration of differences from *O. cyonoides*. Webb's (1969b) *B. galushai* is generally in the same stage of evolution as *B. pugnator*. One complete mandible (UF 20047) from Withlacoochee River 4X locality, however, has significantly longer lower carnassials than does the topotypic sample from Mixson's Bone Bed. UF 20047 has the primitive morphology of only slightly shortened anterior part of ramus (corresponding to a slightly shortened rostrum) and the p2–p3 are not severely imbricated, characters indicating its primitive status in the *Borophagus* clade. We thus refer this mandible to *B. pugnator*.

Materials from the Jack Swayze Quarry of Kansas are significantly smaller than those from other localities. Average m1 length in the Kansas sample is 15% smaller than those from the topotypic series in Colorado. The difference in limb length is even greater, up to 28% for total length of the humerus or tibia. The smaller Kansas individuals are otherwise similar in stage of evolution to the Colorado samples. Based on our phylogeny that the earlier *Borophagus littoralis* is ancestral to *B. pugnator*, the small individuals from Swayze Quarry must represent a size reduction (as opposed to being primitively small). Whether this size reduction leads to *B. orc* and *B. parvus* (discussed below) cannot be answered definitively because the Swayze individuals display none of the derived features of the latter two species.

Borophagus orc (Webb, 1969)

Figure 122I–L

Osteoborus orc Webb, 1969b: 287, figs. 3, 4. Richey, 1979: 107. Leite, 1990: 15. Munthe, 1998: 137.

HOLOTYPE: UF 13180 (AMNH cast 98085), right ramus with c1–p2 alveoli and p3–m2 (fig. 122I, J), from UF locality 4A, Withlacoochee River, 8 mi southeast of Dunnellon, Alachua Formation (late early Hemphillian), Marion County, Florida.

REFERRED SPECIMEN: From the type locality: UF 12313 (AMNH cast 98086) (Webb, 1969b: fig. 4), left maxillary with P2–M1 and M2 alveolus (fig. 122K, L); UF 12314, right maxillary with P2–M1 and M2 alveolus; UF 12317, left P4; UF 12320, right ramus with p2 alveolus, p3–p4, m1 alveolus, m2, and m3 alveolus; UF 12321, left ramal fragment with m2 and m3 alveolus; UF 12326, left ramal fragment with p2–p3 alveoli and p4 broken; UF 12350, left maxillary with P1 alveolus and P2–P4 broken; UF 13181, left ramus with p3–m1 and m3 alveolus; UF 14781, right p4; UF 14784, left m1; UF 14785, right ramal fragment with i1–c1 alveoli, p2, p3 alveolus, and p4; UF 17439a, left ramal fragment with p4; UF 17439b, right P4; UF 17439c, left P4 broken; UF 17439d, right m1 broken; and UF 27380, right ramal fragment with c1 and p2 alveoli, and p3–p4 (all broken).

DISTRIBUTION: Late early Hemphillian of Florida.

EMENDED DIAGNOSIS: In addition to its small size, derived features that distinguish *Borophagus orc* from *B. pugnator* and *B. littoralis* include a greater reduction (shorter) of premolars and loss of p1 in the former. Primitive features of *B. orc* that distinguish it from *B. parvus* and more advanced species are P4 strong parastyle; p4 posterior accessory cusplet strong, posterior cingulum moderate, and transverse diameter less than that of m1 trigonid; and p4 transverse diameter near posterior end only slightly greater than that at main cusp, and lack of a strong posterolingual cingulum and shelf at the crown base.

DESCRIPTION AND COMPARISON: Except the questionable reference of a few dental fragments from the Lemoyne Quarry of Nebraska (Leite, 1990; see Discussion below), no additional material of *Borophagus orc* has been referred to this rare species since its establishment. Thus, Webb's detailed description of *B. orc* is still current and need not be duplicated here. We only highlight relevant features within the present phylogenetic framework.

Borophagus orc is known mostly by maxillary and ramal fragments. A p1 is present in only one of four individuals, a ratio much lower than that for *B. parvus*. The premolars are more reduced than in *B. pugnator*, not only in absolute size but also in relative terms seen in the ratio diagram (fig. 119). On

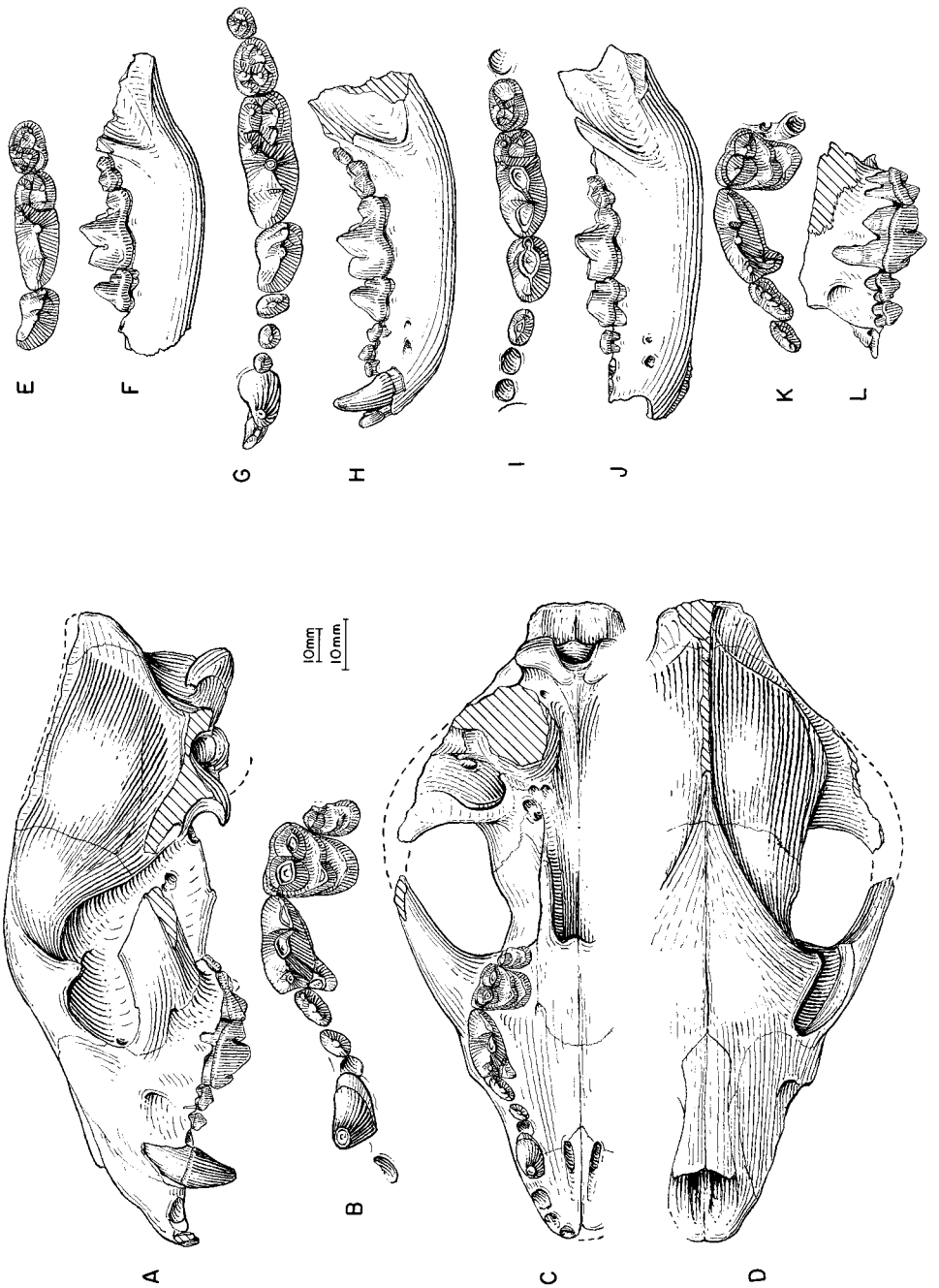

Fig. 122. **A**, Lateral, **B**, enlarged occlusal (M1 reversed from right side), **C**, ventral, and **D**, dorsal views of skull and upper teeth, *Borophagus parvus*, F:AM 75857, holotype, Old Cabin Quarry, Quibiris Formation (late Hemphillian), Pima County, Arizona. **E**, Lower teeth and **F**, ramus, *B. parvus*, F:AM 75877, Old Cabin Quarry. **G**, Lower teeth (m2–m3 reversed from right side) and **H**, ramus, *B. parvus*, F:AM 75881, Old Cabin Quarry. **I**, Lower teeth and **J**, ramus (reversed from right side), *B. orc*, UF 13180, holotype, Withlacoochee River, 8 mi southeast of Dunnellon, Alachua Formation (late early Hemphillian), Marion County, Florida. **K**, Upper teeth and **L**, lateral view of maxillary, *B. orc*, UF 12313, Withlacoochee River. The shorter (upper) scale is for A, C, D, F, H, J, and L, and the longer (lower) scale is for the rest.

the other hand, *B. orc* lacks an anteriorly extended M1 lingual cingulum, more enlarged p4, and unreduced m2, characters that appear in advanced species of *Borophagus*.

DISCUSSION: Webb (1969b: 296) noted the rather mixed primitive and derived morphology of *B. orc* compared to various species of the *Osteoborus-Borophagus* lineage, and concluded that, ''while not so likely ancestral to some or all species of *Borophagus* as are *O. hilli* and *O. progressus*, it [*B. orc*] is nearly as advanced.'' Since our knowledge of this species has not improved since Webb's original description, our phylogenetic interpretation is nearly as uncertain as his nearly 30 years ago. If our placement of this species within the *Borophagus* clade is correct, its diminutive size is definitely an autapomorphy pertaining to dwarfism. It is also tempting to see *B. orc* as an end member of a *B. parvus-orc* lineage in a morphocline of decreasing size. However, the more reduced P2–P3 and p2–p3, wider and more robust p4, and reduced m2 in *B. parvus* indicate a slightly more advanced status. Furthermore, the coexistence of *B. pugnator* and *B. orc* in the Withlacoochee 4A Local Fauna hints at a cladogenetic event in Florida, and the smaller *B. orc* may be a size displacement in response to the larger *B. pugnator*.

Leite (1990: 15) listed three specimens (UNSM 96223, 96225, 96296; all three are represented by talonid fragments of m1s) from the Lemoyne Quarry of Nebraska as *Osteoborus* sp. Noting their small size, he further compared these early Hemphillian materials to *O. orc* without definite taxonomic conclusions. While UNSM 96225 (the size of a large *Leptocyon*) is too small to be even a small *Osteoborus*, the other two talonid fragments (UNSM 96223 and 96296) are within the same size range as *O. orc*. However, so little material is available that any further comment would be speculative.

Borophagus parvus, new species

Figure 122A–H

?*Osteoborus* (Stirton and VanderHoof, 1933): Stirton, 1939b: 372, fig. 38.

Osteoborus cyonoides (Martin, 1928): Wagner, 1981: 193, figs. 29, 30A.

HOLOTYPE: F:AM 75857, skull with I1, I2 broken, I3 alveolus, C1, and P1 alveolus–M2 (fig. 122A–D) from Old Cabin Quarry, Quibiris Formation (late Hemphillian), near Redington, Pima County, Arizona.

ETYMOLOGY: Latin: *parvus*, little, minor.

REFERRED SPECIMENS: Quibiris Formation (late Hemphillian), Pima County, Arizona: Old Cabin Quarry: F:AM 75855, right and left partial maxillae with P4–M2 and both partial rami with i1–c1 all broken and p2 root–m3; F:AM 75856, left maxillary fragment with P4 broken–M2; F:AM 75858, crushed anterior part skull with C1 broken and P3–M2 (P4 broken); F:AM 75859, left partial maxillary with P4–M2 and left partial ramus with c1–p4 and m1 broken; F:AM 75860, crushed anterior part skull with I1–C1 and P2–M2; F:AM 75861, right partial maxillary with P2–M2; F:AM 75862, crushed partial skull with C1–M2 (all worn and broken); F:AM 75863, crushed fragmentary skull with C1 broken, isolated P1 and P2, P4–M1 both broken, and M2; F:AM 75864, crushed partial skull with incisors broken or alveoli, C1 alveolus, P2–M2 (P4 broken), and both partial rami with p2–m3 (m1 broken); F:AM 75865, crushed partial skull with fragmentary C1 and P3–M1; F:AM 75866, crushed anterior part skull; F:AM 75867, crushed anterior skull fragment with I1–P3, P4–M1 both broken, and M2; F:AM 75868, crushed skull fragment with C1 broken, P1–P3, and P4–M2 all badly broken; F:AM 75869, left maxillary fragment with C1 and P2–P4 all broken; F:AM 75870, left partial maxillary with P2–P3, P4–M1 both broken, and M2; F:AM 75871, crushed partial skull with C1 alveolus and P2–M2; F:AM 75872, crushed anterior part skull with I2–C1 alveoli and P1–M1 (P4–M1 broken); F:AM 75875, right ramus with c1 and p2–m3; F:AM 75876, right ramal fragment with m1–m2; F:AM 75877, left partial ramus with p4–m2 (fig. 122E, F); F:AM 75878, mandible with i1–i3, c1 broken, and p1 alveolus–m3; F:AM 75879, right and left partial rami with p4–m2; F:AM 75880, left ramal fragment with m1; F:AM 75881, right and left rami with i1 broken–m3 (fig. 122G, H); F:AM 75882, right and left rami with c1 and p2–m2; F:AM 75883, left ramal fragment with p4–m1; F:AM 75884, right partial ramus with p4 broken–m3; F:AM 75885, both

rami with c1 and p2–m2 all broken; F:AM 75886, left ramal fragment with p3–p4 and m1 broken; F:AM 75887, both partial rami with c1, p3 broken–m1, m2 broken, and both partial ulnae and radii, tibia, and astragalus; F:AM 75888, both partial rami with p4–m1 and m2 broken; F:AM 75889, right ramus with i1–i3, c1–p1 both broken, and p2–m3; F:AM 75890, left ramus with c1 and p2–m1 all broken; F:AM 75891, right partial ramus with c1 broken–m1, m2 broken, and m3; F:AM 75892, left partial ramus with c1, p2 root–m2, and m3 alveolus; F:AM 75893, right partial ramus with c1 and p4–m1; F:AM 75894, left ramal fragment with m1–m2; F:AM 75895, right partial ramus with c1, p1 alveolus, and p2–m1 all broken; F:AM 75896, right ramus with c1–m3 (p1 broken); F:AM 75897, left ramus with right partial ramus with i1–c1 and p1 broken–m3; F:AM 75898, right ramus with c1 broken, p1 alveolus–p4, m1 broken, and m2–m3 alveoli; F:AM 75899, right ramus with p1–p2 broken and p3–m1; F:AM 75900, right partial ramus with i2–p4 and m1 broken; F:AM 75901, left partial ramus with p3–m2; F:AM 75902, right partial ramus with p4–m2 (m1 broken); F:AM 75908, right partial ramus with p3–m2; F:AM 75909, right partial ramus with c1, p2 alveolus–m2, and m3 alveolus; F:AM 75910, right partial ramus with c1 broken and p1 alveolus–m2 (p4–m1 broken and m3 alveolus); F:AM 75911, left ramus with c1, p1 alveolus–p4, and m1–m2 both broken; F:AM 97785A, left ramus fragment with m1–m3; F:AM 97785B, premaxillary-maxillary fragment with I1–I2, I3 alveolus, and C1–P2; F:AM 97786, crushed adolescent skull fragment with C1 erupting, ?P2 or P3 erupting, and P4 and M2 erupting; F:AM 97787A, right maxillary fragment with M1 broken; F:AM 97788, left m1; F:AM 108396, crushed partial skull with I1–M2; F:AM 108397, crushed anterior half of skull with I1 alveolus–M2; F:AM 108398, crushed skull fragment with P3–M2; F:AM 108399, crushed skull fragment with P2–M1 (M2 broken); F:AM 108400, skull fragment with P4–M1 both broken; F:AM 108401, right maxillary fragment with P4–M2 (M1 broken); F:AM 108402, left ramal fragment with c1 broken and p2–p3; F:AM 108403, left isolated P4; F:AM 108404, broken left P4; F:AM 108405, left isolated M1; F:AM 108406, left ramus with i1–i3 all broken, c1–p4, m1 broken, m2 alveolus, and m3; F:AM 108407, partial mandible with i1 broken–c1 and p1–m2 (p3–m2 all broken); F:AM 108408, left partial ramus with c1 broken and p1 alveolus–m2 (p4–m1 broken); F:AM 108409, right partial ramus with c1 and p3–m2; F:AM 108410, right partial ramus with p3–m2 (p4–m1 both broken); F:AM 108411, right partial ramus with broken symphysis, i3 broken, and p3–m2; F:AM 108412, left partial ramus with m1–m2; F:AM 108413, left ramal fragment with m1; F:AM 108414, right partial ramus with p4–m2; F:AM 108415, right partial ramus with p3–m2; F:AM 108416, right partial ramus with c1 broken–p1 alveolus and p2–m2 (p4–m1 both broken); F:AM 108417, right ramal fragment with m1 and m2 broken; F:AM 108418, left premaxillary with I1–I3; F:AM 108419, right p2; F:AM 108420, left ramal fragment with p4; F:AM 108421, right isolated m1; F:AM 108422, right isolated m1; F:AM 108423, left broken isolated m1; F:AM 108424, left m2; F:AM 108425, right m3; F:AM 75904, partial radius with distal end missing; F:AM 75905, right femur; F:AM 75906 and 75906A–C, metacarpals II, III, IV, and V; F:AM 75907, metatarsal III and proximal ends of metatarsals II, IV, and V; F:AM 108426, right crushed humerus; F:AM 108428, right distal end humerus; F:AM 108429, left proximal part ulna; F:AM 108431, right femur; F:AM 108432, proximal end metacarpal V and calcaneum; and F:AM 108433, calcaneum and distal end of metapodial. Redington Quarry: F:AM 67399, crushed skull and mandible with left P4–M2 exposed and right i3–m2; F:AM 67400, crushed skull with I3–M2 (all teeth badly worn) and left ramus with c1 broken, p2–p4, and m1–m2 both broken; and F:AM 108430, articulated incomplete ulna, radius, carpals, metacarpals II–V, and first phalanges. Least Camel Quarry: F:AM 61583, crushed partial skull with I1–I3 (I2 broken), C1, and P2–M2; F:AM 61584, crushed anterior fragment of skull with P2–M2; F:AM 61584A, crushed skull fragment; and F:AM 61584B, crushed cervical and right and left rami with i3–m2 (p2 alveolus).

Big Sandy Formation (late Hemphillian), Mohave County, Arizona: Clay Bank Quar-

ry: F:AM 61585, left partial ramus with c1 and p2–m2; F:AM 61586, right ramus with i1–c1, p1–m1, and m2 broken; F:AM 61588, left ramus with c1, p3–m2, and m3 alveolus; F:AM 61590, left partial ramus with p4–m2; F:AM 61591, left ramus with c1 and p3–m2; F:AM 61593, left ramus with c1, p3 alveolus–m2, and m3 alveolus; F:AM 61594, left ramus with c1 alveolus and p3 broken–m3; F:AM 61597, right ramus with c1 alveolus and p3–m3; F:AM 61598, right partial ramus with c1 and p3–m2; F:AM 61600, left partial ramus with p2 alveolus–m2 (m1 broken); F:AM 61601, left ramal fragment with p4–m1; F:AM 61602, right and left ramal fragments with p4–m2 and detached canine and incisors; F:AM 61604, left ramus with c1, p2–m1, and m2 broken; F:AM 61605 (?same individual as F:AM 61604), right ramus with p3–m3 all broken and m3 alveolus; F:AM 61606, right partial ramus with c1 and p2 alveolus–m1; F:AM 61607, right ramal fragment with p4–m1 both broken; F:AM 61608, right partial ramus with c1 root, p2, and p3–m1 all broken; F:AM 61609 and 61609A, left partial maxillary with P4–M1 and associated ramal fragment with m1 broken; F:AM 61610, left maxillary fragment with P4; F:AM 61611, left and right maxillary fragments with P4–M2 all broken; F:AM 63037, adolescent partial skull with C1 erupting, P4–M2, both incomplete jaws with c1 erupting, p4–m3, immature humerus, ulna, femur, partial tibia, and partial pelvis; F:AM 63055, right adolescent partial ramus with c1, p3, and p4 all erupting, and m1 and m3; F:AM 97783, right partial ramus with c1 broken, p2–p3, p4–m2 all broken and m3; F:AM 97784, right ramal fragment with detached broken p4, m1, and m2 broken–m3 alveolus; F:AM 67955, right humerus with proximal end missing; F:AM 67955A–C, right radius, and right and left radii with distal end incomplete; F:AM 67955D, left ulna; F:AM 67956, right metacarpal I; F:AM 67956A, right metacarpal II; F:AM 67956P, left metacarpal II; F:AM 67956C, right metacarpal III; F:AM 67956C, left metacarpal III; F:AM 67956E, proximal part metacarpal III; F:AM 67956F, left metacarpal IV; F:AM 67956G, left metacarpal V; F:AM 67956H, right calcaneum; F:AM 67956I, first phalanx; and F:AM 67957, right calcaneum. Bird Bone Quarry: F:AM 61592, left ramus with i1–p1 alveoli and p2 alveolus–m2; F:AM 61596, left partial ramus with c1 alveolus, p1 root, p2, and p3 alveolus–m1; F:AM 61599, left partial ramus with c1, p1 and p2 all alveoli, and p3–m2; F:AM 61603, left and right rami with c1 alveolus and p2 alveolus–m3; F:AM 67958C, left calcaneum; and F:AM 105376, right proximal part ulna. Gray Ranch Quarry: F:AM 61587, left ramus with c1, p1–p2 alveoli, p3–m2, and m3 alveolus; F:AM 61589, right ramus with c1, p1 alveolus, and p2–m2; and F:AM 61595, right partial ramus with p4–m3.

Pinole Local Fauna, Pinole Junction Site 1 (UCMP loc. 2572), Pinole Formation (late Hemphillian), Contra Costa County, California: UCMP 22094, left P4 (referred to ?*Osteoborus* by Stirton, 1939b: fig. 38).

Modesto Reservoir Local Fauna, Mehrten Formation (late Hemphillian), Stanislaus County, California: Rock Point (LACM loc. 3908): LACM 61650, right partial ramus with p3 alveolus–m3. Sand Point (LACM loc. 3909): LACM 61690, left ramus with m1–m3; LACM 61691, right ramus with p4 broken–m2 and m3 alveolus; LACM 61692, left ramus with p2 alveolus–m2 and m3 alveolus; and LACM 61693, right ramus with p2 alveolus–m1 and m2–m3 alveoli. Rhino Island (LACM loc. 3942): LACM 62696, left ramus with p4–m2 (Wagner, 1981: fig. 30A); LACM 62697, left ramus with m1; LACM 62698, right ramus with p4; and LACM 62701, right M1. Turlock Lake Site 2 (LACM loc. 3926): UCMP 44670, left ramus with c1 broken, p2 alveolus–m2, and m3 alveolus; and LACM 62519, right ramus with c1, p2–p3 alveoli, and p4–m2 (Wagner, 1981: fig. 29).

DISTRIBUTION: Late Hemphillian of Arizona and California.

DIAGNOSIS: *Borophagus parvus* is small relative to all other species of *Borophagus* (except *B. orc*). *B. parvus* is derived relative to *B. pugnator* and *B. orc* in its anteriorly extended M1 lingual cingulum, more reduced P2–P3 and p2–p3, slightly wider p4, and shortened m2. Primitive features of *B. parvus* compared to *B. secundus* and more derived taxa include muzzle not extremely shortened, palate not abruptly widened at P4 and not wider than it is long, p1 usually pre-

sent, and P2–P3 and p2–p3 not transversely oriented or extremely imbricated.

DESCRIPTION AND COMPARISON: Materials from both the Quibiris and Big Sandy formations form a rather large series of specimens, although their preservation is generally poor. All Arizona specimens suffer from different degrees of crushing, and only occasionally less crushed individuals, such as the holotype, permit confident observations of the cranial morphology.

Borophagus parvus is on average 19% smaller than *B. littoralis*, 13% smaller than *B. secundus*, and 4.3% larger than *B. orc* (all based on basal skull length, except in *B. orc*, which is based on m1 length). Although the frontal is not as prominently vaulted in lateral profile, as it is in more advanced species of *Borophagus*, the forehead is nonetheless highly domed. This is especially evident in anterior view, which shows an arched forehead in the transverse profile as well (i.e., the supraorbital rim is substantially below the highest point of the forehead). This latter feature is invariably developed in all advanced species of *Borophagus*, in contrast to rather flat (in anterior view) foreheads in *B. littoralis* and *B. pugnator*. The rostral shortening is slightly more pronounced than in *B. pugnator* (fig. 118), although the premolars are not severely imbricated. A large contrast in the cranial ratio diagram between *B. littoralis* and *B. parvus* is the latter's shortened temporal fossa (length M2 to bulla in fig. 118), which seems to be a trend within the *Borophagus* clade. The cranial proportions of *B. parvus* are otherwise quite primitive for *Borophagus*. The palate is not dramatically widened at P4 as in *B. secundus* and more derived taxa.

Dentally, the p1 is still present in most Arizona specimens that preserve this part of the ramus (the presence-to-absence ratio of p1 is 29:10), but is lost in the Mehrten sample from California. The P2–P3 and p2–p3 are smaller than those in *B. orc* despite its slightly larger size (fig. 119). Such a precocious premolar reduction prevents the premolars from being imbricated. Although the p4 (8.9 mm average width) is still narrower than the trigonid of m1 (9.6 mm), its relative shortening and widening is unambiguously seen in the ratio diagram (fig. 119), as opposed to that of *B. pugnator* or *B. orc*. The p4 main cusp, on the other hand, is not prominently sloped backward and its tip, when unworn, is usually lower than that of the m1 paraconid, features that are primitive relative to those in *B. secundus*. Also shown in the ratio diagram is the relatively shortened m2 in *B. parvus*.

Samples from the Mehrten Formation of California are in general agreement in size and morphology with those from Arizona but have the following peculiarities of their own: loss of p1, widened p4 at posterior end and a ventrally extended lingual cingular ''lip'' on the crown base of the p4, and a high hypoconid on m2.

DISCUSSION: A small sample of mostly jaw fragments and isolated teeth from the Mehrten Formation of California was described as *Osteoborus cyonoides* by Wagner (1981). From the limited materials, the Mehrten sample exhibits certain transitional features between *Borophagus parvus* and *B. secundus*. It is derived in its loss of p1, but is primitive in its retention of a p4 that is not extremely tall-crowned and prominently reclined as seen in *B. secundus*. Furthermore, the Mehrten materials have some peculiarities of their own: broadened posterior end of p4 with ventrally extended lingual base of the crown and enlarged m2 hypoconid. Although it is conceivable that more complete materials from the Mehrten may prove it to be a distinct taxon, we conservatively refer them to *B. parvus* as a geographic variant from the late Hemphillian of California (see also Discussion under *B. secundus* for a larger form of *Borophagus* from the Mehrten Formation).

A P4 from the Pinole Formation of California matches well, in size and morphology, with those of both *B. orc* and *B. parvus*. We tentatively refer this single carnassial to *Borophagus parvus* because *B. orc* is presently known only in Florida.

Except for its small size, *Borophagus parvus* is morphologically intermediate between the more advanced *B. secundus* and the more primitive *B. pugnator*. Since *B. orc* is smaller in size and more primitive in our phylogenetic analysis, it may be tempting to speculate that *B. parvus* stands at the beginning of a trend toward increasing size in *B. secundus*

and more derived taxa. An alternative to such a scenario is that the small size in *B. orc* and *B. parvus* is the result of character displacement.

Borophagus secundus (Matthew and Cook, 1909)

Figures 123–125

Aelurodon saevus secundus Matthew and Cook, 1909: 372, fig. 3. Matthew, 1918: 185.
Hyaenognathus direptor Matthew, 1924: 100, fig. 20. VanderHoof, 1931: 18. Stirton and VanderHoof, 1933: 177.
Hyaenognathus cyonoides Martin, 1928: 235, figs. 1–3.
Borophagus cyonoides (Martin): Matthew and Stirton, 1930: 173, pls. 21–33. VanderHoof, 1931: 19. Reed and Longnecker, 1932: 66.
Borophagus secundus (Matthew and Cook): VanderHoof, 1931: 18.
Osteoborus cyonoides (Martin): Stirton and VanderHoof, 1933: 177. Savage, 1941: 694, pl. 1, fig. 10. McGrew, 1944a: 75, fig. 25.Dalquest, 1969: 5; 1983: 20. Richey, 1979: 107. Harrison, 1983: 15, figs. 8, 9. Webb and Perrigo, 1984: 241. Munthe, 1998: 137. Miller and Carranza-Castañeda, 1998: 546.
Osteoborus secundus (Matthew and Cook): Stirton and VanderHoof, 1933: 178. Skinner et al., 1977: 358. VanderHoof and Gregory, 1940: 158. Richey, 1979: 114. Munthe, 1998: 137.
Osteoborus cf. *cyonoides* (Martin): Hesse, 1936: 59. Webb and Perrigo, 1984: 247, fig. 10.
Amphicyon sp. Olson and McGrew, 1941: 1236, pl. 4, figs. E, F.
Osteoborus sp. Macdonald, 1959: 877.
Borophagus sp. Cook and Macdonald, 1962: 563.
Osteoborus direptor (Matthew): Richey, 1979: 107. Munthe, 1998: 137.

HOLOTYPE: AMNH 13831, left ramus with c1–p2 alveoli, p3–m2 and m3 alveolus (fig. 123C, D) from the Johnson Member of the Snake Creek Formation (late Hemphillian), Sioux County, Nebraska. In regard to the locality of the type, Skinner et al. (1977: 358) stated, ''The exact site is not known for this specimen. On the basis of morphologic similarities to other taxa from late Hemphillian, AMNH 13831 is tentatively assigned to the ZX Bar Local Fauna.''

REFERRED SPECIMENS: *Aphelops* Draw Fauna, Johnson Member, Snake Creek Formation (early Hemphillian), Sioux County, Nebraska: AMNH 20051, left ramal fragment with p4; AMNH 20065, right ramal fragment with p4; AMNH 20481, left ramus with c1 broken, p2 alveolus–m2 (p4–m1 both broken), and m3 alveolus; and UNSM 4264, left ramal fragment with p4–m2.

Pliohippus Draw, ZX Bar Local Fauna, Johnson Member, Snake Creek Formation (late Hemphillian), Sioux County, Nebraska: AMNH 18919, left ramus with c1, p2–p3 alveoli, and p4–m3 (holotype of *Hyaenognathus direptor* Matthew, 1924) (fig. 125A, B); AMNH 20475, right maxillary with I3–C1 both broken, P1 alveolus, P2, P3 root–P4, and M1–M2 alveoli; and AMNH 81041 (HC 911), left maxillary with C1–P3 and P4–M2 all broken, *Pliohippus* Draw level but a few yd south of *Pliohippus* Draw (referred to *Borophagus* sp. by Cook and Macdonald, 1962: 563).

Turtle Locality (UNSM loc. Cn-103), 2.5 mi southeast of Lodgepole, Ogallala Group (late Hemphillian), Cheyenne County, Nebraska: UNSM 2673, complete skull with I1–M2 (I2 alveolus), cervical vertebrae, and left humerus and ulna.

Rancho Viejo Beds (late Hemphillian), Guanajuato, Mexico (list following Miller and Carranza-Castañeda, 1998): Rancho El Ocote site (Gto. 2), 22 km northeast of San Miguel Allende: IGM 6670, isolated left M1 (Miller and Carranza-Castañeda, 1998: fig. 2.2). Rinconada locality (Gto. 43), 18 km north of San Miguel Allende: IGM 6412, right partial ramus with p4 broken–m3 (m1 incomplete) (Miller and Carranza-Castañeda, 1998: fig. 2.4); IGM 6669, left maxillary fragment with P4–M2 (Miller and Carranza-Castañeda, 1998: fig. 2.1); and IGM 6671, nearly complete right M1 (Miller and Carranza-Castañeda, 1998: fig. 2.3).

Gracias Local Fauna (late early Hemphillian), Honduras (list following Webb and Perrigo, 1984: 241): Rancho Lobo: FMNH P26972, right maxillary with P3–M2 (referred to *Osteoborus cyonoides* by McGrew, 1944a: fig. 25), left maxillary with P4–M2; WM (Walker Museum of University of Chicago) 1766, left ramus with c1 and alveoli of cheekteeth (referred to *Amphicyon* sp. by Olson and McGrew, 1941: pl. 4, figs. E, F); and WM 1767, broken M1. New Year Locality: UF 17771, right M1. Las Culebras: UF 45879, right M1. Tapasuma: F:AM 27020, left ramus with i3–c1, p2–m2 (m1 broken),

and m3 alveolus; and F:AM 27021, left partial ramus with m1–m2 both broken.

Corinto Local Fauna (late early Hemphillian), El Salvador: UF 57481, left M1 (referred to *Osteoborus* cf. *cyonoides* by Webb and Perrigo, 1984: fig. 10).

Edson Quarry, Ogallala Group (late Hemphillian), Marshall Ranch, Sherman County, Kansas: KUVP 3468 (holotype of *Hyaenognathus cyonoides* Martin, 1928), right ramus with i1–c1, p2 alveolus–m2, and m3 alveolus; F:AM 61640, skull with I1 alveolus–M2 and associated mandible with right i2–i3, right and left c1, and p2–m3 (Harrison, 1983: fig. 8; fig. 125C–H); F:AM 61641, skull with I1 alveolus, I2 broken, I3–P2 alveoli, P3–M2, and mandible with c1 alveolus, p2 alveolus–m2, and m3 alveolus; F:AM 61642, anterior part skull with I1–P1 alveoli, P2–M2, and mandible with i1–i2 alveoli, i3–c1, p2–m2, and m3 alveolus; F:AM 61643, right maxillary with I1–I3 alveoli, C1 broken–M1, and M2 alveolus; F:AM 61644, left anterior part of skull with I1 alveolus–C1 and P1 alveolus–M2; F:AM 61645, left detached premaxillary and right and left partial maxillae with I1 alveolus–I3 and C1–M2; F:AM 61646, right maxillary with C1–P1 alveoli and P2–M2 (P3 broken); F:AM 61647, left maxillary with C1–M2 alveoli; F:AM 61648, right maxillary fragment with P4 broken–M1 alveolus; F:AM 61649, posterior part of skull; F:AM 61650, left premaxillary and right and left partial maxillae with I1 alveolus–I3, C1 alveolus, and P3–M2; F:AM 61651, right partial ramus with p4 erupting–m2 and m3 alveolus; F:AM 61652, right and left rami with i1–i3 alveoli, c1, p2 alveolus–m2, and m3 alveolus; F:AM 61653, right and left rami with i1–c1 and p2–m3; F:AM 61654, right partial ramus with c1 broken and p2–m1; F:AM 61655, right partial ramus with i1–i2, i3–c1 both broken, p2–m1, and m2–m3 alveoli; F:AM 61656, left detached m1; F:AM 61657, left ramus with c1 and p4 erupting, m1 alveolus, and m2–m3 erupting; F:AM 61658, right ramus with c1–p4 all broken, m1, and m2–m3 alveoli; F:AM 98088, right and left partial rami with c1 alveolus, p2, p3–m1 alveoli and roots, m2, and m3 alveolus; F:AM 67647, left humerus (Harrison, 1983: fig. 9a, b) and left proximal parts of radius and ulna; F:AM 67646, left radius (Harrison, 1983: fig. 9e, f) and ulna with proximal end broken (Harrison, 1983: fig. 9c, d), left tibia and partial fibula (Harrison, 1983: fig. 9m), metatarsal I, ungular phalanx, and one cervical vertebra; F:AM 67648, left distal part humerus and left tibia with proximal end missing (Harrison, 1983: fig. 9k, l); F:AM 67649, proximal end radius, distal end fibula, calcaneum (Harrison, 1983: fig. 9n), three incomplete metapodials, and four first and one second phalanges and fragments; F:AM 67650, left distal part humerus; F:AM 67650B, right distal part ulna; F:AM 67651, right femur (Harrison, 1983: fig. 9i, j); F:AM 67652, right metatarsal II; F:AM 67654, right metatarsal II; F:AM 67655 and 67655A, right and left metatarsals III (Harrison, 1983: fig. 9q); F:AM 67656, left metatarsal IV; F:AM 67656A, left metatarsal IV (Harrison, 1983: fig. 9r); F:AM 67658, cervical vertebrae and dorsal vertebrae with incomplete ribs; and F:AM 104717, left distal part radius.

Coffee Ranch Local Fauna, Ogallala Group (late Hemphillian), Coffee Ranch Quarry (= Miami Quarry), 8 mi east of Miami, Hemphill County, Texas: F:AM 23350, skull with I1–M2 (fig. 124) and mandible with i1–m3 (fig. 123A, B) (in permanent exhibition); F:AM 23351, right partial maxillary with P3–M1; F:AM 23352, immature partial skull with dP2–dP4 and P4–M2 unerupted; F:AM 23354, right immature ramus with c1 unerupted, dp2–dp4, and p4–m1 unerupted; F:AM 23355, left ramus with p2 alveolus–m2 and m3 alveolus; F:AM 23356, left partial ramus with c1, p2–p3 alveoli, and p4–m2; F:AM 23357, right ramus with c1–m2; F:AM 23357A, right ramus with c1 and p2 alveoli and p3–m3; F:AM 23358, right ramus with c1 alveolus, p3–p4 broken, m1–m2, and m3 alveolus; F:AM 23359, right maxillary with P2–M2; F:AM 23360, left partial maxillary with P4–M1; F:AM 23361, left partial maxillary with P2–M1; F:AM 23362, right maxillary fragment with P4; F:AM 23363, left partial maxillary with P4–M1; F:AM 23372A, right immature ramal fragment with dp3–dp4; F:AM 23372B, right immature ramal fragment with dp3–dp4; F:AM 23372C, right immature ramal fragment with dp4; F:AM 23372D, isolated right dp4; F:AM 23372E, isolated left dP4; F:AM

31000, left partial maxillary with P4–M1 and M2 broken; F:AM 31001, right ramus with i2–i3 alveoli, c1–m2 (p1 absent), and m3 alveolus; F:AM 31002, right ramus with c1 and p2–p3 alveoli and p4–m2; F:AM 31003, right partial ramus with p3–m2; F:AM 31004, skull with I1–C1 alveoli and P1–M2; F:AM 31005, partial skull with I1–I2 alveoli and I3–M2; F:AM 31006, partial skull with I1–I2 alveoli and I3–M2 (P1 alveolus); F:AM 31007, anterior part of skull with I1–I2 alveoli and I3–M2 (P1 area broken); F:AM 31008, right maxillary with P2–M2; F:AM 31009, left partial ramus with p2 alveolus–m2 and m3 alveolus; F:AM 31010, left partial maxillary with P2–M2; F:AM 31011, left ramus with c1 broken, p2 alveolus–p3, p4 broken, m1, m2 broken, and m3 alveolus; F:AM 31012, left immature partial maxillary with dP3 root, dP4, and M1 erupting; F:AM 31013, right maxillary with P1 alveolus–M2; F:AM 31014, right partial maxillary with P4 and M1 broken; F:AM 31015, right partial ramus with c1–m1 (p1 absent); F:AM 31016, right partial ramus with p4–m2; F:AM 31017, left ramus with p2–m3; F:AM 31018, left ramus with p4–m1; F:AM 61700, right maxillary with C1–P1 alveoli and P2–M2; F:AM 61701, left partial maxillary with P4–M1; F:AM 61701-1, left partial maxillary with P4–M1; F:AM 61701-2, left partial maxillary with P2–P3 alveoli, P4, and M1–M2 alveoli; F:AM 61701-3, left partial maxillary with P4–M1; F:AM 61701-4, left partial maxillary with P4–M1; F:AM 61701-5, right partial maxillary with P4–M1 and M2 alveolus; F:AM 61701-6, left partial maxillary with P4–M2; F:AM 61701-7, right maxillary fragment with P4; F:AM 61701-8, right detached P4; F:AM 61702, left ramus with c1 and p2 alveolus–m2; F:AM 61702-1, right ramus with c1–m3 (p1 absent, p2 alveolus, and m2 broken); F:AM 61702-2, right partial ramus with p4–m1 and m2 alveolus; F:AM 61702-3, right partial ramus with c1 and p2 alveoli, p3–m1, and m2–m3 alveoli; F:AM 61702-4, left ramus with p4 broken–m2; F:AM 61702-5, right partial ramus with p2 alveolus–m2; F:AM 61702-6, right partial ramus with p4–m1; F:AM 61702-7, right partial ramus with p2–m2 and m3 alveolus; F:AM 61702-8, right partial ramus with p3 alveolus–m1 and m2–m3 alveolus; F:AM 61702-9, right ramus with p4–m3; F:AM 61703, right ramus with c1–m3 (p1 and p3 alveoli); F:AM 61703-1, left partial ramus with p3–m1; F:AM 61703-2, left ramus with c1 broken alveolus, p2–m1, and m2–m3 alveoli; F:AM 61703-3, left ramus with c1, p2–p3 alveoli, and p4–m2; F:AM 61703-4, right partial ramus with p2 alveolus–m1 and m2–m3 alveoli; F:AM 61703-5, right partial ramus with c1 and p2–m1; F:AM 61703-6, right ramus with c1, p2–m1, and m2 alveolus; F:AM 61703-7, right ramus with p3–m2, and m3 alveolus; F:AM 61703-8, left ramus with p2 alveolus–m2 and m3 alveolus; F:AM 61703-9, right ramus with c1 alveolus, p2–m1, and m2 alveolus; F:AM 61704, right ramus with c1 and p2 alveoli, p3–m1, and m2–m3 alveoli; F:AM 61704-1, left ramus with c1 and p2 alveoli and p3–m3; F:AM 61704-2, right ramal fragment with p4 broken–m1; F:AM 98717, right partial ramus with p2–p3 alveoli and p4–m1; F:AM 98718, right partial ramus with p4–m2; F:AM 98719, right partial ramus with p2–p3 alveoli and p4 broken–m1; F:AM 98720, left partial ramus with p3 alveolus, p4 broken–m1, and m2 broken–m3; F:AM 98721, right ramus with c1 and p3 alveoli, p4–m2, and m3 alveolus; F:AM 98722, right ramus with c1 and p2–p3 alveoli, p4–m1, and m2–m3 alveoli; F:AM 98723, right partial ramus with c1, p2–p3 alveoli, and p4–m1; F:AM 98724, left partial ramus with p2 alveolus–m1; F:AM 98725, right ramus with c1 alveolus, p3–m1, and m2–m3 alveolus; F:AM 108209, left partial ramus with p4–m1 and m2 broken; F:AM 108210, right partial ramus with p4–m2 all broken; F:AM 108211, left partial maxillary with P3 broken–M1 and M2 alveolus; F:AM 108212, left partial maxillary with P4–M1; F:AM 108213, right partial maxillary with P3–M1; F:AM 108214, right partial ramus with m1 and m2–m3 alveoli; F:AM 108215, left partial ramus with c1 and p2–p3 alveoli, p4, and m1–m2 alveoli; F:AM 108216, right partial ramus with c1 and p2–p3 alveoli and p4–m1 alveolus; F:AM 108217, left partial ramus with m1; F:AM 108218, right partial ramus with p3 alveolus, p4, and m1 broken; DMNH 1322 (F:AM 108208), right partial maxillary with P4–M2; DMNH 1323 (F:AM 108207), left partial maxillary with P4–M1; DMNH 1324

(F:AM 108199), right ramus with c1, p2–p3 alveoli, p4–m1, and m2 alveolus; DMNH 1325 (F:AM 108200), right ramus with p2–p3 alveoli and p4–m3; DMNH 1326 (F:AM 108201), left ramus with c1 and p2–p3 alveoli, p4–m1, and m2–m3 alveoli; DMNH 1327 (F:AM 108196), left ramus with c1 alveolus, p2–m2, and m3 alveolus; DMNH 1328 (F:AM 108197), left ramus with c1 and p2 alveoli, p3–m2, and m3 alveolus; DMNH 1329 (F:AM 108202), left ramus with p3–m2, and m3 alveolus; DMNH 1329A (F:AM 108203), left partial ramus with p4–m2 and m3 alveolus; DMNH 1329B (F:AM 108204), left partial ramus with p3 alveolus–m1 and m2–m3 alveoli; DMNH 1329 (F:AM 108198), right partial ramus with c1, p2–p3 alveoli, p4–m1, and m2–m3 alveoli; and UCMP 30663 (AMNH cast 55563), right ramus with c1, p2–p3 alveoli, and p4–m3.

''Goodnight beds,'' Ogallala Group (late Hemphillian), near Goodnight, Armstrong County, Texas: Horace Baker Pit: F:AM 67389, immature skull with dP3–dP4, P2, P4 unerupted, M1–M2 both erupting. Hill Quarry: F:AM 67386, left m1; and F:AM 67390, right immature right ramus with dp2 broken, dp3, dp4 broken, and m1 erupting. Sebit, 14 mi northeast of Matthew's North Pit: F:AM 61579, left partial maxillary with P4 broken–M2. Center Hill Pit, McGehee Place: F:AM 67388, two maxillary fragments with P1 broken–P2 and P4. Hubbard Place Quarry: F:AM 67386A, right detached m1; F:AM 67386B, left partial ramus with p4–m2; and F:AM 67387, right ramus with c1–p1 alveoli, p2–m2, and m3 alveolus. Christian Pit 2: F:AM 67387B, right ramal fragment with p4–m1.

Channing area, Ogallala Group (late Hemphillian), Hartley County, Texas: Holt, 4.5 mi west and 1 mi south of Channing: F:AM 61581, right ramus with c1 and p2 alveoli and p3–m3 all broken. Burson Ranch Pit: F:AM 61582, immature right maxillary fragment with C1 erupting and dP3.

Optima Local Fauna, Ogallala Group (late Hemphillian), Optima (= Guymon) quarries, near Guymon, Texas County, Oklahoma: F:AM 61679, anterior part of skull with I1–C1, dP3, and P4–M1, partial left and right rami with i3–c1, and p3–m2; F:AM 61679-1, anterior part of skull with I2–C1 and P2–M2; F:AM 61679-2, left partial maxillary with P4–M2; F:AM 61679-3, crushed anterior part of skull with I1–I3 alveoli and C1–M2; F:AM 61679-4, anterior half of skull with I1–M2 and both jaws with c1, p2–m2, and m3 alveolus; F:AM 61679-5, right premaxillary and partial maxillary with I3, C1 alveolus, P2, P4, detached C1, and broken M1; F:AM 61679-6, anterior part of skull with I1–M1 and M2 broken; F:AM 61679-7, crushed anterior part of skull with I1–M2 (P4–M1 broken); F:AM 61679-8, crushed anterior fragment of skull with I1–C1 and P4–M2; F:AM 61679-9, right maxillary with C1 alveolus and P2 broken–M1; F:AM 61680, crushed anterior part skull with I1–C1 and P1 root–M2; F:AM 61680-1, anterior part of skull with I1–I3 alveoli, C1, P2–P4, and M1 broken; F:AM 61680-2, right partial maxillary with P4–M1 and M2 alveolus; F:AM 61680-3, crushed anterior part of skull with I3–M2 (P1 alveolus); F:AM 61680-4, crushed partial palate with P2–P4 and M1 broken; F:AM 61680-5, anterior fragment of skull with P2–M2; F:AM 61680-6, right partial maxillary with P4–M1; F:AM 61680-7, crushed anterior part of skull with I1, C1 broken, P2–M2, and both rami with c1, p2 alveolus–m2, and m3 alveolus; F:AM 61680-8, crushed partial skull with I1–M2, both partial rami with c1 and p2–m3; F:AM 61680-9, crushed skull with I1–M2; F:AM 61681, right partial maxillary with P2–M1; F:AM 61681-1, right premaxillary-maxillary with I1–P1 alveoli, P2–P4, and M1 alveolus; F:AM 61681-2, right and left maxillae with I1–M2; F:AM 61681-3, crushed anterior part of skull with I1–I2 alveoli, I3–M1, and M2 alveolus; F:AM 61681-4, right partial maxillary with P4–M1 and M2 alveolus; F:AM 61681-5, crushed partial skull with I1–I3 alveoli, C1, P1 alveolus, P2–M1 (P4 broken), and M2 alveolus; F:AM 61681-6, anterior part of skull with I1–I2 alveolus and I3–M2; F:AM 61681-7, crushed anterior fragment of skull with C1–M2 (M1 broken); F:AM 61681-8, partial palate with C1 and P2–M2; F:AM 61681-9, left partial maxillary with P4–M2; F:AM 61682, right partial maxillary with P4–M1; F:AM 61682-1, partial palate with I1–I2 both broken and I3–M2; F:AM 61682-2, right maxillary with I3, C1, P1 detached, P2–M1, and M2 broken; F:AM

61682-3, right maxillary with P1 alveolus–M2; F:AM 61682-4, right partial maxillary with P2–M1; F:AM 61682-5, partial palate with P2–M2; F:AM 61682-6, left partial maxillary with P4–M2; F:AM 61682-7, crushed anterior part of skull with I1–M2; F:AM 61682-8, left maxillary with C1–M2; F:AM 61682-9, crushed skull fragment with I2–C1 all erupting, P2 erupting, and P4–M2; F:AM 61683, right maxillary fragment with P4–M2; F:AM 61683-1, right maxillary with I1–P1 alveoli, P2–P4, and M1–M2 alveoli; F:AM 61683-2, left maxillary fragment with P4; F:AM 61683-3, right maxillary with P2 alveolus–M2; F:AM 61683-4, skull fragment with P4–M2; F:AM 61683-5, left maxillary fragment with P3–P4; F:AM 61683-6, skull fragment with P2 and P4–M2; F:AM 61683-7, right and left partial maxillae with I3–C1 and P4–M1; F:AM 61683-8, crushed anterior part skull with I1–P2 alveoli and P3–M2; F:AM 61683-9, right and left partial maxillary with P3–M1; F:AM 61684, crushed partial skull with I1–M2; F:AM 61684-1, crushed skull fragment with P3–M2; F:AM 61684-2, crushed anterior part skull with C1 and P2–M2 (P3 and M1 broken); F:AM 61684-3, skull fragment with I1–M2; F:AM 61684-4, crushed anterior part skull with I1–M2; F:AM 61684-5, right maxillary fragment with C1, P4, M1 broken, and M2; F:AM 61684-6, right maxillary fragment with P4–M1; F:AM 61684-7, crushed skull with I1–M2 and both rami with p4–m3; F:AM 61684-8, right and left maxillae with I3–M2; F:AM 61684-9, crushed anterior part skull with I1–M2; F:AM 61685, crushed anterior fragment of skull with I1–P2 and P4–M2; F:AM 61685-1, left maxillary with I3–M1 and M2 broken; F:AM 61685-2, right partial maxillary with P3–P4 and M1 broken; F:AM 61685-3, crushed partial palate with P2–M2; F:AM 61685-4, crushed partial skull with P4–M2 and both rami with i1–c1 and p2–m3; F:AM 61685-5, crushed partial skull with I1–C1 alveoli and P4–M2; F:AM 61685-6, crushed anterior part of skull with I1–C1, P2–M2, mandible with c1 broken, and p2–m3; F:AM 61685-7, anterior part of skull with I1 alveolus–C1 and P1 alveolus–M2; F:AM 61685-8, crushed fragment of skull with I3–C1 and P2–M2; F:AM 61685-9, palate with I3–C1 and P2–M2; F:AM 61686, partial palate with I1 alveolus, I2, I3 alveolus–C1, and P3–M2; F:AM 61686-1, palate with I3–C1, and P2 root–M2; F:AM 61686-2, associated detached upper teeth including P2–M2; F:AM 61686-3, crushed anterior part of skull with C1 and P1 alveolus–M2; F:AM 61686-4, crushed palate with I2 broken and I3–M2; F:AM 61686-5, left maxillary with P3–M1; F:AM 61686-6, right maxillary fragment with P4–M1; F:AM 61686-7, right maxillary with C1 alveolus–M2, both rami with i1–c1, and p2–m2; F:AM 61686-8, left maxillary fragment with C1, P1–P2 roots, P3–P4, M1 broken, and right and left ramal fragments with p4–m3; F:AM 61686-9, crushed skull with I3–M2 (P4–M1 broken), and both partial rami with i3 broken–c1, and p2–m2 (m1 broken); F:AM 61687, anterior part skull with I1 alveolus–M2; F:AM 61688, right partial ramus with p4–m1; F:AM 61688-1, left ramus with c1 and p2 alveolus–m3; F:AM 61688-2, left partial ramus with p4–m1 and m2–m3 alveoli; F:AM 61688-3, right ramus with i1–i3 alveoli, c1, p1 alveolus–m1, and m2–m3 alveoli; F:AM 61688-4, right ramus with c1, p2–m2, and m3 alveolus; F:AM 61688-5, right ramus with c1 root, p2–p3 alveoli, p4–m2, and m3 alveolus; F:AM 61688-6, left partial ramus with p3–m2; F:AM 61688-7, right ramus with c1 and p2–m2; F:AM 61688-8, left partial ramus with p3–m2; F:AM 61688-9, right partial ramus with i1 broken–c1, p2–p3 alveoli, and p4–m1; F:AM 61689, left partial ramus with c1 and p2 alveolus–m1; F:AM 61689-1, left ramus with c1 and p2–m2; F:AM 61689-2, right ramus with c1 and p3–m1; F:AM 61689-3, left partial ramus with p3 broken–m1 and m2–m3 alveoli; F:AM 61689-4, right and left rami with i3–c1, p2 alveolus–m2, and m3 alveolus; F:AM 61689-5, left ramus with c1, p2–p3 alveoli, p4–m2, and m3 alveolus; F:AM 61689-6, right and left rami with i2–c1, p2–m2, and m3 alveolus; F:AM 61689-7, right ramus with c1 alveolus, p2 alveolus–m2, and m3 alveolus; F:AM 61689-8, left ramus with c1 alveolus, p2–m2, and m3 alveolus; F:AM 61689-9, left ramus with c1 and p2–m3; F:AM 61690, right ramus with c1, p1–p2 alveoli, p4–m2, and m3 alveolus; F:AM 61690-1, right ramus with c1, p2–m2, and m3 alveolus; F:AM 61690-2, left ramus with i3–c1, p2 broken–m2, and m3

alveolus; F:AM 61690-3, right and left rami with i2–c1 and p3–m3 alveolus; F:AM 61690-4, left ramus with c1, p2–p3 alveolus, p4–m2, and m3 alveolus; F:AM 61690-5, left ramus with c1, p2–m2, and m3 alveolus; F:AM 61690-6, right and left rami with i3–c1, p2 alveolus–m2, and m3 alveolus; F:AM 61690-7, right ramus with p4–m2 and m3 alveolus; F:AM 61690-8, left partial ramus with p4–m2 and m3 alveolus; F:AM 61690-9, left ramus with i1 broken–c1, p2 alveolus–m2, and m3 alveolus; F:AM 61691, left ramus with c1 alveolus, p3–m2, and m3 alveolus; F:AM 61691-1, left partial ramus with c1 broken, p3–m1, and m2–m3 alveoli; F:AM 61691-2, right ramus with c1, p2–m1, and m2–m3 alveoli; F:AM 61691-3, right ramus with c1 and p2 alveoli, p3–m2, and m3 alveolus; F:AM 61691-4, right partial ramus with c1 and p2 alveolus–m1 (p4 broken); F:AM 61691-5, right ramus with c1 alveolus, p2–m2, and m3 alveolus; F:AM 61691-6, left ramus with c1 alveolus and p2–m2; F:AM 61691-7, right ramus with c1 alveolus, p2–m2, and m3 alveolus; F:AM 61691-8, right ramus with c1, p2–m2 and associated metatarsals I and IV, and first and second phalanges; F:AM 61691-9, right ramus with c1, p2–m2, and m3 alveolus; F:AM 61692, right and left partial rami with c1 and p2 alveolus–m3; F:AM 61692-1, left ramus with i1–c1 and p2–m1; F:AM 61692-2, right and left partial rami with p2 alveolus–m2 and m3 alveolus; F:AM 61692-3, left ramus with c1, p2–p3 alveoli, and p4–m1; F:AM 61692-4, left ramus with c1 and p4–m2; F:AM 61692-5, left ramus with c1 and p2–m3; F:AM 61692-6, right ramus with i3–c1, p2–m1, and detached m2; F:AM 61692-7, left ramus with c1 broken and p2–m2; F:AM 61692-8, left ramus with c1 and p2 alveolus–m2; F:AM 61692-9, right immature ramus with dp3–dp4 and m1–m2; F:AM 61693, left ramus with c1 and p3–m2; F:AM 61693-1, right ramus with c1, p2–m2, and m3 alveolus; F:AM 61693-2, right partial ramus with p3–m1; F:AM 61693-3, right ramus with c1 and p2 alveolus–m3; F:AM 61693-4, right ramus with i3–c1 and p2–m2; F:AM 61693-5, left ramus with c1 and p2–p3 alveoli, p4–m1, and m2–m3 alveoli; F:AM 61693-6, right ramus with i1–i2, c1, p2–m2, and m3 alveolus; F:AM 61693-7, right and left rami with i1–c1 and p2–m2; F:AM 61693-8, left ramus with c1 and p2–m3 alveolus; F:AM 61693-9, left ramus with i1–c1, p2 alveolus–m2, and m3 alveolus; F:AM 61694, right and left rami with c1, p2 alveolus–m2, and m3 alveolus; F:AM 61694-1, left partial ramus with c1, p2 alveolus–m1, and m2 alveolus; F:AM 61694-2, left partial ramus with c1 and p2–m1; F:AM 61694-3, right and left rami with i1–c1, p2–m2, and m3 alveolus; F:AM 61694-4, right and left rami with c1, p2–m2, and m3 alveolus; F:AM 61694-5, right maxillary with C1–M1, right and left rami with c1, and p2–m2; F:AM 61694-6, right and left rami with i3–c1 and p2–m3; F:AM 61694-7, left partial ramus with i1–c1 and p2–m1; F:AM 61694-8, right ramus with c1 and p2–m3; F:AM 61694-9, right ramus with i1–c1 and p2–m2; F:AM 61695, left ramus with i3–c1, p1–p2 alveoli, p4–m2, and m3 alveolus; F:AM 61695-1, right partial ramus with p4–m2; F:AM 61695-2, left partial ramus with c1 and p2–m2; F:AM 61695-3, left partial ramus with c1, p2–p3 alveoli, p4–m2, and m3 alveolus; F:AM 61695-4, left partial ramus with p4 broken–m3; F:AM 61695-5, right and left partial rami with i2–c1 and p2–m2; F:AM 61695-6, right partial ramus with p4–m2; F:AM 61695-7, left ramus with c1 and p2 alveoli, p3–m2, and m3 alveolus; F:AM 61695-8, right partial ramus with c1 and p3–m2; F:AM 61695-9, right partial ramus with c1 broken and p2 (detached)–m2; F:AM 61696, right ramus with p4–m1 and m2–m3 alveoli; F:AM 61696-1, left ramus with c1 broken, p2–m2, and m3 alveolus; F:AM 61696-2, left ramus with i1–c1 and p2 alveolus–m1; F:AM 61696-3, left partial ramus with m1–m2 and m3 alveolus; F:AM 61696-4, right ramus with p4–m2 and m3 alveolus; F:AM 61696-5, left ramus with p3–m1 and m2–m3 alveoli; F:AM 61696-6, left ramus with p4–m3; F:AM 61696-7, left and right rami with i3–c1, p3–m2, and m3 alveolus; F:AM 61696-8, right ramal fragment with p4–m1; F:AM 61696-9, left ramus with c1 broken, p3–m1, and m2 alveolus; F:AM 61697, left ramus with c1 alveolus, p2, p3 alveolus, p4–m1, and m2–m3 alveoli; F:AM 61697-1, left ramus with c1 and p2–m1; F:AM 61697-2, right ramus with c1 and p2–m2; F:AM 61697-3, right ramus with p4–m1; F:AM 61698, immature skull with I3–

C1 erupting, dP2–dP4, P3–M1, and M2 erupting; F:AM 61698-1, crushed immature skull with dC1, dP3–dP4, I3–C1 erupting, and M1 erupting, and both rami with i1–i2, di3–dc1, p1, and dp3–dp4; F:AM 61698-2, immature anterior part skull with dI3, dP2–dP4, and P4–M1 erupting; F:AM 61698-3, left maxillary fragment with dP3–dP4; F:AM 61698-4, right immature ramus with dp3–dp4 and m1–m2 erupting; F:AM 61698-5, left immature ramus with c1 erupting, dp3–dp4, and m1 erupting; F:AM 61698-6, right immature ramal fragment with i1, di3, and dp2–dp4; F:AM 61698-7, left immature ramus with dp3–dp4; F:AM 61698-8, left immature ramus with dp3–dp4 and m1–m2 erupting; F:AM 61698-9, left immature ramus with dp4 broken and m1 erupting; F:AM 61699, left immature ramus with dp3–dp4; F:AM 98090, left ramus with p3–m1; F:AM 98091, left ramus with p2 alveolus–m1 and m2 alveolus; F:AM 98092, left ramus with p3–m2; F:AM 98093, right ramus with p3–m1; F:AM 98094, left and right rami with p4–m2; F:AM 98095, left ramus with p4–m1; F:AM 98096, right ramus with p4–m2 and m3 alveolus; F:AM 98097, right ramus with c1 and p3 broken–m1; F:AM 98098, left ramus with c1 and p4–m2; F:AM 98099, right ramus with p3–m2; F:AM 98100, right ramus with p4–m1; F:AM 98101, right ramus with m1–m2; F:AM 98102, right ramus with p4–m1 and m2 alveolus; F:AM 98103, left ramus with m1–m2; F:AM 98104, left ramus with p3–m2 and m3 alveolus; F:AM 98105, left ramus with c1 and p2 alveolus–m2; F:AM 98106, right ramus with p4–m2 and m3 alveolus; F:AM 98107, right ramus with p4–m2; F:AM 98108, right ramus with p4 broken–m2 and m3 alveolus; F:AM 98109, left ramus with p4–m2 and m3 alveolus; F:AM 98110, right ramus with p4–m2; F:AM 98111, right ramus with m1–m2; F:AM 98112, left ramus with p4–m1; F:AM 98113, right ramus with i3–c1 and p4–m2; F:AM 98114, left ramus with p4–m2 and m3 alveolus; F:AM 98115, right ramus with p2–p3 alveoli, p4–m2, and m3 alveolus; F:AM 98116, left ramus with p4–m2; F:AM 98117, right ramus with p4–m2 and m3 alveolus; F:AM 98118, left ramus with p4–m2 and m3 alveolus; F:AM 98119, left ramus with i3–c1 and p2–m3; F:AM 98120, left ramus with p4–m1 and m2–m3 alveoli; F:AM 98121, left and right rami with p4–m2 and m3 alveolus; F:AM 98122, right ramus with c1 and p3–m2; F:AM 98123, right immature ramus with c1 erupting, p3, dp3–dp4, and m1 erupting; F:AM 98124, left ramus with p4–m2; F:AM 98125, left and right rami with p2–m2; F:AM 98126, right ramus with c1 and p4–m1; F:AM 98127, right ramus with p3–m1 broken; F:AM 98128 right ramus with c1 and p3–m2; F:AM 98129, right ramus with p4–m2; F:AM 98130, left ramus with m1–m2; F:AM 98131, left ramus with c1 and p2–m1 broken; F:AM 98132, left ramus with p4–m3; F:AM 98133, right ramus with c1 and p4–m1; F:AM 98134, right ramus with c1 and p4–m2; F:AM 98135, left and right rami with i1–c1 and p3–m3; F:AM 98136, right ramal fragment with p4–m1; F:AM 98137 and 98137A, left and right rami (one individual) with p3–m2; F:AM 98138, left ramus with p4–m2; F:AM 98139, right ramus with p4–m2; F:AM 98140, left ramus with m1–m2; F:AM 98141 left ramus with p4–m2; F:AM 98142, right ramus with p4–m1; F:AM 98143, right ramus with p4–m2; F:AM 98144, left and right rami with i1–c1 and p3–m2; F:AM 98145, left ramus with c1 and p2–m3; F:AM 98146, left ramus with p3–m2; F:AM 98147, right ramus with p4–m2; F:AM 98148, left ramus with p4–m2; F:AM 98149, left ramus with p3–m3; F:AM 98150, left ramus with p4–m2; F:AM 98151, left ramus with p4–m2; F:AM 98152, right ramus with c1, p2, and p4; F:AM 98153 left and right rami with i2–c1, p3–m1, and m2–m3 alveoli; F:AM 98154, right maxillary with P2–M1; F:AM 98155, right maxillary with P4–M1; F:AM 98156, left maxillary with P3–M2; F:AM 98157, right maxillary with P4–M1; F:AM 98158, left maxillary with P4–M1; F:AM 98159, left maxillary with P4–M1; F:AM 98160, partial crushed palate with C1–M1; F:AM 98161, left maxillary with P3–P4; F:AM 98162, left ramus with p3–p4; F:AM 98163, left maxillary with P4–M2; F:AM 98164, crushed skull with I3, P1–M1, and both rami with c1 and p2–m3; F:AM 98165, left maxillary with P4–M1; F:AM 98166, left maxillary with P4–M1; F:AM 98167, anterior part skull with I1–M2; F:AM 98168, crushed partial skull with C1, P2 bro-

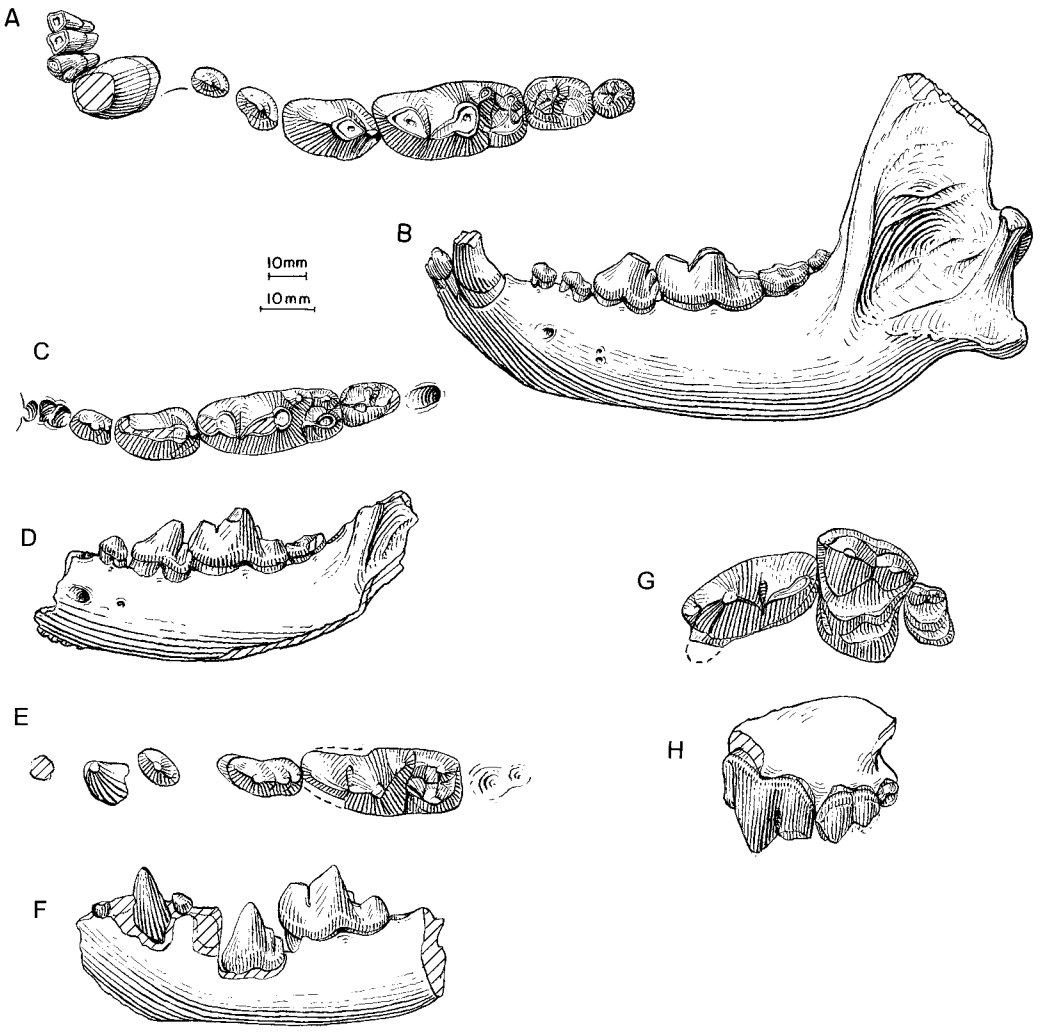

Fig. 123. *Borophagus secundus*. **A**, Lower teeth and **B**, ramus, F:AM 23350, Coffee Ranch Quarry, Ogallala Group (late Hemphillian), Hemphill County, Texas. **C**, Lower teeth and **D**, ramus, AMNH 13831, holotype, Johnson Member, Snake Creek Formation (late Hemphillian), Sioux County, Nebraska. **E**, Lower teeth and **F**, ramus (reversed from right side), F:AM 18126, Mt. Eden Fauna, Mt. Eden Formation (late Hemphillian), Riverside County, California. **G**, Upper teeth and **H**, lateral view of maxillary (reversed from right side), F:AM 18130, Mt. Eden Fauna. The shorter (upper) scale is for B, D, F, and H, and the longer (lower) scale is for the rest.

ken–M1, and left ramus with i2–c1 and p4–m3; F:AM 98169, crushed skull with I1, I3, C1 broken, and P4–M2; F:AM 98170, crushed articulated skull and mandible with all upper and lower teeth; F:AM 98171, anterior part skull with C1 broken and P4 broken–M2; F:AM 98172, partial palate with C1 and P3 broken–M2; F:AM 98173, left premaxillary-maxillary with I2–P2 and P4–M2; F:AM 98174, right immature maxillary with C1 erupting, dP4, P4 erupting and M1; F:AM 98175, right maxillary with M1–M2; F:AM 98176, right immature ramus with c1, dp3, and p4 erupting; F:AM 98177, right ramus with p4–m1 and m2 alveolus; F:AM 67917 and 67917A–C, left humerus and three right distal part humeri; F:AM 67916, left radius and ulna with distal ends missing;

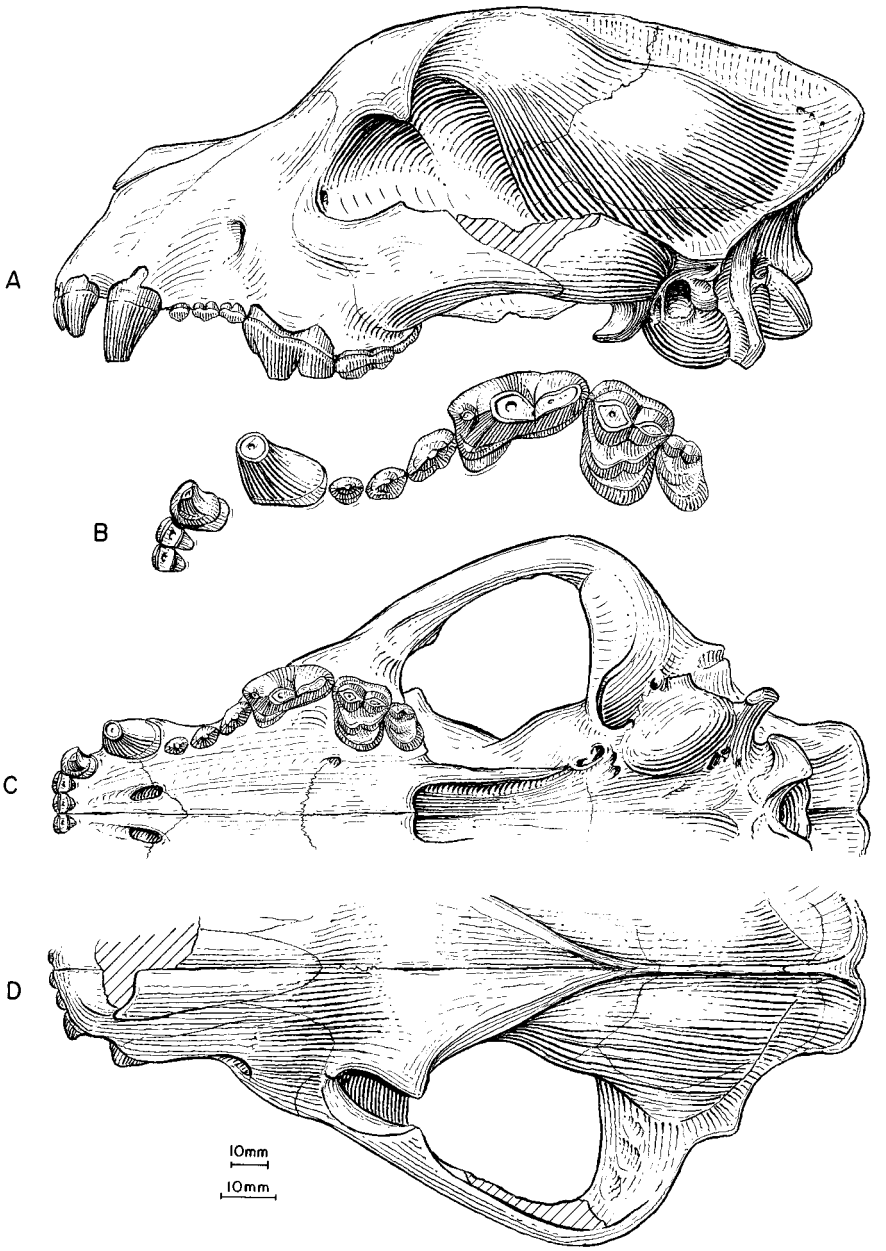

Fig. 124. *Borophagus secundus*. **A**, Lateral, **B**, enlarged occlusal, **C**, ventral, and **D**, dorsal views of skull and upper teeth, F:AM 23350, Coffee Ranch Quarry, Ogallala Group (late Hemphillian), Hemphill County, Texas. The shorter (upper) scale is for A, C, and D, and the longer (lower) scale is for B.

F:AM 67918 and 67918A–D, two right and three left radii; F:AM 67918E–H, one right and three left incomplete radii with distal ends missing; F:AM 67918I–M, five proximal part radii; F:AM 67919 and 67919A–G, one right, six partial right, and one partial left ulnae; F:AM 67920 and 67920A, B, left femur and right and left incomplete femuri; F:AM 67921 and 67921A, B, right tibia and two right distal part tibiae; F:AM 67927 and

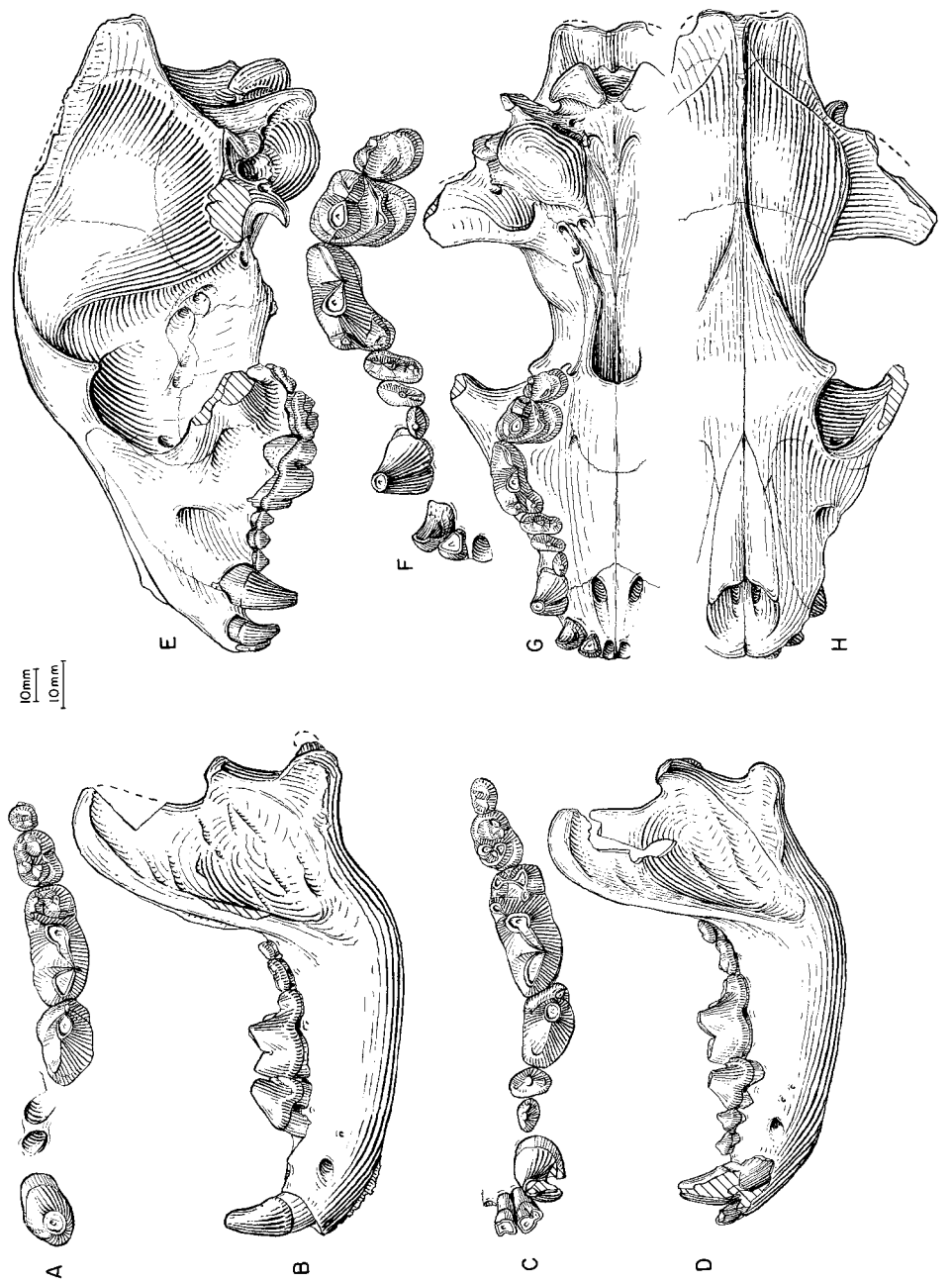

Fig. 125. *Borophagus secundus*. **A**, Lower teeth and **B**, ramus, AMNH 18919 (holotype of *Hyaenognathus direptor*), *Pliohippus* Draw, Johnson Member, Snake Creek Formation (late Hemphillian), Sioux County, Nebraska. **C**, Lower teeth, **D**, ramus, **E**, lateral, **F**, enlarged occlusal, **G**, ventral, and **H**, dorsal views of skull (nasal restored from right side) and upper teeth (I3, P2–P3, and M1 from right side), F:AM 61640, Edson Quarry, Ogallala Group (late Hemphillian), Sherman County, Kansas. The shorter (upper) scale is for B, D, E, G, and H, and the longer (lower) scale is for the rest.

67927A–G, eight metacarpals I; F:AM 67923 and 67923A–L, 13 metacarpals II; F:AM 67924 and 67924A–J, 11 metacarpals III; F:AM 67925 and 67925A–F, seven metacarpals IV; F:AM 67926 and 67926A–E, six metacarpals V; F:AM 67927 and 67927A, B, three metatarsals I; F:AM 67927C–I, seven metatarsals II; F:AM 67928 and 67928A–C, two complete and two proximal part metatarsals III; F:AM 67928D–G, one complete and three partial metatarsals IV; F:AM 67929 and 67929A–G, eight metacarpals V; F:AM 67930 and 67930A–S, 19 calcanea; F:AM 67931 and 67931A–I, 10 astragali; carpals, tarsals and phalanges; OMNH 15165 (OMP 40-1-S21), anterior part of skull and mandible with I3–M1, c1, and p4–m2 (Savage, 1941: pl. 1, fig. 10); and additional 8 OMNH specimens listed by Savage (1939; see Czaplewski et al., 1994).

Leyden Quarry, Chamita Formation (late Hemphillian), Rio Arriba County, New Mexico: F:AM 61637, left ramus with c1, p3 alveolus–m1 (m1 broken), and m2–m3 alveoli.

Mt. Eden Fauna (late Hemphillian), Mt. Eden Formation, Riverside County, California: F:AM 18126, right partial adolescent ramus with detached dp4 and i1–i3 all broken, c1 erupting, p2, p3–p4 erupting and m1 (fig. 123E, F); F:AM 18129, left maxillary fragment with P2–P4, and M1 broken; F:AM 18129A, right isolated M2; F:AM 18130, right partial maxillary with P4–M2 (fig. 123G, H); F:AM 18131, right partial maxillary with P2, and P3 alveolus–M2 (P4 broken); F:AM 18132, right maxillary fragment with P4–M1; F:AM 18123C, left partial ramus with m1–m2 and m3 alveolus; F:AM 18126N, right partial ramus with p2–p3 both broken, p4–m2 and m3 alveolus; F:AM 18126O, right partial ramus with p3–p4 and m1 broken; F:AM 18126P, detached p4 and m1 broken; F:AM 18126Q, right ramal fragment with p4 and m1 broken; and F:AM 18126X, left ramal fragment and symphysis with i1–c1 all broken, p2–p3, and p4 broken.

Rhino Island (LACM loc. 3942), Modesto Reservoir Local Fauna, Mehrten Formation (late Hemphillian), Stanislaus County, California: LACM 62705, left partial premaxillary-maxillary with C1 and P2–M2.

DISTRIBUTION: Early Hemphillian of Nebraska; and late Hemphillian of Nebraska, Kansas, Oklahoma, Texas, New Mexico, California, Mexico, Honduras, and El Salvador.

EMENDED DIAGNOSIS: *B. secundus* is derived relative to *B. parvus* and more primitive species in having a shorter muzzle; palate wider at P4; p1 mostly absent; anterior premolars crowded; p4 more robust, taller crowned, more posteriorly directed, smaller posterior accessory cusplet that is more closely appressed against posterior cingulum, and transverse diameter approaching or exceeding that of trigonid of m1; m1 talonid narrow relative to trigonid; and mandibular ramus short and robust with marked lateral deflection of the dorsal part of the horizontal ramus and the toothrow. *B. secundus* is primitive relative to *B. hilli* and *B. diversidens* in having a frontal sinus not greatly expanded toward inion, paroccipital process not greatly elongated, I3 not prominently enlarged, P4 with strong parastyle and protocone less reduced, P4 and M1 with stronger labial cingulum, P4–M1 not as massive relative to anterior premolars and M2, m2 metaconid equal or higher than protoconid, and mandibular ramus not as massive nor with such lateral curvature of dorsal part of horizontal ramus and toothrow.

DESCRIPTION AND COMPARISON: Abundant materials are available for *Borophagus secundus*, especially from the late Hemphillian of Texas and Kansas, making this species the best represented of any Borophaginae. Excellent cranial and postcranial material from the Coffee Ranch have long been known through Matthew and Stirton's (1930) early study, which provides ample illustrations of this species. More recently, Harrison (1983) has also described the large, exquisitely preserved sample from the Edson Quarry, Kansas.

The most prominent features of this species are its domed forehead and shortened muzzle. Dissection of an undistorted skull (F:AM 61640) from the Edson Quarry reveals a frontal sinus approximately 80 mm long and 25 mm deep. The sinus extends anteriorly to the posterior tip of the nasal process and penetrates posteriorly to the middle part of braincavity (at approximately the same cross-sectional level as the external auditory meatus). The sinus is partitioned by partial

septa but does not penetrate the postorbital process. Shortening of the rostrum causes the posterior tip of the premaxillary process to reach to the level of the antorbital rim, and the posterior border of the palate is contracted anteriorly to lie in front of the posterior border of the M2, although the shortening of rostrum is not very pronounced in the cranial ratio diagram (length of P1–M2 in fig. 118). The facial region lateral to the infraorbital foramen is abruptly widened, as it is in *B. diversidens*. This proportional difference is also reflected in the ratio diagram (fig. 118), which shows a much wider palate width at P4 than that at P1. Another prominent feature of this species is a wide and deep zygomatic arch, also shown in the ratio diagram.

Despite the large amount of material available from widespread geographic areas, dental proportions are rather stable, as shown by the generally low values of the coefficient of variation (appendix III). Exceptions are found in the lower premolars, especially in p2–p3, whose dimensions vary extensively due to the shortening of jaws that causes overcrowding, reduction, and loss of p1 (sometimes p2 as well). The p1 is present in only 3.4% (4 out of 118) of all individuals that have preserved anterior rami (many more are not counted because slight damage in this area can obliterate a very small and shallow alveolus of p1). Richey (1979: 109), on the other hand, found a 16% presence of p1s (total sample of 74 rami) among the Coffee Ranch specimens. The difference seems to lie in Richey's interpretation of certain rami as having had a p1 that was broken off and eventually healed. Our own estimate is thus more conservative. This discrepancy of the estimates aside, the p1 is largely lost both functionally and statistically. The I3 completely lacks lateral accessory cusplets. Because the P1–P3 and p2–p3 are nonoccluding, the shapes of these teeth tend to vary freely. Reflecting the extremely shortened muzzle, the P2–P3 are often entirely transversely oriented to be accommodated in the short space. This imbrication tends to be less severe in the lower premolars because they are shorter than their upper counterparts. The P4 still has a strong parastyle and the M1 a weak labial cingulum, both of which are lost in more derived taxa (e.g., *B. diversidens*). The tip of the main cusp of p4 is generally higher than the m1 paraconid, in contrast to the lowercrowned p4s in *B. parvus*, and it is prominently sloped posteriorly, almost touching the anterior border of the m1 paraconid. This recumbent main body of the p4 tends to compress the posterior accessory cusplet against the posterior cingulum. In occlusal view, the p4 assumes a rather triangular outline due to the broadening of the posterior edge of the tooth. Broadening of the palate at P4 also results in a corresponding lateral displacement of the p4 to the extent that the p4 often overhangs the labial face of the ramus. Continuing the hypercarnivorous trend, the m1 talonid is reduced (both shortened and narrowed). The m1 and m2 metaconids are not especially reduced in height, although the m1 entoconid is smaller than the hypoconid in occlusal view due to the shortening of the talonid on the lingual side. The m2, on the other hand, is relatively unreduced compared to those of *B. hilli* and *B. diversidens*.

DISCUSSION: Matthew and Cook (1909) established a new ''mutant,'' *Aelurodon saevus secundus*, from the Snake Creek Formation of Nebraska. They considered it closely related to *Borophagus* (*Hyaenognathus* in the early days). However, Matthew (1924) subsequently named another species from the Upper Snake Creek beds, *Hyaenognathus direptor*, without comparing it to his earlier taxon (lower teeth of the holotype of *B. direptor*, AMNH 18919, are more robust than those of the type of *B. secundus*, AMNH 13831, although such a difference is within individual variations of *B. secundus* from well-sampled quarries, such as Edson Quarry and Coffee Ranch Quarry). Later, Matthew and Stirton's (1930) study of the excellent Coffee Ranch materials further shifted the attention from *secundus* by referring the Texas materials to *Borophagus cyonoides* Martin, which became the type species of the new genus *Osteoborus* of Stirton and VanderHoof (1933). The latter authors admitted that *secundus* was very closely related to *O. cyonoides* (Stirton and VanderHoof, 1933: 178), but opted to maintain the two species as distinct because of the perceived possibility that most *secundus* specimens from the Snake Creek Formation might have a p1, in contrast

to the general absence of a p1 in individuals from Kansas and Texas. Since then, the Snake Creek names *secundus* and *direptor* were mostly ignored, and *O. cyonoides*, based on more complete materials from Texas and Kansas, came to symbolize this lineage of hyenalike dogs.

Topotype materials of *secundus* and *direptor* from the Snake Creek Formation are still limited to fragmentary upper and lower jaws. However, they preserve enough dental morphology together to confidently identify them as conspecific with the far more numerous materials from Texas and Kansas. Richey (1979: fig. 7) demonstrated that the width of p4 in the holotypes of *secundus* and *direptor* falls within the range of 2 units of standard deviation of the mean of the Coffee Ranch sample. Harrison (1983: 22) further stated that ''future investigation may well indicate that at least *O. secundus*, *O. direptor*, and *O. cyonoides* are conspecific.'' We agree with this latter assessment, and accordingly recognize Matthew and Cook's (1909) subspecific name as having priority (which also implies that *secundus* becomes the type species of *Osteoborus* if the genus is ever used again).

A partial maxillary with C1 and P2–M2 (LACM 62705) from the late Hemphillian Modesto Reservoir Local Fauna of the Mehrten Formation is provisionally referred to *Borophagus secundus*. This specimen has a large M2, found in most *B. secundus*, but possesses a peculiar P4 with a rather reduced parastyle, which is only found in *B. hilli* and *B. diversidens*. This combination of primitive and derived features in LACM 62705 may suggest a distinct species, but such a determination must await additional specimens. In any case, the presence of LACM 62705 in the Mehrten Formation is the only evidence of co-occurrence of two species of *Borophagus* (*B. parvus* and *B. secundus*) in the late Hemphillian of North America.

Borophagus secundus is the earliest taxon to assume the cranial and dental proportions of advanced *Borophagus*: extremely shortened rostrum, broadened palate, imbricated P2–P3 and p2–p3, and robust, high-crowned p4. The abundant fossil record of this species and its wide geographic occurrence attest to the success of this ''hyenoid'' dog.

Borophagus hilli (Johnston, 1939)

Figure 126

Osteoborus hilli Johnston, 1939a: 895, figs. 1–4. Richey, 1979: 107. Munthe, 1998: 137.
Osteoborus progressus Hibbard, 1944: 107, pl. X, figs. 1–4. Richey, 1979: 107.
Osteoborus crassapineatus Olsen, 1956b: 1, pl. 1, figs. 1–3.
Borophagus sp.: Gazin, 1936: 285. Bjork, 1970: 16. Gustafson, 1978: 37, fig. 21B.
Borophagus crassapineatus (Olsen): Richey, 1979: 107.
Borophagus ?*diversidens* (Cope, 1892): Miller, 1980: 786, figs. 12, 13.
Borophagus diversidens Cope, 1892: Lucas and Oakes, 1986: 250, fig. 4C–G.

HOLOTYPE: TWM 1558 (AMNH cast 113946), right anterior part of skull with I1–I2 alveoli, I3–C1, P1 alveolus, and P2–M2, and left ramus with c1 and p2 alveoli and p3–m3 (fig. 126A–E) from the Axtel Ranch Locality, Harrell Ranch, Ogallala Group (late late Hemphillian), Randall County, Texas.

REFERRED SPECIMENS: From the type locality: TWM 1643, partial left ramus with i1–p3 alveoli and p4–m2; TWM 2361, partial left ramus with p2 alveolus–m1; TWM 2418, left and right maxillary fragments with P1 alveolus–M2; TWM 2419, partial left ramus with p2–p3 alveoli and p4–m2; UCMP 43306, right maxillary fragment with P3–M1 (fig. 126F, G).

Saw Rock Canyon Local Fauna, Ogallala Group (late late Hemphillian or early early Blancan), Seward County, Kansas: KUVP 6791 (AMNH cast 45998), right and left rami with p3 and p4 broken–m3 (holotype of *Osteoborus progressus* Hibbard, 1944: figs. 1–4).

Christian Place Quarry, Christian Ranch Local Fauna, Ogallala Group (late late Hemphillian), southwest of Claude, Armstrong County, Texas: F:AM 67387A, left ramus with c1, p2 alveolus–m1, and m2 alveolus (fig. 126H, I).

Palmetto Fauna (''Upper Bone Valley Fauna'' of Tedford et al., 1987), Bone Valley Formation (late late Hemphillian), Polk and Manatee counties, Florida: American Agricultural Chemical Co. Mine: UF V-5644 (AMNH cast 55564), right partial ramus with p4–m1 (holotype of *Osteoborus crassapineatus* Olsen, 1956b: figs. 1–3; referred to *O.*

dudleyi by Webb, 1969b: 283). Four Corners Mine (IMC-Agrico Co.): AMNH 129880, left P4. Fort Green Mine: UF 43573, partial left m1; UF 45974, partial right P4; UF 53979 (cast from private collection of Rick Carter), left ramus with c1 and p2 alveoli, and p3–m1 broken; UF 60822, partial right m1; and UF 114519, partial left m1. Gardinier Mine: UF 100217, partial right m1. CF Industries Mine: UF 130118, partial right m1. District Grade Mine: UF 22912, partial left maxillary with P4–M1; and UF 124526, left ramal fragment with p4. Swift Mine: UF 45940, left and right rami with c1, p2 alveolus, and p3–m2. Whidden Creek: UF 123694, right ramal fragment with erupting m1; UF 131975, left P4; UF 133947, immature right maxillary fragment with erupting P4–M1; UF 133948, right maxillary fragment with M1; and UF 123693, left ramal fragment with m1. Locality unknown: UF 50758, right ramal fragment with m1 alveolus and m2. AgriCo Phosphate Co.: BF OB-16, right maxillary fragment with P4–M1. Cargill (formerly Gardner) Phosphate Mine, Bird Clog Site, near Fort Meade: BF OB-2, right maxillary fragment with P4; BF OB-3, isolated left m1; BF OB-5, isolated right P4; BF OB-7, right ramal fragment with p4–m1; and BF OB-17, left maxillary fragment with P4.

Hagerman Local Fauna, Glenns Ferry Formation (early early Blancan), Hagerman Fossil Beds National Monument, Twin Falls County, Idaho: USNM 12616, edentulous left ramus with p4–m2 alveoli (referred to *Borophagus* sp. by Gazin, 1936: 285; Bjork, 1970: 16). North of Peters Gulch: HAFO 266 (AMNH cast 129877), left ramus with i2–i3 alveoli, c1, p2–p3 alveoli, p4–m1, and m2–m3 alveoli (referred to *Osteoborus hilli* by McDonald, ms).

Ringold Formation (early Blancan), Benton County, Washington: White Bluffs (UWBM loc. A6503): UWBM 35115, left p4, 40 ft above White Bluffs tuff (referred to *Borophagus* sp. by Gustafson, 1978: 37, fig. 21B).

Cuchillo Negro Creek Local Fauna, near Truth or Consequences, Palomas Formation (early Blancan), Sierra County, New Mexico: UNM loc. 303: UNM P-060, right ramus with i2–c1 and p2–m2 (referred to *Borophagus diversidens* by Lucas and Oakes, 1986: fig. 4E–G).

Las Tunas, beds correlated with the Salada Formation (early Blancan), southern Baja California, Mexico: IGM 2297 (AMNH cast 129314), right ramus with p3–m2 (referred to *Borophagus* ?*diversidens* by Miller, 1980: fig. 13); and IGM 2298 (AMNH cast 129315), right ramus fragment with p4–m1 (referred to *Borophagus* ?*diversidens* by Miller, 1980: fig. 12).

DISTRIBUTION: Late late Hemphillian of Kansas, Texas, and Florida; and early Blancan of Idaho, Washington, New Mexico, and Mexico.

EMENDED DIAGNOSIS: Derived characters that distinguish *B. hilli* from *B. secundus* and more primitive species of *Borophagus* are enlarged I3, P4 parastyle further reduced and protocone absent, P4 and M1 lacking labial cingulum, P4–M1 massive and larger relative to premolars and M2, p4 width equal to that of m1 trigonid, shortening of m1 talonid on entoconid side, metaconid of m2 lower than protoconid, and mandibular ramus massive with more lateral curvature of dorsomedial part of horizontal ramus and toothrow. *B. hilli* is more primitive than *B. diversidens* in having low mandibular condyle, I3 less prominently enlarged, P1–P3 and p2–p3 less extremely reduced, P4 less robust and broad, presence of P4 parastyle, M1 metaconule less reduced, presence of posterior accessory cusplet on p4, metaconids and entoconids on lower molars less reduced, m1 trigonid less broadened, and m2 less extremely shortened. *B. hilli* can be distinguished from *B. dudleyi* in its less broadened palate and posterior palatine border anterior to the posterior margin of M2.

DESCRIPTION AND COMPARISON: Except for two fragmentary jaws (UCMP 43306 and F:AM 67387A), most materials presently referred to *Borophagus hilli* have previously been described under different names. Although still represented by a small sample from all localities, a modest gain in knowledge of this species is possible by pooling two previous nominal species (*crassapineatus* and *progressus*) into *B. hilli*.

Knowledge about the cranial morphology of *Borophagus hilli* is still limited to the partial palate of the holotype. It shows a broad-

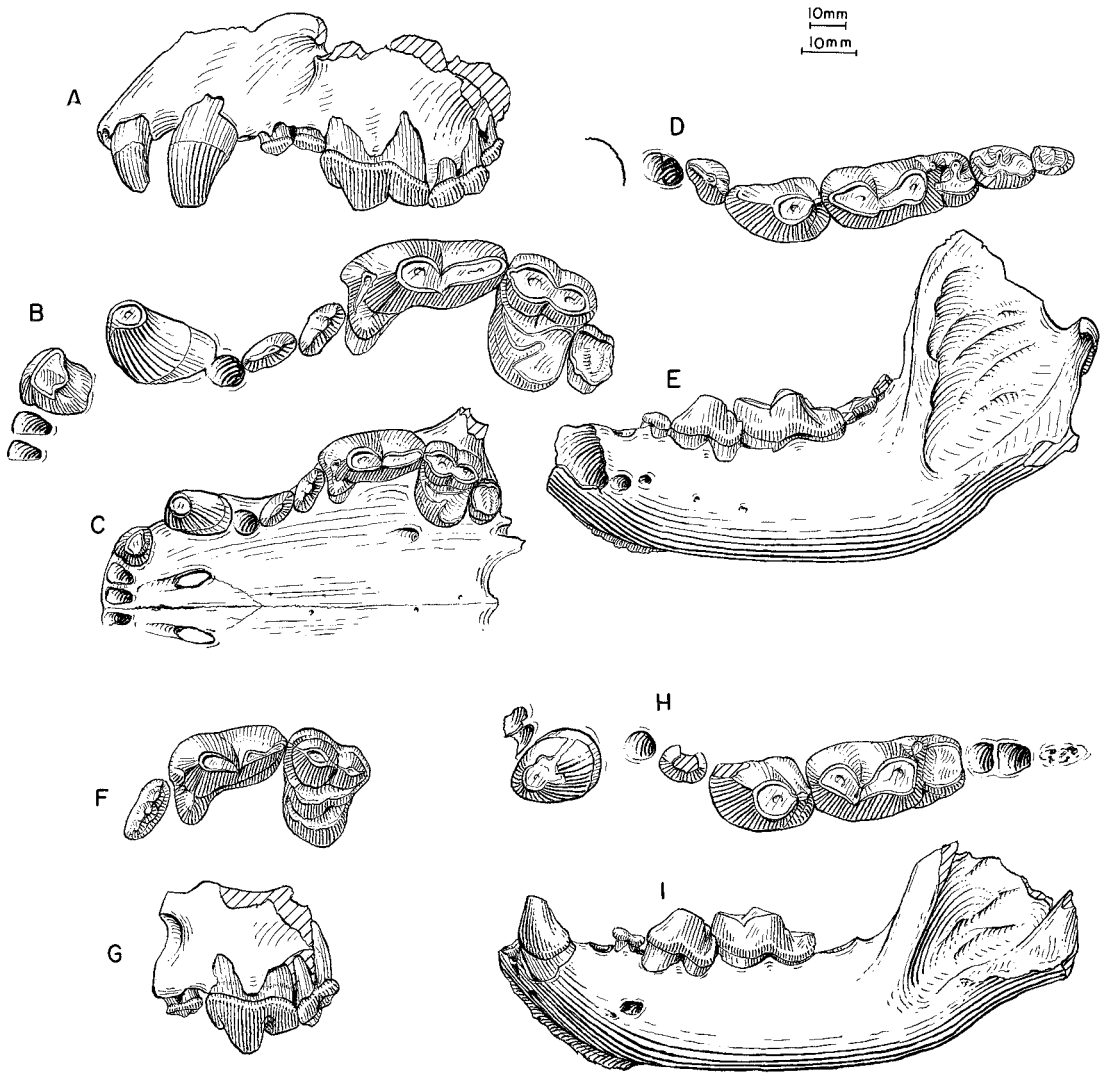

Fig. 126. *Borophagus hilli*. **A**, Lateral, **B**, enlarged occlusal, and **C**, ventral views of partial skull and upper teeth (M2 from right side), **D**, lower teeth, and **E**, ramus, TWM 1558, holotype, Axtel Ranch Locality, Ogallala Group (late late Hemphillian), Randall County, Texas. **F**, Upper teeth and **G**, lateral view of maxillary (reversed from right side), UCMP 43306, Axtel Ranch Locality. **H**, Lower teeth and **I**, ramus, F:AM 67387A, Christian Place Quarry, Ogallala Group (late late Hemphillian), Armstrong County, Texas. The shorter (upper) scale is for A, C, E, G, and I, and the longer (lower) scale is for the rest.

ening of the palate similar to that in *B. secundus* but distinctly less broadened than in *B. dudleyi* and *B. diversidens*. Another feature of *B. hilli* and *B. diversidens* is its anteriorly located posterior palatine border, which is anterior to the posterior border of the M2, in contrast to that in *B. dudleyi*, which has a more posteriorly located palatine border relative to the last molar.

Borophagus hilli is intermediate in most dental measurements between *B. secundus* and *B. diversidens*, as seen in the ratio diagram (fig. 119); it is, on average, 7% larger than *secundus* and 6% smaller than *diversi-*

dens. The I3 is strong and more than twice as large as I2. The P2–P3 are not as extremely reduced as in *B. diversidens*. Although the P4 parastyle is still present, it is relatively smaller than those seen in *B. secundus*. Its protocone has all but disappeared, although its root is still retained. The P4 is rather slender in contrast to the much more robust (wide) P4s in *B. diversidens*. The M1 is completely free of any trace of a labial cingulum. The enlargement of the p4 has reached the stage where the width of p4 is equal to that of the m1 trigonid. The posterior accessory cusp is correspondingly reduced but not totally lost as it is in *B. diversidens*. The metaconid of m1 is still present. The m2 is not as reduced as in *B. diversidens*. The metaconid of m2 on the holotype is very small and little worn and is presumably much lower than the protoconid (worn flat in all specimens). The mandibular condyle is not as prominently elevated above the toothrow as is in *B. diversidens*.

DISCUSSION: Johnston (1939a) compared his *Osteoborus hilli* with *O. secundus* (= *cyonoides*) and *B. diversidens* and considered *hilli* to be intermediate, a conclusion agreed to by all later authors, including us. Shortly afterward, Hibbard (1944) named a new species, *O. progressus*, noting its advanced features shared with *diversidens* but without mention of Johnston's earlier name. Although somewhat later in occurrence (latest Hemphillian or earliest Blancan of Kansas) than that of *B. hilli*, the holotype of *progressus* is easily referable to *B. hilli*.

Dental materials from the Bone Valley Formation compare favorably with the holotype of *Borophagus hilli*. We consider *Osteoborus crassapineatus* to be conspecific with *hilli* (its disproportionately large canine on the holotype probably does not belong to this individual). The presence of a P4 parastyle and a p4 posterior accessory cusplet in *O. crassapineatus* is similar to the condition in the holotype of *B. hilli*, but is clearly more primitive than in *B. diversidens* which has lost both of these structures (see more discussion under *B. dudleyi*).

As presently construed, *Borophagus hilli* spans the late late Hemphillian through early Blancan (mostly Blancan I and II of Repenning, 1987). Although individuals from the early Blancan tend to be referred to *B. diversidens* (e.g., Miller, 1980; Lucas and Oakes, 1986), they are generally closer to *B. hilli* in size and morphology. The extremely derived condition of *B. diversidens* seems to have been acquired in the latest early Blancan.

Borophagus dudleyi (White, 1941)

Figure 127

Pliogulo dudleyi White, 1941a: 67, pls. 10, 11.
Osteoborus dudleyi (White): Webb, 1969b: 281 (in part). Munthe, 1998: 137.

HOLOTYPE: MCZ 3688, skull with only right P3 and alveoli of most other teeth (fig. 127), Phosphate pits near Mulberry, Palmetto Fauna (''Upper Bone Valley Fauna'' of Tedford et al., 1987), Bone Valley Formation (late late Hemphillian), Polk County, Florida.

REFERRED SPECIMENS: Holotype only.

DISTRIBUTION: Late late Hemphillian of Florida.

EMENDED DIAGNOSIS: *Borophagus dudleyi* shares with *B. diversidens* advanced cranial features that are distinguishable from *B. secundus*: highly expanded frontal sinus, widened and posteriorly expanded palate, elongated paroccipital process, and reduced M2. It differs from *B. diversidens* in its extremely posteriorly expanded frontal sinus that almost reaches to the inion, laterally extended postorbital process of frontal, and procumbent upper incisors.

DESCRIPTION AND COMPARISON: The holotype skull, MCZ 3688, is still the only specimen for this species. The excellently preserved skull offers an undistorted view of its cranial morphology. MCZ 3688 is the largest individual among known species of *Borophagus*. It is 12% larger (in basal length of skull) than the only complete skull of *B. diversidens*, MSU 8034. However, MSU 8034 clearly falls within the lower range of *B. diversidens*, as its teeth are generally small, and most individuals of *B. diversidens* have larger teeth than those of MSU 8034 (see appendix III). Therefore, *B. dudleyi* is probably quite close to *B. diversidens* in size. A ratio diagram for cranial measurements (fig. 118) shows that *B. dudleyi* mostly follows the pattern of *B. diversidens*.

The most prominent advancement of the

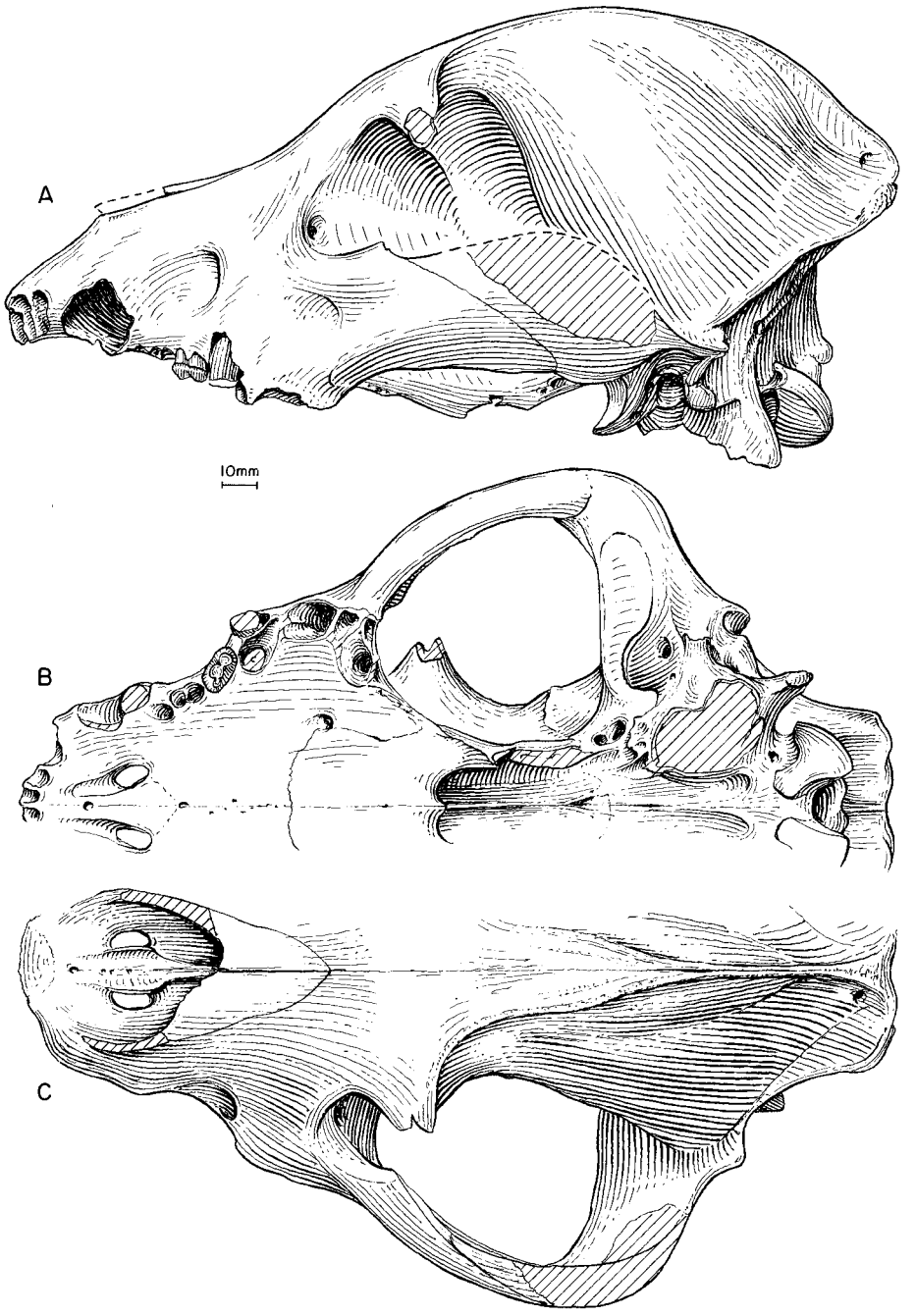

Fig. 127. *Borophagus dudleyi*. **A**, Lateral, **B**, ventral, and **C**, dorsal views of skull (paroccipital process and P3 reversed from right side), MCZ 3688, holotype, Phosphate pits near Mulberry, Bone Valley Formation (late late Hemphillian), Polk County, Florida.

skull of *Borophagus dudleyi* over that of *B. secundus* is its posterior expansion of the frontal sinus (fig. 127). Through small breakages on the skull roof of MCZ 3688, the sinus can be seen to extend far backward, almost to the inion of the skull. Although the frontal–parietal suture is not visible due to complete fusion, the frontal sinus must have penetrated beyond the suture to form a large air space between the braincavity and the top of the skull roof. Externally, the extent of the frontal sinus can also be traced by a slight bulge of the skull roof due to the expansion of sinus beneath it. This posterior expansion of the sinus causes a posterior shift of the forehead dome in lateral profile (fig. 127). Thus, instead of being at a level slightly behind the orbit, such as in *B. secundus* (fig. 124) and *B. diversidens* (fig. 129), the high dome of the skull roof is shifted to the middle of the braincase. The paroccipital process is elongated relative to that in *B. secundus*. The postorbital process of frontal is more laterally expanded than in *B. diversidens*. The posterior border of the palate is expanded behind the posterior border of the last molar.

The essential lack of teeth on the holotype precludes meaningful comparison with other species, and observations can only be made on the alveoli. Judging from their alveoli, the upper incisors are more procumbent than in either *B. secundus* or *B. diversidens*. The P3 is small, both relative to the skull size and the P4 (alveoli only), indicating further reduction of premolars from the condition in *B. hilli*.

DISCUSSION: The identity of *Borophagus dudleyi* (MCZ 3688) is difficult to settle because of its lack of teeth. Contrary to the generally smaller teeth from the Bone Valley materials relative to those of *B. diversidens*, the skull of *B. dudleyi* is 12% larger (in basal length of skull) than the only measurable skull of *B. diversidens*, MSU 8034 (however, note that MSU 8034 may represent a small individual among *B. diversidens*). In addition to its large size and elaborate frontal sinus, the cranial morphology of MCZ 3688 is that of a highly advanced *Borophagus* (e.g., widened palate, elongated paroccipital process). An obvious question is whether MCZ 3688, lacking almost all teeth, belongs to the same species as represented by most dental materials from the Bone Valley (presently referred to *B. hilli*). Based on measurements of the alveoli for MCZ 3688, Webb (1969b) asserted that *B. dudleyi* and *B. crassapineatus* have similar dental dimensions and contended that there is only one large borophagine in the Bone Valley Formation, that is, *dudleyi* is synonymous to *crassapineatus*. We chose to retain *B. dudleyi* as distinct. Its many derived features discussed above seem to indicate that *B. dudleyi* is a unique lineage of its own.

Borophagus diversidens Cope, 1892

Figures 128–130

Borophagus diversidens Cope, 1892: 1028; 1893: 54, pl. XIII, fig. 4. Merriam, 1903: 281, figs. 2, 4, 5. Matthew and Stirton, 1930: 173. VanderHoof, 1931: 18; 1936: 415, fig. 1 (in part); 1937: 389. Johnston, 1939a: 896. Meade, 1945: 520, pl. 48, fig. 4. Hibbard and Riggs, 1949: 838, fig. 1F, H, I. Hibbard, 1950: 159, fig. 18. Dalquest, 1968: 115, figs. 1–4. Skinner et al., 1972: 108, fig. 49. Richey, 1979: 107. Munthe, 1998: 137. Miller and Carranza-Castañeda, 1998: 458.

Felis hillianus Cope, 1893: 55, pl. XIV, figs. 1–11.

Hyaenognathus pachyodon Merriam, 1903: 287, figs. 1, 3, pl. 28, figs. 1, 2. Matthew, 1924: 102. Matthew and Stirton, 1930: 179, figs. 1, 2. VanderHoof, 1931: 19. Colbert, 1939: 65.

Hyaenognathus? (*Porthocyon*?) *dubius* Merriam, 1903: 283, pls. 29, 30. VanderHoof, 1931: 19.

Hyaenognathus (*Porthocyon*) *matthewi* Freudenberg, 1910: 209, figs. 3, 4.

(?) *Hyaenarctos* (*Borophagus*) *diversidens* (Cope): Frick, 1926: 93.

Hyaenognathus cf. *H. pachyodon* (Merriam): Russell and VanderHoof, 1931: 19, fig. 7. VanderHoof, 1933: 382.

Hyaenognathus matthewi (Freudenberg): VanderHoof, 1931: 18. Stock, 1932: 263.

Hyaenognathus solus Stock, 1932: 263, pl. 14, figs. A, B.

Hyaenognathus dubius (Merriam): Stock, 1932: 263.

Canis dirus (Leidy, 1858): VanderHoof, 1936: 415 (TMM 40287-11).

Borophagus pachyodon (Merriam): VanderHoof, 1936: 415. Stirton, 1939b: 389. Richey, 1979: 107. Munthe, 1998: 137.

Borophagus solus (Stock): VanderHoof, 1936: 415. Schultz, 1937: 98. Richey, 1979: 107.

Borophagus matthewi (Freudenberg): VanderHoof, 1936: 415. Richey, 1979: 107.

Borophagus sp.: Shotwell, 1970: 77, fig. 36F.

Osteoborus hillianus (Cope): VanderHoof, 1937: 389.
Canis cf. *C. dirus* (Leidy): VanderHoof, 1937: 389 (in part).
Borophagus –large species: Johnston and Savage, 1955: 39.
Borophagus dubius (Merriam): Richey, 1979: 107.
Borophagus cf. *B. diversidens* (Cope): Conrad, 1980: 212, fig. 14E, E′.

HOLOTYPE: TMM 40287-10 (AMNH cast 129875), left ramal fragment (fig. 128C, D) with c1 alveolus, p2 alveolus, p3, and p4 broken from Mt. Blanco, Blanco Formation (late Blancan), Crosby County, Texas.

REFERRED SPECIMENS: From type locality, Blanco Canyon, Blanco Formation (late Blancan), Crosby County, Texas: TMM 40287-11, paracone and metastyle blade of right P4 and lateral half of right M1 (paratype of *Borophagus diversidens*) (this specimen was identified as milk teeth of *Canis dirus* by VanderHoof, 1936: 415); TMM 18578, ramus fragment with p3–p4; MSU 8034 (Dalquest, 1968: figs. 1–4), skull with I1–M2 (fig. 129), right ramus with i3–c1, p2 alveolus and p3–m3 (fig. 128E, F), axis (Munthe, 1989: fig. 4C), seventh cervical, two caudals, right humerus (Munthe, 1989: figs. 6E, 7E), left partial ulna, partial left and right radii (Munthe, 1989: fig. 9E), pelvis, left femur (Munthe, 1989: fig. 15E), head of right femur, left tibia (Munthe, 1989: fig. 17F), left fibula, and other foot bones (Munthe, 1989: fig. 18B); and AMNH cast 129874 (private collection of Joe Taylor), right ramus with c1, p2 and m2–m3 alveoli and p4–m1. Crawfish ranch house, on south side of draw, 17 ft above basal contact in ''flaggy limestone'' member: TMM 31179-39, right maxillary fragment with P4 and M1 root (Meade, 1945: pl. 48, fig. 4); and TMM 31176-64, right calcaneum. Seven mi northeast of Crosbyton: CMNH 9495, left ramus with c1 broken, p2 alveolus, and p3–m1 (Hibbard, 1950: fig. 18).

Rexroad Formation (late early Blancan), Keefe Canyon Quarry (KUVP loc. 22), Meade County, Kansas: KUVP 7266, right premaxillary-maxillary fragment with C1, P1, P2 alveolus, isolated right P3–P4, and left M1 (Hibbard and Riggs, 1949: fig. 1F, H, I).

Beck Ranch Local Fauna (late early Blancan), Scurry County, Texas: MSU 8644, palate lacking only left I3, both P1s, and right M2 (Dalquest, 1978: fig. 13); MSU 8664 and 9464, two isolated c1s; MSU 8665-6 and 9465-7, five isolated metapodial; MSU 9468, isolated phalanges.

Lisco Local Fauna, Lisco Quarry 1 (UNSM loc. Gd-14), lower part of Broadwater Formation (late early Blancan), Garden County, Nebraska: UNSM 2687, anterior partial skull with I3–M2 and partial mandible with i1–m3; UNSM 25692, crushed anterior partial skull with I1–M2; UNSM 25836, left ramus with c1–p3 alveoli, p4–m2, and m3 alveolus; UNSM 25839, right premaxillary-maxillary with I2–M2; UNSM 25838, partial mandible with i1–m2 (p2 alveolus); UNSM 25840, left and right rami with c1–m3; and UNSM 25841, left maxillary fragment with P4–M1 both broken, right ramus with i1–i3 alveoli, c1, p2–p3 alveoli, and p4–m2.

Rancho Viejo Beds (early Blancan), Guanajuato, Mexico: Arrastracaballos locality (Gto. 6), 10 km north of San Miguel Allende: IGM 6675, right ramus with i1–c1 alveoli, p3–m1, and m2–m3 alveoli (Miller and Carranza-Castañeda, 1998: fig. 3).

Grand View Fauna, Glenns Ferry Formation (late Blancan), Ada County, Idaho: Jackass Butte locality 2404: UO 16343, isolated left p4 (referred to *Borophagus* sp. by Shotwell, 1970: 77, fig. 36F). IMNH loc. 77006: IMNH 29492 (AMNH cast 129878), right ramus with i1–c1 alveoli, p2–m2, and m3 alveolus (Conrad, 1980: fig. 14E, E').

Ringold Formation (late Blancan), Benton County, Washington: Taunton Substation (LACM loc. 6408): LACM 10826, right ramal fragment with m1.

Northern part of Sacramento Valley, Tehama Formation (late Blancan), Tehama County, California: UCMP 31067, broken left M1 (referred to *Hyaenognathus* cf. *H. pachyodon* by Russell and VanderHoof, 1931: fig. 7).

Coso Mountains (late Blancan), Inyo County, California: LACM-CIT loc. 131, 9.5 mi east of Olancha: LACM-CIT 481, partial palate with I1 alveolus and I2–M2 (holotype of *Hyaenognathus solus* Stock, 1932). LACM-CIT loc. 284: LACM-CIT 2024, heel of M1 and roots of P4 (referred to *Borophagus solus* by Schultz, 1937).

Asphalto (Blancan), near foot of Temblor Range, Kern County, California: UCMP 8139 (AMNH cast 30071), left and right rami with c1, p2 alveolus, p3–m2, and m3 alveolus (holotype of *Hyaenognathus pachyodon* Merriam, 1903: pl. 28, figs. 1, 2). One and one-fourth mi southeast of McKittrick: UCMP 29522, right maxillary fragment with broken P4, M1, and M2 alveolus (referred to *Hyaenognathus pachyodon* by Matthew and Stirton, 1930: fig. 1); and UCMP 29523, right ramal fragment with m2 (referred to *Hyaenognathus pachyodon* by Matthew and Stirton, 1930: fig. 2).

Two mi southeast of Cornwall (Blancan), Contra Costa County, California: UCMP 8138 (AMNH cast 30075), partial skull with I3, C1, P1–P3 alveoli, and P4–M2 (holotype of *Hyaenognathus* (*Porthocyon*) *dubius* Merriam, 1903: pls. 29, 30).

Dry Mountain Locality, 111 Ranch Fauna, Gila Group (late Blancan), Graham County, Arizona: F:AM 108446, right partial ramus with m2 broken from base and m3 alveolus.

Three and one-half mi section, Saint David Formation (late Blancan), near Benson, Cochise County, Arizona: F:AM 23399, mandible with i1–c1 and p2–m3.

Post Ranch Fauna, Carnivore Site, Post Ranch area, UA loc. 47-3 (UCMP loc. V6804), Saint David Formation (late Blancan), Cochise County, Arizona: UA 1466 (UCMP cast 80385), partial mandible with i2–m1.

Pima, Gila Group (Blancan), Graham County, Arizona: F:AM 61561, left ramal fragment with m1 broken and m2.

Channel Sands Pocket, Panaca Formation (late Blancan), near Panaca, Lincoln County, Nevada: F:AM 67119, fragmentary palate with P4–M2, mandible with i1 broken–c1, p2–p3 both broken, p4–m3, and two isolated canines and proximal end radius.

From 8 mi east of Broadwater, probably equivalent to Lisco Local Fauna (late early Blancan), Morrill County, Nebraska: UNSM 25891, complete left and partial right rami with c1, p1 alveolus, p2–m2, and m3 alveolus.

Broadwater Local Fauna, Broadwater Formation (early late Blancan), Morrill County, Nebraska: Broadwater Quarry 4 (UNSM loc. Mo-5): UNSM 25837, crushed skull and mandible with crushed upper and lower dentitions; UNSM 25851 (AMNH cast 98083), partial mandible with i1–i3 alveoli, c1, p2 alveolus, and p3–m3; and UNSM 6123-39, crushed upper and lower jaws with right P4–M1 and left p2–p3. Broadwater Quarry 3 (UNSM loc. Mo-6): UNSM 107-12-6-36-SP, left edentulous ramus with c1–m1 alveoli.

Sand Draw Fauna, Keim Formation (late Blancan), Lee Magill Ranch, McGill County, Nebraska: F:AM 67117, right ramus with c1 and p3 alveoli, p4 broken–m2, and m3 alveolus (Skinner et al., 1972: fig. 49); and F:AM 67118, right isolated broken m1.

Hall Gravel Pit, Long Pine Formation (late Blancan), Brown County, Nebraska: F:AM 87485, right partial ramus with p2–p3 alveoli, p4–m2 all broken, and m3 alveolus.

Big Spring Local Fauna (UNSM loc. Ap-103), Long Pine Formation (late late Blancan, i.e., near the end of Blancan V in Repenning, 1987), Antelope County, Nebraska: UNSM 51600, right M1; UNSM 2009-95, right M1; UNSM 2100-79, left ramus with c1–p2 alveoli and p3–m2; and UNSM 2100-91, right ramus with c1 alveolus and p2–m2 (p2 and p4 broken).

Cita Canyon, Ogallala Group (late Blancan), Randall County, Texas: JWT 561, partial left and right rami with p2–m2; JWT 561A, left and right rami with p3–m2; JWT 932, left and right rami with p2–m2; JWT 1558, left maxillary fragment with P4–M1; JWT 2530, m1; WTSU 551 (UCMP cast 80151), partial mandible with i1–m2 (left c1–p2 missing); WTSU 772 (UCMP cast 80252), left ramus with i1–i3 alveoli, c1–m2, and m3 alveolus; WTSU uncataloged, left maxillary fragment with P4–M1; and WTSU uncataloged, right maxillary with P4–M2.

Channing area, Ogallala Group (late Blancan), Oldham County, Texas: Proctor Pit D: F:AM 67364, left ramus with c1 alveolus, p2 alveolus–m2, m3 alveolus (fig. 128A, B) and associated detached right canine; F:AM 67365, crushed fragmentary skull with P4–M1 and isolated teeth including M2 and premolars; and F:AM 129870, left partial maxillary with P4 broken–M1. Bevins Pit 1: F:AM 67332, left partial ramus with p3, p4–m1 both broken, m2, and m3 alveolus. Proctor Pit C: F:AM 67333, right partial ramus with c1 and p3 alveoli, p4–m1 and m2

alveolus, and right isolated m1; and F:AM 129871, left isolated worn m1. Near Proctor Pit A: F:AM 67334, right partial ramus with p3–m2 all broken at bases. Collins Pit 2: F: AM 61580, right ramal fragment with p4–m1 both erupting and left broken m1.

Santa Fe River Locality 1 (late Blancan), Columbia County, Florida: UF 8007, symphyseal part of mandible with i1–p4 alveoli; UF 10469, right M1; UF 10701, partial left P4; and UF 95058, partial right P4.

North Port Charlotte Locality (?late Blancan), Charlotte County, Florida: UF 50759, left maxillary fragment with P4 and roots of M1.

Vicinity of the town of Tequixquiac in the Valley of Mexico (?late Blancan), Mexico: IGM 162 (AMNH cast 14311) (The holotype, IGM 162, was presumably lost some years ago [Miller and Carranza-Castañeda, 1998], but plaster casts are available in some collections. Hibbard and Riggs' [1955] study of the megafauna of the Valley of Mexico found no evidence of a Tertiary fauna, and those in the Valley of Tequixquiac were compared to faunas in the Sangamon interglacial and Wisconsin glacial intervals of the northern Great Plains. However, a Rancholabrean record of *Borophagus* is yet to be found among known faunas, and we consider it likely that IGM 162 was from the latest Blancan, based on its stage of evolution, which is comparable to those from the Big Springs of Nebraska.), anterior part of skull with I1–I2, I3–P1 alveoli, P2–M1, and M2 alveolus (fig. 130) (holotype of *Hyaenognathus matthewi* Freudenberg, 1910: 209, figs. 3, 4).

DISTRIBUTION: Early Blancan of Kansas, Nebraska, Texas, and Mexico; late Blancan of Washington, Idaho, California, Arizona, Nevada, Texas, Nebraska, and Florida; and ?late Blancan of Florida and Mexico.

EMENDED DIAGNOSIS: As the terminal species of the Borophagina, *Borophagus diversidens* is distinguishable from all other species of the genus in its highly derived features: palate abruptly widened at P4; extremely enlarged I3; P1–P3 and p2–p3 small, oval, and buttonlike without cusplets; P4 massive with protocone weak to absent and parastyle absent; M1–M2 small relative to carnassial; M1 paracone exceptionally tall relative to height of metacone, metaconule weak or absent, anterolingual cingulum absent, and lingual cingulum restricted to posterolingual corner; p4 robust and wide with transverse diameter exceeding width of m1 trigonid; p4 tall-crowned, strongly sloped posteriorly, posterior accessory cusp absent, and posterior cingulum compressed; p4 extremely flared laterally; m1 trigonid elongate relative to talonid, metaconid extremely weak or absent, talonid short and narrow, and entoconid greatly reduced or absent; m2 small with paraconid absent, and metaconid either absent or represented by simple crest to protoconid; mandibular condyle high above toothrow; and humerus without entepicondylar foramen.

DESCRIPTION AND COMPARISON: *Borophagus diversidens* is known in many late Blancan localities throughout central and western North America. Although mostly fragmentary, materials from these localities combine to produce a fairly complete picture of its cranial and dental morphology. Variation within a single locality, however, is still poorly known, as no one locality produced a large enough sample. The somewhat crushed skull, MSU 8034, from the topotype area described by Dalquest (1968: figs. 1–4) still provides the best information about the cranial morphology of the species (fig. 129).

As the terminal species of the Borophaginae, *Borophagus diversidens* carries to the extreme some cranial and dental features that canids have explored during their long history. The external morphology of MSU 8034 suggests that it has a highly domed frontal sinus. As in *B. hilli*, the extent of the frontal sinus above the braincase is revealed externally by the gentle inflation of the sinus. On the broken skull of UCMP 8138, the frontal sinus has a maximum depth of 30 mm near the top of the braincase and can be clearly seen to extend to the inion. The bulla is greatly inflated, and the paroccipital process is elongated far beyond the base of the bulla.

The palate is very broad, extremely so in the latest members of this species such as the individuals from the Big Springs of Nebraska and the holotype of *Borophagus matthewi*. The P4 is laterally offset from the P3 in occlusal view, resulting in an abrupt widening of the palate at the P4 and backward. The

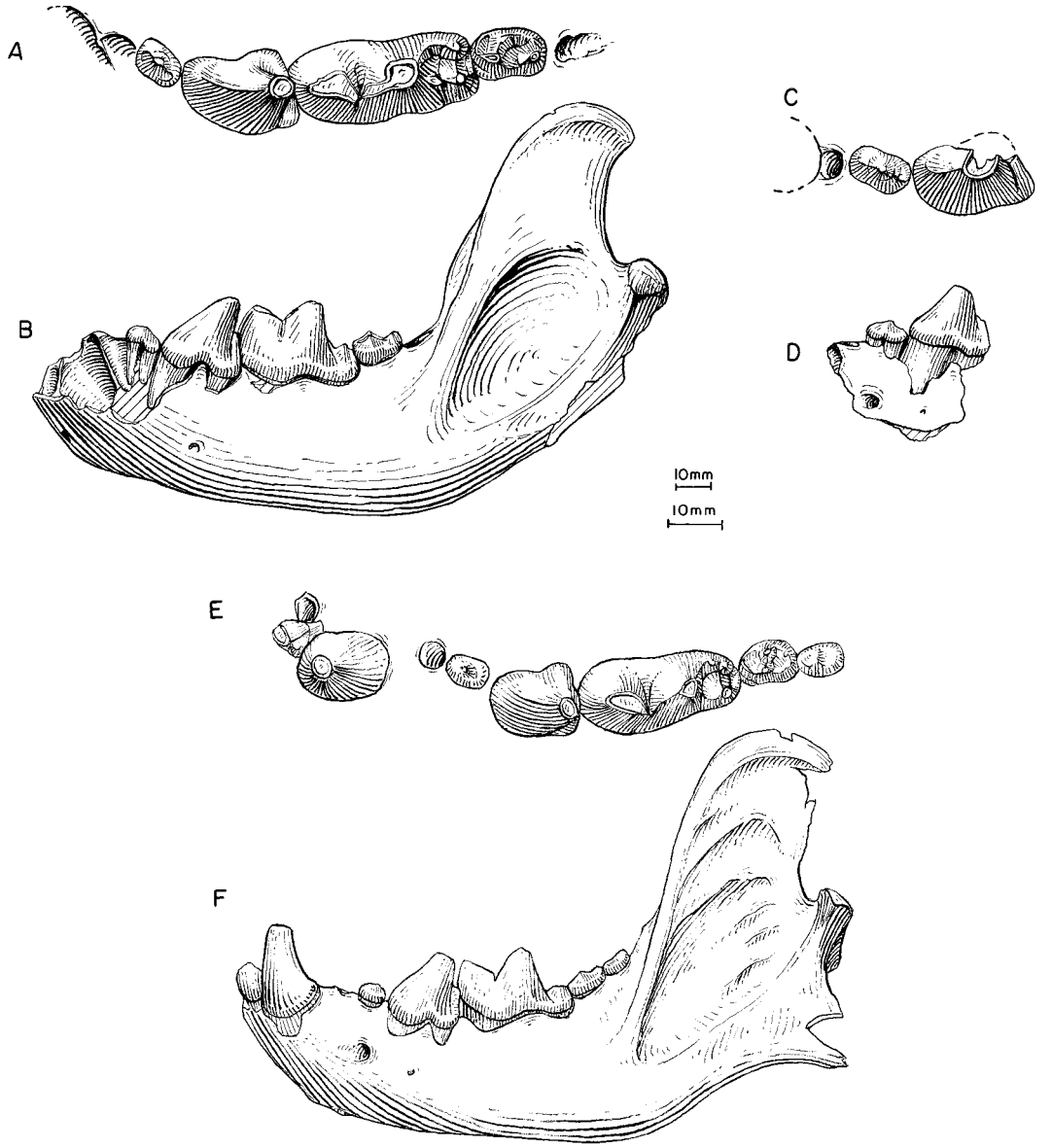

Fig. 128. *Borophagus diversidens*. **A**, Lower teeth and **B**, ramus, F:AM 67364, Proctor Pit D, Ogallala Group (late Blancan), Oldham County, Texas. **C**, Lower teeth and **D**, ramus, TMM 40287-10, holotype, Mt. Blanco, Blanco Formation (late Blancan), Crosby County, Texas. **E**, Lower teeth and **F**, ramus (reversed from right side), MU 8034, Blanco Canyon, Blanco Formation (late Blancan), Crosby County, Texas. The shorter (upper) scale is for B, D, and F, and the longer (lower) scale is for the rest.

palate in UCMP 8138 (holotype of *B. dubius*) is the least widened among known individuals, although it has suffered a certain amount of lateral crushing.

The I3 is greatly enlarged, especially in the holotype of *B. matthewi* (IGM 162; fig. 130). The I3 alveolus is approximately three times as large as those of the I1 and I2, and its posterior border is 12 mm behind those of I1–I2. Extreme reduction of the P1–P3 and p2–p3 left these teeth as no more than small buttons, oval in outline, extremely low

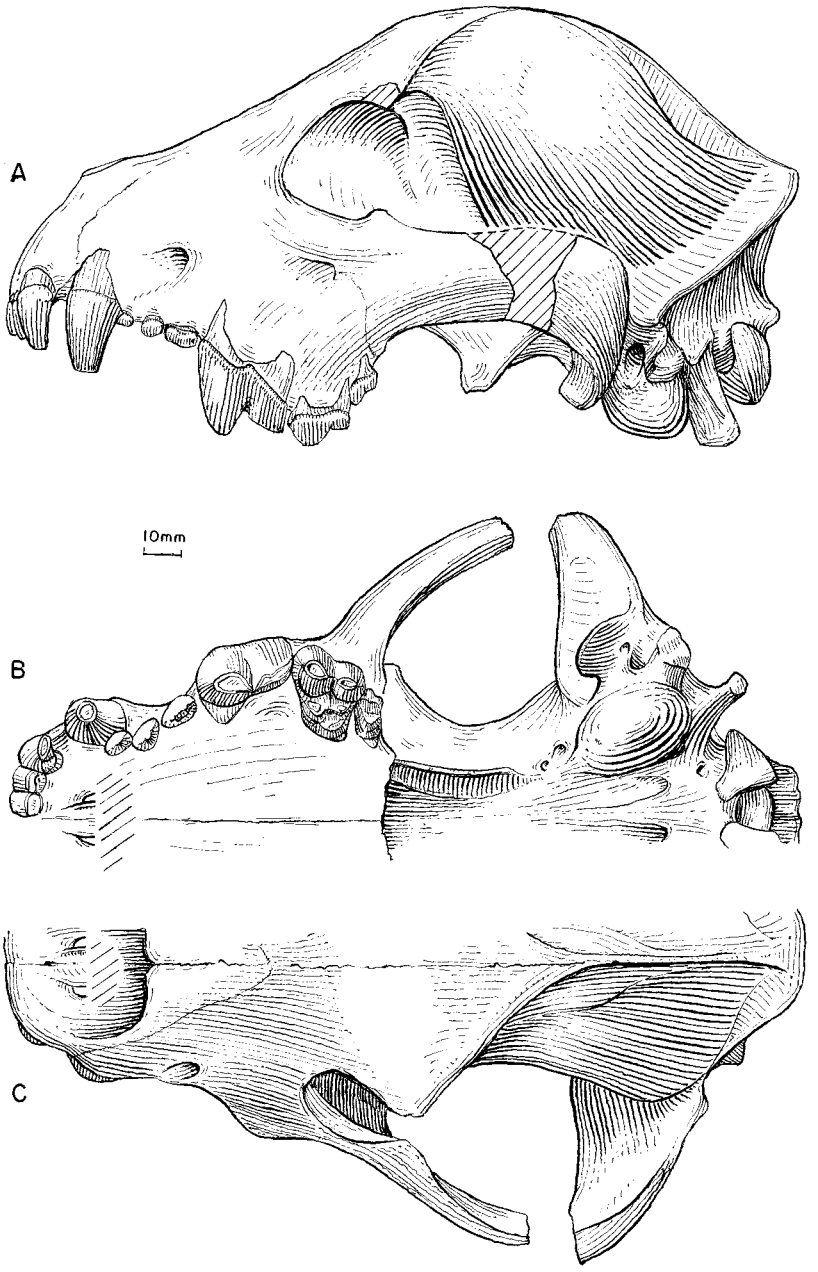

Fig. 129. *Borophagus diversidens*. **A**, Lateral, **B**, ventral, and **C**, dorsal views of skull (P1 reversed from right side), MU 8034, Blanco Canyon, Blanco Formation (late Blancan), Crosby County, Texas.

in crown height, and practically functionless, as they do not occlude. In most individuals, these teeth experience little or no wear even though other teeth (P4–M1 and m1–m2) may have incurred extensive wear. In most individuals, the P4 parastyle and protocone are lost; the root of the latter, however, is still present. The P4 also becomes transversely widened. In contrast to more primitive species, the M1 lingual cingulum is restricted to the posterolingual corner. The M1 labial cingulum is completely lost, and the metaconule

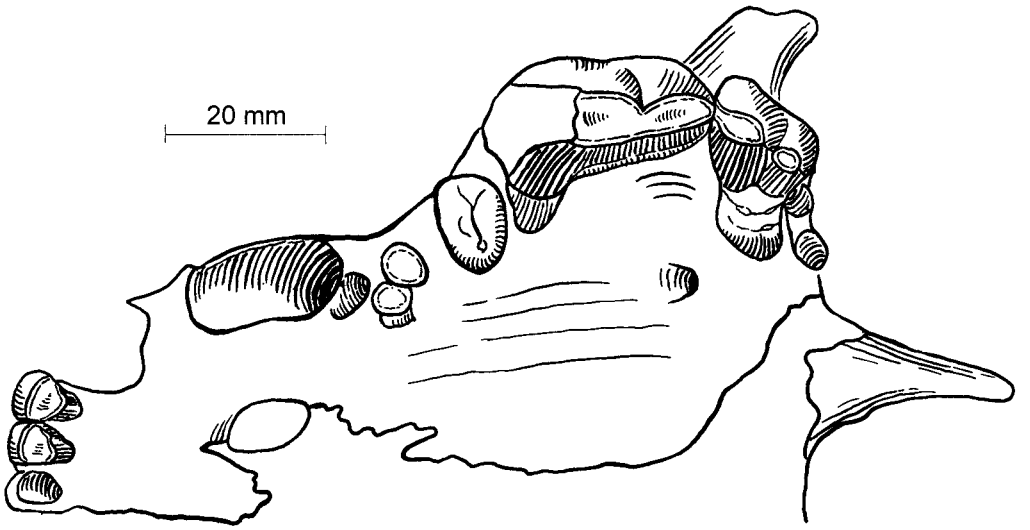

Fig. 130. *Borophagus diversidens*. Ventral view of partial skull, IGM 162 (holotype of *Hyaenognathus matthewi*), vicinity of the town of Tequixquiac, Valley of Mexico (?late Blancan), Mexico. Illustrated from a cast and Freudenberg's (1910: fig. 3) figure by X. Wang.

is reduced or lost. In *B. diversidens*, the p4 width has exceeded that of m1 trigonid and also has highest width-to-length ratio compared to other species (Richey, 1979). The main cusp of the p4 is further reclined, and the extremely elevated posterior cingulum leaves no room for the posterior accessory cusp, which has thus disappeared in all individuals, in contrast to its presence in *B. hilli*. The further reduction of the m1 talonid in *B. diversidens* and the considerable reduction (and occasional loss) of the m1 entoconid indicate a more hypercarnivorous condition than found in *B. hilli*. This is in further contrast to a more widened trigonid. The m1 metaconid is lost in most individuals, and when present is in a low position just slightly above the entoconid. The m2 metaconid is either lost or reduced to a small ridge.

Materials from the Big Springs (late late Blancan) of Nebraska and from Mexico (IGM 162, holotype of *Borophagus matthewi*) represent the most extreme dental modifications toward the ultimate bone-crusher. The palate in IGM 162 is so broadened and the muzzle so shortened that the hard palate is wider than it is long. The broadening of the palate is mainly accomplished through lateral expansion at the level of the P4–M2, causing the P4 to be markedly displaced laterally from the P2–P3 (it is mainly through their extremely laterally flared p4–m1 that the Big Spring's materials are inferred to have reached the corresponding degree of the widening of the palate in IGM 162).

DISCUSSION: The fragmentary holotype of *Borophagus diversidens*, its subsequent ''loss'' and recovery (VanderHoof, 1936), and the lack of appreciation of individual variation combined to inspire a proliferation of names early in the century (see Dalquest [1968] for a summary). In addition to *B. diversidens*, five species were named prior to the 1930s: *Felis hillianus* (Cope, 1892), *Hyaenognathus pachyodon* (Merriam, 1903), *H. dubius* (Merriam, 1903), *H. matthewi* (Freudenberg, 1910), and *H. solus* (Stock, 1932). In a series of papers in the 1930s, VanderHoof and co-authors attempted to reconcile the various names, but failed to escape the typological thinking of the day, leaving essentially all of the then known nominal taxa intact. Since then, the general consensus has seemed to gradually settle on *B. diversidens* as the only and most frequently cited hyenalike dogs in the Blancan of North America. The fact that there is only one form of this dog in a given locality suggests one continuous lineage (anagenetic evolution) in the late early throughout late Blancan.

As the terminal taxon of the Borophaginae clade, *Borophagus diversidens* is clearly the most specialized toward a durophagous dentition, a structure that facilitates the extraction of bone marrow. Morphological trends in this direction generally follow a direction of increasing size, shortening of rostrum and lower jaws, deepening of horizontal ramus, broadening of facial region, reduction of premolars in front of the extremely robust P4, high paracone on M1, enlargement and lateral displacement of p4, elongation of m1, and reduction of m2. Most of these features seem designed to deliver a maximum crushing force between P4 and p4–m1, as well as the necessary remodeling of bones on the lower jaw and skull (see also Werdelin, 1989).

Although specimens of *Borophagus* were sometimes reported in Pleistocene or Plio-Pleistocene ''transitional'' deposits, in most of these cases the deposits were later determined to be late Pliocene (Blancan). A recent report of *B. diversidens* in the basal unit C of the Wellsch Valley Local Fauna, near Swift Current, Saskatchewan (Stalker and Churcher, 1972) places its latest occurrence within the Olduvai subchron (Foster and Stalker, 1976), which coincides closely with the Blancan–Irvingtonian transition (Lundelius et al., 1987: 221). However, our examination of the Saskatchewan specimens, NMC 17824 (left maxillary fragment with M1) and 17825 (right premaxillary fragment with I3), led us to conclude that these do not belong to *Borophagus* but probably represent a large Caninae. In any case, late occurring individuals such as those from the Big Springs (late Blancan V, approximately 2 Ma) of Nebraska, the basal part of the Vallecito Local Fauna (approximately 2.1 Ma; see Cassiliano, 1999: fig. 4a), and the Valley of Mexico (holotype of *B. matthewi*) are just a few rare examples of this powerful dog near the end of its existence. *Borophagus* must have become extinct shortly after that, and thus ended a once extremely successful and, at times, dominant group of carnivorans on the North American continent.

CHARACTER ANALYSIS

Character interpretation is clearly of primary importance in any kind of phylogenetic analysis, be it cladistics or otherwise. Cladistic methodology as is commonly practiced now, however, offers no clear method for how to select characters and divide character states. In general, the coding of a character matrix remains an exercise of considerable subjective judgment. Although we cannot claim exceptions to this rule, our judgments about character variations are derived from a database much larger than any previous attempts and are sometimes grounded in our analysis of living taxa. Imprecision of character interpretations may well cause certain poorly supported clades to flip around if some critical characters are coded slightly differently. For the most part, however, slight changes in the ways we interpreted the characters probably will not significantly alter the topology. One may choose to more finely divide the character states than we have done and the clades may be supported by more or less synapomorphies. After all, the numbers of synapomorphies at different parts of the cladogram are only a rough reflection of the weight of evidence. It is hoped that the overall pattern of our cladogram will remain stable despite the difficulties inherent in the character interpretations.

Most characters used here have been noted by previous authors, although often in a different context and thus with different meanings. Our own contribution is mainly in the examination of these characters on a much broader comparative basis than has previously been possible, thus providing a different perspective about character evolution under the rules of parsimony.

Dental features comprise more than half of the characters selected. This is not only because of practical necessity (i.e., preservational biases against less durable bones), but because of their obvious functional importance. Although it is often true that there is a close relationship of morphology to functionality that leads to independent development of similar structures, these homoplasies

do not necessarily always overwhelm the topology and obscure true relationships. Given a sufficiently dense fossil record and enough intermediate forms, homoplasies can be revealed, especially in combination with other cranial characters (see Phylogenetic Analysis below). Postcranial characters are not included in the cladistic analysis because of the rarity of associated skeletons, although they are sometimes useful in the diagnoses when adjacent taxa have comparable materials.

Some dental characters, particularly those related to hyper- or hypocarnivory, tend to co-vary both between upper and lower dentitions and among adjacent teeth (e.g., among M1–M2 or m1–m2), a common problem in most groups of carnivorans. We code the co-varying features as one character if they are completely correlated. On the other hand, even when two features appear to be completely correlated within a small clade, we may still code them as separate characters if they do not strictly co-vary in other clades. Such a practice has the undesired appearances of ''stronger'' support of certain clades because of the duplication of these co-varying characters, but it offers the benefit of more objective coding in other part of the phylogeny, that is, closer reflection of actual steps in the evolution of other clades in which the relevant characters do not strictly co-vary. When this problem is suspected, we can isolate its effect by analyzing individual clades separately.

Character polarities are determined by the method of outgroup comparison (see Maddison et al., 1984). The closest sister-group of the Borophaginae is *Leptocyon* (a basal Caninae), followed successively by *Hesperocyon* (a basal hesperocyonine) and *Prohesperocyon* (a primitive cynoid) (Tedford, 1978; Wang, 1990, 1994; Wang and Tedford, 1994, 1996); the latter two taxa are the primary outgroups. Primitive *Archaeocyon* is very close to the ancestral morphotype of the Borophaginae, and only a few subtle synapomorphies separate basal borophagines from *Hesperocyon*. This overall closeness in morphology and stratigraphic occurrence between *Archaeocyon* and the hesperocyonines suggests phylogenetic continuity and greatly reduces the uncertainties about the primitive states of the borophagines.

Intraspecific variation of characters is a major source of imprecision in character coding. Even a rigorously defined quantitative character state can fail in variable species whose morphology overlaps broadly with its ancestral or descendent species. Furthermore, most species also vary, sometimes in predictable fashions toward certain specializations, during their geological span. These problems reflect the nature of phylogenetic analysis of fossil taxa, and certain allowance of aberrant features and other such subjective judgments are impossible to avoid.

As is the convention, a character state of ''0'' is generally primitive, except in reversals, and a ''1'' is derived. In multistate characters, however, higher numbers do not necessarily always correspond to more derived states. The numbering of the characters corresponds to numbers in the character matrix in table 2. The following descriptions of characters are grouped under anatomical regions to facilitate easy comparison of related characters.

SKULL

1. Skull proportion: The primitive canid skull has a relatively long and narrow snout. Some hyper- or hypocarnivorous taxa tend to develop a brachycephalic skull that involves a combination of overall shortening and broadening of the skull. These proportional differences are best revealed through ratio diagrams.

Polarity: 0, skull normal proportioned; 1, skull slightly brachycephalic; 2, further shortening of skull.

2. Premaxillary meeting frontal: Primitively, the posterior process of the premaxillary is a thin strip of bone tapering off to a tip and wedged between the nasal and maxillary. It does not come in contact with the frontal bone. In *Desmocyon matthewi* and more derived taxa, the premaxillary process begins to widen and extend posteriorly. This enlarged premaxillary is in contact with an anteriorly extended nasal process of the frontal and thus excludes the contact between the nasal and maxillary. In advanced *Aelurodon*, the premaxillary process is further widened, a feature that seems to be related to the en-

larged I3 with well-developed lateral accessory cusplets.

Polarity: 0, premaxillary does not meet frontal; 1, premaxillary just meets frontal; 2, widened contact between premaxillary and frontal (fig. 131).

3. Postorbital process of frontal: The enlargement of the frontal sinus (see below) results in the frontal shield being widened in many borophagines. The broadening of the shield is often accompanied by enlargement of the postorbital process of the frontal.

Polarity: 0, frontal shield narrow and postorbital process not enlarged; 1, frontal shield widened and postorbital process enlarged (fig. 131).

4. Posterior expansion of frontal sinus: Presence of frontal sinuses in the frontal bone in living canids has long been used in classification (Huxley, 1880). In separate studies, we have demonstrated the usefulness of this feature in the phylogenetic analyses of hesperocyonines and living canines (Wang, 1994; Tedford et al., 1995). In borophagines the frontal sinus has achieved its most extensive development, culminating in advanced species of *Borophagus* in which the sinus extends to the back of the skull over the top of the entire braincase. We have dissected the frontal areas in many key taxa, but exhaustive observation is clearly not possible. As a general guide, a flat forehead and the presence of a small depression above the postorbital process can be taken as indication of lack of a frontal sinus. The extent of the sinus can often be accurately judged by the outline of the inflation of the frontals and parietals on the exterior of the skull.

Polarity: 0, no frontal sinus; 1, small frontal sinus that does not invade the postorbital process and does not extend beyond the postorbital constriction; 2, frontal sinus invades the postorbital process and expands posteriorly to the frontal–parietal suture; 3, frontal sinus extends posteriorly beyond the frontal–parietal suture; 4, frontal sinus penetrates far back beyond the frontal–parietal suture over the top of the entire braincase (fig. 131).

5. Dorsal inflation of frontal sinus: Beginning in *Paratomarctus*, the frontal is dorsally inflated to form a small dome above the orbit. The forehead is prominently domed in the *Borophagus* clade. Although doming of the forehead is mostly caused by enlargement of the underlying frontal sinus, it is here viewed as a different process from the horizontal development of frontal sinus described above (character 4). The dome is the result of dorsal expansion of the sinuses, whereas character 4 above mainly describes the posterior expansion of the sinuses. As seen in the character distribution table (table 2), these two characters do not always coevolve.

Polarity: 0, flat forehead without dorsal inflation of frontal sinus; 1, a small dome on forehead due to underlying inflation of frontal sinus; 2, prominently domed forehead (fig. 132).

6. Masseteric scar on zygomatic arch: The long horizontal scar on the anterior portion of the zygomatic arch is the place of origin for the masseteric muscle. This scar is primitively deep and commonly occupies more than half of the lateral surface of the arch. The derived condition in certain brachycephalic taxa is a narrowed scar that is restricted mostly to the narrow ventral face of the arch, and in lateral view is no more than one-third of the total breath of the arch.

Polarity: 0, masseteric scar wide; 1, masseteric scar narrowed (fig. 132).

7. Lateral flare of zygomatic arch: Primitively in small borophagines, there is a flat facet on the dorsal face of the anterior zygomatic arch just below the orbit. This facet is flared laterally. Beginning in *Cormocyon copei*, this facet is replaced by a rounded dorsal surface of the arch and the lateral flare is absent.

Polarity: 0, lateral flare of zygoma present; 1, flare absent (fig. 131).

8. Zygomatic arch wide posteriorly: In dorsal view, the zygomatic arch primitively forms a gentle curve with its widest point somewhere near the middle of the arch. In *Aelurodon*, however, the widest point is shifted posteriorly toward the level of the postglenoid fossa. Thus, there tends to be a sharp angle at this point, and the outline of the zygomatic arch becomes angled rather than arched.

Polarity: 0, zygomatic arch gently curved laterally; 1, zygomatic arch widened near posterior end (fig. 131).

9. Temporal crest: A single sagittal crest

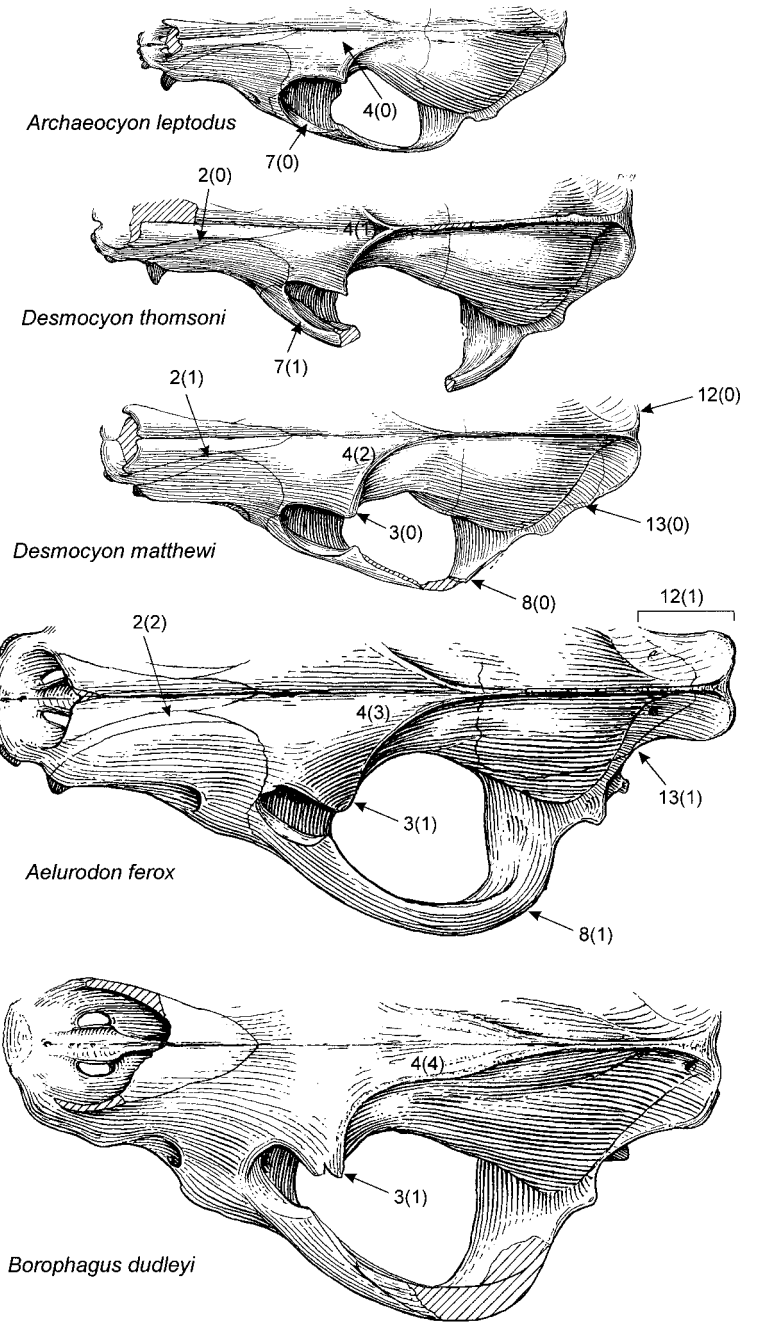

Fig. 131. Comparative dorsal views of skulls of representative borophagines showing the extent of frontal sinuses (shaded areas, character number 4) and other cranial characteristics used in the phylogenetic analysis. Selected taxa include (from top down) *Archaeocyon leptodus* (F:AM 49448), *Desmocyon thomsoni* (AMNH 12874), *Desmocyon matthewi* (F:AM 49177), *Aelurodon ferox* (UNSM 1093), and *Borophagus dudleyi* (MCZ 3688). Character numbers and state numbers (in parentheses) correspond to those listed in the character analysis and data matrix. The skulls are not drawn to the same scale.

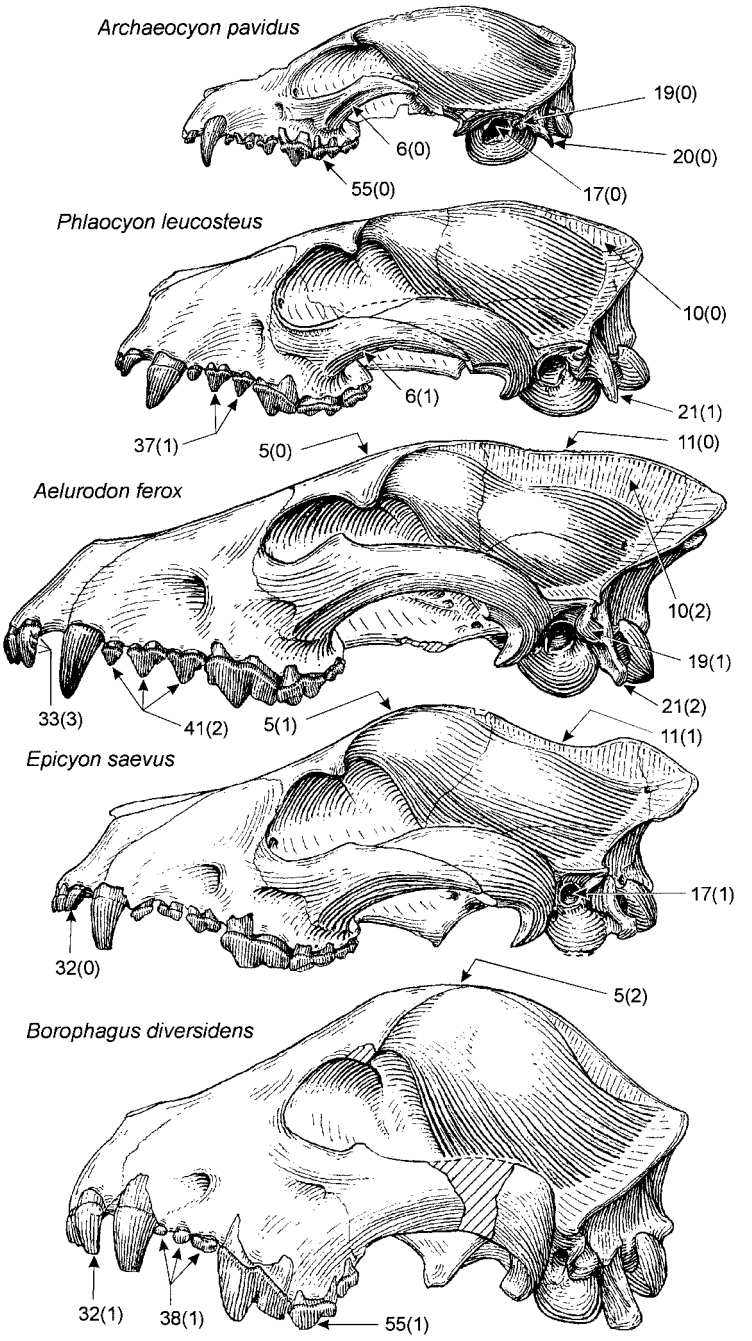

Fig. 132. Comparative lateral views of skulls of representative borophagines showing cranial and dental characteristics used in the phylogenetic analysis. Selected taxa include (from top down) *Archaeocyon pavidus* (F:AM 63970), *Phlaocyon leucosteus* (AMNH 8768), *Aelurodon ferox* (UNSM 1093), *Epicyon saevus* (AMNH 8305), and *Borophagus diversidens* (MSU 8034). Character numbers and state numbers (in parentheses) correspond to those listed in the character analysis and data matrix. The skulls are not drawn to the same scale.

formed by merging of the temporal crests behind the postorbital process is clearly the primitive condition, although separated crests can be a juvenile condition. *Otarocyon* not only possess the double-crested condition in the adult but further strengthens and raises the crests to enclose a shallow valley on top of the skull.

Polarity: 0, single-crested; 1, double-crested, often lyrate, in adults but with little or no reinforcement of the crests; 2, strong, widely separated, and parallel temporal crests enclosing a longitudinal valley (figs. 16, 17).

10. Height of sagittal crest: The height of the sagittal crest varies with sex and age—males and older individuals tend to have higher crests. In *Aelurodon*, the sagittal crest is prominently heightened and can be as tall as 20 mm. This enlarged crest clearly exceeds normal intraspecific variation and is in contrast to lower crests in *Epicyon*.

Polarity: 0, sagittal crest low; 1, sagittal crest high; 2, sagittal crest very high (fig. 132).

11. Sagittal crest profile: In *Epicyon*, the lateral profile of the sagittal crest is concave rather than the primitively dorsally arched or straight profile.

Polarity: 0, sagittal crest dorsally arched or straight; 1, sagittal crest concave (fig. 132).

12. Nuchal crest expansion: Primitively, the nuchal crest is a low ridge with a fan-shaped profile in posterior view. Posterior extension of the nuchal crest is a derived condition most extremely developed in *Aelurodon*. The extended crest often overhangs the occipital condyle.

Polarity: 0, nuchal crest not expanded; 1, nuchal crest extended posteriorly beyond occipital condyle (fig. 131).

13. Lambdoidal crest narrowing: Some species in the Aelurodontina clade have a laterally constricted lambdoidal crest in which the nuchal portion of the crest is narrowed to a rectangular plate.

Polarity: 0, lambdoidal crest not constricted; 1, lambdoidal crest laterally constricted (fig. 131).

14. Palate width: The palate is primitively narrow. A broadened muzzle and widened palate is characterized by some hypercarnivorous taxa, such as *Euoplocyon*, the Aelurodontina clade, and some members of the Borophagina. Measurements of maximum palatal width between the P4s and P1s are listed in appendix II (PWP4 and PWP1), and their relative proportions among related taxa are best compared in the ratio diagrams.

Polarity: 0, palate unwidened; 1, palate moderately widened; 2, palate further widened; 3, palate extremely widened such that it is wider than it is long.

15. Bulla size: In canids, inflation of the bulla is commonly achieved through expansion of the caudal entotympanic. To increase volume, the bulla often inflates anteriorly beyond the posterior border of the postglenoid fossa, or posteriorly toward the paroccipital process. In more extreme cases, such as in *Otarocyon*, the bulla also expands toward the midline of skull such that the interbullar space is narrowed and the partial septum at the ecto- and entotympanic suture is obliterated. The bullar lengths (LB) in appendix II provide a measure of the bulla size, and their proportions relative to other cranial dimensions are illustrated in the ratio diagrams.

Polarity: 0, bulla not inflated; 1, bulla hypertrophied (figs. 17, 18).

16. Ectotympanic ring: Primitively, the ectotympanic forms a half ring and the external auditory meatus is composed of the ectotympanic in the ventral half and the squamosal in the dorsal half. Beginning in *Desmocyon thomsoni*, the ectotympanic forms a full circle superimposed on the squamosal shelf.

Polarity: 0, ectotympanic ring incomplete; 1, ectotympanic forming a full ring.

17. Opening of auditory meatus: The opening of the external auditory meatus is large primitively, sometimes with a V-shaped notch pointing anteroventrally. The opening in *Cynarctus* and many advanced borophagines is small relative to the bulla size.

Polarity: 0, external auditory meatus with large opening; 1, small opening of the external auditory meatus (fig. 132).

18. Auditory meatus tube: In general, canids lack or have shorter external auditory meatal tubes than found in arctoids. The formation of a short tube is subject to ontogenetic and intraspecific variation and its elongation is almost a continuous trend in certain clades. Despite the imprecision of its definition, such a character provides a useful de-

scription of the morphological transformation.

Polarity: 0, absence of a tubular auditory meatus; 1, presence of a short tube for auditory meatus; 2, auditory meatus tube elongated.

19. Mastoid process: From a small, knoblike process in the primitive condition, the mastoid process is ventrally elongated and bears a thin lateral ridge in *Aelurodon*. In *Epicyon aelurodontoides*, the mastoid has an expanded ventral facet that protrudes posteriorly.

Polarity: 0, mastoid process not enlarged; 1, mastoid process ventrally elongated and with a thin lateral ridge; 2, mastoid process with enlarged ventral facet (fig. 132).

20. Paroccipital process orientation: Primitively, the paroccipital process is oriented posteriorly and is free from contact with the bulla. In most derived canids, the process rotates ventrally to point downward, bringing its base or its entire length into contact with the posterior face of the bulla.

Polarity: 0, paroccipital process posteriorly oriented; 1, paroccipital process ventrally oriented (fig. 132).

21. Paroccipital process shape: Primitively the paroccipital process has a triangular or rodlike cross section, and this is true even when it is ventrally directed and fused with the bulla. From this primitive condition, the process may be flattened to closely hug the bulla, whereas in other instances, especially in hypercarnivorous taxa, the process is elongated to expose a long free tip extending beyond the part that is fused with the bulla.

Polarity: 0, paroccipital process rodlike; 1, paroccipital process platelike, hugging bulla, and possibly with short free tip; 2, paroccipital process with elongated free tip.

22. Suprameatal fossa: Presence of a shallow suprameatal fossa in *Hesperocyon* is a primitive condition in canids and Caniformia in general (Wang and Tedford, 1994). This fossa is lost in most canids. Enlargement of this fossa was formerly thought to be restricted to procyonids (Riggs, 1942, 1945; Segall, 1943; Hough, 1944, 1948), but recently it has been demonstrated to occur in a wider array of arctoids (Schmidt-Kittler, 1981; Wolsan, 1993). Presence of a large suprameatal fossa in *Otarocyon* illustrates that canids, too, can have an enlarged fossa, further demonstrating the homoplastic nature of this trait in caniform carnivorans.

Polarity: 0, suprameatal fossa shallow or absent; 1, fossa enlarged.

MANDIBLE

23. Horizontal ramus of mandible: Primitively, the mandibular ramus is moderately deep without significant anterior tapering as in most hesperocyonines and borophagines, in contrast to the slender, anteriorly tapering ramus of canines. A shallow, slender mandible also occurs in *Cynarctoides* and in some species of *Paracynarctus* and *Cynarctus*.

Polarity: 0, horizontal ramus deep and strong; 1, ramus shallow and slender (fig. 133).

24. Symphyseal flange on ramus: An extensive ossification of the symphyseal joint may result in a weak symphyseal flange on the anteroventral border of the ramus in some highly derived borophagines.

Polarity: 0, ramus without a flange; 1, ramus with a symphyseal flange (fig. 133).

25. Height of masseteric fossa: The lower border of the masseteric fossa is primitively near the lower border of the ramus. In advanced species of *Cynarctus*, however, the lower border of the masseteric fossa is elevated and further separated from the lower border of the ramus.

Polarity: 0, masseteric fossa low; 1, masseteric fossa high (fig. 133).

26. Anterior excavation of masseteric fossa: Advanced Borophagina sometimes have a deep masseteric fossa that expands anteriorly and results in a deep excavation of the anterior border of the fossa.

Polarity: 0, masseteric fossa not excavated; 1, masseteric fossa excavated anteriorly (fig. 133).

27. Subangular lobe: Canids primitively lack a subangular lobe. Presence of this lobe in some hypocarnivorous borophagine clades is derived. The subangular lobe in the borophagines is generally smaller than those in some canines.

Polarity: 0, subangular lobe absent or weak; 1, subangular lobe present (fig. 133).

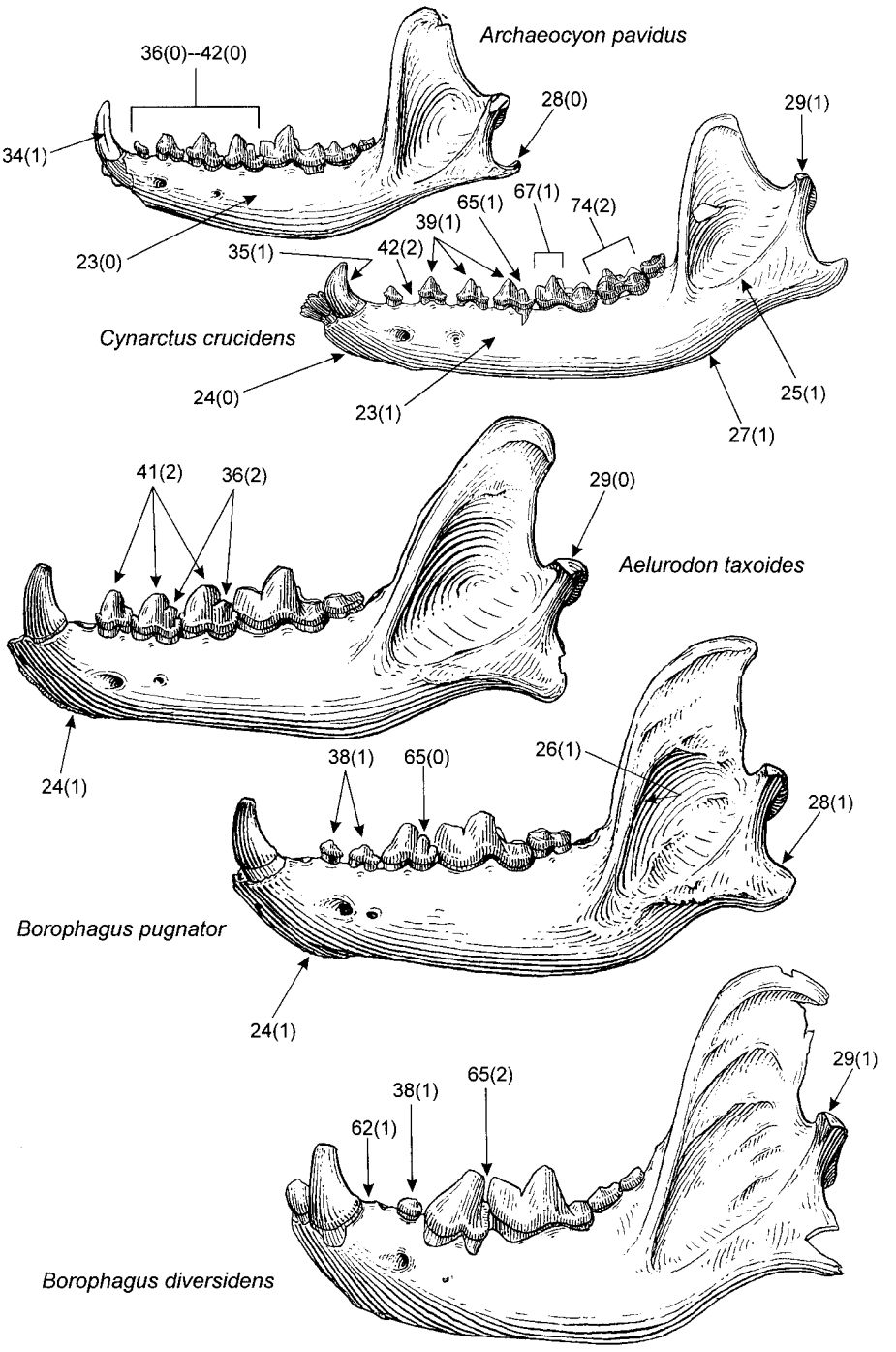

Fig. 133. Comparative lateral views of mandibles of representative borophagines showing ramal and dental characteristics used in the phylogenetic analysis. Selected taxa include (from top down) *Archaeocyon pavidus* (F:AM 63222), *Cynarctus crucidens* (F:AM 49172), *Aelurodon taxoides* (F:AM 61781), *Borophagus pugnator* (F:AM 61662), and *Borophagus diversidens* (MSU 8034). Character numbers and state numbers (in parentheses) correspond to those listed in the character analysis and data matrix. The mandibles are not drawn to the same scale.

28. Angular process: Angular processes in borophagines generally have a broad shelf on the medial side but do not show much variation from this basic pattern, as compared to the more diverse morphology in canines and hesperocyonines. There is a deepening of the process in the *Borophagus* clade compared to a relatively shallow process in most borophagines.

Polarity: 0, angular process shallow; 1, angular process deep (fig. 133).

29. Mandibular condyle: Primitively, the mandibular condyle is near the same level as the lower toothrow and is elevated above the toothrow in the cynarctine clade and *Borophagus diversidens*.

Polarity: 0, mandibular condyle low; 1, mandibular condyle elevated above toothrow (fig. 133).

DENTITION

30. Bladelike cheekteeth: Sharp, bladelike cheekteeth, especially for anterior and posterior edges of the premolars, is an autapomorphy for *Psalidocyon*, as opposed to more blunt cheekteeth in the primitive condition.

Polarity: 0, cheekteeth not bladelike; 1, cheekteeth bladelike (fig. 134).

31. Incisor row: The upper incisor row primitively forms a curved, outwardly protruding outline. In advanced *Aelurodon*, the incisor row forms a straight transverse line.

Polarity: 0, incisor row curved; 1, incisor row straight.

32. I3 size: Primitively, the I3 is approximately the same size as the I1 or I2, or only slightly larger. Enlargement of the I3 is a derived feature occurring in some lineages of hypo- and hypercarnivorous borophagines.

Polarity: 0, I3 not enlarged; 1, I3 enlarged relative to I1–I2; 2, I3 greatly enlarged (figs. 132, 134).

33. I3 lateral cusp: Complex lateral accessory cusplets on the I3 is an easily recognizable characteristic of many borophagine canids. This is especially true for the Aelurodontina clade, which trends toward a steady increase in the complexity of the I3. Beginning in *Epicyon*, and later in *Borophagus*, this trend is reversed toward decreasing the number of lateral cusplets.

Polarity: 0, I3 without lateral cusplet; 1, I3 with one lateral cusplet; 2, I3 with two lateral cusplets; 3, I3 with three lateral cusplets (figs. 132, 134).

34. c1 lateral groove: Presence of a lateral groove along much of the lateral side of the lower canine is a derived feature in *Archaeocyon* and two species of *Phlaocyon*.

Polarity: 0, c1 without lateral groove; 1, c1 with a lateral groove (fig. 133).

35. Recurved c1: A short and markedly recurved lower canine is a synapomorphy of *Cynarctus*, as compared to relatively straight canines in most other canids.

Polarity: 0, c1 not recurved; 1, c1 recurved (fig. 133).

36. reduction or enlargement of premolar cusplets: A posterior accessory cusp and anterior and/or posterior cingular cusps in the upper and lower premolars (especially the posterior ones, i.e., P3, p3–p4) are present in most primitive canids. Reduction and loss of these cusplets occur frequently in canines and in several borophagine lineages. On the other hand, the premolar cusplets in some hypercarnivorous lineages become more distinct.

Polarity: 0, premolar cusplets moderately developed; 1, cusplets reduced or lost; 2, cusplets enlarged (figs. 133, 136).

37. Premolars high-crowned: Disproportionally high-crowned premolars characterize two advanced species of *Phlaocyon*.

Polarity: 0, premolars normal crown height; 1, premolars high-crowned (figs. 132, 133).

38. Anterior premolars low-crowned: Starting in *Epicyon*, and especially in *Borophagus*, the anterior premolars become progressively lower-crowned compared to the crown height of P4 and p4.

Polarity: 0, anterior premolars normal crown height; 1, anterior premolars low-crowned (figs. 132, 133).

39. Premolars shortened: Premolars are shortened in several meso- and hypocarnivorous lineages, such as *Otarocyon*, *Phlaocyon*, *Cynarctus*, and *Paratomarctus*.

Polarity: 0, premolars unshortened; 1, premolars shortened (figs. 133, 136).

40. Premolars slender: One of the prominent characters of the Caninae is long, slender premolars with weak or no accessory

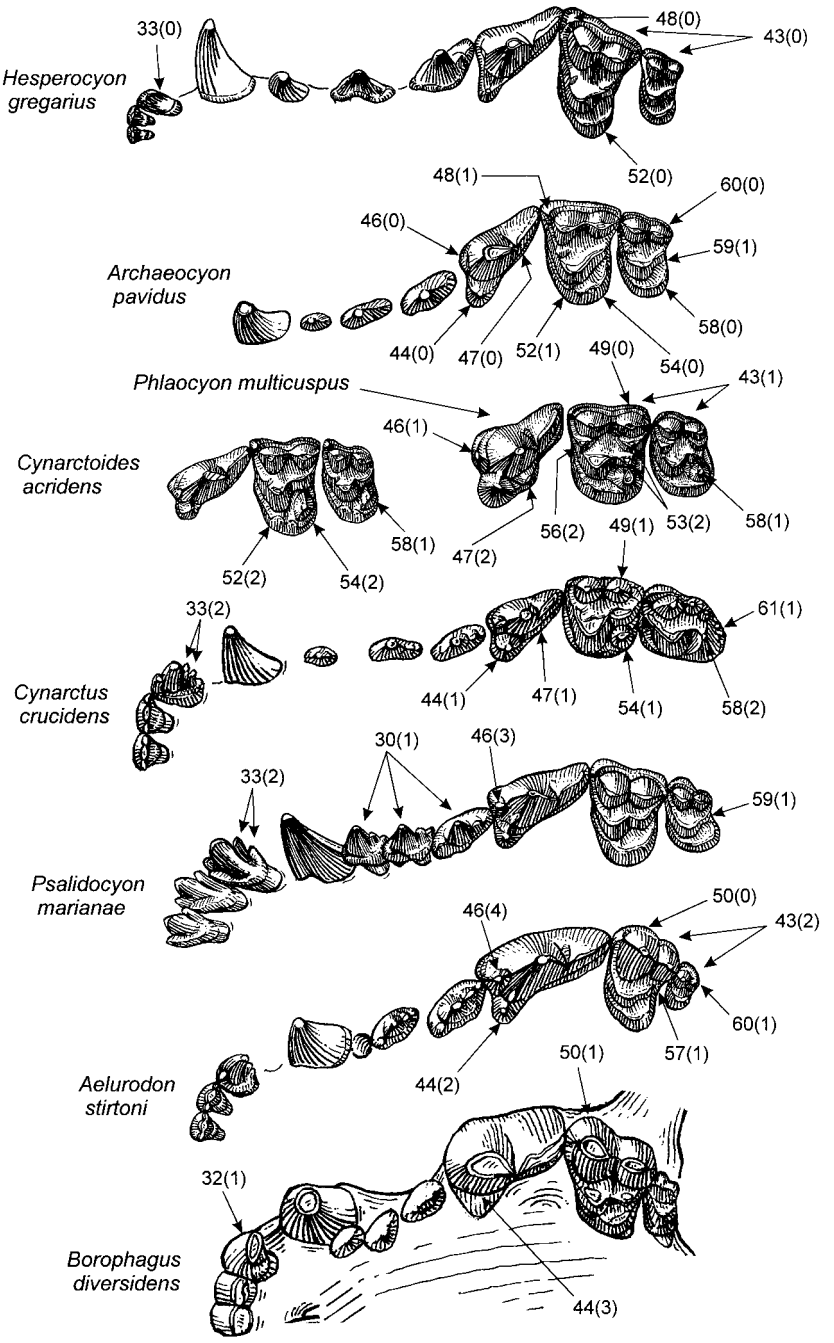

Fig. 134. Comparative occlusal views of upper teeth of representative borophagines and *Hesperocyon* (as outgroup) showing dental characteristics used in the phylogenetic analysis. Selected borophagine taxa include (from top down) *Archaeocyon pavidus* (F:AM 63222), *Cynarctoides acridens* (F:AM 99360), *Phlaocyon multicuspus* (FMNH UC1482), *Cynarctus crucidens* (F:AM 49172), *Psalidocyon marianae* (F:AM 27397), *Aelurodon stirtoni* (UNSM 25789), and *Borophagus diversidens* (MSU 8034). Character numbers and state numbers (in parentheses) correspond to those listed in the character analysis and data matrix. The cheekteeth are not drawn to the same scale.

cusps. Slender premolars, however, also occur in advanced species of *Cynarctoides*.

Polarity: 0, premolars not slender; 1, premolars slender.

41. Premolars massive: In the aelurodontine clade and two hypercarnivorous species of *Phlaocyon*, the premolars are enlarged relative to the molars. This enlargement is uniform throughout the premolar series, in contrast to the differently enlarged p4 compared with the other premolars in *Epicyon* through *Borophagus*. The latter feature is here considered a different character (character 63 below).

Polarity: 0, premolar not enlarged; 1, premolar moderately enlarged; 2, premolars massive (figs. 132, 133, 136).

42. Premolar diastema: In an unelongated skull in the primitive condition of the canids, there is usually a very short or no diastemata between premolars. Elongation of premolar diastemata is a synapomorphy for the Caninae, but also occurs in the Cynarctina clade as a result of shortening of the premolars and lengthening of the lower jaws.

Polarity: 0, no diastemata between premolars; 1, long diastemata; 2, further lengthening of diastemata (fig. 133).

43. Relative size of P4 vs. M1–M2: Hypocarnivorous taxa tend to have large molars for increased grinding area, whereas hypercarnivorous taxa tend to reduce the molars and emphasize the shearing part of the dentition. Both these trends are derived conditions compared to the primitive mesocarnivorous condition.

Polarity: 0, normally proportioned P4 and upper molars; 1, upper molars enlarged relative to P4; 2, upper molars reduced relative to P4 (fig. 134).

44. P4 protocone size: Enlargement of the P4 protocone is adopted by some hypocarnivorous taxa to increase the grinding area of the cheekteeth. Such enlargement may also be associated with a widening of the lingual cingulum or development of a hypocone (character 48). On the other hand, reduction of the P4 protocone is commonly associated with hypercarnivory in the Borophagina clade.

Polarity: 0, P4 protocone not enlarged; 1, protocone enlarged; 2, protocone reduced; 3, protocone further reduced to a mere bulge or an indistinct ridge (fig. 134).

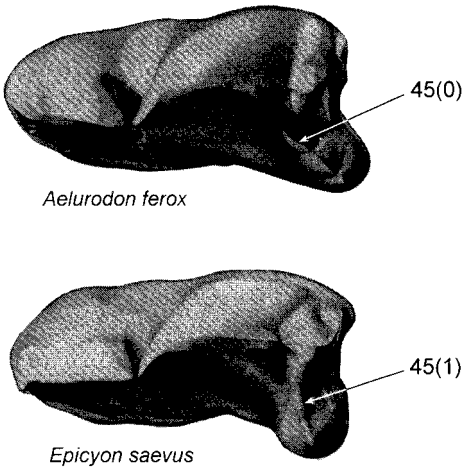

Fig. 135. Occlusal views of upper P4s of *Aelurodon ferox* (USNM 523, holotype) and *Epicyon saevus* (UF 24524) showing the connecting ridge (and lack of it) between the protocone and parastyle. The character number and states (in parentheses) correspond to those listed in the character analysis and data matrix. Illustration adopted from Baskin (1980: fig. 1).

45. P4 protocone and parastyle connection: Baskin (1980) pointed out the connection of these two cusps by a ridge in *Epicyon*, as opposed to the lack of such connection in *Aelurodon*, is a feature with consistent utility in the systematics of large ''*Aelurodon*-like'' taxa. However, he did not determine the polarity of this character. As shown in transitional individuals of *Epicyon*, this ridge primitively leads from the protocone to the apex of paracone in most primitive borophagines. The derived condition is thus a lateral shift of this ridge toward the parastyle.

Polarity: 0, protocone not connected to parastyle by a ridge; 1, protocone connected to parastyle (fig. 135).

46. P4 parastyle: Throughout the history of the borophagines, there are lineages that develop and enlarge their P4 parastyles in different ways. In some *Phlaocyon* and in *Cynarctus crucidens*, the P4 parastyle is simply an enlarged and elevated anterior cingulum. In most borophagines, however, the homology of the P4 parastyle is unclear. It may be a matter of definition whether the parastyle was derived by budding from the lon-

gitudinal ridge on the anterior face of paracone (i.e., development of a notch along the anterior ridge) or from elevating the anterior cingulum along the anterior face of paracone. In favor of the former scenario is the fact that development of a discrete parastyle is often preceded by an enlargement of the anterior ridge on the paracone apart from the anterior cingulum. On the other hand, most parastyles (except some in advanced species of *Aelurodon*) have a distinctly triangular outline in anterior view with the lateral edges converging to the apex of the parastyle, with the base of this triangle (in top-down view) being the anterior cingulum. This latter construction of the parastyle leaves a distinct impression of an elevated cingulum. Since the parastyle is almost always situated at the juncture of the anterior cingulum and anterior ridge of the paracone, it is sometimes difficult to distinguish between the above scenarios. In practice, we assume a transformation series following the first scenario. Furthermore, the size of the parastyle undergoes a reversal in advanced species of *Borophagus*.

Polarity: 0, no P4 parastyle on the anterior cingulum; 1, parastyle originating from the anterior cingulum separate from the anterior ridge of paracone; 2, strong ridge on anterior face of paracone; 3, a distinct parastyle as delineated by a notch on the anterior ridge of paracone; 4, parastyle prominently enlarged (fig. 134).

47. P4 lingual cingulum or hypocone: The P4 hypocones in hypocarnivorous borophagines are derived through progressive enlargement of the internal cingulum behind the protocone. The entire spectrum of intermediate stages can often be observed.

Polarity: 0, P4 internal cingulum week or absent; 1, cingulum thickened; 2, cingulum raised to become a hypocone (fig. 134).

48. M1 parastyle: A strong M1 parastyle is present in most miacids. Although much reduced in hesperocyonines, the parastyle is further reduced in all borophagines and canines, which serves as one of the key synapomorphies for a sister relationship of the two clades.

Polarity: 0, M1 parastyle moderately large; 1, parastyle extremely reduced (fig. 134).

49. M1 labial cingulum at metacone: A labial cingulum lateral to the M1 metacone is primitively present in most borophagines. In advanced species of *Cynarctus*, however, this cingulum, especially the segment lateral to the metacone, is reduced or lost. The labial cingulum is also lost in advanced species of *Borophagus*, which, however, is the result of continued reduction of the labial cingulum beginning anteriorly (paracone).

Polarity: 0, M1 labial cingulum present at metacone; 1, cingulum absent lateral to the metacone (fig. 134).

50. M1 labial cingulum at paracone: Primitively, all borophagines have a well-developed cingulum lateral to the M1 paracone. Reduction or loss of this segment of the cingulum occurs in the most hypercarnivorous borophagines in the *Epicyon–Borophagus* clade.

Polarity: 0, M1 labial cingulum present at paracone; 1, cingulum absent lateral to the paracone (fig. 134).

51. M1 shape: Miacids and hesperocyonine canids have a transversely elongated M1 with an asymmetrical labial border because of a large parastyle (vs. a much smaller metastyle) and posterolingually enlarged internal cingulum. Beginning with *Rhizocyon*, borophagines have acquired a more quadrate appearance of the M1 by reduction of the parastyle and enlargement of the metacone, as well as anterior expansion of the internal cingulum around the protocone. In the *Cynarctus* clade, on the other hand, the outline of the M1 is anteroposteriorly elongated to occlude with an enlarged m1 talonid.

Polarity: 0, M1 short but transversely wide; 1, M1 subquadrate; 2, M1 longitudinally elongated.

52. M1 lingual cingulum: Most hesperocyonines have the lingual cingulum (sometimes produced as a hypocone) well developed at the posterolingual corner of M1 but poorly developed anteriorly. In the primitive condition (as seen in *Hesperocyon*), the cingulum does not surround the protocone. In borophagines and canines the cingulum is extended anteriorly to fully surround the protocone, resulting in a more symmetrical appearance of the tooth. In *Paracynarctus*, advanced species of *Cynarctoides*, and *Carpocyon*, the anterior segment of the cingulum is further thickened, sometimes forming a small cingular cusp distinct from hypocone.

In the hypercarnivorous taxa, however, such as in the *Aelurodon* clade, the lingual cingulum is restricted to the posterolingual corner of the tooth, a reversal to the hesperocyonine condition.

Polarity: 0, M1 lingual cingulum posteriorly positioned and not surrounding protocone; 1, M1 lingual cingulum anteriorly extended to surround protocone; 2, anteriorly thickened lingual cingulum of M1 (fig. 134).

53. M1 metaconule: Primitively, the M1 metaconule is little more than a slight bulge near the lateral end of the postprotocrista. An enlarged metaconule in many meso- and hypocarnivorous taxa is a derived state. In the *Phlaocyon multicuspus–achoros* clade, the metaconule is further enlarged and split into two small cusps.

Polarity: 0, M1 metaconule weak or absent; 1, M1 metaconule large; 2, M1 metaconule split into two cusps (fig. 134).

54. M1 hypocone: Most canids lack a conate hypocone on the lingual cingulum of the M1. The primitive condition is a broad lingual cingulum. A conate hypocone, usually differentiated from the lingual cingulum by a weak notch anteriorly, is independently developed in some hypocarnivorous clades. In advanced species of *Cynarctoides*, the hypocone is further surrounded by a narrow cingulum on the lingual side.

Polarity: 0, conical M1 hypocone absent; 1, conical M1 hypocone present; 2, M1 conical hypocone surrounded by cingulum (fig. 134).

55. M1 paracone: Primitively, the M1 paracone is of approximately the same height and size as the metacone. In hypercarnivorous clades, the paracone is much higher and larger than the metacone, acting as a shearing facet against the hypoconid of m1.

Polarity: 0, M1 paracone low-crowned and subequal to metacone; 1, M1 paracone higher-crowned and markedly larger than metacone (fig. 132).

56. M1 paraconule: Most borophagines have very weak or no paraconule on M1. *Phlaocyon multicuspus* and *P. achoros*, however, share a distinct paraconule on M1.

Polarity: 0, M1 paraconule absent or weakly developed; 1, M1 paraconule enlarged (fig. 134).

57. M1 posterior border: Most borophagines have a gently curved posterior border of the M1. In *Aelurodon stirtoni*, the M1 is sharply concave due to posterior extension of the lingual cingulum.

Polarity: 0, M1 posterior border slightly curved; 1, M1 posterior border sharply concave (fig. 134).

58. M2 hypocone: As in the case of M1, there is no conate hypocone in M2s of most canids, but a broad lingual cingulum in its place. Some hypocarnivorous taxa, however, tend to develop a distinct, conical hypocone, and in extreme cases, such as advanced species of *Cynarctus*, the hypocones are further enlarged and posteriorly expanded.

Polarity: 0, conical M2 hypocone absent; 1, M2 conical hypocone present; M2 hypocone enlarged and posteriorly expanded (fig. 134).

59. M2 metaconule and cingulum: Primitively the M2 metaconule and lingual cingulum are separated by a valley. Most borophagines are derived in that a ridge connects the metaconule and cingulum.

Polarity: 0, M2 metaconule and internal cingulum not connected; 1, M2 metaconule and internal cingulum connected by a ridge (fig. 134).

60. M2 metacone: In most borophagines, a small metacone is present on the M2s. This cusp is extremely reduced or lost in the *Aelurodon mcgrewi–stirtoni* clade.

Polarity: 0, M2 metacone present; 1, M2 metacone very reduced or absent (fig. 134).

61. M2 posterior cingulum: A posterior cingulum on M2 is usually absent or weak in borophagines. This cingulum becomes strong in some hypercarnivorous clades.

Polarity: 0, M2 posterior cingulum absent or weakly developed; 1, M2 posterior cingulum well developed (fig. 97K).

62. Reduction of p1: A small p1 is primitively present in most canids. This tooth is lost in some hypercarnivorous forms due to shortening of the ramus and crowding of cheekteeth.

Polarity: 0, p1 present; 1, p1 absent (figs. 133, 136).

63. p4 size relative to p3: The p4s in most borophagines are the largest of premolars along a gradual gradient from p1 backward. Differential enlargement of the p4 relative to p1–p3 occurs in the *Epicyon–Borophagus*

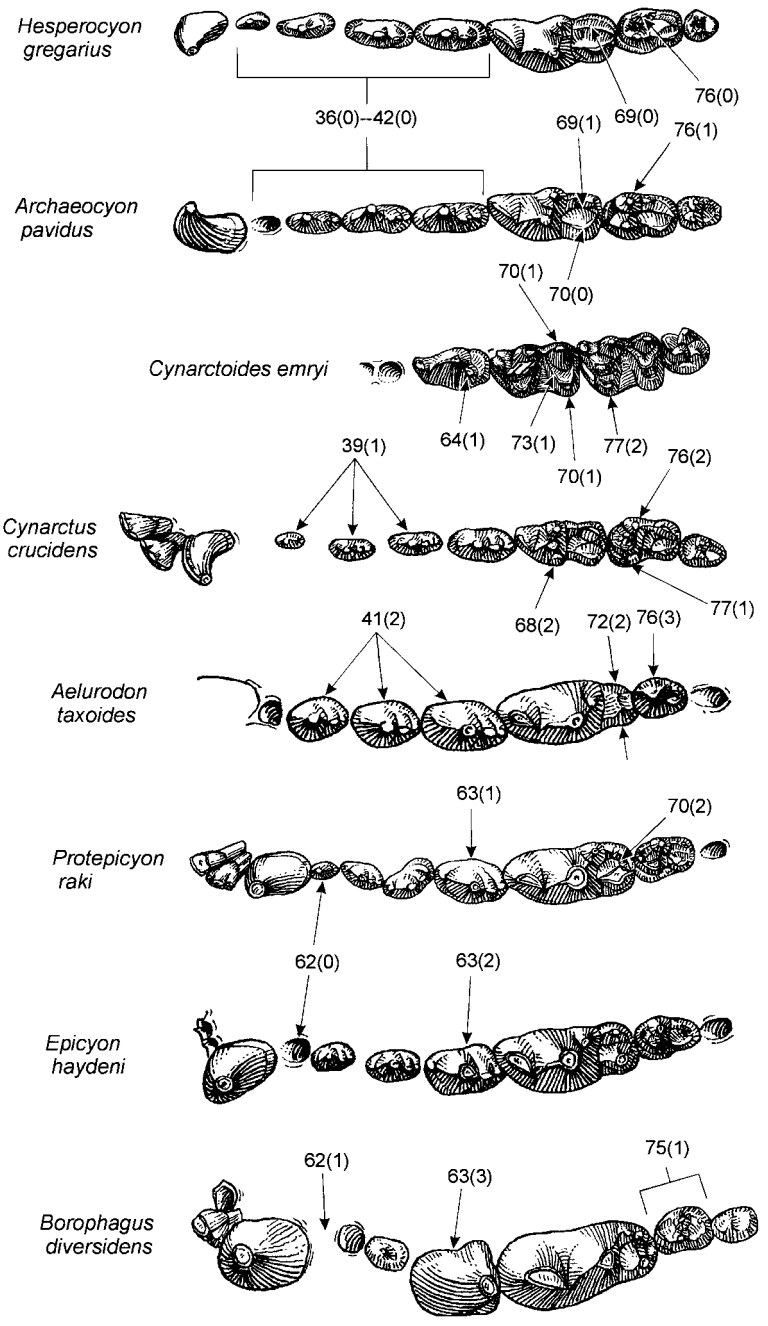

Fig. 136. Comparative occlusal views of the lower teeth of representative borophagines and *Hesperocyon* (as outgroup) showing dental characteristics used in the phylogenetic analysis. Selected borophagine taxa include (from top down) *Archaeocyon pavidus* (F:AM 63970), *Cynarctoides emryi* (UNSM 81-7-8-37), *Cynarctus crucidens* (F:AM 49172), *Aelurodon taxoides* (F:AM 25111), *Protepicyon raki* (F:AM 61738), *Epicyon haydeni* (F:AM 61453), and *Borophagus diversidens* (MSU 8034). Character numbers and state numbers (in parentheses) correspond to those listed in the character analysis and data matrix. The cheekteeth are not drawn to the same scale.

clade, and is developed to the extreme in advanced species of *Borophagus*.

Polarity: 0, p4 not disproportionally enlarged relative to p3; 1, p4 enlarged relative to p3; 2, p4 further widened to nearly the width of m1; 3, p4 wider than m1 (fig. 136).

64. p4 posterior accessory cusp position: Borophagines primitively have a p4 posterior accessory cusp that lies along the midline. From this morphotypical condition, the accessory cusp is shifted laterally in advanced species of *Cynarctoides*.

Polarity: 0, p4 posterior accessory cusp located along midline of tooth; 1, p4 accessory cusp shifted laterally (fig. 136).

65. p4 posterior accessory cusp size: A moderate-size p4 posterior accessory cusp is present in all primitive borophagines. The p4 (but not more anterior premolars) accessory cusp becomes enlarged in most species of *Cynarctus*. On the other hand, this cusp is completely lost in *Borophagus diversidens* due to the reclined principal cusp.

Polarity: 0, moderate-size posterior accessory cusp; 1, p4 accessory cusp enlarged; 2, p4 accessory cusp lost (fig. 133).

66. m1 trigonid elongation: The m1 trigonids in basal borophagines are short and the shearing facets are oriented obliquely. Independently in the Caninae, *Archaeocyon leptodus*, and in *Cormocyon* and more derived borophagine taxa, the trigonid is elongated and the paraconid blade is more open (longitudinally oriented).

Polarity: 0, m1 trigonid short; 1, m1 trigonid elongated and open.

67. m1 trigonid shortening: Shortening of the m1 trigonid occurs in some hypocarnivorous clades as the functional emphasis is shifted from shearing to grinding.

Polarity: 0, m1 trigonid not shortened; 1, m1 trigonid shortened (fig. 133).

68. m1 protostylid: Presence of a small protostylid on m1 is a derived state in contrast to the lack of this cusp in most borophagines. In the more hypocarnivorous species within the *Cynarctoides* and *Cynarctus* clades, the protostylid becomes strong and isolated from the protoconid.

Polarity: 0, m1 protostylid absent or presence of a weak ridge; 1, m1 protostylid small; 2, m1 protostylid large and isolated from protoconid (fig. 136).

69. m1 talonid basin: Primitively in most hesperocyonines and basal cynoids, the talonid of m1 is trenchant, dominated by a high hypoconid, and the entoconid, if present, is a low crest or a narrow shelf far lower than the hypoconid. As one of the fundamental synapomorphies for the Borophaginae–Caninae clade, the entoconid ridge begins to rise and enlarge to nearly the same height as the hypoconid enclosing the talonid basin. This initial trend toward mesocarnivory is further developed in more derived borophagines and canines. The basined talonid, however, is also subject to reversals in hypercarnivorous taxa, such as in *Euoplocyon* and, to a lesser extent, in *Aelurodon* in the Borophaginae, and in *Speothos* and *Cuon–Lycaon* clades of the living Caninae.

Polarity: 0, m1 talonid trenchant; 1, m1 talonid basined (fig. 136).

70. m1 talonid cusp shape: The talonid cusps, the hypoconid and entoconid, are primitively crestlike in borophagines. These cusps progressively become more conate in more derived forms. The next step is the formation of a transverse cristid between these two cusps, closing off the talonid basin posteriorly. This transformation is independently developed in different clades.

Polarity: 0, m1 talonid cusps crestlike; 1, talonid cusps conical; 2, talonid cusps with transverse cristid (figs. 136, 137).

71. m1 entoconid: Primitively, the entoconid, sometimes split into an entoconulid anteriorly, extends forward to connect with the posterior face of the metaconid. A deep notch at the anterior end of the entoconid, resulting in a lingually opened talonid, is characteristic of *Oxetocyon* and *Otarocyon*. In some extreme forms within hypocarnivorous clades, on the other hand, the entoconulid is enlarged to superficially resemble a metastylid.

Polarity: 0, m1 entoconid crestlike or connected to a small entoconulid anteriorly; 1, m1 entoconid deeply notched anteriorly; 2, elevated entoconulid (fig. 137).

72. m1 talonid width: The talonids of most borophagines are subequal in width to the trigonid. Widening of the talonid relative to the trigonid is a hypocarnivorous adaptation to enlarge the grinding area. Conversely, a narrow talonid and reduction of the ento-

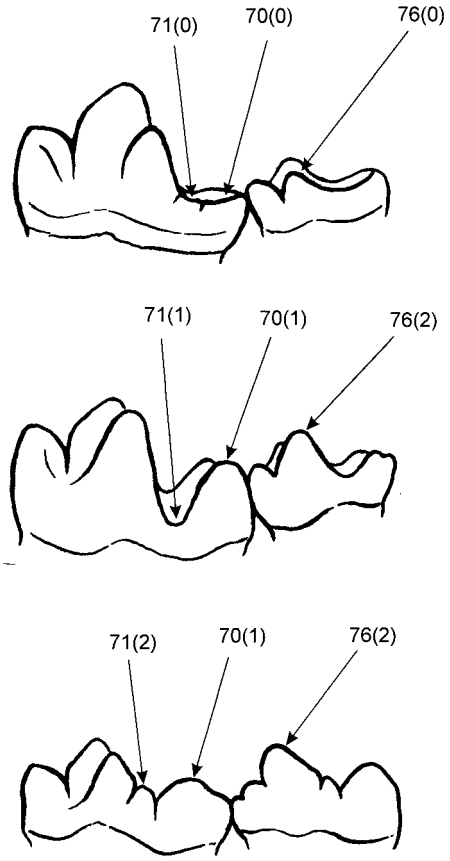

Fig. 137. Lingual views of m1s and m2s showing lower molar characters used in the phylogenetic analysis. Illustrated taxa are (from top down) *Archaeocyon pavidus* (LACM-CIT 466), *Otarocyon cooki* (F:AM 49043), and *Cynarctus crucidens* (F:AM 49172). Character numbers and state numbers (in parentheses) correspond to those listed in the character analysis and data matrix. The lower teeth are not drawn to the same scale.

conid are generally related to hypercarnivory.

Polarity: 0, m1 talonid width subequal to that of trigonid; 1, m1 talonid widened relative to trigonid; 2, m1 talonid narrow relative to trigonid (fig. 136).

73. m1–m2 selenodont: In one of the most striking examples of herbivory by a carnivoran, the lower molars of *Cynarctoides emryi* are selenodont by development of crescentic labial talonid cusps.

Polarity: 0, lower molars not selenodont; 1, lower molars selenodont (fig. 136).

74. m2 enlargement: As part of the grinding dentition, the m2 in canids is sensitive to adaptations toward hypocarnivory. Various stages of m2 enlargement are thus characteristic of most hypocarnivorous clades.

Polarity: 0, m2 not enlarged; 1, m2 enlarged; 2, m2 extremely enlarged (fig. 133).

75. m2 reduction: Different degrees of m2 reductions are characteristic of some hypercarnivorous clades.

Polarity: 0, m2 not reduced; 1, m2 reduced; 2, m2 further reduced (fig. 136).

76. m2 metaconid: Often covarying with its m1 counterpart, the size of the m2 metaconid is an indication of hypo-vs. hypercarnivory. Primitively, the metaconid is slightly lower than the protoconid in *Hesperocyon*. As taxa trend toward hypocarnivory, metaconids become progressively higher, whereas they may be reduced or lost in hypercarnivorous taxa.

Polarity: 0, m2 metaconid lower than protoconid; 1, metaconid equal to or higher than protoconid; 2, metaconid much higher and larger than protoconid; 3, metaconid absent (figs. 136, 137).

77. m2 protostylid: As in m1, m2 protostylids are related to hypocarnivory but do not necessarily strictly covary with the former. The development of m2 protostylids is thus coded as a separate character.

Polarity: 0, m2 protostylid absent; 1, m2 protostylid small; 2, m2 protostylid large (fig. 136).

78. Stratigraphic rank (not used in the PAUP analysis): Rank order of stratigraphic occurrences of each taxa are the earliest appearances of the taxa in the North American Land Mammal ages, and the procedure is defined in the MacClade program (Maddison and Maddison, 1992). Divisions of the NALMa follow that in the Materials and Methods section. No rigorous search procedure is available by the MacClade program, and the stratigraphic character cannot be used in the PAUP analysis. Inclusion of this character is thus mostly of heuristic values of the manual manipulations of the MacClade program.

Polarity: 0, Chadronian; 1, Orellan; 2, Whitneyan; 3, early Arikareean; 4, medial Arikareean; 5, late Arikareean; 6, early Hemingfordian; 7, late Hemingfordian; 8, early

Barstovian; 9, late Barstovian; A, early Clarendonian; B, late Clarendonian; C, early Hemphillian; D, late Hemphillian; E, Blancan.

PHYLOGENY

Although there is no compelling reason that a parsimony method is better at finding the true phylogeny, we adopted the cladistic analysis for its explicit presentation that facilitates hypothesis testing. We thus sought to explain the character distribution by shortest tree(s), which offers the most efficient summary of characters with a minimum number of untested hypotheses.

A 68 taxa (including outgroups) by 77 character (78 if the last character, stratigraphic rank, is included) matrix, representing 191 character states (excluding stratigraphic rank), was compiled for our phylogenetic analysis (table 2). The data matrix has 13.1% missing data (in question marks). Most searching for shortest trees was done by the PAUP program (version 3.0, Swofford, 1990), and parts of the results were verified by the HENNIG86 program (version 1.5, Farris, 1989).

Of the 66 borophagine species, four are known by fragmentary jaws or isolated teeth only (*Archaeocyon roii*, *A. harlowi*, *Cynarctus marylandica*, *Carpocyon limosus*), and their inclusion in the parsimony analysis invariably decreases resolution to the point of collapsing many branches of the trees because of the lack of information for these taxa. An initial heuristic search on the entire data matrix (excluding the stratigraphic character) yielded 14,038 trees with a length of 265 steps. Most of these trees are caused by the free movement of the above four taxa to many positions. Our subsequent parsimony analyses were thus conducted on a subset of the matrix excluding the above four species. These poorly preserved taxa were later manually inserted into the resulting trees using the MacClade program (version 3.0, Maddison and Maddison, 1992) to explore their phylogenetic position.

After the above exclusion, a core data matrix of 64 taxa by 77 characters was subjected to computer programs to search for the shortest trees. The large data set makes it impractical to use search methods that guarantee shortest trees (such as Exhaustive or Branch and Bound methods in PAUP). Instead, the Heuristic method in the PAUP program is employed. To ensure that the results from the Heuristic search did not miss important topologies, we divided the data matrix into several overlapping subsets of taxa and applied the Branch and Bound method to each of the subsets. For example, in a top-down pass, all Borophagina were searched for shortest trees. In the next run, *Carpocyon* through *Borophagus* were excluded from the matrix and an approximately equal number of taxa more basal to the Borophagina clade (in this case Aelurodontina) were added to the matrix for analyses. The process was repeated until the entire data set was exhausted. The same procedure was then applied in a bottom-up pass with a different overlapping subset of taxa. The selection of the subsets was such that different parts of the clades found by the Heuristic search could be thoroughly analyzed to ensure that no new topology had been missed.

A total of 282 shortest trees were recovered by PAUP from the core data matrix (all characters are unordered), with a total length of 261 steps. The large number of trees are the result of multiplications of just a few alternative topologies at a few nodes, and most taxa are fully resolved without ambiguity. For example, at the base of the Borophaginae clade, species of *Archaeocyon*, *Oxetocyon*, and *Otarocyon* are so primitive that lack of derived characters permits them to be freely associated with many other taxa or among themselves. Four of the unresolved segments, each featuring a few alternative trees, are summarized in figure 138.

Figure 139 shows a strict consensus tree derived from the above 282 equally parsimonious topologies. Lack of consistent synapomorphies for the basal borophagines causes near total collapse of the tree at its base. Conservative taxa near the base of

TABLE 2

Character Matrix of the Borophaginae

Character numbers and states corresponds to those listed under Character Analysis. Question marks indicate missing data.

```
                                1         2         3         4         5         6         7
                       1234567890123456789012345678901234567890123456789012345678901234567890123456789012345678

Hesperocyoninae        0000000000000000000000000000000000000000000000000000000000000000000000000000000000000000
Caninae                0000010000000000000000010000000000001000101000001000100000000000001001000000101
Archaeocyon pavidus    0000000000000000000000000000000001000000000000010001000000000000000000001000000102
Archaeocyon leptodus   0000000000000000000000000000000000000000000000010001000000000000010010000000102
Archaeocyon falkenbachi 1000000000000000000000???????0?????0000000000001000100000?????????????????????4
Oxetocyon cuspidatus   0000000?0000000?????????000000?0?????0000000100101001211000000?0000001110000202
Otarocyon macdonaldi   1000010010000010000111000000000000001001000010101000100000000000000101110000201
Otarocyon cooki        1000010020000010000111000000000000001001000010101000100000000000000101110000203
Rhizocyon oregonensis  0000000000000000000000000?0000000000000000000001001100000010000000001000000103
Cynarctoides lemur     0000000010000000001001000?0000???000000000000100111000001000000001100000103
Cynarctoides roii      0?????????????????????10??0??0????000000000000100111000001000000000100000113
Cynarctoides harlowi   0?????????????????????10??0??0?????000000?????????????????????000000?1?000001?5
Cynarctoides luskensis 0000000010000000001001000000000?0000001000000010011100000100000000111000000115
Cynarctoides gawnae    0000000010000001000?1?010000000?????000010000000100111100011000000001110000126
Cynarctoides acridens  0000000010000001000?0?1000000000000000100100001001212000110000100121120000125
Cynarctoides emryi     ???????????????0?????????00000?00?????0000?001000010012120001100001000000001121220110126
Phlaocyon minor        0000000010000000000100000000000000000100010000100111000001000000001100101010 3
Phlaocyon latidens     0000000000000010000100000000?00?????000100010001100111100001000000001100101010 3
Phlaocyon annectens    1?000?????????0?????????00000?0000000010010001000110011110000100000000111010000105
Phlaocyon achoros      1?????????????????????????00000??0?????1001000110121001121010010?0000011101000114
Phlaocyon multicuspus  0001000000000000000100????????000?????01?0011012100112101011007?????????????????5
Phlaocyon marslandensis 1001010000000?????????00000?0001010?1010001100210011111000010000000011201000116
Phlaocyon leucosteus   1000010000000000000100000000000101011010001100210011110000100000000112010001 5
Phlaocyon yatkolai     1???????????????0?????????0000000???0010000?0?????????????????????1000000120100010 6
Phlaocyon mariae       1???????????????0?????????000??0??0??1000010010?2100011100?100????????201001106
Cormocyon haydeni      0000000000000000000100000000000000000000000010011100000100000010010000001 3
Cormocyon copei        0000001000000000000100000??0000000000000000000100111000001000000100100000010 3
Desmocyon thomsoni     0001001000000001000100000000000000000000000000100111000001000000100110000105
Desmocyon matthewi     0102001000000001000100000000000000000000000000100111000001000000100120000010 6
Paracynarctus kelloggi 010200??000000010001000000101000100000000110001100121000001000000101110101010 7
Paracynarctus sinclairi 0102001000000001000100100010100??0?0000001100021001210000010000001011101010?8
Cynarctus galushai     0102001000000001100100000010100010100000001000010021100000100000001011201010108
Cynarctus marylandica  ?????????????????????????????????0?????000000?????????????????????????001011201000118
Cynarctus saxatilis    01020???0????001100100000010100010100010011100011021110002101000101212210202 9
Cynarctus voorhiesi    0?????????????0?????????00101010???010001002?????????????????2101000101212210202 9
Cynarctus crucidens    010?????????00110010010101010002010001002110211102111000210100010121221020 1A
Metatomarctus canavus  0102001 0?????0?????????000000000010000000000020100111000001000000100120000010 6
Euoplocyon spissidens  ???????????????0?????????00000?00?????000000000020100111000001000000100?02001006
Euoplocyon brachygnathus 0102001000000101000120000007000120020000002002010011100000100000010007?02001308
Psalidocyon marianae   0102001000000001000110000000010020001000000003010011100000100000010012000002 8
Microtomarctus conferta 1102001000010001000100000000000100000000000030100111000001000000100120000010 7
Protomarctus optatus   0103001000010001100100000000000020000000000030100111000001000000100120000010 6
Tephrocyon rurestris   0113001?000100011001000000000?????000000000030100111000001000000100120001010 8
Tomarctus hippophaga   0113001000010001100100000000000020000000100003010011100000100000010012000001 8
Tomarctus brevirostris 0113001000011101100100000000000020000000100003010011101000100000010012000001 8
Aelurodon asthenostylus 0113001?0101121110110000000000002000000010220401001010100010000001001202001008
Aelurodon mcgrewi      0113001101011111101120000000000120020000202204010010001000110000010012020010 9
Aelurodon stirtoni     0113001100001111101120000000000120020000202204010010001010110000010012020023 9
Aelurodon ferox        0213001102011211101120000000001130020000202204010010001000100000010012020010 9
Aelurodon taxoides     0213001102011211101120010000001130020000202304010010001000100000010012020013 0A
Paratomarctus temerarius 0113101000010001100100000000000200100100002030100111000001000000100120000010 8
Paratomarctus euthos   0113101000010101100100010000000020010010000203010011100000100000010012000001 9
Carpocyon compressus   0113101000010011110100000000000010010000012040100121000001000000100120001010 8
Carpocyon webbi        0113101?000100111010000001000??001000000120401001210000010000001001200010108
Carpocyon robustus     0113101000010011110100000110000??001000000120401001210000010000100100120001010A
Carpocyon limosus      ?????0?????????????????????????0????????????1204010012100001101?????????????????B
Proepicyon raki        0113101000010011110100000100000200100000002040100111010001000100100120000010 8
Epicyon aelurodontoides 0?031010010111111112??0???????002???10100000???0101111010007?????????????????C
Epicyon saevus         0113101000110111110120000100000000101000002140101111010001000200100120000110A
Epicyon hayleni        0113101000110111120120000100000000010100003140101111010001000200100120000100B
Borophagus littoralis  1113201000010111110?0000????0000??10100000314010112101000100020010012000001 A
Borophagus pugnator    1113201??????1?????????0101010000000101000031401011210100010002001001200000 0C
Borophagus orc         111?????????1?????????01010??0?????101100003140101121010??????200100120000 0C
Borophagus parvus      1113201000010111110?001010100000001011000031401011210100010003001001200001 0D
Borophagus secundus    2113201000010211110100010101000000001011000031401011210100010013001001200001 0C
Borophagus hilli       2?????????????2?????????010101000100010111000031301111210100?001300100120000 0D
Borophagus dudleyi     2114201000010311110120???????001???10110002?????????????????????????????????????D
Borophagus diversidens 2114201000010311110120010101100200010110000310011111001000100130210012000020 0E

                       1234567890123456789012345678901234567890123456789012345678901234567890123456789012345678
                                1         2         3         4         5         6         7
```

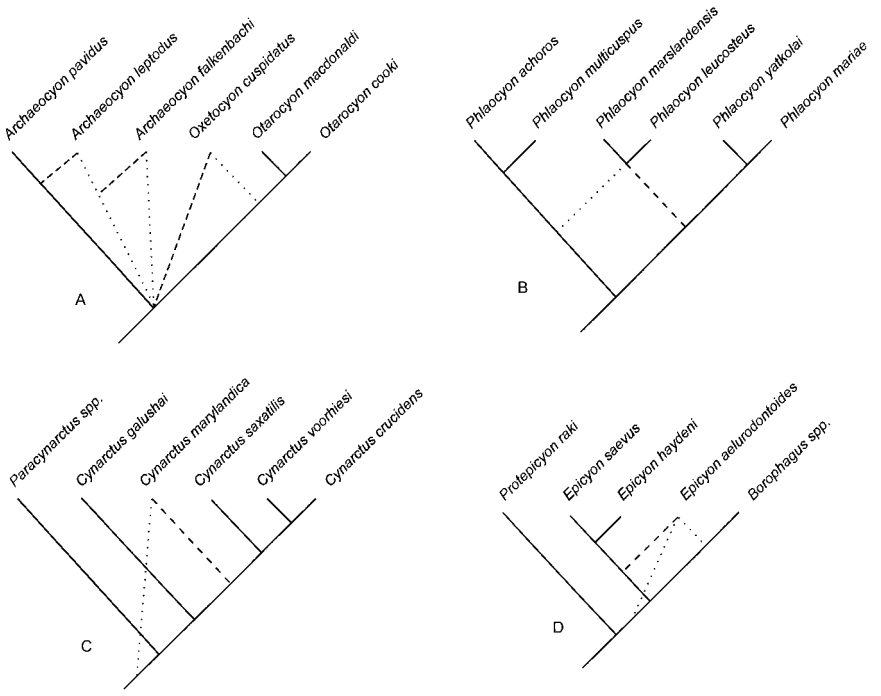

Fig. 138. Examples of some alternative trees for four of the least stable segments of the borophagine phylogeny. Dashed or dotted lines indicate equally parsimonious arrangements. The dashes represents preferred topologies that are further explained in the text.

clades (e.g., *Archaeocyon pavidus* and *A. leptodus*) often lack clear tendencies toward particular directions and are poorly resolved. Beyond this basal cluster, however, taxa more derived than *Rhizocyon* are for the most part quite resolvable. Taxa with many missing data are not necessarily difficult to resolve. Possession of certain critical synapomorphies are sufficient to consistently place some of the most poorly known taxa (e.g., *Phlaocyon achoros*). On the other hand, taxa with few or no missing data can be quite elusive in their cladistic relationships if they are defined mainly by plesiomorphic characteristics.

From the above equally parsimonious trees, we chose a single topology (fig. 140) that represents the best fit in overall consideration, with the four poorly known species (*Archaeocyon roii*, *A. harlowi*, *Cynarctus marylandica*, *Carpocyon limosus*) added in. In the few cases where we must select among equally parsimonious alternatives, our choice, admittedly subjective, was based mainly on subtle morphological features of the uncertain taxa that cannot be objectively coded as discrete characters (such as size relationships) but nonetheless offered clues about initial tendencies toward certain clades (see discussions below for individual cases). In certain cases, stratigraphic occurrences are also taken into considerations mainly through the MacClade program. The following narrative discusses the various nodes along the cladogram (usually from primitive to derived) and details how we view these relationships and how we justified certain relationships where the parsimony analysis was ambiguous.

At the most basal level, the evidence for a monophyletic Canidae is treated in greater depth elsewhere (Wang and Tedford, 1994; Wang, 1994). In those studies, we attempted to establish that *Hesperocyon* is a basal canid just slightly more advanced than *Prohesperocyon*. Our present analysis is built on the earlier studies and assumes that *Hesperocyon* is the closest sister-taxon to the Caninae–

Borophaginae clade and is an ideal outgroup because it possesses the right combination of primitive morphology and occurs at the right time.

The basic relationships of the three subfamilies of Canidae first proposed by Tedford (1978) are largely confirmed by this analysis, although certain basal taxa, such as *Archaeocyon*, *Oxetocyon* and *Otarocyon*, cannot be unambiguously demonstrated to belong to the Borophaginae (see below), a problem that also occurs in *Hesperocyon* within the subfamily Hesperocyoninae (Wang, 1994). The sister relationship between the Borophaginae and Caninae is supported by a few subtle but important synapomorphies mostly related to mesocarnivorous dentitions in contrast to more hypercarnivorous dental morphology of the Hesperocyoninae: reduced M1 parastyle, anteriorly expanded lingual cingulum of M1, basined talonid of m1, and relatively tall m2 metaconid. Apparently shortly after this initial dichotomy from the Hesperocyoninae, the Caninae clade began to differentiate from the Borophaginae. Synapomorphies that support the Caninae clade are mostly related to elongations of the cheekteeth and jaws and simplifications of premolars. The combination of these characters (e.g., slender ramus, long diastemata between premolars, reduction of premolar accessory cusps, long m1 trigonid) easily distinguishes the Caninae and permits recognition of this clade in the early Oligocene (Wang and Tedford, 1996).

Three basal genera, *Archaeocyon*, *Oxetocyon*, and *Otarocyon*, are presently included in our Borophaginae, but in the parsimony analysis they form a multichotomous bush at the base of the Caninae–Borophaginae clade. Although no derived character is found to place these genera on either side of the Caninae–Borophagine dichotomy, it is likely that they are on the borophagine side for the following reasons. First, in contrast to the canines, borophagines such as *Rhizocyon* through *Cormocyon* tend to be more conservative in their dental morphology, that is, they are closer to the primitive morphotype of the canids (as exemplified by *Hesperocyon*) than their counterparts in the Caninae (e.g., *Leptocyon*). The overall morphology of *Archaeocyon* is thus a better candidate for an ancestral borophagine than for a canine. Second, primitive borophagines have several groups that developed hypocarnivorous adaptations (e.g., *Cynarctoides* and *Phlaocyon*), a tendency not seen in the canines until much later (e.g., *Urocyon*, *Otocyon*, and *Nyctereutes* in the Pliocene). Therefore, hypocarnivorous taxa, such as *Oxetocyon* and *Otarocyon*, seem more likely examples of these trends within the borophagines. Third, *Leptocyon*, the earliest taxon with typical synapomorphies of the Caninae, is from the Orellan (Wang and Tedford, 1996). With the exception of a single specimen of *Otarocyon macdonaldi* from the Orellan of South Dakota, records of primitive borophagines (*Archaeocyon* and *Oxetocyon*) begin in the Whitneyan. Compared to the Caninae, such a late appearance for these basal taxa is more congruent with their being on the borophagine rather than canine side of the dichotomy. The overall evidence cited above seems to point toward a borophagine affinity for these basal genera, even though cladistic proof is lacking. Another alternative is a literal interpretation of the parsimony analysis, that is, *Archaeocyon*, *Oxetocyon*, and *Otarocyon* are neither canines nor borophagines, but represent a basal multichotomy of the Caninae–Borophaginae clade. Such an interpretation runs counter to the circumstantial evidence listed above and is considered less likely.

Both monophyly and specific relationships of *Archaeocyon* are also unresolved in the cladistic analysis (fig. 138A). Once again, this is because of the conservative morphology that reveals no consistent pattern of relationships. On the basis of size trends and stratigraphic sequence, we postulate that *A. pavidus* probably gave rise to *A. leptodus*, which in turn gave rise to *A. falkenbachi*. *Archaeocyon leptodus* possesses an elongated m1, a character present in the Caninae and in later borophagines (*Cormocyon* and up). In the present parsimony analysis, this single derived character is sufficient to pull *A. leptodus* within the canine side of the clade. However, our coding of the Caninae is based on a composite taxon, *Leptocyon*, that does not take into account an early individual of *Leptocyon* from the Orellan of Nebraska (see Wang and Tedford, 1996). This specimen, UNSM 25354, has the morphology of the most primitive canine but is too poorly

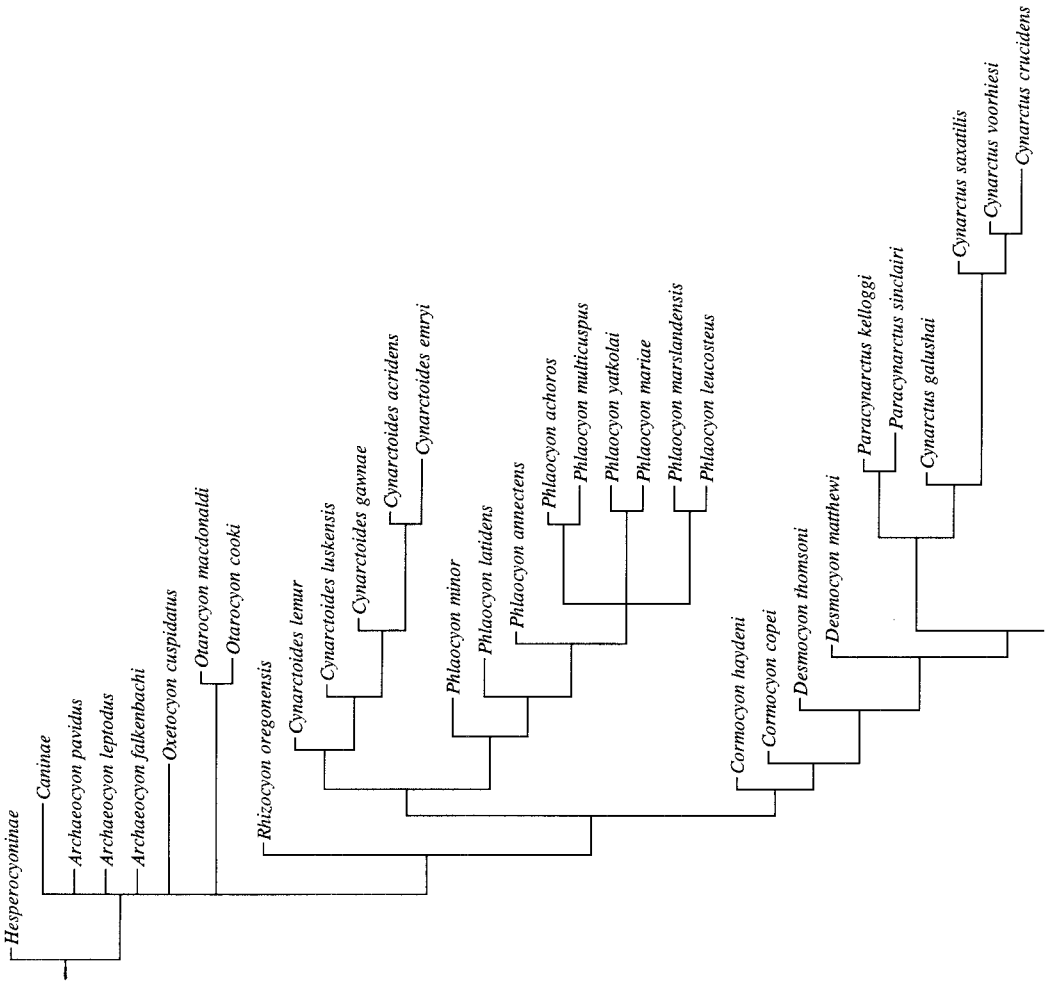

Fig. 139. Strict consensus tree of borophagine canids, based on 282 equally parsimonious trees calculated by PAUP from a core data matrix of 64 taxa by 77 characters. Tree statistics: length, 297; consistency index, 40; retention index, 82.

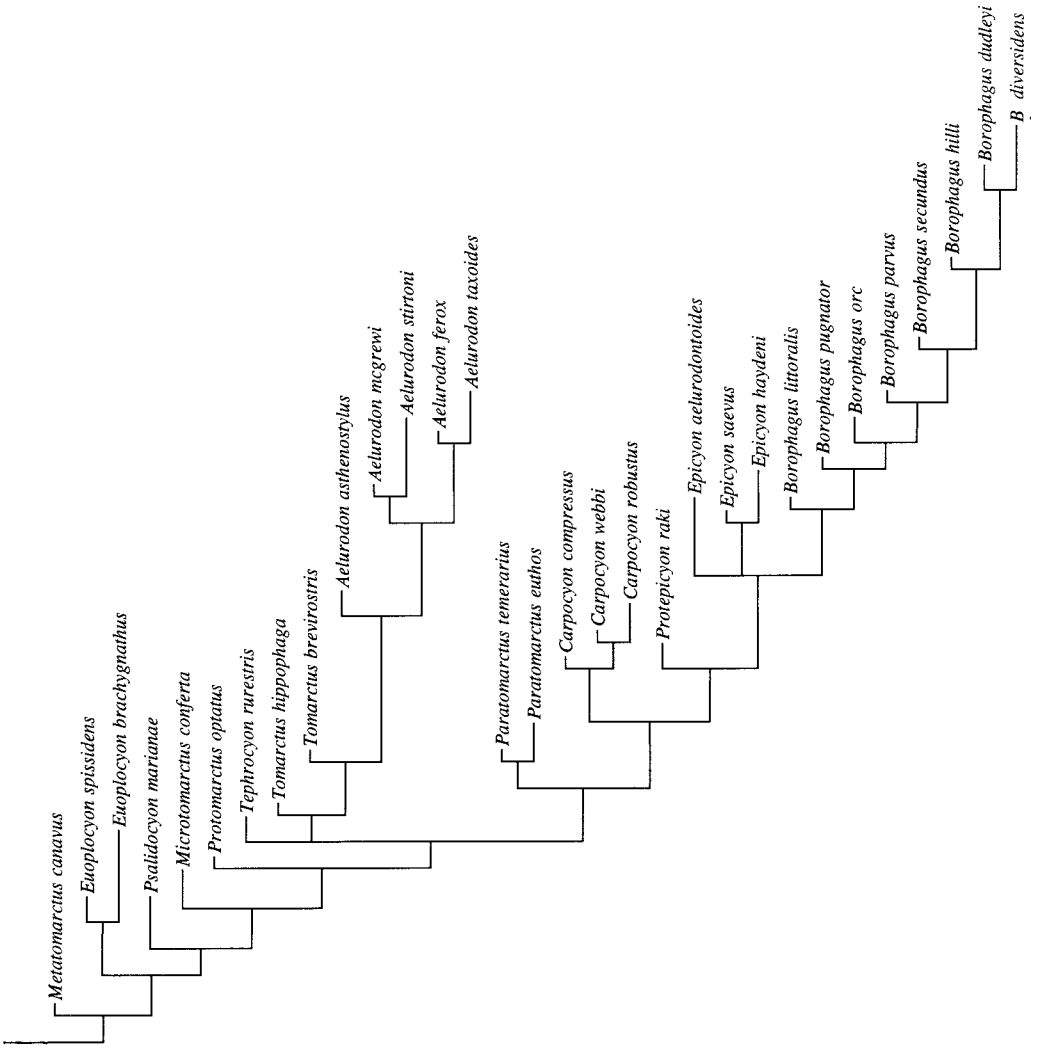

Fig. 139. *(Continued)*

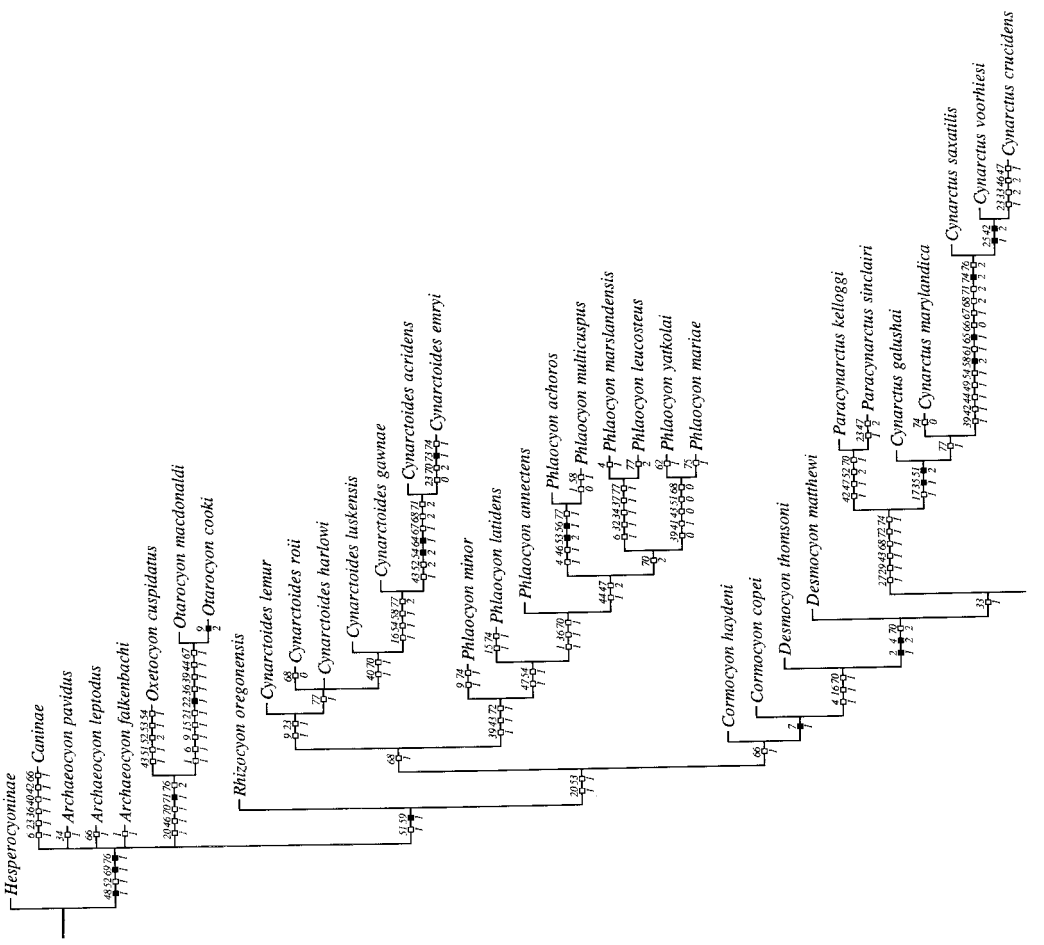
Hesperocyoninae
Caninae
Archaeocyon pavidus
Archaeocyon leptodus
Archaeocyon falkenbachi
Oxetocyon cuspidatus
Otarocyon macdonaldi
Otarocyon cooki
Rhizocyon oregonensis
Cynarctoides lemur
Cynarctoides roii
Cynarctoides harlowi
Cynarctoides luskensis
Cynarctoides gawnae
Cynarctoides acridens
Cynarctoides emryi
Phlaocyon minor
Phlaocyon latidens
Phlaocyon annectens
Phlaocyon achoros
Phlaocyon multicuspus
Phlaocyon marslandensis
Phlaocyon leucosteus
Phlaocyon yatkolai
Phlaocyon mariae
Cormocyon haydeni
Cormocyon copei
Desmocyon thomsoni
Desmocyon matthewi
Paracynarctus kelloggi
Paracynarctus sinclairi
Cynarctus galushai
Cynarctus marylandica
Cynarctus saxatilis
Cynarctus voorhiesi
Cynarctus crucidens

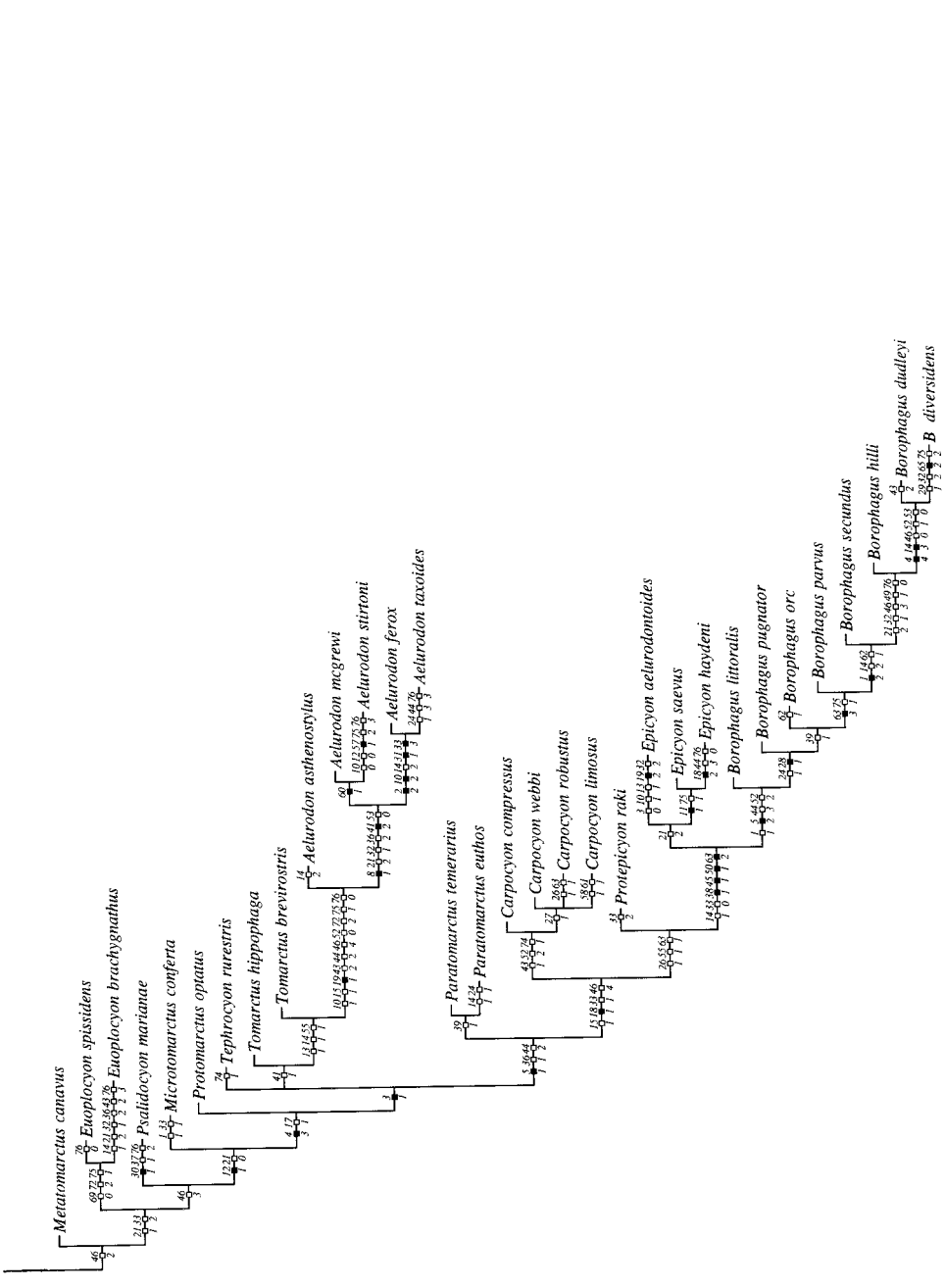

Fig. 140. Proposed cladogram for the borophagine canids. Character distributions are mapped by ClaDos (version 1.2 by Kevin C. Nixon). All characters are nonadditive (unordered). Numbers above the branches represent characters and those below represent character states (all numbers correspond to those in table 2 and Character Descriptions above). Solid bars represent synapomorphies, and empty boxes represent homoplasies (parallelisms or reversals). Tree statistics: length, 296; consistency index, 40; retention index, 82.

known (a partial ramus only) to be properly coded into the matrix. As discussed under *A. leptodus*, this basal *Leptocyon* ramal fragment has a morphology that suggests that the elongated m1 occurs after the appearance of the simplified and elongated premolars in the Caninae. Thus, if UNSM 25354 were included as a distinct species in this analysis, there would be two equally parsimonious solutions of either placing *A. leptodus* within the Caninae or within the Borophaginae (in either case, the elongated m1 is a homoplastic character). We chose to view the latter option as more probable.

The monophyletic genus *Otarocyon* is secure with numerous special synapomorphies found in no others. Furthermore, available evidence from stratigraphy and morphology strongly suggests that the two species, *O. macdonaldi* and *O. cooki*, form a chronospecies pair, with *O. macdonaldi* being ancestral to *O. cooki*.

Although supported by several characters in the cladistic analysis, a sister relationship between *Oxetocyon* and *Otarocyon* is not as strong as it may seem (an alternative arrangement is to collapse *Oxetocyon* to the base, as in the strict consensus tree in fig. 139). Some of these shared characters represent hypocarnivorous adaptations in both genera, and as these occur in other primitive borophagines, they can be the result of parallelisms. The fact that the two genera differ in numerous details suggests independent acquisitions of some of these characters. However, in the absence of evidence to the contrary (lacking transitional taxa for both genera), we tentatively accept a sister relationship for *Oxetocyon* and *Otarocyon* as a hypothesis to be further tested, and we retain *Oxetocyon* as a monotypic genus.

Beginning with *Rhizocyon*, borophagines become more recognizable as members of a monophyletic group through consistent shared-derived characters, even though these characters are still in their initial development. Standing close to the base of the borophagine clade, *Rhizocyon* is little different from *Hesperocyon* beyond the few characters cited in the cladogram. Such primitive similarities had long been observed by early students of canids, who linked these two forms (often called *Galecynus* or *Cynodictis*) together in the historical literature (Cope, 1879a, 1879b, 1884; Merriam, 1906).

Members of the tribe Phlaocyonini consist of hypocarnivorous taxa that were thought to play a significant role in the origin of the Procyonidae (Wortman and Matthew, 1899; McGrew, 1938a, 1941). Monophyly of the phlaocyonine clade is weakly supported by a derived character of m1 protostylid, which is still somewhat inconsistently present among early members of the clade, especially in primitive species of *Phlaocyon*. Within the phlaocyonine clade, two genera form a sister relationship, *Cynarctoides* and *Phlaocyon*. Although their primitive species are quite similar to one another, their advanced members took quite different paths toward hypocarnivory.

The genus *Cynarctoides* is much larger in scope than previously recognized and forms a clade of its own. Membership of its most primitive species, *C. lemur*, is weakly supported by two characters, a slender horizontal ramus and separate temporal crests, both of which were subject to repeated development in canids. Long known in the literature and represented by reasonably complete materials, *C. lemur* possesses few of the typical dental features traditionally identified with *Cynarctoides*, but if correctly identified, as was earlier suggested by Matthew (1932), it helps to bridge the large morphological gap between advanced members of the genus and other basal borophagines. Ignored since their original description, *C. roii* and *C. harlowi* are still too poorly known to be certain of their identity, and their placement within *Cynarctoides* is only weakly suggested by a slender ramus and an m2 protostylid (in *C. roii* only), features that could be independently derived.

Cynarctoides unambiguously begins with *C. luskensis*, which offers a rare opportunity to glimpse a transitional form. In almost every respects, *C. luskensis* stands in an intermediate position between more advanced (*C. gawnae* and up) and more primitive species (*C. lemur* and others). The presence of such typical *Cynarctoides* characters as slender premolars and conical m1 talonid cusps clearly allies *C. luskensis* with the *Cynarctoides* clade, but the lack of more derived features such as a conical hypocone on M1–

M2 permits its identification as a perfectly transitional taxon. The latter feature, along with the first appearance of a strong m2 protostylid, is first seen in *C. gawnae*. As another intermediate taxon in the pectinate clade, *C. gawnae* lacks the large number of characters shared by the most advanced *Cynarctoides*, *C. acridens* and *C. emryi*. The latter two species are easily recognizable because of their unusual tendency toward selenodonty. Their relationships to each other and to *C. gawnae* seem secure.

Compared to *Cynarctoides*, the *Phlaocyon* clade is slightly better supported, not only by more recognizable characters, but also by greater consistency in the occurrence of these characters. Short premolars and a wide m1 talonid are present in all species of *Phlaocyon*, a taxon now much broader in scope than traditionally recognized. Although parsimony analysis suggests a basal position for *P. minor* followed by *P. latidens*, the latter is smaller in size and possibly earlier in occurrence than the former. Since size increase is a trend in most other *Phlaocyon*, it is possible that homoplasies may have obscured the true relationship. If *P. latidens* is at the base of the *Phlaocyon* clade, instead of *P. minor*, a cladogenetic event within the Phlaocyonini separates the two small John Day forms, *C. lemur* and *P. latidens*, and led to their respective clades (genera). The next step, represented by *P. annectens*, is transitional to *Phlaocyon*, and its phylogenetic position seems clear among the known taxa.

The node above *P. annectens* marks a divergence point where three small clades of *Phlaocyon* arise. The earliest clade is the *P. achoros–multicuspus* species pair. Their multiple-cusped upper molars are unique characteristics not seen elsewhere in canids and thus offer reasonable support for this clade. A sister relationship between *P. marslandensis* and *leucosteus* is strongly supported by synapomorphies mostly derived from their highly hypocarnivorous dentition. This relationship has never been in doubt ever since McGrew (1941) first described *P. marslandensis*. Contrary to McGrew (1941), however, *P. marslandensis* is not descendent from *P. leucosteus*. Morphologically, the latter is actually more apomorphous than the former. Although we are inclined toward a sister relationship between the *P. marslandensis–leucosteus* clade and the *P. yatkolai–mariae* clade, support for such a relationship is weak and there is an equally parsimonious tree that links the *P. marslandensis–leucosteus* clade with the *P. achoros–multicuspus* clade (fig. 138B).

Finally, the newly described *P. yatkolai* and *P. mariae* are still poorly known with each species being represented by a single individual with only partial or fragmentary jaws. Our present proposal to link these rather hypercarnivorous species as sister-taxa is likely to be controversial. Uncertainty arises not only from the common frustration of poorly preserved materials, but also from the implication that a hypercarnivorous clade could have been derived from within a largely hypocarnivorous clade. However, available evidence seems to hint at a *Phlaocyon* affinity, including robust premolars and a P4 hypocone. Our proposed position for these two species can only be viewed as a tentative interpretation based on meager evidence, testable only by future discoveries.

Most borophagines form a clade that is a sister to the Phlaocyonini. This large clade, tribe Borophagini, begins with the small, fox-size *Cormocyon*, whose sole feature indicating its membership within this clade is an elongated m1 with an open trigonid. However trivial this character may seem (it independently occurs in the Caninae and *Archaeocyon leptodus*), it initiates a long series of morphological modifications that led to the evolution of a diverse group of taxa that were the dominant canids in the late Tertiary of North America. Between *Cormocyon* and the Cynarctina clade there is a series of transitional taxa in the late Arikareean and Hemingfordian characterized by trends toward larger size and more complex molars. Through *Cormocyon* and *Desmocyon*, the skulls begin to add air spaces in the form of frontal sinuses, and the grinding part of their dentition becomes more cuspidate.

The subtribe Cynarctina marks the third (after *Oxetocyon* and the Phlaocyonini) clade of hypocarnivorous borophagines. Primitive members of the Cynarctina possess a combination of derived and primitive dental morphology (presence of a single accessory cusp on I3 and lack of an enlarged P4 parastyle)

that places them between *Desmocyon matthewi* and *Metatomarctus*. Within the cynarctine clade, we recognize a basal dichotomy represented by *Paracynarctus* and *Cynarctus*. On the *Cynarctus* side, *C. galushai* is grouped with the *Cynarctus* clade by such subtle dental features as a recurved lower canine and slight elongation of upper molars. The poorly known *C. marylandica* is difficult to place in cladistic analysis due to the large amount of missing data (fig. 138C). Among the possible alternatives based on its size and morphology, we chose to placed it near the base of the *Cynarctus* clade because of its possession of a m2 protostylid.

Extremely hypocarnivorous dental characters make advanced species of *Cynarctus* easily distinguishable, as indicated by a long list of synapomorphies below *C. saxatilis*. From *C. saxatilis* and above, there appears to be a linear progression toward smaller size and more complex bunodont dentitions, terminating in *C. crucidens*. If this is the case, the presently recognized three species appear to represent a chronocline. Partition of this lineage (i.e., how many species to be recognized) becomes an exercise of finding convenient morphological or stratigraphic gaps.

As in *Cynarctus*, the *Paracynarctus* clade also trends toward hypocarnivory, although to a lesser degree and in a different fashion. This is most clearly seen in the terminal species *P. sinclairi*, which possesses a P4 hypocone and large, quadrate upper molars, characters not seen or differently developed in *Cynarctus*. Some of the characters uniting the *Paracynarctus* clade also occur at various nodes within the *Cynarctus* clade. However, these characters (e.g., development of diastemata between the premolars and P4 cingulum) seem to be located at different nodes of the *Cynarctus* clade, indicating independent acquisitions along a different path. We thus regard *P. kelloggi* as more likely a *Paracynarctus*.

Taxa immediately above the Cynarctina (from *Metatomarctus* through *Protomarctus*) form another transitional series toward later borophagines. The phyletic order of these taxa is mostly determined by their development of frontal sinuses, I3 lateral accessory cusps, and a P4 parastyle. Lack of a uniform dental pattern among these taxa is the most prominent feature in this segment of the clade. The extremely hypercarnivorous clade, *Euoplocyon*, is in sharp contrast with taxa on either side of the clade (*Metatomarctus* and *Psalidocyon*). *Euoplocyon* appears suddenly in the fossil record and has no intermediate form that would permit confident analysis of its relationship with other taxa. *Psalidocyon* is another form with unique dental features. Its sharply bladed cheekteeth represent autapomorphies that do not suggest relationships to other taxa. Although the distinct P4 parastyle of *Psalidocyon* may indicate advanced status relative to *Metatomarctus* and *Euoplocyon* as postulated by the cladogram, it is conceivable that the development of a parastyle may have been related to its rather cuspidate cheekteeth (that is, independent development of a distinct P4 parastyle remains a possibility to be tested by future discoveries). Further up in the phylogeny is the genus *Microtomarctus*, which is constrained to its present position in the cladogram by the initial development of a posteriorly expanded nuchal crest (derived relative to *Psalidocyon*), but without elaborate frontal sinuses and a small auditory meatus (primitive relative to *Protomarctus*). If our proposal about its phylogenetic position is correct, *Microtomarctus* clearly represents a dwarf lineage, because taxa both below and above *Microtomarctus* are larger in size.

Protomarctus in the next node up is closest to the Aelurodontina–Borophagina dichotomy. It is marked by derived (relative to *Microtomarctus* and below) characters of a well-formed frontal sinus that extends posteriorly behind the frontal–parietal suture and a small opening of the external auditory meatus. On the other hand, *Protomarctus* lacks either the uniformly robust premolars, broad palates, and high sagittal crests in the Aelurodontina clade, or the highly domed foreheads and reduced premolars in the Borophagina clade. *Tephrocyon* in the next node up is slightly more derived than *Protomarctus* in its large postorbital process. The exact relationship of *Tephrocyon* is not cladistically resolved. It lacks the derived characters for the Aelurodontina and Borophagina clades and appears to be a transitional taxon at the base of these two great clades.

The most primitive member of the Aelu-

rodontina clade is represented by *Tomarctus hippophaga*, a transitional taxon that quickly gave rise to *T. brevirostris*. The only character of *T. hippophaga* that marks the beginning of the aelurodontine clade is its tendency toward uniformly enlarged premolars, in contrast to the reduction of premolars and differential size of p3 and p4 in the Borophagina clade. Showing more aelurodontine characters, *T. brevirostris* occurs in the following node. It shows a slightly broadened palate, narrowed nuchal crest, and high-crowned M1 paracone, features that are further developed in *Aelurodon*.

Characters associated with *Aelurodon* begin to appear in its basal species *A. asthenostylus*, as shown by the numerous synapomorphies uniting the genus. These derived characters are mostly associated with the increasing hypercarnivory of the lineage. Cranial modifications probably related to masticatory enhancements include a high sagittal crest and ventrally elongated mastoid process. Molars and carnassials become more trenchant, as occurs in other hypercarnivorous canids (that is, reduced upper molars relative to P4, reduced P4 protocone, prominent P4 parastyle, M1 lingual cingulum restricted to posterior corner, narrow m1 talonid, reduced m2, and reduced m2 metaconid). Additional derived characters are developed in more advanced species of *Aelurodon*. Most of these characters, however, are culminations of morphological trends that occurred earlier: widened posterior end of zygomatic arch, elongated paroccipital process, enlarged I3, more enlarged premolars and their accessory and cingular cusps, and reduced M1 metaconule.

Two lineages diverged within the *Aelurodon* in the late Barstovian: the *A. mcgrewi–stirtoni* clade and the *A. ferox–taxoides* clade. The first evidence of this dichotomy is found in *A. mcgrewi* in its extreme reduction or loss of the M2 metacone, which is shared with *A. stirtoni* (formerly the genotype of *Strobodon*). The *A. mcgrewi–stirtoni* lineage is marked by its reduction in size and extreme development of hypercarnivorous dentition, such as trenchant cheekteeth and reduced last molars. Implied by our proposed phylogenetic relationships are two character reversals in *A. stirtoni*: low sagittal crest and short nuchal crest. *A. stirtoni* is also characterized by an autapomorphy of its own: sharply concave posterior border of M1.

The traditional concept of the genus *Aelurodon* is represented by the *A. ferox–taxoides* lineage. Representing the first attempt at gigantism by the borophagines, this clade is present in most late Barstovian through Clarendonian faunas, and is numerically more dominant than other species of *Aelurodon*. Besides the large number of characters shared with the *A. mcgrewi–stirtoni* clade (wide zygomatic arch, long paroccipital process, large I3, large premolars and accessory cusps, reduced M1 metaconule), the *A. ferox–taxoides* lineage also acquired derived characters: broad contact of premaxillary and frontal, extremely high sagittal crest, further widened palate, transversely straight incisor row, and multiple (usually three) lateral accessory cusps on I3. The *A. ferox–taxoides* species pair appears to be a continuous anagenetic lineage, and as such, there is no natural way of dividing it. The decision to divide it can be questioned in a strict cladistic sense. Besides size increase, however, there is enough morphological modification to encompass more than one morphospecies in the traditional sense. We chose to divide the lineage into two species at the Barstovian–Clarendonian boundary (sensu Tedford et al., 1987), although an alternative division might be possible in regions with well-studied stratigraphy (e.g., Voorhies, 1990a). In the present division, the terminal species *A. taxoides* progressively acquires additional derived features such as a symphyseal boss, more reduced P4 protocone, and loss of m2 metaconid.

We recognize three synapomorphies uniting members of the subtribe Borophagina: dorsally inflated frontal sinus that forms a dome on the forehead, reduction of premolar cusplets, and reduction of P4 protocone. Although the last character, reduction of P4 protocone, also occurs independently in the Aelurodontina, the first two characters are unique for the Borophagina. The progressively more domed forehead in the Borophagina is in sharp contrast to the flat-headed Aelurodontina, and the reduced premolar accessory and cingular cusps in the Borophag-

ina are opposite to the trend of increased cusplets in the Aelurodontina.

The most primitive taxon of the Borophagina is *Paratomarctus*. Monophyly of the genus is suggested by a single synapomorphy of shortened premolars. The more primitive species *P. temerarius* from the Barstovian appears to have given rise to *P. euthos* from the latest Barstovian through Clarendonian as a descendant chronospecies. If so, the division of these two species becomes an exercise of taxonomic convenience. We chose to recognize a different species in the latest Barstovian in order to avail ourselves to the name *euthos*, for a well-known taxon from the Burge Member of the Valentine Formation. Thus defined, *P. euthos* is more derived than *P. temerarius* in its moderately widened palate and weak symphyseal boss.

The next clade above *Paratomarctus* is the genus *Carpocyon*. *Carpocyon* and the *Protepicyon–Borophagus* clade share four synapomorphies that distinguish them from *Paratomarctus*: enlarged bulla, a short tube for auditory meatus, one lateral accessory cusp on I3 (a reversal), and a prominent P4 parastyle. In addition, three autapomorphies ally *Carpocyon* species in a monophyletic group: enlarged upper molars relative to P4, M1 lingual cingulum anteriorly thickened so that the tooth has a quadrate outline, and enlarged m2. These autapomorphies are typical of hypocarnivorous dentitions. *Carpocyon* is apparently the last borophagine to explore hypocarnivory, but it is only moderately successful in this regard as compared with previous lineages (e.g., Phlaocyonini and Cynarctina).

We recognize four species within the *Carpocyon* clade. At the base of the clade is *C. compressus* from Barstovian of the Great Plains. The slightly more derived *C. webbi* is the largest species of the genus and has a more marked mandibular subangular lobe than the former. The relationship of *C. robustus* within the clade is still somewhat uncertain, despite its apparent sister relationship with *C. limosus* in the parsimony analysis. Such a relationship is only weakly supported by a vague posterior cingulum on M2. On the other hand, *C. robustus* has two derived characters (a deeply excavated anterior rim of masseteric fossa and a widened p4 relative to reduced p2–p3) that are commonly associated with the *Protepicyon–Borophagus* clade. It is thus still possible that *C. robustus* has a more derived position than is presently proposed.

The transitional taxon *Protepicyon* shows the initial steps in the evolution of large bone-crushing canids, *Epicyon* and *Borophagus*. Derived characters that signal its advanced status relative to *Carpocyon* include deeply excavated anterior rim of masseteric fossa, high-crowned M1 paracone, and widened p4 relative to reduced anterior premolars. On the other hand, *Protepicyon* is still primitive relative to *Epicyon* in retention of a number of characters: unbroadened palate, presence of a lateral accessory cusp on I3, premolars not low-crowned, P4 protocone not connected to parastyle through a ridge, presence of M1 buccal cingulum, and p4 less enlarged relative to anterior premolars.

A monophyletic *Epicyon–Borophagus* clade is strongly supported by derived states of characters listed above for *Protepicyon*. Most of these characters are related to a bone-crushing dentition (wide palate, reduced p2–p3, enlarged p4, and high M1 paracone). At the base of this clade is *Epicyon*, whose monophyly is supported by a single character, the elongation of its paroccipital process. Within *Epicyon*, *E. aelurodontoides* is clearly a lineage of its own with its unique combination of derived characters, some of which parallel morphologies of *Aelurodon*: high sagittal crest, laterally compressed nuchal crest, posteroventrally expanded mastoid process, and reduced M2. Incomplete information about its morphology (especially its lower dentition) and its peculiar development of *Aelurodon*-like characters do not permit a stable resolution of its phylogenetic position (fig. 138D). We tentatively place it in the *Epicyon* clade. The sister species *E. saevus* and *E. haydeni* are united by two synapomorphies: concave dorsal edge of sagittal crest and reduced m2. *E. haydeni* has further evolved additional autapomorphies that distinguish it from *E. saevus*: elongated auditory meatus, reduced P4 protocone, and low m2 metaconid, features that commonly occur in large hypercarnivorous carnivorans and are homoplastic within the Borophaginae as well.

The terminal clade *Borophagus* is relatively easy to recognize. Besides its shared characters with *Epicyon*, *Borophagus* has the following autapomorphies: short rostrum, highly domed forehead, extreme reduction of P4 protocone, and anteriorly expanded M1 lingual cingulum. Presence of these characters signals the beginning of this clade at *B. littoralis* from the early Clarendonian of California. The California progenitor of *Borophagus* is followed by *B. pugnator* in the Hemphillian of Great Plains and Gulf Coast, which is only slightly more advanced in its development of a weak boss at the symphyseal joint. Although a deep angular process also first appears at *B. pugnator*, lack of preservation of this structure in known materials of *B. littoralis* leaves the possibility open that it may occur there as well.

Further shortening of its anterior premolars indicates a slightly more advanced position for *Borophagus orc*. This dwarf Florida species also has a tendency to lose its p1 (as compared to *B. parvus*), here considered to be an autapomorphy. Extreme widening of p4 relative to p2–p3 and reduction of m2 are the next steps in the *Borophagus* phylogeny, as represented by *B. parvus* from the late Hemphillian of Arizona and California. Another small species of *Borophagus*, this form is rather similar to *B. orc* in its overall primitive morphology.

Beginning in *B. secundus*, advanced species of *Borophagus* are signified by their highly derived morphology relative to *B. parvus*: extreme shortening of snout, prominent widening of palate at P4 and corresponding lateral flare of lower jaw, higher crowned and more posteriorly reclined p4, and loss of p1. These derived characters, along with some proportional differences in skull and dentition, mark a more conspicuous transformation when compared with the differences among primitive species. Toward the latest Hemphillian, further morphological modifications are acquired in *B. hilli* that are shared with *B. diversidens* (and presumably *B. dudleyi*, which may not preserve these features): enlarged I3, reduced P4 parastyle, loss of M1 buccal cingulum at metacone, and low m2 metaconid relative to protoconid. *B. dudleyi* in the latest Hemphillian of Florida is a highly derived taxon with extreme posterior expansion of frontal sinus to inion, a long paroccipital process, and a wide palate. Although these characters are apparently shared by *B. diversidens*, *B. dudleyi* does not appear to be a transitional taxon between *B. hilli* and *B. diversidens*. The cranial morphology of *B. dudleyi* is unique with its posteriorly reclined lateral profile of the frontal sinus, laterally expanded postorbital process, and long palate. Unfortunately, we know very little about the dental morphology of this species (dental characters mapped on the common stem of *B. dudleyi* and *B. diversidens* [fig. 140] are optimizations of the ClaDos programs). The terminal species *B. diversidens* in the late early through late Blancan has the most derived dental conditions among all borophagines. Much of the morphological modifications (autapomorphies) within *B. diversidens* are continuations of trends developed in *B. secundus* through *B. hilli*: further widening of palate, higher mandibular condyle, further enlargement of I3, loss of P4 parastyle, M1 lingual cingulum restricted to posterior corner (a reversal), reduced M1 metaconule, loss of p4 posterior accessory cusp, and further reduction of m2.

COMMENTS ON STRATIGRAPHY, GEOGRAPHY, AND DIVERSITY

STRATIGRAPHY

As a result of the Frick Collection, fossil records of the borophagines have moved from one of largely scattered occurrences in time and space to one of exceptional stratigraphic continuity and broad geographic coverage (fig. 141). During the late Tertiary of North America, borophagines certainly rank as one of the best represented group of carnivorans. With this extraordinary record, it is now possible not only to test ideas about phylogenetic relationships, the main focus of this volume, but also to explore issues related to temporal range, geographic distribution,

and tempo and mode of evolution. While these latter subjects will be the focus of further research that considers examples from the entire family Canidae, we briefly touch on some of these issues as a conclusion to this study.

With the exception of *Oxetocyon*, the *Phlaocyon yatkolai–mariae* clade, the *Euoplocyon* clade, and *Psalidocyon*, which appear in the fossil record rather suddenly without immediate close predecessors, most borophagines have rather continuous fossil records. This continuity of record, with numerous transitional morphologies, permits a higher confidence in the phylogenetic reconstruction than has been possible in the past. The postulated relationships are bridged by numerous transitional forms that substantiate our phylogeny in great detail. In some instances, the record is so continuous that partitioning lineages into more than one species becomes an exercise of arbitrary decisions resolved by cutting along certain chronologic boundaries in order to maintain coefficients of variation comparable to those of living canid species (such as the *Aelurodon ferox-taxoides* and *Paratomarctus temerarius-euthos* species pairs).

Despite such an exceptional record, however, there are weaknesses that either place constraints on our phylogenetic analysis or limit our confidence in stratigraphic representations. The most significant shortcoming in our overall stratigraphic representation occurs in strata of medial Arikareean age (28–24 Ma), which are under-represented by chronologically well-constrained samples. Further collection and study of this interval may significantly refine our taxonomic coverage this period. This is especially true for *Cynarctoides* and *Phlaocyon*, which essentially lack medial Arikareean records, but, judging from the phylogenetic pattern (fig. 141), must have undergone critical parts of their diversification during this period.

Among the different borophagine clades, hypocarnivorous taxa appear to have worse records than do hypercarnivorous taxa. With the exception of *Cynarctoides acridens*, most hypocarnivorous species are represented by no more than a handful of specimens, in contrast to the usually much larger samples of meso- and hypercarnivorous taxa. It remains to be determined whether this difference is a reflection of original abundances of the respective taxa or is affected by preservational biases, either because of the property of hard tissues (i.e., more delicate bones of small omnivores are less likely to be preserved than those of heavily built large predators) or because of habitat preferences (i.e., terrestrial deposits in the late Tertiary may favor open habitats where large pursuit predators are more likely present, as opposed to more wooded areas, which smaller omnivores prefer).

In the presently recognized chronological units (subdivisions of the North American Land Mammal ages), most borophagine taxa have unbroken records during their existence (obviously the quality of the records are far from even). There are, however, noticeable gaps in the fossil record, indicating the presence of unrecorded or ghost lineages (Norell, 1992) in the intervening strata. Besides the large gaps in the medial Arikareean for *Cynarctoides* and *Phlaocyon*, the following two examples are unlikely to have been influenced by taxonomic determinations (both examples involve morphologically distinct lineages unlikely to be confused with other taxa). One involves a ghost lineage in the Whitneyan between the presently recognized *Otarocyon cooki* (early Arikareean) and *O. macdonaldi* (Orellan). Morphologically, a moderate gap exists between these two species that conceivably can be filled by a transitional form in the Whitneyan. A similar situation involves the *Euoplocyon brachygnathus–spissidens* clade, which is missing in the late Hemingfordian, although morphological distance between these two species is small and a late Hemingfordian transitional form is not expected to be greatly different from species on either side.

As an approximate measure of the correspondence between the phylogenetic order of borophagines and their stratigraphic sequence, figure 142 plots this relationship between clade ranks and stratigraphic ranks. With a correlation coefficient of 0.939 ($R^2 = 0.881$), there is a remarkable congruence between phylogeny and stratigraphy in the borophagine records. Certain incongruence between first occurrences and phylogenetic ranks may be due either to incorrect recon-

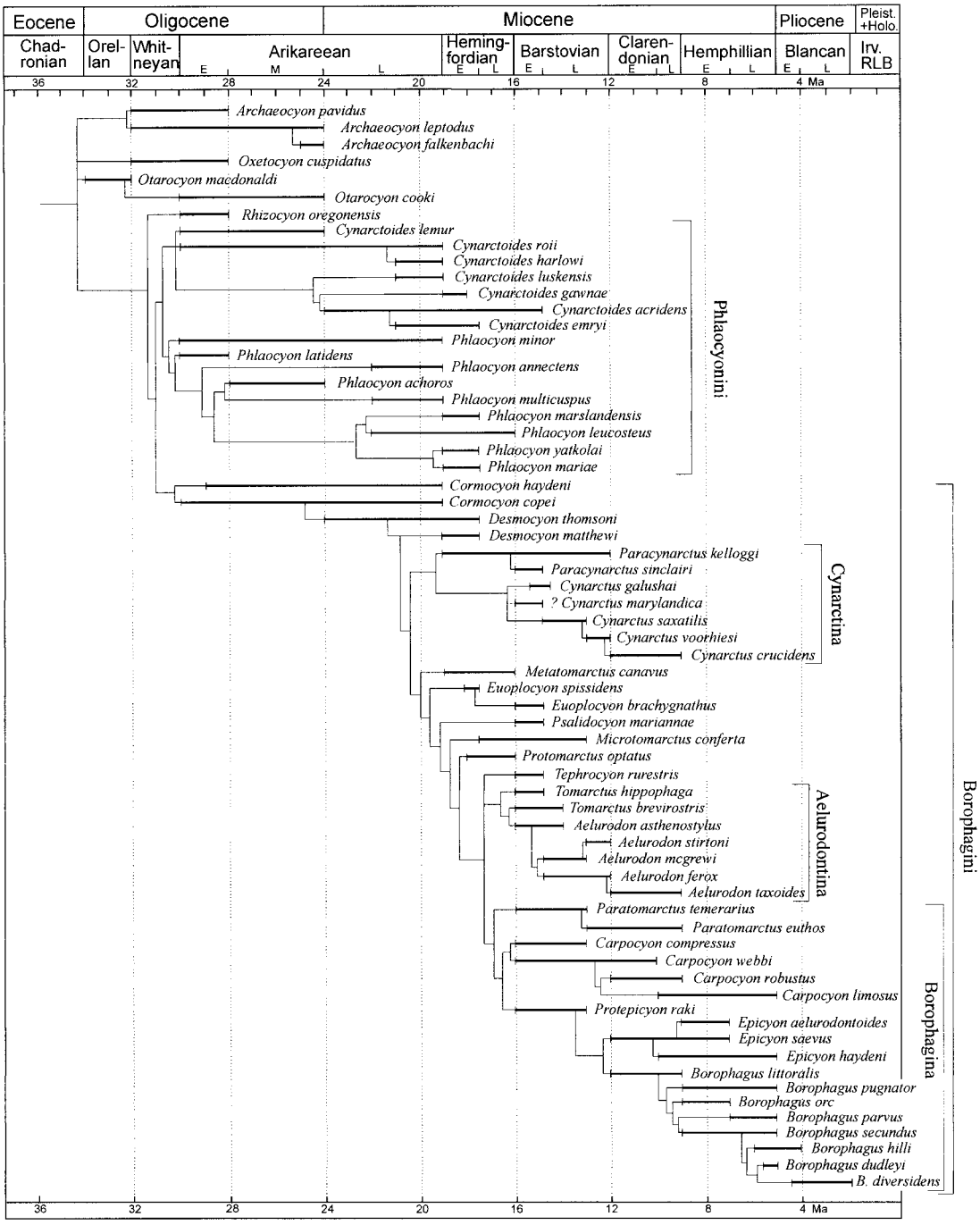

Fig. 141. Stratigraphic distribution and postulated phyletic relationships for the Borophaginae. Although essentially based on our cladistic analyses, the phyletic relationships represent further speculations about the cladogenetic or anagenetic events, based on our assessment of their morphology and stratigraphy. Chronological framework is based on a revision of those proposed in Emry et al. (1987), Tedford et al. (1987), and Lundelius et al. (1987), as explained in the Materials and Methods section.

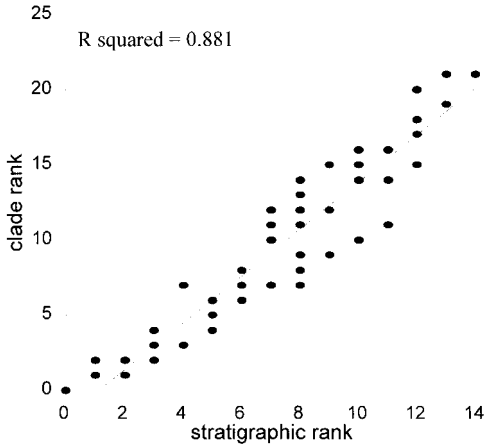

Fig. 142. Bivariate plot of phylogenetic vs. stratigraphic ranks, following the method by Gauthier et al. (1988). Stratigraphic ranks follow that in Character Analysis (character 78). Linear regression produces an R^2 of 0.881 (R = 0.939) and a regression line of y = 1.57 − 1.766 (straight line among dots), where y indicates clade ranks and x indicates stratigraphic ranks.

struction of some part of the cladogram because of homoplasies or to incorrect assignment of ages. An example of the former may be in *Phlaocyon latidens*, which greatly predates all of the descendent taxa (fig. 141). It is possible that *P. latidens* may be a precociously advanced species that is actually ancestral to *P. minor*. If such is the case, the late Arikareean *P. annectens* could have been arisen from within *P. minor*, which has a long stratigraphic record. An example of the problems of age assignment may be in *Epicyon aelurodontoides*, whose age estimate of early Hemphillian is based on poorly documented assemblages and adjacent faunas that may or may not be coeval (i.e., an earlier occurrence for this taxon is possible). To further complicate the issue, *E. aelurodontoides* possesses several homoplastic characters to obscure its real phylogenetic position (the peculiar combination of its derived characters implies that some of them must be homoplasies no matter what topology is settled on), hence its specific name.

ZOOGEOGRAPHY

Knowledge of geographic distribution of the borophagines is constrained by the fact that most of the Tertiary terrestrial deposits are exposed in the western half of North America and in the middle latitudes. Within the western United States, records from the West Coast are not comparable in quantity and quality to those of the Great Plains until the early Barstovian. Given such physical limitations, it is possible to discern only broad zoogeographic patterns that are often consistent with the distributions of other components of the fauna from which the canids are derived.

As in the case of many other late Tertiary groups, records from the northern Great Plains often provide the yardstick by which everything else is measured, despite frequent hiatuses in the Plains deposits. Out of 65 borophagine species recognized in this study, 51 are either exclusively found in the Great Plains or occur there during parts of their existence.

During the Barstovian and Clarendonian, deposits on the West Coast and southwestern United States seem to contain the earliest appearances of all of the large-size, bone-crushing clades. The *Aelurodon* clade first appeared in the early Barstovian of California and Nevada in the form of *Aelurodon asthenostylus*, which quickly expanded eastward to the Great Plains, where it is first recorded in the late early Barstovian of Colorado and then in the late Barstovian of Nebraska. Also in the early Barstovian of California and New Mexico, the *Epicyon* clade is represented by its precursor *Protepicyon raki*. After a significant hiatus in the late Barstovian, true *Epicyon* appears in the Clarendonian of the Great Plains. In the early Clarendonian of California, the *Borophagus* clade evolved its first member *Borophagus littoralis*, which appears to have been confined to California during the entire Clarendonian. The earliest record of the genus outside California is the more derived species *B. pugnator*, which appears in the early Hemphillian of the Great Plains.

In the Gulf Coast, the Florida record may register the latest occurrence of certain clades (i.e., relics), such as *Carpocyon limosus*, in the latest Hemphillian when records of these taxa have all disappeared in the Great Plains and elsewhere. This may also be true of *Epicyon haydeni* and *Borophagus pugnator* in

the Upper Bone Valley deposits, although this is less certain due to possibilities of faunal mixing in these phosphate mines. A possible case of dwarfism is seen in the late early Hemphillian of Florida in the form of *Borophagus orc*. In addition, Florida may be the place of origin for the small *Phlaocyon achoros–multicuspus* clade, although chronological order in this case is not certain.

DIVERSITY

With the present addition of 18 new species, the total number of borophagine species now reaches to 66, a 38% increase over the previous known diversity of 48. The overall canid record in North America (approximately 141 species; fig. 143) exceeds that of the Eurasian hyenids in terms of number of species (Werdelin and Solounias, 1991, listed 79 species), in part because canids have a much longer history that dates back to the late Eocene more than 37 Ma. Hyenids, on the other hand, have a more recent history in the Miocene and later, that is, from 24 Ma to the present. Even after discounting the Paleogene records, the number of North American canids from the Neogene (more than 110) is still more than the Old World hyenids.

As an approximate measure of dental diversity, we adopt the concepts of hyper- and hypocarnivory to describe morphological adaptation in carnivorans. In a broader definition than was originally proposed by Crusafont-Pairó and Truyols-Santonja (1956), we classify a taxon as hypercarnivorous if it possesses any dental tendency toward increased efficiency in shearing, which in canids commonly involves the elongated shearing blades of carnassial teeth, reduction or loss of m1 metaconid, shortened and simplified m1 talonid, and reduction of M2 and m2–m3 (bone-crushing forms are thus included as hypercarnivores in our definition, in contrast to that by Van Valkenburgh [1991], who adopted a narrower definition in order to be more strictly comparable to the catlike adaptations). In contrast, hypocarnivorous forms tend to shorten the shearing blade, and to enlarge and increase complexity of the grinding part of the dentition (m1 talonid and m2–m3). As a coordinate term, mesocarnivory is used to indicate a dentition lacking either of these specializations.

Thus defined, borophagines are roughly composed of 20 hypocarnivorous, 21 hypercarnivorous, and 25 mesocarnivorous species (the boundaries between these categories are not sharply delimited, and the above figures are thus subjective estimates). Hypocarnivorous taxa are concentrated in the Hemingfordian and Barstovian, in the earlier half of the borophagine history, and are all small to medium in size. Only one moderately hypocarnivorous species (*Carpocyon limosus*) was present in the Hemphillian when borophagines were completely dominated by hypercarnivorous taxa. Besides the hypercarnivorous *Euoplocyon* in the Hemingfordian, the vast majority of hypercarnivorous species are in Barstovian through Blancan in age and are all medium- to large-size individuals. Many of these hypercarnivores are further specialized in the durophagous direction, that is, cranial and dental modifications that are adapted for cracking bones. Species in the Aelurodontina clade are the modern equivalent of the African hunting dog (*Lycaon*) or Asiatic dhole (*Cuon*), whereas advanced taxa in the Borophagina clade are ecologically more comparable with modern hyenids, especially the spotted hyena (*Crocuta*). Mesocarnivorous taxa maintain a rather constant presence throughout the history of the Borophaginae except during the latest Tertiary when borophagines had become consistently large in size and decidedly hypercarnivorous. The mesocarnivorous species always provide the ancestral stocks for hypo- and hypercarnivorous lineages.

Postcranial materials for the Borophaginae remain quite limited. Munthe's (1979, 1989) study of borophagine postcranial diversity is in need of updating in light of the present systematic revision, although her basic conclusion is still valid. Her finding of a diverse array of postcranial adaptations, in contrast to the stereotypical view that these hyenoid dogs were noncursorial, bone-crushing scavengers only, is consistent with our own systematic conclusions. Her analysis, however, was confined to medium- to large-size hypercarnivorous borophagines (generally the traditional concept of the group), and she did not consider the richly diverse small and hy-

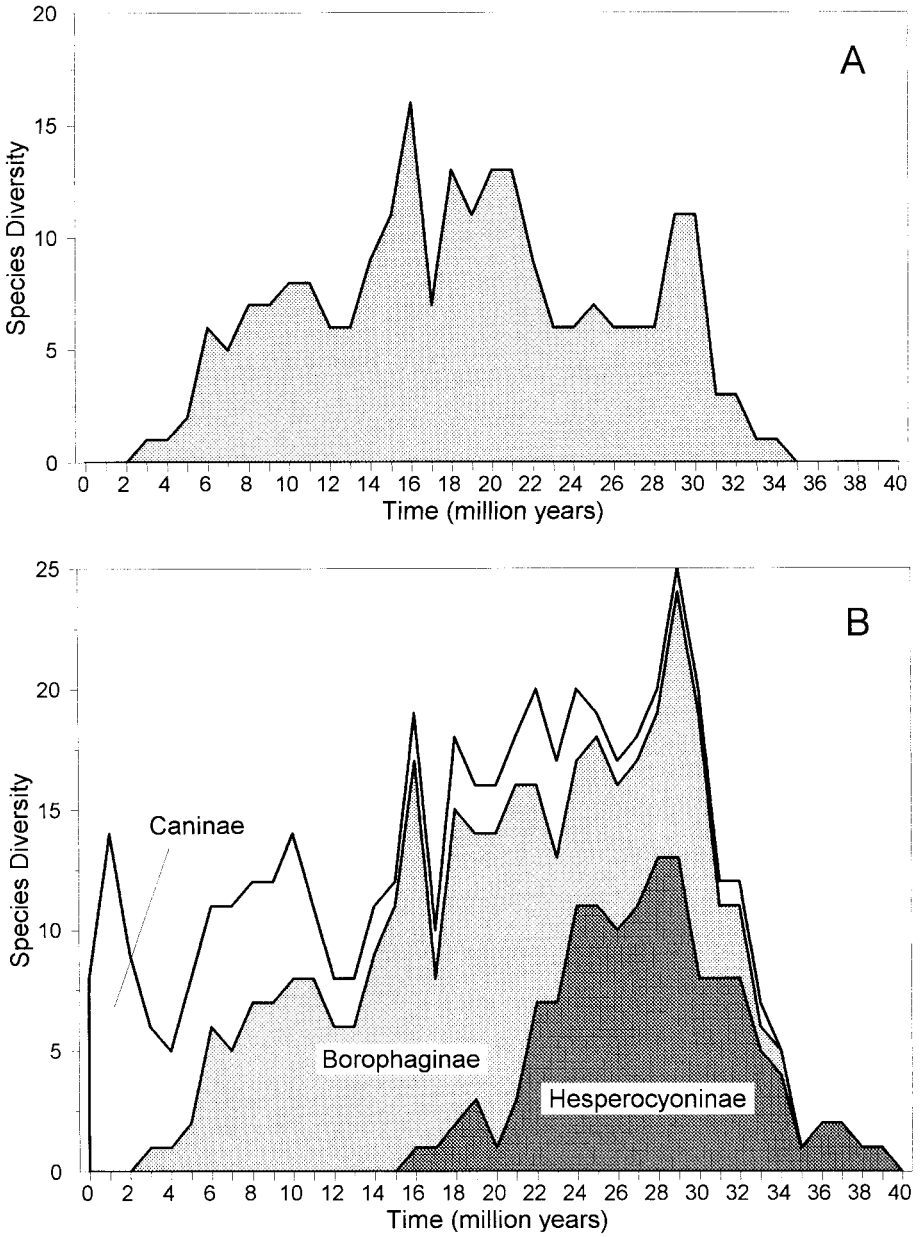

Fig. 143. Patterns of fluctuating species diversity in the Borophaginae (**A**) and in three subfamilies of North American Canidae during the Cenozoic (**B**). Data for the Hesperocyoninae are based on Wang (1994) and those for the Caninae are from unpublished data.

pocarnivorous groups. Figure 144 shows a log-ratio diagram for a few species of borophagines for which postcranial skeletons are relatively complete. One obvious trend in this diagram is that front limbs are proportionally more elongated than the hindlimbs in larger, more hypercarnivorous taxa, a tendency also prominent in the modern hyenids.

Of the 66 recognized species, the average species longevity is approximately 3.4 m.y. (a figure dependent on how hypodigms for each species are assembled, i.e., researchers'

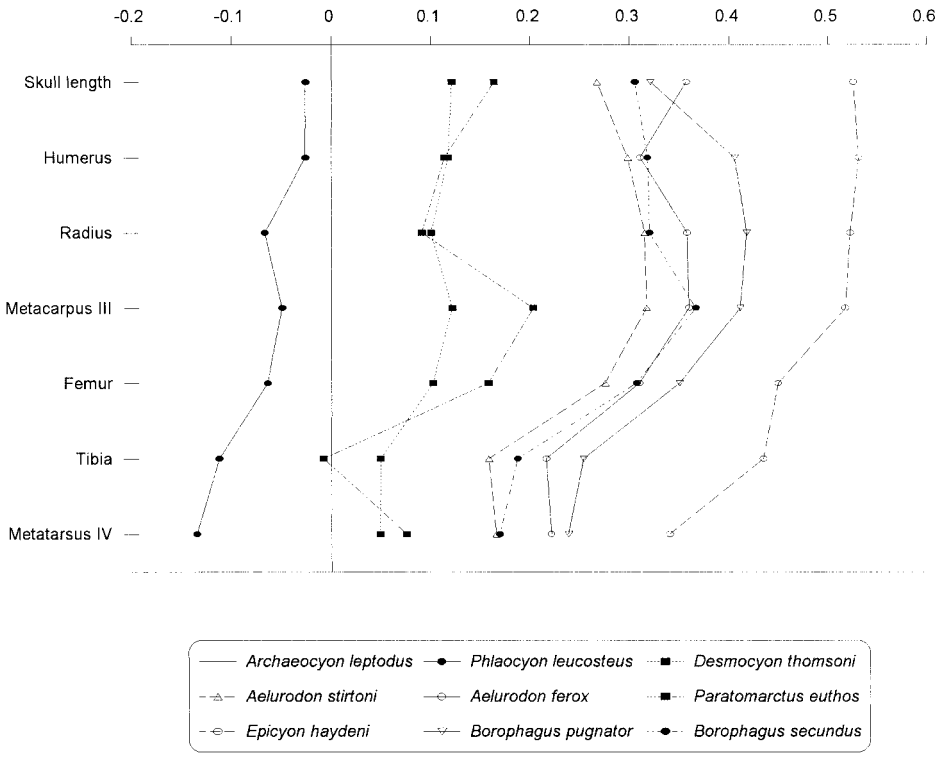

Fig. 144. Log-ratio diagram of six measurements of limb bones from selected borophagine species for which postcranial skeletons are relatively complete. Measurements as defined in Munthe (1989) and data combined from Munthe (1989) and personal measurements.

views of paleospecies as well as their notion of morphological breadth for morphospecies). Given that our treatment of species includes both cladogenetic and anagenetic lineages, the species longevity may be more of a reflection of the rate of morphological evolution than the actual duration of the species. Small mesocarnivorous taxa tend to have a longer species longevity—their rate of morphological evolution seems slower than the larger, more specialized taxa. The chronological limits of each taxon are also influenced by the precision of assignment of the limits of the geochron for each hypodigm. Perhaps a more meaningful measure is the longevity of clades. Again, clades of small- to medium-size hypocarnivores (Phlaocyonini, 15.2 m.y.; Cynarctina, 9.5 m.y.) seem to slightly outlive clades of large hypercarnivores (Aelurodontina, 7 m.y.; hypercarnivorous part of Borophagina, 14 m.y.).

Early in the Oligocene (about 30 Ma) both hesperocyonines and borophagines achieved near maximum species diversity (fig. 143), probably within the first 6 m.y. of the existence of the borophagines. This rapid cladogenesis yielded the basis for the Phlaocyonini as well as seeing the continuation of a number of archaic clades of some adaptive diversity. At this time the Canidae were more diverse in terms of species numbers than during any other period. This seems largely due to the mostly opposite adaptive pathways followed by these subfamilies: the Hesperocyoninae were largely hypercarnivorous, the Borophaginae largely exploited hypocarnivorous adaptations, and the rare Caninae were mesocarnivorous. It may be significant that this diversity coincided with a major environmental change (a long episode of Antarctic glaciation) and a corresponding chronofaunal reorganization (Tedford et al. 1996). The Oligocene (28–24 Ma) drop in borophagine diversity is partly an artifact of the

poor record of the group in the Great Plains during an interval whose paleontological history is not well understood.

Hypocarnivorous adaptations continued to be dominant among borophagines into the early Miocene (late Arikareean) and to involve the appearance of additional lineages as hesperocyonines took a drastic drop in diversity. The appearance of early members of the Borophagini (*Cormocyon* and *Desmocyon*) in the late Oligocene and early Miocene augmented the diverse phlaocyonines to initiate the major phase of borophagine diversity during the early Miocene. This was largely brought about by rapid cladogenesis of meso- to hypercarnivorous borophagines, the basal stocks of both the Aelurodontina and Borophagina, and a further development of another hypocarnivorous group, the Cynarctina. This diverse array of species flourished from the late Hemingfordian into the Barstovian during the organization of the Miocene chronofauna that produced the greatest ungulate diversity in North America (Webb et al., 1995). Borophagine species diversity drops rapidly after 16 Ma, at the Barstovian–Hemingfordian boundary, tracking but peaking before the high point of ungulate diversity. In the Barstovian and Clarendonian, cladogenesis is largely confined to the Borophagina, especially within *Borophagus* during the Hemphillian (late Miocene). In the Hemphillian, competition with immigrants felids, large mustelids, and giant ursids intensified, leading to durophagous adaptations among the borophagines as a vital survival strategy. The presence of the ecomorph Eurasian procyonid *Simocyon* (Wang, 1997) in North America at this time gives further evidence of openings in the niche for bone-processing carnivores in the late Miocene. In the Blancan, the highly derived *Borophagus diversidens*, last of the subfamily, continues in the face of competition from hyenas (*Chasmaporthetes*) and the rise of pack hunting wolves (*Canis edwardi*) as the Caninae enter their rapid phase of cladogenesis during the Pliocene and Pleistocene.

As a subfamily of canids, the Borophaginae, although confined to the Tertiary of North America, is notable among families of carnivorans in its richness of morphological adaptations. Borophagines encompassed the combined ecological roles played by modern canids, hyenids, and procyonids, a reflection of the evolutionary flexibility of canids and their ability for rapid diversification given proper opportunities (Van Valkenburgh, 1991). In the later Tertiary, borophagines are about equal to hyenids in their range of meso- and hypercarnivorous adaptations, although the borophagines have fewer bone-crushing (durophagous) clades. There is a close parallel in the ecological roles played by the North American borophagines and the late Tertiary hyenids in Eurasia. While there are some durophagous canids (*Epicyon*, *Borophagus*, and possibly certain *Aelurodon*) that are the Tertiary trophic equivalent of modern hyenas, there are also a large number of extinct hyenids (e.g., *Ictitherium*, *Thalassictis*, *Hyaenictitherium*) that are the Tertiary equivalent of mesocarnivorous canids. This largely overlapping trophic status may have been a reason that the Eurasian hyenid and North American canid faunas were confined to their own continents despite the evidence of considerable interchange of other carnivorans and ungulates during the Tertiary (Tedford et al., 1987). Only when the borophagines were nearly extinct did a single hyenid lineage (*Chasmaporthetes*) establish itself in North America. To date, no such record of a borophagine has been found in the Tertiary of Eurasia.

REFERENCES

Addicott, W. O.
1972. Provincial middle and late Tertiary molluscan stages, Temblor Range, California. Proc. Pac. Coast Miocene Biostratigraphic Symp. Pac. Section S.E.P.M. Meeting., Bakersfield, Ca: 1–26.

Adegoke, O. S.
1969. Stratigraphy and paleontology of the marine Neogene formations of the Coalinga region, California. Univ. California Publ. Geol. Sci. 80: 1–269.

Barbat, W. F., and A. A. Weymouth
1931. Stratigraphy of the *Borophagus littor-*

alis locality, California. Univ. California Publ. Bull. Dep. Geol. Sci. 21: 25–36.

Barbour, E. H., and H. J. Cook
1914. Two new fossil dogs of the genus *Cynarctus* from Nebraska. Nebraska Geol. Surv. 4: 225–227.
1917. Skull of *Aelurodon platyrhinus* sp. nov. Ibid. 7: 173–180.

Baskin, J. A.
1980. The generic status of *Aelurodon* and *Epicyon* (Carnivora, Canidae). J. Paleontol. 54: 1349–1351.
1998. Evolutionary trends in the late Miocene hyena-like dog *Epicyon* (Carnivora, Canidae). *In* Y. Tomida, L. J. Flynn, and L. L. Jacobs (eds.), Advances in vertebrate paleontology and geochronology. National Science Museum, Tokyo, Monogr. 14: 191–214.

Baskin, J. A., and R. H. Tedford
1996. Small arctoid and feliform carnivorans. *In* D. R. Prothero and R. J. Emry, (eds.), The terrestrial Eocene–Oligocene transition in North America, Pt. II: Common vertebrates of the White River chronofauna, pp. 486–497. Cambridge: Cambridge Univ. Press.

Beaumont, G. de
1964. Essai sur la position taxonomique des genres *Alopecocyon* Viret et *Simocyon* Wagner (Carnivora). Eclogae Geol. Helv. 57: 829–836.

Becker, J. J.
1980. The Star Valley Local Fauna (early Hemphillian), southwestern Idaho. Master's thesis, Dept. Zool., Univ. of Idaho, 71 pp.

Berry, C. T.
1938. A Miocene dog from Maryland. Proc. U.S. Natl. Mus. 85: 159–161.

Berta, A.
1988. Quaternary evolution and biogeography of the large South American Canidae (Mammalia: Carnivora). Univ. California Publ. Geol. Sci. 132: 1–149.

Bjork, P. R.
1970. The Carnivora of the Hagerman local fauna (late Pliocene) of southwestern Idaho. Trans. Am. Philos. Soc. 60: 1–54.

Bode, F. D.
1935. The fauna of *Merychippus* zone, north Coalinga district, California. Contrib. Carnegie Inst. Washington Publ. 453: 65–96.

Cande, S. C., and D. V. Kent
1992. A new geomagnetic polarity time scale for the late Cretaceous and Cenozoic. J. Geophys. Res. 97: 13,917–13,951.
1995. Revised calibration of the geomagnetic polarity timescale for the late Cretaceous and Cenozoic. Ibid. 100: 6,093–6,095.

Cassiliano, M. L.
1999. Biostratigraphy of Blancan and Irvingtonian mammals in the Fish Creek-Vallecito section, southern California, and a review of the Blancan-Irvingtonian boundary. J. Vert. Paleontol. 19: 169–186.

Chorn, J., and K. N. Whetstone
1978. On the use of the term nomen vanum in taxonomy. J. Paleontol. 52: 494.

Churcher, C. S.
1960. Cranial variation in the North American red fox. J. Mamm. 41: 349–360.

Clutton-Brock, J., G. B. Corbet, and M. Hills
1976. A review of the family Canidae, with a classification by numerical methods. Bull. British Mus. (Nat. Hist.) Zool. 29: 119–199.

Colbert, E. H.
1939. Carnivora of the Tung Gur Formation of Mongolia. Bull. Am. Mus. Nat. Hist. 76: 47–81.

Condon, T.
1896. Scientific description of two new fossil dogs. Bull. Univ. Oregon 2: 11.

Conrad, G. S.
1980. The biostratigraphy and mammalian paleontology of the Glenns Ferry Formation from Hammett to Oreana, Idaho. Ph.D. diss., Idaho State Univ., Pocatello.

Cook, H. J.
1909. Some new carnivora from the lower Miocene beds of western Nebraska. Nebraska Geol. Surv. 3: 262–272.
1912. Faunal lists of the Tertiary formations of Sioux County, Nebraska. Ibid. 7: 33–45.
1914. A new canid from the lower Pliocene of Nebraska. Ibid. 7: 49–50.
1922. A Pliocene fauna from Yuma County, Colorado, with notes on the clearly related Snake Creek beds from Nebraska. Proc. Colorado Mus. Nat. Hist. 4: 3–30.
1930. New rhinoceroses from the Pliocene of Colorado and Nebraska. Ibid. 9: 44–51.

Cook, H. J., and J. R. Macdonald
1962. New Carnivora from the Miocene and Pliocene of western Nebraska. J. Paleontol. 36: 560–567.

Cope, E. D.
1873. Third notice of extinct vertebrata from the Tertiary of the plains. Palaeontol. Bull. 16: 1–8.
1877. The extinct vertebrate obtained in New Mexico by parties of the expedition of 1874. U.S. Geogr. Surv. W. 100th Merid. (Wheeler), Rep. 4: 1–370.
1878. On some of the characters of the Miocene fauna of Oregon. Paleontol. Bull. 30: 1–16.
1879a. Observations on the faunae of the Miocene Tertiaries of Oregon. Bull. U.S. Geol. Geogr. Surv. Territories 1880, 5: 55–69.
1879b. Second contribution to a knowledge of the Miocene Fauna of Oregon. Proc. Am. Philos. Soc. 18: 370–376.
1881a. On the Canidae of the Loup Fork Epoch. Bull. U.S. Geol. Geogr. Surv. Territories 6: 387–390.
1881b. On the Nimravidae and Canidae of the Miocene period. Ibid. 6: 165–181.
1883. On the extinct dogs of North America. Am. Nat. 17: 235–249.
1884. The Vertebrata of the Tertiary formations of the West, book I. Rep. U.S. Geol. Surv. Territories 3: 1–1009.
1889. The mechanical cause of the development of the hard parts of the Mammalia. J. Morph. 3: 137–280.
1890. A new dog from the Loup Fork Miocene. Am. Nat. 24: 1067–1068.
1892. A hyena and other Carnivora from Texas. Ibid. 26: 1028–1029.
1893. A preliminary report on the vertebrate paleontology of the Llano Estacado. 4th Annu. Rep. Geol. Surv. Texas: 1–136.

Cope, E. D., and W. D. Matthew
1915. Hitherto unpublished plates of Tertiary Mammalia and Permian Vertebrata. Am. Mus. Nat. Hist. Monogr. Ser. 2.

Corner, R. G.
1976. An early Valentinian vertebrate local fauna from southern Webster County, Nebraska. Master's thesis, Univ. Nebraska, Lincoln, 311 pp.

Crusafont-Pairó, M., and J. Truyols-Santonja
1956. A biometric study of the evolution of fissiped carnivores. Evolution 10: 314–332.

Czaplewski, N. J., R. L. Cifelli, and W. Langston, Jr.
1994. Catalog of type and figured fossil vertebrates, Oklahoma Museum of Natural History. Oklahoma Geol. Surv. Spec. Publ. 94-1: 1–35.

Dahr, E.
1949. On the systematic position of *Phlaocyon leucosteus* Matthew and some related forms. Arkiv för Zool. 41A: 1–15.

Dalquest, W. W.
1968. The bone-eating dog, *Borophagus diversidens* Cope. Q. J. Florida Acad. Sci. 31: 115–129.
1969. Pliocene carnivores of the Coffee Ranch (type Hemphill) Local Fauna. Bull. Texas Mem. Mus. 15: 1–44.
1978. Early Blancan mammals of the Beck Ranch Local Fauna of Texas. J. Mamm. 59: 269–298.
1983. Mammals of the Coffee Ranch Local Fauna, Hemphillian of Texas. Pearce-Sellards Ser. Texas Mem. Mus. 38: 1–41.

Dalquest, W. W., and J. T. Hughes
1966. A new mammalian local fauna from the lower Pliocene of Texas. Trans. Kansas Acad. Sci. 69: 79–87.

Dalquest, W. W., J. A. Baskin, and G. E. Schultz
1996. Fossil mammals from a late Miocene (Clarendonian) site in Beaver County, Oklahoma. *In* Contributions in mammalogy: a memorial volume honoring Dr. J. Knox Jones, Jr., pp. 107–137. Mus. Texas Tech Univ.

Dayan, M., D. Simberloff, E. Tchernov, and Y. Yom-Tov
1992. Canine carnassials: character displacement in the wolves, jackals, and foxes of Israel. Biol. J. Linn. Soc. 45: 315–331.

Dayan, M., E. Tchernov, Y. Yom-Tov, and D. Simberloff
1989. Ecological character displacement in Saharo-Arabian *Vuples*: outfoxing Bergmann's rule. Oikos 55: 263–272.

Douglass, E.
1903. Vertebrates from Montana Tertiary. Ann. Carnegie Mus. 2: 145–199.

Downs, T.
1956. The Mascall Fauna from the Miocene of Oregon. Univ. California Publ. Geol. Sci. 31: 199–354.

Emry, R. J., P. R. Bjork, and L. S. Russell
1987. The Chadronian, Orellan, and Whitneyan North American land mammal ages. *In* M. O. Woodburne (ed.), Cenozoic mammals of North America, geochronology and biostratigraphy, pp. 118–152. Berkeley: Univ. California Press.

Emry, R. J., and R. E. Eshelman
1998. The early Hemingfordian (early Miocene) Pollack Farm Local Fauna: first

Tertiary land mammals described from Delaware. *In* R. N. Benson (ed.), Geology and paleontology of the lower Miocene Pollack Farm fossil site, Delaware, pp. 153–173. Delaware Geological Survey Special Publication No. 21.

Evander, R. L.
1986. Carnivores of the Railway Quarries Local Fauna. Trans. Nebraska Acad. Sci. 14: 25–34.

Evans, H. E., and G. C. Christensen
1979. Miller's anatomy of the dog. Philadelphia: W. B. Saunders.

Farris, J. S.
1989. HENNIG86, version 1.5. Port Jefferson Station, NY.

Fejfar, O., and N. Schmidt-Kittler
1984. *Sivanasua* and *Euboictis* n. gen.—zwei pflanzenfressende Schleichkatzen-vorläufer (Viverridae, Carnivora, Mammalia) im europäischen Untermiozän. Mainz. Geowiss. Mitt. 13: 49–72.
1987. *Lophocyon carpathicus* nov. gen. nov. sp. aus dem Jungtertiär der Ostslowakei und eine neue unterfamilie dershleikatzen (Viverridae). Palaeontographica 199: 1–22.

Forsten, A.
1970. The late Miocene Trail Creek mammalian fauna. Contrib. Geol. Univ. Wyoming 9: 39–51.

Foster, J. H., and A. M. Stalker
1976. Paleomagnetic stratigraphy of the Wellsch Valley site, Saskatchewan. Geol. Surv. Canada Pap. 76-1c: 191–193.

Frailey, D.
1978. An early Miocene (Arikareean) fauna from northcentral Florida (the SB-1A Local Fauna). Univ. Kansas Mus. Nat. Hist. Occas. Pap. 75: 1–20.
1979. The large mammals of the Buda Local Fauna (Arikareean: Alachua County, Florida). Bull. Florida State Mus. Biol. Sci. 24: 123–173.

Fremd, T. J., E. A. Bestland, and G. J. Retallack
1994. John Day Basin paleontology field trip guide and road log. For 1994 Society of Vertebrate Paleontology Annual Meeting, Seattle, Washington. John Day Fossil Beds National Monument 94-1.

Fremd, T. J., and X. Wang
1995. Resolving blurred faunas: biostratigraphy in John Day Fossil Bed National Monument. *In* V. L. Santucci and L. McClelland (eds.), National Park Service paleontological research, United States Department of the Interior, pp. 73–76.

Freudenberg, W.
1910. Die Säugetierfauna dies Pliocäns und Postpliocäns von Mexiko, I: carnivoren. Geol. Palaeontol. Abh. Jena 9: 193–231.

Frick, C.
1926. The Hemicyoninae an American Tertiary bear. Bull. Am. Mus. Nat. Hist. 56: 1–119.

Galbreath, E. C.
1953. A contribution to the Tertiary geology and paleontology of northeastern Colorado. Univ. Kansas Paleontol. Contrib. 4: 1–120.
1956. Remarks on *Cynarctoides arcidens* from the Miocene of northeastern Colorado. Trans. Kansas Acad. Sci. 59: 373–378.

Galusha, T.
1966. The Zia Sand Formation, new early to medial Miocene beds in New Mexico. Am. Mus. Novitates 2271: 12 pp.
1975a. Childs Frick and the Frick Collection of fossil mammals. Curator 18: 5–15.
1975b. Stratigraphy of the Box Butte Formation, Nebraska. Bull. Am. Mus. Nat. Hist. 156: 1–68.

Gauthier, J. A., A. G. Kluge, and T. Rowe
1988. Amniote phylogeny and the importance of fossils. Cladistics 4: 105–209.

Gawne, C. E.
1973. Faunas and sediments of the Zia Sand, medial Miocene of New Mexico. Unpubl. Ph.D. diss., Columbia University, New York, 359 pp.
1975. Rodents from the Zia Sand Miocene of New Mexico. Am. Mus. Novitates 2586: 25 pp.

Gazin, C. W.
1932. A Miocene mammalian fauna from southeastern Oregon. Carnegie Inst. Washington Publ. 418: 37–86.
1936. A study of the fossil horse remains from the upper Pliocene of Idaho. Proc. U.S. Natl. Mus. 83: 281–320.

Gingerich, P. D., and D. A. Winkler
1979. Patterns of variation and correlation in the dentition of the red fox, *Vulpes vuples*. J. Mamm. 60: 691–704.

Ginsburg, L.
1966. Les amphicyons des Phosphorites du Quercy. Ann. Paléontol. 52: 23–64.

Gittleman, J. L., and B. Van Valkenburgh
1997. Sexual dimorphism in the canines and skulls of carnivores: effects of size,

phylogeny, and behavioural ecology. J. Zool. London 242: 97–117.

Green, M.
1948. A new species of dog from the lower Pliocene of California. Univ. California Publ. Bull. Dept. Geol. Sci. 28: 81–90.
1954. A cynarctine from the upper Oligocene of South Dakota. Trans. Kansas Acad. Sci. 57: 218–220.
1971. Addition to the Mission vertebrate fauna, lower Pliocene of South Dakota. J. Paleontol. 45: 486–490.

Gregory, J. T.
1942. Pliocene vertebrates from Big Spring Canyon, South Dakota. Univ. California Publ. Bull. Dept. Geol. Sci. 26: 307–446.

Gustafson, E. P.
1978. The vertebrate faunas of the Pliocene Ringold Formation, south-central Washington. Bull. Mus. Nat. Hist. Univ. Oregon 23: 1–62.

Hall, E. R., and W. W. Dalquest
1962. A new doglike carnivore, genus *Cynarctus*, from the Clarendonian, Pliocene, of Texas. Univ. Kansas Publ. Mus. Nat. Hist. 14: 137–138.

Hall, E. R., and H. T. Martin
1930. A skull of *Nothocyon* from the John Day Oligocene. Univ. Kansas Sci. Bull. 19: 283–287.

Harrison, J. A.
1983. The Carnivora of the Edson Local Fauna (late Hemphillian), Kansas. Smithson. Contrib. Paleobiol. 54: 1–42.

Hatcher, J. B.
1893. On a small collection of vertebrate fossils from the Loup Fork beds of northwestern Nebraska, with note on the geology of the region. Am. Nat. 28: 236–248.

Hay, O. P.
1902. Bibliography and catalogue of fossil Vertebrata of North America. Bull. U.S. Geol. Surv. 179: 1–868.
1924. Description of some fossil vertebrates from the upper Miocene of Texas. Proc. Biol. Soc. Washington 37: 1–20.

Hayden, F. V.
1858. Explorations under the War Department, explanations of a second edition of a geological map of Nebraska and Kansas, based upon information obtained in an expedition to the Black Hills, under the command of Lieut. G. K. Warren. Proc. Acad. Nat. Sci. Philadelphia 10: 139–158.

Henshaw, P. C.
1942. A Tertiary mammalian fauna from the San Antonio Mountains near Tonopah, Nevada. Carnegie Inst. Washington Publ. 530: 77–168.

Hesse, C. J.
1936. A Pliocene vertebrate fauna from Optima, Oklahoma. Univ. California Publ. Bull. Dept. Geol. Sci. 24: 57–70.
1940. A Pliocene vertebrate fauna from Higgins, Lipscomb County, Texas. Univ. Texas Publ. 3945: 671–698.

Hibbard, C. W.
1944. Two new mammals from the middle Pliocene of Seward County, Kansas. Bull. Univ. Kansas 30: 107–114.
1950. Mammals of the Rexroad Formation from Fox Canyon, Kansas. Contrib. Mus. Paleontol. Univ. Michigan 8: 113–192.

Hibbard, C. W., and E. S. Riggs
1949. Upper Pliocene vertebrates from Keefe Canyon, Meade County, Kansas. Bull. Geol. Soc. Am. 60: 829–860.
1955. Pleistocene vertebrates from the Upper Becerra Formation (Becerra Superior), Valley of Tequixquiac, Mexico, with notes on other Pleistocene forms. Univ. Michigan Mus. Paleont. Contrib. 12: 47–96.

Honey, J. G., and G. A. Izett
1988. Paleontology, taphonomy, and stratigraphy of the Browns Park Formation (Oligocene and Miocene) near Maybell, Moffat County, Colorado. U.S. Geol. Surv. Prof. Pap. 1358: 1–52.

Hough, J. R.
1944. The auditory region in some Miocene carnivores. J. Paleontol. 22: 573–600.
1948. The auditory region in some members of the Procyonidae, Canidae, and Ursidae. Bull. Am. Mus. Nat. Hist. 92: 73–118.

Hunt, R. M., Jr.
1974. The auditory bulla in Carnivora: an anatomical basis for reappraisal of carnivore evolution. J. Morphol. 143: 21–76.
1977. Basicranial anatomy of *Cynelos* Jourdan (Mammalia: Carnivora), an Aquitanian amphicyonid from the Allier Basin, France. J. Paleontol. 51: 826–843.

Hunter, J. P., and J. Jernvall
1995. The hypocone as a key innovation in mammalian evolution. Proc. Natl. Acad. Sci. USA 92: 10,718–10,722.

Huxley, T. H.
1880. On the cranial and dental characters of

the Canidae. Proc. Zool. Soc. London 16: 238–288.

International Commission on Zoological Nomenclature
1985. International Code of Zoological Nomenclature, 3rd ed. Adopted by the XX General Assembly of the International Union of Biological Sciences, Helsinki, August 1979. London: Int. Trust Zool. Nomencl., 338 pp.

Johnston, C. S.
1939a. Preliminary report on the late middle Pliocene Axtel locality, and the description of a new member of the genus *Osteoborus*. Am. J. Sci. 237: 895–898.
1939b. A skull of *Osteoborus validus* from the early middle Pliocene of Texas. J. Paleontol. 13: 526–530.

Johnston, C. S., and D. E. Savage
1955. A survey of various late Cenozoic vertebrate faunas of the Panhandle of Texas, Pt. I, Introduction, description of localities, preliminary faunal lists. Univ. California Publ. Geol. Sci. 31: 27–50.

Jolicoeur, P.
1975. Sexual dimorphism and geographical distance as factors of skull variation in the wolf *Canis lupus* L. *In* M. W. Fox (ed.), The wild canids, their systematics, behavioral ecology and evolution, pp. 54–61. New York: Van Nostrand Reinhold.

Kitts, D. B.
1957. A Pliocene vertebrate fauna from Ellis County, Oklahoma. Oklahoma Geol. Surv. Circ. 48: 1–26.
1964. *Aelurodon*, an addition to the Durham local fauna, Roger Mills County, Oklahoma. Oklahoma Geol. Notes 24: 76–78.

Kolenosky, G. B., and R. O. Standfield
1975. Morphological and ecological variation among gray wolves (*Canis lupus*) of Ontario, Canada. *In* M. W. Fox (ed.), The wild canids, their systematics, behavioral ecology and evolution, pp. 62–72. New York: Van Nostrand Reinhold.

Koufos, G. D., L. de Bonis, and S. Sen
1994. *Lophocyon paraskevaidisi*, a new viverrid (Carnivora, Mammalia) from the middle Miocene of Chios Island, Greece. Geobios 28: 511–523.

Kretzoi, M.
1968. New generic names for homonyms. Vert. Hungarica 10: 163–166.

Lawrence, B., and W. H. Bossert
1967. Multiple character analysis of *Canis lupus latrans* and *familiaris*, with a discussion of the relationships of *Canis niger*. Am. Zool. 7: 223–232.
1975. Relationships of North American *Canis* shown by a multiple character analysis of selected populations. *In* M. W. Fox (ed.), The wild canids, their systematics, behavioral ecology and evolution, pp. 73–86. New York: Van Nostrand Reinhold.

Lay, D. M.
1972. The anatomy, physiology, and functional significance and evolution of specialized hearing organs of gerbilline rodents. J. Morph. 138: 41–120.

Leidy, J.
1858. Notice of remains of extinct Vertebrata, from the valley of the Niobrara River, collected during the exploring expedition of 1857, in Nebraska, under the command of Lieut. G. K. Warren, U.S. Top. Eng., by Dr. F. V. Hayden, Geologist to the expedition. Proc. Acad. Nat. Sci. Philadelphia 1858: 20–29.
1869. The extinct mammalian fauna of Dakota and Nebraska, including an account of some allied forms from other localities, together with a synopsis of the mammalian remains of North America. J. Acad. Nat. Sci. Philadelphia 7: 1–472.
1871. Report on the vertebrate fossils of the Tertiary formations of the West. U.S. Geol. Surv. Wyoming 2nd Annu. Rep. F. V. Hayden, U.S. Geol. pp. 340–370.

Leite, M. B.
1990. Stratigraphy and mammalian paleontology of the Ash Hollow Formation (Upper Miocene) on the north shore of Lake McConaughy, Keith County, Nebraska. Contrib. Geol. Univ. Wyoming 28: 1–29.

Loomis, F. B.
1932. The small carnivores of the Miocene. Am. J. Sci. 24: 316–329.
1936. Three new Miocene dogs and their phylogeny. J. Paleontol. 10: 44–52.

Lucas, S. G., and W. Oakes
1986. Pliocene (Blancan) vertebrates from the Palomas Formation, south-central New Mexico. New Mexico Geol. Soc. guidebook, 37th Field Conf.: 249–255.

Lundelius, E. L., C. S. Churcher, T. Downs, C. R. Harington, E. H. Lindsay, G. E. Schultz, H. A. Semken, S. D. Webb, and R. J. Zakrzewski
1987. The North American Quaternary sequence. *In* M. O. Woodburne (ed.), Cenozoic mammals of North America,

geochronology and biostratigraphy, pp. 211–235. Berkeley: Univ. California Press.

Macdonald, J. R.
1948. The Pliocene carnivores of the Black Hawk Ranch Fauna. Univ. California Publ. Bull. Dept. Geol. Sci. 28: 53–80.
1956. A new Clarendonian mammalian fauna from the Truckee Formation of western Nevada. J. Paleontol. 30: 186–202.
1959. The middle Pliocene mammalian fauna from Smiths Valley, Nevada. Ibid. 33: 872–887.
1960. An early Pliocene fauna from Mission, South Dakota. Ibid. 34: 961–982.
1963. The Miocene faunas from the Wounded Knee area of western South Dakota. Bull. Am. Mus. Nat. Hist. 125: 141–238.
1970. Review of the Miocene Wounded Knee faunas of southwestern South Dakota. Bull. Los Angeles Cty Mus. Nat. Hist. 8: 1–82.

Maddison, W. P., and D. R. Maddison
1992. MacClade: analysis of phylogeny and character evolution. Sunderland, MA: Sinauer.

Maddison, W. P., M. J. Donoghue, and D. R. Maddison
1984. Outgroup analysis and parsimony. Syst. Zool. 33: 83–103.

Martin, H. T.
1928. Two new carnivores from the Pliocene of Kansas. J. Mamm. 9: 233–236.

Martin, L. D.
1989. Fossil history of the terrestrial Carnivora. *In* J. L. Gittleman (ed.), Carnivore behavior, ecology, and evolution, pp. 536–568. Ithaca, NY: Cornell Univ. Press.

Matthew, W. D.
1899. A provisional classification of the freshwater Tertiary of the West. Bull. Am. Mus. Nat. Hist. 12: 19–75.
1901. Fossil mammals of the Tertiary of northeastern Colorado. Mem. Am. Mus. Nat. Hist. 1: 355–448.
1902. New Canidae from the Miocene of Colorado. Bull. Am. Mus. Nat. Hist. 16: 281–290.
1907. A lower Miocene fauna from South Dakota. Ibid. 23: 169–219.
1909. Faunal lists of the Tertiary Mammalia of the West. *In* H. F. Osborn (ed.), Cenozoic mammal horizons of western North America, with faunal lists of the Tertiary Mammalia of the West, by W. D. Matthew. Bull. U.S. Geol. Surv. 361: 1–138.
1918. Contributions to the Snake Creek fauna with notes upon the Pleistocene of western Nebraska, American Museum Expedition of 1916. Bull. Am. Mus. Nat. Hist. 38: 183–229.
1924. Third contribution to the Snake Creek fauna. Ibid. 50: 59–210.
1930. The phylogeny of dogs. J. Mamm. 11: 117–138.
1932. New fossil mammals from the Snake Creek quarries. Am. Mus. Novitates 540: 8 pp.

Matthew, W. D., and H. J. Cook
1909. A Pliocene fauna from western Nebraska. Bull. Am. Mus. Nat. Hist. 26: 361–414.

Matthew, W. D., and G. W. Gidley
1904. New or little known mammals from the Miocene of South Dakota, American Museum Expedition of 1903. Bull. Am. Mus. Nat. Hist. 20: 241–268.

Matthew, W. D., and R. A. Stirton
1930. Osteology and affinities of *Borophagus*. Univ. California Publ. Bull. Dept. Geol. Sci. 19: 171–216.

Mawby, J. E.
1964. Species groups of the canid genus *Aelurodon*. Geol. Soc. Am. Cordilleran Sect., 60th Annu. Meeting Prog.: 43 (abstract).
1965. Pliocene vertebrates and stratigraphy in Stewart and Ione valleys, Nevada. Ph.D. diss., Univ. California, Berkeley.

McDonald, G.
MS. Hemphillian to Blancan borophagine dogs (Mammalia: Carnivora) from Idaho.

McGrew, P. O.
1935. A new *Cynodesmus* from the lower Pliocene of Nebraska with notes on the phylogeny of dogs. Univ. California Publ. Bull. Dept. Geol. Sci. 23: 305–312.
1937. The genus *Cynarctus*. J. Paleontol. 11: 444–449.
1938a. Dental morphology of the Procyonidae with a description of *Cynarctoides*, gen. nov. Field Mus. Nat. Hist. Geol. Ser. 6: 323–339.
1938b. The Burge Fauna, a lower Pliocene mammalian assemblage from Nebraska. Univ. California Publ. Bull. Dept. Geol. Sci. 24: 309–328.
1939. *Phlaocyon*—a correction. J. Paleontol. 13: 365.
1941. A new procyonid from the Miocene of

Nebraska. Field Mus. Nat. Hist. Geol. Ser. 8: 33–36.
1944a. An *Osteoborus* from Honduras. Ibid. 8: 75–77.
1944b. The *Aelurodon saevus* group. Ibid. 8: 79–84.

McKenna, M. C.
1966. Synopsis of Whitneyan and Arikareean camelid phylogeny. Am. Mus. Novitates 2253: 11 pp.

McKenna, M. C., and S. K. Bell
1997. Classification of mammals above the species level. New York: Columbia Univ. Press.

Meade, G. E.
1945. The Blanco Fauna. Univ. Texas Publ. 4401: 509–556.

Merriam, J. C.
1903. The Pliocene and Quaternary Canidae of the Great Valley of California. Univ. California Publ. Bull. Dept. Geol. Sci. 3: 277–290.
1906. Carnivora from the Tertiary formations of the John Day region. Ibid. 5: 1–64.
1911. Tertiary mammal beds of Virgin Valley and Thousand Creek in northwestern Nevada. Ibid. 6: 199–306.
1913. Notes on the canid genus *Tephrocyon*. Ibid. 7: 359–372.
1916. Tertiary vertebrate fauna from the Cedar Mountain region of western Nevada. Ibid. 9: 161–198.
1919. Tertiary mammalian faunas of the Mohave desert. Univ. California Publ. Bull. Dept. Biol. Sci. 11: 437–585.

Merriam, J. C., and W. J. Sinclair
1907. Tertiary faunas of the John Day region. Univ. California Publ. Bull. Dep. Geol. Sci. 5: 171–205.

Messenger, K. K., and C. L. Messenger
1977. Carnivores from the Jamber Local Fauna (Pliocene, Valentinian), Boyd County, Nebraska. Trans. Nebraska Acad. Sci. 4: 95–101.

Miller, W. E.
1980. The late Pliocene Las Tunas Local Fauna from southernmost Baja California, Mexico. J. Paleontol. 54: 762–805.

Miller, W. E., and O. Carranza-Castañeda
1998. Late Tertiary canids from central Mexico. J. Paleontol. 72: 546–556.

Mones, A.
1989. Nomen dubium vs. nomen vanum. J. Vertebr. Paleontol. 9: 232–234.

Munthe, J.
1988. Miocene mammals of the Split Rock area, Granite Mountains Basin, central Wyoming. Univ. California Publ. Dept. Geol. Sci. 126: 1–136.

Munthe, K.
1979. The skeleton of the Borophaginae (Carnivora, Canidae): morphology and function. Ph.D. diss., Univ. California, Berkeley, 274 pp.
1989. The skeleton of the Borophaginae (Carnivora, Canidae), morphology and function. Univ. California Publ. Dept. Geol. Sci. 133: 1–115.
1998. Canidae. *In* C. M. Janis, K. M. Scott, and L. L. Jacobs (eds.), Evolution of Tertiary mammals of North America, Vol. 1: Terrestrial carnivores, ungulates, and ungulatelike mammals, pp. 124–143. Cambridge: Cambridge Univ. Press.

Norell, M. A.
1992. Taxi origin and temporal diversity: the effect of phylogeny. *In* M. J. Novacek and Q. D. Wheeler (eds.), Extinction and phylogeny, pp. 89–118. New York: Columbia Univ. Press.

Nowak, R. M.
1979. North American Quaternary *Canis*. Univ. Kansas Mus. Nat. Hist. Monogr. 6: 1–154.

Olsen, S. J.
1956a. The Caninae of the Thomas Farm Miocene. Breviora 26: 1–12.
1956b. A new species of *Osteoborus* from the Bone Valley Formation of Florida. Florida Geol. Surv. Spec. Publ. 2: 1–5.
1958. Some problematical carnivores from the Florida Miocene. J. Paleontol. 32: 595–602.

Olson, E. C., and P. O. McGrew
1941. Mammalian fauna from the Pliocene of Honduras. Bull. Geol. Soc. Am. 52: 1219–1244.

Patterson, B.
1956. Early Cretaceous mammals and the evolution of mammalian molar teeth. Fieldiana Geol. 13: 1–105.

Peterson, O. A.
1907. The Miocene beds of western Nebraska and eastern Wyoming and their vertebrate faunae. Ann. Carnegie Mus. 4: 21–72.
1910. Description of new carnivores from the Miocene of western Nebraska. Mem. Carnegie Mus. 4: 205–278.
1924. Discovery of fossil mammals in the Brown's Park Formation of Moffatt County, Colorado. Ann. Carnegie Mus. 15: 299–304.

1928. The Brown's Park Formation. Mem. Carnegie Mus. 11: 87–130.

Piveteau, J.
1961. Traité de paléontologie, Tome VI, Vol. I, L'origine des mammifères et les aspects fondamentaux de leur évolution. Paris: Brodard-Taupin Imprimer-Relieur, 1138 pp.

Prothero, D. R., and C. C. Swisher III
1992. Magnetostratigraphy and geochronology of the terrestrial Eocene–Oligocene transition in North America. *In* D. R. Prothero and W. A. Berggren (eds.), Eocene–Oligocene climatic and biotic evolution, pp. 46–73. Princeton, NJ: Princeton Univ. Press.

Reed, L. C., and O. M. Langnecker
1932. The geology of Hemphill County, Texas. Univ. Texas Bull. 3231: 1–98.

Repenning, C. A.
1987. Biochronology of the microtine rodents of the United States. *In* M. O. Woodburne (ed.), Cenozoic mammals of North America, geochronology and biostratigraphy, pp. 236–268. Berkeley: Univ. California Press.

Repenning, C. A. and J. G. Vedder
1961. Continental vertebrates and their stratigraphic correlation with marine mollusks, eastern Caliente Range, California. U.S. Geol. Surv. Prof. Pap. 424: C-235–239.

Retallack, G. J.
1983. A paleopedological approach to the interpretation of terrestrial sedimentary rocks: the mid-Tertiary fossil soils of Badlands National Park, South Dakota. Geol. Soc. Am. Bull. 94: 823–840.

Reynolds, R. E., R. Hunt, Jr., and B. Albright
1995. Rhinoceros in Lanfair Valley. San Bernardino Cty. Mus. Assoc. Q. 42: 107–110.

Richey, K. A.
1938. *Osteoborus diabloensis*, a new dog from the Black Hawk Ranch fauna, Mount Diablo, California. Univ. California Publ. Bull. Dept. Geol. Sci. 24: 303–307.
1979. Variation and evolution in the premolar teeth of *Osteoborus* and *Borophagus* (Canidae). Trans. Nebraska Acad. Sci. 7: 105–123.

Riggs, E. S.
1942. Preliminary description of two lower Miocene carnivores. Field Mus. Nat. Hist. Geol. Ser. 7: 59–62.
1945. Some early Miocene carnivores. Ibid. 9: 69–114.

Robinson, P.
1968. Road log, Craig, Colorado to Kremmling, Colorado. *In* C. C. Black, M. C. McKenna, and P. Robinson (eds.), Field Conference guidebook for the high altitude and mountain basin deposits of Miocene age in Wyoming and Colorado, pp. 1–6. Boulder: Univ. Colorado Museum.

Romer, A. S., and A. H. Sutton
1927. A new arctoid carnivore from the lower Miocene. Am. J. Sci. 14: 459–464.

Russell, R. D., and V. L. VanderHoof
1931. A vertebrate fauna from a new Pliocene formation in northern California. Univ. California Publ. Bull. Dep. Geol. Sci. 20: 11–21.

Savage, D. E.
1939. The Optima Fauna, middle Pliocene, from Texas County, Oklahoma. Unpubl. M.S. thesis, Univ. of Oklahoma, 128 p.
1941. Two new middle Pliocene carnivores from Oklahoma, with notes on the Optima fauna. Am. Midland Nat. 25: 692–710.

Schlaikjer, E. M.
1935. Contributions to the stratigraphy and paleontology of the Goshen Hole area, Wyoming. IV: New vertebrates and the stratigraphy of the Oligocene and early Miocene. Bull. Mus. Comp. Zool. 76: 97–189.

Schlosser, M.
1890. Die affen, lemuren, chiropteren, insectivoren, marsupialier, creodonten und carnivoren des Europäischen Tertiärs, III. Beitr. Paläontol. Österreich-Ungarns und des Orients 8: 1–106.

Schmidt-Kittler, N.
1981. Zur Stammesgeschichte der marderverwandten Raubtiergruppen (Musteloidea, Carnivora). Eclogae Geol. Helv. 74: 753–801.

Schultz, J. R.
1937. A late Cenozoic vertebrate fauna from Coso Mountains, Inyo County, California. Carnegie Inst. Washington Publ. 487: 75–109.

Scott, W. B.
1890. Preliminary account of the fossil mammals from the White River and Loup Fork formations, contained in the Museum of Comparative Zoology, Pt. II. the Carnivora and Artiodactyla. Bull. Mus. Comp. Zool. 20: 65–100.
1893. The mammals of the Deep River Beds. Am. Nat. 27: 659–662.

1895. The mammalia of the Deep River Beds. Trans. Am. Philos. Soc. Philadelphia 18: 55–185.
1898. Notes on the Canidae of the White River Oligocene. Ibid. 19: 325–415.

Segall, W.
1943. The auditory region of the arctoid carnivores. Field Mus. Nat. Hist. Zool. Ser. 29: 33–59.

Sellards, E. H.
1916. Fossil vertebrates from Florida: a new Miocene fauna; new Pliocene species; the Pleistocene fauna. Florida State Geol. Surv. Annu. Rep. 8: 77–160.

Shotwell, J. A.
1968. Miocene mammals of southeast Oregon. Bull. Mus. Nat. Hist. Univ. Oregon 14: 1–67.
1970. Pliocene mammals of southeast Oregon and adjacent Idaho. Ibid. 17: 1–103.

Simpson, G. G.
1932. Miocene land mammals from Florida. Bull. Florida State Geol. Surv. 10: 1–41.
1941. Large Pleistocene felines of North America. Am. Mus. Novitates 1136: 26 pp.
1945. The principles of classification and a classification of mammals. Bull. Am. Mus. Nat. Hist. 8: 1–350.

Sinclair, W. J.
1915. Additions to the fauna of the lower Pliocene Snake Creek beds (results of the Princeton University 1914 Expedition to Nebraska). Proc. Am. Philos. Soc. 54: 73–95.

Skinner, M. F., and F. W. Johnson
1984. Tertiary stratigraphy and the Frick Collection of fossil vertebrates from north-central Nebraska. Bull. Am. Mus. Nat. Hist. 178: 217–368.

Skinner, M. F., C. W. Hibbard, E. D. Gutentag, G. R. Smith, J. G. Lundberg, J. A. Holman, J. A. Feduccia, and P. V. Rich
1972. Early Pleistocene pre-glacial and glacial rocks and faunas of north-central Nebraska, class Mammalia. Bull. Am. Mus. Nat. Hist. 148: 1–148.

Skinner, M. F., S. M. Skinner, and R. J. Gooris
1977. Stratigraphy and biostratigraphy of late Cenozoic deposits in central Sioux County, western Nebraska. Bull. Am. Mus. Nat. Hist. 158: 265–371.

Stalker, A. M., and C. S. Churcher
1972. Glacial stratigraphy of the southwestern Canadian prairies: the Laurentide record. Proc. 24th Int. Geol. Cong., Montreal, Quebec, Quat. Geol. Sect. 12: 110–119.

Stevens, M. S.
1977. Further study of Castolon Local Fauna (early Miocene) Big Bend National Park, Texas. Pearce-Sellards Ser. Texas Mem. Mus. 28: 1–69.

Stevens, M. S., J. B. Stevens, and M. R. Dawson
1969. New early Miocene formation and vertebrate local fauna, Big Bend National Park, Brewster County, Texas. Pearce-Sellards Ser Texas Mem Mus. 15: 1–53.

Stirton, R. A.
1932. Correlation of the Fish Lake Valley and Cedar Mountain beds of the Esmeralda Formation of Nevada. Science 76: 60–61.
1939a. The Nevada Miocene and Pliocene mammalian faunas as faunal units. Proc. Sixth Pac. Sci. Congr. pp. 627–638.
1939b. Cenozoic mammal remains from the San Francisco Bay region. Univ. California Publ. Bull. Dep. Geol. Sci. 24: 339–410.

Stirton, R. A., and V. L. VanderHoof
1933. *Osteoborus*, a new genus of dogs, and its relation to *Borophagus* Cope. Univ. California Publ. Bull. Dept. Geol. Sci. 23: 175–182.

Stock, C.
1928. Canid and proboscidian remains from the Ricardo deposits, Mohave Desert, California. Carnegie Inst. Washington Publ. 393: 39–49.
1932. *Hyaenognathus* from the late Pliocene of the Coso Mountain, California. J. Mamm. 13: 263–266.
1933. Carnivora from the Sespe of the Las Posas Hills, California. Carnegie Inst. Washington Publ. Contrib. Palaeontol. 440: 29–42.

Swofford, D. L.
1990. Phylogenetic analysis using parsimony (PAUP), version 3.0. Urbana: Illinois Nat. Hist. Surv.

Tanner, L. G.
1973. Notes regarding skull characteristics of *Oxetocyon cuspidatus* Green (Mammalia, Canidae). Trans. Nebraska Acad. Sci. 2: 66–69.

Tedford, R. H.
1978. History of dogs and cats: a view from the fossil record. *In* Nutrition and management of dogs and cats, chap. M23. St. Louis, MO: Ralston Purina Co.

Tedford, R. H., and D. Frailey
1976. Review of some Carnivora (Mammalia) from the Thomas Farm local fauna (Hemingfordian: Gilchrist County, Florida). Am. Mus. Novitates 2610: 1–9.
Tedford, R. H., and M. E. Hunter
1984. Miocene marine-nonmarine correlations, Atlantic and Gulf Coastal Plains, North America. Palaeogeogr. Palaeoclimatol. Palaeoecol. 47: 129–151.
Tedford, R. H., and Qiu Z.-x.
1996. A new canid genus from the Pliocene of Yushe, Shanxi Province. Vertebr. PalAsiat. 34: 27–40.
Tedford, R. H., B. E. Taylor, and X. Wang
1995. Phylogeny of the Caninae (Carnivora: Canidae): the living taxa. Am. Mus. Novitates 3146: 37 pp.
MS. Phylogenetic systematics of the North American fossil Caninae (Carnivora, Canidae).
Tedford, R. H., T. Galusha, M. F. Skinner, B. E. Taylor, R. W. Fields, J. R. Macdonald, J. M. Rensberger, S. D. Webb, and D. P. Whistler
1987. Faunal succession and biochronology of the Arikareean through Hemphillian interval (Late Oligocene through earliest Miocene epochs) in North America. *In* M. O. Woodburne (ed.), Cenozoic mammals of North America, geochronology and biostratigraphy, pp. 153–210. Berkeley: Univ. California Press.
Tedford, R. H., J. B. Swinehart, C. C. Swisher III, D. R. Prothero, S. A. King, and T. E. Tierney
1996. The Whitneyan–Arikareean transition in the High Plains. *In* D. R. Prothero and R. J. Emry (eds.), The Terrestrial Eocene–Oligocene transition in North America, Pt. I: The chronostratigraphy of the Uintan through Arikareean, pp. 312–334. Cambridge: Cambridge Univ. Press.
Thorpe, M. R.
1922a. Oregon Tertiary Canidae, with descriptions of new forms. Am. J. Sci. 3: 162–176.
1922b. Some Tertiary carnivora in the Marsh Collection, with descriptions of new forms. Ibid. 3: 423–455.
Untermann, G. E., and B. R. Untermann
1954. Geology of Dinosaur National Monument and vicinity Utah–Colorado. Bull. Utah Geol. Miner. Surv. 42: 1–221.
Van Valen, L.
1966. Deltatheridia, a new order of mammals. Bull. Am. Mus. Nat. Hist. 132: 1–126.
Van Valkenburgh, B. V.
1991. Iterative evolution of hypercarnivory in canids (Mammalia: Carnivora): evolutionary interactions among sympatric predators. Paleobiology 17: 340–362.
VanderHoof, V. L.
1931. *Borophagus littoralis* from the marine Tertiary of California. Univ. California Publ. Bull. Dept. Geol. Sci. 21: 15–24.
1933. Additions to the fauna of the Tehama upper Pliocene of northern California. Am. J. Sci. 25: 382–383.
1936. Notes on the type *Borophagus diversidens* Cope. J. Mamm. 17: 415–516.
1937. Critical observations on the Canidae in Cope's original collection from the Blancho of Texas. Proc. Geol. Soc. Am. 1936: 389 (abstract).
VanderHoof, V. L., and J. T. Gregory
1940. A review of the genus *Aelurodon*. Univ. California Publ. Bull. Dept. Geol. Sci. 25: 143–164.
Voorhies, M. R.
1965. The Carnivora of the Trail Creek Fauna. Contrib. Geol. Univ. Wyoming 4: 21–25.
1990a. Vertebrate paleontology on the proposed Norden Reservoir area, Brown, Cherry, and Keya Paha counties, Nebraska. Div. Archaeol. Res., Univ. Nebraska Lincoln, Tech. Rep. 82-09: 1–A593.
1990b. Vertebrate biostratigraphy of the Ogallala Group in Nebraska. *In* T. C. Gustavson (ed.), Geologic framework and regional hydrology: Upper Cenozoic Blackwater Draw and Ogallala Formations, Great Plains, pp. 115–151. Austin: Univ. Texas Bur. Econ. Geol.
Voorhies, M. R., J. A. Holman, and Xue X.-x.
1987. The Hottell Ranch rhino quarries (basal Ogallala: medial Barstovian), Banner County, Nebraska. Pt. I: Geologic setting, faunal list, lower vertebrates. Contrib. Geol. Univ. Wyoming 25: 55–69.
Wagner, H. M.
1981. Geochronology of the Mehrten Formation in Stanislaus County, California. Unpubl. Ph.D. diss., Dep. Geology, Univ. California, Riverside, 342 pp.
Wang, X.
1990. Systematics, functional morphology, and evolution of primitive Canidae (Mammalia: Carnivora). Ph.D. diss., Univ. Kansas, Lawrence.
1993. Transformation from plantigrady to digitigrady: functional morphology of locomotion in *Hesperocyon* (Canidae:

Carnivora). Am. Mus. Novitates 3069: 23 pp.
1994. Phylogenetic systematics of the Hesperocyoninae (Carnivora: Canidae). Bull. Am. Mus. Nat. Hist. 221: 1–207.
1997. New cranial material of *Simocyon* from China, and its implications for phylogenetic relationship to the red panda (*Ailurus*). J. Vertebr. Paleontol. 17: 184–198.

Wang, X., and R. H. Tedford
1992. The status of genus *Nothocyon* Matthew, 1899 (Carnivora): an arctoid not a canid. J. Vertebr. Paleontol. 12: 223–229.
1994. Basicranial anatomy and phylogeny of primitive canids and closely related miacids (Carnivora: Mammalia). Am. Mus. Novitates 3092: 34 pp.
1996. Canidae. *In* D. R. Prothero and R. J. Emry (eds.), The terrestrial Eocene–Oligocene transition in North America, Pt. II: Common vertebrates of the White River Chronofauna, pp. 433–452. Cambridge: Cambridge Univ. Press.

Wayne, R. K., W. G. Nash, and S. J. O'Brien
1987a. Chromosomal evolution of the Canidae. I. Species with high diploid numbers. Cytogenet. Cell Genet. 44: 123–133.
1987b. Chromosomal evolution of the Canidae. II. Divergence from the primitive carnivore karyotype. Ibid. 44: 134–141.

Wayne, R. K, E. Geffen, D. J. Girman, K. P. Koepfli, L. M. Lau, and C. R. Marshall
1997. Molecular systematics of the Canidae. Syst. Zool. 46: 622–653

Wayne, R. K., and S. J. O'Brien
1987. Allozyme divergence within the Canidae. Ibid. 36: 339–355.

Webb, S. D.
1969a. The Burge and Minnechaduza Clarendonian mammalian fauna of north-central Nebraska. Univ. California Publ. Geol. Sci. 78: 1–191.
1969b. The Pliocene Canidae of Florida. Bull. Florida Sta. Mus. Biol. Sci. 14: 273–308.

Webb, S. D., and S. C. Perrigo
1984. Late Cenozoic vertebrates from Honduras and El Salvador. J. Vertebr. Paleontol. 4: 237–254.

Webb, S. D., B. J. MacFadden, and J. A. Baskin
1981. Geology and paleontology of the Love Bone Bed from the late Miocene of Florida. Am. J. Sci. 281: 513–544.

Webb, S. D., R. C. Hulbert, Jr., and W. D. Lambert
1995. Climatic implications of large-herbivore distributions in the Miocene of North America. *In* E. S. Vrba, G. H. Denton, T. C. Partridge, and L. H. Burckle (eds.), Paleoclimate and evolution: with emphasis on human origins, pp. 91–108. New Haven, CT: Yale Univ. Press.

Webster, D. B., and M. Webster
1980. Morphological adaptations of the ear in the rodent family Heteromyidae. Am. Zool. 20: 247–254.

Werdelin, L.
1989. Constraint and adaptation in the bone-cracking canid *Osteoborus* (Mammalia: Canidae). Paleobiology 15: 387–401.

Werdelin, L., and N. Solounias
1991. The Hyaenidae: taxonomy, systematics and evolution. Fossils and Strata 30: 1–104.

Whistler, D. P., and D. W. Burbank
1992. Miocene biostratigraphy and biochronology of the Dove Spring Formation, Mojave Desert, California, and characterization of the Clarendonian mammal age (late Miocene) in California. Geol. Soc. Am. Bull. 104: 644–658.

White, T. E.
1941a. Additions to the fauna of the Florida Pliocene. Proc. New England Zool. Club 18: 67–70.
1941b. Additions to the Miocene fauna of Florida. Ibid. 18: 91–98.
1942. The lower Miocene mammal fauna of Florida. Bull. Mus. Comp. Zool. 92: 1–49.
1947. Addition to the Miocene fauna of north Florida. Ibid. 99: 497–515.

Williams, C. T.
1967. Classification of the Borophaginae (Canidae). Unpubl. Master's thesis, Dep. Zool., Univ. Kansas, Lawrence, 103 pp.

Wilson, J. A.
1939. A new species of dog from the Miocene of Colorado. Univ. Michigan Contrib. Mus. Paleontol. 5: 315–318.
1960. Miocene carnivores, Texas coastal plain. J. Paleontol. 34: 983–1000.

Wolsan, M.
1993. Phylogeny and classification of early European Mustelida (Mammalia: Carnivora). Acta Theriol. 38: 345–384.

Wood, H. E., and A. E. Wood
1937. Mid-Tertiary vertebrates from the Texas coastal plain: fact and fable. Am. Midland Nat. 18: 129–146.

Woodburne, M. O., and C. C. Swisher, III
1995. Land mammal high-resolution geochronology, intercontinental overland dispersals, sea level, climate, and vicariance. *In* W. A. Berggren, D. V. Kent, and J. A. Hardenbol (eds.), Geochronology, time scales and global stratigraphic correlation: a unified framework for a historical geology. SEPM (Soc. Sediment. Geol.) Spec. Publ. 54: 335–364.

Wortman, J. L., and W. D. Matthew
1899. The ancestry of certain members of the Canidae, the Viverridae, and Procyonidae. Bull. Am. Mus. Nat. Hist. 12: 109–139.

APPENDIX I

List of Taxa by Localities

Unless otherwise noted, biochronologic terminology and correlations follow those of Emry et al. (1987) for Orellan through Whitneyan strata, Tedford et al. (1987) for Arikareean through Hemphillian strata, and Lundelius et al. (1987) and Repenning (1987) for Blancan strata. We follow Tedford et al. (1987: fig. 6.2) for the informal subdivisions within the Land Mammal ages (e.g., early or late Hemingfordian). In the case of the long interval for the Arikareean, we adopt a tripartite division of early, medial, and late Arikareean that correspond to Tedford et al.'s (1987: fig. 6.2) early early (e.g., Gering Fauna and equivalent), late early (e.g., Monroe Creek Fauna and equivalent), and late (e.g., Harrison Fauna plus Agate Spring Local Fauna) Arikareean. In the case of the Blancan age, which was either undivided by Lundelius et al. (1987: fig. 7.3) or subdivided into five biochrons based on microtine rodents by Repenning (1987: fig. 8.1), we arbitrarily divide the early and late Blancan at the boundary between the Blancan II and III of Repenning. For further explanations about the chronological calibrations, see the Materials and Methods section. An asterisk indicates that the holotype of the designated taxon is from the locality noted.

Orellan

Scenic Member, Brule Formation, Shannon County, South Dakota: **Otarocyon macdonaldi*.

Toston Formation, Lewis and Clark County, Montana: *Otarocyon macdonaldi*.

Whitneyan

Whitney Member, Brule Formation, Dawes, Morrill, Scotts Bluff, and Sioux counties, Nebraska: *Archaeocyon pavidus*, *Archaeocyon leptodus*, and *Oxetocyon cuspidatus*.

Whitney Member, Brule Formation, Three Tubs locality, north side of 66 Mountain, Goshen County, Wyoming: *Archaeocyon leptodus*.

Poleslide Member, Brule Formation, Jackson and Shannon counties, South Dakota: *Archaeocyon pavidus* and **Oxetocyon cuspidatus*.

?Whitneyan

?Poleslide Member, Brule Formation, Cedar Pass, South Dakota: *Cynarctoides lemur*.

Latest Whitneyan or earliest Arikareean

Kew Quarry Local Fauna, Sespe Formation, Las Posas Hills, Ventura County, California: **Archaeocyon pavidus*.

Early Arikareean

Horn Member, Brule Formation, Banner and Morrill counties, Nebraska: *Archaeocyon leptodus*.

Lower part of Sharps Formation, Shannon County, South Dakota: *Archaeocyon pavidus* and *Cynarctoides lemur*.

Upper part of Sharps Formation, Jackson and Shannon counties, South Dakota: *Archaeocyon leptodus*, **Otarocyon cooki*, *Cynarctoides lemur*, **Cynarctoides roii*, and *Cormocyon haydeni*.

Gering Formation, Morrill County, Nebraska: *Oxetocyon cuspidatus*.

Lower Arikaree Group, White Butte (Chalky Buttes), Slope County, North Dakota: *Archaeocyon leptodus*.

Lower Arikaree Group, Little Muddy Creek, Niobrara County, Wyoming: *Archaeocyon leptodus*, *Otarocyon cooki*, and *Phlaocyon minor*.

Lower Arikaree Group, Willow Creek, Niobrara County, Wyoming: *Archaeocyon leptodus*.

Lower Arikaree Group, south side of Bear Mountain, Goshen County, Wyoming: *Archaeocyon leptodus*.

Lower Arikaree Group, Horse Creek area, Goshen County, Wyoming and Banner County, Nebraska: *Archaeocyon leptodus* and *Cynarctoides roii*.

Lower Arikaree Group, Goshen Hole, Goshen County, Wyoming: **Archaeocyon leptodus*.

Toston Formation, Canyon Ferry area, Lewis and Clark County, Montana: *Archaeocyon leptodus*.

Turtle Cove Member, John Day Formation, Wheeler and Grant counties, Oregon: *Archaeocyon pavidus*, **Rhizocyon oregonensis*, **Cynarctoides lemur*, **Phlaocyon latidens*, and **Cormocyon copei*.

Medial Arikareean

Lower Arikaree Group, Muddy Creek, Niobrara and Platte counties, Wyoming: *Archaeocyon leptodus*, **Archaeocyon falkenbachi*, and *Otarocyon cooki*.

Lower Arikaree Group, north of Jeriah, Niobrara County, Wyoming: *Otarocyon cooki*.

Upper part of the lower Arikaree Group, west of Spanish Diggings, Niobrara County, Wyoming: *Cormocyon haydeni*.

Lower Rosebud beds, equivalent to Monroe Creek Formation, Wounded Knee area, Shannon County, South Dakota: *Cormocyon haydeni*.

Turtle Butte Formation, Tripp County, South Dakota: *Phlaocyon minor*.

Medial or late Arikareean

Lower Rosebud beds, equivalent to Monroe Creek Formation or Harrison Formation, Wounded Knee area, east of Porcupine Creek, Shannon County, South Dakota: *Cynarctoides acridens*.

Browns Park Formation, Moffat County, Colorado: *Cynarctoides lemur* and *Phlaocyon annectens*.

Late Arikareean

Harrison Formation, Agate area, Sioux County, Nebraska: *Cynarctoides acridens*, *Phlaocyon minor*, and *Desmocyon thomsoni*.

Rocks referred to Harrison Formation, north of Lusk area, Niobrara County, Wyoming: *Cormocyon haydeni*.

Rocks equivalent to Harrison Formation, Eagle Nest Butte, 260 ft above the base of the exposed section, Washabaugh County, South Dakota: **Cormocyon haydeni*.

Upper Harrison beds, Agate area, Sioux County, Nebraska: **Cynarctoides acridens*, *Cynarctoides emryi*, **Phlaocyon annectens*, and *Desmocyon thomsoni*.

Upper Harrison beds, south side of Dry Creek, Box Butte County, Nebraska: *Phlaocyon leucosteus*.

Upper Harrison beds, north of Lusk, Niobrara County, Wyoming: *Desmocyon thomsoni*.

Upper Harrison beds, south of Lusk, Niobrara County, Wyoming: *Phlaocyon minor* and *Desmocyon thomsoni*.

Upper Harrison beds, south of Lusk, Goshen County, Wyoming: **Cynarctoides luskensis*, *Cynarctoides acridens*, *Phlaocyon minor*, **Phlaocyon multicuspus*, and *Desmocyon thomsoni*.

Upper Harrison beds, Spoon Buttes area, Goshen County, Wyoming: *Desmocyon thomsoni*.

Upper Harrison beds, Wheatland area, Platte County, Wyoming: *Desmocyon thomsoni*.

Upper Harrison beds, Van Tassel area, Niobrara County, Wyoming and Sioux County, Nebraska: **Cynarctoides harlowi*, *Phlaocyon minor*, and *Phlaocyon annectens*.

Upper Harrison beds, 7 mi southeast of Chugwater, Platte County, Wyoming: *Cynarctoides luskensis*.

Upper Harrison beds, Guernsey area, Platte County, Wyoming: *Phlaocyon minor* and *Desmocyon thomsoni*.

Upper Harrison beds, Cherry County, Nebraska: *Desmocyon thomsoni*.

Rosebud Formation, Wounded Knee area, Shannon County, South Dakota: **Phlaocyon minor* and **Desmocyon thomsoni*.

Troublesome Formation, Grand County, Colorado: *Cormocyon copei*.

?Haystack Valley Member, John Day Formation, Oregon: *Desmocyon thomsoni*,

Lower part of Piedra Parada Member, Zia Formation, Standing Rock Quarry, Sandoval County, New Mexico: *Cynarctoides acridens*.

Cedar Run Local Fauna, Oakville Formation, Cedar Creek, Washington County, Texas: *Phlaocyon minor*.

Castolon Local Fauna, lower part of Delaho Formation, Big Bend National Park, Brewster County, Texas: *Phlaocyon annectens*.

Buda Local Fauna, Alachua County, Florida: *Cynarctoides lemur*, **Phlaocyon achoros*, and *Cormocyon copei*.

SB-1A Local Fauna, 1 mi north of Live Oak, Suwannee County, Florida: *Phlaocyon leucosteus*.

Early Hemingfordian

Runningwater Formation, Box Butte, Cherry and Dawes counties, Nebraska: *Cynarctoides acridens*, **Cynarctoides emryi*, **Phlaocyon marslandensis*, *Phlaocyon leucosteus*, **Phlaocyon yatkolai*, *Desmocyon thomsoni*, **Desmocyon matthewi*, *Paracynarctus kelloggi*, and *Metatomarctus canavus*.

Runningwater Formation, Stamen Ranch, Sioux County, Nebraska: *Cynarctoides emryi*.

Runningwater Formation, Bridgeport Quarry, Morrill County, Nebraska: *Cynarctoides acridens*, *Desmocyon thomsoni*, and *Metatomarctus canavus*.

Runningwater Formation, *Aletomeryx* Quarry and vicinity, near Antelope Creek, Cherry County, Nebraska: *Cynarctoides acridens*, *Phlaocyon leucosteus*, **Phlaocyon mariae*, and *Desmocyon matthewi*.

Runningwater Formation, 2 mi west of Pole Creek, Cherry County, Nebraska: *Metatomarctus canavus* and *Desmocyon matthewi*.

Runningwater Formation, Clinton Highway Locality, Sheridan County, Nebraska: *Phlaocyon marslandensis* and *Metatomarctus canavus*.

?Runningwater Formation, Spiers Quarry, Dawes County, Nebraska: *Desmocyon thomsoni*.

Martin Canyon Local Fauna, Martin Canyon beds, Logan County, Colorado: *Cynarctoides acridens*, **Phlaocyon leucosteus*, and *Protomarctus optatus*.

Geertson Formation, Lemhi Valley, 40 mi south of Salmon, Lemni County, Idaho: *Cynarctoides acridens*.

Near middle of Chamisa Mesa Member, Zia Formation, Blick and *Cynarctoides* quarries, Sandoval County, New Mexico: *Cynarctoides acridens* and *Protomarctus optatus*.

Near middle of Chamisa Mesa Member, Zia Formation, Jemez Creek drainage, southwest corner of *Blickomylus* Hill, local green zone near base of hill, Sandoval County, New Mexico: *Cynarctoides gawnae*.

Upper part of Chamisa Mesa Member, Zia Formation, Jeep Quarry, Sandoval County, New Mexico: **Cynarctoides gawnae*, *Desmocyon thomsoni*, and *Metatomarctus canavus*.

Canyada Pilares Member, Zia Formation, Canyada Pilares, Northern Ceja del Rio Puerco area, New Mexico: *Paracynarctus kelloggi*.

Oakville Formation, Hidalgo Bluff, Washington County, Texas: *Cynarctoides acridens*.

Thomas Farm Local Fauna, Hawthorn Formation, Gilchrist County, Florida: **Metatomarctus canavus*, and **Euoplocyon spissidens*.

Pollack Farm Site, lower Calvert Formation, near Cheswold, Delaware: *Paracynarctus kelloggi* and *Metatomarctus canavus*.

Miller Locality, ?Dixie County, Florida: *Desmocyon matthewi*.

Late Hemingfordian

Box Butte Formation, Box Butte and Dawes counties, Nebraska: *Cynarctoides acridens*, *Phlaocyon leucosteus*, and *Protomarctus optatus*.

Sheep Creek Fauna, Sheep Creek Formation, Sioux County, Nebraska: *Cynarctoides acridens* and **Protomarctus optatus*.

?Sheep Creek Formation, Whistle Creek, Sioux County, Nebraska: *Protomarctus optatus*.

Rocks temporally equivalent to the Sheep Creek Formation, Ginn Quarry, Dawes County, Nebraska: *Cynarctoides acridens* and *Protomarctus optatus*.

Split Rock Formation, Granite Mountain, Fremont County, Wyoming: *Cynarctoides acridens*, *Paracynarctus kelloggi*, *Metatomarctus canavus*, and *Protomarctus optatus*.

Nambe Member, Tesuque Formation, south of Santa Cruz River, 50 ft below the Nambe White Ash Stratum, Santa Fe County, New Mexico: *Cynarctoides acridens*.

Nambe Member, Tesuque Formation, White Operation Wash, Santa Fe County, New Mexico: *Paracynarctus kelloggi*.

Nambe Member, Tesuque Formation, Santa Fe County, New Mexico: *Microtomarctus conferta*.

Zia Formation, Kiva Quarry near the divide between Canyada de Zia and Canyada Piedra Parada, Jemez Creek area, Sandoval County, New Mexico: *Paracynarctus kelloggi* and *Microtomarctus conferta*.

Massacre Lake Local Fauna, Big Basin, Washoe County, Nevada: *Paracynarctus kelloggi*.

Hackberry Local Fauna, Lanfair Valley, eastern Mohave, California: *Metatomarctus canavus*.

Phillips Ranch Local Fauna, Bopesta Formation, Kern County, California: *Paracynarctus kelloggi*.

Third Division Fauna, Barstow Formation, San Bernardino County, California: *Protomarctus optatus*.

Late Hemingfordian or early Barstovian

North Park Formation, Spruce Gulch, 5 mi south of State Bridge, Eagle County, Colorado: *Paracynarctus kelloggi*.

Early Barstovian

Lower Snake Creek Fauna, Olcott Formation, Sioux and Dawes counties, Nebraska: *Cynarctoides acridens*, **Paracynarctus sinclairi*, *Euoplocyon brachygnathus*, *Psalidocyon marianae*, **Microtomarctus conferta*, **Tomarctus hippophaga*, and *Tomarctus brevirostris*.

Sand Canyon Formation, Dawes County, Nebraska: *Tomarctus hippophaga*.

Sand Canyon Formation, Observation Quarry, Dawes County, Nebraska: *Cynarctoides acridens*, *Paracynarctus sinclairi*, and *Tomarctus hippophaga*.

Sand Canyon Formation, Surprise Quarry, Hay Springs Creek Drainage, Dawes County, Nebraska: *Aelurodon asthenostylus*.

Lower part of Pawnee Creek Formation, Weld County, Colorado: *Microtomarctus conferta*, **Tomarctus brevirostris*, and *Aelurodon asthenostylus*.

Skull Ridge Member, Tesuque Formation, Santa Fe County, New Mexico: *Cynarctoides acridens*, *Paracynarctus kelloggi*, **Psalidocyon marianae*, *Microtomarctus conferta*, *Tomarctus hippophaga*, and *Tomarctus brevirostris*.

Skull Ridge Member, Tesuque Formation, Third District, Santa Fe County, New Mexico: *Tomarctus brevirostris*.

Undifferentiated beds in Zia Formation, Jemez Creek area, Sandoval County, New Mexico: *Microtomarctus conferta*.

Pointblank Local Fauna, Fleming Formation, near Pointblank, San Jacinto County, Texas: *Paratomarctus temerarius*.

Trinity River Local Fauna, Fleming Formation, San Jacinto County, Texas: *Paratomarctus temerarius*.

Green Hills Fauna, Barstow Formation, San Bernardino County, California: *Paracynarctus kelloggi*, *Euoplocyon brachygnathus*, *Microtomarctus conferta*, and *Tomarctus hippophaga*.

Barstow Formation, Yermo Quarry, San Bernardino County, California: *Cynarctoides acridens*, *Microtomarctus conferta*, and *Tomarctus hippophaga*.

Second Division Fauna, Barstow Formation, San Bernardino County, California: *Cynarctoides acridens*, **Cynarctus galushai*, *Microtomarctus conferta*, *Tomarctus brevirostris*, *Aelurodon asthenostylus*, *Paratomarctus temerarius*, and *Protepicyon raki*.

Caliente Formation, Kent Quarry, Ventura County, California: *Tomarctus hippophaga*.

Caliente Formation, East Caliente Range, San Luis Obispo County, California: *Tomarctus brevirostris*.

Virgin Valley Formation, Virgin Valley, Humboldt County, Nevada: **Paracynarctus kelloggi*.

Carlin Formation, 3.5 mi south of Carlin, Elko County, Nevada: *Microtomarctus conferta*.

High Rock Canyon, Humboldt County, Nevada: *Metatomarctus* sp. A and *Metatomarctus* sp. B.

Mascall Fauna, Mascall Formation, Grant County, Oregon: **Tephrocyon rurestris*.

Red Basin Local Fauna, Butte Creek Volcanic Sandstone, Juntura Formation, Malheur County, Oregon: *Tephrocyon rurestris*.

Skull Spring Local Fauna, Butte Creek Formation, Malheur County, Oregon: *Euoplocyon brachygnathus*.

Flint Creek beds, near New Chicago, Granite County, Montana: **Euoplocyon brachygnathus*, and *Paratomarctus temerarius*.

Smith River Valley, ''Upper beds'' or ''*Cyclopidius* beds,'' in Deep River beds, Meagher County, Montana: *Paratomarctus temerarius*.

Tonopah Local Fauna, Siebert Formation, San Antonio Mountains, Nye County, Nevada: *Paracynarctus kelloggi*, *Microtomarctus conferta*, and **Aelurodon asthenostylus*.

Stewart Spring Fauna, Esmeralda Formation, Cedar Mountain, Mineral County, Nevada: *Paratomarctus temerarius* and *Carpocyon compressus*.

Calvert Formation, Calvert County, Maryland: **Cynarctus marylandica*.

Late Barstovian

Cornell Dam Member, Valentine Formation, Norden Bridge Quarry, Niobrara River, Brown County, Nebraska: *Cynarctus saxatilis*, *Aelurodon ferox*, *Paratomarctus temerarius*, and *Carpocyon compressus*.

Crookston Bridge Member, Valentine Formation, Railway Quarry A, Cherry County, Nebraska: *Cynarctus saxatilis*, *Aelurodon mcgrewi*, *Aelurodon ferox*, *Paratomarctus temerarius*, and *Carpocyon compressus*.

Devils Gulch Member, Valentine Formation, Devil's Gulch, Brown, Cherry, and Keya Paha counties, Nebraska: *Cynarctus saxatilis*, **Aelurodon mcgrewi*, *Aelurodon ferox*, *Paratomarctus temerarius*, and *Carpocyon compressus*.

Burge Member, Valentine Formation, Brown and Cherry counties, Nebraska: **Cynarctus voorhiesi*, **Aelurodon stirtoni*, *Aelurodon ferox*, **Paratomarctus euthos*, and **Carpocyon webbi*.

Ogallala Group temporally equivalent to Burge Member of Valentine Formation, Extension Quarry and Paleo Channel Quarry, Sheridan County, Nebraska: *Paratomarctus euthos*.

Ogallala Group temporarily equivalent to Burge Member of Valentine Formation, Hardin Bridge, Niobrara River, Sheridan County, Nebraska: *Aelurodon ferox*.

Valentine Formation, H. A. Davis Ranch, east side of Snake River, Cherry County, Nebraska: *Carpocyon compressus*.

Ogallala Group temporarily equivalent to upper part of Valentine Formation, 2.9 mi east of White Clay, along the Nebraska–South Dakota state line, Nebraska and South Dakota: *Aelurodon ferox*.

Valentine Formation, Elliot Place, Brown County, Nebraska: *Paratomarctus temerarius*.

Valentine Formation, Myers Farm, Webster County, Nebraska: *Cynarctus saxatilis*, *Paratomarctus temerarius*.

Valentine Formation, Tihen Locality, Keya Paha County, Nebraska: *Aelurodon ferox*.

Valentine Formation, Antelope Creek and Minnechaduza Creek, Cherry County, Nebraska: *Aelurodon ferox*.

Ogallala Group, temporally equivalent to Valentine Formation, Niobrara River, Sheridan County, Nebraska: *Aelurodon ferox*.

Ogallala Group, Driftwood Creek, Hitchcock County, Nebraska: *Aelurodon asthenostylus*.

Ogallala Group, Spatz Quarry, Knox County, Nebraska: *Aelurodon ferox*.

Ogallala Group, Devil's Nest road, Knox County, Nebraska: *Aelurodon ferox*.

Ogallala Group, temporally equivalent to the Cornell Dam Member of the Valentine Formation, Hottell Ranch Quarry, Banner County, Nebraska: *Aelurodon ferox*.

Ogallala Formation, temporally equivalent to Crookston Bridge Member of Valentine Formation, Hazard Homestead, Driftwood Creek, Hitchcock County, Nebraska: *Aelurodon ferox* and *Carpocyon compressus*.

Republican River beds, Red Willow County, Nebraska: *Aelurodon mcgrewi*.

Pawnee Creek Formation, Horse Quarry, Weld County, Colorado: *Microtomarctus conferta*, *Tomarctus brevirostris*, *Aelurodon asthenostylus*, and *Carpocyon compressus*.

Cedar Springs Draw Local Fauna, Browns Park Formation, Moffat County, Colorado: *Microtomarctus conferta*.

Trail Creek Fauna, Ogallala Group, Laramie County, Wyoming: *Paratomarctus temerarius*.

Ogallala Group, Cedar Creek, 40 mi north of Sterling, Logan County, Colorado: **Cynarctus saxatilis*.

Cold Spring Fauna, Fleming Formation, 8 mi south of Livingston, Polk County, Texas: *Microtomarctus conferta* and *Aelurodon ferox*.

?Cold Spring Fauna, Fleming Formation, J. Niscavit Farm, Grimes County, Texas: *Tomarctus brevirostris*.

Pojoaque Member, Tesuque Formation, Santa Fe and Rio Arriba counties, New Mexico: *Microtomarctus conferta*, *Aelurodon stirtoni*, *Aelurodon ferox*, *Paratomarctus temerarius*, and *Carpocyon webbi*.

Chama El Rito Member, Tesuque Formation, South fork of Three Sands Hills Wash, Rio del Oso–Abiquiu locality, Rio Arriba County, New Mexico: *Microtomarctus conferta*, *Aelurodon ferox*, *Aelurodon stirtoni*, and *Paratomarctus temerarius*.

Ojo Caliente Member, Tesuque Formation, Rio Arriba County, New Mexico: *Aelurodon ferox*, *Paratomarctus temerarius*, and *Carpocyon webbi*.

Dixon Member, Tesuque Formation, Rio Arriba County, New Mexico: *Aelurodon taxoides*.

Undifferentiated beds, Zia Formation, Jemez Creek area, Sandoval County, New Mexico: *Microtomarctus conferta*, *Aelurodon ferox*, *Paratomarctus temerarius*, and *Protepicyon raki*.

Unnamed member, Zia Formation, North Rio Puerco area, Sandoval County, New Mexico: *Paratomarctus temerarius* and *Protepicyon raki*.

Unnamed formation, Home Station Pass, Pershing County, Nevada: *Paracynarctus kelloggi*.

First Division Fauna, Barstow Formation, San Bernardino County, California: *Cynarctus galushai*, *Microtomarctus conferta*, *Aelurodon asthenostylus*, *Paratomarctus temerarius*, and **Protepicyon raki*.

?Late Barstovian

"Valley of the Niobrara River," Nebraska: **Aelurodon ferox*.

"Sands of the Niobrara River, Loup Fork," Nebraska: **Paratomarctus temerarius*.

"Loup Fork," presumably Valentine Formation, Cherry County, Nebraska: **Carpocyon compressus*.

Republic River beds, Silica Mine, Calvert, Kansas: *Carpocyon compressus*.

Noble Farm, Moore County, Texas: *Tomarctus brevirostris*.

Late Barstovian–Clarendonian

Pojoaque Member, Tesuque Formation, Santa Fe County, New Mexico: *Epicyon saevus*.

Unnamed beds of Zia Formation, Santa Ana Wash, Jemez Creek area, Sandoval County, New Mexico: *Epicyon saevus*.

Early Clarendonian

Cap Rock Member, Ash Hollow Formation, Williams Canyon, tributary of Plum Creek, Brown County, Nebraska: **Cynarctus crucidens*.

Cap Rock Member, Ash Hollow Formation, Clayton and East Clayton quarries, Brown County, Nebraska: *Cynarctus crucidens*, *Aelurodon taxoides*, *Paratomarctus euthos*, and *Epicyon saevus*.

Cap Rock Member, Ash Hollow Formation, Medicine Creek, Brown County, Nebraska: *Cynarctus crucidens*.

Cap Rock Member, Ash Hollow Formation, Cherry and Keyapaha counties, Nebraska: *Aelurodon taxoides*.

Beds temporally equivalent to the Cap Rock Member of Ash Hollow Formation, Driftwood Creek, 16 mi southeast of Trenton, south side of Republic River, Hitchcock County, Nebraska: *Paratomarctus euthos*, *Carpocyon robustus*, and *Epicyon saevus*.

Marly zone, base of Cap Rock Member of Ash Hollow Formation, first canyon above the Boiling Springs Bridge, south side of Niobrara River, Cherry County, Nebraska: *Carpocyon robustus*.

Ogallala Group, temporally equivalent to lower part of Ash Hollow Formation, Patton Ranch, Banner County, Nebraska: *Epicyon saevus*.

Ash Hollow Formation, Gallup Gulch, 35 ft above spring level, massive sand, Cherry County, Nebraska: *Carpocyon robustus*.

Undifferentiated beds of Ogallala Group equivalent to Cap Rock Member of Ash Hollow Formation, Hollow Horn Bear Quarry, Todd County, South Dakota: *Cynarctus crucidens*, *Aelurodon taxoides*, *Paratomarctus euthos*, *Carpocyon robustus*, and *Epicyon saevus*.

Mission Local Fauna, undifferentiated beds of Ogallala Group temporarily equivalent to Ash Hollow Formation, Thomas Fox Ranch, Mellette County, South Dakota: *Aelurodon taxoides*, *Paratomarctus euthos*, and *Carpocyon robustus*.

Undifferentiated beds of Ogallala Group equivalent to Ash Hollow Formation, Canyon of Little White River and Rosebud Agency Quarry, South Dakota: *Aelurodon taxoides* and *Epicyon saevus*.

Undifferentiated beds of Ogallala Group equivalent to Ash Hollow Formation, Big Spring Canyon, Bennett County, South Dakota: *Aelurodon taxoides* and *Epicyon saevus*.

Undifferentiated beds of Ogallala Group equivalent to Cap Rock Member of Ash Hollow Formation, 2.5 mi west of Wounded Knee Creek, 0.5 mi south of South Dakota state line, Cherry County, Nebraska: *Aelurodon taxoides*.

Laucomer Member, Snake Creek Formation, Kilpatrick Quarry (= Quarry 7), Sioux County, Nebraska: *Cynarctus crucidens*.

Beaver Local Fauna, Laverne Formation, Whisenhunt Quarry, Beaver County, Oklahoma: *Aelurodon taxoides*.

Clarendon beds, Donley County, Texas: *Cynarctus crucidens* and *Carpocyon robustus*.

Clarendon beds, MacAdams Quarry, 10 mi north of Clarendon, Donley County, Texas: *Paratomarctus euthos*, *Aelurodon taxoides*, and *Epicyon saevus*.

Clarendon beds, White Fish Creek, Donley County, Texas: *Aelurodon taxoides*, *Paratomarctus euthos*, *Epicyon saevus*, and *Epicyon haydeni*.

Ogallala Group, Turkey Creek, Mill Iron Ranch, Hall County, Texas: *Aelurodon taxoides*.

Ogallala Group, Amarillo area, Texas: *Aelurodon taxoides*.

Lapara Creek Fauna, Goliad Formation, near Normanna, Bee County, Texas: *Aelurodon taxoides*.

Agricola Fauna, Bone Valley Formation, Agricola Road Locality, Polk County, Florida: *Aelurodon taxoides*.

Chamita Formation, Round Mountain Quarry, Rio Arriba County, New Mexico: *Aelurodon taxoides* and *Epicyon saevus*.

Fish Lake Valley Fauna, Esmeralda Formation, Esmeralda County, Nevada: *Epicyon saevus*.

Esmeralda Formation, Snowball Valley North, Cedar Mountain, Mineral County, California: *Aelurodon taxoides*.

Monterey Formation, Crocker Springs, Kern County, California: **Borophagus littoralis*.

South Tejon Hills Local Fauna, Santa Margarita Formation, Kern County, California: *Borophagus littoralis*.

?Early Clarendonian

''Sands of the Niobrara River,'' ?Cap Rock Member, Ash Hollow Formation, north-central Nebraska: **Epicyon saevus*.

Late Clarendonian

Merritt Dam Member, Ash Hollow Formation, Brown, Cherry, Hitchcock, and Sheridan counties, Nebraska: *Cynarctus crucidens*, *Aelurodon taxoides*, *Paratomarctus euthos*, *Carpocyon robustus*, *Epicyon saevus*, and *Epicyon haydeni*.

Ash Hollow Formation, Turtle Canyon, upper sandstone layer, Sheridan County, Nebraska: *Epicyon haydeni*.

Ash Hollow Formation, North Shore Locality, Keith County, Nebraska: *Epicyon haydeni*.

Laucomer Member, Snake Creek Formation, Sioux County, Nebraska: *Aelurodon taxoides*, *Epicyon saevus*, and *Epicyon haydeni*.

Browns Park Formation, near Craig, 75 ft below the Weller Cap, upper end of Swelter Draw, Moffat County, Colorado: *Carpocyon robustus*.

Alachua Formation, Love Bone Bed, Alachua County, Florida: *Epicyon saevus* and *Epicyon haydeni*.

Truckee Formation, Churchill County, Nevada: *Epicyon saevus*.

Green Valley Formation, Black Hawk Ranch Quarry, south side of Mount Diablo, Contra Costa County, California: *Aelurodon taxoides* and *Borophagus littoralis*.

San Pablo Group, Ingram Creek 8, Stanislaus County, California: *Borophagus littoralis*.

Clarendonian

''Valley of the Niobrara River,'' ?Merritt Dam Member, Ash Hollow Formation, Nebraska: **Epicyon haydeni*.

''Loup Fork,'' Ash Hollow Formation, south side of the Niobrara River, midway between the mouths of Pine and Box Butte creeks, Sheridan County, Nebraska: **Aelurodon taxoides*.

''Loup Fork,'' Madison River, Montana: *Epicyon haydeni*.

The Dalles Formation, Oregon: *Epicyon saevus*.

Driftwood Creek, Hitchcock County, Nebraska: *Epicyon haydeni*.

Lower part of Ash Hollow Formation, Harrisburg Locality A1, Banner County, Nebraska: *Aelurodon taxoides*.

Lower part of Ash Hollow Formation, south side of Niobrara River, northeast of River View School, Sheridan County, Nebraska: *Aelurodon taxoides*.

Thayer Ranch, 2 mi below Lion Bridge on Niobrara River, ?Cap Rock Member, Ash Hollow Formation, Cherry County, Nebraska: *Carpocyon webbi*.

Ogallala Group, Republican River beds, Bow Creek, 12.5 mi southeast of Logan, Kansas: *Aelurodon taxoides*.

Durham Local Fauna, Ogallala Group, Roger Mills County, Oklahoma: *Epicyon haydeni*.

Ogallala Group, Channing area, Texas: *Aelurodon taxoides*.

Excell Local Fauna, Ogallala Group, north of Canadian River, Texas: *Aelurodon taxoides*.

Ogallala Group, Highway Pit, 0.75 mi north of Lipscomb, Lipscomb County, Texas: *Cynarctus crucidens*.

Ogallala Group, Sanford Pit, 12 mi southwest of Borger, Carson County, Texas: *Aelurodon taxoides*.

Ogallala Group, Noble Ranch, Moore County, Texas: *Aelurodon taxoides*.

Upper part of Pojoaque Member, Tesuque Formation, Rio Arriba and Santa Fe counties, New Mexico: *Aelurodon ferox* and *Epicyon haydeni*.

Beds referred to the Chamita Formation, Black Mesa, San Ildefonso, Rio Arriba County, New Mexico: *Carpocyon webbi*.

Bidahochi Formation, President Wilson Springs, Jeddito Valley, Navajo County, Arizona: *Epicyon haydeni*.

Milk Creek Formation, Milk Creek area, Yavapai County, Arizona: *Carpocyon robustus* and *Epicyon haydeni*.

Ricardo Fauna, Dove Spring Formation, Red Rock Canyon, Kern County, California: **Carpocyon robustus*, *Epicyon saevus*, and *Epicyon haydeni*,

Clarendonian or Hemphillian

South of Coso Mountains, Inyo County, California: *Epicyon saevus*.

Early Hemphillian

Aphelops Draw Fauna, Johnson Member, Snake Creek Formation, Sioux County, Nebraska: *Epicyon saevus*, *Epicyon haydeni*, and *Borophagus secundus*.

Ash Hollow Formation, Lemoyne Quarry, Keith County, Nebraska: *Epicyon haydeni*.

Ogallala Group, Head of Blue Creek, Garden County, Nebraska: *Borophagus pugnator*.

Ogallala Group, Turtle-Carnivore Quarry, Frontier County, Nebraska: *Epicyon saevus*.

Ogallala Group, Medicine Creek, Frontier County, Nebraska: *Borophagus pugnator*.

Ogallala Group, Wray area, Yuma County, Colorado: *Epicyon haydeni*, and **Borophagus pugnator*.

Ogallala Group, Rhino Hill Quarry, Wallace County, Kansas: *Borophagus pugnator*.

Ogallala Group, Jack Swayze Quarry, Clark County, Kansas: *Epicyon haydeni* and *Borophagus pugnator*.

Ogallala Group, Rhino Quarry, Young Brothers Ranch, Vicinity of Ashland, Clark County, Kansas: *Epicyon haydeni*.

Ogallala Group, 2 mi south of Young Brothers Ranch, vicinity of Ashland, Clark County, Kansas: **Epicyon aelurodontoides*.

Ogallala Group, vicinity of John Dakin Quarry, Clark County, Kansas: *Borophagus pugnator*.

Ogallala Group, F. Sebastian Place, 1 mi southwest of Oberlin, Decatur County, Kansas: *Epicyon haydeni*.

Ogallala Group, Vicinity of Hall Cope's Ranch, 6 mi southwest of Norton, Norton County, Kansas: *Epicyon haydeni*.

Ogallala Group, Port of Entry Pit (Arnett Locality), 5 mi east of Higgins, Texas, in Ellis County, Oklahoma: *Carpocyon limosus*, *Epicyon saevus*, and *Epicyon haydeni*.

Ogallala Group, North Pit, Schwab Place, and Fritzler Place, Ellis County, Oklahoma: *Epicyon saevus* and *Epicyon haydeni*.

Hemphill Beds, Ogallala Group, Bridge Creek, Box T Ranch, north of Higgins, Lipscomb County, Texas: *Epicyon saevus*, *Epicyon haydeni*, and *Borophagus pugnator*.

Ogallala Group, V. V. Parker Place, Pit 1, 10 mi northeast of Higgins, Lipscomb County, Texas: *Epicyon saevus* and *Epicyon haydeni*.

McGehee Farm Locality, 5 mi north of Newberry, Alachua County, Florida: *Epicyon saevus* and *Epicyon haydeni*.

Alachua Formation, Haile 19A Locality, Alachua County, Florida: *Epicyon haydeni*.

Alachua Formation, Mixson's Bone Bed, Levy County, Florida: *Epicyon haydeni* and *Borophagus pugnator*.

Alachua Formation, Withlacoochee River 4A and 4X, Citrus County, Florida: *Borophagus pugnator* and **Borophagus orc*.

Star Valley Quarry, unnamed beds in Banbury Basalt, Little Owyhee River, Owyhee County, Idaho: *Epicyon haydeni*.

Rome Fauna, Rome beds, Dry Creek, Malheur County, Oregon: *Epicyon haydeni* and *Borophagus pugnator*.

Thousand Creek Fauna, Thousand Creek Formation, Humboldt County, Nevada: *Epicyon saevus*.

Gracias Local Fauna, Honduras: *Borophagus secundus*.

Corinto Local Fauna, El Salvador: *Borophagus secundus*.

?Early Hemphillian

Ogallala Group, Sanford Pit, 12 mi southwest of Borger, Channing area, Carson County, Texas: *Epicyon saevus*.

Poison Creek Formation, Reynolds Creek, Owyhee County, Idaho: *Borophagus pugnator*.

Late Hemphillian

ZX Bar Local Fauna, Johnson Member, Snake Creek Formation, Sioux County, Nebraska: **Borophagus secundus*.

Ogallala Group, Turtle Locality, Cheyenne County, Nebraska: *Borophagus secundus*.
Ogallala Group, Edson Quarry, Sherman County, Kansas: *Borophagus secundus*.
Optima Local Fauna, Ogallala Group, Optima (= Guymon) quarries, Texas County, Oklahoma: *Borophagus secundus*.
Coffee Ranch Local Fauna, Ogallala Group, Coffee Ranch Quarry (= Miami Quarry), Hemphill County, Texas: *Borophagus secundus*.
Ogallala Group, ''Goodnight beds,'' Armstrong County, Texas: *Borophagus secundus*.
Ogallala Group, Channing area, Hartley County, Texas: *Borophagus secundus*.
Axtel Local Fauna, Ogallala Group, Axtel Ranch Locality, Randall County, Texas: **Borophagus hilli*.
Christian Ranch Local Fauna, Ogallala Group, Christian Place Quarry, Armstrong County, Texas: *Borophagus hilli*.
Palmetto Fauna, Bone Valley Formation, Hardee and Polk counties, Florida: **Carpocyon limosus*, *Epicyon haydeni*, *Borophagus pugnator*, *Borophagus hilli*, and **Borophagus dudleyi*.
Chamita Formation, Leyden Quarry, Rio Arriba County, New Mexico: *Borophagus secundus*.
Quibiris Formation, Old Cabin, Redington, and Least Camel quarries, Pima County, Arizona: **Borophagus parvus*.
Big Sandy Formation, Clay Bank, Bird Bone, and Gray Ranch quarries, Mohave County, Arizona: *Borophagus parvus*.
Pinole Local Fauna, Pinole Formation, Pinole Junction Site, Contra Costa County, California: *Borophagus parvus*.
Modesto Reservoir Local Fauna, Mehrten Formation, Rock Point, Sand Point, Rhino Island, and Turlock Lake sites, Stanislaus County, California: *Borophagus parvus* and *Borophagus secundus*.
Mt. Eden Fauna, Mt. Eden Formation, Riverside County, California: *Borophagus secundus*.
Rancho Viejo Beds, Guanajuato, Mexico: *Borophagus secundus*.

?Hemphillian

Prison Farm Gravel Pit, Powell County, Montana: *Epicyon haydeni*.

Latest Hemphillian or earliest Blancan

Saw Rock Canyon Local Fauna, Ogallala Group, Seward County, Kansas: *Borophagus hilli*.

Early Blancan

Hagerman Local Fauna, Glenns Ferry Formation, Twin Falls County, Idaho: *Borophagus hilli*.
Ringold Formation, White Bluffs, Benton County, Washington: *Borophagus hilli*.
Cuchillo Negro Creek Local Fauna, Palomas Formation, Sierra County, New Mexico: *Borophagus hilli*.
Beds correlated with Salada Formation, Las Tunas, southern Baja California, Mexico: *Borophagus hilli*.
Rexroad Formation, Keefe Canyon Quarry, Meade County, Kansas: *Borophagus diversidens*.
Beck Ranch Local Fauna, Scurry County, Texas: *Borophagus diversidens*.
Lisco Local Fauna, Lower part of Broadwater Formation, Lisco Quarry 1, Garden County, Nebraska: *Borophagus diversidens*.
From 8 mi east of Broadwater, probably equivalent to Lisco Local Fauna, Morrill County, Nebraska: *Borophagus diversidens*.
Rancho Viejo beds, Guanajuato, Mexico: *Borophagus diversidens*.

Late Blancan

Grand View Fauna, Glenns Ferry Formation, Ada County, Idaho: *Borophagus diversidens*.
Taunton Fauna, Ringold Formation, Benton County, Washington: *Borophagus diversidens*.
Tehama Formation, northern Sacramento Valley, Tehama County, California: *Borophagus diversidens*.
Coso Mountains, Inyo County, California: *Borophagus diversidens*.
Post Ranch Fauna, Saint David Formation, Carnivore Site, Post Ranch area, Cochise County, Arizona: *Borophagus diversidens*.
Saint David Formation, 3.5 mi section, near Benson, Cochise County, Arizona: *Borophagus diversidens*.
Gila Group, Dry Mountain Locality, Graham County, Arizona: *Borophagus diversidens*.
Panaca Formation, Channel Sands Pocket, near Panaca, Lincoln County, Nevada: *Borophagus diversidens*.
Broadwater Local Fauna, Broadwater Formation, Morrill County, Nebraska: *Borophagus diversidens*.
Sand Draw Fauna, Keim Formation, Lee Magill Ranch, McGill County, Nebraska: *Borophagus diversidens*.
Long Pine Formation, Hall Gravel Pit, Brown County, Nebraska: *Borophagus diversidens*.
Big Spring Local Fauna, Long Pine Formation, Antelope County, Nebraska: *Borophagus diversidens*.
Blanco Formation, Mt. Blanco, Crosby County, Texas: **Borophagus diversidens*.
Cita Canyon, Randall County, Texas: *Borophagus diversidens*.
Ogallala Group, Channing area, Red Corral (Proctor Pits), Oldham County, Texas: *Borophagus diversidens*.

Santa Fe River Locality 1, Columbia County, Florida: *Borophagus diversidens*.

?Late Blancan

Vicinity of the town of Tequixquiac in the Valley of Mexico, Mexico: *Borophagus diversidens*.

North Port Charlotte Locality, Charlotte County, Florida: *Borophagus diversidens*.

Blancan

Asphalto, near foot of Temblor Range, Kern County, California: *Borophagus diversidens*.

Two miles southeast of Cornwall, Contra Costa County, California: *Borophagus diversidens*.

Gila Group, Pima, Graham County, Arizona: *Borophagus diversidens*.

APPENDIX II

Cranial Measurements of Borophaginae
(Units are in millimeters)

To minimize ontogenetic variation and postmortem distortion, only adult individuals (permanent dentitions fully erupted) and specimens that have not suffered excessive distortion were measured in the present study. As a result, only selected specimens are included for measurement, and they are presented in original measurements instead of in summary form (as in the case of the dental measurements). A slightly modified system of the cranial measurements used by Nowak (1979) is adopted in this study (figs. 145, 146), so that those who are interested can carry out comparative biometrical studies using his data and ours, which are also broadly comparable to those in the Hesperocyoninae monograph (Wang, 1994). The following list details the cranial variates used in this study; all cranial measurements are by Wang. Abbreviations of measurements are in parentheses. For visual comparison, log-ratio diagrams (sensus Simpson, 1941) are presented for all species throughout the text (sometime more than once under different clusters of species).

1. Length of posterior C1 foramen magnum notch (LCM)—Distance from posterior border of upper canine alveolus to foramen magnum notch.
2. Greatest skull length (GSL)—Length from anterior tip of premaxillary to posterior tip of inion.
3. Zygomatic width (ZW)—Greatest distance across zygomata.
4. Braincase width (BW)—Greatest width of cranium across level of parietosquamosal sutures (can be difficult to locate when sutures are fully fused).
5. Maxillary toothrow length from P1 to M2 (LPM)—Distance from anterior edge of alveolus of P1 to posterior edge of alveolus of M2.
6. Maximum palate width across cheekteeth (PWP4)—Greatest breadth between labial sides of most widely separated upper cheekteeth (P4 or M1).
7. Palatal width at P1 (PWP1)—Minimum width between lingual margins of alveoli of the P1s.
8. Frontal shield width (FSW)—Maximum breadth across postorbital processes of frontals.
9. Postorbital constriction width (PCW)—Least width across frontals at constriction behind postorbital processes.
10. Length of M2 to bulla (M2B)—Minimum distance from posterior edge of alveolus of M2 to depression in front of bulla.
11. Height of maxillary toothrow to orbit (MOH)—Minimum distance from outer alveolar margin of M1 to most ventral point of orbit (the alveolar margin of the M1 often varies extensively among individuals or on either side of an individual).
12. Depth of jugal (JD)—Minimum depth of jugal anterior to postorbital process, at right angle to its anteroposterior axis.
13. P4 length (P4L)—Maximum anteroposterior length of crown measured on labial side.
14. M2 width (M2W)—Maximum transverse diameter.
15. Bulla length (LB)—Length from median lacerate foramen to suture of bulla with paraoccipital process.

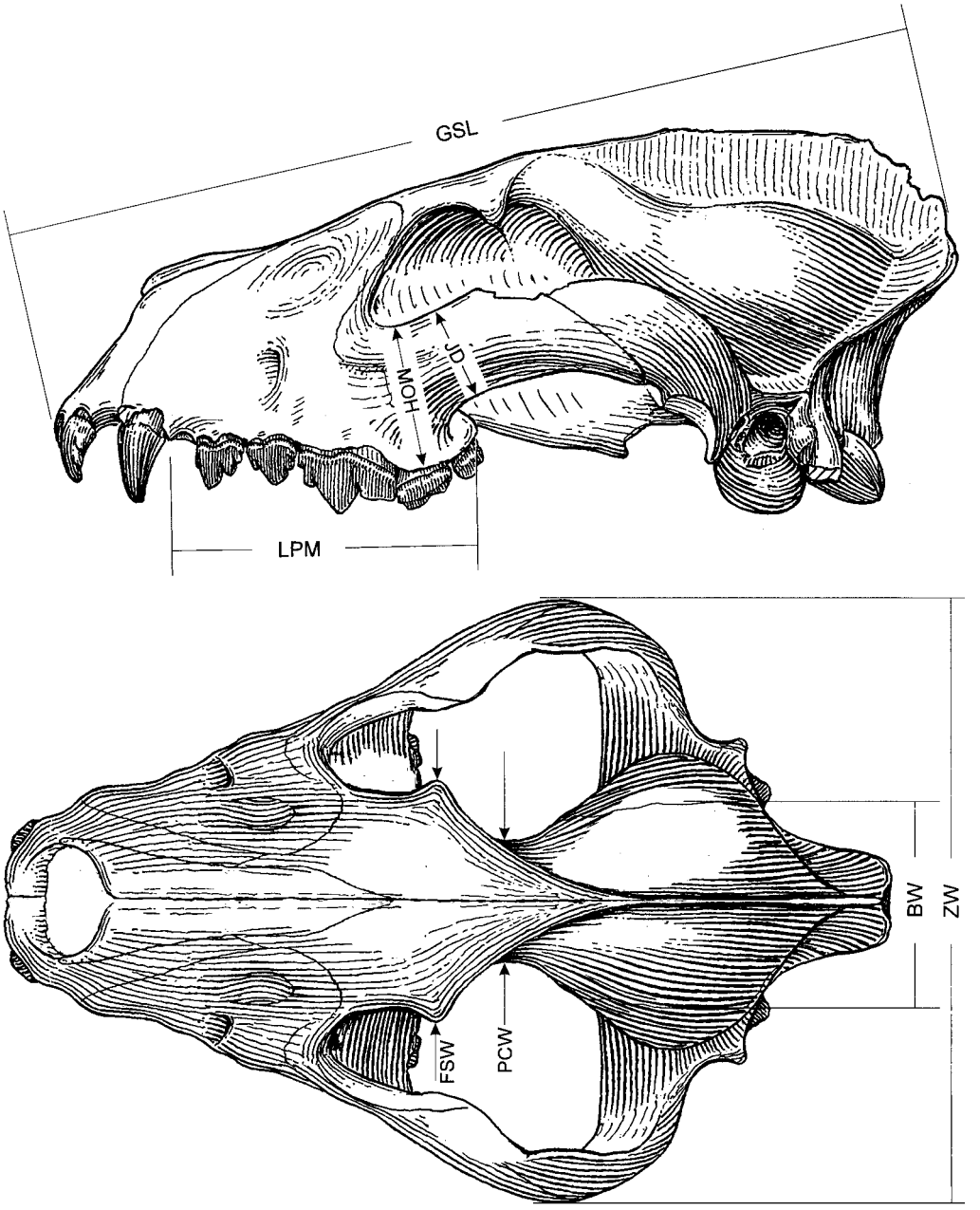

Fig. 145. Definition of cranial measurements, lateral and dorsal aspects of skull. See text for further explanations.

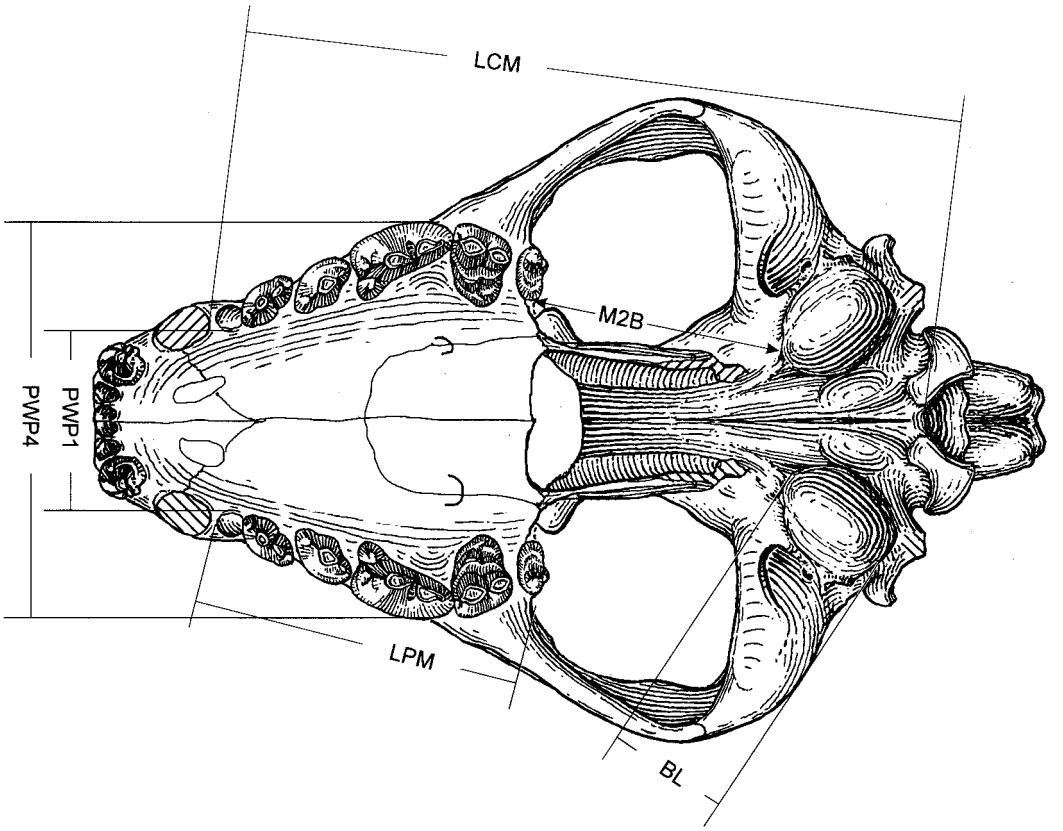

Fig. 146. Definition of cranial measurements, ventral aspect of skull. See text for further explanations.

APPENDIX II. Cranial Measurements of Borophaginae

	LCM	GSL	ZW	BW	LPM	PWP4	PWP1	FSW	PCW	M2B	MOH	JD	P4L	M2W	LB
Archaeocyon pavidus															
F:AM 63970	62.5	76.0	34.0	24.5	26.0	19.6	5.8	15.0	7.5	20.5	9.5	4.6	6.3	5.2	12.5
F:AM 63221	62.0	74.0	44.0		26.3	22.5	7.5	20.0	11.7	18.0	9.5	4.5	6.7	5.6	14.5
F:AM 63222	59.5	72.5	40.0	28.0	25.2	21.0	8.0	18.5	10.5	16.0	9.0	4.6	6.7	5.6	15.5
Mean	61.33	74.17	39.33	26.25	25.83	21.03	7.10	17.83	9.90	18.17	9.33	4.57	6.57	5.47	14.17
Standard Deviation	1.31	1.43	4.11	1.75	0.46	1.18	0.94	2.09	1.77	1.84	0.24	0.05	0.19	0.19	1.25
Coefficent of Variation	2.14	1.93	10.45	6.67	1.80	5.63	13.26	11.75	17.84	10.13	2.53	1.03	2.87	3.45	8.80
Archaeocyon leptodus															
FMNH P14797	71.0	84.5	53.5		30.0	28.0	10.0	22.0	14.0	19.0	11.5	6.0	7.6	7.5	16.8
F:AM 49030			56.0			30.1			14.0	26.5	11.0	6.4	9.2	6.5	18.2
F:AM 49033	82.3	101.0	50.0		34.5	28.5	9.3	22.5	11.2	23.7	9.5		8.7	7.5	18.8
F:AM 49045	74.0	88.5		29.5	31.0	25.5	9.1	20.0	12.5	19.5	11.2	5.5	8.0	7.0	17.3
F:AM 49060											12.5		9.2	6.5	19.3
F:AM 49447	79.0	98.4		32.5	34.1	26.9	10.1	19.6	13.1	24.0	10.0		8.7		16.9
F:AM 50221					30.5	26.7	9.1				12.0	6.1	7.7	6.3	
F:AM 50298	73.0	88.0			29.7	25.5		24.0		20.2	11.5	5.3	8.1		
F:AM 63971	72.0				28.5	25.5	8.8	18.4	12.9	21.0	11.0	5.9	7.0	5.7	14.7
KUVP 32380	86.2	101.0	56.0	35.0	36.7	31.8	11.0	22.9	14.7	25.1	11.9	7.0	9.6	7.4	17.8
UNSM 25399	82.0	98.0			33.0		10.0	21.0	13.0	23.5			8.6	6.9	20.0
UNSM 25707	82.0	101.7			34.2			23.2		23.1	12.9	5.6	8.7	6.9	19.1
UNSM 26097					32.2	26.3	8.5				12.5	6.1	8.0	6.6	
Mean	77.94	95.14	53.88	32.33	32.22	27.48	9.54	21.51	13.18	22.56	11.46	5.99	8.39	6.80	17.89
Standard Deviation	5.21	6.51	2.46	2.25	2.39	2.02	0.74	1.77	1.01	2.38	0.97	0.48	0.71	0.53	1.47
Coefficent of Variation	6.69	6.84	4.56	6.95	7.42	7.36	7.76	8.21	7.66	10.54	8.43	8.04	8.44	7.78	8.20
Archaeocyon falkenbachi															
F:AM 49029 (holotype)	69.4	88.0	54.3	33.0	31.0	27.3	9.7	22.4	11.0	18.5	11.5	5.5	8.7		15.8
Rhizocyon oregonensis															
AMNH 6879 (holotype)	70.0	86.0	44.0	31.0	30.0	27.8	10.5	21.0	13.0	20.5	10.6	5.5	8.3	6.8	14.5
Otarocyon macdonaldi															
AMNH 38986 (holotype)	54.4	63.8	40.8	27.0	21.7	21.4	6.6	15.9	12.2	13.2	7.7		5.6	4.4	17.8
Otarocyon cooki															
F:AM 49020	63.0	65.0	48.0	30.0	22.0	23.0	9.5	20.0	12.5	13.0	9.8	4.6	5.9	5.2	22.5
F:AM 49023	63.0			28.5				20.0	10.0						24.5

APPENDIX II. Cranial Measurements *continued*

	LCM	GSL	ZW	BW	LPM	PWP4	PWP1	FSW	PCW	M2B	MOH	JD	P4L	M2W	LB
Otarocyon cooki continued															
F:AM 49042					24.5	23.9	10.8		12.3		8.9	4.3	6.7	5.6	
F:AM 49043				32.2					13.2						24.4
Mean	63.00	65.00	48.00	30.23	23.25	23.45	10.15	20.00	12.00	13.00	9.35	4.45	6.30	5.40	23.80
Standard Deviation	0.00	0.00	0.00	1.52	1.25	0.45	0.65	0.00	1.20	0.00	0.45	0.15	0.40	0.20	0.92
Coefficent of Variation	0.00	0.00	0.00	5.03	5.38	1.92	6.40	0.00	10.02	0.00	4.81	3.37	6.35	3.70	3.87
Cynarctoides lemur															
AMNH 6888 (holotype)	72.0	80.0	45.0	27.0	26.0	22.5	8.0	19.0		17.0	10.0	5.2	6.8	5.1	16.5
AMNH 6889			38.0	28.0		21.8			11.7	15.2	8.2	4.1	6.8	5.2	14.7
UCMP 10208				30.1			9.0								15.7
Mean	72.00	80.00	41.50	28.37	26.00	22.15	8.50	19.00	11.70	16.10	9.10	4.65	6.80	5.15	15.63
Standard Deviation	0.00	0.00	3.50	1.29	0.00	0.35	0.50	0.00	0.00	0.90	0.90	0.55	0.00	0.05	0.74
Coefficent of Variation	0.00	0.00	8.43	4.55	0.00	1.58	5.88	0.00	0.00	5.59	9.89	11.83	0.00	0.97	4.71
Cynarctoides luskensis															
F:AM 49005 (holotype)	66.4	78.0			30.4				13.0	17.3	9.6	4.6	7.0	6.3	16.2
Cynarctoides gawnae															
F:AM 49249 (holotype)	58.4				27.4	20.4	6.0			12.0			6.6	5.8	15.2
Cynarctoides acridens															
F:AM 49203	66.0				37.5	23.2		23.2	14.0	18.0	10.5	5.5	8.3	8.0	
F:AM 63140					36.3								8.0	6.4	
Mean	66.00				36.90	23.20		23.20	14.00	18.00	10.50	5.50	8.15	7.20	
Standard Deviation	0.00				0.60	0.00		0.00	0.00	0.00	0.00	0.00	0.15	0.80	
Coefficent of Variation	0.00				1.63	0.00		0.00	0.00	0.00	0.00	0.00	1.84	11.11	
Phlaocyon minor															
F:AM 49004	65.0	80.0	52.0	35.5	29.0	28.5	10.8	22.0	16.0	16.2	12.6	6.3	8.3	7.3	16.2
Phlaocyon latidens															
AMNH 6896 (holotype)					23.0	23.4		18.0	13.3	18.7	11.5	7.7	7.4	5.8	19.5
Phlaocyon multicuspus															
FMNH 1482 (holotype)	92.0	114.8	66.0	36.0	37.5	32.9	14.1	25.9	18.6	29.0	15.3	8.0	9.8	8.3	22.8
Phlaocyon marslandensis															
UNSM 26153		124.4	75.0	42.0	46.5	42.6	17.8	34.5	21.5		18.5	11.5	10.0		
Phlaocyon leucosteus															
AMNH 8768 (holotype)	75.5	93.8	66.0	35.2	31.0	34.0	14.5	28.5	15.8	22.7	12.7	7.5	9.2	6.8	18.0

APPENDIX II. Cranial Measurements *continued*

	LCM	GSL	ZW	BW	LPM	PWP4	PWP1	FSW	PCW	M2B	MOH	JD	P4L	M2W	LB
Phlaocyon leucosteus continued															
UNSM 26524			54.0		34.3			19.6	14.0		11.7	6.4	8.1	6.5	
Mean	75.50	93.80	60.00	35.20	32.65	34.00	14.50	24.05	14.90	22.70	12.20	6.95	8.65	6.65	18.00
Standard Deviation	0.00	0.00	6.00	0.00	1.65	0.00	0.00	4.45	0.90	0.00	0.50	0.55	0.55	0.15	0.00
Coefficent of Variation	0.00	0.00	10.00	0.00	5.05	0.00	0.00	18.50	6.04	0.00	4.10	7.91	6.36	2.26	0.00
Cormocyon haydeni															
F:AM 49448 (holotype)	82.0	100.4	53.0	35.7	36.5	29.9	10.7	21.0	15.0	22.0	12.5	6.2	10.0	8.2	18.7
KUVP 32380	85.5	100.5	57.0	35.5	36.5	31.7	11.0	22.9	14.8	25.1	12.4	6.5	9.7	7.5	18.4
Mean	83.75	100.45	55.00	35.60	36.50	30.80	10.85	21.95	14.90	23.55	12.45	6.35	9.85	7.85	18.55
Standard Deviation	1.75	0.05	2.00	0.10	0.00	0.90	0.15	0.95	0.10	1.55	0.05	0.15	0.15	0.35	0.15
Coefficent of Variation	2.09	0.05	3.64	0.28	0.00	2.92	1.38	4.33	0.67	6.58	0.40	2.36	1.52	4.46	0.81
Cormocyon copei															
AMNH 6885 (holotype)	92.0	113.0	55.6	37.2	39.5	35.2		25.0	16.0	28.6	13.4	8.4	8.9	7.5	20.5
AMNH 6887				37.2				26.0	13.1	31.0					18.8
UCMP 76748				39.5		36.6		25.7	18.0	28.7	13.3		10.4	7.7	18.5
UCMP 77161	96.5	123.0		38.2	42.0	36.5	13.0	26.1	14.5	29.8	15.5	8.6	10.2	8.6	19.2
UCMP 112181					35.3	29.0	11.0								
YPM 12679				36.3	35.6		12.5		13.4	29.7			9.3	8.2	
Mean	94.25	118.00	55.60	37.68	38.10	34.33	12.17	25.70	15.00	29.56	14.07	8.50	9.70	8.00	19.25
Standard Deviation	2.25	5.00	0.00	1.09	2.80	3.12	0.85	0.43	1.81	0.87	1.01	0.10	0.62	0.43	0.76
Coefficent of Variation	2.39	4.24	0.00	2.89	7.34	9.10	6.98	1.67	12.08	2.95	7.21	1.18	6.40	5.38	3.96
Desmocyon thomsoni															
AMNH 12874 (holotype)	108.0	135.0	78.0	41.0	44.0	38.8	18.0	31.0	18.0	36.5	21.0	12.0	12.9	9.5	21.5
F:AM 49067	95.0		76.0	41.2	43.8	45.2	19.6	34.0		29.6	16.0		11.9	9.1	18.2
F:AM 49096A	108.0	136.0			45.5	38.7				35.5	17.0		12.5	9.5	
F:AM 49096B	100.0	138.0			44.0			28.0	16.0	35.0	18.5		12.1	9.7	21.0
F:AM 49096C	98.0	130.0	70.0	39.8	42.5	40.5	18.0	30.4		32.0	18.6	9.5	12.3	9.2	22.0
F:AM 49097	98.0	136.0	81.0	39.0	46.5	46.0	21.0	31.0	16.5	32.5	19.0	11.0	12.3	10.0	22.0
UNSM 26550	95.3	117.8	69.1	41.5	42.0	38.8	15.5	29.5	20.7	27.7	15.1	8.3	11.7	8.9	22.1
UNSM 26664	94.3	119.6	71.0	40.5	43.7	39.9	16.0	30.0	20.2	27.8	15.7	7.8	12.0	9.2	20.9
Mean	99.58	130.34	74.18	40.50	44.00	41.13	18.02	30.56	18.28	32.08	17.61	9.72	12.21	9.39	21.10
Standard Deviation	5.17	7.72	4.43	0.86	1.36	2.90	1.91	1.70	1.90	3.23	1.87	1.59	0.35	0.33	1.27
Coefficent of Variation	5.20	5.92	5.97	2.13	3.10	7.06	10.58	5.56	10.38	10.08	10.64	16.32	2.88	3.55	6.01

APPENDIX II. Cranial Measurements *continued*

	LCM	GSL	ZW	BW	LPM	PWP4	PWP1	FSW	PCW	M2B	MOH	JD	P4L	M2W	LB
Desmocyon matthewi															
F:AM 49177 (holotype)	103.0	134.0	78.3	43.3	45.8	46.0	21.8	38.6	26.0	30.8	20.0	9.7	13.3	10.0	21.8
F:AM 61300	114.0	138.7			46.0	45.0	20.5	35.0	23.5	39.0	20.2	9.8	12.8	10.1	23.0
Mean	108.50	136.35	78.30	43.30	45.90	45.50	21.15	36.80	24.75	34.90	20.10	9.75	13.05	10.05	22.40
Standard Deviation	5.50	2.35	0.00	0.00	0.10	0.50	0.65	1.80	1.25	4.10	0.10	0.05	0.25	0.05	0.60
Coefficent of Variation	5.07	1.72	0.00	0.00	0.22	1.10	3.07	4.89	5.05	11.75	0.50	0.51	1.92	0.50	2.68
Paracynarctus kelloggi															
F:AM 61001	125.0	164.5			52.4	45.0	25.6		33.5	45.0	17.0		12.2		
Paracynarctus sinclairi															
F:AM 61009 (holotype)	131.5	170.0	90.0	51.0	54.0	48.0	22.0	40.2	31.3	45.0	22.5	13.0	12.7	12.7	26.0
Cynarctus galushai															
F:AM 27543 (holotype)	134.0	174.0		56.0	60.3	55.5	23.7			46.8	17.8		13.8	11.4	22.8
F:AM 27550					50.5	42.2	18.0						11.8	10.2	
Mean	134.00	174.00		56.00	55.40	48.85	20.85			46.80	17.80		12.80	10.80	22.80
Standard Deviation	0.00	0.00		0.00	4.90	6.65	2.85			0.00	0.00		1.00	0.60	0.00
Coefficent of Variation	0.00	0.00		0.00	8.84	13.61	13.67			0.00	0.00		7.81	5.56	0.00
Cynarctus saxatilis															
FMNH P25537					63.0	55.4	25.3						13.1	10.8	25.0
Cynarctus crucidens															
F:AM 49172					50.9	40.7	24.3						9.7	8.2	
Euoplocyon brachygnathus															
F:AM 50120	120.0	156.0		57.0	45.0	54.0	32.0	40.0	30.4	42.0	25.6	14.5	14.5	9.0	24.2
Psalidocyon marianae															
F:AM 27397 (holotype)	112.0	149.0		41.0	48.5	46.0	22.0		25.0	36.0	20.5	11.4	13.5	9.8	22.0
Microtomarctus conferta															
AMNH 18253	91.3			42.0	42.2	38.0	15.0	31.6	23.5	27.4	13.2	9.6	12.2	9.3	18.0
F:AM 27398	98.0			42.5	46.0	41.6		38.0	24.0	28.7	18.0		13.8	9.2	21.8
F:AM 27473	102.0	128.0	72.0	42.0	47.0	44.2	16.5	34.5	21.8	28.8	17.0	9.5	14.5	10.3	23.4
F:AM 27533	101.0	133.3			48.0	40.0	18.0	35.2	24.5	31.4	16.4		14.3	9.8	18.5
F:AM 27548	98.5	124.0			46.5	40.0	15.5	28.4	22.4	29.8			12.8	10.3	19.3
F:AM 61031	102.0			43.0	44.0	45.0	16.4	38.0	24.0	31.0					21.5
F:AM 61038	105.0			44.0	48.0			37.0	26.0	31.5	17.0		15.0	9.2	24.0
F:AM 61039	99.0		69.7	39.4	47.5	43.3			25.0	25.8	17.7	10.8	14.5	10.2	21.2

APPENDIX II. Cranial Measurements *continued*

	LCM	GSL	ZW	BW	LPM	PWP4	PWP1	FSW	PCW	M2B	MOH	JD	P4L	M2W	LB
Microtomarctus conferta continued															
F:AM 61057	103.0	127.0			51.8	49.3	16.8	37.0		28.0	17.3		15.5	10.9	12.5
LACM 138651	103.0	120.0	76.0	48.0	48.0	45.7	17.5	35.7	20.0	31.1	17.7	11.0	13.0	10.0	22.8
Mean	100.28	126.46	72.57	42.99	46.90	43.01	16.53	35.04	23.47	29.35	16.79	10.23	13.96	9.91	20.30
Standard Deviation	3.66	4.41	2.60	2.43	2.44	3.29	0.97	3.02	1.71	1.84	1.44	0.68	1.03	0.55	3.23
Coefficent of Variation	3.65	3.49	3.59	5.64	5.20	7.65	5.87	8.61	7.29	6.26	8.56	6.65	7.38	5.60	15.92
Protomarctus optatus															
AMNH 20498	116.7		90.4		50.0	50.0	20.7			32.0	19.5	11.8	14.8	11.5	23.7
F:AM 61274	120.0	152.0	86.0		54.2	50.2	21.8			35.0	23.1	13.5	16.4	11.1	26.1
F:AM 61278	123.5	162.0	94.3	46.0	56.0	53.3	22.5	42.0	30.0	42.0	21.8	14.5	16.8	11.8	25.5
F:AM 61280	137.0	179.0	114.0	45.0	57.5	54.8	25.8			49.5	27.0	14.3	15.6	12.2	25.0
F:AM 61281	119.0	148.0		48.0	52.0	50.0	20.6	38.0	27.3	36.5	20.5		14.6		22.0
Mean	123.24	160.25	96.18	46.33	53.94	51.66	22.28	40.00	28.65	39.00	22.38	13.53	15.64	11.65	24.46
Standard Deviation	7.22	11.97	10.70	1.25	2.69	2.01	1.90	2.00	1.35	6.17	2.61	1.06	0.86	0.40	1.46
Coefficent of Variation	5.86	7.47	11.13	2.69	4.99	3.89	8.51	5.00	4.71	15.83	11.66	7.87	5.51	3.46	5.98
Tephrocyon rurestris															
UO 23077 (holotype)	138.8			49.4	58.4	55.0	25.0	56.0	27.0	48.5	23.5	14.6	17.5	13.4	24.7
Tomarctus hippophaga															
AMNH 18242	158.0	176.0	110.0	48.0	58.5	60.3	23.5	46.0	25.0	46.0	25.0	16.5	19.0	12.3	25.0
AMNH 18243	133.0	166.7	97.5	55.4	60.0	56.5	23.1		32.6	40.6	24.5	15.0	17.4	13.0	27.1
AMNH 18244	136.0	181.0	107.7	52.0	61.7	62.0	24.5	56.0	37.0	45.0	24.5	13.0	17.8	12.7	26.0
F:AM 61156	132.0	177.4	94.5	52.0	56.0	57.6	22.5	43.0	34.4	48.0	22.5	13.0	18.1	12.5	26.0
F:AM 61181				50.7											26.0
F:AM 61215	137.0	172.0		50.0	59.0		22.0	42.0	30.2	44.0	23.0		16.5	12.6	25.5
F:AM 61216				47.5		54.0				37.8			16.2	13.2	
F:AM 61220	160.0	199.0			65.0					61.0	26.6	16.5	16.2	14.0	26.0
Mean	142.67	178.68	102.43	50.80	60.03	58.08	23.12	46.75	31.84	46.06	24.35	14.80	17.31	12.90	25.94
Standard Deviation	11.69	10.13	6.56	2.49	2.80	2.82	0.86	5.54	4.08	6.87	1.34	1.57	0.99	0.53	0.59
Coefficent of Variation	8.19	5.67	6.41	4.90	4.67	4.85	3.71	11.85	12.81	14.92	5.50	10.60	5.71	4.10	2.27
Tomarctus brevirostris															
F:AM 27379				53.0	59.2	58.0		43.0	34.0	43.5	22.3	14.0	16.9	13.3	25.0
F:AM 27470	151.0	180.5		49.0	63.5		24.0	54.0	34.0	51.0	25.5	18.0	17.0	12.3	26.0
F:AM 61158	143.0	187.0	110.0	55.0	61.5	67.5	29.0	58.0	38.5	50.0	26.5	18.2	19.8	13.0	24.5

APPENDIX II. Cranial Measurements *continued*

	LCM	GSL	ZW	BW	LPM	PWP4	PWP1	FSW	PCW	M2B	MOH	JD	P4L	M2W	LB
Tomarctus brevirostris continued															
Mean	147.00	183.75	110.00	52.33	61.40	62.75	26.50	51.67	35.50	48.17	24.77	16.73	17.90	12.87	25.17
Standard Deviation	4.00	3.25	0.00	2.49	1.76	4.75	2.50	6.34	2.12	3.32	1.79	1.93	1.34	0.42	0.62
Coefficent of Variation	2.72	1.77	0.00	4.77	2.86	7.57	9.43	12.28	5.98	6.90	7.23	11.56	7.51	3.26	2.48
Aelurodon asthenostylus															
F:AM 27159	149.5	195.0		61.7	69.0	73.0	32.3	49.0	35.0	49.0	26.6	17.1	23.3	11.8	33.5
F:AM 27161				54.5	69.0	79.6	33.0	66.6	44.2	52.6	30.2	19.1	23.5	11.6	
F:AM 28351	179.0	229.0	156.0	62.0	78.0	90.0	45.6		34.0	53.5	37.2	23.3	26.5	13.6	37.7
Mean	164.25	212.00	156.00	59.40	72.00	80.87	36.97	57.80	37.73	51.70	31.33	19.83	24.43	12.33	35.60
Standard Deviation	14.75	17.00	0.00	3.47	4.24	7.00	6.11	8.80	4.59	1.94	4.40	2.58	1.46	0.90	2.10
Coefficent of Variation	8.98	8.02	0.00	5.84	5.89	8.65	16.53	15.22	12.17	3.76	14.05	13.03	5.99	7.29	5.90
Aelurodon mcgrewi															
F:AM 22410 (holotype)	188.0	243.0	156.0	55.0	74.8	82.2	37.0			60.8	38.0	24.7	27.1	11.7	35.8
F:AM 61778	170.0	225.0	151.5	57.0	74.0	81.4	34.8	64.0	38.0	54.0	33.0	22.5	26.6	11.1	37.2
Mean	179.00	234.00	153.75	56.00	74.40	81.80	35.90	64.00	38.00	57.40	35.50	23.60	26.85	11.40	36.50
Standard Deviation	9.00	9.00	2.25	1.00	0.40	0.40	1.10	0.00	0.00	3.40	2.50	1.10	0.25	0.30	0.70
Coefficent of Variation	5.03	3.85	1.46	1.79	0.54	0.49	3.06	0.00	0.00	5.92	7.04	4.66	0.93	2.63	1.92
Aelurodon stirtoni															
F:AM 25175	150.0	201.0	123.0	53.0	65.6	71.5		50.0	34.0	45.3	28.0	19.0	23.8	10.0	38.0
F:AM 27492	151.0	195.0			54.5		30.0	51.5	32.0	43.5	30.0	21.4	24.5	9.6	31.6
UNSM 25789	143.0	190.0	124.0	51.0	63.0	72.4	30.0	40.0	24.0	47.0	27.5	18.0	24.6	8.9	32.8
Mean	148.00	195.33	123.50	52.00	61.03	71.95	30.00	47.17	30.00	45.27	28.50	19.47	24.30	9.50	34.13
Standard Deviation	3.56	4.50	0.50	1.00	4.74	0.45	0.00	5.10	4.32	1.43	1.08	1.43	0.36	0.45	2.78
Coefficent of Variation	2.40	2.30	0.40	1.92	7.77	0.63	0.00	10.82	14.40	3.16	3.79	7.33	1.46	4.79	8.14
Aelurodon ferox															
F:AM 25230	195.0	244.0	156.0	57.0	88.0	85.0	40.0	77.0	39.0	60.0	36.5	23.0	24.9	13.5	37.0
F:AM 27346	192.0	249.0	166.0	62.0	82.0	92.0	47.0	77.0	41.7	70.0	37.0	26.3	27.0	14.7	41.2
F:AM 27490					79.0	87.0	38.0	72.0	39.3	63.8			29.6	11.2	
F:AM 61720					82.2	91.0	41.2						26.5	14.2	
F:AM 61746	169.0	227.0	153.0	59.0	80.7	91.2	40.5	73.0	38.4	55.5	36.0	22.3	25.0	14.5	34.7
F:AM 61753	192.0	251.0	176.0	65.0	88.0	96.0	46.0	81.0	39.0	62.0	38.0	25.6	26.6	14.1	41.2
F:AM 61754	210.0	276.0		55.0	92.0		48.2	78.0	36.0	81.0	41.0	27.0	27.6	13.2	38.2
F:AM 61755	180.0		160.0		85.0	95.3	47.0		35.0	59.0	37.0	23.0	27.9	13.7	33.0

APPENDIX II. Cranial Measurements *continued*

	LCM	GSL	ZW	BW	LPM	PWP4	PWP1	FSW	PCW	M2B	MOH	JD	P4L	M2W	LB
Aelurodon ferox continued															
F:AM 61757	192.0	254.0	164.0	65.0	91.5	95.3	44.0	73.0	35.0	60.3	42.0	27.5	28.8	16.0	39.0
F:AM 70624					91.0	96.0	45.5	82.0			41.0	26.0	27.2	14.0	
UNSM 1093	185.0	251.0	164.0	60.0	83.5	96.3	47.7	76.0	39.5	61.5	42.6	26.0	27.5	15.0	34.0
UNSM 2330-87	177.0	231.0	150.0	57.5	81.0	87.3	37.6	65.2	35.0	60.0	36.5	24.2	26.6	13.0	35.0
UNSM 2126-90	178.0	239.0		58.0	83.0			71.0	36.0		37.5	22.7	25.0	14.3	30.5
UNSM 46185	174.0	230.0	163.0	57.0	78.5	94.0	41.5		38.5	57.0	37.0	24.5	26.5	11.2	37.0
UW 2427	173.0	231.0	155.0	56.0	80.6			69.0	34.5	56.0	36.7	23.5	25.2	13.5	32.7
Mean	184.75	243.91	160.70	59.23	84.40	92.20	43.40	74.52	37.45	62.18	38.37	24.74	26.79	13.74	36.13
Standard Deviation	11.29	13.80	7.20	3.27	4.44	3.80	3.62	4.70	2.21	6.78	2.27	1.69	1.35	1.23	3.25
Coefficent of Variation	6.11	5.66	4.48	5.52	5.25	4.12	8.34	6.31	5.90	10.90	5.91	6.83	5.03	8.97	8.99
Aelurodon taxoides															
F:AM 61781	178.0	246.0	154.0	63.0	85.0	91.3	45.0	64.0	30.0	60.5	37.4	22.7	27.0	11.8	37.0
F:AM 61782	165.0	226.0	166.0		71.5	94.3	43.2			58.0	34.5	24.5	24.5		32.0
F:AM 67013	210.0	275.0		68.0	89.0	95.0	48.5	88.0			45.0	39.1	27.7	14.7	
F:AM 67036	215.0	280.0	188.0		93.2	103.5	53.0			80.0	43.8	27.8	29.8	13.0	44.0
F:AM 67047	218.0		196.0	65.0	104.0	103.5	46.2	81.0	38.0	70.0	42.0	24.6	34.5	14.4	42.5
F:AM 67328			180.0		82.0	105.0					38.4	24.6	29.3	14.0	39.0
F:AM 70755	208.0		191.0		93.0	105.5	50.3	101.2	48.3	74.0	41.0	24.2	28.7	16.0	37.0
F:AM 79775	209.0		182.0		93.0					79.0	45.0	23.4		14.3	40.3
UCMP 59272	201.0	266.0		61.5	100.4			89.0	35.2	71.0	45.0	31.5	30.7	14.0	34.6
UNSM 1486	216.0	287.0	190.0		98.0	104.4	50.0			75.8	43.3	30.1	34.0	15.5	32.0
UNSM 25933	211.0	282.0	187.0	60.0	94.0	113.0	47.0	87.3	38.5	75.5	44.6	27.4	33.0		
Mean	203.10	266.00	181.56	63.50	91.19	101.72	47.90	85.08	38.00	71.53	41.82	27.26	29.92	14.19	37.60
Standard Deviation	16.69	20.61	12.67	2.79	8.68	6.45	2.97	11.18	5.97	7.26	3.43	4.61	3.04	1.18	4.04
Coefficent of Variation	8.22	7.75	6.98	4.40	9.52	6.34	6.21	13.14	15.71	10.16	8.21	16.89	10.16	8.31	10.74
Paratomarctus temerarius															
F:AM 27244	115.4	144.5	80.0	42.0	49.6	45.6	16.7	34.3	26.2	38.0	21.0		14.7	9.8	24.8
F:AM 27255	128.5	165.0		47.0	53.0	55.6	21.4	43.0	31.4	41.0	22.8	11.6	15.0	11.8	26.0
F:AM 61069	129.0	164.7	95.0	46.0	54.5	51.0		46.0	34.0	43.5	23.0	13.4	16.2	11.2	23.0
F:AM 61070	124.0	157.7		50.5	55.0	54.5	22.1	45.0		43.0	21.5	12.7			21.5
F:AM 67121	113.0	145.0			52.5		18.0			34.0			14.7	10.0	23.0
F:AM 67142	118.0	153.3	83.5	43.0	55.3	49.6	18.4		25.0	35.5	22.0	13.2	16.3	11.0	24.4

APPENDIX II. Cranial Measurements *continued*

	LCM	GSL	ZW	BW	LPM	PWP4	PWP1	FSW	PCW	M2B	MOH	JD	P4L	M2W	LB
Paratomarctus temerarius continued															
F:AM 67394	148.0			45.4	62.0			44.8	26.2	52.7			14.6	12.5	27.7
Mean	125.13	155.03	86.17	45.65	54.56	51.26	19.32	42.62	28.56	41.10	22.06	12.73	15.25	11.05	24.34
Standard Deviation	10.98	8.31	6.41	2.77	3.53	3.58	2.07	4.27	3.51	5.80	0.76	0.70	0.72	0.94	1.92
Coefficent of Variation	8.77	5.36	7.44	6.06	6.48	6.99	10.74	10.02	12.28	14.11	3.44	5.48	4.71	8.55	7.90
Paratomarctus euthos															
F:AM 61089	140.0		110.0	53.5	57.6	60.1	30.0	52.0	39.0	48.0	25.3	17.0	17.9	11.5	31.0
F:AM 61101	128.0	175.0		57.5	52.5	61.0	32.8	58.0	31.0	47.0	25.0	15.6	17.0	10.2	23.0
F:AM 67350		180.0		50.0			30.0	52.0	36.0				18.7		25.0
F:AM 70753		184.0	99.2	47.0	62.5	58.2		47.2	30.0		29.0	16.0	18.1	13.0	
Mean	134.00	179.67	104.60	52.00	57.53	59.77	30.93	52.30	34.00	47.50	26.43	16.20	17.93	11.57	26.33
Standard Deviation	6.00	3.68	5.40	3.92	4.08	1.17	1.32	3.83	3.67	0.50	1.82	0.59	0.61	1.14	3.40
Coefficent of Variation	4.48	2.05	5.16	7.54	7.10	1.95	4.27	7.32	10.81	1.05	6.88	3.63	3.40	9.89	12.91
Carpocyon compressus															
UNSM 2556-90	144.5	187.0	98.0	51.0	60.5	58.5	23.2	57.5	33.7	50.5	26.6	15.7	17.8	11.6	29.0
Carpocyon webbi															
F:AM 61328 (holotype)	177.0	227.0		56.0	88.7	71.1	29.4	66.0	43.0	63.5	34.0	19.7	21.5	15.3	32.2
Carpocyon robustus															
F:AM 61350	148.0	186.0	120.0	48.0	62.0	62.4			36.8	55.0	25.5	16.7	17.0	13.5	
F:AM 70758	179.0		116.0		71.0					61.0	31.3	21.3	21.3	12.6	33.5
Mean	163.50	186.00	118.00	48.00	66.50	62.40			36.80	58.00	28.40	19.00	19.15	13.05	33.50
Standard Deviation	15.50	0.00	2.00	0.00	4.50	0.00			0.00	3.00	2.90	2.30	2.15	0.45	0.00
Coefficent of Variation	9.48	0.00	1.69	0.00	6.77	0.00			0.00	5.17	10.21	12.11	11.23	3.45	0.00
Protepicyon raki															
F:AM 61705 (holotype)					73.5						31.0	20.5	25.8	16.0	
F:AM 61738	162.0	214.0	124.0		73.0	70.8	30.5			54.4	25.0	19.0	25.1	12.3	35.4
F:AM 61739				57.7	71.7	76.5	33.0		38.5		27.0	18.7	23.6	12.6	34.0
Mean	162.00	214.00	124.00	57.70	72.73	73.65	31.75		38.50	54.40	27.67	19.40	24.83	13.63	34.70
Standard Deviation	0.00	0.00	0.00	0.00	0.76	2.85	1.25		0.00	0.00	2.49	0.79	0.92	1.68	0.70
Coefficent of Variation	0.00	0.00	0.00	0.00	1.04	3.87	3.94		0.00	0.00	9.02	4.06	3.70	12.31	2.02
Epicyon aelurodontoides															
F:AM 67025 (holotype)			168.0	66.0	93.2			63.0			40.0	32.0	31.4	12.9	40.0

APPENDIX II. Cranial Measurements *continued*

	LCM	GSL	ZW	BW	LPM	PWP4	PWP1	FSW	PCW	M2B	MOH	JD	P4L	M2W	LB
Epicyon saevus															
AMNH 8305	173.0	225.0	147.0	58.5	77.7	81.0	27.2	71.6	42.6	59.2	31.4	22.8	24.8	13.7	30.0
F:AM 61381	180.0	241.4	133.0	60.0	82.2	80.2	26.6			60.0	38.0	24.3	27.5	16.2	34.0
F:AM 61402	175.0	231.0	144.0	56.0	80.3	73.6	32.0	73.7	49.5	57.0	41.5	25.0	25.7	15.1	31.0
F:AM 61420	210.0	282.0	190.0	65.0	93.0	98.7	48.0	95.0	63.0	74.5	44.0	29.3	29.8	16.6	
F:AM 67331	176.0	228.0	144.0	56.0	81.0	81.3	30.2	71.0	40.3	56.0	31.6	20.0	25.3	14.6	34.4
F:AM 70767	178.0	233.0	138.0	55.0	79.7	81.2	28.5	72.0	44.0	60.0	35.3	22.6	24.5	14.2	35.5
UF 24566					70.5						35.0	21.2	25.1	13.3	
UF 24580					80.0								25.0	13.5	
UF 33301	170.0				73.0			76.0	44.0	57.0	30.0	19.5	24.5		
UF 37283					77.0	88.8	32.0				31.2		27.0	14.0	
Mean	180.29	240.07	149.33	58.42	79.44	83.54	32.07	76.55	47.23	60.53	35.33	23.09	25.92	14.58	32.98
Standard Deviation	12.50	19.43	18.76	3.40	5.70	7.41	6.80	8.41	7.57	5.89	4.66	2.96	1.61	1.11	2.11
Coefficent of Variation	6.93	8.09	12.56	5.81	7.18	8.87	21.20	10.99	16.03	9.73	13.18	12.81	6.22	7.60	6.39
Epicyon haydeni															
F:AM 25141	225.0				93.0		38.0			84.0	48.5	31.5	30.0	16.3	41.0
F:AM 30901					91.0	100.0	43.5				44.0	37.7	30.0	12.1	
F:AM 61443			200.0		98.5	109.0	47.0	106.0			50.6	31.8	34.4	16.0	
F:AM 61474					100.0	107.0	45.0	118.0	53.8		53.0		36.7		
F:AM 61501	255.0	340.0	206.0	80.0	114.0	106.5	47.0	113.0	55.0	88.0	55.0	40.0	36.8	17.2	39.5
F:AM 61503	255.0	338.0		88.0	111.0	126.0	58.0	94.0	60.0	100.0	57.0				
F:AM 61558	233.0	298.0			99.0						50.5	30.0	33.7	15.2	38.0
LACM 131855	208.0	278.0	168.0	60.0	87.0	88.0	34.5	93.5	50.6	79.2	39.7	26.0	16.2	16.1	32.6
UCMP 29638	198.0	258.0	150.0	56.0	91.0	78.0	34.3	73.0	41.5	64.0	41.0	22.9	29.0	14.8	37.5
UF 92000	217.0	282.0	178.0	62.0	89.5	101.0	40.0			82.0	42.0	26.8	30.0	16.0	
UNSM 9499-89	241.0	310.0	215.0	75.0	99.5	111.5	47.7	110.0	63.0	92.0	47.5	34.5	35.0	17.0	43.5
LACM 127790					91.3	109.6	48.8				48.7		29.9		
Mean	229.00	300.57	186.17	70.17	97.07	103.66	43.98	101.07	53.98	84.17	48.13	31.24	31.06	15.63	38.68
Standard Deviation	19.60	28.58	22.81	11.61	8.08	12.52	6.66	14.28	6.90	10.44	5.31	5.25	5.46	1.44	3.37
Coefficent of Variation	8.56	9.51	12.25	16.55	8.32	12.08	15.15	14.13	12.79	12.40	11.04	16.79	17.58	9.20	8.71
Borophagus littoralis															
UCMP 31503 (holotype)	166.0	220.0		56.0	74.5	76.3	35.0	68.0	40.8	59.0	37.5	21.4	25.8	14.6	30.0
UCMP 34515	151.0	199.0	120.0	52.0	68.5	74.5	26.6			50.0	35.0	19.4	24.5	13.5	

APPENDIX II. Cranial Measurements *continued*

	LCM	GSL	ZW	BW	LPM	PWP4	PWP1	FSW	PCW	M2B	MOH	JD	P4L	M2W	LB
Borophagus littoralis continued															
Mean	158.50	209.50	120.00	54.00	71.50	75.40	30.80	68.00	40.80	54.50	36.25	20.40	25.15	14.05	30.00
Standard Deviation	7.50	10.50	0.00	2.00	3.00	0.90	4.20	0.00	0.00	4.50	1.25	1.00	0.65	0.55	0.00
Coefficent of Variation	4.73	5.01	0.00	3.70	4.20	1.19	13.64	0.00	0.00	8.26	3.45	4.90	2.58	3.91	0.00
Borophagus pugnator															
CM 182					67.0	83.8	38.0				36.0	25.8	25.1	13.5	
CM 184 (holotype)					71.7	84.4	34.2	67.3	41.1		36.5		25.4	15.0	
F:AM 61662					65.6	69.7	28.5	60.0	36.3		29.4		22.7	12.3	
Mean					68.10	79.30	33.57	63.65	38.70		33.97	25.80	24.40	13.60	
Standard Deviation					2.61	6.79	3.90	3.65	2.40		3.24	0.00	1.21	1.10	
Coefficent of Variation					3.83	8.57	11.63	5.73	6.20		9.53	0.00	4.95	8.12	
Borophagus orc															
UF 12313					51.2										
Borophagus parvus															
F:AM 75857 (holotype)	135.5	186.0	116.0	59.0	54.5	68.2	28.0	66.0	48.0	45.5	23.8	21.5	20.6	11.4	27.0
Borophagus secundus															
F:AM 31004	158.0	215.0	154.0	61.0	67.5	91.8	35.5	75.5	40.3	46.0	36.2	27.0	26.9	14.5	35.0
F:AM 61640	142.3	200.3		57.0	61.2	77.5	29.3	57.1	37.0	46.0	32.5		25.1	14.5	35.5
F:AM 61641	158.0	220.2		55.0	70.2	82.5	32.0	63.2	35.5	50.4	38.5	26.4	28.1	15.5	33.3
F:AM 61642					64.1	76.6	30.3				32.2	24.8	24.3	13.6	
F:AM 61680-9	154.0	211.0		58.0	65.5	80.9	31.0	59.0	40.0	47.6	33.0	22.0	25.2	15.6	33.0
F:AM 61687					71.8	89.8	33.2				34.5		27.5	17.2	
UNSM 2673	178.0	238.0	149.0	51.0	73.5	82.1	36.0	70.0	35.0	59.0	37.0	22.7	25.7	14.6	37.5
Mean	158.06	216.90	151.50	56.40	67.69	83.03	32.47	64.96	37.56	49.80	34.84	24.58	26.11	15.07	34.86
Standard Deviation	11.51	12.41	2.50	3.32	4.08	5.35	2.37	6.88	2.22	4.87	2.26	1.97	1.30	1.07	1.63
Coefficent of Variation	7.28	5.72	1.65	5.89	6.03	6.44	7.30	10.60	5.90	9.78	6.50	8.02	4.97	7.11	4.68
Borophagus hilli															
WT 1558 (holotype)					68.2	91.7	35.5						29.9	12.7	
Borophagus dudleyi															
MCZ 3688 (holotype)	183.0	247.0	188.0	64.0	74.0	112.0	46.0	94.0	53.0	68.0	39.0	36.0	32.0		33.0
Borophagus diversidens															
IGN 162					65.3	116.3	43.2						30.4		
LACM-CIT 481					68.5	91.4	33.0						28.5	12.2	

APPENDIX II. Cranial Measurements *continued*

	LCM	GSL	ZW	BW	LPM	PWP4	PWP1	FSW	PCW	M2B	MOH	JD	P4L	M2W	LB
Borophagus diversidens continued															
MSU 8034	165.4	212.0	166.0	59.4	71.3	98.9	34.3	66.8	44.9	60.4	47.4	28.5	28.7	13.2	32.9
UCMP 8138					68.5	92.5							29.9	13.6	
Mean	165.40	212.00	166.00	59.40	68.40	99.78	36.83	66.80	44.90	60.40	47.40	28.50	29.38	13.00	32.90
Standard Deviation	0.00	0.00	0.00	0.00	2.12	9.96	4.53	0.00	0.00	0.00	0.00	0.00	0.80	0.59	0.00
Coefficent of Variation	0.00	0.00	0.00	0.00	3.10	9.98	12.31	0.00	0.00	0.00	0.00	0.00	2.72	4.53	0.00

APPENDIX III

Statistical Summaries of Dental Measurements of Borophaginae (units are in millimeters)

Most specimens were measured by Taylor, and the rest were measured by Wang. Problems in consistency are minimal for most measurements, especially longitudinal measurements, which are well defined and highly reproducible (fig. 147). Some transverse measurements (e.g., P4 width, M2 width, m1 trigonid width), on the other hand, may be sensitive to location and angle of the caliper, and are inherently less precise and subject to variations in individual habits. A skull-length measurement is added to provide a sense of overall size. Abbreviations of measurements are in parentheses. For a visual comparison, log-ratio diagrams (sensu Simpson, 1941) are presented for all species throughout the text (sometimes more than once under different clusters of species).

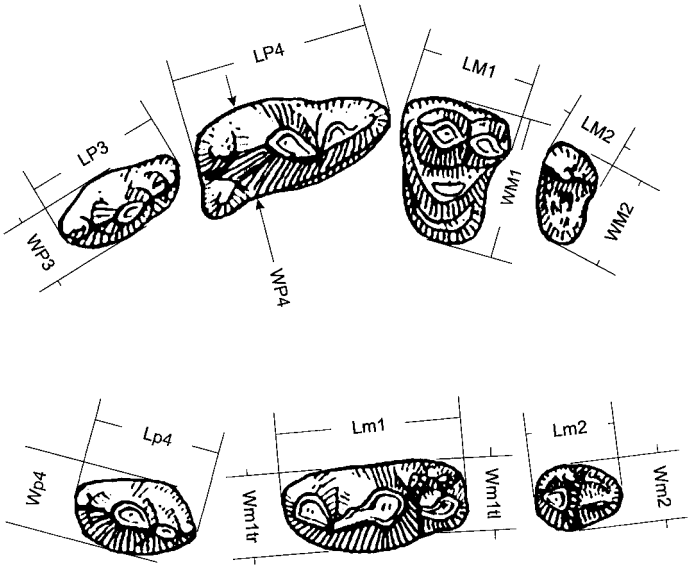

Fig. 147. Definition of dental measurements for P3–M2 (upper) and p4–m2 (lower). See text for further explanations.

Basal length of skull (BL)—Maximum distance from anterior tip of premaxillary to foramen magnum notch.

P1–P3 lengths (e.g., LP1)—Maximum anteroposterior diameter on the major axis of each tooth.

P4 length (LP4)—Maximum anteroposterior diameter from the parastyle to the metastyle corners with calipers held parallel to the base of the tooth.

P4 width (WP4)—Maximum transverse diameter taken just posterior to the protocone.

M1 length (LM1)—Maximum anteroposterior diameter from the parastyle to the metastyle with the calipers held parallel to the labial border.

M1 width (WM1)—Maximum transverse diameter from the labial cingulum to the lingual border with caliper held perpendicular to the paracone and metacone.

M2 length (LM2)—Maximum anteroposterior diameter from the parastyle to the metastyle with the calipers held parallel to the labial border.

M2 width (WM2)—Maximum transverse diameter on the major axis of the tooth from the labial cingulum to the lingual border.

p1–p4 lengths (e.g., Lp1)—Maximum anteroposterior diameter on the major axis of each tooth.

p4 width (Wp4)—Maximum transverse diameter of p4.

m1 length (Lm1)—Maximum anteroposterior diameter of each tooth.

m1 trigonid width (Wm1tr)—Maximum transverse diameter at the carnassial notch.

m1 talonid width (Wm1tl)—Maximum transverse diameter of the talonid at hypoconid.

m2 length (Lm2)—Maximum anteroposterior diameter on the main axis of the tooth from the paraconid to the posterior cingulum or hypoconulid.

m2 width (Wm2)—Maximum transverse diameter.

APPENDIX III. Statistical Summaries of Dental Measurements

	BL	LP1	LP2	LP3	LP4	WP4	LM1	WM1	LM2	WM2	Lp1	Lp2	Lp3	Lp4l	Wp4	Lm1	Wm1tr	Wm1tl	Lm2	Wm2
Archaeocyon pavidus																				
Holotype (LACM 466)			3.8	4.3	6.4	3.0	4.5	6.8	3.3	5.2		3.6	4.4	5.2	2.4	7.0	3.0	3.2	4.3	2.9
Mean	69.67	2.03	3.68	4.44	6.73	3.14	5.20	6.94	3.47	5.22	2.14	3.71	4.49	5.18	2.23	7.36	2.95	3.13	4.28	2.76
Standard Deviation	1.25	0.18	0.15	0.27	0.45	0.27	0.37	0.24	0.17	0.46	0.23	0.34	0.42	0.40	0.23	0.38	0.28	0.25	0.28	0 17
Coefficent of Variation	1.79	8.82	3.99	6.12	6.72	8.45	7.02	3.48	4.80	8.88	10.90	9.18	9.42	7.73	10.56	5.13	9.54	8.14	6.49	6.24
Maximum	71.0	2.3	3.8	5.0	7.6	3.5	5.5	7.3	3.8	5.8	2.5	4.2	5.5	6.1	2.6	7.9	3.5	3.7	4.7	3.0
Minimum	68.0	1.8	3.4	4.1	6.3	2.8	4.5	6.6	3.3	4.4	1.8	3.0	4.0	4.6	1.8	6.5	2.5	2.7	3.8	2.3
Number	3	4	5	7	8	5	6	5	7	6	5	8	10	12	12	16	13	14	16	14
Archaeocyon leptodus																				
Holotype (MCZ 2878)														6.2	2.1	9.6	3.2	3.6	5.2	3.2
Mean	87.89	2.83	4.78	5.46	8.42	4.09	6.71	8.25	4.09	6.44	2.55	4.46	5.30	5.97	2.58	9.34	3.60	3.85	5.30	3.33
Standard Deviation	6.65	0.21	0.46	0.55	0.65	0.36	0.54	0.55	0.45	0.53	0.30	0.50	0.52	0.49	0.19	0.73	0.24	0.27	0.47	0.26
Coefficent of Variation	7.56	7.42	9.66	10.01	7.67	8.87	8.02	6.61	10.97	8.27	11.80	11.16	9.82	8.21	7.21	7.86	6.61	7.02	8.83	7.85
Maximum	97.0	3.3	6.0	6.8	9.7	5.1	7.7	9.5	5.0	7.2	3.0	5.3	6.1	6.9	2.8	10.9	4.2	4.5	6.3	3.9
Minimum	80.0	2.5	4.3	4.7	7.3	3.5	5.5	7.2	3.3	5.5	2.0	3.1	4.4	5.0	2.1	7.8	3.1	3.3	4.2	2.9
Number	11	10	14	19	30	29	30	28	25	24	10	18	29	36	28	53	43	47	41	38
Archaeocyon falkenbachi																				
Holotype (AMNH 49029)			4.5		8.5	4.2	6.8	8.9												
Oxetocyon cuspidatus																				
Holotype (SDSM 2980)							4.9	6.0												
Mean					6.95	3.55	5.40	6.73	4.10	6.40				5.07	2.33	7.63	2.97	3.47	4.80	3.40
Standard Deviation					0.65	0.45	0.57	0.66	0.20	0.00				0.12	0.17	0.21	0.12	0.12	0.00	0.00
Coefficent of Variation					9.35	12.68	10.58	9.80	4.88	0.00				2.46	7.28	2.69	4.20	3.60	0.00	0.00
Maximum					7.6	4.0	6.2	7.6	4.3	6.4				5.2	2.5	7.9	3.1	3.6	4.8	3.4
Minimum					6.3	3.1	4.9	6.0	3.9	6.4				4.9	2.1	7.4	2.8	3.3	4.8	3.4
Number					2	2	3	3	2	2				3	3	3	3	3	1	1
Otarocyon macdonaldi																				
Holotype (AMNH 38986)	62.0	1.9	2.4	3.6	5.6	2.7	4.6	5.9	2.8	4.7	1.7	2.7	3.5	4.0	2.1	6.3	2.6	2.8	3.7	2.6
Mean	62.00	1.90	2.85	3.65	5.60	2.75	4.70	6.00	3.10	4.85	1.70	2.70	3.50	4.00	2.10	6.30	2.60	2.80	3.70	2.60
Standard Deviation	0.00	0.00	0.45	0.05	0.00	0.05	0.10	0.10	0.30	0.15	0.00	0.00	0.00	0.00	0.00	0.00	0.00	0.00	0.00	0.00
Coefficent of Variation	0.00	0.00	15.79	1.37	0.00	1.82	2.13	1.67	9.68	3.09	0.00	0.00	0.00	0.00	0.00	0.00	0.00	0.00	0.00	0.00
Maximum	62.0	1.9	3.3	3.7	5.6	2.8	4.8	6.1	3.4	5.0	1.7	2.7	3.5	4.0	2.1	6.3	2.6	2.8	3.7	2.6
Minimum	62.0	1.9	2.4	3.6	5.6	2.7	4.6	5.9	2.8	4.7	1.7	2.7	3.5	4.0	2.1	6.3	2.6	2.8	3.7	2.6
Number	1	1	2	2	2	2	2	2	2	2	1	1	1	1	1	1	1	1	1	1
Otarocyon cooki																				
Holotype (SDSM 54308)														4.1	2.0	6.2	2.4	2.9	4.1	2.5
Mean	64.00	1.80	3.00	3.80	6.50	3.23	5.10	6.97	3.36	5.42	1.93	3.10	3.78	4.34	2.31	6.51	2.83	3.15	3.95	2.75
Standard Deviation	0.00	0.30	0.30	0.30	0.26	0.39	0.11	0.56	0.27	0.23	0.09	0.33	0.23	0.22	0.24	0.36	0.26	0.26	0.38	0.24
Coefficent of Variation	0.00	16.67	10.00	7.89	4.03	12.07	2.10	8.07	8.12	4.27	4.88	10.80	5.99	5.10	10.29	5.56	9.11	8.26	9.63	8.70
Maximum	64.0	2.1	3.3	4.1	6.8	3.8	5.2	7.5	3.8	5.8	2.0	3.4	4.1	4.7	2.7	7.0	3.3	3.6	4.6	3.1
Minimum	64.0	1.5	2.7	3.5	5.9	2.5	4.9	5.7	3.0	5.1	1.8	2.5	3.5	4.1	2.0	5.9	2.4	2.7	3.5	2.4
Number	1	2	2	2	7	6	7	7	5	5	3	5	6	9	9	12	9	11	11	11

APPENDIX III. Dental Measurements *continued*

	BL	LP1	LP2	LP3	LP4	WP4	LM1	WM1	LM2	WM2	Lp1	Lp2	Lp3	Lp4l	Wp4	Lm1	Wm1tr	Wm1tl	Lm2	Wm2
Rhizocyon oregonensis																				
Holotype (AMNH 6879)	80.0	3.0	4.8	5.3	8.0	4.0	6.6	8.0	3.2	6.5	2.6	4.7	5.5	6.2	2.5	9.3	3.4	3.7	5.3	3.2
Mean	80.00	3.00	4.80	5.50	8.13	3.80	6.40	7.88	3.70	5.88	2.60	4.43	5.25	6.14	2.80	9.09	3.47	3.71	5.20	3.32
Standard Deviation	0.00	0.00	0.00	0.36	0.19	0.28	0.21	0.08	0.33	0.49	0.00	0.31	0.26	0.30	0.18	0.73	0.17	0.18	0.42	0.29
Coefficent of Variation	0.00	0.00	0.00	6.47	2.32	7.44	3.31	1.05	8.96	8.37	0.00	6.97	4.95	4.83	6.52	8.06	4.90	4.75	8.16	8.72
Maximum	80.0	3.0	4.8	6.0	8.4	4.0	6.6	8.0	4.0	6.5	2.6	4.7	5.5	6.5	3.1	10.0	3.7	3.9	5.8	3.7
Minimum	80.0	3.0	4.8	5.2	8.0	3.4	6.1	7.8	3.2	5.3	2.6	4.0	4.9	5.6	2.5	8.0	3.3	3.3	4.5	2.9
Number	1	1	1	3	3	3	4	4	4	4	1	3	4	7	9	11	6	8	8	9
Cynarctoides lemur																				
Holotype (AMNH 6888)	72.0	1.8		5.1	6.4	3.8	5.0	6.8	3.5	4.8										
Mean	72.00	1.80	3.80	4.92	6.81	3.61	5.51	6.89	3.57	5.34	2.30		4.57	5.47	2.56	7.43	3.24	3.38	4.30	2.87
Standard Deviation	0.00	0.00	0.20	0.27	0.34	0.16	0.46	0.39	0.21	0.56	0.00		0.21	0.31	0.25	0.26	0.35	0.13	0.33	0.23
Coefficent of Variation	0.00	0.00	5.26	5.43	4.95	4.42	8.26	5.62	5.98	10.43	0.00		4.50	5.65	9.94	3.48	10.94	3.92	7.71	7.97
Maximum	72.0	1.8	4.0	5.2	7.3	3.9	6.4	7.6	4.0	6.4	2.3		4.8	6.1	3.1	7.8	3.9	3.7	4.6	3.2
Minimum	72.0	1.8	3.6	4.5	6.2	3.4	4.5	6.2	3.2	4.7	2.3		4.3	4.9	2.2	6.7	2.7	3.2	3.5	2.5
Number	1	1	2	6	14	9	22	22	12	11	1		3	9	8	16	12	10	8	6
Cynarctoides roii																				
Holotype (SDSM 53321)													4.1	4.5	2.2	6.4	2.5	2.8	3.9	2.6
Mean												3.20	3.90	4.53	2.10	6.52	2.67	2.97	4.05	2.54
Standard Deviation												0.00	0.32	0.34	0.11	0.27	0.16	0.32	0.15	0.24
Coefficent of Variation												0.00	8.11	7.53	5.09	4.16	6.19	10.95	3.70	9.51
Maximum												3.2	4.3	5.1	2.3	6.9	3.0	3.9	4.3	2.8
Minimum												3.2	3.5	4.1	2.0	5.8	2.4	2.5	3.9	2.1
Number												1	4	7	7	12	12	12	6	5
Cynarctoides harlowi																				
Holotype (ACM 31-34)												3.3	4.0	4.1	1.9	6.6	2.4	2.8	3.7	2.6
Cynarctoides luskensis																				
Holotype (F:AM 49005)	75.0			5.1	7.0	3.7	6.3	7.5	4.3	6.5				5.3	2.3	7.6	3.0	3.4	4.8	3.0
Mean	75.00			5.05	7.10	3.85	6.15	7.75	4.30	6.70		4.00	4.70	5.30	2.50	7.55	3.00	3.35	5.00	3.10
Standard Deviation	0.00			0.05	0.10	0.15	0.15	0.25	0.00	0.20		0.00	0.00	0.00	0.20	0.05	0.00	0.05	0.20	0.10
Coefficent of Variation	0.00			0.99	1.41	3.90	2.44	3.23	0.00	2.99		0.00	0.00	0.00	8.00	0.66	0.00	1.49	4.00	3.23
Maximum	75.0			5.1	7.2	4.0	6.3	8.0	4.3	6.9		4.0	4.7	5.3	2.7	7.6	3.0	3.4	5.2	3.2
Minimum	75.0			5.0	7.0	3.7	6.0	7.5	4.3	6.5		4.0	4.7	5.3	2.3	7.5	3.0	3.3	4.8	3.0
Number	1			2	2	2	2	2	2	2		1	1	2	2	2	2	2	2	2
Cynarctoides gawnae																				
Holotype (F:AM 49249)		2.2	4.2	4.7	6.6	3.1	5.0	6.7	3.6	5.9		3.8	4.4	4.8	1.9	7.5	2.6	3.2	4.3	3.1
Mean		2.20	4.20	4.70	6.60	3.10	5.00	6.70	3.60	5.90	2.30	3.80	4.60	5.00	1.95	8.00	2.73	3.27	4.50	3.10
Standard Deviation		0.00	0.00	0.00	0.00	0.00	0.00	0.00	0.00	0.00	0.00	0.00	0.20	0.20	0.05	0.37	0.12	0.09	0.20	0.00
Coefficent of Variation		0.00	0.00	0.00	0.00	0.00	0.00	0.00	0.00	0.00	0.00	0.00	4.35	4.00	2.56	4.68	4.56	2.89	4.44	0.00
Maximum		2.2	4.2	4.7	6.6	3.1	5.0	6.7	3.6	5.9	2.3	3.8	4.8	5.2	2.0	8.4	2.9	3.4	4.7	3.1
Minimum		2.2	4.2	4.7	6.6	3.1	5.0	6.7	3.6	5.9	2.3	3.8	4.4	4.8	1.9	7.5	2.6	3.2	4.3	3.1
Number		1	1	1	1	1	1	1	1	1	1	1	2	2	2	3	3	3	2	2

APPENDIX III. Dental Measurements *continued*

	BL	LP1	LP2	LP3	LP4	WP4	LM1	WM1	LM2	WM2	Lp1	Lp2	Lp3	Lp4l	Wp4	Lm1	Wm1tr	Wm1tl	Lm2	Wm2
Cynarctoides acridens																				
Holotype (AMNH 82558)																9.0	3.3	4.3		
Mean	80.20	2.50	4.85	5.40	7.55	3.74	5.97	7.76	4.88	7.03	2.23	4.38	5.05	5.62	2.47	8.44	3.25	3.83	5.69	3.59
Standard Deviation	0.00	0.00	0.23	0.57	0.67	0.38	0.60	0.76	0.63	0.49	0.25	0.39	0.35	0.40	0.29	0.60	0.29	0.36	0.36	0.39
Coefficent of Variation	0.00	0.00	4.72	10.53	8.89	10.15	9.97	9.79	12.95	6.96	11.05	8.91	6.94	7.10	11.69	7.07	8.87	9.41	6.35	10.93
Maximum	80.2	2.5	5.2	6.1	8.8	4.5	7.0	9.4	6.0	7.7	2.7	5.1	5.8	6.7	3.1	10.0	4.0	4.8	6.5	4.5
Minimum	80.2	2.5	4.6	4.4	6.2	3.2	4.8	6.3	4.1	6.3	1.7	3.4	4.3	5.0	2.0	6.7	2.5	3.1	5.0	3.0
Number	1	1	4	6	13	12	22	23	10	7	14	33	39	49	50	75	66	74	53	52
Cynarctoides emryi																				
Holotype (UNSM 25455)														5.5	2.6	7.0			6.0	
Mean							6.00	8.00	4.80	7.30			4.73	5.15	2.60	7.62	3.38	4.00	5.97	3.75
Standard Deviation							0.00	0.00	0.00	0.00			0.31	0.30	0.16	0.58	0.15	0.23	0.21	0.15
Coefficent of Variation							0.00	0.00	0.00	0.00			6.53	5.74	6.28	7.67	4.38	5.86	3.44	4.00
Maximum							6.0	8.0	4.8	7.3			5.0	5.5	2.8	8.6	3.6	4.2	6.2	3.9
Minimum							6.0	8.0	4.8	7.3			4.3	4.7	2.4	7.0	3.2	3.6	5.7	3.6
Number							1	1	1	1			3	4	3	5	4	4	3	2
Phlaocyon minor																				
Holotype (AMNH 12877)					8.6	4.6	7.0	9.2	5.5	8.2		5.1	6.0	7.0	3.3	9.7	3.8	4.4		
Mean	72.00	2.40	4.40		8.33	4.40	6.83	8.88	5.00	7.40	2.13	4.54	5.37	6.32	2.89	9.32	3.76	4.26	6.03	3.83
Standard Deviation	0.00	0.00	0.00		0.21	0.20	0.20	0.43	0.36	0.57	0.24	0.47	0.42	0.46	0.31	0.62	0.41	0.33	0.44	0.39
Coefficent of Variation	0.00	0.00	0.00		2.47	4.55	3.00	4.87	7.12	7.64	11.05	10.39	7.75	7.28	10.63	6.69	10.85	7.63	7.33	10.14
Maximum	72.0	2.4	4.4		8.6	4.6	7.0	9.3	5.5	8.2	2.3	5.1	6.0	7.1	3.5	10.5	4.8	4.8	7.1	4.2
Minimum	72.0	2.4	4.4		8.1	4.2	6.5	8.2	4.7	7.0	1.8	3.8	4.7	5.5	2.5	8.5	3.3	3.7	5.5	3.2
Number	1	1	1		3	2	4	4	3	3	3	5	7	10	9	12	10	11	9	7
Phlaocyon latidens																				
Holotype (AMNH 6896)					7.4	4.5	6.5	7.6	3.9	5.9			4.7	5.6	2.8	8.5	3.4	4.0	5.1	3.2
Mean				5.40	7.24	4.23	6.11	7.39	4.11	5.77	2.10	4.15	4.83	5.68	2.79	8.20	3.43	4.12	5.17	3.45
Standard Deviation				0.00	0.32	0.28	0.40	0.47	0.24	0.38	0.00	0.05	0.14	0.26	0.20	0.28	0.18	0.71	0.32	0.23
Coefficent of Variation				0.00	4.42	6.56	6.52	6.33	5.73	6.53	0.00	1.20	2.84	4.62	7.24	3.38	5.14	17.26	6.18	6.64
Maximum				5.4	7.8	4.5	6.9	8.2	4.4	6.6	2.1	4.2	5.0	6.0	3.2	8.5	3.7	6.3	5.6	3.8
Minimum				5.4	6.8	3.9	5.4	6.8	3.8	5.4	2.1	4.1	4.7	5.1	2.5	7.7	3.0	3.5	4.5	3.2
Number				1	7	4	9	9	7	7	1	2	6	11	11	18	11	18	7	6
Phlaocyon annectens																				
Holotype (CMNH 1602)		2.7	4.3	4.5	8.6	5.1	6.4	7.6	4.0	6.5	2.4	4.1	4.7	5.7	2.8	9.7	3.4	4.2	5.1	3.5
Mean		2.40	4.25	4.77	8.08	5.25	6.00	7.55	3.47	5.87	2.40	4.15	4.57	5.80	3.05	9.30	3.77	4.08	4.85	3.50
Standard Deviation		0.30	0.05	0.38	0.40	0.34	0.45	0.05	0.41	0.69	0.00	0.05	0.09	0.10	0.25	0.71	0.26	0.28	0.25	0.00
Coefficent of Variation		12.50	1.18	7.91	4.90	6.39	7.55	0.66	11.85	11.84	0.00	1.20	2.06	1.72	8.20	7.64	6.97	6.80	5.15	0.00
Maximum		2.7	4.3	5.3	8.6	5.8	6.5	7.6	4.0	6.5	2.4	4.2	4.7	5.9	3.3	10.1	4.0	4.3	5.1	3.5
Minimum		2.1	4.2	4.5	7.6	4.9	5.5	7.5	3.0	4.9	2.4	4.1	4.5	5.7	2.8	8.2	3.4	3.6	4.6	3.5
Number		2	2	3	4	4	4	2	3	3	1	2	3	2	2	4	3	4	2	1
Phlaocyon achoros																				
Holotype (UF 18389)					6.8	4.1														

APPENDIX III. Dental Measurements *continued*

	BL	LP1	LP2	LP3	LP4	WP4	LM1	WM1	LM2	WM2	Lp1	Lp2	Lp3	Lp4l	Wp4	Lm1	Wm1tr	Wm1tl	Lm2	Wm2
Phlaocyon achoros continued																				
Mean					6.95	4.25	6.50	7.60	3.93	5.50			3.70	5.10	2.60	8.50	3.10	3.87	5.15	3.45
Standard Deviation					0.15	0.15	0.00	0.00	0.24	0.57			0.00	0.10	0.10	0.10	0.10	0.31	0.15	0.05
Coefficent of Variation					2.16	3.53	0.00	0.00	5.99	10.39			0.00	1.96	3.85	1.18	3.23	7.99	2.91	1.45
Maximum					7.1	4.4	6.5	7.6	4.1	6.0			3.7	5.2	2.7	8.6	3.2	4.3	5.3	3.5
Minimum					6.8	4.1	6.5	7.6	3.6	4.7			3.7	5.0	2.5	8.4	3.0	3.6	5.0	3.4
Number					2	2	1	1	3	3			1	2	2	2	2	3	2	2
Phlaocyon multicuspus																				
Holotype (FMNH UC1482)					9.7	6.7	7.8	10.1	5.7	9.1										
Phlaocyon marslandensis																				
Holotype (FMNH P26314)					9.8	8.1	8.6	10.3												
Mean		2.70	5.75	6.55	9.96	7.80	8.92	10.82	5.20	6.90		6.30	6.20	7.30	4.50	11.20	5.20	6.00	6.93	5.27
Standard Deviation		0.00	0.25	0.25	0.23	0.57	0.36	0.70	0.00	0.00		0.70	0.30	0.60	0.20	0.80	0.30	0.20	0.26	0.57
Coefficent of Variation		0.00	4.35	3.82	2.34	7.33	4.04	6.44	0.00	0.00		11.11	4.84	8.22	4.44	7.14	5.77	3.33	3.79	10.89
Maximum		2.7	6.0	6.8	10.4	8.3	9.5	12.0	5.2	6.9		7.0	6.5	7.9	4.7	12.0	5.5	6.2	7.3	6.0
Minimum		2.7	5.5	6.3	9.8	7.0	8.5	10.0	5.2	6.9		5.6	5.9	6.7	4.3	10.4	4.9	5.8	6.7	4.6
Number		1	2	2	5	3	5	5	1	1		2	2	2	2	2	2	2	3	3
Phlaocyon leucosteus																				
Holotype (AMNH 8768)	88.5	2.5	4.5	5.0	9.2	6.8	7.2	10.0	4.5	6.6	2.2	4.6	5.2	6.6	3.9	9.4	4.9	5.5	5.9	4.4
Mean	88.50	2.60	4.60	5.10	8.76	6.70	7.50	9.54	4.55	6.83	2.35	4.40	5.07	6.33	3.78	9.76	4.73	5.20	5.70	4.33
Standard Deviation	0.00	0.08	0.29	0.45	0.45	0.33	0.28	0.37	0.09	0.28	0.15	0.20	0.42	0.39	0.37	0.65	0.23	0.31	0.24	0.08
Coefficent of Variation	0.00	3.14	6.40	8.91	5.14	4.99	3.68	3.84	1.90	4.06	6.38	4.55	8.27	6.16	9.80	6.69	4.82	5.93	4.30	1.92
Maximum	88.5	2.7	5.0	5.7	9.2	7.2	8.0	10.0	4.7	7.3	2.5	4.6	5.5	6.7	4.3	10.6	5.0	5.5	5.9	4.4
Minimum	88.5	2.5	4.3	4.6	7.9	6.2	7.2	9.0	4.5	6.6	2.2	4.2	4.5	5.7	3.3	9.1	4.5	4.8	5.3	4.2
Number	1	3	3	3	5	5	5	5	4	4	2	2	3	4	4	5	4	4	4	4
Phlaocyon yatkolai																				
Holotype (UNSM 62546)												8.3	9.2	11.0	6.3	16.2	7.2	7.8	8.8	5.8
Phlaocyon mariae																				
Holotype (F:AM 25466)			11.1	11.8	19.2	12.3	13.1	16.2	6.2	9.4								9.0	9.2	6.1
Cormocyon haydeni																				
Holotype (F:AM 49448)	91.5	3.3	5.5	6.7	10.0	4.9	7.9	9.8	5.3	8.2	2.8	5.3	6.7	7.5	3.1	11.0	4.0	4.5	6.0	4.0
Mean	93.75	3.30	5.45	6.48	9.58	4.75	7.53	9.33	4.70	7.28	2.67	5.23	6.45	6.85	3.10	10.48	4.02	4.25	5.78	3.64
Standard Deviation	2.25	0.00	0.05	0.28	0.66	0.21	0.33	0.42	0.35	0.57	0.19	0.09	0.22	0.46	0.16	0.78	0.29	0.36	0.20	0.39
Coefficent of Variation	2.40	0.00	0.92	4.28	6.86	4.34	4.34	4.51	7.52	7.86	7.07	1.80	3.38	6.73	5.27	7.44	7.10	8.56	3.53	10.79
Maximum	96.0	3.3	5.5	6.8	10.2	5.0	7.9	9.8	5.3	8.2	2.8	5.3	6.7	7.5	3.3	11.8	4.6	4.9	6.0	4.2
Minimum	91.5	3.3	5.4	6.2	8.5	4.5	7.2	8.7	4.4	6.8	2.4	5.1	6.1	6.2	2.9	9.7	3.7	3.9	5.5	3.2
Number	2	1	2	4	4	4	4	4	4	4	3	3	4	4	3	6	6	6	5	5
Cormocyon copei																				
Holotype (AMNH 6885)	103.0	3.0	5.4	6.0	8.9	4.9	8.0	9.1	4.9	7.7	2.3	5.2	6.0	6.8	3.2	11.0	4.0	4.5	6.2	4.0
Mean	103.00	2.95	5.43	6.36	9.35	5.11	7.82	9.46	5.06	7.58	2.65	5.55	6.28	7.26	3.43	11.09	4.38	4.96	6.48	4.36
Standard Deviation	0.00	0.05	0.39	0.60	0.51	0.36	0.61	0.84	0.46	0.65	0.35	0.47	0.41	0.47	0.30	0.77	0.46	0.41	0.43	0.21
Coefficent of Variation	0.00	1.69	7.18	9.40	5.50	6.97	7.79	8.84	9.12	8.56	13.21	8.50	6.48	6.46	8.65	6.95	10.58	8.30	6.63	4.73

APPENDIX III. Dental Measurements *continued*

	BL	LP1	LP2	LP3	LP4	WP4	LM1	WM1	LM2	WM2	Lp1	Lp2	Lp3	Lp4l	Wp4	Lm1	Wm1tr	Wm1tl	Lm2	Wm2
Cormocyon copei continued																				
Maximum	103.0	3.0	6.0	7.5	10.3	5.6	9.1	10.7	5.9	9.0	3.0	6.3	7.0	7.8	3.9	12.2	5.2	5.6	7.3	4.7
Minimum	103.0	2.9	4.9	5.6	8.6	4.6	6.7	8.0	4.3	6.8	2.3	5.1	5.6	6.4	3.0	9.4	3.7	4.5	5.9	4.0
Number	1	2	4	7	10	7	11	11	11	11	2	4	10	8	10	10	8	8	8	7
Desmocyon thomsoni																				
Holotype (AMNH 12874)	126.0	4.0	7.0	7.8	13.0	7.0	10.5	12.8	6.8	9.6	3.5	7.0	7.6	9.0	4.5	14.2	6.0	6.5	8.0	5.2
Mean	114.05	4.05	6.59	7.57	12.05	6.00	9.54	11.89	5.98	8.72	3.50	6.37	7.42	8.51	4.17	13.56	5.39	5.67	7.89	4.94
Standard Deviation	7.22	0.30	0.44	0.51	0.61	0.46	0.63	0.77	0.44	0.63	0.21	0.62	0.49	0.53	0.39	0.86	0.47	0.46	0.54	0.38
Coefficent of Variation	6.33	7.48	6.68	6.77	5.09	7.67	6.65	6.49	7.33	7.23	5.91	9.72	6.56	6.17	9.47	6.34	8.68	8.20	6.80	7.71
Maximum	126.0	4.5	7.7	8.8	13.4	7.1	10.8	13.0	6.8	10.0	3.9	7.7	8.3	10.0	5.4	15.5	6.3	6.5	9.0	6.0
Minimum	104.0	3.3	6.0	6.5	10.8	5.3	8.5	10.4	5.3	7.8	3.0	5.3	6.6	7.8	3.5	11.6	4.5	4.8	6.5	4.1
Number	11	17	24	29	33	30	33	32	24	22	14	23	30	41	38	58	45	52	37	31
Desmocyon matthewi																				
Holotype (F:AM 49177)	121.0	4.0	7.0	7.9	13.0	5.9	10.8	12.9	6.3	8.4	3.6	6.2	7.0	8.7	4.5	14.7	6.0	6.2	8.1	5.6
Mean	126.50	4.15	6.83	7.55	12.83	6.57	10.20	12.44	6.15	8.95	3.37	6.32	7.40	9.07	4.57	14.83	5.70	6.09	8.35	5.27
Standard Deviation	5.50	0.15	0.25	0.38	0.66	0.57	0.44	0.45	0.15	0.55	0.26	0.78	0.55	0.57	0.33	1.12	0.42	0.49	0.61	0.56
Coefficent of Variation	4.35	3.61	3.64	5.00	5.18	8.73	4.30	3.62	2.44	6.15	7.80	12.28	7.43	6.28	7.17	7.57	7.37	8.05	7.30	10.67
Maximum	132.0	4.3	7.0	7.9	13.8	7.3	10.8	12.9	6.3	9.5	3.6	7.8	8.8	10.0	5.1	17.5	6.7	7.3	9.3	6.3
Minimum	121.0	4.0	6.4	7.0	12.0	5.9	9.6	11.8	6.0	8.4	3.0	5.2	6.7	8.1	4.1	13.0	5.0	5.4	7.5	4.5
Number	2	2	4	4	4	3	5	5	2	2	3	6	9	16	12	20	16	15	14	10
Paracynarctus kelloggi																				
Holotype (UCMP 11562)											4.6	6.1		8.5	4.7	14.6	5.7	7.3	10.5	
Mean		4.73	7.34	8.28	12.72	7.37	11.25	13.24	8.04	11.49	4.46	6.72	7.51	9.17	4.83	14.95	5.96	6.97	10.31	6.28
Standard Deviation		0.55	0.56	0.53	1.27	0.69	0.72	0.69	0.54	1.07	0.47	0.56	0.72	0.82	0.49	1.36	0.64	0.52	0.58	0.46
Coefficent of Variation		11.63	7.64	6.42	10.00	9.33	6.36	5.25	6.78	9.33	10.64	8.41	9.60	8.90	10.12	9.12	10.71	7.52	5.65	7.26
Maximum		5.5	8.0	9.0	14.2	8.5	12.3	14.2	9.0	12.6	5.5	7.8	9.4	10.8	5.6	18.2	7.5	8.0	11.5	7.1
Minimum		4.0	6.5	7.5	10.0	6.2	9.7	12.0	7.4	9.5	3.8	5.4	6.3	7.5	4.0	12.8	5.0	5.8	9.6	5.3
Number		4	5	4	9	6	10	8	11	11	9	16	12	21	19	24	18	22	14	13
Paracynarctus sinclairi																				
Holotype (F:AM 61009)	156.5		8.0	8.3	12.7	8.4	12.0	14.0	9.5	12.0										
Mean	156.50		8.00	8.30	11.30	7.57	10.93	12.93	8.50	10.93		6.63	8.00	9.60	5.20	14.70	6.70	7.20		
Standard Deviation	0.00		0.00	0.00	1.02	0.60	0.90	0.90	0.73	0.90		0.46	0.00	0.30	0.00	1.47	0.20	0.10		
Coefficent of Variation	0.00		0.00	0.00	9.02	7.95	8.23	6.95	8.54	8.23		7.00	0.00	3.12	0.00	10.02	2.99	1.39		
Maximum	156.5		8.0	8.3	12.7	8.4	12.0	14.0	9.5	12.0		7.1	8.0	9.9	5.2	17.0	6.9	7.3		
Minimum	156.5		8.0	8.3	10.3	7.0	9.8	11.8	7.8	9.8		6.0	8.0	9.3	5.2	13.0	6.5	7.1		
Number	1		1	1	3	3	3	3	3	3		3	1	2	1	4	2	2		
Cynarctus galushai																				
Holotype (F:AM 27543)	206.5		8.0	9.1	13.8	6.3	11.5	13.1	7.8	10.8	3.6	7.2	8.7	9.4	4.6	16.2	6.0	6.6	10.5	
Mean	206.50	5.10	7.20	8.35	12.37	6.07	10.80	11.70	7.70	9.90	3.60	7.24	8.13	9.51	4.79	15.88	6.05	6.38	10.06	5.81
Standard Deviation	0.00	0.00	0.80	0.75	1.02	0.26	0.50	0.99	0.10	0.90	0.00	0.10	0.49	0.49	0.17	0.72	0.27	0.34	0.42	0.25
Coefficent of Variation	0.00	0.00	11.11	8.98	8.26	4.33	4.60	8.46	1.30	9.09	0.00	1.41	6.05	5.16	3.47	4.53	4.54	5.27	4.13	4.35
Maximum	206.5	5.1	8.0	9.1	13.8	6.3	11.5	13.1	7.8	10.8	3.6	7.4	8.7	10.2	5.0	17.2	6.5	7.0	10.9	6.1

APPENDIX III. Dental Measurements *continued*

	BL	LP1	LP2	LP3	LP4	WP4	LM1	WM1	LM2	WM2	Lp1	Lp2	Lp3	Lp4l	Wp4	Lm1	Wm1tr	Wm1tl	Lm2	Wm2
Cynarctus galushai continued																				
Minimum	206.5	5.1	6.4	7.6	11.5	5.7	10.4	11.0	7.6	9.0	3.6	7.1	7.5	8.7	4.5	14.5	5.7	5.7	9.5	5.5
Number	1	1	2	2	3	3	3	3	2	2	1	5	3	9	9	11	11	12	8	7
Cynarctus marylandica																				
Holotype (USNM 15561)																		7.1	9.1	6.1
Mean														9.70	5.10			7.10	9.10	6.10
Standard Deviation														0.00	0.00			0.00	0.00	0.00
Coefficent of Variation														0.00	0.00			0.00	0.00	0.00
Maximum														9.7	5.1			7.1	9.1	6.1
Minimum														9.7	5.1			7.1	9.1	6.1
Number														1	1			1	1	1
Cynarctus saxatilis																				
Holotype (AMNH 9453)											4.2		8.7	10.4	5.5	16.0	6.5	7.3	12.2	7.0
Mean			7.70	9.10	13.63	6.97	12.13	13.10	10.15	11.45	4.45	7.80	9.00	10.37	5.57	16.68	5.98	7.28	11.98	7.93
Standard Deviation			0.00	0.60	0.69	0.78	0.28	0.90	0.96	0.42	0.25	0.10	0.22	0.05	0.09	0.43	0.58	0.60	0.39	0.62
Coefficent of Variation			0.00	6.59	5.09	11.14	2.29	6.89	9.49	3.63	5.62	1.28	2.40	0.45	1.69	2.59	9.71	8.27	3.25	7.85
Maximum			7.7	9.7	14.5	7.9	12.6	14.5	11.8	12.1	4.7	7.9	9.2	10.4	5.7	17.2	6.5	7.9	12.2	8.7
Minimum			7.7	8.5	12.8	6.0	11.9	12.0	9.4	11.0	4.2	7.7	8.7	10.3	5.5	16.0	5.0	6.3	11.3	7.0
Number			1	2	3	3	4	4	4	4	2	2	3	3	3	4	4	4	4	4
Cynarctus voorhiesi																				
Holotype (F:AM 105094)													7.5	9.4	4.9	13.7	5.0	6.0	12.2	6.6
Mean									9.60	9.60		6.00	7.54	8.90	4.70	13.90	4.77	6.28	11.63	6.40
Standard Deviation									0.00	0.00		0.00	0.16	0.39	0.14	0.23	0.33	0.28	0.42	0.22
Coefficent of Variation									0.00	0.00		0.00	2.15	4.40	3.01	1.69	6.92	4.42	3.60	3.38
Maximum									9.6	9.6		6.0	7.8	9.4	4.9	14.3	5.0	6.6	12.2	6.6
Minimum									9.6	9.6		6.0	7.3	8.3	4.6	13.7	4.3	6.0	11.2	6.1
Number									1	1		1	5	6	3	4	3	4	3	3
Cynarctus crucidens																				
Holotype (UNSM 25465)												4.8	5.7	7.0	3.6	10.7	4.1	5.5	9.4	5.5
Mean		3.85	5.57	6.44	8.88	6.04	9.25	8.85	9.79	8.21	3.08	5.32	6.15	7.63	3.73	11.25	4.01	5.50	10.22	5.72
Standard Deviation		0.15	0.54	0.62	1.23	0.58	0.59	0.68	0.88	0.56	0.39	0.48	0.46	0.69	0.27	0.61	0.31	0.34	0.77	0.41
Coefficent of Variation		3.90	9.77	9.55	13.82	9.63	6.37	7.69	8.99	6.86	12.56	8.94	7.42	9.10	7.15	5.45	7.76	6.24	7.49	7.16
Maximum		4.0	6.0	7.1	10.2	6.9	10.3	10.3	11.2	9.2	3.7	6.0	6.8	8.9	4.2	12.7	4.5	6.1	12.2	6.6
Minimum		3.7	4.8	5.4	7.1	5.2	8.2	7.8	7.8	7.3	2.6	4.7	5.4	6.5	3.4	10.2	3.6	4.5	9.0	5.2
Number		2	3	5	6	5	17	17	11	11	5	9	10	13	11	22	19	20	16	13
Protomarctus canavus																				
Holotype (UF V-5260)												6.9		7.5	4.9	15.6	6.3	6.3	8.8	5.7
Mean	155.00	5.70	8.59	9.60	15.54	7.70	11.77	14.51	7.00	11.23	4.74	7.63	8.62	10.34	5.46	17.45	6.98	7.09	9.23	6.00
Standard Deviation	0.00	0.00	0.70	0.69	0.74	0.60	0.65	0.74	0.69	0.97	0.40	0.48	0.48	0.75	0.53	1.06	0.60	0.54	0.70	0.54
Coefficent of Variation	0.00	0.00	8.10	7.24	4.77	7.74	5.55	5.09	9.83	8.60	8.50	6.33	5.53	7.24	9.77	6.06	8.66	7.58	7.57	9.02
Maximum	155.0	5.7	9.8	10.5	16.8	9.1	13.0	15.7	8.0	13.1	5.3	8.9	10.2	12.3	6.5	19.7	8.4	8.4	10.6	7.2
Minimum	155.0	5.7	7.5	8.7	14.0	6.6	10.5	13.1	5.7	9.4	4.1	6.8	7.9	7.5	4.0	15.5	5.2	5.6	8.0	5.0

APPENDIX III. Dental Measurements *continued*

	BL	LP1	LP2	LP3	LP4	WP4	LM1	WM1	LM2	WM2	Lp1	Lp2	Lp3	Lp4l	Wp4	Lm1	Wm1tr	Wm1tl	Lm2	Wm2
Protomarctus canavus continued																				
Number	1	1	7	7	26	24	35	36	23	23	5	35	39	62	57	62	55	57	40	38
Protomarctus sp. A																				
Mean																19.70	6.60	6.00	10.40	
Standard Deviation																0.40	0.00	0.00	0.00	
Coefficent of Variation																2.03	0.00	0.00	0.00	
Maximum																20.1	6.6	6.0	10.4	
Minimum																19.3	6.6	6.0	10.4	
Number																2	1	1	1	
Protomarctus sp. B																				
Mean														12.60	6.15	23.60	7.30	8.55		
Standard Deviation														0.40	0.25	0.90	0.40	0.15		
Coefficent of Variation														3.17	4.07	3.81	5.48	1.75		
Maximum														13.0	6.4	24.5	7.7	8.7		
Minimum														12.2	5.9	22.7	6.9	8.4		
Number														2	2	2	2	2		
Euoplocyon spissidens																				
Holotype (MCZ 4246)														9.4	4.9	16.5	6.5	5.7		
Mean					14.20	6.80	9.70	12.00	5.40	7.60				9.60	4.95	16.40	6.30	5.75	7.80	4.80
Standard Deviation					0.00	0.00	0.00	0.00	0.00	0.00				0.20	0.05	0.10	0.20	0.05	0.00	0.00
Coefficent of Variation					0.00	0.00	0.00	0.00	0.00	0.00				2.08	1.01	0.61	3.17	0.87	0.00	0.00
Maximum					14.2	6.8	9.7	12.0	5.4	7.6				9.8	5.0	16.5	6.5	5.8	7.8	4.8
Minimum					14.2	6.8	9.7	12.0	5.4	7.6				9.4	4.9	16.3	6.1	5.7	7.8	4.8
Number					1	1	1	1	1	1				2	2	2	2	2	1	1
Euoplocyon brachygnathus																				
Holotype (CMNH 752)																18.0		5.4		
Mean	146.00	6.10	8.72	9.30	15.70	7.80	10.23	12.98	4.93	7.90	5.88	7.33	8.46	10.46	5.58	17.75	6.46	5.77	7.39	4.90
Standard Deviation	0.00	0.43	0.32	0.49	0.46	0.22	0.75	0.43	0.44	0.10	0.33	0.52	0.40	0.47	0.22	0.65	0.51	0.50	0.45	0.31
Coefficent of Variation	0.00	7.08	3.66	5.22	2.95	2.77	7.33	3.33	8.89	1.27	5.56	7.06	4.76	4.46	3.93	3.68	7.83	8.61	6.03	6.27
Maximum	146.0	6.5	9.3	10.0	16.3	8.0	11.0	13.5	5.5	8.0	6.4	8.2	9.2	11.5	6.0	19.0	7.3	6.5	8.2	5.2
Minimum	146.0	5.5	8.4	8.5	15.0	7.5	9.0	12.3	4.3	7.8	5.5	6.7	8.0	9.8	5.3	17.0	5.4	5.0	6.7	4.2
Number	1	3	5	5	4	3	4	4	4	2	4	7	5	8	6	11	9	9	7	7
Psalidocyon marianae																				
Holotype (F:AM 27397)	135.0	6.7	7.6	8.7	13.5	7.0	10.5	12.6	7.0	9.7	4.9		6.8	9.0	5.0	16.0	5.8	5.8	8.3	5.3
Mean	135.00	6.70	7.60	8.70	13.50	7.00	10.50	12.60	7.00	9.70	5.20	7.00	7.70	9.53	4.83	15.38	5.48	5.68	8.30	5.30
Standard Deviation	0.00	0.00	0.00	0.00	0.00	0.00	0.00	0.00	0.00	0.00	0.30	0.00	0.63	0.48	0.24	0.53	0.45	0.21	0.00	0.00
Coefficent of Variation	0.00	0.00	0.00	0.00	0.00	0.00	0.00	0.00	0.00	0.00	5.77	0.00	8.16	5.06	4.94	3.45	8.27	3.76	0.00	0.00
Maximum	135.0	6.7	7.6	8.7	13.5	7.0	10.5	12.6	7.0	9.7	5.5	7.0	8.5	10.3	5.1	16.0	6.2	6.0	8.3	5.3
Minimum	135.0	6.7	7.6	8.7	13.5	7.0	10.5	12.6	7.0	9.7	4.9	7.0	6.8	9.0	4.5	14.7	5.0	5.4	8.3	5.3
Number	1	1	1	1	1	1	1	1	1	1	2	2	4	4	4	5	5	5	1	1
Microtomarctus conferta																				
Holotype (AMNH 17203)												5.5	6.4	7.4	4.1	14.5	5.5	5.5	7.5	5.1

APPENDIX III. Dental Measurements *continued*

	BL	LP1	LP2	LP3	LP4	WP4	LM1	WM1	LM2	WM2	Lp1	Lp2	Lp3	Lp4l	Wp4	Lm1	Wm1tr	Wm1tl	Lm2	Wm2
Microtomarctus conferta continued																				
Mean	113.00	3.87	6.79	8.07	13.56	6.30	10.21	12.31	6.02	9.16	3.20	5.90	7.09	8.33	4.43	15.46	5.73	5.95	8.00	5.27
Standard Deviation	5.08	0.36	0.78	0.59	0.89	0.59	0.73	0.86	0.43	0.59	0.42	0.46	0.47	0.57	0.38	0.90	0.38	0.43	0.65	0.36
Coefficent of Variation	4.50	9.20	11.45	7.26	6.58	9.45	7.12	7.01	7.20	6.41	13.26	7.80	6.66	6.84	8.56	5.83	6.71	7.22	8.17	6.84
Maximum	120.0	4.5	8.8	9.4	15.0	7.8	11.5	14.3	7.1	10.9	4.3	7.0	8.3	9.7	5.5	18.0	6.7	7.2	9.2	6.0
Minimum	100.0	3.5	5.4	6.9	11.5	5.0	8.5	10.6	5.2	8.1	2.5	4.5	5.8	6.9	3.9	13.0	4.8	5.2	5.2	4.6
Number	11	9	19	23	52	42	53	49	48	46	14	46	68	88	71	108	72	70	63	48
Protomarctus optatus																				
Holotype (AMNH 18916)												6.8	8.3	10.3	5.0	17.3	6.8	7.3	9.1	6.5
Mean	143.46	5.23	8.24	9.48	15.86	7.54	12.26	14.59	7.39	11.23	4.01	7.27	8.36	10.40	5.47	17.73	6.90	7.25	9.83	6.15
Standard Deviation	12.31	0.41	0.54	0.74	0.75	0.53	0.67	1.02	0.53	1.10	0.48	0.55	0.40	0.65	0.42	0.99	0.43	0.45	0.59	0.44
Coefficent of Variation	8.58	7.93	6.55	7.84	4.73	7.06	5.43	6.97	7.13	9.83	11.85	7.58	4.82	6.28	7.69	5.59	6.29	6.17	6.04	7.10
Maximum	164.0	5.9	9.5	11.4	17.0	8.8	13.3	16.5	8.4	13.3	5.0	9.0	9.0	11.5	6.3	20.5	8.0	8.2	11.0	7.1
Minimum	127.0	4.8	7.3	8.5	14.1	6.5	11.0	12.9	6.5	8.5	3.5	6.0	7.3	9.0	4.5	15.5	5.7	6.5	8.8	5.4
Number	5	4	14	12	34	34	33	33	26	24	8	26	31	46	45	58	52	53	36	33
Tephrocyon rurestris																				
Holotype (UO 23077)			8.1	10.2	17.2	7.6	13.0	14.6	7.7	10.0		7.2	8.7	11.3	6.1	20.0	7.4	7.9	11.5	6.9
Mean			8.20	9.90	17.15	8.70	12.08	14.95	7.55	11.50		7.20	8.70	11.30	6.20	19.20	6.85	7.10	11.03	6.25
Standard Deviation			0.00	0.20	0.05	0.00	0.86	0.65	0.55	0.00		0.00	0.00	0.00	0.00	1.54	0.47	0.66	0.40	0.54
Coefficent of Variation			0.00	2.02	0.29	0.00	7.11	4.35	7.28	0.00		0.00	0.00	0.00	0.00	8.04	6.89	9.29	3.65	8.65
Maximum			8.2	10.1	17.2	8.7	13.0	15.6	8.1	11.5		7.2	8.7	11.3	6.2	21.9	7.6	8.2	11.5	7.0
Minimum			8.2	9.7	17.1	8.7	10.8	14.3	7.0	11.5		7.2	8.7	11.3	6.2	17.6	6.4	6.5	10.4	5.5
Number			1	2	2	1	4	2	2	1		1	1	1	1	5	4	4	4	4
Tomarctus hippophaga																				
Holotype (AMNH 13836)												8.2	9.5	11.8	6.6	19.8	8.2	8.2	10.3	6.6
Mean	161.63	5.47	9.14	10.40	17.20	8.36	12.70	15.33	7.95	11.93	4.35	7.99	9.30	11.19	6.23	19.84	7.72	8.07	10.52	6.75
Standard Deviation	11.54	0.21	0.61	0.68	1.24	0.65	0.62	0.90	0.53	0.79	0.49	0.49	0.53	0.62	0.52	1.22	0.57	0.48	0.68	0.44
Coefficent of Variation	7.14	3.76	6.71	6.55	7.22	7.74	4.85	5.87	6.70	6.60	11.20	6.09	5.69	5.51	8.40	6.14	7.42	5.94	6.47	6.52
Maximum	186.0	5.7	10.5	11.6	21.0	10.1	14.0	17.5	9.5	13.2	5.7	8.8	10.3	12.5	7.4	22.5	9.1	9.2	12.5	7.5
Minimum	145.0	5.2	8.3	8.8	14.6	7.2	11.0	13.6	7.0	9.3	3.4	6.0	8.0	9.4	4.9	16.5	6.3	7.1	8.6	5.8
Number	8	3	15	24	59	49	57	51	46	42	22	60	69	90	82	113	94	97	73	59
Tomarctus brevirostris																				
Holotype (AMNH 8302)																23.0	8.2	8.6		
Mean	171.00		9.96	11.58	19.94	9.37	14.48	17.34	8.04	12.29	4.83	8.70	10.29	12.52	7.39	22.54	8.69	8.77	10.95	7.28
Standard Deviation	0.00		0.47	0.61	1.03	0.65	0.79	0.89	0.30	0.64	0.85	0.59	0.50	0.65	0.59	0.78	0.50	0.44	0.92	0.54
Coefficent of Variation	0.00		4.69	5.24	5.15	6.89	5.44	5.12	3.76	5.19	17.58	6.76	4.90	5.20	7.97	3.44	5.76	4.98	8.40	7.42
Maximum	171.0		10.4	12.6	21.7	10.6	15.7	19.1	8.5	13.0	6.0	9.3	11.3	13.8	9.5	24.8	9.7	9.8	13.0	8.5
Minimum	171.0		9.3	11.0	18.2	8.0	13.4	15.5	7.5	11.0	4.0	7.0	9.0	11.0	6.6	21.0	8.0	8.0	9.5	6.2
Number	1		5	6	12	11	13	11	9	8	3	17	23	30	27	36	31	30	20	17
Aulurodon asthenostylus																				
Holotype (LACM-CIT 781)					21.8	10.6	15.9	18.8	8.6	12.0	5.7	9.4	11.1	14.6	8.6	25.7	9.9	9.5	12.1	8.1
Mean	186.00	7.08	11.03	13.52	23.28	11.09	14.93	18.26	7.57	12.23	5.47	9.56	11.31	13.94	8.44	25.58	9.81	9.12	11.14	7.58

APPENDIX III. Dental Measurements *continued*

	BL	LP1	LP2	LP3	LP4	WP4	LM1	WM1	LM2	WM2	Lp1	Lp2	Lp3	Lp4l	Wp4	Lm1	Wm1tr	Wm1tl	Lm2	Wm2
Aulurodon asthenostylus continued																				
Standard Deviation	9.00	0.86	0.88	1.09	1.00	0.62	0.82	1.07	0.63	1.02	0.44	0.66	0.70	0.99	0.47	1.31	0.73	0.75	0.84	0.46
Coefficent of Variation	4.84	12.18	7.96	8.05	4.28	5.57	5.48	5.86	8.33	8.30	8.05	6.94	6.18	7.10	5.59	5.14	7.42	8.20	7.51	6.11
Maximum	195.0	8.8	13.4	16.5	26.0	13.3	17.0	20.5	8.8	14.5	6.3	11.0	13.1	17.8	9.7	28.5	11.2	11.3	13.7	8.6
Minimum	177.0	6.5	9.9	11.5	21.0	10.0	13.3	16.0	6.8	10.8	4.5	8.5	10.4	12.2	7.6	22.0	8.3	8.0	9.3	6.6
Number	2	6	12	22	33	29	34	32	30	29	10	33	38	45	36	52	36	39	40	35
Aelurodon mcgrewi																				
Holotype (F:AM 22410)	210.0	7.2	12.1	15.0	27.0	11.2	16.7	17.2	7.7	10.4		10.8	12.6	16.5	9.7	27.2	10.5		10.1	8.2
Mean	206.00	7.53	11.80	14.70	26.25	11.33	16.00	17.80	7.05	10.40	5.85	9.95	11.58	14.83	8.80	25.67	10.07	8.70	10.40	7.68
Standard Deviation	4.00	0.25	0.25	0.64	0.91	0.66	0.62	0.73	0.48	1.06	0.55	0.93	0.93	1.41	1.02	1.37	0.85	0.94	0.47	0.44
Coefficent of Variation	1.94	3.31	2.16	4.36	3.48	5.84	3.88	4.13	6.77	10.15	9.40	9.39	8.03	9.52	11.64	5.35	8.42	10.76	4.51	5.79
Maximum	210.0	7.8	12.1	15.2	27.0	12.0	16.7	18.8	7.7	11.5	6.4	10.9	12.7	16.6	10.6	27.5	11.8	10.5	11.2	8.2
Minimum	202.0	7.2	11.5	13.6	24.7	10.3	15.2	17.0	6.5	8.7	5.3	8.7	10.4	13.0	7.8	23.5	9.2	7.4	9.8	7.1
Number	2	3	4	4	4	4	4	4	4	4	2	4	5	6	6	7	7	6	5	5
Aelurodon stirtoni																				
Holotype (UCMP 33474)				13.7	25.1	9.5	14.1	16.7												
Mean	174.33	6.30	10.30	13.90	24.20	10.34	13.74	16.80	5.72	8.80	6.25	9.16	11.18	14.18	9.25	24.69	10.13	8.48	8.90	7.12
Standard Deviation	2.05	0.50	0.56	0.57	1.29	0.62	0.39	0.48	0.49	0.94	0.75	0.59	0.70	0.89	0.59	1.13	0.66	0.44	0.92	0.50
Coefficent of Variation	1.18	7.94	5.46	4.09	5.32	5.96	2.85	2.84	8.52	10.71	12.00	6.45	6.25	6.30	6.38	4.57	6.54	5.18	10.35	6.96
Maximum	177.0	6.8	10.7	15.0	25.3	11.1	14.2	17.7	6.2	9.7	7.0	10.4	12.1	15.7	10.0	26.2	11.6	9.1	10.0	7.8
Minimum	172.0	5.8	9.2	13.2	21.3	9.4	13.2	16.1	5.0	7.1	5.5	8.3	10.0	12.6	8.3	22.3	9.4	7.8	7.5	6.2
Number	3	2	5	7	8	7	7	8	5	5	2	9	11	11	11	12	11	12	10	10
Aelurodon ferox																				
Holotype (USNM 523)					27.1	12.7														
Mean	216.21	8.65	13.37	16.20	26.42	12.03	16.58	19.66	8.37	12.95	7.55	11.39	13.42	16.52	9.46	28.24	10.96	9.94	12.01	8.24
Standard Deviation	12.68	0.88	1.08	1.37	1.71	1.02	1.06	1.23	0.89	1.16	1.19	1.00	1.13	1.35	0.87	1.59	0.75	0.65	0.92	0.58
Coefficent of Variation	5.86	10.22	8.05	8.46	6.47	8.49	6.38	6.26	10.67	8.95	15.79	8.75	8.45	8.15	9.15	5.64	6.86	6.53	7.65	7.01
Maximum	243.0	10.3	16.0	19.5	31.2	15.0	18.8	21.9	10.5	15.5	9.6	13.5	16.2	21.0	11.6	32.5	12.7	11.5	14.5	9.8
Minimum	197.0	7.0	11.3	13.2	22.3	9.1	14.3	16.5	6.4	9.7	5.3	9.4	11.0	13.9	7.8	24.2	9.4	8.5	9.7	7.2
Number	14	15	38	38	60	50	56	55	44	44	18	58	68	80	70	86	70	74	66	61
Aelurodon taxoides																				
Holotype (YPM-PU 10635)												13.5	16.2	20.5	11.5	32.0	12.5	11.5	12.8	9.5
Mean	245.25	9.40	15.47	18.63	28.17	12.97	16.99	19.93	8.41	12.56	9.05	13.10	15.54	19.22	10.97	30.05	11.82	10.33	12.84	9.08
Standard Deviation	14.91	1.00	1.40	1.47	2.58	1.03	1.40	1.73	0.91	1.86	0.82	1.17	1.51	1.68	0.98	2.50	1.17	1.22	1.37	0.84
Coefficent of Variation	6.08	10.69	9.02	7.91	9.15	7.97	8.21	8.68	10.76	14.80	9.08	8.96	9.69	8.76	8.90	8.33	9.92	11.81	10.66	9.25
Maximum	264.0	10.5	17.7	22.0	34.5	15.3	20.2	23.5	10.0	15.5	10.7	16.7	20.3	23.9	13.6	36.5	14.5	13.0	18.0	11.6
Minimum	211.0	7.0	13.2	16.0	24.5	11.0	14.3	16.8	7.0	8.4	7.4	11.0	13.0	15.9	9.4	26.0	10.0	8.0	10.8	7.8
Number	8	8	23	29	35	31	36	36	21	20	13	46	49	60	58	62	55	54	41	40
Paratomarctus temerarius																				
Holotype (USNM 768)																16.0	6.0	6.4		
Mean	139.86	4.68	7.70	9.13	15.18	7.31	11.66	13.79	7.09	10.21	3.73	6.78	7.86	9.50	5.10	17.87	6.65	7.18	9.55	6.06
Standard Deviation	8.85	0.39	0.57	0.65	1.30	0.71	0.94	1.05	0.56	0.86	0.53	0.53	0.60	0.79	0.47	1.23	0.54	0.63	0.81	0.55

APPENDIX III. Dental Measurements *continued*

	BL	LP1	LP2	LP3	LP4	WP4	LM1	WM1	LM2	WM2	Lp1	Lp2	Lp3	Lp4l	Wp4	Lm1	Wm1tr	Wm1tl	Lm2	Wm2
Paratomarctus temerarius continued																				
Coefficent of Variation	6.33	8.41	7.46	7.15	8.57	9.71	8.06	7.63	7.91	8.39	14.12	7.83	7.67	8.28	9.17	6.91	8.13	8.80	8.49	9.15
Maximum	155.0	5.4	8.8	11.1	18.0	9.0	14.5	16.5	8.8	11.8	5.0	7.8	9.3	11.5	6.1	21.0	8.0	8.7	11.5	7.2
Minimum	129.0	4.0	6.5	8.2	13.1	5.8	10.0	11.9	6.3	8.2	3.2	5.7	6.6	8.0	4.0	15.5	5.5	5.5	8.2	5.0
Number	11	13	27	36	60	49	61	56	54	51	9	53	63	89	80	110	93	94	79	68
Paratomarctus euthos																				
Holotype (UCMP 29282)			8.0	10.0	17.5		13.3	16.6	7.1	11.4										
Mean	152.00	5.10	7.73	9.24	17.83	8.13	12.70	14.46	7.15	10.69	4.76	6.96	8.09	10.48	5.81	20.34	7.44	7.81	9.63	6.36
Standard Deviation	9.03	0.10	0.33	0.68	1.14	0.69	0.75	1.21	0.41	0.81	0.45	0.86	0.75	0.82	0.54	1.19	0.61	0.65	0.76	0.63
Coefficent of Variation	5.94	1.96	4.27	7.40	6.40	8.49	5.92	8.35	5.74	7.58	9.54	12.29	9.26	7.87	9.29	5.87	8.18	8.32	7.84	9.94
Maximum	160.0	5.2	8.3	10.2	21.0	10.0	14.5	16.6	7.5	12.0	5.3	9.5	10.1	12.4	7.2	23.5	9.0	9.3	11.1	7.7
Minimum	137.0	5.0	7.3	8.4	15.5	7.3	11.1	12.8	6.1	9.2	4.3	5.5	6.3	8.5	4.5	17.5	6.0	6.8	8.4	5.4
Number	4	2	9	8	21	15	15	12	10	10	5	17	23	32	29	41	34	34	23	22
Carpocyon compressus																				
Holotype (AMNH 8543)														10.0	5.5	19.5		8.0		
Mean	167.00	5.50	8.25	10.07	17.20	8.68	13.43	15.36	7.70	10.22	4.70	7.94	9.12	11.13	6.26	20.94	7.88	8.44	11.86	7.58
Standard Deviation	0.00	0.00	0.25	1.07	1.63	0.74	1.16	1.38	0.37	0.64	0.10	0.34	0.56	0.69	0.40	1.29	0.41	0.52	0.73	0.40
Coefficent of Variation	0.00	0.00	3.03	10.59	9.47	8.49	8.65	8.97	4.74	6.23	2.13	4.26	6.12	6.19	6.41	6.18	5.14	6.13	6.12	5.30
Maximum	167.0	5.5	8.5	11.3	19.3	9.5	15.0	17.0	8.2	11.1	4.8	8.5	10.0	12.3	7.0	22.5	8.8	9.4	13.1	8.2
Minimum	167.0	5.5	8.0	8.7	14.8	7.5	11.6	12.8	7.1	9.4	4.6	7.5	8.5	10.0	5.5	18.4	7.0	7.6	10.6	7.0
Number	1	1	2	3	4	4	6	7	6	6	2	5	6	16	15	17	13	18	12	12
Carpocyon webbi																				
Holotype (F:AM 61328)	205.0	6.8	10.5	12.5	21.0	10.5	15.8	19.0	10.5	13.7										
Mean	205.00	6.20	9.83	12.34	20.62	10.34	15.34	18.11	9.65	13.60	5.90	9.51	11.22	13.45	7.60	24.65	9.55	9.65	13.29	8.26
Standard Deviation	0.00	0.60	0.81	1.01	1.26	0.87	0.86	1.21	0.44	0.64	0.10	0.79	0.90	0.86	0.44	1.70	0.65	0.56	0.74	0.24
Coefficent of Variation	0.00	9.68	8.19	8.21	6.10	8.41	5.61	6.66	4.55	4.72	1.69	8.34	8.06	6.37	5.80	6.90	6.84	5.84	5.57	2.95
Maximum	205.0	6.8	10.5	13.2	23.0	12.0	16.5	20.5	10.5	14.5	6.0	10.7	12.2	14.8	8.2	27.5	10.6	10.5	14.5	8.6
Minimum	205.0	5.6	8.7	10.4	18.5	9.3	14.0	16.5	9.2	12.5	5.8	8.3	9.5	11.5	6.7	21.5	8.5	8.5	11.8	7.9
Number	1	2	3	5	10	7	9	8	8	8	2	10	6	13	11	16	11	13	16	13
Carpocyon robustus																				
Holotype (UCMP 33569)											5.0	8.0	8.5	12.5	7.6	22.3	8.7	8.6	10.8	7.0
Mean	166.00	5.30	9.00	10.75	19.30	9.53	13.73	16.87	8.60	11.73	4.70	8.09	9.55	13.06	7.90	23.84	9.18	9.24	11.40	7.82
Standard Deviation	0.00	0.00	0.00	0.75	1.78	0.81	0.70	0.98	0.37	0.81	0.29	0.70	0.77	0.60	0.58	1.61	0.66	0.52	0.57	0.55
Coefficent of Variation	0.00	0.00	0.00	6.98	9.25	8.48	5.08	5.84	4.27	6.89	6.26	8.67	8.11	4.56	7.38	6.77	7.17	5.68	5.01	7.06
Maximum	166.0	5.3	9.0	11.5	20.9	10.3	14.5	18.0	9.0	12.5	5.0	9.8	11.0	14.0	8.6	26.9	9.8	10.0	12.5	8.5
Minimum	166.0	5.3	9.0	10.0	16.5	8.3	12.6	15.6	8.0	10.5	4.3	7.0	8.2	12.0	6.5	20.0	7.8	8.3	10.5	7.0
Number	1	1	1	2	4	4	4	3	4	4	3	9	10	12	11	14	12	11	9	6
Carpocyon limosus																				
Holotype (UF 12069)				9.7	15.7	8.0	11.4	13.8	8.6	11.2										
Mean				9.70	15.70	8.00	12.25	15.10	9.30	13.15										
Standard Deviation				0.00	0.00	0.00	0.85	1.10	0.70	0.05										
Coefficent of Variation				0.00	0.00	0.00	6.94	7.28	7.53	0.38										

APPENDIX III. Dental Measurements *continued*

	BL	LP1	LP2	LP3	LP4	WP4	LM1	WM1	LM2	WM2	Lp1	Lp2	Lp3	Lp4l	Wp4	Lm1	Wm1tr	Wm1tl	Lm2	Wm2
Carpocyon limosus continued																				
Maximum				9.7	15.7	8.0	13.1	16.2	10.0	13.2										
Minimum				9.7	15.7	8.0	11.4	14.0	8.6	13.1										
Number				1	1	1	2	2	2	2										
Protepicyon raki																				
Holotype (F:AM 61705)			11.0	13.5	25.0	10.9	17.5	20.5	8.8	15.5	6.3	9.9	13.0	16.5	9.6	29.5	9.8	10.9		
Mean	209.67	7.10	11.23	13.86	24.37	11.00	16.12	19.54	8.29	13.79	5.90	9.84	11.58	14.81	8.99	26.61	9.95	10.04	12.26	8.28
Standard Deviation	16.34	0.00	0.43	0.91	0.93	0.65	0.80	1.06	0.74	1.36	0.34	0.59	0.60	0.96	0.60	1.36	0.53	0.60	1.00	0.59
Coefficent of Variation	7.79	0.00	3.83	6.54	3.83	5.87	4.94	5.42	8.95	9.84	5.71	5.95	5.20	6.49	6.62	5.12	5.30	5.95	8.11	7.08
Maximum	230.0	7.1	11.8	15.0	25.5	11.8	17.5	21.5	9.5	16.0	6.3	10.7	13.0	16.5	10.1	29.5	10.8	11.0	14.5	9.2
Minimum	190.0	7.1	10.5	12.3	22.0	10.0	14.5	18.0	7.0	11.7	5.4	8.8	10.8	13.5	8.0	24.0	9.2	9.2	11.0	7.3
Number	3	1	8	8	14	12	12	12	12	12	6	14	17	18	14	19	11	12	13	13
Epicyon aelurodontoides																				
Holotype (F:AM 67025)			12.0		31.3	13.7	20.2	20.6	8.2	11.7										
Epicyon saevus																				
Holotype (USNM 126)																26.7	10.2	9.9	11.0	8.0
Mean	211.47	6.76	11.16	14.61	25.92	11.48	17.45	20.32	9.40	13.07	5.45	9.25	11.27	16.82	9.97	29.09	11.42	10.66	13.04	8.90
Standard Deviation	18.14	0.62	0.72	1.44	2.19	1.06	1.30	1.49	0.94	1.35	0.70	0.77	0.81	1.49	0.92	1.84	0.78	0.83	1.14	0.77
Coefficent of Variation	8.58	9.23	6.47	9.85	8.44	9.24	7.43	7.35	9.98	10.30	12.75	8.29	7.23	8.83	9.20	6.33	6.82	7.80	8.77	8.70
Maximum	248.0	7.7	12.6	17.1	32.3	13.5	20.5	25.0	11.4	16.0	6.7	11.0	13.0	20.3	12.5	34.0	13.3	13.3	15.4	11.6
Minimum	195.0	5.5	10.0	12.0	21.8	9.4	15.0	17.8	7.3	11.0	4.4	7.0	8.2	13.0	7.8	24.5	9.0	9.2	8.9	7.2
Number	7	9	25	29	66	64	67	64	43	40	21	87	106	140	124	173	147	143	98	89
Epicyon haydeni																				
Holotype (USNM 127)													14.7	20.5	11.8	35.0	15.1	13.6		
Mean	276.86	8.55	13.63	17.31	32.97	15.00	20.63	24.34	10.84	15.15	6.67	11.27	13.96	21.91	13.11	36.25	14.39	13.07	15.68	10.13
Standard Deviation	32.27	1.08	1.32	1.97	2.74	1.18	1.57	2.06	1.04	1.75	0.68	1.10	1.38	2.01	1.23	2.69	1.14	0.97	1.02	0.80
Coefficent of Variation	11.66	12.62	9.65	11.39	8.30	7.88	7.60	8.44	9.64	11.52	10.15	9.78	9.86	9.16	9.37	7.42	7.90	7.40	6.53	7.94
Maximum	315.0	10.0	16.5	20.3	40.0	17.1	24.0	28.0	12.8	17.8	7.6	13.5	18.0	26.1	15.8	42.5	17.2	15.2	18.0	11.6
Minimum	215.0	6.6	11.0	14.0	26.2	12.5	18.0	20.5	8.8	9.9	5.2	8.0	10.5	18.0	9.9	31.5	12.0	11.0	13.2	8.5
Number	7	11	27	33	48	41	43	40	25	26	18	64	72	95	83	104	84	89	50	41
Borophagus littoralis																				
Holotype (UCMP 31503)	197.0		11.0	12.7	25.6	11.2	16.7	19.7	9.0	12.9										
Mean	187.00	6.90	11.07	13.74	24.31	10.61	16.55	19.33	9.68	12.43	5.50	8.40	9.90	16.12	9.48	26.50	10.76	10.11	12.88	8.83
Standard Deviation	10.00	0.85	0.55	0.81	1.79	1.03	0.57	1.20	0.67	0.36	0.00	0.25	0.07	1.31	0.57	1.10	0.59	0.50	0.65	0.60
Coefficent of Variation	5.35	12.35	5.01	5.87	7.37	9.73	3.47	6.21	6.91	2.87	0.00	3.04	0.71	8.15	6.03	4.13	5.46	4.94	5.04	6.81
Maximum	197.0	7.6	11.9	15.0	28.0	12.8	17.7	23.0	10.6	12.9	5.5	8.7	10.0	18.3	10.4	28.0	11.2	10.6	13.7	9.4
Minimum	177.0	5.7	10.0	12.6	21.6	8.7	15.5	17.9	8.5	12.0	5.5	8.0	9.8	14.5	9.0	25.1	9.4	9.1	11.9	8.0
Number	2	3	7	7	11	11	15	15	8	8	1	4	4	5	4	12	7	7	4	3
Borophagus pugnator																				
Holotype (CMNH 184)		6.5	10.0	13.0	25.0	12.1	17.8	20.6	8.8	14.3										
Mean		6.18	9.10	11.75	24.57	11.20	16.90	18.74	9.61	13.78	4.78	7.81	9.72	16.04	9.83	26.88	10.75	10.15	12.10	8.07
Standard Deviation		0.20	0.66	0.77	2.22	1.25	0.98	3.11	0.97	1.38	0.40	0.77	1.10	1.55	1.11	1.81	0.90	0.72	1.23	0.80

APPENDIX III. Dental Measurements *continued*

	BL	LP1	LP2	LP3	LP4	WP4	LM1	WM1	LM2	WM2	Lp1	Lp2	Lp3	Lp4l	Wp4	Lm1	Wm1tr	Wm1tl	Lm2	Wm2
Borophagus pugnator continued																				
Coefficent of Variation		3.31	7.29	6.55	9.05	11.12	5.77	16.62	10.10	9.99	8.29	9.91	11.29	9.67	11.29	6.74	8.33	7.13	10.13	9.91
Maximum		6.5	10.0	13.0	28.1	12.4	18.0	21.1	11.4	16.6	5.4	8.6	11.9	18.3	11.7	31.1	12.4	11.3	14.1	9.6
Minimum		6.0	8.0	10.9	20.3	9.0	14.5	8.8	8.0	11.5	4.3	6.1	7.9	13.0	8.0	23.5	8.9	8.7	10.5	7.2
Number		4	5	4	9	8	14	14	10	10	4	10	20	26	23	29	28	26	11	10
Borophagus orc																				
Holotype (UF 13180)													6.7	13.6	8.1	21.2	9.3	8.3	10.0	7.3
Mean			8.10	10.37	20.37	9.05	12.70	15.30				6.50	7.20	14.07	8.63	22.15	9.27	8.35	10.13	7.07
Standard Deviation			0.33	0.54	0.29	0.32	0.10	0.20				0.00	0.37	0.39	0.28	0.65	0.17	0.05	0.09	0.29
Coefficent of Variation			4.03	5.24	1.41	3.54	0.79	1.31				0.00	5.20	2.80	3.25	2.93	1.83	0.60	0.93	4.06
Maximum			8.5	10.8	20.7	9.5	12.8	15.5				6.5	7.7	14.5	9.1	22.8	9.5	8.4	10.2	7.4
Minimum			7.7	9.6	20.0	8.7	12.6	15.1				6.5	6.8	13.4	8.3	21.5	9.1	8.3	10.0	6.7
Number			3	3	3	4	2	2				1	3	6	6	2	3	2	3	3
Borophagus parvus																				
Holotype (F:AM 75857)	166.0		7.0	8.9	19.8	10.3	15.0	17.3	6.5	10.8										
Mean	166.00	4.58	7.45	9.47	20.21	9.32	14.08	17.18	6.51	10.76	3.84	5.56	6.54	12.63	8.95	23.76	9.66	9.46	10.31	7.67
Standard Deviation	0.00	0.31	0.72	0.52	0.91	0.53	0.69	0.97	0.52	0.69	0.21	0.47	0.58	0.82	0.57	0.94	0.63	0.52	0.61	0.47
Coefficent of Variation	0.00	6.80	9.72	5.48	4.52	5.67	4.87	5.63	7.99	6.37	5.36	8.48	8.79	6.48	6.36	3.97	6.58	5.49	5.96	6.09
Maximum	166.0	4.9	8.3	10.8	22.0	10.5	15.3	18.9	7.4	12.0	4.1	6.6	8.1	14.8	10.8	26.0	11.2	10.5	11.6	8.4
Minimum	166.0	4.1	6.1	8.7	18.0	8.3	13.0	14.8	5.6	9.5	3.5	4.9	5.4	10.6	8.2	21.8	8.2	8.2	9.0	6.6
Number	1	4	13	14	27	18	23	19	17	17	5	18	38	59	48	72	56	54	46	39
Borophagus secundus																				
Holotype (AMNH 13831)													8.5	15.5	9.8	26.1	11.0	9.5	10.5	7.7
Mean	190.30	6.07	9.08	11.76	25.02	11.37	16.26	19.56	9.55	13.79	3.50	7.14	8.67	16.14	10.91	26.92	11.26	10.41	11.85	8.65
Standard Deviation	10.41	0.48	0.64	0.82	1.34	0.76	0.84	1.12	0.74	0.93	0.00	0.60	0.68	0.97	0.65	1.19	0.59	0.60	0.71	0.52
Coefficent of Variation	5.47	7.87	6.99	6.97	5.34	6.67	5.18	5.70	7.79	6.71	0.00	8.44	7.80	6.03	5.97	4.41	5.21	5.73	5.95	6.01
Maximum	202.0	7.2	11.0	13.5	28.6	13.8	19.4	22.6	11.5	15.5	3.5	8.6	10.5	18.7	12.7	32.0	12.9	12.2	13.9	10.5
Minimum	172.0	5.2	7.8	9.6	21.5	9.6	14.0	17.2	7.4	11.6	3.5	5.5	7.0	14.0	8.5	23.8	10.0	8.3	10.0	7.2
Number	5	32	76	88	148	134	128	121	83	78	1	66	139	233	228	250	236	229	164	153
Borophagus hilli																				
Holotype (WTM 1558)			10.7	11.1	29.6	11.8	16.6	21.7	9.5	10.6			9.0	18.2	11.4	29.7	11.8	10.1	11.6	8.1
Mean			10.10	11.50	28.46	12.41	16.71	20.93	9.25	10.75		8.30	9.10	18.51	13.18	29.88	12.52	10.83	12.17	8.61
Standard Deviation			0.60	0.37	2.10	1.02	0.73	1.49	0.25	0.15		0.00	0.57	0.83	1.14	1.54	1.16	1.04	0.99	0.48
Coefficent of Variation			5.94	3.25	7.37	8.25	4.38	7.12	2.70	1.40		0.00	6.22	4.47	8.65	5.16	9.24	9.60	8.10	5.53
Maximum			10.7	12.0	31.1	14.6	17.5	23.4	9.5	10.9		8.3	9.8	20.5	15.8	34.0	14.6	13.2	13.6	9.4
Minimum			9.5	11.1	24.5	11.2	15.5	19.3	9.0	10.6		8.3	8.0	17.4	11.4	27.8	11.1	9.0	11.0	7.9
Number			2	3	10	9	7	7	2	2		1	8	17	16	17	17	15	9	7
Borophagus dudleyi																				
Holotype (MCZ 3688)	220.0			12.3	32.2															
Borophagus diversidens																				
Holotype (TMM 40287-10)													11.5	20.2						
Mean	206.50	7.73	9.88	11.80	30.48	14.32	17.93	21.64	9.82	11.98	7.50	9.18	10.10	20.68	15.32	32.91	14.53	11.44	12.03	8.48

APPENDIX III. Dental Measurements *continued*

	BL	LP1	LP2	LP3	LP4	WP4	LM1	WM1	LM2	WM2	Lp1	Lp2	Lp3	Lp4l	Wp4	Lm1	Wm1tr	Wm1tl	Lm2	Wm2
Borophagus diversidens continued																				
Standard Deviation	10.50	0.16	0.36	0.84	2.12	1.08	1.06	1.37	1.36	1.16	0.00	0.90	0.91	1.12	1.09	1.79	0.86	0.84	0.99	0.64
Coefficent of Variation	5.08	2.12	3.67	7.14	6.95	7.52	5.91	6.34	13.81	9.72	0.00	9.81	8.98	5.42	7.08	5.45	5.89	7.34	8.25	7.60
Maximum	217.0	8.0	10.5	13.4	34.5	16.2	19.4	24.4	13.3	13.2	7.5	11.2	12.0	23.5	18.0	37.5	17 0	13.1	14.5	10.1
Minimum	196.0	7.6	9.3	10.4	27.0	11.8	15.8	19.4	8.6	9.8	7.5	7.7	8.0	18.1	13.3	29.2	13.0	9.7	10.3	7.3
Number	2	4	6	8	21	15	19	18	9	9	1	10	26	32	27	32	28	26	23	23